

Applied Mathematical Sciences

Christian Kuehn

Multiple Time Scale Dynamics

 Springer

Applied Mathematical Sciences

Volume 191

Founding Editors

Fritz John, Joseph Laselle and Lawrence Sirovich

Editors

S.S. Antman

ssa@math.umd.edu

Leslie Greengard

greengard@cims.nyu.edu

P.J. Holmes

pholmes@math.princeton.edu

Advisors

J. Keener

R.V. Kohn

B. Matkowsky

P. Newton

R. Pego

C. Peskin

L. Ryzhik

A. Singer

A. Stevens

A. Stuart

More information about this series at <http://www.springer.com/series/34>

Christian Kuehn

Multiple Time Scale Dynamics

Christian Kuehn
Institute for Analysis
and Scientific Computing
Vienna University of Technology
Vienna, Austria

ISSN 0066-5452 ISSN 2196-968X (electronic)
ISBN 978-3-319-12315-8 ISBN 978-3-319-12316-5 (eBook)
DOI 10.1007/978-3-319-12316-5
Springer Cham Heidelberg New York Dordrecht London

Library of Congress Control Number: 2014955212

Mathematics Subject Classification: 34-01, 34-02, 34A26, 34A34, 34C26, 34C45, 37-01, 37-02, 34Exx,
37Gxx

© Springer International Publishing Switzerland 2015

This work is subject to copyright. All rights are reserved by the Publisher, whether the whole or part of the material is concerned, specifically the rights of translation, reprinting, reuse of illustrations, recitation, broadcasting, reproduction on microfilms or in any other physical way, and transmission or information storage and retrieval, electronic adaptation, computer software, or by similar or dissimilar methodology now known or hereafter developed. Exempted from this legal reservation are brief excerpts in connection with reviews or scholarly analysis or material supplied specifically for the purpose of being entered and executed on a computer system, for exclusive use by the purchaser of the work. Duplication of this publication or parts thereof is permitted only under the provisions of the Copyright Law of the Publisher's location, in its current version, and permission for use must always be obtained from Springer. Permissions for use may be obtained through RightsLink at the Copyright Clearance Center. Violations are liable to prosecution under the respective Copyright Law.

The use of general descriptive names, registered names, trademarks, service marks, etc. in this publication does not imply, even in the absence of a specific statement, that such names are exempt from the relevant protective laws and regulations and therefore free for general use.

While the advice and information in this book are believed to be true and accurate at the date of publication, neither the authors nor the editors nor the publisher can accept any legal responsibility for any errors or omissions that may be made. The publisher makes no warranty, express or implied, with respect to the material contained herein.

Printed on acid-free paper

Springer is part of Springer Science+Business Media (www.springer.com)

Preface

This book aims to provide an introduction to dynamical systems with multiple time scales. As in any overview book, several topics are covered only quite briefly. My aim was to focus on topics that seem to be less available in introductory form. However, I try to give a global view of the subject by covering a broad spectrum of ideas and tools. The detailed bibliography aims to direct the reader to further topics. To explain it with a simple metaphor: using this book should make you more familiar with a country’s map, culture, and main attractions rather than imparting details of every street in just one city. Both things are useful at times.

The term “multiple time scale dynamics” is rather modern. The subject and many of its core ideas are much older. For example, “singular perturbation theory” or “multiscale systems” encompass a larger variety of topics than what I present here. On the one hand, no serious multidimensional spatial problems are considered in this book. Furthermore, there are many singularly perturbed problems that have very little to do with dynamical systems. On the other hand, ordinary differential equations (ODEs) with multiple time scales already contain motivation, technique, and intuition for more complicated scenarios.

Classical singular perturbation theory for multiple time scale systems provides many asymptotic techniques centered on series expansions, matching, and averaging. These methods are still indispensable today, and this book gives an overview of them. However, the details are not covered, since many excellent introductory texts are available. The last two decades have brought major additional progress with a particular focus on geometric ideas as well as powerful numerical algorithms. A major goal of this book was to merge several viewpoints with a wide variety of different techniques into a unified framework. Another reason for the broad choice of topics was to make it easier for students and researchers new to the field to get a much quicker overview.

Again, I would like to warn the reader that this book is obviously not a mathematical monograph aiming at a complete treatment of the entire field of multiple time scales. Some readers, particularly students, may wonder how a book of over 700 pages can be only an “introduction,” but let me point out that most chapters, and even many five-page sections, in this book in fact deserve their own mathematical monograph of 300 pages or more. A few such books have

been written, while many exist only in a distant, happier future. I encourage my colleagues working in the field—you know who you are—to begin work on such projects and fill in the missing mathematical details that I decided to leave out in order to make the subject much more accessible to beginners. Despite the simplifications, there seem to be several advantages of the style of presentation. The great diversity of the subject, ranging from mathematical theory in dynamics, analysis, geometry, topology, stochastics, and numerics to virtually all fields in science and engineering applications, easily becomes visible. The unity and interconnections between different approaches to multiple time scale problems can be identified much more readily. Also, scientists with particular applications in mind should find it easier to spot many potential tools right away, while a “purer” mathematician can use this text as a source book of open mathematical problems. The target audience of the book is senior undergraduates, graduate students, as well as researchers interested in using the theory of multiple time scale dynamics in nonlinear science, either from a theoretical or a mathematical modeling perspective. Section 1.1 provides a more detailed guide to the book.

Now I have the pleasure of thanking several colleagues, collaborators, and institutions that have helped to get this book started, keep it on track, and eventually push it over the finish line. First and foremost, I would like to thank my thesis adviser, John Guckenheimer, for introducing me to the field during my time as a graduate student. Undoubtedly, he shaped my view of the field, and without his support and encouragement, I would never have attempted to undertake a book project on multiple time scale systems. Important influences on this book during my postdoctoral years have come from my colleagues Thilo Gross, Peter Szmolyan, Nils Berglund, and Barbara Gentz. Thilo helped me to form bridges from multiscale dynamics to such seemingly distant areas as ecology, networks, systems biology, and statistical physics. I would like to thank Peter for sharing his tremendous insights into all aspects of geometric multiscale dynamics. Nils and Barbara have been constant sources of inspiration on everything stochastic. Although it is clear that I am responsible for all potential errors that may remain within this version, I would like to thank several colleagues who responded with valuable feedback—alerting me to anything from tiny typos to blatant blunders—in various draft versions of this book: Nils Berglund, Alan Champneys, Hayato Chiba, Mike Cortez, Peter De Maesschalck, John Guckenheimer, Pavel Gurevich, Annalisa Iuorio, Mike Jeffrey, Hans Kaper, Daniel Karrasch, Chris Jones, Ilona Kosiuk, Steven Lade, Gabriel Lord, Anatoly Neishtadt, Clare Perryman, Sofia Piltz, Nikola Popovic, Jens Rademacher, Martin Rasmussen, Martin Riedler, Stephen Schechter, Jan Sieber, Eric Siero, Peter Szmolyan, Frits Veerman, Martin Wechselberger, and Antonios Zagaris.

Furthermore, I would like to thank the production staff at Springer for the handling of my manuscript. In particular, Achi Dosanjh has been extremely important and tremendously helpful in leading the entire editorial process. Regarding the formatting of the book, I would also like to thank Yuri Kuznetsov,

who shared his L^AT_EX book formatting preamble with me, from which I took some inspiration for the format of this book. Several anonymous referees also provided very valuable feedback, which helped to improve the book.

During the writing of this book I have also benefited from the generous hospitality and financial support of various institutions, including Cornell University, the Max Planck Institute for Physics of Complex Systems, and the Vienna University of Technology. Furthermore, I would like to thank the Austrian Academy of Sciences for support via the “Austrian Programme for Advanced Research and Technology” and the European Commission for support via a “Marie Curie International Reintegration Grant.” The final push of this project has been supported through the program “Oberwolfach Leibniz Fellows” by the Mathematisches Forschungsinstitut Oberwolfach.

Although it is obvious for an overview book on a topic, let me stress that I do not make any claims to novelty of its content. I have tried to summarize and condense the extensive literature on multiple time scale dynamics into a more accessible expository format. However, I can certainly say that during the writing of this book, several very natural new ideas arose. I hope that the research-oriented reader will have a similar experience and that this book will provide a starting point for new ideas in multiscale dynamics.

Vienna, Austria
2014

Christian Kuehn

Contents

Preface	v
1 Introduction	1
1.1 User's Guide	1
1.2 Fast–Slow Systems	8
1.3 The van der Pol Equation	9
1.4 The FitzHugh–Nagumo Equation	10
1.5 Terminology: Fast–Slow Systems	11
1.6 Terminology: Asymptotic Analysis	14
1.7 References	16
2 General Fenichel Theory	19
2.1 Invariant Manifolds	20
2.2 Perturbations of Invariant Manifolds	28
2.3 Normal Hyperbolicity	40
2.4 Specialization to Fast–Slow Systems	47
2.5 References	50
3 Geometric Singular Perturbation Theory	53
3.1 Fenichel's Theorem	53
3.2 The Slow Flow	58
3.3 Singularities	61
3.4 Examples	65
3.5 References	70
4 Normal Forms	71
4.1 The Normally Hyperbolic Case	71
4.2 Fold Points	77
4.3 Fold Curves	80
4.4 Systems of First Approximation	82
4.5 A Note on Linear Systems	85
4.6 References	88

5	Direct Asymptotic Methods	91
5.1	Elementary Results	91
5.2	Basics of Relaxation Oscillations	95
5.3	Normally Hyperbolic Planar Systems	98
5.4	Generic Folds in Planar Systems	103
5.5	The Period of Relaxation Oscillations	108
5.6	References	111
6	Tracking Invariant Manifolds	113
6.1	Simple Jumps and Transversality	114
6.2	The FitzHugh–Nagumo Equation	120
6.3	The C^0 Exchange Lemma	124
6.4	The C^1 Exchange Lemma	129
6.5	Fast Waves in the FitzHugh–Nagumo Equation	141
6.6	Strong Exchange Lemmas	145
6.7	BVPs and Periodic Orbits	149
6.8	References	155
7	The Blowup Method	159
7.1	Basics	160
7.2	Local Computation	167
7.3	The Quasihomogeneous Case	171
7.4	Blowup Analysis of the Generic Fold	178
7.5	Relaxation Oscillations in \mathbb{R}^2	187
7.6	Relaxation Oscillations in \mathbb{R}^3	190
7.7	Remarks on Rescaling	194
7.8	References	196
8	Singularities and Canards	197
8.1	Folded Singularities in Planar Systems	198
8.2	Singular Hopf Bifurcation in \mathbb{R}^2	205
8.3	The First Lyapunov Coefficient	208
8.4	Canard Explosion	210
8.5	Canards in \mathbb{R}^3	213
8.6	Secondary Canards at Folded Nodes	223
8.7	Singularities beyond Folds	228
8.8	Curvature	233
8.9	References	235
9	Advanced Asymptotic Methods	239
9.1	Matched Asymptotic Expansions	240
9.2	Further Concepts and Terminology	251
9.3	The Boundary Function Method	255
9.4	WKB Theory	259
9.5	Asymptotics and Blowup	262
9.6	Averaging	265

9.7	Gevrey Asymptotics	268
9.8	Poincaré–Lindstedt and Two-Timing	274
9.9	The Renormalization Group I	279
9.10	The Renormalization Group II	285
9.11	References	290
10	Numerical Methods	295
10.1	Stiff Equations	295
10.2	A-Stability	299
10.3	Boundary Value Problems (BVPs)	303
10.4	Two Standard BVP Methods	306
10.5	Conditioning	308
10.6	Continuation	312
10.7	Heterogeneous Multiscale Methods	315
10.8	Error Analysis for HMM	319
10.9	References	322
11	Computing Manifolds	327
11.1	Basic Techniques	327
11.2	The CSP Method	331
11.3	The ZDP Method	342
11.4	Other Reduction Methods	344
11.5	Saddle-Type Slow Manifolds	348
11.6	Manifolds and Singularities	353
11.7	References	356
12	Scaling and Delay	359
12.1	The Fold Revisited	359
12.2	Delayed Hopf Bifurcation	361
12.3	Delayed Bifurcation and WKB	370
12.4	The Newton Polygon	373
12.5	Power Transformations	376
12.6	Parameterizing Critical Manifolds	379
12.7	Slowly Time-Dependent Systems	384
12.8	Other Newton Polygon Applications	392
12.9	References	395
13	Oscillations	397
13.1	Overview	398
13.2	Folded Nodes	400
13.3	Singular Hopf and Hyperbolic Equilibria	403
13.4	Tourbillon	407
13.5	The Koper Model	408
13.6	Square-Wave / Fold-Homoclinic Bursting	413
13.7	Elliptic / subHopf–Foldcycle Bursting	416
13.8	Three Time-Scale Systems	417
13.9	References	425

14 Chaos in Fast-Slow Systems	431
14.1 A Basic Idea	432
14.2 Chaotic Dynamics	434
14.3 Smale Horseshoes	436
14.4 Chaos in van der Pol's Equation I	442
14.5 Chaos in van der Pol's Equation II	448
14.6 Hénon-Type Maps	455
14.7 Chaotic Forced Oscillations	460
14.8 Constructing Chaotic Attractors	468
14.9 Stochastic Replacement	471
14.10 References	473
15 Stochastic Systems	477
15.1 Motivation and Viewpoints	478
15.2 Fenichel Theory for SDEs	482
15.3 Noisy Fold with Slow Drift	488
15.4 Direct Asymptotics	493
15.5 Stochastic Reduction	497
15.6 Random Dynamical Systems	505
15.7 Markov Chains	510
15.8 Large Deviations	512
15.9 Dynkin's Equation and WKB	517
15.10 References	520
16 Topological Methods	525
16.1 Decomposition of Invariant Sets	525
16.2 Conley Index	530
16.3 Connecting Orbits	535
16.4 Singular Index Pairs	540
16.5 Further Techniques	546
16.6 References	550
17 Spatial Dynamics	553
17.1 Stability of Traveling Waves I	553
17.2 Stability of Traveling Waves II	558
17.3 Conservation Laws	562
17.4 Lattice Dynamical Systems	573
17.5 Adaptive Neural Fields	578
17.6 References	580
18 Infinite Dimensions	583
18.1 Semigroups	584
18.2 Invariant Manifolds	587
18.3 Homogenization	595
18.4 Delay Equations with Small Delay	600
18.5 Differential Inclusions	605

18.6	Amplitude Equations	611
18.7	References	615
19	Other Topics	619
19.1	Differential-Algebraic Equations I	620
19.2	Differential-Algebraic Equations II	624
19.3	Nonsmooth Dynamical Systems	627
19.4	Hysteresis	633
19.5	Nonstandard Analysis: Introduction	637
19.6	Nonstandard Analysis: An Application	642
19.7	Averaging and Adiabatic Invariants	646
19.8	Singular Bifurcation Diagrams	649
19.9	Critical Transitions	654
19.10	References	661
20	Applications	665
20.1	Engineering	665
20.2	Neuroscience	668
20.3	Chemical Oscillations	673
20.4	Lasers	676
20.5	Ecology	679
20.6	Pattern Formation	681
20.7	Celestial Mechanics	685
20.8	Systems Biology	688
20.9	Fluid Dynamics	691
20.10	Quantum Mechanics	694
20.11	Networks	696
20.12	References	700
Bibliography		705
Index		799

Chapter 1

Introduction

In this chapter, we begin in Section 1.1 with a practical guide to orient the reader to how the book is structured and how it can be utilized. Several notational conventions are introduced as well. Section 1.2 covers some basic terminology for systems with two time scales. Sections 1.3 and 1.4 introduce various versions of the van der Pol and FitzHugh–Nagumo equations. We shall use these models throughout the book as examples. Additional basic terms and definitions are considered in Section 1.5, while Section 1.6 is a very brief survey of some concepts and notation in asymptotic analysis.

Background: Throughout this book, it is assumed that the reader is comfortable with the basics of analysis/calculus as well as linear algebra. The relevant topics are discussed in many standard first- and second-year university mathematics courses. There are many excellent texts available on analysis/calculus [EP02, Pug10, Rud76, Spi06] as well as on linear algebra [Gel89, Jän94, Kör12, Str09]. Furthermore, a first course in differential equations is required, preferably with some focus on qualitative dynamics of ordinary differential equations (ODEs); some recommended basic texts are [Arn73, Bra93, Gle94, HSD03, Str00], while more advanced treatments are [Arn83, Chi10, Mei07, Tes12, Ver06]. Knowledge of asymptotic analysis and perturbation methods is not required. Some chapters may require a bit of additional background, which is described at the beginning of each chapter.

1.1 User’s Guide

The main goal of this book is to introduce the area of multiple time scale dynamical systems from a broad perspective. Although this is quite a bold statement, I hope that readers with widely varying backgrounds ranging from second- and third-year undergraduate students up to senior researchers, as well as from “pure mathematicians” to “applied scientists,” will find the book useful in discovering the beauty and utility of multiscale differential equations.

Structure: Although any author’s perfect reader diligently reads an advanced mathematics book cover to cover and carefully tracks all the introduced notation and conventions, such a reader rarely exists in the real world. In fact, I would be delighted if you read the book in front of you in this way, but there definitely is an interplay between the length of the book and your time and topical-interest constraints. Hence, I have deviated from a linear storyline.

Notation and conventions are repeated at several places in the book, in particular at the beginning of each chapter or section. Although this adds a little bit of extra “weight,” it sometimes does not even make a difference. For example, consider two different versions of the same equation:

$$\frac{dx}{dt} = x' = \dots, \quad t \in \mathbb{R}, \quad x = x(t) \in \mathbb{R}^m, \quad (1.1)$$

and

$$x' = \dots. \quad (1.2)$$

The first, (1.1), recalls the notational convention that $(\cdot)'$ means derivative with respect to t and that we often write x instead of $x(t)$. It also recalls the domains and ranges of the variables. The second version (1.2) does none of this but would still take up one line.

The book is designed so that it is possible to browse in it. More precisely, if a particular chapter is of interest to you, then reading that chapter is possible with relatively minimal backtracking. Of course, it is sometimes necessary to look at some main theorem from a previous chapter or go to another section to obtain a broad perspective of the topic.

The presentation has been limited to the basic principles and key technical tricks of the subject. That is, the focus is on highlighting the main concepts and ideas of proofs instead of presenting the latest elaborate tweak of a method. Although this eases the presentation, the drawback is that several statements are not “sharp” or “optimal” in the sense that stronger results could be obtained if more space were available.

Topics: There are many perspectives from which one could approach multiscale dynamical systems. One may start from highly complex systems, such as a global climate-socioecological system or many other “multiphysics” models, and then try to reduce those systems. Obviously, multiple time scales of the various components as well as multiple spatial scales are going to play a crucial role for the reduction. In this process, a focus could be on the physical modeling principle, the numerical methods, asymptotic analysis, or mathematical theorems to go from one scale to the next. All these views are extremely important. However, here we shall take a much more modest approach in terms of our starting point.

I have chosen to follow the paradigm of dynamical systems and abstract genericity theory. This implies that we begin with the simplest possible low-dimensional models that are generic; loosely speaking, they are so frequent that they cannot be avoided, even in arbitrary dimensions or in models of

bewildering complexity. A very intuitive case of scale separation occurs for processes with multiple time scales. Time scale separation is a phenomenon that occurs on the microscale (chemical reactions; quantum tunneling; particles in fluids; single-neuron models) as well as on the macroscale (forest fires and tree growth; climate and weather; ecology and evolution). In fact, it is quite difficult to think of a complex open physical system in which time scale separation never plays a role. From a mathematical perspective, one of the simplest ways to capture multiple time scales is to start with an **ordinary differential equation** (ODE) with just two time scales, so-called fast–slow systems, and two or three phase space variables. It is quite remarkable how many phenomena can be explained on this level, which then, by genericity, reappear in higher-dimensional models. Hence, we try to build the theory and the main ideas from the ground up. Of course, this has the disadvantage that we may not immediately tackle some complex systems, but it definitely contributes to the main goal of this book to make the core ideas visible and accessible.

This approach is also reflected in the topics and their ordering:

Part I: The first main focus is to build some basic geometric/asymptotic intuition and cover the regular (“normally hyperbolic”) theory. Chapter 3 provides the cornerstone result; the proof is in Chapter 2, which may be skipped at first reading. Essentially, one may reduce a fast–slow system that satisfies suitable normal hyperbolicity conditions to the slow variables if the time scale separation is infinite. In Chapter 4, several standard forms are computed for the general hyperbolic case and the simplest nonhyperbolic singularities. Then Chapter 5 covers direct asymptotic techniques to obtain correction terms to the infinite-scale separation assumption.

Part II: The next step is to focus on the slow variables and the normal hyperbolicity condition. Chapter 6 examines transitions from fast motion to slow motion using geometric methods when we are still in a normally hyperbolic setup. Then Chapters 7 and 8 deal extensively with resolving generic singularities that appear once the normal hyperbolicity assumption is violated. The focus is on a geometric desingularization technique and on slow-to-fast transitions. Furthermore, we analyze several classes of initially counterintuitive solutions that arise near singularities.

Part III: Having gained sufficient geometric intuition for the main phenomena, it is time to fill our toolbox. Chapter 9 provides an exposition of a wide variety of asymptotic expansion methods that can be used to obtain series expansions to trajectories and to more general invariant dynamical objects. Chapters 10 and 11 deal with the numerical aspects and also cover a relatively broad range of algorithms. Asymptotic and numerical methods can be employed for various dynamical regimes covered in Parts I and II. In fact, Chapter 12 adds even more tools with an algebraic/combinatorial flavor into the mix and covers another generic singularity from different perspectives.

Part IV: The tools acquired are now put to quite spectacular use by explaining the mechanisms behind oscillatory patterns such as mixed-mode and bursting oscillations in Chapter 13, as well as explaining the origin of chaotic dynamics in fast–slow systems in Chapter 14. Naturally, we are also led to analyze the effect of noise, and Chapter 15 illustrates why there is an intricate interplay between multiple time scales and noise in dynamical systems.

Part V: A few advanced topics are covered briefly. Topological methods are discussed in Chapter 16 with a focus on how we may translate geometric conditions into algebraic questions. Chapter 17 deals with systems between the finite-dimensional ODE case and several classes of infinite-dimensional differential equations such as **partial differential equations (PDEs)**. Finally, in Chapter 18, we venture briefly into the fully infinite-dimensional multiple time scales case and illustrate the major challenges.

Part VI: Several topics that did not fit immediately within the scope of the elementary topics have been included in Chapter 19. Basically, this collection should be viewed as an augmentation and enrichment of the discussions in Parts I through V. In Chapter 20, several applications of various methods we have developed are sketched, and we also illustrate how time scale separation arises in a wide variety of contexts. Since Chapter 20 is based purely on examples, it also provides a playground for further study.

Overall, I would like to emphasize again that there is often no strong dependence between chapters but that there is considerable powerful interaction. For example, one may prove the existence of a periodic orbit by a topological argument, establish its scaling via geometric desingularization, and then look at its parameter dependence via numerical methods. However, the order of these methods and discoveries could easily be interchanged.

Notation: Union and intersections between two sets V, W will be denoted by $V \cup W$ and $V \cap W$, respectively, while we use $V - W$ to denote set difference. The empty set is denoted by \emptyset . In the context of topological spaces, we use V° for interior, \overline{V} for closure, and ∂V for the boundary. We denote the integers by \mathbb{Z} , the positive integers (or natural numbers) by \mathbb{N} , the rational numbers by \mathbb{Q} , the real numbers by \mathbb{R} , and the complex numbers by \mathbb{C} . The subscript 0 will be employed to explicitly include the zero, and a superscript + indicates positive parts. For instance,

$$\mathbb{N}_0 := \{0, 1, 2, 3, \dots\}, \quad (\mathbb{R}^m)^+ := \{x \in \mathbb{R}^m : x_i > 0 \text{ for all } i = 1, 2, \dots, m\}.$$

Furthermore, in formulas, we reserve $e \approx 2.71828\dots$ for Euler's constant, $i = \sqrt{-1}$ for the imaginary unit, and $\pi \approx 3.14159\dots$ for the ratio of a circle's circumference to its diameter. For the absolute value of elements from \mathbb{R} or \mathbb{C} we simply write $| \cdot |$, while **norms** are denoted by $\| \cdot \|$. As a standard norm for $x \in \mathbb{R}^m$, we use the **Euclidean norm**

$$\|x\| = \|x\|_2 := \sqrt{x_1^2 + x_2^2 + \cdots + x_m^2}.$$

The same convention applies to matrix norms, where no index denotes the matrix norm associated with the Euclidean norm. For spaces that cannot be naturally identified with a finite-dimensional real vector space, the norms for vectors and operators will be introduced explicitly. Vectors are usually regarded as column vectors, and we shall emphasize this sometimes by writing $(x_1, x_2, \dots, x_m)^\top \in \mathbb{R}^m$, where $(\cdot)^\top$ denotes the transpose, especially when the standard Euclidean **inner product** is involved:

$$x^\top w = x \cdot w = \sum_{j=1}^m x_j w_j, \quad \text{for } x, w \in \mathbb{R}^m,$$

i.e., it is sometimes nice to avoid the use of the centered-dot symbol. We shall write Id for the identity operator acting on a vector space and use the usual notation for matrix groups e.g., $\text{SL}(n, \mathbb{R})$ for the special linear group of real $n \times n$ matrices with determinant one. Furthermore, as a shorthand notation, we shall often just write 0 , instead of $(0, 0, \dots, 0)^\top$ or $(0, 0, \dots, 0)$, for the zero vector and the origin of the coordinate system. For maps $f : \mathbb{R}^m \rightarrow \mathbb{R}^m$, the **(total) derivative** at a point $p \in \mathbb{R}^m$ is a linear map denoted by $Df|_p : \mathbb{R}^m \rightarrow \mathbb{R}^m$ or $(Df)(p) : \mathbb{R}^m \rightarrow \mathbb{R}^m$. For maps of multiple variables $f : \mathbb{R}^m \times \mathbb{R}^n \rightarrow \mathbb{R}^m$, $f = f(x, y)$, we shall also write $(D_x f)(p) : \mathbb{R}^m \rightarrow \mathbb{R}^m$ to emphasize with respect to which variable we differentiate. Of course, the simpler notation $f'(p)$ will be used if $m = 1$. The class of continuous functions is denoted by $C^0(\mathbb{R}^m, \mathbb{R})$ or just $C^0(\mathbb{R}^m)$ (respectively C^0) if the range (respectively the domain and the range) are understood from the context. The subscript “b” indicates boundedness; for example, $C_b^0(\mathbb{R}^m, \mathbb{R})$ are continuous globally bounded functions. Similarly, we use $C^r(\mathbb{R}^m, \mathbb{R})$ to denote r -times continuously differentiable functions.

If $f : \mathbb{R}^m \rightarrow \mathbb{R}$, then $\frac{\partial f}{\partial x_j}$ and f_{x_j} denote partial derivatives, and standard conventions for the **gradient** and the **Laplacian** are employed:

$$\nabla f = \left(\frac{\partial f}{\partial x_1}, \dots, \frac{\partial f}{\partial x_m} \right)^\top, \quad \Delta f = \sum_{j=1}^m \frac{\partial^2 f}{\partial x_j^2}.$$

All other relevant notation will be introduced as needed; please consult the beginning of each section for the major definitions and also refer to the chapter introductions for more background on various concepts that you may be unsure about. This brings us neatly to the next issue.

Background: At the beginning of each chapter, there is a section on required background material for that chapter. The basic requirements necessary throughout the book are laid out above, at the beginning of this chapter. Basically, you should be comfortable with analysis, linear algebra, and a first course on differential equations.

However, it is important to point out that some sections may require a bit of additional background. I have tried to use only the basic concepts of each area, but how does this work in practice? Let me give you an example: Suppose you are not familiar with the terminology of a **(smooth) manifold**. Of course, one may study smooth manifolds for many years, but for our purpose that is unnecessary. Instead, you should be comfortable with looking up just the basic definition, and you will soon realize that for our 1- and 2-dimensional examples, it suffices to think of smooth curves and smooth surfaces. Near each point, these manifolds can be described by the graph of a smooth function. This viewpoint actually extends to arbitrary dimensions. So thinking in terms of classical objects from low-dimensional geometry and analysis such as curves, spheres, and cylinders can get you a long way.

Although a basic definition often suffices, it is hoped that this book may also be a motivation to study the mathematical concepts you have just learned about “by the way” in more detail. The same aspect can also work in exactly the opposite way if you in fact knew all the abstract concepts but have never really used them in concrete examples arising in applications. In summary, this book has also been written in the hope that it might bridge backgrounds between different groups of mathematically inclined readerships.

Textbook: This book can be used as a textbook for a second course on differential equations and dynamical systems. If there is just one semester available, I suggest spending roughly one-half of the time on basic topics. First, it is necessary to introduce some of the terminology from Chapter 1 and discuss Fenichel’s theorem from Chapter 3. To balance the geometric view, it is also recommended to spend some time exploring asymptotics (i.e., cover the less-technical parts of Chapters 5 and 9) and providing a basic guide to numerical issues (i.e., cover some elementary parts of Chapter 10). With this toolkit in hand, there should still be around one-half of the semester left, and I would recommend just selecting what looks most exciting and fits best with the backgrounds of the students.

There are also many exercises spread throughout the book, which range from rather straightforward verifications and the use of standard software packages up to serious research projects; a very rough distinction has been made by using “Exercise/Project” to indicate when the initial steps may be easy but giving a complete solution may take substantial additional time.

Arguably, there are very few courses dedicated to multiple time scale dynamics in curricula at the time of writing, but I believe that one could quickly learn a remarkably large amount about mathematics and its applications by covering various aspects of multiscale dynamics.

Research: This book can be used for self-study and as a research starting point in the area of multiscale dynamical systems. There is enough self-contained material and food for thought to accomplish anything from a first undergraduate research project or seminar presentation up to a major research breakthrough. Hence, you should also ask yourself before continuing with this book which direction you aim for. In terms of mini-projects, this is quite easy. Just shop around in the book up to a point that really catches your attention

and then delve into the details. It may be helpful to start right in the chapter you are most interested in to get an overview of the results and then go back to relevant technical background chapters afterward.

For the cutting-edge research aspect, the situation in the area of **multiscale systems** is very involved. Connections between different mathematical and application subdisciplines have often not been bridged completely, and we still have substantial gaps in our understanding of many multiscale systems. I hope that this book provides some groundwork to cover the simplest low-dimensional multiple time scale scenario in enough detail to get you started. However, finishing the important open questions in multiscale dynamics should still occupy several future generations of scientists.

References: To make it easier to catch up with current research topics, each chapter concludes with a literature review. First, I have featured the original sources on which the chapter has been built. In the second part of the literature reviews, additional directions are suggested. The reference list has been driven by the principles of “collection” and “categorization” instead of “selection.” Furthermore, if a citation appears in the statement of a theorem, then that is the source from which I have taken the result. Very frequently, the citation is also the source where the result was first established, but there are several cases in which I have not been able to determine the precise history of a theorem. In those cases, I have used as a first citation the textbook, expository book chapter, or survey article from which I have taken the result, so that it is entirely obvious that one should look for further history to attribute the result correctly; then I have sometimes added a few older references to indicate where to search for the historical details.

Despite the serious effort I have invested in the references, there are, unfortunately, several serious shortcomings. Firstly, the reference list is necessarily incomplete, so please feel encouraged to send those references to me via email that I have missed. Please note that the reference list “cutoff” for this edition was December 31, 2013. Only references available as an electronic preprint or published form at that time have been added. Secondly, I have restricted myself to include only references whose abstract and basic introduction I could actually read; unfortunately, this means that certain parts of the literature in Russian, particularly work from the 1960s and 1970s, as well as in Chinese, particularly work in the last 15 years, have not been included. I have to admit that my mathematical language proficiency does not extend beyond English, French, and German. However, I did highlight many reviews of Russian-language papers and would strongly encourage any reader who speaks Russian to dig through those reviews, since they certainly contain many gems that have not been translated. Thirdly, there is some additional focus on recent developments in the subject. Older work, regardless of the language, predating the 1980s, is potentially underrepresented. Fourthly, if a reference was available neither electronically nor by walking into the closest library, then I decided not to include it. Clearly, such reasoning is flawed, but it is extraordinarily time-consuming to hunt for a source if you do not even have an abstract to tell you whether it might be relevant.

1.2 Fast–Slow Systems

We shall begin by studying ordinary differential equations (ODEs) in which some variables have derivatives of much larger magnitude than those of other variables. This scenario yields a system with different time scales. The easiest case is a separation, which splits the variables into two groups.

Definition 1.2.1. A **fast–slow vector field** (or (m, n) -**fast–slow system**) is a system of ordinary differential equations taking the form

$$\begin{aligned}\varepsilon \frac{dx}{d\tau} &= \varepsilon \dot{x} = f(x, y, \varepsilon), \\ \frac{dy}{d\tau} &= \dot{y} = g(x, y, \varepsilon),\end{aligned}\tag{1.3}$$

where $f : \mathbb{R}^m \times \mathbb{R}^n \times \mathbb{R} \rightarrow \mathbb{R}^m$, $g : \mathbb{R}^m \times \mathbb{R}^n \times \mathbb{R} \rightarrow \mathbb{R}^n$, and $0 < \varepsilon \ll 1$. Furthermore, the x variables are called **fast variables**, and the y variables are called **slow variables**. Setting $t = \tau/\varepsilon$ gives the equivalent form

$$\begin{aligned}\frac{dx}{dt} &= x' = f(x, y, \varepsilon), \\ \frac{dy}{dt} &= y' = \varepsilon g(x, y, \varepsilon).\end{aligned}\tag{1.4}$$

We refer to t as the **fast time scale** or **fast time** and to τ as the **slow time scale** or **slow time**.

The parameter ε can be thought of as the “separation” of time scales and is sometimes called the **time-scale parameter**. If the notation $0 < \varepsilon \ll 1$ follows an equation, it will indicate that we are interested only in the case that ε is small and positive. If it appears in a statement or theorem, then it indicates that ε is **sufficiently small**, i.e., $0 < \varepsilon \ll 1$ means that there exists some $\varepsilon_0 > 0$ such that for all $\varepsilon \in (0, \varepsilon_0]$, the statement of the theorem holds.

In many situations, f and g are independent of ε , and we can write the fast–slow vector field as

$$\begin{aligned}\varepsilon \dot{x} &= f(x, y), \\ \dot{y} &= g(x, y),\end{aligned}\tag{1.5}$$

with the analogous obvious reformulation on the fast time scale.

Remark: The notation for fast–slow systems has not been uniform, and authors use different conventions. Sometimes, one finds that the x variables are slow and the y variables are fast with similar or no changes regarding the notation for the functions f and g . Similar remarks apply to the time scale notation t and τ as well as the notation for the dimensions m and n .

We are going to adhere to the conventions introduced here as far as possible throughout this book. There are simple mnemonics for our notation. It will become clear in working with fast–slow systems that if we pick an initial condition “at random,” then the first motion of a trajectory is “usually” fast, and eventually the trajectory might move slowly, i.e., fast–slow. We also have $\text{fast} < \text{slow}$ in alphabetical order and $m < n$, $f < g$ as well as $x < y$, which makes it possible to memorize the choices we made in Definition 1.2.1. There is no claim made that this choice is best, but it will be convenient for this book.

There are two compelling facts that should encourage one to study fast–slow systems. The first is that the mathematical structure of fast–slow systems is very intricate due to the small parameter ε . Many techniques ranging from classical asymptotic methods and nonstandard analysis to geometric methods and numerical treatments have been used successfully alongside the toolbox of dynamical systems theory. Although the first reason alone would clearly suffice to command further investigation, fast–slow systems also regularly appear in mathematical modeling across many areas of the natural sciences. Some classical examples will be our starting point in familiarizing the reader with the setup before we proceed to more advanced mathematical ideas.

1.3 The van der Pol Equation

One of the classical equations that motivated research in nonlinear dynamics is the **van der Pol (vdP)** equation. The equation was first introduced by Balthasar van der Pol in [vdP20] as a second-order equation given by

$$x'' + \mu(x^2 - 1)x' + x = 0, \quad (1.6)$$

where $\mu \gg 1$. Van der Pol was a pioneer in the fields of radio and telecommunications. He used equation (1.6) to study a vacuum tube triode circuit. The circuit was constructed experimentally, and the observed periodic orbit was modeled using (1.6). We can convert (1.6) into a fast–slow system. First set $t = \mu\tau$. Then x' is replaced by \dot{x}/μ , and x'' is replaced by \ddot{x}/μ^2 . Furthermore, we define $y = \dot{x}/\mu^2 + x^3/3 - x$ (also called the **Liénard transformation**) so that $\dot{y} = -x$. Hence, we can convert (1.6) into the first-order system

$$\begin{aligned} \frac{1}{\mu^2}\dot{x} &= y - \frac{x^3}{3} + x, \\ \dot{y} &= -x. \end{aligned} \quad (1.7)$$

Setting $\varepsilon = 1/\mu^2$ gives a fast–slow system with dimensions $(m, n) = (1, 1)$ according to Definition 1.2.1. There are several variations of van der Pol's equation. Variants with forcing terms are of considerable interest:

$$x'' + \mu(x^2 - 1)x' + x = a, \quad (1.8)$$

where $a > 0$ is a constant forcing term. As we shall see later, equation (1.8) played an important role in the development of multiple-time-scale dynamics. It can be written as a first-order system using a similar rescaling and definition of y , which leads to

$$\begin{aligned} \varepsilon\dot{x} &= y - \frac{x^3}{3} + x, \\ \dot{y} &= a - x. \end{aligned} \quad (1.9)$$

If the forcing is periodic, we get another variant of van der Pol's equation:

$$x'' + \mu(x^2 - 1)x' + x = a \sin(2\pi\nu t), \quad (1.10)$$

where ν represents the frequency and a the amplitude of the forcing. We can transform (1.10) by the same procedure as above and get

$$\begin{aligned}\varepsilon \dot{x} &= y - \frac{x^3}{3} + x, \\ \dot{y} &= a \sin(2\pi\nu\mu\tau) - x.\end{aligned}\tag{1.11}$$

Defining a new parameter $\omega = \mu\nu$ and setting $\theta = \omega\tau$, we obtain

$$\begin{aligned}\varepsilon \dot{x} &= y - \frac{x^3}{3} + x, \\ \dot{y} &= a \sin(2\pi\theta) - x, \\ \dot{\theta} &= \omega,\end{aligned}\tag{1.12}$$

as a vector field on $\mathbb{R}^2 \times S^1$, where we view S^1 as $[0, 1]$ with endpoints identified, i.e., $S^1 = \mathbb{R}/\mathbb{Z}$. Hence, we have obtained a $(1, 2)$ -fast–slow system in which $(y, \theta) =: (y_1, y_2)$ are the slow variables.

Equation (1.12) was originally introduced in [vdP34]. Van der Pol studied all different versions of his equation in considerable detail [vdP20, vdP26, vdP34, vdPvdM27, vdPvdM28] and pointed out many important dynamical features. Due to the limited availability of mathematical methods, he could not analyze the equations fully. We shall discuss the dynamics of all versions of van der Pol's equation in quite some detail; see Sections 1.5, 5.2, 5.3, 5.5, 7.5, 7.6, 8.2, 8.4, 8.5, 8.8, 9.2, 10.3, 10.4, 11.1, 14.1, 14.4, 14.5, 14.1, 15.4, and 19.6.

1.4 The FitzHugh–Nagumo Equation

The FitzHugh equation is a simplification of the Hodgkin–Huxley model for an electric potential of a nerve axon [HH52d]. The first version was developed by FitzHugh [Fit55] and is a $(1, 1)$ -fast–slow system:

$$\begin{aligned}\varepsilon \dot{u} &= w - \frac{u^3}{3} + u + q_1, \\ \dot{w} &= -\frac{1}{q_2}(w + q_3u - q_4),\end{aligned}\tag{1.13}$$

where $(u, w) \in \mathbb{R}^2$ are phase space variables and q_i are parameters. We can view (1.13) as a generalization of van der Pol's equation (1.9). Nagumo and his coworkers [NAY62] added a diffusion term to FitzHugh's equation and considered the following partial differential equations (PDEs):

$$\begin{aligned}\frac{\partial u}{\partial \tau} &= \frac{\partial^2 u}{\partial x^2} + f(u) - w + I, \\ \frac{\partial w}{\partial \tau} &= \varepsilon(u - \gamma w),\end{aligned}\tag{1.14}$$

where $f(u) = u(u - a)(1 - u)$ and I, a, γ are parameters. Suppose we assume a **traveling wave** solution to (1.14) and set $u(x, \tau) = u(x + s\tau) =: u(t)$ and $w(x, \tau) = w(x + s\tau) =: w(t)$, where s represents the **wave speed**. By the chain rule, we get $u_\tau = su'$, $u_{xx} = u''$, and $w_\tau = sw'$. We set $v = u'$ and substitute into (1.14) to obtain

$$\begin{aligned}u' &= v, \\ v' &= sv - u(u - a)(1 - u) + w - I, \\ w' &= \frac{\varepsilon}{s}(u - \gamma w).\end{aligned}\tag{1.15}$$

We change from the fast time t to the slow time τ and relabel variables $x_1 = u$, $x_2 = v$, and $y = w$. This gives a $(2, 1)$ -fast–slow system

$$\begin{aligned}\varepsilon \dot{x}_1 &= x_2, \\ \varepsilon \dot{x}_2 &= sx_2 - x_1(x_1 - a)(1 - x_1) + y - I, \\ \dot{y} &= \frac{1}{s}(x_1 - \gamma y).\end{aligned}\tag{1.16}$$

Often, all the related equations presented here are referred to as “the” **FitzHugh–Nagumo (FHN)** equation. Sometimes, we adopt this common terminology if it is clear from the context which version of the FitzHugh–Nagumo family we are studying; we shall adopt the same practice for “the” van der Pol equation.

Historically, van der Pol’s equation and the FitzHugh–Nagumo equation are two of the most important examples of fast–slow systems. Trying to understand their dynamics has provided a driving force in the general development of multiple time scale dynamics. Both families of equations exhibit a wide variety of interesting dynamical phenomena and appear frequently in various applications including—but not limited to—neuroscience, seismology, electrical circuits, networks, and systems biology. The FitzHugh–Nagumo equation is extensively studied in Sections 3.4, 6.2, 6.5, 6.7, 8.8, 11.5, 12.3, 13.3, 16.2, 16.5, 17.1, 17.4, and 19.8.

1.5 Terminology: Fast–Slow Systems

The first natural attempt to analyze a fast–slow system is to consider the case $\varepsilon = 0$. Since we have two basic scales to formulate our equations, slow time τ and fast time t , we get two cases.

Definition 1.5.1. The differential-algebraic equation obtained by setting $\varepsilon = 0$ in the formulation of the slow time scale (1.3) is called the **slow subsystem** or **slow vector field**:

$$\begin{aligned}0 &= f(x, y, 0), \\ \dot{y} &= g(x, y, 0).\end{aligned}\tag{1.17}$$

The flow generated by (1.17) is called the **slow flow**.

Remark: A **flow** $\phi : \mathbb{R}^{m+n} \times \mathbb{R} \rightarrow \mathbb{R}^{m+n}$ is just the solution map $\phi(z(0), \tau) = z(\tau)$ for $z(\tau) = (x(\tau), y(\tau))$. Abstractly, one may define a flow as a map that satisfies $\phi(z, 0) = z$ for every z and $\phi(\phi(z, \tau_1), \tau_2) = \phi(z, \tau_1 + \tau_2)$ for every $\tau_{1,2} \in \mathbb{R}$.

The slow subsystem is also referred to as the **reduced problem** and its flow as the **reduced flow**. Note that (1.17) is not an ODE, but an ODE with an algebraic constraint $f(x, y, 0) = 0$. Therefore, we have a **differential-algebraic equation (DAE)**. Initial conditions $x(0) = x_0$ and $y(0) = y_0$ must satisfy the constraint for solutions to exist.

Definition 1.5.2. The parameterized system of ODEs obtained by setting $\varepsilon = 0$ on the fast time scale formulation (1.4) is called a **fast subsystem** or **fast vector field**:

$$\begin{aligned} x' &= f(x, y, 0), \\ y' &= 0. \end{aligned} \quad (1.18)$$

The flow of (1.18) is called the **fast flow**.

The set of equations (1.18) is also referred to as the **layer equations** or the **layer problem**. This terminology encodes the geometric idea that each fixed y describes one “layer” of the fast subsystem. To distinguish the slow and fast systems from the original equations given by (1.3) and/or (1.4), we sometimes refer to (1.3) and/or (1.4) as the **full system**.

Definition 1.5.3. The case $\varepsilon = 0$ is also called the **singular limit**.

The slow and fast formulations give a hint as to how we should analyze the full system with $0 < \varepsilon \ll 1$. The natural strategy is to decompose solution curves of a fast–slow system into singular limit segments. The idea is that depending on the region in phase space, we should use either the fast or the slow subsystems. Near the set described by the algebraic equation $f(x, y, 0) = 0$, a trajectory should be given approximately by solutions of the slow flow. Sufficiently far away from $\{f(x, y, 0) = 0\}$, we expect the slow motion of the variables y to be irrelevant and hope to approximate trajectories by the fast flow. Clearly, the set $\{(x, y) \in \mathbb{R}^m \times \mathbb{R}^n : f(x, y, 0) = 0\}$ deserves a special name.

Definition 1.5.4. We call the set

$$C_0 = \{(x, y) \in \mathbb{R}^m \times \mathbb{R}^n : f(x, y, 0) = 0\}$$

the **critical set**. If C_0 is a submanifold of $\mathbb{R}^m \times \mathbb{R}^n$, we refer to C_0 as the **critical manifold**.

We are mostly interested in the case that C_0 is a sufficiently smooth manifold and shall use the term “critical set” only when we want to emphasize that C_0 is not smooth. Often, the critical manifold is also denoted by C , S , or S_0 (for reasons we shall discuss in Chapter 3). The relation between equilibrium points of the fast flow and the critical manifold C_0 is particularly simple.

Proposition 1.5.5. *Equilibrium points of the fast flow are in one-to-one correspondence with points in C_0 .*

Proof. Fix any y_0 . If x_0 is an equilibrium point of the fast flow

$$x' = f(x, y_0, 0),$$

then $f(x_0, y_0, 0) = 0$, and we conclude that $(x_0, y_0) \in C_0$. The converse is clear. \square

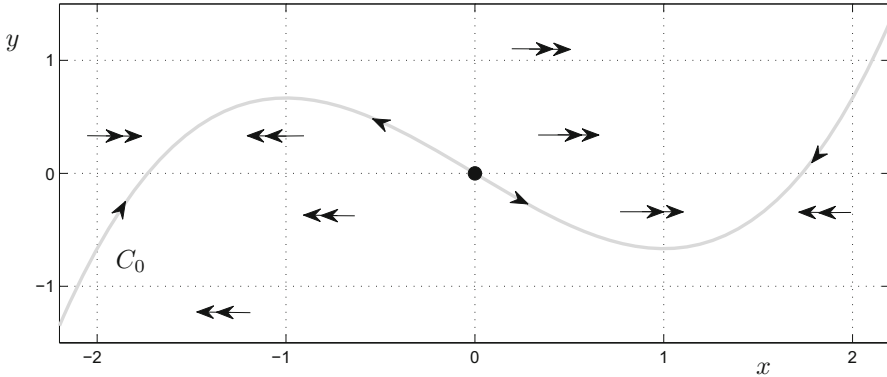


Figure 1.1: Critical manifold C_0 (gray) of the van der Pol equation (1.19). The slow flow and fast flow are indicated by single and double arrows respectively. The equilibrium $(x, y) = (0, 0)$ of the full system is marked as well (black dot).

Example 1.5.6. Let us review the previous concepts with an example. Consider the (unforced) van der Pol equation given on the slow time scale by

$$\begin{aligned}\varepsilon \dot{x} &= y - \frac{x^3}{3} + x, \\ \dot{y} &= -x.\end{aligned}\tag{1.19}$$

We obtain the critical manifold C_0 by setting $\varepsilon = 0$ in this formulation, so that

$$C_0 = \left\{ (x, y) \in \mathbb{R} \times \mathbb{R} : y = \frac{x^3}{3} - x \right\}.$$

We see that C_0 is a smooth manifold, since it is (even globally) the graph of a smooth function; see Figure 1.1. The slow flow $\dot{y} = -x$ is constrained to C_0 . Just looking at the sign of x gives the slow flow direction shown in Figure 1.1 by single arrows. The fast subsystems are arranged as horizontal layers parameterized by different y -values

$$\begin{aligned}x' &= y - \frac{x^3}{3} + x, \\ y' &= 0.\end{aligned}\tag{1.20}$$

There are either one, two, or three equilibrium points for (1.20), and the double arrows show the direction of the fast flow. ♦

Example 1.5.7. Consider the periodically forced van der Pol equation

$$\begin{aligned}\varepsilon \dot{x} &= y - \frac{x^3}{3} + x, \\ \dot{y} &= a \sin(2\pi\theta) - x, \\ \dot{\theta} &= \omega.\end{aligned}$$

We find that the critical manifold is given by

$$C_0 = \left\{ (x, y, \theta) \in \mathbb{R}^2 \times S^1 : y = \frac{x^3}{3} - x \right\}, \quad (1.21)$$

which is just a smooth surface. ♦

Exercise 1.5.8. Use a computer to produce a visualization of the critical manifold (1.21). As a basic exercise, it suffices to regard S^1 as $[0, 1]$ and plot a surface with boundary in \mathbb{R}^3 . As a more difficult exercise, try to view $S^1 = \mathbb{R}/\mathbb{Z}$ and embed the topological cylinder into \mathbb{R}^3 . ◇

1.6 Terminology: Asymptotic Analysis

In this section, we briefly review some notation from asymptotic analysis that will be used throughout the book. In particular, it is probably best to refer back to this section when working with concrete examples. It is not a detailed introduction to asymptotic analysis.

For the time scale separation parameter ε , we have assumed $0 < \varepsilon \ll 1$, so any limit $\varepsilon \rightarrow 0$ is understood as ε tending to zero from above. We shall not use other common notation such as $\varepsilon \rightarrow 0^+$ or $\varepsilon \downarrow 0$. Let \mathcal{D} be a domain in \mathbb{R}^n and consider functions $v, w : \mathcal{D} \times (0, \varepsilon_0) \rightarrow \mathbb{R}$ for ε_0 sufficiently small.

Definition 1.6.1. The **order** of $v(x, \varepsilon)$ is **not lower than** that of $w(x, \varepsilon)$ at a point $x = x_0 \in \mathcal{D}$ if for $\varepsilon \rightarrow 0$, there exist positive functions $k(x)$ and $\varepsilon(x)$ such that

$$|v(x_0, \varepsilon)| < k(x_0)|w(x_0, \varepsilon)|, \quad \text{for } 0 < \varepsilon < \varepsilon(x_0) \leq \varepsilon_0. \quad (1.22)$$

This relation is denoted by the “big-O” **Landau notation** $v(x_0, \varepsilon) = \mathcal{O}(w(x_0, \varepsilon))$. If (1.22) holds for each $x \in \mathcal{D}$, then we write $v(x, \varepsilon) = \mathcal{O}(w(x, \varepsilon))$. If $k(x)$ and $\varepsilon(x)$ are independent of x , then $v(x, \varepsilon) = \mathcal{O}(w(x, \varepsilon))$ uniformly in \mathcal{D} .

Definition 1.6.2. The **order** of $v(x, \varepsilon)$ is **higher than** that of $w(x, \varepsilon)$ at a point $x = x_0 \in \mathcal{D}$ if for $\varepsilon \rightarrow 0$ and every $\kappa > 0$, there exists a positive function $\varepsilon_\kappa(x)$ such that

$$|v(x_0, \varepsilon)| < \kappa|w(x_0, \varepsilon)|, \quad \text{for } 0 < \varepsilon < \varepsilon_\kappa(x_0) \leq \varepsilon_0. \quad (1.23)$$

This relation is denoted by the “little-o” **Landau notation** $v(x_0, \varepsilon) = o(w(x_0, \varepsilon))$. If (1.23) holds for each $x \in \mathcal{D}$, then we write $v(x, \varepsilon) = o(w(x, \varepsilon))$. If $\varepsilon_\kappa(x)$ is independent of x , then $v(x, \varepsilon) = o(w(x, \varepsilon))$ uniformly in \mathcal{D} .

Quite often, we shall also employ the condensed notation $v = \mathcal{O}(w)$ or $v = o(w)$ as $\varepsilon \rightarrow 0$ when it is understood that results are uniformly valid on a domain that is being currently considered. Sometimes, we even use a notation like $v = \mathcal{O}(\varepsilon^N)$ without further reference to $\varepsilon \rightarrow 0$, since the form of the function $w = \varepsilon^N$ already clearly indicates which asymptotic limit we are considering. Also, other notational conventions exist such as

$$v = o(w) \Leftrightarrow v \ll w \Leftrightarrow v \prec w.$$

It is very convenient to use $v \ll w$, since it makes many statements easy to read.

Exercise 1.6.3. Prove that $e^{-1/\varepsilon} = \mathcal{O}(\varepsilon^n)$ for all $n \in \mathbb{N}$ as $\varepsilon \rightarrow 0$. \diamond

Functions like $e^{-1/\varepsilon}$ from Exercise 1.6.3 are often called **beyond all orders** or **asymptotically equal to zero**. Note that this property is measured against the sequence ε^n , so that we should formally use the terminology “beyond all orders with respect to $\{\varepsilon^n\}_{n=0}^\infty$.”

Definition 1.6.4. A **gauge function** $\delta(\varepsilon)$ is a function that is monotonically decreasing (as $\varepsilon \rightarrow 0$), continuously differentiable in $(0, \varepsilon_0)$, and positive.

Beyond the standard example ε^n , other useful gauge functions are ε^α for $\alpha \in \mathbb{R}$ (often $\alpha \in \mathbb{Q}$) and $\varepsilon^\alpha |\ln \varepsilon|^\beta$; see, e.g., Chapter 5. Gauge functions become extremely useful as sequences.

Definition 1.6.5. The sequence $\{\delta_n(\varepsilon)\}_{n=0}^\infty$ is called an **asymptotic sequence** if

$$\delta_{n+1}(\varepsilon) = o(\delta_n(\varepsilon)), \quad \text{for all } n \text{ as } \varepsilon \rightarrow 0.$$

The classical asymptotic sequence that we are going to use most of the time is $\{\varepsilon^n\}_{n=0}^\infty$. Another sequence in which we shall be interested is $\{\varepsilon^{n/3} |\ln \varepsilon|^m\}_{m,n}$.

Definition 1.6.6. Let $v(x, \varepsilon)$ be defined on $\mathcal{D} \times (0, \varepsilon_0)$, and let $\{\delta_n(\varepsilon)\}_{n=0}^\infty$ be an asymptotic sequence as $\varepsilon \rightarrow 0$. If there exist functions $b_N(x)$ and $\{a_n(x)\}_{n=0}^N$, finite in $x_0 \in \mathcal{D}$, such that

$$v(x_0, \varepsilon) = \sum_{n=0}^N a_n(x_0) \delta_n(\varepsilon) + b_N(x_0) \cdot o(\delta_N(\varepsilon)), \quad (1.24)$$

then the right-hand side in (1.24) is called the **asymptotic expansion** of v at x_0 up to order $\delta_N(\varepsilon)$ as $\varepsilon \rightarrow 0$. If (1.24) is valid for all x_0 , the reference to the point is dropped. If $b_N(x)$ is uniformly bounded, then

$$v(x, \varepsilon) = \sum_{n=0}^N a_n(x) \delta_n(\varepsilon) + o(\delta_N(\varepsilon)) \quad (1.25)$$

is the uniformly valid asymptotic expansion of v up to order $\delta_N(\varepsilon)$.

Asymptotic expansions encapsulate the concept that the next term in the expansion is “smaller” than the previous one. It is also quite common to write

$$v(x, \varepsilon) = \sum_{n=0}^N a_n(x_0) \delta_n(\varepsilon) + \mathcal{O}(\delta_{N+1}(\varepsilon))$$

to give some additional information about the higher-order remainder. When equalities of the form (1.24)–(1.25) hold for all $n \in \mathbb{N}$, then

$$v(x, \varepsilon) \sim \sum_{n=0}^\infty a_n(x) \delta_n(\varepsilon) \quad (1.26)$$

is also called an **asymptotic series** of v . Under suitable conditions, the standard linear operations of addition, differentiation, and integration can be applied term by term, at least on a formal level, to an asymptotic series. Sometimes, one refers to the series in (1.26) as “asymptotically convergent,” which could be confusing, because the series may not, and often will not, converge in the classical sense. A convergent series is also an analytic function, and by taking larger and larger partial sums, we can obtain more and more accurate approximations to the function. An asymptotic series also provides an approximation to a function, but it might not converge, and the approximation becomes more accurate only near a certain value x_0 and if $\varepsilon \rightarrow 0$. A priori, it is not clear how many terms we have to sum to get a “good” or “best” approximation with an asymptotic series.

Exercise 1.6.7. Find different functions with the same asymptotic series. ◇

1.7 References

Section 1.2: There are several other brief introductions that provide some elements of the fast–slow terminology: [Ber01, Guc02, Guc96, Hek10, Kap99, O’M08, Ver05a]. Unfortunately, notation and terminology are not uniform in the literature (and this book tries to improve this situation). For recent surveys on the Russian-language literature, we refer to [BNS04, Vas63, Vas76, Vas94]; many papers in this community also cite a combination of [Tik52, Pon57, PR60], so a citation search will reveal many more relevant publications. Some other surveys are [CO99, KR89]. Many nice examples on the difficulties of singular perturbation problems are discussed in [O’M01, O’M68b]. If further motivation for multiscale problems is required, one may turn to [EE03b, ELVE04]. For books focusing on numerics and modeling aspects for certain classes of multiscale problems, consider [E11, Ste07].

Section 1.3: The original references for the work of van der Pol (vdP) are [vdP20, vdP26, vdP34, vdPvdM27, vdPvdM28]. There has been extensive work on vdP-type equations investigating their bifurcations [BEG⁺03, Guc03, GHW03, HB12, HR78, KO00, MPL93]. The first detailed mathematical analysis of the forced vdP can be found in [Car52, CL45, CL47, Lit57a, Lit57b]. There are many variants of the vdP equation such as Bonhoeffer-vdP-type models [SSSI12], coupled vdP equations [Bi04, CR88, KS91a, RH80, SR82, SR86], nonsmooth vdP [BLM09], self-excitation models [GB10, Ver05c], time-delayed vdP [Mac01, XC03], the vdP-Duffing oscillator [ML93], and the vdP-Mathieu equation [VV09]. Furthermore, in the analysis of the vdP dynamics, one may focus on various aspects such as a priori estimates [Hab78], asymptotics [Ros86], fast–slow decomposition [Lev47], jumps [Gou13], and periodic orbits [Lou59].

Section 1.4: The Hodgkin–Huxley model for the squid giant axon has been developed in [HH52c, HH52b, HH52a, HH52d]. The original papers by FitzHugh and Nagumo (FHN) are [Fit55, Fit60, Fit61, NAY62]. For the planar system without diffusion, a detailed bifurcation analysis has been carried out [RGG00]. Waves in FHN and associated basic problems are outlined nicely in [Has75, Has76a, McK70, RK83]. Nagumo worked quite extensively on singular perturbation problems [Nag39, Nag93]. Of course, there are many FHN variants [FDS12, FDS13], including a buffered FHN

[TS11c], piecewise linear [KTS11], and various neuron models [HR82]. There has also been a great deal of research on various fully spatial FHN equations [DS06, Lop82, RS99, WW05] that we do not cover here. The one-dimensional traveling wave case is covered extensively in Chapters 6 and 17).

Section 1.5: The terminology introduced in this section can be found in virtually every source on multiple time scale systems, so we shall not provide further detailed references here.

Section 1.6: This section is based on the singular perturbation books [EdJ82, JF96, Mil06]. A more theoretical approach is considered in [HS99]. In fact, asymptotic techniques for differential equations have a history of over 100 years [Bir08b, Bir08a, BL23]. A book with a focus on asymptotic analysis and multiple time-scale problems is [Ver05b]. More detailed references on asymptotic analysis can be found in Sections 5.6 and 9.11.

Chapter 2

General Fenichel Theory

Important Remark: This chapter provides a proof of the perturbation of normally hyperbolic invariant manifolds due to Fenichel. Chapter 3 specializes the general case to fast–slow systems, so that the current chapter is necessary only for readers interested in the proof and its strategy. It is possible to skip this chapter at first reading, get an idea how the theorem is used, and then return to the proof.

In this chapter, we develop some of the major results for general normally hyperbolic manifolds, which will be specialized to the fast–slow case in Chapter 3. The presentation follows [Fen71, Fen74, Fen77, Wig94] and is shorter than [Wig94] but still contains more details than [Fen71]. Therefore, it is hoped that an intermediate alternative may add some expository value. Readers familiar with [Fen71, Wig94], or [HPS77] can easily skip the entire chapter.

Section 2.1 outlines the basics of invariant manifold theory. We also introduce the generalized Lyapunov-type numbers, which control the strength of the flow in the tangent and normal directions to the manifold. Section 2.2 describes the perturbation problem for invariant manifolds and outlines the main proof strategy involving the graph transform. Section 2.3 defines the concept of normal hyperbolicity, states the main theorem, and completes the proof by combining the auxiliary results from the previous sections. We also discuss the technically subtle issue of asymptotic rate foliations. Section 2.4 provides a transition to fast–slow systems by specializing the general normally hyperbolic case to critical and slow manifolds, thereby providing a natural connection to Chapter 3.

Background: The basic definitions for smooth manifolds are required; the introductory parts of any differential geometry book up to the definition of tangent bundles will suffice. The books [Lee06, Jän01] are highly recommended. Another good choice

with a concrete low-dimensional focus is [Kue02]. Of course, one may also go more encyclopedic [Spi99], focus on physics and calculations [AMR88, Fra11, Nak03], or consider other good alternatives [Mil97b, Mun97].

2.1 Invariant Manifolds

Invariant manifold theory is one of the cornerstones of the geometric approach to multiple time scale dynamics. To illustrate the main issue, we begin with the simplest nontrivial example.

Example 2.1.1. Consider the linear constant-coefficient ODE in \mathbb{R}^2 given by

$$\dot{z} = Az \quad \text{with } A = \begin{pmatrix} \lambda_1 & 0 \\ 0 & \lambda_2 \end{pmatrix}, z \in \mathbb{R}^2, \lambda_1 < 0 \text{ and } \lambda_2 > 0. \quad (2.1)$$

Observe that (2.1) has a hyperbolic saddle equilibrium point at the origin. The system (2.1) together with an initial condition $z(0)$ has the solution

$$z(t) = \begin{pmatrix} e^{\lambda_1 t} & 0 \\ 0 & e^{\lambda_2 t} \end{pmatrix} z(0) =: \phi_t(z(0)). \quad (2.2)$$

If $z(0) = (a, 0)^\top$ for $a \in \mathbb{R} - \{0\}$, the flow decays toward $(0, 0)$ in forward time, and if $z(0) = (0, a)^\top$ for $a \in \mathbb{R} - \{0\}$, the flow decays toward zero in negative time. The spaces $E^s = \{z \in \mathbb{R}^2 : z_2 = 0\}$ and $E^u = \{z \in \mathbb{R}^2 : z_1 = 0\}$ are called the **stable** and **unstable subspaces** of the equilibrium point $(0, 0)$. Observe that E^s and E^u are **globally invariant** under the flow, i.e., $\phi_t(E^s) \subset E^s$ and $\phi_t(E^u) \subset E^u$ for all $t \in \mathbb{R}$. Now perturb equation (2.1) to obtain

$$\dot{z} = Az + Bz \quad \text{with } A \text{ as above, } B = \begin{pmatrix} \varepsilon & 0 \\ 0 & \varepsilon \end{pmatrix} \text{ and } 0 < \varepsilon \ll 1. \quad (2.3)$$

For ε small enough, the previous analysis still applies, and we have the stable and unstable subspaces E^s and E^u for the perturbed system. ♦

The major question to be addressed is how far the previous observation can be generalized. A first answer is the important **stable manifold theorem**.

Theorem 2.1.2 ([KH95, Tes12]; see also [Kel67, HP70, Per29]). *Consider the ODE*

$$\dot{z} = H(z) \quad \text{for } z \in \mathbb{R}^N \text{ and } H \in C^r(\mathbb{R}^N, \mathbb{R}^N) \text{ with } r \geq 1 \quad (2.4)$$

with z^ a hyperbolic fixed point for (2.4), i.e., the associated linearized system*

$$\dot{z} = [DH(z^*)]z \quad (2.5)$$

has a matrix $DH(z^)$ with k real-part-negative and $N-k$ real-part-positive eigenvalues with corresponding eigenspaces E^s and E^u . Then there exists a neighborhood U of z^* containing local stable and unstable manifolds $W_{loc}^s(z^*)$ and $W_{loc}^u(z^*)$ given by*

$$W_{loc}^s(z^*) = \{z \in U : \phi_t(z) \rightarrow z^* \text{ as } t \rightarrow \infty \text{ and } \phi_t(z) \in U \text{ for all } t \geq 0\},$$

$$W_{loc}^u(z^*) = \{z \in U : \phi_t(z) \rightarrow z^* \text{ as } t \rightarrow -\infty \text{ and } \phi_t(z) \in U \text{ for all } t \leq 0\}.$$

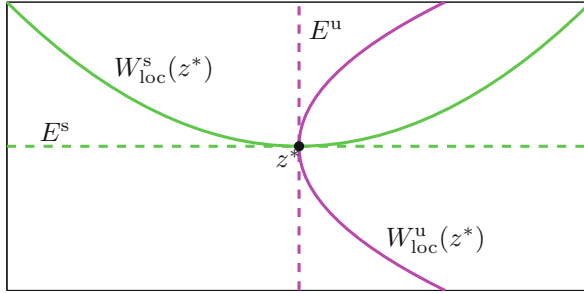


Figure 2.1: Sketch of the situation in the stable manifold theorem.

Furthermore, $W_{\text{loc}}^s(z^*)$ and $W_{\text{loc}}^u(z^*)$ are tangent to E^s and E^u at z^* , i.e., we have $T_{z^*}(W_{\text{loc}}^s(z^*)) = E^s$ and $T_{z^*}(W_{\text{loc}}^u(z^*)) = E^u$. The manifolds $W_{\text{loc}}^s(z^*)$ and $W_{\text{loc}}^u(z^*)$ are at least as smooth as H .

The situation of the stable manifold theorem is shown in Figure 2.1. Theorem 2.1.2 generalizes Example 2.1.1 as it applies to nonlinear problems, and it yields locally invariant manifolds. The key statement in Theorem 2.1.2 is that near a hyperbolic equilibrium point z^* , the nonlinear stable and unstable manifolds are well approximated by eigenspaces of the linearized system. But what if we do not restrict to the case of a static equilibrium point and allow the equilibrium to move slowly?

Example 2.1.3. Consider the $(1, 1)$ -fast–slow system given by

$$\begin{aligned} x' &= f(x, y, \varepsilon) = -x + \varepsilon, \\ y' &= g(x, y, \varepsilon) = \varepsilon y^2. \end{aligned} \tag{2.6}$$

Observe that the critical manifold $C_0 = \{(x, y) \in \mathbb{R}^2 : x = 0\}$ is just the y -axis. It is invariant under the flow, since it consists of equilibrium points for the fast subsystem. Now consider $\varepsilon > 0$. Then the line $C_\varepsilon = \{(x, y) \in \mathbb{R}^2 : x = \varepsilon\}$ is an invariant manifold for the flow of (2.6); see Figure 2.2. Note that C_ε contains the single equilibrium point $(x, y) = (\varepsilon, 0)$ for (2.6), which is not hyperbolic; such points are the main theme of Chapters 7 and 8. ♦

Next, we want to investigate what happens to invariant manifolds for the general ODE

$$z' = H(z) \quad \text{for } z \in \mathbb{R}^N, H \in C^r(\mathbb{R}^N, \mathbb{R}^N) \text{ with } r \geq 1 \tag{2.7}$$

under a perturbation.

Definition 2.1.4. Let M be a compact connected C^r -manifold with boundary embedded in \mathbb{R}^N . Let $\phi_t(\cdot)$ denote the flow defined by the vector field (2.7).

- M is called an **inflowing invariant manifold** if for every $p \in \partial M$, the vector field is pointing strictly inward and for all $p \in M$, $\phi_t(p) \in M$ for all $t \geq 0$.

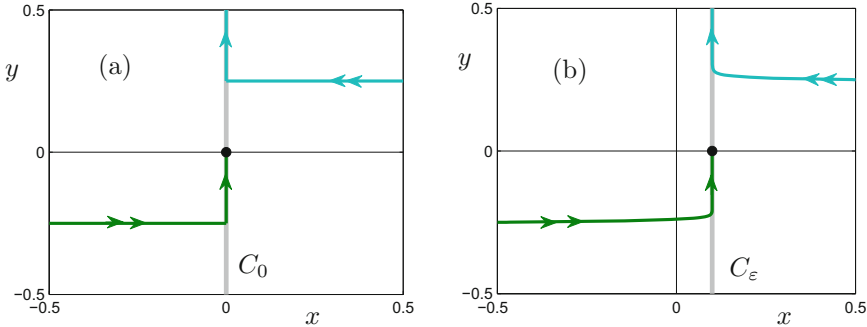


Figure 2.2: Perturbation of a critical manifold in the fast–slow system (2.6). (a) $\varepsilon = 0$: critical manifold C_0 (gray) and two trajectories (green and cyan) concatenated from fast and slow subsystem trajectories are shown. (b) $\varepsilon = 0.1$: perturbed manifold C_ε (gray), two full system trajectories (green and cyan) of (2.6) and the equilibrium (black dot) are shown.

- M is called an **overflowing invariant manifold** if for every $p \in \partial M$, the vector field is pointing strictly outward and for all $p \in M$, $\phi_t(p) \in M$ for all $t \leq 0$.
- M is called an **invariant manifold** if for every $p \in M$, we have $\phi_t(p) \in M$ for all $t \in \mathbb{R}$.
- M is called a **locally invariant manifold** if for each $p \in M$, there exists a time interval $I_p = (t_1, t_2)$ such that $0 \in I_p$ and $\phi_t(p) \in M$ for all $t \in I_p$.

See Figure 2.3 for an illustration of the definitions.

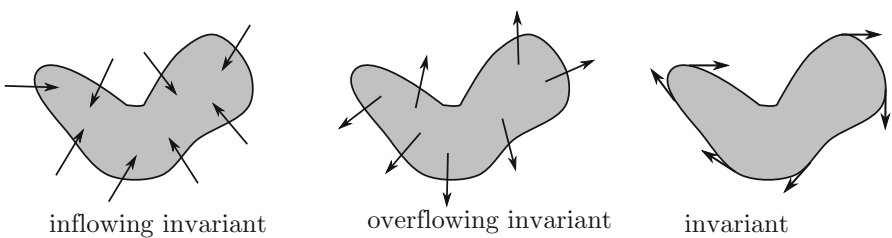


Figure 2.3: Examples of inflowing invariant, overflowing invariant, and invariant manifolds (gray) with boundary (black closed curve). The flow is indicated by arrows.

Note that reversing the time direction in (2.7) turns an overflowing invariant manifold into an inflowing invariant manifold and conversely. Therefore, we shall restrict to overflowing invariant manifolds for the remaining discussion. Furthermore, we emphasize again the assumption that M is compact, which is made throughout this chapter.

The tangent bundle

$$TM = \bigcup_{p \in M} \{p\} \times T_p M$$

collects all the tangent spaces, i.e., elements in TM are pairs $(p, T_p M)$ consisting of a point $p \in M$ and its associated tangent space. Since $M \subset \mathbb{R}^N$, the Euclidean inner product of the ambient space induces a splitting at each point $T_p \mathbb{R}^N|_M = T_p M \oplus \mathcal{N}_p$, where \mathcal{N}_p denotes the **normal space** to $T_p M$ consisting of all vectors orthogonal to $T_p M$ and \oplus is the usual **direct sum**. Hence, there is also a splitting $T \mathbb{R}^N|_M = TM \oplus \mathcal{N}$, where \mathcal{N} denotes the **normal bundle**, which collects all normal spaces. Using the Euclidean inner product, we also have an associated norm $\|\cdot\|$ measuring the length of vectors in the tangent and normal bundles; see [Lee06] for more on general **vector bundles**.

Remark: Since M can have a boundary, some constructions make sense only if we allow an extension of the overflowing invariant manifold M slightly under the flow, i.e., if we consider $\phi_t(M)$ for t sufficiently small. Since M is compact, this causes no problems. We shall not introduce new manifolds that represent extensions and refer to M and its suitable extensions by the same notation.

Let $\Pi : T \mathbb{R}^N|_M \rightarrow \mathcal{N}$ denote the projection of a vector onto the normal component to M fixing the base point. To compare the flows in the tangential and normal directions, we need the following maps defined for every $p \in M$:

$$\begin{aligned} A_t(p) &= D\phi_{-t}(p)|_M : T_p M \rightarrow T_{\phi_{-t}(p)} M, \\ B_t(p) &= \Pi \circ D\phi_t(\phi_{-t}(p))|_M : \mathcal{N}_{\phi_{-t}(p)} \rightarrow \mathcal{N}_p, \end{aligned}$$

where the restriction notation $(\cdot)|_M$ will often be dropped. Here A_t is the linearization of the (backward) tangential flow, and B_t is the linearization of the flow in the normal direction. It is also helpful to introduce the following notation for nonzero vectors:

$$w_0 \in \mathcal{N}_p \quad \text{and} \quad v_0 \in T_p M.$$

The corresponding vectors obtained under the linearized flow based at the point $\phi_{-t}(p)$ will be denoted by

$$w_{-t} = (\Pi \circ D\phi_{-t}(p))w_0 \quad \text{and} \quad v_{-t} = D\phi_{-t}(p)v_0.$$

The point p is frequently suppressed in the notation. Figure 2.4 provides an overview of the notation.

Definition 2.1.5. Let $p \in M$. The **generalized Lyapunov-type numbers** are defined by

$$\nu(p) = \inf \left\{ a : \frac{1}{\|w_{-t}\|^a} \rightarrow 0 \quad \text{as } t \rightarrow \infty, \quad \forall w_0 \in \mathcal{N}_p \right\} \quad (2.8)$$

and, if $\nu(p) < 1$,

$$\sigma(p) = \inf \left\{ b : \frac{\|v_{-t}\|}{\|w_{-t}\|^b} \rightarrow 0 \quad \text{as } t \rightarrow \infty \quad \forall w_0 \in \mathcal{N}_p, v_0 \in T_p M \right\}. \quad (2.9)$$

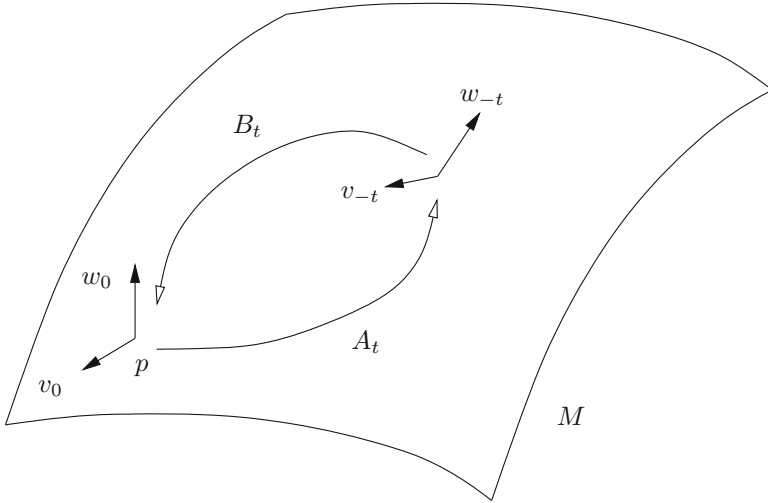


Figure 2.4: Setup for the linearized dynamics near the manifold M .

Remark: It will turn out that additional generalized Lyapunov-type numbers are needed in Section 2.3, but for now, Definition 2.1.5 will suffice.

Definition 2.1.5 may not be very intuitive, so we look at some easy cases. If $a = 1$ in (2.8), we ask whether

$$\frac{1}{\|w_{-t}\|} \rightarrow 0 \quad \text{as } t \rightarrow \infty. \quad (2.10)$$

Geometrically, this corresponds to contraction of vectors in the normal direction to M in forward time. Hence, equation (2.10) holds if M is attracting in the normal direction and therefore $\nu(p)$ is a quantitative measure of stability with smaller $\nu(p)$ implying faster contraction in the normal direction. Similarly, we find that $\sigma(p)$ describes the relation between components normal and tangential to M , with small $\sigma(p)$ indicating that the normal direction dominates the tangent direction. Before we can compute the generalized Lyapunov-type numbers in an example, we need an auxiliary result.

Lemma 2.1.6 ([Wig94]).

$$\begin{aligned} \nu(p) &= \limsup_{t \rightarrow \infty} \|B_t(p)\|^{1/t}, \\ \sigma(p) &= \limsup_{t \rightarrow \infty} \frac{\log \|A_t(p)\|}{-\log \|B_t(p)\|} \quad \text{if } \nu(p) < 1. \end{aligned} \quad (2.11)$$

The proof of Lemma 2.1.6 is a relatively direct argument involving limits.

Example 2.1.7. Consider the linear ODE given by

$$\dot{z} = \begin{pmatrix} \lambda & 0 \\ 0 & -\mu \end{pmatrix} z \quad \text{for } z \in \mathbb{R}^2 \text{ and } \lambda, \mu > 0. \quad (2.12)$$

Clearly, $M = \{z = (z_1, z_2)^\top \in \mathbb{R}^2 : z_1 \in (-1, 1), z_2 = 0\}$ is an overflowing invariant manifold inducing the splitting

$$\mathrm{T}\mathbb{R}^2|_M = \mathrm{T}M \oplus \mathcal{N}, \quad (2.13)$$

where the two-dimensional bundles are given by

$$\begin{aligned} \mathrm{T}M &= \{(z_1, 0) \times (\mathbb{R}, 0) : z_1 \in (-1, 1)\}, \\ \mathcal{N} &= \{(z_1, 0) \times (0, \mathbb{R}) : z_1 \in (-1, 1)\}. \end{aligned} \quad (2.14)$$

To calculate A_t and B_t , we need the (linearized) flow for (2.12) and the projection Π onto \mathcal{N} . Direct calculation yields

$$\mathrm{D}\phi_t = \begin{pmatrix} e^{\lambda t} & 0 \\ 0 & e^{-\mu t} \end{pmatrix} \quad \text{and} \quad \Pi = \begin{pmatrix} 0 & 0 \\ 0 & 1 \end{pmatrix}. \quad (2.15)$$

This gives the tangential and normal dynamics

$$\begin{aligned} A_t(p) &= \mathrm{D}\phi_{-t}|_M(p) &= \begin{pmatrix} e^{-\lambda t} & 0 \\ 0 & 0 \end{pmatrix}, \\ B_t(p) &= \Pi \circ \mathrm{D}\phi_t|_M(\phi_{-t}(p)) &= \begin{pmatrix} 0 & 0 \\ 0 & e^{-\mu t} \end{pmatrix}. \end{aligned}$$

Therefore, the generalized Lyapunov-type numbers are given by

$$\begin{aligned} \nu(p) &= \limsup_{t \rightarrow \infty} |e^{-\mu t}|^{1/t} &= e^{-\mu} < 1, \\ \sigma(p) &= \limsup_{t \rightarrow \infty} \frac{\log |e^{-\lambda t}|}{-\log |e^{-\mu t}|} &= -\frac{\lambda}{\mu}. \end{aligned}$$

Hence calculating the generalized Lyapunov-type numbers for linear systems is a relatively easy task. ♦

Exercise 2.1.8. Prove that the numbers $\nu(p)$ and $\sigma(p)$ are independent of the choice of inner product in \mathbb{R}^N and in particular independent of the splitting $\mathrm{T}\mathbb{R}^N|_M = \mathrm{T}M \oplus \mathcal{N}$ obtained from the inner product. Hint: Take two such inner products and splittings and recall that all norms on \mathbb{R}^N are equivalent. ◇

The following auxiliary results were developed by Fenichel [Fen71] with additional explanations found in [Wig94] leading up to Theorem 2.2.2 below.

Lemma 2.1.9. *The generalized Lyapunov-type numbers are constant on orbits under the flow ϕ_t , i.e., $\nu(p) = \nu(\phi_{-t}(p))$ and $\sigma(p) = \sigma(\phi_{-t}(p))$.*

Proof. We shall prove the result only for $\nu(p)$, since it contains the relevant idea. Fix $\tau > 0$, fix a point p , and write $B_t(p) = B_t$ for the following calculation:

$$\begin{aligned} B_{\tau+t} &= \Pi \circ \mathrm{D}\phi_{t+\tau}(\phi_{-(t+\tau)}) \\ &= \Pi \circ \mathrm{D}\phi_\tau(\phi_{-\tau}) \circ \mathrm{D}\phi_t(\phi_{-(t+\tau)}) \\ &= \Pi \circ \mathrm{D}\phi_\tau(\phi_{-\tau}) \circ \Pi \circ \mathrm{D}\phi_t(\phi_{-(t+\tau)}) = B_\tau B_t(\phi_{-\tau}), \end{aligned}$$

where we can put in the projection Π in the last step because $T_{\phi_{-\tau}(p)}M$ is in the nullspace of $\Pi \circ D\phi_\tau(\phi_{-\tau})$. We get the equation

$$B_{\tau+t}(p) = B_\tau(p)B_t(\phi_{-\tau}(p)), \quad (2.16)$$

and using (2.16), it follows that

$$\|B_{\tau+t}(p)\|^{1/t} \leq \|B_\tau(p)\|^{1/t} \|B_t(\phi_{-\tau}(p))\|^{1/t}. \quad (2.17)$$

Since $B_\tau(p)$ is bounded, we have that $\limsup_{t \rightarrow \infty} \|B_\tau(p)\|^{1/t} = 1$, and so taking limits in (2.17) gives

$$\limsup_{t \rightarrow \infty} \|B_{\tau+t}(p)\|^{1/t} \leq \limsup_{t \rightarrow \infty} \|B_t(\phi_{-\tau}(p))\|^{1/t} = \nu(\phi_{-\tau}(p)).$$

But since

$$\limsup_{t \rightarrow \infty} \|B_{\tau+t}(p)\|^{1/t} = \limsup_{t+\tau \rightarrow \infty} \|B_{\tau+t}(p)\|^{1/(t+\tau)} = \nu(p),$$

it follows that $\nu(p) \leq \nu(\phi_{-\tau}(p))$. Also observe that $B_\tau(p)$ acting on \mathcal{N} is invertible, since ϕ_t is invertible, and therefore (2.16) implies

$$(B_\tau(p))^{-1}B_{\tau+t}(p) = B_t(\phi_{-\tau}(p)).$$

Now applying the same procedure and taking limits leads to the opposite inequality $\nu(\phi_{-\tau}(p)) \leq \nu(p)$, which proves the result. \square

Let us look again at the definition of the generalized Lyapunov-type number $\nu(p)$,

$$\nu(p) = \inf \left\{ a : \frac{1}{a^t \|w_{-t}\|} \rightarrow 0 \quad \text{as } t \rightarrow \infty, \quad \forall w_0 \in \mathcal{N}_p \right\}, \quad (2.18)$$

and recall that $w_0 = B_t(p)w_{-t}$. Since $\|w_0\|$ is a constant, we can rewrite (2.18) as

$$\begin{aligned} \nu(p) &= \inf \left\{ a : \left(\frac{\|B_t(p)w_{-t}\|}{\|w_{-t}\|} \right) / a^t \rightarrow 0 \quad \text{as } t \rightarrow \infty, \quad \forall w_0 \in \mathcal{N}_p \right\} \\ &= \inf \left\{ a : \|B_t(p)\| / a^t \rightarrow 0 \quad \text{as } t \rightarrow \infty \right\}. \end{aligned}$$

This implies that if we know $\nu(p)$, then we get a bound on the linearized flow in the normal direction. The same reasoning obviously applies to $\sigma(p)$ and a suitable combination of A_t and B_t . One key observation made by Fenichel in [Fen71] is that this is the correct way to control the normal and tangential flows. By substantially modifying an argument from [Sac69], he obtained the following result.

Lemma 2.1.10 (Uniformity lemma). *Suppose $\|B_t(p)\| / a^t \rightarrow 0$ as $t \rightarrow \infty$ for every $p \in M$ and some $a > 0$. Then there are constants $\hat{a} < a$ and $\kappa > 0$ such that*

$$\|B_t(p)\| < \kappa \hat{a}^t \quad \text{for every } p \in M \text{ and } t \geq 0. \quad (2.19)$$

If we suppose in addition that $a \leq 1$ and $\|A_t(p)\|\|B_t(p)\|^b \rightarrow 0$ as $t \rightarrow \infty$ for every $p \in M$, then there exist constants $\hat{b} < b$ and K such that

$$\|A_t(p)\|\|B_t(p)\|^{\hat{b}} < K \quad \text{for every } p \in M \text{ and } t \geq 0. \quad (2.20)$$

Proof. We shall prove only (2.19) and note that the argument applies with minor modifications to proving (2.20). Using the hypothesis, we get that for each $p \in M$, there exists $T(p)$ such that $\|B_{T(p)}(p)\| < a^{T(p)}$, and by continuity of the flow, we have a neighborhood $U(p)$ such that for all $p' \in U(p)$,

$$\|B_{T(p)}(p')\| < a^{T(p)}.$$

By compactness of M , we can find a finite covering $M \subset U(p_1) \cup \dots \cup U(p_K)$. Choose $\hat{a} < a$ such that for $p' \in \overline{U(p_i)}$,

$$\|B_{T(p_i)}(p')\| < \hat{a}^{T(p_i)}.$$

Fix $p \in M$ and let i_k with $i_k \in \{1, 2, \dots, K\}$ be such that

$$p \in U(p_{i_1}), \quad \phi_{-T(p_{i_1})}(p) \in U(p_{i_2}), \quad \dots, \quad \phi_{-(T(p_{i_1})+\dots+T(p_{i_{j-1}}))}(p) \in U(p_{i_j}).$$

Define $\tau(j) = T(p_{i_1}) + \dots + T(p_{i_j})$, fix any $t > 0$, and write it as

$$t = \tau(j) + r \quad \text{for some } j \geq 0 \text{ (with } \tau(0) = 0 \text{) and } 0 \leq r \leq \max_{i \in \{1, \dots, K\}} T(p_i).$$

By construction, we have $B_t(p) = B_{T(p_{i_1})+\dots+T(p_{i_j})+r}(p)$. This can be written as a product

$$B_t(p) = B_{T(p_{i_1})}(p) \cdot B_{T(p_{i_2})}(\cdot) \cdots B_{T(p_{i_j})}(\cdot) \cdot B_r(\phi_{-(T(p_{i_1})+\dots+T(p_{i_{j-1}}))}(p)),$$

where some points of evaluation for the maps $B_{T(p_{i_k})}(\cdot)$ are omitted for brevity. On taking the norm, this gives

$$\begin{aligned} \|B_t(p)\| &< \|B_r(\phi_{-(T(p_{i_1})+\dots+T(p_{i_{j-1}}))}(p))\| \left(\frac{\hat{a}^r}{\hat{a}^r}\right) \hat{a}^{T(p_{i_1})} \cdots \hat{a}^{T(p_{i_j})} \\ &\leq \kappa \hat{a}^{T(p_{i_1})+\dots+T(p_{i_j})+r} = \kappa \hat{a}^t, \end{aligned}$$

where the constant is given by $\kappa = \max_{p \in M, r \in [0, T(p_i)]} \frac{\|B_r(p)\|}{\hat{a}^r}$. \square

The result gives several important corollaries. The first two follow directly.

Corollary 2.1.11. *If $\nu(p) < a \leq 1$ for every $p \in M$, then $\|B_t(p)\| \rightarrow 0$ as $t \rightarrow \infty$ uniformly for every $p \in M$.*

Corollary 2.1.12. *If $\nu(p) < a \leq 1$ and $\sigma(p) < b$ for every $p \in M$, then it follows that $\|A_t(p)\|\|B_t(p)\|^b \rightarrow 0$ as $t \rightarrow \infty$ uniformly for every $p \in M$.*

Corollary 2.1.13. *$\nu(\cdot)$ and $\sigma(\cdot)$ attain their suprema on M .*

Proof. Suppose $\nu(\cdot)$ does not attain its supremum. Set $a = \sup_{p \in M} \nu(p)$. By the uniformity lemma, there exists $\hat{a} < a$ such that $\|B_t(p)\| < \kappa \hat{a}^t$ for all $p \in M$ and $t \geq 0$. Now pick any a' such that $\hat{a} < a' < a$. Then

$$\frac{\|B_t(p)\|}{(a')^t} \rightarrow 0 \quad \text{as } t \rightarrow \infty,$$

and so $\nu(p) < a'$, which is a contradiction. \square

2.2 Perturbations of Invariant Manifolds

With estimates on the linearized tangential and normal flows in hand, the goal is to prove a perturbation result for invariant manifolds. A definition is needed to state the result concisely.

Definition 2.2.1. Let H and H^{pert} be two C^1 vector fields on \mathbb{R}^N , and let \mathcal{K} be a compact set. Then we say that H is C^1 **θ -close** to H^{pert} (on \mathcal{K}) if

$$\begin{aligned} \sup_{z \in \mathcal{K}} \|H(z) - H^{\text{pert}}(z)\| &\leq \theta, \\ \sup_{z \in \mathcal{K}} \|DH(z) - DH^{\text{pert}}(z)\| &\leq \theta. \end{aligned}$$

We shall refer to H as the **unperturbed vector field** and H^{pert} as the **perturbed vector field**.

The definition is just a different way of stating that the unperturbed and perturbed vector fields are C^1 -close in the sup-norm. Now we can state Fenichel's major perturbation result for overflowing invariant manifolds.

Theorem 2.2.2 ([Fen71]; see also [HPS77]). *Consider*

$$\dot{z} = H(z) \quad \text{with } H \in C^r \text{ and } z \in \mathbb{R}^N. \quad (2.21)$$

Let M be a C^r compact connected manifold that is overflowing invariant under the flow ϕ_t defined by (2.21). Assume that

$$\nu(p) < 1 \quad \text{and} \quad \sigma(p) < \frac{1}{r} \quad \text{for all } p \in M. \quad (2.22)$$

Then for every C^r vector field H^{pert} that is C^1 θ -close to H , with θ sufficiently small, there is a manifold M^{pert} that is overflowing invariant under H^{pert} and C^r -diffeomorphic to M .

Roughly speaking, if the linearized dynamics for an invariant manifold M induce a splitting into fast normal dynamics and slow tangential dynamics, we can perturb the system a bit and get a distorted version M^{pert} of the invariant manifold M ; see Figure 2.5. We shall from now on always assume that the hypothesis (2.22) is satisfied. The strategy of the proof is as follows:

- (S1) Choose a nice **atlas** for M , i.e., a nice collection of coordinate **charts**, which are maps from M to a Euclidean space and which parameterize M locally.
- (S2) Obtain estimates for the tangential and normal flows.
- (S3) Set up the “graph-transform” G .
- (S4) Obtain M^{pert} as a fixed point of G in a suitable function space.
- (S5) Show that M^{pert} is indeed C^r .

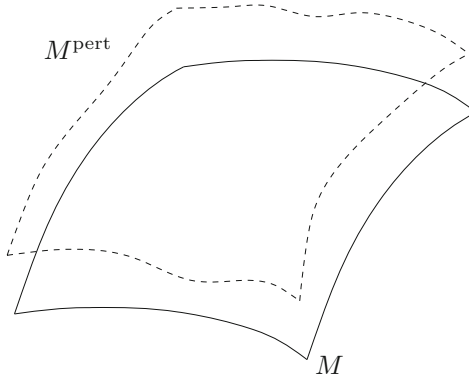


Figure 2.5: Perturbation of an invariant manifold illustrating Theorem 2.2.2.

There are other very important strategies for proving the persistence of invariant manifolds; see Section 2.5 for comments and references. We shall focus on the key ideas contained in parts (S2)–(S4) and also omit some technical steps needed for the general proof. However, the construction will be kept general enough to show how an extension of the proof could be carried out. The first simplification is that we are dealing only with a single chart, i.e., let $U \subset M$ be open in M . Suppose M has dimension $N - k$. Consider a chart

$$\mu : U \rightarrow \mathcal{D} \subset \mathbb{R}^{N-k},$$

where \mathcal{D} is a disk centered at 0 and μ is a **diffeomorphism**, i.e., μ is smooth and invertible with smooth inverse. Clearly, we can assume that μ has a bounded total derivative on U . To prove the entire result for M , we would have to choose a “nice” atlas with several coordinate charts and then use the compactness of M .

By standard properties of the normal bundle, we know that $\mathcal{N}|_U$ has a C^{r-1} orthonormal basis. Note that since M has dimension $N - k$, the fibers of \mathcal{N} have dimension k . By moving the normal bundle a bit, differentiability can be improved.

Remark: Before stating the detailed result, recall that two manifolds M_1 and M_2 are **transversal** (or **intersect transversally**) in \mathbb{R}^N if the tangent spaces $T_p M_1$ and $T_p M_2$ span $T_p \mathbb{R}^N \cong \mathbb{R}^N$ at each point $p \in M_1 \cap M_2$. As an aside, it should be noted that the word “recall” in this book is used in the usual mathematical sense, i.e., if you know the concept, then you may skip to the next aspect, and if you do not know the concept, then please try to learn it quickly.

Proposition 2.2.3 ([Whi36, Wig94]). *There exists a C^r k -dimensional bundle $\mathcal{N}' \subset T\mathbb{R}^N|_M$ transversal to TM . Given any $\varepsilon > 0$, there exist orthonormal bases*

$$\{\tilde{e}_1(p), \dots, \tilde{e}_k(p)\} \quad \text{for } \mathcal{N}|_U \quad \text{and} \quad \{\tilde{f}_1(p), \dots, \tilde{f}_k(p)\} \quad \text{for } \mathcal{N}'|_U$$

such that $\|\tilde{e}_l(p) - \tilde{f}_l(p)\| < \varepsilon$ for $l \in \{1, 2, \dots, k\}$.

The set \mathcal{N}' is called the **transversal bundle**, and we denote its elements by (p, v) with $p \in M$ and $v \in T\mathbb{R}^N$ transversal to $T_p M$. We want to consider the elements of the transversal bundle to lie in \mathbb{R}^N , which formally requires a map

$$h : \mathcal{N}' \rightarrow \mathbb{R}^N \quad \text{defined by} \quad h(p, v) = p + v.$$

Proposition 2.2.4. *Let $\mathcal{K} \subset M$ be any compact subset. On a neighborhood of the zero section of $\mathcal{N}'|_{\mathcal{K}}$, the map h is a C^r -diffeomorphism to a neighborhood of $\mathcal{K} \subset \mathbb{R}^N$.*

The proof of Proposition 2.2.4 can be found in [Whi36]. Also, recall that a **section** of a vector bundle is a map from the base manifold into the bundle such that the image at each base point belongs to a corresponding fiber [Lee06]; the **zero section** selects the zero vector in each fiber. Next, consider the set

$$\mathcal{N}'_\varepsilon = \{(p, v) \in \mathcal{N}' : \|v\| < \varepsilon\}.$$

Formally, we should use the map h to view \mathcal{N}' as a subset of \mathbb{R}^N , but it should be clear from Figure 2.6 that we just have defined a nice neighborhood of M in \mathbb{R}^N . Choose an orthonormal basis of \mathcal{N}'_ε and define

$$\tau : \mathcal{N}'_\varepsilon \rightarrow \mathbb{R}^k \quad \text{by} \quad \tau(p, v) = \{\text{coordinates of } v \text{ in chosen basis}\}.$$

Since the basis is orthonormal and τ is linear, we have $\|\tau(p, v)\| = \|v\|$. Define $\mu \times \tau : \mathcal{N}'_\varepsilon \rightarrow \mathbb{R}^{N-k} \times \mathbb{R}^k$ by

$$(\mu \times \tau)(p, v) = (\mu(p), \tau(p, v)) =: (y, x).$$

Using the **inverse function theorem**, we can prove that $\mu \times \tau$ is a C^r diffeomorphism; for a statement and proof of the inverse function theorem, see [Rud76]. Hence we have constructed a local coordinate system in \mathbb{R}^N for points in a neighborhood of M ; see Figure 2.6. Since $(\mu \times \tau)^{-1}(y, 0) = (p, 0)$, we see that a vanishing second coordinate means that the point lies in M .

Remark: All objects and maps introduced have a suitable smoothness level, i.e., they are C^r , so that there is the chance that all following constructions can produce C^r objects. Since we are dealing only with a single chart $\mu : U \rightarrow \mathcal{D}$, we could disregard the maps μ and τ and pretend to work in \mathbb{R}^{N-k} and \mathbb{R}^k . This would no longer work in the general case for many charts, since we have to keep track of more than just one identification of U and fibers of \mathcal{N}' with subsets of \mathbb{R}^{N-k} and \mathbb{R}^k .

Lemma 2.2.5. *Let $\Pi' : T\mathbb{R}^N|_M \rightarrow \mathcal{N}'$ be the projection onto the transversal bundle. Define $B'_t = \Pi' \circ D\phi_t(\phi_{-t}(p))$. Then there exists $T > 1$ such that*

$$\|B'_T(p)\| < \frac{1}{4}, \tag{2.23}$$

$$c^{2k+1} \|A_T(p)\|^k \|B'_T(p)\| < \frac{1}{4}, \tag{2.24}$$

for all $p \in U$, $0 \leq k \leq r$, and a constant $c > 0$.

Proof. Note that the generalized Lyapunov-type numbers for the splitting $T\mathbb{R}^N|_M = TM \oplus \mathcal{N}'$ are the same as those for the splitting $T\mathbb{R}^N|_M = TM \oplus \mathcal{N}$, by Exercise 2.1.8. Now apply the corollaries to the uniformity lemma (see Corollary 2.1.11 and Corollary 2.1.12). \square

Notice that we can increase the constant c if necessary by taking T larger. We shall see later that this constant is introduced for computational convenience. We fix the $T > 1$ given in Lemma 2.2.5 in what follows. The estimate in equation (2.23) shows that the linearized flow contracts vectors in the direction transversal to M by a factor of $1/4$. For a suitable small neighborhood of M , we can, of course, make a statement about the nonlinear flow too.

Lemma 2.2.6. *For $\varepsilon > 0$ sufficiently small, one has $\phi_T : \mathcal{N}'_\varepsilon \rightarrow \mathcal{N}'_{\varepsilon/3}$, i.e., the nonlinear flow contracts locally by at least $1/3$.*

Proof. (Sketch) Locally, the difference between the linear and nonlinear flows in the transversal direction is at most $\mathcal{O}(\varepsilon^2)$ for the finite time T by a direct Taylor expansion of the nonlinear flow. Since $\frac{\varepsilon}{4} + \mathcal{O}(\varepsilon^2) < \frac{\varepsilon}{3}$ for ε small, we get the result. \square

The next step is to move all involved maps to local coordinates, so we set

$$\begin{aligned} g^0(y, x) &= \mu \circ h^{-1} \circ \phi_T \circ h \circ (\mu \times \tau)^{-1}(y, x), \\ f^0(y, x) &= \tau \circ h^{-1} \circ \phi_T \circ h \circ (\mu \times \tau)^{-1}(y, x). \end{aligned}$$

These maps define the time T -map of the flow in local coordinates

$$(y, x) \mapsto (g^0(y, x), f^0(y, x)) \in \mathbb{R}^{N-k} \times \mathbb{R}^k.$$

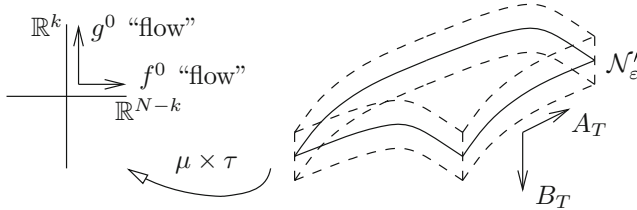


Figure 2.6: Linearized flows on M and locally in $\mathbb{R}^{N-k} \times \mathbb{R}^k$.

In principle, we should think of g^0 as giving the flow along M and of f^0 as the transversal flow; see Figure 2.6. Denote the total derivatives with respect to the first $N - k$ variables by D_1 , and for the remaining k variables by D_2 . We see that the local representation of A_T is $(D_1 g^0(x, 0))^{-1}$ and that B_T is given by $D_2 f^0(x, 0)$.

Suppose that H is C^1 θ -close to a perturbed vector field H^{pert} . The same construction can be carried out, and we define

$$\begin{aligned} g^\theta(y, x) &= \mu \circ h^{-1} \circ \phi_T^{\text{pert}} \circ h \circ (\mu \times \tau)^{-1}(y, x), \\ f^\theta(y, x) &= \tau \circ h^{-1} \circ \phi_T^{\text{pert}} \circ h \circ (\mu \times \tau)^{-1}(y, x). \end{aligned}$$

These maps define the time T map of the perturbed flow in local coordinates

$$(y, x) \rightarrow (g^\theta(y, x), f^\theta(y, x)) \in \mathbb{R}^{N-k} \times \mathbb{R}^k.$$

The following result is a local coordinate version of the uniformity lemma.

Lemma 2.2.7. *Let $\eta > 0$ and suppose that H is C^1 θ -close to H^{pert} . Assume that θ and ε are sufficiently small. Then*

$$\|(\mathbf{D}_1 g^\theta(y, x))^{-1}\|^k \| \mathbf{D}_2 f^\theta(y, x) \| < \frac{1}{2} \quad \text{for } 0 \leq k \leq r, \quad (2.25)$$

$$\|f^\theta(y, x)\| < \varepsilon, \quad (2.26)$$

$$\|\mathbf{D}_1 f^\theta(y, x)\| < \eta. \quad (2.27)$$

Furthermore, the norms of all total derivatives of $g^0, f^0, g^\theta, f^\theta$ and $(g^\theta)^{-1}$ are bounded on $(\mu \times \tau)\mathcal{N}'_\varepsilon$ by some constant Q .

Proof. First notice that the last statement follows directly, since continuous functions are bounded on compact sets. Let us begin by comparing the unperturbed and perturbed flows. For $t \in [-T, T]$, using that H and H^{pert} are C^1 θ -close on \bar{U} leads to an estimate for $\|\phi_t(z) - \phi_t^{\text{pert}}(z)\| =$

$$\begin{aligned} &= \left\| \phi_0(z) - \phi_0^{\text{pert}}(z) + \int_0^t H(\phi_s(z)) - H^{\text{pert}}(\phi_s^{\text{pert}}(z)) \, ds \right\| \\ &\leq \int_0^t \|H(\phi_s(z)) - H^{\text{pert}}(\phi_s(z)) + H^{\text{pert}}(\phi_s(z)) - H^{\text{pert}}(\phi_s^{\text{pert}}(z))\| \, ds \\ &\leq \theta T + L \int_0^t \|\phi_s(z) - \phi_s^{\text{pert}}(z)\| \, ds, \end{aligned}$$

where L is the Lipschitz constant for H^{pert} . Now we can apply **Gronwall's lemma** (see [Hal09, HSD03] for a statement and proof of Gronwall's lemma) to get that

$$\|\phi_t(z) - \phi_t^{\text{pert}}(z)\| \leq \theta T e^{LT}. \quad (2.28)$$

Similarly, it follows that

$$\|\mathbf{D}\phi_t(z) - \mathbf{D}\phi_t^{\text{pert}}(z)\| \leq \theta T e^{L'T} \quad (2.29)$$

for some constant L' . Recall that Lemma 2.2.5 provides the estimates

$$\|B'_T(p)\| < \frac{1}{4}, \quad (2.30)$$

$$c^{2k+1} \|A_T(p)\|^k \|B'_T(p)\| < \frac{1}{4}, \quad (2.31)$$

for all $p \in U$ and $0 \leq k \leq r$. Also, the coordinate chart μ has been constructed carefully to have bounded total derivative, say

$$\|\mathbf{D}\mu\| < c \quad \text{and} \quad \|(\mathbf{D}\mu)^{-1}\| < c.$$

Recall that we can increase the constant c in (2.31) if necessary so that we can indeed assume that the c 's used so far are the same. Furthermore, the choice of orthonormal basis of \mathcal{N}'_ε implies that

$$\|\mathrm{D}\tau\| = 1 = \|(\mathrm{D}\tau)^{-1}\|.$$

Since $\|\mathrm{D}h\| = 1 = \|(\mathrm{D}h)^{-1}\|$, the estimates (2.31) and (2.29) imply that

$$\|(\mathrm{D}_1 g^\theta(y, x))^{-1}\|^k \|\mathrm{D}_2 f^\theta(y, x)\| < \frac{1}{4}$$

for θ small enough to make the perturbed linearization close to the unperturbed one. Note that the constants involving c cancel out nicely. This establishes (2.25). For the second desired inequality (2.26), we recall that Lemma 2.2.6 states that vectors in the transversal direction are contracted by a factor of $\varepsilon/3$ by the unperturbed flow. One can use (2.28) to make this estimate close to the unperturbed flow. Choosing θ and ε appropriately, one concludes that in the local coordinate form,

$$\|g^\theta(y, x)\| < \varepsilon,$$

so we have proved (2.26). The last inequality states that

$$\|\mathrm{D}_1 f^\theta(y, x)\| < \eta. \quad (2.32)$$

Notice that the overflowing invariance of M implies that $f^\theta(y, 0) = 0$, and so by making ε small enough, we can use continuity of the derivative for f to justify (2.32). \square

Having finished the main estimates for step (S2), we can now proceed to define the ‘‘graph transform.’’ Let S denote the space of sections of $\mathcal{N}'_\varepsilon|_U$. Hence if $v \in S$, then it assigns, in a continuous way, to each point in $M|_U$ a vector in $\mathcal{N}'_\varepsilon|_U$. If we think of v in local coordinates, we obviously look at

$$u := \tau \circ v \circ \mu^{-1} : \mathcal{D} \rightarrow \mathbb{R}^k.$$

The **graph** of u is defined as $\text{graph}(u) = \{(y, x) \in \mathbb{R}^{N-k} \times \mathbb{R}^k : u(y) = x\}$. One wants to restrict the space S to a more tractable set and so considers

$$\text{Lip}(v) := \sup_{y, y' \in \mathcal{D}} \frac{\|u(y) - u(y')\|}{\|y - y'\|},$$

where u is the local coordinate representation of v , and defines

$$S_\delta := \{v \in S : \text{Lip}(v) \leq \delta\}. \quad (2.33)$$

This singles out all the sections that have a local coordinate expression with Lipschitz constant less than δ . In particular, if $v \in S_\delta$, then $\text{graph}(v)$ is a Lipschitz manifold in \mathbb{R}^N .

Definition 2.2.8. Consider $v \in S_\delta$ with local coordinate representation $u = \tau \circ v \circ \mu^{-1}$. The perturbed time T flow ϕ_T^{pert} defines a map on $\text{graph}(u)$ given by

$$(y, u(y)) \mapsto (g^\theta(y, u(y)), f^\theta(y, u(y))) =: (\xi, (Gu)(\xi)),$$

where the function G is the local coordinate representation of a map $G : S_\delta \rightarrow S$, called the **graph transform**.

The graph transform G provides a way to connect the flow of the perturbed equation to invariant manifolds described as graphs. In fact, the desired perturbed overflowing invariant manifold will be obtained as a fixed point of G in S_δ .

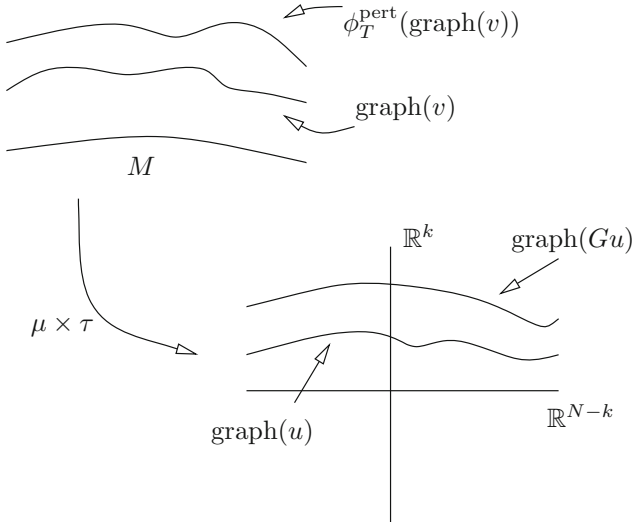


Figure 2.7: Illustration of the graph transform.

Note that the notation G describing the graph transform on the manifold as well as in local coordinates is intentionally overloaded; see Figure 2.7. A priori, we do not know whether G is really well defined, since there is no immediate reason why the image $(g^\theta(y, u(y)), f^\theta(y, u(y)))$ should be described by a graph of a function. The precise argument is a bit technical (see [Wig94] for details), but we can give an intuitive argument.

Lemma 2.2.9. *The graph transform G is well defined, i.e., its image consists of sections in S .*

Proof. (Sketch) Note first that uniqueness of solutions for ODEs implies that $\phi_T^{\text{pert}}(p) = \phi_T^{\text{pert}}(p')$ if and only if $p = p'$, so moving the graph by the flow cannot “collapse” points, so we get a manifold; see also Figure 2.8(a).

The major problem is that two points of $\phi_T^{\text{pert}}(\text{graph}(v))$ might lie in the same fiber, so that the new manifold could not be described by a graph. The function

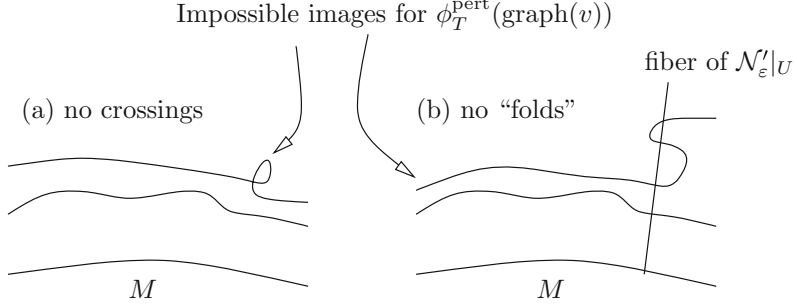


Figure 2.8: Illustration for the proof of Lemma 2.2.9.

describing it would have to be “multivalued”; see Figure 2.8(b). Now imagine decreasing the parameter θ , which controls the perturbation. The smaller we choose it, the closer the image is to the unperturbed invariant manifold for which we have assumed that it is locally given by a graph. Hence, at some point, the “foldings” in Figure 2.8(b) are gone. Since we are free to make θ small, the result follows. \square

Now write the graph of u as $u(y) = x$ and apply G , which yields a new graph

$$(Gu)(g^\theta(y, x)) = f^\theta(y, x) \quad \text{i.e.} \quad (Gu)(g^\theta(y, u(y))) = f^\theta(y, u(y)),$$

so that a fixed point u of G satisfies

$$u(g^\theta(y, u(y))) = f^\theta(y, u(y)). \quad (2.34)$$

One should think of (2.34) as a condition that u has to satisfy for $\text{graph}(u)$ to remain invariant under ϕ_T^{pert} . This finishes step (S3). The next goal is to apply the Banach contraction mapping theorem to G , so we must first show that the range of G is also suitably Lipschitz; details about the **Banach contraction mapping theorem** and its proof can be found in [Kör04].

Lemma 2.2.10. *For ε , δ , and θ sufficiently small, $G : S_\delta \rightarrow S_\delta$.*

Proof. We have to prove that for $u \in S_\delta$,

$$\|(Gu)(\xi) - (Gu)(\xi')\| \leq \delta \|\xi - \xi'\| \quad (2.35)$$

for $\xi, \xi' \in \mathcal{D}$. Notice that one can choose ξ close to ξ' and cover \mathcal{D} with a finite number of smaller disks of radius $\|\xi - \xi'\|$ if necessary. On each disk, the Lipschitz inequality (2.35) will hold. Recall that the graph transform is given by

$$\begin{aligned} (Gu)(\xi) &= f^\theta(y, u(y)) && \text{with} && \xi = g^\theta(y, u(y)), \\ (Gu)(\xi') &= f^\theta(y', u(y')) && \text{with} && \xi' = g^\theta(y', u(y')), \end{aligned}$$

for $y, y' \in \mathcal{D}$. Lemma 2.2.7 gave us the following estimates:

$$\begin{aligned} \|\mathrm{D}g^\theta\|, \|(\mathrm{D}g^\theta)^{-1}\| &< Q, \\ \|\mathrm{D}_1f^\theta\| &< \eta, \\ \|\mathrm{D}_1f^\theta\| \|(\mathrm{D}g^\theta)^{-1}\| &< \frac{1}{2}. \end{aligned} \quad (2.36)$$

First we want to bound $\|\xi - \xi'\|$ from below in terms of $\|y - y'\|$, so

$$\begin{aligned} \|\xi - \xi'\| &= \|g^\theta(y, u(y)) - g(y', u(y'))\| \\ &\geq \underbrace{\|g^\theta(y, u(y)) - g(y', u(y))\|}_{=: A^*} - \underbrace{\|g^\theta(y', u(y)) - g(y', u(y'))\|}_{=: B^*}. \end{aligned} \quad (2.37)$$

The terms A^* and B^* can be treated separately. We need a lower bound for A^* . Let us regard g^θ for now as a function of \mathbb{R}^{N-k} variables and suppress $u(y) = x$ as parameters. Then let $w = g^\theta(y)$ and $w' = g^\theta(y')$. Choosing y close to y' , the inverse function theorem allows us to invert g^θ , so

$$\begin{aligned} y &= (g^\theta)^{-1}(w), \\ y' &= (g^\theta)^{-1}(w'). \end{aligned}$$

Taylor expanding the right-hand sides around 0 and subtracting gives

$$y - y' = \mathrm{D}_1(g^\theta)^{-1}(w - w') + \mathcal{O}(\|w - w'\|^2) \quad \text{as } \|w - w'\| \rightarrow 0.$$

On taking norms and dividing by $\|\mathrm{D}_1(g^\theta)^{-1}\|$, it follows that

$$\begin{aligned} A^* &= \|g^\theta(y, u(y)) - g^\theta(y', u(y))\| \\ &\geq \|\mathrm{D}_1g^\theta\|^{-1}\|y - y'\| + \mathcal{O}(\|y - y'\|^2), \end{aligned}$$

as $\|y - y'\| \rightarrow 0$. This gives the required lower bound. We need an upper bound for B^* , and using Taylor expansion again yields

$$\begin{aligned} B^* &= \|g^\theta(y', u(y)) - g^\theta(y', u(y'))\| \\ &\leq \|\mathrm{D}_2g^\theta\| \|u(y) - u(y')\| + \mathcal{O}(\|u(y) - u(y')\|^2) \\ &\leq \delta \|\mathrm{D}_2g^\theta\| \|y - y'\| + \mathcal{O}(\|y - y'\|^2) \end{aligned}$$

as $\|y - y'\| \rightarrow 0$. Putting both estimates together leads to

$$\begin{aligned} \|\xi - \xi'\| &\geq A^* - B^* \\ &\geq \|\mathrm{D}_1g^\theta\|^{-1}(1 - \delta \|\mathrm{D}_1g^\theta\|^{-1} \|\mathrm{D}_2g^\theta\|) \|y - y'\| \\ &\quad + \mathcal{O}(\|y - y'\|^2). \end{aligned} \quad (2.38)$$

From (2.36), one knows that $\|\mathrm{D}_1g^\theta\|^{-1} \|\mathrm{D}_2g^\theta\| < Q^2$ and $\|\mathrm{D}_1g^\theta\|^{-1} < Q$. Furthermore, $\mathcal{O}(\|y - y'\|^2) < \delta Q \|y - y'\|$ by choosing y sufficiently close to y' . Combining these observations with (2.38) yields

$$\|\xi - \xi'\| \leq \|\mathrm{D}_1g^\theta\|^{-1}(1 - 2\delta Q^2) \|y - y'\|.$$

Fortunately, the main estimate we are aiming at is not far away. Indeed, consider

$$\begin{aligned} \|(Gu)(\xi) - (Gu)(\xi')\| &= \|f(y, u(y)) - f(y', u(y'))\| \\ &\leq \|f^\theta(y, u(y)) - f^\theta(y', u(y))\| \\ &\quad + \|f^\theta(y', u(y)) - f^\theta(y', u(y'))\|. \end{aligned}$$

Each of the terms on the right-hand side can be Taylor-expanded:

$$\|(Gu)(\xi) - (Gu)(\xi')\| \leq (\|D_1 f^\theta\| + \delta \|D_2 f^\theta\|) \|y - y'\| + \mathcal{O}(\|y - y'\|^2). \quad (2.39)$$

Again invoking (2.36), we know that $\|D_1 f\| < \eta$. Making y and y' sufficiently close gives $\mathcal{O}(\|y - y'\|^2) < \eta \|y - y'\|$. Using the last two observations, one can rewrite (2.39) as

$$\begin{aligned} \|(Gu)(\xi) - (Gu)(\xi')\| &\leq (2\eta + \|D_2 f^\theta\| \delta) \|y - y'\| \\ &\leq \frac{(2\eta + \|D_2 f^\theta\| \delta)}{1 - 2\delta Q^2} \| (D_1 g^\theta)^{-1} \| \|\xi - \xi'\|, \end{aligned} \quad (2.40)$$

where we have used (2.38) in the last inequality. Making δ small ensures that

$$1 - 2\delta Q^2 > \frac{3}{4}.$$

Also η can be chosen sufficiently small that

$$2\eta Q < \frac{2\delta}{8}.$$

Since we have not used the omnipresent (2.36) for a while, let us recall that it also gives $\|D_2 f^\theta\| \| (Dg^\theta)^{-1} \| < 1/2$. Putting the last three observations together yields

$$\frac{(2\eta + \|D_2 f^\theta\| \delta)}{1 - 2\delta Q^2} \| (D_1 g^\theta)^{-1} \| < \frac{\frac{2\delta}{8} + \frac{\delta}{2}}{\frac{3}{4}} = \delta. \quad (2.41)$$

Combining (2.40) and (2.41) finally gives the required result. \square

The next step consists in setting up the Banach contraction mapping theorem for G on S_δ with the sup-norm. Recall that this norm is given by

$$\|u\|_\infty = \sup_{z \in M} \|u(z)\|.$$

Lemma 2.2.11. *For ε , δ , and η sufficiently small and $v, v' \in S_\delta$ with $v \neq v'$,*

$$\|Gv - Gv'\|_\infty \leq \kappa \|v - v'\|_\infty$$

for some constant $\kappa < 1$, i.e., G is a contraction in the Banach space of continuous sections into \mathcal{N}'_ε .

Remark: A **Banach space** is a complete normed vector space; see [Fol99, Rud91]. Since the norm $\|\cdot\|_\infty$, and in fact any norm, also induces a metric d via $d(v, v') := \|v - v'\|_\infty$, we can apply the Banach contraction mapping theorem for complete metric spaces on any Banach space.

Proof. (of Lemma 2.2.11) Since $v \neq v'$, it follows that $\|v - v'\|_\infty \neq 0$. Let u be the local coordinate representation of v . Let $\xi \in \mathcal{D}$ and choose y, y' such that $\xi = g(y, u(y)) = g(y', u(y'))$. The main estimate is

$$\begin{aligned} & \| (Gu)(\xi) - (Gu')(\xi) \| = \| f^\theta(y, u(y)) - f^\theta(y', u'(y')) \| \\ & \leq \| f^\theta(y, u(y)) - f^\theta(y', u(y)) \| + \| f^\theta(y', u(y)) - f^\theta(y', u(y')) \| \\ & \quad + \| f^\theta(y', u(y')) - f^\theta(y', u'(y')) \| . \end{aligned} \quad (2.42)$$

Recalling that $\|D_1 f\| < \eta$ and $\|D_2 f\| < \frac{1}{2}$, one can easily estimate the last three terms using Taylor expansion, so (2.42) becomes

$$\| (Gu)(\xi) - (Gu')(\xi) \| \leq (2\eta + \frac{1}{2}\delta) \|y - y'\| + \frac{1}{2} \|u - u'\|_\infty + O(\|u - u'\|_\infty^2). \quad (2.43)$$

Since $\|u(\cdot)\|_\infty < \varepsilon$, we can make ε small and conclude that

$$O(\|u - u'\|_\infty^2) < \frac{1}{16} \|u - u'\|_\infty. \quad (2.44)$$

Furthermore, we know that $\|y - y'\|$ is bounded by some suitably large constant, and so in particular,

$$\|y - y'\| \leq K \|u - u'\|_\infty \quad (2.45)$$

for some $K > 0$. Using (2.44) and (2.45) in the estimate (2.43) gives

$$\| (Gu)(\xi) - (Gu')(\xi) \| \leq \left(\left(2\eta + \frac{1}{2}\delta \right) K + \frac{9}{16} \right) \|u - u'\|_\infty.$$

Now choose η and δ small to ensure that

$$\left(2\eta + \frac{1}{2}\delta \right) K + \frac{9}{16} \leq \kappa < 1.$$

This implies

$$\| (Gu)(\xi) - (Gu')(\xi) \| \leq \kappa \|u - u'\|_\infty,$$

and taking the supremum of ξ gives the result. \square

Exercise 2.2.12. Prove that the space S_δ from (2.33) is a Banach space under the sup-norm. \diamond

Corollary 2.2.13. *There exists a unique $v \in S_\delta$ such that*

$$\text{graph}(v) \subseteq \phi_t^{\text{pert}}(\text{graph}(v)) \quad \text{for all } t \geq 0.$$

Proof. By Exercise 2.2.12, we know that S_δ is a Banach space under the sup-norm. Using Lemma 2.2.11, we apply the Banach contraction mapping theorem to get a unique fixed point v of the graph transform G . Note that this implies

$$\text{graph}(v) \subseteq \phi_T^{\text{pert}}(\text{graph}(v)), \quad (2.46)$$

since M is overflowing. Then for $t > 0$ with t small enough, we know from the proof of Lemma 2.2.9 that there exists v_t giving $\phi_t^{\text{pert}}(\text{graph}(v)) \cap \mathcal{N}'_\varepsilon|_U$ as a graph. The next goal is to show that $v = v_t$. Using (2.46), we get

$$\phi_t^{\text{pert}}(\text{graph}(v)) \subseteq \phi_t^{\text{pert}}(\phi_T^{\text{pert}}(\text{graph}(v))) = \phi_T^{\text{pert}}(\phi_t^{\text{pert}}(\text{graph}(v))).$$

Therefore, $v_t = v$ by the uniqueness of the fixed point for G . Now apply the argument inductively to get the result for all $t \geq 0$. \square

The section v (or locally the function u) gives us the desired overflowing invariant manifold M^{pert} , at least for the piece of M covered by our single chart $\mu : U \rightarrow \mathcal{D}$. Hence, we have finished step (S4). In principle, we just have to rewrite the argument for an atlas of M and make sure that all different domains and maps “fit nicely together.” This is an important, but tedious, step that we decide to skip here.

Theorem 2.2.14 ([Fen71, Wig94]; see also [HPS77]). *M^{pert} is C^r (as claimed in Theorem 2.2.2).*

The proof can be found in an abbreviated version in [Fen71] and in very detailed form in [Wig94]. We shall only outline the main idea.

Proof. (Sketch) Let u denote the fixed point of the graph transform in local coordinates and recall that u satisfies

$$u(\xi) = f^\theta(y, u(y)) \quad \text{with } \xi = g^\theta(y, u(y)). \quad (2.47)$$

Formally differentiating (2.47) yields

$$(Du(\xi))(D\xi) = D_1 f^\theta(y, u(y)) + D_2 f^\theta(y, u(y))Du(y).$$

Using the definition of ξ and rearranging the last equation gives

$$(Du(\xi)) = [D_1 f^\theta(y, u(y)) + D_2 f^\theta(y, u(y))Du(y)] \cdot [D_1 g^\theta(y, u(y)) + D_2 g^\theta(y, u(y))Du(y)]^{-1}. \quad (2.48)$$

With the notation $Du(\xi) = w$ and $\mathcal{H}w$ for the right-hand side in (2.48), we can express (2.48) simply as

$$\mathcal{H}w = w. \quad (2.49)$$

This implies that if the derivative exists, then it must satisfy the **functional equation** (2.49). But we do not know that w exists, so consider the iteration

$$w^0 = 0 \quad \text{and} \quad \mathcal{H}w^n = w^{n+1}. \quad (2.50)$$

It can be shown that \mathcal{H} is contracting in a suitable space. The techniques for this step are similar to those used in the proof of existence of the invariant manifold. The Banach contraction mapping theorem guarantees a unique solution to (2.50). A direct calculation using the definition of the derivative shows that this solution is indeed the derivative of u . The argument can now be applied inductively to achieve C^r differentiability. \square

2.3 Normal Hyperbolicity

We have assumed up to now the condition

$$\nu(p) = \inf \left\{ a : \frac{1}{\|w_{-t}\|a^t} \rightarrow 0 \quad \text{as } t \rightarrow \infty \quad \forall w_0 \in \mathcal{N}_p \right\} < 1. \quad (2.51)$$

As illustrated previously, (2.51) is an asymptotic stability condition for the flow in the direction normal to the overflowing invariant manifold M . An analogous condition will be needed if we are dealing with an inflowing invariant manifold, just that the time direction will be reversed and asymptotic stability holds in backward time. This requires a refined definition of generalized Lyapunov-type numbers.

As in Section 2.2, it is assumed that M is a compact, connected, invariant manifold of class C^r for some $r \geq 1$. Suppose there exists a continuous splitting

$$\mathbb{T}\mathbb{R}^N|_M = \mathcal{N}^u \oplus TM \oplus \mathcal{N}^s$$

with the projections $\Pi^s : \mathbb{T}\mathbb{R}^N|_M \rightarrow \mathcal{N}^s$ and $\Pi^u : \mathbb{T}\mathbb{R}^N|_M \rightarrow \mathcal{N}^u$. Assume that the subbundles $TM \oplus \mathcal{N}^s$ and $TM \oplus \mathcal{N}^u$ are invariant under $D\phi_t$. Let $u_0 \in \mathcal{N}_p^u$, $v_0 \in T_p M$, and $w_0 \in \mathcal{N}_p^s$. As usual, we shall denote by

$$u_{-t} = \Pi^u \circ D\phi_{-t}(p)u_0, \quad v_{-t} = D\phi_{-t}(p)v_0, \quad w_{-t} = \Pi^s \circ D\phi_{-t}(p)w_0,$$

the images of the linearized flow.

Definition 2.3.1. The **generalized Lyapunov-type numbers** are

$$\begin{aligned} \nu^u(p) &= \inf \left\{ a : \frac{\|u_{-t}\|}{a^t} \rightarrow 0 \quad \text{as } t \rightarrow \infty, \quad \forall u_0 \in \mathcal{N}_p^u \right\}, \\ \nu^s(p) &= \inf \left\{ a : \frac{1}{\|w_{-t}\|a^t} \rightarrow 0 \quad \text{as } t \rightarrow \infty, \quad \forall w_0 \in \mathcal{N}_p^s \right\}, \end{aligned}$$

and if $\nu^u(p) < 1$ and $\nu^s(p) < 1$, one also defines

$$\begin{aligned} \sigma^u(p) &= \inf \left\{ b : \|v_{-t}\| \|u_{-t}\|^b \rightarrow 0 \quad \text{as } t \rightarrow \infty, \quad \forall u_0 \in \mathcal{N}_p^u, v_0 \in T_p M \right\}, \\ \sigma^s(p) &= \inf \left\{ b : \frac{\|v_{-t}\|}{\|w_{-t}\|^b} \rightarrow 0 \quad \text{as } t \rightarrow \infty, \quad \forall w_0 \in \mathcal{N}_p^s, v_0 \in T_p M \right\}. \end{aligned}$$

The definitions are compatible with those previously given, i.e., $\nu^s(p) = \nu(p)$ and $\sigma^s(p) = \sigma(p)$ in the notation of Definition 2.1.5. As in Lemma 2.1.6, we can rely on the following way to calculate the generalized Lyapunov-type numbers:

$$\begin{aligned} \nu^u(p) &= \limsup_{t \rightarrow \infty} \|\Pi^u \circ D\phi_{-t}(\phi_t(p))|_{\mathcal{N}^u}\|^{1/t}, \\ \nu^s(p) &= \limsup_{t \rightarrow \infty} \|\Pi^s \circ D\phi_t(\phi_{-t}(p))|_{\mathcal{N}^s}\|^{1/t}, \\ \sigma^u(p) &= \limsup_{t \rightarrow \infty} \frac{\log \|D\phi_t|_M(p)\|}{-\log \|\Pi^u \circ D\phi_{-t}(\phi_t(p))|_{\mathcal{N}^u}\|}, \\ \sigma^s(p) &= \limsup_{t \rightarrow \infty} \frac{\log \|D\phi_t|_M(p)\|}{-\log \|\Pi^s \circ D\phi_t(\phi_{-t}(p))|_{\mathcal{N}^s}\|}. \end{aligned}$$

As before, it is helpful to calculate the generalized Lyapunov-type numbers for a simple example. We begin with the numbers ν^u and ν^s .

Example 2.3.2. Consider the ODE

$$\dot{z} = \begin{pmatrix} \lambda & 0 \\ 0 & -\mu \end{pmatrix} z \quad \text{for } z \in \mathbb{R}^2 \text{ and } \lambda, \mu > 0. \quad (2.52)$$

As an invariant manifold M choose the equilibrium point $(0, 0) =: 0$. Let us choose the splitting $T\mathbb{R}^2|_0 = \mathcal{N}^u \oplus \mathcal{N}^s$ with $\mathcal{N}^u = \{\{0\} \times (z_1, 0) : z_1 \in \mathbb{R}\}$ and $\mathcal{N}^s = \{\{0\} \times (0, z_2) : z_2 \in \mathbb{R}\}$. Obviously, the two bundles \mathcal{N}^u and \mathcal{N}^s should just be viewed as the coordinate axes in \mathbb{R}^2 . The projections are

$$\Pi^u = \begin{pmatrix} 1 & 0 \\ 0 & 0 \end{pmatrix} \quad \text{and} \quad \Pi^s = \begin{pmatrix} 0 & 0 \\ 0 & 1 \end{pmatrix}.$$

The linearized flow and its derivative are easily found:

$$\phi_t(p) = \begin{pmatrix} p_1 e^{\lambda t} & 0 \\ 0 & p_2 e^{-\mu t} \end{pmatrix} \quad \text{and hence} \quad D\phi_t(p) = \begin{pmatrix} e^{\lambda t} & 0 \\ 0 & e^{-\mu t} \end{pmatrix}.$$

Therefore, it follows that

$$\begin{aligned} \nu^u(p) &= \limsup_{t \rightarrow \infty} \|\Pi^u \circ D\phi_{-t}(\phi_t(p))|_{\mathcal{N}^u}\|^{1/t} \\ &= \limsup_{t \rightarrow \infty} |e^{-\lambda t}|^{1/t} = e^{-\lambda}, \\ \nu^s(p) &= \limsup_{t \rightarrow \infty} \|\Pi^s \circ D\phi_t(\phi_{-t}(p))|_{\mathcal{N}^s}\|^{1/t} \\ &= \limsup_{t \rightarrow \infty} |e^{-\mu t}|^{1/t} = e^{-\mu}. \end{aligned}$$

This shows that the conditions $\nu^u(p) < 1$ and $\nu^s(p) < 1$ precisely require that 0 be a hyperbolic equilibrium point. ♦

Definition 2.3.3. Let M be a compact connected invariant manifold in \mathbb{R}^N . A splitting $T\mathbb{R}^N|_M = \mathcal{N}^u \oplus TM \oplus \mathcal{N}^s$ is called **hyperbolic** if $\nu^u(p) < 1$ and $\nu^s(p) < 1$ for all $p \in M$.

Remark: It is tempting to call M a **hyperbolic manifold** if there exists a hyperbolic splitting as given in Definition 2.3.3. Unfortunately, this conflicts with the terminology in differential geometry of “hyperbolic manifolds” as those Riemannian manifolds that have constant sectional curvature -1 ; see [Rat06]. For our scenario, Definition 2.3.4, given below, has become the common terminology.

Recall that $\sigma(p) < \frac{1}{r}$ for all $p \in M$ was the condition that guaranteed that the flow in the normal direction dominated the flow in the tangential direction. The equivalent conditions needed now are $\sigma^u(p) < \frac{1}{r}$ and $\sigma^s(p) < \frac{1}{r}$ for all $p \in M$.

Definition 2.3.4. Let M be a compact connected invariant manifold in \mathbb{R}^N . A splitting $T\mathbb{R}^N|_M = \mathcal{N}^u \oplus TM \oplus \mathcal{N}^s$ is called **normally hyperbolic** if $\nu^u(p) < 1$, $\nu^s(p) < 1$, $\sigma^u(p) < 1$, and $\sigma^s(p) < 1$ for all $p \in M$. If an invariant manifold M admits a normally hyperbolic splitting, then it is called a **normally hyperbolic invariant manifold**.

The notion of a normally hyperbolic manifold is one of the most important concepts in the geometric theory of dynamical systems. It is helpful to keep

the colloquial version of Definition 2.3.4 in mind, which says that a manifold is normally hyperbolic if the linearized flow in the normal direction dominates the linearized flow in the tangential direction.

Intuitively, this should hold for multiple time-scale systems: In some parts of the phase space, the dynamics are slow (tangential direction) and are dominated by the fast dynamics (normal direction). This idea is explained in more detail in Chapter 3. We are now in a position to state another version of the perturbation theorem for invariant manifolds; see also Theorem 2.2.2.

Theorem 2.3.5 (Fenichel [Fen71]; see also [HPS77]). *Let H be a C^r vector field on \mathbb{R}^N with $r \geq 1$. Let M be a compact, connected C^r -manifold properly embedded in \mathbb{R}^N . Suppose that M is invariant and normally hyperbolic under the flow of H . Given any C^r -vector field H^{pert} sufficiently C^1 -close to H , there exists a C^r -manifold M^{pert} that is invariant under the flow of H^{pert} and diffeomorphic to M .*

In [Fen71], Fenichel derived not only the perturbation of the invariant manifold but also a variety of related results. We shall not discuss their proofs here, and restrict ourselves to statements as well as illustrative examples.

Theorem 2.3.6 (Fenichel [Fen71, Wig94]; see also [HPS77]). *Let H be a C^r vector field on \mathbb{R}^N with $r \geq 1$. Let M be a compact, connected C^r -manifold properly embedded in \mathbb{R}^N . Suppose that M is invariant and normally hyperbolic under the flow of H . Then there are C^r -manifolds*

$$W^u \text{ tangent to } \mathcal{N}^u \oplus TM \quad \text{and} \quad W^s \text{ tangent to } \mathcal{N}^s \oplus TM$$

with W^u overflowing invariant, W^s inflowing invariant, and $W^u \cap W^s = M$. Given any C^r vector field H^{pert} sufficiently C^1 -close to H , there exist C^r -manifolds

$$W_{\text{pert}}^u \text{ overflowing invariant} \quad \text{and} \quad W_{\text{pert}}^s \text{ inflowing invariant}$$

under the flow of H^{pert} ; W_{pert}^u and W_{pert}^s are diffeomorphic to W^u and W^s respectively.

If one requires in addition that the subbundles $\mathcal{N}^u \oplus TM$ and $TM \oplus \mathcal{N}^s$ be invariant under the linearized flow $D\phi_t$, one obtains new invariant subbundles for the perturbed invariant manifold. We can memorize Theorem 2.3.6 by the simple slogan that stable and unstable manifolds of a normally hyperbolic manifold persist under perturbation.

The graph transform can be used to establish the existence of W_{pert}^u and W_{pert}^s . The easiest example to illustrate Theorem 2.3.6 is the case of an equilibrium point.

Example 2.3.7. Consider the 2-dimensional ODE

$$\dot{z} = H(z) + \varepsilon I(z) \quad \text{for } z \in \mathbb{R}^2 \text{ and } \varepsilon \in (-\varepsilon_0, \varepsilon_0), \tag{2.53}$$

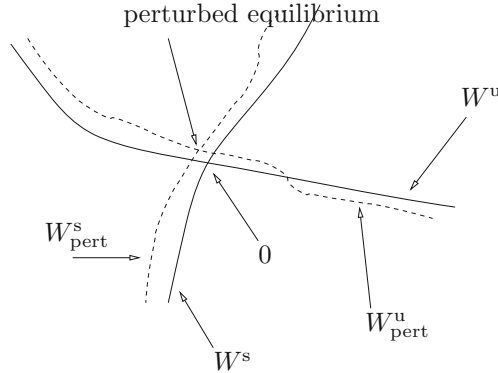


Figure 2.9: Perturbation of a hyperbolic equilibrium point for (2.53).

where H and I are smooth. Set $\varepsilon = 0$ and suppose that the origin $(0, 0) =: 0$ is a hyperbolic saddle equilibrium of

$$\dot{z} = H(z). \quad (2.54)$$

Looking at Theorem 2.3.6, we can view 0 as a normally hyperbolic invariant manifold; cf. Example 2.3.2. The tangent space to 0 is the zero vector by convention. Linearizing the system gives

$$\dot{z} = [DH(0)]z.$$

The statement of the existence of W^u and W^s can now be concluded either from Theorem 2.3.6 or from the stable manifold theorem 2.1.2; see Figure 2.9. ♦

Exercise 2.3.8. Prove directly that the equilibrium point in (2.54) persists (slightly moved) in equation (2.53) without using Theorem 2.3.6. ◇

Suppose we want to decompose the stable and unstable manifolds into submanifolds. The next example illustrates how this could be done.

Example 2.3.9. Consider the linear $(1, 1)$ -fast–slow system given by

$$\begin{aligned} x' &= -x, \\ y' &= -\varepsilon(x + y). \end{aligned} \quad (2.55)$$

Consider a point $p = (p_1, p_2)$. Then (2.55) is easily solved, and the trajectory through p is

$$\begin{aligned} x(t; p) &= p_1 e^{-t}, \\ y(t; p) &= p_1 \frac{\varepsilon}{1-\varepsilon} e^{-t} + \left(p_2 - p_1 \frac{\varepsilon}{1-\varepsilon}\right) e^{-\varepsilon t}. \end{aligned} \quad (2.56)$$

Exercise 2.3.10. Sketch or plot the solutions (2.56) for $\varepsilon = 0$ and $0 < \varepsilon \ll 1$. ◇

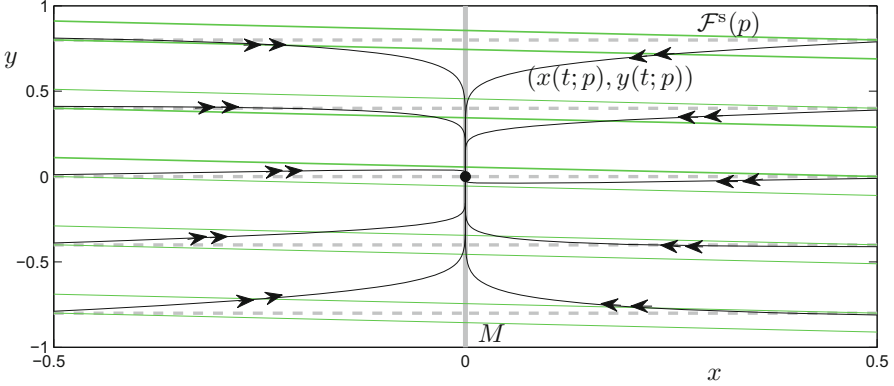


Figure 2.10: Illustration for the fast–slow system (2.55). The critical manifold M (thick solid gray line) is in this special case also the perturbed manifold $M = M_\varepsilon$. The global equilibrium at the origin is plotted as well (black dot). Furthermore, part of the foliation for $\varepsilon = 0$ (gray dashed lines) and the foliation \mathcal{F}^s (green curves) for $\varepsilon = 0.1$ are shown. Note that the trajectories (black curves, double arrows) for $\varepsilon = 0.1$ do not coincide with \mathcal{F}^s . In this figure, the initial points for each trajectory have also been used as points through which a fiber is drawn; compare, for example, the trajectory and the fiber, which both contain the point $p = (0.5, 0.8)$.

Observe that the y -axis $M = \{(x, y) \in \mathbb{R}^2 : x = 0\}$ is an invariant manifold for (2.55); M_0 is also a critical manifold in the terminology of Definition 1.5.4. It is normally hyperbolic and invariant for every small ε , and in particular for $\varepsilon = 0$. Hence, we have a special case whereby the perturbed manifold M_ε coincides with the original one $M = M_\varepsilon$. The stable manifold of M is the whole plane $W^s(M) = \mathbb{R}^2$. Let us take another initial condition $q = (q_1, q_2)$ and consider the difference of the two solution curves

$$\begin{aligned} x(t; q) - x(t; p) &= (q_1 - p_1)e^{-t}, \\ y(t; q) - y(t; p) &= (q_1 - p_1)\frac{\varepsilon}{1-\varepsilon}e^{-t} + \left((q_2 - p_2) - (q_1 - p_1)\frac{\varepsilon}{1-\varepsilon}\right)e^{-\varepsilon t}. \end{aligned} \quad (2.57)$$

If we view q as a fixed initial condition, we can distinguish between different points p by requiring that the trajectory through p approach the trajectory through q “at the fastest rate.” From (2.57), we see that there are two natural rates at which the trajectories approach each other, namely $e^{-\varepsilon t}$ and e^{-t} . If we aim to find the “fastest approach,” we should eliminate the coefficient in front of the term $e^{-\varepsilon t}$. This gives the algebraic constraint

$$(q_2 - p_2) - (q_1 - p_1)\frac{\varepsilon}{1-\varepsilon} = 0.$$

Expressing this as a line with independent variable p_1 yields

$$\left\{ \left(p_1, q_2 + (q_1 - p_1)\frac{\varepsilon}{1-\varepsilon} \right) \in \mathbb{R}^2 \right\}.$$

The point q was arbitrary, and it seems reasonable to choose it on M to organize the lines we have just obtained, i.e., to choose $q = (0, q_2)$. This gives

$$\mathcal{F}^s(q) := \left\{ \left(p_1, q_2 + (q_1 - p_1) \frac{\varepsilon}{1 - \varepsilon} \right) \in \mathbb{R}^2 \right\}. \quad (2.58)$$

The manifold $\mathcal{F}^s(q)$ is called the **stable fiber** through q . Note that $\mathcal{F}^s(q)$ is not an invariant manifold (draw it), since it is not a trajectory. One can view the decomposition of $W^s(M)$ into the submanifolds $\mathcal{F}^s(q)$ abstractly in two ways:

- $\{(q, \mathcal{F}^s(q)) : q \in M\}$ is a **fiber bundle** over M with fibers \mathbb{R}^1 . This fiber bundle is clearly isomorphic to the trivial bundle $\mathbb{R}^1 \times \mathbb{R}^1$; for more on general fiber bundles, see [Mic08].
- The lines $\mathcal{F}^s(q)$ describe a foliation of \mathbb{R}^2 by 1-dimensional submanifolds (the **leaves** of the foliation). Warning: This is not the foliation induced by integral curves of the vector field! See also Figure 2.10.

We remark that the foliation of \mathbb{R}^2 persists for all ε sufficiently small. For more details on the abstract theory of **foliations**, see [Lee06]; it is helpful to think of a foliation just as a nice subdivision of a manifold into submanifolds (also called leaves). ♦

Exercise 2.3.11. Find an example of a 2-dimensional vector field that has \mathbb{R}^2 as a stable manifold W^s but W^s is not foliated/fibered by submanifolds defined by “fastest rates.” Hint: When does normal hyperbolicity fail in Example 2.3.9? ◇

The general situation is more complicated, e.g., we cannot expect to obtain a global foliation of the ambient space as in Example 2.3.9. Nevertheless, the basic construction of decomposing stable and unstable manifolds can be carried out locally. Before we state the theorem, recall that we denote the splitting for a normally hyperbolic invariant manifold by $T\mathbb{R}^N = \mathcal{N}^u \oplus TM \oplus \mathcal{N}^s$.

Theorem 2.3.12 (Fenichel [Fen74, Fen77]). *Consider a C^r vector field H on \mathbb{R}^N and the associated ODE $\dot{z} = H(z)$. Suppose M is a normally hyperbolic invariant manifold under the flow ϕ_t given by H . Then there exists a manifold $\mathcal{F}^u(p)$ for each $p \in M$ such that*

- $\bigcup_{p \in M} \mathcal{F}^u(p) = W_{loc}^u(M).$
- $\mathcal{F}^u(p)$ is **negatively invariant**, i.e., $\phi_{-t}(\mathcal{F}^u(p)) \subseteq \mathcal{F}^u(\phi_{-t}(p))$ for all $t \geq 0$ and $p \in M$.
- $\mathcal{F}^u(p)$ is tangent to \mathcal{N}_p^u at p .
- There exist constants C_u, λ_u such that if $q \in \mathcal{F}^u(p)$, then

$$\|\phi_{-t}(p) - \phi_{-t}(q)\| < C_u e^{-\lambda_u t} \quad \text{for every } t \geq 0. \quad (2.59)$$

(e) Suppose $q \in \mathcal{F}^u(p)$ and $q' \in \mathcal{F}^u(p')$. Then

$$\frac{\|\phi_{-t}(p) - \phi_{-t}(q)\|}{\|\phi_{-t}(p) - \phi_{-t}(q')\|} < C_u e^{-\lambda_u t} \quad \text{for every } t \geq 0 \text{ unless } p = p'.$$

(f) $\mathcal{F}^u(p) \cap \mathcal{F}^u(p') = \emptyset$ unless $p = p'$.

(g) $\mathcal{F}^u(p)$ is C^r with respect to the base point p .

The same conclusions hold with obvious modifications for manifolds $\mathcal{F}^s(p)$ with $\bigcup_{p \in M} \mathcal{F}^s(p) = W_{loc}^s(M)$ (e.g., replace negatively invariant with **positively invariant**, so that $\phi_t(\mathcal{F}^s(p)) \subseteq \mathcal{F}^s(\phi_t(p))$ for all $t \geq 0$ and $p \in M$).

Furthermore, if H^{pert} is θ C^1 -close to H for θ sufficiently small, then H^{pert} has a foliation with all properties given above and diffeomorphic to the one for H .

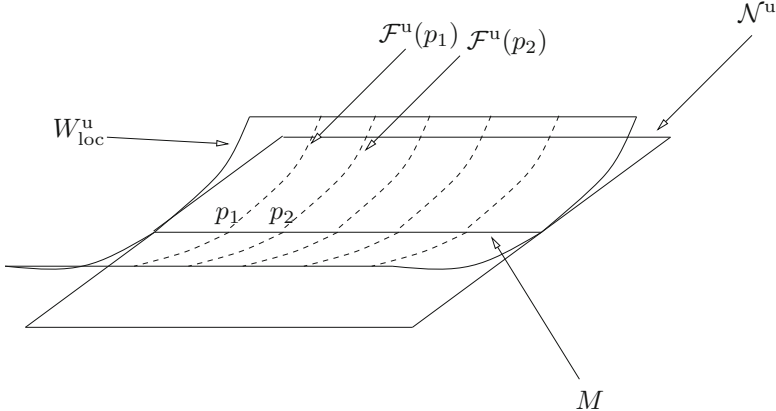


Figure 2.11: Foliation of an unstable manifold $W_{loc}^u(M)$.

The situation of the theorem is illustrated in Figure 2.11; see also Figure 2.10. Note that equation (2.59) is precisely the decomposition of the unstable manifold by submanifolds $\mathcal{F}^u(p)$ that are characterized by initial conditions approaching each other at the fastest rate in backward time.

Definition 2.3.13. We call foliations \mathcal{F}^u and \mathcal{F}^s over M as described in Theorem 2.3.12 **asymptotic rate foliations**.

Theorem 2.3.12 can be summarized by the mnemonic that stable and unstable manifolds of a normally hyperbolic manifold can be decomposed into submanifolds that are characterized by asymptotic rate conditions and that this foliation persists under perturbation.

Remark: If we supposed only that M is overflowing invariant, we would have to assume the extra technical condition that the stable directions in a suitable splitting

can be “compared nicely” to the unstable directions. This can be expressed by another generalized Lyapunov-type number and a corresponding requirement on its magnitude. Since we are dealing with a normally hyperbolic invariant manifold, this condition (as used, e.g., in [Fen74] or [Wig94]) is automatically satisfied.

2.4 Specialization to Fast–Slow Systems

This section aims to connect the general theory of normally hyperbolic invariant manifolds from Sections 2.1–2.3 to fast–slow systems following [Fen79]. Recall from Section 1.2 that our goal is to study fast–slow systems of the form

$$\begin{aligned} \varepsilon \frac{dx}{d\tau} &= \varepsilon \dot{x} = f(x, y, \varepsilon), \\ \frac{dy}{d\tau} &= \dot{y} = g(x, y, \varepsilon), \end{aligned} \quad (2.60)$$

where $f : \mathbb{R}^m \times \mathbb{R}^n \times \mathbb{R} \rightarrow \mathbb{R}^m$, $g : \mathbb{R}^m \times \mathbb{R}^n \times \mathbb{R} \rightarrow \mathbb{R}^n$, and $0 \leq \varepsilon \ll 1$. Setting $\tau = \varepsilon t$ yields the formulation on the fast time scale

$$\begin{aligned} \frac{dx}{dt} &= x' = f(x, y, \varepsilon), \\ \frac{dy}{dt} &= y' = \varepsilon g(x, y, \varepsilon). \end{aligned} \quad (2.61)$$

The strategy is to adapt the invariant manifold theorems from Sections 2.1, 2.2, and 2.3 to equations (2.60) and (2.61). Denote the vector field defined on the fast time scale in (2.61) by X_ε for $0 \leq \varepsilon \ll 1$, i.e.,

$$X_\varepsilon : \mathbb{R}^{m+n} \rightarrow T\mathbb{R}^{m+n} \cong \mathbb{R}^{m+n} \quad \text{with } X_\varepsilon(x, y) = (f(x, y, \varepsilon), \varepsilon g(x, y, \varepsilon)).$$

Considering $\varepsilon = 0$, we obtain $X_0(x, y) = (f(x, y, 0), 0)$, which is the vector field defining the fast flow (cf. Definition 1.5.2). The equilibrium points of X_0 are given by solving $f(x, y, 0) = 0$. Recall that we defined the critical set/manifold as $C_0 = \{(x, y) \in \mathbb{R}^n \times \mathbb{R}^m : f(x, y, 0) = 0\}$. We showed in Proposition 1.5.5 that the critical manifold C_0 consists of equilibria of the fast flow.

As outlined in Chapter 1, one would like to combine solutions of the fast subsystem, defined by the vector field X_0 , with solutions of the slow subsystem (2.60). From these two different singular limits ($\varepsilon = 0$) we hope to recover information about the case $0 < \varepsilon \ll 1$. Let X_R denote the slow (or reduced) flow on C_0 . Recall that this flow is defined by the differential-algebraic equation (DAE)

$$\begin{aligned} 0 &= f(x, y, 0), \\ y &= g(x, y, 0). \end{aligned}$$

The next step to connect the slow flow X_R to X_ε is to linearize X_ε on C_0 in the phase space variables. Fix some $p \in C_0$. Then

$$DX_\varepsilon(p)|_{\varepsilon=0} = \begin{pmatrix} D_x f(p, 0) & D_y f(p, 0) \\ 0 & 0 \end{pmatrix}. \quad (2.62)$$

Therefore, $\lambda_0 = 0$ is always an eigenvalue of multiplicity n . We call λ_0 the **trivial eigenvalue** and all other m eigenvalues of (2.62) the **nontrivial eigenvalues**. Assume that the number of nontrivial eigenvalues in the right complex

half-plane, on the imaginary axis, and in the left complex half-plane are m^u , m^c , and m^s respectively. As usual, we denote the corresponding unstable, center, and stable eigenspaces by E^u , E^c , and E^s with

$$\dim(E^u) = m^u, \quad \dim(E^c) = m^c + n, \quad \dim(E^s) = m^s.$$

Now we can apply invariant manifold theory as developed in Sections 2.1–2.3. The first question is, when is a critical manifold C_0 normally hyperbolic in the context of fast–slow systems?

Definition 2.4.1. A compact submanifold $M_0 \subset C_0$ is called **normally hyperbolic** if for all $p \in M_0$, the $m \times m$ matrix $(D_x f)(p)$ has no eigenvalues with zero real part.

A matrix with no eigenvalues with zero real part is called a **hyperbolic matrix**. Hence, one could also define normal hyperbolicity by requiring the fast subsystem linearization $(D_x f)(p)$ to be a hyperbolic matrix for each $p \in M_0$.

It is not difficult to see that Definition 2.4.1 is a special case of the general Definition 2.3.4 (with $m^c = 0$). Intuitively, we can think of this fact as follows. First note that $(D_x f)(p)$ describes the linearized flow in the fast/normal direction to M_0 , and $(D_y g)(p)$ gives the linearized slow/tangential flow. Since there are no eigenvalues with zero real part for $(D_x f)(p)$, we can make $\frac{1}{\varepsilon}(D_x f)(p)$ as large as we want—by taking ε sufficiently small—compared to $(D_y g)(p)$. Therefore, the normal flow dominates the tangential flow, as required for the general definition of normal hyperbolicity.

Theorem 2.4.2 (Fenichel’s Theorem, classical version, [Fen79]). *Let X_ε be a family of vector fields given by a C^r -fast–slow vector field ($r \geq 2$) as given in (2.61). Let $M_0 \subset C_0$ be an n -dimensional properly embedded C^r -submanifold of \mathbb{R}^{m+n} . Suppose that M_0 is normally hyperbolic, i.e., $D_x f(p)$ is a hyperbolic matrix for all $p \in M_0$ and has m^s eigenvalues with negative real part and m^u eigenvalues with positive real part. Then for ε sufficiently small,*

- (R1) *there exists a family of C^r -manifolds M_ε such that M_ε is a normally hyperbolic locally invariant manifold for X_ε ;*
- (R2) *there exist families of $(n + m^s)$ - and $(n + m^u)$ -dimensional local stable and unstable manifolds $W_{loc,\varepsilon}^s$ and $W_{loc,\varepsilon}^u$ with $W_{loc,\varepsilon}^s = W_{loc}^s(M_\varepsilon)$ and $W_{loc,\varepsilon}^u = W_{loc}^u(M_\varepsilon)$;*
- (R3) *the local stable and unstable manifolds have families $\mathcal{F}_\varepsilon^s$ and $\mathcal{F}_\varepsilon^u$ of asymptotic rate foliations consisting of C^r -leaves $\mathcal{F}_\varepsilon^s(p)$ and $\mathcal{F}_\varepsilon^u(p)$ for $p \in M_\varepsilon$;*
- (R4) *all previously mentioned families of manifolds are C^{r-1} in ε ;*
- (R5) *the vector field given by*

$$X_{C,\varepsilon}(p) := \begin{cases} \frac{1}{\varepsilon} X_\varepsilon(p) & \text{if } \varepsilon \neq 0 \text{ and } p \in M_\varepsilon, \\ X_R(p) & \text{if } \varepsilon = 0 \text{ and } p \in M_0, \end{cases} \quad (2.63)$$

is a C^r -vector field on M_ε ; $X_{C,\varepsilon}$ is a C^{r-1} family of vector fields in ε .

Remark: Furthermore, note that the **local invariance** of M_ε is due to possible boundaries through which trajectories can leave. Therefore, M_ε is not invariant in general. It is helpful to think of the tangential directions to the critical manifold as center directions and view Theorem 2.4.2 as a **center-manifold**-type result; see [Car81, GH83].

Proof. (of Theorem 2.4.2, Sketch) The assertions (R1), (R2), and (R3) follow directly from the invariant manifold Theorems 2.3.5, 2.3.6, and 2.3.12. To prove continuity in ε in (R5), one has to show that for a sequence of points $p_\varepsilon \in M_\varepsilon$,

$$X_R(p_\varepsilon) = \lim_{\varepsilon \rightarrow 0} \frac{1}{\varepsilon} X_\varepsilon(p_\varepsilon).$$

Note that $\frac{1}{\varepsilon} X_\varepsilon = (f/\varepsilon, g)$, so that the limit as $\varepsilon \rightarrow 0$ is just the limit of the fast-slow system written on the slow time scale. Indeed, consider

$$\begin{aligned}\dot{x} &= \frac{1}{\varepsilon} f(x, y, \varepsilon), \\ \dot{y} &= g(x, y, \varepsilon),\end{aligned}$$

and so the limit as $\varepsilon \rightarrow 0$ is

$$\begin{aligned}0 &= f(x, y, 0), \\ \dot{y} &= g(x, y, 0).\end{aligned}\tag{2.64}$$

It is relatively easy to see that equation (2.64) defines the flow X_R . The proof of differentiability in ε is similar. For C^1 -differentiability, consider

$$\frac{\partial}{\partial \varepsilon} \left(\frac{X_\varepsilon}{\varepsilon} \right) = \left(-\frac{f}{\varepsilon^2} + \frac{f_\varepsilon}{\varepsilon}, g_\varepsilon \right).$$

Hence, the derivative for $\varepsilon \neq 0$ defines a vector field

$$\begin{aligned}\varepsilon^2 \dot{x} &= -f(x, y, \varepsilon) + \varepsilon f_\varepsilon(x, y, \varepsilon), \\ \dot{y} &= g_\varepsilon(x, y, \varepsilon).\end{aligned}\tag{2.65}$$

Taking the limit as $\varepsilon \rightarrow 0$ in equation (2.65) yields

$$\begin{aligned}0 &= f(x, y, 0), \\ \dot{y} &= g_\varepsilon(x, y, 0).\end{aligned}$$

This is the same as differentiating the defining equation of the slow flow

$$\dot{y} = g(x, y, \varepsilon)$$

directly in ε . The same procedure works for higher derivatives in ε . The fact that all families depending on ε are C^{r-1} is proven in [Fen77] (Theorems 1–4), so that (R4) and the upper bound on differentiability in (R5) follow. \square

Parts (R1)–(R4) of Theorem 2.4.2 should not be surprising if we look back at the general theory of normally hyperbolic invariant manifolds. The key observation is part (R5). Normal hyperbolicity allows us to extend the fast–slow system written on the slow time scale as

$$\begin{aligned}\dot{x} &= \frac{1}{\varepsilon} f(x, y, \varepsilon), \\ \dot{y} &= g(x, y, \varepsilon),\end{aligned}$$

“smoothly” (in fact, C^{r-1}) to the slow flow X_R on the critical manifold. Therefore, one can treat singular perturbations as $\varepsilon \rightarrow 0$ near normally hyperbolic parts of the critical manifold as regular perturbations; for more details, see Chapters 3 and 5. Sometimes, a slightly more general version of Theorem 2.4.2 is helpful whereby M_0 is a normally hyperbolic manifold of the slow flow X_0 with $\dim(M_0) < n$. Roughly speaking, a normally hyperbolic equilibrium or periodic orbit of the slow vector field X_0 inside a normally hyperbolic manifold C_0 perturbs to corresponding objects for the full system.

The distinction in differentiability of C^{r-1} families and C^r members of the family will not concern us any further here. The key aspect is that we might have to deal with finite smoothness of the family of manifolds M_ε and vector fields defined on them. This problem is completely analogous to the one encountered in classical center manifold theory (see, e.g., [Car81]). As in center manifold theory, the manifold M_ε is also not unique in general, and Fenichel’s theorem shows only the existence of M_ε .

A natural generalization of the previous results is to allow center directions for the nontrivial eigenvalues of $(D_x f)(p, 0)$ for $p \in C_0$. In this case, we obtain center manifolds at hyperbolic and nonhyperbolic points. The key problem with this approach is that we cannot conclude the convergence $X_\varepsilon \rightarrow X_R$ as $\varepsilon \rightarrow 0$ at nonhyperbolic equilibria of the fast subsystem.

2.5 References

Most of this chapter is based on a combination of [Fen71, Fen74, Fen77, Fen79, Wig94] with a little dose of [Jon95].

Section 2.1: Another very important source for invariant manifolds is [HPS77], where the case of maps [PS70] is treated in full detail. There is also quite substantial work [Sac69] predating Fenichel’s work, most notably Tikhonov’s results on attracting slow manifolds [Tik52]. Another more abstract version of the theory can be found in [BK94]. The approach via the graph transform is usually quite robust [BB13], but there are other standard techniques such as the Lyapunov–Perron method [Car81, Lya47, Per29]. For an introductory account of the basic case of the stable manifold theorem, we also refer to [KH95, Tes12] and to the short survey in the introduction of [BLZ98]. More details on the stable manifold theorem can be found in the articles [HP70, Irw70, Irw80, Kel67, MS87, MS96c, Sma67].

Section 2.2: Note that we always made the compactness assumption on the manifold, and this may be lifted under certain conditions [Hop66, KK91]. Noncompact normally hyperbolic invariant manifolds in Riemannian manifolds of bounded geometry are treated in [Eld12, Eld13]. The theory is also consistently linked with the question of structural stability [PT77].

Section 2.3: A nice illustration of exponentially small nonuniqueness for center manifolds can be found in [Sij85]; however, the nonuniqueness is not a major issue in the vast majority of cases [Osi97]. Essentially, the construction of the manifolds as center manifolds is quite standard by now [BF96]. However, one may also go an operator-theoretic route [Wel76] to establish perturbations of invariant manifolds. It is very important to point out that the converse to the result “normal hyperbolicity implies persistence” is also true [Man78], so we cannot really avoid the concept of normally hyperbolic invariant manifolds once perturbation problems are considered. Even weakening it turns out to be problematic in certain cases [vS87]. However, there have been very successful attempts to play with some of the hypotheses. For example, partial hyperbolicity [HP05, Pes04] allows certain uniform center directions, while nonuniform hyperbolicity requires a hyperbolic splitting without uniformity. To check whether a manifold is normally hyperbolic, it is usually crucial to study a spectral problem [Swa83].

Section 2.4: Another recent approach to bridging general invariant manifolds to fast–slow systems is [NS13b]; see also [Sak90].

One may apply normally hyperbolic invariant manifolds not only to fast–slow ODEs but to many other cases, for example Axiom A dynamical systems [PS75c], bifurcation unfoldings [BCHV93, Han98], discrete-time nonautonomous fast–slow systems [Poe03], entropy in billiards [KS86], geodesic flows on the two-torus [DLS00], geoscience applications [Kop85], persistence of invariant tori [CL00, Wig88], scattering maps [DLS08], shadowing [DGR13, Fis06], singular equations [BS11b], synchronization [KPB00], and certainly many other topics not mentioned here, some of which will appear many times in the rest of this book such as traveling waves [Gar93]. For infinite-dimensional problems [Mie90], normal hyperbolicity can be quite subtle [MPSS93], and we refer to Chapter 18 for a possible generalization of Fenichel’s Theorem to semigroups.

Chapter 3

Geometric Singular Perturbation Theory

This chapter introduces some of the core elements, definitions, and theorems of the theory of normally hyperbolic invariant manifold theory for fast–slow systems. Several other chapters build on this material.

Section 3.1 states Fenichel’s theorem for perturbations of the critical manifold C_0 ; roughly speaking, if the fast flow transverse to C_0 dominates the slow flow on C_0 , then C_0 perturbs to a nearby slow manifold C_ε . Section 3.2 calculates the slow flow on the critical manifold in various ways. Section 3.3 defines the simplest generic cases in which normal hyperbolicity breaks down locally at certain singularities, while Section 3.4 goes through a few classical examples to illustrate the previously discussed fundamental ideas of **geometric singular perturbation theory** (GSPT).

Background: Some basic ideas about the geometry of curves and surfaces are very helpful; for more details on general smooth manifolds, see the introduction to Chapter 2. To get a better view on fast–slow system singularities, it is helpful to have some, even very elementary, glimpse at classical **bifurcation theory**. Recommended introductions are [Str00, HK91], while [GH83, Kuz04] are more advanced—but incredibly useful—books. Other excellent options include [ASY96, Sey94, Per01a, Wig03], which have quite widely varying focus themes but still center on bifurcations.

3.1 Fenichel’s Theorem

This section states the results developed in Section 2.4 in a slightly simpler terminology and format. These results are going to be used throughout this book. The reader who followed Chapter 2 should easily see how the results

stated here are proved, since they are direct adaptations from the classical versions; however, all the statements and descriptions in this section are self-contained. We begin with the general formulation of an (m, n) -fast–slow system

$$\begin{aligned}\varepsilon \frac{dx}{d\tau} &= \varepsilon \dot{x} = f(x, y, \varepsilon), \\ \frac{dy}{d\tau} &= \dot{y} = g(x, y, \varepsilon),\end{aligned}\tag{3.1}$$

where $(x, y) \in \mathbb{R}^m \times \mathbb{R}^n$ and $0 < \varepsilon \ll 1$ is a small parameter representing the ratio of time scales. The functions $f : \mathbb{R}^m \times \mathbb{R}^n \times \mathbb{R} \rightarrow \mathbb{R}^m$ and $g : \mathbb{R}^m \times \mathbb{R}^n \times \mathbb{R} \rightarrow \mathbb{R}^n$ are assumed to be sufficiently smooth. On the fast time scale $t = \tau/\varepsilon$, the system (3.1) reads

$$\begin{aligned}x' &= \frac{dx}{dt} = f(x, y, \varepsilon), \\ y' &= \frac{dy}{dt} = \varepsilon g(x, y, \varepsilon).\end{aligned}\tag{3.2}$$

We quickly recall a few definitions and facts from Section 1.5. The slow subsystem is defined by considering $\varepsilon = 0$ in (3.1), which yields

$$\begin{aligned}0 &= f(x, y, 0), \\ \dot{y} &= g(x, y, 0).\end{aligned}\tag{3.3}$$

The slow flow defined by (3.3) is restricted to the critical manifold

$$C_0 = \{(x, y) \in \mathbb{R}^{m+n} : f(x, y, 0) = 0\}.$$

Points on the critical manifold are equilibria of the fast subsystem

$$\begin{aligned}x' &= f(x, y, 0), \\ y' &= 0.\end{aligned}\tag{3.4}$$

The next definition, which is the same as Definition 2.4.1, is a key regularity assumption of the subject.

Definition 3.1.1. A subset $S \subset C_0$ is called **normally hyperbolic** if the $m \times m$ matrix $(D_x f)(p, 0)$ of first partial derivatives with respect to the fast variables has no eigenvalues with zero real part for all $p \in S$.

It will often be necessary to assume compactness of S . If S is also sufficiently regular—for example if S is a **smooth manifold** so that it can be locally written as the graph of a smooth map—then a uniform estimate on the eigenvalues of $(D_x f)$ can be used. Hence, we shall often make the assumption that S is a smooth compact manifold. There is also a relationship between the equilibria of the fast subsystem and normal hyperbolicity.

Proposition 3.1.2. *A subset $S \subset C_0$ is normally hyperbolic if and only if for each $p = (x^*, y^*) \in S$, we have that x^* is a hyperbolic equilibrium point of $x' = f(x, y^*, 0)$.*

Proof. This follows immediately from Definition 3.1.1 and the definition of a hyperbolic equilibrium point; cf. Proposition 1.5.5. \square

The type of equilibrium points for the fast subsystem lying in S determines whether S is stable or unstable. Since the terms “stable” and “unstable” usually refer to actual equilibrium points or invariant sets in the full system for $\varepsilon > 0$, it seems wise to avoid them.

Definition 3.1.3. A normally hyperbolic subset $S \subset C_0$ is called **attracting** if all eigenvalues of $(D_x f)(p, 0)$ have negative real part for $p \in S$; similarly, S is called **repelling** if all eigenvalues have positive real part. If S is normally hyperbolic and neither attracting nor repelling, it is of **saddle type**.

The next theorem will be used throughout this book on many occasions. For the statement of the theorem as presented in this chapter, we need the notion of **Hausdorff distance** between two nonempty sets $V, W \subset \mathbb{R}^{m+n}$, which is defined by

$$d_H(V, W) := \max \left\{ \sup_{v \in V} \inf_{w \in W} \|v - w\|, \sup_{w \in W} \inf_{v \in V} \|v - w\| \right\}.$$

Theorem 3.1.4 (Fenichel's theorem, “frequently used fast–slow version” [Fen79, Jon95]; see also [Tik52]). Suppose $S = S_0$ is a compact normally hyperbolic submanifold (possibly with boundary) of the critical manifold C_0 of (3.1) and that $f, g \in C^r$ ($r < \infty$). Then for $\varepsilon > 0$ sufficiently small, the following hold:

- (F1) There exists a locally invariant manifold S_ε diffeomorphic to S_0 . Local invariance means that trajectories can enter or leave S_ε only through its boundaries.
- (F2) S_ε has Hausdorff distance $\mathcal{O}(\varepsilon)$ (as $\varepsilon \rightarrow 0$) from S_0 .
- (F3) The flow on S_ε converges to the slow flow as $\varepsilon \rightarrow 0$.
- (F4) S_ε is C^r -smooth.
- (F5) S_ε is normally hyperbolic and has the same stability properties with respect to the fast variables as S_0 (attracting, repelling, or of saddle type).
- (F6) S_ε is usually not unique. In regions that remain at a fixed distance from ∂S_ε , all manifolds satisfying (F1)–(F5) lie at a Hausdorff distance $\mathcal{O}(e^{-K/\varepsilon})$ from each other for some $K > 0$, $K = \mathcal{O}(1)$.

Note that all asymptotic notation refers to $\varepsilon \rightarrow 0$. The same conclusions as for S_0 hold locally for its stable and unstable manifolds:

$$W_{\text{loc}}^s(S_0) = \bigcup_{p \in S_0} W_{\text{loc}}^s(p), \quad W_{\text{loc}}^u(S_0) = \bigcup_{p \in S_0} W_{\text{loc}}^u(p),$$

where we view points $p \in S_0$ as equilibria of the fast subsystem. These manifolds also persist for $\varepsilon > 0$ sufficiently small: there exist local stable and unstable manifolds $W_{\text{loc}}^s(S_\varepsilon)$ and $W_{\text{loc}}^u(S_\varepsilon)$, respectively, for which conclusions (F1)–(F6) hold if we replace S_ε and S_0 by $W_{\text{loc}}^s(S_\varepsilon)$ and $W_{\text{loc}}^s(S_0)$ (or similarly by $W_{\text{loc}}^u(S_\varepsilon)$ and $W_{\text{loc}}^u(S_0)$).

For a proof of Theorem 3.1.4, as well as sharper statements on modes of convergence and regularity, see Chapter 2 and Theorem 2.4.2. Fenichel published his general invariant manifold theory during the 1970s and then applied the theory to fast–slow systems in a 1979 paper [Fen79] with the title

Geometric Singular Perturbation Theory for Ordinary Differential Equations.

It is common to abbreviate **geometric singular perturbation theory** as **GSPT**; today, GSPT encompasses not only the results of Fenichel [Fen79] but a much wider range of geometric techniques. Therefore, we shall avoid general references to GSPT and try to point exactly to the theorems that are used.

Theorem 3.1.4 can also be called **Tikhonov’s theorem** or, perhaps even better, the **Fenichel–Tikhonov theorem**. Tikhonov [Tik52] showed that for a compact attracting normally hyperbolic submanifold $S \subset C_0$, every solution starting sufficiently close to S approaches S in a slow time $\mathcal{O}(\varepsilon |\log \varepsilon|)$ and then stays $\mathcal{O}(\varepsilon)$ -close to S . Since Fenichel’s theorem seems to be the most common term at the time of writing, we adopt it here, but see Section 3.5 for additional historical background. It is customary to give the manifolds S_ε a special name.

Definition 3.1.5. A manifold S_ε , as obtained in the conclusion of Theorem 3.1.4, is called a **slow manifold**.

Often, a representative of the manifolds S_ε is called “the” slow manifold. Formally, this is incorrect, since S_ε is not unique, but since all possible choices lie $\mathcal{O}(e^{-K/\varepsilon})$ -close, it will often be arbitrary in most analytical and numerical considerations which choice we make. For example, $\mathcal{O}(e^{-K/\varepsilon})$ -terms are beyond all order for the asymptotic sequence $\{\varepsilon^j\}_{j=1}^\infty$. Furthermore, normally hyperbolic submanifolds of the slow subsystem, such as equilibria and periodic orbits, persist in every slow manifold; cf. the discussion at the end of Section 2.4. From a numerical perspective, an exponentially small error can often simply be disregarded. Therefore, we just adopt the convention to refer to C_ε as “the” slow manifold.

Remark: Sometimes, the letters C and S are used interchangeably for the critical manifold, i.e., there is no standard notational convention in the literature. Therefore, one should always check which notation is currently in use.

In any case, it is important to distinguish between a critical manifold obtained in the singular limit $\varepsilon = 0$ and a slow manifold that is obtained via Fenichel’s theorem for $\varepsilon > 0$. After all, a major theorem has been applied to go from a critical to a slow manifold. Unfortunately, “slow manifold” is often used quite freely for historical reasons. Another issue is that we can extend slow manifolds under the flow of the full system, where the extension may not have anything to do with a critical manifold.

Via a simple example, we are going to illustrate Fenichel’s theorem 3.1.4.

Example 3.1.6. Consider the following $(1, 1)$ -fast–slow system:

$$\begin{aligned} x' &= y^2 - x, \\ y' &= -\varepsilon y. \end{aligned} \tag{3.5}$$

Our goal is to find the slow manifold. The critical manifold is given by

$$C_0 = \{(x, y) \in \mathbb{R}^2 : x = y^2\}.$$

We observe that C_0 is normally hyperbolic and attracting everywhere, since

$$\frac{\partial}{\partial x}(y^2 - x) = -1 < 0.$$

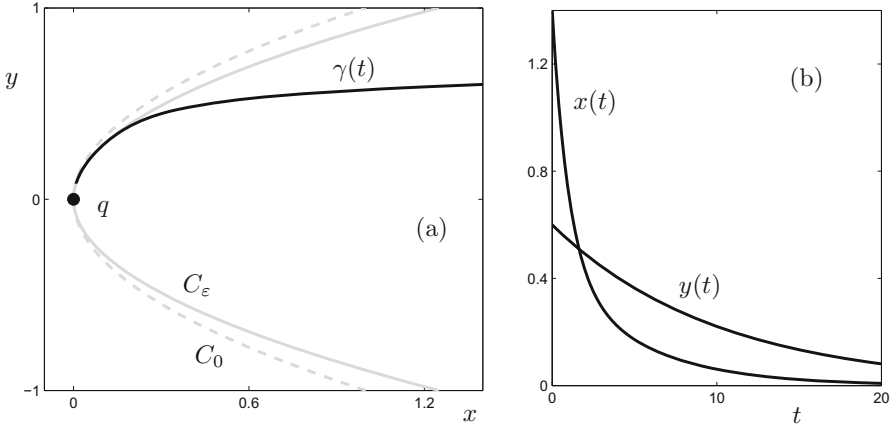


Figure 3.1: Illustration for (3.5). (a) Phase space: the critical manifold C_0 (dashed gray), the slow manifold C_ε (solid gray), the equilibrium $q = (0, 0)$, and a trajectory segment $\gamma(t) = (x(t), y(t))$ are shown for $\varepsilon = 0.1$. (b) Time series for both components of $\gamma(t)$.

Observe that (3.5) can be solved explicitly by

$$(x(t), y(t)) = \left(\left[x(0) - \frac{y(0)^2}{1 - 2\varepsilon} \right] e^{-t} + \frac{y(0)^2}{1 - 2\varepsilon} e^{-2\varepsilon t}, y(0)e^{-\varepsilon t} \right). \quad (3.6)$$

If $x(0) = \frac{y(0)^2}{1 - 2\varepsilon}$, then the solution (3.6) evolves only on the slow time scale $\tau = \varepsilon t$:

$$(x(t), y(t)) = \left(\frac{y(0)^2}{1 - 2\varepsilon} e^{-2\varepsilon t}, y(0)e^{-\varepsilon t} \right).$$

In particular, we observe that

$$x(t) = \frac{y(t)^2}{1 - 2\varepsilon} \quad \text{for all } t \geq 0.$$

Hence the slow manifold is given by

$$C_\varepsilon = \left\{ (x, y) \in \mathbb{R}^2 : x = \frac{y^2}{1 - 2\varepsilon} \right\}.$$

Figure 3.1 illustrates the situation and shows a typical trajectory $\gamma(t)$ that approaches the slow manifold. Note that we can simply talk about “the” slow manifold here, since any compact submanifold $S_0 = S \subset C_0$ could have been chosen to which to apply Fenichel’s theorem. Furthermore, the full system (3.1.6) has a global equilibrium point $q = (0, 0)$. ♦

Exercise 3.1.7. Show that for $0 < \varepsilon \ll 1$, the equilibrium q is globally asymptotically stable. ◇

The general problem of computing slow manifolds analytically or numerically is highly nontrivial. Only the simplicity of equations (3.5) saved us in the last example.

3.2 The Slow Flow

The next goal is to obtain an analytical expression for the slow flow on the critical manifold C_0 . An important case distinction is encoded in the next definition.

Definition 3.2.1. Let C_0 be the critical manifold. We call

$$C_{0,s} = \{p \in C_0 : (\mathrm{D}_x f)(p, 0) \text{ is not invertible}\}$$

(fast–slow) singular points and $C_{0,r} := C_0 - C_{0,s}$ (fast–slow) regular points.

The modifier “fast–slow” has been added to the notion of singular point, since possible confusion could arise with the notion from singularity theory [Lu76]. In this context, one might want to view $f : \mathbb{R}^{m+n} \rightarrow \mathbb{R}^m$ and define singular points p as points where $(\mathrm{D}f)(p)$, the total derivative with respect to both variables, does not have maximal rank m . Therefore, $f(x, y) = y^2 - x$ would yield a singular point at $(0, 0)$, but it is not a singular point in the sense of Definition 3.2.1. We shall see in Proposition 3.2.4 below why such a distinction is helpful.

Example 3.2.2. Note that regularity is weaker than normal hyperbolicity. For example, consider a point $p^* \in C_0$ and suppose the fast subsystem linearization is

$$(\mathrm{D}_x f)(p^*, 0) = \begin{pmatrix} 0 & -1 \\ 1 & 0 \end{pmatrix} \quad \Rightarrow \quad (\mathrm{D}_x f)(p^*, 0)^{-1} = \begin{pmatrix} 0 & 1 \\ -1 & 0 \end{pmatrix},$$

so p^* is a regular point. However, at $p^* \in C_{0,r}$, the matrix $(\mathrm{D}_x f)(p^*, 0)$ has a complex conjugate pair of eigenvalues $\pm i$ with zero real part, so C_0 is not normally hyperbolic at p^* . ♦

As a general result, $p \in C_{0,s}$ implies that C_0 is not normally hyperbolic at p , since $(\mathrm{D}_x f)(p, 0)$ has zero as an eigenvalue with multiplicity at least one.

Suppose now that C_0 is a manifold and $p \in C_0$ is a regular point. Then the **implicit function theorem** (see [Rud76] for a statement and the proof of the implicit function theorem) yields the existence of a map

$$h : \mathbb{R}^n \rightarrow \mathbb{R}^m$$

describing C_0 , locally near p , as a graph, and $f(h(y), y, 0) = 0$ holds near p . The map h can be used to reduce the slow subsystem

$$\begin{aligned} 0 &= f(x, y, 0), \\ \dot{y} &= g(x, y, 0), \end{aligned}$$

to the simpler form

$$\dot{y} = g(h(y), y, 0). \quad (3.7)$$

Sometimes, it is convenient to use some (or all) of the fast x -variables to parameterize the slow subsystem instead of some (or all) of the slow y -variables. We illustrate a very important calculation to achieve this in the next example.

Example 3.2.3. Consider the (unforced) van der Pol equation:

$$\begin{aligned} \varepsilon \dot{x} &= y - \frac{x^3}{3} + x, \\ \dot{y} &= -x, \end{aligned} \quad (3.8)$$

with critical manifold $C_0 = \{(x, y) \in \mathbb{R}^2 : y = \frac{x^3}{3} - x\}$. The singular limit $\varepsilon = 0$ in (3.8) leads to

$$\begin{aligned} 0 &= y - \frac{x^3}{3} + x, \\ \dot{y} &= -x. \end{aligned} \quad (3.9)$$

Differentiating the equation $f(x, y) = y - \frac{x^3}{3} + x = 0$ with respect to τ , we obtain

$$\frac{\partial f}{\partial x} \dot{x} + \frac{\partial f}{\partial y} \dot{y} = (1 - x^2) \dot{x} + \dot{y} = 0.$$

It follows from (3.9) that $\dot{y} = -x$, and so

$$\dot{x} = \frac{x}{1 - x^2}. \quad (3.10)$$

Hence, we have derived an explicit form for the slow flow on the critical manifold C_0 ; see Figure 3.2(c). Note carefully that the ODE (3.10) has an unstable equilibrium at $x = 0$ and is not defined at the points $x = 1$ and $x = -1$; see Figure 3.2. In fact, the points $x = \pm 1$ split the critical manifold into three parts:

$$\begin{aligned} C_0^{a-} &= C_0 \cap \{(x, y) \in \mathbb{R}^2 : x < -1\}, \\ C_0^r &= C_0 \cap \{(x, y) \in \mathbb{R}^2 : -1 < x < 1\}, \\ C_0^{a+} &= C_0 \cap \{(x, y) \in \mathbb{R}^2 : x > 1\}, \end{aligned}$$

where $C_0^{a\pm}$ are normally hyperbolic attracting and C_0^r is normally hyperbolic repelling, since $D_x f|_{C_0} = -x^2 + 1$. The slow subsystem can also be expressed in terms of the independent variable y if we solve $y = \frac{x^3}{3} - x$ for x and substitute it into (3.9). By the implicit function theorem, this is possible if $x \neq \pm 1$. The situation is shown in Figure 3.2(b). ♦

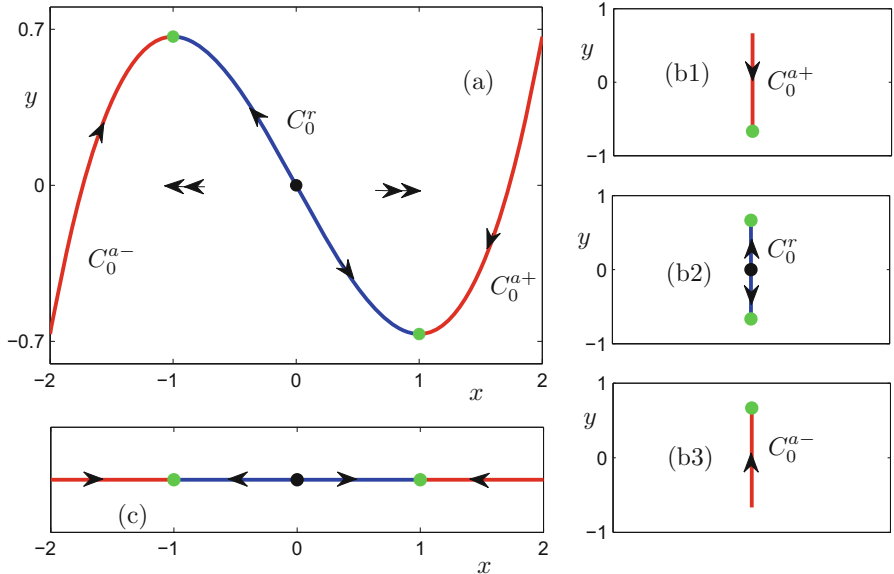


Figure 3.2: Illustration for the singular limit of (3.8). The critical manifold C_0 consists of three submanifolds: $C_0^{a\pm}$ (red) are attracting parts, while C_0^r (blue) is repelling. The equilibrium point at the origin (black dot) and the two nonnormally hyperbolic points $(x, y) = (\pm 1, \mp 2/3)$ (green) are shown as well. Double arrows indicate fast flow, and single arrows slow flow. (a) Phase space. (b) Slow flow in the variable y . (c) Slow flow in the variable x given by (3.10).

A slight problem in formulating the slow subsystem as (3.7) is that it does not describe a vector field in \mathbb{R}^{n+m} . Therefore, we cannot compare the singular limit with the full system for $0 < \varepsilon \ll 1$ directly. In practice, this rarely turns out to be a problem, since we know that the slow subsystem must be tangent to the critical manifold, and hence one can always embed it into \mathbb{R}^{m+n} . One can also derive a suitable expression directly, as shown in the next proposition.

Proposition 3.2.4. *Assume that the critical set C_0 is a smooth manifold, let $p = (x_0, y_0) \in C_0 \subset \mathbb{R}^m \times \mathbb{R}^n$, and assume that $(D_x f)(p, 0)$ has maximal rank, so that $p \in C_{0,r}$. Then there exists a neighborhood $V \subset C_0$ of p such that the slow subsystem for $\varepsilon = 0$ on V is given by*

$$\begin{aligned}\dot{x} &= -(D_x f(q, 0))^{-1}(D_y f(q, 0))g(q, 0), \\ \dot{y} &= g(q, 0),\end{aligned}\tag{3.11}$$

for all $q \in V$. In shorthand notation, we sometimes write

$$\begin{aligned}\dot{x} &= -(D_x f)^{-1}(D_y f)g, \\ \dot{y} &= g.\end{aligned}$$

Proof. By continuity of the determinant, we can find a neighborhood of p , say $V \subset C_0$, such that $(D_x f)(q, 0)$ is invertible for all $q \in V$. Implicit differentiation of $0 = f(x, y, 0)$ with respect to τ yields

$$(D_x f)\dot{x} + (D_y f)\dot{y} = (D_x f)\dot{x} + (D_y f)g = 0.$$

The result follows on direct algebraic manipulation and evaluation at q . \square

We have derived several expressions for the slow flow that allow us to calculate it efficiently for simple problems. However, it can be very difficult for higher-dimensional problems to find the slow flow analytically. This difficulty results from the fact that at least in principle, we always have to deal with the solution of a general system of nonlinear equations

$$0 = f(x, y, 0). \quad (3.12)$$

To solve (3.12) analytically or numerically is a large topic. A few possible approaches are explained in Sections 10.6, 12.6, 19.1, 19.2, and Chapter 11. For now, we can postpone this problem, since our first goal is to understand low-dimensional fast–slow systems, where dealing with (3.12) is often no problem.

3.3 Singularities

So far, we have focused on the case in which the critical set is a manifold consisting of regular points or the even stronger assumption that C_0 is normally hyperbolic. A large part of multiple time scale dynamics deals with loss of regularity and normal hyperbolicity. We are going to provide an overview of some cases that can occur. Suppose first that $p \in C_0$ is a singular point, i.e., $p \in C_{0,s}$, so that

$$(D_x f)(p, 0) : \mathbb{R}^m \rightarrow \mathbb{R}^m \quad (3.13)$$

is not of maximal rank. The simplest possible rank deficiency arises when (3.13) has rank $m - 1$ with zero as an eigenvalue of multiplicity one.

Example 3.3.1. The simplest example in which (3.13) is rank deficient is a $(1, 1)$ -fast–slow system

$$\begin{aligned} x' &= y - x^2 &= f(x, y, \varepsilon), \\ y' &= \varepsilon g(x, y, \varepsilon), \end{aligned} \quad (3.14)$$

where $(x, y) \in \mathbb{R} \times \mathbb{R}$. The critical manifold is a parabola

$$C_0 = \{(x, y) \in \mathbb{R}^2 : y = x^2\};$$

see Figure 3.3(a). We consider the origin $(x, y) = (0, 0)$ and obtain

$$(D_x f)(0, 0, 0) = \frac{\partial f}{\partial x}(0, 0, 0) = -2x|_{x=0} = 0. \quad (3.15)$$

Therefore, $(0, 0) \in C_0$ is not regular and not normally hyperbolic. Observe that

$$\frac{\partial^2 f}{\partial x^2}(0, 0, 0) = f_{xx}(0, 0, 0) \neq 0, \quad (3.16)$$

which is a nondegeneracy condition. In fact, the reader should check that the two nonnormally hyperbolic points in Example 3.2.3 satisfy conditions analogous to (3.15)–(3.16). The fast subsystem of (3.14) is

$$x' = y - x^2, \quad (3.17)$$

$$y' = 0. \quad (3.18)$$

In this case, $y \in \mathbb{R}$ is a parameter and (3.17) is the normal form for a **fold bifurcation** at $y = 0$; alternative terms for a fold bifurcation are **saddle-node bifurcation**, **turning point**, and **limit point**. ♦

The last example can be extended to a general (m, n) -fast–slow system (3.1).

Definition 3.3.2. Suppose $p \in C_0$, so that $f(p, 0) = 0$ holds. Then p is a **fold point** if

$$(D_x f)(p, 0) \quad \text{is of rank } m - 1.$$

A fold point is called **nondegenerate** if for vectors w and v , which are in the left and right nullspaces of $(D_x f)(p, 0)$ respectively, one has

$$w \cdot [(D_{xx} f)(p, 0)(v, v)] \neq 0 \quad \text{and} \quad w \cdot [(D_y f)(p, 0)] \neq 0.$$

We have remarked already in Example 3.3.1 that fold points can be viewed as fold (or saddle-node) bifurcations of the fast subsystem. For a $(1, 1)$ -fast–slow system, the fast subsystem is

$$x' = f(x, y), \quad x \in \mathbb{R}, y \in \mathbb{R}. \quad (3.19)$$

In bifurcation theory, $f(x, y)$ is viewed as defining a 1-parameter family of vector fields. It can be shown that although a fold bifurcation point can be made to disappear for $x' = f(x)$ with $x \in \mathbb{R}$ by a perturbation, a nondegenerate fold bifurcation is stable under perturbations in 1-parameter families of vector fields (3.19), i.e., it has “codimension one.” The major conclusion of this viewpoint is that fold bifurcations are “generic” in 1-parameter families of sufficiently smooth vector fields.

Remark: More precisely, a property is **generic** in a topological space if it holds in a countable intersection of open dense sets; see also [Lu76, Wig03, GG74, Arn83] and Section 3.5.

Since fast–slow systems have at least one fast and one slow variable, it is very likely that we will encounter a fold singularity. Therefore, folds are studied extensively in this book in Sections 4.2, 4.4, 5.4, 7.4, 8.1–8.6, 9.5, 11.6, 13.2, 15.3, and 19.6.

In fact, fast–slow systems go beyond the bifurcation theory approach, since the slow variables are true dynamical variables. If the fast subsystem has a

bifurcation and one considers the full system dynamics for $0 < \varepsilon \ll 1$, then the situation is also referred to as **dynamic bifurcation**.

There are many other singularities/bifurcations beyond the important fold point. We give a few examples.

Example 3.3.3. Consider the following $(1, 1)$ -fast–slow system:

$$\begin{aligned} x' &= x(y - x), \\ y' &= \varepsilon g(x, y, \varepsilon). \end{aligned} \quad (3.20)$$

The critical set $C_0 = \{(x, y) \in \mathbb{R}^2 : x = 0 \text{ or } y = x\}$ is a manifold except at the origin $(x, y) = (0, 0) := 0$. It is easy to see that C_0 is not a manifold at 0, since the two lines $\{x = 0\}$ and $\{y = x\}$ cross. This yields a **transcritical point**, or **transcritical singularity**; see Figure 3.3(b) and Section 8.7. ♦

Example 3.3.4. Consider the $(1, 2)$ -fast–slow system

$$\begin{aligned} x' &= y_1 + y_2 x - x^3 = f(x, y, \varepsilon), \\ y'_1 &= \varepsilon g_1(x, y, \varepsilon), \\ y'_2 &= \varepsilon g_2(x, y, \varepsilon). \end{aligned} \quad (3.21)$$

The critical set $C_0 = \{(x, y) \in \mathbb{R}^2 : y_1 = -y_2 x + x^3\}$ is a manifold, but it contains a curve of fold points given by

$$L = \left\{ (x, y) \in C_0 : \frac{\partial f}{\partial x} = y_2 - 3x^2 = 0 \right\}.$$

It is easy to check that the folds are nondegenerate except at $(x, y_1, y_2) = (0, 0, 0)$, which is a **cusp point** or **cusp singularity**; see Figure 3.3(c). It is known from bifurcation theory [Kuz04] that the cusp has codimension two, and two parameters are required to understand its dynamics. Therefore, two slow variables should be considered. ♦

Example 3.3.5. Consider the $(2, 1)$ -fast–slow system

$$\begin{aligned} x'_1 &= yx_1 - x_2 - x_1(x_1^2 + x_2^2) = f_1(x, y), \\ x'_2 &= x_1 + yx_2 - x_2(x_1^2 + x_2^2) = f_2(x, y), \\ y' &= \varepsilon g(x, y, \varepsilon), \end{aligned} \quad (3.22)$$

where $f := (f_1, f_2)$. The critical manifold $C_0 = \{(x, y) \in \mathbb{R}^2 : x_1 = 0 = x_2\}$ is simply the y -axis. The linearization with respect to the fast variables is

$$D_x f|_{C_0} = \left(\begin{pmatrix} \frac{\partial f_1}{\partial x_1} & \frac{\partial f_1}{\partial x_2} \\ \frac{\partial f_2}{\partial x_1} & \frac{\partial f_2}{\partial x_2} \end{pmatrix} \right) \Bigg|_{C_0} = \begin{pmatrix} y & -1 \\ 1 & y \end{pmatrix}.$$

Therefore, C_0 consists only of regular points, but $D_x f|_{C_0}$ has a pair of complex eigenvalues $\pm i$ at $y = 0$, so that C_0 is not normally hyperbolic at the origin, which is a Hopf bifurcation of the fast subsystem; see Figure 3.3(d). Details on Hopf bifurcations of the fast subsystem are contained in Sections 12.2, 12.3, 13.6, and 13.7. ♦

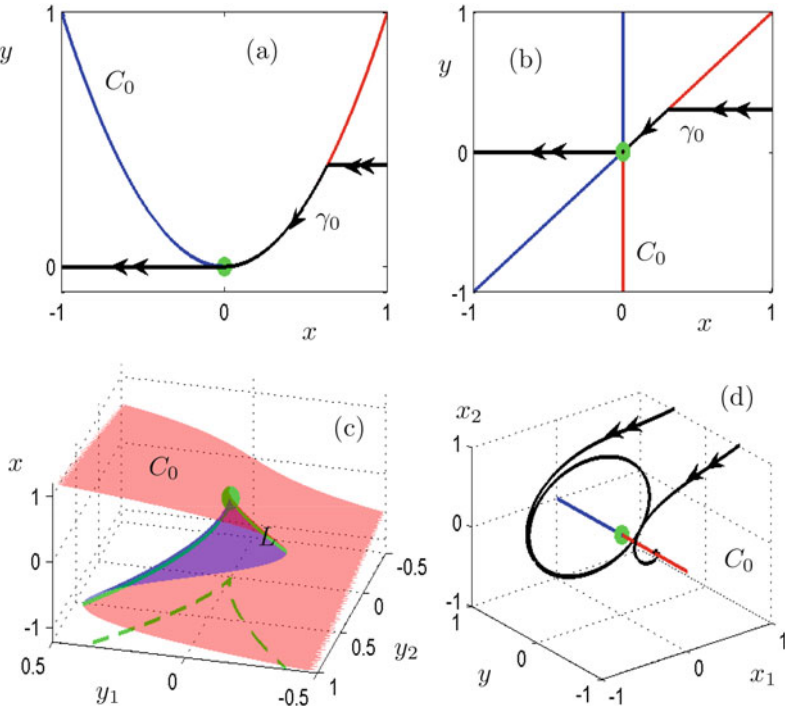


Figure 3.3: Singularities of the critical manifold C_0 (attracting parts = red, repelling parts = blue). (a) Fold point (green dot) at the origin for (3.14) with $g(x, y, \varepsilon) = -1$. A candidate orbit γ_0 is also shown. (b) Transcritical point (green dot) for (3.20) with $g(x, y, \varepsilon) = -1$ and a candidate γ_0 . (c) Cusp surface from Example 3.3.4 containing a curve of folds L (green, solid); a projection of the curve of folds onto the slow variables is also shown (green dashed curve), which explains the name cusp. The cusp point itself (green dot) is at the origin. (d) Hopf bifurcation (green dot) of the fast subsystem for (3.22). Two fast subsystem trajectory segments starting at $(x_1, x_2, y) = (1, 1, \pm\frac{1}{2})$ are shown.

Another important concept relevant for most singularities is that they are natural transition points from the slow to the fast subsystem or vice versa. Figures 3.3(a) and 3.3(b) show trajectories γ_0 , so-called **candidates**, that have been obtained as concatenations of fast and slow subsystem trajectories. The next definition makes the concept more precise.

Definition 3.3.6. A **candidate trajectory** (or **candidate orbit**) is defined as a homeomorphic image $\gamma_0(t)$ of a real interval (a, b) with $a < b$, where

- the interval is partitioned as $a = t_0 < t_1 < \dots < t_m = b$;
- the image of each subinterval $\gamma_0(t_{j-1}, t_j)$ is a trajectory of either the fast or the slow subsystem;

- the image $\gamma_0(a, b)$ has an orientation that is consistent with the orientations on each subinterval $\gamma_0(t_{j-1}, t_j)$ induced by the fast and slow flows.

Often, candidates are called **singular trajectories**. The term “candidate” stresses the fact that it is a trajectory that we want to perturb for $\varepsilon > 0$, while using “singular trajectory” emphasizes the construction via concatenating fast and slow subsystem segments.

3.4 Examples

In this section, we consider a few examples to illustrate Fenichel’s Theorem 3.1.4 as well as singular points and candidate trajectories.

Example 3.4.1. We have already seen in Example 3.1.6 that the critical manifold and a slow manifold have to be distinguished carefully. An even simpler example is the following affine $(1, 1)$ -fast–slow system:

$$\begin{aligned} \varepsilon \frac{dx}{d\tau} &= \varepsilon \dot{x} = y - x, \\ \frac{dy}{d\tau} &= \dot{y} = 1, \end{aligned} \tag{3.23}$$

with critical manifold $C_0 = \{(x, y) \in \mathbb{R}^2 : y = x\}$. The solution of (3.23) can be calculated explicitly:

$$(x(\tau), y(\tau)) = \left(y(0) + \tau - \varepsilon + (x(0) - y(0) + \varepsilon)e^{-\tau/\varepsilon}, y(0) + \tau \right).$$

Observe that $x(0) - y(0) + \varepsilon = 0$ implies that $x(\tau) - y(\tau) + \varepsilon = 0$ for all times. Therefore, the curve

$$C_\varepsilon = \{(x, y) \in \mathbb{R}^2 : y = x + \varepsilon\}$$

is a slow manifold. Also, $C_0 \neq C_\varepsilon$ for $\varepsilon > 0$ and $d_H(C_0, C_\varepsilon) = \mathcal{O}(\varepsilon)$ as $\varepsilon \rightarrow 0$ in the Hausdorff distance. These observations reflect very well the properties (F1), (F2), and (F5) of Fenichel’s Theorem 3.1.4. One can also consider the situation whereby

$$x(0) - y(0) + \varepsilon = e^{-K/\varepsilon},$$

for some fixed $K > 0$, to see that the different slow manifolds lie within a band of size $\mathcal{O}(e^{-K/\varepsilon})$, illustrating the nonuniqueness (F6) from Fenichel’s theorem. However, it is often convenient to work with C_ε and not to carry around the exponentially small terms, since many results are independent of these terms; but see Section 9.7. ♦

The next example illustrates the subtle issue of finite smoothness for slow manifolds; see (F4) in Theorem 3.1.4.

Example 3.4.2. Consider the $(1, 1)$ -fast–slow system

$$\begin{aligned} \varepsilon \dot{x} &= -(x + y^{1/\varepsilon}) = f(x, y, \varepsilon), \\ \dot{y} &= -y = g(x, y, \varepsilon), \end{aligned} \tag{3.24}$$

in a small fixed neighborhood $\mathcal{N} = \{|x| < \delta, |y| < \delta\}$ of $(x, y) = (0, 0)$. For fixed $\delta \in (0, 1)$, we have that $y \in \mathcal{N}$ implies $|y|^{1/\varepsilon} < \delta^{1/\varepsilon} \rightarrow 0$ as $\varepsilon \rightarrow 0$. Therefore, the critical manifold of (3.24) is formally given by

$$C_0 = \{(x, y) \in \mathcal{N} : x = 0\}.$$

Certainly C_0 is a smooth curve, since it is just a line. For the full system (3.24), one has $y(\tau) = y(0)e^{-\tau}$, so that

$$\dot{x} = -\frac{1}{\varepsilon} \left(x + y(0)^{1/\varepsilon} e^{-\tau/\varepsilon} \right) \quad \Rightarrow \quad x(\tau) = x(0)e^{-\tau/\varepsilon} - y(0)^{1/\varepsilon} \frac{\tau}{\varepsilon} e^{-\tau/\varepsilon},$$

which can be checked by direct differentiation. Since $-\tau = \ln(y(\tau)/y(0))$, the trajectories can be rewritten as solution curves

$$\begin{cases} x = x(0) \left(\frac{y}{y(0)} \right)^{1/\varepsilon} + \frac{y^{1/\varepsilon}}{\varepsilon} \ln \left(\frac{y}{y(0)} \right) & \text{if } y(0) \neq 0, \\ y = 0 & \text{if } y(0) = 0. \end{cases} \quad (3.25)$$

Hence, the x -axis is a smooth invariant manifold along which the fast dynamics $x(\tau) = x(0)e^{-\tau/\varepsilon} = x(0)e^{-t}$ take place; see Figure 3.4. Any slow manifold C_ε , which exists by Fenichel's theorem, near the origin is constructed from two curves

$$x = x(0) \left(\frac{y}{y(0)} \right)^r + ry^r \ln \left(\frac{y}{y(0)} \right), \quad r := \frac{1}{\varepsilon} \quad (3.26)$$

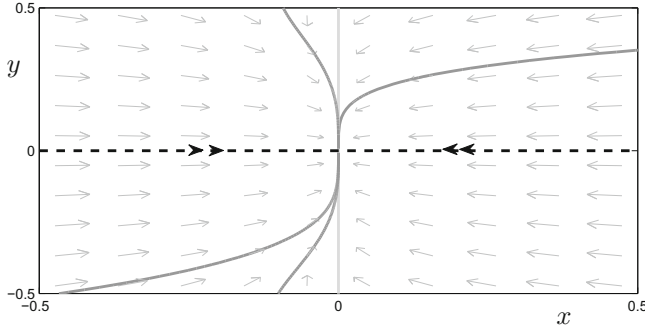


Figure 3.4: Illustration for the ODE (3.24). The critical manifold C_0 (light gray), several solution curves (gray) that can be pieced together locally near $(x, y) = (0, 0)$ to form a slow manifold C_ε and the purely fast fiber (black dashed) are shown with $\varepsilon = 1/4$.

for two different values $y(0)$ of opposite sign, since these curves are the only other possible solution curves by (3.25). Observe that

$$\frac{\partial^r}{\partial y^r} \left(y^r \ln \left(\frac{y}{y(0)} \right) \right) = r! \ln \left(\frac{y}{y(0)} \right) + \dots,$$

so that the r th derivative of the curve (3.26) becomes unbounded as $y \rightarrow 0$. Hence, C_ε has finite smoothness. The level of smoothness increases when $r = 1/\varepsilon$ increases. When $\varepsilon \rightarrow 0$, the better dynamical separation of fast and slow directions leads to better smoothness properties. ♦

So far, we have dealt only with normally hyperbolic manifolds that are attracting or repelling. The next example shows that saddle-type normally hyperbolic manifolds are important as well.

Example 3.4.3. Consider the 3-dimensional FitzHugh–Nagumo equation (1.16) from Section 1.4 (with parameter $I = 0$) given by

$$\begin{aligned} x'_1 &= x_2 &= f_1(x, y), \\ x'_2 &= sx_2 - x_1(x_1 - a)(1 - x_1) + y = f_2(x, y), \\ y' &= \frac{\varepsilon}{s}(x_1 - \gamma y) &= \varepsilon g(x, y). \end{aligned} \quad (3.27)$$

We easily find that the one-dimensional critical manifold is given by

$$C_0 = \{(x_1, x_2, y) \in \mathbb{R}^2 \times \mathbb{R}^1 : x_2 = 0, y = x_1(x_1 - a)(1 - x_1) =: c_a(x_1)\}.$$

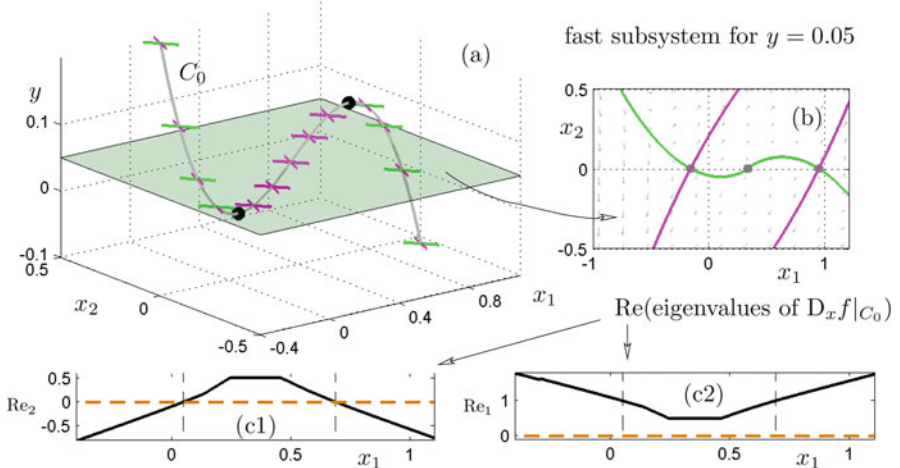


Figure 3.5: Illustration for the fast subsystem of the FitzHugh–Nagumo equation (3.27). (a) Phase space with critical manifold C_0 (gray). The green and magenta lines indicate the attracting and repelling eigendirections for C_0 , showing that the critical manifold has two unbounded branches of saddle type. The transparent plane is a fast subsystem domain for $y = 0.05$. (b) Fast subsystem phase portrait with stable (green) and unstable (magenta) manifolds of the three equilibria (gray dots). (c) Real parts of the eigenvalues of $D_x f(p)$ for $p \in C_0$. Vertical lines indicate the folds, and the horizontal (brown) line indicates a change of stability where the real part is zero.

There are two nondegenerate fold points in the critical manifold

$$\left\{ (x_{1,\pm}, 0, c_a(x_{1,\pm})) : x_{1,\pm} = \frac{1}{3} \left(1 + a \pm \sqrt{1 - a + a^2} \right) \right\},$$

where $x_{1,\pm}$ are found by solving $c'_a(x_1) = 0$. Some typical parameters considered in the FitzHugh–Nagumo equation are $(s, a, \gamma) = (1, 1/10, 1)$, in which case the linearization for $p = (x_1, x_2, y) \in C_0$, viewed as an equilibrium point of the fast subsystem, is

$$D_x f(p) = \begin{pmatrix} 0 & 1 \\ 3x_1^2 - \frac{11}{5}x_1 + \frac{1}{10} & 1 \end{pmatrix}.$$

We can easily compute the eigenvalues $\lambda_{1,2}$ of $D_x f(p)$ depending on x_1 . Figure 3.5(a) indicates the eigendirections and shows that C_0 has two unbounded branches of saddle type:

$$C_0^{a-} = \{(x, y) \in \mathbb{R}^3 : x_1 < x_{1,-}\} \cap C_0 \quad \text{and} \quad C_0^{a+} = \{(x, y) \in \mathbb{R}^3 : x_1 > x_{1,+}\} \cap C_0.$$

The middle branch $C_0^r = \{(x, y) \in \mathbb{R}^3 : x_{1,-} < x_1 < x_{1,+}\}$ is repelling; see also Figure 3.5(c). One of the domains $\{y = 0.05\}$ of the fast subsystem

$$\begin{aligned} x'_1 &= x_2, \\ x'_2 &= sx_2 - x_1(x_1 - a)(1 - x_1) + y, \end{aligned} \tag{3.28}$$

is shown in Figure 3.5(a), and the associated phase portrait in Figure 3.5(b). Although (3.27) has no attractor, we shall see in Sections 6.5 and 19.8 that it has many interesting bounded invariant sets corresponding to traveling waves of the associated PDE (see Sections 6.2 and 1.4). In fact, certain waves for the FitzHugh–Nagumo PDE are stable, which can be shown using the methods from Section 17.1. ♦

Another definition from this chapter that is important to illustrate is that of candidate orbits, which are concatenations of fast and slow subsystem trajectory segments; see Definition 3.3.6. It is best to explore this notion by discovering which candidate orbits are possible in a given system. Examples are given in Figure 3.3(a)–(b). The following exercise is not only excellent practice, but it already hints at complications that we are going to resolve in later chapters.

Exercise 3.4.4. Identify different (classes of) candidate orbits for (a) the unforced van der Pol equation and the van der Pol equation with constant forcing (see Section 1.3) and (b) the three-dimensional FitzHugh–Nagumo system (3.27) from Example 3.4.3. ◇

The following example occupies an important historical role in the development of singular perturbation theory.

Example 3.4.5. Suppose $s \in [a, b]$ for some $a < 0 < b$. Consider the second-order boundary value problem (BVP)

$$\varepsilon \frac{d^2y}{ds^2} + p(s, \varepsilon, \delta) \frac{dy}{ds} + q(s, \varepsilon, \delta)y = 0, \quad y(a) = A, \quad y(b) = B, \tag{3.29}$$

where p, q are assumed to be sufficiently smooth, $0 < \varepsilon \ll 1$, and $\delta \in \mathbb{R}$ are parameters. Typical assumptions are

$$\begin{aligned} p(0, \varepsilon, \delta) &= 0, & \frac{\partial p}{\partial s}(0, \varepsilon, \delta) &< 0, \\ p(s, \varepsilon, \delta) &> 0 \text{ for } s < 0, & p(s, \varepsilon, \delta) &< 0 \text{ for } s > 0, \end{aligned} \quad (3.30)$$

for all ε, δ sufficiently small. Often, one refers to $s = 0$, where (3.30) holds as a **turning point**. However, there are several variations of this definition, and one also uses “turning point” frequently to refer to a classical saddle-node (or fold) bifurcation. So some care is needed when reading the literature. There are several ways to rewrite (3.29) as a first-order system. One possibility is to consider

$$x := p(s, \varepsilon, \delta) \frac{dy}{ds} + q(s, \varepsilon, \delta).$$

After a bit of calculation and setting $\frac{ds}{d\tau} = 1$, we get

$$\begin{aligned} \varepsilon \frac{dx}{d\tau} &= -xp + \varepsilon \left[\frac{(p_s+q)(x-qy)}{p} + q_s y \right], \\ \frac{dy}{d\tau} &= (x - qy)/p, \\ \frac{ds}{d\tau} &= 1, \end{aligned} \quad (3.31)$$

where the subscript s for p, q indicates partial derivatives. The critical manifold is given by

$$C_0 = \{(x, y, s) \in \mathbb{R}^3 : x = 0\}.$$

Note that C_0 is normally hyperbolic as long as $p(s, 0, \delta) \neq 0$. At the turning point $s = 0$, the condition (3.30) implies that normal hyperbolicity is lost. This effect has been studied intensively using various asymptotic methods to be discussed in Chapter 9. A particularly interesting case occurs when the condition

$$\frac{-q(0, 0, 0)}{p_s(0, 0, 0)} = N \in \mathbb{N}_0 \quad (3.32)$$

is satisfied for some nonnegative integer N . It turns out that (3.32) is a necessary condition for a “resonance effect,” which yields a solution converging as $\varepsilon \rightarrow 0$ to a nontrivial solution of the BVP (3.29). This effect is also referred to as **Ackerberg–O’Malley resonance**. Although we shall not discuss the details here, we mention that combining (3.32) with

$$\frac{\partial}{\partial \delta} \left[\frac{q(0, 0, \delta)}{(p_s(0, 0, \delta))} \right] \Big|_{\delta=0} \neq 0$$

yields a sufficient condition for resonance, i.e., it can be obtained by varying a single parameter δ . ♦

3.5 References

Section 3.1: This section is partially based on [DGK⁺12, Jon95]. The original work is due to [Fen79, Tik52], with more background in [Fen71, Fen74, Fen77, Wig94]. Some other important historical contributions are [CL52, HL55, Hop71, Lev56, NS98, Sak90], where asymptotic matching was a key component [Hop68, Hop74, KK62]; see also Section 9.1. A very popular exposition can be found in [Jon95]. There are also several mini-introductions [Guc02, Guc96, Klo83, Nip85, Szm92, Szm91, Ver07b] as well as longer surveys [Kap99] and variations on the same theme [Ano99, Ike89, KS94, WPJ11, CG92]. There has been a long historical interest to build a coherent theory of fast–slow systems [CC69, Kre79, Kre80] and to decouple the fast and slow components [OA82]. The critical manifold approximation for $\varepsilon = 0$ is often also referred to as quasi-steady-state approximation [NW11, NW07, SW00a] in many applications.

Section 3.2: The section is mainly based on [Fen79]. After the main paper [Fen79], Fenichel continued to work on fast–slow systems [Fen85, Fen83b] and tackled, e.g., slow subsystem oscillations [Cha69, Fen83a]. We also remark, although the terminology we used is quite well established, that the nonstandard analysis literature sometimes prefers the term “rivers” for slow/critical manifolds [Sam91, vdB91]. Also, another natural question one may ask is what happens when the critical manifold is neutrally stable over a large subset e.g., when it is elliptic [LZ11].

Section 3.3: This section is a collection of standard singularities in fast–slow systems [BKK13, DGK⁺12] that link directly to classical (static) bifurcation theory [GH83, Kuz04]. The definition of candidates is taken from [Ben90, Hai05]. The breakdown of normal hyperbolicity is probably the biggest theoretical challenge in dynamics of multiscale systems [Nip86b, Nip86a], since linear methods cannot work immediately. A singularity we will not cover in this book is the blue-sky catastrophe [KMR08, SST05, SK08] (unfortunately, sometimes the fold is also called a blue-sky bifurcation). Also, we are going to restrict ourselves to codimension-one and codimension-two singularities, but one may go to codimension-three [HMD13].

Section 3.4: The example for finite differentiability is taken from [Guc04]. The fast–slow decomposition of the three-dimensional FHN equation is discussed extensively in [GK09b, GK10b]. The turning point example is taken from [Kop79, Kop80, KP81]. There has been a great deal of work on turning points [Kaz58, Lan49, O'M70b, Was85, Wat71] and related phenomena such as overstability [FS03c] and resonances [Kop79, Kop80, Kre81, KP74]. Differential inequalities have also been used successfully near turning points [How75, How78d, How78a, How78c]; see also work on sub- and supersolutions [CH06].

A topic that could be explored further is fast–slow maps [MS05], where one expects that standard invariant manifold theory for maps can still be applied [HPS77]. Furthermore, fast–slow maps can often be embedded into flows [IS01]. Also, the complex analysis viewpoint on singularly perturbed systems [FS05] as well as slow manifolds for fast–slow Hamiltonian systems [KW12, KPR12, Mac04] are not covered in this book in any considerable detail.

Chapter 4

Normal Forms

Having developed the main theorems of perturbations of invariant manifolds, we aim to bring a fast–slow system into **normal form**. As this book was written, there was no complete general theory for what a “normal form” for a fast–slow system should be. In the following, we indicate some possibilities and transformations to simplify fast–slow system and shall use the term “normal form” loosely for all systems of equations that have been obtained as the result of a simplifying transformation procedure.

Section 4.1 covers the normal form transformation for the normally hyperbolic case, also referred to as Fenichel normal form. Basically, the transformations rectify the normally hyperbolic invariant manifold and its stable and unstable manifolds. Section 4.2 examines the simplest generic fold singularity and illustrates that the leading-order fast variable approximation is just a second-order quadratic nonlinearity. This case is extended to a parabolic cylinder for a line of fold points in three dimensions in Section 4.3. Section 4.4 discusses systems of first approximation that can be viewed as nicely scaled leading-order truncations of normal forms near singularities. Section 4.5 deals with the problem of how to bring a system into a standard fast–slow form; the technique is illustrated in the linear context.

Background: Sufficient patience to track coordinate changes and Taylor expansions. Knowledge of classical normal form theory for differential equations is not required but could be beneficial for a bigger picture; see Section 4.6.

4.1 The Normally Hyperbolic Case

Suppose we consider—as usual—the (m, n) -fast–slow system

$$\begin{aligned}\frac{dx}{dt} &= x' = f(x, y, \varepsilon), \\ \frac{dy}{dt} &= y' = \varepsilon g(x, y, \varepsilon),\end{aligned}\tag{4.1}$$

where $(x, y) \in \mathbb{R}^m \times \mathbb{R}^n$ and f, g are smooth maps. Let $S = S_0$ be a compact contractible normally hyperbolic submanifold of the critical manifold C_0 . By Fenichel's Theorem 3.1.4, there exists a family of slow manifolds S_ε . Assume that the slow manifolds are given as graphs, i.e., there is a compact set $V \subset \mathbb{R}^n$ such that

$$v : V \times [0, \varepsilon_1] \subset \mathbb{R}^n \times \mathbb{R} \rightarrow \mathbb{R}^m \quad \text{for } \varepsilon_1 > 0 \text{ sufficiently small}$$

and S_ε is given as a graph $S_\varepsilon = \{(v(y, \varepsilon), y) \in \mathbb{R}^{m+n}\}$. It will be convenient to formulate the transformation into a local normal form under the assumption that f, g and S are sufficiently smooth. Recall that the slow manifolds S_ε of a smooth fast-slow system will in general not be C^∞ . We know only that v is C^r in (y, ε) and r can be made larger by choosing ε_1 smaller. Therefore, we shall simply use the shorthand term **C^r -smooth** to indicate that we can find an object or map with C^r -smoothness for any $r \geq 2$ in what follows.

We are going to establish a local normal form for (4.1) near $p \in S_0$ in a series of propositions. By normal hyperbolicity, we know that $D_x f(p, 0)$ has m eigenvalues λ_j with nonzero real part, say

$$\operatorname{Re}(\lambda_j) > 0 \quad \text{for } j \in \{1, \dots, m^u\} \quad \text{and} \quad \operatorname{Re}(\lambda_j) < 0 \quad \text{for } j \in \{m^u + 1, \dots, m\}.$$

If we set $m^s = m - m^u$, this just means that we have m^u repelling and m^s attracting directions normal to S_0 .

Proposition 4.1.1. *There exists a C^r -smooth coordinate change in a neighborhood of $S_0 \times \{0\} \subset \mathbb{R}^{m+n} \times [0, \varepsilon_1]$ such that the fast-slow system (4.1) near S_0 can be written as*

$$\begin{aligned} a'_1 &= A_1(y)a_1 + F_1(a, y, \varepsilon), \\ a'_2 &= A_2(y)a_2 + F_2(a, y, \varepsilon), \\ y' &= \varepsilon g(a, y, \varepsilon), \end{aligned} \tag{4.2}$$

where $(a_1, a_2) \in \mathbb{R}^{m^u} \times \mathbb{R}^{m^s}$, $A_1(y)$ is an $m^u \times m^u$ matrix with eigenvalues having positive real part, $A_2(y)$ is an $m^s \times m^s$ matrix with eigenvalues having negative real part; A_j , F_j ($j = 1, 2$), and g are maps that are at least C^{r-1} in all arguments. Furthermore, $F_j(0, y, 0) = 0$ and $D_a F_j(0, y, 0) = 0$ for $j = 1, 2$.

Remark: In this book, we shall not discuss the sharp smoothness results for (4.2). Instead, we always adopt the viewpoint that f, g are sufficiently smooth and $\varepsilon > 0$ is sufficiently small. In this case, Proposition 4.1.1 provides a vector field (4.2) of any desired finite smoothness.

Proof. Let $p = (v(y, 0), y) \in S_0$. Note that one can assume without loss of generality that $v(y, 0) = 0$, so that $S_0 = \{(0, y) \in \mathbb{R}^{m+n}\}$, since we can set $\tilde{x} = x - v(y, 0)$ and recompute the equations if necessary. For each $(0, y) \in S_0$, we know by normal hyperbolicity that $D_x f(0, y, 0)$ has m eigenvalues λ_i with $\operatorname{Re}(\lambda_i) \neq 0$. Since S_0 is simply connected, the number of eigenvalues with positive (respectively negative) real part is independent of y . Hence, we can smoothly choose bases of the corresponding eigenspaces. Therefore, there exists a smooth coordinate change $T_0(x) = a$ giving (4.2).

By Fenichel's theorem, we know that S_ε is normally hyperbolic and diffeomorphic to S_0 . Since the manifolds are diffeomorphic, we conclude that S_ε is also simply connected. Therefore, the same construction works for every ε sufficiently small, and we can find a coordinate change $T_\varepsilon(x) = a$. \square

The last proof gives a smooth family T_ε of coordinate changes simplifying (4.1). Assume from now on that the slow manifold has been straightened as demonstrated in the proof of Proposition 4.1.1, i.e.,

$$S_\varepsilon = \{(0, y) \in \mathbb{R}^{m+n}\},$$

and that we have shifted the coordinate system along y so that $(0, 0) \in S_\varepsilon$. One also writes (4.2) in the more compact form

$$\begin{aligned} a' &= A(y)a + F(a, y, \varepsilon), \\ y' &= \varepsilon g(a, y, \varepsilon), \end{aligned} \tag{4.3}$$

where it is understood that $a = (a_1, a_2)$ and

$$A = \begin{pmatrix} A_1 & 0 \\ 0 & A_2 \end{pmatrix}.$$

An obvious problem of (4.3) is that we have to deal with a possibly very complicated function $F = F(a, y, \varepsilon)$. To simplify the equation even further, we can transform (4.3) by straightening the stable and unstable manifolds $W_{\text{loc}}^s(S_\varepsilon)$ and $W_{\text{loc}}^u(S_\varepsilon)$.

Theorem 4.1.2 (Fenichel normal form, [Fen79, Jon95, JKK96]). *There exists a C^r -smooth coordinate change in a neighborhood of $S_0 \times \{0\} \subset \mathbb{R}^{m+n} \times [0, \varepsilon_1]$ such that the fast-slow system (4.3) near a normally hyperbolic slow manifold S_ε can be written as*

$$\begin{aligned} a'_1 &= \Lambda_1(a, y, \varepsilon)a_1, \\ a'_2 &= \Lambda_2(a, y, \varepsilon)a_2, \\ y' &= \varepsilon(h(y, \varepsilon) + H(a_1, a_2, y, \varepsilon)(a_1, a_2)), \end{aligned} \tag{4.4}$$

for $\|a\| = \|(a_1, a_2)\|$ sufficiently small; Λ_j (for $j = 1, 2$), h , and H are maps that are at least C^{r-1} in all arguments; $\Lambda_1(a, y, \varepsilon)$ is a matrix with eigenvalues having positive real part, $\Lambda_2(a, y, \varepsilon)$ is a matrix with eigenvalues having negative real part, and $H(a_1, a_2, y, \varepsilon)$ is bilinear when applied to (a_1, a_2) .

Proof. Note that locally, for $\|a\|$ small enough, one can write the stable and unstable manifolds $W_{\text{loc}}^s(S_\varepsilon)$ and $W_{\text{loc}}^u(S_\varepsilon)$ also as graphs, i.e., there exist C^r -smooth maps h_s and h_u such that

$$\begin{aligned} W_{\text{loc}}^s(S_\varepsilon) &= \{(a_1, a_2, y) : a_1 = h_s(a_2, y, \varepsilon)\}, \\ W_{\text{loc}}^u(S_\varepsilon) &= \{(a_1, a_2, y) : a_2 = h_u(a_1, y, \varepsilon)\}. \end{aligned}$$

The interpretation is that we can write $W_{\text{loc}}^s(S_\varepsilon)$ as a graph over the stable-normal and slow directions and $W_{\text{loc}}^u(S_\varepsilon)$ as a graph over the unstable-normal

and slow directions. To straighten the stable manifold, define the coordinate change

$$a_1^{\text{new}} = a_1 - h_s(a_2, y, \varepsilon),$$

leaving the other variables unchanged. This transforms $W_{\text{loc}}^s(S_\varepsilon)$ to $\{a_1^{\text{new}} = 0\}$. Then set

$$a_2^{\text{new}} = a_2 - h_u(a_1^{\text{new}} + h_s(a_2, y, \varepsilon), a_2, \varepsilon).$$

This transforms $W_{\text{loc}}^u(S_\varepsilon)$ to $\{a_2^{\text{new}} = 0\}$. Obviously, both transformations are as smooth as h_s and h_u and can be inverted. For convenience, suppose that the transformations have been carried out. Then we revert to the old notation, so that $(a_1^{\text{new}}, a_2^{\text{new}}) = (a_1, a_2)$. Since $W_{\text{loc}}^s(S_\varepsilon)$ and $W_{\text{loc}}^u(S_\varepsilon)$ are locally invariant, all trajectories in a neighborhood U_ε of S_ε satisfy

$$a_1 = 0 \text{ implies } a_1' = 0 \quad \text{and} \quad a_2 = 0 \text{ implies } a_2' = 0.$$

Therefore, one can factor a_1 and a_2 in equation (4.2), respectively in (4.3), so that

$$\begin{aligned} a_1' &= A_1(y)a_1 + F_1(a, y, \varepsilon) = \Lambda_1(a, y, \varepsilon)a_1, \\ a_2' &= A_2(y)a_2 + F_2(a, y, \varepsilon) = \Lambda_2(a, y, \varepsilon)a_2, \\ y' &= \varepsilon g(a, y, \varepsilon). \end{aligned}$$

It remains to simplify the slow directions y . Recall that Fenichel's theorem provides foliations \mathcal{F}^s and \mathcal{F}^u of the stable and unstable manifolds. Let Π^- denote the map sending a point $(0, a_2, y) \in \mathcal{F}^s((0, \hat{a}_2, \hat{y}))$ to the y -coordinate of the base point $\Pi^-(0, a_2, y) = \hat{y}$. Construct Π^+ in the same way for the foliation \mathcal{F}^u . Consider the coordinate change

$$y^{\text{new}} = \Pi^-(0, a_2, y, \varepsilon). \tag{4.5}$$

Hence, each leaf $\mathcal{F}^s(\cdot)$ is transformed under (4.5) so that all points in it have the same y -coordinate; see also Figure 4.1. The same works for the foliation \mathcal{F}^u , because we can now use the transformation

$$y^{\text{brand-new}} = \Pi^+(a_1, 0, y^{\text{new}}, \varepsilon).$$

After the transformations, we revert, as before, to the old y -coordinate and set $y = y^{\text{brand-new}}$. Positive invariance of \mathcal{F}^s and negative invariance of \mathcal{F}^u imply that if $a_1 = 0$ or $a_2 = 0$, then $g(a, y, \varepsilon)$ is a function of y and ε only. It follows that

$$g(a_1, a_2, y, \varepsilon) = h(y, \varepsilon) + H(a_1, a_2, y, \varepsilon)(a_1, a_2),$$

where h, H are C^r -smooth functions and $H(a_1, a_2, y, \varepsilon)$ is bilinear when applied to (a_1, a_2) . \square

Equation (4.4) was termed **Fenichel normal form** by Jones in [Jon95], and it has a simple geometric interpretation, shown in Figure 4.1. Sometimes, the differential equation for the slow variables is written as

$$y' = \varepsilon [h(y, \varepsilon) + H(a_1, a_2, y, \varepsilon) \otimes a_1 \otimes a_2], \tag{4.6}$$

which emphasizes that H is a C^r -smooth rank-three tensor acting on the vectors $a_1 \in \mathbb{R}^{m_u}$ and $a_2 \in \mathbb{R}^{m_s}$. The componentwise notation of (4.6) is

$$y'_j = \varepsilon \left[h_j(y, \varepsilon) + \sum_{u=1}^{m_u} \sum_{s=1}^{m_s} H_{jus} a_{1,u} a_{2,s} \right],$$

which is convenient for explicit computations and to clarify the bilinearity of H .

Fenichel normal form can be simplified even further under some additional assumptions. The **flow-box theorem** or **rectification lemma** from classical ODE theory allows us to straighten a flow locally under suitable conditions; see [Chi10, Arn73, HSD03]. Hence, the proof of Theorem 4.1.2 can be modified easily to obtain another version of Fenichel normal form.

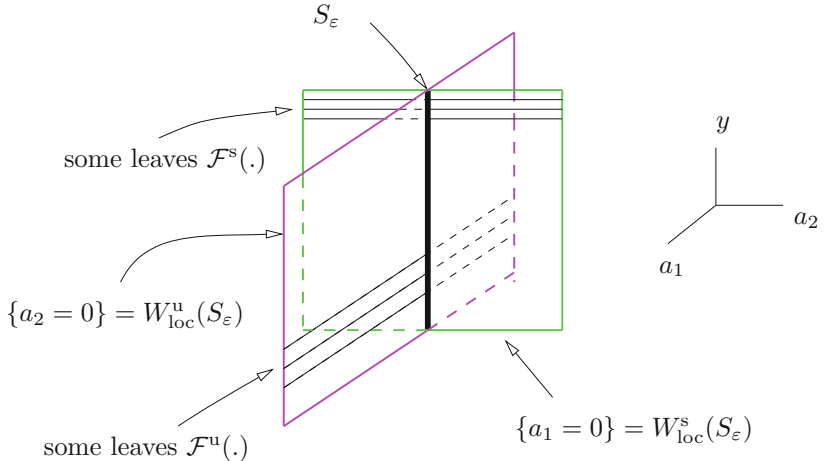


Figure 4.1: Illustration of Fenichel normal form from Theorem 4.1.2. There are fast dynamics toward S_ε in $W_{\text{loc}}^s(S_\varepsilon)$ (green) in forward time, and similarly for $W_{\text{loc}}^u(S_\varepsilon)$ (magenta) in backward time. However, note that the fast fibers are given by the asymptotic rate foliation as described in Section 2.3 and illustrated in Figure 2.10; in particular, these fibers are usually not trajectories.

Corollary 4.1.3. *Suppose the flow on the normally hyperbolic slow manifold S_ε is rectifiable. Then there exists a C^r -smooth coordinate change such that a fast-slow system can be written as*

$$\begin{aligned} a'_1 &= \Lambda_1(a, y, \varepsilon)a_1, \\ d'_2 &= \Lambda_2(a, y, \varepsilon)a_2, \\ y' &= \varepsilon(e_1 + \tilde{H}(a, y, \varepsilon)a_1), \end{aligned}$$

for $\|a\| = \|(a_1, a_2)\|$ sufficiently small, where $e_1 = (1, 0, \dots, 0)^\top \in \mathbb{R}^n$ and $\tilde{H}(a, y, \varepsilon)$ is a matrix.

Corollary 4.1.3 will be of particular importance in our development of the exchange lemma in Section 6.3. We shall mention that one can use more advanced technical tools than direct coordinate changes to prove normal form results. For example, Ilyashenko [Ily97] refers to the Takens saddle suspension theorem to derive a result analogous to Corollary 4.1.3. The next example shows that even though a given singularly perturbed problem looks simple, it may not be obvious whether and how it can be converted into Fenichel normal form.

Example 4.1.4. Consider the linear two-point boundary value problem (BVP) on $\tau \in [0, 1]$ given by

$$\varepsilon \frac{d^2 u}{d\tau^2} + \frac{du}{d\tau} + u = \varepsilon \ddot{u} + \dot{u} + u = 0, \quad u(0) = 1, \quad u(1) = -1, \quad (4.7)$$

where $0 < \varepsilon \ll 1$. The first step is to convert (4.7) into a first-order system. There are several possibilities, and we use a transformation—which can be motivated by asymptotic methods from Section 9.1—given by

$$\begin{pmatrix} x \\ y \end{pmatrix} = \begin{pmatrix} \varepsilon & \varepsilon \\ 1 & \varepsilon \end{pmatrix} \begin{pmatrix} u \\ \dot{u} \end{pmatrix} \quad \Rightarrow \quad \begin{pmatrix} u \\ \dot{u} \end{pmatrix} = \begin{pmatrix} \frac{1}{\varepsilon-1} & \frac{1}{1-\varepsilon} \\ \frac{1}{\varepsilon-\varepsilon^2} & \frac{1}{\varepsilon-1} \end{pmatrix} \begin{pmatrix} x \\ y \end{pmatrix}. \quad (4.8)$$

Differentiating x and y with respect to τ , replacing the second derivatives using (4.7), and applying the coordinate change (4.8) yields

$$\begin{aligned} \varepsilon \dot{x} &= [-1 + \varepsilon + \mathcal{O}(\varepsilon^2)]x + [\mathcal{O}(\varepsilon^2)]y, \\ \dot{y} &= [1 + \mathcal{O}(\varepsilon)]x + [-1 + \mathcal{O}(\varepsilon)]y, \end{aligned} \quad (4.9)$$

and the boundary conditions are

$$u(0) = \frac{-x(0) + y(0)}{1 - \varepsilon} = 1 \quad \text{and} \quad u(1) = \frac{-x(1) + y(1)}{1 - \varepsilon} = -1.$$

The $(1, 1)$ -fast–slow system has a normally hyperbolic attracting critical manifold $C_0 = \{(x, y) \in \mathbb{R}^2 : x = 0\}$. Fenichel’s theorem guarantees the existence of a slow manifold $C_\varepsilon = \{(x, y) \in \mathbb{R}^2 : x = h_\varepsilon(y) = 0 + \mathcal{O}(\varepsilon)\}$. Changing to the fast time scale $t = \tau/\varepsilon$ in (4.9) yields

$$\begin{aligned} x' &= [-1 + \varepsilon + \mathcal{O}(\varepsilon^2)]x + [\mathcal{O}(\varepsilon^2)]y, \\ y' &= [\varepsilon + \mathcal{O}(\varepsilon^2)]x + [-\varepsilon + \mathcal{O}(\varepsilon^2)]y. \end{aligned} \quad (4.10)$$

Introducing a new coordinate as in the proof of Theorem 4.1.2 by $a = x - h_\varepsilon(y)$ yields the Fenichel normal form near C_ε

$$\begin{aligned} a' &= [-1 + \mathcal{O}(\varepsilon)]a, \\ y' &= \varepsilon[(1 + \mathcal{O}(\varepsilon))a - (1 + \mathcal{O}(\varepsilon))y]. \end{aligned} \quad (4.11)$$

Let us point out that this example raises many important questions that are going to be addressed in this book. For example, it still remains to solve the BVP, which is discussed in more detail in Sections 9.1 and 9.2 as well as Sections 10.3 and 10.4. One may also want to compute $h_\varepsilon(y)$, which is considered in Sections 11.1–11.4. ♦

4.2 Fold Points

In addition to normally hyperbolic parts of the critical manifold, one can also ask whether there are “normal forms” for singularities of the critical manifold. In this section, we demonstrate the analysis for the fold point. Consider a $(1, 1)$ -fast–slow system given by

$$\begin{aligned}\varepsilon \frac{dx}{d\tau} &= \varepsilon \dot{x} = f(x, y), \\ \frac{dy}{d\tau} &= \dot{y} = g(x, y),\end{aligned}\tag{4.12}$$

with $(x, y) \in \mathbb{R}^2$. To simplify the discussion, we have assumed that the right-hand side of the fast–slow system is independent of ε . Recall from Definition 3.3.2 that the critical manifold $C_0 = \{f(x, y) = 0\}$ has a nondegenerate fold point at $P = (x_0, y_0)$ if

$$f_x(x_0, y_0) = 0 \quad f_{xx}(x_0, y_0) \neq 0, \quad f_y(x_0, y_0) \neq 0.\tag{4.13}$$

Remark: In classical bifurcation theory [Kuz04], one refers to $f_{xx}(x_0, y_0) \neq 0$ as a nondegeneracy condition and to $f_y(x_0, y_0) \neq 0$ as a transversality condition. Here we shall reserve the term “transversality” for a crossing condition of the slow dynamics. In particular, we emphasize that we shall always assume (4.13) for fold points in this book, so confusion will be, we hope, avoided.

In addition, it is natural to assume a (slow dynamics) **transversality condition** given by

$$g(x_0, y_0) < 0 \quad \text{or} \quad g(x_0, y_0) > 0.\tag{4.14}$$

The first three conditions (4.13) prescribe the folding of C_0 ; see also Figure 4.2. The condition (4.14) prevents the existence of equilibria of the slow flow near a fold point; the case with an equilibrium is discussed in Sections 8.1–8.4.

Definition 4.2.1. A fold point satisfying (4.13) and (4.14) is called a **generic fold point**.

Theorem 4.2.2 ([MR80]). *Consider a generic fold point P . There exists a change of coordinates $\phi(x, y) = (\xi, \eta)$ such that the critical manifold near $\phi(P) = (0, 0)$ is given by*

$$\eta = \xi^2 \quad \text{or} \quad \eta = -\xi^2.$$

One can choose ϕ such that the slow vector field near $(0, 0)$ has either positive or negative sign; in particular, there are no equilibria for the slow flow near $(0, 0)$.

Remark: The coordinate change can be chosen such that the parabola opens upward or downward. It is merely a matter of convenience which form to select. The same remark applies to the sign of the slow vector field.

Proof. We aim to transform the critical manifold to the parabola $\eta = -\xi^2$ with slow flow of positive sign. We can assume without loss of generality,

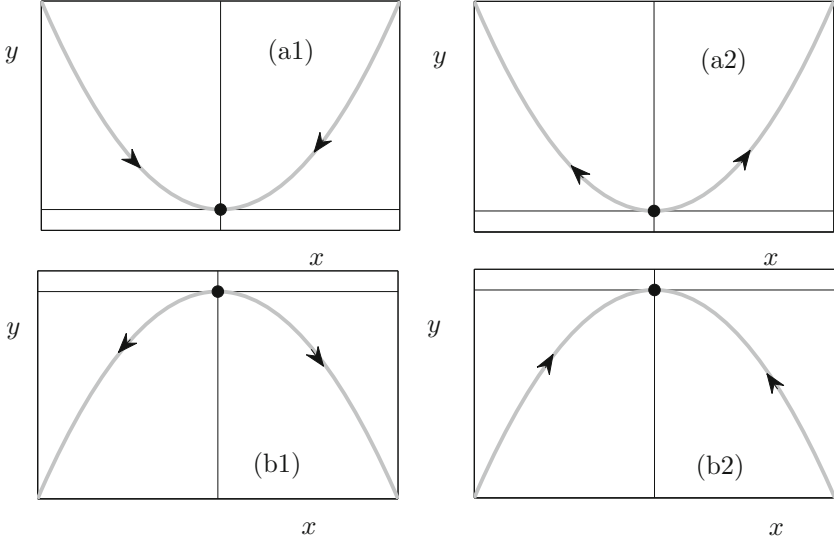


Figure 4.2: The critical manifold C_0 (gray curve) near a nondegenerate fold point (black dot) and the associated slow flow. All four possible local cases are shown. For the slow flow, (a1) and (b1) show $g(x_0, y_0) < 0$, while (a2) and (b2) show $g(x_0, y_0) > 0$.

on using a translation coordinate change, that $P = (x_0, y_0) = (0, 0)$. Since $f_y(P) = f_y(0, 0) \neq 0$, the implicit function theorem yields that $y = Y(x)$ for x near 0 and some smooth function Y with $Y(0) = 0$. By definition of the critical manifold, it follows that

$$f(x, Y(x)) = 0 \quad \text{for } x \text{ near 0.} \quad (4.15)$$

Differentiating (4.15) and evaluating the derivative at $(0, 0)$ leads to

$$0 = f_x(0, Y(0)) + f_y(0, Y(0))Y'(0) = f_x(0, 0) + f_y(0, 0)Y'(0).$$

By genericity of the fold, we have $f_x(0, 0) = 0$ and $f_y(0, 0) \neq 0$, so it follows that $Y'(0) = 0$. Differentiating (4.15) twice and using $f_{xx}(0, 0) \neq 0$, one easily deduces

$$Y''(0) = -\frac{f_{xx}(0, 0)}{f_y(0, 0)} \neq 0.$$

Therefore, Taylor's theorem applied to $Y(x)$ at $x = 0$ reads

$$y = Y(x) = -\frac{f_{xx}(0, 0)}{2f_y(0, 0)}x^2 + \frac{1}{6}Y'''(vx)x^3 \quad \text{for some } v \in [0, 1].$$

To construct the coordinate change explicitly, define the function

$$y = \varphi(x) = x \sqrt{\left| \frac{f_{xx}(0, 0)}{2f_y(0, 0)} \right| - \frac{1}{6}xY'''(vx) \operatorname{sign}[f_{xx}(0, 0)f_y(0, 0)]}. \quad (4.16)$$

Note that $\varphi(x)$ is smooth in a neighborhood of $x = 0$. Furthermore, $\varphi(0) = 0$ and

$$\varphi'(0) = \sqrt{\left| \frac{f_{xx}(0,0)}{2f_y(0,0)} \right|} > 0.$$

Hence φ is invertible near 0, and we denote its inverse by $\psi(y) = x$. The coordinate change can now be defined:

$$\begin{aligned} (\xi, \eta) &= (\varphi(x) \operatorname{sign}[f_{xx}(0,0)], y \operatorname{sign}[g(0,0)]), \\ (x, y) &= (\psi(\xi \operatorname{sign}[f_{xx}(0,0)]), \eta \operatorname{sign}[g(0,0)]). \end{aligned} \quad (4.17)$$

It is clear that (4.17) transforms the critical manifold near $(0,0)$ into the parabola $\eta = -\xi^2$. The equations for the full fast–slow system now read

$$\begin{aligned} \varepsilon \dot{\xi} &= \frac{\xi^2 + \eta}{\alpha(\xi, \eta)}, \\ \dot{\eta} &= \beta(\xi, \eta), \end{aligned} \quad (4.18)$$

where

$$\begin{aligned} \alpha(\xi, \eta) &= \frac{(\xi^2 + \eta)\psi'(\xi \operatorname{sign}[f_{xx}(0,0)]) \operatorname{sign}[f_{xx}(0,0)]}{f(\psi(\xi \operatorname{sign}[f_{xx}(0,0)]), \eta \operatorname{sign}[g(0,0)])}, \\ \beta(\xi, \eta) &= |g(\psi(\xi \operatorname{sign}[f_{xx}(0,0)]), \eta \operatorname{sign}[g(0,0)])|. \end{aligned} \quad (4.19)$$

Since $\beta(\xi, \eta) > 0$, the proof is finished. \square

Equations (4.16)–(4.19) provide an explicit method for transforming any $(1,1)$ fast–slow system near a generic fold into an equation with parabolic critical manifold and unidirectional slow flow. This transformation will be particularly useful for developing explicit asymptotic expansions near a fold point; see Chapter 5. It is possible to bring the slow subsystem into a normal form as well.

Theorem 4.2.3 ([Arn94]). *In a neighborhood of a generic fold point, the slow subsystem may be transformed by a coordinate change to*

$$y = \pm x^2 \quad \text{and} \quad \dot{y} = \pm 1 + xA(y).$$

The function $A(y)$ is invariant under any such coordinate change. The slow flow may be transformed by a C^∞ change of time to $y = \pm t + t^{3/2}$.

The proof can be found in [Arn94, I.4], but it should not be surprising that such a simplification is possible by looking at Theorem 4.2.2 and Figure 4.2.

Exercise/Project 4.2.4. Instead of starting from system (4.12), consider

$$\begin{aligned} \varepsilon \dot{x} &= f(x, y, \varepsilon), \\ \dot{y} &= g(x, y, \varepsilon). \end{aligned} \quad (4.20)$$

What changes in the statement and in the proof of Theorem 4.2.2? Also, use your results to prove Theorem 4.2.5, stated below. \diamond

Theorem 4.2.5 ([KS01b]; see also [MR80]). *Suppose (4.20) has a generic fold point P . Then there exists a smooth change of coordinates $\phi(x, y) = (\xi, \eta)$ such that locally near $\phi(P) = (0, 0)$, the system (4.20) is given by*

$$\begin{aligned} \frac{d\xi}{dt} &= \xi' = \eta + \xi^2 + \mathcal{O}(\xi^3, \xi\eta, \eta^2, \varepsilon), \\ \frac{d\eta}{dt} &= \eta' = \varepsilon(\pm 1 + \mathcal{O}(\xi, \eta, \varepsilon)). \end{aligned} \quad (4.21)$$

4.3 Fold Curves

The next step is to check whether a normal form approach can be applied to folds in systems with more than one slow variable. We focus on the $(1, 2)$ -fast–slow system

$$\begin{aligned} \varepsilon \dot{x} &= f(x, y_1, y_2, \varepsilon), \\ \dot{y}_1 &= g_1(x, y_1, y_2, \varepsilon), \\ \dot{y}_2 &= g_2(x, y_1, y_2, \varepsilon). \end{aligned} \quad (4.22)$$

The critical manifold $C_0 = \{(x, y_1, y_2) \in \mathbb{R}^3 : f(x, y_1, y_2, 0) = 0\}$ is now generically a surface, and points P that are not normally hyperbolic ($f_x(P, 0) = 0$) are usually not isolated but form a one-dimensional curve L inside C_0 . Suppose points in L are fold points, i.e.,

$$L = \{(x, y_1, y_2) \in C_0 : f_x(x, y_1, y_2, 0) = 0, f_{xx}(x, y_1, y_2, 0) \neq 0\}.$$

An example is shown in Figure 4.3(a). For nondegenerate fold points $P \in C_0$, we have $f_{y_1}(P, 0) \neq 0$ or $f_{y_2}(P, 0) \neq 0$ (or both). In any case, we can assume without loss of generality that a nondegenerate fold curve can be parameterized, at least locally, by y_2 , so that

$$L = \{(\theta(y_2), \psi(y_2), y_2) : y_2 \in I\}, \quad (4.23)$$

where I is a suitable interval. Next, we introduce a function

$$l(y_2) := \left(\begin{array}{c} f_{y_1} \\ f_{y_2} \end{array} \right) \cdot \left(\begin{array}{c} g_1 \\ g_2 \end{array} \right) \Big|_{(\theta(y_2), \psi(y_2), y_2)},$$

where \cdot denotes the usual dot product in \mathbb{R}^2 . The key assumption, in addition to nondegeneracy, is

$$l(y_2) \neq 0 \quad \text{for all } y_2 \in I. \quad (4.24)$$

The geometric interpretation of (4.24) is that if we project the slow flow into the (y_1, y_2) -plane, then it is not tangent to the fold curve L at the origin $(0, 0)$. This is analogous to the condition in a $(1, 1)$ -fast–slow system whereby we required that the slow flow be nonzero at a nondegenerate fold point. The condition (4.24) is referred to as a **transversality condition** or the **normal switching condition**.

Theorem 4.3.1 ([SW04]; see also [MKKR94, Ben82]). *Suppose a nondegenerate fold curve L of (4.22) satisfies the normal switching condition. Then there*

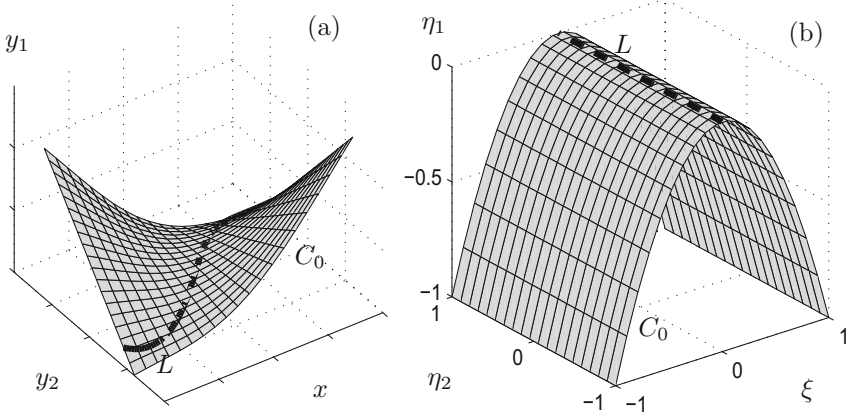


Figure 4.3: The critical manifold C_0 (gray surface) for a $(1, 2)$ -fast–slow system containing a nondegenerate fold curve L (dashed black curve) is shown. (a) General case associated with (4.22). (b) Normal form (4.25).

exists a smooth change of coordinates $\phi(x, y_1, y_2) = (\xi, \eta_1, \eta_2)$ such that locally near the fold curve, the system (4.22) is given by

$$\begin{aligned} \frac{d\xi}{dt} &= \xi' = \eta_1 + \xi^2 + \mathcal{O}(\xi^3, \xi\eta_1\eta_2, \xi\eta_1^2, \varepsilon), \\ \frac{d\eta_1}{dt} &= \eta'_1 = \varepsilon g_1(\xi, \eta_1, \eta_2, \varepsilon), \\ \frac{d\eta_2}{dt} &= \eta'_2 = \varepsilon g_2(\xi, \eta_1, \eta_2, \varepsilon), \end{aligned} \quad (4.25)$$

where $t = \tau/\varepsilon$ and $g_1(\xi, \eta_1, \eta_2, \varepsilon) = 1 + g_{11}(\xi, \eta_1, \eta_2, \varepsilon)$, where $g_{11}(0, 0, \eta_2, 0) = 0$ and $g_2(0, 0, \eta_2, 0) = 0$ for $y \in I$; see also Figure 4.3(b).

Proof. (Sketch; [SW04, Wec98]) Rectifying the fold curve along the η_2 -axis works as in the proofs of Theorem 4.1.2 and Theorem 4.2.2 by introducing new coordinates $(\hat{x}, \hat{y}_1, \hat{y}_2)$ and utilizing the functions $\theta(y_2)$, $\psi(y_2)$ from (4.23). Then a direct Taylor expansion, as for previous normal form results, yields

$$\begin{aligned} \hat{x}' &= \hat{y}_1 + \hat{x}^2 + \mathcal{O}(\hat{x}^3, \hat{x}\hat{y}_1\hat{y}_2, \hat{x}\hat{y}_2, \varepsilon), \\ \hat{y}'_1 &= \varepsilon \hat{g}_1(\hat{x}, \hat{y}_1, \hat{y}_2, \varepsilon), \\ \hat{y}'_2 &= \varepsilon \hat{g}_2(\hat{x}, \hat{y}_1, \hat{y}_2, \varepsilon), \end{aligned} \quad (4.26)$$

with $\hat{g}_1(0, 0, \hat{y}_2, 0) > 0$ for all $\hat{y}_2 \in \hat{I}$. Observe that the normal switching condition implies that $\hat{g}_2(0, 0, \hat{y}_2, 0) = 0$ for all $\hat{y}_2 \in \hat{I}$. Let $\hat{g}_1(\hat{x}, \hat{y}_1, \hat{y}_2, \varepsilon) = g(\hat{y}_2) + g_{11}(\hat{x}, \hat{y}_1, \hat{y}_2, \varepsilon)$, where $g(\hat{y}_2) := \hat{g}_1(0, 0, \hat{y}_2, 0) > 0$. Since $g(\hat{y}_2) > 0$, the following scaling transformation is well defined:

$$\xi = \hat{x}g(\hat{y}_2)^{-\frac{1}{3}}, \quad \eta_1 = \hat{y}_1g(\hat{y}_2)^{-\frac{2}{3}}, \quad \eta_2 = \hat{y}_2.$$

It yields, on its being used in (4.26), that

$$\begin{aligned} \xi' &= g(\hat{y}_2)^{\frac{1}{3}} (\eta_1 + \xi^2 + \mathcal{O}(\xi^3, \xi\eta_1\eta_2, \xi\eta_1^2, \varepsilon)), \\ \eta'_1 &= \varepsilon g(\hat{y}_2)^{\frac{1}{3}} (1 + g_{11}(\xi, \eta_1, \eta_2, \varepsilon)), \\ \eta'_2 &= \varepsilon g(\hat{y}_2)^{\frac{1}{3}} g_2(\xi, \eta_1, \eta_2, \varepsilon). \end{aligned} \quad (4.27)$$

The positive factor $g(\hat{y}_2)^{1/3}$ in (4.27) can be removed by a time rescaling. \square

Example 4.3.2. The periodically forced van der Pol equation

$$\begin{aligned}\varepsilon \dot{x} &= y - \frac{x^3}{3} + x, \\ \dot{y} &= a \sin(2\pi\theta) - x, \\ \dot{\theta} &= \omega,\end{aligned}$$

is an example of a critical manifold C_0 containing two fold curves

$$\begin{aligned}L^\pm &= \left\{ (x, y, \theta) \in \mathbb{R}^2 \times S^1 : y = \frac{x^3}{3} - x, -x^2 + 1 = 0 \right\} \\ &= \left\{ (x, y, \theta) \in \mathbb{R}^2 \times S^1 : x = \pm 1, y = \mp \frac{2}{3} \right\},\end{aligned}$$

which are already nicely aligned with the θ -axis. ♦

Exercise 4.3.3. Determine, depending upon the parameter ω , for which points $P \in L^\pm$ the normal switching condition (4.24) is satisfied. ◇

The normal form (4.25) from Theorem 4.3.1 is a typical example of how the analysis of singularities of fast–slow systems begins. Certain nondegeneracy and transversality conditions are first assumed; then the singular object is transformed so that it is nicely aligned in standard coordinates near the origin; and finally, a Taylor expansion is employed and the lowest-order terms are retained.

4.4 Systems of First Approximation

So far, the normal form results have been quite intuitive if one is familiar with the calculations for a fold (or saddle-node) bifurcation in single time scale systems. The next results truly separate the theory of fast–slow systems from classical bifurcation theory.

Theorem 4.4.1 ([Arn94]; see also [MR80]). *There exists a coordinate change such that a $(1, 1)$ -fast–slow system sufficiently close to a generic fold point in (x, y) -variables can be transformed into a system on a single time scale*

$$\begin{aligned}\frac{dX}{dT} &= X^2 \pm Y + \mathcal{O}(\varepsilon^{1/3}), \\ \frac{dY}{dT} &= \pm 1 + \mathcal{O}(\varepsilon^{1/3}),\end{aligned}\tag{4.28}$$

defined in a region of size $\mathcal{O}(1)$ as $\varepsilon \rightarrow 0$ around $(X, Y) = (0, 0)$.

Before proving the result, let us motivate parts of the construction required in the proof. Suppose we start with the system

$$\begin{aligned}\varepsilon \frac{dx}{d\tau} &= \varepsilon \dot{x} = x^2 \pm y, \\ \frac{dy}{d\tau} &= \dot{y} = \pm 1,\end{aligned}\tag{4.29}$$

which is motivated by the normal form for the fold point in Theorem 4.2.3. We want to write (4.29), locally, as a system on a single time scale. Observe that ε always occurs, on the slow time scale τ and on the fast time scale $t = \tau/\varepsilon$,

as a multiplicative factor. This suggests that we **rescale** phase space and time. One possible choice of rescaling is

$$(x, y, \tau) \mapsto (\varepsilon^{1/3} X, \varepsilon^{2/3} Y, \varepsilon^{2/3} T). \quad (4.30)$$

Substituting (4.30) into (4.29) is an easy calculation:

$$\begin{aligned} \varepsilon \dot{x} &= \varepsilon \frac{\varepsilon^{1/3} dX}{\varepsilon^{2/3} dT} = \varepsilon^{2/3} X^2 \pm \varepsilon^{2/3} Y, \\ \dot{y} &= \frac{\varepsilon^{2/3} dY}{\varepsilon^{2/3} dT} = \pm 1. \end{aligned}$$

For $\varepsilon > 0$, the factor $\varepsilon^{2/3}$ cancels, so that the result is

$$\begin{aligned} \frac{dX}{dT} &= X^2 \pm Y, \\ \frac{dY}{dT} &= \pm 1, \end{aligned}$$

where the four different combinations of signs are equivalent up to a coordinate change. Note carefully that the rescaling (4.30) is singular when $\varepsilon \rightarrow 0$. The neighborhood of $(x, y) = (0, 0)$ in original coordinates, where Theorem 4.4.1 is valid, shrinks as $\varepsilon \rightarrow 0$; see also the discussion near (4.38) below.

Proof. (of Theorem 4.4.1) By Theorem 4.2.5, there exists a smooth change of coordinates that transforms the system to

$$\begin{aligned} \frac{d\xi}{dt} &= \xi' = \eta_1 \pm \xi^2 + \mathcal{O}(\xi^3, \xi\eta, \eta^2, \varepsilon), \\ \frac{d\eta}{dt} &= \eta' = \varepsilon(\pm 1 + \mathcal{O}(\xi, \eta, \varepsilon)). \end{aligned} \quad (4.31)$$

Using $(\xi, \eta, t) = (\varepsilon^{1/3} X, \varepsilon^{2/3} Y, \varepsilon^{-1/3} T)$ in (4.31) involves a direct computation:

$$\begin{aligned} \frac{dX}{dT} &= \eta_1 \pm \xi^2 + \frac{1}{\varepsilon^{2/3}} \mathcal{O}(\varepsilon X^3, \varepsilon^{4/3} Y^2, \varepsilon) = \eta_1 \pm \xi^2 + \mathcal{O}(\varepsilon^{1/3}), \\ \frac{dY}{dT} &= \pm 1 + \mathcal{O}(\varepsilon^{1/3} X, \varepsilon^{2/3} Y, \varepsilon) = \pm 1 + \mathcal{O}(\varepsilon^{1/3}), \end{aligned}$$

where $\varepsilon \ll \varepsilon^{2/3} \ll \varepsilon^{1/3}$, since $\varepsilon \rightarrow 0$ has been used. \square

In some dynamical regimes (see Section 5.4 and Section 7.4), the precise size of the error term in ε is not of interest, and one can simply drop it.

Definition 4.4.2. The truncated system from Theorem 4.4.1 given by

$$\begin{aligned} \frac{dX}{dT} &= X^2 \pm Y, \\ \frac{dY}{dT} &= \pm 1, \end{aligned}$$

is called the **system of first approximation** for a generic fold point in a $(1, 1)$ -fast–slow system.

Similar results exist for $(1, 2)$ -fast–slow systems.

Theorem 4.4.3 ([Arn94]). *There exists a coordinate change such that a (1, 2)-fast–slow system in an open neighborhood of a curve of nondegenerate fold points L that satisfy the normal switching condition can be transformed into a system on a single time scale,*

$$\begin{aligned}\frac{dX}{dT} &= X^2 \pm Y_1 + \mathcal{O}(\varepsilon^{1/3}), \\ \frac{dY_1}{dT} &= \pm 1 + \mathcal{O}(\varepsilon^{1/3}), \\ \frac{dY_2}{dT} &= 0 + \mathcal{O}(\varepsilon),\end{aligned}\tag{4.32}$$

since $\varepsilon \rightarrow 0$ defined in an $\mathcal{O}(1)$ region near $(X, Y_1, Y_2) = (0, 0, Y_2)$ with $Y_2 \in I$ for some interval I .

Proof. (Sketch, [SW04]) The result follows from Theorem 4.3.1 and the transformation

$$(\xi, \eta_1, \eta_2, \tau) \mapsto (\varepsilon^{1/3}X, \varepsilon^{2/3}Y_1, Y_2, \varepsilon^{2/3}T),\tag{4.33}$$

which is just a rescaling. \square

The scaling (4.33) leaves the second slow variable unchanged. The slow flow crosses the fold curve transversally, as prescribed by the normal switching condition, and this should lead to a situation similar to the (1, 1)-fast–slow generic fold. However, at each point on the fold curve, one can aim for a finer analysis that takes into account the terms in the map g_2 from Theorem 4.3.1. In (4.32), these terms are hidden in $\mathcal{O}(\varepsilon)$ in the Y_2 equation.

Alternative rescalings can be applied if one just focuses on a single point $P \in L$. For example, consider the system

$$\begin{aligned}\varepsilon \frac{dx}{d\tau} &= x^2 + y_1, \\ \frac{dy_1}{d\tau} &= -1, \\ \frac{dy_2}{d\tau} &= k_x x + k_y y_1 + k_\varepsilon \varepsilon,\end{aligned}\tag{4.34}$$

near $(x, y_1, y_2) = (0, 0, 0)$, where the normal switching condition for (4.34) is certainly satisfied and k_x , k_y , and k_ε are constants. Now consider the rescaling

$$(x, y_1, y_2, \tau) \mapsto (\varepsilon^{1/3}X, \varepsilon^{2/3}Y_1, \varepsilon Y_2, \varepsilon^{2/3}T)\tag{4.35}$$

and apply it to (4.34). This yields

$$\begin{aligned}\frac{dX}{dT} &= X^2 + Y_1, \\ \frac{dY_1}{dT} &= -1, \\ \frac{dY_2}{dT} &= k_x X + \mathcal{O}(\varepsilon^{1/3}).\end{aligned}\tag{4.36}$$

This calculation hints at the fact that the system near a nondegenerate fold point satisfying the normal switching condition can be simplified into a form slightly different from (4.32).

Theorem 4.4.4. ([Arn94]) There exists a coordinate change such that a “generic” $(1, 2)$ -fast–slow system near a nondegenerate fold point P that satisfies the normal switching condition can be transformed into a system on a single time scale,

$$\begin{aligned}\frac{dX}{dT} &= X^2 - Y_1 + \mathcal{O}(\varepsilon^{1/3}), \\ \frac{dY_1}{dT} &= -1 + \mathcal{O}(\varepsilon^{1/3}), \\ \frac{dY_2}{dT} &= -X + \mathcal{O}(\varepsilon^{1/3}),\end{aligned}\tag{4.37}$$

as $\varepsilon \rightarrow 0$ defined in an $\mathcal{O}(1)$ region near $(X, Y_1, Y_2) = (0, 0, 0)$.

The genericity condition required in Theorem 4.4.4 is technically involved; it is detailed in [Arn94]. However, the example (4.34) shows that it relates to a genericity condition for the slow flow, since for $k_x = 0$, the systems (4.36) and (4.32) may not have the same lowest-order ε -dependent error terms.

Definition 4.4.5. The truncated system obtained from Theorem 4.4.4 and given by

$$\begin{aligned}\frac{dX}{dT} &= X^2 - Y_1, \\ \frac{dY_1}{dT} &= -1, \\ \frac{dY_2}{dT} &= -X,\end{aligned}$$

is called a **system of first approximation** for a nondegenerate fold point satisfying the normal switching condition in a $(1, 2)$ -fast–slow system.

From the previous calculations, several natural questions arise. The first problem is to find a good geometric interpretation for the coordinate changes. Since all the original (x, y) -variables are scaled by some negative power of ε , one can view the coordinate change as a **zoom** or **magnifying glass** near the fold point. For example, consider the fast coordinate

$$x = \varepsilon^{1/3} X \quad \Rightarrow \quad x\varepsilon^{-1/3} = X \quad \Rightarrow x = \mathcal{O}(1) \text{ implies } X = \mathcal{O}(\varepsilon^{-1/3}).\tag{4.38}$$

In Chapter 7, we are going to discuss the blowup method, whereby the rescaling strategy and systems of first approximation will reappear.

The second natural question arising from the previous discussion is this: what happens when the normal switching condition (4.24) fails? Such failure will happen generically at isolated points on the fold curve. Do we still have a nice theory of normal forms and systems of first approximation? Sections 8.5, 8.6, 13.2, and 13.3 cover this situation in some detail.

4.5 A Note on Linear Systems

So far, we have applied simplifying transformations to fast–slow systems that were given in a standard form

$$\begin{aligned}\varepsilon \frac{dx}{d\tau} &= \varepsilon \dot{x} = f(x, y, \varepsilon), \\ \frac{dy}{d\tau} &= \dot{y} = g(x, y, \varepsilon).\end{aligned}\tag{4.39}$$

Obviously, (4.39) is convenient, but not all systems may be directly brought into this form. In this section, we are going to solve this problem for linear systems. For nonlinear systems, we refer the reader to Sections 11.1–11.4 and 20.2.

As a starting point, consider a general linear system of the form

$$\varepsilon \frac{dz}{d\tau} = \varepsilon \dot{z} = F(\varepsilon)z, \quad (4.40)$$

where $z \in \mathbb{R}^N$ and $F(\varepsilon)$ is an $N \times N$ matrix. For notational convenience, a decomposition of the form $F(\varepsilon) = F_0 + \varepsilon F_1(\varepsilon)$ is introduced. The goal is to find a coordinate change that identifies the fast and slow variables and brings (4.39) into the standard form

$$\begin{aligned} \varepsilon \dot{x} &= A_{11}(\varepsilon)x + \varepsilon A_{12}(\varepsilon)y, \\ \dot{y} &= A_{21}(\varepsilon)x + A_{22}(\varepsilon)y, \end{aligned} \quad (4.41)$$

where $A_{11}(0) \in \mathbb{R}^{m \times m}$ is nonsingular, $A_{12}(\varepsilon) \in \mathbb{R}^{m \times n}$, $A_{21}(\varepsilon) \in \mathbb{R}^{n \times m}$, and $A_{22}(\varepsilon) \in \mathbb{R}^{n \times n}$. If we can achieve the transformation to (4.41), it will follow from the invertibility of $A_{11}(0)$ that the variables $x \in \mathbb{R}^m$ are fast and the variables $y \in \mathbb{R}^n$ are slow.

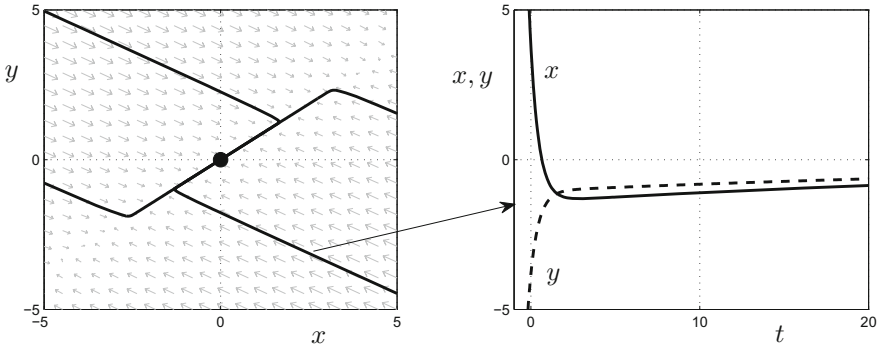


Figure 4.4: Phase portrait and time series for (4.42) with $\varepsilon = 0.05$. (a) Four trajectories are shown converging to the stable equilibrium $(0, 0)$ as $t \rightarrow \infty$. (b) Time series for x (solid curve) and y (dashed curve). Both variables show a clear multiple time scale structure with an initial fast transient.

Example 4.5.1. As a simple example, consider $N = 2$ and the linear system

$$\frac{dz}{dt} = z' = \underbrace{\begin{pmatrix} -1.2 & 1.6 \\ 0.6 & -0.8 \end{pmatrix}}_{=:F_0} z + \varepsilon \underbrace{\begin{pmatrix} 0.2 & -0.6 \\ 0.4 & -1.2 \end{pmatrix}}_{=:F_1} z, \quad (4.42)$$

where $t = \tau/\varepsilon$. Clearly, the system (4.42) is not in a standard form. Figure 4.4(a) shows the phase portrait of (4.42), and Figure 4.4(b) shows time series for one trajectory. The fast–slow system structure is clearly visible in the

phase portrait as well as in the time series. Calculating the eigenvalues of F_0 , we find one eigenvalue -2 and one zero eigenvalue. This gives an algebraic hint that the system has a fast–slow structure. ♦

We continue with the general case of the system (4.40). Suppose the dimension of the null space of F_0 is n , and assume that there exists a decomposition

$$\text{range}(F_0) \oplus \text{nullspace}(F_0) = \mathbb{R}^{m+n}, \quad N = m + n. \quad (4.43)$$

This should remind the reader of the classical splitting for Fenichel theory from Section 2.3. The helpful difference for linear systems is that one can construct a normal form structure globally in a completely algebraic and easily computable way. First, choose m linearly independent vectors orthogonal to the null space of F_0 and use them as rows for a matrix $Q \in \mathbb{R}^{m \times (m+n)}$, so that

$$\nu \in \text{nullspace}(F_0) \Leftrightarrow F_0\nu = 0 \Leftrightarrow Q\nu = 0.$$

Example 4.5.2. (Example 4.5.1 continued) A direct computation shows that

$$\text{nullspace}(F_0) = \text{span}((-0.8, -0.6)^\top).$$

A vector orthogonal to this 1-dimensional subspace is $(0.6, -0.8)^\top$, so that $Q = (0.6, -0.8) : \mathbb{R}^2 \rightarrow \mathbb{R}$. Observe from Figure 4.4(a) that $x := Q\nu$ looks like a good candidate for a fast variable to reach the form (4.41), since x vanishes on the line that we would guess is the critical manifold. ♦

Therefore, $x = Q\nu$ is a good candidate for the m fast variables. It is natural to consider the matrix $P \in \mathbb{R}^{n \times (m+n)}$ constructed from row vectors in the left null space of F_0 , so that $PF_0 = 0$. The guess for the n slow variables is $y = P\nu$.

Theorem 4.5.3 ([KKO99]). *Suppose $F(0) = F_0$ satisfies (4.43). Then the coordinate change*

$$x = Q\nu, \quad y = P\nu, \quad T := \begin{pmatrix} Q \\ P \end{pmatrix} \in \mathbb{R}^{(m+n) \times (m+n)}$$

transforms the system (4.40) into the normal form

$$\begin{aligned} \varepsilon \dot{x} &= A_{11}(\varepsilon)x + \varepsilon A_{12}(\varepsilon)y, \\ \dot{y} &= A_{21}(\varepsilon)x + A_{22}(\varepsilon)y, \end{aligned} \quad (4.44)$$

where $A_{11}(0) \in \mathbb{R}^{m \times m}$ is nonsingular, $A_{12}(\varepsilon) \in \mathbb{R}^{m \times n}$, $A_{21}(\varepsilon) \in \mathbb{R}^{n \times m}$, and $A_{22}(\varepsilon) \in \mathbb{R}^{n \times n}$.

Proof. Let $(x, y)^\top = Tz$ and observe that $T^{-1} = (V \ W)$, where the columns of V and W are bases of the range and null space of F_0 , respectively. Then one computes

$$\begin{aligned} \begin{pmatrix} \dot{x} \\ \dot{y} \end{pmatrix} &= T \left(\frac{1}{\varepsilon} F_0 + F_1(\varepsilon) \right) T^{-1} \begin{pmatrix} x \\ y \end{pmatrix} \\ &= \begin{pmatrix} \frac{1}{\varepsilon} QF_0V + QF_1(\varepsilon)V & QF_1(\varepsilon)W \\ PF_1(\varepsilon)V & PF_1(\varepsilon)W \end{pmatrix} \begin{pmatrix} x \\ y \end{pmatrix}. \end{aligned}$$

Hence, let $A_{11}(\varepsilon) := QF_0V + \varepsilon QF_1(\varepsilon)V$, $A_{12}(\varepsilon) := QF_1(\varepsilon)W$, $A_{21}(\varepsilon) := PF_1(\varepsilon)V$, and $A_{22}(\varepsilon) := PF_1(\varepsilon)W$. The matrix $A_{11}(0) = QF_0V\mathbb{R}^{m \times m}$ is nonsingular by construction, and it is the only nonzero block of TF_0T^{-1} . \square

Exercise 4.5.4. Finish the computations from Examples 4.5.1–4.5.2 by computing the normal form (4.44) for (4.42). \diamond

The main lesson from Theorem 4.5.3 is that it can pay off to consider a linear(ized) system, identify a small parameter, and consider the eigenvalue structure of the singular limit system. This can yield important clues as to whether the system has a multiple time scale structure. Furthermore, it often helps to identify the fast and slow variables.

4.6 References

Section 4.1: This section is based mostly on [Fen79, Jon95]; see also [KJ01, Kap99]. The idea of normal form transformations for the normally hyperbolic case is always to simplify the algebraic expressions and to separate the variables [Rob08] as much as possible. However, the way in which we pursued the topic, according to Fenichel, is not the only possibility [Oka87]. The main problems tend to arise on the nonlinear level [VCCD06], although the linear theory is already highly nontrivial [BP91].

Section 4.2: The section mainly follows [MR80], but the ideas can already be found in classical (static) bifurcation theory [Kuz04]. The case of one fast variable can also be partially covered using singularity theory [Arn92, BG92, GG74, Lu76], which relates to classical catastrophe theory [Gil93, Pos78, Sau80, WP74, Zee77]. There are also many books available that contain background on normal forms for the single-time-scale case [GH83, Mur02a, Nay11]. The method of multiple scales [ZY05, ZY06], as well as other asymptotic analysis methods, can also be used to derive normal forms; see Chapter 9.

Section 4.3: This section is based on [Wec98, SW04]. Note that not only are normal form transformations relevant for mathematical analysis, but they can be very useful in applications as well e.g., in chemistry [KCD98]. Another direction to consider is fast–slow systems with additional structure such as Hamiltonian systems and the associated normal forms [ACV13]. There seems to be relatively little work on normal forms for symmetric systems [GS85, GSS85] with a multiple time scale structure.

Section 4.4: The idea of first approximation systems can be found in many contexts [Arn94]; we based the fold case on [Ily97]. The idea that the first-approximation system plays a key role in the dynamics near singularities will reappear several times throughout this book; see, e.g., Chapter 8.

Section 4.5: This section has been modified from [KKO99], which is also one of the main reference books on fast–slow systems in control theory; see [Don83, GPS90] for other books with different perspectives. It is particularly useful to have a standard form [SHK89] available for linear systems [Cam78, CR79, DV83b] in control theory [CD96], but one may also consider the nonstandard-form case [Kha89]. Essentially, the goal is to group the variables in some form [SS83, SW83]. In this context, even the size of ε [Abe86a, SD93, Sha04] and the case of more than two time scales [Kha79, LS83] have been considered. Key themes have been feedback

control [CK78b, O'R79a, O'R80, Sab87, San83b], optimal control problems in various versions [DG79, GG97, WK73, BD86], and the associated asymptotic solutions [O'M75, OK75, O'M72b, O'M72a, O'M76a, San74, San75]; often, the focus has been on the linear case [Por74b, Por74a, Por77, Por76, SK69a].

Since we do not cover fast–slow systems control theory in this book, we provide a very brief literature survey here. Several other surveys are also available [DK06, KJS76, Kok84, Nai02, NR85, O'M78b, SOK84, VD86]. For general background on control theory, we refer to [Son98, Son04]. The idea that singularly perturbed systems are natural in control theory [KH75, San78] is quite old [CK76, ISKB92, MK88]. One interesting concept that appears in this context is D-stability [Abe86b, Abe85a, EA86, vV81]. Also, there is a natural relation to classical singularly perturbed BVPs [FK76], to averaging [Gai04, Ser13], to boundary layers [O'M74], and to the geometric approach via slow manifolds [KRP85, RK86, SO88, SO87]. Another nice topic in this context is matrix Riccati equations [CG00, Gaj88, GG88, HK71, KBG99, Kok75, KY72, KCG10, SGS92, YK73], their relation to fast–slow systems [NP87, NP88], and to asymptotic solutions [Phi83]. Furthermore, there are many fast–slow stochastic control systems [AB02, Ben84, BB87, BG07b, Gaj86, GK86, HK77, KR96, KP91b, KP91a, KG84, PK81, Sin82, TS77] in which noisy fluctuations may also occur in the time scale [GT03].

There are many control theory topics in which the fast–slow structure helps to simplify the problem, such as algorithmic aspects [BG88, QG92], asymptotics [Cho78, Cho77, Cho79, CK78a, FG76], attainable sets [KP97], closed-loop optimization [FFH97], composite control [KK86, KH89, SK85a, Suz81], descriptor systems [Fri01], difference equations [Bla81, LK84, LK85a, Mah82, MCS86, Phi80, Vor08, VS06], distribution theory [Fra82], fast subsystem oscillations [Gai92, Vig97], feedback control [CPS90, MC85, SPC92], frequency-domain methods [PS75a, PS75b], functional optimization [AG97b], global Lyapunov stability [SK84], H-infinity control [KC92, LG00, OSS92, SD99], high-gain nonlinear systems [Mar85, YKU77], high-gain observer stabilization [AK00], hybrid systems [FGH01], input–output relations [MS84], input-to-state stability [Chr00, TMN03], iterative algorithms [DK84, Jav78a, JK77], measures in bang-bang control [Art05, Art09], multimodeling [Kok81], nonautonomous systems [O'R79b, San77], nonlinear optimal control [Dmi78, Shi83], norm-bounded uncertainties [Fri06a], optimal control Hamiltonian systems [AG00, GL01, RM00], quadratic cost functions [SS87], quadratic regulator problems [SW85], reachable sets [Don92, DS88, GO10], reduced controllers [SR88], reduced-order models [IK85], Riccati gain methods [Kun76], sampling [BDMNC96], smoothing problems [AH78], stabilization of nonlinear systems [DH82, Kho89, SK69b, Vid85], and tracking problems [TS97]. The range of applications is extremely broad as well, including the aircraft time-to-climb problem [Ard80], distributed parameter systems [Bal82], manufacturing systems [Son93], synchronous machine models [AZSPS82], and various industrial applications [KS68].

Chapter 5

Direct Asymptotic Methods

In this chapter, we shall just attempt to compute asymptotic expansions for fast–slow systems by more or less brute force. It is a very instructive technique: just substitute an asymptotic expansion for the solution and see what happens. In other words, where does such a substitution seem to give a good approximation, and where are modifications required?

Section 5.1 distinguishes regular and singular perturbation problems and states the elementary results for the regular case. In Section 5.2, we introduce relaxation oscillations, which provide an excellent motivational, and surprisingly complicated, example of how asymptotic expansions can be used in fast–slow systems. The difficulty is that fold points are involved. Section 5.3 treats the normally hyperbolic region approaching a fold, which can be analyzed asymptotically by direct substitution of an asymptotic series. Near a fold, one has to piece different expansions together. The general results are stated in Section 5.4. A more abstract introduction to this approach is given in Section 9.1. In Section 5.5, the results from Sections 5.3 and 5.4 are then combined to state the expansion of the relaxation oscillation period for the van der Pol equation.

Background: No additional background is required.

5.1 Elementary Results

The basic definitions from asymptotic analysis and perturbation methods are given in Section 1.6. Here we start with a general (i.e., not necessarily fast–slow) system of ODEs,

$$\frac{dz}{dt} = z' = F(z; \varepsilon), \quad (5.1)$$

with $z \in \mathbb{R}^N$ and a small parameter $0 < \varepsilon \ll 1$. The flow of (5.1) will be denoted by $\phi(z, t; \varepsilon)$. Assume that it is defined and sufficiently smooth in a domain $\mathcal{D} \subset \mathbb{R}^N$. The limiting problem as $\varepsilon \rightarrow 0$ associated with (5.1) is

$$z' = F(z, 0). \quad (5.2)$$

The flow of (5.2) is denoted by $\phi_0(z, t)$. We assume that both flows are defined at least for some time $t \in [0, T]$ when the initial condition z is in \mathcal{D} . The following classical result relates the flow for $\varepsilon = 0$ to a small perturbation as defined by (5.1).

Theorem 5.1.1 ([MR80]; see also [Was02]). *Fix an initial condition $z \in \mathcal{D}$. Define $\mathcal{D}_\varepsilon := \mathcal{D} \times [0, \varepsilon_1]$ for ε_1 sufficiently small and assume $F \in C^k(\mathcal{D}_\varepsilon, \mathbb{R}^N)$. Then the solution of (5.1) has a representation*

$$\phi(z, t; \varepsilon) = \phi_0(z, t) + \varepsilon \phi_1(z, t) + \cdots + \varepsilon^{k-1} \phi_{k-1}(z, t) + \mathcal{O}(\varepsilon^k) \quad (5.3)$$

uniformly on $[0, T]$ as $\varepsilon \rightarrow 0$. If F is analytic in \mathcal{D}_ε , there exists a uniformly convergent series on $[0, T]$,

$$\phi(z, t; \varepsilon) = \sum_{k=0}^{\infty} \phi_k(z, t) \varepsilon^k. \quad (5.4)$$

If (5.4) holds, then we certainly have an asymptotic series

$$\phi(z, t; \varepsilon) \sim \sum_{k=0}^{\infty} \phi_k(z, t) \varepsilon^k$$

for the asymptotic sequence $\{\varepsilon^k\}_{k=0}^{\infty}$ uniformly as $\varepsilon \rightarrow 0$ on $[0, T]$, i.e., we have a regular perturbation expansion of the solution. At first, Theorem 5.1.1 looks like the solution to all multiple time scale problems, but unfortunately, the situation is often much more complicated. Consider a fast–slow system on the slow time scale

$$\begin{aligned} \varepsilon \frac{dx}{d\tau} &= \varepsilon \dot{x} = f(x, y, \varepsilon), \\ \frac{dy}{d\tau} &= \dot{y} = g(x, y, \varepsilon). \end{aligned} \quad (5.5)$$

This formulation is not amenable to Theorem 5.1.1, since on dividing (5.5) by ε , we end up with

$$F(z; \varepsilon) = \begin{pmatrix} \frac{1}{\varepsilon} f(x, y, \varepsilon) \\ g(x, y, \varepsilon) \end{pmatrix}.$$

In general, this vector field has no limit for $\varepsilon \rightarrow 0$ due to the term $\frac{1}{\varepsilon}$. One is forced to transform (5.5) into the fast time $t = \tau/\varepsilon$, which yields

$$\begin{aligned} \frac{dx}{dt} &= x' = f(x, y, \varepsilon), \\ \frac{dy}{dt} &= y' = \varepsilon g(x, y, \varepsilon). \end{aligned} \quad (5.6)$$

Theorem 5.1.1 applies to (5.6) on an interval $t \in [0, t_0] = I$. Transforming I back to the slow time scale yields the validity of the asymptotic series for $\tau \in [0, \varepsilon t_0]$, but $\varepsilon t_0 \rightarrow 0$ as $\varepsilon \rightarrow 0$. Therefore, Theorem 5.1.1 does not help us to determine an asymptotic solution of a general fast–slow system.

We shall now present two examples to highlight a key difference between problems in which a direct asymptotic expansion works and those in which it does not.

Example 5.1.2 ([Hol95]). Consider the second-order ODE with $0 < \delta \ll 1$

$$\frac{d^2u}{dt^2} = u'' = -\frac{1}{(1 + \delta u)^2} \quad \text{for } t \geq 0 \text{ and } u(0) = 0, u'(0) = 1. \quad (5.7)$$

We look for a formal asymptotic expansion for the solution $u(t)$ as $\delta \rightarrow 0$. Assume that the solution of (5.7) has an asymptotic expansion of the form

$$u(t) = u_0(t) + \delta u_1(t) + \mathcal{O}(\delta^2). \quad (5.8)$$

Our goal is to find the coefficient functions $u_i(t)$. Substituting (5.8) into (5.7) yields

$$\begin{aligned} u_0''(t) + \delta u_1''(t) + \mathcal{O}(\delta^2) &= (1 + \delta(u_0(t) + \dots))^{-2}, \\ &= -1 + 2\delta u_0(t) + \mathcal{O}(\delta^2), \end{aligned} \quad (5.9)$$

where $(1 + z)^{-2} \sim 1 - 2z$ as $z \rightarrow 0$ has been used. The initial conditions become

$$u_0(0) + \delta u_1(0) + \mathcal{O}(\delta^2) = 0 \quad \text{and} \quad u_0'(0) + \delta u_1'(0) + \mathcal{O}(\delta^2) = 1. \quad (5.10)$$

How do we continue? The standard idea is that in (5.9) and (5.10), terms with different powers of δ should match. Collecting terms of order $\mathcal{O}(\delta^0) = \mathcal{O}(1)$ leads to

$$u_0''(t) = -1 \quad \text{with } u_0(0) = 0 \text{ and } u_0'(0) = 1. \quad (5.11)$$

This equation can be solved explicitly and has a solution $u_0(t) = -\frac{1}{2}t^2 + t$. Looking at terms of order $\mathcal{O}(\delta)$ in (5.9) and (5.10), ones finds that

$$u_1''(t) = 2u_0(t) = -t^2 + 2t \quad \text{with } u_1(0) = 0 \text{ and } u_1'(0) = 0. \quad (5.12)$$

It is an easy exercise to show that this is solved by $u_1(t) = \frac{1}{3}t^3 - \frac{1}{12}t^4$. Therefore, we expect that the asymptotic expansion of $u(t)$ is

$$u(t) = -\frac{1}{2}t^2 + t + \delta \left(\frac{1}{3}t^3 - \frac{1}{12}t^4 \right) + \mathcal{O}(\delta^2). \quad (5.13)$$

It can be shown that (5.13) is indeed an asymptotic solution as $\delta \rightarrow 0$. We compare the zeroth-order approximation $u_0(t)$ and the first-order approximation $u_0(t) + \delta u_1(t)$ with a numerical solution in Figure 5.1.

The first-order approximation is virtually indistinguishable from the numerical solution. The advantage in comparison to numerical computation is that we have an explicit formula for $u(t)$ for small δ . ♦

The procedure in Example 5.1.2 is typical for the solution of differential equations by asymptotic methods. One substitutes a formal asymptotic series into the differential equation, collects terms of equal order, and attempts to determine the coefficients of the series. Then one can try to prove that the formal series is indeed asymptotic. Let us contrast Example 5.7 with a multiple time scales problem.

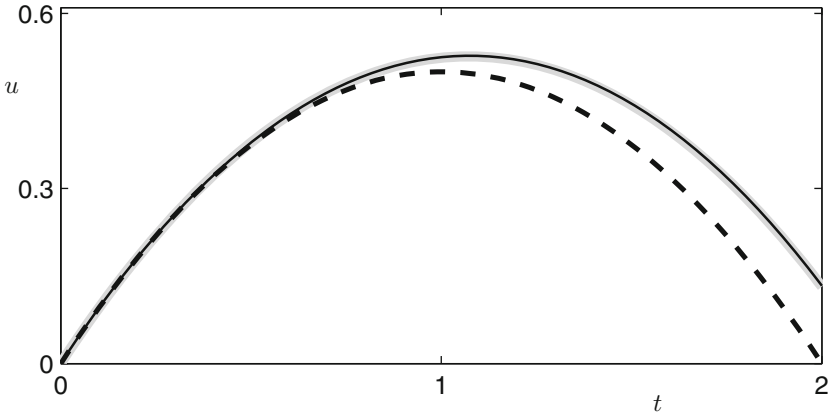


Figure 5.1: Comparison of solutions for (5.7) with $\delta = 0.1$. The numerical solution (thick gray), the zeroth-order asymptotic solution $u_0(t)$ (dashed black), and first-order asymptotic solution $u_0(t) + \delta u_1(t)$ (thin solid black) curves are shown.

Example 5.1.3. Consider the classical linear two-point boundary value problem (BVP)

$$\varepsilon \frac{d^2y}{d\tau^2} + y = \varepsilon \ddot{y} + y = 0 \quad \text{with } y(0) = A \text{ and } y(1) = B, \quad (5.14)$$

which has already been discussed in Example 4.1.4 for $A = 1$ and $B = -1$. Recall from Example 4.1.4 that (5.14) can be viewed as a $(1, 1)$ -fast-slow system. Here, we attempt to find an asymptotic series solution to (5.14) by the same method as in Example 5.1.2. Hence, let $y(\tau) = y_0(\tau) + \varepsilon y_1(\tau) + \mathcal{O}(\varepsilon^2)$, and substitute this expansion into equation (5.14). Then

$$\varepsilon \ddot{y}_0 + y_0 + \varepsilon y_1 + \mathcal{O}(\varepsilon^2) = 0. \quad (5.15)$$

The lowest-order term in (5.15) is $\mathcal{O}(1)$, and it yields the equation $y_0(\tau) \equiv 0$. Substituting this back into (5.15) and collecting the $\mathcal{O}(\varepsilon)$ terms, we have $y_1(\tau) \equiv 0$. Hence, this procedure has not gone well. In fact, it is going nowhere, and we get only an asymptotic sequence of the form

$$y(\tau) \sim 0 \quad \text{as } \varepsilon \rightarrow 0. \quad (5.16)$$

This solution is obviously false: take, for example, $A = 1$ and $B = -1$; then (5.16) does not satisfy the boundary conditions. ♦

Example 5.1.3 shows the frequent case in perturbation theory that the problems to be solved at different orders to determine the coefficients are not of the same type as the original problem, i.e., in Example 5.1.3, we ended up with algebraic equations instead of a second-order ODE when trying to perturb the lowest-order solution.

It would be nice if we could group all perturbation problems into classes “regular” and “singular.” Unfortunately, there is no universally accepted definition, and we shall list a few formal as well as informal approaches.

Definition 5.1.4. A differential equation problem involving a small parameter $0 < \varepsilon \ll 1$ can be called a **singular perturbation problem** under one of the following definitions:

- (D1) The asymptotic series is not a power series in ε , or if it is, the power series has a vanishing radius of convergence.
- (D2) The solution does not converge uniformly as $\varepsilon \rightarrow 0$ to a singular solution for $\varepsilon = 0$.
- (D3) Substituting a power series expansion in ε yields problems of a “different type” from that of the original differential equation.
- (D4) Substituting a (regular) power series expansion in ε “fails,” i.e., a problem is singular if it is not regular.

Definitions (D3)–(D4) are good for practical purposes by trial and error, while (D1)–(D2) are sufficiently precise mathematical definitions for the purposes of this book. In the context of fast–slow systems (5.5)–(5.6), definition (D1) centers on a **regular asymptotic (or power series) series ansatz**

$$x \sim x_0 + x_1 \varepsilon + x_2 \varepsilon^2 + \dots, \quad y \sim y_0 + y_1 \varepsilon + y_2 \varepsilon^2 + \dots, \quad (5.17)$$

which fails either by being the wrong ansatz or because the series does not converge for any $\varepsilon > 0$. We shall see, e.g., in Section 5.3, that Fenichel’s theorem implies that solutions on normally hyperbolic slow manifolds can be obtained via (5.17). Perturbing the slow flow on a normally hyperbolic critical manifold is a regular perturbation problem. However, the vast majority of topics in the remainder of this book deal with how fast–slow systems give rise to singular perturbation problems.

5.2 Basics of Relaxation Oscillations

We know from Section 3.1 that trajectories of the slow flow on a normally hyperbolic critical manifold C_0 are going to be good approximations to the full fast–slow system with $0 < \varepsilon \ll 1$. We also defined singularities of C_0 as well as candidate orbits and considered examples in Section 3.3. In this section, we introduce one of the most important classes of periodic orbits in fast–slow systems consisting of passages near singular as well as regular points on C_0 .

Example 5.2.1. Recall from Section 1.3 that the unforced van der Pol's equation is given by

$$\begin{cases} \varepsilon \frac{dx}{d\tau} = \varepsilon \dot{x} = y - \frac{x^3}{3} + x, \\ \frac{dy}{d\tau} = \dot{y} = -x. \end{cases} \quad (5.18)$$

The critical manifold is $C_0 = \{(x, y) \in \mathbb{R}^2 : y = \frac{x^3}{3} - x\}$. It has two fold points given by $P_{\pm} = (\pm 1, \mp 2/3)$, which split C_0 into three normally hyperbolic parts,

$$C_0^{a-} = C_0 \cap \{x < -1\}, \quad C_0^r = C_0 \cap \{-1 < x < 1\}, \quad C_0^{a+} = C_0 \cap \{x > 1\},$$

where $C_0^{a\pm}$ are attracting and C_0^r is repelling; see Figure 5.2.

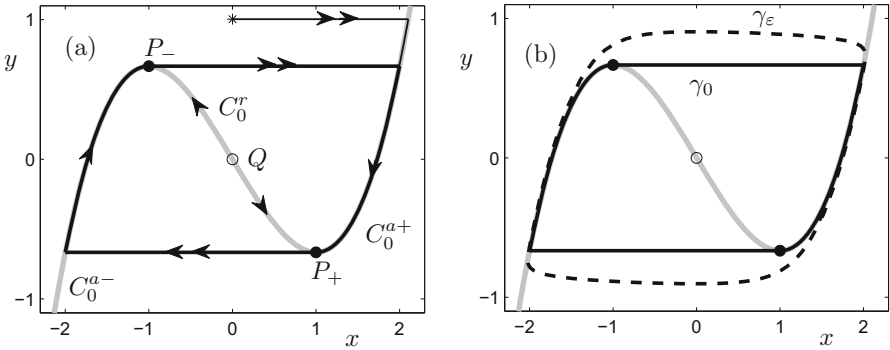


Figure 5.2: Illustration of relaxation oscillations in van der Pol's equation (5.18). (a) Fast–slow decomposition for $\varepsilon = 0$ with the critical manifold C_0 (gray), the two fold points P_{\pm} (black dots), the unstable equilibrium at the origin (black circle), a periodic candidate orbit (thick black), another candidate (thin black, started at the star), and fast and slow flows (double and single arrows) are shown. (b) Comparison of the periodic candidate relaxation oscillation orbit γ_0 with an actual attracting limit cycle relaxation oscillation γ_ε for $\varepsilon = 0.05$.

Let us try to understand from the singular limit $\varepsilon = 0$ what types of trajectories and attractors should exist for (5.18). The fast subsystem and slow subsystem are

$$\begin{cases} \frac{dx}{dt} = x' = y - \frac{x^3}{3} + x, \\ \frac{dy}{dt} = y' = 0, \end{cases} \quad \begin{cases} 0 = y - \frac{x^3}{3} + x, \\ \dot{y} = -x. \end{cases}$$

The fast subsystem has either one, two, or three equilibrium points depending on the value of y . For $|y| > 2/3$, corresponding to fast subsystems above and below the fold points at $y = \pm 2/3$, there is only one stable equilibrium point. For $|y| < 2/3$, the branch C_0^r consists of repelling equilibrium points for the fast subsystem. We conclude, therefore, that almost all candidate trajectories start with a fast motion toward C_0^{a+} or C_0^{a-} ; the thin black curve in Figure 5.2(a) is a typical example.

After reaching $C_0^{a\pm}$, a candidate orbit γ_0 continues via the slow flow $\dot{y} = -x$, which is obviously directed downward on C_0^{a+} and upward on C_0^{a-} . Suppose γ_0 continues via the slow flow on C_0^{a+} . Then it must reach the fold P_+ , since although the slow flow is not defined at P_+ , it is directed toward P_+ on C_0^{a+} and C_0^r . Therefore, the candidate **jumps** from P_+ in the fast subsystem at $y = -2/3$ to the **drop point** $(x, y) = (-2, -2/3) \in C_0^{a-}$. A similar analysis shows that γ_0 then continues to P_- and jumps back to $(x, y) = (2, 2/3) \in C_0^{a+}$. Hence, the candidate orbit is periodic. This is a prime example of a **relaxation oscillation** for $\varepsilon = 0$. Based on this analysis, we would guess that the relaxation oscillation candidate γ_0 persists as an attracting relaxation oscillation limit cycle γ_ε for $0 < \varepsilon \ll 1$; see Figure 5.2(b). ♦

Exercise 5.2.2. (a) Sketch the time series of a typical relaxation oscillation.
 (b) Numerically integrate van der Pol's equation (5.18) for $\varepsilon = 0.05, 0.1, 1$. Compare your results with the analysis in Example 5.2.1 and your sketch from part (a). ◇

One can try to phrase the previous observations in a definition.

Definition 5.2.3. A periodic solution γ_ε of a fast–slow system is called a **relaxation oscillation** if it converges (with respect to Hausdorff distance) in the singular limit $\varepsilon \rightarrow 0$ to a candidate γ_0 consisting of alternating fast and slow segments forming a closed loop.

As we shall see, particularly in Chapter 13, Definition 5.2.3 is slightly too general. It includes the classical case from Figure 5.2 but also other types of fast–slow oscillations that are traditionally not referred to as relaxation oscillations.

Definition 5.2.4. A periodic solution γ_ε of a fast–slow system is called a **simple relaxation oscillation** if it converges in the singular limit $\varepsilon \rightarrow 0$ to a candidate γ_0 consisting of alternating fast and slow segments in which jumps occur only at generic fold points and the drop points are normally hyperbolic.

We shall prove the existence and the stability of a simple relaxation oscillation using geometric methods in Sections 7.5 and 7.6. For the remainder of this chapter, we focus on direct asymptotic methods to establish an asymptotic series solution for relaxation oscillations with a view toward the unforced van der Pol equation. However, before the reader continues, it is an interesting exercise to think about relaxation oscillations in various examples.

Exercise/Project 5.2.5. Consider the periodically forced van der Pol equation (1.11) and sketch a relaxation oscillation candidate orbit. As a more advanced question, consider the examples in Chapter 20 and determine which ones have a relaxation oscillation candidate orbit. ◇

Exercise 5.2.6. Consider the $(1, 1)$ -fast–slow system suggested by Vidal and Françoise,

$$\begin{aligned}\varepsilon \dot{x} &= (1 - x^2)(x - y), \\ \dot{y} &= x(y + p_1)(p_2 - y),\end{aligned}\tag{5.19}$$

for parameters $p_1, p_2 > 0$. (a) Sketch a relaxation oscillation candidate orbit for (5.19). (b) Find a small perturbation of $(1 - x^2)(x - y)$ such that (5.19) has a simple relaxation oscillation candidate orbit. \diamond

5.3 Normally Hyperbolic Planar Systems

The discussion of van der Pol's equation in Example 5.2.1 and Figure 5.2(b) raises the question how to develop an asymptotic series for relaxation oscillations, in particular, an asymptotic series for the solution as well as the period depending upon $0 < \varepsilon \ll 1$. This section develops asymptotics for $(1, 1)$ -fast-slow systems

$$\begin{aligned} \varepsilon \frac{dx}{d\tau} &= \varepsilon \dot{x} = f(x, y), \\ \frac{dy}{d\tau} &= \dot{y} = g(x, y), \end{aligned} \quad (5.20)$$

near a normally hyperbolic attracting submanifold S_0 of the critical manifold $C_0 = \{(x, y) \in \mathbb{R}^2 : f(x, y) = 0\}$. In this section, it will always be assumed that

- f, g are sufficiently smooth;
- $g(x, y) \neq 0$ for all $(x, y) \in S_0$, so that the slow flow has no equilibria on S_0 , i.e., we may even assume without loss generality that $g(x, y) > 0$ on S_0 ;
- the initial condition $(x(0; \varepsilon), y(0; \varepsilon))$ for the trajectory $(x(\tau; \varepsilon), y(\tau; \varepsilon))$ to be approximated is $\mathcal{O}(e^{-K/\varepsilon})$ close to the attracting slow manifold S_ε .

A typical example for S_0 is a compact subset of C_0^{a+} or C_0^{a-} as in Example 5.2.1. Since $f_x(x, y)|_{S_0} < 0$ the implicit function theorem yields the existence of a function $x_0(y)$ such that

$$S_0 = \{(x, y) \in \mathbb{R}^2 : x = x_0(y) \text{ for } y \in (a, b)\} \quad (5.21)$$

for some interval (a, b) ; see Figure 5.2(a).

Fenichel's theorem and the implicit function theorem also yield the existence of a solution curve $x(y; \varepsilon)$ representing the solution $(x(t; \varepsilon), y(t; \varepsilon))$ as a graph over y . The disadvantage of this formulation is that finding $x(y; \varepsilon)$ does not provide an immediate time parameterization. The advantage is that in the planar case, we can rewrite (5.20) as a one-dimensional ODE,

$$\varepsilon \frac{dx}{dy} = \frac{f(x, y)}{g(x, y)} =: h(x, y), \quad (5.22)$$

since we have assumed that $g(x, y) \neq 0$ on S_0 , which extends by continuity to a suitable neighborhood of S_0 . Solving (5.22) using an asymptotic series allows for a convenient computation of $x(y; \varepsilon)$.

Theorem 5.3.1 ([MR80]). *There exists a formal series solution*

$$x(y; \varepsilon) = x_0(y) + x_1(y)\varepsilon + x_2(y)\varepsilon^2 + \dots \quad (5.23)$$

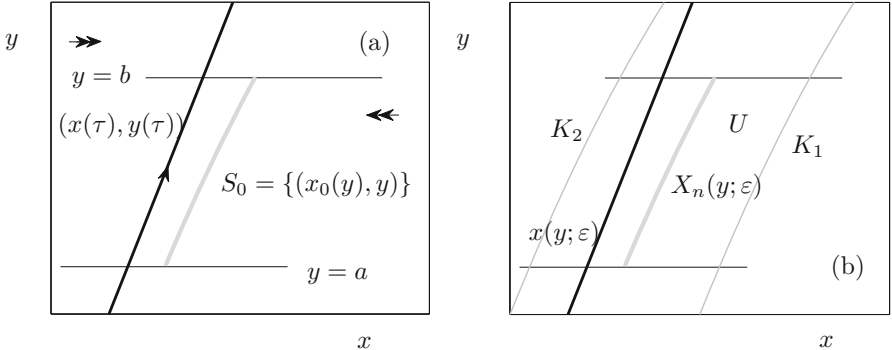


Figure 5.3: Asymptotics near a normally hyperbolic attracting manifold S_0 (thick gray). The true solution $(x(\tau), y(\tau)) = (x(\tau; \varepsilon), y(\tau; \varepsilon))$ (thick black) is shown as well. Both parts of the figure should be viewed abstractly, but they were generated using van der Pol's equation (5.18) with $\varepsilon = 0.05$ by zooming into a rectangle $[-1.6, -1.2] \times [0.38, 0.54]$. (a) Boundaries (thin black) in the definition (5.21) at $y = a$ and $y = b$ delimit the region of interest, chosen as $a = 0.4$ and $b = 0.5$. (b) Illustration for the proof of Theorem 5.3.3. The boundaries K_1 and K_2 as well as $X_n(y; \varepsilon)$ are shown for $n = 0$.

satisfying (5.22). Furthermore, all coefficient functions $x_i(y)$ can be calculated using function values and derivatives of f and g only.

Proof. We substitute (5.23) into equation (5.22). On the left-hand side, differentiate term by term, and on the right-hand side, use the multidimensional Taylor formula

$$F(z_0 + \sum_{n=1}^{\infty} z_n \varepsilon^n) = F(z_0) + \sum_{n=1}^{\infty} \varepsilon^n \sum_{k=1}^n \frac{F^{(k)}(z_0)}{k!} \sum_{i_1 + \dots + i_k = n, i_j \geq 1} z_{i_1} \cdots z_{i_k}.$$

To ensure that the series (5.23) formally satisfies (5.22), one can just compare coefficients for different powers of ε on each side. This results in the following equation for $\mathcal{O}(\varepsilon^0) = \mathcal{O}(1)$:

$$h(x_0(y), y) = 0.$$

Therefore, we have that $x_0(y)$ is not only the defining equation of S_0 , but also the (formal) zeroth-order approximation to $x(y; \varepsilon)$. For terms involving $\mathcal{O}(\varepsilon)$, a direct calculation shows that

$$x'_0(y) = x_1(y) h_x(x_0(y), y).$$

Since $x_0(y)$ is known already and

$$h_x(x_0(y), y) = \frac{f_x(x_0(y), y)}{g(x_0(y), y)} + \frac{h(x_0(y), y) g_x(x_0(y), y)}{g(x_0(y), y)} = \frac{f_x(x_0(y), y)}{g(x_0(y), y)},$$

it follows that $x_1(y)$ is explicitly given by

$$x_1(y) = \frac{x'_0(y)}{h_x(x_0(y), y)} = -\frac{f_y(x_0(y), y)g(x_0(y), y)}{(f_x(x_0(y), y))^2}. \quad (5.24)$$

This procedure can be continued, and the result is the following rather lengthy general formula for $n \geq 2$:

$$\begin{aligned} x_n(y) &= \frac{1}{f_x} \left[x'_{n-1}g - \sum_{v=2}^n \frac{1}{v!} \frac{\partial^v f}{\partial x^v} \sum_{i_1+\dots+i_v=n, i_j \geq 1} x_{i_1} \cdots x_{i_v} \right] + \quad (5.25) \\ &\quad \frac{1}{f_x} \left[\sum_{i+k=n-1, i \geq 0, k \geq 1} x'_i \sum_{v=1}^k \frac{1}{v!} \frac{\partial^v g}{\partial x^v} \sum_{i_1+\dots+i_v=k, i_j \geq 1} x_{i_1} \cdots x_{i_v} \right], \end{aligned}$$

where all functions are evaluated at $(x_0(y), y)$ or y ; see [MR80] for more details on the computation leading to (5.25). Obviously, the last formula depends only on function values and derivatives of f and g , which finishes the proof. \square

Fenichel's theorem 3.1.4 shows that for a normally hyperbolic part of the critical manifold, we can apply regular perturbation theory to compute the slow manifold, so that the formal series (5.23) is an asymptotic series. However, it is very instructive to prove directly that the formal series for $x(y; \varepsilon)$ is an asymptotic series as $\varepsilon \rightarrow 0$.

Lemma 5.3.2. *There exist constants M_n such that $|x_n(y)| \leq M_n$ for $y \in (a, b)$.*

Proof. The proof proceeds by induction. The base step is clear, since $x_0(y)$ describes a finite piece of the critical manifold, since $a, b < \pm\infty$. The induction step follows using the explicit expression for $x_n(y)$ given by (5.25) and smoothness of f and g . \square

Knowing the outcome of our discussion, we overload notation and write $x(y; \varepsilon)$ for the true solution of (5.22) with initial condition (\bar{x}, a) as well as the asymptotic series. Furthermore, it is helpful to introduce the partial sums

$$X_n(y; \varepsilon) := \sum_{k=0}^n x_k(y) \varepsilon^k.$$

Theorem 5.3.3 ([MR80]). *The formal power series developed in Theorem 5.3.1 is an asymptotic series of the solution $x(y; \varepsilon)$ to (5.22) as $\varepsilon \rightarrow 0$. More precisely, for each fixed $n \geq 0$,*

$$|X_n(y; \varepsilon) - x(y; \varepsilon)| < C_n \varepsilon^{n+1} \quad \text{for some constant } C_n > 0.$$

In particular, the inequality (5.3.3) implies that

$$|X_n(y; \varepsilon) - x(y; \varepsilon)| = o(\varepsilon^{n+1}) \quad \text{for any } n \in \mathbb{N}_0 \text{ as } \varepsilon \rightarrow 0,$$

which satisfies the definition of asymptotic expansion/series (see Definition 1.6.6).

Proof. (Sketch, [MR80]) Fix some $n \in \mathbb{N}_0$. The strategy of the proof is to trap the true solution curve $x(y; \varepsilon)$ in a neighborhood U of size $\mathcal{O}(\varepsilon^{n+1})$ of the curve described by $X_n(y; \varepsilon)$. We define this neighborhood by the two curves (with constants C_n to be chosen later)

$$\begin{aligned} K_1 &= \{(x, y) : x = X_n(y; \varepsilon) - C_n \varepsilon^{n+1}\} && \text{for } y \in (a, b), \\ K_2 &= \{(x, y) : x = X_n(y; \varepsilon) + C_n \varepsilon^{n+1}\} && \text{for } y \in (a, b), \end{aligned}$$

where one may take a as the x -coordinate of the initial condition. The neighborhood U is then given by restricting y to (a, b) . The situation is shown in Figure 5.3(b). If we can show that every trajectory starting inside U stays inside U for some choice of constant C_n , it will follow that

$$|x(y; \varepsilon) - X_n(y; \varepsilon)| < C_n \varepsilon^{n+1},$$

which will give the result. The first step is to prove that

$$\frac{dK_1}{d\tau} > 0 \quad \text{uniformly for all } (x, y) \in K_1.$$

This implies that the trajectory $x(y; \varepsilon)$ can never leave U through K_1 . By direct computation, it follows that on K_1 ,

$$\begin{aligned} \frac{dK_1}{d\tau} &= \frac{dx}{d\tau} - \frac{dy}{d\tau} \cdot \frac{dX_n}{dy} = \frac{1}{\varepsilon} f - g \frac{dX_n}{dy}, \\ &= \frac{g(X_n(y; \varepsilon - C_n \varepsilon^{n+1}), y)}{\varepsilon} \left[h(X_n(y; \varepsilon - C_n \varepsilon^{n+1}), y) - \varepsilon \frac{dX_n(y; \varepsilon)}{d\tau} \right]. \end{aligned} \quad (5.26)$$

Lemma 5.3.2 implies boundedness of the functions $x_n(y)$, so that Taylor's formula can be employed to simplify two terms:

$$\begin{aligned} g(X_n(y; \varepsilon - C_n \varepsilon^{n+1}), y) &= g(x_0(y), y) + \mathcal{O}(\varepsilon), \\ h(X_n(y; \varepsilon - C_n \varepsilon^{n+1}), y) &= h(X_n(y; \varepsilon), y) \\ &\quad - C_n \varepsilon^{n+1} h_x(x_0(y), y) + \mathcal{O}(\varepsilon^{n+2}). \end{aligned} \quad (5.27)$$

The remaining term involves a time derivative of X_n , which can be constructed by a similar iterative process to that by which X_n itself was constructed. The result turns out to be

$$\varepsilon \frac{dX_n(y; \varepsilon)}{dy} = h(X_n(y; \varepsilon), y) + \varepsilon^{n+1} x_{n+1}(y) h_x(x_0(y), y) + \mathcal{O}(\varepsilon^{n+1}). \quad (5.28)$$

Substituting (5.27) and (5.28) back into (5.26) yields

$$\frac{dK_1}{d\tau} = -\varepsilon^n (C_n + x_{n+1}(y)) f_x(x_0(y), y) + \mathcal{O}(\varepsilon^{n+1}).$$

The first term in this expression determines its sign as $\varepsilon \rightarrow 0$. Using Lemma 5.3.2 again, we know that $|x_{n+1}(y)|$ is bounded. Since $f_x < 0$ in U by one of our initial assumptions, we can choose C_n large enough that

$$\frac{dK_1}{d\tau} > 0 \quad \text{uniformly on } K_1.$$

This implies, as can be seen after a bit of thought, that the true solution $x(y; \varepsilon)$ starting inside U cannot exit through K_1 . A similar argument gives that

$$\frac{dK_2}{d\tau} < 0 \quad \text{uniformly on } K_2.$$

Therefore, the solution must stay inside U . Since there are no equilibrium points of the slow flow inside U (since $g(x, y) > 0$), the trajectory eventually reaches $y = b$. This corresponds to the situation in Figure 5.3(b) and concludes the proof. \square

One very important insight from the previous discussion is that a normally hyperbolic critical manifold C_0 can be viewed as the **zeroth-order approximation** to a slow manifold C_ε . The last viewpoint holds not only in two dimensions. From an asymptotic analysis viewpoint, the trajectories on normally hyperbolic critical manifolds are single-term asymptotic expansions of solutions to the full system with $\varepsilon > 0$.

Example 5.3.4. We are going to apply the previous theory of asymptotic expansions to the unforced van der Pol equation

$$\begin{aligned} \varepsilon \dot{x} &= y - \frac{x^3}{3} + x = f(x, y), \\ \dot{y} &= -x = g(x, y). \end{aligned} \tag{5.29}$$

See Example 5.2.1 for details on the fast–slow decomposition of (5.29). Suppose we are interested in a solution starting near the stable part of the critical manifold C_0 to the right of the fold point $P_+ = (1, -2/3)$. This part C_0^{a+} of C_0 is given by the function

$$x_0(y) = \left(\frac{2}{3y + \sqrt{9y^2 - 4}} \right)^{1/3} + \left(\frac{3y + \sqrt{9y^2 - 4}}{2} \right)^{1/3}.$$

This is also the zeroth-order approximation to the trajectory. By (5.24), the first-order term is

$$x_1(y) = -\frac{f_y(x_0(y), y)g(x_0(y), y)}{(f_x(x_0(y), y))^2} = \dots = \frac{x_0(y)}{(1 - x_0(y)^2)^2}.$$

The first-order asymptotic expansion is

$$x(y; \varepsilon) = x_0(y) + x_1(y)\varepsilon + \mathcal{O}(\varepsilon^2).$$

We compare this curve to a solution obtained by numerical integration in Figure 5.4 for the case $\varepsilon = 0.01$. The result shows that the asymptotic expansion near the normally hyperbolic attracting part C_0^{a+} matches the numerical solution quite well but that it looks like a really poor approximation close to the fold point $P_+ = (1, -2/3)$. ♦

Exercise/Project 5.3.5. (a) Use Theorem 5.3.3 to compute one more term of the asymptotic expansion derived in the previous example. (b) Compare your results with numerical integration for $\varepsilon = 0.01$. What number of terms in the asymptotic expansion seems “optimal”? ◇

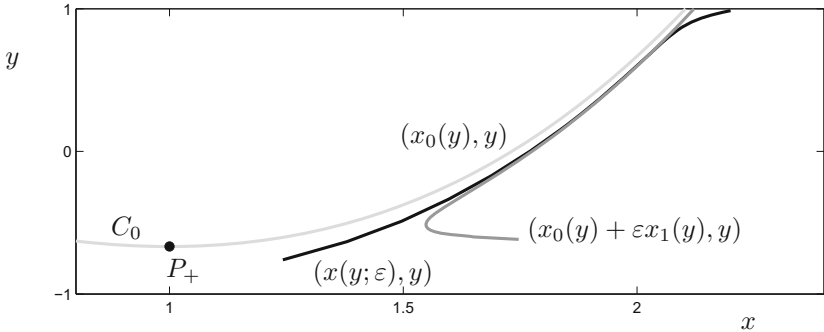


Figure 5.4: Comparison of numerical and asymptotic solutions to van der Pol's equation (5.29). The zeroth-order approximation C_0 (light gray), the first-order approximation (dark gray), the numerical solution (black), and the fold point P_+ (black dot) are shown.

5.4 Generic Folds in Planar Systems

Figure 5.4 indicates that we should not be able to use a regular expansion near a fold point. The next example gives a nice algebraic illustration of this observation.

Example 5.4.1. Consider the simple fold normal form

$$\begin{aligned} \varepsilon \frac{dx}{d\tau} &= \varepsilon \dot{x} = y + x^2, \\ \frac{dy}{d\tau} &= \dot{y} = 1, \end{aligned} \tag{5.30}$$

derived in Section 4.2. Clearly, $y(\tau) = \tau + y(0)$, so that (5.30) can also be viewed as a **nonautonomous** ODE,

$$\varepsilon \dot{x} = \tau + y(0) + x^2. \tag{5.31}$$

Substituting the ansatz $x(\tau; \varepsilon) = x_0(\tau) + x_1(\tau)\varepsilon + x_2(\tau)\varepsilon^2 + \mathcal{O}(\varepsilon^3)$ into (5.31) yields

$$\varepsilon \dot{x}_0 + \varepsilon^2 \dot{x}_1 + \mathcal{O}(\varepsilon^3) = \tau + y(0) + x_0^2 + 2x_0 x_1 \varepsilon + (2x_0 x_1 + x_1^2) \varepsilon^2 + \mathcal{O}(\varepsilon^3),$$

where we have omitted the argument τ from $x_j(\tau)$ for notational convenience. At order $\mathcal{O}(1)$, it follows that $x_0 = \pm\sqrt{-y(0) - \tau}$, and we select the negative square root for now, since it corresponds to the attracting critical manifold of (5.30); the calculations for the positive root are similar. At order $\mathcal{O}(\varepsilon)$, we obtain

$$\dot{x}_0 = 2x_0 x_1 \quad \Rightarrow \quad x_1(\tau) = \frac{1}{4(y(0) + \tau)}.$$

Proceeding to order $\mathcal{O}(\varepsilon^2)$ gives

$$\dot{x}_1 = 2x_0 x_2 + x_1^2 \quad \Rightarrow \quad x_2(\tau) = \frac{5}{32(-y(0) - \tau)^{5/2}}.$$

Therefore, the asymptotic expansion up to and including second order of the attracting normally hyperbolic slow manifold is

$$\begin{aligned} x(\tau; \varepsilon) &= -\sqrt{-y(0) - \tau} + \frac{\varepsilon}{4(y(0) + \tau)} + \frac{5\varepsilon^2}{32(-y(0) - \tau)^{5/2}} + \mathcal{O}(\varepsilon^3) \\ &= c_0 \bar{y}^{1/2} + c_1 \bar{y}^{-1} \varepsilon + c_2 \bar{y}^{-5/2} \varepsilon^2 + \mathcal{O}(\varepsilon^3), \end{aligned} \quad (5.32)$$

where we have defined $\bar{y} := -y(0) - \tau$, and c_j are constant coefficients. Let us look at the asymptotics of the first two terms in (5.32). If the series is asymptotic, we must have $c_0 \bar{y}^{1/2} \ll c_1 \bar{y}^{-1} \varepsilon$ as $\varepsilon \rightarrow 0$. This condition fails if

$$c_0 \bar{y}^{1/2} \sim c_1 \bar{y}^{-1} \varepsilon \Leftrightarrow \bar{y}^{1/2} \sim \bar{y}^{-1} \varepsilon \Leftrightarrow \bar{y} \sim \varepsilon^{2/3}.$$

So if we choose an initial condition, say $y(0) = -1$, then the series is asymptotic for some time, but eventually it becomes **disordered** when the solution $y(\tau; \varepsilon)$ reaches a regime at $\mathcal{O}(\varepsilon^{2/3})$ -distance in the y -coordinate to the fold point $P = (0, 0)$. From (5.32), it is easy to check that the same conclusion about disordering applies if we compare the first and third or the second and third terms of the asymptotic expansion. In fact, the entire asymptotic series exhibits this behavior. From $x_0^2 = \bar{y}$, it follows that the relevant scaling for x is $\mathcal{O}(\varepsilon^{1/3})$; see also Section 4.2, where we have previously encountered this scaling. ♦

Example 5.4.1 indicates that the dynamics near a fold point lead to a singularly perturbed problem. The next step is to determine asymptotic expansions of trajectories in the neighborhood of a general generic fold point $P = (x_0, y_0)$ for a $(1, 1)$ -fast–slow system

$$\begin{aligned} \varepsilon \dot{x} &= f(x, y), \\ \dot{y} &= g(x, y). \end{aligned} \quad (5.33)$$

Recall that genericity for folds that satisfy $f(P) = 0$ and $f_x(P) = 0$ requires the additional conditions $f_{xx}(P) \neq 0$, $f_y(P) \neq 0$, and $g(P) \neq 0$. Assume without loss of generality that $f_{xx}(P) > 0$, $f_y(P) > 0$ and $g(P) > 0$. By Theorem 4.2.2 (and its proof), there exists a local coordinate change $(\xi, \eta) = \phi(x, y)$ of (5.33) near P with $\phi(P) = (0, 0)$ such that

$$\begin{aligned} \varepsilon \dot{\xi} &= \frac{\xi^2 + \eta}{\alpha(\xi, \eta)}, \\ \dot{\eta} &= \beta(\xi, \eta), \end{aligned} \quad (5.34)$$

where the critical manifold C_0 is given by the parabolic equation $-\xi^2 = \eta$. We have also seen in Section 4.2 that genericity of the fold allows us to assume $\alpha(\xi, \eta) > 0$ and $\beta(\xi, \eta) > 0$ uniformly in a neighborhood of $(\xi, \eta) = (0, 0)$. Define rescaled variables

$$\xi = \mu u, \quad \eta = \mu^2 v, \quad t = \mu^2 T, \quad \text{with } \mu^3 = \gamma \varepsilon.$$

Substituting this into (5.34) yields (cf. the proof of Theorem 4.4.1)

$$\begin{aligned} \frac{du}{dT} &= \gamma \frac{u^2 + v}{\alpha(\mu u, \mu^2 v)}, \\ \frac{dv}{dT} &= \beta(\mu u, \mu^2 v). \end{aligned} \quad (5.35)$$

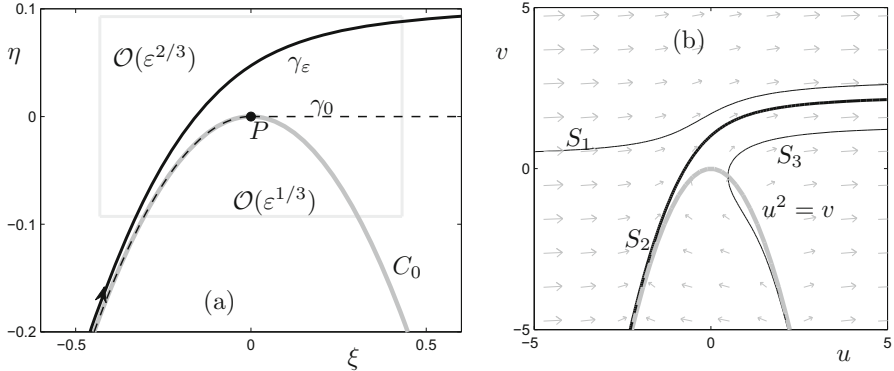


Figure 5.5: Illustration of dynamics near a generic fold. (a) Phase space dynamics for the normal form (5.35); see also (5.30). The critical manifold C_0 (thick gray), a candidate orbit γ_0 (thin dashed black), a numerical solution γ_ε (thick black) for $\varepsilon = 0.01$, the fold point P (black dot), as well as a neighborhood of P (light gray rectangle) with $(x, y) \in [-2\varepsilon^{1/3}, 2\varepsilon^{1/3}] \times [-2\varepsilon^{2/3}, 2\varepsilon^{2/3}]$ are shown. (b) Phase space portrait for the Riccati equation (5.44), where three solution curves S_j are shown. The curve S_2 (thick black) has the key asymptotic behavior as $u, v \rightarrow -\infty$.

A neighborhood of P in the ξ -coordinate can be given by requiring

$$\xi \in (-q, q) \quad \text{for some fixed and sufficiently small } q > 0. \quad (5.36)$$

Under the rescaling, this gives $u \in (-q/\mu, q/\mu)$. Since $\mu \rightarrow 0$ as $\varepsilon \rightarrow 0$, the neighborhood of P expands as ε approaches zero. Hence, one must develop asymptotics in the limit $u \rightarrow \pm\infty$ and $\mu \rightarrow 0$ for equation (5.35) to understand the region near P . Obviously, similar reasoning holds for the η and v coordinates. Note that v and u are monotonically increasing near P , since it was assumed that $\alpha(\cdot, \cdot) > 0$ and $\beta(\cdot, \cdot) > 0$ near P . The situation is illustrated in Figure 5.5(a).

To approximate trajectories of (5.35), consider the equation

$$\frac{dv}{du} = \frac{1}{\gamma} \frac{\alpha(\mu u, \mu^2 v) \beta(\mu u, \mu^2 v)}{u^2 + v} =: \frac{\tilde{\gamma}(u, v)}{u^2 + v}. \quad (5.37)$$

Finding an asymptotic expansion of a solution $v(u, \mu)$ of (5.37) provides an asymptotic expansion of our original problem after a conversion to the original variables. This yields a function $\eta(\xi, \mu)$ approximating trajectories flowing toward a generic fold point. The asymptotic expansion has to be split into two regions near the fold.

Theorem 5.4.2 ([MR80]). Let $\mu^3 = \gamma\varepsilon$ for some positive constant $\gamma > 0$. Define the (formal) power series

$$V_n\left(\frac{\xi}{\mu}, \mu\right) = v_0\left(\frac{\xi}{\mu}\right) + \mu v_1\left(\frac{\xi}{\mu}\right) + \mu^2 v_2\left(\frac{\xi}{\mu}\right) + \cdots + \mu^n v_n\left(\frac{\xi}{\mu}\right) \quad (5.38)$$

with coefficient functions v_i to be described below. Then a trajectory that is an extension of the attracting slow manifold of (5.34) into the fold region has an asymptotic expansion near the generic fold point $(0, 0)$ given by

$$\eta(\xi, \mu) = \begin{cases} -\xi^2 & + \mathcal{O}(\varepsilon^{2/3}) \\ \mu^2 v_0\left(\frac{\xi}{\mu}\right) & + \mathcal{O}(\varepsilon) \\ \mu^2 V_N\left(\frac{\xi}{\mu}, \mu\right) & + \mathcal{O}(\varepsilon^{1+N/3}) \end{cases} \quad (5.39)$$

for values $\xi \in [-\varepsilon^{1/3}, 0]$. For $\xi \in [0, \varepsilon^{1/3}]$, the asymptotic approximation is

$$\eta(\xi, \mu) = \begin{cases} 0 & + \mathcal{O}(\varepsilon^{2/3}) \\ \mu^2 v_0\left(\frac{\xi}{\mu}\right) & + \mathcal{O}(\varepsilon \ln \frac{1}{\varepsilon}) \\ \mu^2 V_M\left(\frac{\xi}{\mu}, \mu\right) & + \mathcal{O}(\varepsilon^{1+M/3}) \end{cases} \quad (5.40)$$

for $N > M$. The different terms in equations (5.39)–(5.40) give the 0-, 1-, N -, and M -term approximations.

Proof. (Sketch, [MR80]) We shall only outline very briefly the strategy employed, since the mechanics of the proof are very similar to the proofs of Theorems 5.3.1 and 5.3.3. First, substitute the formal series (5.38) for $\xi/\mu = u$ into equation (5.37), which is given by

$$\frac{dv}{du} = \frac{\tilde{\gamma}(u, v)}{u^2 + v}. \quad (5.41)$$

Expanding and collecting terms in different powers of μ gives a sequence of equations for the functions $v_i(u)$. This sequence can be solved iteratively starting at $v_0(u) = v_0(\xi/\mu)$. As a result, we get a power series formally satisfying (5.41). Define two curves displaced slightly from a (formal) power series expansion. It can be shown that the two curves trap the solution as in the proof of Theorem 5.3.3 and provide the claimed asymptotics as $\mu \rightarrow 0$. This shows that the representation of the solution is indeed an asymptotic series. \square

A detailed procedure for finding the functions $v_i(u)$ and their asymptotic behavior is given in [MR80] (see Chapter II, Sections 8–12). We shall only indicate what happens in the process of finding $v_0(u)$.

Exercise/Project 5.4.3. Show that

$$\frac{\tilde{\gamma}(\mu u, \mu^2 \sum_{k=0}^{\infty} \mu^k v_k(u))}{u^2 + v_0(u) + \sum_{k=1}^{\infty} \mu^k v_k(u)} = \frac{1}{u^2 + v_0(u)} + \mathcal{O}(\mu) \quad (5.42)$$

for $\mu \rightarrow 0$. \diamond

The expansion (5.42) shows that the ODE for $v_0(u) =: v$ to be solved is

$$\frac{dv}{du} = \frac{1}{u^2 + v}. \quad (5.43)$$

Instead of trying to find v as a function of u , we can try to find u as a function of v and invert later. Hence, we view (5.43) as

$$\frac{du}{dv} = u^2 + v. \quad (5.44)$$

It is now very important to note that (5.44) is a (**special**) **Riccati equation**. Its solution can be expressed in terms of special functions (see [AS65]) and the initial fast–slow singularly perturbed fold point is reduced to a classical problem from asymptotic analysis. But what solution should we choose if we do not have an initial condition? Figure 5.5(b) displays three of the solution curves of the special Riccati equation.

Exercise 5.4.4. Show that the Riccati equation (5.44) can be transformed into the **Airy equation** $\frac{d^2\tilde{u}}{d^2\tilde{v}} = \tilde{v}\tilde{u}$. ◇

It turns out after some analysis [MR80] that the solution curve S_2 of (5.44) (see also Figure 5.5) is the only one asymptotic to the parabola $v = -u^2$ as $u, v \rightarrow -\infty$. Reflection along the diagonal transforms back to the original equation (5.43). Denote the solution obtained from S_2 by $v_0(u)$. As suggested already by Figure 5.5, one concludes that $v_0(u)$ is the only solution asymptotic to the parabola describing the critical manifold. Hence, $v_0(u)$ is the zeroth-order term in a formal power series used in Theorem 5.4.2 for the part to the left of the fold point.

Similar judicious choices have to be made for higher-order terms, which complicates the derivation of the asymptotic expansion. Theorem 5.4.2 gives an asymptotic expansion for different sides of the fold point. Unfortunately, their validity is limited, since the interval of definition requires $\xi \in [-\varepsilon^{1/3}, \varepsilon^{1/3}]$, which shrinks with ε . A different asymptotic sequence has to be considered. As it turns out, one has to replace $\{\mu^n\}_n = \{\varepsilon^{n/3}\}_n$ by logarithmic terms

$$\left\{ \mu^n \ln^m \left(\frac{1}{\mu} \right) \right\}_{n,m} = \left\{ \frac{\varepsilon^{n/3}}{3} \ln^m \left(\frac{1}{\varepsilon} \right) \right\}_{n,m}.$$

This asymptotic sequence works inside an interval $(\varepsilon^{1/3}, q]$, where $q > 0$ is fixed.

Theorem 5.4.5 ([MR80]). *Consider a normal form for a fold point the origin*

$$\frac{d\eta}{d\xi} = \varepsilon \frac{\tilde{\gamma}(\xi, \eta)}{\xi^2 + \eta}. \quad (5.45)$$

Let $\lambda \in (0, 1/3)$. Define a (formal) series

$$Z_n(\xi, \varepsilon) = \sum_{k=2}^n \varepsilon^{k/3} \sum_{m=1}^{\varpi(k-2)} c_{n,m}(\xi) \ln^m \frac{1}{\varepsilon},$$

where $\varpi(k) = s$ for $k = 3s$ or $k = 3s + 2$ and $\varpi(k) = k + 1$ if $k = 3s + 1$. Then the solution $\eta(\xi, \varepsilon)$, which is an extension of the attracting slow manifold into the fold region, to equation (5.45) has an asymptotic expansion as $\varepsilon \rightarrow 0$ given by

$$\eta(\xi, \varepsilon) = \begin{cases} 0 & + \mathcal{O}(\varepsilon^{2/3}) \\ Z_2(\xi, \varepsilon) & + \mathcal{O}(\varepsilon^{1/3}) \\ Z_3(\xi, \varepsilon) & + \mathcal{O}\left(\varepsilon^{\min\left(\frac{4}{3}, \frac{5}{3}-3\lambda\right)}\right) \\ Z_{N+3}(\xi, \varepsilon) & + \mathcal{O}\left(\varepsilon^{\frac{N+4}{3}-\lambda(N+2)}\right) \end{cases} \quad (5.46)$$

for $\xi \in (\varepsilon^\lambda, q]$ and some arbitrary positive integer N . The coefficient functions $c_{n,m}(\xi)$ can be calculated from $\tilde{\gamma}(\cdot, \cdot)$ and its derivatives only.

The detailed proof and the calculation of the coefficients $c_{n,m}$ are impressive [MR80] but also lengthy, and we omit them here. Although we do not present the proof, let us note that the first approximation in (5.46) is $\eta = \mathcal{O}(\varepsilon^{2/3})$ and not $\mathcal{O}(1)$, since the asymptotic expansion is calculated in the normal form (5.35), which has to be scaled back to the original variables. A three-dimensional version of Theorem 5.4.5 is discussed in Section 7.6.

Exercise/Project 5.4.6. A more formal approach to deriving a single asymptotic expansion valid in multiple scaling regions is discussed in Section 9.1. Can you find the leading-order terms in (5.46) using the background from Section 9.1? ◇

Remark: The asymptotic series obtained by extending slow manifolds under the flow into a region near planar fold points are already highly nontrivial. We expect asymptotic solutions to increase in complexity for higher dimensions and singularities that are generic only for (m, n) -fast–slow systems with $m + n \geq 3$. In such cases, the full asymptotic series are often not known. Even if they were known, they would probably be too complicated to yield important insights. Therefore, one should often just look for the leading-order terms and the first ε -dependent correction.

5.5 The Period of Relaxation Oscillations

Once we have asymptotic expressions for the solution curves near a fold point as given in Theorem 5.4.5, it is possible to find asymptotic formulas for the period of a relaxation oscillation. Before we state this result, we look at a classical example.

Example 5.5.1. Consider the unforced van der Pol equation

$$\begin{aligned} \varepsilon \frac{dx}{d\tau} &= \varepsilon \dot{x} = y - \frac{x^3}{3} + x, \\ \frac{dy}{d\tau} &= \dot{y} = -x. \end{aligned} \quad (5.47)$$

From the fast–slow decomposition in Example 5.2.1 and Figure 5.2, we expect that van der Pol’s equation has a relaxation oscillation periodic orbit γ_ε close

to a candidate periodic orbit γ_0 consisting of two fast and two slow segments. For the zeroth-order approximation T_0 to the period T_ε of the relaxation limit cycle, we simply neglect the fast pieces and consider only the slow flow on the critical manifold

$$C_0 = \left\{ (x, y) \in \mathbb{R}^2 : y = \frac{x^3}{3} - x \right\}.$$

The slow flow can be written explicitly, as discussed in Section 3.2, via the calculation

$$y = \frac{x^3}{3} - x \quad \Rightarrow \quad -x = \dot{y} = \dot{x}x^2 - \dot{x} \quad \Rightarrow \quad \dot{x} = \frac{x}{1-x^2}. \quad (5.48)$$

Luckily, the ODE can be solved by separation of variables. If we want to know the time T^{a+} it takes for the flow on $C_0^{a+} = C_0 \cap \{x > 1\}$, we have to integrate (5.48) between the fast jump at $x = 2$ and the fold point P_+ at $x = 1$; see Figure 5.2. Therefore, the problem is

$$T^{a+} = \int_0^{T^{a+}} dt = \int_2^1 \frac{1-x^2}{x} dx = \int_2^1 \left(\frac{1}{x} - x \right) dx = \frac{3}{2} - \ln 2.$$

Obviously, the calculation on $C_0^{a-} = C_0 \cap \{x < -1\}$ will be the same by symmetry, so we have for the zeroth-order approximation of the period,

$$T_0 = T^{a+} + T^{a-} = 2T^{a+} = 3 - 2\ln 2.$$

This result gives a good approximation to $T_\varepsilon = T_0 + \mathcal{O}(\varepsilon^{2/3})$ if ε is small. ♦

The example can be generalized to a $(1, 1)$ -fast–slow system

$$\begin{aligned} \varepsilon \dot{x} &= f(x, y), \\ \dot{y} &= g(x, y), \end{aligned} \quad (5.49)$$

with critical manifold C_0 . Assume that (5.49) has periodic candidate orbit Λ_0 that perturbs to a relaxation oscillation Λ_ε for $0 < \varepsilon \ll 1$. Suppose Λ_0 consists of M fast and M slow segments.

Definition 5.5.2. A point $P \in C_0$ at which a slow and a fast segment are concatenated is called

- a **jump point** if the fast flow is directed away from C_0 ,
- a **drop point** if the fast flow is directed toward C_0 .

Typical jump points are generic fold points, and sometimes the terminology is used interchangeably in the literature. A candidate relaxation oscillation Λ_0 having three fast and three slow segments is shown in Figure 5.6. The jump points are denoted by J_i and the drop point following J_i is denoted by D_i . In the case of Figure 5.6, we have $i = 1, 2, 3$ with $M = 3$.

Suppose Λ_ε is a simple relaxation oscillation of (5.49) (see Definition 5.2.4; jumps occur only at generic folds, and the slow segments contain no equilibria).

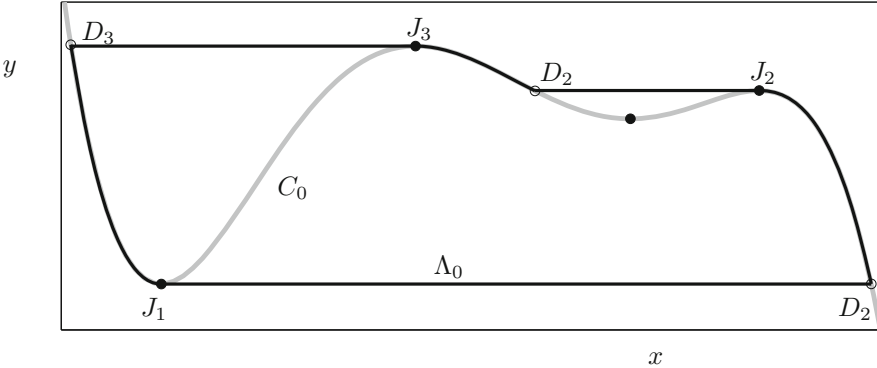


Figure 5.6: A six-segment simple relaxation oscillation. The critical manifold C_0 (gray), fold points (black dots), and the candidate/singular relaxation oscillation Λ_0 (thin black) are shown, and the jump points J_i and drop points D_i for ($i = 1, 2, 3$) are indicated. The critical manifold was generated by choosing $f(x, y) = y + (x - 1)(x - 2)(x + 1)(x + 4)(x + 7)$.

The zeroth-order approximation T_0 of the period T_ε of Λ_ε is found simply by integrating the slow flow on Λ_0 . Away from the folds, the slow flow can be expressed using the description of C_0 as a graph $x = h(y)$, so that

$$\dot{y} = g(h(y), y), \quad (5.50)$$

which corresponds to a projection of the slow flow onto the y -axis.

Remark: As shown in Example 5.5.1, it might sometimes be more convenient to project onto the x -axis instead.

For the parameterization (5.50), one obtains

$$T_0 = \int_{\Lambda_0} \frac{1}{g(h(y), y)} dy, \quad (5.51)$$

where the fast jumps are regarded as instantaneous. A more precise computational formula is

$$T_0 = \sum_{i=1}^{M-1} \int_{y(D_i)}^{y(J_{i+1})} \frac{1}{g(h_{i+1}(y), y)} dy + \int_{y(D_M)}^{y(J_1)} \frac{1}{g(h_1(y), y)} dy,$$

where $y(D_i)$, $y(J_i)$ denote the y -coordinates of the points, and h_i is a function describing C_0 between the drop point D_i and the jump point J_{i+1} for $i = 2, 3, \dots, M$, while h_1 describes it between D_M and J_1 . The formula for T_0 is often relatively easy to compute. Unfortunately, once we consider what the corrections for $0 < \varepsilon \ll 1$ are, the situation becomes far more involved. This is to be expected based on results in Sections 5.3 and 5.4, which have to be used to derive the period T_ε . To state the main result, the convention $\varpi(k) := s$ for $k = 3s$ or $k = 3s + 2$ and $\varpi(k) = k + 1$ if $k = 3s + 1$ is used again.

Theorem 5.5.3 ([MR80]). Suppose Λ_ε is a simple relaxation oscillation with M fast and M slow segments. Then the period T_ε has an asymptotic representation,

$$T_\varepsilon = T_0 + \sum_{m=1}^M T(m) + \mathcal{O}\left(\varepsilon^{(N+2)/3} \ln^{\varpi(N)} \frac{1}{\varepsilon}\right), \quad \text{as } \varepsilon \rightarrow 0,$$

where T_0 is given by (5.51) and $N \in \mathbb{N}$ specifies the number of terms used in the expansion for the summands $T(m)$, which are

$$T(m) = \sum_{n=2}^{N+1} \varepsilon^{n/3} \sum_{r=0}^{\varpi(n-2)} K(m, n, r) \ln^r \frac{1}{\varepsilon}.$$

The coefficients $K(m, n, r)$ can be calculated from the function values and derivatives of f and g . The natural number N can be chosen arbitrarily; it specifies how many terms of the asymptotic series are used.

Remark: We do not consider the calculation of the coefficients $K(m, n, r)$ here, since the formulas are rarely of practical help due to their high complexity. The impressive detailed calculation is contained in [MR80].

The problem of the relaxation oscillation period has been included here mostly for highlighting one of the original questions posed at the beginning of the theory of multiple time scales. For van der Pol's equation (5.47), the result in Theorem 5.5.3 was preceded by the classical **Dorodnitsyn's formula**

$$T_\varepsilon = 3 - 2 \ln 2 + C_1 \varepsilon^{2/3} - \frac{\varepsilon}{3} \ln \frac{1}{\varepsilon} + C_2 \varepsilon + \mathcal{O}(\varepsilon^{4/3}). \quad (5.52)$$

Exercise/Project 5.5.4. Try to determine the constants in (5.52) numerically, using, for example, one of the numerical methods discussed in Sections 10.1, 10.2, and 10.6. ◇

For more detailed information on the constants C_1 , C_2 and the history of Dorodnitsyn's formula, see Section 5.6.

5.6 References

Section 5.1: The basic results can be found in some form in many books [JF96, EdJ82, Hol95, Mil06, Smi85] on singular perturbations. For a more specialized approach for fast-slow systems, we refer to the excellent monographs [MR80, MKKR94], while [Lom92, LE88] present a more abstract operator-theoretic viewpoint. Two well-known classic books have substantially influenced the area [BM61, Was02]. There is also a book available directed more toward formal power series [Bal00]. Even for linear systems, the singular perturbation asymptotic analysis is interesting [O'M79]. Another important aspect to keep in mind is the comparison between numerical and asymptotic solutions [DA67, OF80]. Furthermore, there are many applications such as chemical reactor theory [COT74]; we shall encounter many more applications in Section 9.11.

Section 5.2: This section is based mostly on relaxation oscillations surveys [Guc04, MR80], but there are many excellent sources in which relaxation oscillations are described, e.g., [Gra87]. For some historical perspectives, see the articles [Bre60, GL12]; the book [Min47] also provides a very good context for the early history of the field. The geometric viewpoint was developed relatively early during the analysis [Kon08, Lef57]. In fact, a solid mathematical analysis of relaxation oscillations in a quite general class of van der Pol (vdP)-type equations was known already in the 1940s [Car52, LaS49, LS42], and their broad relevance for applications was also realized at that time [DS49, Kar49, Wes39]. Relaxation oscillators are a cornerstone of the classical field of nonlinear oscillations [Min62]. There are many directions that have been studied based on relaxation oscillations, such as bifurcation scenarios [GHW05, Tro76], biological clocks [FK02], catalysis [Has83], chemical reactions [GER78, Tys84], combustion [EM92], exactly solvable toy models [GP87], fluid dynamics [LR84b], lasers [GK91, KvdGL97], neural nets [CE01], piecewise-linear systems [Ana83, Hog03], plastic deformation models [Brø12], pursuit systems [SY10], satellite motion [QGNR97], single-neuron models [ADF90], stick-slip phenomena [PB11] and various predator-prey systems [GV73, HS09, KK95, Kol92, MLSA07, RWV11, SM08].

Section 5.3: This section and the next are based mostly on [MR80], but see also [PR64, Roz62]; consider [Gil83, Nip83] for related results. The basic idea of matching different regimes will be discussed much more formally in Section 9.1, but see also [BG74, Gil90]. Asymptotics analysis for singularly perturbed problems has a long history [Fin83, Mac68, O'M78a], in particular for periodic solutions [Mis61]. Even double asymptotics was considered relatively early on [Fra98, Jr60]. Quite general asymptotic results for fast-slow systems have been available for various problems [Che50, Che49, Jr62, Sib63a] for quite some time.

Section 5.4: The fold is dealt with in various other parts of this book, so we do not provide additional references here; see in particular Sections 7.4, 9.5, 12.1 and the associated reference sections.

Section 5.5: The results are taken from [MR80], which, in turn, is partially based on [Dor47, Mis58, Roz64]. One may also extend the asymptotic analysis approach to the forced vdP equation [Gra80, GNV84] and higher-dimensional relaxation oscillations [KM89, MK93b]. There has also been a bit of a debate in the literature regarding the exact coefficients of Dorodnitsyn's formula [AG82, Arn94, DG90, DGA84]. Extending asymptotics into the complex domain is another interesting direction [HT90].

Another direction that takes advantage of relaxation oscillators is that of coupled systems, in which interesting patterns can emerge [LT13, SS13b, TLRB11]. There are also many applications of coupled relaxation oscillators, for example to central pattern generators [RS93], genetic oscillations [KKK04], heterogeneous oscillators [LZSK12], neural phase equations [Izh00b], phase locking [Coo01], pulse-coupled systems [Bot95] and small-network synchronizations [Gra84, GJ79, TL97]. It is also natural to compare relaxation and other classes of oscillators [SK93b, SK95a, KS95].

Furthermore, a classical topic involving asymptotics is second-order boundary-value problems (BVPs), e.g., topics such as asymptotics/existence [How76b, How78b, How76a], difference equations [CH76], extensions to fourth-order problems [LR60, Rab57], infinite intervals [MR83], initial value problems [How79a], mixed boundary conditions [LS86], nonexistence results [O'M76b, O'M68a] and nonlinear problems [O'M70c].

Chapter 6

Tracking Invariant Manifolds

The main goal of this chapter is to discuss the tracking of invariant manifolds when they transition from a fast to a slow motion and vice versa. That is, we would like to understand how trajectories or more general objects enter and leave the vicinity of a normally hyperbolic critical manifold. The main application is to show how the geometric theory of fast–slow systems can be used to prove the persistence of candidate orbits for $0 < \varepsilon \ll 1$.

Section 6.1 covers the case in which only one fast jump is involved and also highlights the usefulness of Melnikov-type calculations. Section 6.2 discusses a motivating example arising in the FitzHugh–Nagumo equation whereby pulse solutions may consist of fast and slow parts. Sections 6.3 and 6.4 state and prove the main technical result, the exchange lemma, which describes accurately how invariant objects behave near normally hyperbolic fast-to-slow and slow-to-fast transitions. Finally, we have enough tools to prove the existence of the pulse solutions of the FitzHugh–Nagumo equation in Section 6.5. A technical improvement to the exchange lemma is considered in Section 6.6, which deals with exponentially small terms. Section 6.7 shows the flexibility of the results by pointing out that we are not restricted to (homoclinic) pulse solutions but can tackle rather general boundary value problems.

Background: Regarding various proofs that use differential-geometric terminology, the same comments as for Chapter 2 apply, i.e., the basic definitions for smooth manifolds are required; however, here we also need a bit of differential forms for the proof in Section 6.4. As before, the books [Lee06, Jän01] are very helpful, with more details in [Spi99, AMR88, Mun97].

6.1 Simple Jumps and Transversality

In this chapter we consider an (m, n) -fast–slow system

$$\begin{aligned}\varepsilon \frac{dx}{d\tau} &= \varepsilon \dot{x} = f(x, y, \varepsilon), \\ \frac{dy}{d\tau} &= \dot{y} = g(x, y, \varepsilon),\end{aligned}\tag{6.1}$$

where f, g are smooth, and the critical manifold $C_0 = \{(x, y) \in \mathbb{R}^{m+n} : f(x, y, 0) = 0\}$ is normally hyperbolic. Since C_0 is normally hyperbolic, it follows that $D_x f|_{C_0}$ is invertible. The implicit function theorem yields (locally) that $C_0 = \{(h(y), y) \in \mathbb{R}^{m+n}\}$ is a graph, where $h : \mathbb{R}^n \rightarrow \mathbb{R}^m$ is a map such that $f(h(y), y, 0) = 0$; see also Chapter 3. Then the slow subsystem is

$$\dot{y} = g(h(y), y, 0) \quad \text{on } C_0.\tag{6.2}$$

If the slow flow (6.2) has two hyperbolic equilibrium points p_0 and q_0 , there might be a **heteroclinic orbit** γ_0 between p_0 and q_0 for (6.2),

$$\lim_{\tau \rightarrow -\infty} \gamma_0(\tau) = p_0, \quad \lim_{\tau \rightarrow +\infty} \gamma_0(\tau) = q_0 \quad \text{or} \quad \lim_{\tau \rightarrow +\infty} \gamma_0(\tau) = p_0, \quad \lim_{\tau \rightarrow -\infty} \gamma_0(\tau) = q_0.$$

When $p_0 = q_0$, then γ_0 is called a **homoclinic orbit**. The heteroclinic situation is shown in Figure 6.1, where the stable manifold $W^s(p_0)$ and the unstable manifold $W^u(q_0)$ for the slow flow defined via (6.2) intersect transversally in a heteroclinic orbit γ_0 .

Perturbing the system for $0 < \varepsilon \ll 1$ should also yield a heteroclinic connection γ_ε between two equilibria of the full system (6.1). This can be roughly justified by Fenichel's theorem as follows: C_0 perturbs to a slow manifold C_ε , the flow on C_ε is close to the slow flow on C_0 , and the stability of transversal intersection implies that the flow on the slow manifold still has a heteroclinic connection between two slightly perturbed equilibrium points p_ε and q_ε . This result will be formalized below.

The next step is to ask for the best possible generalizations of the previous situation. Clearly, we also want to include the case in which a heteroclinic or homoclinic orbit involves both fast and slow dynamics. The simplest case for this situation is to assume the existence of two n -dimensional normally hyperbolic invariant manifolds C^1 and C^2 that are contained in the critical manifold $C_0 =: C$ of (6.1). Suppose C^1 and C^2 contain hyperbolic invariant sets P^1 and P^2 for the slow flow (6.2); to simplify the abstract setting, one can simply think of P^1 and P^2 as equilibrium points. The fast subsystem will be used to find a heteroclinic orbit between P^1 and P^2 .

Remark: All following results will be applicable in the case $C^1 = C^2$ and $P^1 = P^2$, which yields homoclinic orbits, as well as the case $C^1 = C^2$ and $P^1 \neq P^2$ shown in Figure 6.1.

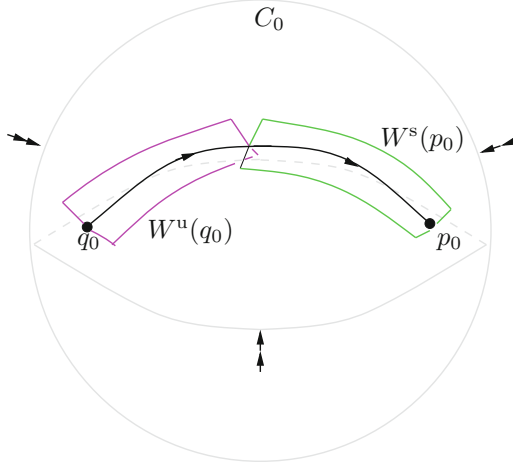


Figure 6.1: The phase space is \mathbb{R}^4 with three slow variables and one fast variable. The critical manifold C_0 is a three-dimensional ball in \mathbb{R}^4 . The equilibria $p_0, q_0 \in C_0$ are shown together with the transversal intersection of their stable and unstable manifolds $W^s(p_0)$ and $W^u(q_0)$ for the slow flow (6.2). The transversal intersection gives a heteroclinic connection from q_0 to p_0 . The fast flow is indicated by double arrows and is directed toward C_0 .

The stable and unstable manifolds of P^1 and P^2 with respect to the slow flow have to be defined more formally. Without loss of generality, let us assume that we are interested in the unstable manifold of P^1 and the stable manifold of P^2 :

$$\begin{aligned} W^u(P^1) &= \{p \in C^1 : \phi_\tau^{\text{slow}}(p) \rightarrow P^1 \text{ as } \tau \rightarrow -\infty\}, \\ W^s(P^2) &= \{p \in C^2 : \phi_\tau^{\text{slow}}(p) \rightarrow P^2 \text{ as } \tau \rightarrow +\infty\}, \end{aligned} \quad (6.3)$$

where ϕ_τ^{slow} is the slow flow for equation (6.2). Furthermore, certain submanifolds of the stable and unstable manifolds of the critical manifold C have to be defined:

$$\begin{aligned} N^1 &= \bigcup_{p \in W^u(P^1)} \{q \in \mathbb{R}^{n+m} : \phi_t^{\text{fast}}(q) \rightarrow p \text{ as } t \rightarrow -\infty\}, \\ N^2 &= \bigcup_{p \in W^s(P^2)} \{q \in \mathbb{R}^{n+m} : \phi_t^{\text{fast}}(q) \rightarrow p \text{ as } t \rightarrow +\infty\}, \end{aligned} \quad (6.4)$$

where ϕ_t^{fast} is the flow of the fast subsystem (for $t = \tau/\varepsilon$)

$$\begin{aligned} \frac{dx}{dt} &= x' = f(x, y, 0), \\ \frac{dy}{dt} &= y' = 0. \end{aligned}$$

The y -coordinates to be used for a particular flow in (6.4) are determined by the y -coordinates of p . Instead of requiring a transversal intersection of manifolds defined entirely by the slow flow as in Figure 6.1, one can require a transversal intersection of N^1 and N^2 . The situation is shown in Figure 6.2.

The candidate heteroclinic orbit consists of a slow segment on C^1 starting at P^1 . This segment connects to a fast segment that lies in the transversal intersection of N^1 and N^2 . The last slow segment lies on C^2 connecting to P^2 .

Theorem 6.1.1 ([Szm91]). *Suppose P^1 and P^2 are normally hyperbolic invariant manifolds for the slow flow and that the two manifolds N^1 and N^2 , as defined by (6.4), intersect transversally. Then there exists $\varepsilon_0 > 0$ such that for all $\varepsilon \in (0, \varepsilon_0]$, the fast-slow system (6.1) has a transversal heteroclinic orbit between P^1 and P^2 .*

Proof. By Fenichel's theorem (Theorem 3.1.4), the manifolds N^1 and N^2 perturb to unstable and stable manifolds N_ε^1 and N_ε^2 . The stability of transversal intersection implies that N_ε^1 and N_ε^2 still intersect transversally for ε sufficiently small. The result follows. \square

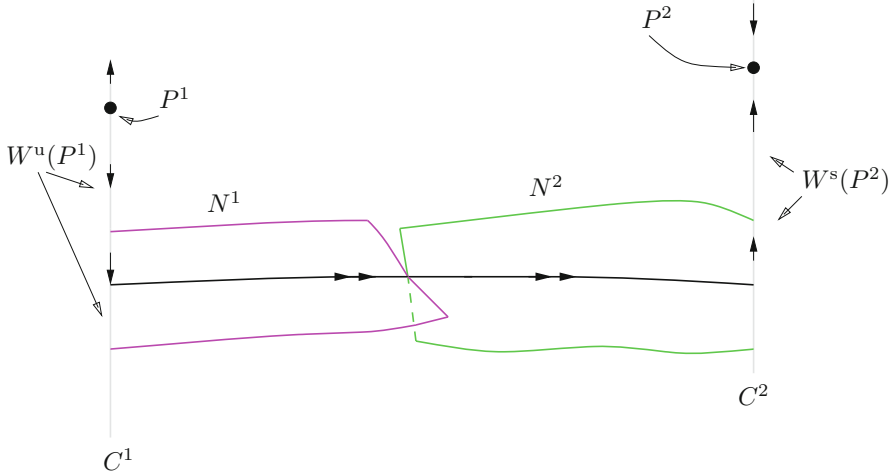


Figure 6.2: Transversal intersection of N^1 and N^2 yields a heteroclinic connection between P^1 and P^2 consisting of two slow segments and one fast segment. Note that the y -coordinate is actually constant on each fast orbit.

It is possible to weaken the hypotheses on P^1 and P^2 . One needs only that P^1 is a compact normally hyperbolic overflowing invariant manifold with boundary for the slow flow and that P^2 is a compact normally hyperbolic inflowing invariant manifold with boundary for the slow flow. Although this is only a slight modification, it is necessary, since often one is confronted with systems of the form

$$\begin{aligned} \varepsilon \dot{x} &= f(x, y, \mu, \varepsilon), \\ \dot{y} &= g(x, y, \mu, \varepsilon), \\ \dot{\mu} &= 0, \end{aligned} \tag{6.5}$$

where $\mu \in \mathbb{R}^p$ arise as parameters. The **extended system** (6.5) does not satisfy the invariance assumptions, but it is easy to modify the equation $\dot{\mu} = 0$ near the boundary of the manifolds

$$\tilde{P}^i := \{(P^i(\mu), \mu)\} \quad \text{for } i = 1, 2$$

to make the manifold \tilde{P}^1 overflowing invariant and \tilde{P}^2 inflowing invariant.

Suppose we are in the situation described in Theorem 6.1.1. Then a major problem in applying it is to check the transversality condition. Since N^1 and N^2 intersect, there exists a value $y = y_0$ such that in the fast subsystem

$$x' = f(x, y_0, 0), \quad (6.6)$$

there is a heteroclinic orbit between two equilibrium points $p_1 = (x_1(y_0), y_0) \in W^u(P^1)$ and $p_2 = (x_2(y_0), y_0) \in W^s(P^2)$. Denote the heteroclinic orbit by $(x_0(t), y_0) \in \mathbb{R}^{m+n}$. The intersection between N^1 and N^2 at a point $p = (x_0(t), y_0)$ for some t is transverse if and only if

$$T_p N^1 \oplus T_p N^2 = \mathbb{R}^{m+n}.$$

Direct dimension counting always gives

$$\dim(T_p N^1 + T_p N^2) = \dim(T_p N^1) + \dim(T_p N^2) - \dim(T_p N^1 \cap T_p N^2).$$

Based upon the definition

$$d := \dim(T_p N^1) + \dim(T_p N^2) - m - n, \quad (6.7)$$

it follows that that N^1 and N^2 intersect transversally if and only if

$$d = \dim(T_p N^1 \cap T_p N^2).$$

From now on, we shall assume that the intersection of the fast subsystem unstable manifold of p_1 and the fast subsystem stable manifold of p_2 is just a single one-dimensional heteroclinic connection $(x_0(t), y_0)$. Furthermore, we assume that the intersection of the tangent spaces to the fast subsystem unstable manifold of p_1 and the fast subsystem stable manifold of p_2 is one-dimensional as well. This situation is equivalent to the assumption that x'_0 is the only (up to a scalar multiple) nontrivial bounded solution to the **variational equation**

$$x' = D_x f(x_0(t), y_0, 0)x.$$

Let ψ denote the unique (up to a scalar multiple) nontrivial solution to the adjoint equation

$$\psi' = -(D_x f(x_0(t), y_0, 0))^\top \psi. \quad (6.8)$$

Now we can state an important theorem.

Theorem 6.1.2 ([Szm91]). *Let P^1 and P^2 be normally hyperbolic manifolds of the slow subsystem with $W^u(P^1)$, $W^s(P^2)$ and N^1 , N^2 defined in (6.3) and (6.4) respectively. Let Π denote the projection onto the y -coordinate. Then N^1 and N^2 intersect transversally if and only if there are exactly $d-1$ linearly independent solutions $\xi \in T_{y_0}\Pi(W^u(P^1)) \cap T_{y_0}\Pi(W^s(P^2))$ to the equation*

$$M \cdot \xi = 0, \quad (6.9)$$

where $M \in \mathbb{R}^n$ is defined by

$$M = \int_{-\infty}^{\infty} \psi(t) \cdot D_y f(x_0(t), y_0, 0) dt. \quad (6.10)$$

To illustrate how the result works, we are going to discuss a toy model. We need a lemma, whose proof is left as an exercise.

Exercise/Project 6.1.3. Verify that the solution of the adjoint variational equation (6.8) for two fast variables $m = 2$ is

$$\psi(t) = e^{-\int_0^t \text{Tr}(D_x f(x_0(s), y_0, 0)) ds} (-x'_2(t), x'_1(t))^{\top}, \quad (6.11)$$

where Tr denotes the trace of a matrix. What about higher-dimensional cases? ◇

Example 6.1.4. Consider the $(2, 1)$ -fast–slow system

$$\begin{aligned} \varepsilon \dot{x}_1 &= 1 - (x_1)^2, \\ \varepsilon \dot{x}_2 &= y + x_1 x_2, \\ \dot{y} &= y^2 - (x_1)^2. \end{aligned} \quad (6.12)$$

The critical manifold C_0 is easily found. It consists of two lines L_{\pm} ,

$$\begin{aligned} C_0 &= \{(x_1, x_2, y) \in \mathbb{R}^3 : x_1 = -1 \text{ and } y = x_2 \quad \text{or} \quad x_1 = 1 \text{ and } y = -x_2\} \\ &= L_{x_1=-1} \cup L_{x_1=+1} =: L_- \cup L_+. \end{aligned}$$

A projection onto the (x_1, y) -plane of the situation with the singular flows of the fast and slow subsystems is shown in Figure 6.3. A singular heteroclinic orbit connects the two saddle equilibria $p_1 = (-1, 1, 1)$ and $p_2 = (1, 1, -1)$. Define the manifolds N^1 and N^2 as two planes

$$\begin{aligned} N_1 &= \{(x_1, x_2, y) \in \mathbb{R}^3 : x_1 \in [-1, 1], y = x_2\}, \\ N_2 &= \{(x_1, x_2, y) \in \mathbb{R}^3 : x_1 \in [-1, 1], y = -x_2\}. \end{aligned}$$

These are precisely the manifolds checked for transversal intersection in Theorem 6.1.2. Here N^1 is part of the unstable manifold of L_- , and N^2 is part of the stable manifold of L_+ . Geometrically, it is clear that they intersect transversally in the segment

$$H_{\text{fast}} = \{(x_1, x_2, x_3) \in \mathbb{R}^3 : x_1 \in [-1, 1], x_2 = 0, y = 0\}.$$

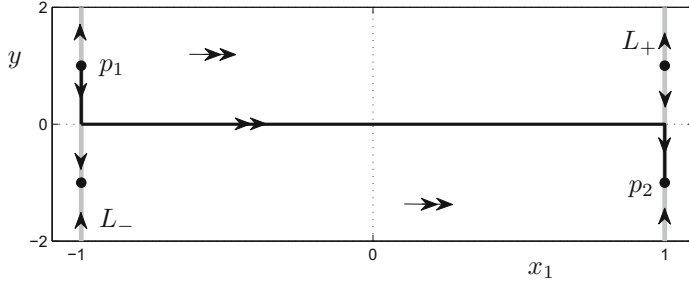


Figure 6.3: Projection of the fast–slow structure of (6.12) onto the (x_1, y) -plane. The singular heteroclinic connection (black) and the critical manifold C_0 (gray) are shown.

The segment H_{fast} is a heteroclinic connection for the fast subsystem with $y = y_0 = 0$; see Figure 6.3. Hence, Theorem 6.1.1 implies that the singular heteroclinic orbit H consisting of

$$\{x_1 = -1, x_2 \in [0, 1], y = x_2\} \cup H_{\text{fast}} \cup \{x_1 = 1, x_2 \in [0, 1], y = -x_2\}$$

persists for $\varepsilon > 0$ sufficiently small and (6.12) has a heteroclinic orbit. This geometric observation can be verified algebraically. First, one has to calculate the dimension d as given in equation (6.7). Let p be a point on the heteroclinic orbit H . Then

$$d = \dim(T_p N^1) + \dim(T_p N^2) - m - n = 2 + 2 - 2 - 1 = 1.$$

The equation $M \cdot \xi = 0$ is a scalar equation, and we aim to show that it has $d - 1 = 1 - 1 = 0$ nontrivial solutions, i.e., that $M \neq 0$. Let H_{fast} be denoted in parameterized form by $(x_1(t), x_2(t), y_0) = (x_0(t), 0)$; formally, one should denote, e.g., $x_1(t)$ by $(x_1)_0(t)$, since it is a coordinate along the heteroclinic orbit, but we drop the 0 subscript for notational convenience. The solution of the adjoint equation is obtained from (6.11):

$$\psi(t) = e^{\int_0^t x_1(s) ds} (-y_0 - x_1(t)x_2(t), 1 - (x_1(t))^2)^\top. \quad (6.13)$$

Exercise 6.1.5. Check (6.13) by calculating $D_x f(x_0(s), y_0, 0)$ and its trace. \diamond

Furthermore, a direct calculation yields

$$D_y f(x_0(t), y_0, 0) = (0, 1)^\top.$$

Putting the previous results into (6.10) gives

$$\begin{aligned} M &= \int_{-\infty}^{\infty} \psi(t) \cdot D_y f(x_0(t), y_0, 0) dt \\ &= \int_{-\infty}^{\infty} e^{\int_0^t x_1(s) ds} (-y_0 - x_1(t)x_2(t), 1 - (x_1(t))^2)^\top \cdot (0, 1)^\top dt \\ &= \int_{-\infty}^{\infty} e^{\int_0^t x_1(s) ds} (1 - (x_1(t))^2) dt. \end{aligned}$$

Note that $x_1(t)$ describes the fast segment of the heteroclinic orbit lying between $x_1 = -1$ and $x_1 = 1$. Hence, $1 - x_1(t)^2 > 0$ for all $t \in \mathbb{R}$. The exponential function is positive as well, and we conclude that $M > 0$. This implies the existence of the heteroclinic orbit. ♦

Unfortunately, Theorem 6.1.2 does not cover all cases occurring in practice. In the next chapter, we shall give a more detailed introduction to the FitzHugh–Nagumo equation and shall explain why certain heteroclinic and homoclinic orbits are much more difficult to obtain.

6.2 The FitzHugh–Nagumo Equation

The FitzHugh–Nagumo equation is a simplification of the Hodgkin–Huxley model for the electric potential of a nerve axon. In this section, we consider the PDE version developed by Nagumo, as introduced in Section 1.4, for the electric potential $u = u(x, \tau)$ and an auxiliary variable $w = w(x, \tau)$:

$$\begin{aligned} u_\tau &= \delta u_{xx} + c_a(u) - w, \\ w_\tau &= \varepsilon(u - \gamma w), \end{aligned} \tag{6.14}$$

where $(x, \tau) \in \mathbb{R} \times [0, \infty)$, $0 < \varepsilon \ll 1$, $c_a(u) := u(u - a)(1 - u)$, and $\gamma > 0$, $\delta > 0$, $0 < a < 1/2$ are parameters; for a biophysical interpretation of nerve impulse equations, such as the FitzHugh–Nagumo equation, see Section 20.2.

Of particular interest are **traveling wave** solutions to (6.14), so we make the ansatz $u(x, \tau) = u(x + s\tau) =: u(t)$ and $w(x, \tau) = w(x + s\tau) =: w(t)$, where s represents the **wave speed**. By the chain rule, it follows that $u_\tau = su'$, $u_{xx} = u''$, and $w_\tau = sw'$, where $'$ denotes derivatives with respect to t . Now set $v = u'$ and substitute into (6.14). Then

$$\begin{aligned} u' &= v, \\ v' &= \frac{1}{\delta}(sv - c_a(u) + w), \\ w' &= \frac{\varepsilon}{s}(u - \gamma w). \end{aligned} \tag{6.15}$$

A homoclinic orbit of (6.15) corresponds to a **traveling pulse** solution of (6.14), a heteroclinic orbit to a **traveling front or back** solution, and a periodic orbit to a **traveling wave train**; see Figure 6.4. Changing from the fast time t to the slow time τ and relabeling variables $x_1 = u$, $x_2 = v$, and $y = w$ in (6.15), one gets a $(2, 1)$ -fast–slow system in standard form:

$$\begin{aligned} \varepsilon \dot{x}_1 &= x_2, \\ \varepsilon \dot{x}_2 &= \frac{1}{\delta}(sx_2 - c_a(x_1) + y), \\ \dot{y} &= \frac{1}{s}(x_1 - \gamma y). \end{aligned} \tag{6.16}$$

For now, we shall refer to (6.16) as *the* FitzHugh–Nagumo equation. It is one of the goals of this chapter to provide the tools for existence proofs of various traveling wave solutions that correspond to certain bounded invariant sets of

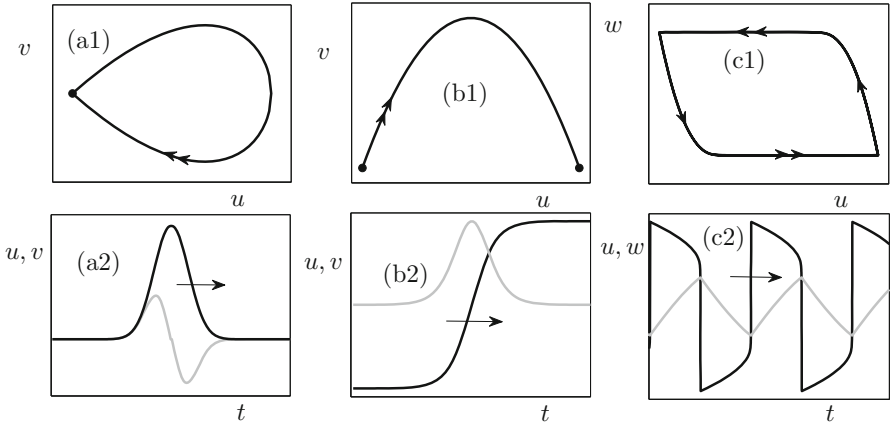


Figure 6.4: Sketch of the correspondence between ODE phase space (top row) for (6.15) and traveling wave solutions (bottom row) for the PDE (6.14). (a1) Sketch of a homoclinic orbit lying entirely in a fast subsystem. (a2) Corresponding pulse solution for the variables u (black) and $v = u'$ (gray). (b1) Sketch of a heteroclinic orbit lying entirely in a fast subsystem. (b2) Corresponding traveling back solution for the variables u (black) and $v = u'$ (gray). (c1) Sketch of a relaxation oscillation periodic solution. Note carefully that here the projection onto a fast variable u and a slow variable w is shown. (c2) Corresponding wave train solution for the variables u (black) and w (gray).

the ODE (6.16). The equilibrium points of (6.16) are given by the intersection of the y -nullcline $\{y = x_1/\gamma\}$ and the critical manifold

$$C_0 = \{(x_1, x_2, y) \in \mathbb{R}^3 : x_2 = 0, y = c_a(x_1) = x_1(1 - x_1)(x_1 - a)\}.$$

There are two nondegenerate fold points on C_0 found by solving $c'_a(x_1) = 0$:

$$x_1 = x_{1,\pm} = \frac{1}{3}(1 + a \pm \sqrt{1 - a + a^2}), \quad x_2 = 0, \quad y = c_a(x_{1,\pm}).$$

We denote the folds by $q_\pm = (x_{1,\pm}, 0, c_a(x_{1,\pm}))$. They split the critical manifold into three branches:

$$\begin{aligned} C_0^{a-} &= \{x_1 < x_{1,-}\} \cap C_0, \\ C_0^r &= \{x_{1,-} < x_1 < x_{1,+}\} \cap C_0, \\ C_0^{a+} &= \{x_{1,+} < x_1\} \cap C_0, \end{aligned}$$

where $C_0^{a\pm}$ are of saddle type and C_0^r is repelling; see also Example 3.4.3. The next exercise gives guidance on how Theorems 6.1.1 and 6.1.2 can be used to prove the existence of a heteroclinic orbit if there is more than one equilibrium point for (6.16). It is helpful to recall the fast–slow decomposition of the FitzHugh–Nagumo equation presented in Example 3.4.3 before continuing with the rest of this section and the next exercise.

Exercise/Project 6.2.1. Assume that the parameter γ is selected such that (6.16) has three hyperbolic equilibrium points. Denote the equilibrium point on C_0^{a-} by $p_1 = (0, 0, 0)$ and the equilibrium point on C_0^{a+} by p_2 . Both points are saddles, and the goal is to prove that a heteroclinic candidate between p_1 and p_2 persists. Hints:

1. Draw the situation with three equilibrium points (e.g., modify Figure 6.5(a) by changing the slope of the y -nullcline).
2. Extend the system by the equation $s' = 0$ as described in the remarks after Theorem 6.1.1.
3. Define N^1 for p_1 and N^2 for p_2 with $\dim(N^1) = 2$ and $\dim(N^2) = 3$.
4. Use the following fact [McK70]: there exists $s = (1 - 2a)/\sqrt{2}$ such that the fast subsystem at $y = y_0 = 0$ has a heteroclinic connection between C_0^{a-} and C_0^{a+} .
5. Now consider the second component of M in (6.10). \diamond

We proceed to the situation in which Theorems 6.1.1 and 6.1.2 no longer work. Suppose γ is chosen large enough that the full system (6.16) has a unique equilibrium point at $(0, 0, 0)$, e.g., it can be checked that this is the case for $\gamma = 1$.

Exercise 6.2.2. Determine the values of γ for which (6.16) has a unique global equilibrium point. \diamond

We assume from now on that $\delta = 5$, $\gamma = 1$, and $a = 1/10$ and write $c_{1/10}(x_1) = c(x_1)$. From the linearization of (6.16) at $(0, 0, 0)$, it follows that the origin is of saddle type with one unstable and two stable directions for the full system. The fold points can be described more explicitly:

$$x_{1,\pm} = \frac{1}{30} (11 \pm \sqrt{91}) \quad \text{or numerically: } x_{1,+} \approx 0.6846, \quad x_{1,-} \approx 0.0487.$$

The geometry of the system for one equilibrium point is illustrated in Figure 6.5(a). The sign of \dot{y} is given by $(x_1 - y)$. It is positive below $y = x_1$ and negative above, so the slow flow on C_0^{a-} is directed toward the unique equilibrium point. The slow subsystem orbits flow in the positive y -direction on the branches C_0^r and C_0^{a+} . The fast subsystem is

$$\begin{aligned} x'_1 &= x_2, \\ x'_2 &= sx_2 - x_1(1 - x_1)(x_1 - a) + y. \end{aligned} \tag{6.17}$$

The phase spaces of the fast subsystems, parameterized by the slow variable y , are planes $\{y = \text{constant}\}$. There are three different regions for (6.17) depending on the number of equilibrium points. There is one equilibrium for (6.17) for $y > c_a(x_{1,+})$ or $y < c_a(x_{1,-})$, two equilibria if $y = c_a(x_{1,\pm})$, and three equilibria if $c_a(x_{1,-}) < y < c_a(x_{1,+})$, so that the plane intersects C_0 three times;

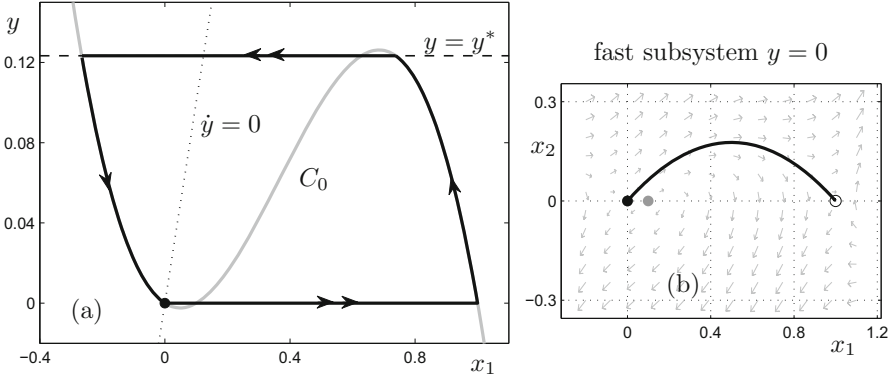


Figure 6.5: Singular ($\varepsilon = 0$) homoclinic orbit (pulse) for the FitzHugh–Nagumo equation (6.16) for $\delta = 5$, $a = 1/10$, $\gamma = 1$, $s = (1 - 2a)/\sqrt{2}$. (a) Projection into the (x_1, y) -plane. The unique global equilibrium at the origin (black dot), the critical manifold C_0 (gray), the y -nullcline (dotted), the fast subsystem domain at $y = y^* \approx 0.123$ (dashed), and the singular homoclinic orbit (black curve) are shown. (b) Fast subsystem phase portrait for the first fast jump with the heteroclinic orbit from C_0^{a-} to C_0^{a+} (black curve). The three equilibria of the fast subsystem (6.17) are shown as well; the two saddle points on $C_0^{a\pm}$ (black solid dot and black circle) are saddles, while the equilibrium on C_0^r (gray) is a spiral source. For three-dimensional illustrations, see also the related Figures 3.5, 11.4, 11.5, and 17.7.

see Figure 6.5(b). Let us focus on the last case, in which (6.17) has two saddle equilibria located on C_0^{a-} and C_0^{a+} and an unstable spiral on C_0^r .

It is shown analytically in [AW74] that there exists a wave speed s^* such that (6.17) has a heteroclinic connection between the two saddles at $y = 0$ and another heteroclinic connection for a value y^* with $0 < y^* < c_a(x_1, \cdot)$. The heteroclinic connection at $y = 0$ involves the unstable manifold of the equilibrium point $(0, 0)$ on C_0^{a-} , which is also the unique equilibrium of the full system; see Figure 6.5(b). Knowing the directions of the slow flow on each of the pieces of the critical manifold, one can construct a candidate consisting of alternating pieces of fast and slow motion, as shown in Figure 6.5(a).

Exercise/Project 6.2.3. Check several statements made so far in the fast–slow analysis of the FitzHugh–Nagumo equation. ◇

Looking at Figure 6.5(a), we are tempted to conclude that the FitzHugh–Nagumo equation has a homoclinic orbit to $(0, 0, 0)$, since we have just exhibited one in the singular limit. Unfortunately, it does not suffice to check just a transversality condition in the fast subsystems. The problem is that our singular orbit now contains two fast segments. We have to follow the unstable manifold $M = W^u(0, 0, 0)$ of the equilibrium point until it reaches a neighborhood close to the slow manifold C_ε^{a+} . Then we must follow M as it evolves near (but not

on) C_ε^{a+} ; indeed, if we were on C_ε^{a+} , or inside its stable manifold, then we would not be able to jump at the second heteroclinic connection at $y = y^*$, which occurs before the fold at $x_{1,+}$.

The next step is to consider the exit of M in a neighborhood of the second jump point at height $y = y^*$ and the fast connection to a neighborhood of C_ε^{a-} . Then we can follow it back near C_ε^{a-} to conclude that it reaches the stable manifold of $(0, 0, 0)$. So we must track how M evolves under the flow. In particular, a new tool is needed to track the evolution of M near C_ε^{a+} .

6.3 The C^0 Exchange Lemma

Before we begin the general discussion of the exchange lemma, we look at a low-dimensional, but very instructive, example.

Example 6.3.1. Consider the $(2, 1)$ -fast–slow system

$$\begin{aligned}\frac{da}{dt} &= a' = \lambda a, \\ \frac{db}{dt} &= b' = \gamma b, \\ \frac{dy}{dt} &= y' = \varepsilon,\end{aligned}\tag{6.18}$$

for fixed constants $\gamma < 0 < \lambda$, $0 < \varepsilon \ll 1$. The explicit solution of (6.18) is

$$a(t) = a_0 e^{\lambda t}, \quad b(t) = b_0 e^{\gamma t}, \quad y(t) = \varepsilon t + y_0,$$

where $(a_0, b_0, y_0) = (a(0), b(0), y(0))$. The geometry of the problem is shown in Figure 6.6 with saddle-type normally hyperbolic critical manifold $C_0 = \{(a, b, y) \in \mathbb{R}^3 : a = 0 = b\}$, the stable manifold $W^s(C_0) = \{(a, b, y) \in \mathbb{R}^3 : a = 0\}$, and the unstable manifold $W^u(C_0) = \{(a, b, y) \in \mathbb{R}^3 : b = 0\}$. Consider two sections

$$\Sigma_0 := \{(a, b, y) \in \mathbb{R}^3 : b = 1\} \quad \text{and} \quad \Sigma_1 := \{(a, b, y) \in \mathbb{R}^3 : a = 1\}$$

that are transverse to the stable and unstable manifolds of C_0 . The Poincaré map $\Pi : \Sigma_0 \rightarrow \Sigma_1$ induced by the flow can be calculated as

$$\Pi(a_0, 1, y_0) = (a_0 e^{\lambda t}, e^{\gamma t}, \varepsilon t + y_0) \quad \text{with} \quad a_0 e^{\lambda t} \stackrel{!}{=} 1 \quad \Rightarrow \quad t = -\frac{1}{\lambda} \ln a_0.$$

Therefore, a direct calculation yields that

$$b_1 = a_0^{-\gamma/\lambda}, \quad y_1 = y_0 - \frac{\varepsilon}{\lambda} \ln a_0 \quad \Rightarrow \quad a_0 = e^{-\frac{\lambda}{\varepsilon}(y_1 - y_0)}.\tag{6.19}$$

Under the assumption that we want to travel a distance $y_1 - y_0 = \mathcal{O}(1)$ as $\varepsilon \rightarrow 0$ near C_0 , it follows that a_0 has to be exponentially small, i.e., of order $\mathcal{O}(e^{-K/\varepsilon})$ for some constant $K > 0$ independent of ε . Geometrically, this means that the initial condition has to be exponentially close to the stable manifold $W^s(C_0)$. Furthermore, $b_1 = \mathcal{O}(e^{-K/\varepsilon})$, so that trajectories flowing for a long

time near a saddle-type manifold leave near the unstable manifold with exponentially small distance. Of course, similar conclusions apply if we consider families of trajectories starting on a submanifold $M \subset \Sigma_0$. The previous “ C^0 -information” is insufficient to track a tangent space $T_{(\cdot)}M$. To treat this case, formally differentiating in (6.19) leads to

$$\begin{aligned} \frac{dy_1}{da_0} &= -\frac{\varepsilon}{\lambda a_0}, \\ \frac{db_1}{da_0} &= -\frac{\gamma}{\lambda} a_0^{-(\gamma/\lambda+1)}, \end{aligned} \quad \Rightarrow \quad \frac{db_1}{dy_1} = \left(-\frac{\gamma}{\lambda} a_0^{-1-\gamma/\lambda} \right) \left(-\frac{\lambda a_0}{\varepsilon} \right) = \frac{\gamma}{\varepsilon} a_0^{-\gamma/\lambda}.$$

Using the result $a_0 = e^{-\frac{\lambda}{\varepsilon}(y_1-y_0)}$ in the last differential equation, we get

$$\frac{db_1}{dy_1} = \frac{\gamma}{\varepsilon} e^{\frac{\gamma}{\varepsilon}(y_1-y_0)},$$

which implies that the tangent space $T_{(a_1, 1, y_1)}M$ is also exponentially close to the tangent space of the unstable manifold $T_{(a_1, 1, y_1)}W^u(C_0)$ if the traveled distance is $y_1 - y_0 = \mathcal{O}(1)$. ♦

We want to extend the last example to a general fast–slow system

$$\begin{aligned} \varepsilon \frac{dx}{d\tau} &= \varepsilon \dot{x} = f(x, y, \varepsilon), \\ \frac{dy}{d\tau} &= \dot{y} = g(x, y, \varepsilon), \end{aligned} \tag{6.20}$$

for $x \in \mathbb{R}^m$, $y \in \mathbb{R}^n$ with $m \geq 2$.

Remark: Parameters in the system such as the wave speed s in the FitzHugh–Nagumo equation (6.16) can be included in the vector y as slow variables. In the FitzHugh–Nagumo equation, this would mean including the equation for the wave speed $\dot{s} = 0$ and relabeling s to a suitably indexed y -coordinate.

Let S_0 denote some compact normally hyperbolic subset of the critical manifold and let S_ε be the corresponding slow manifold. Recall from Section 4.1 that a fast–slow system near a normally hyperbolic critical manifold S_0 can be transformed into Fenichel normal form (cf. Theorem 4.1.2 and Figure 6.6):

$$\begin{aligned} \frac{da}{dt} &= a' = \Lambda(a, b, y, \varepsilon)a, \\ \frac{db}{dt} &= b' = \Gamma(a, b, y, \varepsilon)b, \\ \frac{dy}{dt} &= y' = \varepsilon(h(y, \varepsilon) + H(a, b, y, \varepsilon)(a, b)), \end{aligned} \tag{6.21}$$

with $t = \tau\varepsilon$, $a \in \mathbb{R}^k$, $b \in \mathbb{R}^l$, $y \in \mathbb{R}^n$, and $k + l = m$; Λ and Γ are matrix-valued functions, and H is a bilinear-form-valued function that can be written explicitly as

$$y'_i = \varepsilon \left(h_i(y, \varepsilon) + \sum_{u=1}^k \sum_{s=1}^l H_{ius} a_u b_s \right).$$

Recall that the matrix-valued functions Λ and Γ are constructed by separating the fast unstable and fast stable directions. More precisely, in (6.21), the manifold S_0 is given by

$$S_0 = \{(a, b, y) \in \mathbb{R}^{m+n} : a = 0, b = 0\},$$

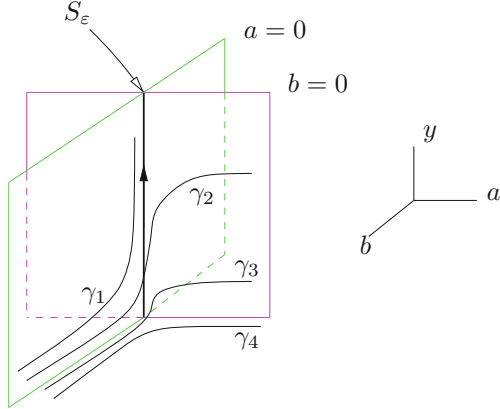


Figure 6.6: Sketch of a fast–slow system near a compact subset S_0 of a normally hyperbolic critical manifold. For the linear system (6.18) from Example 6.3.1, the view holds globally. For a general fast–slow system (6.20), Fenichel normal form is only local, and in the picture, several coordinates have been suppressed. We have also drawn in several sample trajectories γ_i for $i \in \{1, 2, 3, 4\}$ for the full system $0 < \varepsilon \ll 1$. Note that γ_1 lies inside the stable manifold $W^s(S_\varepsilon)$ (green); the trajectory has a fast phase toward S_ε and then follows S_ε slowly (draw the arrows). The other trajectories have initial values further away from the $W^s(S_\varepsilon)$ and stay close to S_ε for only a certain time, or do not even come close to it, such as γ_4 . Those trajectories $\gamma_{2,3}$ that stay close to S_ε for a while then leave the neighborhood of S_ε very close to $W^u(S_\varepsilon)$ (magenta). To compute trajectories near a saddle-type manifold numerically, we refer to Section 11.5.

where we recall our convention to abbreviate the zero vector $(0, 0, \dots, 0)^\top =: 0$ for notational convenience. Normal hyperbolicity implies that there are λ_0, γ_0 such that every eigenvalue λ_i of $\Lambda(0, 0, y, 0)$ and every eigenvalue γ_i of $\Gamma(0, 0, y, 0)$ satisfies

$$\operatorname{Re}(\lambda_i) > \lambda_0 > 0, \quad \operatorname{Re}(\gamma_i) < \gamma_0 < 0$$

in a region (or box)

$$\mathfrak{B} := \{(a, b, y) : \|a\| < \delta, \|b\| < \delta, y \text{ in a given compact region}\}$$

with $\delta > 0$ sufficiently small. The same holds for $\varepsilon > 0$ sufficiently small, so that (6.21) is still valid and we can find $\lambda_\varepsilon > 0$ and $\gamma_\varepsilon < 0$, which are the weak unstable and weak stable eigenvalues near S_ε . In equations (6.21), we can rectify the slow flow (see Section 4.1) so that

$$\begin{aligned} a' &= \Lambda(a, b, y, \varepsilon)a, \\ b' &= \Gamma(a, b, y, \varepsilon)b, \\ y' &= \varepsilon(U + H(a, b, y, \varepsilon)(a, b)), \end{aligned} \tag{6.22}$$

where $U = (1, 0, \dots, 0)^\top$. Observe that the stable and unstable manifolds W^s and W^u of S_ε are given by $\{a = 0\}$ and $\{b = 0\}$ respectively.

Let M be a $(k+1)$ -dimensional invariant manifold; M may depend smoothly on ε , but we do not display this in the notation; M is the manifold that we want to follow in phase space. We remark that the dimensional requirement on M can be generalized (see Section 6.6), but for simplicity, we shall consider only the case of $(k+1)$ dimensions for now. Suppose M intersects the boundary of the box \mathfrak{B} in $\{b = \delta\}$ at some point q . If q is close enough to the stable manifold $W^s(S_\varepsilon) = \{a = 0\}$, then a trajectory starting at q stays near S_ε for a long time, e.g., $t \sim 1/\varepsilon$ (cf. Example 6.3.1).

Lemma 6.3.2 ([JK94b]). *There exists constants $c_a, c_b, K > 0$ such that for $s \leq t$, the following three results hold:*

$$(R1) \quad \|b(t)\| \leq c_b \|b(s)\| e^{\gamma_0(t-s)};$$

$$(R2) \quad \|a(t)\| \geq c_a \|a(s)\| e^{\lambda_0(t-s)};$$

$$(R3) \quad \left\| \int_s^t a(\sigma) d\sigma \right\| \leq K \quad (\text{independent of } \varepsilon, t, s);$$

as long as a trajectory remains in \mathfrak{B} .

Proof. We begin by proving (R1). Since the eigenvalues of $\Gamma(a, b, y, \varepsilon)$ are close to those of $\Gamma(0, 0, y, \varepsilon)$, it follows that near each point $z = (a, b, y) \in \mathfrak{B}$, there is a neighborhood N of z such that

$$\|b(t)\| \leq C_N \|b(s)\| e^{\gamma_0(t-s)}$$

holds if $b(\sigma) \in N$ with $\sigma \in (s, t)$ and ε sufficiently small. By compactness of \mathfrak{B} , we can cover \mathfrak{B} by a finite number of such neighborhoods. In fact, considering all segments, the trajectories lying in \mathfrak{B} cover each segment by an open cover. The union of those sets covers \mathfrak{B} , and then a finite subcover exists by compactness. Therefore, an estimate for an arbitrary trajectory is

$$\|b(t)\| \leq C_{N_1} C_{N_2} \cdots C_{N_m} \|b(s)\| e^{\gamma_0(t-s)}$$

for some finite fixed $m \in \mathbb{N}$. Now (R1) follows, and (R2) is immediate by the same method of proof as for (R1). This leaves the estimate (R3). Using (R2) yields

$$\|a(\sigma)\| \leq \frac{1}{c_a} \|a(t)\| e^{\lambda_0(\sigma-t)} \quad \text{for } \sigma \leq t.$$

Integrating both sides of the last equation leads to

$$\int_s^t \|a(\sigma)\| d\sigma \leq \frac{1}{c_a} \|a(t)\| \int_s^t e^{\lambda_0(\sigma-t)} d\sigma \leq \frac{\|a(t)\|}{c_a \lambda_0} (1 - e^{\lambda_0(s-t)}).$$

Since $\|a(t)\| \leq \delta$ and $\lambda_0 > 0$, we can conclude that (R3) holds. \square

Now we can track trajectories inside \mathfrak{B} and follow a neighborhood of q in M under the flow, as shown by the next result; see also Figure 6.7.

Theorem 6.3.3 ([JK94b]). Let $\bar{q} \in M \cap \{\|a\| = \delta\}$ be the exit point of a trajectory starting at $q \in M \cap \{\|b\| = \delta\}$ that spends time t that is $\mathcal{O}(1/\varepsilon)$ in \mathfrak{B} . Let V be a neighborhood of q in M . If V is sufficiently small, then the image of V under the time t map is $\mathcal{O}(\varepsilon)$ -close to

$$\{\|b\| = 0, y_i - y_i(0) = 0, i > 1\}$$

in the C^0 -norm, where $y_i(0)$ denotes the y -coordinates of q .

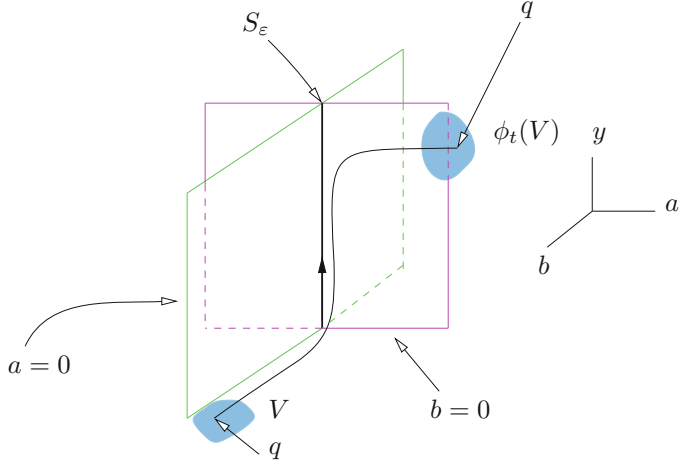


Figure 6.7: In this figure, all coordinates y_i with $i > 1$ are suppressed. The image of the neighborhood V (light blue, shaded) near the exit point \bar{q} is denoted by $\phi_t(V)$ (light blue, shaded); it is very close to the unstable manifold $W^u(S_\varepsilon) = \{\|b\| = 0\}$ (magenta) near the exit point \bar{q} .

Proof. By (R1) from Lemma 6.3.2, it follows that $b(t)$ is small. Hence, we are left with the y_i coordinates with $i > 1$. Since $b(t)$ is small, one obtains

$$y'_i \leq \varepsilon \left(\sum_{u=1}^k H_{iu} a_u \right) =: \varepsilon \bar{H}_i \cdot a,$$

where \bar{H}_i is a k -vector of functions. Since \bar{H}_i is smooth and \mathfrak{B} is compact, let d_i be a bound for $\|\bar{H}_i\|$. Therefore,

$$\int_0^t y_i \, d\sigma \leq \varepsilon \int_0^t \bar{H}_i \cdot a \, d\sigma$$

implies, using the fundamental theorem of calculus, that

$$|y_i(t) - y_i(0)| \leq \varepsilon \int_0^t d_i \|a(\sigma)\| \, d\sigma. \quad (6.23)$$

Using Lemma 6.3.2, part (R3), we can conclude that the right-hand side of (6.23) is $\mathcal{O}(\varepsilon)$. \square

A natural name for Theorem 6.3.3 is the **C^0 -exchange lemma**.

6.4 The C^1 Exchange Lemma

Having the C^0 exchange lemma, one may wonder why there is any need to consider a refined version of it? The problem is that every trajectory exits near \bar{q} almost tangent to the unstable manifold $W^u(S_\varepsilon)$. Hence, we have no information about the part of the tangent spaces of M in the slow centerlike directions.

As an example, suppose we know results about transversality in the singular limit $\varepsilon = 0$ for an intersection of $W^u(S_0)$ with some other manifold, say N . Then we cannot conclude yet that M from Theorem 6.3.3 is transversal to N for $0 < \varepsilon \ll 1$. Theorem 6.3.3 provides information about the location of the manifold M itself (“ C^0 -information”) but not about its tangent spaces (“ C^1 -information”). Since the tangent spaces determine whether an intersection is transversal, the C^0 -exchange lemma is insufficient.

Remark: Note carefully that the situation just described occurs for the FitzHugh–Nagumo equation (6.16) if we try to follow the unstable manifold of the unique equilibrium point during its second jump; see Figure 6.5.

The C^1 -closeness result for (6.22) is the following (cf. Figure 6.7):

Theorem 6.4.1 (Exchange lemma, [JK94b]). *Let M be a $(k+1)$ -dimensional invariant manifold. Assume that $M \cap \{\|b\| = \delta\}$ intersects $\{a = 0\}$ transversely. Let $\bar{q} \in M \cap \{\|a\| = \delta\}$ be the exit point of a trajectory starting at $q \in M \cap \{\|b\| = \delta\}$ that spends time $t = \mathcal{O}(1/\varepsilon)$ in \mathfrak{B} . Let V be a neighborhood of q in M . The image of V under the time t map is $\mathcal{O}(\varepsilon)$ -close in the C^1 -norm to*

$$\{\|b\| = 0, y_i - y_i(0) = 0, i > 1\}, \quad (6.24)$$

where $y_i(0)$ denotes the y -coordinates of q .

The key point of the exchange lemma is to trade information about transversality and variation of certain center directions (here y_i with $y_i > 1$) near q with new information near the exit point \bar{q} given by a C^1 -closeness result to a certain submanifold of the unstable manifold $W^u(S_\varepsilon)$. Any proof of Theorem 6.4.1 is going to involve technical calculations, but we remind the reader that the one key idea has already been discussed in Example 6.3.1.

The idea of proof used by Jones and Kopell [JK94b] to achieve a tracking of the tangent spaces to M is to consider **$(k+1)$ -differential forms** that are dual to $(k+1)$ planes in $k+l+n$ space and describe their evolution by a differential equation.

Remark: For technical background on differential forms, see [Lee06, Jän01], where basic k -forms and the **wedge product** \wedge are defined and the **exterior product space** is discussed. Furthermore, recalling (in the sense of the remark before Proposition 2.2.3) the notions of **pushforward** and **pullback** of differential forms will be helpful.

As usual, we shall write simply $(k+1)$ -form with the implicit assumption that all forms are sufficiently differentiable. A **basic $(k+1)$ -form** is given by

$$P_{\sigma_1 \dots \sigma_{k+1}} := d\sigma_1 \wedge \dots \wedge d\sigma_{k+1},$$

where $\sigma_j \in \{a_i, b_i, y_i\}$. A basis for all $(k+1)$ -forms is given by restricting to increasing indices, where we agree on the index ordering

$$a_1 < a_2 < \dots < a_k < b_1 < \dots < b_l < y_1 < \dots < y_n.$$

It will be convenient to use a projectivized version of the $P_{\sigma_1 \dots \sigma_{k+1}}$,

$$\hat{P}_{\sigma_1 \dots \sigma_{k+1}} := \frac{P_{\sigma_1 \dots \sigma_{k+1}}}{P_{a_1 \dots a_k y_1}}.$$

A priori, \hat{P} might not be well defined, since $P_{a_1 \dots a_k y_1}$ might be zero. But we shall see that near S_ε , one has $P_{a_1 \dots a_k y_1} \neq 0$, i.e., the components of tangent planes of M at points of trajectories in \mathfrak{B} always have nonvanishing components in the a_i and the y_1 directions. In fact, the hyperplane H spanned by the a_i and the y_1 coordinates can be defined by requiring that

$$P_{\sigma_1 \dots \sigma_{k+1}}(v) = 0 \quad \text{for all } v \in H \text{ and } (\sigma_1, \dots, \sigma_{k+1}) \neq (a_1, \dots, a_k, y_1).$$

Now the exchange lemma can be restated in an equivalent version using differential forms.

Theorem 6.4.2 (Exchange lemma, differential form conclusion [JK94b]). *Under the same assumptions as in Theorem 6.4.1, we conclude that at \bar{q} ,*

$$\hat{P}_{\sigma_1 \dots \sigma_{k+1}} = \mathcal{O}(\varepsilon)$$

for all $(\sigma_1, \dots, \sigma_{k+1}) \neq (a_1, \dots, a_k, y_1)$.

Considerable technical checking arises in the proof. Here we restrict attention to the lowest nontrivial case with respect to dimensions of all objects involved. Despite the simplifications, the proof contains all necessary techniques to prove Theorem 6.4.2 in full generality (see [JK94b] for the general proof). More precisely, we aim to prove Theorem 6.4.2 for a $(2, 2)$ -fast–slow system in Fenichel normal form near the slow manifold S_ε with $z := (a, b, y_1, y_2)$ and $a, b, y_1, y_2 \in \mathbb{R}$:

$$\begin{aligned} a' &= \Lambda(z, \varepsilon)a, \\ b' &= \Gamma(z, \varepsilon)b, \\ y'_1 &= \varepsilon g_1(z, \varepsilon) = \varepsilon(1 + H_1(a, b, y, \varepsilon)ab), \\ y'_2 &= \varepsilon g_2(z, \varepsilon) = \varepsilon(H_2(a, b, y, \varepsilon)ab). \end{aligned} \tag{6.25}$$

In view of the previous notation, we have $k = 1 = l$ and $n = 2$, and we still work in a suitable neighborhood (or box)

$$\mathfrak{B} := \{(a, b, y) \in \mathbb{R}^4 : |a| < \delta, |b| < \delta, y \text{ in a given compact region}\}. \quad (6.26)$$

The proof can be divided into six steps:

- *Step 1:* To track tangent planes to a two-dimensional invariant manifold M , one can develop evolution equations for differential 2-forms that are dual to planes in \mathbb{R}^4 .
- *Step 2:* The evolution equations derived in Step 1 are of a special form due to the structure of Fenichel normal form and they “split” the coordinates of 2-forms into two groups. One is formed by P_{ay_1} , P_{ay_2} , and the other by the four other basic 2-forms spanning $\Lambda^2 \mathbb{R}^4$. Both groups will satisfy fundamental estimates under the flow.
- *Step 3:* The assumptions of the exchange lemma on transversality at the entry point to \mathfrak{B} and spending time of order $\mathcal{O}(1/\varepsilon)$ in \mathfrak{B} are used. They provide estimates on the initial conditions at the entry point q .
- *Step 4:* In \mathfrak{B} , we are going to follow a reference solution that starts at the entry point q , stays close to (or “tracks”) the slow manifold, and then exits near \bar{q} . The first key component is to show that the form P_{ay_1} never vanishes inside \mathfrak{B} . This allows one to consider forms projectivized/divided by P_{ay_1} . Then the reference solution is tracked through a compact neighborhood inside \mathfrak{B} . One shows that inside \mathfrak{B} , all estimates we want from the evolution equations hold and then extends this procedure by compactness of \mathfrak{B} .
- *Step 5:* This step provides the basic estimates to control the evolution of all 2-forms inside \mathfrak{B} . The estimates appear to be rather involved, but the essential tool is just Gronwall’s lemma.
- *Step 6:* The last step collects all the previous results and derives from estimates at q the final estimates at \bar{q} . This final part of the proof is subdivided into three parts. The first tracks M from q to S_ε , the second follows M near S_ε , and the third deals with the exit from S_ε toward \bar{q} . The overall patching strategy is the same as in Step 4.

Step 1: We begin with a remark on 2-forms in \mathbb{R}^4 . Let σ_i for $i = 1, 2, 3, 4$ be coordinates in \mathbb{R}^4 . Observe that if P is a 2-plane, then the evaluation of a 2-form on P is defined only up to a multiple, since we can scale basis vectors inside P . To avoid this ambiguity, consider a unit rectangle R of P and, for example, define $(d\sigma_1 \wedge d\sigma_2)(P)$ by projecting R onto the (σ_1, σ_2) -plane along the coordinate axes σ_3, σ_4 and by taking the area of this projection. Note that this defines the evaluation of 2-forms up to orientation; this ambiguity will not matter for us in the following, since we will consider only absolute values in

evaluating 2-forms on planes. Furthermore, observe that, e.g., the (σ_1, σ_2) -plane is characterized by vanishing of all basic 2-forms except $d\sigma_1 \wedge d\sigma_2$ and $d\sigma_2 \wedge d\sigma_1$.

The variational equations describing a flow of the differential forms da , db , dy_1 , and dy_2 associated with (6.25) are

$$\begin{aligned} da' &= \Lambda(z, \varepsilon)da + a(\nabla\Lambda \cdot dz), \\ db' &= \Gamma(z, \varepsilon)db + b(\nabla\Gamma \cdot dz), \\ dy'_1 &= \varepsilon\nabla g_1(z, \varepsilon) \cdot dz, \\ dy'_2 &= \varepsilon\nabla g_2(z, \varepsilon) \cdot dz, \end{aligned}$$

where $dz = (da, db, dy_1, dy_2)^\top$ and ∇ denotes the usual **gradient operator**. The calculation of the evolution equations for the two-form $P_{\sigma_1 \sigma_2}$ just uses the product rule

$$\begin{aligned} P'_{ay_1} &= (da \wedge dy_1)' = da' \wedge dy_1 + da \wedge dy'_1 \\ &= (\Lambda(z, \varepsilon)da + a\nabla\Lambda \cdot dz) \wedge dy_1 + \varepsilon da \wedge (\nabla g_1 \cdot dz) \\ &=: \Lambda(z, \varepsilon)P_{ay_1} + aR_1 + \varepsilon R_2, \end{aligned}$$

where \cdot denotes the usual dot product between vectors in \mathbb{R}^4 . We drop the argument (z, ε) for simplicity from now on. The calculations for the other 2-forms are similar, and the desired evolution equations are

$$\begin{aligned} P'_{ay_1} &= \Lambda P_{ay_1} + aR_1 + \varepsilon R_2, \\ P'_{ay_2} &= \Lambda P_{ay_2} + aR_3 + \varepsilon R_4, \\ P'_{ab} &= (\Lambda + \Gamma)P_{ab} + aR_5 + bR_6, \\ P'_{by_1} &= \Gamma P_{by_1} + bR_7 + \varepsilon R_8, \\ P'_{by_2} &= \Gamma P_{by_2} + bR_9 + \varepsilon R_{10}, \\ P'_{y_1 y_2} &= \varepsilon(R_{11} + R_{12}), \end{aligned} \tag{6.27}$$

where

$$\begin{aligned} R_1 &= (\nabla\Lambda \cdot dz) \wedge dy_1, & R_7 &= (\nabla\Gamma \cdot dz) \wedge dy_1, \\ R_2 &= da \wedge (\nabla g_1 \cdot dz), & R_8 &= db \wedge (\nabla g_1 \cdot dz), \\ R_3 &= (\nabla\Lambda \cdot dz) \wedge dy_2, & R_9 &= (\nabla\Gamma \cdot dz) \wedge dy_2, \\ R_4 &= da \wedge (\nabla g_2 \cdot dz), & R_{10} &= db \wedge (\nabla g_2 \cdot dz), \\ R_5 &= (\nabla\Lambda \cdot dz) \wedge db, & R_{11} &= dy_1 \wedge (\nabla g_1 \cdot dz), \\ R_6 &= da \wedge (\nabla\Gamma \cdot dz), & R_{12} &= (\nabla g_2 \cdot dz) \wedge dy_2. \end{aligned}$$

Note that we considered only the six 2-forms $P_{ay_1}, P_{ay_2}, P_{ab}, P_{by_1}, P_{by_2}, P_{y_1 y_2}$ as they span the space of two-forms $\wedge^2 \mathbb{R}^4$.

Exercise 6.4.3. Derive the equation for P'_{by_1} . Prove that $\wedge^2 \mathbb{R}^4 \cong \mathbb{R}^6$. \diamond

To simplify notation, let

$$\begin{aligned} Z &:= (P_{ay_1}, P_{ay_2})^\top &= (Z_1, Z_2)^\top, \\ X &:= (P_{ab}, P_{by_1}, P_{by_2}, P_{y_1 y_2})^\top &= (X_1, X_2, X_3, X_4)^\top. \end{aligned}$$

Step 2: The next lemma provides fundamental estimates used throughout the entire proof of the exchange lemma.

Lemma 6.4.4. *The equations for (Z, X) can be written in the form*

$$\begin{aligned} Z' &= \Lambda Z + \eta_1(Z, X, t), \\ X' &= BX + \eta_2(Z, X, t), \end{aligned} \quad (6.28)$$

where $B = B(z, \varepsilon)$ is a 4×4 -matrix-valued function. The following hold:

(i) At $a = 0, b = 0, \varepsilon = 0$, we have $\eta_1 = 0, \eta_2 = 0$.

(ii) The matrix B satisfies

$$\left\| \exp \left(\int_s^t (B - \Lambda(\text{Id})) \, d\xi \right) \right\| \leq \bar{M} \exp(-\mu(t-s)) \quad (6.29)$$

for some $\bar{M} \geq 1, \mu > 0$, and $t > s$.

(iii) Denote by η_{1i} the i th row of η_1 . Then

$$\eta_{1i} = F_i(Z_i, X, t) + G_i(Z, X, t),$$

where the following estimates are satisfied:

$$\begin{aligned} |F_i(Z_i, X, t)| &\leq \tilde{C}|a|(|Z_i| + \|X\|), \\ |G_i(Z, X, t)| &\leq \varepsilon \tilde{K}|a|(\|Z\| + \|X\|), \end{aligned}$$

for some fixed constants $\tilde{C}, \tilde{K} < \infty$.

(iv) Furthermore, one has

$$\eta_2 = P(X, t) + Q(Z, X, t),$$

where the following estimates are satisfied:

$$\begin{aligned} \|E(X, t)\| &\leq \hat{C}|a|\|X\| \\ \|H(Z, X, t)\| &\leq \hat{K}(\varepsilon + |b|)(\|Z\| + \|X\|) \end{aligned}$$

for some fixed constants $\hat{C}, \hat{K} < \infty$.

Proof. From the evolution equations (6.27), we find that

$$\begin{aligned} Z' &= \Lambda Z + \begin{pmatrix} aR_1 + \varepsilon R_2 \\ aR_3 + \varepsilon R_4 \end{pmatrix} \\ &= \Lambda Z + \begin{pmatrix} a(\Lambda_a Z_1 + \Lambda_b X_2 - \Lambda_{y_2} X_4) + \varepsilon(g_{1b} X_1 + g_{1y_1} Z_1 + g_{1y_2} Z_2) \\ a(\Lambda_a Z_2 + \Lambda_b X_3 + \Lambda_{y_1} X_4) + \varepsilon(g_{2b} X_1 + g_{2y_1} Z_1 + g_{2y_2} Z_2) \end{pmatrix}, \end{aligned} \quad (6.30)$$

where letter subscripts denote the partial derivative with respect to the indicated variable; note that the antisymmetry property of differential forms has been used

extensively in the calculation (6.30). From (6.30), we see that $Z' = \Lambda Z$ when $a = 0$ and $\varepsilon = 0$. We also have

$$\begin{aligned} X' &= \begin{pmatrix} \Lambda + \Gamma & 0 & 0 & 0 \\ 0 & \Gamma & 0 & 0 \\ 0 & 0 & \Gamma & 0 \\ 0 & 0 & 0 & 0 \end{pmatrix} \begin{pmatrix} X_1 \\ X_2 \\ X_3 \\ X_4 \end{pmatrix} + \begin{pmatrix} aR_5 + bR_6 \\ bR_7 + \varepsilon R_8 \\ bR_9 + \varepsilon R_{10} \\ \varepsilon R_{11} + \varepsilon R_{12} \end{pmatrix} \\ &= BX + \begin{pmatrix} a(\Lambda_a X_1 - \Lambda_{y_1} X_2 - \Lambda_{y_2} X_3) + b(\Gamma_b X_1 + \Gamma_{y_1} X_1 + \Gamma_{y_2} X_2) \\ b(\Gamma_a Z_1 + \Gamma_b X_2 - \Gamma_{y_2} X_4) + \varepsilon(-g_{1a} X_1 + g_{1y_1} X_2 + g_{1y_2} X_3) \\ b(\Lambda_a Z_2 + \Lambda_b X_3 + \Lambda_{y_1} X_4) + \varepsilon(-g_{2a} X_1 + g_{2y_1} X_2 + g_{2y_2} X_3) \\ \varepsilon(-g_{1a} Z_1 - g_{1b} X_2 + g_{1y_2} X_4 + g_{1a} Z_2 + g_{2b} X_3 + g_{2y_1} X_4) \end{pmatrix}. \end{aligned} \quad (6.31)$$

Hence, for $a = 0$, $b = 0$, and $\varepsilon = 0$, we must have $\eta_2 = 0$, which completes the proof of (i). For (ii), note that

$$B - \Lambda \text{ Id} = \begin{pmatrix} \Gamma & 0 & 0 & 0 \\ 0 & \Gamma - \Lambda & 0 & 0 \\ 0 & 0 & \Gamma - \Lambda & 0 \\ 0 & 0 & 0 & -\Lambda \end{pmatrix}. \quad (6.32)$$

Recall that $\Lambda \geq \Lambda_0 > 0$ and $\Gamma \leq \Gamma_0 < 0$ for (z, ε) in a suitable compact subset, which we called \mathfrak{B} , near the critical manifold by Fenichel normal form theory. Therefore, the matrix in (6.32) has eigenvalues bounded above by some negative fixed number, say $-\mu$ with $\mu > 0$; using this observation, (ii) follows. We can group the terms on the right-hand side in (6.30) as follows:

$$\begin{aligned} F_1(Z_1, X, t) &:= a(\Lambda_a Z_1 + \Lambda_b X_2 - \Lambda_{y_2} X_4), \\ G_1(Z, X, t) &:= \varepsilon(g_{1b} X_1 + g_{1y_1} Z_1 + g_{1y_2} Z_2), \\ F_2(Z_2, X, t) &:= a(\Lambda_a Z_2 + \Lambda_b X_3 + \Lambda_{y_1} X_4), \\ G_2(Z, X, t) &:= \varepsilon(g_{2b} X_1 + g_{2y_1} Z_1 + g_{2y_2} Z_2). \end{aligned}$$

Using the triangle inequality, the estimates required in (iii) follow. Now set $E(X, t)$ equal to all the terms of $X' - BX$ that do not vanish at $b = 0$ and $\varepsilon = 0$. Then let $H(Z, X, t) := X' - BX - E(X, t)$ and use the triangle inequality again. This proves (iv) and completes the proof. \square

Step 3: We want to incorporate the assumptions of the exchange lemma into estimates on the initial conditions of Z_i and X_i at q . In particular, the trajectory spends at least $t = \mathcal{O}(1/\varepsilon)$ in a box \mathfrak{B} , and there is a transversality condition at the entry point q . This will constrain the values of (Z, X) on $T_q M$. Let $\hat{X}_i := X_i/Z_1$ and $\hat{Z}_2 := Z_2/Z_1$ as suggested in the differential form version of the exchange lemma in Theorem 6.4.2.

Lemma 6.4.5. *There exists $\bar{K} > 0$ such that at $T_q M$, we have $|Z_1| > \bar{K}\varepsilon$, $|\hat{X}_i| < 1/(\bar{K}\varepsilon)$, and $|\hat{Z}_2|$ is exponentially small.*

Proof. Evaluating forms on $T_q M$ is defined as evaluating them on a projection to a unit hypercube. Therefore, we must have $|X_i(T_q M)| \leq 1$. Since $T_q M$ is

transverse with respect to $\{a = 0\}$, there is a \bar{K} such that $|Z_1(T_q M)| > \bar{K}\varepsilon$. Hence, it follows that

$$|\hat{X}_i(T_q M)| = \frac{|X_i(T_q M)|}{|Z_1(T_q M)|} < 1/(\bar{K}\varepsilon).$$

It remains to show that $|\hat{Z}_2|$ is exponentially small, and so one has to estimate $|Z_2|$. We view $T_q M$ as spanned by two vectors, one defined by the vector field (6.25), denoted by v , and a vector orthogonal to it in $T_q M$, say v^\perp . Up to a scalar multiple,

$$|Z_2(T_q M)| = \text{const} \cdot \left| \det \begin{pmatrix} v_1 & v_4 \\ v_1^\perp & v_4^\perp \end{pmatrix} \right| = \text{const} \cdot |v_1 v_4^\perp - v_4 v_1^\perp|, \quad (6.33)$$

since evaluating the differential form $da \wedge dy_2 = Z_2$ on two vectors amounts to picking out the a and y_2 components and then applying the determinant. By definition of v , we look at equation (6.25) and see that $|v_1|$ is $\mathcal{O}(|a|)$. Since $|v_4^\perp|$ is bounded by a constant, we have an $\mathcal{O}(|a|)$ estimate on the first term of (6.33). Next, recall that the equation for y'_2 in Fenichel normal form is

$$y'_2 = \varepsilon g_2(z, \varepsilon) = \varepsilon(H_2(a, b, y, \varepsilon)ab).$$

This means that v_4 also contains a multiplicative factor of $\mathcal{O}(|a|)$ when we estimate it. If one shows that $|a|$ is exponentially small at q , then the result follows easily. Indeed, Lemma 6.3.2 says that the a -coordinate will expand at least by a positive rate $\Lambda_0 > 0$ inside \mathfrak{B} . Now use the hypothesis that the trajectory through q stays an $\mathcal{O}(1/\varepsilon)$ time in \mathfrak{B} and hence $|a|$ must have been exponentially small at q ,

$$|a| < k_1 e^{-k_2/\varepsilon} \quad \text{for some constants } k_i > 0.$$

Hence, $|Z_2|$ is exponentially small, which immediately yields that $|\hat{Z}_2|$ is exponentially small. \square

Step 4: The next goal is to estimate the size of \hat{Z}_i and \hat{X}_i evaluated on the tangent space to M that evolves under the flow. The reference trajectory starts at q and ends at \bar{q} . From Lemma 6.4.5, we know that $|Z_1| > \bar{K}\varepsilon$ in a neighborhood of q , so the projectivized forms are well defined (i.e., the denominator is nonzero) in this region. The next lemma provides this well-definedness inside \mathfrak{B} .

Lemma 6.4.6. *There is a constant $C > 0$ such that*

$$|Z_1'|' \geq (\Lambda - C|a|(1 + \|\hat{X}\| + \varepsilon\|\hat{Z}\|))|Z_1|. \quad (6.34)$$

Proof. Near q , it is known that $|Z_1| \neq 0$, and so we calculate

$$\begin{aligned} |Z_1'|' &= \frac{d}{dt} \sqrt{Z_1^2} = \frac{2Z_1'Z_1}{2\sqrt{Z_1^2}} \\ &= \frac{\Lambda Z_1^2}{|Z_1|} + \frac{\eta_{11}Z_1}{|Z_1|} = \Lambda|Z_1| + \frac{\eta_{11}Z_1}{|Z_1|}. \end{aligned}$$

Using Lemma 6.4.4, we find that

$$\begin{aligned} |Z_1'| &\geq \Lambda|Z_1| - (|F_1| + |G_1|) \\ &\geq (\Lambda - \tilde{C}|a|)|Z_1| - \tilde{C}|a|\|X\| - \varepsilon\tilde{K}|a|(\|Z\| + \|X\|). \end{aligned}$$

Now choose C such that $C > \tilde{C} + \varepsilon\tilde{K}$ and $C > \tilde{K}$, and we obtain (6.34) near q . Making the box \mathfrak{B} sufficiently small, we can make $|a|$ small enough that since $\Lambda \geq \Lambda_0 > 0$, we always have

$$(\Lambda - C|a|(1 + \|\hat{X}\| + \varepsilon\|\hat{Z}\|)) > 0.$$

Near q , we conclude that $|Z_1'| > 0$, and so $|Z_1|$ is increasing. If the reference trajectory leaves a neighborhood of q then we still have $|Z_1| > \bar{K}\varepsilon$. Repeating the argument above in a compact set away from q and covering \mathfrak{B} by finitely many compact sets yields $|Z_1| \neq 0$ inside \mathfrak{B} . The estimate (6.34) follows. \square

Step 5: The next lemma is fundamental for controlling \hat{Z}_i inside \mathfrak{B} .

Lemma 6.4.7. *There are constants $C, K > 0$, where C is as in Lemma 6.4.6, such that the following inequalities hold:*

$$|\hat{Z}_i'| \leq (\alpha(t) + 2C|a|)|\hat{Z}_i| + \alpha(t) \quad (6.35)$$

$$\|\hat{X}\| \leq \bar{M} \left[\|\hat{X}_0\| e^{\int_0^t \beta_1(s) ds} + \int_0^t e^{\int_s^t \beta_1(r) dr} \beta_2(s) ds \right], \quad (6.36)$$

where α , β_1 , and β_2 are as follows:

$$\begin{aligned} \alpha(t) &= C|a|(\|\hat{X}\| + \varepsilon(1 + \|\hat{Z}\|)), \\ \beta_1(t) &= -\mu + C(\delta + |a|\|\hat{X}\|), \\ \beta_2(t) &= K[(\varepsilon + |b| + \varepsilon|a|\|\hat{X}\|)\|\hat{Z}\| + \varepsilon + |b|]. \end{aligned}$$

The constant $\mu > 0$ carries over from Lemma 6.4.4, and $\delta > 0$ defines the neighborhood size of \mathfrak{B} as given in (6.26).

Proof. We start by proving (6.35). A direct calculation as in the previous lemma gives

$$|\hat{Z}_i'| = -\frac{\eta_{11}\hat{Z}_i^2}{Z_1|\hat{Z}_i|} + \frac{\eta_{1i}\hat{Z}_i}{Z_1|\hat{Z}_i|}. \quad (6.37)$$

The chain and quotient rules used for calculating (6.37) are valid only for $|Z_i| \neq 0$; when $Z_i = 0$, we obtain only left and right limits for the derivative of opposite sign. If we estimate the right-hand side of (6.37), then we obtain

$$|\hat{Z}_i'| \leq \left| \frac{\eta_{11}}{Z_1} \right| |\hat{Z}_i| + \left| \frac{\eta_{1i}}{Z_1} \right|,$$

which is independent of such left and right limits. Using Lemma 6.4.4, one obtains

$$\begin{aligned} \left| \frac{\eta_{11}}{Z_1} \right| &\leq \tilde{C}|a|(1 + \|\hat{X}\|) + \varepsilon\tilde{K}|a|(1 + \|\hat{Z}\| + \|\hat{X}\|), \\ \left| \frac{\eta_{1i}}{Z_1} \right| &\leq \tilde{C}|a|(|\hat{Z}_i| + \|\hat{X}\|) + \varepsilon\tilde{K}|a|(1 + \|\hat{Z}\| + \|\hat{X}\|). \end{aligned}$$

The desired estimate (6.35) now follows if we choose C , as before, such that $C > \tilde{C} + \varepsilon\tilde{K}$ and $C > \tilde{K}$. This completes the first part of the proof. For the second part, a direct calculation yields

$$\begin{aligned}\hat{X}'_i &= \frac{d}{dt} \left(\frac{X_i}{Z_1} \right) = \frac{Z_1 X'_i - X_i Z'_1}{Z_1^2} \\ &= \frac{Z_1(B_{ii}X_i + \eta_{2i}) - X_i(\Lambda Z_1 + \eta_{11})}{Z_1^2} \\ &= (B_{ii} - \Lambda)\hat{X}_i + \left[\frac{\eta_{2i}}{Z_1} - \frac{\eta_{11}}{Z_1}\hat{X}_i \right].\end{aligned}$$

This result can be written more compactly in vector form as

$$\hat{X}' = (B - \Lambda)\hat{X} + \left[\frac{\eta_2}{Z_1} - \frac{\eta_{11}}{Z_1}\hat{X} \right].$$

From Lemma 6.4.4, we get that

$$\left\| \frac{\eta_2}{Z_1} \right\| \leq \hat{C}|a|\|\hat{X}\| + \hat{K}(\varepsilon + |b|)(1 + \|\hat{Z}\| + \|\hat{X}\|).$$

Since we already found an estimate on $|\eta_{11}/Z_1|$ above, it now follows that

$$\left| \frac{\eta_2}{Z_1} - \frac{\eta_{11}}{Z_1}\hat{X} \right| \leq \beta_3(t)\|\hat{X}\| + \beta_2(t), \quad (6.38)$$

where $\beta_3(t) = C^*|a|(1 + \|\hat{X}\|) + K(\varepsilon + |b|)$ and the constants are chosen such that $C^* > \tilde{C} + \varepsilon\tilde{K} + \tilde{C}$ and $K > \max(\tilde{K}, \hat{K})$. Basically, the estimate (6.38) controls the nonlinear term for the equations of \hat{X} . Next, consider an **integrating factor**

$$J(t) := \exp \left(- \int_0^t (B - \Lambda \text{ Id}) \, ds \right).$$

A standard integrating factor calculation then reads

$$\begin{aligned}\hat{X}' J - (B - \Lambda)\hat{X} J &= J \left[\frac{\eta_2}{Z_1} - \frac{\eta_{11}}{Z_1}\hat{X} \right] \\ \Rightarrow \quad (\hat{X} J)' &= J \left[\frac{\eta_2}{Z_1} - \frac{\eta_{11}}{Z_1}\hat{X} \right] \\ \Rightarrow \quad \int_0^t (\hat{X} J)' \, ds &= \int_0^t J \left[\frac{\eta_2}{Z_1} - \frac{\eta_{11}}{Z_1}\hat{X} \right] \, ds \\ \Rightarrow \quad \hat{X} &= J(t)^{-1}\hat{X}_0 + J(t)^{-1} \int_0^t J \left[\frac{\eta_2}{Z_1} - \frac{\eta_{11}}{Z_1}\hat{X} \right] \, ds.\end{aligned}$$

The inverse of the matrix $J(t)$ is

$$J(t)^{-1} = \exp \left(\int_0^t (B - \Lambda \text{ Id}) \, ds \right).$$

Recall from Lemma 6.4.4 that we have the estimate

$$\exp\left(\int_s^t (B - \Lambda \text{ Id}) \, dr\right) \leq \bar{M} e^{-\mu(t-s)}.$$

Therefore, $\|\hat{X}\|$ can be estimated as follows:

$$\begin{aligned} \|\hat{X}\| &\leq \|J(t)^{-1}\hat{X}_0\| + \int_0^t \|J(t)^{-1}J(s)\| \left\| \frac{\eta_2}{Z_1} - \frac{\eta_{11}}{Z_1}\hat{X} \right\| ds \\ &\leq \bar{M} \left[e^{-\mu t} \|\hat{X}_0\| + \int_0^t e^{-\mu(t-s)} (\beta_3(s) \|\hat{X}\| + \beta_2(s)) \, ds \right]. \end{aligned} \quad (6.39)$$

The last equation is in a form such that we may apply a **generalized Gronwall inequality**, which states that if $u, v, c \geq 0$, c is differentiable, and $v(t) \leq c(t) + \int_0^t u(s)v(s) \, ds$, then

$$v(t) \leq c(0) \exp \int_0^t u(s) \, ds + \int_0^t c'(s) \left[\exp \int_s^t u(r) \, dr \right] ds.$$

For a proof, see [CL55]. Multiplying (6.39) by $e^{\mu t}$ and applying the generalized Gronwall inequality gives

$$e^{\mu t} \|\hat{X}\| \leq \bar{M} \left[\|\hat{X}_0\| e^{\int_0^t \beta_3(s) \, ds} + \int_0^t e^{\mu s} \beta_2(s) e^{\int_s^t \beta_3(r) \, dr} \, ds \right].$$

Since the size of the box \mathfrak{B} is such that $|a| < \delta$ and $|b| < \delta$, it follows that

$$-\mu + \beta_3 \leq -\mu + C(\delta + |a| \|\hat{X}\|) = \beta_1,$$

where C is chosen such that $C > C^* + 2K\delta$ and ε is sufficiently small, in particular less than δ . Since we have that

$$e^{-\mu(t-s)} = \exp \left[\int_s^t (-\mu) \, dr \right],$$

the final result (6.36) follows. □

Step 6: Having all the estimates in place, we proceed to the proof of the exchange lemma.

Proof. (of Theorem 6.4.2) The argument consists of three parts:

1. Follow the trajectory from q for an $\mathcal{O}(1/\varepsilon)$ time until $|b|$ is exponentially small near the slow manifold $S_\varepsilon = \{a = 0, b = 0\}$.
2. Follow the trajectory while $|a|$ and $|b|$ stay exponentially small near S_ε .
3. Consider the region where $|a|$ grows to $\delta > 0$ capturing departure from S_ε .

Let $T = \mathcal{O}(1/\varepsilon)$ denote the time the trajectory from q to \bar{q} takes to pass through \mathfrak{B} . We can assume without loss of generality that q corresponds to $t = 0$.

Part 1: Let $T_1 \in (0, T)$ be a time of order $\mathcal{O}(1/\varepsilon)$ such that $|a|$ is exponentially small for $t < T_1$. Then at $t = T_1$, we have that $\|\hat{Z}\|$ is exponentially small and $\|\hat{X}\| = \mathcal{O}(\varepsilon + \delta)$.

Proof of Part 1: Clearly, there is such a time T_1 by Lemma 6.3.2, since if T_1 did not exist, then the trajectory would already leave \mathfrak{B} before T . Assume that $\|\hat{Z}\| \leq 1$ and $\|\hat{X}\| \leq 1/(\bar{K}\varepsilon)$ for $t \in (0, T_1)$; this will be justified at the end of the proof of Part 1. Recall from Lemma 6.4.5 that $\|\hat{X}(0)\| \leq 1/(\bar{K}\varepsilon)$. Note that we have

$$\beta_1(t) \leq -\mu/2 \quad (6.40)$$

$$\beta_2(t) \leq 2K(\varepsilon + \delta), \quad (6.41)$$

since $|a|$ is exponentially small, $|b| \leq \delta$, and $\|\hat{Z}\| \leq 1$ (see Lemma 6.4.7). Then we can use (6.36) and get

$$\begin{aligned} \|\hat{X}_i\| &\leq \bar{M} \left[\|\hat{X}_0\| e^{\int_0^t \beta_1(s) ds} + \int_0^t e^{\int_s^t \beta_1(r) dr} \beta_2(s) ds \right] \\ &\leq \bar{M} \left[\frac{1}{\bar{K}\varepsilon} e^{-\frac{\mu}{2}t} + \int_0^t e^{-\frac{\mu}{2}(t-s)} 2K(\varepsilon + \delta) ds \right] \\ &\leq \bar{M} \left[\frac{1}{\bar{K}\varepsilon} e^{-\frac{\mu}{2}t} + \frac{4K}{\mu} (\varepsilon + \delta) \right]. \end{aligned} \quad (6.42)$$

Looking at (6.42), observe that the first term is exponentially small for $T_1 = \mathcal{O}(1/\varepsilon)$, and so we have $\|\hat{X}\| \leq \mathcal{O}(\varepsilon + \delta)$. Since $|a|$ is exponentially small, we also have

$$\alpha(t) + 2C|a| \leq K_2 e^{-c_2/\varepsilon} =: \kappa \quad (6.43)$$

for some $K_2, c_2 > 0$. Using (6.35) and the usual Gronwall lemma yields

$$\begin{aligned} |\hat{Z}_i(t)| &\leq |\hat{Z}_i| e^{\kappa t} + \int_0^t e^{\kappa(t-s)} \kappa ds \\ &= |\hat{Z}_i(0)| e^{\kappa t} + e^{\kappa t} - 1. \end{aligned} \quad (6.44)$$

But since κ is exponentially small and $t \leq \mathcal{O}(1/\varepsilon)$, it follows that κt must be exponentially small. But $e^{\kappa t} - 1 \approx \kappa t$, which means that the second term of (6.44) is exponentially small. In Lemma 6.4.5, it is shown that $|\hat{Z}_i(0)|$ is exponentially small, and this implies that $|\hat{Z}_i|$ is exponentially small. This establishes the two estimates we want for Part 1 as long as we can show that $\|\hat{Z}\| \leq 1$ and $\|\hat{X}\| \leq 1/(\bar{K}\varepsilon)$. Indeed, $|\hat{Z}_i(0)|$ is exponentially small, and so there is a time $0 < t^* \leq T_1$ such that $\|\hat{Z}\| \leq 1$ for $t \in [0, t^*]$. Up to this time, the estimates derived so far hold, which means that at $t = t^*$, we have

$\|\hat{Z}\|$ exponentially small; now cover $[0, T_1]$ by a finite number of time intervals. Applying a similar argument to the assumed estimate for $\|\hat{X}\|$ finishes Part 1.

Part 2: Let $T_1 < T_2 < T$ be any time $T_2 = \mathcal{O}(1/\varepsilon)$ such that $T - T_2 = \mathcal{O}(1/\varepsilon)$, and for $t \in [T_1, T_2]$, we have $|a|$ and $|b|$ exponentially. Then at $t = T_2$, $\|\hat{X}\| = \mathcal{O}(\varepsilon)$, and $\|\hat{Z}\|$ is still exponentially small.

Proof of Part 2: We can repeat the argument of Part 1 and observe that we can improve on the estimate of β_2 , since $|b|$ is now exponentially small, to get $\beta_2 \leq 2K\varepsilon$. Looking at (6.42), we find that

$$\|\hat{X}\| \leq 4\bar{M}K\varepsilon/\mu + \text{exponentially small terms} \quad (6.45)$$

With respect to $\|\hat{Z}\|$, the estimate (6.44) is still valid, which completes the proof of Part 2.

Note that the strategy so far was to assume some a priori bounds on $\|\hat{Z}\|$ and $\|\hat{X}\|$. Then in Parts 1 and 2, it was shown that the a priori bounds can be refined on a compact time interval. Hence, we were able to cover the desired time intervals $[0, T_1]$ and $[T_1, T_2]$ by a finite number of subintervals; at the left endpoints of the subintervals, the a priori bounds hold. The third step is proven by precisely the same strategy.

Part 3: For $t \in [T_2, T]$, we have that $|b|$ is exponentially small and $|a| = \mathcal{O}(\delta)$. Then it follows that at $t = T$, $\|\hat{X}\| = \mathcal{O}(\varepsilon)$ and $\|\hat{Z}\| = \mathcal{O}(\varepsilon)$.

Proof of Part 3: Consider the a priori bounds $\|\hat{Z}\| \leq 1$ and $\|\hat{X}\| \leq K_3\varepsilon$ for some $K_3 > 0$ that are satisfied at T_2 . Observe that for $\|\hat{X}\| = \mathcal{O}(\varepsilon)$, one finds that $|a|\|\hat{X}\| = \mathcal{O}(\varepsilon)$, since $|a| \leq \delta$. This implies that for ε and δ sufficiently small, the estimates (6.40) and (6.45) are valid. Using (6.36) as in Part 1 gives

$$\|\hat{X}\| \leq \bar{M} \left[e^{-(\frac{\mu}{2})(t-T_2)} \|\hat{X}(T_2)\| + \frac{4K\varepsilon}{\mu} + \text{exp. small terms} \right]. \quad (6.46)$$

Therefore, it follows that $\|\hat{X}\| = \mathcal{O}(\varepsilon)$. For $\|\hat{Z}\|$, observe that the left-hand side of (6.43) no longer satisfies an exponential estimate, since $\alpha(t) + 2C|a| = \mathcal{O}(\delta)$. We have to look at $\alpha(t)$ again, which is given by

$$\begin{aligned} \alpha(t) &= C|a|(\|\hat{X}\| + \varepsilon(1 + \|\hat{Z}\|)) \\ &\leq C|a|(K_3\varepsilon + \varepsilon(1 + 1)) = 3C|a|\varepsilon(K_3 + 2). \end{aligned}$$

Applying Gronwall's lemma again to (6.35) yields

$$|\hat{Z}_i(t)| \leq |\hat{Z}_i(T_2)| e^{3C \int_{T_2}^t |a| ds} + \varepsilon \int_{T_2}^t e^{3C \int_s^t |a| dr} C(K_3 + 2)|a| ds. \quad (6.47)$$

From Lemma 6.3.2, we know that $\int_{T_2}^t |a| ds$ and $\int_s^t |a| dr$ stay finite. Hence, the first term on the right-hand side of (6.47) is exponentially small, and the

second term is $\mathcal{O}(\varepsilon)$. This is precisely what is required for the differential form conclusion of the exchange lemma, i.e., $\|\hat{X}\| = \mathcal{O}(\varepsilon)$ and $\|\hat{Z}\| = \mathcal{O}(\varepsilon)$ near the exit point \bar{q} . \square

Remark: The proof presented here applies only to \mathbb{R}^4 , but it contains all necessary steps for more general cases. In particular, observe that the low dimensionality significantly simplifies Lemma 6.4.4, which calculates the equations of motion for the differential forms. Once this lemma is proved in higher-dimensional cases, the rest of the proof can be carried over.

Exercise/Project 6.4.8. Prove Lemma 6.4.4 as required for the general case of the exchange lemma. \diamond

In the next section, the exchange lemma is applied to prove the existence of a homoclinic orbit in the FitzHugh–Nagumo (FHN) equation. Although for this purpose, Theorem 6.4.1 is sufficient, in some cases, stronger versions of the exchange lemma are needed. This will be the subject of Section 6.6.

6.5 Fast Waves in the FitzHugh–Nagumo Equation

Having the exchange lemma available, we can proceed with the idea developed in Section 6.2. Recall that the goal is to prove the existence of a homoclinic orbit in a version of the FitzHugh–Nagumo (FHN) equation

$$\begin{aligned}\frac{dx_1}{dt} &= x'_1 = x_2, \\ \frac{dx_2}{dt} &= x'_2 = \frac{1}{\delta}(sx_2 - c_a(x_1) + y), \\ \frac{dy}{dt} &= y' = \frac{\varepsilon}{s}(x_1 - \gamma y),\end{aligned}\tag{6.48}$$

where $c_a(x_1) = x_1(1-x_1)(x_1-a)$. As in Section 6.2, we assume that γ is chosen small enough that (6.48) has a unique global equilibrium at $(0, 0, 0)$. Also, we assume that

$$0 < a < \frac{1}{2}.$$

For simplicity, one may think simply of the case $\gamma = 1$ and $a = 1/10$. In contrast to the ideas developed in Section 6.1, the candidate homoclinic orbit for $\varepsilon = 0$ consists of two fast and two slow segments, as shown in Figure 6.5(a). Consider (6.48) in the singular limit $\varepsilon = 0$. As discussed in Section 6.2, we know that there exists a wave speed s^* such that the fast subsystem defined by $y = 0$ at the height of the global equilibrium has a heteroclinic connection between its two saddle equilibria $(x_1, x_2) = (0, 0)$ and $(x_1, x_2) = (1, 0)$. Then we follow the slow flow on the critical manifold C_0^{a+} until we reach another fast subsystem with $y = y^* > 0$ that has another heteroclinic connection. Denote the two equilibria of this system by $(x_{1,r}^*, 0) \in C_0^{a+}$ and $(x_{1,l}^*, 0) \in C_0^{a-}$. After traversing the second heteroclinic connection, we follow the slow flow on C_0^{a-} down to the equilibrium $(0, 0, 0)$.

Theorem 6.5.1 ([JKL01]; see also [Car77, Has82]). *If $\varepsilon > 0$ is sufficiently small, the FitzHugh–Nagumo equation (6.48) has a homoclinic orbit for a wave speed s that is $\mathcal{O}(\varepsilon)$ -close to s^* . The homoclinic orbit lies within $\mathcal{O}(\varepsilon)$ Hausdorff distance of the singular orbit with two fast and two slow segments. The orbit is locally unique.*

Remark: The homoclinic orbit corresponds to a so-called **fast (traveling) wave**, since $s^* > 0$, in contrast to the **slow waves** for $s \approx 0$ considered in Section 6.1. See Figure 6.4 for the correspondence between traveling waves and bounded global orbits of (6.48).

Before describing the detailed proof, we outline the strategy. Regarding $s \in [s^* - \delta, s^* + \delta]$ as a parameter, we see that the origin $0 := (0, 0, 0) = (x_1, x_2, y)$ in (6.48) has a one-dimensional unstable manifold $W^u(0, s)$; here $\delta > 0$ is assumed to be sufficiently small. Taking the union over all these parameter values yields a center-unstable manifold

$$W^{cu} = \bigcup_{s \in [s^* - \delta, s^* + \delta]} W^u(0, s).$$

This manifold can be viewed as the center-unstable manifold of the global equilibrium of the FitzHugh–Nagumo equation extended by $s' = 0$:

$$\begin{aligned} x'_1 &= x_2, \\ x'_2 &= \frac{1}{5}(sx_2 - c_a(x_1) + y), \\ y' &= \frac{\varepsilon}{s}(x_1 - y), \\ s' &= 0. \end{aligned} \tag{6.49}$$

Similarly, a three-dimensional center-stable manifold W^{cs} for the global equilibrium exists. The goal is to show that W^{cu} intersects W^{cs} transversely in (x_1, x_2, y, s) -space. Counting dimensions, it follows that if the intersection is transverse, then the manifolds must intersect in a curve for some s_0 near s^* . Note that this value s_0 is fixed, since there is no flow in the s -direction in (6.49). Hence, we have a homoclinic orbit for $s = s_0$ that is locally unique. This “simplifies” the problem to demonstrating the transversality of W^{cu} and W^{cs} .

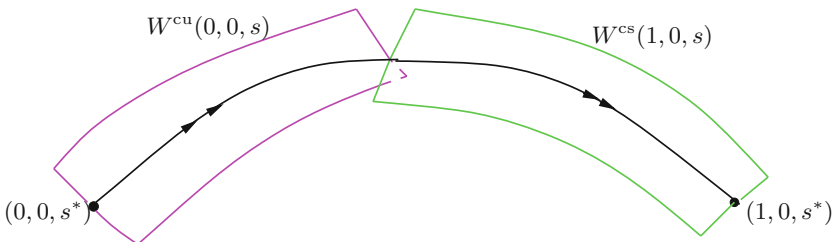


Figure 6.8: Sketch of transversal intersection of the manifolds $W^{cu}(0, 0, s)$ (magenta) and $W^{cs}(1, 0, s)$ (green) as s varies close to s^* .

Obviously, information about the singular limit versions of these manifolds has to be used. Setting $\varepsilon = 0$ and $y = 0$ in (6.49), we obtain a three-dimensional

system that has a two-dimensional center-unstable manifold $W^{cu}(0, 0, s)$ to $(x_1, x_2) = (0, 0)$. Similarly, there exists a two-dimensional center-stable manifold $W^{cs}(1, 0, s)$ to the second saddle equilibrium of the fast subsystem $(x_1, x_2) = (1, 0)$. These two manifolds should intersect along the heteroclinic connection for $s = s^*$. The situation is abstractly shown in Figure 6.8. We shall just state the result.

Lemma 6.5.2. $W^{cu}(0, 0, s)$ intersects $W^{cs}(1, 0, s)$ transversely in (x_1, x_2, s) -space along the curve defined by $s = s^*$.

A similar result should hold for the second heteroclinic connection from C_0^{a+} to C_0^{a-} . Now fix $s = s^*$ and let y vary in a neighborhood of y^* .

Lemma 6.5.3. $W^{cu}(x_{1,r}^*, 0, y)$ intersects $W^{cs}(x_{1,l}^*, 0, y)$ transversely in (x_1, x_2, y) -space along the heteroclinic orbit that exists for $y = y^*$.

Both lemmas will be proven later using differential forms. There are multiple other techniques to prove them, but for now, the following exercise should suffice to continue the argument.

Exercise/Project 6.5.4. Investigate the heteroclinic connections in the fast subsystem(s) numerically and check whether the heteroclinic connections break when we perturb away from $s = s^*$ and $y = y^*$ respectively. \diamond

The next step is to define $\overline{C_0^{a+}}$ as the compact part of C_0^{a+} given by $y \in [-\delta, y^* + \delta]$ and set $I_\delta := [s^* - \delta, s^* + \delta]$. We want to follow W^{cu} close to the slow manifold, denoted by S_ε^{a+} , associated to $\overline{C_0^{a+}} \times I_\delta$ using the exchange lemma. Having all definitions and preliminaries in place, we can outline the proof of Theorem 6.5.1.

Proof. (of Theorem 6.5.1, sketch; see [JKL01]) The setting is the four-dimensional space (x_1, x_2, y, s) for equation (6.49). For $\varepsilon > 0$ sufficiently small, the center-unstable manifold W^{cu} is close to the singular object $W^{cu}(0, 0, s)$. The stability of transverse intersection under perturbation and Lemma 6.5.2 imply that W^{cu} intersects the stable manifold $W^s(S_\varepsilon^{a+})$ of the slow manifold S_ε^{a+} transversely. Now we can apply the exchange lemma to follow W^{cu} close to S_ε^{a+} and conclude that it can be followed for ε sufficiently small up to $y \approx y^*$ and that it leaves the vicinity of S_ε^{a+} C^1 -close to $W^u(S_\varepsilon^{a+})$. Note that the C^1 conclusion is crucial here for the following step.

Since W^{cu} is now C^1 -close to $W^u(S_\varepsilon^{a+})$, it is also C^1 -close to the singular object $W^{cu}(x_{1,r}^*, 0, y)$. Hence, we can use Lemma 6.5.3 and the stability of transversal intersection (transversality is defined by a C^1 condition!) to conclude that W^{cu} intersects the stable manifold $W^s(S_\varepsilon^{a-})$ of the compact part of the slow manifold S_ε^{a-} associated to $C_0^{a-} \times I_\delta$ transversely. Now follow W^{cu} close to S_ε^{a-} . Since S_ε^{a-} is very close to $C_0^{a-} \times I_\delta$ for $\varepsilon > 0$ sufficiently small by Fenichel theory, we have that W^{cu} —after we have followed it around—is close to the center-stable manifold of the origin W^{cs} . Hence, there exists a transversal intersection of the two-dimensional manifold W^{cu} and the three-dimensional manifold W^{cs} . \square

Note that the proof not only defined a one-dimensional intersection curve fixing s_0 close to s^* but also fixed a value y_0 close to y^* determining where the second fast jump occurred in the homoclinic orbit.

It remains to prove Lemmas 6.5.2 and 6.5.3. Since their proofs are very similar, we prove only Lemma 6.5.2.

Proof. (of Lemma 6.5.2) Differential forms are used as in the proof of the exchange lemma. The variational equations for the fast subsystem with $s' = 0$ appended are

$$\begin{aligned} (\mathrm{d}x_1)' &= \mathrm{d}x_2, \\ (\mathrm{d}x_2)' &= s \, \mathrm{d}x_2 + x_2 \, \mathrm{d}s - c'_a(x_1) \, \mathrm{d}x_1, \\ (\mathrm{d}s)' &= 0. \end{aligned}$$

Define 2-forms by the same notation as in Section 6.4, e.g., $P_{x_1 x_2} = \mathrm{d}x_1 \wedge \mathrm{d}x_2$. The equation on 2-forms to use for the transversality argument is

$$P'_{x_1 x_2} = s P_{x_1 x_2} + x_2 P_{x_1 s}. \quad (6.50)$$

This equation can be derived, as usual, by differentiating the form $\mathrm{d}x_1 \wedge \mathrm{d}x_2$ using the chain rule. We want to look at $P_{x_1 x_2}$ and $P_{x_1 s}$ evaluated on tangent planes to the manifolds $W^{cu}(0, 0, s) =: M_u$ and $W^{cs}(1, 0, s) =: M_s$. It will be assumed that the tangent vectors have been normalized before we evaluate the forms. Denote values of the forms on these planes by $P_{x_1 x_2}^\pm$ and $P_{x_1 s}^\pm$, where $+$ indicates unstable and $-$ indicates stable. Suppose we can show that $P_{x_1 x_2}^+$ and $P_{x_1 s}^+$ have the same sign and $P_{x_1 x_2}^-$ and $P_{x_1 s}^-$ have opposite signs. Now look at the vectors $(P_{x_1 x_2}, P_{x_1 s}, P_{x_2 s})$. In this scenario, they are linearly independent tangent vectors to M_u and M_s . This means that M_u and M_s intersect transversely.

Hence, the problem is reduced to checking signs. Obviously, M_u and M_s have the vector field $(x_2, sx_2 - c_a(x_1), 0)$ as a tangent vector. Consider another tangent vector given by $(a^\pm, b^\pm, 1)$. We want to take the third coordinate to be 1 to ensure that the vector is linearly independent of the vector field, and this is justified, since $(\mathrm{d}s)' = 0$ (check this). The two vectors can be made orthonormal using the Gram–Schmidt algorithm. Hence, the forms P_{\dots}^\pm are equal, up to a positive normalization factor $N > 0$, to the corresponding 2×2 subdeterminant of the 2×3 matrix

$$\begin{pmatrix} x_2 & sx_2 - c_a(x_1) & 0 \\ a^\pm & b^\pm & 1 \end{pmatrix}.$$

In particular, for $P_{x_1 s}^\pm$, this means that

$$P_{x_1 s}^\pm = N \begin{vmatrix} x_2 & 0 \\ a^\pm & 1 \end{vmatrix} = Nx_2.$$

From the fast subsystem, it follows that $x_2 > 0$ on M_u and M_s . Therefore, $P_{x_1 s}^\pm = Nx_2 > 0$, and equation (6.50) can be simplified to

$$P_{x_1 x_2}^\pm = s P_{x_1 x_2}^\pm + N(x_2)^2. \quad (6.51)$$

The last step is to look at the signs of $P_{x_1 x_2}^\pm$. Observe that M_u and M_s both contain a line of equilibrium points with a tangent vector in the s -direction; this follows directly from the construction, since the equation $s' = 0$ has been appended. For every plane containing such a line, the form $P_{x_1 x_2}$ must vanish. Recall that the time variable in the differential equations we have written down so far is t . Then if $t \rightarrow \infty$, we must have $P_{x_1 x_2}^- \rightarrow 0$ due to the location of the line of equilibrium points. This implies that $P_{x_1 x_2}^- < 0$, since equation (6.51) has a positive right-hand side for t sufficiently large. Similarly, it follows that if $t \rightarrow -\infty$, then $P_{x_1 x_2}^+ \rightarrow 0$, and so $P_{x_1 x_2}^+ > 0$. This establishes the sign condition. \square

6.6 Strong Exchange Lemmas

In the previous sections, we obtained the exchange lemma and applied it to prove the existence of homoclinic orbits in the FitzHugh–Nagumo equation. The version of the exchange lemma stated in Theorem 6.4.1 can be strengthened. The goal of this section is to state some possible generalizations.

Recall that the heuristic idea of the exchange lemma is to follow an invariant manifold M during its passage near a slow manifold S_ε . The transversality information given by the intersection of M and $W^s(S_\varepsilon)$ is interchanged with information about closeness to $W^u(S_\varepsilon)$ when M exits a neighborhood of S_ε . Several hypotheses in Theorem 6.4 can be weakened:

- The manifold M to be tracked had a fixed dimension given by the number of unstable directions of S_ε plus one. This can be improved.
- We usually proved that M is $\mathcal{O}(\varepsilon)$ -close to some submanifold of $W^u(S_\varepsilon)$. This can be improved to an exponential closeness result.
- Furthermore, the manifold S_ε was assumed to have only slow directions. This is not necessary as long as all the directions in S_ε are dominated by the fast directions, so that S_ε remains normally hyperbolic.

To make these modifications precise, consider an ODE on \mathbb{R}^N that has a normally hyperbolic invariant slow/centerlike manifold S_ε of dimension l . Assume that the stable and unstable manifolds $W^s(S_\varepsilon)$ and $W^u(S_\varepsilon)$ have dimensions m and k respectively such that $l + k + m = N$. Assume that normal hyperbolicity holds for $\varepsilon \in (0, \varepsilon_0]$ and that the manifolds are sufficiently smooth. In a neighborhood \mathfrak{B} of S_ε , we can convert the equations into Fenichel normal form; cf. (6.21). In addition to the usual Fenichel normal form, there can be “fast dynamics” on S_ε that are dominated by the normal directions as well:

$$\begin{aligned} a' &= \Lambda(a, b, y, \varepsilon), \\ b' &= \Gamma(a, b, y, \varepsilon), \\ w' &= \varepsilon[h_1(y, \varepsilon) + H_1(a, b, y, \varepsilon) \otimes a \otimes b], \\ \theta' &= h_2(y, \varepsilon) + H_2(a, b, y, \varepsilon) \otimes a \otimes b, \end{aligned} \tag{6.52}$$

where $a \in \mathbb{R}^k$, $b \in \mathbb{R}^l$, $y = (w, \theta) \in \mathbb{R}^{l_w + l_\theta} = \mathbb{R}^l$, and Λ , Γ are the usual matrix-valued functions in Fenichel normal form; regarding the tensor notation \otimes , consider the explanation following equation (6.21). As a convention, let $h := (h_1, h_2)^\top$ and $H := (H_1, H_2)^\top$. We can consider the variables y in this case to be center-type variables and make the following first explicit assumption:

- (H1) $\Lambda(0, 0, y, 0)$, $\Gamma(0, 0, y, 0)$ and $D_y h_2(y, 0)$ are independent of the fast center variable θ .

For fixed δ , ε_0 , and U , we define the neighborhood \mathfrak{B} of S_ε , similar to the situation of the construction in Section 6.4, by

$$\mathfrak{B} := \{(a, b, y) \in \mathbb{R}^N : \|a\|, \|b\| < \delta, y \in U, \varepsilon \in (0, \varepsilon_0]\},$$

where $\delta > 0$ is sufficiently small and U is a suitable compact set. The invariant manifold to track is one manifold of a smooth family $\{M_\varepsilon\}_{\varepsilon \in (0, \varepsilon_0]}$, each of dimension $k + \sigma$, where $1 \leq \sigma \leq l$. This generalizes the case $\sigma = 1$ considered so far. To quantify the tracking result, it is helpful to introduce the spectral bounds on the linear terms in Fenichel normal form:

$$\begin{aligned} \lambda_0 &= \inf \bigcup_{y \in \bar{U}} \text{Re}(\text{spec } \Lambda(0, 0, y, 0)), \\ \gamma_0 &= \sup \bigcup_{y \in \bar{U}} \text{Re}(\text{spec } \Gamma(0, 0, y, 0)), \\ \hat{\alpha}_0 &= \sup \bigcup_{y \in \bar{U}} \text{Re}(\text{spec } D_y h(0, y)), \\ \alpha_0 &= \sup \bigcup_{y \in \bar{U}} \text{Re}(\text{spec } (D_y h(0, y))^{(\sigma)}), \\ \beta_0 &= \inf \bigcup_{y \in \bar{U}} \text{Re}(\text{spec } (D_y h(0, y))^{(\sigma)}), \end{aligned} \tag{6.53}$$

where $A^{(p)}$ denotes the induced derivation of the linear map $A : V \rightarrow V$ for some vector space V . In particular, if V is of dimension q and $1 \leq p \leq q$ we can define a map on p -forms by

$$A^{(p)}(v_1 \wedge \cdots \wedge v_p) := \sum_{i=1}^p v_1 \wedge \cdots \wedge A v_i \wedge \cdots \wedge v_p.$$

This map $A^{(p)}$ has a matrix representation, and so it makes sense to consider its spectrum. The definitions (6.53) are just a slightly more refined way of talking about the spectrum associated to $D_y h(0, y)$ matching the dimension of the manifold to be tracked ($\dim M_\varepsilon = k + \sigma$). The next step is to collect more detailed assumptions about the manifold(s) M_ε . The transversality at the entry to the neighborhood of S_ε can be stated as follows:

- (H2) For each $\varepsilon \in (0, \varepsilon_0]$, there is a point $q_\varepsilon \in M_\varepsilon \cap \partial \mathfrak{B}$ such that q_ε is smooth in ε and the manifold M_ε intersects $W^s(S_\varepsilon)$ transversely at q_ε .

The situation is shown in Figure 6.9. From (H2), it follows that there exists a point q_0 in $M_0 \cap W^s(S_0)$; the last intersection is not necessarily transverse and does not have to be for the theory to apply.

To define the length of time trajectories spend in the region \mathfrak{B} , consider the augmented system of (6.52) with $\varepsilon' = 0$ appended. Let V_{r_0} be the ball of radius r_0 around q_0 in the phase space of the augmented system. Define

$$Q_\varepsilon := M_\varepsilon \cap V_{r_0} \quad \text{and} \quad \tau_q^\mathfrak{B} := \inf\{\tau > 0 : \phi_t(q) \notin \mathfrak{B}\},$$

where q is some point in \mathfrak{B} and $\phi_t(\cdot)$ is the flow of (6.52). The next hypothesis quantifies the time that points in Q_ε remain inside \mathfrak{B} :

(H3) Fix $v_0 > 0$. Assume that for each $\varepsilon \in (0, \varepsilon_0]$, there exists $Q_\varepsilon^v \subset Q_\varepsilon$ such that $\inf_{q \in Q_\varepsilon^v} \tau_q^\mathfrak{B}$ is monotonically increasing as v decreases and

$$\lim_{v \rightarrow \infty} \inf_{q \in Q_\varepsilon^v} \tau_q^\mathfrak{B} = \infty. \quad (6.54)$$

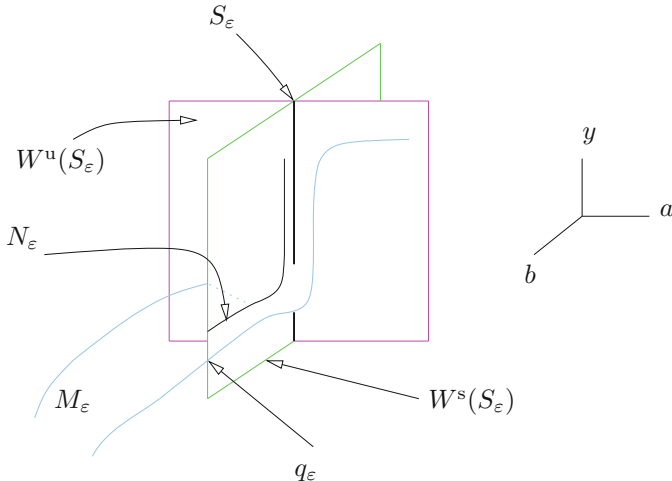


Figure 6.9: Sketch of the transversal intersection of M_ε (light blue) and $W^s(S_\varepsilon)$ (green).

The sets Q_ε^v should be interpreted as neighborhoods of q_ε that shrink closer and closer toward the stable manifold $W^s(S_\varepsilon)$. In fact, we can construct them using the distance to $W^s(S_\varepsilon)$ as a metric. The smaller v gets, the longer points inside Q_ε^v will remain inside \mathfrak{B} , i.e., close to S_ε . For the last hypothesis, define

$$N_\varepsilon = W^s(S_\varepsilon) \cap Q_\varepsilon.$$

For each fixed $\varepsilon \in (0, \varepsilon_0]$, the set N_ε is a σ -dimensional submanifold of $W^s(S_\varepsilon)$; see Figure 6.9.

Exercise 6.6.1. Prove that σ is the right dimension. Hint: What are the dimensions of all the manifolds involved? \diamond

Now let Π_- denote the projection of M_ε along $W^s(S_\varepsilon)$ onto S_ε . This projection acts along the “stable fibers” of S_ε . Define

$$J_\varepsilon := \Pi_-(N_\varepsilon)$$

as the projection of the submanifold N_ε onto S_ε . Basically, this projects a piece of M_ε onto S_ε . We want the projected object J_ε to be a σ -dimensional submanifold of S_ε . Therefore, we assume the following:

(H4) The linear map $(\Pi_-|_{N_\varepsilon})_* : T_{q_\varepsilon} N_\varepsilon \rightarrow T_{\Pi_-(q_\varepsilon)} S_\varepsilon$ is injective.

This implies the desired conclusion about J_ε . In particular, the manifold J_ε can now be transported along the “slow flow” on S_ε given by the $y = (w, \theta)$ -variables. Using this flow, the desired submanifold of $W^u(S_\varepsilon)$, to which the manifold M_ε is C^1 -close on exiting from \mathfrak{B} , can be identified. Also, let $\rho_0 := \hat{\alpha}_0$ if $\sigma < l$ and $\rho_0 := |\gamma_0|$ if $\sigma = l$.

Theorem 6.6.2 (Strong exchange lemma, [KJ01, JKK96, JT09]). *Fix any integer $1 \leq \sigma \leq l$. Assume that the conditions (H1)–(H4) are satisfied and that*

$$\begin{aligned} \lambda_0 &> \max(\hat{\alpha}_0, \rho_0 + \alpha_0 - \beta_0, \alpha_0 - \beta_0), \\ |\gamma_0| &> \alpha_0 - \beta_0. \end{aligned}$$

Choose $\kappa > 0$ such that

$$\kappa < \min(\lambda_0 - \hat{\alpha}_0, |\gamma_0|, \lambda_0 - (\rho_0 + \alpha_0 - \beta_0), \lambda_0 - \alpha_0 + \beta_0, |\gamma_0| - \alpha_0 + \beta_0).$$

Then there exist $\delta_0, \varepsilon_0 > 0$ such that whenever $\delta \in (0, \delta_0)$, then for each $\varepsilon \in (0, \varepsilon_0)$, there is $v_0 = v_0(\varepsilon) > 0$ such that for each $v \in [0, v_0]$ and $q \in Q_\varepsilon^v$,

$$\phi_{\tau_q^\mathfrak{B}}(M_\varepsilon) \text{ is } C^1\text{-}\mathcal{O}(e^{-\kappa\tau_q^\mathfrak{B}})\text{-close to } W^u(S_\varepsilon)|_{\phi_{\tau_q^\mathfrak{B}}(J_\varepsilon)} \text{ at } \phi_{\tau_q^\mathfrak{B}}(q).$$

Remark: Sometimes the terminology **exchange lemma with exponentially small error (ELESE)** is used for Theorem 6.6.2. Since this terminology focuses only on the error and does not include all the generalizations, the term **strong exchange lemma** seems adequate, i.e., Theorem 6.6.2 is one of the available stronger versions (due to weaker hypotheses and stronger conclusions) of the classical exchange lemma 6.4.1.

The spectral conditions derived from the linearization of the system look complicated, but they are just ensuring that the tangential directions are dominated by the normal directions in a suitable way. Also, the spectral conditions are easy to check, since this requires only the calculation of eigenvalues of matrices in the singular limit $\varepsilon = 0$. The version of the strong exchange lemma presented here is taken from [KJ01]. Originally, it was proven by Tin and Jones, and the proof can be found in [Tin94]. For a more detailed discussion of why an exponentially small error in the last estimate might be needed, we refer to [JKK96]; this relates in particular to the case of Hamiltonian singular limit systems.

6.7 BVPs and Periodic Orbits

Although the exchange lemma was initially developed to prove the existence of homoclinic and heteroclinic connections in fast–slow systems, it can be applied in other situations. In particular, quite general **boundary value problems (BVPs)** and existence results for periodic orbits will be discussed in this section. Consider a fast–slow system for a time $\xi \in [0, 1]$ of the form

$$\begin{aligned}\varepsilon \frac{dx}{d\xi} &= F(x, z, \tau, \varepsilon), \\ \frac{dz}{d\xi} &= G(x, z, \tau, \varepsilon),\end{aligned}\tag{6.55}$$

for $(x, z) \in \mathbb{R}^m \times \mathbb{R}^\eta$ with boundary conditions

$$B_0(x(0), z(0), \varepsilon) = 0 \quad \text{and} \quad B_1(x(1), z(1), \varepsilon) = 0,\tag{6.56}$$

where B_i takes values in \mathbb{R}^{d_i} with $d_0 + d_1 = m + \eta$. It is very helpful to think of the simple case $\eta = 1$, $m = 2$, and $d_0 = 1, d_1 = 2$ (or $d_0 = 2, d_1 = 1$) for illustration purposes. Observe that the BVP (6.55)–(6.56) is not yet in the standard form of a fast–slow system due to time-dependence. Adjoining time as another variable yields

$$\begin{aligned}\varepsilon \frac{dx}{d\tau} &= \varepsilon \dot{x} = F(x, z, \varepsilon), \\ \frac{dz}{d\tau} &= \dot{z} = G(x, z, \varepsilon), \\ \frac{d\xi}{d\tau} &= \dot{\xi} = 1,\end{aligned}\tag{6.57}$$

where setting $y := (z, \xi)^\top \in \mathbb{R}^n = \mathbb{R}^{\eta+1}$, $f = F$, and $g = (G, 1)^\top$ recovers our usual setup. The boundary conditions are then transformed to conditions on a solution to lie in two particular submanifolds of (x, z, ξ) -phase space,

$$\mathcal{B}_0 := \{B_0(x, z, \varepsilon) = 0, \xi = 0\} \quad \text{and} \quad \mathcal{B}_1 := \{B_1(x, z, \varepsilon) = 0, \xi = 1\}.\tag{6.58}$$

The ε -dependence is suppressed, and we use the shorthand notation \mathcal{B}_i instead of the more formal $\mathcal{B}_i^\varepsilon$. Assume that the maps B_i are smooth and have maximal rank, so that \mathcal{B}_i has dimension

$$b_i := m + \eta - d_i \quad \text{for } i = 0, 1.$$

For the case $d_0 = 1$ and $d_1 = 2$, this means that $b_0 = 2$ and $b_1 = 1$, which yields proper submanifolds inside the hyperplanes $\xi = 0$ and $\xi = 1$ as boundary conditions; see Figure 6.10.

Definition 6.7.1. The reformulation of a (BVP) given by (6.55)–(6.56) into an autonomous system with submanifold constraints (6.57)–(6.58) is called the **connection problem**. The manifolds \mathcal{B}_i in (6.58) are called **boundary manifolds**.

This terminology makes sense, since the solution connects two given submanifolds that form the boundaries of the solution trajectory. In Figure 6.10,

the situation we want to focus on is illustrated: a trajectory starting from \mathcal{B}_0 follows some number of intermediate normally hyperbolic slow manifolds S_i for slow times $\tau_i = \mathcal{O}(1)$ before it reaches \mathcal{B}_1 . Obviously, there are more difficult versions of the connection problem that occur in applications, but we restrict ourselves to the situation of Figure 6.10. More precisely, assume that the solution follows slow manifolds S_i for times $\tau_i = \mathcal{O}(1)$ with $i = 1, \dots, N$.

Remark: Boundary value problems that have solutions with fast transition layers away from \mathcal{B}_0 and \mathcal{B}_1 are said to have **interior layers**; see Section 9.1, on matched asymptotic expansions, for more details. In this section, the existence of solutions for a special type of interior layer is proven.

The strategy is to write down all the conditions needed to apply a suitable version of the exchange lemma near each S_i . Then a singular solution consisting of heteroclinic connections in the fast subsystem

$$\begin{aligned} \frac{dx}{dt} &= x' = F(x, z, \varepsilon), & (\text{with } t = \tau/\varepsilon, y = (z, \xi)^\top \in \mathbb{R}^n), \\ \frac{dy}{dt} &= y' = 0, \end{aligned}$$

and segments of the slow flow on each S_i should perturb to a solution for $0 < \varepsilon \ll 1$ if suitable transversality hypotheses are satisfied.

Assume that a candidate/singular solution of concatenated fast and slow subsystem segments to 6.57 exists that starts in \mathcal{B}_0 and ends in \mathcal{B}_1 . Let $\bar{p}_0 \in \mathcal{B}_0$

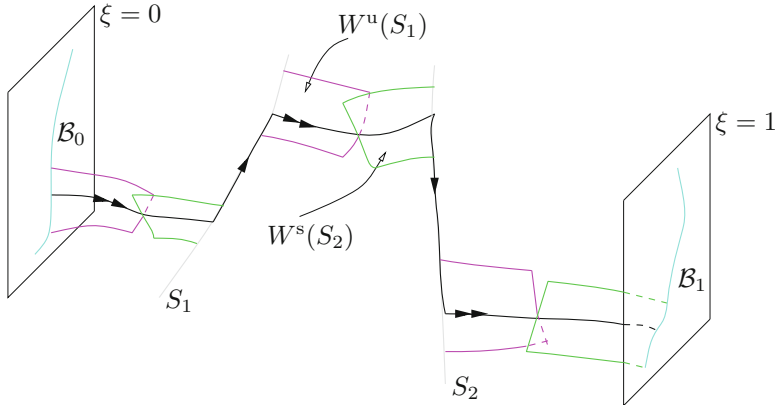


Figure 6.10: Sketch of a connection problem derived from a BVP. Two intermediate slow manifolds S_i for $i = 1, 2$ are shown. A trajectory (black), the critical manifold (gray), its stable and unstable manifolds (green/magenta), and the boundary condition (cyan) are shown. Note that at least one dimension has been suppressed, since the problem (6.57) is posed in \mathbb{R}^4 .

be the starting point and $p_{N+1} \in \mathcal{B}_1$ the final point of the singular solution. Denote by p_i and \bar{p}_i the first and last points of the singular solution γ_0 in the intermediate critical manifold S_i . The assumptions we need are (see also Figure 6.10) as follows:

- (A1) Each critical manifold S_i is normally hyperbolic with m_a attracting and m_r repelling directions with $m = m_a + m_r$. Furthermore, assume $b_0 \geq m_r$, $b_1 \geq m_a$, and $b_0 + b_1 + 1 = m + n$.
- (A2) On each critical manifold S_i , the singular solution γ_0 spends time $t_i = \mathcal{O}(1/\varepsilon)$ on the fast time scale.
- (A3) Let $N_0 := \mathcal{B}_0 \cap W^s(S_1)$. Define a map $N_0 \rightarrow \omega(N_0) =: J_1$ taking each point on N_0 to its forward limit set (or ω -limit set) under the fast subsystem flow on S_1 . Assume that this map is injective and that its image is a smooth submanifold of S_1 of dimension $b_0 - m_r$.
- (A4) The fast flow at \bar{p}_0 is not tangent to \mathcal{B}_0 , and \mathcal{B}_0 intersects $W^s(S_1)$ transversally at \bar{p}_0 .

Note that J_1 can be viewed as the **jump-on set** in S_1 . Clearly, we can build further sets of this type. Let $\phi_\tau^s(\cdot)$ denote the slow flow. Then define

$$\begin{aligned} U_i &:= \phi_{1/\varepsilon(\tau_i-\delta, \tau_i+\delta)}^s(J_i), \\ J_{i+1} &:= \omega(W^u(U_i) \cap W^s(S_{i+1})), \end{aligned}$$

for some suitable small $\delta > 0$. The last definition takes the last jump-on set, flows it via the slow flow, expands it a bit further to make room for the perturbation, and then transports it via the fast subsystem to generate the next jump-on set.

- (A5) $W^u(U_i) = W^u(S_i)|_{U_i}$ intersects $W^s(S_{i+1})$ transversally along the fast subsystem trajectory from \bar{p}_i to p_{i+1} for $i = 1, 2, \dots, N-1$ and $\dim(J_{i+1}) = b_0 - k$.
- (A6) The slow flow on S_i for $i = 1, 2, \dots, N$ at p_i is not tangent to J_i .
- (A7) $W^u(U_N)$ intersects \mathcal{B}_1 transversally at p_{N+1} .

Note that all the assumptions we have made are very natural, and some are even immediately satisfied in the case $\eta = 1 = d_1 = d_2$ and $m = 2$. The assumptions (A1)–(A3) guarantee that we have the correct setup for the exchange lemma near each critical manifold S_i . Using (A4)–(A7) gives the required transversality hypotheses of the manifolds involved in the construction. Using the ideas in the proof of Theorem 6.5.1, it is relatively straightforward to establish the next result.

Theorem 6.7.2 ([TKJ94]). *Suppose a singular solution exists for the boundary value problem (6.57)–(6.58) satisfying assumptions (A1)–(A7). Then for $\varepsilon > 0$ sufficiently small, there is a locally unique solution to the connection problem converging to the singular solution as $\varepsilon \rightarrow 0$.*

To prove the existence of the homoclinic orbit in the FitzHugh–Nagumo equation (see Section 6.5), one also had to calculate explicitly whether the transversality assumptions hold. Often, this check is nontrivial. Hence, it is helpful to illustrate the situation with an example.

Example 6.7.3. Consider the boundary value problem

$$\begin{aligned} \varepsilon^2 \frac{d^2 u}{d\xi^2} &= F(u, v), & \frac{d^2 v}{d\xi^2} &= G(u, v) \\ \text{boundary conditions } u(i) &= \alpha_i, & v(i) &= \beta_i \end{aligned} \quad (6.59)$$

for $\xi \in [0, 1]$ and $i = 0, 1$. We restrict to the case $u, v \in \mathbb{R}$, although a more general situation can be analyzed. The connection problem is given by

$$\begin{aligned} \varepsilon \dot{u} &= w, \\ \varepsilon \dot{w} &= F(u, v), \\ \dot{v} &= z, \\ \dot{z} &= G(u, v), \\ \dot{\xi} &= 1. \end{aligned}$$

In our usual fast–slow variables, we have $(u, w) =: x$ and $(v, z, \xi) =: y$. The associated boundary manifolds are

$$\mathcal{B}_i = \{(u, w, v, z, \xi) \in \mathbb{R}^5 | u = \alpha_i, v = \beta_i, \xi = i\}$$

for $i = 0, 1$. Observe that $\dim(\mathcal{B}_i) = 2$. The critical manifold of (6.7.3) is

$$C_0 = \{(u, w, v, z, \xi) \in \mathbb{R}^5 | w = 0, F(u, v) = 0\}.$$

Assume that C_0 has two compact subsets S_j for $j = 1, 2$ that are normally hyperbolic with one attracting and one repelling direction, so that $m = m_a + m_r = 1 + 1 = 2$. Furthermore, assume that each manifold S_j is given by a graph with $u = h_j(v)$, so that

$$S_j = \{h_j(v) = u, w = 0\} \quad \text{for } j = 1, 2.$$

A classical situation in which these assumptions hold is provided by the case $F(u, v) = c(u) - v$ and $c(u)$ is a cubic polynomial, but it is not too difficult to keep the situation more general. Suppose a singular solution to the connection problem exists that has one slow segment on S_1 and a second one on S_2 . The situation is illustrated in Figure 6.11.

We shall not verify all assumptions (A1)–(A7) but focus on the specific transversality assumptions (A5) and (A7). Observe that instead of flowing the manifold \mathcal{B}_0 forward and checking the required transversality conditions, we can also try to flow \mathcal{B}_1 backward and to meet the forward image of \mathcal{B}_0 at a suitable position. A good position seems to be the jump between S_1 and S_2 . Hence, define

$$\begin{aligned} J &= \omega(N_0) = \omega(\mathcal{B}_0 \cap W^s(S_1)), \\ U &= \phi_{(t_1-\delta, t_1+\delta)}^s(J) \subset S_1. \end{aligned}$$

Since we are interested in the backward flow as well, we define the map $N_1 \rightarrow \alpha(N_1)$ that sends a set N_1 to its backward limit set (or α -limit set) under the fast flow. Then set

$$\begin{aligned} \tilde{J} &= \alpha(\mathcal{B}_1 \cap W^u(S_2)), \\ \tilde{U} &= \phi_{-(t_2-\delta, t_2+\delta)}^s(\tilde{J}) \subset S_2. \end{aligned}$$

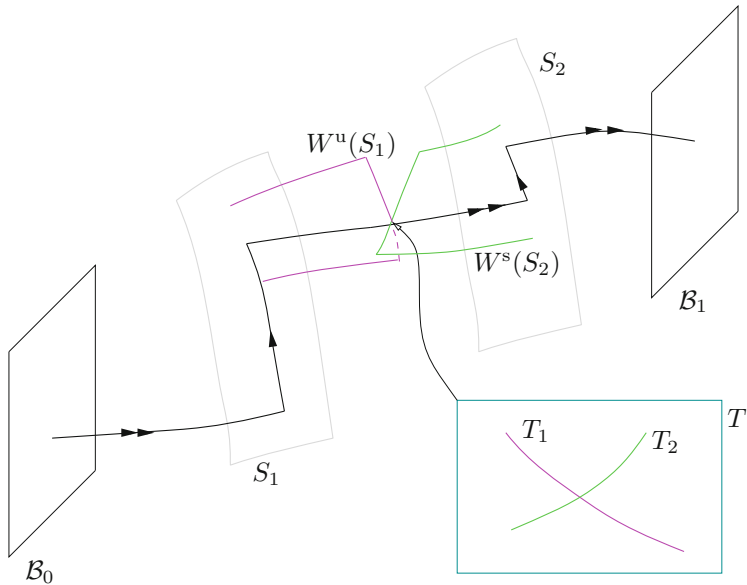


Figure 6.11: Sketch of the connection problem for equation (6.7.3). The singular solution is shown in black. Note that not all dimensions are shown, since phase space is five-dimensional.

The key property to show is that

$$W^u(U) \text{ intersects } W^s(\tilde{U}) \text{ transversally.} \quad (6.60)$$

We do not discuss the calculations required between \mathcal{B}_0 and S_1 as well as between \mathcal{B}_1 and S_2 . Instead, let us focus on the region between S_1 and S_2 . Pick a point q on the heteroclinic fast subsystem connection between S_1 and S_2 and let P_q be a hyperplane transverse to the heteroclinic connection between S_1 and S_2 . The fast subsystem is given by

$$\begin{aligned} u' &= w, \\ w' &= F(u, v), \\ v' &= 0. \end{aligned}$$

Observe that v is constant, so that the heteroclinic connection between S_1 and S_2 occurs for a fixed value $v = v^*$. The idea is to “split” the condition (6.60) into one part depending only on the fast variables and another part depending only on the slow variables. Hence, we just start looking at

$$\begin{aligned} T &:= T_q(W^u(S_1) \cap W^s(S_2) \cap P_q), \\ T_1 &:= T_q(W^u(U) \cap W^s(S_2) \cap P_q), \\ T_2 &:= T_q(W^s(\tilde{U}) \cap W^u(S_1) \cap P_q). \end{aligned}$$

See also Figure 6.11. Counting dimensions gives that $\dim(T) = 2$ and $\dim(T_j) = 1$ for $j = 1, 2$. A rather lengthy but elementary argument shows that if we satisfy a certain transversality condition in the fast variables along the heteroclinic connection between S_1 and S_2 , then it suffices to show that T_1 intersects T_2 transversally in T . Intuitively, this makes sense, since the slow variables do not change along the heteroclinic. Hence, we would like to compute the slopes of the curves T_1 and T_2 inside T from the slow subsystems

$$\begin{aligned}\dot{v} &= z, \\ \dot{z} &= G(\phi_j(v), v), \\ \dot{\xi} &= 1.\end{aligned}\tag{6.61}$$

Let $\Pi : \mathbb{R}^5 \rightarrow \mathbb{R}^3$ denote the projection onto the slow variables $\Pi(u, w, v, z, \xi) = (v, z, \xi)$. Note that Π is injective on the critical manifolds S_j and that

$$\Pi(J) = \{(v, z, \xi) \in \mathbb{R}^3 \mid v = \beta_0, \xi = 0\}, \quad \Pi(\tilde{J}) = \{(v, z, \xi) \in \mathbb{R}^3 \mid v = \beta_1, \xi = 1\}.$$

Follow $\Pi(J)$ forward under the slow flow until it reaches $v = v^*$ and also follow $\Pi(\tilde{J})$ backward up to $v = v^*$, where we know the heteroclinic jump occurs. Then define

$$\varphi_j(v) := \int_{\beta_j}^v G(\phi_j(\alpha), \alpha) \, d\alpha \quad \text{for } j = 1, 2.$$

The equation $\ddot{v} = G(\phi_j(v), v)$ derived from the first two equations in (6.61) can be formally integrated. With initial conditions (β_0, z_0) for (v, z) , we have at $v = v^*$,

$$\begin{aligned}z &= \sigma \sqrt{(z_0)^2 + 2\varphi_1(v^*)} \\ \xi &= \sigma \int_{\beta_0}^{v^*} \frac{1}{\sqrt{(z_0)^2 + 2\varphi_1(\alpha)}} \, d\alpha,\end{aligned}\tag{6.62}$$

where $\sigma = \pm 1$ is chosen such that $\xi > 0$. Note that (6.62) describes a curve in the heteroclinic jump set $\{v = v^*\}$ parameterized by z_0 . Hence, we have followed $\Pi(J)$ under the slow flow.

Exercise 6.7.4. Verify and/or derive (6.62). Hint: Verification works via direct differentiation if one replaces v^* by $v(\tau)$ in (6.62). \diamond

Similarly, one can track $\Pi(\tilde{J})$ under the backward flow in the slow variables with initial conditions (β_1, z_1) for (v, z) :

$$\begin{aligned}z &= \tilde{\sigma} \sqrt{(z_1)^2 + 2\varphi_2(v^*)} \\ \xi &= 1 - \tilde{\sigma} \int_{\beta_1}^{v^*} \frac{1}{\sqrt{(z_1)^2 + 2\varphi_2(\alpha)}} \, d\alpha,\end{aligned}\tag{6.63}$$

where $\tilde{\sigma} = \pm 1$ is chosen such that $\xi \in [0, 1]$. The slopes of the curves T_{i+1} for $i = 0, 1$ are therefore given by

$$\frac{d\xi}{dz} = \frac{d\xi/dz_i}{dz/dz_i} = \frac{-z_i \int_{\beta_i}^{v^*} [(z_i)^2 + 2\varphi_{i+1}(\alpha)]^{-3/2} \, d\alpha}{z_i [(z_i)^2 + 2\varphi_{i+1}(v^*)]^{-1/2}}.\tag{6.64}$$

As long as the two slopes in (6.64) are not equal, one can conclude transversality of T_1 and T_2 . A possible sufficient condition to reach this conclusion is that z be of one sign on both critical manifolds S_j and that β_0, β_1 be on opposite sides of v^* . Hence, the geometric approach leads to an understanding of why algebraic conditions of the form (6.64) can arise for the solvability of classical boundary value problems. ♦

Example 6.7.3 and the homoclinic orbit construction in the FitzHugh–Nagumo equation lead to the observation that we can group many of the applications of the exchange lemma in the framework of boundary value problems, since a homoclinic orbit for an ODE to a equilibrium point q is the solution of a boundary value problem:

$$z' = F(z) \quad \text{with boundary conditions } z(-\infty) = q = z(\infty).$$

Another problem that fits into this framework is that of periodic orbits of ODEs that satisfy the BVP

$$z' = F(z) \quad \text{with boundary conditions } z(0) = z(T),$$

where T is the period of the periodic orbit.

Remark: In Sections 10.6, 11.5, and 19.8, the BVP framework will be used effectively in conjunction with numerical methods.

For periodic orbits, we have an analogue of Theorem 6.7.2.

Theorem 6.7.5 ([ST01]). *Suppose a fast–slow system has a singular periodic orbit consisting of alternating fast and slow segments. Suppose that the slow segments lie on normally hyperbolic critical manifolds and suitable transversality conditions hold. Then there exists a locally unique periodic orbit for $\varepsilon > 0$ sufficiently small, and this orbit converges to the singular solution as $\varepsilon \rightarrow 0$.*

It is important to point out that proving the existence of special global trajectories (periodic, homoclinic, heteroclinic, etc.) is often the first step in the analysis of a problem. Once a special trajectory has been obtained, one may want to study its bifurcations under parameter variation or use the basic existence result to conclude the existence of more complicated, e.g., chaotic, invariant sets; see Section 6.8.

6.8 References

Section 6.1: This section is based mostly on [Szm92, Szm91]. For a classical introduction to singular perturbations and waves, consider [TK88]. Heteroclinic connections are a well-studied theme in fast–slow systems [Bat94, Lin90a, Sak90], and the goal is usually to establish the transversal intersection of invariant manifolds [BP01]. The same remark applies to homoclinic orbits and their bifurcations [KMR95, DH00b, XHZ05b]. Homoclinic orbits to a saddle focus are naturally of particular interest [BP03, BP08, BS99a], since they can be used to prove the existence of chaos [Kuz04, Shi65]. It should be noted that homoclinic and heteroclinic bifurcation theory is itself a very large field [CDF90, CDT90, Den93a, Den90, Den93b, Den95b, GTGN97, Gru98,

[HKN01b](#), [HK00](#), [KKO96a](#), [KKO96b](#), [Nii96](#), [Rad05](#), [San95](#)] with many applications [[WK05](#), [KFR01](#)]. For an excellent survey of the topic, we refer to [[HS10b](#)]. Another important related topic is Melnikov theory [[Feč00](#), [GH83](#), [MS96d](#), [SBJM00](#), [Wec02](#)]; however, sometimes one may avoid the use of Melnikov theory to show transversality [[KL88](#)]. Homoclinics can also exist for resonant structures in perturbed Hamiltonian systems [[HW93](#), [HW95](#), [Kov95](#), [Kov92](#), [Kov93](#)] and play a key role in various versions of the nonlinear Schrödinger equation [[GC04](#)].

Section 6.2: This section is based on [[GK09b](#)], but the fast–slow decomposition of the FitzHugh–Nagumo (FHN) equation has been known for quite some time; see, e.g., [[Jon84](#)]. The original papers by FitzHugh and Nagumo [[Fit55](#), [Fit60](#), [Fit61](#), [NAY62](#)] already illustrate that the FHN equation was bound to become an important standard model in nonlinear science [[Cro87](#)]. For an overview of Nagumo’s equation, which is basically FHN without the slow variable, we refer to [[McK70](#)]. Sometimes a piecewise-linear version is used to make the analysis more explicit [[Fer78](#), [Fer81](#), [Rin77](#), [RK73](#), [Rin75](#)]. Even numerical methods may sometimes not show immediately which type of dynamics is relevant for the FHN equation [[CKK⁺09](#)]. For asymptotics of waves and pulses, we refer to [[RT82a](#)] and for radial solutions to [[DRS07](#)]. Instead of the FHN model, another excellent motivating example for heteroclinic connections is that of gas dynamics equations [[GS01a](#), [GS95](#), [GS93](#)].

Section 6.3: The basic view on the exchange lemma is outlined well in [[KJ01](#)]. An introduction to the exchange lemma can be found in [[Jon95](#)]. One has to keep in mind that there is always the fundamental idea [[Cop78](#)] of exponential dichotomies [[CL95](#), [Pal82](#), [Pal84](#), [Pal88](#)] in the background, which can be extended to algebraic dichotomies [[Lin09](#)]. As expected, the exchange lemma also immediately links to other topics, such as turning points [[Liu06](#)].

Section 6.4: The proof we presented was first considered in [[JK94b](#)]. There are several further studies on the exchange lemma available [[JK94b](#), [JT09](#), [KJ01](#), [Tin94](#), [TKJ94](#)], including versions with turning points [[Liu00](#), [Sch08b](#)]. Differential forms can be avoided in the proof by making use of shooting [[Bru96](#)] or contraction maps in weighted spaces [[Bru99](#)]; we decided to use differential forms because they provide another useful tool for the analysis of fast–slow systems that has probably not been utilized to its full potential. There is also Deng’s lemma, which relates to the exchange lemma [[Sch08a](#), [Sch08b](#)].

Section 6.5: The section was based on the result in [[JKL01](#)]. The existence of the fast FHN pulse has been established via various methods. For example, we mention the series of studies [[Has75](#), [Has76a](#), [Has82](#), [Has76b](#)] and [[Yan87](#), [Yan88](#), [Yan89](#), [aKM89](#)]. Double-pulse solutions in nerve axon equations [[EFF82](#)] and other multipulse solutions [[Fer82](#)] exist as well. Other topics are asymptotic methods [[SP96](#)], bifurcation of multipulses from a double heteroclinic [[BD02](#), [San98](#)], breathers [[IN94](#)], coexistence of different waves [[HY09](#), [LV06](#)], control theory [[AAA12](#)], existence of infinitely many waves [[Den91](#), [KT84](#)], related FHN-type models [[ZE10](#)], Riesz–Feller operators [[AK13c](#)], standing pulses via Hamiltonian methods [[CC12](#)], and threshold surfaces [[MR90](#)].

Section 6.6: The exponentially-small-error version can be found in [JKK96], but see also [Sch08a, Sch08b] for other generalizations. The topic of exponentially small splittings in fast–slow systems is quite classical [Eck92, KJK00]. For multipulse homoclinic orbits in adiabatic systems in connection with an application of Melnikov theory, we refer to [STK96]. The various versions for the exchange lemma have been applied, e.g., to coupled nerve equations [Bos95], the Lorenz–Krishnamurthy model [FK96, Tin95, Van08], multibump orbits in Hamiltonian systems [KK96], Poisson–Nernst–Planck systems [EL07, Liu05, Liu05, LW10a], semiconductor models [JR98], solitary waves in the cubic–quintic nonlinear Schrödinger equation [Kap98], and waves in a plasma model [Kaz00b].

Section 6.7: For the application of the exchange lemma to BVPs, we have built on [HKKO98], and the application to periodic orbits is found in [ST01]. In fact, one could also move to multipoint BVPs [Xie12] and use them for the bifurcation analysis of BVPs [Bru98].

Chapter 7

The Blowup Method

This chapter deals with geometric desingularization of nonhyperbolic equilibrium points using the so-called blowup method. The main insight, due to Dumortier and Roussarie, is that singularities at which fast and slow directions interact may be converted into partially hyperbolic problems using the blowup method. The method inserts a suitable manifold, e.g., a sphere, at the singularity.

Section 7.1 introduces the technical tools for the case of single-time-scale systems starting from classical polar coordinates applied to planar vector fields. In Section 7.2, polar coordinates are replaced by local Euclidean coordinates to simplify the computational effort. The blowup method does not work for all classes of vector fields equally well, but Section 7.3 discusses the case of quasihomogeneous vector fields, for which the computation can be carried out very efficiently. In Section 7.4, we return to fast–slow systems and outline the blowup analysis of the planar fold, which is a key component in the geometric theory of fast–slow systems. Sections 7.5 and 7.6 cover applications of the fold singularity results to prove the existence of relaxation oscillations in two and three dimensions. Section 7.7 covers a rescaling procedure that occurs at a crucial step in the blowup method when a reparameterization of time is required.

It should be noted that the presentation in this chapter is quite detailed, although one may certainly introduce the blowup procedure more quickly. However, the method can look quite opaque at first sight, so an elementary introduction seems to be justified.

Background: Just being able to calculate with polar coordinates and other coordinate transformations of vector fields already conveys the essence of the method. For the abstract viewpoint, it may be helpful to get used to the geometric language of differential equations involving vector fields, tangent spaces, etc.; see the introduction to Chapter 2 for references.

7.1 Basics

Initially, the blowup method was a technique developed separately from the geometric study of multiple-time-scale equations. For clarity of exposition, we shall introduce it for single-time-scale systems following [Dum78, Dum93].

Remark: The term “blowup” is also used in the context of finite-time existence of solutions for differential equations, e.g., $z' = z^2$ has solutions blowing up in finite time. This is a completely different use of the term and is not immediately related to geometric desingularization as developed in this chapter.

Let us begin with an example to see which problem the blowup method addresses.

Example 7.1.1. Consider the planar ODE given by

$$\begin{aligned}\dot{z}_1 &= z_1^2 - 2z_1z_2 = F_1(z_1, z_2), \\ \dot{z}_2 &= z_2^2 - 2z_1z_2 = F_2(z_1, z_2).\end{aligned}\tag{7.1}$$

We define $F(z_1, z_2) = (F_1(z_1, z_2), F_2(z_1, z_2))^\top$. Hence, $F(0, 0) = 0$ and

$$DF_{(z_1, z_2)} = \begin{pmatrix} 2z_1 - 2z_2 & -2z_1 \\ -2z_2 & 2z_2 - 2z_1 \end{pmatrix} \Rightarrow DF_{(0, 0)} = \begin{pmatrix} 0 & 0 \\ 0 & 0 \end{pmatrix}.$$

Therefore, $(0, 0)$ is a nonhyperbolic equilibrium point. The blowup method will allow us to construct a vector field with hyperbolic singularities out of (7.1). We shall return to this example after introducing the general construction. ♦

Beginning with the simplest case, consider a planar ODE given by $\dot{z} = F(z)$ for $z \in \mathbb{R}^2$ and $F \in C^\infty$ with $F(0) = 0$. The next definition provides the most basic blowup transformation, which is illustrated by an example below.

Definition 7.1.2. Let S^1 be the unit circle. Consider the polar coordinate transformation

$$\phi : S^1 \times I \rightarrow \mathbb{R}^2, \quad \phi(\theta, r) = (r \cos \theta, r \sin \theta),$$

where I is a (possibly infinite) interval in \mathbb{R} with $0 \in I$, and $\theta \in [0, 2\pi)$ parameterizes S^1 . The **polar blowup** \hat{F} of the vector field F is defined by

$$\hat{F}(\theta, r) := (D\phi_{(\theta, r)}^{-1} \circ F \circ \phi)(\theta, r)\tag{7.2}$$

for $r \neq 0$ and by the continuous extension of (7.2) to $r = 0$. Obviously, \hat{F} is a vector field on $S^1 \times I$.

The choice of I is somewhat arbitrary. In most practical cases, one uses $I = \mathbb{R}$, $I = [0, s]$ for some $s > 0$ or $I = (-a, \infty)$ for some $0 \leq a < \infty$. Each choice has certain advantages and disadvantages, e.g., the case $I = \mathbb{R}$ implies that we have to view \hat{F} as a vector field on the cylinder. The other choices make it easier to visualize \hat{F} as a vector field on \mathbb{R}^2 , as we will see by working through several examples.

Notice from equation (7.2) that we have just expressed the vector field F in a different coordinate system. One key point is that the polar coordinate change is not one-to-one at the origin. Therefore, Definition 7.1.2 has to be investigated further for $r = 0$. Before giving a proof that the definition is indeed a good idea, it is helpful to explain the polar blowup construction from a geometric viewpoint.

Example 7.1.3. (Example 7.1.1 continued...) Let us just figure out \hat{F} in our example. This is a direct calculation:

$$\begin{aligned}\hat{F}(\theta, r) &= (\mathrm{D}\phi_{(\theta, r)}^{-1} \circ F \circ \phi)(\theta, r) \\ &= \begin{pmatrix} -\frac{\sin \theta}{r} & \frac{\cos \theta}{r} \\ \cos \theta & \sin \theta \end{pmatrix} \begin{pmatrix} r^2(\cos^2 \theta - 2 \cos \theta \sin \theta) \\ r^2(\sin^2 \theta - 2 \cos \theta \sin \theta) \end{pmatrix} \\ &= \begin{pmatrix} 3r \cos \theta \sin \theta(\sin \theta - \cos \theta) \\ \frac{1}{4}r^2(\cos \theta + 3 \cos(3\theta) + \sin \theta - 3 \sin(3\theta)) \end{pmatrix}.\end{aligned}$$

Dividing by $\frac{1}{r}$ is not going to change the qualitative structure (see Section 7.7) of the phase portrait of \hat{F} outside the circle $S^1 \times \{r = 0\}$. In particular, consider

$$\bar{F}(\theta, r) := \frac{1}{r} \hat{F}(\theta, r) = \begin{pmatrix} 3 \cos \theta \sin \theta(\sin \theta - \cos \theta) \\ \frac{1}{4}r(\cos \theta + 3 \cos(3\theta) + \sin \theta - 3 \sin(3\theta)) \end{pmatrix}.$$

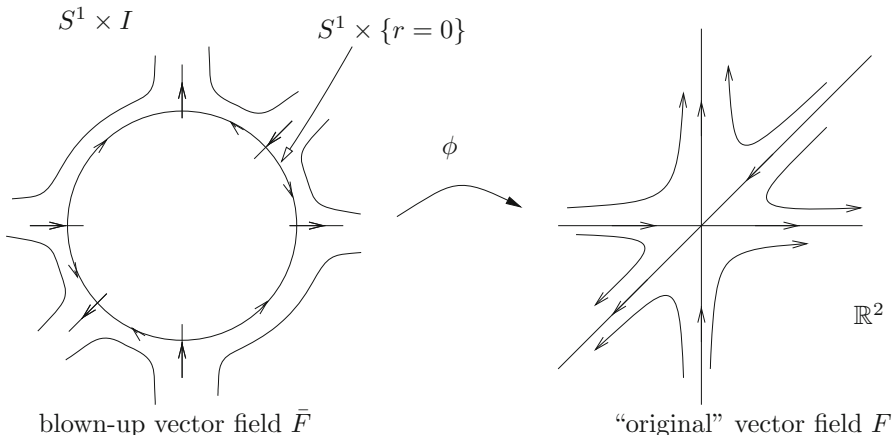


Figure 7.1: Polar blowup at $(0, 0)$ of equation (7.1).

The phase portrait of \bar{F} on $S^1 \times [0, \infty)$ is illustrated in Figure 7.1. There are six equilibrium points on $S^1 \times \{r = 0\}$. For example, we obtain $\bar{F}(\frac{\pi}{2}, 0) = (0, 0)$ and that

$$\mathrm{D}\bar{F}_{(\frac{\pi}{2}, 0)} = \begin{pmatrix} -3 & 0 \\ 0 & 1 \end{pmatrix}.$$

So $(\frac{\pi}{2}, 0)$ is a hyperbolic saddle. It is easy to check that the other five equilibrium points on $S^1 \times \{r = 0\}$ are also hyperbolic saddles. Therefore, we have

desingularized the vector field. The price paid is that a single equilibrium is blown up to a full circle, which has six equilibrium points on it. ♦

Exercise 7.1.4. Complete the phase portrait in Figure 7.1 to include arrows on flow lines for $S^1 \times (0, \infty)$. Now draw a schematic picture of typical representatives of directed flow lines for $S^1 \times (-\frac{1}{2}, 0)$. ◇

Since ϕ is a diffeomorphism on $S^1 \times (0, \infty)$, the vector field \hat{F} is conjugate to F on $S^1 \times \{r > 0\}$, so no information outside of an equilibrium point is lost by blowing up. To motivate the blowup algebraically, consider the diagram

$$\begin{array}{ccc} T(S^1 \times I) & \xrightarrow{D\phi} & T\mathbb{R}^2 \\ \hat{F} \uparrow \wedge & & F \uparrow \\ S^1 \times I & \xrightarrow{\phi} & \mathbb{R}^2 \end{array}$$

Hence, \hat{F} is the map that makes the diagram induced by the polar coordinate change commute. This can be expressed concisely by defining \hat{F} as the vector field such that $\phi_*(\hat{F}) = F$, where ϕ_* is the **pushforward** of a vector field. The last two statements give the formula $D\phi \circ \hat{F} = F \circ \phi$, which recovers the initial definition in (7.2). The construction can be generalized, and we denote by S^{n-1} the $(n-1)$ -dimensional unit sphere in \mathbb{R}^n ; instead of choosing an explicit polar parameterization, we just use the ambient coordinates in the next definition.

Definition 7.1.5. Let F be a C^∞ vector field on \mathbb{R}^n with $F(0) = 0$. Consider the generalized polar coordinate transformation

$$\phi : S^{n-1} \times I \rightarrow \mathbb{R}^n \quad \phi(\bar{z}_1, \dots, \bar{z}_n, r) = (r\bar{z}_1, \dots, r\bar{z}_n),$$

where $\sum_{k=1}^n \bar{z}_k^2 = 1$ and I is a (possibly infinite) interval in \mathbb{R} with $0 \in I$. The **polar blowup** \hat{F} of the vector field F is defined by

$$\hat{F}(\bar{z}_1, \dots, \bar{z}_n, r) := (D\phi_{(\bar{z}_1, \dots, \bar{z}_n, r)}^{-1} \circ F \circ \phi)(\bar{z}_1, \dots, \bar{z}_n, r) \quad (7.3)$$

for $r \neq 0$ and by the continuous extension of (7.3) to $r = 0$.

The next theorem shows that the blowup indeed gives a well-defined vector field on $S^{n-1} \times \{r = 0\}$, as claimed in the definition, i.e., the continuous extension to $r = 0$ works.

Theorem 7.1.6 ([Dum78]). *Let F be a C^∞ vector field on \mathbb{R}^n with $F(0) = 0$. Then the polar blowup \hat{F} given in Definition 7.1.5 is a C^∞ vector field on $S^{n-1} \times I$.*

Proof. Define two vector fields on \mathbb{R}^n :

$$R = \sum_{i=1}^n z_i \frac{\partial}{\partial z_i}, \quad V_{ij} = \frac{1}{2} \left(z_i \frac{\partial}{\partial z_j} - z_j \frac{\partial}{\partial z_i} \right).$$

Observe that $V_{ij} = -V_{ji}$ and $V_{ii} = 0$. Using these facts, it is an easy calculation to show that

$$r^2 F = \left(\sum_{i=1}^n z_i^2 \right) F = \langle R, F \rangle R + 2 \sum_{i,j} \langle V_{ij}, F \rangle V_{ij}. \quad (7.4)$$

Here R represents the radial component and V_{ij} the rotational components of the vector field F . On $S^{n-1} \times I$, we define \hat{R} and \hat{V}_{ij} by $\phi_*(\hat{R}) = R$ and $\phi_*(\hat{V}_{ij}) = V_{ij}$. Next, define auxiliary functions $\alpha_r := \langle R, F \rangle$ and $\alpha_{ij} := \langle V_{ij}, F \rangle$. On taking the pushforward in equation (7.4), we get the relation

$$r^2 F = \phi_* \left((\alpha_r \circ \phi) \hat{R} + 2 \sum_{i,j} (\alpha_{ij} \circ \phi) \hat{V}_{ij} \right)$$

and therefore

$$F = \phi_* \left(\frac{1}{r^2} \left((\alpha_r \circ \phi) \hat{R} + 2 \sum_{i,j} (\alpha_{ij} \circ \phi) \hat{V}_{ij} \right) \right).$$

Hence, an explicit equation for the desired vector field is

$$D\phi^{-1} \circ F \circ \phi = \frac{1}{r^2} \left((\alpha_r \circ \phi) \hat{R} + 2 \sum_{i,j} (\alpha_{ij} \circ \phi) \hat{V}_{ij} \right). \quad (7.5)$$

This equation is defined for $r = 0$ by the following argument. At $0 \in \mathbb{R}^n$, we know that F, R and V_{ij} vanish. Using the product rule, observe that α_r and α_{ij} have no linear terms in their Taylor expansions (i.e., their 1-jet vanishes); for more on jets see [Lu76]. Therefore, $\alpha_r \circ \phi$, $\alpha_{ij} \circ \phi$, $\frac{\partial(\alpha_r \circ \phi)}{\partial r}$, and $\frac{\partial(\alpha_{ij} \circ \phi)}{\partial r}$ are zero. This implies that $(1/r^2)(\alpha_r \circ \phi)$ and $(1/r^2)(\alpha_{ij} \circ \phi)$ are C^∞ for $r = 0$. Hence, the vector field (7.5) is a well-defined vector field for $r = 0$. \square

The last proof is not only a technical detail; it provides us with another explicit way of calculating the polar blowup using equation (7.5). Furthermore, one can guess how to desingularize the blown-up vector field \hat{F} , since dividing it by r^k with k as large as possible appears to be useful. In Example 7.1.1, we had $F(0) = 0$ and $DF(0) = 0$ with a nonzero **Hessian** ($D^2 F(0)$); recall that the Hessian is just the matrix of second partial derivatives. In the language of **jets**, this reads $j_1(F) = 0$ with $j_2(F) \neq 0$ (where the 2-jet $j_2(F)$ can be thought of as the second-order truncated Taylor expansion of F).

Remark: The k -jet of a function $f : \mathbb{R} \rightarrow \mathbb{R}$ at a point $p \in \mathbb{R}$ may be defined as its truncated Taylor polynomial

$$[j_k(f)](x) = f(p) + f'(p)x + \cdots + \frac{1}{k!} \left[\frac{d^k f}{dx^k}(p) \right] x^k, \quad (7.6)$$

and this definition naturally generalizes to Taylor series in higher dimensions. There are various ways to introduce jets, but one should just think of the k -jet as an object that collects the Taylor coefficients of a function up to and including order k ; hence we may view the k -jets also as vectors in the space of coefficients. We shall often just suppress the point p in the notation if $p = 0$ and omit the argument x in (7.6), since we may either use the polynomial viewpoint or just focus on the vector formed by its coefficients.

Definition 7.1.7. Let F be a C^∞ vector field with $j_l(F) = 0$ for $l \in \{0, 1, \dots, k\}$ and $j_{k+1}(F) \neq 0$. We define the **(rescaled) polar blowup** $\bar{F} := \frac{1}{r^k} \hat{F}$.

Using the same arguments as in the proof of Theorem 7.1.6, it follows that \bar{F} is defined on $S^{n-1} \times \{r = 0\}$.

Remark: There is no standard terminology to distinguish between the vector fields \hat{F} and \bar{F} . We have introduced the term “rescaled” to emphasize that scaling by a factor $1/r^k$ does not change the qualitative structure of the vector field near the singularity at $r = 0$. However, the times on orbits of \hat{F} and \bar{F} are not comparable; see Section 7.7. We drop the term “rescaled” if it is clear that we want to desingularize the vector field under consideration.

Example 7.1.8. Consider the differential equation given by

$$\begin{aligned}\dot{z}_1 &= z_2 &= F_1(z_1, z_2), \\ \dot{z}_2 &= z_1^2 + z_1 z_2 &= F_2(z_1, z_2),\end{aligned}\tag{7.7}$$

with $F(z_1, z_2) = (F_1(z_1, z_2), F_2(z_1, z_2))^\top$. We find that $F(0) = 0$ and $DF_{(0,0)}$ has a double zero eigenvalue. Attempting a polar blowup at $(0, 0)$ yields

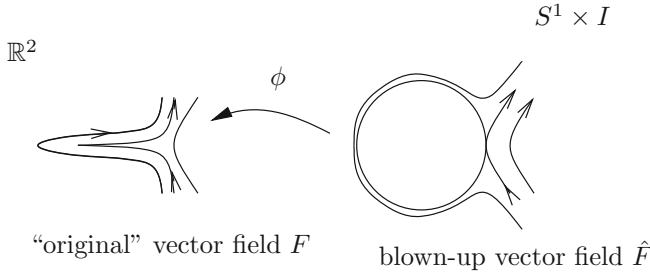
$$\begin{aligned}\hat{F}(\theta, r) &= (D\phi_{(\theta, r)}^{-1} \circ F \circ \phi)(\theta, r) \\ &= \begin{pmatrix} -\frac{\sin \theta}{r} & \frac{\cos \theta}{r} \\ \cos \theta & \sin \theta \end{pmatrix} \begin{pmatrix} r \sin \theta \\ r^2(\cos^2 \theta + \cos \theta \sin \theta) \end{pmatrix} \\ &= \begin{pmatrix} r \cos^3 \theta + r \cos^2 \theta \sin \theta - \sin^2 \theta \\ r \cos \theta \sin \theta (1 + r \cos \theta + r \sin \theta) \end{pmatrix}.\end{aligned}$$

So we cannot divide by any power of r . This is expected, since $DF_{(0,0)} \neq 0$, and so $j_1(F)(0) \neq 0$, which yields $\hat{F} = \bar{F}$. There are two singular points for \bar{F} on the set $S^1 \times \{r = 0\}$ given by $(\pi, 0)$ and $(-\pi, 0)$. A direct calculation gives

$$D\bar{F}_{(\pi, 0)} = \begin{pmatrix} 0 & -1 \\ 0 & 0 \end{pmatrix} = D\bar{F}_{(-\pi, 0)}.\tag{7.8}$$

The only thing we have achieved so far is to make our differential equation more complicated. The two new equilibrium points are still not hyperbolic. The situation is shown in Figure 7.2. The natural question is whether blowing up at $(\pi, 0)$ and $(-\pi, 0)$ is going to improve anything. ♦

To deal with repeated blowups, we need a way to consider the vector field \hat{F} as defined on an open subset of \mathbb{R}^2 . Let us consider the case $I = (-\frac{1}{2}, \infty)$. For $S^1 \times (-\frac{1}{2}, \infty)$, we know how to define the blowup map ϕ as a change to polar coordinates. The next proposition gives a nice map of $I = (-\frac{1}{2}, \infty)$ into a subset of \mathbb{R}^2 and shows what the formula for the blowup map should be in this case.

Figure 7.2: One polar blowup at $(0,0)$ of (7.7).

Proposition 7.1.9. Define $T_1 : S^1 \times (-\frac{1}{2}, \infty) \rightarrow S^1 \times (\frac{1}{2}, \infty)$ by $T_1(\alpha, r) = (\alpha, r+1)$ and $\psi : \mathbb{R}^2 \rightarrow \mathbb{R}^2$ by $\psi(z) = z - \frac{z}{\|z\|}$. Then

$$\begin{array}{ccc} & \mathbb{R}^2 & \\ \psi \nearrow & & \downarrow \phi \\ \{z : \|z\| > \frac{1}{2}\} & \xleftarrow[\phi^{-1} \circ T_1]{} & S^1 \times (-\frac{1}{2}, \infty) \end{array}$$

is a commutative diagram, i.e., $\psi \circ \phi^{-1} \circ T_1 = \phi$. Furthermore, blowing up by ϕ and dividing by r^k is equivalent to blowing up by ψ and dividing by $(\|z\| - 1)^k$.

From a geometric perspective, we just have identified a semi-infinite annulus with the subset $\{z : \|z\| > \frac{1}{2}\}$, i.e., ‘‘unrolled the annulus’’ on the plane. The commutativity of the diagram shows that there exists a well-defined blowup map on $\{z : \|z\| > \frac{1}{2}\}$.

Exercise 7.1.10. Prove Proposition 7.1.9. \diamond

Hence, one may perform repeated blowups in \mathbb{R}^2 using ψ . This gives equilibrium points on the circle $\{z \in \mathbb{R}^2 : \|z\| = 1\}$. Let z_1 be such an equilibrium point and use the map $T_{z_0}(z) = z + z_0$ to blow up using $T_{z_0} \circ \psi$. The situation is shown in Figure 7.3, where two blowups are carried out. Clearly, this construction can be iterated. Denote by $\psi_n = T_{z_n} \circ \psi$ the n th blowup map and by $\hat{F}_{[n]}$ and $\bar{F}_{[n]}$ the sequences of blown-up and rescaled blown-up vector fields.

Proposition 7.1.11 ([Dum78]). Let $\Gamma_n = (\psi_1 \circ \cdots \circ \psi_n)^{-1}(0)$. Then the following hold:

- (R1) There exists only one connected component of $(\mathbb{R}^2 - \Gamma_n)$ that is unbounded. Call it A_n .
- (R2) $\partial A_n \subset \Gamma_n$ and ∂A_n is homeomorphic to S^1 .
- (R3) A_n consists of finitely many smooth arcs meeting transversally.
- (R4) $(\psi_1 \circ \cdots \circ \psi_n)|_{A_n}$ is an analytic diffeomorphism sending A_n onto $\mathbb{R}^2 - \{0\}$.

(R5) $\hat{F}_{[n]}$ restricted to A_n is analytically equivalent to F restricted to $\mathbb{R}^2 - \{0\}$.

(R6) Up to rescaling by a positive function, the analytic equivalence on A_n holds also for $\bar{F}_{[n]}$.

The proof of statements (R1)–(R5) in Proposition 7.1.11 follows by looking at Figure 7.3 and induction on n . Statement (R6) is relatively straightforward to prove as well, but it is involved from the viewpoint of notation (see [Dum78] for details). To state the final result for repeated blowups, another definition is needed.

Definition 7.1.12. A vector field F on \mathbb{R}^n with $F(0) = 0$ satisfies a **Łojasiewicz inequality** if there exist $k \in \mathbb{N}$ (with $k > 0$) and $c > 0$ such that

$$\|F(z)\| \geq c\|z\|^k \quad \text{for all } z \in U, \quad (7.9)$$

where U is some neighborhood of 0.

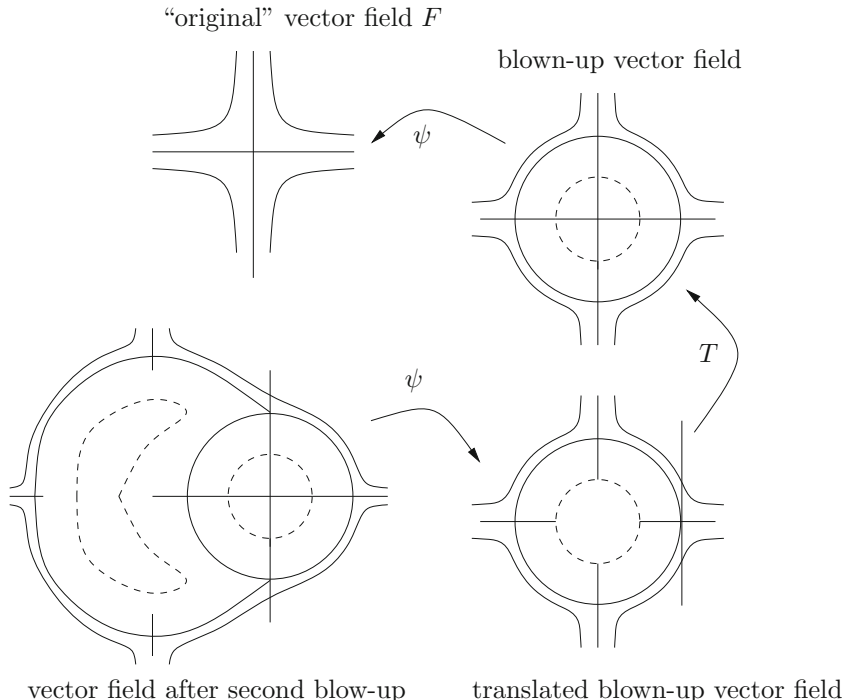


Figure 7.3: Sketch of a repeated blowup: first blow up by ψ and then translate (here we have $T(z_1, z_2) = (z_1 - 1, z_2)$) to blow up at $(1, 0)$. The translated blown-up vector field can be blown up by ψ again.

Analytic vector fields satisfy a Łojasiewicz inequality at an isolated equilibrium point. Therefore, the following theorem can be applied in a large number of cases. Note that the notation from Proposition 7.1.11 is used for the statement.

Theorem 7.1.13 ([Dum78, Dum93]). *If F is a vector field on \mathbb{R}^2 that satisfies a Lojasiewicz inequality, then there is a finite sequence of blowups desingularizing F . More precisely, there is a sequence $\psi_1 \circ \dots \circ \psi_n$ defining a rescaled blown-up vector field $\bar{F}_{[n]}$ such that the equilibrium points of $\bar{F}_{[n]}$ on ∂A_n are either*

- hyperbolic or partially hyperbolic isolated equilibrium points \bar{z} , so that $j_\infty(\bar{F}_{[n]}|_{W^c})(\bar{z}) \neq 0$, where W^c is a center manifold for $\bar{F}_{[n]}$ at \bar{z} , or
- regular smooth closed curves with boundary along which $\bar{F}_{[n]}$ is normally hyperbolic.

No analogous statement is known for arbitrary dimensions, but see Section 7.8. Nevertheless, the techniques clearly generalize, so that we can hope to desingularize at least some specific higher-dimensional equations.

Definition 7.1.14. The rescaled blown-up vector field $\bar{F}_{[n]}$ in Theorem 7.1.13 is called the **desingularization** of F .

The main message is that geometric desingularization techniques allow the study of degenerate equilibrium points with hyperbolic methods on a more complicated space.

7.2 Local Computation

Example 7.2.1. (Example 7.1.8 continued) Consider the blowup begun above for the equation

$$\begin{aligned}\dot{z}_1 &= z_2 &= F_1(z_1, z_2), \\ \dot{z}_2 &= z_1^2 + z_1 z_2 = F_2(z_1, z_2).\end{aligned}\tag{7.10}$$

In this case, the result is the sequence of rescaled blown-up vector fields given in Figure 7.4; this is still to be justified by a calculation. It may seem easy to perform the calculations using the blowup map ψ using a computer algebra system. ♦

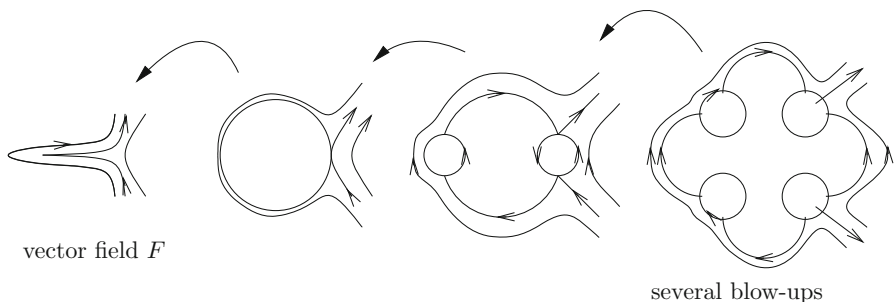


Figure 7.4: Sketch of the repeated (polar) blowup at $(0, 0)$ of a “cusp-type” singularity; see (7.10).

Exercise/Project 7.2.2. Calculate as many steps as you can of the blowup for equation (7.10) at $(0, 0)$ using the map $\psi : \mathbb{R}^2 \rightarrow \mathbb{R}^2$ given by $\psi(z) = z - z/\|z\|$. More precisely, use a computer algebra system to calculate

$$\left(D\psi_{(z_1, z_2)}^{-1} \circ F \circ \psi \right) (z_1, z_2). \quad (7.11)$$

Then desingularize by dividing by an appropriate power of $(\|z\| - 1)^k$ and find the equilibrium points on $\{z : \|z\| = 1\}$. Blow up each equilibrium point if it is not partially hyperbolic. Try to obtain a plot of the desingularized vector field. Don't try too hard! \diamond

Having done Exercise 7.2.2, you should have identified the bottleneck in this direct calculation. The algebraic equations for finding the equilibrium points in the blown-up equation are hard to solve, even numerically. The main limitation is that a global analytical formula for the blowup is often not available. Instead, focusing on a local calculation turns out to be feasible.

Definition 7.2.3. Let F be a C^∞ vector field on \mathbb{R}^n with $F(0) = 0$. Define the map $\mu_i : \mathbb{R}^n \rightarrow \mathbb{R}^n$ by

$$\mu_i(z_1, \dots, z_n) = (z_i z_1, z_i z_2, \dots, z_i z_{i-1}, z_i, z_i z_{i+1}, \dots, z_i z_n). \quad (7.12)$$

Then define the **directional blowup** of F in direction z_i by

$$\hat{F}^i(z) := ((D\mu_i)_z^{-1} \circ F \circ \mu_i)(z). \quad (7.13)$$

Note that there is again a problem in that \hat{F}^i might not be defined everywhere. In that case, the problematic set is $\{z_i = 0\}$, since we cannot invert μ_i on $\{z_i = 0\}$. The same techniques as in Theorem 7.1.6 can be used to show that the vector field can be extended to $\{z_i = 0\}$. Also notice that we have abused the superscript notation \hat{F}^i , which has the obvious ambiguities of iteration, powers, and differentiation already. Since neither of these operations is commonly performed on the blown-up vector field, confusion should not arise.

Definition 7.2.4. Let \hat{F}^i be the directional blowup of F in direction i at 0. Suppose $j_l(F)(0) = 0$ for $l \in \{0, 1, \dots, k\}$ and $j_{k+1}(F)(0) \neq 0$. Define the **rescaled directional blowup** in direction i by $\bar{F}^i(z) := \frac{1}{z_i^k} \hat{F}^i(z)$.

It is useful to compare the polar and directional blowups in an example.

Example 7.2.5. We know (see Example 7.1.3) how to calculate the polar blowup of

$$\begin{aligned} \dot{z}_1 &= z_1^2 - 2z_1 z_2 = F_1(z_1, z_2), \\ \dot{z}_2 &= z_2^2 - 2z_1 z_2 = F_2(z_1, z_2). \end{aligned}$$

In \mathbb{R}^2 , there are directions available. In the z_1 -direction, one gets

$$\begin{aligned} \bar{F}^1(z) &= \frac{1}{z_1} ((D\mu_1)_z^{-1} \circ F \circ \mu_1)(z) \\ &= \frac{1}{z_1} \begin{pmatrix} 1 & 0 \\ -\frac{z_2}{z_1} & \frac{1}{z_1} \end{pmatrix} \begin{pmatrix} z_1^2 - 2z_1^2 z_2 \\ (z_1 z_2)^2 - 2z_1^2 z_2 \end{pmatrix} \\ &= \begin{pmatrix} z_1(1 - 2z_2) \\ 3z_2(z_2 - 1) \end{pmatrix}. \end{aligned}$$

In the z_2 -direction, we obtain

$$\bar{F}^2(z) = \begin{pmatrix} 3z_1(z_1 - 1) \\ z_2(1 - 2z_1) \end{pmatrix}.$$

In Figure 7.5, the polar blowup is compared with the two-directional blowups.

Observe that the directional blowup in the z_1 -direction turns the singularity $(0, 0)$ into a whole line of singularities given by $\{z_1 = 0\}$. Bending this line into a semicircle, we can imagine that the z_1 -direction blowup represents, at least, the half-plane $\{z_1 > 0\}$. Similarly, the z_2 -directional blowup represents at least the half-plane $\{z_2 > 0\}$. Figure 7.5 suggests that the complete structure of the polar blowup can be determined by directional blowups. ♦

The observations of the previous example are not accidental, and we can recover the complete structure by directional blowups.

Proposition 7.2.6 ([Dum78, Dum93]). *Up to change of coordinates, the directional and polar blowup methods are equivalent. More precisely, let \hat{F} denote the polar blowup of a C^∞ vector field F on \mathbb{R}^2 with $F(0) = 0$. Denote by \hat{F}^i the directional blowups. Then given a sufficiently small $V \subset \mathbb{R}^2$, we can find $U \subset S^1 \times (-\frac{1}{2}, \infty)$ such that \hat{F} and \hat{F}^i are equivalent up to a diffeomorphism $C : U \rightarrow V$.*

Proof. A slightly stronger statement will be proved. In fact, let $V = \mathbb{R}^2 - \{z : z_1 \neq 0\}$ and define

$$U := \left\{ (\theta, r) \in S^1 \times \left(-\frac{1}{2}, \infty\right) : \theta \in \left[0, \frac{\pi}{2}\right) \cup \left(\frac{3\pi}{2}, 2\pi\right) \right\}.$$

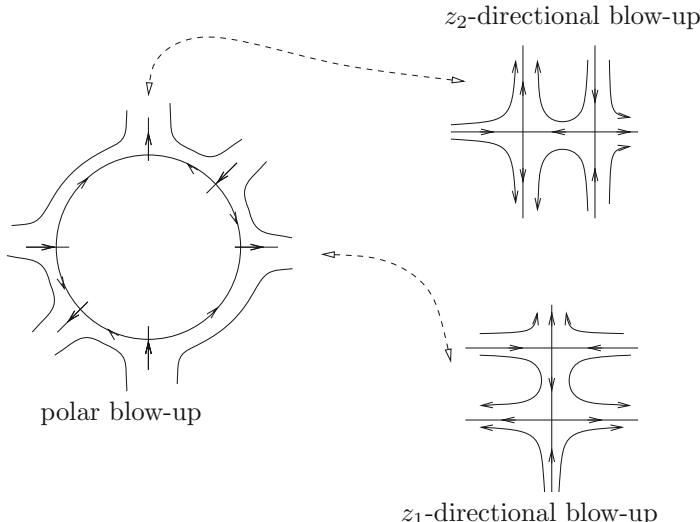


Figure 7.5: Polar blowup at 0 of (7.1) compared to directional blowups

Viewing S^1 embedded in \mathbb{R}^2 , it follows that U covers at least the half-plane $\{z_1 > 0\}$. Define an analytic change of coordinates $C : U \rightarrow V$ given by $C(r, \theta) = (r \cos \theta, \tan \theta)$. Then consider the diagram

$$\begin{array}{ccc} U & \xrightarrow{\phi} & \mathbb{R}^2 \\ C \downarrow & \nearrow \mu_1 & \\ V & & \end{array} \quad (7.14)$$

A direct calculation yields

$$(\mu_1 \circ C)(\theta, r) = (r \cos \theta, r \tan \theta \cos \theta) = (r \cos \theta, r \sin \theta),$$

and therefore, diagram (7.14) commutes. We conclude that on U and V , the vector fields \hat{F} and \hat{F}^1 are diffeomorphic with $C_*(\hat{F}) = \hat{F}^1$. Also, the rescaled blowups are equivalent. Suppose the rescaled polar blowup is given by division with $\frac{1}{r^k}$. Then

$$C_*(\bar{F}) = C_*\left(\frac{1}{r^k}\hat{F}\right) = \frac{1}{(z_1^2 + (z_1 z_2)^2)^{\frac{k}{2}}} C_*(\hat{F}) = \frac{1}{(1+z_2^2)^{\frac{k}{2}}} \frac{1}{z_1^k} \hat{F}^1 = \frac{1}{(1+z_2^2)^{\frac{k}{2}}} \bar{F}^1.$$

So the orbits of \bar{F}^1 and \bar{F} are equivalent with correct orientations, since we have rescaled by an everywhere positive function. Now one can use $U' = \{(\theta, r) \in S^1 \times (-\frac{1}{2}, \infty) : \theta \in [\frac{\pi}{2}, \frac{3\pi}{2}]\}$, $V = \{z_1 < 0\}$ and the same mapping C to find that \bar{F}^1 and \bar{F} are equivalent for this case as well. Using the z_2 -directional blowup \bar{F}^2 takes care of the remaining sets $\{\frac{\pi}{2}\} \times (-\frac{1}{2}, \infty)$ and $\{\frac{3\pi}{2}\} \times (-\frac{1}{2}, \infty)$. \square

In the previous proof, the coordinate change C played the role of the geometric construction we described as “bending” the directional blowup and mapping it to a suitable half-plane. The next example demonstrates that the directional blowups are extremely helpful for iterated blowups.

Example 7.2.7. Recall that in Example 7.1.8 and Exercise 7.2.2, we tried to find the blowup of

$$\begin{aligned} \dot{z}_1 &= z_2 &= F_1(z_1, z_2), \\ \dot{z}_2 &= z_1^2 + 2z_1 z_2 = F_2(z_1, z_2). \end{aligned}$$

Although we have given an answer already, we have not yet justified Figure 7.4. Consider blowing up the origin in the z_1 -direction:

$$\hat{F}_{[1]}^1(z) = \bar{F}_{[1]}^1(z) = (z_1 z_2, z_1 + 2z_1 z_2 - z_2^2)^\top.$$

Another blowup at the origin in the z_1 -direction gives

$$\hat{F}_{[2]}^1(z) = \bar{F}_{[2]}^1(z) = (z_1^2 z_2, 1 + 2z_1 z_2(1 - z_2))^\top.$$

There are no equilibrium points in $\bar{F}_{[2]}^1$. So let us try the z_2 -direction instead in the last step. Since the notation gets cumbersome with separate indices, we

only write the number of blowups as a subscript and the last direction as a superscript. Therefore,

$$\hat{F}_{[2]}^2(z) = \bar{F}_{[2]}^2(z) = (-z_1(z_1 - 2z_2 + 2z_1z_2), z_2(z_1 - z_2 + 2z_1z_2))^{\top}, \quad (7.15)$$

which has an equilibrium point at the origin. Notice that the failure of the z_1 -direction would have been expected if we had known the result in Figure 7.4. The second polar blowup does not have equilibria except on the vertical lines intersecting a circle. Those lines are precisely the parts of the plane not covered by the z_1 -directional blowup. Calculating the derivatives, we obtain $(D\bar{F}_{[2]}^2)_{(0,0)} = 0$. So we continue with another z_2 -directional blowup:

$$\begin{aligned}\hat{F}_{[3]}^2(z) &= (z_1z_2(3 - 2z_1(1 + 2z_2), z_2^2(z_1 + 2z_1z_2 - 1))^{\top}, \\ \bar{F}_{[3]}^2(z) &= (z_1(3 - 2z_1(1 + 2z_2), z_2(z_1 + 2z_1z_2 - 1))^{\top}.\end{aligned}$$

The vector field $\bar{F}_{[3]}^2$ has two equilibrium points given by $p_1 = (0, 0)$ and $p_2 = (\frac{3}{2}, 0)$. Calculating the linearizations at p_1 and p_2 , we finally have

$$(D\bar{F}_{[3]}^2)_{p_i} = \begin{pmatrix} 3 & 0 \\ 0 & -1 \end{pmatrix} \quad \text{for } i \in \{1, 2\}.$$

So p_1 and p_2 are hyperbolic saddles. The remaining calculations to determine Figure 7.4 are almost identical to the sequence of blowups in directions z_1 , z_2 , and z_2 that we have done so far. ♦

Exercise 7.2.8. Prove that the blowup $\hat{F}_{[2]}^2$ in Example 7.2.7 is indeed given by equation (7.15), i.e., check the calculation. ◇

7.3 The Quasihomogeneous Case

Although the directional blowup method gives us a computable method of desingularization, it is still quite laborious to keep track of all the charts. In some cases, we can employ yet another improvement of the blowup map, one that requires even fewer calculations. The next example illustrates why one may hope to find something better.

Example 7.3.1. Consider the following ODE:

$$\begin{aligned}\dot{z}_1 &= z_2 = F_1(z_1, z_2), \\ \dot{z}_2 &= z_1^2 = F_2(z_1, z_2).\end{aligned}$$

Observe that $F(0, 0) = 0$ and that $DF(0, 0)$ has two zero eigenvalues. The polar blowup is readily calculated:

$$\hat{F}(\theta, r) = \bar{F}(\theta, r) = (r \cos^3 \theta - \sin^2 \theta, r \cos \theta \sin \theta(1 + r \cos \theta))^{\top}.$$

It has two equilibrium points given by $p_1 = (0, 0)$ and $p_2 = (\pi, 0)$. Both points are not hyperbolic, and it is easy to check that the linearizations $D\bar{F}_{p_i}$ each have

two zero eigenvalues. So one would have to blow up again, preferably using the directional blowup to desingularize F . Instead, let us modify the polar blowup map and define

$$\varphi(\theta, r) := (r^2 \cos \theta, r^3 \sin \theta). \quad (7.16)$$

The choice of exponents for r will be explained in Sections 12.4–12.8, where combinatorial tools are developed to calculate the exponents for polynomial vector fields. Of course, the same formula for blowing up can still be used:

$$\hat{F}(\theta, r) := ((D\varphi)^{-1}_{(\theta, r)} \circ F \circ \varphi)(\theta, r).$$

Another calculus exercise leads to the vector field

$$\bar{F}(\theta, r) = \frac{1}{r} \hat{F}(\theta, r) = \left(\frac{6 \sin^2 \theta - 4 \cos^3 \theta}{\cos(2\theta) - 5}, -\frac{2r \cos \theta \sin \theta (1 + \cos \theta)}{\cos(2\theta) - 5} \right). \quad (7.17)$$

Observe that \bar{F} has two equilibria given in polar coordinates in the blown-up space by $p_3 \approx (0.63, 0)$ and $p_4 \approx (-0.63, 0)$, which are found to be hyperbolic saddles. Therefore, F has been desingularized in one step. The phase portrait of \bar{F} from equation (7.17) is given in Figure 7.6. ♦

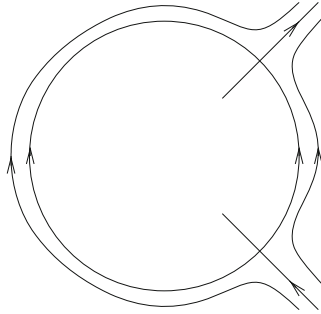


Figure 7.6: Blowup at $(0, 0)$ of equation (7.17).

It is helpful to introduce some additional concepts to explain how the map φ in Example 7.3.1 is chosen.

Definition 7.3.2. A function $f : \mathbb{R}^n \rightarrow \mathbb{R}$ is called **quasihomogeneous** of type $(a_1, \dots, a_n) \in \mathbb{N}^n$ and degree k if for every $r \in \mathbb{R}$,

$$f(r^{a_1} z_1, \dots, r^{a_n} z_n) = r^k f(z_1, \dots, z_n). \quad (7.18)$$

A vector field F is called **quasihomogeneous** of type (a_1, \dots, a_n) and degree $k+1$ if its j th component function $F_j(z_1, \dots, z_n)$ is quasihomogeneous of type (a_1, \dots, a_n) and degree $k+a_j$.

Remark: There seems to be no agreement in the literature on the terminology for quasihomogeneous vector fields. Some authors refer to degree k in a situation in which we say degree $k+1$.

Example 7.3.3. Consider the vector field

$$F(z_1, z_2) = (z_1^2 - 2z_1z_2, z_2^2 - 2z_1z_2)^\top. \quad (7.19)$$

One checks that $F_1(z_1, z_2) = z_1^2 - 2z_1z_2$ is quasihomogeneous of type $(1, 1)$ and degree 2. Since the same holds for $F_2(z_1, z_2)$, we can conclude that F is quasihomogeneous of type $(1, 1)$ and degree 2. ♦

Example 7.3.4. Now let us consider the vector field from Example 7.3.1 given by $F(z_1, z_2) = (z_2, z_1^2)$. Writing out the conditions for quasihomogeneity gives

$$\begin{aligned} F_1(r^{a_1}z_1, r^{a_2}z_2) &= r^{a_2}z_2 = r^{k+a_1}z_2 = r^{k+a_1}F_1(z_1, z_2), \\ F_2(r^{a_1}z_1, r^{a_2}z_2) &= r^{2a_1}z_1^2 = r^{k+a_2}z_1^2 = r^{k+a_2}F_2(z_1, z_2). \end{aligned}$$

Solving the algebraic equations yields $3a_1 = 2a_2$, so choosing a_1 and a_2 as small as possible, we find that F is quasihomogeneous of type $(2, 3)$ and degree 2. This special property of F explains why $\varphi(\theta, r) = (r^2 \cos \theta, r^3 \sin \theta)$ is a good choice for the blowup map in Example 7.3.1. ♦

Combining the insights from the examples leads to another definition.

Definition 7.3.5. Let F be a C^∞ vector field on \mathbb{R}^n with $F(0) = 0$. Let $a_i \in \mathbb{N}$ for $i = \{1, 2, \dots, n\}$ and consider the generalized polar coordinate transformation

$$\varphi : S^{n-1} \times I \rightarrow \mathbb{R}^n, \quad \varphi(\bar{z}_1, \dots, \bar{z}_n, r) = (r^{a_1}\bar{z}_1, \dots, r^{a_n}\bar{z}_n),$$

where I is a (possibly infinite) interval in \mathbb{R} with $0 \in I$ and $\sum_{k=1}^n \bar{z}_k^2 = 1$. The **weighted polar blowup** \hat{F} of the vector field F is defined by

$$\hat{F}(\bar{z}_1, \dots, \bar{z}_n, r) = (\mathrm{D}\varphi_{(\bar{z}_1, \dots, \bar{z}_n, r)}^{-1} \circ F \circ \varphi)(\bar{z}_1, \dots, \bar{z}_n, r) \quad (7.20)$$

for $r \neq 0$ and by the continuous extension of (7.2) to $r = 0$. Suppose that $j_l(F) = 0$ for $l \in \{0, 1, \dots, k\}$ and $j_{k+1}(F) \neq 0$. We define the (**rescaled**) **weighted polar blowup** by $\bar{F} = \frac{1}{r^k} \hat{F}$.

Remark: Instead of “weighted,” it is common to call the blowup from Definition 7.3.5 a **quasihomogeneous blowup**; see also [Dum78, Dum93] for background on the quasihomogeneous terminology and [Kol07] for the weighted blowup in algebraic geometry.

It again turns out that the computation in polar coordinates can be cumbersome, and it helps to introduce directional blowups. Let us look at a detailed example before the definition.

Example 7.3.6. Consider the vector field F given in \mathbb{R}^2 with coordinates $(z_1, z_2) = (x, y)$ by

$$\begin{aligned} \dot{x} &= y, \\ \dot{y} &= x^2. \end{aligned} \quad (7.21)$$

The blowup of (7.21) was discussed in Example 7.3.1. In Example 7.3.4, it was demonstrated that (7.21) is quasihomogeneous of type $(2, 3)$. So we try to use the weighted (or quasihomogeneous) blowup with coefficients $(2, 3)$:

$$\varphi : S^1 \times I \rightarrow \mathbb{R}^2, \quad \text{where } \varphi(\bar{x}, \bar{y}, r) = (r^2\bar{x}, r^3\bar{y}).$$

A blowup in the x -direction only should combine this with the map $(\bar{x}, \bar{y}) \mapsto (\bar{x}, \bar{x}\bar{y})$, so that

$$(\bar{x}, \bar{y}, r) \mapsto (r^2 \bar{x}, r^3 \bar{x}\bar{y}). \quad (7.22)$$

Recall that the directional blowup in the x -direction can be defined away from $\bar{x} = 0$ and that it extends automatically to the set $\{\bar{x} = 0\}$, which represents the blown-up point. Therefore, we should be able to eliminate the variable \bar{x} entirely in this case and “divide by \bar{x} ” in (7.22) to end up with a blowup map on \mathbb{R}^2 . This idea has to be made more precise. The main idea is that away from the set $\{(\bar{x}, \bar{y}) \in S^1 : \bar{x} = 0\}$, we can consider the coordinate chart

$$\kappa_1 : S^1 \times I \rightarrow \mathbb{R}^2 \quad \text{where} \quad \kappa_1(\bar{x}, \bar{y}, r) = \left(\frac{\bar{y}}{\bar{x}^{b_1}}, \frac{r}{\bar{x}^{b_2}} \right) =: (y_1, r_1)$$

for some coefficients $b_i \in \mathbb{R}$ to be determined. The b_i are going to work as weights to obtain the expressions of the blowup map in local coordinates without \bar{x} . Note that the chart κ_1 is reminiscent of the map

$$(z_1, \dots, z_{i-1}, z_i, z_{i+1}, \dots, z_n) \mapsto \left(\frac{z_1}{z_i}, \dots, \frac{z_{i-1}}{z_i}, 1, \frac{z_{i+1}}{z_i}, \dots, \frac{z_n}{z_i} \right). \quad (7.23)$$

The last map is recognized as the change from homogeneous to affine coordinates for **projective space**. This should not be surprising, since one can construct (real) projective space \mathbb{PR}^n by identifying antipodal points on S^n ; see also [Lee06] for background on projective space. This also hints that we should be careful whether we consider the transformation (7.23) using division by z_i or the map

$$(z_1, \dots, z_{i-1}, z_i, z_{i+1}, \dots, z_n) \mapsto \left(-\frac{z_1}{z_i}, \dots, -\frac{z_{i-1}}{z_i}, -1, -\frac{z_{i+1}}{z_i}, \dots, -\frac{z_n}{z_i} \right)$$

using division by $-z_i$. It is helpful to look at some explicit calculations for our example to see how the idea of “switching to (weighted) affine coordinates” in combination with the directional blowup works. The main target is that the following diagram should commute:

$$\begin{array}{ccc} & S^1 \times I & \\ \kappa_1 \swarrow & & \searrow \varphi \\ \mathbb{R}^2 & \xrightarrow{\mu_1} & \mathbb{R}^2 \end{array}$$

where μ_1 is the polar blowup in local coordinates, which we would like to be given by

$$\mu_1(y_1, r_1) := (r_1^2, r_1^3 y_1) = (x, y).$$

We have the following data:

$$\begin{aligned} \text{from } \kappa_1 \quad & y_1 = \bar{y}\bar{x}^{-b_1}, \quad r_1 = r\bar{x}^{-b_2}, \\ \text{from } \varphi \quad & x = r^2\bar{x}, \quad y = r^3\bar{y}, \end{aligned} \quad (7.24)$$

and μ_1 maps (y_1, r_1) -space to (x, y) -space. From (7.24), we get

$$\begin{aligned} x &= r^2 \bar{x} = (r_1 \bar{x}^{b_2})^2 \bar{x} \stackrel{!}{=} r_1^2, \\ y &= r^3 \bar{y} = (r_1 \bar{x}^{b_2})^3 y_1 \bar{x}^{b_1} \stackrel{!}{=} r_1^3 y_1. \end{aligned}$$

So we can simply choose $b_2 = -\frac{1}{2}$ and $b_1 = \frac{3}{2}$ to get the desired result. The next step is to find the new vector field on \mathbb{R}^2 that is given by the blowup via μ_1 :

$$\begin{aligned} x &= r_1^2, \\ y &= r_1^3 y_1. \end{aligned}$$

Since this change of coordinates just represents a mapping on \mathbb{R}^2 , the calculation has been reduced from many coordinate changes to just one:

$$r_1^3 y_1 = y = \dot{x} = 2r_1 \dot{r}_1 \Rightarrow \dot{r}_1 = \frac{1}{2} r_1^2 y_1. \quad (7.25)$$

To derive the flow for y_1 requires another calculation:

$$r_1^4 = x^2 = \dot{y} = 3r_1^2 \dot{r}_1 y_1 + r_1^3 \dot{y}_1 \Rightarrow \dot{y}_1 = r_1 \left(1 - \frac{3}{2} y_1^2 \right). \quad (7.26)$$

Desingularizing (7.25) and (7.26) by dividing by r_1 and rescaling time (see Section 7.7) removes r_1 , and we obtain the blown-up vector field

$$\begin{aligned} \dot{r}_1 &= \frac{1}{2} r_1 y_1, \\ \dot{y}_1 &= 1 - \frac{3}{2} y_1^2. \end{aligned} \quad (7.27)$$

Looking at Figure 7.6 as computed in Example 7.3.1, observe that (7.27) precisely represents the polar blown-up vector field in the right half-plane $\{(x, y) \in \mathbb{R}^2 : x > 0\}$ if we embed S^1 as the unit circle in \mathbb{R}^2 . To cover all parts near the embedded circle S^1 in Figure 7.6, which represents the blown-up equilibrium point $(0, 0)$, additional coordinate charts are required:

$$\begin{aligned} \kappa_{-1}(\bar{x}, \bar{y}, r) &=: (y_{-1}, r_{-1}), \\ \kappa_2(\bar{x}, \bar{y}, r) &=: (x_2, r_2), \\ \kappa_{-2}(\bar{x}, \bar{y}, r) &=: (x_{-2}, r_{-2}). \end{aligned} \quad (7.28)$$

Choosing the charts using the same procedure by which we constructed κ_1 and μ_1 yields the directional blowup maps

$$\begin{aligned} \mu_{-1}(y_{-1}, r_{-1}) &= (-r_{-1}^2, r_{-1}^3 y_{-1}), \\ \mu_2(x_2, r_2) &= (r_2^2 x_2, r_2^3), \\ \mu_{-2}(x_{-2}, r_{-2}) &= (r_{-2}^2 x_{-2}, -r_{-2}^3). \end{aligned} \quad (7.29)$$

Note that there is formally no need to calculate the blown-up vector field for μ_2 and μ_{-2} , since we can consider the map $r \mapsto -r$ that interchanges between the two blown-up vector fields induced by μ_2 and μ_{-2} . This is geometrically clear

from the reflection symmetry around the x -axis in Figure 7.6. The calculations give the three rescaled blown-up vector fields

$$\begin{cases} \dot{r}_{-1} = -\frac{1}{2}r_{-1}y_{-1} \\ \dot{y}_{-1} = 1 - \frac{3}{2}y_{-1}^2 \end{cases} \quad \begin{cases} \dot{r}_2 = \frac{1}{3}r_2x_2^2 \\ \dot{x}_2 = 1 - \frac{2}{3}x_2^3 \end{cases} \quad \begin{cases} \dot{r}_{-2} = \frac{1}{3}r_{-2}x_{-2}^2 \\ \dot{x}_{-2} = 1 + \frac{2}{3}x_{-2}^3 \end{cases}.$$

The previous three vector fields represent the left half-plane, upper half-plane, and lower half-plane of the vector field defined by the polar blowup φ on $S^1 \times I$ if we embed S^1 as the unit circle in \mathbb{R}^2 . ♦

Exercise 7.3.7. Find the three coordinate charts κ_{-1} , κ_2 , and κ_{-2} as indicated in (7.28) that induce the vector fields given in (7.29). ◇

The key idea is that the directional blowup together with coordinate charts on the blown-up space $S^{n-1} \times I$ reduces the computations for weighted blowups. The weighted blowups are usually given by a map from $S^{n-1} \times I$ to \mathbb{R}^n , and then the situation is reduced to a simple coordinate change on \mathbb{R}^n . Although there is a serious price to pay—working in *several* charts—it turns out that this local approach is preferable. The practical approach to using the blowup is to define charts on the sphere, use the directional blowup, and hence reduce the problem to a coordinate change on \mathbb{R}^n . The situation is illustrated in a schematic view in Figure 7.7.

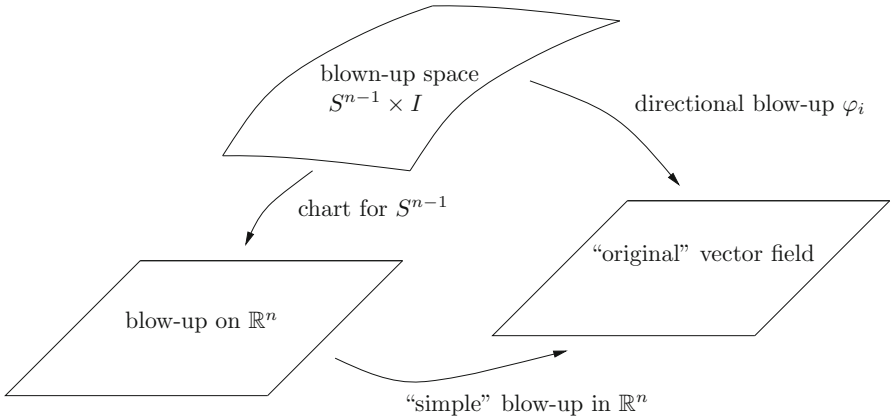


Figure 7.7: Coordinate changes to simplify the blowup method.

Definition 7.3.8. Let F be a C^∞ vector field on \mathbb{R}^n such that $F(0) = 0$ and $DF(0) = 0$. Let $a_i \in \mathbb{N}$ for $i = \{1, 2, \dots, n\}$ and consider the directional blowup map in the i -direction $\varphi_i : S^{n-1} \times I \rightarrow \mathbb{R}^n$:

$$\varphi_i(\bar{z}_1, \dots, \bar{z}_n, r) = (r^{a_1} \bar{z}_1 \bar{z}_i, \dots, r^{a_{i-1}} \bar{z}_{i-1} \bar{z}_i, r^{a_i} \bar{z}_i, r^{a_{i+1}} \bar{z}_{i+1} \bar{z}_i, \dots, r^{a_n} \bar{z}_n \bar{z}_i),$$

where I is a (possibly infinite) interval in \mathbb{R} with $0 \in I$ and $\sum_{k=1}^n \bar{z}_k^2 = 1$. The **weighted directional blowup** \hat{F} of the vector field F is defined by

$$\hat{F}(\bar{z}_1, \dots, \bar{z}_n, r) := ((D\varphi_i)^{-1}_{(\bar{z}_1, \dots, \bar{z}_n, r)} \circ F \circ \varphi_i)(\bar{z}_1, \dots, \bar{z}_n, r) \quad (7.30)$$

for $r \neq 0$ and by the continuous extension of (7.2) to $r = 0$. Suppose that $j_k(F) = 0$ and $j_{k+1}(F) \neq 0$. Define the **(rescaled) weighted directional blowup** by $\bar{F} = \frac{1}{r^k} \hat{F}$.

Definition 7.3.9. We continue in the setup of the previous definition. Let $\kappa_a : S^{n-1} \times I$ be a chart and use $\mu_a : \mathbb{R}^n \rightarrow \mathbb{R}^n$ to denote the blowup/coordinate change induced by the following commutative diagram:

$$\begin{array}{ccc} & S^{n-1} \times I & \\ \kappa_a \swarrow & & \searrow \varphi_i \\ \mathbb{R}^n & \xrightarrow{\mu_a} & \mathbb{R}^n \end{array}$$

If κ_a is a suitably chosen (weighted) affine chart for the i th coordinate given by

$$(\bar{z}_1, \dots, \bar{z}_n, r) \mapsto \left(\frac{\bar{z}_1}{\bar{z}_i^{b_1}}, \dots, \frac{\bar{z}_{i-1}}{\bar{z}_i^{b_{i-1}}}, \frac{\bar{z}_{i+1}}{\bar{z}_i^{b_{i+1}}}, \dots, \frac{\bar{z}_n}{\bar{z}_i^{b_n}}, r \right),$$

then one may write the map μ_a as

$$\mu_a(w_1, \dots, w_n, r) := (r^{a_1} w_1, \dots, r^{a_{i-1}} w_{i-1}, r^{a_i}, r^{a_{i+1}} w_{i+1}, \dots, r^{a_n} w_n),$$

where $w = (w_1, \dots, w_n)^\top \in \mathbb{R}^n$ denotes coordinates for the domain of μ_a and the range of κ_a , i.e., for the space \mathbb{R}^3 in the lower left-hand corner of the diagram above. We also call μ_a the **weighted directional blowup** in the direction i , since it is a local coordinate expression for the weighted directional blowup given in Definition 7.3.8.

Each directional blowup covers only one part of the new phase space $S^{n-1} \times I$. Hence, one should think of patching each of the directional blowup vector fields together to form one vector field \bar{X} . Formally, this is often encoded in the next definition.

Definition 7.3.10. Let M be a smooth compact manifold with a finite open covering $\{B_i\}$. A **local vector field** \bar{X} is defined by smooth vector fields \bar{X}_i on each B_i such that if $B_i \cap B_j \neq \emptyset$, then there exists a smooth function ϕ_{ij} defined and strictly positive in $B_i \cap B_j$ such that $X_i = \phi_{ij} X_j$ on $B_i \cap B_j$.

The functions ϕ_{ij} are obtained from **transition maps** of the charts of the manifold; a transition map between two charts ψ_1 and ψ_2 is just $\psi_1 \circ \psi_2^{-1}$. It has the class of the manifold (e.g., smooth manifolds are defined via smooth transition maps [Lee06]). In practice, the definition of a local vector field provides only a framework and rarely has to be checked, since we usually start with a polar blowup and use directional blowups to simplify the calculations. In this case, we always have a local vector field.

In getting used to the calculations, it is often forgotten that one difficult problem is to determine the coefficients a_i ; see Section 7.8. Most algorithmic methods are based on the Newton polygon and are not trivial to carry out; see Section 12.4.

7.4 Blowup Analysis of the Generic Fold

To get used to the blowup technique in multiple time scale dynamics, it is helpful to consider a concrete low-dimensional example. In this section, the generic fold point in a planar fast–slow system is considered. The geometric desingularization will complement the asymptotic analysis of the fold discussed in Section 5.4. Consider the $(1, 1)$ -fast–slow system

$$\begin{aligned} \frac{dx}{dt} &= x' = f(x, y, \varepsilon), \\ \frac{dy}{dt} &= y' = \varepsilon g(x, y, \varepsilon). \end{aligned} \quad (7.31)$$

Suppose (7.31) has a generic fold point. Without loss of generality, we may assume that this point is at $(x, y) = (0, 0)$ and

$$\begin{aligned} f(0, 0, 0) &= 0, & f_x(0, 0, 0) &= 0, & f_{xx}(0, 0, 0) &> 0, \\ f_y(0, 0, 0) &< 0, & g(0, 0, 0) &< 0, \end{aligned} \quad (7.32)$$

where subscripts denote partial derivatives; cf. the discussion of normal forms for (7.31) in Section 4.2 for more details. By the smoothness of all functions involved, the conditions (7.32) hold in a neighborhood U of $(0, 0)$. We shall work only in this neighborhood from now on. Denote the normally hyperbolic branches of the critical manifold C_0 by

$$S_0^a = \{(x, y) \in C_0 : f_x < 0\} \cap U \quad \text{and} \quad S_0^r = \{(x, y) \in C_0 : f_x > 0\} \cap U.$$

By Fenichel’s theorem, there exist associated slow manifolds S_ε^a and S_ε^r for $0 < \varepsilon \ll 1$. The situation is illustrated in Figure 7.8; see also Sections 5.3 and 5.4. Using the theory of normal forms for planar fast–slow systems developed in Section 4.2, we may restrict attention to the (extended) system

$$\begin{aligned} x' &= -y + x^2 + h(x, y, \varepsilon), \\ y' &= \varepsilon g(x, y, \varepsilon), \\ \varepsilon' &= 0, \end{aligned} \quad (7.33)$$

where the terms in g and h can be written as

$$\begin{aligned} h(x, y, \varepsilon) &= axy + bx^3 + \mathcal{O}(y^2, \varepsilon x, \varepsilon y), \\ g(x, y, \varepsilon) &= -1 + cx + \mathcal{O}(x^2, y, \varepsilon). \end{aligned}$$

Denote the vector field defined via (7.33) by X . The reason for keeping only certain terms with explicit coefficients is that only those terms are going to matter in the analysis of the dynamics. The main goal is to describe the attracting slow manifold S_ε^a and how it passes near the fold point. Here S_ε^a consists of exponentially close trajectories, and we select a single such trajectory; see also Section 3.1. Define two sections for $\rho > 0$ small:

$$\Delta^{\text{in}} := \{(x, \rho^2) \in U : x \in J_{\text{in}}\} \quad \text{and} \quad \Delta^{\text{out}} := \{(\rho, y) \in U : y \in J_{\text{out}}\},$$

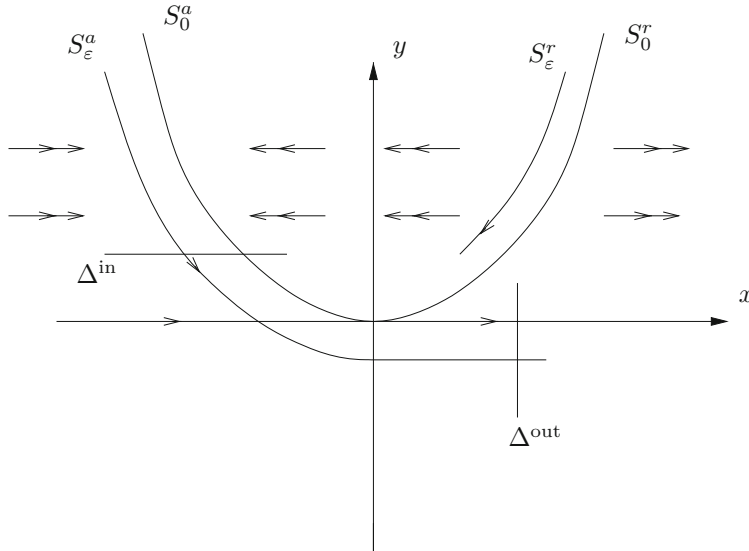


Figure 7.8: Sketch of the situation near a generic fold point of a planar fast–slow system (7.33).

where J_{in} and J_{out} are intervals chosen such that a mapping $\Pi : \Delta^{\text{in}} \rightarrow \Delta^{\text{out}}$ is well defined as the transition map for the flow of all trajectories close to S_ε^a near the fold point. The goal of this section is to sketch the main ideas for a geometric proof of the next theorem.

Theorem 7.4.1 ([KS01b, DR96b]). *There exists $\varepsilon_0 > 0$ such that for all $\varepsilon \in (0, \varepsilon_0]$, the following hold:*

(R1) *The manifold S_ε^a passes through Δ^{out} at $(\rho, H(\varepsilon))$ with $H(\varepsilon) = \mathcal{O}(\varepsilon^{2/3})$.*

(R2) *Δ^{in} is mapped by Π to an interval of size $\mathcal{O}(e^{-C/\varepsilon})$ for some $C > 0$.*

(R3) *The function $H(\varepsilon)$ has asymptotic expansion*

$$H(\varepsilon) = c_1 \varepsilon^{2/3} + c_2 \ln \varepsilon + c_3 \varepsilon + \mathcal{O}(\varepsilon^{4/3} \ln \varepsilon) \quad \text{as } \varepsilon \rightarrow 0.$$

Remark: Basically, Theorem 7.4.1 is another version of Theorems 5.4.2 and 5.4.5.

The fact that $H(\varepsilon) = \mathcal{O}(\varepsilon^{2/3})$ implies that the approximation given by the critical manifold and the vertical fast flow is of order $\mathcal{O}(\varepsilon^{2/3})$ in the y -coordinate. Note that the term $\mathcal{O}(e^{-C/\varepsilon})$ from (R2) is irrelevant for the explicit asymptotic expansion for $H(\varepsilon)$, since it is transcendentally small compared to the leading-order terms. Hence, the nonuniqueness of S_ε^a does not affect the main asymptotic result (R3).

The key point, noticed first by Dumortier and Roussarie [DR96b] in the context of van der Pol's equation, is that $(x, y, \varepsilon) = (0, 0, 0)$ is a nonhyperbolic

equilibrium point of (7.33), and hence the blowup method applies. Therefore, a proof [KS01b] may consist of the following steps:

- *Step 1:* Find a suitable blowup map to desingularize the fold point.
- *Step 2:* Find charts to express the blowup in local coordinates.
- *Step 3:* Calculate all the local data of the problem.
- *Step 4:* Investigate the dynamics of the blown-up vector fields.
- *Step 5:* Connect the results from different charts and “blow down.”

Step 1: The important spaces are two manifolds $B := S^2 \times \mathbb{R}$ and $B_0 := S^2 \times [0, r_0]$ for some $r_0 > 0$. The blowup is a map

$$\varphi : B_0 \rightarrow \mathbb{R}^3,$$

which induces a vector field \bar{X} by $\varphi_*(\bar{X}) = X$. Denote coordinates induced on S^2 by the ambient space by $(\bar{x}, \bar{y}, \bar{\varepsilon})$ and the coordinate on $[0, r_0]$ by \bar{r} . The general structure of a weighted (or quasihomogeneous) blowup is

$$\varphi(\bar{x}, \bar{y}, \bar{\varepsilon}, \bar{r}) = (\bar{r}^{a_1} \bar{x}, \bar{r}^{a_2} \bar{y}, \bar{r}^{a_3} \bar{\varepsilon}). \quad (7.34)$$

It turns out that one blowup that works to desingularize the fold point is

$$\varphi(\bar{x}, \bar{y}, \bar{\varepsilon}, \bar{r}) := (\bar{r}\bar{x}, \bar{r}^2\bar{y}, \bar{r}^3\bar{\varepsilon}) = (x, y, \varepsilon). \quad (7.35)$$

But how would we find the coefficients $(a_1, a_2, a_3) = (1, 2, 3)$? Let us use a heuristic approach that turns out to be very useful in practice. The fast–slow system has two singular limits, namely the slow (or reduced) subsystem and the fast flow (or layer problem). The smallest-order nontrivial approximations to this system are

$$\frac{dy}{d\tau} = -\varepsilon \quad \text{and} \quad \frac{dx}{dt} = x^2 - y,$$

where $\tau = \varepsilon t$. Hence, we might guess that the truncated normal form (or system of first approximation; see Section 4.4) given by

$$\begin{aligned} x' &= x^2 - y, \\ y' &= -\varepsilon, \\ \varepsilon' &= 0, \end{aligned} \quad (7.36)$$

suffices to determine the blowup coefficients. Denote by $F = F(x, y, \varepsilon) : \mathbb{R}^3 \rightarrow \mathbb{R}^3$ the vector field given by (7.36). We can now check whether F is quasihomogeneous of type (a_1, a_2, a_3) and degree $k + 1$; see Definition 7.3.2. Overloading the meaning of the a_i already hints at the fact that they will turn out to be correct coefficients for the weighted (or quasihomogeneous) blowup. Indeed, a direct calculation applying the definition of quasihomogeneity yields

$$\begin{aligned} r^{2a_1}x^2 - r^{a_2}y &\stackrel{!}{=} r^{a_1+k}(x^2 - y), \\ -r^{a_3}\varepsilon &\stackrel{!}{=} -r^{a_2+k}\varepsilon. \end{aligned}$$

This translates into solving the following algebraic equations:

$$2a_1 = a_2 = a_1 + k \quad \text{and} \quad a_3 = a_2 + k.$$

Since the third equation $\varepsilon' = 0$ in (7.36) does not contribute any algebraic relation, we have some choices. Setting $a_1 = 1$ implies that $a_2 = 2$ and $k = 1$. This leads to $a_3 = 3$, and therefore it is a reasonable attempt to consider the blowup (7.35), which induces a blown-up vector field on B respectively on B_0 .

Step 2: To find charts to express the blowup in local coordinates, a good notation is essential. Following the conventions introduced in [KS01d], let $B_{\bar{y}}^+ := B \cap \{\bar{y} > 0\}$ be a submanifold of B ; similarly, introduce $B_{\bar{\varepsilon}}^+$ and $B_{\bar{x}}^+$. Covering only parts of B will be sufficient, since not the whole blown-up vector field on B is relevant for the subsequent analysis. Define three charts for $B = S^2 \times \mathbb{R}$:

$$K_1 : B_{\bar{y}}^+ \rightarrow \mathbb{R}^3 \quad \text{given by} \quad x_1 = \bar{x}\bar{y}^{-1/2}, \quad \varepsilon_1 = \bar{\varepsilon}\bar{y}^{-3/2}, \quad r_1 = \bar{r}\bar{y}^{1/2}.$$

$$K_2 : B_{\bar{\varepsilon}}^+ \rightarrow \mathbb{R}^3 \quad \text{given by} \quad x_2 = \bar{x}\bar{\varepsilon}^{-1/3}, \quad y_2 = \bar{y}\bar{\varepsilon}^{-2/3}, \quad r_2 = \bar{r}\bar{\varepsilon}^{1/3}.$$

$$K_3 : B_{\bar{x}}^+ \rightarrow \mathbb{R}^3 \quad \text{given by} \quad y_3 = \bar{y}\bar{x}^{-2}, \quad \varepsilon_3 = \bar{\varepsilon}\bar{x}^{-3}, \quad r_3 = \bar{r}\bar{x}.$$

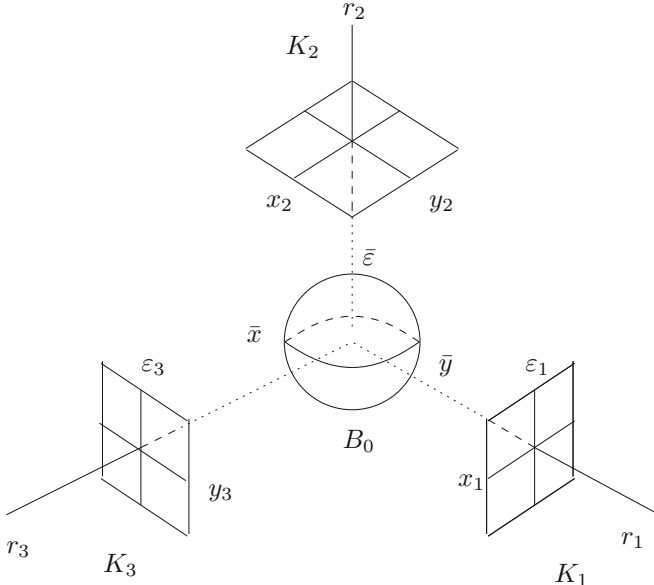


Figure 7.9: Sketch of the coordinate charts for submanifolds of B .

The situation is illustrated in Figure 7.9. The reasoning regarding the choice of charts follows the pattern illustrated in Example 7.3.6. We show only how to obtain the chart K_1 for $B_{\bar{y}}^+$ such that in its coordinates $(x_1, \varepsilon_1, r_1)$, the blowup is given by

$$x = r_1 x_1, \quad y = r_1^2, \quad \varepsilon = r_1^3 \varepsilon_1. \quad (7.37)$$

As in Section 7.3, we attempt a weighted change to affine coordinates

$$x_1 = \bar{x}\bar{y}^{-b_1}, \quad \varepsilon_1 = \bar{\varepsilon}\bar{y}^{-b_2}, \quad r_1 = \bar{r}\bar{y}^{-b_3}. \quad (7.38)$$

Using the blowup transformation φ described in (7.35), we can write it in the chart (7.38) as

$$\begin{aligned} x &= \bar{r}\bar{x} = r_1\bar{y}^{b_3}x_1\bar{y}^{b_1}, \\ y &= \bar{r}^2\bar{y} = r_1^2\bar{y}^{2b_3}\bar{y}, \\ \varepsilon &= \bar{r}^3\bar{\varepsilon} = r_1^3\bar{y}^{3b_3}\varepsilon_1\bar{y}^{b_2}. \end{aligned}$$

To match (7.37), one must solve the resulting system of linear equations

$$\begin{aligned} b_1 + b_3 &= 0, \\ 2b_3 &= -1, \\ b_2 + 3b_3 &= 0. \end{aligned}$$

The result is easily found to be $(b_1, b_2, b_3) = (1/2, 3/2, -1/2)$, and this defines the chart K_1 , as claimed above.

Exercise 7.4.2. Carry out the calculations for K_2 and K_3 . \diamond

Step 3: The three key components to calculate for K_i (for $i = 1, 2, 3$) are the blowup maps, the transition functions between K_i , and the blown-up vector fields. The best way to get used to the relevant calculations is to do some of them as exercises. Hence, we introduce only types of calculations not discussed previously.

Lemma 7.4.3. *The (directional) blowups induced from the charts K_i and the weighted polar blowup φ are*

$$\begin{aligned} \text{for } K_1: \quad x &= r_1 x_1, & y &= r_1^2, & \varepsilon &= r_1^3 \varepsilon_1, \\ \text{for } K_2: \quad x &= r_2 x_2, & y &= r_2^2 y_2, & \varepsilon &= r_2^3, \\ \text{for } K_3: \quad x &= r_3, & y &= r_3^2 y_3, & \varepsilon &= r_3^3 \varepsilon_3. \end{aligned}$$

The three charts can be viewed, on a purely formal level, to correspond to conditions of the form $\bar{y} = 1$, $\bar{\varepsilon} = 1$, and $\bar{x} = 1$ respectively. Geometrically, this means that we want to cover the sphere with charts with rectangular coordinate systems placed in certain directions. In Figure 7.9, we may think of moving the rectangular coordinate systems along the dashed lines toward the sphere and wrapping them onto the sphere.

In fact, this viewpoint can also be used as a, again purely formal but practical, shortcut to obtaining the directional blowup maps in Lemma 7.4.3. For example, setting $\bar{y} = 1$ in (7.34) and relabeling the bar variables with a subscript 1 precisely yields K_1 in Lemma 7.4.3. We refer to Example 7.3.6 for further information on how this process actually leads to a good definition of charts when we know only the main weighted blowup map.

Exercise 7.4.4. Prove Lemma 7.4.3 using the methods of Section 7.3. \diamond

Lemma 7.4.5. Let κ_{ij} denote the transition maps from K_i to K_j . Then

$$\begin{aligned}\kappa_{12} : \quad & x_2 = x_1 \varepsilon_1^{-1/3}, \quad y_2 = \varepsilon_1^{-2/3}, \quad r_2 = r_1 \varepsilon_1^{1/3}, \quad \text{for } \varepsilon_1 > 0, \\ \kappa_{12}^{-1} : \quad & x_1 = x_2 y_2^{-1/2}, \quad \varepsilon_1 = y_2^{-3/2}, \quad r_1 = r_2 y_2^{1/2}, \quad \text{for } y_2 > 0, \\ \kappa_{23} : \quad & y_3 = y_2 x_2^{-2}, \quad \varepsilon_3 = x_2^{-3}, \quad r_3 = r_2 x_2, \quad \text{for } x_2 > 0, \\ \kappa_{23}^{-1} : \quad & x_2 = \varepsilon_3^{-1/3}, \quad y_2 = y_3 \varepsilon_3^{-2/3}, \quad r_2 = r_3 \varepsilon_3^{1/3}, \quad \text{for } \varepsilon_3 > 0.\end{aligned}$$

Proof. (Sketch) In the case of κ_{12} , we get from the definitions of the maps,

$$x_2 = \bar{x} \varepsilon^{-1/3} = x_1 \bar{y}^{1/2} \varepsilon_1^{-1/3} \bar{y}^{-1/2} = x_1 \varepsilon_1^{-1/3}.$$

Similar calculations can be applied to the coordinates y_2 and r_2 and to the other three charts. \square

Exercise 7.4.6. Fill in more details in the proof of Lemma 7.4.5. \diamond

The last, and most important, part is to calculate the blown-up vector fields.

Lemma 7.4.7. In the chart K_1 , the blown-up vector field is

$$\begin{aligned}x'_1 &= r_1 \left(-1 + x_1^2 + \frac{1}{2} \varepsilon_1 x_1 + r_1 (ax_1 + bx_1^3 - \frac{c}{2} \varepsilon_1 x_1^2) + \mathcal{O}(r_1^2) \right), \\ r'_1 &= \frac{1}{2} r_1^2 \varepsilon_1 \left(-1 + cr_1 x_1 + \mathcal{O}(r_1^2) \right), \\ \varepsilon'_1 &= \frac{3}{2} r_1 \varepsilon_1^2 \left(1 - cr_1 x_1 + \mathcal{O}(r_1^2) \right).\end{aligned}$$

In the chart K_2 , the blown-up vector field is

$$\begin{aligned}x'_2 &= r_2 (x_2^2 - y_2 + \mathcal{O}(r_2)), \\ y'_2 &= r_2 (-1 + \mathcal{O}(r_2)), \\ r'_2 &= 0.\end{aligned}$$

In the chart K_3 , the blown-up vector field is

$$\begin{aligned}r'_3 &= r_3^2 (1 - y_3 + br_3 + ar_3 y_3 + \mathcal{O}(r_3^3)), \\ y'_3 &= r_3 (-\varepsilon_3 - 2y_3 + cr_3 \varepsilon_3 + 2y_3^2 - 2by_3 r_3 + 2ar_3 y_3^2 + \mathcal{O}(r_3^2(y_3 + \varepsilon_3))), \\ \varepsilon'_3 &= -3\varepsilon_3 r_3 (1 - y_3 + br_3 + ar_3 y_3 + \mathcal{O}(r_3^2)).\end{aligned}$$

Proof. (Sketch) We show the calculation only for K_2 and omit the algebraic manipulations for the other two charts. Recall that our fast-slow system is

$$\begin{aligned}x' &= -y + x^2 + axy + bx^3 + \mathcal{O}(y^2, \varepsilon x, \varepsilon y), \\ y' &= \varepsilon(-1 + cx + \mathcal{O}(x^2, y, \varepsilon)), \\ \varepsilon' &= 0.\end{aligned}\tag{7.39}$$

The blowup in K_2 is (see Lemma 7.4.3)

$$x = r_2 x_2, \quad y = r_2^2 y_2, \quad \varepsilon = r_2^3.$$

Since $r_2 = \varepsilon^{1/3}$ is a constant, the map is just a rescaling of x and y . Therefore, the blowup vector field can be calculated as

$$\begin{aligned}x' &= r_2 x'_2 = r_2^2 x_2^2 - r_2^2 y_2 + h(r_2 x_2, r_2^2 y_2, r_2^3) = r_2^2 (x_2^2 - y_2 + \mathcal{O}(r_2)), \\ y' &= r_2^2 y'_2 = r_2^3 g(r_2 x_2, r_2^2 y_2, r_2^3) = -r_2^3 + \mathcal{O}(r_2^4), \\ r'_2 &= 0.\end{aligned}$$

and the result follows. \square

Exercise 7.4.8. Verify Lemma 7.4.7 in the case of the chart K_1 . Hint: Differentiate $\varepsilon = r_1^3 \varepsilon_1$ to get the equation for ε_1 . \diamond

In each case, we have blown up the fold point $(0, 0, 0)$ to the plane $\{r_i = 0\}$ in K_i . Looking at the vector fields of Lemma 7.4.7, we see that each such plane consists of equilibrium points. Dividing by r_i desingularizes the vector fields as in Sections 7.1–7.3; see also Section 7.7. For example, in K_2 , one obtains

$$\begin{aligned} x'_2 &= x_2^2 - y_2 + \mathcal{O}(r_2), \\ y'_2 &= -1 + \mathcal{O}(r_2), \\ r'_2 &= 0, \end{aligned} \tag{7.40}$$

which is precisely the system of first approximation for a fold as derived in Section 4.4.

Step 4: Investigating the dynamics of the blown-up vector fields is often the most difficult aspect. The reason is that although additional hyperbolicity has been gained at equilibria, one still has to understand the flow of the blown-up space. Often, this requires a combination of tools from dynamical systems theory. As before, we shall describe the analysis of only one blown-up vector field here. We have already discussed the Riccati equation arising for (7.40) in chart K_2 in Section 5.4. Therefore, we consider the analysis in the chart K_1 here. Recall that the desingularized flow in the chart K_1 is given by

$$\begin{aligned} x'_1 &= -1 + x_1^2 + \frac{1}{2}\varepsilon_1 x_1 + r_1 (ax_1 + bx_1^3 - \frac{c}{2}\varepsilon_1 x_1^2) + \mathcal{O}(r_1^2), \\ r'_1 &= \frac{1}{2}r_1\varepsilon_1 (-1 + cr_1x_1 + \mathcal{O}(r_1^2)), \\ \varepsilon'_1 &= \frac{3}{2}\varepsilon_1^2 (1 - cr_1x_1 + \mathcal{O}(r_1^2)). \end{aligned} \tag{7.41}$$

The dynamics in the chart K_1 describe the approach and departure slightly away from the generic fold point involving the slow manifolds S_ε^j for $j = a, r$; see Figure 7.8.

For the analysis of the flow defined by (7.41), all relevant objects are shown in Figure 7.10. It is helpful to refer to Figure 7.10 whenever a new definition or notation is introduced.

Observe that (7.41) has the invariant subspaces $\{r_1 = 0\}$ and $\{\varepsilon_1 = 0\}$. They intersect in the line $l_1 = \{(x_1, 0, 0) : x_1 \in \mathbb{R}\}$, which corresponds to the generic fold point. Looking at (7.41), we see that the dynamics on l_1 are described by $x'_1 = -1 + x_1^2$. They have two equilibrium points,

$$p_a := (-1, 0, 0) \quad \text{and} \quad p_r := (1, 0, 0).$$

Obviously, both points are hyperbolic for the one-dimensional flow on l_1 . The eigenvalue for p_a is -2 , so that it is attracting, while the eigenvalue for p_r is 2 , and hence it is repelling. Let us restrict attention to the dynamics in a rectangular box

$$\mathcal{D}_{1,-} := \{(x_1, r_1, \varepsilon_1) : x_1 < 0, 0 \leq r_1 \leq \rho, 0 \leq \varepsilon_1 \leq \delta\},$$

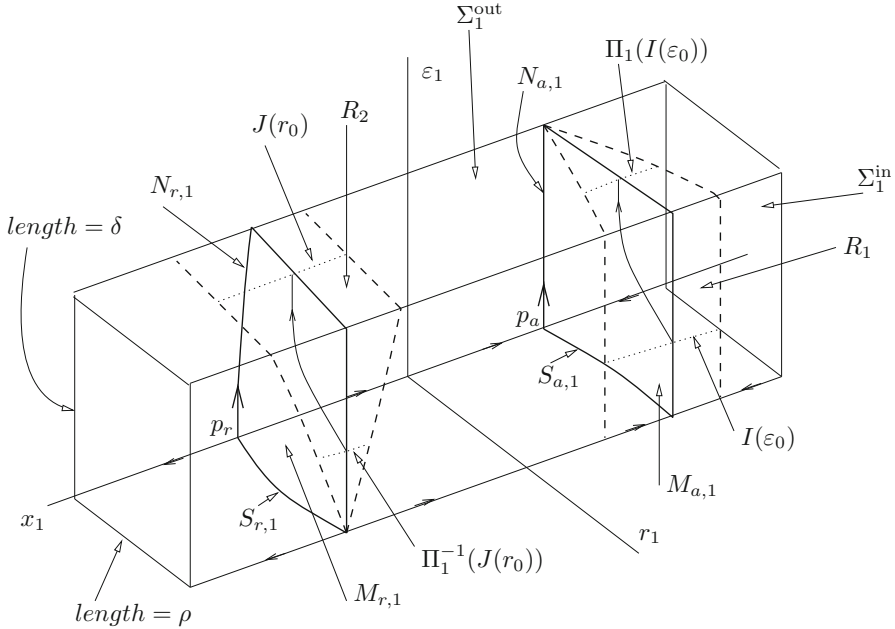


Figure 7.10: Sketch of the objects involved in the analysis of the vector field (7.41) in the chart K_1 .

where the constants δ and ρ are chosen suitably small that all local theorems we want to apply hold, i.e., the focus is on the dynamics in the vicinity of the equilibrium point p_a . The dynamics in the invariant plane $\{\varepsilon_1 = 0\}$ are given by

$$\begin{aligned} x'_1 &= -1 + x_1^2 + r_1 (ax_1 + bx_1^3) + \mathcal{O}(r_1^2), \\ r'_1 &= 0. \end{aligned} \quad (7.42)$$

Upon choosing $\rho > 0$ sufficiently small, the implicit function theorem yields that the system (7.42) has a curve of equilibria emanating from p_a ; call this curve $S_{a,1}$.

Exercise 7.4.9. Show that $S_{a,1}$ corresponds to the branch S_ε^a of the slow manifold using the coordinate chart map K_1 . \diamond

Note that the curve $S_{a,1}$ always has one hyperbolic attracting direction. In the system (7.42), the point p_a is again an equilibrium, but it has a zero eigenvalue in the direction tangent to the curve $S_{a,1}$. The equations in the invariant plane $r_1 = 0$ are

$$\begin{aligned} x'_1 &= -1 + x_1^2 + \frac{1}{2}\varepsilon_1 x_1, \\ \varepsilon'_1 &= \frac{3}{2}\varepsilon_1^2. \end{aligned}$$

Again p_a is an equilibrium. It has the expected hyperbolic direction in l_1 , but in the invariant plane $\{r_1 = 0\}$, it has another zero eigenvalue from the equation

$\varepsilon'_1 = \frac{3}{2}\varepsilon_1^2$ and a corresponding eigenvector $(-1, 4)$. Hence, there exists a unique one-dimensional center manifold $N_{a,1}$ at p_a tangent to the eigenspace spanned by $(-1, 4)$ at p_a ; see Figure 7.10. In summary, we have the following result.

Lemma 7.4.10. *The analysis of the blown-up vector field (7.41) yields, on choosing δ and ρ sufficiently small, that*

- $p_a = (-1, 0, 0)$ is an equilibrium point with eigenvalues $\lambda_1 = -2, \lambda_2 = 0 = \lambda_3$. It has corresponding eigenvectors $(1, 0, 0), (-1, 0, 4)$, and the tangent vector to $S_{a,1}$ at p_a .
- There exists a two-dimensional center-stable manifold $M_{a,1}$ at p_a that contains $N_{a,1}$ and $S_{a,1}$.
- There exists a stable invariant foliation \mathcal{F}^s with base $M_{a,1}$ and one-dimensional fibers. For every $c > -2$, the contraction along \mathcal{F}^s is stronger than e^{ct_1} .

Proof. (Sketch) Standard center manifold theory (see [GH83] or [Car81]) and the previous observations suffice to prove the result. \square

Observe also that the center manifold $M_{a,1}$ corresponds to a neighborhood of the attracting branch of the slow manifold. The next step is to look at trajectories in and close to $M_{a,1}$. Define two sections

$$\begin{aligned}\Sigma_1^{\text{in}} &:= \{(x_1, r_1, \varepsilon_1) \in \mathcal{D}_{1,-} : r_1 = \rho\}, \\ \Sigma_1^{\text{out}} &:= \{(x_1, r_1, \varepsilon_1) \in \mathcal{D}_{1,-} : \varepsilon_1 = \delta\}.\end{aligned}$$

Let R_1 be the rectangle in Σ_1^{in} defined by $|1 + x_1| \leq \beta$ for sufficiently small $\beta > 0$. For $0 \leq \varepsilon\delta$, define the line $I(\varepsilon_0) := R_1 \cap \{\varepsilon = \varepsilon_0\}$. The equation

$$\varepsilon'_1 = \frac{3}{2}\varepsilon_1^2(1 - \mathcal{O}(r_1)) \tag{7.43}$$

can be used to determine the transition time for the map $\Pi_1 : \Sigma_1^{\text{in}} \rightarrow \Sigma_1^{\text{out}}$. Direct integration of (7.43) yields that a point $p = (x_1, \rho, \varepsilon_1) \in \Sigma_1^{\text{in}}$ maps to the point $\Sigma_1(p) \in \Sigma_1^{\text{out}}$ in the time

$$T = \frac{2}{3} \left(\frac{1}{\varepsilon_1} - \frac{1}{\delta} \right) (1 + \mathcal{O}(\rho)).$$

From the last calculation and Lemma 7.4.10, one can conclude the final result on the behavior of the transition map.

Proposition 7.4.11. *The transition map $\Pi_1 : \Sigma_1^{\text{in}} \rightarrow \Sigma_1^{\text{out}}$ for the vector field (7.41) takes R_1 to a wedge-shaped region $\Pi_1(R_1) \subset \Sigma_1^{\text{out}}$. In particular, for fixed $c < 2$, there exists a constant $K = K(c, \rho, \delta, \beta)$ such that for $\varepsilon_1 \in (0, \delta]$, the image $\Pi_1(I(\varepsilon_1))$ is an interval around $M_{a,1} \cap \Sigma_1^{\text{out}}$ with width bounded by*

$$K \exp \left(-\frac{2c}{3} \left(\frac{1}{\varepsilon_1} - \frac{1}{\delta} \right) \right).$$

Therefore, one part of the relevant asymptotics to describe the flow past a generic fold point has been computed. The other parts of the flow map are obtained by analyzing the ODEs in the charts K_2 and K_3 . In fact, the techniques required for chart K_3 are quite different from the computations for K_1 . In K_3 , the logarithmic correction terms that we encountered already in Theorem 5.4.5 arise, but we shall not consider the details here; see also Section 9.5. In K_2 , the Riccati equation described in Section 5.4 is the primary tool; see also [KS01d] for details.

Exercise/Project 7.4.12. Carry out the same analysis for the neighborhood of the equilibrium p_r . Use the notation introduced in Figure 7.10 and the results in Lemma 7.4.10 and Proposition 7.4.11 to guide you. \diamond

Step 5: To connect the results from different charts, a “blowdown” transformation is required. We shall only indicate the strategy of the final proof. The goal is to analyze the full flow map $\Pi : \Delta^{\text{in}} \rightarrow \Delta^{\text{out}}$; see Figure 7.8. Splitting the problem into three maps $\Pi_i : K_i \rightarrow K_i$ in the charts K_i (for $i = 1, 2, 3$), we see that there exists a blown-up version $\tilde{\Pi} : K_1 \rightarrow K_3$ of Π given by

$$\Pi := \Pi_3 \circ \kappa_{23} \circ \Pi_2 \circ \kappa_{12} \circ \Pi_1.$$

Once results about each map Π_i have been computed, as demonstrated for Π_1 in Proposition 7.4.11, one has the behavior of Π . Formally, a **blowdown transformation** of Π given by

$$\tilde{\Pi} = \varphi \circ \Pi \circ \varphi^{-1},$$

from which the result in Theorem 7.4.1 can then be concluded. Note carefully that the entire procedure requires careful bookkeeping as well as a detailed understanding of the individual, usually quite nontrivial, parts of the flow in each chart.

Many blowup method calculations follow the five steps outlined here for the generic fold point. However, each individual step often requires creative solutions. After all, we are dealing with nonlinear dynamical systems, and there is no “complete method” applicable to every nonlinear differential equation. One should rather view the blowup method as a technique that helps to make additional tools for (partially) hyperbolic invariant sets available.

7.5 Relaxation Oscillations in \mathbb{R}^2

Recall from Section 5.2 that certain $(1, 1)$ -fast–slow systems with an S-shaped critical manifold can exhibit relaxation oscillations. Relaxation oscillations can occur in higher-dimensional systems as well (see Section 7.6), but we shall restrict attention here to the planar case. As the starting point, consider a $(1, 1)$ -fast–slow system (7.31) under the following assumptions:

- (A1) The critical manifold C_0 is S-shaped, i.e., it can be written in the form $y = h(x)$ for a function $h : \mathbb{R} \rightarrow \mathbb{R}$ with precisely two critical points, one nondegenerate maximum and one nondegenerate minimum. One can shift the minimum by a change of coordinates to the origin. Assume that the maximum occurs at $x = x_m$. The critical manifold has three normally hyperbolic pieces:

$$C_0^{a-} = \{x < 0\} \cap C_0, \quad C_0^r = \{0 < x < x_m\} \cap C_0, \quad C_0^{a+} = \{x_m < x\} \cap C_0.$$

- (A2) The branches $C_0^{a\pm}$ are attracting, while C_0^r is repelling.
- (A3) Both fold points $(0, h(0))$ and $(x_m, h(x_m))$ of C_0 are generic. Recall that this means for $\varepsilon = 0$ that C_0 is locally quadratic near the fold with nonzero slow flow at the fold point p ,
- $$f(p, 0) = 0, \quad f_x(p, 0) = 0, \quad f_{xx}(p, 0) \neq 0, \quad f_y(p, 0) \neq 0, \quad g(p, 0) \neq 0.$$
- (A4) The slow flow on C_0^{a-} points to the right ($\dot{x} > 0$), and it points to the left on C_0^{a+} ($\dot{x} < 0$).

The situation is shown in Figure 7.11, where also some additional notation is introduced. Recall from Definition 5.5.2 that a generic fold point $p \in C_0$ is called a **jump point** if the fast flow is directed away from p . By (A4), a candidate orbit of the slow flow can reach this jump point. Hence, one can define a candidate trajectory γ_0 consisting of the fast connections from $(0, 0)$ to $(x_r, 0)$ and (x_m, y_m) to (x_l, y_m) and slow segments on C_0^{a-} and C_0^{a+} connecting (x_l, y_m) to $(0, 0)$ and $(x_r, 0)$ to (x_m, y_m) respectively. Recall from Definition 5.2.3 that a continuous family of periodic orbits γ_ε is a **relaxation oscillation** if γ_ε converges to the singular orbit γ_0 as $\varepsilon \rightarrow 0$.

Theorem 7.5.1 ([KS01e]; see also [Car52, MR80]). *Assume (A1)–(A4) and let U be a (small) tubular neighborhood of γ_0 . Then for each fixed $\varepsilon > 0$ sufficiently small, there exists a unique limit cycle $\gamma_\varepsilon \subset U$. The cycle is strongly attracting with Floquet exponent bounded above by $-K/\varepsilon$ for some constant $K > 0$. Furthermore, γ_ε converges to γ_0 in the Hausdorff distance as $\varepsilon \rightarrow 0$.*

Remark: Here it just suffices to think of a **tubular neighborhood** of a manifold M as a “tube” around M . More precisely, it is a neighborhood in the ambient space of M that is diffeomorphic to a suitable open subset of the normal bundle [Lee06]. It can be shown that an embedded submanifold M in \mathbb{R}^N always has a tubular neighborhood.

Proof. By Fenichel’s theorem (suitable compact submanifolds of), $C_0^{a\pm}$ perturb to nearby slow manifolds $C_\varepsilon^{a\pm}$. By Theorem 7.4.1 on the analysis of a generic fold, the slow manifolds can be continued past the fold points, and they then follow approximately a layer of the fast subsystem until they arrive at another slow manifold. Consider a horizontal section Δ as shown in Figure 7.11 and assume that $\varepsilon > 0$ is sufficiently small. We want to follow two trajectories $\gamma_\varepsilon^{1,2}$ starting on Δ . By Fenichel’s theorem,

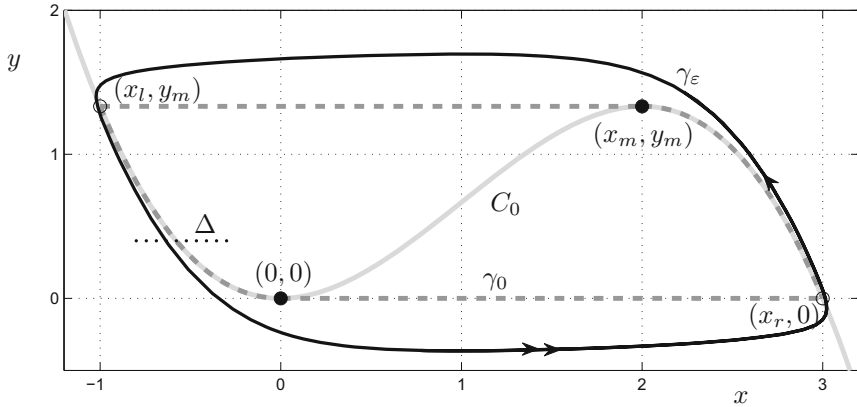


Figure 7.11: S-shaped critical manifold C_0 (light gray) for a system with relaxation oscillations. The figure was generated using the model system $x' = -y + x^2 - \frac{1}{3}x^3$, $y' = \varepsilon(x - 1)$ with $\varepsilon = 0.1$ for the numerical integration of the relaxation oscillation periodic orbit γ_ε (black curve). The two fold points (black dots) are also jump points with two associated drop points (circles). The candidate orbit (dashed gray) switches between fast and slow motion at these four special points.

$\gamma_\varepsilon^{1,2}$ are attracted (exponentially with rate $\mathcal{O}(e^{-1/\varepsilon})$) to C_ε^{a-} . By Theorem 7.4.1, $\gamma_\varepsilon^{1,2}$ pass by the fold $(0, 0)$ contracting exponentially toward each other until they reach a neighborhood of C_ε^{a+} . Again using Fenichel's theorem and Theorem 7.4.1, we may conclude that $\gamma_\varepsilon^{1,2}$ are attracted toward C_ε^{a+} , pass by the fold (x_m, y_m) , and return near C_ε^{a-} to Δ .

Therefore, the return map $\Pi : \Delta \rightarrow \Delta$ is a contraction (with exponential rate $\mathcal{O}(e^{-1/\varepsilon})$), and the contraction mapping theorem implies that Π has a unique fixed point. This fixed point is a point on the desired limit cycle γ_ε . Due to the exponential contraction near the limit cycle, it follows that its Floquet multiplier is bounded above by $-K/\varepsilon$ for some constant $K > 0$. Again using Theorem 7.4.1 and Fenichel's theorem, one may conclude that in the singular limit $\varepsilon \rightarrow 0$, the periodic orbits converge to the singular orbit, i.e., $\gamma_\varepsilon \rightarrow \gamma_0$ in the Hausdorff distance. \square

Although the proof of Theorem 7.5.1 is quite straightforward, it illustrates an important point regarding how a local result from the blowup method can be used. In fact, there are several proofs for the existence of special orbits passing near nonnormally hyperbolic parts of a critical manifold that proceed by a similar strategy; see Section 7.8.

Exercise 7.5.2. Consider the 2D FitzHugh–Nagumo equation (1.13) and check for which range of parameters Theorem 7.5.1 can be applied. \diamond

7.6 Relaxation Oscillations in \mathbb{R}^3

It has been proven in Section 7.5 that relaxation oscillations can occur under certain assumptions in $(1, 1)$ -fast–slow systems. In this section, this result is generalized to the case of two slow and one fast variable. It helps to begin with an example.

Example 7.6.1. Consider the periodically forced van der Pol equation

$$\begin{aligned}\varepsilon \frac{dx}{d\tau} &= \varepsilon \dot{x} = y - \frac{x^3}{3} + x, \\ \frac{dy}{d\tau} &= \dot{y} = a \sin(2\pi\theta) - x, \\ \frac{d\theta}{d\tau} &= \dot{\theta} = \omega,\end{aligned}\tag{7.44}$$

where $(x, y) \in \mathbb{R}^2$, $\theta \in S^1 = [0, 1]/(0 \sim 1)$ (i.e., view the circle as the interval $[0, 1]$ with 0 and 1 identified), a, ω are parameters, and $0 < \varepsilon \ll 1$. The critical manifold $C_0 = \{(x, y, \theta) \in \mathbb{R}^2 \times S^1 : y = \frac{x^3}{3} - x\}$ is again S-shaped; see Figure 7.12. The numerically computed trajectory in Figure 7.12 clearly looks like a relaxation oscillation. The natural question now is to prove a result that states that this relaxation oscillation can be obtained from singular orbits consisting of concatenations of trajectories for the fast and slow subsystems similar to the situation in \mathbb{R}^2 . ♦

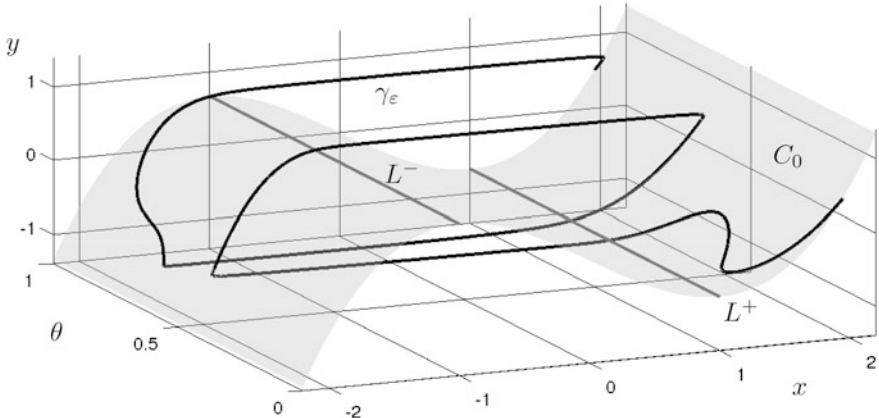


Figure 7.12: Relaxation oscillation for (7.44) with $\varepsilon = 0.01$, $a = 1.8$, and $\omega = 0.1$. The critical manifold C_0 is shown in light gray, and the two fold lines L^\pm are shown in dark gray. The relaxation cycle γ_ε (black) consists of four fast and four slow segments. Note that the phase space is $\mathbb{R}^2 \times S^1$, and the θ -coordinate has to be identified via $0 \sim 1$. Sometimes, one also refers to the global return mechanism as induced via an “S-shaped” critical manifold, which is illustrated in Figure 7.13.

We begin with a general $(1, 2)$ -fast–slow system:

$$\begin{aligned}\varepsilon \dot{x} &= f(x, y_1, y_2, \varepsilon), \\ \dot{y}_1 &= g_1(x, y_1, y_2, \varepsilon), \\ \dot{y}_2 &= g_2(x, y_1, y_2, \varepsilon).\end{aligned}\tag{7.45}$$

Recall from Section 4.3 that the critical manifold $C_0 = \{(x, y) \in \mathbb{R}^3 : f(x, y, 0) = 0\}$ of (8.44) is generically a surface, and points P that are not normally hyperbolic ($f_x(P, 0) = 0$) are usually not isolated but form one-dimensional curves L inside C_0 . Suppose that all the points P are nondegenerate fold points

$$f(P, 0) = 0, \quad f_x(P, 0) = 0, \quad f_{xx}(P, 0) \neq 0, \quad f_{y_1}(P, 0) \neq 0.\tag{7.46}$$

The fold curve L can be parameterized by y_2 under the previous assumptions,

$$L = \{(\theta(y_2), \psi(y_2), y_2) : y_2 \in I\},$$

where $I \subset \mathbb{R}$ is a suitable interval. In addition, introduce the function

$$l(y_2) := \left(\begin{array}{c} f_{y_1} \\ f_{y_2} \end{array} \right) \cdot \left(\begin{array}{c} g_1 \\ g_2 \end{array} \right) \Big|_{(\theta(y_2), \psi(y_2), y_2)}.$$

The key additional regularity assumption for a fold point P of a $(1, 2)$ -fast–slow system is that

$$l(\text{ } y_2\text{-component of } P) \neq 0.\tag{7.47}$$

Recall from Section 4.3 that (7.47) is called the **normal switching condition**. Geometrically, the condition means that the desingularized slow flow is not tangent to the fold curve at P .

Remark: In Sections 8.5, 8.6, 14.4, 14.5, 13.2, and 13.5, the failure of (7.47) is discussed in considerable detail.

Nondegenerate fold points satisfying (7.47) are also called **jump points** in the context of relaxation oscillations. As for the two-dimensional case, we list the assumptions for obtaining relaxation oscillations from a candidate orbit with alternating fast–slow segments:

(A1) The critical manifold C_0 is S-shaped, i.e., it can be decomposed as

$$C_0 = C_0^{a-} \cup L^- \cup C_0^r \cup L^+ \cup C_0^{a+}.$$

(A2) The branches $C_0^{a\pm}$ are normally hyperbolic attracting, and C_r is normally hyperbolic repelling.

(A3) All fold points on $L^+ \cup L^-$ are nondegenerate and satisfy the normal switching condition. The slow flow is directed toward and the fast slow away from the fold points.

(A4) Denote by $P(L^\pm) \subset C_0^{a\mp}$ the projections of L^\pm along the fast directions to the opposite attracting branch. Assume that the slow flow is transverse to $P(L^\pm)$.

(A5) There exists a singular hyperbolic periodic orbit γ_0 .

It is important to note that (A1)–(A4) can be weakened to suitable local statements, e.g., if all the fold points in the neighborhood of γ_0 satisfy (A3)–(A4), then the discussions to follow remain unchanged. Hyperbolicity of γ_0 is computed from a return map obtained from the singular limit to be described below in more detail.

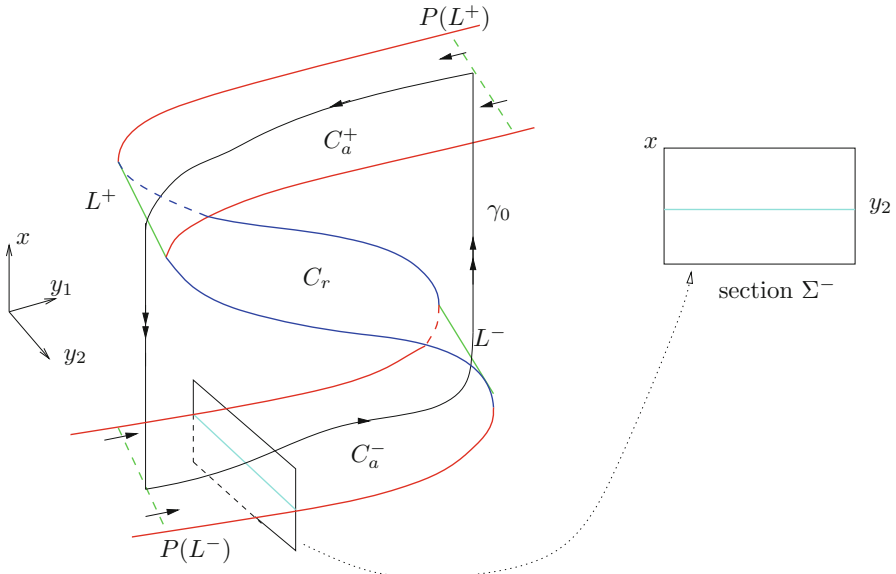


Figure 7.13: Sketch of the classical situation for relaxation oscillations in \mathbb{R}^3 . The viewpoint explains the terminology “S-shaped return mechanism.”

Assuming (A1)–(A5), one expects the singular periodic orbit γ_0 to persist. The fast flow along the x -coordinates ensures that the fast segments are arbitrarily close to γ_0 in this component. Near $C_0^{a\pm}$, the slow flow is close to the flow on the slow manifolds $C_\varepsilon^{a\pm}$ by Fenichel’s theorem. The transversality assumption (A4) ensures that the fast-to-slow transitions perturb for $\varepsilon > 0$.

The problem occurs near the two fold lines L^\pm . The assumptions on the fold points should guarantee that a regular jump to a different sheet occurs. As discussed previously for the planar situation, there are two well-known approaches to this problem. One employs asymptotic methods to derive the perturbation result from the asymptotic expansions, and the other uses a blowup technique on the fold curves L^\pm . Here, we only state the result of these calculations.

Introduce the section Σ^- , which is transverse to C_0^{a-} ; see Figure 7.13. Then straighten out the intersection between Σ^- and the manifold C_0^{a-} along a coordinate axis. In fact, a coordinate transformation can be used such that $C_0^{a-} \cap \Sigma^-$ corresponds to the y_2 -axis; see Section 4.1 for various similar straightening transformations. Without loss of generality, Σ^- is defined by $y_1 = \text{const}$ near C_0^{a-} ,

as shown in the right panel in Figure 7.13. Let $G_0(y)$ denote the singular return map induced on $C_0^{a-} \cap \Sigma^-$ by concatenating segments of the slow flow and the fast flow. Then the next theorem states that G_0 is a very good approximation to the actual return map on $C_\varepsilon^{a-} \cap \Sigma^-$.

Theorem 7.6.2 ([MKKR94, SW04]). *Suppose (A1)–(A4) hold as stated above. Then there exists an open neighborhood V of the point $\Sigma \cap \gamma_0$ such that the Poincaré return map $\Pi : V \rightarrow \Sigma^-$ induced by (7.45) is well defined for ε sufficiently small. It is given by*

$$\Pi(y_2, x) = (G(y_2, x, \varepsilon), R(y_2, x, \varepsilon)),$$

where $|R|$ and its partial derivatives are bounded by $e^{-\alpha/\varepsilon}$ for some constant $\alpha > 0$, i.e., $R(y_2, x, \varepsilon)$ is exponentially small. Furthermore,

$$G(y_2, x, \varepsilon) = G_0(y) + \mathcal{O}(\varepsilon \ln \varepsilon),$$

so that the return map is well approximated by the singular return map.

The main statement of Theorem 7.6.2 is that the singular return map approximates, up to some ε -dependent error terms, the full return map. Indeed, note that additional ε -dependent terms are introduced in the x -coordinate of the map Π if the section is not aligned with $\{x = 0\}$.

We can now also clarify assumption (A5), i.e., a singular periodic orbit γ_0 is hyperbolic if $G'_0(y_2^*) \neq 0$, where y_2^* denotes the y_2 -coordinate of $\Sigma^- \cap \gamma_0$. From the description of the map Π , the next result follows immediately.

Theorem 7.6.3 ([MKKR94, SW04]). *Suppose (A1)–(A5) hold. Then a candidate trajectory γ_0 persists for $\varepsilon > 0$ sufficiently small as a relaxation oscillation of (7.45). It is stable if $G'(y_2^*) < 1$ and unstable if $G'(y_2^*) > 1$.*

In addition to proving the existence of the relaxation oscillation, it is also possible to derive asymptotic formulas. The results are similar to the two-dimensional case presented in Chapter 5. Let $h^-(y) = x$ define the critical manifold C_0^{a-} as a graph. Consider $(x_0, y_0) = (h^-(y_0), y_0) \in C_0^{a-}$ and let T_0 denote the period of the singular relaxation cycle γ_0 where the fast jumps are instantaneous. Denote by $(x(\varepsilon), y(\varepsilon)) = (x(\varepsilon), y_1(\varepsilon), y_2(\varepsilon)) \in \mathbb{R}^3$ the coordinate representation of the relaxation curve depending on ε . The period of the relaxation cycle will be denoted by $T(\varepsilon)$. Recall that we defined $\varpi(k) = s$ for $k = 3s$ or $k = 3s + 2$ and $\varpi(k) = k + 1$ if $k = 3s + 1$ in Theorem 5.4.5.

Theorem 7.6.4 ([MKKR94]). *The following asymptotic series representations hold for the relaxation cycle:*

$$\begin{aligned} y(\varepsilon) &= y_0 + \sum_{k=2}^{\infty} \varepsilon^{k/3} \sum_{j=0}^{\varpi(k-2)} y_{k,j} \ln^j \frac{1}{\varepsilon}, \\ x(\varepsilon) &= h^-(y(\varepsilon)) + \sum_{k=1}^{\infty} \varepsilon^n F_n(y(\varepsilon)), \\ T(\varepsilon) &= T_0 + \sum_{k=2}^{\infty} \varepsilon^{k/3} \sum_{j=0}^{\varpi(k-2)} T_{k,j} \ln^j \frac{1}{\varepsilon}, \end{aligned}$$

where the coefficients $y_{k,j}$ and $T_{k,j}$ can be computed from function values and derivatives of the vector field, and the functions F_n can be computed from derivatives of the critical manifold.

Theorem 7.6.4 is similar in many aspects to the two-dimensional relaxation oscillation asymptotics described in Chapter 5. This is not surprising, since the essential part of the calculation is the flow past fold points. The important message from Theorems 7.6.2–7.6.4 is that techniques such as geometric desingularization via blowup and direct asymptotic analysis via matching can often be carried over from lower- to higher-dimensional fast–slow systems.

7.7 Remarks on Rescaling

The blowup method always requires a desingularization step such as

$$\begin{aligned} \dot{r} &= r^k(\dots), \quad \dot{r} = (\dots), \quad \text{or} \quad \dot{x} = x^k(\dots), \quad \dot{x} = (\dots), \\ \dot{\theta} &= r^k(\dots), \quad \dot{\theta} = (\dots), \quad \text{or} \quad \dot{y} = x^k(\dots), \quad \dot{y} = (\dots), \end{aligned}$$

involving multiplication/division by certain prefactors. Another situation in which a multiplication transformation is important is discussed in the next example.

Example 7.7.1. Consider the van der Pol equation (again)

$$\begin{aligned} \varepsilon \frac{dx}{d\tau} &= \varepsilon \dot{x} = y - \frac{x^3}{3} + x, \\ \frac{dy}{d\tau} &= \dot{y} = -x. \end{aligned} \tag{7.48}$$

Setting $\varepsilon = 0$ in (7.48) yields $C_0 = \{y = \frac{x^3}{3} - x\}$. Differentiating the algebraic constraint gives $\dot{y} = (x^2 - 1)\dot{x}$. Therefore, the slow subsystem can be written as

$$\dot{x} = \frac{x}{1 - x^2}. \tag{7.49}$$

Away from the two fold points at $x = \pm 1$, one expects that the ODE (7.49) is related to the ODEs $\dot{x} = x$ or $\dot{x} = -x$ obtained from multiplication by $\pm(1 - x^2)$.



This motivates us to consider the general relation between the ODE

$$z' = F(z) \quad \text{for } z \in \mathbb{R}^N, F : \mathbb{R}^N \rightarrow \mathbb{R}^N \text{ smooth} \quad (7.50)$$

and a rescaling via a smooth positive function $G : \mathbb{R}^N \rightarrow (0, \infty)$ given by

$$z' = G(z)F(z). \quad (7.51)$$

Intuitively, the systems should have the same phase portrait, since multiplying by a positive function just changes the length of the vectors at each point in phase space but not their direction. Observe that multiplying by a smooth negative function $G : \mathbb{R}^N \rightarrow (-\infty, 0)$ and then reversing the direction of time gets us back to the positive function case.

Theorem 7.7.2 ([Chi10]). *Let $J \subset \mathbb{R}$ be an interval with $0 \in J$ and suppose $\gamma = \gamma(t)$ solves (7.50). Then the function $B : J \rightarrow \mathbb{R}$ defined by*

$$B(t) := \int_0^t \frac{1}{G(\gamma(s))} \, ds \quad (7.52)$$

is invertible on its range $K \subseteq \mathbb{R}$. Let $\beta : K \rightarrow J$ denote the inverse of B . Then

$$\beta'(t) = G(\gamma(\beta(t))), \quad \text{holds for all } t \in K.$$

Furthermore, $\tilde{\gamma}(t) := \gamma(\beta(t))$ solves (7.51).

Proof. Note that $B'(t) = 1/G(\gamma(t))$ is a continuous positive function. Hence, $B(t)$ is invertible. For the inverse $\beta(t)$, one obtains

$$\beta'(t) = \frac{1}{B'(\beta(t))} = G(\gamma(\beta(t))).$$

To check the last statement involves another direct calculation:

$$\tilde{\gamma}'(t) = \beta'(t)\gamma'(\beta(t)) = G(\gamma(\beta(t)))F(\gamma(\beta(t))) = G(\tilde{\gamma}(t))F(\tilde{\gamma}(t)). \quad \square$$

Theorem 7.7.2 states that the ODEs (7.50) and (7.51) have the same solution curves, up to a **time rescaling** (or **time reparameterization**). This result can be applied immediately to the desingularization step for the blowup method as well as desingularization of the slow flow as in Example 7.7.1. However, it is usually not possible to find an explicit formula for the time rescaling, e.g., consider

$$z' = F(z) \quad \text{and} \quad z' = z_j^k F(z) = G(z)F(z)$$

for some $j \in \{1, 2, \dots, N\}$ that occurs for the weighted (or quasihomogeneous) directional blowup. In this case, we have

$$\beta'(t) = ([\gamma(\beta(t))]_j]^k \quad \text{and} \quad B(t) = \int_0^t (\gamma_j)^{-k}(s) \, ds,$$

where the subscript j indicates the j th component. If there are special solutions for which γ or $\tilde{\gamma}$ are known, one might be able to work out the time rescaling formula, but this case rarely occurs. Nevertheless, a statement of equivalence up to time rescaling is already strong enough for most purposes.

7.8 References

Section 7.1: This section, as well as the next two sections, is based upon a reexposition of material in [Dum78, Dum93]. The desingularization of planar vector fields after a finite number of blowups is sometimes called the Bendixson–Seidenberg–Dumortier theorem [Kal03]. It has the same flavor as the resolution of singularities in algebraic geometry. The famous Hironaka theorem states that for algebraic varieties over a field of characteristic zero, there exists a resolution after a finite number of blowups to a nonsingular variety [Hir64a, Hir64b, Wlo05]. Some references on the blowup method for analytic vector fields are collected in [IY08].

Section 7.2: Of course, there is the question how one would determine the blowup weights. This is discussed in Bruno [Bru89] and Panazzolo [Pan06] as well as in Chapter 12. Blowup techniques are useful in various contexts for single-time-scale systems such as analytic differential equations [IY08], bifurcation unfoldings [Guc84, Zol87], degenerate differential equations [DRS97, GLMM00], integrable systems [DLZ97], stability analysis for PDEs [SS04a, SS05a], wave speeds [DPK07b], and Yang–Mills theory [BFM06].

Section 7.3: In addition to [Dum93, Dum77], there are details on the weighted blowup in [BM90]. There is also a relation to normal form theory for fast–slow vector fields [BMD11]. The rescaling step in the blowup method is also directly related to Poincaré compactification [GPCS06, DH99, Wec02]. It is important to mention that one should not confuse “blowup” of singularities and finite-time “blowup” of solutions [Bal77, Gla77, JL92, Lev90]. Another confusion could arise for the period blowup (blue-sky catastrophe) for a $(1, 2)$ -fast–slow system as treated in [GKR08]. Furthermore, there is a technique with functional-analysis flavor for PDEs that is also sometimes called the “blowup method” [BMS08, FM92].

Section 7.4: The blowup analysis of the fold point is based on [KS01d, KS01b], which, in turn, was based on the fundamental ideas first considered in [DR96b]. For further details on higher-order asymptotics, see Sections 5.4, 9.5 as well as [MR80].

Section 7.5: The relatively straightforward proof is taken from the first part of [KS01e]. The Ackerberg–OMalley resonance problem can be analyzed using blowup techniques [Mae07a]. For an application to planar systems with unbounded manifolds, see [Kue14]. Many more applications are referenced in Chapter 8, Section 5.6, and many other places throughout this book.

Section 7.6: This section is based mainly on [SW04], but see also the references in Sections 1.7 and 5.6 for more on the historical background. The existence of relaxation oscillations in higher dimensions has been established by various geometric methods [Bon87]. For relaxation oscillations in a $(1, 2)$ -fast–slow predator–prey system, see [LXY03]. The existence of tori of relaxation oscillations in fast–slow systems is considered in [Kol94, KM89].

Chapter 8

Singularities and Canards

In this chapter, we put our previous tools such as Fenichel’s theorem and the blowup method to good use. The main goal is to delve even further into the analysis of singularities where normal hyperbolicity is lost and to track trajectories through a region near the singularity.

In Section 8.1, a nondegenerate fold is considered whereby a transversality condition of the slow flow is violated. This reveals so-called canard orbits, which transition in or near repelling slow manifolds for long times. Section 8.2 connects this phenomenon to Hopf bifurcation, while Section 8.3 illuminates how canards and Hopf bifurcations can be related in parameter space. In Section 8.4, we proceed to the global picture generated by rapidly growing canard periodic orbits in the plane, the so-called canard explosion. Instead of a nongeneric fold in a two-dimensional system, it is highly relevant to look at generic folded singularities in three-dimensional systems where the canard phenomenon reappears. Sections 8.5 and 8.6 cover the generation of canards in a three-dimensional normal form in quite some detail. To emphasize that there are many other relevant problems involving loss of normal hyperbolicity beyond folded singularities, we deal with the transcritical case in Section 8.7. We also refer the reader to Chapter 12, where the fast subsystem Hopf singularity is covered in more detail. Section 8.8 concludes this chapter by explaining how curvature can be used to improve our understanding of canard orbits.

Background: It would be helpful to have a very solid understanding of Section 7.4 to comprehend one possible strategy for carrying out the details of the proofs that we omit in this chapter. Otherwise, the same requirements as for Chapter 3 apply, i.e., some elementary understanding of classical bifurcation theory would be helpful [Str00, HK91].

8.1 Folded Singularities in Planar Systems

Consider a $(1, 1)$ -fast–slow system with a parameter $\lambda \in \mathbb{R}$ given by

$$\begin{aligned}\frac{dx}{dt} &= x' = f(x, y, \lambda, \varepsilon), \\ \frac{dy}{dt} &= y' = \varepsilon g(x, y, \lambda, \varepsilon).\end{aligned}\tag{8.1}$$

Assume that $(x_0, y_0) = p$ is a fold point for all values of λ . In all previous chapters, we have considered the generic case that the slow flow is nonzero at p , i.e., $g(p, \lambda, 0) \neq 0$; see also Definition 4.2.1. This implied that the slow subsystem is singular at the fold point, since it is given by

$$\dot{x} = \frac{g(x, h(x), \lambda, 0)}{h'(x)},\tag{8.2}$$

where the function $h : \mathbb{R} \rightarrow \mathbb{R}$ describes the critical manifold locally as a graph $C_0 = \{(x, y) \in \mathbb{R}^2 : y = h(x)\}$ and $h'(x_0) = 0$. The parameter λ turns (8.1) into a 1-parameter family of vector fields that generically satisfy $g(x_0, h(x_0), \lambda_0, 0) = 0$ for an isolated value λ_0 . This means that the slow flow (8.2) may be well defined for λ_0 if the zeros in the numerator and denominator of the vector field (8.2) cancel. Clearly, we expect dynamics distinct from the case of a generic fold. Assume without loss of generality that the fold point is $p = (0, 0)$ and $\lambda_0 = 0$.

Definition 8.1.1. The fold point $(x_0, y_0) = (0, 0)$ is called a **folded singularity** at $\lambda_0 = 0$ if it satisfies the assumptions of a nondegenerate fold,

$$\begin{aligned}f(0, 0, 0, 0) &= 0, & f_x(0, 0, 0, 0) &= 0, \\ f_{xx}(0, 0, 0, 0) &\neq 0, & f_y(0, 0, 0, 0) &\neq 0\end{aligned}\tag{8.3}$$

(where subscripts denote partial derivatives), and it satisfies the condition

$$g(0, 0, 0, 0) = 0.\tag{8.4}$$

The term “folded singularity” arises from the fact that $g(0, 0, 0, 0) = 0$ implies that the origin is an equilibrium (or “singular”) point of (8.1).

Definition 8.1.2. A folded singularity of (8.1) is called **generic** if

$$g_x(0, 0, 0, 0) \neq 0 \quad \text{and} \quad g_\lambda(0, 0, 0, 0) \neq 0.$$

The assumption $g_x \neq 0$ implies a transversal intersection of the nullcline $g(x, y, \lambda, 0) = 0$ and the critical manifold C_0 . The assumption $g_\lambda \neq 0$ yields that the nullcline $g(x, y, \lambda, 0) = 0$ passes through the fold point at nonzero speed as λ varies through $\lambda_0 = 0$. As in the analysis of the generic fold, we shall assume without loss of generality that

$$f_y(0, 0, 0, 0) < 0 \quad \text{and} \quad f_{xx}(0, 0, 0, 0) > 0.\tag{8.5}$$

Therefore, the basic geometric picture is a parabolic critical manifold C_0 with an attracting left branch C_0^a and a repelling right branch C_0^r and corresponding slow manifolds C_ε^a and C_ε^r . The situation is illustrated in Figure 8.1(a).

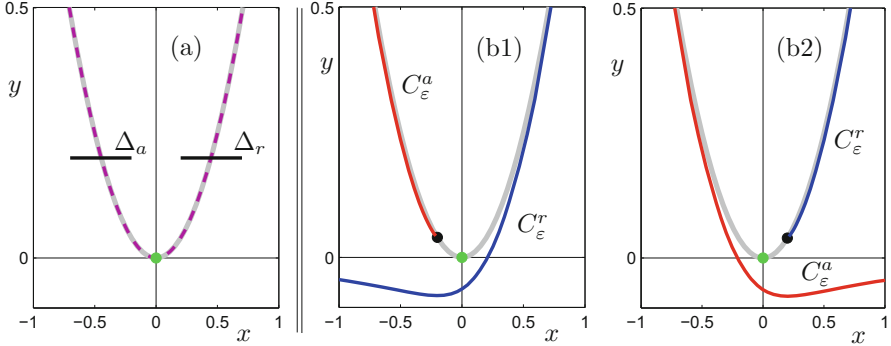


Figure 8.1: Situation near a nondegenerate folded singularity point in a \$(1,1)\$-fast–slow system for the model system \$x' = -y + x^2\$, \$\dot{y} = \varepsilon(\lambda + x)\$. (a) Singular limit \$\varepsilon = 0\$ with the candidate maximal canard (dashed violet) connecting \$C_0^a\$ and \$C_0^r\$. The folded singularity at the origin (green dot) and the critical manifold \$C_0\$ (gray) are shown as well. (b) For \$\varepsilon = 0.05\$, the global equilibrium (black dot) is shown for two cases. The attracting and repelling slow manifolds (red and blue) were obtained by numerical integration. (b1) \$\lambda = 0.2\$ with a stable global equilibrium. (b2) \$\lambda = -0.2\$ with an unstable global equilibrium. From (b), it is a reasonable guess that there should exist \$\lambda_c\$ depending on \$\varepsilon\$ such that a maximal canard in \$C_\varepsilon^a \cap C_\varepsilon^r\$ exists.

It will turn out that for particular choices of \$\lambda\$ and \$\varepsilon\$, it is possible to connect \$C_\varepsilon^a\$ to \$C_\varepsilon^r\$ past the folded singularity; see Figure 8.1. In the following, we shall state precisely when such a scenario is possible. Observe that the assumptions (8.3), (8.4), and (8.5) imply that the system (8.1) can be transformed into a normal form

$$\begin{aligned} x' &= -yh_1(x, y, \lambda, \varepsilon) + x^2h_2(x, y, \lambda, \varepsilon) + \varepsilon h_3(x, y, \lambda, \varepsilon), \\ y' &= \varepsilon(\pm xh_4(x, y, \lambda, \varepsilon) - \lambda h_5(x, y, \lambda, \varepsilon) + yh_6(x, y, \lambda, \varepsilon)), \end{aligned} \quad (8.6)$$

where

$$\begin{aligned} h_3(x, y, \lambda, \varepsilon) &= \mathcal{O}(x, y, \lambda, \varepsilon), \\ h_j(x, y, \lambda, \varepsilon) &= 1 + \mathcal{O}(x, y, \lambda, \varepsilon), \quad j = 1, 2, 4, 5. \end{aligned}$$

The proof is just a slight modification of the derivation of the normal form of the generic fold point; see Section 4.2. The signs of the different terms in (8.6) depend on the signs chosen for the imposed inequality conditions. Let us assume without loss of generality that the sign in front of the term \$xh_4\$ is positive. This implies that the flow is downward on \$C_\varepsilon^a\$ and upward on \$C_\varepsilon^r\$. Hence, one may attempt to search for a solution that connects \$C_\varepsilon^a\$ to \$C_\varepsilon^r\$. To simplify notation, the following shorthand conventions are helpful:

$$\begin{aligned} a_1 &= \frac{\partial h_3}{\partial x}(0, 0, 0, 0), \quad a_2 = \frac{\partial h_1}{\partial x}(0, 0, 0, 0), \quad a_3 = \frac{\partial h_2}{\partial x}(0, 0, 0, 0), \\ a_4 &= \frac{\partial h_4}{\partial x}(0, 0, 0, 0), \quad a_5 = h_6(0, 0, 0, 0), \quad A = -a_2 + 3a_3 - 2a_4 + 2a_5. \end{aligned} \quad (8.7)$$

Also for $j = a, r$, let $\Delta_j = \{(x, \rho^2) : x \in I_j\}$ be the horizontal sections illustrated in Figure 8.1 for suitably small intervals I_j . Let Π be the transition map of the flow from Δ_a to Δ_r and introduce the notation $q_{j,\varepsilon} = \Delta_j \cap C_\varepsilon^j$.

Theorem 8.1.3 ([KS01b, DR96b]). *Suppose a $(1,1)$ -fast–slow system has a generic folded singularity and assume that the slow flow connects the two branches of the critical manifold C_0^a and C_0^r . Then there exist $\varepsilon_0 > 0$ and a smooth function $\lambda = \lambda_c(\sqrt{\varepsilon})$ defined on $[0, \varepsilon_0]$ such that the following hold:*

$$(R1) \quad \Pi(q_{a,\varepsilon}) = q_{r,\varepsilon} \text{ if and only if } \lambda = \lambda_c(\sqrt{\varepsilon});$$

$$(R2) \quad \text{the function } \lambda_c \text{ has the expansion}$$

$$\lambda_c(\sqrt{\varepsilon}) = -\left(\frac{a_1 + a_5}{2} + \frac{A}{8}\right)\varepsilon + \mathcal{O}(\varepsilon^{3/2}); \quad (8.8)$$

$$(R3) \quad \text{the transition map } \Pi \text{ is defined only for } \lambda \text{ in an interval around } \lambda_c(\sqrt{\varepsilon}) \text{ of width } \mathcal{O}(e^{-c/\varepsilon}) \text{ for some } c > 0;$$

$$(R4) \quad \frac{\partial}{\partial \lambda}(\Pi(q_{a,\varepsilon}) - q_{r,\varepsilon})|_{\lambda=\lambda_c(\sqrt{\varepsilon})} > 0.$$

Remark: The notation $\sqrt{\varepsilon}$ for $\lambda_c(\sqrt{\varepsilon})$ emphasizes the fact that the asymptotic expansion (8.8) is based on the asymptotic sequence $\{\varepsilon^{k/2}\}_{k=0}^\infty$ and that λ_c is smooth as a function of $\sqrt{\varepsilon}$.

Before we sketch some ideas for the proof of Theorem 8.1.3, we discuss and apply it. The major result is the construction of a special solution of a planar fast–slow system due to the presence of a singularity.

Definition 8.1.4. A solution lying in the intersection of the slow manifolds C_ε^a and C_ε^r is called a **maximal canard**.

Note that a maximal canard is a quite unexpected phenomenon. It follows a branch of the slow manifold, which is *repelling*. This explains the use of the word “canard,” which can mean “false news” in French. The alternative interpretation of “canard,” which also means “duck” in French, will be explained in Section 8.4; interestingly, there are even more linguistic relations, since “false news” is colloquially known as ‘Ente’ (or “Zeitungssente”) in German, but “Ente” also means “duck” in German.

Definition 8.1.5. A trajectory segment of a fast–slow system is a **canard** if it stays within $\mathcal{O}(\varepsilon)$ distance to a repelling branch of a slow manifold for a time that is $\mathcal{O}(1)$ on the slow time scale $\tau = t\varepsilon$.

Remark: Theorem 8.1.3 shows that canards occur near a folded singularity. Hence, sometimes the terminology **canard point** is used. However, it seems reasonable to use canard point also beyond the case of folds, since other singularities can also create canard orbits; see Sections 8.7, 12.2, and 12.3. Furthermore, we remark that we just use the word “maximal” to distinguish the canards from Definitions 8.1.4 and 8.1.5; in particular, no mathematical ordering, where an object can be “maximal,” of different canards will be used in this book.

Another key observation is encoded in (R3) of Theorem 8.1.3, which shows that canard solutions occur in exponentially small regions in parameter space in planar fast–slow systems. This makes canards very difficult to detect in practice, since direct forward numerical integration will not be able to generate canard solutions easily; see Section 11.5 for a detailed discussion of the numerical issues.

Example 8.1.6. To understand the necessary steps in applying Theorem 8.1.3, consider the van der Pol equation with constant forcing

$$\begin{aligned} x' &= y - \left(\frac{x^3}{3} - x \right), \\ y' &= \varepsilon(a - x). \end{aligned} \quad (8.9)$$

We are interested in only one of the two fold points of (8.9) located at $(1, -2/3)$. It is easy to put the system into the standard normal form (8.6). After shifting the fold point to the origin, reversing time $t \rightarrow -t$, and setting $a-1 =: \lambda$, we get

$$\begin{aligned} x' &= -y + x^2(1 + \frac{x}{3}), \\ y' &= \varepsilon(x - \lambda). \end{aligned}$$

In this standard form, the relevant parameters a_i defined in (8.7) are

$$a_1 = 0, \quad a_2 = 0, \quad a_3 = \frac{1}{3}, \quad a_4 = 0, \quad a_5 = 0, \quad A = 1.$$

Hence, a maximal canard exists on a curve λ_c in (ε, λ) -space with the expansion

$$\lambda_c(\sqrt{\varepsilon}) = -\frac{\varepsilon}{8} + \mathcal{O}(\varepsilon^{3/2}).$$

It is interesting at this point to think about what should happen to the maximal canard once it reaches the neighborhood of the second fold; see Section 8.4 for details. ♦

Exercise 8.1.7. Extend the calculations in Example 8.1.6 to the planar FitzHugh–Nagumo model; see Section 1.4. ◇

We return to Theorem 8.1.3 and sketch a few important ideas for the proof. As for the fold, a blowup is required to desingularize the system

$$\begin{aligned} x' &= -yh_1(x, y, \lambda, \varepsilon) + x^2h_2(x, y, \lambda, \varepsilon) + \varepsilon h_3(x, y, \lambda, \varepsilon), \\ y' &= \varepsilon(xh_4(x, y, \lambda, \varepsilon) - \lambda h_5(x, y, \lambda, \varepsilon) + yh_6(x, y, \lambda, \varepsilon)), \\ \varepsilon' &= 0, \\ \lambda' &= 0, \end{aligned} \quad (8.10)$$

near the origin $(x, y, \varepsilon, \lambda) = (0, 0, 0, 0)$. A good choice for the blowup is

$$x = \bar{r}\bar{x}, \quad y = \bar{r}^2\bar{y}, \quad \varepsilon = \bar{r}^2\bar{\varepsilon}, \quad \lambda = \bar{r}\bar{\lambda},$$

where overbars denote coordinates in the blown-up space; see Sections 7.3 and 7.4 as well as Chapter 12 for how to derive the choice of coefficients. It turns out that two charts K_1, K_2 suffice for the directional blowup

$$\begin{aligned} K_1, \quad \bar{y} = 1 : \quad x &= r_1 x_1, & y &= r_1^2, & \varepsilon &= r_1^2 \varepsilon_1, & \lambda &= r_1 \lambda_1, \\ K_2, \quad \bar{\varepsilon} = 1 : \quad x &= r_2 x_2, & y &= r_2^2 y_2, & \varepsilon &= r_2^2, & \lambda &= r_2 \lambda_2. \end{aligned} \quad (8.11)$$

Here we focus on the chart K_2 , where the blowup reduces to a rescaling

$$x = \sqrt{\varepsilon}x_2, \quad y = \varepsilon y_2, \quad \lambda = \sqrt{\varepsilon}\lambda_2. \quad (8.12)$$

Inserting (8.12) into (8.10) and using definitions for h_j yields the next result.

Lemma 8.1.8 ([KS01b]). *The vector field in the chart K_2 can, after a desingularization by $r_2 = \sqrt{\varepsilon}$, be expressed as*

$$\begin{aligned} x'_2 &= -y_2 + x_2^2 + \sqrt{\varepsilon}G_1(x_2, y_2) + \mathcal{O}(\sqrt{\varepsilon}(\lambda_2 + \sqrt{\varepsilon})), \\ y'_2 &= x_2 - \lambda_2 + \sqrt{\varepsilon}G_2(x_2, y_2) + \mathcal{O}(\sqrt{\varepsilon}(\lambda_2 + \sqrt{\varepsilon})), \end{aligned} \quad (8.13)$$

where

$$G(x_2, y_2) = \begin{pmatrix} G_1(x_2, y_2) \\ G_2(x_2, y_2) \end{pmatrix} = \begin{pmatrix} a_1x_2 - a_2x_1y_2 + a_3x_2^3 \\ a_4x_2^2 + a_5y_2 \end{pmatrix}.$$

The folded singularity occurs in the original system when $\varepsilon = 0$ and $\lambda = 0$, so we are interested in a perturbation argument from this singular limit case. Setting $\varepsilon = 0$ and $\lambda_2 = 0$ in (8.13) yields the important planar ODE

$$\begin{aligned} x'_2 &= -y_2 + x_2^2, \\ y'_2 &= x_2. \end{aligned} \quad (8.14)$$

Analyzing (8.14) is a relatively straightforward task if one has the next result available.

Proposition 8.1.9. *A first integral for (8.14) is given by*

$$H(x_2, y_2) = \frac{1}{2}e^{-2y_2} \left(y_2 - x_2^2 + \frac{1}{2} \right). \quad (8.15)$$

The solution associated with $H(x_2, y_2) = 0$ has algebraic growth and is given by

$$\gamma_c(t_2) = \begin{pmatrix} x_{c,2}(t_2) \\ y_{c,2}(t_2) \end{pmatrix} = \begin{pmatrix} \frac{1}{2}t_2 \\ \frac{1}{4}t_2^2 - \frac{1}{2} \end{pmatrix}. \quad (8.16)$$

Proof. For the first integral, we just calculate

$$\begin{aligned} \frac{d}{dt_2} H(x_2, y_2) &= x'_2 \frac{\partial H}{\partial x_2} + y'_2 \frac{\partial H}{\partial y_2} \\ &= -x'_2 x_2 e^{-2y_2} + y'_2 \left[-e^{-2y_2} \left(y_2 - x_2^2 + \frac{1}{2} \right) + \frac{1}{2} e^{-2y_2} \right] \\ &= e^{-2y_2} [(-y_2 + x_2^2)x_2 + x_2(-y_2 + x_2^2)] = 0. \end{aligned}$$

The special solution (8.16) is a level curve associated with $H = 0$, since

$$H(x_{c,2}(t_2), y_{c,2}(t_2)) = \frac{1}{2}e^{-2y_{c,2}(t_2)} \left(\frac{1}{4}t_2^2 - \frac{1}{2} - \left(\frac{t_2}{2} \right)^2 + \frac{1}{2} \right) = 0,$$

and therefore $\gamma_c(t_2)$ also solves (8.14). \square

The level curves of the function H determine the flow of (8.14). Figure 8.2(a) shows that $(0, 0)$ is a center equilibrium with $H(0, 0) = 1/4$. Periodic orbits exist for $H = h$ with $h \in (0, 1/4)$ and terminate at the special solution γ_c when $h = 0$; see also Section 13.8 and Figure 13.14. Since γ_c is of algebraic growth, it is the natural candidate orbit to form the maximal canard from Theorem 8.1.3. In fact, Figure 8.2(b) indicates that γ_c starts at a point p_a on the equator of the sphere $(\bar{x}, \bar{y}, \bar{z}) \in S^2$ (with $\bar{r} = 0$ understood here) corresponding to C_0^a and ends at a point p_r corresponding to C_0^r .

Lemma 8.1.10 ([KS01b]). *The flow for (8.10) in the chart K_1 is*

$$\begin{aligned} x'_1 &= -1 + x_1^2 + r_1(a_1\varepsilon_1x_1 - a_2x_1 + a_3x_1^3) - \frac{\varepsilon_1x_1}{2}F(x_1, r_1, \varepsilon_1, \lambda_1) \\ &\quad + \mathcal{O}(r_1(r_1 + \lambda_1)), \\ r'_1 &= \frac{r_1\varepsilon_1}{2}F(x_1, r_1, \varepsilon_1, \lambda_1), \\ \varepsilon'_1 &= -\varepsilon_1^2F(x_1, r_1, \varepsilon_1, \lambda_1), \\ \lambda'_1 &= -\frac{\lambda_1\varepsilon_1}{2}F(x_1, r_1, \varepsilon_1, \lambda_1), \end{aligned} \tag{8.17}$$

where $F(x_1, r_1, \varepsilon_1, \lambda_1) = x_1 - \lambda_1 + r_1(a_4x_1^2 + a_5) + \mathcal{O}(r_1(r_1 + \lambda_1))$.

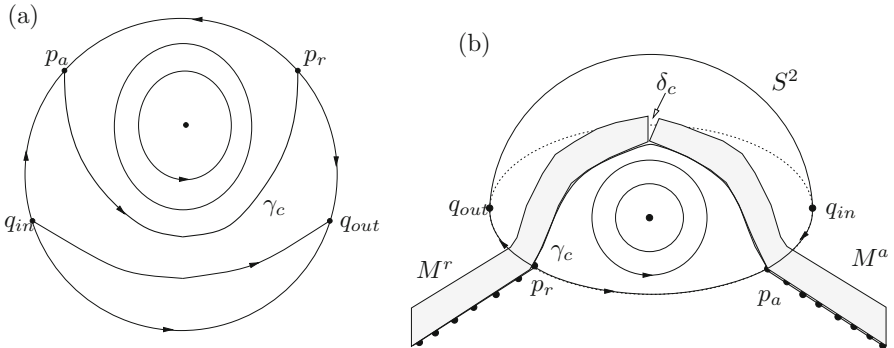


Figure 8.2: Sketch of the blown-up vector field near a folded singularity in \mathbb{R}^2 . (a) Projection onto the upper half-sphere. Note that the level curves of the first integral H from Proposition 8.1.9 have been compactified onto the sphere. For an illustration of H in \mathbb{R}^2 , see also Figure 13.14. (b) Phase space for the blown-up problem.

The calculations to obtain Lemma 8.1.10 are very similar to the detailed calculations in Section 7.4, so we skip them here. Focusing on the dynamical analysis of (8.17), we see that the points $p_a := (-1, 0, 0, 0)$ and $p_r = (1, 0, 0, 0)$ are immediately identified as equilibria lying on the equator of S^2 ; see Figure 8.2. To check that these points are really endpoints of the C_0^a and C_0^r in the chart K_1 , one has to calculate the blown-up critical manifold. For C_0^a , we get

$$C_0^a \cup \{(0, 0)\} = \{y = x^2, x \leq 0\} \xrightarrow{K_1} \{r_1^2 = r_1^2x_1^2, r_1x_1 \leq 0\} = \{x_1 = -1, r_1 \geq 0\},$$

so if $r_1 = 0$, then p_a is indeed the endpoint of the blown-up manifold $\bar{C}^{a,1}$ corresponding to the origin $(x, y) = (0, 0)$. Moreover, $\varepsilon_1 = 0 = \lambda_1$ defines an invariant subspace for the system (8.17), which reduces to

$$\begin{aligned} x'_1 &= -1 + x_1^2 + r_1(-a_2x_1 + a_3x_1^3) + \mathcal{O}(r_1^2), \\ r'_1 &= 0. \end{aligned} \quad (8.18)$$

For fixed r_1 , we can solve $-1 + x_1^2 + r_1(-a_2x_1 + a_3x_1^3) + \mathcal{O}(r_1^2) = 0$, at least locally near $x_1 = -1$, for a curve of equilibrium points ending at p_a ; $\bar{C}^{a,1}$ can be identified with this curve. In a similar way, the point p_r can be treated that satisfies the sketch in Figure 8.2(b). Then, one can construct attracting and repelling center manifolds $\bar{M}^{a,r}$ in blown-up space corresponding to $C_\varepsilon^{a,r}$ and based along γ_c . The distance between these manifolds has to be calculated, where a zero of the distance function will correspond to a maximal canard; see Figure 8.2(b).

Lemma 8.1.11 ([KS01b]). *The distance δ_c between \bar{M}^a and \bar{M}^r in K_2 is*

$$\delta_c(r_2\lambda_2) = d_{r_2}r_2 + d_{\lambda_2}\lambda_2 + \mathcal{O}(r_2^2), \quad (8.19)$$

where

$$\begin{aligned} d_{r_2} &= \int_{-\infty}^{\infty} \nabla H(\gamma_c(t))^\top G(\gamma_c(t)) dt, \\ d_{\lambda_2} &= \int_{-\infty}^{\infty} \nabla H(\gamma_c(t))^\top \begin{pmatrix} 0 \\ -1 \end{pmatrix} dt, \end{aligned}$$

where G is defined as in Lemma 8.1.8.

We shall skip the detailed proof of Lemma 8.1.11 here and just note that the integrals d_{r_2} and d_{λ_2} arise as Melnikov-type integrals in the calculation [KS01b, Wec02].

Proof. (of Theorem 8.1.3, sketch) A maximal canard lying inside $C_\varepsilon^a \cap C_\varepsilon^r$ exists if and only if $\delta_c = 0$. By Lemma 8.1.11, we have

$$0 = d_{r_2}r_2 + d_{\lambda_2}\lambda_2 + \mathcal{O}(r_2^2). \quad (8.20)$$

Under the assumption $d_{\lambda_2} \neq 0$, the implicit function theorem yields that (8.20) can be solved for λ_2 :

$$\lambda_2 = -\frac{d_{r_2}}{d_{\lambda_2}}r_2 + \mathcal{O}(r_2^2). \quad (8.21)$$

Hence, one can calculate d_{r_2} and d_{λ_2} using the formulas in Lemma 8.1.11 as well as the explicit singular canard solution $\gamma_c(t)$ from Proposition 8.1.9. The result for d_{λ_2} is straightforward:

$$\begin{aligned} d_{\lambda_2} &= \int_{-\infty}^{\infty} \nabla H(\gamma_c(t))^\top \begin{pmatrix} 0 \\ -1 \end{pmatrix} dt = - \int_{-\infty}^{\infty} \frac{\partial H}{\partial y_2}(\gamma_c(t)) dt \\ &= - \int_{-\infty}^{\infty} -e^{-2y_{c,2}(t)} (y_{c,2}(t) - x_{c,2}(t)^2) dt \\ &= - \int_{-\infty}^{\infty} -e^{-(t^2/2-1)} \left(\frac{1}{4}t^2 - \frac{1}{2} - \frac{1}{4}t^2 \right) dt = -\frac{e}{2} \int_{-\infty}^{\infty} e^{-\frac{t^2}{2}} dt < 0, \end{aligned}$$

which also confirms the assumption $d_{\lambda_2} \neq 0$. The calculation for d_{r_2} is similar but quite lengthy, with the two major steps

$$\begin{aligned} d_{r_2} &= \int_{-\infty}^{\infty} e^{-2y_{c,2}(t)} \left[-a_1 x_{2,c}(t)^2 + (a_2 - a_4 + a_5) x_{2,c}(t)^2 y_{2,c}(t) \right. \\ &\quad \left. + (a_4 - a_3) x_{2,c}(t)^4 - a_5 y_{2,c}(t)^2 \right] dt \end{aligned} \quad (8.22)$$

$$= -\frac{e}{4} \left(a_1 + a_5 + \frac{A}{4} \right) \int_{-\infty}^{\infty} e^{-\frac{t^2}{2}} dt, \quad (8.23)$$

where repeated integration by parts is used for the second equality and A is defined in (8.7); see Exercise 8.1.12. Now (R1)–(R2) follow, since

$$\begin{aligned} \lambda_2 &= - \left(\frac{a_1 + a_5}{2} + \frac{A}{8} \right) r_2 + \mathcal{O}(r_2^2) \\ \Rightarrow \lambda_c(\sqrt{\varepsilon}) &= - \left(\frac{a_1 + a_5}{2} + \frac{A}{8} \right) \varepsilon + \mathcal{O}(\varepsilon^{3/2}), \end{aligned}$$

using the blowdown transformation $\lambda = r_2 \lambda_2$, $\sqrt{\varepsilon} = r_2$ from (8.11). It is relatively straightforward to prove (R3), since the manifolds must be exponentially close for the flow map Π to be defined; (R4) holds, since $d_{\lambda_2} < 0$, so that the manifolds split as claimed. \square

Exercise 8.1.12. Use integration by parts to derive (8.23) from (8.22). \diamond

8.2 Singular Hopf Bifurcation in \mathbb{R}^2

Here we continue the analysis of the folded singularity begun in the last section. In particular, the main system studied is the normal form

$$\begin{aligned} x' &= -yh_1(x, y, \lambda, \varepsilon) + x^2 h_2(x, y, \lambda, \varepsilon) + \varepsilon h_3(x, y, \lambda, \varepsilon), \\ y' &= \varepsilon(xh_4(x, y, \lambda, \varepsilon) - \lambda h_5(x, y, \lambda, \varepsilon) + yh_6(x, y, \lambda, \varepsilon)), \end{aligned} \quad (8.24)$$

where

$$\begin{aligned} h_3(x, y, \lambda, \varepsilon) &= \mathcal{O}(x, y, \lambda, \varepsilon), \\ h_j(x, y, \lambda, \varepsilon) &= 1 + \mathcal{O}(x, y, \lambda, \varepsilon), \quad j = 1, 2, 4, 5, \end{aligned}$$

and we consider, as already defined in (8.7), the notation

$$\begin{aligned} a_1 &= \frac{\partial h_3}{\partial x}(0, 0, 0, 0), \quad a_2 = \frac{\partial h_1}{\partial x}(0, 0, 0, 0), \quad a_3 = \frac{\partial h_2}{\partial x}(0, 0, 0, 0), \\ a_4 &= \frac{\partial h_4}{\partial x}(0, 0, 0, 0), \quad a_5 = h_6(0, 0, 0, 0), \quad A = -a_2 + 3a_3 - 2a_4 + 2a_5. \end{aligned} \quad (8.25)$$

Theorem 8.2.1 ([KS01e]). *Suppose $(x, y) = (0, 0)$ is a generic folded singularity at $(x, y) = (0, 0)$ for $\lambda = 0$ with normal form (8.24). Then there exist $\varepsilon_0 > 0$ and $\lambda_0 > 0$ such that for $0 < \varepsilon < \varepsilon_0$ and $|\lambda| < \lambda_0$, in a suitable neighborhood of the origin, the system (8.24) has precisely one equilibrium point p with*

$p \rightarrow (0, 0)$ as $(\lambda, \varepsilon) \rightarrow (0, 0)$. Furthermore, there exists a curve $\lambda = \lambda_H(\sqrt{\varepsilon})$ of Hopf bifurcations such that p is stable for $\lambda < \lambda_H(\sqrt{\varepsilon})$ and

$$\lambda_H(\sqrt{\varepsilon}) = -\frac{a_1 + a_5}{2}\varepsilon + \mathcal{O}(\varepsilon^{3/2}). \quad (8.26)$$

The Hopf bifurcation is nondegenerate when $A \neq 0$, where A is defined in (8.25). It is supercritical if $A < 0$ and subcritical if $A > 0$.

The reason why the Hopf bifurcation, which occurs at $\mathcal{O}(\varepsilon)$ -distance from the fold point, in Theorem 8.2.1 is a so-called **singular Hopf bifurcation** will be explained below. The meaning and utility of the constant A is explored further in Section 8.3.

Proof. (of Theorem 8.2.1, sketch) The result can be proven just using the “scaling chart” K_2 defined in (8.12). Recall from Lemma 8.1.8 that the vector field in K_2 can be expressed as

$$\begin{aligned} x'_2 &= -y_2 + x_2^2 + \sqrt{\varepsilon}G_1(x_2, y_2) + \mathcal{O}(\sqrt{\varepsilon}(\lambda_2 + \sqrt{\varepsilon})), \\ y'_2 &= x_2 - \lambda_2 + \sqrt{\varepsilon}G_2(x_2, y_2) + \mathcal{O}(\sqrt{\varepsilon}(\lambda_2 + \sqrt{\varepsilon})), \end{aligned} \quad (8.27)$$

where

$$G(x_2, y_2) = \begin{pmatrix} G_1(x_2, y_2) \\ G_2(x_2, y_2) \end{pmatrix} = \begin{pmatrix} a_1x_2 - a_2x_1y_2 + a_3x_2^3 \\ a_4x_2^2 + a_5y_2 \end{pmatrix}.$$

Observe that (8.27) has an equilibrium point $p_2 = (x_{2,e}, y_{2,e})$ with $x_{2,e} = \lambda_2 + \mathcal{O}(2)$ and $y_{2,e} = \mathcal{O}(2)$, where we temporarily define $\mathcal{O}(2) := \mathcal{O}(\lambda_2^2 + \sqrt{\varepsilon}|\lambda_2| + \varepsilon)$. The point p from the theorem corresponds to p_2 in the blowup coordinates. Computing the linearization at p_2 yields the matrix

$$A_2 := \begin{pmatrix} 2\lambda_2 + a_1\sqrt{\varepsilon} + \mathcal{O}(2) & -1 + \mathcal{O}(2) \\ 1 + \mathcal{O}(2) & a_5\sqrt{\varepsilon} + \mathcal{O}(2) \end{pmatrix}. \quad (8.28)$$

Computing the Hopf bifurcation condition $0 = \text{Tr}(A_2) = 2\lambda_2 + [a_1 + a_5]\sqrt{\varepsilon} + \mathcal{O}(2)$ and applying the blowdown map $\lambda = \lambda_2\sqrt{\varepsilon}$ yields (8.26). To prove the remaining part involving the constant A , we must compute the first Lyapunov coefficient \bar{l}_1 at the Hopf bifurcation point. Results stated in [CLW94, Chapter 3] and a direct calculation, which we skip here, give

$$\bar{l}_1 = \frac{1}{8}A\sqrt{\varepsilon} + \mathcal{O}(\varepsilon), \quad (8.29)$$

which establishes the remaining part of the result. \square

The family of small limit cycles generated in the Hopf bifurcation correspond to perturbations of the closed level curves of the function

$$H(x_2, y_2) = \frac{1}{2}e^{-2y_2} (y_2 - x_2^2 + 1/2)$$

considered in Proposition 8.1.9; see also Figure 8.2(a). In Section 8.3, we give more details regarding the computation of the first Lyapunov coefficient (8.29).

Hence, it remains to explain the terminology ‘‘singular Hopf bifurcation.’’ Consider a simpler version of (8.24) given by

$$\begin{aligned} x' &= -y + x^2, \\ y' &= \varepsilon(x - \lambda). \end{aligned} \quad (8.30)$$

Clearly, (8.30) has an equilibrium point at $p_0 = (\lambda, \lambda^2)$ with associated linearization given by the matrix

$$A_0(\lambda) := \begin{pmatrix} 2\lambda & -1 \\ \varepsilon & 0 \end{pmatrix}.$$

The Hopf bifurcation occurs at $\lambda = 0$. The eigenvalues of $A_0(0)$ at the Hopf bifurcation are $\sigma_{\pm} = \pm i\sqrt{\varepsilon}$ and $\sigma_{\pm} \rightarrow 0$ as $\varepsilon \rightarrow 0$. Alternatively, we can also look at (8.30) on the slow time scale $\tau = \varepsilon t$ with linearization $\frac{1}{\varepsilon}A_0$ and eigenvalues $\frac{1}{\varepsilon}\sigma_{\pm}$, which tend to infinity as $\varepsilon \rightarrow 0$. On both time scales, the eigenvalues at the Hopf bifurcation are ‘‘singular.’’ Note very carefully that this is in contrast to the eigenvalues of the matrix A_2 from (8.28), where the blowup has already resolved the singularity. The situation just encountered can be encoded in a more general definition.

Definition 8.2.2 ([Bra98]). Suppose that a multiple time scale system has a Hopf bifurcation on varying a parameter λ . Consider the system on the two-dimensional center manifold. Then we say that a **singular Hopf bifurcation occurs** if the linearized center manifold system has a pair of **singular eigenvalues** at the Hopf bifurcation point $\lambda = \lambda_H$, that is,

$$\sigma(\lambda; \varepsilon) = \alpha(\lambda; \varepsilon) + i\beta(\lambda; \varepsilon),$$

so that $\alpha(\lambda_H; \varepsilon) = 0$, $\alpha_{\lambda}(\lambda_H; \varepsilon) \neq 0$, with

$$\begin{aligned} \lim_{\varepsilon \rightarrow 0} |\beta(\lambda_H; \varepsilon)| &= \infty, \text{ on the slow time scale } \tau, \text{ and} \\ \lim_{\varepsilon \rightarrow 0} \beta(\lambda_H; \varepsilon) &= 0, \text{ on the fast time scale } t. \end{aligned}$$

In short, a **singular Hopf bifurcation** occurs when the eigenvalues become singular as $\varepsilon \rightarrow 0$.

Example 8.2.3. Consider the van der Pol-type (1, 1)-fast–slow system

$$\begin{aligned} x' &= -y + x^2 - x^3, \\ y' &= \varepsilon(x - \lambda + y). \end{aligned} \quad (8.31)$$

The critical manifold is $C_0 = \{y = x^2 - x^3\}$ with fold points $(x, y) = (0, 0) =: 0$ and $(x, y) = (2/3, 4/27)$. The origin becomes a generic folded singularity when $\lambda = 0$, and we shall focus on this case. Comparing (8.31) and (8.24), we find that

$$h_3 = 0, \quad h_1 = 1, \quad h_2 = 1 - x, \quad h_4 = 1, \quad h_5 = 1, \quad h_6 = 1.$$

Furthermore, from (8.25), it follows that

$$a_1 = 0, \quad a_2 = 0, \quad a_3 = -1, \quad a_4 = 0, \quad a_5 = 1, \quad A = -1.$$

Therefore, the Hopf bifurcation is supercritical. According to Theorem 8.1.3, a maximal canard occurs when

$$\lambda_c(\sqrt{\varepsilon}) = -\left(\frac{a_1 + a_5}{2} + \frac{A}{8}\right)\varepsilon + \mathcal{O}(\varepsilon^{3/2}) = -\frac{3}{8}\varepsilon + \mathcal{O}(\varepsilon^{3/2}).$$

From Theorem 8.2.1, it follows that

$$\lambda_H(\sqrt{\varepsilon}) = -\frac{a_1 + a_5}{2}\varepsilon + \mathcal{O}(\varepsilon^{3/2}) = -\frac{1}{2}\varepsilon + \mathcal{O}(\varepsilon^{3/2})$$

is the location of the singular Hopf bifurcation. ♦

Exercise/Project 8.2.4. Consider the FitzHugh–Nagumo (FHN) equation from Section 1.4 and use Theorem 8.1.3 and Theorem 8.2.1 to compute the location of the maximal canard and the singular Hopf bifurcation depending on the FHN system parameters. ◇

The calculations in Example 8.2.3 are quite short and elegant. However, Exercise 8.2.4 shows that computations can get quite cumbersome due to the required preliminary normal form transformations. If one suspects that a higher-dimensional system has a (two-dimensional) singular Hopf bifurcation, one has to calculate the center manifold and the normal form (8.24) of the vector field on the center manifold to apply Theorems 8.1.3 and 8.2.1. The next section discusses a possible shortcut for this situation.

8.3 The First Lyapunov Coefficient

We continue with the setup of the normal form (8.24) and in particular with the definitions of the coefficients (8.25). The location of the Hopf bifurcation λ_H (Theorem 8.2.1) and the maximal canard λ_c (Theorem 8.1.3) can be computed:

$$\begin{aligned}\lambda_H &= -\frac{a_1+a_5}{2}\varepsilon + \mathcal{O}(\varepsilon^{3/2}), \\ \lambda_c &= -\left(\frac{a_1+a_5}{2} + \frac{A}{8}\right)\varepsilon + \mathcal{O}(\varepsilon^{3/2}).\end{aligned}\tag{8.32}$$

The equilibrium is stable for $\lambda < \lambda_H$ and unstable for $\lambda > \lambda_H$. The Hopf bifurcation is nondegenerate for $A \neq 0$, supercritical for $A < 0$, and subcritical for $A > 0$. Unfortunately, the computation of the normal form coefficients is not immediately obvious. Most bifurcation software packages (see also Section 10.9) can detect Hopf bifurcations, so that given a fixed ε , one can approximate λ_H numerically. It is important to observe that to approximate λ_c , it suffices to compute A , since

$$\lambda_H - \lambda_c = \frac{A}{8}\varepsilon + \mathcal{O}(\varepsilon^{3/2}).\tag{8.33}$$

Knowing A , we can easily approximate the location of the maximal canard by $\lambda_c = \lambda_H - \frac{A}{8}\varepsilon + \mathcal{O}(\varepsilon^{3/2})$.

The main point is to recognize that A is just a scaled version of the first Lyapunov coefficient l_1 at a Hopf bifurcation. Unfortunately, there are many

different conventions for the first Lyapunov coefficient at a Hopf bifurcation, all being scaled versions of one another; see Section 8.9. For example, suppose $(x, y) \in \mathbb{R}^2$ and consider a system at a Hopf bifurcation point

$$\begin{pmatrix} x' \\ y' \end{pmatrix} = M \begin{pmatrix} x \\ y \end{pmatrix} + \begin{pmatrix} f(x, y) \\ g(x, y) \end{pmatrix}, \quad (8.34)$$

where M is a matrix with eigenvalues $\pm i\omega_0$ for some $\omega_0 > 0$, and $f(x, y), g(x, y)$ are the nonlinear terms. Then a convention for l_1 is [CLW94, p. 211]

$$\begin{aligned} l_1^{CLW} = & \frac{m_{12}}{16\omega_0^4} [\omega_0^2 [(f_{xxx} + g_{xxy}) + 2m_{22}(f_{xxy} + g_{xyy}) - m_{21}(f_{xyy} + g_{yyy})] \\ & - m_{12}m_{22}(f_{xx}^2 - f_{xx}g_{xy} - f_{xy}g_{xx} - g_{xx}g_{yy} - 2g_{xy}) \\ & - m_{21}m_{22}(g_{yy}^2 - g_{yy}f_{xy} - g_{xy}f_{yy} - f_{xx}f_{yy} - 2f_{xy}^2) \\ & + m_{12}^2(f_{xx}g_{xx} + g_{xx}g_{xy}) - m_{21}^2(f_{yy}g_{yy} + f_{xy}f_{yy}) \\ & - (\omega_0^2 + 3m_{22}^2)(f_{xx}f_{xy} - g_{xy}g_{yy})], \end{aligned} \quad (8.35)$$

where all evaluations in (8.35) are at $(x, y) = (0, 0)$. If we apply a preliminary linear coordinate change $(x, y)^\top = N(x^*, y^*)^\top$ to bring M from (8.34) into Jordan normal form and then drop the stars for (x^*, y^*) , then we will be looking at

$$\begin{pmatrix} x' \\ y' \end{pmatrix} = \begin{pmatrix} 0 & -\omega_0 \\ \omega_0 & 0 \end{pmatrix} \begin{pmatrix} x \\ y \end{pmatrix} + \begin{pmatrix} f^*(x, y) \\ g^*(x, y) \end{pmatrix} \quad (8.36)$$

for some new functions f^* and g^* . Then another convention for the Lyapunov coefficient is [GH83, p. 152]

$$\begin{aligned} l_1^{GH} = & \frac{1}{16}[f_{xxx}^* + f_{xyy}^* + g_{xxy}^* + g_{yyy}^*] + \frac{1}{16\omega_0}[f_{xy}^*(f_{xx}^* + f_{yy}^*) \\ & - g_{xy}^*(g_{xx}^* + g_{yy}^*) - f_{xx}^*g_{xx}^* + f_{yy}^*g_{yy}^*]. \end{aligned} \quad (8.37)$$

The Hopf bifurcation theorem holds for every version of l_1 , since only the sign is relevant in this case.

Theorem 8.3.1 (see, e.g., [GH83, Kuz04, MM76, Per01a, CLW94]). *A Hopf bifurcation is supercritical if $l_1 < 0$ and subcritical if $l_1 > 0$.*

The upshot is that for a positive scaling factor $\rho_v > 0$, we must have an equation of the form

$$l_1^v = \rho_v A$$

for each different version, such as $l_1^v = l_1^{GH}$ or $l_1^v = l_1^{CLW}$. One can calculate the scaling factor ρ_v by computing A and l_1^v for the same normal form (8.24). This yields a numerical strategy based on bifurcation software tools to analyze singular Hopf bifurcations in \mathbb{R}^2 :

- (S1) Compute the location of the Hopf bifurcation. This gives λ_H .
- (S2) Find the first Lyapunov coefficient at the Hopf bifurcation.
- (S3) Compute the location of the maximal canard by (8.33).

In most numerical codes, the steps (S1)–(S2) are already implemented. Therefore, it often suffices just to use step (S3). The problem is to check which convention for the first Lyapunov coefficient is used, i.e., to find the scaling factor $\rho_v > 0$.

Remark: We do not state any current software conventions here, since they might change on a more rapid time scale than this text. However, it is usually quite easy to determine from a manual, or the source code, which convention for the first Lyapunov coefficient is used.

Exercise/Project 8.3.2. Apply a numerical software bifurcation toolbox to the FitzHugh–Nagumo equation (1.13) to find periodic orbits undergoing canard explosion and to determine the first Lyapunov coefficient; see also Section 10.6. ◇

8.4 Canard Explosion

In Sections 8.1–8.3, we discussed planar fast–slow systems and how to find the singular Hopf bifurcation point as well as the maximal canard. These calculations are local near the folded singularity. Here we outline one possibility for the global dynamics. Consider a standard $(1, 1)$ -fast–slow system

$$\begin{aligned}\varepsilon \dot{x} &= f(x, y, \lambda), \\ \dot{y} &= g(x, y, \lambda),\end{aligned}\tag{8.38}$$

with parameter $\lambda \in \mathbb{R}$, where f, g are sufficiently smooth. We make the following assumptions:

- (A1) The critical manifold $C_0 = \{(x, y) \in \mathbb{R}^2 : f(x, y) = 0, y = h(x)\}$ is a smooth S-shaped curve with two generic fold points p_{\pm} . More precisely, assume that the critical manifold splits as follows:

$$C_0 = C_0^{a-} \cup \{p_-\} \cup C_0^r \cup \{p_+\} \cup C_0^{a+},$$

where $C_0^{a\pm}$ are normally hyperbolic attracting and C_0^r is normally hyperbolic repelling.

- (A2) p_- is a local maximum of h , while p_+ is a local minimum. For $\lambda = \lambda_c$, one of the folds, say p_+ , becomes a generic folded singularity, while the other fold, p_- , is a generic fold point, i.e., for $\lambda \in \mathbb{R}$, we have

$$\begin{aligned}f_x(p_{\pm}, \lambda) &= 0, \quad f_y(p_{\pm}, \lambda) \neq 0 \quad f_{xx}(p_-, \lambda) > 0, \quad f_{xx}(p_+, \lambda) < 0, \\ g_x(p_-, \lambda_c) &\neq 0, \quad g_{\lambda}(p_-, \lambda_c) \neq 0, \quad g(p_+, \lambda_c) = 0, \quad g(p_-, \lambda) \neq 0.\end{aligned}$$

- (A3) For $\lambda = \lambda_c$, the slow flow satisfies $\dot{x} < 0$ on $C_0^{a+} \cup C_0^r$, while $\dot{x} > 0$ on C_0^{a-} .

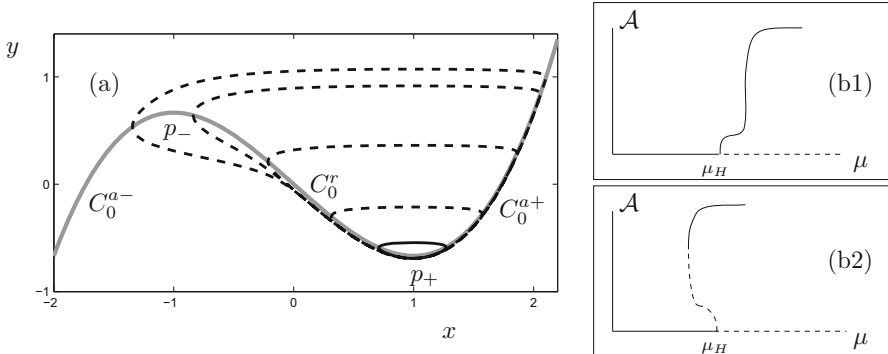


Figure 8.3: Canard explosion. (a) Periodic orbits generated in a singular Hopf bifurcation; here we used van der Pol's equation (8.40) for $\varepsilon = 0.05$. A typical small limit cycle near the Hopf bifurcation at $\lambda = \lambda_H$ is shown as a solid curve, whereas all the other periodic orbits (dotted curves) occur in a very small parameter interval at $\lambda \approx 0.993491$. Panels (b1) and (b2) show general sketches of the bifurcation diagrams corresponding to the supercritical (which is the case for van der Pol's equation) and the subcritical singular Hopf bifurcations. Here, \mathcal{A} denotes the amplitude of the limit cycle.

One should think of the planar van der Pol and FitzHugh–Nagumo systems, see Sections 1.3 and 1.4, as classical examples where the assumptions can be applied. Assumption (A2) allows us to apply the results from Sections 7.4 and 8.1 about folds. Figure 8.3(a) shows an example in which several periodic orbits are shown for different parameter values λ near the canard point value λ_c . After the singular Hopf bifurcation, the periodic orbits are small. When λ reaches the maximal canard value $\lambda = \lambda_c$, rapid growth of the periodic orbits occurs, as shown by the dashed periodic orbits in Figure 8.3(a). A further variation of the parameter leads to relaxation oscillations. In Figures 8.3(b1)–(b2), the possible bifurcation diagrams under variation of λ are shown.

It can be shown that the periodic orbits of “intermediate size” can be characterized as perturbations of so-called **singular canard cycles** for $\varepsilon = 0$. For the relaxation oscillations, we know this already from Sections 5.2 and 7.5, while the small Hopf cycles are covered in Sections 8.2 and 8.3.

Definition 8.4.1. Under the assumptions (A1)–(A3), define the continuous family $\gamma(s)$ of **singular canard cycles** consisting of candidate orbits for $s \in [0, 2s^*]$, where

- $\gamma(0)$ is the folded singularity p_+ , and $\gamma(2s^*)$ is a relaxation cycle;
- $\gamma(s)$ for $s \in (0, s^*]$ consists of candidates with slow segments on C_0^{a+} and C_0^r with one fast jump; these candidate cycles are also called **canards without head** or **jump-back canards** (see Figure 8.4(a));
- $\gamma(s)$ for $s \in (s^*, 2s^*)$ consists of candidates with slow segments on $C_0^{a\pm}$ and C_0^r with one fast jump from C_0^r to C_0^{a-} ; these candidate cycles are

also called **canards with head** or **jump-forward canards** (see Figure 8.4(b)).

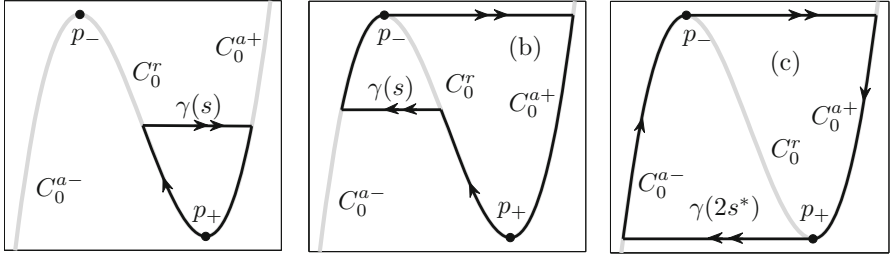


Figure 8.4: Singular canard cycles from Definition 8.4.1. (a) Canards without head. (b) Canards with head. (c) Relaxation oscillation. The periodic orbit in (b) gives another explanation of the translation canard (French = duck) if one draws an “eye” inside the upper left part, “legs” on the lower right, and some “feathers” in the upper right part.

The most important result about singular canard cycles is how they facilitate the transition between small and large limit cycles.

Theorem 8.4.2 ([KS01e]; see also [Die84, DR96b, Eck83]). *Suppose (A1)–(A3) hold, $0 < \varepsilon \ll 1$, and $\lambda_c(\sqrt{\varepsilon})$ is the maximal canard value (see Theorem 8.1.3). Then there exists a smooth parameterized family $s \mapsto (\lambda(s, \sqrt{\varepsilon}), \gamma(s, \sqrt{\varepsilon}))$ of periodic orbits (or **canard cycles**) growing from $\mathcal{O}(\varepsilon)$ amplitude to a relaxation oscillation within an exponentially small parameter interval*

$$|\lambda(s, \sqrt{\varepsilon}) - \lambda_c(\sqrt{\varepsilon})| = \mathcal{O}(e^{-K/\varepsilon}), \quad \text{for some } K > 0 \text{ as } \varepsilon \rightarrow 0.$$

Furthermore, $\gamma(s, \sqrt{\varepsilon}) \rightarrow \gamma(s, 0) = \gamma(s)$ in the Hausdorff distance as $\varepsilon \rightarrow 0$.

The result shows that the transition from small to large limit cycles is bound to look instantaneous in many applications due to the exponentially small parameter interval within which it occurs. Hence, the situation in Theorem 8.4.2 is referred to as a **canard explosion**.

To prove the bifurcation diagrams in Figure 8.3(b1)–(b2), one also has to investigate the stability of the canard cycles. Note that the parameterization $s \in [0, 2s^*] = [0, s^*) \cup [s^*, 2s^*]$ can be mapped, or chosen, so that the slow variable y is used as a parameter:

$$s \mapsto y \in [y(p_+), y(p_-)] \cup [y(p_-), 2y(p_-)],$$

where y marks the slow variable value at which the fast jump away from C_0^r occurs, i.e., $[y(p_+), y(p_-)]$ parameterizes canards without head, and $[y(p_-), 2y(p_-)]$ canards with head. With this convention, Theorem 8.4.2 can be made more precise to distinguish the super- and sub-critical singular Hopf bifurcations.

Theorem 8.4.3 ([KS01e]). Suppose (A1)–(A3) hold, $0 < \varepsilon \ll 1$, and $\nu \in (0, 1)$. Then there exists a smooth family of periodic orbits $s \mapsto (\lambda(s, \sqrt{\varepsilon}), \gamma(s, \sqrt{\varepsilon}))$. The canard explosion always occurs when $s \in [y(p_+) + \varepsilon^\nu, 2y(p_-) - \varepsilon^\nu]$,

$$|\lambda(s, \sqrt{\varepsilon}) - \lambda_c(\sqrt{\varepsilon})| \leq e^{-1/\varepsilon^\nu}, \quad (8.39)$$

where $\lambda_c(\sqrt{\varepsilon})$ is the maximal canard value. If the singular Hopf bifurcation is

- supercritical, then for $s \in (y(p_+), y(p_+) + \varepsilon^\nu)$, the family $\gamma(s, \sqrt{\varepsilon})$ is attracting, uniformly $\mathcal{O}(\varepsilon^\nu)$ -close to the folded singularity, and $\lambda(s, \sqrt{\varepsilon})$ is strictly increasing;
- subcritical, then for $s \in (y(p_+), y(p_+) + \varepsilon^\nu)$, the family $\gamma(s, \sqrt{\varepsilon})$ is uniformly $\mathcal{O}(\varepsilon^\nu)$ -close to the folded singularity and $\lambda(s, \sqrt{\varepsilon})$ is strictly decreasing. There exists a unique parameter value in the region (8.39) at which the family $\gamma(s, \sqrt{\varepsilon})$ undergoes a saddle node of limit cycles.

For $s \in [2y(p_-) - \varepsilon^\nu, 2y(p_-)]$, the orbit $\gamma(s, \sqrt{\varepsilon})$ is a relaxation oscillation, and $\lambda(s, \sqrt{\varepsilon})$ is strictly increasing.

The results in Theorem 8.4.3 are sketched in Figure 8.3(b1)–(b2). It should be pointed out that the stability of the periodic orbits in the subcritical case can again be computed using the constant A introduced in (8.25), since A is a scaled version of the first Lyapunov coefficient, as shown in Section 8.3.

To prove Theorems 8.4.2 and 8.4.3, several techniques exist; see Section 8.9. We shall not develop the details of the proof here. If one uses the blowup method, the previous results on generic and singular fold point blowups can be used. The family of periodic orbits can be constructed by piecing together dynamics in two blowup regions near p_\pm with fast jumps and slow flow on normally hyperbolic parts of the critical manifold.

Example 8.4.4. The classical example for canard explosion is van der Pol's equation with constant forcing λ , which is given as a (1, 1)-fast–slow system by

$$\begin{aligned} \varepsilon \dot{x} &= y - \frac{x^3}{3} + x, \\ \dot{y} &= \lambda - x. \end{aligned} \quad (8.40)$$

Theorems 8.4.2 and 8.4.3 apply immediately, since the critical manifold $C_0 = \{(x, y) \in \mathbb{R}^2 : y = x^3/3 - x\}$ is S-shaped when viewed in (y, x) -phase space. The fold points are $p_\pm = \pm 1$. It is easily checked that at $\lambda = 1$, the fold p_- is generic and p_+ is a folded singularity. The singular Hopf bifurcation is supercritical. The numerical calculations for (8.40) in Figure 8.3(a) were carried out using numerical continuation as described in Section 10.6. The numerics nicely match the theoretical predictions. ♦

8.5 Canards in \mathbb{R}^3

In planar systems in \mathbb{R}^2 , canards occur only generically in one-parameter families. The situation is different in three-dimensional fast–slow systems. To get a basic understanding of what can happen in this situation, we begin with a simple example.

Example 8.5.1. Consider the $(1, 2)$ -fast–slow system

$$\begin{aligned}\varepsilon \frac{dx}{d\tau} &= \varepsilon \dot{x} = x^2 + y_1, \\ \frac{dy_1}{d\tau} &= y_1 = -2y_2, \\ \frac{dy_2}{d\tau} &= y_2 = 1.\end{aligned}\tag{8.41}$$

The critical manifold $C_0 = \{(x, y) \in \mathbb{R}^3 : y_1 = -x^2\}$ is a parabolic cylinder containing a line of fold points $L = \{(x, y_1, y_2) \in \mathbb{R}^3 : x = 0 = y_1\}$; see Figure 8.5. The left branch of C_0 given by $C_0 \cap \{x < 0\}$ is normally hyperbolic attracting, while the right branch $C_0 \cap \{x > 0\}$ is repelling. The slow subsystem on C_0 in (x, y_2) -coordinates is given by

$$\begin{aligned}\dot{x} &= \frac{y_2}{x}, \\ \dot{y}_2 &= 1.\end{aligned}\tag{8.42}$$

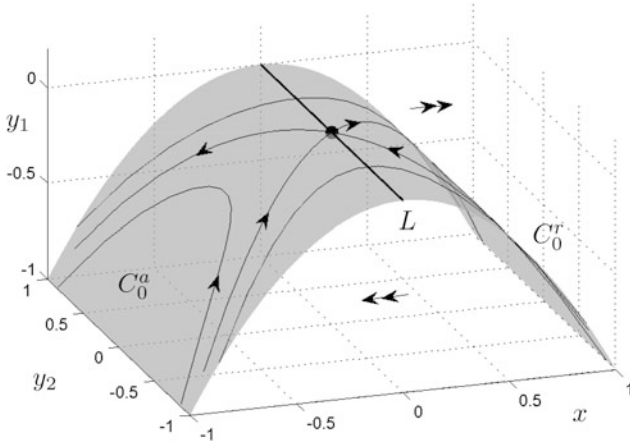


Figure 8.5: Illustration of the geometry for (8.41). The critical manifold C_0 (gray), the fold curve L (thick black line), and the slow flow of (8.42) (thin black curves, single arrows) are shown. The origin $(x, y_1, y_2) = (0, 0, 0)$ (black dot) is an equilibrium point for the desingularized slow flow (8.43).

We can desingularize the slow flow, multiplying the vector field by x and rescaling time. This reverses the orientation of time for the slow flow on the left attracting branch on C_0 ; see Section 7.7. The desingularized slow flow is

$$\begin{aligned}\dot{x} &= y_2, \\ \dot{y}_2 &= x.\end{aligned}\tag{8.43}$$

The slow flow (8.42) and its desingularized version (8.43) are shown in Figure 8.6. Note that (8.43) has a usual saddle point at the origin, whereas the origin in (8.42) is part of two special trajectories that cross each other and pass straight through the singularity at nonzero speed. Similar to the discussion of

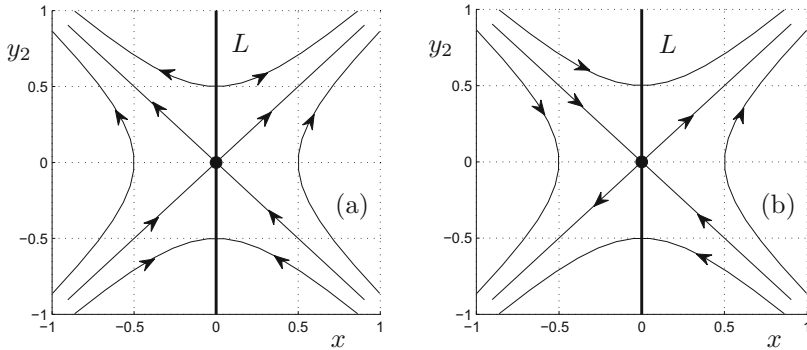


Figure 8.6: (a) Slow flow (8.42). (b) Desingularized slow flow (8.43).

folded singularities in \mathbb{R}^2 in Sections 8.1 and 8.2, these trajectories indicate that there is a possibility for canards in the full system (8.41). Indeed, it is easy to check that (8.41) has two exact solutions:

$$(x(\tau), y_1(\tau), y_2(\tau)) = (-\tau^2 \pm \varepsilon, \tau, \pm\tau).$$

Both solutions have algebraic growth and hence must lie on the slow manifold of the system C_ε for all time. They turn out to be the perturbations of the two special trajectories in (8.42). ♦

For $(1, 1)$ -fast–slow systems, one has only to consider a single candidate trajectory as a candidate for a canard orbit. However, Example 8.5.1 shows that multiple candidate trajectories can be relevant, which makes the following terminology useful:

Definition 8.5.2. Trajectories of the slow flow lying in the attracting and repelling parts of the critical manifold are called **singular canards**. If the slow flow trajectory passes from a repelling to an attracting branch of the critical manifold, it is called a **singular faux canard**.

A reasonable strategy is to classify the singularities that can occur in the slow flow and check which ones admit singular canard solutions. Then one has to determine which of the singular canard solutions persist and what they correspond to in the full system. We begin with a general $(1, 2)$ -fast–slow system:

$$\begin{aligned} \varepsilon \dot{x} &= f(x, y_1, y_2, \varepsilon), \\ \dot{y}_1 &= g_1(x, y_1, y_2, \varepsilon), \\ \dot{y}_2 &= g_2(x, y_1, y_2, \varepsilon). \end{aligned} \tag{8.44}$$

Recall from Section 4.3 that the critical manifold

$$C_0 = \{(x, y_1, y_2) \in \mathbb{R}^3 : f(x, y_1, y_2, 0) = 0\}$$

of (8.44) is generically a surface, and points P with $f_x(P, 0) = 0$ are usually not isolated but form a one-dimensional curve L inside C_0 . Obviously, we may

translate a single point of interest in L to the origin $(x, y_1, y_2) = (0, 0, 0)$. Hence, assume without loss of generality that the origin is a fold point. With the usual shorthand notation $(0, 0, 0, 0) =: 0$, the conditions for a nondegenerate fold point are

$$f(0) = 0, \quad f_x(0) = 0, \quad f_{xx}(0) \neq 0, \quad f_{y_1}(0) \neq 0. \quad (8.45)$$

The fold curve L can be parameterized by y_2 under the previous assumptions (see Section 4.3):

$$L = \{(\theta(y_2), \psi(y_2), y_2) \in \mathbb{R}^3 : y_2 \in I\},$$

where I is a sufficiently small interval around 0. In addition, recall that the function

$$l(y_2) := \begin{pmatrix} f_{y_1} \\ f_{y_2} \end{pmatrix} \cdot \begin{pmatrix} g_1 \\ g_2 \end{pmatrix}_{(\theta(y_2), \psi(y_2), y_2)}$$

played a key role in defining the normal switching condition $l(0) \neq 0$. It is easy to check that this condition is violated in Example 8.5.1 at the origin. Therefore, we can extend the definition of a folded singularity, given in Definition 8.1.1 for $(1, 1)$ -fast–slow systems, to $(1, 2)$ -fast–slow systems.

Definition 8.5.3. The origin $0 \in C_0$ is called a **folded singularity** of a $(1, 2)$ -fast–slow system if it satisfies (8.45) and

$$l(0) = 0. \quad (8.46)$$

Remark: The concept of folded singularities naturally extends to more general (m, n) -fast–slow systems. In fact, Definition 3.3.2 still applies, and the normal switching condition can also be expressed abstractly as a transversality hypothesis of slow flow trajectories to submanifolds of fold points.

Lemma 8.5.4 ([Wec98]). *Assume that the origin is a folded singularity for (8.44). Then there exists a coordinate change such that near the origin, we can write (8.44) in the form*

$$\begin{aligned} \varepsilon \dot{x} &= y_1 + x^2 + \mathcal{O}(\varepsilon x, \varepsilon y_1, \varepsilon y_2, \varepsilon^2, y_1^2 x, x^3, x y_1 y_2), \\ \dot{y}_1 &= b y_2 + c x + \mathcal{O}(y_1, \varepsilon, y_2^2, x y_2, x^2), \\ \dot{y}_2 &= a + \mathcal{O}(x, y_1, y_2, \varepsilon). \end{aligned} \quad (8.47)$$

The constants a, b, c are computable from the Taylor expansion of the original vector field.

Proof. First, use the fold point conditions to get the normal form for the critical manifold (see Section 4.3, Theorem 4.3.1). This yields the equation for $\varepsilon \dot{x}$. The parameterization $(\theta(y_2), \psi(y_2), y_2)$ of the fold curve can be used to rectify it along the y_2 -axis using the map $(x, y_1, y_2) \mapsto (x - \theta(y_2), y_1 - \psi(y_2), y_2)$. Then we can Taylor expand f, g_1 and g_2 and use the canard point condition (8.46) to conclude that $g_1(0) = 0$. \square

More detailed higher-order terms and/or additional parameters in (8.47) will be needed in certain situations. For now, we shall work with (8.47). The critical manifold near the origin is given by

$$C_0 = \{(x, y_1(x, y_2), y_2) \in \mathbb{R}^3 : y_1(x, y_2) = -x^2(1 + \mathcal{O}(x, y_2))\},$$

where $y_1(x, y_2)$ is a function obtained from the implicit function theorem. Observe that C_0 is split into a repelling part C_0^r for $x > 0$, an attracting branch for C_0^a for $x < 0$, and the fold line L along the y_2 -axis; see Figure 8.5.

Lemma 8.5.5. *The desingularized slow flow of (8.47) is given by*

$$\begin{aligned}\dot{x} &= by_2 + cx + \mathcal{O}(y_2^2, xy_2, x^2), \\ \dot{y}_2 &= -2ax + \mathcal{O}(xy_2, x^2).\end{aligned}\tag{8.48}$$

Proof. First, differentiate $y_1(x, y_2)$ implicitly with respect to time, which yields the slow subsystem

$$\begin{aligned}-2x(1 + \mathcal{O}(\dots))\dot{x} &= by_2 + cx + \mathcal{O}(\dots), \\ y_2 &= a + \mathcal{O}(\dots),\end{aligned}\tag{8.49}$$

where $\mathcal{O}(\dots)$ denotes the higher-order terms. Next, multiplying the right-hand side of (8.49) by $-2x(1 + \mathcal{O}(\dots))$ and using a time rescaling (see also Section 7.7) yields the result. \square

Note very carefully that the time for (8.48) is reversed on C_0^r in comparison to the slow subsystem (8.49) without desingularization. The origin is now an equilibrium point for (8.48). The linearization A and eigenvalues of (8.48) at the origin are

$$A = \begin{pmatrix} c & b \\ -2a & 0 \end{pmatrix} \quad \Rightarrow \quad \lambda_{\pm} = \frac{c \pm \sqrt{c^2 - 8ab}}{2}.\tag{8.50}$$

It is straightforward to classify equilibria at the origin based on the eigenvalues. However, for planar vector fields, an even simpler tool is available using $\text{tr}(A) = c$ and $\det(A) = 2ab$ to draw the trace-determinant plane with the parabola $[\text{tr}(A)]^2 = 4\det(A)$; see [HSD03, Str00]. The next two results follow immediately.

Lemma 8.5.6. *For $ab > 0$, the origin in (8.48) has the following nondegenerate types:*

$$\begin{array}{ll} c > 0, \ 8ab < c^2 & \text{unstable node}; \quad c > 0, \ c^2 < 8ab & \text{unstable focus/spiral}; \\ c < 0, \ 8ab < c^2 & \text{stable node}; \quad c < 0, \ c^2 < 8ab & \text{stable focus/spiral}; \end{array}$$

while for $ab < 0$, the equilibrium is a saddle point.

The nondegenerate types are of codimension zero and occur generically in $(1, 2)$ -fast–slow vector fields; see Figure 8.7. The degenerate types in the next lemma are of codimension one and occur generically in one-parameter families of $(1, 2)$ -fast–slow vector fields.

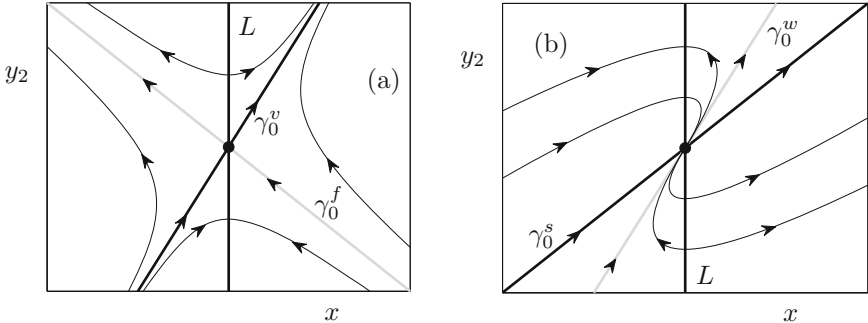


Figure 8.7: Equilibria for the slow flow (8.42) (i.e., without desingularization); the trajectories were generated using the linear system $(\dot{x}, y_2)^\top = A(x, y_2)^\top$ with matrix A given in (8.50). (a) Folded saddle: two singular canard orbits γ_0^f (gray, “faux canard”) and γ_0^v (black, “vrai canard”) are shown. (b) Folded node: two singular canard orbits γ_0^w (gray, “weak canard”) and γ_0^s (black, “strong canard”) are shown.

Lemma 8.5.7. *The origin in (8.48) has the following (codimension-one) degenerate types for $c \neq 0$:*

$$\begin{aligned} ab = 0, \quad a \neq 0 & \quad \text{saddle-node type I,} \\ ab = 0, \quad b \neq 0 & \quad \text{saddle-node type II,} \\ 8ab = c^2, & \quad \text{degenerate node.} \end{aligned}$$

For $c = 0$, the only degenerate type occurs for $ab > 0$, which is a center.

Lemma 8.5.7 contains an implicit definition distinguishing two different types of saddle node; see also Figure 8.8.

Definition 8.5.8. An equilibrium point of the desingularized slow flow is called a **folded saddle**, **folded node**, **folded focus**, **folded saddle-node** or **folded center** depending on which of the cases in Lemma 8.5.6 or Lemma 8.5.7 applies. We also refer to the corresponding points in the nondesingularized slow flow (8.49) with the same terminology.

Remark: In this section we shall not discuss the degenerate cases from Lemma 8.5.7 or any cases of higher codimension. However, since the folded saddle-node case will be important in Section 13.3, the geometry is shown in Figure 8.8.

For the folded saddle, there exist two singular canards γ_0^v and γ_0^f , as shown in Figure 8.7. Observe that γ_0^v (the “**vrai canard**” or just the “canard”) corresponds to the stable manifold of the saddle and passes from C_0^a to C_0^r . The singular canard γ_0^f (the “**faux canard**”) corresponds to the unstable manifold of the saddle and passes from C_0^r to C_0^a . For the folded node, there exist a singular canard γ_0^s corresponding to the strong eigenvalue of the node and a singular canard γ_0^w corresponding to the weak eigenvalue. The other solutions of the desingularized slow flow are tangent to the weak eigendirection. A folded

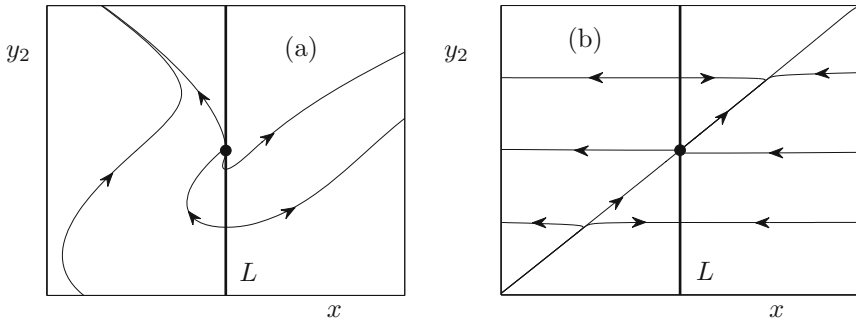


Figure 8.8: Degenerate equilibria for the slow flow (8.42) (i.e., without desingularization). (a) Folded saddle node of type I. (b) Folded saddle node of type II.

focus does not have singular canards. The folded saddle nodes have a singular canard corresponding to the hyperbolic eigendirection of the desingularized slow flow.

It helps to introduce additional notation for the eigenvalues to indicate immediately which case is under discussion. For the folded saddle, denote the eigenvalues associated with γ_0^v and γ_0^f by λ_v and λ_f respectively.

Proposition 8.5.9 ([SW01]). *A singular faux canard corresponds to a positive eigenvalue, i.e., $\lambda_v < 0 < \lambda_f$.*

Exercise 8.5.10. Prove Proposition 8.5.9. \diamond

For the folded node, denote the eigenvalues associated with γ_0^s and γ_0^w by λ_s and λ_w respectively, i.e., $|\lambda_s| > |\lambda_w|$. Also, denote the ratio of the eigenvalues by

$$\mu := \frac{\lambda_w}{\lambda_s} \in (0, 1).$$

Obviously, one is interested in perturbations of singular canards for $0 < \varepsilon \ll 1$.

Theorem 8.5.11 ([Ben82, Ben90, SW01]). *The following hold for a given a (1, 2)-fast-slow vector field (8.47) with a nondegenerate folded singularity and ε sufficiently small:*

- (R1) *For a folded saddle or a folded node, the singular canard solutions γ_0^v and γ_0^s always perturb to maximal canard solutions in $C_\varepsilon^a \cap C_\varepsilon^r$.*
- (R2) *For a folded node, the weak singular canard γ_0^w perturbs to a maximal canard as long as $\mu^{-1} \notin \mathbb{N}$.*

We shall discuss in Section 8.6 what happens in the case of resonances $\mu^{-1} \in \mathbb{N}$ for a folded node.

Proof. (of Theorem 8.5.11, sketch; see [SW01]) The general strategy demonstrated in Section 7.4 applies to (8.47). The main idea is to show that the slow

manifolds C_ε^a and C_ε^r intersect transversally along perturbations of singular canards. The correct weighted polar blowup $\varphi : S^3 \times I \rightarrow \mathbb{R}^4$ is

$$x = r\bar{x}, \quad y_1 = r^2\bar{y}_1, \quad y_2 = r\bar{y}_2, \quad \varepsilon = r^2\bar{\varepsilon} \quad (8.51)$$

with $(\bar{x}, \bar{y}_1, \bar{y}_2, \bar{\varepsilon}) \in S^3$ and $r \in I$ for a suitable interval I containing 0. It turns out to be sufficient to consider two directional blowups in charts κ_1 and κ_2 corresponding to $\bar{y}_1 = -1$ and $\bar{\varepsilon} = 1$. In the chart κ_2 , sometimes also called the **classical chart** or the **rescaling chart**, one can obtain special solutions to the blown-up vector field that are extensions of singular canards. In the chart κ_1 , these solutions can be connected to the normally hyperbolic slow manifolds. Using the variational equation in the chart κ_2 along the special solutions will establish the required transversality. The situation is shown abstractly in Figure 8.9.

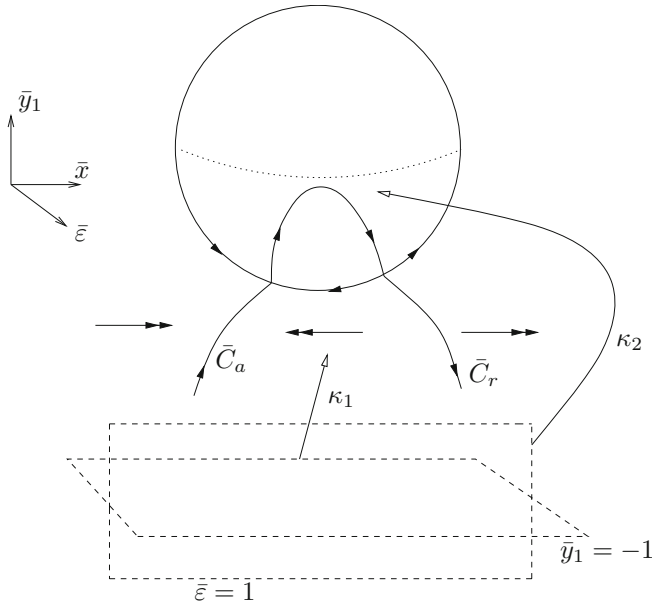


Figure 8.9: Partial sketch of blowup (8.51). The two charts will be used for different parts of the dynamics; κ_2 covers dynamics on the sphere, and κ_1 covers dynamics outside of it.

In the chart κ_2 , we have $\bar{\varepsilon} = 1$. This means that $\varepsilon = r^2$, so that $r = \sqrt{\varepsilon}$. Hence we just have a rescaling of the vector field (8.47) given by

$$(x, y_1, y_2) \mapsto (\varepsilon^{1/2}\bar{x}, \varepsilon\bar{y}_1, \varepsilon^{1/2}\bar{y}_2).$$

It turns out that the higher-order terms will not matter for our analysis in κ_2 ,

so we just apply the rescaling to

$$\begin{aligned} x' &= y_1 + x^2, \\ y'_1 &= \varepsilon(by_2 + cx), \\ y'_2 &= \varepsilon a. \end{aligned}$$

After the rescaling, the result is

$$\begin{aligned} \bar{x}' &= \varepsilon^{1/2}(\bar{y}_1 + \bar{x}^2), \\ \bar{y}_1 &= \varepsilon^{1/2}(b\bar{y}_2 + c\bar{x}), \\ \bar{y}_2 &= \varepsilon^{1/2}a, \end{aligned} \quad (8.52)$$

and the desingularization (dividing by $r = \varepsilon^{1/2}$) yields

$$\begin{aligned} \bar{x}' &= \bar{y}_1 + \bar{x}^2, \\ \bar{y}_1 &= b\bar{y}_2 + c\bar{x}, \\ \bar{y}_2 &= a. \end{aligned} \quad (8.53)$$

It is a crucial observation made by Benoit that (8.53) has special solutions γ_{\pm} for $b \neq 0$, real $\lambda_{\pm} \neq 0$ (cf. Example 8.5.1),

$$(\bar{x}(t), \bar{y}_1(t), \bar{y}_2(t)) = \left(\frac{\lambda_{\pm}}{2}t, -\frac{\lambda_{\pm}^2}{4}t^2 - \frac{\lambda_{\pm}}{2}, at \right). \quad (8.54)$$

Note that in the case of a folded saddle and a folded node, we have nonzero real eigenvalues and $b \neq 0$. The importance of the special solutions is that they are of algebraic growth and form key connections between the attracting and repelling slow manifolds. After quite a few calculations, the variational equation along the transformed special solutions in κ_2 reduces to

$$\frac{d^2u}{dT^2} - 2T \frac{du}{dT} + 2(\mu_{\pm} - 1)u = 0 \quad \text{with } \mu_{\pm} := \frac{\lambda_+ \lambda_-}{\lambda_{\pm}^2}. \quad (8.55)$$

Sometimes, (8.55) is also called the **Weber equation**. However, there are several families of differential equations that are called Weber equations. It turns out that the special solutions γ_{\pm} in the chart κ_2 are transformed to the trivial solution with respect to the variational equation (8.55). Hence, the slow manifolds will intersect along the special solutions representing the singular canards transversally if and only if (8.55) has only nontrivial solutions that grow exponentially in forward or backward time. Now facts about the Weber equation (8.55) (see [AS65]) can be used. It has only nontrivial exponentially growing solutions in either forward or backward time for $\mu_{\pm} \notin \mathbb{N}$.

Next, recall the eigenvalue notation conventions introduced before Theorem 8.5.11 and consider the folded node and folded saddle cases separately. In the folded saddle case, we have $\lambda_v < 0 < \lambda_f$, and so $\mu_{\pm} < 0$. Therefore, the singular canard always perturbs to a maximal canard in this case. In the folded node case, we have $|\lambda_s| > |\lambda_w|$ and $\lambda_s \lambda_w > 0$, which implies that $\mu_s \in (0, 1)$. Therefore, the singular strong canard γ_0^s again perturbs to a maximal canard.

For μ_w in the folded node case, we know only that $\mu_w > 1$, which implies that the singular canard γ_0^w corresponding to the weak eigendirection for a folded node perturbs to a maximal canard as long as $\mu_w \notin \mathbb{N}$.

In the chart κ_1 , we can again derive a differential equation in blown-up coordinates. Using a coordinate change from κ_2 to κ_1 , one can match the special solutions to the slow manifolds in the chart κ_1 . This completes the outline of the proof. \square

In addition to the existence of the canard solutions, one may say quite a bit more about geometry in the case of the folded node.

Theorem 8.5.12 ([SW01, BKW06]). *In the case of a folded node with $n - 1 < \mu^{-1} < n$, the slow manifolds C_ε^a and C_ε^r twist $n - 1$ times around the maximal canard solution associated with the weak eigendirection. A twist corresponds to a rotation by 180° .*

Theorem 8.5.12 follows from a more detailed analysis of the solutions to (8.55). It will be very useful when we discuss mixed-mode oscillations in Section 13.2. It is also worth noting that (8.55) is solved by **Hermite polynomials** $H_{n-1}(T)$ for $n = \mu_\pm \in \mathbb{N}$; see [AS65]. These particular solutions to the variational equation can be used to determine the geometry of the canards near and at the resonances; see Section 8.6.

Remark: The rescaled vector field (8.53) can be viewed as a **system of first approximation** for a generic folded singularity. We developed the basic ideas of systems of first approximation in the case of nondegenerate fold point in Section 4.4. Very similar ideas were used to derive (8.53). A rescaling of the variables leads to equations (8.52). Then dividing by $r = \varepsilon^{1/2}$ yields the result that corresponds to the time rescaling used to derive the systems of first approximation in Section 4.4. In fact, it is often a good guiding principle that the desingularized blown-up system in the rescaling chart should be the system of first approximation.

Example 8.5.13. For a classical example that exhibits folded singularities, consider the periodically forced van der Pol equation

$$\begin{aligned} \varepsilon \dot{x} &= y - \frac{x^3}{3} + x, \\ \dot{y} &= a \sin(2\pi\theta) - x, \\ \dot{\theta} &= \omega, \end{aligned} \tag{8.56}$$

where $(x, y, \theta) \in \mathbb{R}^2 \times S^1$ and $a, \omega > 0$ are parameters. Here we describe S^1 as $[0, 1]$ with endpoints identified. The critical manifold is

$$C_0 = \left\{ (x, y, \theta) \in \mathbb{R}^2 \times S^1 : y = \frac{1}{3}x^3 - x \right\}.$$

It is easy to check that it has two attracting sheets $C_0^{a-} = C_0 \cap \{x < -1\}$, $C_0^{a+} = C_0 \cap \{x > 1\}$ and a repelling sheet $C_0^r = C_0 \cap \{-1 < x < 1\}$. There are fold points on two lines:

$$L_- = \left\{ \left(-1, \frac{2}{3}, \theta \right) \in \mathbb{R}^2 \times S^1 \right\} \quad \text{and} \quad L_+ = \left\{ \left(1, -\frac{2}{3}, \theta \right) \in \mathbb{R}^2 \times S^1 \right\}.$$

Differentiating the equation $y = \frac{1}{3}x^3 - x$ implicitly with respect to time leads to the slow subsystem

$$\begin{aligned}(x^2 - 1)\dot{x} &= a \sin(2\pi\theta) - x, \\ \dot{\theta} &= \omega.\end{aligned}$$

The desingularized slow flow is obtained via multiplication by $(x^2 - 1)$ and by a time rescaling that reverses the orientation of time on C_0^r :

$$\begin{aligned}\dot{x} &= a \sin(2\pi\theta) - x, \\ \dot{\theta} &= \omega(x^2 - 1).\end{aligned}\tag{8.57}$$

All equilibrium points of (8.57) lie on the fold lines L_{\pm} , and hence they are folded singularities. We focus on the line L_+ and henceforth assume $x = 1$. One has to solve $1/a = \sin(2\pi\theta)$ to locate the folded singularities. Therefore, $a < 1$ yields no solution. For $a = 1$, we have one folded singularity at $(x, \theta) = (1, 1/4)$, and for $a > 1$, we get two folded singularities,

$$\begin{aligned}p_1 &= (1, \theta_1), \quad \text{where } \theta_1 = \frac{1}{2\pi} \sin^{-1}(1/a) \text{ and } \theta_1 < 1/4, \\ p_2 &= (1, \theta_2), \quad \text{where } \theta_2 = \frac{1}{2\pi} \sin^{-1}(1/a) \text{ and } \theta_2 > 1/4.\end{aligned}$$

To check the types of equilibria we calculate the linearization of (8.56):

$$A := \begin{pmatrix} -1 & 2\pi a \cos(2\pi\theta) \\ 2\omega x & 0 \end{pmatrix}.$$

For $a = 1$, $x = 1$, and $\theta = 1/4$, it follows that A has eigenvalues -1 and 0 , which implies a saddle node. For $a > 1$, the eigenvalues of A are real as long as $a < \sqrt{1 + 1/(16\pi\omega)^2}$. A direct eigenvalue calculation shows that in this case, p_1 is a folded node and p_2 is a folded saddle. Therefore, Theorem 8.5.11 shows that (8.56) has maximal canards lying close to the repelling slow manifold C_ε^r for ε sufficiently small. The bifurcation structure of the van der Pol equation with periodic forcing turns out to be very complicated. In Sections 14.4 and 14.5, several visualizations are computed, and it is proved that the periodically forced van der Pol equation can exhibit chaotic behavior for certain ranges of parameters. ♦

Exercise/Project 8.5.14. Show that the folded saddle node for $a = 1$, $x = 1$, and $\theta = 1/4$ is of type I (see Lemma 8.5.7 for the definition). What happens for $a > \sqrt{1 + 1/(16\pi\omega)^2}$ and which folded singularities occur on the line L_- ? ◊

8.6 Secondary Canards at Folded Nodes

We continue with the notation introduced in the last section. Theorem 8.5.11 classifies maximal canards near a folded saddle. For folded nodes, the key condition is the absence of resonances, i.e., $\mu^{-1} = \lambda_s/\lambda_w \notin \mathbb{N}$ for the eigenvalues $\lambda_{s,w}$ of the linearization of the desingularized slow subsystem at the folded node. Away from resonances, the two singular canards $\gamma_0^{s,w}$ perturb to maximal canards $\gamma_\varepsilon^{s,w}$. It remains to determine what happens at a resonance for a folded node.

Observe that the normal form (8.47) contains three parameters a, b, c , which is too general for the case of a folded node. A folded node is generic in $(1, 2)$ -fast–slow systems. Hence, a normal form should not contain any parameters. However, since the ratio of the eigenvalues matters for the quantitative structure such as twisting of the slow manifolds, one should retain at least one parameter. The next theorem confirms this logic.

Theorem 8.6.1 ([Arn94]). *The system of first approximation for a $(1, 2)$ -fast–slow system (8.44) near a generic folded singularity is given by*

$$\begin{aligned}\frac{dX}{dT} &= Y_1 - X^2, \\ \frac{dY_1}{dT} &= 2X + A(\varepsilon)Y_2, \\ \frac{dY_2}{dT} &= \pm 1,\end{aligned}\tag{8.58}$$

which is valid for $|X| < 1$, $|Y_1| < 1$, $|Y_2| < 1$, and error terms of order $\mathcal{O}(\varepsilon^{1/2})$.

Proof. (Sketch, [Arn94]) The equation for X follows from Theorem 4.3.1. To remove the ε -dependence, apply the rescaling

$$(x, y_1, y_2, t) \mapsto (\varepsilon^{1/2}X, \varepsilon Y_1, \varepsilon^{1/2}Y_2, \varepsilon^{1/2}T).\tag{8.59}$$

The result follows by direct calculation, where the ε -dependence for the free parameter arises due to the ε -dependent transformations. \square

The details of the proof for Theorem 8.6.1 are similar to the generic fold point in Theorem 4.4.3. Note that the rescaling (8.59) is the same as that used to obtain the classical chart κ_2 in the proof of Theorem 8.5.11; see the discussion following the proof of that theorem. Exercise 8.6.2 also helps to understand how to transition from (8.47) to (8.58).

Exercise 8.6.2. Determine the transformations that reduce

$$\begin{aligned}\varepsilon\dot{x} &= y_1 - x^2, \\ \dot{y}_1 &= p_1x + p_2y_2, \\ \dot{y}_2 &= p_3,\end{aligned}\tag{8.60}$$

to the system of first approximation (8.58). What assumptions do you have to make on the parameters p_i ? \diamond

It is interesting to use numerical simulation to understand canards near a folded node.

Example 8.6.3. Consider a time-reversed version of the system of first approximation (8.58) written in the form

$$\begin{aligned}\dot{x} &= -x^2 + y_1, \\ \dot{y}_1 &= -2x + ay_2, \\ \dot{y}_2 &= 1.\end{aligned}\tag{8.61}$$

Observe that (8.61) has a time-reversing symmetry σ given by

$$\sigma(x, y_1, y_2, t) = (-x, y_1, -y_2, -t).\tag{8.62}$$

This symmetry will be used later on to simplify the numerical calculations. The geometry of the slow manifolds near the folded node at the origin is particularly intriguing. The desingularized slow subsystem is

$$\begin{aligned}\dot{x} &= -2x + ay_2, \\ \dot{y}_2 &= 2x.\end{aligned}$$

The eigenvalues of the linear desingularized slow flow are

$$\lambda_- = -1 - \sqrt{1+2a} = \lambda_s \quad \text{and} \quad \lambda_+ = -1 + \sqrt{1+2a} = \lambda_w.$$

Therefore, we have a stable folded node for $a \in (-1/2, 0)$. The inverse ratio of the eigenvalues $\mu^{-1} = \lambda_s/\lambda_w$ runs through all natural numbers if we start with $a = -1/2$ and approach $a = 0$, i.e., we go through all possible resonances. The critical manifold $C_0 = \{(x, y_1, y_2) \in \mathbb{R}^3 : x^2 = y_1\}$ of (8.61) splits into attracting and repelling parts,

$$C_0^a = \{(x, y_1, y_2) \in \mathbb{R}^3 : x > 0\} \quad \text{and} \quad C_0^r = \{(x, y_1, y_2) \in \mathbb{R}^3 : x < 0\}.$$

Figure 8.10 shows trajectories in the slow manifolds C_ε^a and C_ε^r up to the cross section $\{y_2 = 0\}$. The trajectory in C_ε^a was obtained by forward integration, and the trajectory in C_ε^r by applying the symmetry σ from (8.62). Alternatively, one also may use integration backward in time in this context. To understand the canards, consider the intersection of C_ε^a and C_ε^r on a section

$$\Sigma := \{(x, y_1, y_2) \in \mathbb{R}^3 : y_2 = 0\}.$$

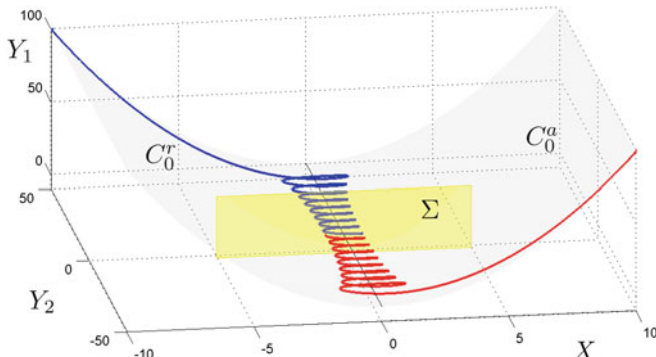


Figure 8.10: Partial trajectories of (8.61) in red and blue for $a = -0.001$. The red trajectory is contained in the slow manifold C_ε^a , and the blue one is in C_ε^r . The critical manifold C_0 is shown in gray and a part of the section $\Sigma = \{y_2 = 0\}$ in yellow, where the trajectories are truncated. The fold points lie on the y_2 -coordinate axis. Note carefully that the system of first approximation is a zoom-in near the folded node, so the scale might be misleading at first.

Numerical integration for a grid of values $(x, x^2, -50)$ for $x \in (0, 25)$ yields trajectories which were computed up to Σ . This gives a numerical representation

of the intersection $C_\varepsilon^a \cap \Sigma$. To obtain $C_\varepsilon^r \cap \Sigma$, the symmetry σ has been applied. The results in (x, y_1) -coordinates on Σ are shown in Figure 8.11.

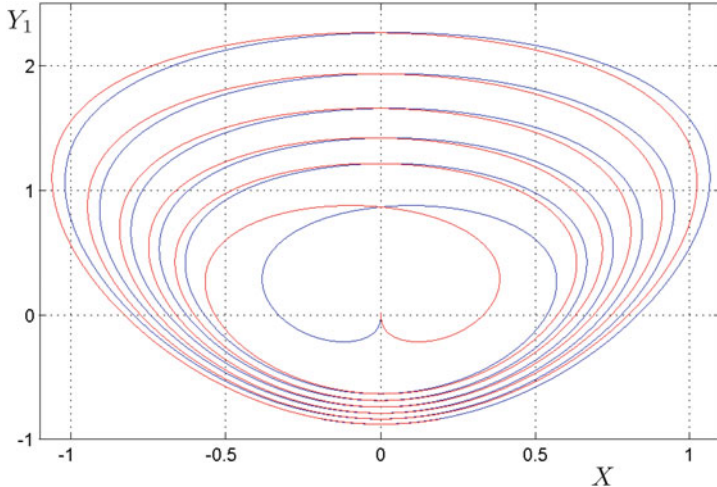


Figure 8.11: Intersection of the slow manifolds on the section Σ ; $C_{a,\varepsilon}$ is in red and $C_{r,\varepsilon}$ is in blue.

It is clearly visible from Figure 8.11 that there are more than two intersections between the two slow manifolds, i.e., we observe more canards than just the two maximal canards from Theorem 8.5.11. Since the parameter a for the numerical simulation was quite small ($a = -0.001$), many resonances have been encountered, since $a = -1/2$ is the starting point for resonances. Therefore, one conjectures that additional maximal canards are generated at resonant values.

♦

Exercise/Project 8.6.4. Use a numerical integration routine to reproduce Figure 8.11; see also Chapter 10. Now vary the parameter a and try to determine the number of intersection points in $C_\varepsilon^a \cap C_\varepsilon^r$. ♦

Definition 8.6.5. All maximal canards not obtained as a perturbation of the two singular canards $\gamma_0^{s,w}$ using Theorem 8.5.11 are called **secondary canards**.

Secondary canards are actually visible as singular canards for the desingularized slow flow. Figure 8.7(b) shows a folded node with the strong and weak eigendirections for the equation

$$\begin{aligned}\dot{x} &= by_2 + cx, \\ \dot{y}_2 &= -2ax,\end{aligned}\tag{8.63}$$

with $0 < 8ab < c^2$. This leads to the observation that there are two special trajectories $\gamma_0^{s,w}$ that pass at nonzero speed through a folded node. In fact, a closer look at the situation leads to the improved observation that a whole sector $S_0 \subset C_0^a$, bounded by the strong singular canard γ_0^s and the fold line L ,

of trajectories passes through the folded node; see Figure 8.7(b). Perturbations of slow subsystem trajectories lying in \mathcal{S}_0 are also good candidates for obtaining maximal canards. Here we restrict ourselves to statements of the known results and a geometric description of the situation. The first result gives already a broad view that many additional maximal canards are generated.

Theorem 8.6.6 ([GH05]). *For the system of first approximation (8.61), the number of maximal canards becomes unbounded as $a \rightarrow 0^-$. More precisely, the number of trajectories that remain at a bounded distance from the critical manifold for all time is $\mathcal{O}(-1/a)$.*

A more detailed classification can be given that relies on bifurcations at resonances. We outline the steps of this analysis, which basically continues the proof of Theorem 8.5.11. Beginning with Theorem 8.6.1 or with the truncated system in the classical chart κ_2 in the proof of Theorem 8.5.11, the next lemma follows after a few calculations.

Lemma 8.6.7. *The system of first approximation given by (8.58) for a $(1, 2)$ -fast-slow system near a generic folded node singularity can be transformed to*

$$\begin{aligned} X' &= X^2 + Y_1, \\ Y'_1 &= -Y_2 - (\mu + 1)X, \\ Y'_2 &= -\frac{1}{2}\mu, \end{aligned} \tag{8.64}$$

where $\mu = \frac{\lambda_w}{\lambda_s}$ is the ratio of the eigenvalues for the linear desingularized slow flow of (8.64).

One can now observe that (8.64) has two special algebraic solutions:

$$\Gamma_w(t) = \left(\frac{\mu}{2}t, -\frac{\mu^2}{4}t^2 + \frac{\mu}{2}, -\frac{\mu}{2}t \right) \quad \text{and} \quad \Gamma_s(t) = \left(\frac{1}{2}t, -\frac{1}{4}t^2 + \frac{1}{2}, -\frac{\mu}{2}t \right),$$

where $\Gamma_{s,w}$ correspond to the strong and weak singular canards in a rescaled coordinate system, i.e., in the classical chart of the blowup. The system (8.64) has been investigated for bifurcations at resonant values when $\mu^{-1} \in \mathbb{N}$. In particular, one wants a bifurcation equation for the blown-up versions of the slow manifolds describing their intersections. Let ρ denote the distance between the manifolds at $\Gamma_w(0)$. Then the next result can be proved analytically.

Theorem 8.6.8 ([Wec05]). *If $\mu = \mu_0$ and μ_0^{-1} is odd, there exists a transcritical bifurcation of singular canards for (8.64) near Γ_w . The bifurcation equation is locally equivalent to the normal form*

$$\rho^2 + (-1)^{\frac{\mu_0^{-1}+1}{2}} \rho(\mu^{-1} - \mu_0^{-1}) = 0$$

for $\mu_0^{-1} = 2n - 1$ and $n \in \mathbb{N}$.

Theorem 8.6.8 can be “blown down” to give the same bifurcation result for the original manifolds C_ε^a and C_ε^r .

Remark: The proof uses an extension of the **Melnikov method** [Wec02] to heteroclinic orbits connecting nonhyperbolic equilibria at infinity. The proof continues along similar lines as in the proof of Theorem 8.5.11, and we shall not detail it here.

The result of Theorem 8.6.8 describes what we expect to happen at odd resonance values and confirms that there are more than two maximal canards. A numerical study shows that for even values of μ^{-1} , we expect a pitchfork bifurcation of canards. The bifurcation diagram is shown in Figure 8.12. We see from that figure that only certain secondary canards survive beyond a small neighborhood of the resonance values. Despite the generation of extra canards in the pitchfork and transcritical bifurcations, some of the secondary canards exist only in a small region in parameter space. The mechanism eliminating them has been called a **turning point bifurcation of canards**.

Regardless of the technical details, the main message is that secondary maximal canards are generated at resonances. Their number depends on the ratio of the eigenvalues of the linearized desingularized slow subsystem.

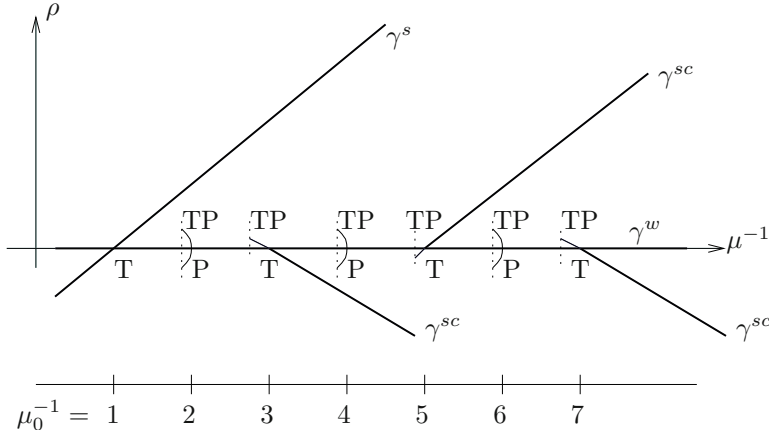


Figure 8.12: Sketch of the bifurcation diagram for (8.64): T = Transcritical, P = Pitchfork and TP = Turning point bifurcation. All bifurcations are for maximal canards, i.e., for the transversal intersections of slow manifolds. Only the maximal canards with bold lines persist outside of a small neighborhood of each bifurcation point defined by a resonance $\mu \in \mathbb{N}$.

Theorem 8.6.9 ([Wec05, BKW06]). *For folded nodes, suppose $k \in \mathbb{N}$ is such that $2k+1 < \mu^{-1} = \frac{\lambda_s}{\lambda_s'} < 2k+3$ and $\mu^{-1} \neq 2(k+1)$. Then in addition to $\gamma_{\varepsilon}^{s,w}$, there are k secondary maximal canards $\gamma_{\varepsilon}^{sc}$ for $0 < \varepsilon \ll 1$.*

8.7 Singularities beyond Folds

Although fold points are extremely important due to their generic occurrence in fast-slow systems, there are obviously many other interesting singularities

possible. As an example, this section outlines the transcritical singularity for planar $(1, 1)$ -fast–slow systems

$$\begin{aligned}\frac{dx}{dt} &= x' = f(x, y, \varepsilon), \\ \frac{dy}{dt} &= y' = \varepsilon g(x, y, \varepsilon),\end{aligned}\quad (8.65)$$

where f, g are sufficiently smooth. Transcritical singularities occur when two branches of the critical set $C_0 = \{(x, y) \in \mathbb{R}^2 : f(x, y, 0) = 0\}$ cross transversally. As typical examples, it is helpful to keep the following two cases in mind:

$$\begin{aligned}f_1(x, y, \varepsilon) &= x(x + y), \\ f_2(x, y, \varepsilon) &= x^2 - y^2 + \mathcal{O}(\varepsilon),\end{aligned}$$

which both have transcritical points at $(x, y) = (0, 0)$. The fast vector field f_1 is often encountered in applications for which a trivial branch of solutions represented by the critical manifold $x = 0$ often exists. Typical examples are ecological models with a zero population level and chemical reactions that never have negative concentrations, so that $x = 0$ should be invariant. The fast vector field f_2 is essentially a normal form for the transcritical point, and we shall describe how to reach this form next.

Definition 8.7.1. The system (8.65) has a nondegenerate **transcritical singularity** at $(x, y) = (0, 0)$ if the following conditions are satisfied:

$$f(0, 0, 0) = 0, \quad \frac{\partial f}{\partial x}(0, 0, 0) = 0, \quad \frac{\partial f}{\partial y}(0, 0, 0) = 0, \quad (8.66)$$

$$\frac{\partial^2 f}{\partial x^2}(0, 0, 0) = 0, \quad \det \begin{pmatrix} \frac{\partial^2 f}{\partial x^2}(0, 0, 0) & \frac{\partial^2 f}{\partial x \partial y}(0, 0, 0) \\ \frac{\partial^2 f}{\partial x \partial y}(0, 0, 0) & \frac{\partial^2 f}{\partial y^2}(0, 0, 0) \end{pmatrix} < 0. \quad (8.67)$$

From now on, we also require the additional transversality condition

$$g_0 := g(0, 0, 0) \neq 0. \quad (8.68)$$

Obviously, the assumption that the transcritical singularity/point occurs at the origin is not a restriction, since this can always be achieved by translating coordinates. Furthermore, the restriction to planar systems is also not severe, since transversal crossing points of the critical set for (m, n) -fast–slow systems can be treated as well, as long as a suitable center manifold reduction is possible.

Before using the conditions (8.66)–(8.68) to transform (8.65) to normal form, it is convenient to define a few additional constants:

$$\begin{aligned}k_{xx} &:= \frac{1}{2} \frac{\partial^2 f}{\partial x^2}(0, 0, 0), & k_{xy} &:= \frac{1}{2} \frac{\partial^2 f}{\partial x \partial y}(0, 0, 0), \\ k_{yy} &:= \frac{1}{2} \frac{\partial^2 f}{\partial y^2}(0, 0, 0), & k_\varepsilon &:= \frac{\partial f}{\partial \varepsilon}(0, 0, 0).\end{aligned}$$

Proposition 8.7.2. *In a sufficiently small neighborhood of the transcritical point $(x, y) = (0, 0)$, there exists a coordinate change transforming (8.65) into*

$$\begin{aligned}x' &= x^2 - y^2 + \lambda \varepsilon + h_1(x, y, \varepsilon), \\ y' &= \varepsilon(1 + h_2(x, y, \varepsilon)),\end{aligned}\quad (8.69)$$

where the form of the higher-order terms is

$$\begin{aligned} h_1(x, y, \varepsilon) &= \mathcal{O}(x^3, x^2y, xy^2, y^3, \varepsilon x, \varepsilon y, \varepsilon^2), \\ h_2(x, y, \varepsilon) &= \mathcal{O}(x, y, \varepsilon), \end{aligned}$$

and the computable constant λ is given by

$$\lambda = \frac{1}{|g_0| \sqrt{k_{xy}^2 - k_{xx}k_{yy}}} (k_\varepsilon k_{xx} + g_0 k_{xy}).$$

Proof. (Sketch; [KS01c]) First, use a Taylor series for (8.65) and apply the conditions for a transcritical singularity from Definition (8.7.1). Then let

$$\hat{x} = k_{xx}x - k_{xy}y, \quad \hat{y} = \text{sign}(g_0)y\sqrt{k_{xy}^2 - k_{yy}k_{xx}}, \quad \hat{\varepsilon} = \varepsilon|g_0|\sqrt{k_{xy}^2 - k_{yy}k_{xx}}$$

and check that this coordinate change indeed yields (8.69). \square

Proposition 8.7.2 and its proof are quite typical for several other singularities; see Chapter 4. Based on the geometric conditions of the singularity, one determines which terms are of leading order for the fast–slow system and then transforms it into a suitable normal form such as (8.69).

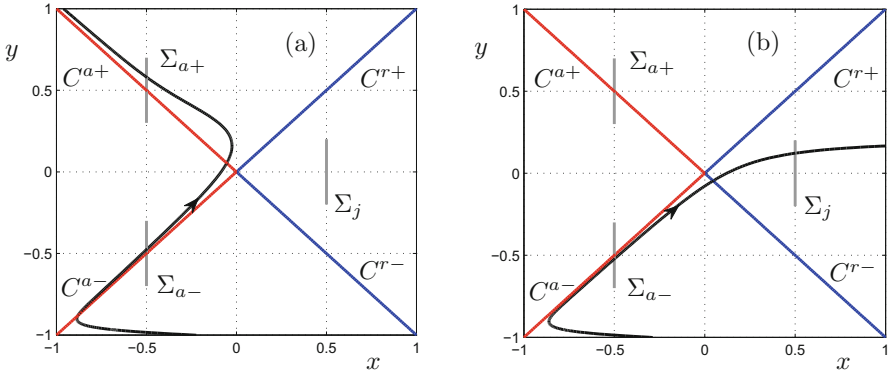


Figure 8.13: Transcritical singularity with attracting (red) and repelling (blue) submanifolds defined in (8.70) and sections (gray) given by (8.71). Trajectories are calculated for $\varepsilon = 0.05$. (a) $\lambda < 1$ showing exchange of stability. (b) $\lambda > 1$ yielding a fast jump.

The next step is to analyze (8.69). The higher-order terms $h_{1,2}$ will not affect the analysis, and we will drop them from now on. The parameter λ switches (8.69) between two dynamical regimes, as shown in Figure 8.13. The critical set $C_0 = \{(x, y) \in \mathbb{R}^2 : x^2 = y^2\}$ has four normally hyperbolic submanifolds:

$$\begin{aligned} C_0^{a-} &= \{x < 0, y < 0\} \cap C_0, & C_0^{a+} &= \{x < 0, y > 0\} \cap C_0, \\ C_0^{r-} &= \{x > 0, y < 0\} \cap C_0, & C_0^{r+} &= \{x > 0, y > 0\} \cap C_0, \end{aligned} \tag{8.70}$$

where $C_0^{a\pm}$ are attracting and $C_0^{r\pm}$ are repelling. Fenichel theory provides the associated slow manifolds. Trajectories starting near the slow manifold C_ε^{a-} will come exponentially close to it. Then the slow flow

$$\frac{dy}{d\tau} = \dot{y} = 1 \quad \text{on } C_0^{a-} \text{ for } \tau = \varepsilon t$$

implies that these trajectories will be transported toward the transcritical singularity at $(0, 0)$. Hence, we have to track C_ε^{a-} through a neighborhood of $(0, 0)$. As usual, we also use the notation C_ε^{a-} for the extension of the slow manifold under the flow. Fix $\rho > 0$ and consider the following three sections located at $\mathcal{O}(1)$ -distance from the origin:

$$\begin{aligned} \Sigma_{a-} &= \{(-\rho, y) : y \in [-\rho - \delta, -\rho + \delta]\}, \\ \Sigma_{a+} &= \{(-\rho, y) : y \in [\rho - \delta, \rho + \delta]\}, \\ \Sigma_j &= \{(\rho, y) : y \in [-\delta, \delta]\}, \end{aligned} \tag{8.71}$$

for a suitable $\delta > 0$ with $\delta = \mathcal{O}(1)$ as shown in Figure 8.13. Let $\Pi_a : \Sigma_{a-} \rightarrow \Sigma_{a+}$ and $\Pi_j : \Sigma_{a-} \rightarrow \Sigma_j$ be the two possible transition maps of the flow.

Theorem 8.7.3 ([KS01c]). *Suppose $\lambda \neq 1$ is fixed. Then there exists ε_0 such that for $\varepsilon \in (0, \varepsilon_0]$, two cases can occur:*

- (a) *If $\lambda > 1$, then C_ε^{a-} passes through Σ_j at a point $(\rho, \nu(\varepsilon))$, where $\nu(\varepsilon) = \mathcal{O}(\sqrt{\varepsilon})$ and $\Pi_j(\Sigma_{a-})$ has size $\mathcal{O}(e^{-K/\varepsilon})$ for a constant $K > 0$.*
- (b) *If $\lambda < 1$, then C_ε^{a-} passes through Σ_{a+} , and $\Pi_j(\Sigma_{a-})$ has size $\mathcal{O}(e^{-K/\varepsilon})$ for a constant $K > 0$.*

Theorem 8.7.3 distinguishes between the case $\lambda > 1$ of a fast jump away from the singularity and the case $\lambda < 1$ where a transfer (or **exchange of stability**) between the two attracting branches of the critical set occurs; see Figure 8.13. Near $\lambda = 1$, canards occur, but we shall not consider this case here and refer the reader to Section 8.9.

Proof. (of Theorem 8.7.3, sketch; [KS01c]) Define $\bar{B} = S^2 \times [0, r_0]$, $r_0 > 0$, and consider the system

$$\begin{aligned} x' &= x^2 - y^2 + \lambda\varepsilon, \\ y' &= \varepsilon, \\ \varepsilon' &= 0, \end{aligned} \tag{8.72}$$

under the blowup $(x, y, \varepsilon) = (\bar{r}\bar{x}, \bar{r}\bar{y}, \bar{r}^2\bar{\varepsilon})$, where $(\bar{x}, \bar{y}, \bar{\varepsilon}, \bar{r}) \in \bar{B}$. It can be checked that the invariant circle $\{\bar{r} = 0 = \bar{\varepsilon}\}$ contains six equilibria (as shown in Figure 8.14). Four of the equilibria correspond to the four branches of the critical set $C_\varepsilon^{a\pm}$, $C_\varepsilon^{r\pm}$. Two of the equilibria represent the incoming fast fiber $\{y = 0, x < 0\}$ and the outgoing fast fiber $\{y = 0, x > 0\}$. Observe that the dynamics and stability of equilibria on $\{\bar{r} = 0 = \bar{\varepsilon}\}$ are inherited from the fast flow of the original system; see Figure 8.14.

Formally, one must employ three charts to analyze the dynamics, but we shall restrict attention to the chart defined by $\bar{\varepsilon} = 1$, in which the flow on the sphere

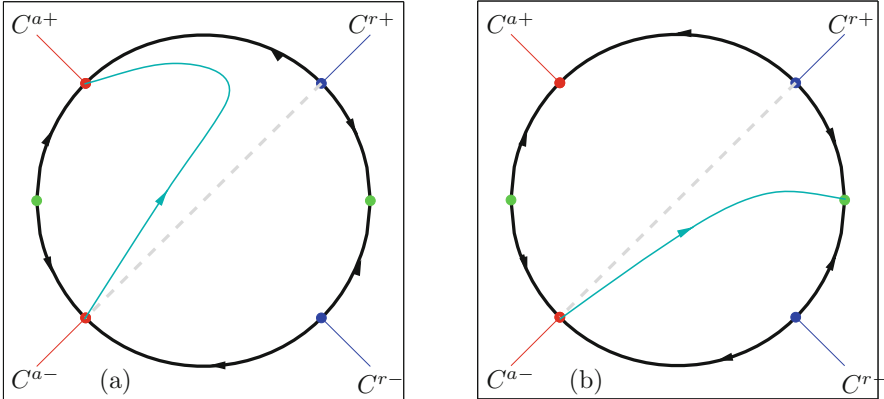


Figure 8.14: Sketch of the blown-up vector field near the transcritical singularity shown in a projection as viewed from the top of the sphere S^2 . The invariant circle $\{\bar{r} = 0 = \bar{\varepsilon}\}$ (black), the equilibria for the attracting and repelling manifolds (red/blue), and the two equilibria for the fast fibers (green) are shown. The dashed line (gray) is the special trajectory γ , which exists only for $\lambda = 1$. The cyan trajectory is the continuation of the attracting critical manifold C_ε^{a+} over the sphere. (a) $\lambda < 1$. (b) $\lambda > 1$.

can be resolved. In this chart, the blowup is a rescaling $(\sqrt{\varepsilon}x, \sqrt{\varepsilon}y) = (X, Y)$, which, after setting $T = \sqrt{\varepsilon}t$, yields on applying it in (8.72) that

$$\begin{aligned} \frac{dX}{dT} &= X^2 - Y^2 + \lambda, \\ \frac{dY}{dT} &= 1. \end{aligned} \quad (8.73)$$

For $\lambda = 1$, a special solution of (8.73) is $\gamma(T) = (X(T), Y(T)) = (T, T)$, which is a maximal canard solution between C_ε^{a-} and C_ε^{r+} . Changing λ so that $\lambda < 1$ means that a trajectory starting near C_ε^{a-} will miss C_ε^{r-} and converge to C_ε^{a+} instead, as shown in Figure 8.14(a). The case $\lambda > 1$ implies that the trajectory will end up at the outgoing fast critical fiber instead; see Figure 8.14(b). \square

Locally, the results for a transcritical point are relatively straightforward. However, note carefully that in the case $\lambda = 1$, a maximal canard occurs.

Example 8.7.4. Consider the following $(1, 1)$ -fast-slow system:

$$\begin{aligned} x' &= (x - y)(1 - x^2) + \mu\varepsilon, \\ y' &= \varepsilon x, \end{aligned} \quad (8.74)$$

which is a modification of an example originally suggested in [FPV08]. The critical set $C = \{x = y\} \cup \{x = \pm 1\}$ clearly has two transcritical points located at $(1, 1)$ and $(-1, -1)$. ♦

Exercise/Project 8.7.5. Analyze the existence, stability, and scaling properties of the equilibria and periodic orbits for (8.74) based on varying the parameter μ for $0 < \varepsilon \ll 1$. ◇

8.8 Curvature

So far, we have dealt mostly with the existence of canard orbits for sufficiently small $\varepsilon > 0$. Here we briefly describe how curvature can be used to quantify canard cycles in planar systems. Consider the $(1, 1)$ -fast–slow system

$$\begin{aligned}\varepsilon \frac{dx}{d\tau} &= \varepsilon \dot{x} = y - f(x), \\ \frac{dy}{d\tau} &= \dot{y} = g(x),\end{aligned}\tag{8.75}$$

for functions $f, g : \mathbb{R} \rightarrow \mathbb{R}$ that may depend on additional parameters. As concrete examples, one should think of (8.75) as the van der Pol equation with constant forcing or the FitzHugh–Nagumo equation; Sections 1.3 and 1.4. Trajectories of (8.75) can be expressed as curves $y(x)$ satisfying

$$(y - f(x)) \frac{dy}{dx} = \varepsilon g(x).\tag{8.76}$$

The **curvature** $\kappa(x)$ of a plane curve $y(x)$ is defined by

$$\kappa(x) := \frac{y''(x)}{(1 + y'(x)^2)^{3/2}}.\tag{8.77}$$

From Sections 8.1–8.4, we know that canard cycles occur in an exponentially small parameter region near a singular Hopf bifurcation and that they can enclose a convex area (“ducks without head”) or a nonconvex area (“ducks with head”). For the nonconvex case, an inflection point appears near the repelling critical manifold. It was suggested in [DJ11b] to take this observation as a definition to distinguish a canard explosion for small ε from the usual Hopf bifurcation for larger ε . A nonconvex area can be enclosed if and only there is at least one **inflection point** at which the curvature (8.77) vanishes. Denote the set of inflection points on trajectories by

$$\mathcal{I} := \{(x, y(x)) \in \mathbb{R}^2 : \kappa(x) = 0, \text{ i.e., } y''(x) = 0\}.$$

To calculate the inflection points, it is natural to differentiate the defining relation (8.76) with respect to x , which gives

$$-\left(\frac{dy}{dx}\right)^2 + f'(x)\frac{dy}{dx} + \varepsilon g'(x) = (y - f(x))\frac{d^2y}{dx^2}.\tag{8.78}$$

So if $h := y - f(x) \neq 0$, then $y''(x) = 0$ and (8.78) lead to

$$0 = \left(\frac{dy}{dx}\right)^2 - f'(x)\frac{dy}{dx} - \varepsilon g'(x).\tag{8.79}$$

Inserting dy/dx from (8.76) into (8.79) and calculating a bit yields

$$g'(x)h^2 + f'(x)g(x)h - \varepsilon g(x)^2 = 0.\tag{8.80}$$

Equation (8.80) is quadratic in h with two solutions h_{\pm} and respective associated solutions $y_{\pm}(x)$ given by

$$y_{\pm}(x) = f(x) - \frac{g(x)}{2g'(x)} \left[f'(x) \pm \sqrt{f'(x)^2 + 4\varepsilon g'(x)} \right]. \quad (8.81)$$

Note that the solutions depend on ε and are real-valued if and only if

$$f'(x)^2 + 4\varepsilon g'(x) \geq 0. \quad (8.82)$$

The next example shows how to apply the criterion (8.82) in practice.

Example 8.8.1. Consider the van der Pol equation with constant forcing where we have

$$f(x) = \frac{x^3}{3} - x \quad \text{and} \quad g(x) = a - x \quad (8.83)$$

for a parameter $a \in \mathbb{R}$. Using the tools from Section 8.2, one checks that a singular Hopf bifurcation with associated canard cycles occurs at $a = 1$ for $\varepsilon > 0$ sufficiently small. From (8.82), it follows that $(x^2 - 1)^2 - 4\varepsilon \geq 0$, which means that

$$\text{either } x^2 > 1 + 2\sqrt{\varepsilon} \quad (8.84)$$

$$\text{or } x^2 < 1 - 2\sqrt{\varepsilon}. \quad (8.85)$$

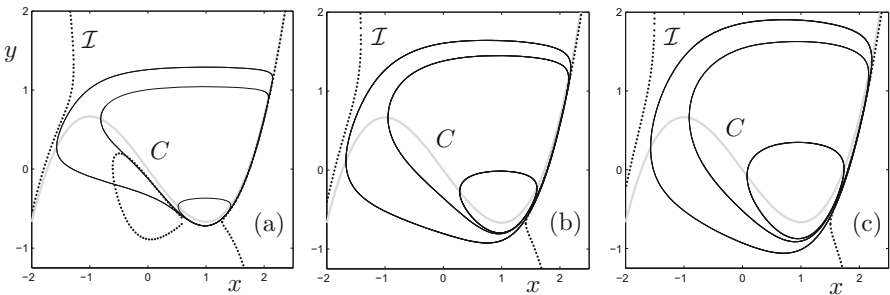


Figure 8.15: Curvature and periodic orbits for van der Pol's equation (8.75), (8.83). The critical manifold C (gray curve, thick), the inflection curves I (dotted black, for $q = 1$) and periodic orbits for three different values of q (thin black curves) are shown. (a) $\varepsilon = 0.1$, periodic orbits for $q = 0.988, 0.98631, 0.985$. The inflection curve has a clear component inside $\{|x| < 1\}$, and there are canard cycles enclosing a nonconvex set. (b) $\varepsilon = 0.25$, limit cycles for $q = 0.97, 0.95, 0.75$. At the critical case, the limit cycles all enclose convex sets. (c) $\varepsilon = 0.4$, limit cycles for $q = 0.95, 0.9, 0.7$.

For the first condition (8.84), there are always x values for which it holds, giving inflection curves in the region $|x| > \sqrt{1 + 2\sqrt{\varepsilon}}$. However, this region does not contain any part of the repelling critical manifold $C^r = \{(x, y) \in \mathbb{R}^2 :$

$|x| < 1, y = f(x)\}$, which is the region in which inflection points should lie for the canard cycles. The second condition (8.85) holds inside the region $|x| < 1$ for some real value of x if and only if

$$1 - 2\sqrt{\varepsilon} > 0 \quad \Rightarrow \quad \varepsilon < \frac{1}{4} =: \varepsilon_0.$$

Hence for $\varepsilon < \varepsilon_0$, the periodic orbits generated in the Hopf bifurcation can have inflection points lying near C^r . Figure 8.15 shows periodic orbits under the variation of a for three different values of ε . The predicted transition from convex to nonconvex limit cycles can be observed. ♦

Let us point out that the criterion for canard cycles discussed here is only one possible way to distinguish different regimes for finite ε . Other possibilities based on various geometric properties of solutions in phase space are certainly conceivable. Furthermore, the use of curvature for fast–slow systems is not restricted to the canard case, and more references are given in Section 8.9.

8.9 References

Section 8.1: This section is based mostly on [KS01b]. There is a well-known asymptotic analysis approach to planar canards that has been published with a creative title [Eck83]. The transition to relaxation oscillations and associated bifurcations are also described in [DR07]. Further abstract work on desingularization and canards can be found in [Pan02]. In addition, much work on canards can be found in the nonstandard analysis literature [Die94]; see also Section 19.10. For more on canard asymptotics, see [For08, FM05, GI91]. An interesting generalization of the planar case is to canards on the two-dimensional torus [GI01, Sch10, Sch11], where they occur generically without parameters. Note very carefully that there is also the phenomenon of torus canards [BBK⁺11, BDB⁺12, DBKK12, KTK08], which is not the same as “canards on the 2-torus.” A survey of canards based on the Russian literature is available [Kol89]. Of course, several works on canards have been published under the headline of turning points [MD10]; see also Section 5.6.

Section 8.2: The discussion is extracted from [KS01e] as well as [Kue10b]. The singular Hopf bifurcation in \mathbb{R}^2 is a classical topic in fast–slow systems [Sob13]. It can be treated using asymptotic methods [BE86, BE92]. For the higher-dimensional case, one of the first basic works was [Bra98], and we also refer to [Guc08b, GM12b]. In Section 13.3, the oscillations near a singular Hopf bifurcation in \mathbb{R}^3 are covered [GW00, MY07, MY08]. The theory has been applied in various further directions, e.g., the Brusselator model [Mat06], chemical systems [PGS91], coupled neural fields [Cur10, CR11, CSRR08, SCCR07], delay equations [KE14], laser dynamics [KE03], power systems [Bea00], self-replicating chemical models [Bro11] and thermal explosion problems [GS92, GS91].

Section 8.3: The explanations follow [Kue10b]. Details on the definitions of various first Lyapunov coefficients are contained in most books on bifurcation theory [CLW94, GH83, Kuz04, Per01a]. It is expected that the results also carry through to higher-dimensional singular Hopf bifurcations in a suitable form [YZ04a]. For more details on the computational relevance, we refer to Section 10.6.

Section 8.4: The section is based on [KS01e] as well as [DR96b]. The case of subcritical Hopf bifurcation and the associated number of limit cycles is quite intricate [Dum13]. There are several applications of canard theory such as autocatalytic reactions [BS01, GSS06, GS09c, KS11], the BZ reaction [BBE91, RKZE03b], control of canards [DM08], coupled neurons [LWH07], Faraday waves [HKG05] the Hodgkin–Huxley model [Moe06, RW08, RW07], optical systems [SK13, SK11a], plastic deformation models [Brø12], predator–prey models [LZ13, Ver07a], the Schrödinger equation [Ben96, KMR99], and surface oxidation reactions [Moe02, XHZ05a]. The theory can be pushed further in several directions, such as additional fast variables [Wec12, XHZ06b], complex solutions [FS99b, Mat00], nonsmooth systems [DFH⁺13, PT13, RG13], difference equations [ER03], discrete quadratic maps [Fru88, Fru92], Gevrey asymptotics [CD91], iteration approaches [Brø12], multiple repelling segments [KOPR13], nonsmooth models [TL13], parametric families [dS99a, MR12b], and topological methods [PPZ09]. Due to the natural occurrence of periodic orbits in planar systems involving canards, there are connections to Hilbert’s 16th problem [Rou98, Ily02, DRR94, Fra12] and slow divergence integrals [MD11, Dum11, SH13] with a focus on Liénard systems [CDP13].

Section 8.5: The section was compiled from [SW01, DGK⁺12]. Much of the fundamental work on canards and folded singularities in \mathbb{R}^3 was originally carried out in the language of nonstandard analysis [Ben82, Ben90, Ben01, BL82, Ben85], and one should highlight the excellent contributions obtained in [Ben85]. For a numerical perspective centering on return maps, we refer to [Guc08a]. More on canards with two slow variables can be found in [BKR02, KT97]. The theory also extends to higher-dimensional problems with additional fast and slow variables [BS91, KM91, Wec12]. It has been suggested that surfaces of canards be referred to as black swans [SS01, Shc03, SS05b, XHZ06a]. Some applications are given by bursting mechanisms [TTB12], interneuron models [EW09], and splitting for globally coupled oscillators [ZREK03]; see also Chapter 13.

Section 8.6: In this section, we have followed [Wec05]. Even more details and generalizations are discussed in [Wec98, Wec12, Wec02] as well as [KW10]. The asymptotic case of many maximal canards has been covered in [GH05]. Beyond the three-dimensional case, one actually finds canards also in spatially extended systems, e.g., in advection–reaction–diffusion systems [WP10], reaction–diffusion systems [MPK09, Su93], scalar balance laws [Har03], spatial predator–prey models [BKP06], and for various other classes of traveling waves [SSS03]. One may also approach the canard problem from the abstract algebraic-geometric viewpoint [Pan00].

Section 8.7: The results here follow the presentation in [KS01c]. There are several important classical results regarding exchange of stability [LS75, LS77], which may occur near transcritical and pitchfork singularities [NS99, Sch85a]. The transcritical case involving canards is also discussed in [BS09b, BG01, FPV08, VF12]. For the pitchfork case, there are additional references as well [KR99, Mar96]. For an abstract approach to intersecting critical manifolds and loss of normal hyperbolicity, we refer to [BNS99, NS08, Sti98c]. Another interesting case that can be resolved using geometric methods is the Lagerstrom problem [PS04a, PS04b].

Section 8.8: This section is based mostly on [DJ11b, DJ11a], which also discusses the size of ε [Jav78b]. In particular, a key concept employed was the inflection line [BBE94, DKR13]. There is a more general view on curvature and fast–slow systems with a focus on normally hyperbolic structures [Gin09, GL11, GRC08] but also some aspects of canards [GLC13]. Viewing canards as thresholds for excitable systems is discussed in [Bra92].

Chapter 9

Advanced Asymptotic Methods

Asymptotic analysis is a key ingredient in capturing multiscale dynamics. In this chapter, a collection of asymptotic and perturbation methods is presented. The focus is on the basic principles of methods and key examples to understand their application. All methods can be applied in many other circumstances, and although the algebraic manipulations change, the principles of the methods tend to carry over.

Sections 9.1 and 9.2 cover the topic of matched asymptotic expansions and its variants. The idea of matching different asymptotic expansions on an overlap domain is one of the core principles of asymptotic analysis and perturbation methods. Section 9.3 deals with the boundary function method, which exploits an *a priori* structural assumption to develop uniformly valid expansions. Another classical approach is the WKB approach, presented in Section 9.4, where a certain exponential ansatz is made. WKB theory covers a surprisingly wide array of problems, even involving loss of normal hyperbolicity. The relation between asymptotics and the blowup method near a fold point is considered in Section 9.5, which yields a unified view on parts of Chapters 5 and 7. Section 9.6 gives a very compressed exposition of averaging. The idea is to average the fast motion and use the averaged quantity as an effective input for the slow variables. Exponential asymptotics can also play an important role in fast–slow systems and is discussed in Section 9.7, with a focus on introducing the basic definitions of Gevrey order. Section 9.8 contains an exposition to the two-timing method (or “method of multiple scales”). It makes the *a priori* assumption in the asymptotic expansion that the coefficients depend on two time scales. Unsurprisingly, this turns out to be a useful ansatz for fast–slow systems. In Section 9.9, the renormalization group is introduced, and its relation to normal form transformations is sketched (and hence it is also directly related to averaging). In Section 9.10, another application of renormalization is given to compute slow manifold expansions.

It is also very important to note that many of the methods turn out to be “essentially” equivalent. Section 9.9 is an example of such an equivalence, since it relates the method of normal forms to the renormalization group. Normal forms are also directly related to averaging, which in turn is “equivalent” to the method of multiple scales in many cases. Although we shall not detail all the connections here, it is not really surprising from a geometric viewpoint that several asymptotic methods work similarly. For example, we know that the asymptotic expansion in powers ε^k of a normally hyperbolic slow manifold is unique when the differences between slow manifolds are exponentially small. Hence, every asymptotic method for slow manifolds that calculates up to k th-order accuracy must eventually lead to the same result; therefore, similarities in the computational procedures are bound to occur. Of course, it may be beneficial to think and calculate via several different viewpoints.

Background: This chapter is essentially self-contained but requires a willingness to try out the presented expansion methods on various problems. In fact, trial and error for slight modifications of the examples given in this chapter is almost certainly a successful strategy for acquiring the necessary computational techniques. However, some algebraic manipulations are tedious, so knowledge of a symbolic computer algebra package can be beneficial.

9.1 Matched Asymptotic Expansions

One of the most classical techniques for understanding multiple time scale dynamics is the method of **matched asymptotic expansions**. Implicitly, this method was used in Chapter 5. Here, we develop the method on a more formal level. Also, it will be instructive to see how the method of matched asymptotic expansions relates to the geometric theory of multiple time scales.

The general concept of matched asymptotic expansions is to glue asymptotic series from different fast–slow regions together. To understand this principle, we will consider an example in detail given by the linear second-order differential equation

$$\varepsilon \frac{d^2y}{d\tau^2} + \frac{dy}{d\tau} + y = \varepsilon \ddot{y} + \dot{y} + y = 0 \quad (9.1)$$

for a function $y = y(\tau; \varepsilon)$ with initial conditions

$$y(0; \varepsilon) = 0 \quad \text{and} \quad \dot{y}(0; \varepsilon) = \frac{1}{\varepsilon}. \quad (9.2)$$

Before we begin with an asymptotic approach for solving (9.1)–(9.2), we use a basic geometric analysis. Let $\dot{y} = x$. Then we obtain

$$\begin{aligned} \varepsilon \dot{x} &= -(x + y) =: f(x, y), \\ \dot{y} &= x, \end{aligned} \quad (9.3)$$

with initial conditions $x(0; \varepsilon) = \frac{1}{\varepsilon}$ and $y(0; \varepsilon) = 0$. The critical manifold of (9.3) is $C_0 = \{y = -x\}$. It is normally hyperbolic attracting, since $f_x \equiv -1$. By Fenichel’s theorem, C_0 perturbs to a slow manifold C_ε that is $\mathcal{O}(\varepsilon)$ away from C_0 . Since $x(0; \varepsilon) = \frac{1}{\varepsilon}$ and $y(0; \varepsilon) = 0$, we start far away from C_0 respectively

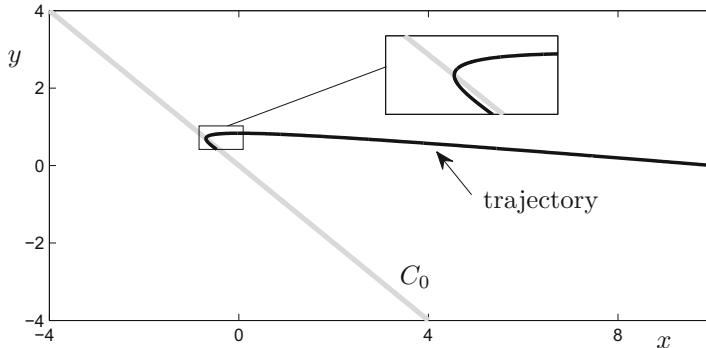


Figure 9.1: Solution to equation (9.3) for a time $\tau \in [0, 1]$ and $\varepsilon = 0.1$.

C_ε . The slow subsystem on the critical manifold expressed in the x -variable is $\dot{x} = -x$. The situation is shown in Figure 9.1. First, the solution has a fast transition until it reaches the vicinity of the slow manifold C_ε , which it then tracks at a slow speed.

Definition 9.1.1. An asymptotic expansion valid for perturbations of the fast flow is called an **inner expansion**. An asymptotic expansion valid for perturbations of the slow flow is called an **outer expansion**.

Remark: The terminology is slightly confusing, since one may intuitively think of an “outer region” as one that is away from the critical manifold. The reason for Definition 9.1.1 becomes obvious once we look at a time series to solutions of singular perturbation problems.

A solution to (9.1) can also be shown as a time series in the original spatial variable y ; see Figure 9.2. The solution first makes a fast transition, which means that the time series has only a small segment describing this “inner part.” Then the “outer part” takes much longer, due to slow evolution near the slow manifold.

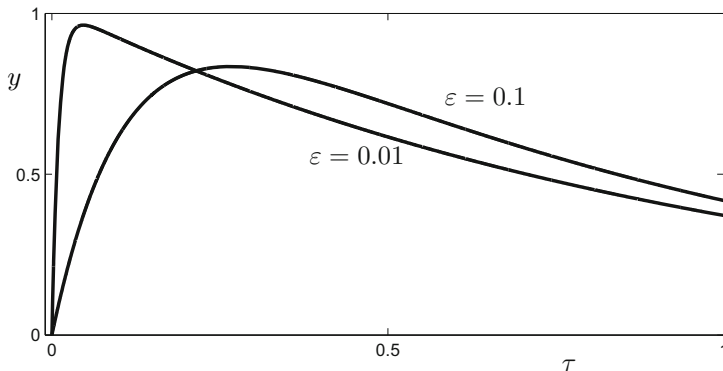


Figure 9.2: Solution to equation (9.1) for a time $\tau \in [0, 1]$ and two different values of ε . Smaller values of ε induce an even sharper transition near $y = 0$.

The region of large derivative \dot{y} is also called the **inner layer** or **boundary layer** (since it appears on the boundary of the time domain). The regime of comparatively small derivative \dot{y} is called the **outer layer**. Note that an inner layer can also occur at a point in the interior of the parameterized time domain. In this case, it is also called an **interior layer**. The terminology of layers is not much used in this book, since we usually refer to “fast motion” and “slow motion.” However, almost all papers and books on asymptotic analysis use the layer terminology, and the reader may try to practice translating in the remaining part of this chapter where the “layer” terminology is still used.

To analyze the solution of (9.1) in more detail, we use the exact solution as a starting point:

$$y(\tau; \varepsilon) = \frac{1}{\sqrt{1 - 4\varepsilon}} \left(\exp \left[-(1 - \sqrt{1 - 4\varepsilon}) \frac{\tau}{2\varepsilon} \right] - \exp \left[-(1 + \sqrt{1 - 4\varepsilon}) \frac{\tau}{2\varepsilon} \right] \right). \quad (9.4)$$

The explicit solution (9.4) helps to develop the correct intuition as to what asymptotic expansions should look like. A technique to calculate asymptotic expansions without the knowledge of the exact solution will be developed later on. The ε -dependent factors in (9.4) have the expansions

$$\begin{aligned} -(1 - \sqrt{1 - 4\varepsilon})/(2\varepsilon) &= -1 - \varepsilon + \mathcal{O}(\varepsilon^2), \\ -(1 + \sqrt{1 - 4\varepsilon})/(2\varepsilon) &= -\frac{1}{\varepsilon} + 1 + \mathcal{O}(\varepsilon), \\ \frac{1}{\sqrt{1 - 4\varepsilon}} &= 1 + 2\varepsilon + \mathcal{O}(\varepsilon^2). \end{aligned}$$

Using those formulas, one may write the exact solution (9.4) asymptotically as

$$y(\tau; \varepsilon) = (1 + 2\varepsilon + \dots)(e^{-\tau - \varepsilon\tau + \dots} - e^{-\tau/\varepsilon + \tau + \dots}). \quad (9.5)$$

Ideally, one would like to find a single expansion for the solution with asymptotic sequence $\{\varepsilon^k\}_{k=0}^\infty$. Fixing $\tau \neq 0$ and letting $\varepsilon \rightarrow 0$ in (9.5) yields that the term $e^{-\tau/\varepsilon + \tau + \dots}$ is transcendently small. Since we aim to expand the solution as a power series in ε , a transcendently small term will not play a role at any order, and we neglect it here. Computing the asymptotic expansion of the remaining term inside the second bracket of (9.5), employing the usual Taylor expansion, yields

$$e^{-\tau - \varepsilon\tau} = e^{-\tau}(1 - \varepsilon\tau + \dots).$$

Therefore, a formal result valid up to order $\mathcal{O}(\varepsilon^2)$ is the expansion

$$y(\tau; \varepsilon) = e^{-\tau} + \varepsilon(2 - \tau)e^{-\tau} + \mathcal{O}(\varepsilon^2). \quad (9.6)$$

The result (9.6) is the outer expansion, and it describes the approximation to the flow near the slow manifold. Note that the zeroth-order term turns out as expected, since the slow subsystem in the y -coordinate is just $\dot{y} = -y$, which has the solution $y(\tau; 0) = e^{-\tau}$.

However, the result (9.6) cannot be uniformly valid. For $\tau \rightarrow 0$, it satisfies neither initial condition in (9.2). This problem is not unexpected, since (9.6) is just an expansion on the slow time scale τ . Hence, we consider the fast time scale $t = \tau/\varepsilon$ in the expansion (9.5) of the exact solution

$$y(t; \varepsilon) = (1 + 2\varepsilon + \dots)(e^{-\varepsilon t - \varepsilon^2 t + \dots} - e^{-t + \varepsilon t + \dots}). \quad (9.7)$$

For t fixed and finite, there is no transcendentally small term in (9.7) as $\varepsilon \rightarrow 0$. A direct calculation gives the expansion

$$y(t; \varepsilon) = (1 - e^{-t}) + \varepsilon(2 - t - (2 + t)e^{-t}) + \mathcal{O}(\varepsilon^2). \quad (9.8)$$

Note that in the case $\varepsilon \rightarrow 0$, one has $y(0; \varepsilon) \sim 0$ and

$$\frac{dy}{dt}(t = 0; \varepsilon) \sim 1 \quad \text{as } \varepsilon \rightarrow 0 \quad \Rightarrow \quad \frac{dy}{d\tau}(\tau = 0; \varepsilon) \sim \frac{1}{\varepsilon} \quad \text{as } \varepsilon \rightarrow 0,$$

so that both boundary conditions are satisfied asymptotically by (9.8). Recall that the fast or inner expansion (9.8) and the slow or outer expansion (9.6) are expressed in terms of the asymptotic sequence

$$\{1, \varepsilon, \varepsilon^2, \dots, \varepsilon^n, \dots\}. \quad (9.9)$$

To simplify the following calculations, it helps to introduce functions for the coefficients of the two asymptotic series. For the outer/slow series (9.6), we have

$$h_0(\tau) := e^{-\tau} \quad \text{and} \quad h_1(\tau) := (2 - \tau)e^{-\tau}.$$

For the inner/fast series (9.8), let

$$g_0(t) := 1 - e^{-t} \quad \text{and} \quad g_1(t) = 2 - t - (2 + t)e^{-t}.$$

The solutions (9.8) and (9.6) are valid on different time scales. The key idea of **matched asymptotic expansions** is to find a common time scale. On this common scale, one can then “match” the two series solutions. This process will work only if each asymptotic series is valid for time scales slightly different from the fast t -scale and the slow τ -scale. We begin with the slow series (9.6). For fixed $\tau \neq 0$, it follows that

$$\lim_{\varepsilon \rightarrow 0} y(\tau; \varepsilon) = h_0(\tau) \quad (9.10)$$

and

$$\lim_{\varepsilon \rightarrow 0} \frac{y(\tau; \varepsilon) - h_0(\tau)}{\varepsilon} = h_1(\tau). \quad (9.11)$$

Now consider the new intermediate time scale τ_η and set $\tau = \eta(\varepsilon)\tau_\eta$. To satisfy (9.10), we must have, for $\tau_\eta \neq 0$ fixed,

$$\lim_{\varepsilon \rightarrow 0} y(\eta\tau_\eta; \varepsilon) - h_0(\eta\tau_\eta) = 0. \quad (9.12)$$

Knowing the exact solution, one may just substitute it into (9.12):

$$\lim_{\varepsilon \rightarrow 0} (1 + 2\varepsilon + \dots)(e^{\eta\tau_\eta - \varepsilon\eta\tau_\eta + \dots} - e^{-\eta\tau_\eta/\varepsilon + \eta\tau_\eta + \dots}) - e^{-\eta\tau_\eta} = 0.$$

As long as the term $e^{-\eta\tau_\eta/\varepsilon + \eta\tau_\eta + \dots}$ is transcendentally small, we certainly get (9.12). This will be the case if $\varepsilon|\log \varepsilon| \ll \eta(\varepsilon)$. Under this assumption, one also verifies that

$$\lim_{\varepsilon \rightarrow 0} \frac{y(\eta\tau_\eta; \varepsilon) - h_0(\eta\tau_\eta)}{\varepsilon} - h_1(\eta\tau_\eta) = 0.$$

Therefore, the outer asymptotic solution is valid, including order $\mathcal{O}(\varepsilon)$, if

$$\varepsilon |\log \varepsilon| \ll \eta(\varepsilon) \ll 1. \quad (9.13)$$

Sometimes, the range of time scales over which an asymptotic expansion is valid is called an **extended domain of validity**; for example, the extended domain of validity of the outer expansion (9.6) is then given by (9.13). This domain can be considered graphically, as shown in Figure 9.3.

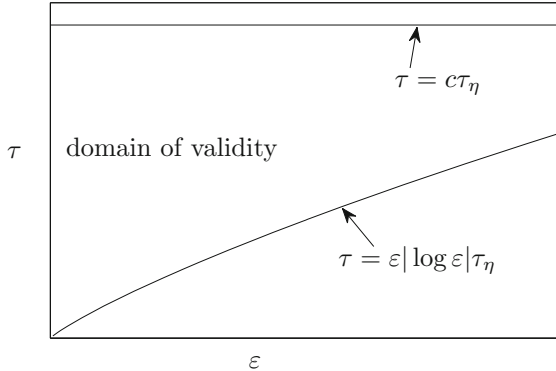


Figure 9.3: Sketch of the domain of validity (9.13). Here c is a constant, and the two curves bound the domain given by (9.13). Note that we assume for this figure that τ_η is fixed to some constant, as required for the limiting operation $\varepsilon \rightarrow 0$.

The same procedure works for the inner asymptotic solution. Let $t = \eta\tau_\eta/\varepsilon$, and then we require for the inner expansion to be valid including order $\mathcal{O}(\varepsilon)$ that for fixed $\tau_\eta \neq \infty$,

$$\lim_{\varepsilon \rightarrow 0} y(\eta\tau_\eta; \varepsilon) - g_0(\eta\tau_\eta/\varepsilon) = 0, \quad (9.14)$$

$$\lim_{\varepsilon \rightarrow 0} \frac{y(\eta\tau_\eta; \varepsilon) - g_0(\eta\tau_\eta/\varepsilon)}{\varepsilon} - g_1(\eta\tau_\eta/\varepsilon) = 0. \quad (9.15)$$

It can be checked that to satisfy (9.14), it is sufficient to have

$$\varepsilon \ll \eta(\varepsilon) \ll 1. \quad (9.16)$$

To have a valid expansion including the $\mathcal{O}(\varepsilon)$ term (i.e., a two-term expansion), we have to satisfy (9.14) and (9.15), and this gives the following extended domain of validity:

$$\varepsilon \ll \eta(\varepsilon) \ll \varepsilon^{1/2}. \quad (9.17)$$

Exercise/Project 9.1.2. Verify that (9.16) is an extended domain of validity for the inner expansion. Is this region optimal, i.e., can it be enlarged? ◇

Definition 9.1.3. A time scale on which the inner/fast and outer/slow expansions are simultaneously valid is called an **overlap domain**.

We can now use (9.13), (9.16), and (9.17) so that up to order $\mathcal{O}(1)$ and order $\mathcal{O}(\varepsilon)$, we have the following overlap domains:

$$\mathcal{O}(1) : \quad \varepsilon |\log \varepsilon| \ll \eta(\varepsilon) \ll 1, \quad (9.18)$$

$$\mathcal{O}(\varepsilon) : \quad \varepsilon |\log \varepsilon| \ll \eta(\varepsilon) \ll \varepsilon^{1/2}. \quad (9.19)$$

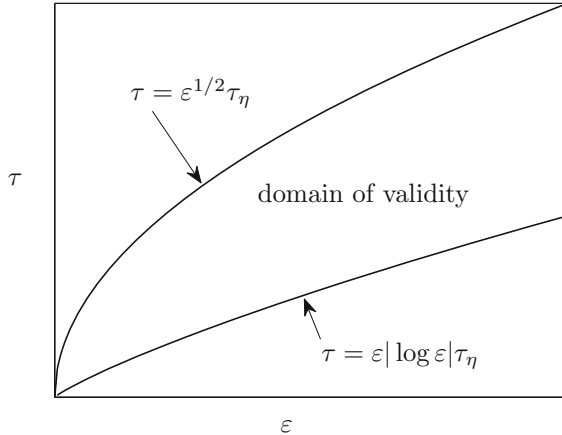


Figure 9.4: Sketch of the domain of validity (9.19). Note that we assume for this figure that τ_η is fixed to some constant value, as required for the limiting operation $\varepsilon \rightarrow 0$.

The domain (9.19) is shown in Figure 9.4. It can be checked from the known formulas for the coefficients of the asymptotic expansions that with fixed $\tau_\eta \neq 0$ and $\tau_\eta \neq \infty$,

$$\lim_{\varepsilon \rightarrow 0} h_0(\eta\tau_\eta) - g_0(\eta\tau_\eta/\varepsilon) = 0 \quad (9.20)$$

for (9.18) and also

$$\lim_{\varepsilon \rightarrow 0} \frac{h_0(\eta\tau_\eta) + \varepsilon h_1(\eta\tau_\eta) - g_0(\eta\tau_\eta/\varepsilon) - g_1(\eta\tau_\eta/\varepsilon)}{\varepsilon} = 0 \quad (9.21)$$

for (9.21). The conditions (9.20) and (9.21) are usually referred to as **asymptotic matching conditions**. In the example, they are satisfied automatically, since we derived them from the exact solution. However, we shall see that those conditions can be used to find the coefficients of the asymptotic series and to verify the overlap domain.

The next goal is to combine the two expansions into a single asymptotic expansion. We know that the slow and fast expansions are

$$h_0 + \varepsilon h_1 + \mathcal{O}(\varepsilon^2) = e^{-\tau} + \varepsilon(2 - \tau)e^{-\tau} + \mathcal{O}(\varepsilon^2),$$

$$g_0 + \varepsilon g_1 + \mathcal{O}(\varepsilon^2) = (1 - e^{-t}) + \varepsilon((2 - t)e^{-t} - (2 + t)e^{-t}) + \mathcal{O}(\varepsilon^2).$$

One idea would be simply to add the two results, but this is dangerous, since two equal terms appear, and one has to remove one of them get a correct asymptotic series. For example, from the matching condition of order $\mathcal{O}(1)$, we have on the overlap domain

$$0 = \lim_{\varepsilon \rightarrow 0} h_0(\eta\tau_\eta) - g_0(\eta\tau_\eta/\varepsilon) = \lim_{\varepsilon \rightarrow 0} e^{\eta\tau_\eta} - (1 - e^{-\eta\tau_\eta/\varepsilon}) = \lim_{\varepsilon \rightarrow 0} e^{-\eta\tau_\eta} - 1.$$

We get the correct matching result only because the terms $\lim_{\varepsilon \rightarrow 0} e^{-\eta\tau_\eta} = 1$ and -1 cancel. These terms will appear twice if we do not subtract correctly. A similar calculation for $\mathcal{O}(\varepsilon)$ yields that we should subtract the common terms

$$1 + \varepsilon(2 - \tau).$$

Therefore, we get as a result that

$$\begin{aligned} y(\tau; \varepsilon) &= (h_0 + g_0 - 1) + \varepsilon(h_1 + g_1 - (2 - t)) + \mathcal{O}(\varepsilon^2) \\ &= (e^{-\tau} - e^{-t}) + \varepsilon((2 - \tau)e^{-\tau} - (2 + t)e^{-t}) + \mathcal{O}(\varepsilon^2). \end{aligned} \quad (9.22)$$

The asymptotic expansion $y(\tau; \varepsilon)$ is uniformly valid up to order $\mathcal{O}(\varepsilon^2)$. It is easily verified that the relevant conditions (9.10), (9.11), (9.14), and (9.15) hold. The asymptotic expansion is compared to the exact solution in Figure 9.5.

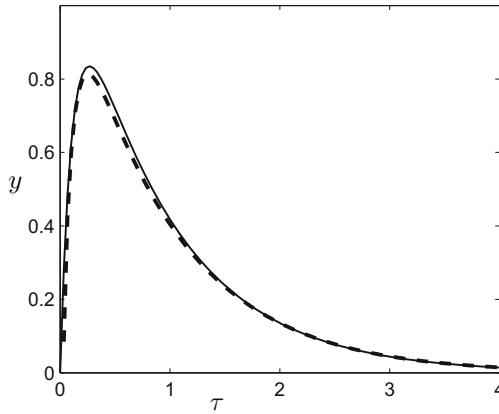


Figure 9.5: Comparison between the exact solution (solid black) and the asymptotic solution (dashed black) for $\tau \in [0, 4]$ and $\varepsilon = 0.1$. The asymptotic solution is a very good approximation despite the use of only two terms and a relatively large ε .

Definition 9.1.4. A combination of inner/fast and outer/slow expansions that is an asymptotic expansion valid beyond the inner and outer solutions is called a **composite expansion**.

The last essential aspect to address is how one can calculate the inner, outer, and composite expansions without the exact solution. Although this is not

the most important conceptual step, it is the most important computational one. Again, we illustrate the procedure for our example of the linear singularly perturbed second-order differential equation

$$\varepsilon \frac{d^2y}{d\tau^2} + \frac{dy}{d\tau} + y = \varepsilon \ddot{y} + \dot{y} + y = 0 \quad (9.23)$$

for a function $y = y(\tau; \varepsilon)$ with initial conditions

$$y(0; \varepsilon) = 0 \quad \text{and} \quad \dot{y}(0; \varepsilon) = \frac{1}{\varepsilon}. \quad (9.24)$$

In general, one should try an ansatz of the form

$$y(\tau; \varepsilon) = h_0(\tau)\gamma_0(\varepsilon) + h_1(\tau)\gamma_1(\varepsilon) + \mathcal{O}(\gamma_1(\varepsilon)),$$

where the asymptotic sequence $\gamma_k(\varepsilon)$ is undetermined. It is often possible to derive the correct asymptotic sequence during the process of matching. Here we shall simply start with the usual first guess $\gamma_k(\varepsilon) = \varepsilon^k$, so that

$$y(\tau; \varepsilon) = h_0(\tau) + h_1(\tau)\varepsilon + \mathcal{O}(\varepsilon^2) \quad (9.25)$$

up to second order. As long as the critical manifold is normally hyperbolic, we expect a direct regular perturbation computation to yield the correct outer/slow expansion. Substituting (9.25) into (9.23) and collecting terms of different orders gives

$$\dot{h}_0 + h_0 = 0, \quad (9.26)$$

$$\ddot{h}_0 + \dot{h}_1 + h_1 = 0. \quad (9.27)$$

From the fast–slow decomposition, we know that the solution starts far away from the slow manifold for ε sufficiently small. Since we have only initial conditions (9.24), there are no initial and/or boundary conditions for (9.26)–(9.27) available. Still, we can easily write down the general solution of both equations:

$$\begin{aligned} h_0(\tau) &= A_1 e^{-\tau}, \\ h_1(\tau) &= A_2 e^{-\tau} - A_1 \tau e^{-\tau}. \end{aligned}$$

The constants A_i with $i = 1, 2$ will be determined later. Regarding the inner/fast expansion, one has to change the time scale of the original problem to $\tau = \varepsilon t$, so that we try to solve

$$\frac{d^2y}{dt^2} + \frac{dy}{dt} + \varepsilon y = y'' + y' + \varepsilon y = 0 \quad (9.28)$$

for a function $y = y(t; \varepsilon)$ with initial conditions

$$y(0; \varepsilon) = 0 \quad \text{and} \quad y'(0; \varepsilon) = 1. \quad (9.29)$$

Again, a direct perturbation technique is expected to work:

$$y(t; \varepsilon) = g_0(t) + g_1(t)\varepsilon + \mathcal{O}(\varepsilon^2). \quad (9.30)$$

Note that the initial conditions (9.29) can now be used. Substitution of (9.30) into (9.28)–(9.29) and collecting terms of different orders yields

$$\begin{aligned} g_0'' + g_0' &= 0, \\ g_1'' + g_1' + g_1 &= 0, \end{aligned}$$

with initial conditions $g_0(0) = 0$, $g_0'(0) = 1$ and $g_1(0) = 0$, $g_1'(0) = 0$. The equations for g_0 and g_1 are straightforward to solve:

$$\begin{aligned} g_0(t) &= 1 - e^{-t}, \\ g_1(t) &= (2-t) - (2+t)e^{-t}. \end{aligned}$$

The next step is to determine the unknown constants A_i . To do so, we use the two matching conditions on the time scale $\tau = \eta\tau_\eta$:

$$\lim_{\varepsilon \rightarrow 0} h_0(\eta\tau_\eta) - g_0(\eta\tau_\eta/\varepsilon) = 0, \quad (9.31)$$

$$\lim_{\varepsilon \rightarrow 0} \frac{h_0(\eta\tau_\eta) + \varepsilon h_1(\eta\tau_\eta) - g_0(\eta\tau_\eta/\varepsilon) - g_1(\eta\tau_\eta/\varepsilon)}{\varepsilon} = 0. \quad (9.32)$$

To apply condition (9.31), the trick is to expand $h_0(\eta\tau_\eta)$ and $g_0(\eta\tau_\eta/\varepsilon)$ for small η in a Taylor series:

$$\begin{aligned} h_0(\eta\tau_\eta) &= A_1(1 - \eta\tau_\eta + \mathcal{O}(\eta^2)), \\ g_0(\eta\tau_\eta/\varepsilon) &= 1 - e^{-\eta\tau_\eta/\varepsilon}. \end{aligned}$$

Substituting the last two expressions into (9.31), we can look at different orders of η . For the constant term $\mathcal{O}(1) = \mathcal{O}(\eta^0)$, it follows that

$$\lim_{\varepsilon \rightarrow 0} A_1 - 1 = 0.$$

Clearly, this implies that $A_1 = 1$. The second-order term yields

$$\lim_{\varepsilon \rightarrow 0} \eta\tau_\eta = 0.$$

Therefore, we must have $\eta \ll 1$. Since the term $e^{-\eta\tau_\eta/\varepsilon}$ does not match any term in our asymptotic sequence ε^k , it must be beyond all orders (or transcendentally small). This implies that $\varepsilon|\log\varepsilon| \ll \eta$. In summary, we have

$$A_1 = 1 \quad \text{and} \quad \varepsilon|\log\varepsilon| \ll \eta(\varepsilon) \ll 1.$$

These results for the unknown coefficient and the overlap domain agree precisely with the earlier calculations.

Exercise 9.1.5. Using the matching condition (9.32), show that $A_2 = 2$ and verify that an overlap domain for the asymptotic expansion up to order $\mathcal{O}(\varepsilon)$ is given by $\varepsilon|\log\varepsilon| \ll \eta(\varepsilon) \ll \varepsilon^{1/2}$. ◇

We can now summarize the key elements of the method of **matched asymptotic expansions**:

1. Understand the decomposition into different asymptotic regimes.
2. Consider a general or explicit ansatz with an asymptotic sequence.
3. Compute by regular perturbation the inner and outer expansions.
4. Determine the unknown constants, the domains of validity, and if necessary, the asymptotic sequence from matching conditions.
5. Derive a composite expansion by subtracting common terms.

Our introduction to matched asymptotic expansions so far has been very formal to illustrate the connection to fast–slow systems. Now we shall illustrate a fast computational method that works well on many classical problems taking several nonrigorous shortcuts. Consider the second-order singularly perturbed problem

$$\varepsilon \frac{d^2y}{d\tau^2} + (1 + \tau) \frac{dy}{d\tau} + y = \varepsilon \ddot{y} + (1 + \tau)\dot{y} + y = 0, \quad (9.33)$$

which is time-dependent, with boundary conditions

$$y(0) = 1 \quad \text{and} \quad y(1) = 1. \quad (9.34)$$

A good geometric understanding of the problem would tell us where the boundary layer is, but let us just guess that there is an inner/fast layer near $\tau = 0$ and the rest of the solution consists of an outer/slow layer. Equation (9.33) is written on the slow time scale τ , and the standard ansatz is

$$y(\tau; \varepsilon) = h_0(\tau) + h_1(\tau)\varepsilon + \mathcal{O}(\varepsilon^2). \quad (9.35)$$

Substituting (9.35) into (9.33) and collecting terms of different orders in ε gives the equations

$$(1 + \tau)\dot{h}_0 + h_0 = 0 \quad \text{and} \quad (1 + \tau)\dot{h}_1 + h_1 + \ddot{h}_0 = 0,$$

where we must satisfy the boundary conditions $h_0(1) = 1$ and $h_1(1) = 0$. The equations are easily solved:

$$h_0(\tau) = 2(1 + \tau)^{-1} \quad \text{and} \quad h_1(\tau) = 2(1 + \tau)^{-3} - \frac{1}{2}(1 + \tau)^{-1}.$$

Considering (9.33) on the time scale $\tau = t\varepsilon$, we get

$$\frac{d^2y}{dt^2} + (1 + \varepsilon t) \frac{dy}{dt} + \varepsilon y = y'' + (1 + \varepsilon t)y' + \varepsilon y = 0. \quad (9.36)$$

The standard ansatz for the inner/fast asymptotic expansion is

$$y(t; \varepsilon) = g_0(t) + g_1(t)\varepsilon + \mathcal{O}(\varepsilon^2). \quad (9.37)$$

Substituting (9.37) into (9.36) and collecting terms again, we obtain

$$g_0'' + g_0 = 0 \quad \text{and} \quad g_1'' + g_1' + tg_0' + g_0 = 0.$$

Taking into account the boundary conditions $g_0(0) = 1$ and $g_1(0) = 0$ yields

$$g_0(t) = 1 + A_0(e^{-t} - 1) \quad \text{and} \quad g_1(t) = -t + A_0 \left(-\frac{1}{2}t^2 e^{-t} + t \right) + A_1(e^{-t} - 1).$$

Next, we could employ the formal asymptotic matching conditions for an intermediate time scale $\tau = \eta\tau_\eta$:

$$\begin{aligned} \lim_{\varepsilon \rightarrow 0} h_0(\eta\tau_\eta) - g_0(\eta\tau_\eta/\varepsilon) &= 0, \\ \lim_{\varepsilon \rightarrow 0} \frac{h_0(\eta\tau_\eta) + \varepsilon h_1(\eta\tau_\eta) - g_0(\eta\tau_\eta/\varepsilon) - g_1(\eta\tau_\eta/\varepsilon)}{\varepsilon} &= 0. \end{aligned} \quad (9.38)$$

This procedure will give the overlap domains and determine the constants A_i for $i = 1, 2$. Instead, we are going to apply another argument. Consider the outer/slow solution $y(\tau; \varepsilon)$, which is clearly not valid at $\tau = 0$. However, one can just expand the solution in a series under the assumption $\tau \rightarrow 0^+$, i.e., this is an expansion for the slow/outer solution in the fast/inner limit and requires $\tau \ll 1$. This idea yields

$$y(\tau; \varepsilon) = 2 + \mathcal{O}(\varepsilon, \tau) \quad \text{as } \tau \rightarrow 0^+.$$

Similarly, one can expand the fast/inner solution in the outer/slow limit $t \rightarrow \infty$. As long as $1 \ll \tau/\varepsilon = t$ and $\tau \ll 1$ hold, we also have $\varepsilon t \rightarrow 0^+$. Therefore, expanding the fast solution in terms of $\varepsilon t \approx 0$ leads to

$$y(t; \varepsilon) = 1 - A_0 + \mathcal{O}(\varepsilon t) = 1 - A_0 + \mathcal{O}(\tau).$$

The expressions $1 - A_0 + \mathcal{O}(\tau)$ and $2 + \mathcal{O}(\varepsilon, \tau)$ should agree, so that we must have $A_0 = -1$. During the process, we also had to require that $\varepsilon \ll \tau \ll 1$, which, in our previous notation, is the condition $\varepsilon \ll \eta \ll 1$ on the intermediate time scale, i.e., it is the common domain of validity for an expansion up to order $\mathcal{O}(1)$. It can be shown that for the expansion up to order $\mathcal{O}(\varepsilon)$, we get

$$\varepsilon \ll \eta \ll \varepsilon^{1/2} \quad \text{and} \quad A_1 = -\frac{3}{2}.$$

Exercise 9.1.6. Calculate the domains of validity and the constants A_i for $i = 1, 2$ using the asymptotic matching conditions (9.38). Compare your computations to the ad hoc method of reexpanding inner and outer solutions in the limits $t \rightarrow \infty$ and $\tau \rightarrow 0^+$. \diamond

Note that the computational ideas described here avoid some complications and are based on the observation that one should be able to match solutions by expanding them on a suitable time scale into a domain where they were not originally valid. Exercise 9.1.6 should convince you that the computations to be carried out are basically the same for each approach.

Exercise 9.1.7. Show that the composite expansion

$$y(\tau; \varepsilon) = \left(\frac{2}{1 + \tau} - e^{-t} \right) + \left(\frac{2}{(1 + \tau)^3} - \frac{1}{2(1 + \tau)} + \left(\frac{1}{2}t^2 - \frac{3}{2} \right)e^{-t} \right)\varepsilon + \mathcal{O}(\varepsilon^2)$$

is uniformly valid for (9.33) up to order two. \diamond

9.2 Further Concepts and Terminology

There are many other standard concepts in asymptotic analysis and perturbation theory. The goal of this section is to introduce a few of these ideas and the required notation in the context of examples and then relate them to the geometric viewpoint of fast–slow systems.

Recall the linear second-order differential equation we solved in the last section using matched asymptotic expansions:

$$\varepsilon \frac{d^2y}{d\tau^2} + \frac{dy}{d\tau} + y = \varepsilon \ddot{y} + \dot{y} + y = 0. \quad (9.39)$$

From geometric fast–slow analysis, we were able to determine that asymptotic expansions should involve the slow time scale τ and a fast time scale $t = \tau/\varepsilon$. Classical asymptotic analysis derives this statement by setting $\tau_\eta = \tau/\eta(\varepsilon)$ in (9.39), which yields

$$\frac{\varepsilon}{\eta^2} \frac{d^2y}{d\tau_\eta^2} + \frac{1}{\eta} \frac{dy}{d\tau_\eta} + y = 0. \quad (9.40)$$

If $\eta(\varepsilon) = \mathcal{O}(1)$, so, e.g., we pick $\eta(\varepsilon) = 1$, then for ε sufficiently small, the two largest terms in (9.40) yield the outer/slow limiting equation

$$\frac{dy}{d\tau_\eta} + y = 0. \quad (9.41)$$

The two terms on the left-hand side of (9.41) are in a so-called **dominant balance**, i.e., they are the largest terms as $\varepsilon \rightarrow 0$ and they have the same order.

Definition 9.2.1. Let $\tau_\eta = \tau/\eta(\varepsilon)$ be a time rescaling. If $\eta(\varepsilon) = \mathcal{O}(h(\varepsilon))$ for some fixed function h as $\varepsilon \rightarrow 0$, then we call the differential equation obtained by this time rescaling a **distinguished limit**.

If we assume only a range for the magnitude of a time rescaling such as $\varepsilon \ll \eta(\varepsilon) \ll 1$, we can still consider (9.40), but it would not be written in a distinguished limit. Looking at (9.40), we could also try to find $\eta(\varepsilon)$ such that the second and first derivative terms are in dominant balance. This requires

$$\frac{\varepsilon}{\eta^2} = \frac{1}{\eta} \Rightarrow \eta(\varepsilon) = \mathcal{O}(\varepsilon).$$

For definiteness, we choose $\eta(\varepsilon) = \varepsilon$, and substituting this into (9.40) yields the inner/fast limiting equation

$$\frac{d^2y}{d\tau_\eta^2} + \frac{dy}{d\tau_\eta} = 0. \quad (9.42)$$

Again we see that (9.42) is obtained from a dominant balance using a distinguished limit. Note that other choices of $\eta(\varepsilon)$ are possible but do not yield a dominant balance. For example, if we set $\eta(\varepsilon) = \varepsilon^2$, we find that (9.40) degenerates into

$$\frac{d^2y}{d\tau_\eta^2} = 0.$$

Often it is understood that if a distinguished limit appears, then a dominant balance argument has been used to choose it. In terms of geometric fast–slow systems theory, the two distinguished limits we have obtained in (9.41) and (9.42) correspond respectively to the slow and fast subsystems. To see this, we begin with the fast subsystem. Consider the equation (9.40) with $t = \tau/\varepsilon$:

$$y'' + y' + \varepsilon y = 0. \quad (9.43)$$

Then set $\frac{1}{\varepsilon}y' =: x$, which transforms (9.43) into

$$\begin{aligned} \varepsilon x' + \varepsilon x + \varepsilon y &= 0, \\ y' &= \varepsilon x, \end{aligned}$$

which is just the fast subsystem if we cancel ε in the first equation and then let $\varepsilon \rightarrow 0$. Similarly, consider the second-order equation on the slow scale τ :

$$\varepsilon \ddot{y} + \dot{y} + y = 0. \quad (9.44)$$

Setting $\dot{y} =: x$ and letting $\varepsilon \rightarrow 0$ gives the differential algebraic system defining the slow flow

$$\begin{aligned} 0 &= -x - y, \\ \dot{y} &= x. \end{aligned}$$

Obviously, the ideas of dominant balance and distinguished limit can be used for much more general equations than just the linear problem we considered here.

Another important concept is that of interior layers, already mentioned in the last section. As an example, consider the unforced van der Pol equation

$$\begin{aligned} \varepsilon \dot{x} &= y - \left(\frac{x^3}{3} - x \right), \\ \dot{y} &= -x. \end{aligned} \quad (9.45)$$

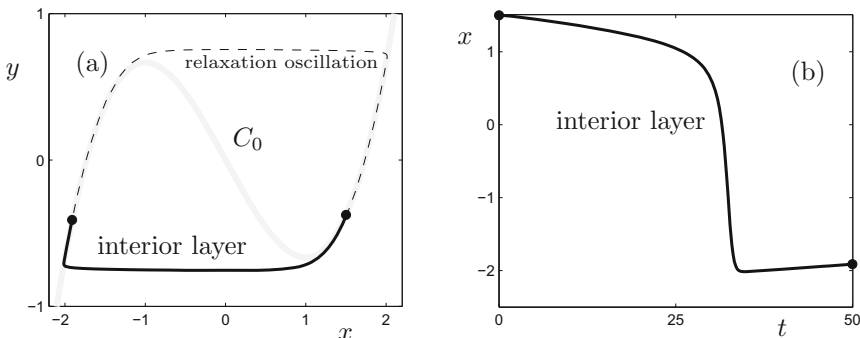


Figure 9.6: Interior layer in a relaxation oscillation for van der Pol's equation (9.45) ($\varepsilon = 0.01$). (a) Phase portrait with the relaxation oscillation (thin black dashed) and an interior layer (thick black). (b) Time series for the interior layer with initial point and endpoint for the finite time interval $t \in [0, 50]$.

The critical manifold of (9.45) is $C_0 = \left\{y = \frac{x^3}{3} - x =: c(x)\right\}$. We know from Sections 5.2 and 7.5 that (9.45) exhibits periodic relaxation oscillations consisting of two fast and two slow segments; see Figure 9.6(a). Instead of looking at the full periodic orbit, let us consider the initial value problem defined by (9.45) and initial conditions

$$x(0) = \frac{3}{2} \quad \text{and} \quad y(0) = c\left(\frac{3}{2}\right) = -\frac{3}{8}.$$

If we consider the solution on the finite time interval $t \in [0, 50]$, then we obtain the time series shown in Figure 9.6(b). The trajectory starts $\mathcal{O}(\varepsilon)$ -close to the slow manifold C_ε obtained as a perturbation of C_0 using Fenichel's theorem; see Figure 9.6(a). Hence, there is no long initial fast transient, and the solution lies close to the attracting critical manifold $C_0 \cap \{x > 1\}$ until it reaches the vicinity of the fold point $(1, -2/3)$, where it jumps close to the other attracting branch $C_0 \cap \{x < -1\}$. Then another slow segment occurs before $t = 50$. Therefore, the time series has a fast jump somewhere around the middle of the time interval. Note that we could also pose (9.45) with boundary conditions instead of initial conditions and obtain a similar time series, as shown in Figure 9.6(b).

Definition 9.2.2. An asymptotic solution of a fast–slow system on a fixed fast-scale time interval $[T_0, T_1]$ has an **interior layer** if a fast subsystem asymptotic expansion is required for $t \in [t_0, t_1]$ with $T_0 < t_0 < t_1 < T_1$ and t_i is at least $\mathcal{O}(1)$ bounded away from T_i for $i = 1, 2$.

Definition 9.2.2 is obviously quite broad, but it captures the essence of the intuitive idea of what an interior layer should be. On the slow time scale $\tau = t\varepsilon$, the requirement that the times t_i be $\mathcal{O}(1)$ away from the fixed time interval boundaries translates into the statement that the times $\tau_i = t_i\varepsilon$ are at least $\mathcal{O}(\varepsilon)$ away from εT_i . The next example shows that special asymptotic expansions in the interior of a time domain are not necessarily connected to “standard” fast jumps.

Example 9.2.3. Consider the two-point boundary value problem on $\tau \in [-1, 1]$

$$\varepsilon \ddot{y} + \tau \dot{y} - y = 0, \quad y(-1) = 1, \quad y(1) = 2. \quad (9.46)$$

As usual, we will first transform the problem into a fast–slow system to understand what to expect. So set $\dot{y} =: x$. Then we get

$$\begin{aligned} \varepsilon \dot{x} &= -\tau x + y, \\ \dot{y} &= x. \end{aligned} \quad (9.47)$$

Note that (9.47) is a nonautonomous system of ODEs, so we add $\dot{\tau} = 1$ to the system to make it autonomous. This yields

$$\begin{aligned} \varepsilon \dot{x} &= -\tau x + y, \\ \dot{y} &= x, \\ \dot{\tau} &= 1. \end{aligned} \quad (9.48)$$

Using the boundary conditions of (9.46), it follows that the phase space of (9.48) is limited to $P := \{(x, y, \tau) \in \mathbb{R}^3 : \tau \in [-1, 1]\}$. Every solution of (9.48) has to

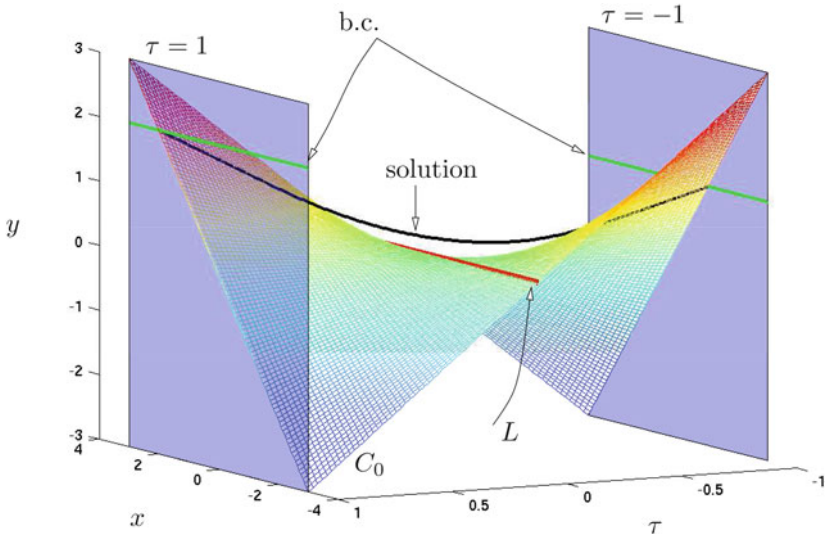


Figure 9.7: Solution (black) of the boundary value problem (9.46) from the viewpoint of fast–slow systems for $\varepsilon = 0.05$. The critical manifold C_0 is shown as a colored surface, where the color is derived from a “height”-function of the y -coordinate. The singular points $L \subset C_0$ (red) form a line. The boundary conditions (b.c., green) lie inside two planes given by the starting time $\tau = -1$ and the final time $\tau = 1$.

satisfy the boundary conditions, so it has to start on the line $\{\tau = -1, y = 1\}$ and end on the line $\{\tau = 1, y = 2\}$. The critical manifold of (9.48) is

$$C_0 = \{(x, y, \tau) \in P : y = \tau x\}.$$

The key observation is that C_0 is not normally hyperbolic for $\tau = 0$. Denote these singular points by

$$L = C_0 \cap \{\tau = 0\} = \{(x, y, \tau) \in P : \tau = 0 = y\}.$$

Hence, there is the possibility that a solution might enter a neighborhood of L near or on a slow manifold, but then normal hyperbolicity fails to hold at $\tau = 0$. This implies that regular perturbation theory for a single solution in the interior of $[\tau = -1, \tau = 1]$ will usually not suffice, even if we make a clever choice of time scale. The exact solution of (9.46) can be computed in integral form:

$$y(\tau) = K_1 \tau + K_2 \left(e^{-\tau^2/(2\varepsilon)} + \frac{\tau}{\varepsilon} \int_{-1}^{\tau} e^{-s^2/(2\varepsilon)} ds \right),$$

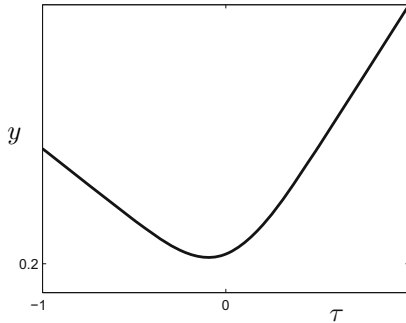


Figure 9.8: Time series of the corner-layer solution of (9.46) for $\varepsilon = 0.05$.

where the boundary conditions determine the constants K_i ,

$$K_1 = -1 + \frac{3e^{-1/(2\varepsilon)}}{2e^{-1/(2\varepsilon)} + I(\varepsilon)\varepsilon},$$

$$K_2 = \frac{3}{2e^{-1/(2\varepsilon)} + I(\varepsilon)/\varepsilon},$$

and $I(\varepsilon) = \int_{-1}^1 e^{-s^2/(2\varepsilon)} ds$. The solution is illustrated in Figure 9.7. It is visible that the solution departs slightly from the vicinity of C_0 near the singular points L .

The example shows that asymptotic solutions of rather simple-looking boundary value problems can be very intricate. Classical asymptotic terminology calls the part of the solution shown in Figure 9.7 near $\tau = 0$ a **corner layer**. This terminology again stems from the viewpoint of time series as seen by looking at the $(\tau, y(\tau))$ -plot of the solution shown in Figure 9.8. ♦

Exercise 9.2.4. Find an asymptotic expansion for (9.46) valid up to $\mathcal{O}(\varepsilon)$. ◊

9.3 The Boundary Function Method

The method of matched asymptotics requires, even for a normally hyperbolic problem, quite substantial calculations. In general, there are multiple layers with different time scales that have to be matched. Given an (m, n) -fast–slow system

$$\begin{aligned} \varepsilon \frac{dx}{d\tau} &= \varepsilon \dot{x} = f(x, y), \\ \frac{dy}{d\tau} &= \dot{y} = g(x, y), \end{aligned} \tag{9.49}$$

for $z := (x, y) \in \mathbb{R}^{m+n}$ and $0 < \varepsilon \ll 1$ with normally hyperbolic attracting critical manifold $C_0 = \{f = 0\}$, we already know the structure of the solutions and the second important time scale $t = \tau/\varepsilon$. The **boundary function method** makes use of this knowledge to develop asymptotic expansions. The first main idea is to write the solution of (9.49) as

$$\begin{pmatrix} x(\tau; \varepsilon) \\ y(\tau; \varepsilon) \end{pmatrix} = z(\tau; \varepsilon) = \bar{z}(\tau; \varepsilon) + Z(t; \varepsilon) = \begin{pmatrix} \bar{x}(\tau; \varepsilon) \\ \bar{y}(\tau; \varepsilon) \end{pmatrix} + \begin{pmatrix} X(t; \varepsilon) \\ Y(t; \varepsilon) \end{pmatrix} \tag{9.50}$$

to represent the two time scales explicitly. Then \bar{z} and Z are expanded asymptotically with asymptotic sequence $\{\varepsilon^k\}_{k=0}^\infty$ as $\varepsilon \rightarrow 0$:

$$\begin{aligned}\bar{z}(\tau; \varepsilon) &\sim \bar{z}_0(\tau) + \bar{z}_1(\tau)\varepsilon + \bar{z}_2(\tau)\varepsilon^2 + \dots, \\ Z(t; \varepsilon) &\sim Z_0(t) + Z_1(t)\varepsilon + Z_2(t)\varepsilon^2 + \dots.\end{aligned}\quad (9.51)$$

Substituting (9.50) into (9.49) yields

$$\begin{aligned}\varepsilon \frac{d\bar{x}}{d\tau} + \frac{dX}{dt} &= f(\bar{x} + X, \bar{y} + Y), \\ \frac{d\bar{y}}{d\tau} + \frac{1}{\varepsilon} \frac{dY}{dt} &= g(\bar{x} + X, \bar{y} + Y).\end{aligned}\quad (9.52)$$

The next step is to represent the right-hand side of (9.52) also as a sum, e.g., $f = \bar{f} + F$, to take the two time scales into account. For example, for the fast variables, we obtain

$$\begin{aligned}f(\bar{x} + X, \bar{y} + Y) &= f(\bar{x}(\tau; \varepsilon), \bar{y}(\tau; \varepsilon)) + \\ &\quad [f(\bar{x}(\varepsilon t; \varepsilon) + X(t; \varepsilon), \bar{y}(\varepsilon t; \varepsilon) + Y(t; \varepsilon)) - f(\bar{x}(\varepsilon t; \varepsilon), \bar{y}(\varepsilon t; \varepsilon))] \\ &=: \bar{f} + F.\end{aligned}$$

Once we treat g in a similar way, the system (9.52) reads

$$\begin{aligned}\varepsilon \dot{\bar{x}} + X' &= \bar{f} + F, \\ \dot{\bar{y}} + \frac{1}{\varepsilon} Y' &= \bar{g} + G,\end{aligned}\quad (9.53)$$

where $' = d/dt$ as usual. Each term on the right-hand side of (9.53) can be expanded asymptotically again:

$$\begin{aligned}\bar{f} &\sim \bar{f}_0 + \bar{f}_1\varepsilon + \bar{f}_2\varepsilon^2 + \dots, & F &\sim F_0 + F_1\varepsilon + F_2\varepsilon^2 + \dots, \\ \bar{g} &\sim \bar{g}_0 + \bar{g}_1\varepsilon + \bar{g}_2\varepsilon^2 + \dots, & G &\sim G_0 + G_1\varepsilon + G_2\varepsilon^2 + \dots.\end{aligned}\quad (9.54)$$

The asymptotics in (9.54) work by straightforward Taylor expansion, e.g.,

$$\begin{aligned}\bar{f} &= f(\bar{x}_0(\tau) + \bar{x}_1(\tau)\varepsilon + \dots, \bar{y}_0(\tau) + \bar{y}_1(\tau)\varepsilon + \dots) \\ &= f(\bar{x}_0(\tau), \bar{y}_0(\tau)) + \left[\bar{x}_1(\tau) \frac{\partial \bar{f}}{\partial x}(\bar{x}_0(\tau), \bar{y}_0(\tau)) + \bar{y}_1(\tau) \frac{\partial \bar{f}}{\partial y}(\bar{x}_0(\tau), \bar{y}_0(\tau)) \right] \varepsilon \\ &\quad + \dots + \left[\bar{x}_k(\tau) \frac{\partial \bar{f}}{\partial x}(\bar{x}_0(\tau), \bar{y}_0(\tau)) + \bar{y}_k(\tau) \frac{\partial \bar{f}}{\partial y}(\bar{x}_0(\tau), \bar{y}_0(\tau)) + r_k \right] \varepsilon^k + \dots,\end{aligned}$$

where the terms r_k depend only on $\bar{x}_j(\tau)$ and $\bar{y}_j(\tau)$ for $j < k$. It will be best to see the dependencies in an example.

Exercise 9.3.1. Suppose $f(x, y) = y^2 - x$. Calculate the asymptotic series (9.54) for \bar{f} and F . \diamond

The second step for the boundary function method is to write down the hierarchy of equations that have to be solved to obtain the asymptotic series coefficients. The idea is to consider terms in (9.54) depending on τ and t separately and collect equal powers of ε . Hence, the leading-order term $\bar{z}_0(\tau) = (\bar{x}_0(\tau), \bar{y}_0(\tau))^\top$ on the slow scale τ satisfies

$$\begin{aligned}0 &= \bar{f}_0 = f(\bar{x}_0(\tau), \bar{y}_0(\tau)), \\ \frac{d\bar{y}_0}{d\tau} &= \bar{g}_0 = g(\bar{x}_0(\tau), \bar{y}_0(\tau)),\end{aligned}\quad (9.55)$$

which is just the slow subsystem of the original problem (9.49). This result is completely expected, since $\bar{x}_0(\tau)$ is the leading-order term for the slow dynamics. Similarly, we obtain the anticipated result that $Z_0(t) = (X_0(t), Y_0(t))^\top$ satisfies

$$\begin{aligned}\frac{dX_0}{dt} &= F_0 = f(\bar{x}_0(0) + X_0, \bar{y}_0(0) + Y_0) - f(\bar{x}_0(0), \bar{y}_0(0)), \\ &\quad = f(\bar{x}_0(0) + X_0, \bar{y}_0(0) + Y_0), \\ \frac{dY_0}{dt} &= G_0 = 0,\end{aligned}\tag{9.56}$$

which is the fast subsystem to which the condition $f(\bar{x}_0(\tau), \bar{y}_0(\tau)) = 0$ from (9.55) has already been applied. Collecting the different $\mathcal{O}(\varepsilon^k)$ -terms for each $k \geq 1$ gives the remaining equations

$$\begin{aligned}\dot{\bar{x}}_{k-1} &= \bar{f}_k, & X'_k &= F_k, \\ \dot{\bar{y}}_k &= \bar{g}_k, & Y'_k &= G_{k-1}.\end{aligned}\tag{9.57}$$

The remaining step of the boundary function method is to include the initial condition $z_0 = (x_0, y_0)$ in a suitable way. Using the expansions (9.51) yields

$$\begin{aligned}x_0 &= \bar{x}_0(0) + \bar{x}_1(0)\varepsilon + \cdots + X_0(0) + X_1(0)\varepsilon + \cdots, \\ y_0 &= \bar{y}_0(0) + \bar{y}_1(0)\varepsilon + \cdots + Y_0(0) + Y_1(0)\varepsilon + \cdots,\end{aligned}\tag{9.58}$$

which immediately imply, on collecting equal powers of ε , that

$$x_0 = \bar{x}_0(0) + X_0(0) \quad \text{and} \quad y_0 = \bar{y}_0(0) + Y_0(0).\tag{9.59}$$

The higher-order terms must vanish, which yields for $k \geq 1$ that

$$0 = \bar{x}_k(0) + X_k(0) \quad \text{and} \quad 0 = \bar{y}_k(0) + Y_k(0).\tag{9.60}$$

Let us first focus on (9.59). Since we know only (x_0, y_0) , additional conditions must be imposed to determine the four terms $\bar{x}_0(0)$, $X_0(0)$, $\bar{y}_0(0)$, and $Y_0(0)$. The algebraic equation $f(\bar{x}_0(\tau), \bar{y}_0(\tau)) = 0$ from (9.55) allows us to determine from, say $\bar{y}_0(0)$, the corresponding base point $\bar{x}_0(0)$ on the normally hyperbolic attracting critical manifold C , so that $\bar{x}_0(0)$ does not have to be treated as an unknown. In a similar way, $\bar{x}_k(0)$ can be determined via algebraic equations arising from (9.57). The next step is key, and it imposes conditions on the **boundary functions** $Y_k(t)$ at $t = 0$. Since C_0 is normally hyperbolic and attracting, we expect the fast terms $Z_k(t) = (X_k(t), Y_k(t))^\top$ to decay exponentially as $t \rightarrow \infty$. It turns out that it suffices to impose this constraint on the t -dependent terms of the slow variables

$$Y_k(\infty) = 0, \quad \text{for all } k = 0, 1, 2, \dots\tag{9.61}$$

As a simple consistency check, we look at $k = 0$, where $Y'_0 = 0$ from (9.56) and $Y_0(\infty) = 0$ imply that $Y_0(t) \equiv 0$. This is correct, since the slow variables do not change to lowest order on the fast time scale for trajectories approaching a normally hyperbolic critical manifold. In the classical terminology, this corresponds to the fact that the function $y(\tau; \varepsilon)$ does not have a boundary layer to lowest order.

Theorem 9.3.2 ([VBK95]). Consider (9.49), where f, g are smooth, and suppose the critical manifold C_0 is normally hyperbolic attracting. Then the scheme defined via (9.55)–(9.61) yields an asymptotic expansion for $z(\tau; \varepsilon) = (x(\tau; \varepsilon), y(\tau; \varepsilon))^\top$ uniformly valid for $0 \leq \tau \leq T$, for a fixed final time $T > 0$, as $\varepsilon \rightarrow 0$, i.e.,

$$\max_{0 \leq \tau \leq T} \left\| z(\tau; \varepsilon) - \sum_{k=0}^K [\bar{z}_k(\tau) + Z_k(t)] \varepsilon^k \right\| = \mathcal{O}(\varepsilon^{K+1}) \quad \text{for each } k \in \mathbb{N}_0.$$

Obviously, the conditions on C_0 can be relaxed to be normally hyperbolic attracting in a certain compact region, since the trajectory segment $z(\tau; \varepsilon)$ is approximated only for a compact time interval $0 \leq \tau \leq T$.

Example 9.3.3. Let us consider the simple $(1, 1)$ -fast–slow system

$$\begin{aligned} \varepsilon \dot{x} &= y^2 - x = f(x, y), \\ \dot{y} &= 1 = g(x, y), \end{aligned} \tag{9.62}$$

which is a test example that we will encounter again in Chapter 11. The initial condition for (9.62) is given by $(x(0), y(0)) = (x_0, y_0)$. The critical manifold $C_0 = \{y^2 = x\}$ is normally hyperbolic attracting everywhere in \mathbb{R}^2 . Direct calculations show that

$$\begin{aligned} \bar{f} &= f(\bar{x}(\tau; \varepsilon), \bar{y}(\tau; \varepsilon)) = \bar{y}(\tau; \varepsilon)^2 - \bar{x}(\tau; \varepsilon) \\ &\sim \bar{y}_0^2 - \bar{x}_0 + [2\bar{y}_0\bar{y}_1 - \bar{x}_1]\varepsilon + \dots = \bar{f}_0 + \varepsilon \bar{f}_1. \\ F &= [f(\bar{x}(\varepsilon t; \varepsilon) + X(t; \varepsilon), \bar{y}(\varepsilon t; \varepsilon) + Y(t; \varepsilon)) - f(\bar{x}(\varepsilon t; \varepsilon), \bar{y}(\varepsilon t; \varepsilon))] \\ &= Y(t; \varepsilon)^2 + 2\bar{y}(\varepsilon t; \varepsilon)Y(t; \varepsilon) - X(t; \varepsilon) \\ &\sim Y_0^2 - X_0 + 2Y_0\bar{y}_0 + \varepsilon[2(Y_0Y_1 + \bar{y}_0Y_1 + \bar{y}_1Y_0) - X_1] + \dots = F_0 + \varepsilon F_1 + \dots, \end{aligned}$$

where we have omitted higher-order terms, since we want to calculate the asymptotic series solutions only up to order $\mathcal{O}(\varepsilon)$. Obviously, $\bar{g} \equiv 1 = \bar{g}_0$ and $G \equiv 0$, so that $\bar{g}_k \equiv 0$ for $k \geq 1$ and $G_k \equiv 0$ for $k \geq 0$. Starting with the slow subsystem (9.55), we obtain

$$\begin{aligned} 0 &= \bar{f}_0 = \bar{y}_0^2 - \bar{x}_0 &\Rightarrow \bar{y}_0(\tau)^2 &= \bar{x}_0(\tau), \\ \dot{\bar{y}}_0 &= 1 &\Rightarrow \bar{y}_0(\tau) &= \tau + \bar{y}_0(0). \end{aligned}$$

The fast subsystem (9.56) yields

$$\begin{aligned} X'_0 &= F_0 = Y_0^2 - X_0 + 2Y_0\bar{y}_0, \\ Y'_0 &= G_0 = 0 &\Rightarrow Y_0(t) &= \text{const.} \end{aligned} \tag{9.63}$$

The boundary function condition (9.61) implies that $Y_0(t) \equiv 0$. This simplifies the equation for X_0 , yielding

$$X'_0 = Y_0^2 - X_0 + 2Y_0\bar{y}_0 = -X_0 \Rightarrow X_0(t) = X_0(0)e^{-t}.$$

From the initial conditions (9.59), it follows that $y_0 = \bar{y}_0(0) + Y_0(0) = \bar{y}_0(0)$ and $x_0 = \bar{x}_0 + X_0(0) = y_0^2 + X_0(0)$. Hence, the zeroth-order asymptotic solution is

$$\begin{aligned} x(\tau; \varepsilon) &= (y_0 + \tau)^2 + [x_0 - y_0^2]e^{-\tau/\varepsilon} + \mathcal{O}(\varepsilon), \\ y(\tau; \varepsilon) &= \tau + y_0 + \mathcal{O}(\varepsilon). \end{aligned} \tag{9.64}$$

Examining the solution (9.64), we see that it is exact for the slow variable. It also has the right behavior for the fast variable with an exponentially fast decay toward the critical manifold and then a slow flow evolution. We proceed to the slow time scale equations (9.57) for the first-order expansion

$$\begin{aligned} 2(y_0 + \tau) = \dot{\bar{x}}_0 &= \bar{f}_1 = 2\bar{y}_0\bar{y}_1 - \bar{x}_1 \Rightarrow \bar{x}_1(\tau) = 2(\tau + y_0)\bar{y}_1(\tau) - 2(y_0 + \tau), \\ \dot{\bar{y}}_1 &= \bar{g}_1 = 0 \Rightarrow \bar{y}_1(\tau) = \bar{y}_1(0). \end{aligned}$$

The fast time scale equations (9.57) for the first-order expansion are

$$\begin{aligned} X'_1 &= F_1 = -X_1 + 2(Y_0Y_1 + \bar{y}_0Y_1 + \bar{y}_1Y_0) = -X_1 + 2(\varepsilon t + y_0)Y_1(0), \\ Y'_1 &= G_0 = 0. \end{aligned} \quad (9.65)$$

Obviously, we get $Y_1(t) = 0$ using the boundary function conditions $Y_1(\infty) = 0$. This implies that $X_1(t) = X_1(0)e^{-t}$. From the initial conditions, we have (9.60), and we obtain

$$0 = \bar{y}_1(0) + Y_1(0) = \bar{y}_1(0) \Rightarrow \bar{y}_1(\tau) \equiv 0, \quad \bar{x}_1(\tau) = -2(y_0 + \tau).$$

The initial condition $0 = \bar{x}_1(0) + X_1(0)$ then implies that $X_1(0) = 2y_0$, so

$$X_1(t) = 2y_0e^{-t}, \quad Y_1(t) \equiv 0, \quad \bar{x}_1(\tau) = -2(y_0 + \tau), \quad \bar{y}_1(\tau) \equiv 0.$$

Hence, the first-order asymptotic solution is

$$\begin{aligned} x(\tau; \varepsilon) &= (y_0 + \tau)^2 + [x_0 - y_0^2]e^{-\tau/\varepsilon} + [2y_0e^{-\tau/\varepsilon} - 2(y_0 + \tau)]\varepsilon + \mathcal{O}(\varepsilon^2), \\ y(\tau; \varepsilon) &= \tau + y_0 + \mathcal{O}(\varepsilon^2), \end{aligned}$$

which is uniformly valid on compact time intervals as $\varepsilon \rightarrow 0$. ♦

Exercise/Project 9.3.4. Consider (9.62) from Example 9.3.3 and compute the second-order asymptotic expansion using the boundary function method. Compare your result with the exact solution of (9.62). What about higher-order expansions? ◇

As a concluding remark, we see that the boundary function method takes advantage of the a priori known structure of the fast-slow system in its setup to compute asymptotic expansions. This theme will occur several times in the remaining parts of this chapter.

9.4 WKB Theory

Another important classical asymptotic method is the **Wentzel, Kramers, Brillouin (WKB)** approximation. Often, the name WKB encompasses a rather wide class of ideas. Here we shall just restrict ourselves to the classical case. Suppose we want to solve a higher-order ODE written in one variable y :

$$F\left(\frac{d^n y}{d\tau^n}, \frac{d^{n-1} y}{d\tau^{n-1}}, \dots, \frac{dy}{d\tau}, y, \tau; \varepsilon\right) = 0. \quad (9.66)$$

Obviously, not all problems of the form (9.66) can be treated using WKB theory. One potential application occurs when the highest derivative in (9.66) is multiplied by ε . The central ansatz of the WKB method is to try an approximation of the form

$$y(\tau) \sim \exp \left(\frac{1}{\gamma(\varepsilon)} \sum_{j=0}^{\infty} \gamma(\varepsilon)^j S_j(\tau) \right) \quad \text{with } \gamma(\varepsilon) \rightarrow 0 \text{ as } \varepsilon \rightarrow 0, \quad (9.67)$$

where the functions S_j and γ are to be determined. The motivation of the ansatz (9.67) can be given by various arguments. For example, looking at the very simple linear equation

$$\varepsilon \dot{y} = \pm y \quad \Rightarrow \quad y(\tau) = y(0) e^{\pm \tau/\varepsilon},$$

one may conjecture that it is a good idea to build in an exponential-type solution in the asymptotic ansatz, since it appears naturally in a very simple version of (9.66). Before we discuss the validity conditions for the WKB method, it helps to consider an example.

Example 9.4.1. A second-order homogeneous linear differential equation is said to be of **Schrödinger type** if the first derivative term \dot{y} is not present:

$$\varepsilon^2 \frac{d^2 y}{d\tau^2} = \varepsilon^2 \ddot{y} = Q(\tau)y, \quad Q(\tau) \neq 0. \quad (9.68)$$

At first glance, (9.68) looks to be quite a degenerate problem from a fast–slow systems point of view. For example, consider the case $Q(\tau) = 1$. Then one possible associated first-order $(1, 1)$ -fast–slow system is

$$\begin{aligned} \varepsilon^2 \dot{x} &= y, \\ \dot{y} &= x. \end{aligned} \quad (9.69)$$

The critical manifold $C_0 = \{y = 0\}$ of (9.69) is nowhere normally hyperbolic; however, see Exercise 5.4.4 for a better coordinate change. In any case, the WKB ansatz easily produces a solution by a direct application, as we shall now demonstrate. Differentiating (9.67) twice, we get

$$\begin{aligned} \dot{y} &\sim \left[\frac{1}{\gamma(\varepsilon)} \sum_{j=0}^{\infty} \gamma(\varepsilon)^j \dot{S}_j(\tau) \right] \exp \left(\frac{1}{\gamma(\varepsilon)} \sum_{j=0}^{\infty} \gamma(\varepsilon)^j S_j(\tau) \right), \\ \ddot{y} &\sim \left[\frac{1}{\gamma(\varepsilon)^2} \left(\sum_{j=0}^{\infty} \gamma(\varepsilon)^j \dot{S}_j(\tau) \right)^2 + \frac{1}{\gamma(\varepsilon)} \sum_{j=0}^{\infty} \gamma(\varepsilon)^j \ddot{S}_j(\tau) \right] \exp \left(\frac{1}{\gamma(\varepsilon)} \sum_{j=0}^{\infty} \gamma(\varepsilon)^j S_j(\tau) \right), \end{aligned}$$

with $\gamma(\varepsilon) \rightarrow 0$ as $\varepsilon \rightarrow 0$. Substituting the second derivative and the WKB ansatz into (9.68) gives

$$\frac{\varepsilon^2}{\gamma(\varepsilon)^2} (\dot{S}_0)^2 + \frac{2\varepsilon^2}{\gamma(\varepsilon)} \dot{S}_0 \dot{S}_1 + \frac{\varepsilon^2}{\gamma(\varepsilon)} \ddot{S}_0 + \dots = Q(\tau), \quad (9.70)$$

where the exponential terms already have been canceled. Dominant balance requires that $Q(\tau)$ has the same order as the largest term on the left-hand side of (9.70). This requires choosing $\gamma(\varepsilon) = \varepsilon$, and it also explains why we have begun with an equation having ε^2 in it, since this avoids many square roots. The usual regular perturbation approach of comparing different powers of ε in (9.70) then yields

$$Q(\tau) = (\dot{S}_0)^2, \quad (9.71)$$

$$0 = 2\dot{S}_0\dot{S}_1 + \ddot{S}_0, \quad (9.72)$$

$$0 = 2\dot{S}_0\dot{S}_k + \ddot{S}_{k-1} + \sum_{j=1}^{k-1} \dot{S}_j\dot{S}_{k-j} \quad \text{for } k \geq 2. \quad (9.73)$$

Equation (9.71) is an **eikonal equation** with the two symbolic solutions

$$S_0(\tau) = \pm \int^\tau \sqrt{Q(s)} \, ds. \quad (9.74)$$

The equation for S_1 given by (9.72) is a **transport equation**; it has a solution given by

$$S_1(\tau) = -\frac{1}{4} \ln Q(\tau). \quad (9.75)$$

If we use only the first two terms S_0 and S_1 in the WKB approximation for the Schrödinger equation, we get two solutions, one for each sign of (9.74). Forming the linear combination yields

$$y(\tau) \sim \frac{K_1}{Q(\tau)^{1/4}} \exp\left(\frac{1}{\varepsilon} \int_{\tau_0}^\tau \sqrt{Q(s)} \, ds\right) + \frac{K_2}{Q(\tau)^{1/4}} \exp\left(-\frac{1}{\varepsilon} \int_{\tau_0}^\tau \sqrt{Q(s)} \, ds\right)$$

as a leading-order approximation for $y(\tau)$, where the constants K_i for $i = 1, 2$ are to be determined from initial and/or boundary conditions, and τ_0 is an arbitrary fixed integration limit. ♦

It should be clear from Example 9.4.1 that the actual calculations for the WKB method are relatively straightforward. However, the method has a remarkable range of applications; see Section 9.11. It can even be used to recover a large part of the boundary layer theory that we treated using matched asymptotic expansions.

Exercise 9.4.2. Consider the **quartic oscillator**

$$\varepsilon^2 \frac{d^2 y}{d\tau^2} = q(\tau) y^3 \quad (9.76)$$

and calculate its asymptotic solution using the WKB method. ◇

The main conditions for the validity of the WKB method, which we just state here, are as follows:

- (C1) The sequence of functions $\gamma(\varepsilon)^{j-1} S_j(\tau)$ has to be an asymptotic sequence as $\gamma(\varepsilon) \rightarrow 0$ for $\varepsilon \rightarrow 0$. Preferably, this should hold uniformly in τ .

- (C2) If we want a good approximation by truncating at the term $\gamma(\varepsilon)^{N-1} S_N(\tau)$, we must have

$$\gamma(\varepsilon)^N S_{N+1}(\tau) \ll 1 \quad \text{as } \varepsilon \rightarrow 0. \quad (9.77)$$

If $\gamma(\varepsilon)^N S_{N+1}(\tau)$ is not much smaller than 1, the exponential of the neglected terms will be large.

In particular, if (C1) and (C2) hold, the relative error will be

$$\frac{y(\tau) - \exp\left(1/\gamma(\varepsilon) \sum_{j=0}^N \gamma(\varepsilon)^j S_s(\tau)\right)}{y(\tau)} \sim \gamma(\varepsilon)^N S_{N+1}(\tau) \quad \text{as } \varepsilon \rightarrow 0.$$

Before we finish our very brief discussion of the WKB method, we mention that retaining only the S_0 term is called the **geometrical optics approximation**. Keeping S_0 and S_1 is called the **physical optics approximation**.

9.5 Asymptotics and Blowup

It is interesting to ask how asymptotic matching and the blowup method are related. Recall that in Section 5.4, the asymptotic expansion near a generic fold point was derived using asymptotic matching. In Section 7.4, the blowup method was used to derive a similar result, which we now recall. As we saw in Section 4.2, the normal form for a generic planar fold at the origin is

$$\begin{aligned} \frac{dx}{dt} &= x' = -y + x^2 + F(x, y, \varepsilon), \\ \frac{dy}{dt} &= y' = \varepsilon(-1 + G(x, y, \varepsilon)), \end{aligned} \quad (9.78)$$

where the higher-order terms can be written explicitly as

$$\begin{aligned} F(x, y, \varepsilon) &= axy + bx^3 + \mathcal{O}(y^2, \varepsilon x, \varepsilon y, x^2 y, x^4), \\ G(x, y, \varepsilon) &= cx + \mathcal{O}(x^2, y, \varepsilon x). \end{aligned}$$

Let C_0 denote the critical manifold of (9.78). Then C_0 naturally splits into two parts: $C_0^a = C_0 \cap \{x < 0\}$ and $C_0^r = C_0 \cap \{x > 0\}$; see also Figure 7.8 or Figure 9.9. Consider two sections for $\rho > 0$ small,

$$\Delta^{\text{in}} := \{(x, \rho^2) : x \in J_{\text{in}}\} \quad \text{and} \quad \Delta^{\text{out}} = \{(\rho, y) : y \in J_{\text{out}}\},$$

where J_{in} and J_{out} are two intervals to be chosen such that $\Pi : \Delta^{\text{in}} \rightarrow \Delta^{\text{out}}$ is a well-defined transition map for the flow of all trajectories close to C_ε^a near the fold point. Theorem 7.4.1 will be restated here for convenience:

Theorem 9.5.1. *There exists $\varepsilon_0 > 0$ such that for $\varepsilon \in (0, \varepsilon_0]$, the following hold:*

1. *The manifold C_ε^a passes through Δ^{out} at $(\rho, h(\varepsilon))$ with $h(\varepsilon) = \mathcal{O}(\varepsilon^{2/3})$.*
2. *Δ^{in} is mapped by Π to an interval of size $\mathcal{O}(e^{-K/\varepsilon})$ for some $K > 0$.*

3. The function $h(\varepsilon)$ has asymptotic expansion

$$h(\varepsilon) = c_1 \varepsilon^{2/3} + c_2 \ln \varepsilon + c_3 \varepsilon + \mathcal{O}(\varepsilon^{4/3} \ln \varepsilon) \quad \text{as } \varepsilon \rightarrow 0. \quad (9.79)$$

Recall that in Section 4.2, we stated a more general version of the asymptotic expansion (9.79). Here we outline how to get this more detailed result using a combination of blowup and asymptotic matching. Define the following function:

$$\varpi(j) := \begin{cases} \left[\frac{j+2}{3} \right] - 1 & \text{if } j+1 = 3m \text{ for some } m \in \mathbb{N}_0, \\ \left[\frac{j+2}{3} \right] & \text{otherwise.} \end{cases}$$

Theorem 9.5.2 ([vGKS05]; see also [MR80]). *There exist smooth functions $c_{jl}(\rho)$ such that for every $N \geq 1$,*

$$h(\varepsilon) = \rho^2 \sum_{j=0}^N \sum_{l=0}^{\varpi(j)} c_{jl}(\rho) \left(\frac{\varepsilon}{\rho^3} \right)^{\frac{2+j}{3}} \left(\ln \frac{\varepsilon}{\rho^3} \right)^l + \mathcal{O} \left(\left(\frac{\varepsilon}{\rho^3} \right)^{\frac{N+3}{3}} \right). \quad (9.80)$$

The detailed computation of (9.80) is relatively long and quite involved. However, the overall idea, which we will describe below, is very interesting; see Chapter 7 for more details on the background required for the following argument.

Proof. (Sketch; [vGKS05]) First, augment the system (9.78) by $\varepsilon' = 0$ and consider the blowup at $(x, y, \varepsilon) = (0, 0, 0)$ defined by

$$\varphi : S^2 \times [0, r_0] \rightarrow \mathbb{R}^3, \quad \varphi(\bar{x}, \bar{y}, \bar{\varepsilon}, \bar{r}) = (\bar{r}\bar{x}, \bar{r}^2\bar{y}, \bar{r}^3\bar{\varepsilon}) = (x, y, \varepsilon),$$

where $r_0 > 0$ is suitably chosen. The singularity $(0, 0, 0)$ corresponds to the two-sphere $\{\bar{r} = 0\}$ in the blowup coordinates. As usual, it is better to consider directional blowups to parameterize $S^2 \times [0, r_0]$ given in the three charts

$$\begin{aligned} K_1 : \quad &x = r_1 x_1, \quad y = r_1^2, \quad \varepsilon = r_1^3 \varepsilon_1, \\ K_2 : \quad &x = r_2 x_2, \quad y = r_2^2 y_2, \quad \varepsilon = r_2^3, \\ K_3 : \quad &x = r_3, \quad y = r_3^2 y_3, \quad \varepsilon = r_3^3 \varepsilon_3. \end{aligned} \quad (9.81)$$

Recall that the three charts parameterize different regions V_ε^i in (x, y, ε) -space. In particular, K_1 covers V_ε^1 , which is a neighborhood of C_ε^a with $y > K\varepsilon^{\frac{2}{3}}$ for some constant $K > 0$; K_2 covers V_ε^2 , which is a neighborhood of the origin of size $((\mathcal{O}(\varepsilon^{\frac{1}{3}}), \mathcal{O}(\varepsilon^{\frac{2}{3}}))$; K_3 covers V_ε^3 , which is a neighborhood of the critical fiber $\{(x, 0) : x \in \mathbb{R}\}$ with $x > K\varepsilon^{\frac{1}{3}}$.

The situation is illustrated in Figure 9.9. Recall that in the proof of Theorem 9.5.1, one uses (9.81) to find three vector fields that can be desingularized by dividing out a suitable power of r_i . In K_1 , a center manifold M_1^a is found that corresponds to C_ε^a in the blown-up coordinates. This manifold can be extended into K_2 as M_2^a via a coordinate change. The same applies to extend M_2^a into K_3 as M_3^a . All three manifolds together define a manifold \tilde{M}^a , which can be viewed as a blown-up version of C_ε^a ; see Figure 9.10.

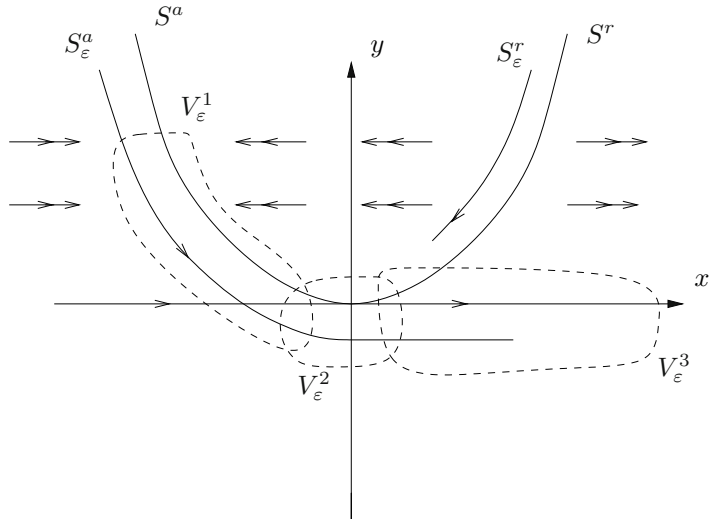


Figure 9.9: Covering of S_ε^a and its extension under the flow by regions V_ε^i associated with directional blowups in charts K_i for $i = 1, 2, 3$; see equation (9.81) and Section 7.4.

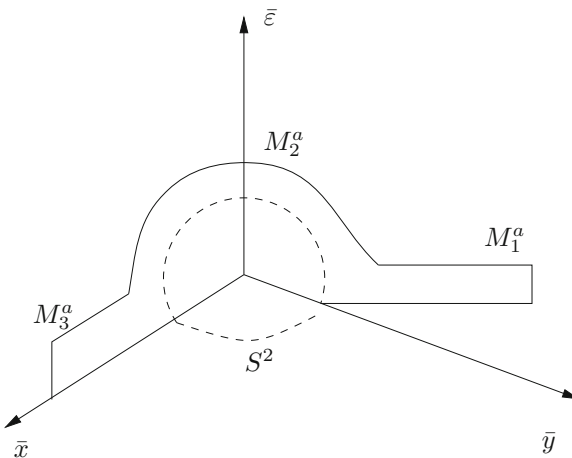


Figure 9.10: Sketch of blown-up version $\tilde{M}^a = M_1^a \cup M_2^a \cup M_3^a$ of the slow attracting manifold S_ε^a for equation (9.78).

The main idea is to derive an asymptotic expansion of M_i^a in each chart. It can be shown that M_1^a will not contribute to the final expansion (9.80); since in V_ε^1 , there is an exponential contraction toward C_ε^a for all trajectories, it is intuitive that the expansion of $h(\varepsilon)$ can depend at most on exponentially small

terms coming from M_1^a . For M_2^a in K_2 , one can make the ansatz

$$y_2 = \sum_{j=0}^{\infty} m_{2,j}^a(x_2) r_2^j.$$

For M_3^a in K_3 , the following asymptotic series works:

$$y_3 = \sum_{j=0}^{\infty} m_{3,j}^a(\varepsilon_3) r_3^j.$$

Then it turns out, after quite substantial calculation, that the special form of (9.80) is due to a resonance phenomenon in K_3 . The center manifold M_3^a contains a saddle equilibrium point. The blown-up linearized vector field at this point has eigenvalues λ_i that satisfy the resonance relation $\lambda_1 + \lambda_2 = \lambda_3$. \square

Remark: Note very carefully that the idea in the last proof was implicitly present in the ad hoc calculations in Section 4.2. There we considered the slow manifold C_ε^a in different regimes and applied scaling transformations in each regime to compute locally valid asymptotic expansions. The blowup provides a geometric viewpoint of these ideas.

The idea in the last proof also suggests a more general strategy for using the blowup and asymptotic calculations in tandem. Suppose we face a singular perturbation problem for which the asymptotic expansion of a special trajectory or an invariant manifold is not known. One could guess what the right expansion is in sufficiently small subdomains and use asymptotic matching. The problem is that some guesswork is involved in this procedure. Instead, using quasihomogeneity and a blowup, the problem is naturally structured into several subdomains where the dynamics are (partially) hyperbolic. Then an expansion of the desired trajectory can be obtained in each directional blowup chart using a regular expansion ansatz. The resulting expansions can be matched via either overlap domains or invariant manifold methods. Carrying this program out in practice is nontrivial, as the next, very difficult, exercise shows.

Exercise/Project 9.5.3. Consider the fast–slow **pitchfork bifurcation** normal form

$$\begin{aligned} x' &= -yx - x^3, \\ y' &= \varepsilon, \end{aligned} \tag{9.82}$$

and try to prove a result similar to Theorem 9.5.2 using asymptotic expansions in blowup charts; see also Section 12.7. \diamond

9.6 Averaging

The method of averaging is introduced here from an asymptotics viewpoint. We begin with a brief review of classical averaging theory. Consider an ODE of the form

$$\frac{dy}{d\tau} = \dot{y} = \delta G(Y, \tau, \delta) \tag{9.83}$$

for $y \in \mathbb{R}^m$, $0 < \delta \ll 1$, and G is assumed to be sufficiently smooth and periodic in τ with period $T > 0$. Define the **averaged equation** (or the **averaged system**) as

$$\dot{Y} = \frac{\delta}{T} \int_0^T G(Y, s, 0) \, ds =: \delta \bar{G}(y). \quad (9.84)$$

In this case, the classical averaging theorem relates the solutions $y(\tau)$ of (9.83) and $Y(\tau)$ of (9.84).

Theorem 9.6.1 (see, e.g., [GH83, SVM07]). *There exists a change of coordinates $y = Y + \delta w(Y, \tau, \delta)$ such that (9.83) becomes*

$$\dot{Y} = \delta \bar{G}(Y) + \delta^2 G_1(Y, \tau, \delta),$$

where G_1 is of period T in τ . Furthermore, if $\|y(0) - Y(0)\| = \mathcal{O}(\delta)$, then

$$\|y(\tau) - Y(\tau)\| = \mathcal{O}(\delta) \quad (9.85)$$

on a time scale $\tau = \mathcal{O}(1/\delta)$, i.e., there exists a constant $K > 0$ independent of δ such that (9.85) is valid for $0 \leq \tau\delta \leq K$.

The main idea is that the averaged system is close for a long time to the original system. One can actually obtain further conclusions about the averaged system; see Section 9.11.

Notice that a fast–slow system does not have to be in the form (9.83) suitable for averaging with $\varepsilon = \delta$, since we usually have

$$\begin{aligned} \dot{x} &= \frac{1}{\varepsilon} f(x, y), \\ \dot{y} &= g(x, y). \end{aligned} \quad (9.86)$$

However, the averaging idea is still extremely useful, since it may be of interest to understand the slow dynamics on a family of fast subsystem periodic orbits. Normally, hyperbolic parts of the critical manifold C_0 are families of fast subsystem hyperbolic equilibria. For the equilibrium case, we know that there is a slow flow on a slow manifold that is $\mathcal{O}(\varepsilon)$ -close to C_0 . We want an analogue of the result for periodic orbits of the fast subsystem. The idea is to find a flow that approximates the flow on the family of periodic orbits. Consider the fast subsystem

$$\frac{dx}{dt} = x' = f(x, y) \quad (9.87)$$

such that (9.87) has a continuous family of periodic orbits $\gamma(t, y)$ for each value of y in some neighborhood \mathcal{D}_0 of $y = y(0) =: y_0$ with period $T(y)$ that is uniformly bounded so that there are constants $T_1, T_2 > 0$ such that $T_1 \leq T(y) \leq T_2$. For simplicity, we shall also assume that each orbit $\gamma(t, y)$ is asymptotically stable with respect to the fast variables. It seems plausible that the full fast–slow system (9.86) should have solutions $(x(\tau), y(\tau))$ such that the fast motion is approximated by the family of fast subsystem periodic orbits

$$x(\tau) \approx \gamma\left(\frac{\tau}{\varepsilon}, y(\tau)\right).$$

Formally, substituting this result into the slow subsystem yields

$$\dot{y} = g(\gamma(\tau/\varepsilon, y), y).$$

The idea is that the slow motion on the family of periodic orbits can be obtained by averaging out the fast oscillations. Hence, we are led to consider

$$\dot{Y} = \bar{g}(Y) := \frac{1}{T(Y)} \int_0^{T(Y)} g(\gamma(t, Y), Y) dt. \quad (9.88)$$

It will be convenient to make a change of variable $t = T(Y)\theta$ and to set $\Gamma(\theta, Y) = \gamma(T(Y)\theta, Y)$. This transforms (9.88) into

$$\dot{Y} = \int_0^1 g(\Gamma(\theta, Y), Y) d\theta. \quad (9.89)$$

Assume that the solution $Y(\tau)$ with initial condition $Y(0) = Y_0$ stays inside \mathcal{D}_0 for $0 \leq \tau \leq \tau_1$. The following theorem shows that the averaging procedure produces the correct result with an error of order $\mathcal{O}(\varepsilon)$.

Theorem 9.6.2 ([PR60]; see also [BG06]). *Let x_0 be sufficiently close to $\Gamma(\theta_0, Y_0)$ for some θ_0 . Then there exists a function $\theta(\tau)$ that satisfies a differential equation of the form*

$$\varepsilon \dot{\theta} = \frac{1}{T(Y)} + \mathcal{O}(\varepsilon), \quad \theta(0) = \theta_0,$$

and the following estimates hold:

$$\begin{aligned} x(\tau) &= \Gamma(\theta(\tau), Y(\tau)) + \mathcal{O}(\varepsilon), \\ y(\tau) &= Y(\tau) + \mathcal{O}(\varepsilon), \end{aligned}$$

for $\mathcal{O}(\varepsilon |\log \varepsilon|) \leq \tau \leq \tau_1$.

Proof. (Sketch; [PR60, BG06]) We shall consider only the case of a planar fast variable $x \in \mathbb{R}^2$. Let $n(\theta, y)$ denote the outward unit normal to the periodic orbit $\Gamma(\theta, y)$. Changing to polar coordinates (θ, r) near the periodic orbit can be achieved by the transform

$$x = \Gamma(\theta, y) + rn(\theta, y). \quad (9.90)$$

Then the fast subsystems near the periodic orbits are given by

$$\varepsilon \dot{x} = f(\Gamma(\theta, y), y) + A(\theta, y)n(\theta, y)r + \mathcal{O}(r^2),$$

where $A(\theta, y) = D_x f(\Gamma(\theta, y), y)$ is the linearization along the periodic orbit. Note that we can also express $\varepsilon \dot{x}$ as a function of \dot{r} and $\dot{\theta}$ by differentiating (9.90) and using the equation for \dot{y} . A bit of calculation shows that we will end up with a system

$$\begin{aligned} \varepsilon \dot{\theta} &= \frac{1}{T(y)} + b_\theta(\theta, r, y, \varepsilon), \\ \varepsilon \dot{r} &= f_r(\theta, r, y, \varepsilon), \\ \dot{y} &= g(\Gamma(\theta, y) + rn(\theta, y), y), \end{aligned} \quad (9.91)$$

where the functions b_θ and f_r can be computed explicitly in terms of A , Γ , n , and their derivatives with respect to y . It is not difficult to see that b_θ and f_r will vanish for $r = 0 = \varepsilon$, since in this case, we have precisely the singular limit dynamics on a periodic orbit. In fact, the linearization $D_r f_r(\theta, 0, y, 0)$ depends only on $A(\theta, y)$. Observe that in a neighborhood of $r = 0$, it follows that $\dot{\theta} > 0$, and one can reduce the three equations (9.91) to two:

$$\begin{aligned}\frac{dr}{d\theta} &= T(y) \frac{f_r(\theta, r, y, \varepsilon)}{1 + T(y)b_\theta(\theta, r, y, \varepsilon)}, \\ \frac{dy}{d\theta} &= \varepsilon T(y) \frac{g(\Gamma(\theta, y)) + rn(\theta, y, y)}{1 + T(y)b_\theta(\theta, r, y, \varepsilon)}.\end{aligned}\quad (9.92)$$

Averaging the right-hand side of (9.92) over θ yields

$$\begin{aligned}\frac{dR}{d\theta} &= T(Y)(a(Y)R + \mathcal{O}(\varepsilon)), \\ \frac{dY}{d\theta} &= \varepsilon(\bar{g}(Y) + \mathcal{O}(R) + \mathcal{O}(\varepsilon)),\end{aligned}\quad (9.93)$$

where $a(Y) < 0$; this last fact follows from the asymptotic stability of the periodic orbits. Note that (9.93) is again fast–slow and the angular variable evolves on the fast time scale. Fenichel theory now implies that R approaches a slow manifold in an $\mathcal{O}(\varepsilon)$ -neighborhood of $\{R = 0\}$. For such R , the classical averaging theorem (see Theorem 9.6.1) applies to show that $r(\tau) - R(\tau)$ and $y(\tau) - Y(\tau)$ remain $\mathcal{O}(\varepsilon)$ -close up to times $\theta(\tau) = \mathcal{O}(1/\varepsilon)$. \square

Theorem 9.6.2 shows that up to an error of order $\mathcal{O}(\varepsilon)$, the effective slow dynamics on a family of periodic orbits are determined by an averaged system. For an application of averaging to bursting oscillations, we refer to Section 13.6.

One does not have to stop at periodic orbits and consider more complicated invariant sets such as tori or even chaotic invariant sets; see also Section 14.9. Suppose the fast subsystems support a smooth family of invariant sets (e.g., tori). Then we can often “average” over the attractor similarly to what was done the case of periodic orbits; see also Section 9.11.

Exercise/Project 9.6.3. Consider the Morris–Lecar model discussed in Sections 13.6 and 13.7 and check when Theorem 9.6.2 can be applied to it. Compare your analytical results with the direct simulation and numerical continuation methods presented in Chapter 10. \diamond

9.7 Gevrey Asymptotics

So far, we have dealt mostly with classical asymptotic sequences of the form $\{\varepsilon^k\}_{k=0}^\infty$ as $\varepsilon \rightarrow 0$. In this case, terms of the form $\mathcal{O}(e^{-K/\varepsilon})$ with $0 < K = \mathcal{O}(1)$ are called transcendently small or beyond all orders. Indeed, considering the function

$$a(\varepsilon) = \begin{cases} e^{-1/\varepsilon} & \text{if } \varepsilon > 0, \\ 0 & \text{if } \varepsilon \leq 0,\end{cases}\quad (9.94)$$

we see that a formal (Poincaré) expansion as $\varepsilon \rightarrow 0$ yields

$$a(\varepsilon) = \sum_{k=0}^{\infty} a_k \varepsilon^k = \sum_{k=0}^{\infty} 0 \cdot \varepsilon^k = 0,$$

since $|a(\varepsilon)| \leq K_N |\varepsilon|^N$ for $N = 0, 1, 2, \dots$ and some positive fixed numbers K_N . One also refers to (9.94) as an **asymptotically flat function** in the sense of Poincaré. The major idea of Gevrey asymptotics is to look at a much finer scale. A function $f(\varepsilon)$ is **asymptotically flat of Gevrey order s** if

$$f(\varepsilon) \leq K \exp\left(-\frac{c}{|\varepsilon|^{1/s}}\right)$$

for some positive $c, K = \mathcal{O}(1)$. For example, the function $a(\varepsilon)$ is asymptotically flat of Gevrey order s for every $s \geq 1$ as $\varepsilon \rightarrow 0$. It can actually be shown that this concept of asymptotic flatness characterizes the approach of Gevrey asymptotics that we shall outline here. The next two definitions form the basis of the subject.

Definition 9.7.1. Let $s \geq 0$ and consider a formal power series

$$p = \sum_{m=0}^{\infty} a_m \varepsilon^m.$$

We say that p is of **Gevrey order s** (as $\varepsilon \rightarrow 0$) if there exist constants $K, A \geq 0$ such that

$$|a_m| \leq K(m!)^s A^m, \quad \text{for } m = 0, 1, 2, \dots \quad (9.95)$$

The set of all power series in ε of Gevrey order s is denoted by $\mathbb{C}[[\varepsilon]]_s$.

Observe that $\mathbb{C}[[\varepsilon]]_0$ actually is the set of power series that converge for sufficiently small ε . It is also not difficult to see that $\mathbb{C}[[\varepsilon]]_s$ is a vector space under the natural operations.

Remark: Sometimes, one finds a slightly modified definition of Gevrey order s that replaces (9.95) by

$$|a_m| \leq K \Gamma(1 + sm) A^m,$$

where $\Gamma(\cdot)$ denotes the gamma function, which replaces the factorial; recall that $\Gamma(1 + sm) = (sm)!$ for $sm \in \mathbb{N}$. We shall restrict ourselves to Definition 9.7.1 here.

Definition 9.7.2. A function $f(\varepsilon)$ admits an **asymptotic expansion of Gevrey order s** ($s \geq 0$),

$$p = p(\varepsilon) = \sum_{m=0}^{\infty} a_m \varepsilon^m,$$

as $\varepsilon \rightarrow 0$ on a **sectorial domain**

$$\mathfrak{D}_{r,a,b} := \{\varepsilon \in \mathbb{C} : a < \arg \varepsilon < b, 0 < |\varepsilon| < r\}$$

if the following conditions are satisfied:

(i) f is **holomorphic** (i.e., complex analytic; see [Gam01]) on $\mathfrak{D}_{r,a,b}$.

(ii) There exists a formal power series $p = \sum_{k=0}^{\infty} a_k \varepsilon^k$ such that

$$\left| f(\varepsilon) - \sum_{m=0}^{N-1} a_m \varepsilon^m \right| \leq C_{\rho,\alpha,\beta} (N!)^s (A_{\rho,\alpha,\beta})^N |\varepsilon|^N \quad (9.96)$$

holds on $\mathfrak{D}_{r,a,b}$ for every $N \in \mathbb{N}$ for $0 < \rho < r$ and $a < \alpha < \beta < b$, and $C_{\rho,\alpha,\beta}$ and $A_{\rho,\alpha,\beta}$ are nonnegative constants depending on f and (ρ, α, β) .

We also write $f(\varepsilon) \sim_s p(\varepsilon)$ and let $\mathcal{G}_s(r, a, b)$ denote the set of all functions admitting an asymptotic expansion of Gevrey order s .

Definitions 9.7.1 and 9.7.2 can be easily extended to the case that f depends on another variable or parameter; for example, if $f = f(u, \varepsilon)$, then one has to consider the coefficients $a_k = a_k(u)$ and require all estimates for u in a suitable domain. It follows from Definition 9.7.2 that if $\tilde{s} > s$ and $f(\varepsilon) \sim_s p(\varepsilon)$, then $f(\varepsilon) \sim_{\tilde{s}} p(\varepsilon)$. The key measure of Gevrey asymptotic series is the size of the error terms (9.96). Classical Poincaré asymptotics would require

$$\left| f(\varepsilon) - \sum_{m=0}^{N-1} a_m \varepsilon^m \right| \leq C |\varepsilon|^N \quad (9.97)$$

for some constant $C > 0$ as $\varepsilon \rightarrow 0$. Hence, the Gevrey requirement (9.96) is stricter than the Poincaré one, since the growth of the error terms is restricted. In particular, if $f(\varepsilon) \sim_s p(\varepsilon)$, then we get that $f(\varepsilon) \sim p(\varepsilon)$. Consider the map

$$J : \mathcal{G}_s(r, a, b) \rightarrow \mathbb{C}[[\varepsilon]]_s, \quad J(f) = p,$$

that sends a function f to its Gevrey series. The nullspace of J is

$$\mathcal{G}_{s,0}(r, a, b) := \{f \in \mathcal{G}_s(r, a, b) : J(f) = 0\},$$

and it can be nicely characterized by the following theorem.

Theorem 9.7.3 ([Sib00]). *If $s = 0$, then $\mathcal{G}_{s,0}(r, a, b) = \{0\}$. If $s > 0$, then $f \in \mathcal{G}_{s,0}(r, a, b)$ if and only if f is holomorphic and*

$$|f(\varepsilon)| \leq \tilde{C}_{\rho,\alpha,\beta} \exp(-\tilde{A}_{\rho,\alpha,\beta} |\varepsilon|^{-1/s}) \quad (9.98)$$

holds on $\mathfrak{D}_{r,a,b}$ for $0 < \rho < r$ and $a < \alpha < \beta < b$, and $\tilde{C}_{\rho,\alpha,\beta} \geq 0$ and $\tilde{A}_{\rho,\alpha,\beta} > 0$ are constants.

Theorem 9.7.3 justifies the earlier characterization of Gevrey asymptotics in terms of asymptotic flatness. Before we proceed with the general theory, it will help to consider a classical example in which Gevrey asymptotics arises.

Example 9.7.4. Consider the ODE

$$\varepsilon^2 \frac{df}{d\varepsilon} = f - \varepsilon \quad (9.99)$$

for $f = f(\varepsilon)$. A formal power series solution of (9.99) is given by

$$p(\varepsilon) = \sum_{k=0}^{\infty} (k!) \varepsilon^{k+1} = \varepsilon \sum_{k=0}^{\infty} (k!) \varepsilon^k, \quad (9.100)$$

which can be verified by substitution of f by p from (9.100) into (9.99). The series $\sum_{k=0}^{\infty} (k!) \varepsilon^k$ is of Gevrey order 1. ♦

The appearance of Gevrey asymptotics in Example 9.7.4 is well known. It is also a classical result that ODEs like (9.99) with certain singularities exhibit Gevrey asymptotic solutions with divergent series. The viewpoint of multiple time scale dynamics entered the theory much later. One slight obstacle in the development in this direction is that we are primarily interested in fast–slow systems posed for $(x, y, t, \varepsilon) \in \mathbb{R}^{m+n} \times \mathbb{R} \times \mathbb{R}$, which have to be complexified to apply Gevrey asymptotics. Before we look at particular applications to real fast–slow systems, it is natural to consider

$$\begin{aligned} \varepsilon \frac{dx}{dz} &= f(x, y, \varepsilon) \\ \frac{dy}{dz} &= g(x, y, \varepsilon), \end{aligned} \quad (9.101)$$

where $(x, y) \in \mathbb{C}^{m+n}$, $0 < |\varepsilon| \ll 1$, $z \in \mathbb{C}$ is complex time, and f, g map into \mathbb{C}^m and \mathbb{C}^n respectively. We consider the **complex fast–slow system** (9.101) near the origin $(x, y, \varepsilon) \approx (0, 0, 0)$. To make the following statements easier, we always make the standing assumptions that

$$\|x\| < \delta_x, \quad \|y\| < \delta_y, \quad |\arg \varepsilon| < \delta_a, \quad 0 < |\varepsilon| < \delta_\varepsilon, \quad (9.102)$$

where $\|\cdot\|$ is viewed as the Euclidean norm on \mathbb{R}^{2m} and \mathbb{R}^{2n} respectively and $\delta_{(\cdot)} > 0$ are suitable sufficiently small constants. We shall refer to (9.102) simply as the domain \mathfrak{D} ; for example, we assume that f and g are holomorphic in \mathfrak{D} . It can be shown when (9.101) admits an actual solution that has a Gevrey asymptotic expansion.

Theorem 9.7.5 ([Sib00]). *Suppose f, g admit Gevrey asymptotic expansions s and that*

$$(\mathbf{D}_x f)(0, 0, 0) \quad \text{is invertible.} \quad (9.103)$$

Assume also that the following conditions hold:

$$g(0, 0, 0) = 0, \quad f(0, 0, 0) = 0, \quad (9.104)$$

$$(\mathbf{D}_x g)(0, 0, 0) = 0, \quad (\mathbf{D}_y f)(0, 0, 0) = 0. \quad (9.105)$$

Then (9.101) has a unique formal solution $(x, y) = (q(z, \varepsilon), p(z, \varepsilon))$, where the function $q(0, \varepsilon)$ is Gevrey of order r . Furthermore, (9.101) admits an actual holomorphic solution $(x, y) = (\tilde{x}, \tilde{y})$, which has the formal solution as its Gevrey asymptotic expansion of order $\max(s, r)$. In summary, we have

$$(x(z, \varepsilon), y(z, \varepsilon)) \sim_{\max(r, s)} (q(z, \varepsilon), p(z, \varepsilon))$$

as $\varepsilon \rightarrow 0$ in a suitable domain \mathfrak{D} as given in (9.102).

The condition (9.103) just says that the critical manifold does not have any singularities in \mathfrak{D} ; see Section 3.3. This concludes the basic introduction to Gevrey asymptotics. The next two examples show how these ideas have been used in fast–slow systems.

Consider the $(1, 1)$ -fast–slow system

$$\begin{aligned} \varepsilon \dot{x} &= a + y^3 x, \\ \dot{y} &= 1. \end{aligned} \tag{9.106}$$

Observe that the critical manifold $C_0 = \{(x, y) \in \mathbb{R}^2 : a + xy^3 = 0\}$ has a singularity for $a = 0$ at the origin. Depending on the value of a , we may conjecture that canard trajectories exist near the singularity. The vector field (9.106) can be rewritten as

$$\varepsilon \frac{dx}{dy} = a + y^3 x. \tag{9.107}$$

In fact, (9.107) is just an example of the more general problem

$$\varepsilon \frac{dx}{dy} = a + F(y)x + \varepsilon G(x, y, \varepsilon, a), \tag{9.108}$$

where we assume that F, G are real analytic near $(x, y, \varepsilon, a) = (0, 0, 0, 0)$. As usual, we shall refer to $C_0 = \{x = -a/F(y)\}$ as the critical manifold. Sometimes, points where $F(y)$ has a simple zero are called **generic turning points**; it should be noted, as mentioned previously, that the definition of what classes of points are called “turning points” is not completely uniform across the literature. The following theorem can be proved using a combination of blowup and Gevrey methods.

Theorem 9.7.6 ([Mae07b]). *Suppose $f(y) = \lambda y^p + \mathcal{O}(y^{p+1})$ (as $y \rightarrow 0$) for some $\lambda > 0$ and odd $p \in \mathbb{N}$, and set $s := \frac{1}{p+1}$. Then there exist curves*

$$a = A(\varepsilon^s), \quad x = \psi(y, \varepsilon^s)$$

that solve (9.108). For each fixed y , the function $\psi(y, u)$ is of Gevrey order s with respect to u . The **control curve** $A(u)$ is also of Gevrey order s for u in a suitable sectorial domain near $u = 0$ that contains the positive real axis and $A(0) = 0$. Furthermore, an upper bound for the Gevrey order of $a = A(u)$ is provided by

$$\operatorname{Re} \left(\frac{1}{y^{p+1}} \int_y^0 F(w) \, dw \right).$$

Exercise/Project 9.7.7. What is an upper bound for the Gevrey order of $a = A(\varepsilon^s)$ for equation (9.107)? \diamond

The interesting part of Theorem 9.7.6 is that the Gevrey properties of A can be used to prove when the family of solution curves has canard solutions. The idea is to use the characterization of asymptotic flatness for Gevrey functions.

Corollary 9.7.8 ([Mae07b]). *Equation (9.108) has canard solutions if and only if the Taylor series of $A(u)$ is identically zero. Furthermore, if $A \sim_s 0$, then the constant $\tilde{A}_{\rho,\alpha,\beta}$ in Theorem 9.7.3 can be used to estimate the maximum canard size.*

Theorem 9.7.6 and Corollary 9.7.8 show that canard solutions are intricately connected to Gevrey properties; this should be compared with the exponentially small canard region encountered for a singular Hopf bifurcation and its associated canard explosion in Sections 8.1–8.4.

Another interesting context in which Gevrey asymptotics occurs in fast–slow systems is provided by coordinate transformations. Consider a Hamiltonian system in action-angle coordinates (see also Section 19.7)

$$\begin{aligned} \frac{d\varphi}{dt} &= \varphi' = \omega(y), \\ \frac{dy}{dt} &= y' = 0, \end{aligned} \tag{9.109}$$

where $y \in \mathbb{R}^n$ are the action coordinates (often also denoted by I) and φ are the angles or phases. For simplicity, we shall assume that the phase is one-dimensional with $\varphi \in \mathbb{R}/\mathbb{Z} = S^1$ and that $\omega(y)$ is real analytic. Consider a perturbation of (9.109) of the form

$$\begin{aligned} \varphi' &= \omega(y) + \varepsilon F(y, \varphi, \varepsilon), \\ y' &= \varepsilon G(y, \varphi, \varepsilon), \end{aligned} \tag{9.110}$$

where $0 < \varepsilon \ll 1$, and we assume that F, G are real analytic and periodic in φ with period 1. Note that the perturbation is not necessarily Hamiltonian. Sometimes, (9.110) is called a system with **fast rotating phase** due to the obvious time scale separation between the fast phase and the slow action variables. One natural question is how far we can simplify the $(1, n)$ -fast–slow system (9.110) by a formal **near-identity transformation**

$$\begin{aligned} y &= Y + \varepsilon U(Y, \hat{\varphi}) = Y + \varepsilon U_1(Y, \hat{\varphi}) + \varepsilon^2 U_2(Y, \hat{\varphi}) + \dots, \\ \varphi &= \hat{\varphi} + \varepsilon V(Y, \hat{\varphi}) = \hat{\varphi} + \varepsilon V_1(Y, \hat{\varphi}) + \varepsilon^2 V_2(Y, \hat{\varphi}) + \dots, \end{aligned} \tag{9.111}$$

where we require 1-periodicity of U, V in φ .

Theorem 9.7.9 ([RS96]). *In a sufficiently small neighborhood of the origin, the $(1, n)$ -fast–slow system (9.110) can be transformed by a coordinate change*

$$\begin{aligned} y &= Y + \varepsilon U(Y, \hat{\varphi}), \\ \varphi &= \hat{\varphi} + \varepsilon V(Y, \hat{\varphi}), \end{aligned}$$

into a system of the form

$$\begin{aligned}\hat{\varphi}' &= \omega(y) + \varepsilon \left(\hat{G}(Y, \varepsilon) + \beta(Y, \hat{\varphi}, \varepsilon) \right), \\ Y' &= \varepsilon \left(\hat{F}(Y, \varepsilon) + \alpha(Y, \hat{\varphi}) \right).\end{aligned}$$

The functions U and V are analytic of Gevrey order 1 (on a suitable domain). Moreover, the functions α and β are uniformly exponentially small:

$$\|\alpha\| + |\beta| < K_1 \exp(-K_2/|\varepsilon|) \quad \text{for constants } K_{1,2} > 0.$$

In particular, the transformed system has slow action coordinates independent of the phase up to exponentially small errors.

Theorem 9.7.9 tells us that the transformation that eliminates the fast variable in (9.110) has Gevrey order 1 and that the reduction works with exponentially small error.

9.8 Poincaré–Lindstedt and Two-Timing

In this section, we shall briefly discuss classical asymptotic methods designed for problems of the form

$$\frac{dz}{dt} = z' = F(z, t, \delta), \tag{9.112}$$

where F will be real analytic, $z \in \mathbb{R}^N$, $0 < \delta \ll 1$, and we assume that the problem $z' = F(z, t, 0)$ is easy to solve. Note that (9.112) does not have our usual multiple time scales structure. Recall from Section 5.1 that solutions $z(t; \delta)$ to (9.112) satisfy the estimate

$$\|z(t; \delta) - z(t; 0)\| = \mathcal{O}(\delta)$$

for times $t \in [0, T]$ with $T = \mathcal{O}(1)$. One major question is what happens on a longer time scale and whether asymptotic expansions can be used in this context. A simple example illustrates these issues.

Example 9.8.1. Consider the **damped harmonic oscillator** with small damping $0 < \delta \ll 1$ given by

$$x'' + 2\delta x' + x = 0, \quad x(0) = 1, \quad x'(0) = 0. \tag{9.113}$$

The unperturbed equation for $\delta = 0$ is the classical **harmonic oscillator**. The standard trick $x' =: y$ for (9.113) yields

$$\begin{aligned}x' &= y, \\ y' &= -2\delta y - x.\end{aligned}$$

Obviously, the exact solution can be calculated easily, and solutions decay to zero as $t \rightarrow \infty$. Let us make the regular perturbation ansatz for (9.113):

$$x(t; \delta) = x_0(t) + \delta x_1(t) + \delta^2 x_2(t) + \dots$$

Collecting the $\mathcal{O}(1)$ -terms leads to the equation

$$x_0'' + x_0 = 0, \quad x_0(0) = 1, \quad x_0'(0) = 0,$$

which can be solved easily to yield $x_0(t) = \cos t$. Using this solution and collecting the $\mathcal{O}(\delta)$ -terms yields

$$x_1'' + x_1 = 2 \sin t, \quad x_1(0) = 0, \quad x_1'(0) = 0.$$

Again, the solution is not difficult to find, since $x_1(t) = \sin t - t \cos t$. Therefore, the regular perturbation expansion up to first order is

$$x(t; \delta) \sim \cos t + \delta(\sin t - t \cos t) + \mathcal{O}(\delta^2), \quad \text{as } \delta \rightarrow 0. \quad (9.114)$$

In fact, if $t = \mathcal{O}(1)$, then the regular expansion perfectly fits the theory, and (9.114) stays within $\mathcal{O}(\delta)$ of the harmonic oscillator. For $t = \mathcal{O}(1/\delta)$ and beyond, we note that (9.114) fails rather miserably, since the term $\delta|t \cos t|$ will begin to grow without bound. This effect is caused entirely by the perturbation scheme. ♦

Example 9.8.1 shows that regular perturbation expansions can be good for a short $\mathcal{O}(1)$ time scale but that one may run into serious problems on a long time scale $\mathcal{O}(1/\delta)$. Hence, we are dealing with a multiscale problem in which different time scales are important for the validity of an approximate solution. The appearance of certain growing terms for regular perturbation schemes is a major challenge.

Definition 9.8.2. Terms in an asymptotic expansion that grow without bound as time tends to infinity are called **secular terms**.

There are several approaches to producing expansions that are free of spurious secular terms. We shall outline two possibilities for a classical example. More examples are discussed in specialized texts on asymptotic analysis; see Section 9.11. The main example is the **weakly nonlinear Duffing oscillator**

$$\frac{d^2x}{dt^2} + x + \delta x^3 = x'' + x + \delta x^3 = 0, \quad x(0) = 1, \quad x'(0) = 0, \quad (9.115)$$

where $0 < \delta \ll 1$. One can show that (9.115) is solved by a periodic orbit; see also Figure 9.11(a).

Exercise 9.8.3. Prove that (9.115) is a Hamiltonian system. Prove that the solution of (9.115) is periodic. Show that the first-order regular perturbation expansion of (9.115) is

$$x(t; \delta) \sim \cos t - \delta \frac{\sin t}{16} (6t + \sin(2t)) + \mathcal{O}(\delta^2)$$

as $\delta \rightarrow 0$. Therefore, we have a secular term of the form $t \sin t$. ♦

The first method we are going to discuss is due to Lindstedt and Poincaré and is now called **Lindstedt's method** or the **Poincaré–Lindstedt method**. The main idea is to consider a new time variable, say s , given by

$$s = \omega t = (1 + \delta\omega_1 + \delta^2\omega_2 + \dots)t. \quad (9.116)$$

Sometimes, the time variable s is also called the **strained coordinate**. The undetermined coefficients ω_j will be used to eliminate the secular terms. The perturbation ansatz uses the new strained coordinate as follows:

$$x(t; \delta) = x_0(s) + \delta x_1(s) + \delta^2 x_2(s) + \dots \quad (9.117)$$

From (9.116) and the chain rule, it follows that

$$\frac{d^2x}{dt^2} = \omega^2 \frac{d^2x}{ds^2}.$$

Plugging the last result and (9.116) into (9.115) yields

$$\omega^2 \frac{d^2x}{ds^2} + x + \delta x^3 = (1 + \delta\omega_1 + \delta^2\omega_2 + \dots)^2 \frac{d^2x}{ds^2} + x + \delta x^3 = 0,$$

where we use a dot to denote differentiation with respect to s . Using also the perturbation ansatz (9.117), we end up with

$$(1 + 2\delta\omega_1 + \dots) \left(\frac{d^2x_0}{ds^2} + \delta \frac{d^2x_1}{ds^2} + \dots \right) + (x_0 + \delta x_1 + \dots) + \delta(x_0^3 + \dots) = 0,$$

where we drop terms of order $\mathcal{O}(\delta^2)$; one should keep these terms for higher-order asymptotic expansions, but we are content with the first correction term here. At order $\mathcal{O}(\delta^0) = \mathcal{O}(1)$, the harmonic oscillator appears:

$$\frac{d^2x_0}{ds^2} + x_0 = 0, \quad x_0(0) = 1, \quad x'_0(0) = 0.$$

The solution is $x_0(s) = \cos s$. At order $\mathcal{O}(\delta)$, the equation is

$$\frac{d^2x_1}{ds^2} - 2\omega_1 \cos s + x_1 + \cos^3 s = 0, \quad x_1(0) = 0, \quad \frac{dx_1}{ds}(0) = 0. \quad (9.118)$$

After a bit of calculation (or using a computer algebra system), one finds that (9.118) is solved by

$$x_1(s) = -\frac{1}{8} (s(3 - 8\omega_1) + \cos s \sin s) \sin s.$$

The first term is secular, but it can be eliminated by choosing $\omega_1 = \frac{3}{8}$, so that

$$x_1(s) = -\frac{1}{8} \sin^2 s \cos s = \frac{1}{32} (\cos(3s) - \cos s).$$

Therefore, the first-order asymptotic expansion is

$$x(s; \delta) = \cos s - \frac{\delta}{32} (\cos(3s) - \cos s) + \mathcal{O}(\delta^2).$$

One also has the relation $s = t(1 + \frac{3}{8}\delta) + \mathcal{O}(\delta^2)$, which can be used to write the expansion in the original time variable:

$$x(t; \delta) = \cos \left[t(1 + \frac{3}{8}\delta) \right] - \frac{\delta}{32} \left(\cos \left[3t(1 + \frac{3}{8}\delta) \right] - \cos \left[t(1 + \frac{3}{8}\delta) \right] \right) + \mathcal{O}(\delta^2).$$

Although the result itself is interesting, the key idea to remember is the modified time scale $s = \omega t$.

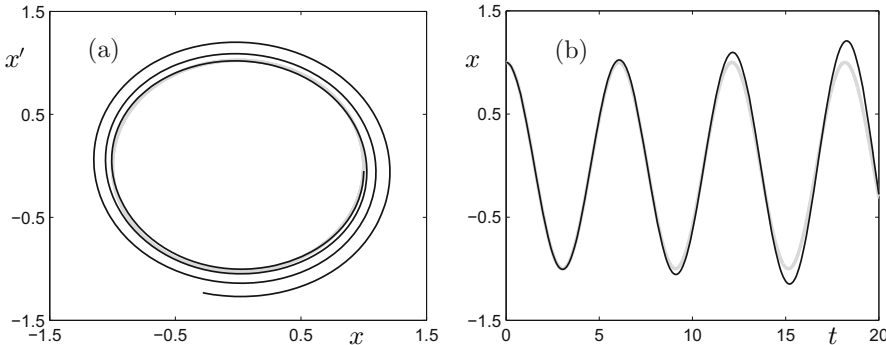


Figure 9.11: Illustration for long time asymptotics of the weakly nonlinear Duffing oscillator (9.115) for $\delta = 0.1$. The thick gray curve represents the numerical solution and the lowest-order asymptotic expansion (9.125), since both curves are virtually indistinguishable on the scale of the plot. The regular perturbation expansion with secular terms is shown as a thin black curve; it diverges from the true solution on a longer time scale. (a) (x, x') -phase space. (b) Time series.

The second method we are going to discuss uses a similar idea and makes the ansatz

$$x(t; \delta) = X_0(t, \tau) + \delta X_1(t, \tau) + \dots, \quad (9.119)$$

where $\tau = \delta t$. In particular, (9.119) assumes that the solution depends on two time scales, a fast time t and a slow time τ . Therefore, one also refers to this ansatz as **two-timing** or the **method of multiple scales**; the last terminology is quite common and also very unfortunate, since there are many methods for multiscale problems. Starting from (9.119), an application of the chain rule leads to the observation

$$\frac{dx}{dt} = \left(\frac{\partial X_0}{\partial t} + \frac{\partial X_0}{\partial \tau} \frac{d\tau}{dt} \right) + \delta \left(\frac{\partial X_1}{\partial t} + \frac{\partial X_1}{\partial \tau} \frac{d\tau}{dt} \right) + \dots,$$

and since $d\tau/dt = \delta$, we obtain

$$\frac{dx}{dt} = \frac{\partial X_0}{\partial t} + \delta \left(\frac{\partial X_0}{\partial t} + \frac{\partial X_1}{\partial t} \right) + \mathcal{O}(\delta^2).$$

Differentiating one more time yields

$$\frac{d^2x}{dt^2} = \frac{\partial^2 X_0}{\partial t^2} + \delta \left(2 \frac{\partial^2 X_0}{\partial \tau \partial t} + \frac{\partial^2 X_1}{\partial t^2} \right) + \mathcal{O}(\delta^2). \quad (9.120)$$

Substituting (9.120) and (9.119) into the weakly nonlinear Duffing oscillator (9.115) gives for the first two orders

$$\mathcal{O}(1) : \frac{\partial^2 X_0}{\partial t^2} + X_0 = 0, \quad (9.121)$$

$$\mathcal{O}(\delta) : \frac{\partial^2 X_1}{\partial t^2} + X_1 = -X_0^3 - 2 \frac{\partial^2 X_0}{\partial \tau \partial t}. \quad (9.122)$$

It looks like major additional complications have been introduced, since (9.122) is a partial differential equation. It is surprising that for several interesting perturbation problems, the resulting PDEs produced by the two-timing method are solvable. The general solution of (9.121) is easy to find:

$$X_0(t, \tau) = A(\tau)e^{it} + \overline{A(\tau)}e^{-it},$$

where $\overline{A(\tau)}$ denotes the complex conjugate of the **amplitude** $A(\tau)$. This yields

$$\begin{aligned} X_0^3 &= A(\tau)^3 e^{3it} + \overline{A(\tau)}^3 e^{-3it} + 3|A(\tau)|^2 A(\tau)e^{it} + 3|A(\tau)|^2 \overline{A(\tau)}e^{-it}, \\ 2 \frac{\partial^2 X_0}{\partial \tau \partial t} &= 2 \left(i e^{it} \frac{dA}{d\tau} - i e^{-it} \frac{d\overline{A}}{d\tau} \right). \end{aligned}$$

Therefore, the right-hand side of (9.122) is

$$e^{it} \left(-3|A|^2 A - 2i \frac{dA}{d\tau} \right) + e^{-it} \left(-3|A|^2 \overline{A} + 2i \frac{d\overline{A}}{d\tau} \right) - e^{3it} A^3 - e^{3it} \overline{A}^3.$$

Since e^{it} and e^{-it} solve the homogeneous problem on the left-hand side of (9.122), we must ensure that their coefficients vanish on the right-hand side to avoid secular terms.

Exercise/Project 9.8.4. Which classes of functions $g(t)$ produce secular terms for the equation $x'' + x = g(t)$? ◇

The additional new time variable can now be used to eliminate secular terms, as suggested above, by requiring

$$0 = -3|A|^2 A - 2i \frac{dA}{d\tau}, \quad (9.123)$$

$$0 = -3|A|^2 \overline{A} + 2i \frac{d\overline{A}}{d\tau}. \quad (9.124)$$

The **amplitude equations** (9.123) and (9.124) are complex conjugates and hence redundant. One may just solve, say (9.123), to find $A(\tau)$. Using polar coordinates for the complex plane and thus writing $A(\tau) = R(\tau)e^{i\theta(\tau)}$ yields

$$\begin{aligned}\frac{dR}{d\tau} &= 0, \\ \frac{d\theta}{d\tau} &= \frac{3}{2}R^2,\end{aligned}$$

which immediately leads to $A(\tau) = R(0)\exp(i\theta(0) + \frac{3}{2}iR^2(0)\tau)$. Therefore, the zeroth-order solution is

$$X_0(t, \tau) = 2R(0) \cos\left(\theta(0) + \frac{3}{2}R^2(0)\tau + t\right).$$

The initial conditions $x(0) = 1$, $x'(0) = 0$ determine $R(0)$ and $\theta(0)$, since $x(0) = 1$ becomes

$$X_0(0, 0) = 1, \quad X_1(0, 0) = 0, \quad \dots,$$

and $x'(0) = 0$ translates into (using $\tau = \delta t$)

$$\frac{\partial X}{\partial t}(0, 0) = 0, \quad \frac{\partial X_1}{\partial t}(0, 0) = -\frac{\partial X_0}{\partial \tau}(0, 0), \quad \dots.$$

To satisfy the initial conditions, we must have $R(0) = \frac{1}{2}$ and $\theta(0) = 0$. It follows that the zeroth-order solution on the original time scale t is given by

$$x_0(t; \delta) = \cos\left[t\left(1 + \frac{3}{8}\delta\right)\right] + \mathcal{O}(\delta) \quad (9.125)$$

as $\delta \rightarrow 0$, which agrees with the solution found previously using the Poincaré–Lindstedt method. A comparison of (9.125) to the true solution and the regular expansion with secular terms is shown in Figure 9.11. It is more complicated to obtain higher-order terms with the method of multiple scales, since we must guess what scales appear at higher order, e.g., $\tau = \delta^3 t$, leading to an “ n -timing method” for n time scales.

The method of multiple scales can also be used to provide results for systems that we treated using averaging in Section 9.6. In particular, one may use two-timing to compute the effective slow dynamics for fast subsystems with periodic orbits and obtain a result consistent with the first-order averaging approximation; see Section 9.11.

9.9 The Renormalization Group I

The **renormalization group (RG)** method provides another approach to perturbation problems. Our discussion will follow the original ideas of Chen, Goldenfeld, and Ono [CGO96, CGO94, DHH⁺08]. The CGO-RG method will be reinterpreted later on. Consider the ODE

$$\frac{dx}{dt} = x' = Ax + \delta G(x), \quad x(T_0) = w(T_0) \quad (9.126)$$

with $x \in \mathbb{R}^m$, $0 < \delta \ll 1$, and we assume that the matrix $A \in \mathbb{R}^{m \times m}$ is diagonal with eigenvalues λ_i on the imaginary axis. Furthermore, $t > T_0 \geq 0$ and $x(T_0) = w(T_0)$ is a way to write the initial condition that will turn out to be convenient later. The assumption on A implies that we want to deal with perturbations of harmonic problems, e.g., one should think of eigenvalues i and $-i$ that give sines and cosines for the unperturbed problem. We also require for simplicity that G be a polynomial

$$G(x) = \sum_{\alpha, j} C_{\alpha, j} x^{\alpha_1} x^{\alpha_2} \cdots x^{\alpha_m} e_j = \sum_{\alpha, j} C_{\alpha, j} x^\alpha e_j,$$

where $\alpha = (\alpha_1, \alpha_2, \dots, \alpha_m) \in (\mathbb{N}_0)^m$ is a **multi-index** and e_j is the j th Euclidean basis vector.

Exercise 9.9.1. Consider Rayleigh's equation

$$x'' + x = \delta \left(x' - \frac{1}{3} (x')^3 \right) \quad (9.127)$$

and show that it can be written in the form (9.126). Furthermore, prove that it has a regular asymptotic expansion containing secular terms. \diamond

The goal of the renormalization procedure for (9.126) is to deal with the secular terms arising in a regular asymptotic expansion and to provide an asymptotic expansion valid up to long time scales of order $\mathcal{O}(1/\delta)$. First, it is easier to understand the method by considering the general procedure for (9.126) and then consider an example. The renormalization procedure consists of six steps:

- (1) Derive a regular/naive asymptotic expansion for the problem and identify all secular terms.
- (2) Apply a transformation that simplifies the nonsecular terms containing the initial condition.
- (3) Introduce an arbitrary time s between T_0 and t .
- (4) Make a change of coordinates, called renormalization, simplifying terms containing $(t - T_0)$.
- (5) Apply the RG condition

$$\left. \frac{dx}{ds} \right|_{s=t} = 0 \quad (9.128)$$

justified by the fact that the solution does not depend on s .

- (6) Solving equation (9.128) and equating t and s in the modified regular perturbation expansion will indeed provide a solution free of secular terms.

It should be noted that the coordinate changes can be carried out to different orders. In the following, we will be interested in obtaining a solution free of

secular terms up to and including order $\mathcal{O}(\delta)$. For the following calculations, it is illuminating to try to use (9.127) as an example in parallel. The starting point is to substitute a regular expansion

$$x(t) = x_0(t) + \delta x_1(t) + \delta^2 x_2(t) + \dots \quad (9.129)$$

into (9.126), where subscripts are viewed as indices for the different orders, i.e., x_1, x_2, \dots in (9.129) are vectors in \mathbb{R}^m . Collecting terms for the first two orders of δ , we get

$$\mathcal{O}(1) : x'_0 = Ax_0, \quad x_0(T_0) = w(T_0), \quad (9.130)$$

$$\mathcal{O}(\delta) : x'_1 = Ax_1 + G(x_0), \quad x_1(T_0) = 0. \quad (9.131)$$

Solving (9.130) and (9.131) yields

$$x_0(t) = e^{(t-T_0)A}w(T_0), \quad (9.132)$$

$$\begin{aligned} x_1(t) &= e^{(t-T_0)A} \int_{T_0}^t e^{-(s-T_0)A} G(e^{(s-T_0)A} w(T_0)) \, ds \\ &= e^{(t-T_0)A} \left[(t-T_0) \sum_{\Lambda_{\alpha,j}=0} C_{\alpha,j} w(T_0)^\alpha e_j \right. \\ &\quad \left. + \sum_{\Lambda_{\alpha,j} \neq 0} \frac{C_{\alpha,j}}{\Lambda_{\alpha,j}} (e^{\Lambda_{\alpha,j}(t-T_0)} - 1) w(T_0)^\alpha e_j \right], \end{aligned} \quad (9.133)$$

where $\Lambda_{\alpha,j} := \sum_{k=1}^m \alpha_k \lambda_k - \lambda_j$. Hence, the solution $x_1(t)$ can produce secular terms, since the expansion to first order is

$$\begin{aligned} x(t) &= e^{(t-T_0)A} \left(w(T_0) + \delta(t-T_0) \sum_{\Lambda_{\alpha,j}=0} C_{\alpha,j} w(T_0)^\alpha e_j \right. \\ &\quad \left. + \delta \sum_{\Lambda_{\alpha,j} \neq 0} \frac{C_{\alpha,j}}{\Lambda_{\alpha,j}} (e^{\Lambda_{\alpha,j}(t-T_0)} - 1) w(T_0)^\alpha e_j \right) + \mathcal{O}(\delta^2), \end{aligned} \quad (9.134)$$

and terms with $\Lambda_{\alpha,j} = 0$ are secular. Note that many terms in (9.134) involve only T_0 and $w(T_0)$, which means that one could aim at defining a new initial condition $v(T_0)$ that is used to absorb those terms. The transformation that works is

$$v(T_0) = e^{-T_0 A} w(T_0) - \delta \sum_{\Lambda_{\alpha,j} \neq 0} \frac{C_{\alpha,j}}{\Lambda_{\alpha,j}} e^{\Lambda_{\alpha,j} T_0} (e^{-T_0 A} w(T_0))^\alpha e_j + \mathcal{O}(\delta^2).$$

After some calculation, one finds that (9.134) becomes

$$\begin{aligned} x(t) &= e^{tA} v(T_0) + \delta(t-T_0) e^{tA} \sum_{\Lambda_{\alpha,j}=0} C_{\alpha,j} v(T_0)^\alpha e_j + \\ &\quad \delta e^{tA} \sum_{\Lambda_{\alpha,j} \neq 0} \frac{C_{\alpha,j}}{\Lambda_{\alpha,j}} e^{\Lambda_{\alpha,j} t} v(T_0)^\alpha e_j + \mathcal{O}(\delta^2), \end{aligned} \quad (9.135)$$

where absorbing higher-order terms into $\mathcal{O}(\delta^2)$ is crucial. Having completed the second step of the CGO-RG method, one may proceed to introduce a new time s into the secular term

$$\begin{aligned} x(t) &= e^{tA}v(T_0) + \delta(t-s+s-T_0)e^{tA} \sum_{\Lambda_{\alpha,j}=0} C_{\alpha,j}v(T_0)^\alpha e_j + \\ &\quad \delta e^{tA} \sum_{\Lambda_{\alpha,j} \neq 0} \frac{C_{\alpha,j}}{\Lambda_{\alpha,j}} e^{\Lambda_{\alpha,j} t} v(T_0)^\alpha e_j + \mathcal{O}(\delta^2). \end{aligned} \quad (9.136)$$

The next idea is to absorb the secular terms with $(s - T_0)$ into another new function $V(s)$, which is going to depend on s instead of T_0 . The transformation that works is

$$V(s) = v(T_0) + \delta(t-T_0) \sum_{\Lambda_{\alpha,j}=0} C_{\alpha,j}v(T_0)^\alpha e_j + \mathcal{O}(\delta^2).$$

After some more direct calculations, one obtains the renormalized expansion

$$\begin{aligned} x(t) &= e^{tA}V(s) + \delta(t-s)e^{tA} \sum_{\Lambda_{\alpha,j}=0} C_{\alpha,j}V(s)^\alpha e_j + \\ &\quad \delta e^{tA} \sum_{\Lambda_{\alpha,j} \neq 0} \frac{C_{\alpha,j}}{\Lambda_{\alpha,j}} e^{\Lambda_{\alpha,j} t} V(s)^\alpha e_j + \mathcal{O}(\delta^2). \end{aligned} \quad (9.137)$$

Note carefully that absorbing higher-order terms into $\mathcal{O}(\delta^2)$ is again a critical step in deriving a renormalized expansion. The RG condition (9.128) tells us to differentiate (9.137) with respect to s , which yields

$$\begin{aligned} \frac{dx}{ds} &= e^{tA} \frac{dV}{ds} - \delta e^{tA} \sum_{\Lambda_{\alpha,j}=0} C_{\alpha,j}V(s)^\alpha e_j + \delta(t-s)e^{tA} \sum_{\Lambda_{\alpha,j}=0} C_{\alpha,j} \frac{d}{ds} V(s)^\alpha e_j \\ &\quad + \delta e^{tA} \sum_{\Lambda_{\alpha,j} \neq 0} \frac{C_{\alpha,j}}{\Lambda_{\alpha,j}} e^{\Lambda_{\alpha,j} s} \frac{d}{ds} V(s)^\alpha e_j + \mathcal{O}(\delta^2). \end{aligned}$$

The CGO-RG method dictates that we evaluate of the last expression at $s = t$, which makes the third term on the right disappear, and then set the result equal to zero. Therefore, we are left with

$$\begin{aligned} 0 &= e^{tA} \frac{dV}{ds} - \delta e^{tA} \sum_{\Lambda_{\alpha,j}=0} C_{\alpha,j}V(s)^\alpha e_j \\ &\quad + \delta e^{tA} \sum_{\Lambda_{\alpha,j} \neq 0} \frac{C_{\alpha,j}}{\Lambda_{\alpha,j}} e^{\Lambda_{\alpha,j} t} \frac{d}{ds} V(s)^\alpha e_j + \mathcal{O}(\delta^2). \end{aligned}$$

Since $\frac{dV}{ds} = \mathcal{O}(\delta)$, one may move the term for $\Lambda_{\alpha,j} \neq 0$ into $\mathcal{O}(\delta^2)$. Multiplying by e^{-tA} yields an ODE for $V = V(s)$,

$$\frac{dV}{ds} = \delta \sum_{\Lambda_{\alpha,j}=0} C_{\alpha,j}V^\alpha e_j + \mathcal{O}(\delta^2). \quad (9.138)$$

The crucial observation is that (9.138) is the first-order **amplitude equation** for our original problem analogous to the amplitude equation derived from the two-timing method; see Section 9.8. Solving (9.138) and using $V(s)$ in the derived regular/naive expansion with $s = t$ will produce a solution free of secular terms up to and including order $\mathcal{O}(\delta)$. Hence, the solution will be valid up to a time of order $\mathcal{O}(1/\delta)$.

Exercise/Project 9.9.2. Reconsider the Rayleigh equation from Exercise 9.9.1. Find the asymptotic expansion of (9.127) free of secularities up to and including first order:

- (a) Use a step-by-step CGO-RG method on the first-order system derived in Exercise 9.9.1. *Warning: This is tedious and lengthy, so it is very instructive to use a computer algebra system to implement the steps.*
- (b) Try to use the CGO-RG method directly on the second-order equation. Compare your solution with the results in [CGO96].

Compare your results to the Poincaré–Lindstedt or two-timing method from Section 9.8. ◇

A couple of observations can be made regarding the CGO-RG method. Note that equations (9.135) and (9.137) are equivalent, since T_0 is just replaced by s and $v(T_0)$ is replaced by $V(s)$. Therefore, steps (2)–(4) of the CGO-RG method are not really necessary, since they serve just to rename variables. A similar observation holds for the RG condition, which requires an evaluation at $s = t$ that is another renaming procedure for the variables. Hence, one can consider a shorter alternative way to renormalization:

RG_1 Begin with a regular/naive perturbation expansion given an arbitrary initial time t_0 and initial condition $w(t_0)$.

RG_2 Renormalize the initial condition by absorbing terms into $w(t_0)$ in the regular perturbation expansion that are time-independent and bounded.

RG_3 Apply the RG condition $\frac{dx}{dt_0} = 0$.

The approach via RG_1 – RG_3 is a simpler procedure, but it will produce an equivalent result. Let \mathcal{V} denote the space of vector fields with which we are trying to deal, e.g., all vector fields of the form (9.126). Let \mathcal{S} denote the space of truncated regular asymptotic expansions for \mathcal{V} . Then one may represent the simplified RG method by the following commutative diagram:

$$\begin{array}{ccc} \mathcal{S} & \xrightarrow{RG_2} & \mathcal{S} \\ RG_1 \uparrow & & \downarrow RG_3 \\ \mathcal{V} & \xrightarrow[NF]{} & \mathcal{V} \end{array} \tag{9.139}$$

The diagram already hints at the fact that the three steps of the simplified RG method are equivalent to a direct transformation on the original vector field

provided by classical Poincaré–Birkhoff **normal form theory**. Indeed, the application of coordinate changes to the regular expansion pushed the secular terms to higher order. This leaves only so-called **resonant terms**. This is precisely what normal form theory tries to accomplish, i.e., eliminate all terms except resonant ones. It is interesting to work out some of the details for the original problem (9.126) using the RG method defined by (9.139) up to first order. Starting with a regular asymptotic expansion gives

$$\begin{aligned} x(t) = & e^{(t-t_0)A} \left(w(t_0) + \delta(t-t_0) \sum_{\Lambda_{\alpha,j}=0} C_{\alpha,j} w(t_0)^{\alpha} e_j \right. \\ & \left. + \delta \sum_{\Lambda_{\alpha,j} \neq 0} \frac{C_{\alpha,j}}{\Lambda_{\alpha,j}} (e^{\Lambda_{\alpha,j}(t-t_0)} - 1) w(t_0)^{\alpha} e_j \right) + \mathcal{O}(\delta^2). \end{aligned} \quad (9.140)$$

The renormalization of the integration constant is provided by

$$w(t_0) = W(t_0) + \delta \sum_{\Lambda_{\alpha,j} \neq 0} \frac{C_{\alpha,j}}{\Lambda_{\alpha,j}} W(t_0)^{\alpha} e_j + \mathcal{O}(\delta^2). \quad (9.141)$$

Using this transformation leads to

$$\begin{aligned} x(t) = & e^{(t-t_0)A} \left(W(t_0) + \delta(t-t_0) \sum_{\Lambda_{\alpha,j}=0} C_{\alpha,j} W(t_0)^{\alpha} e_j \right. \\ & \left. + \delta \sum_{\Lambda_{\alpha,j} \neq 0} \frac{C_{\alpha,j}}{\Lambda_{\alpha,j}} e^{\Lambda_{\alpha,j}(t-t_0)} W(t_0)^{\alpha} e_j \right) + \mathcal{O}(\delta^2). \end{aligned} \quad (9.142)$$

The last step is to differentiate the right-hand side of (9.142) with respect to t_0 and set it equal to zero. After some straightforward, but slightly lengthy, algebraic manipulations, one ends up with the following theorem.

Theorem 9.9.3 ([DHH⁺08]). *After the steps RG₁–RG₃ have been applied to equation (9.126) with initial condition $x(t_0) = w(t_0)$, the RG condition RG₃ gives an ODE*

$$\frac{dW}{dt_0} = AW + \delta \sum_{\Lambda_{\alpha,j}=0} C_{\alpha,j} W^{\alpha} e_j + \mathcal{O}(\delta^2), \quad (9.143)$$

where $W(t_0)$ relates to the initial condition $w(t_0) = x(t_0)$ via (9.141). In particular, after specifying some initial condition $x(T_0)$, one may obtain $W(T_0)$, providing a well-defined problem (9.143). Furthermore, the following conclusions hold:

- (9.143) is the same equation obtained by normal form theory up to and including first order, i.e., it contains only resonant terms up to first order;
- the solution of (9.143) approximates the original problem up to times of order $\mathcal{O}(1/\delta)$.

The key idea of the CGO-RG method is the renormalization of initial conditions. In particular, a coordinate change is applied to solutions of the vector field $x' = Ax + f(x)$, with fixed A and f , parameterized by different initial conditions. Therefore, one treats all solutions simultaneously. Although the initial idea of **renormalization** arose in physics, the mathematical adaptation of the idea is found not only in the RG method but in many other branches of dynamical systems. The idea is always similar and revolves around a rescaling procedure of a whole family of solutions; see Section 9.11.

9.10 The Renormalization Group II

From the discussion in the last section, one may guess that the RG method can be extended to equations of the form

$$\frac{dz}{dt} = z' = F(z) + \varepsilon G(z) \quad (9.144)$$

for $z \in \mathbb{R}^N$, F, G sufficiently smooth, $0 < \varepsilon \ll 1$, and the unperturbed problem $z' = F(z)$ has a flow φ_t that is periodic. For example, an (m, n) -fast–slow system

$$\begin{aligned} x' &= f(x, y), \\ y' &= \varepsilon g(x, y), \end{aligned} \quad (9.145)$$

can be written in the form (9.144). Indeed, if we set $z = (x, y) \in \mathbb{R}^{m+n}$ and

$$F = \begin{pmatrix} f \\ 0 \end{pmatrix} \quad \text{and} \quad G = \begin{pmatrix} 0 \\ g \end{pmatrix},$$

then we obtain (9.144). In this case, the unperturbed system $z' = F(z)$ is the fast subsystem

$$\begin{aligned} x' &= f(x, y) \\ y' &= 0. \end{aligned}$$

If the critical manifold $C_0 = \{(x, y) \in \mathbb{R}^{m+n} : f(x, y) = 0\}$ is nonempty, we know that it represents equilibrium points of $z' = F(z)$; in particular, equilibrium points are periodic solutions, so that we expect RG theory to apply. We are going to illustrate another slightly different way to interpret the CGO-RG method for (9.144). As before, it is assumed for simplicity that G is a polynomial. The regular perturbation ansatz

$$z(t; \varepsilon) = z_0(t) + \varepsilon z_1(t) + \cdots$$

produces at the first two orders the well-known (cf. (9.130)-(9.131)) equations

$$\begin{aligned} z'_0 &= F(z_0), \\ z'_1 &= (\mathrm{D}_z F)(z_1) + G(z_0). \end{aligned}$$

Before we proceed, an auxiliary definition will be helpful.

Definition 9.10.1. Recall that $\varphi_t(w)$ denotes the flow for the unperturbed system $z'_0 = F(z_0)$ with initial condition w . Define

$$R_1(w) := \lim_{t \rightarrow -\infty} \frac{1}{t} \int^t (\mathrm{D}_w \varphi_s)^{-1} G(\varphi_s(w)) \, ds,$$

$$h_t^{(1)}(w) := (\mathrm{D}_w \varphi_t) \int_{-\infty}^t [(\mathrm{D}_w \varphi_s)^{-1} G(\varphi_s(w)) - R_1(w)] \, ds,$$

where \int^t is the indefinite integral with undetermined constants of integration; the constants of integration will not matter in what follows, and basically, they arise due to a free choice of the initial time.

The indices of R_1 and $h^{(1)}$ allude to the fact that there exists a whole family of maps. These higher-order maps will not be needed to carry out the RG method up to and including order $\mathcal{O}(\varepsilon)$. Let us try to understand first how the map R_1 relates to the RG method. Assume for the moment that we are back in case $z' = Az + \varepsilon G(z)$ from Section 9.9, where $A \in \mathbb{R}^{N \times N}$ is a matrix with eigenvalues on the imaginary axis. As discussed already in (9.133), the solution for z_1 can be formally written as

$$z_1(t) = e^{tA} \int^t e^{-sA} G(e^{sA} w) \, ds = (\mathrm{D}_w \varphi_t) \int^t [(\mathrm{D}_w \varphi_s)^{-1} G(\varphi_s(w))] \, ds.$$

This solution may have terms that are secular for order $\mathcal{O}(\varepsilon)$ and grow like $\mathcal{O}(t)$. These terms are precisely the ones picked out by R_1 . We can write

$$z_1(t) = tR_1(w) + h_t^{(1)}(w).$$

It turns out that the amplitude equation, (9.138) can also be written as

$$w' = \varepsilon R_1(w) + \mathcal{O}(\varepsilon^2).$$

In fact, $h_t^{(1)}(w)$ are all the terms that have to be eliminated via the renormalization transformation. The formal steps can be made precise, and one may reinterpret the first-order RG method based on the next definition.

Definition 9.10.2. Define the first-order **RG equation** as

$$w' = \varepsilon R_1(w).$$

Define the first-order **RG transformation** as

$$\alpha_t^{(1)}(w) := \varphi_t(w) + \varepsilon h_t^{(1)}(w), \quad (9.146)$$

where $\varphi_t(w)$ is the flow for $z' = F(z)$ with initial condition w .

Based on Definition 9.10.2, another equivalent version of the RG method can be developed; see also Section 9.11. First, it is helpful to focus on (9.146) in the context of a fast-slow systems example.

Example 9.10.3. Consider the following $(1, 1)$ -fast–slow system:

$$\begin{aligned} x' &= y - x - xy, \\ y' &= \varepsilon(cx - y + xy), \end{aligned} \tag{9.147}$$

where $0 < c < 1$ is a parameter. The critical manifold of (9.147) is

$$C_0 = \left\{ (x, y) \in \mathbb{R}^2 : x = \frac{y}{1+y} \right\}.$$

Since $\frac{\partial}{\partial x}(y - x - xy) = -1 - y$, it follows that C_0 is normally hyperbolic and attracting for $y > -1$. Let us calculate the first-order RG transformation (9.146) restricted to C_0 for $y > -1$. The first step is to consider the flow $\varphi_s(w)$ for the fast subsystem

$$\begin{aligned} x' &= y - x - xy, \\ y' &= 0. \end{aligned}$$

After a bit of calculation, it follows that the flow with initial condition $(w_1, w_2) = (x(0), y(0))$ is

$$\varphi_t(w) = \left(\frac{w_2}{1+w_2} + e^{-t(1+w_2)} \left(w_1 - \frac{w_2}{1+w_2} \right), w_2 \right). \tag{9.148}$$

Note that throughout the following calculations, the condition $y > -1$ will be used several times to ensure that $1 + w_2 > 0$. Differentiating (9.148) and evaluating the result on C_0 yields

$$D_w \varphi_t = \begin{pmatrix} e^{-t(1+w_2)} \frac{1-e^{-t(1+w_2)}}{(1+w_2)^2} & \\ 0 & 1 \end{pmatrix}.$$

It is straightforward to invert the last matrix, so that

$$(D_w \varphi_t)^{-1} = \begin{pmatrix} e^{t(1+w_2)} \frac{1-e^{t(1+w_2)}}{(1+w_2)^2} & \\ 0 & 1 \end{pmatrix}.$$

The map G from Definition 9.10.1 is just

$$G(x, y) = (0, cx - y + xy)^\top.$$

Hence, we have all the information to calculate $R_1(w)$ for $w \in C$, which yields

$$\begin{aligned} R_1(w) &= \lim_{t \rightarrow -\infty} \frac{1}{t} \int^t (D_w \varphi_s)^{-1} G(\varphi_s(w)) \, ds \\ &= \dots \\ &= \left(\frac{w_2(c-1)}{(1+w_2)^3}, \frac{w_2(c-1)}{(1+w_2)} \right)^\top, \end{aligned}$$

where the dots indicate some unpleasant algebraic manipulation carried out via computer algebra. After some more algebra, we obtain

$$\begin{aligned}
h_t^{(1)}(w) &= (\mathrm{D}_w \varphi_t) \int_{-\infty}^t [(\mathrm{D}_w \varphi_s)^{-1} G(\varphi_s(w)) - R_1(w)] \, ds \\
&= \dots \\
&= (\mathrm{D}_w \varphi_t) \int_{-\infty}^t \begin{pmatrix} \frac{e^{s(1+w_2)} w_2(1-c)}{(1+w_2)^3} \\ 0 \end{pmatrix} \, ds \\
&= \begin{pmatrix} e^{-t(1+w_2)} \frac{1-e^{-t(1+w_2)}}{(1+w_2)^2} \\ 0 \end{pmatrix} \begin{pmatrix} \frac{e^{t(1+w_2)} w_2(1-c)}{(1+w_2)^4} \\ 0 \end{pmatrix} \\
&= \begin{pmatrix} \frac{w_2(1-c)}{(1+w_2)^4} \\ 0 \end{pmatrix}.
\end{aligned}$$

Therefore, the first-order RG transform restricted to C is

$$\alpha_t^{(1)}(w) := \begin{pmatrix} \frac{w_2}{1+w_2} \\ w_2 \end{pmatrix} + \varepsilon \begin{pmatrix} \frac{w_2(1-c)}{(1+w_2)^4} \\ 0 \end{pmatrix}. \quad (9.149)$$

The interesting conjecture of the calculation is that (9.149) provides an approximation for the slow manifold

$$C_\varepsilon = \{(x, y) \in \mathbb{R}^2 : x = h_0(y) + \varepsilon h_1(y) + \varepsilon^2 h_2(y) + \dots\}, \quad (9.150)$$

where $h_0(y) = \frac{y}{1+y}$. For example, the first component of the second term in (9.149) yields the correct first-order approximation, as the next exercise shows. ♦

Exercise/Project 9.10.4. Use a method other than the renormalization group to prove that for the slow manifold (9.150), we have $h_1(y) = y(1-c)/(1+y)^4$; see also Chapter 11. ◇

The slow manifold approximation is correct in even more generality. To state the result, one has to introduce higher-order RG equations and RG transformations. As usual, we denote the slow variable dynamics by $g(x, y) = g(z) : \mathbb{R}^{m+n} \rightarrow \mathbb{R}^n$ for a general fast–slow vector field (9.145). The main ansatz is a regular perturbation expansion

$$z = z_0 + \varepsilon z_1 + \varepsilon^2 z_2 + \dots$$

for the z -variable. Define new maps G_j given by the relation

$$\sum_{j=1}^{\infty} \varepsilon^j g(z_0 + \varepsilon z_1 + \varepsilon^2 z_2 + \dots) = \sum_{j=1}^{\infty} \varepsilon^j G_j(z_0, z_1, z_2, \dots). \quad (9.151)$$

For example, the first two maps are

$$\begin{aligned}
G_1(z_0) &= g(z_0), \\
G_2(z_0, z_1) &= [\mathrm{D}_z g(z_0)](z_1),
\end{aligned}$$

and higher-order functions are obtained from a direct Taylor expansion of the left-hand side of (9.151).

Definition 9.10.5. Let $\varphi_t(w)$ denote the flow of the fast subsystem with initial condition in the critical manifold $w \in C$. Define

$$\begin{aligned} R_1(w) &:= \lim_{t \rightarrow -\infty} \frac{1}{t} \int^t (\mathrm{D}_w \varphi_s)^{-1} G_1(\varphi_s(w)) \, ds, \\ h_t^{(1)}(w) &:= (\mathrm{D}_w \varphi_t) \int_{-\infty}^t [(\mathrm{D}_w \varphi_s)^{-1} G_1(\varphi_s(w)) - R_1(w)] \, ds, \end{aligned}$$

where \int^t is the indefinite integral with an undetermined constants of integration; the constants of integration will not matter in what follows. Furthermore, define

$$\begin{aligned} R_j(w) &:= \lim_{t \rightarrow -\infty} \left[\frac{1}{t} \int^t (\mathrm{D}_w \varphi_s)^{-1} G_j(\varphi_s(w), h_s^{(1)}(w), \dots, h_s^{(j-1)}(w)) \right. \\ &\quad \left. - (\mathrm{D}_w \varphi_s)^{-1} \sum_{k=1}^{j-1} (\mathrm{D}_w h_s^{(k)}) R_{j-k}(w) \, ds \right], \\ h_t^{(j)}(w) &:= (\mathrm{D}_w \varphi_t) \left[\int_{-\infty}^t (\mathrm{D}_w \varphi_s)^{-1} G_j(\varphi_s(w), h_s^{(1)}(w), \dots, h_s^{(j-1)}(w)) \right. \\ &\quad \left. - (\mathrm{D}_w \varphi_s)^{-1} \sum_{k=1}^{j-1} (\mathrm{D}_w h_s^{(k)}) R_{j-k}(w) - R_j(w) \, ds \right]. \end{aligned}$$

Then define the **k th-order RG equation** restricted to C_0 by

$$w' = \varepsilon R_1(w) + \varepsilon^2 R_2(w) + \dots + \varepsilon^k R_k(w)$$

and the **k th-order RG transformation** restricted to C_0 by

$$\alpha_t^{(k)}(w) = \varphi_t(w) + \varepsilon h_t^{(1)}(w) + \dots + \varepsilon^k h_t^{(k)}(w).$$

In the context of autonomous fast–slow systems, the transformation $\alpha_t = \alpha^{(k)}$ will turn out to be independent of time. The next theorem guarantees that the RG transformation provides us with an approximation the slow manifold.

Theorem 9.10.6 ([Chi09]). *Suppose C_0 is a normally hyperbolic attracting critical manifold for a fast–slow system. Then the k th-order RG transformation on C_0 provides an $\mathcal{O}(\varepsilon^{k+1})$ -approximation to the slow manifold C_ε , i.e.,*

$$d_H(C_\varepsilon, \alpha^{(k)}(C_0)) = \mathcal{O}(\varepsilon^{k+1}), \quad \text{as } \varepsilon \rightarrow 0,$$

where d_H denotes the Hausdorff distance.

In principle, the same procedure can be extended to find slow manifolds as perturbations from more general invariant sets of the fast subsystem such as periodic orbits. The RG procedure also provides an alternative approach to other reduction methods for fast–slow systems presented in Chapter 11.

9.11 References

Section 9.1: This section and the next are based mainly on [KC96], but see also [BO99, Lag88]. Boundary layers have been a key topic [Eck94, Eck77] motivating the development of asymptotics methods. The same holds for the idea that matching should be employed [Fra69, Hop75, LC72, Ski11]. There are also many examples of BVPs with interior layers; see, e.g., [O'M00, O'M83]. Particularly, second-order equations have played a fundamental role. For example, there have been works on classical boundary layers [O'M69], composite expansions [FS10b, San79] corner layers [KS03, SK97], two coupled second-order equations [AFFS06, ABC⁺06, Fif76, Ita84], heteroclinic connections [SF07], interior layers [Fif74, OW04], and transition time analysis [DS95b]. The approach we have taken to compare the asymptotic solution with the “true” numerical solution is a standard strategy [GNJ89, O'M88]. A quite general asymptotic approach of BVPs is provided by [FJ82, SW86]. A typical motivating example in the area is the so-called Lagerstrom problem, which has been tackled via an integral formulation [CFL78], uniform series expansions [HM09b], and various other asymptotic methods [HTB90b, Mac79, Mac78, RS75b, Ski81]. Another very important motivation for matched asymptotics is turning points [McK55, RW77, Ski94, WR76], which we already referenced in Section 5.6.

Section 9.2: Several surveys on singular perturbation methods exist showing the breadth of the area [O'M91, O'M08]. There are also many classical books [CH84, JF96, Eck79, Eck73, EdJ82, Hin91, Joh05, Mur87, NM95, Nay04, Nay81]. These books often contain more details of the methods that we have introduced such as WKB, two-timing, and/or averaging as well as many further worked examples. There are many other topics we could have featured in more detail, such as bifurcation problems [MR77], computer algebra methods [Ran94], elliptic spatial problems [EdJ66], ε -dependent boundary terms [HKO68, OK68], fourth-order equations [HLM92, LMH92], Kaplun limits involving double asymptotics [Fre72, Mey67], logarithmic switchback terms [LR84a, Mac80], Padé approximation [Att11, AAM98], PDE turbulence [Skr12], the shadowing lemma [Lin88], third-order equations [Hsi65], transformation methods [Sib62a], and weakly coupled nonlinear oscillators [Bos96, Rub77]. For a recent book on composite asymptotic expansions, see [FS13].

Section 9.3: The exposition of the boundary function method was taken from [VBK95]. The reviews [Vas63, Vas76] on asymptotics by the Russian mathematical school are highly recommended. The method can be modified for partial differential equations (PDEs) [Nes93], and we also mention the related Lyusternik–Vishik method for PDEs with a small parameter [Tre07]. There are several applications such as canards in the Schrödinger equation [BHF02], chemical reactions [HK99, KS05], delay equations [Tia03], enzyme kinetics [AIT09], gas bubbles [LK00], moment closure for stochastic equations [Bob07], plasma physics [Fil06], semiconductors [KO92], systems with sliding [Fri02c], and thin-film flows [WLW08].

Section 9.4: This section is based on [BO99]; note that the phase in the ansatz could also be taken as a complex-valued function [Mas94]. The quartic oscillator example is taken from [PR12]. Historically, WKB stands for the work of Wentzel [Wen26], Kramers [Kra26], and Brillouin [Bri26]. Sometimes, one also refers to the method as WKBJ or JWKB, indicating the work of Jeffreys [Jef24]; another alternative terminology is to refer to the ansatz as the Liouville–Green method [Lio37, Gre37, Olv61]. Most modern books on quantum mechanics also contain a treatment of the WKB

method [Hal13, Wei12]. The lowest-order geometric optics expansion is well described in [Bre51]. Turning points, where normal hyperbolicity is lost, have a long history in asymptotic analysis [FS10c], and they motivated parts of WKB theory [AO70, PM00]. The Ackerberg–O’Malley resonance is well described in [Wil81] with some more precise details in [Sib81]. Some early papers on formal asymptotics near a turning point using coordinate transformations are [Sib62b, Sib63b]. There are many other topics related to turning points and resonance, such as classification questions [FS04], Hamiltonian problems [GH88], Raleigh characterization in operator theory [Gro80, Gro77], the Stokes line [BNR82, LK70], uniform expansions [Ski87], and variational asymptotics [GM77]. The Schrödinger equation is deeply linked to WKB, and there is a vast literature on the topic [Bud01, Car08, CK11, CK98, Mar70, MG53, Vor12] including numerical methods [JMS11, AAN11, CK83b]. The field of WKB-type methods is extremely large, and the standard ansatz has turned to be surprisingly robust in a wide variety of situations. The method has been applied to find the asymptotics for many different types of problems, such as biodegradation fronts [XH00], black holes [IW87, Kon03], buckling [FS02b], C^* -algebra-valued equations [SV96], cochlea models [CC03], differential-difference equations with small shifts [LM94a, LM94b], diffusion in a potential [CCR79], elastic bars [DW10], field theories [GS77], genetic switches [ARLS11], geophysical fluid dynamics [Maj03], Hartree-type equations [CMS05], the Helmholtz equation [GV10], hydrogen–oxygen mixing layers [SLW99], hyperbolic PDEs [Rau12], instantons [ZJJ04], KdV equations [Miu76, MK74], nonautonomous systems [HJ01], PT-symmetric equations [BJ12], random matrix theory [DIZ97], recurrence equations [CC96], renormalization-type methods [Woo93, Woo95], the repairman problem [Kne94], Stokes waves [CM70], the supersymmetric standard model [CJK98], wave speeds of reaction–diffusion equations [Fre86], and water waves in a slowly varying channel [Neu83].

Section 9.5: This section is based on [vGKS05]. For more details on matched asymptotics, we refer to the other sections, while the blowup method is discussed in detail in Chapters 7 and 8.

Section 9.6: This section is based mostly on [BG06, GH83] with the example of fast subsystem averaging from [Kue10a, RE89]. For more detailed books on averaging with many examples, we refer to [LM88, PS08, SVM07, GK10a]. In fact, many of the technical averaging results for ordinary differential equations [BM61, Fat28, KB37] are quite classical, and even fine technical refinements were considered already in the early 1980s [Gil82, Mur83, Per82, Per81, San83a]. Historically, there is also a deep link to Hamiltonian systems and classical mechanics [HV97, Kev87, Lev99, Nei03, MPY11]; for a quite detailed history, see the first appendix in [SVM07]. Some of the algebraic manipulations for averaging methods can be simplified using Lie transforms [Hen70, HM77]. The literature on applications of averaging methods are vast, including climate models [Kif01a], control systems [Gra04, Gra99], coupled oscillators [EK91, FK93, Gil75], dispersion-managed solitons [PZ03], excitable cells [Med05], fluid dynamics [HKN01a, PTW05], forced oscillators [GH84], hydrogen atoms in electric fields [BU01], Josephson junctions [SC86], Markov chain mean-field models [LN13], mechanical systems [WKB97], optimal control [Cha87], phase-locked loops [CH13], power systems [CAK78], plasma models [Fre06], separatrix splitting [Tre96], symmetric problems [SB85, VC93] tidal elevation models [DKM02], trapping problems [GW92, Kat83b, Kat83a], and the three-body problem [Féj01]. There is also an immediate connection to highly oscillatory problems [KL93, KL94]. There have been many improvements and variations [DM10] of the averaging framework e.g., advection–

diffusion equations [Kro91], almost periodic cases [Bri09], associated stable manifolds [Sch88], asymptotically autonomous systems [SPT05], averaging on manifolds [DGL94], Axiom A conditions [Kif04a, Kif92], convolution approximation [Bri11], discretized problems [Feč91], various dispersive PDEs [ASS13, ACM08a, Gua13, Hab91b], ergodic fast subsystems [Sch95b], error estimates [Vit79], exponentially small error estimates [Nei84, PT00, Tre97], flows on surfaces [DK13], higher-order averaging [ESD90, Mon86, San80], infinite-dimensional Hamiltonian systems [MS03c], iterated averaging [Per84, PH78], iterated maps [DEV04], mixing conditions [Kif04b, Kif03], multifrequency systems involving Diophantine conditions [Bak86, DRW89], parabolic PDEs [Kou97, Mat01], PDE approximations [MS03d], quasidifferential equations [MP98], relations to Young measures [ALT07], several small parameters [Gai86, GN02, GN01], slowly varying averages [Art10, Art07], sustained resonance [Rob83], and systems with impulses [BM81, FM13]. The upshot is that no matter what type of dynamical system one considers, there is often a set of very reasonable assumptions under which one may average the system. In fact, we shall return to an overview of averaging results in several other reference sections; see, e.g., Sections 15.10 and 19.10.

Section 9.7: The basic definitions of Gevrey analysis can be found in [Sib00], while the two application examples are considered in [Mae07b, RS96]. Similar results to the coordinate transformation result are also obtained in [Con04]. Gevrey techniques have been a staple in the analysis of singularly perturbed problems for quite some time [CD94, CD93, CDMFS07, CDRSS00, Sib00]. An early application to canard theory can be found in [MLK94]. More details on summability and turning points involving a complex equation are discussed in [BFSW98a, BFSW98b]. Another classical topic is multisummability [BMF02, RS96, Wal90b, Wal90a]. There are several related ideas that interface with Gevrey asymptotics [Gil97], such as hyperasymptotics [BH90, Boy99, Boy05], transseries [How10], and Lie–Desprit transformations [COR12, Dep69]. For more details on Hamiltonian fast–slow systems, we refer to Section 19.10 as well as [BS10]. Matching for terms beyond all orders [BSSV98], as well as convergence of asymptotic series [Kal13], relates nicely with complex analysis.

Section 9.8: The example considered can be found in many asymptotic analysis texts [BO99, KC96]. The philosophy of two-timing methods as a two-variable expansion idea is very classical [Lic69, O'M70a]; for some surveys and expositions, see [Hol99, Jak13, Smi75]. As for averaging and WKB, there are many applications of two-timing approaches. For example, the method has been applied to the Boussinesq equation [Kor06], dispersive waves [Hab91a, Has71], gas dynamics [EY91], heat flow in a rod [Edw00], various nonlinear oscillator models [BHK91, BH88, Kri89] the Orr–Sommerfeld equations [Lon87], predator–prey systems [Bra03], quantum optics [Jan03], resonance phenomena [SS04c], thermohaline convection [Mor86], tracing light rays [KW79], vibration absorbers [OCN99], water waves [Dem10], and wave motion [FK85]. Many more references can be found in the literature on nonlinear mechanics and fluid dynamics. One can also extend the method to difference equations [RH12], derive error estimates [Rei71], and consider expanding intervals [Kol74, MW96]. Of course, like all other asymptotic methods [BK08b, Kif08], two-timing approaches may fail [Rei80, Rub78]. A classical problem for the methods of this section is Lighthill's equation [Bur70, Com68, Com72]. Procedures immediately related to two-variable expansion ideas are the von Zeipel method [Kev66] and the reconstitution method [LP99]. As pointed out already at the beginning of this chapter, averaging and the method of multiple scales (two-timing) can be viewed as “equivalent” for certain classes of problems [Mor66, Nay05, Per69, Sar78]; a similar remark applies to

two-timing in comparison averaging, normal form transformations, and matched asymptotics [CMP77, OK11, Wol77]. Two-timing also plays a key role in deriving amplitude equations and in homogenization methods; see Section 18.7 for more references in these directions. In fact, the direct two-scale ansatz has probably played a more important role for spatial multiscale problems than for purely multiple time scale dynamics.

Section 9.9: The equivalence of the renormalization group (RG) to normal forms was based on [DHH⁺08], whereas the original reference for the singularly perturbed ODE application of RG is due to [CGO96, CGO94]. The RG method arose in physics [Fis74] and is often attributed to Wilson [Wil75, Wil83, WK74]. As mentioned already several times, establishing relations between RG, multiple scales, normal forms, averaging, and related methods is a common theme in the area [Che04, Iwa08, MO03, OW06, Set95]. For an expository look at RG from the asymptotic analysis perspective, one may consider [Kir12, OK09]. RG can also be used to derive amplitude equations [CGOP94, Chi13] in a way similar to the method of multiple scales we used in Section 18.6.

Section 9.10: This section was extracted from [Chi09]; see also [Chi08]. For even more references on RG, we refer to [Les98]. The statistical physics view is well described in the textbook [Gol92]; for additional monographs, consider [Ami84, BG95, BDFN92, Car96, ZJ07]. The RG philosophy has been applied in many diverse contexts such as diffusive processes [OC12], elementary particle systems [Sha94], periodically forced nonlinear Schrödinger equations [MP08], and small-world networks [NW99].

A standard asymptotic analysis topic that we have omitted almost completely in this book is methods for integrals [Bru70, Erd56, Mil06, Mur84]; also, Borel summability has not been covered [Cos09]. Other topics we could have included in more detail are the superadiabatic Stokes phenomenon [BU11] and distributional asymptotics [EK02, EK90, EK95].

Chapter 10

Numerical Methods

For the analysis of many nonlinear dynamical systems, numerical methods are indispensable. Fast–slow systems are no exception. In fact, multiscale differential equations provide a big challenge for efficient numerics.

In Section 10.1, we begin with classical forward integration schemes and point out the central role played by multiple time scale systems as prototypical stiff problems. Section 10.2 continues this theme and quantifies the performance by introducing A-stability. Sections 10.3 and 10.4 provide a brief introduction to boundary value problems (BVPs) and their numerical treatment as reformulating many fast–slow systems in terms of a BVP can help substantially. This viewpoint is illustrated in Section 10.5, where the condition number of a linear system arising from a discretized fast–slow problem is considered. Section 10.6 is a mini-introduction to numerical continuation that allows the parameter-tracking of various dynamical objects; in our context, an important application arises when we view the time scale separation as the continuation parameter. Sections 10.7 and 10.8 deal with the construction and error analysis of heterogeneous multiscale methods. Basically, this technique makes use of the time scale separation by partially decoupling the forward integration for the fast and slow subsystems.

Background: Although one may read this chapter without additional further requirements, knowledge of a programming language is highly recommended. Without practicing and testing various methods yourself, there is relatively little chance of deeply understanding its advantages and shortcomings.

10.1 Stiff Equations

Consider the general ODE initial value problem

$$\frac{dz}{dt} = z' = F(z), \quad z(T_0) = z_0, \tag{10.1}$$

for $z \in \mathbb{R}^N$. To solve (10.1) numerically, consider a sequence of times

$$t_0 = T_0, \quad t_1 = T_0 + h, \quad t_2 = T_0 + 2h, \quad \dots,$$

where h is the **time step**. The goal is to find an approximation to $z(t)$ by computing it at discrete times $z_j := z(t_j)$. The simplest method for solving (10.1) numerically is the **(explicit) Euler method**

$$z_{n+1} = z_n + hF(z_n), \quad (10.2)$$

which tries to predict a new point z_{n+1} on the trajectory from the derivative at the current point z_n .

Exercise 10.1.1. Consider Euler's method with $z \in \mathbb{R}^1$ and suppose that F has a (global) Lipschitz constant L_F . Define the **local truncation error** T_n and the **global error** E_n as

$$T_n := \frac{z(t_{n+1}) - z(t_n)}{h} - F(z(t_n)) \quad \text{and} \quad E_n := z(t_n) - z_n,$$

where $z(t_n)$ is the exact solution evaluated at time t_n .

- (a) Show that $\max_{0 \leq n \leq N-1} |T_n| = K_0 h$ and give an estimate of $K_0 > 0$ based on the second derivative of the solution $z(t)$.
- (b) Prove that $|E_n| \leq K_1 [\exp(L_F(t_n - t_0)) - 1]$ for $n = 0, 1, 2, \dots$ and give an estimate of K_1 based on the local truncation error. \diamond

Multiple time scale systems are one major reason why better numerical schemes than Euler's method have been developed. To illustrate this point, we begin with an example.

Example 10.1.2. Consider the linear $(1, 1)$ -fast–slow system

$$\begin{aligned} \frac{dx}{d\tau} &= \dot{x} = -\frac{x}{\varepsilon}, \\ \frac{dy}{d\tau} &= \dot{y} = -y. \end{aligned} \quad (10.3)$$

The solution of (10.3) is $(x(\tau), y(\tau)) = (x(0)e^{-\tau/\varepsilon}, y(0)e^{-\tau})$. Hence, all solutions of (10.3) will decay to the stable node at the origin. In Figure 10.1, we have applied Euler's method (10.2) for $\varepsilon = 0.001$ and a step size $h = 0.01$. The method fails and produces a divergent numerical solution.

A very simple calculation illustrates what went wrong. Denote the vector field (10.3) by $z' = Az$, where $z = (x, y)$ and A is the matrix given by

$$A = \begin{pmatrix} -\frac{1}{\varepsilon} & 0 \\ 0 & -1 \end{pmatrix}.$$

Then Euler's method with step size h at step $n \rightarrow n+1$ is

$$z_{n+1} = z_n + hAz_n = (\text{Id} + hA)z_n.$$

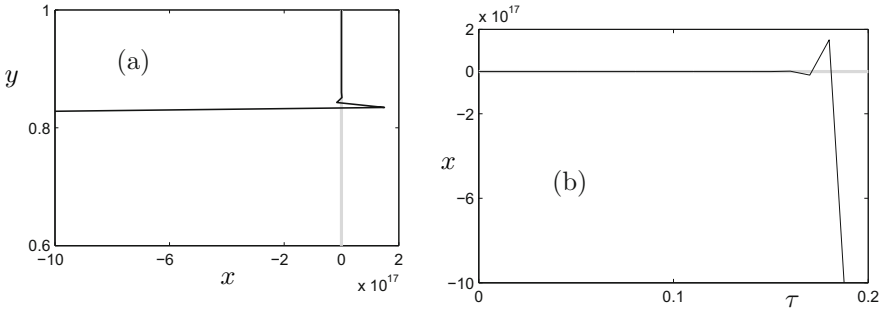


Figure 10.1: Numerical solution of (10.3) with the explicit Euler method for $\varepsilon = 0.001$ (thin black curve, step size $h = 0.01$); initial condition is $(x(0), y(0)) = (1, 1)$. The correct solution is shown in gray and decays toward zero. Obviously, the Euler solution diverges. Note the large scale for the x -coordinate in the phase space plot (a) and the time series plot (b).

Therefore, it follows that the Euler solution at some final step N is

$$z_N = (\text{Id} + hA)^N z_0 = \begin{pmatrix} (1 - \frac{h}{\varepsilon})^N & 0 \\ 0 & (1 - h)^N \end{pmatrix} z_0.$$

We conclude that the Euler solution will converge to zero if

$$|1 - h| < 1 \quad \text{and} \quad \left| 1 - \frac{h}{\varepsilon} \right| < 1.$$

The first condition is easily satisfied, since any step size $h \in (0, 2)$ will work. The difficulty arises for the fast component, where we need $h = k\varepsilon$ for $0 < k < 2$. Hence, the step size has to be extremely small if there is a big separation in time scales. But if we choose the step size very small, it will take a long time to resolve the trajectory, particularly on an attracting slow manifold, where one would like to take bigger steps. ♦

The problem arising in Example 10.1.2 is not the only numerical challenge caused by multiple time scale dynamics. For now, we shall postpone other issues and just focus on methods to solve the problem observed in Example 10.1.2. Multiple time scale systems are the primary examples for so-called **stiff differential equations**. There is no general definition of a stiff differential equation, but for our perspective, the main aspect is that multiple time scale differential equations are a (large) subset of stiff differential equations. To make this idea more precise, one could consider the following construction. Let

$$w' = (DF)w$$

denote the linearization of the ODE (10.1) with $w \in \mathbb{R}^N$. Suppose all the eigenvalues λ_j of DF have negative real parts. Then define the **stiffness ratio**

μ as

$$\mu := \frac{\max_j \{\operatorname{Re}(\lambda_j)\}}{\min_j \{\operatorname{Re}(\lambda_j)\}}. \quad (10.4)$$

A system is then called **stiff** if μ is large. For a multiple time scales system with $F = (f, \varepsilon g)$, we are usually going to find that $\mu = \mathcal{O}(1/\varepsilon)$; note that this result is invariant under changing to the slow time scale $\tau = \varepsilon t$. The standard assumption $0 < \varepsilon \ll 1$ implies that $\mu = \mathcal{O}(1/\varepsilon)$ is always very large.

Remark: The definition of stiffness via the ratio (10.4) for the linearized system might not be appropriate for nonlinear problems; see references in Section 10.9. However, the ratio is helpful in illustrating the key role played by multiple time scales.

We briefly consider a few classical methods that go beyond the explicit Euler scheme. It is well known that the error we make at each step, called the local truncation error, of the explicit Euler method is bounded by $K_0 h$ for some constant $K_0 > 0$; see Exercise 10.1.1. Therefore, the Euler method has **order one** or **order $\mathcal{O}(h)$** (as $h \rightarrow 0$). The **modified Euler method** is given by

$$z_{n+1} = z_n + hF\left(z_n + \frac{1}{2}F(z_n)\right); \quad (10.5)$$

it has order $\mathcal{O}(h^2)$, providing better error control. Another scheme is the **fourth-order Runge–Kutta (RK)** method

$$z_{n+1} = z_n + \frac{1}{6}h(k_1 + 2k_2 + 2k_3 + k_4), \quad (10.6)$$

where

$$\begin{aligned} k_1 &= F(z_n), \\ k_2 &= F(z_n + \frac{1}{2}hk_1), \\ k_3 &= F(z_n + \frac{1}{2}hk_2), \\ k_4 &= F(z_n + hk_3). \end{aligned}$$

The coefficients k_2 and k_3 represent approximations of derivatives z' at intermediate points between t_n and t_{n+1} . It turns out that the fourth-order RK method provides a very good compromise between speed and accuracy for many problems. Some variation of the RK method is often implemented as the default solver for many numerical software packages. However, the next exercise shows that the standard fourth-order RK method is not very efficient for a sufficiently large time scale separation.

Exercise/Project 10.1.3. Implement the modified Euler method (10.5) and the fourth-order RK method (10.6). Apply both methods to the fast–slow test problem (10.3) from Example 10.1.2. How are the time scale separation ε and the step size h related to the convergence? ◇

All methods considered so far compute the new point on a solution curve z_{n+1} from one previous point, i.e., they are **one-step methods**. Furthermore, there is a direct formula that expresses z_{n+1} using z_n that makes the methods **explicit**. There is a generalization available called **linear multistep methods**.

Definition 10.1.4. A linear k -step method is defined by

$$\sum_{j=0}^k a_j z_{n+j} = h \sum_{j=0}^k b_j F(z_{n+j}), \quad (10.7)$$

where we assume, to avoid degenerate cases, that $a_0^2 + b_0^2 \neq 0$ and $a_k \neq 0$.

One also refers to

$$\begin{aligned}\rho(z) &= \sum_{j=0}^k a_j z^j, \\ \sigma(z) &= \sum_{j=0}^k b_j z^j,\end{aligned}$$

as the **first** and **second characteristic polynomials** of the linear k -step method. The **Adams–Bashforth method**

$$z_{n+4} = z_{n+3} + \frac{1}{24}h(55F(z_{n+3}) - 59F(z_{n+2}) + 37F(z_{n+1}) + f(z_n))$$

is an example of an explicit linear four-step method; note that a one-step method can be used to initialize the first three points for a four-step method. Another classical example is the **implicit Euler method**

$$z_{n+1} = z_n + hF(z_{n+1}),$$

where one has to solve a system of algebraic equations to find z_{n+1} , i.e., the scheme defines z_{n+1} only implicitly. The implicit Euler method is a one-step method, as is the **trapezoid rule method**

$$z_{n+1} = z_n + \frac{1}{2}h(F(z_{n+1}) + f(z_n)).$$

Definition 10.1.5. A linear k -step method is **explicit** if $b_k = 0$, i.e., there is a direct formula to obtain z_{n+k} from z_{n+j} for $j < k$. If $b_k \neq 0$, then the method is **implicit**.

Exercise/Project 10.1.6. Pick one or two of your favorite multiple time scale ODEs from this book and experiment with the various methods that we have discussed in this section. Change the step size and the time scale separation and calculate the local truncation and global error for each method you try. ◇

Linear multistep methods can be designed and analyzed based on several important numerical analysis concepts such as zero stability, consistency, and convergence; see Section 10.9. We shall not discuss these classical topics here but focus on so-called A-stability, which is one way to characterize how well a method is expected to cope with stiff equations.

10.2 A-Stability

As a preparation for the discussion to follow, we have to state a standard result about solving linear recurrence relations. Suppose we are given the **k th-order linear recurrence relation**

$$\alpha_k z_{n+k} + \cdots + \alpha_1 z_{n+1} + \alpha_0 z_n = 0, \quad n = 0, 1, 2, \dots, \quad (10.8)$$

with $\alpha_k \neq 0$, $\alpha_0 \neq 0$, and $\alpha_j \in \mathbb{R}$ for $j = 0, 1, \dots, k$. Define the **characteristic polynomial** associated with (10.8) as

$$\rho(w) := \alpha_k w^k + \cdots + \alpha_1 w + \alpha_0.$$

Denote by w_r , $1 \leq r \leq l$, $l \leq k$, the distinct roots of the polynomial ρ and denote by m_r the multiplicity of the root w_r .

Lemma 10.2.1 ([Hen62, SM03]). *If a sequence of complex numbers z_n satisfies (10.8), then*

$$z_n = \sum_{r=1}^l p_r(n) w_r^n,$$

where p_r is a polynomial in n of degree $m_r - 1$; in particular, if all the roots w_r are simple, then the p_r are constants.

A simple test equation will be very helpful in capturing the basic properties of stiff equations.

Definition 10.2.2. The **Dahlquist test equation** is given by

$$z' = \lambda z, \quad z(0) = z_0, \tag{10.9}$$

where $\lambda \in \mathbb{C}$ and $\operatorname{Re}(\lambda) < 0$.

It is clear that solutions of (10.9) must decay to zero as $t \rightarrow \infty$. It seems to be a rather logical requirement that this property of decay to zero should also hold for a numerical solution, i.e.,

$$z_n \rightarrow 0, \quad \text{as } n \rightarrow \infty.$$

Applying the general linear multistep method (10.7) to the Dahlquist test equation yields

$$\sum_{j=0}^k a_j z_{n+j} = h \sum_{j=0}^k b_j \lambda z_{n+j}.$$

The last equation can be rewritten as

$$\sum_{j=0}^k (a_j - \lambda h b_j) z_{n+j} = 0. \tag{10.10}$$

Observe that (10.10) is a linear recurrence relation.

Definition 10.2.3. The associated characteristic polynomial of the recurrence relation (10.10) is

$$\Pi(w; \lambda h) = \sum_{j=0}^k (a_j - \lambda h b_j) w^j. \tag{10.11}$$

One also calls (10.11) the **stability polynomial** of the linear multistep method.

Note that the stability polynomial can be rewritten in terms of the first- and second-order characteristic polynomials of the multistep methods:

$$\Pi(w; \lambda h) = \rho(w) - \lambda h \sigma(w).$$

Lemma 10.2.1 implies that the solution of the recurrence relation (10.10) can be written in terms of the roots w_r of the stability polynomial

$$z_n = \sum_{r=1}^l p_r(n) w_r^n,$$

where the roots are functions of λh and the coefficients a_j, b_j of the stability polynomial. If each root has absolute value less than 1, we easily see that $z_n \rightarrow 0$ as $n \rightarrow \infty$.

Definition 10.2.4. A linear multistep method is called **absolutely stable** for a given value of λh if each root $w_r = w_r(\lambda h)$ of the stability polynomial satisfies $|w_r(\lambda h)| < 1$.

The next step is to classify for which values λh a method is absolutely stable.

Definition 10.2.5. The **region of absolute stability** is the set of points $\lambda h \in \mathbb{C}$ for which the linear multistep method is absolutely stable.

We have seen that λ might be of order $\mathcal{O}(1/\varepsilon)$ for $0 < \varepsilon \ll 1$ in multiple time scale problems. Hence, we would like to have a region of absolute stability that admits every h if $\operatorname{Re}(\lambda) < 0$.

Definition 10.2.6. A linear multistep method is called **A-stable** if its region of absolute stability contains the left half of the complex plane.

The problem is that A-stability is rather difficult to obtain for linear multistep methods. Indeed, the famous **Dahlquist second barrier theorem** shows that there are limitations to linear multistep methods.

Theorem 10.2.7 ([Dah63]; see also [HW91b, Ise02, SM03]). *The following three statements hold:*

- (a) *No explicit linear multistep method is A-stable.*
- (b) *No A-stable linear multistep method can have order greater than 2.*
- (c) *The second-order A-stable linear multistep method with the smallest error constant is the trapezoid method.*

The general proof of Dahlquist's theorem is beyond the scope of this book, but let us at least verify that the trapezoid method is A-stable. The method is defined by

$$z_{n+1} = z_n + \frac{h}{2} (f(z_{n+1}) + f(z_n)). \quad (10.12)$$

Applying (10.12) to the test equation $z' = \lambda z$ leads to

$$z_{n+1} = z_n + \frac{h}{2} \lambda z_{n+1} + \frac{h}{2} \lambda z_n.$$

Therefore, the associated stability polynomial is

$$p(w; \lambda h) = \left(1 - \frac{1}{2}\lambda h\right)w + \left(-1 - \frac{1}{2}\lambda h\right).$$

The only root is easily found as

$$w_r = \frac{1 + \frac{1}{2}\lambda h}{1 - \frac{1}{2}\lambda h}.$$

If $\operatorname{Re}(\lambda h) = h\operatorname{Re}(\lambda) < 0$, then it follows that $|w_r| < 1$, and we conclude that the trapezoid method is A-stable. However, methods of order two might not be sufficient for many purposes, and one could ask for a compromise. Perhaps some higher-order linear multistep methods are not A-stable but have a relatively large region of absolute stability. It would also be highly desirable that the region of absolute stability include the negative real axis. Such methods can be derived; see also Section 10.9. One way to quantify the stability of these methods is to weaken the definition of A-stability.

Definition 10.2.8. A linear multistep method is called **$A(\alpha)$ -stable** if the domain of absolute stability contains a wedge/cone in the left half-plane given by

$$\{\lambda h \in \mathbb{C} : |\arg(\lambda h) - \pi| < \alpha\}.$$

As an example, we shall mention only **backward differentiation formulas**, or **BDF**, methods. These are special linear multistep methods of the form

$$hb_k f(z_{n+k}) = a_k z_{n+k} + \cdots + a_0 z_n.$$

In particular, the requirement on a general linear multistep method is that $b_j = 0$ for $0 \leq j \leq k-1$, $k \geq 1$, and $b_k \neq 0$. One derives the coefficients by requiring the maximum accuracy that the method can possibly achieve; typical examples are the BDF formulas of orders 2, 3, and 4:

$$\begin{aligned} 2hf(z_{n+2}) &= 3z_{n+2} - 4z_{n+1} + z_n, \\ 6hf(z_{n+3}) &= 11z_{n+3} - 18z_{n+2} + 9z_{n+1} - 2z_n, \\ 12hf(z_{n+4}) &= 25z_{n+4} - 48z_{n+3} + 36z_{n+2} - 16z_{n+1} + 3z_n. \end{aligned}$$

The second-order method is A-stable. The third- and fourth-order methods are $A(\alpha)$ -stable with opening angles α approximately given by 86.03 and 73.35 degrees. Essentially all modern textbooks on numerical solutions of ODEs have detailed plots of stability regions; see Section 10.9. However, it is quite instructive to use numerical experiments to try to locate the boundary of the stability region.

Exercise 10.2.9. Determine the domain of absolute stability for the fourth-order Runge–Kutta method (10.6) and the fourth-order BDF method. ◇

Of course, one can also try to move beyond the natural class of linear multistep methods completely and search for A-stable methods in other classes of methods. For example, there are several classes of methods of order higher than two that are A-stable. Of course, one expects the computational complexity to increase for these methods in comparison to linear multistep schemes, but a detailed discussion of these issues is beyond the scope of this book; see Section 10.9.

10.3 Boundary Value Problems (BVPs)

We have seen in the last two sections that initial value problems for fast–slow systems are difficult to solve numerically. Just making a small error in the forward time-stepping algorithm can lead to incorrect global results. Often, it helps tremendously to reformulate the equation in terms of a **boundary value problem (BVP)**. Here we restrict ourselves to **two-point BVPs** given by

$$\frac{dz}{dt} = z' = F(z), \quad (10.13)$$

$$G(z(T_a), z(T_b)) = 0, \quad (10.14)$$

where $z \in \mathbb{R}^N$, $F : \mathbb{R}^N \rightarrow \mathbb{R}^N$, $G : \mathbb{R}^{2N} \rightarrow \mathbb{R}^N$, and $t \in [T_a, T_b]$.

Remark: Note that BVPs include initial value problems (IVPs) as a special case. However, sometimes it helps to prescribe a mixture of conditions at the initial and final times to improve the numerics; see, e.g., Section 11.5.

The boundary conditions (10.14) are very general, and we shall encounter only **separated boundary conditions**

$$G(z(T_a), z(T_b)) = \begin{pmatrix} G_1(z(T_a)) \\ G_2(z(T_b)) \end{pmatrix} = 0,$$

where $G_1 : \mathbb{R}^N \rightarrow \mathbb{R}^p$, $G_2 : \mathbb{R}^N \rightarrow \mathbb{R}^q$, and $p + q = N$. Another simplification that can be made is to translate time to achieve $T_a = 0$. Then one may rescale time $\tilde{t} = \frac{t}{T_b}$, which yields

$$\frac{dz}{d\tilde{t}} = z' = T_b F(z), \quad (10.15)$$

$$G_1(z(0)) = 0, \quad G_2(z(1)) = 0. \quad (10.16)$$

Then define $\tilde{F}(z) := T_b F(z)$ and apply the usual procedure of dropping all the tildes for notational convenience:

$$\frac{dz}{dt} = z' = F(z), \quad (10.17)$$

$$G_1(z(0)) = 0, \quad G_2(z(1)) = 0,$$

which is the standard form of a two-point boundary value problem with separated boundary conditions. Using a standardized form not only is mathematically convenient but also simplifies the development of general-purpose numerical solvers.

Remark: It is often possible to transform BVPs into a standard form. For example, even unseparated boundary conditions and multipoint boundary value problems can be converted into standard form by introducing additional variables; see [AMR87] for details.

A first natural mathematical question to ask is when solutions to the BVP (10.17) exist and if so, when they are unique. The next example shows the scale of the problem one is facing in this regard.

Example 10.3.1. Consider the classical harmonic oscillator ODE

$$\begin{aligned} z'_1 &= 2\pi z_2, \\ z'_2 &= -2\pi z_1, \end{aligned} \tag{10.18}$$

as a boundary value problem for $t \in [0, 1]$ with boundary conditions

$$z_1(0) = 0 \quad \text{and} \quad z_1(1) = k.$$

The general solution of (10.18) with $z_1(0) = 0$ is obviously given by

$$(z_1(t), z_2(t)) = (c \sin(2\pi t), c \cos(2\pi t)),$$

where c is a constant to be determined from the boundary condition $z_1(1) = k$. If $k \neq 0$, then there is no solution, and if $k = 0$, then there are infinitely many solutions, since every constant $c \in \mathbb{R}$ can be chosen. ♦

The example shows that even a simple linear BVP might have no or multiple solutions. The situation seems to look worse than for IVPs, where standard theory of ODEs guarantees short-time existence and uniqueness of solutions under relatively mild assumptions. However, using geometric singular perturbation theory, such as the exchange lemma or the blowup method, we were able to prove in Chapters 6–8 the existence of special trajectories for a fast–slow system. Hence, we may often know, from some a priori geometric arguments, that the trajectory we are trying to approximate numerically exists (or that it should exist).

Exercise/Project 10.3.2. Consider the following two-point BVP for $t \in [T_a, T_b]$:

$$\begin{aligned} 0 &= \varepsilon^2 z'' - zz' + f(t)z, \\ A &= z(T_a) - \varepsilon z'(T_a), \\ B &= z(T_b) - \varepsilon z'(T_b), \end{aligned} \tag{10.19}$$

and determine under what conditions on T_a, T_b, A, B a solution to (10.19) exists. We note that (10.19) is an example from classical turning point theory as discussed in Sections 3.4, 9.11, and 20.10. ◇

The simplest method for solving a standard BVP (10.17) numerically is called **simple shooting**. The idea is to vary the initial condition of an IVP solver until the solution fits the boundary conditions. One should think of having some degrees of freedom available at $t = 0$, shoot/integrate a trajectory forward, and then check whether it matches the boundary conditions at $t = 1$. Regardless of the implementation and details used, we often exclude simple shooting from consideration, since it is basically an IVP approach. However, the idea of shooting can be useful for fast-slow systems.

Example 10.3.3. Consider van der Pol's equation with constant forcing

$$\begin{aligned} x' &= y - \frac{1}{3}x^3 + x, \\ y' &= \varepsilon(a - x). \end{aligned} \quad (10.20)$$

The critical manifold is $C_0 = \{y = \frac{1}{3}x^3 - x\}$ with fold points at $x = \pm 1$. We know from our analysis in Chapter 8 that there is a singular Hopf bifurcation at $a = 1$ with an associated canard explosion. One problem is that even if we knew the exact parameter value for a where a canard occurs, a direct initial value solver approach fails.

In Figure 10.2, we show a numerical trajectory computed for $\varepsilon = 0.01$ and $a = 0.9987404510709979033$ with an IVP solver. The zoom in Figure 10.2 shows that the solution is extremely sensitive along the middle repelling branch $C_0^\text{r} = C_0 \cap \{-1 < x < 1\}$ of the critical manifold. In fact, Figure 10.2 suggests that solutions may cross, which is theoretically impossible by uniqueness of solutions for ODEs, i.e., in the zoomed-in region, the solution has to decide

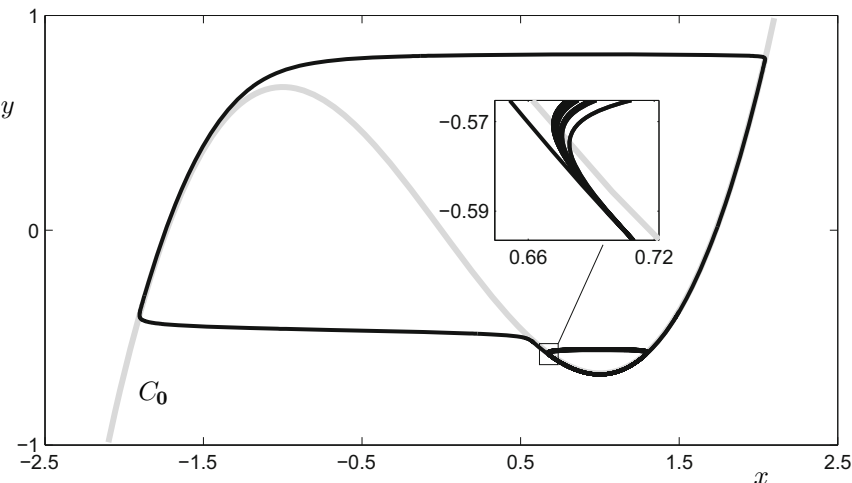


Figure 10.2: Numerical (forward integration) trajectory of van der Pol's equation (10.20) obtained for $a = 0.9987404510709979033$ and $\varepsilon = 0.01$.

whether to jump left or right and cannot alternate. A BVP approach can be used to find the canard orbits and detect the corresponding values of a . Define two sections

$$\begin{aligned}\Sigma_1 &:= \{(x, y) \in \mathbb{R}^2 : x = -1\}, \\ \Sigma_2 &:= \{(x, y) \in \mathbb{R}^2 : x = a\}.\end{aligned}$$

Then we can compute two trajectory segments using shooting, one from Σ_1 to Σ_2 using forward integration and one from Σ_1 to Σ_2 using backward integration. Then we can vary the parameter a and the integration time to match the two segments on both sections, which yields a periodic orbit. This procedure is illustrated in Figure 10.3.

The key idea of this approach is that the computation requires the solution of two boundary value problems, each of which is numerically stable under forward integration, so that shooting is successful. Formally, the approach shown in Figure 10.3 is a **multiple shooting** method, since we considered multiple BVPs. ♦

10.4 Two Standard BVP Methods

In Section 10.5, we are going to explain why certain boundary value problems can be better conditioned than the corresponding initial value problems. Before we proceed to that step, we briefly sketch two ideas for solving the BVP (10.17) numerically without using an initial value solver.

The first classical method is that of **finite differences**. Choose a **mesh**

$$\Pi : \quad 0 = t_1 < t_2 < \dots < t_M < t_{M+1} = 1. \quad (10.21)$$

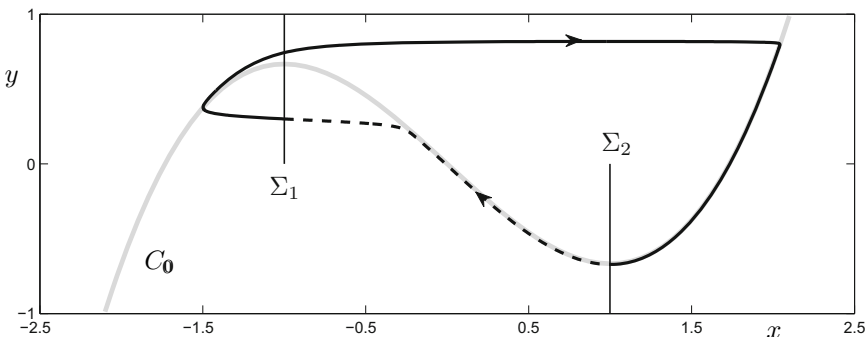


Figure 10.3: Illustration of the idea behind how to find canards via (multiple) shooting in van der Pol's equation (10.20). The dashed black trajectory segment was computed using an IVP solver using backward integration and starting from the section Σ_1 . The solid black trajectory segment was computed with an IVP solver with forward integration. On variation of a and the integration times, we can match the segments on the two sections $\Sigma_{1,2}$ to form a periodic (canard) solution. Note that the canard explosion happens within an exponentially small parameter interval; see Section 8.4.

For simplicity, let us assume that the mesh is uniform, so that $t_k = (k - 1)h$ for $h = 1/M$. The derivatives $z'_j(t_k)$ for $j \in \{1, 2, \dots, N\}$ can be approximated by a (midpoint) finite difference

$$z'_j \left(\frac{t_{k+1} + t_k}{2} \right) = \frac{z_j(t_{k+1}) - z_j(t_k)}{h} + \mathcal{O}(h^2) \approx \frac{z_j(t_{k+1}) - z_j(t_k)}{h}.$$

This yields an approximation of the BVP (10.17) given by

$$\begin{aligned} z_j(t_{k+1}) - z_j(t_k) &= h F_j \left(\frac{z(t_{k+1}) + z(t_k)}{2} \right), \\ G_1(z(t_1)) &= 0, \quad G_2(z(t_{M+1})) = 0. \end{aligned} \tag{10.22}$$

The algebraic equations (10.22) have $(M+1) \times N$ unknowns $z_j(t_k)$. Observe that there are $M \times N$ equations coming from discretizing the differential equation and N equations from the boundary conditions. Then one may attempt to solve the resulting nonlinear algebraic equations for the unknowns $z_j(t_k)$, which provides an approximation z_Π to the solution z . The finite difference scheme presented here is very simple, and higher-order schemes can be found with similar considerations as for IVPs [AMR87].

Remark: We shall not discuss the solution of nonlinear algebraic equations. In many practical cases, it suffices to apply **Newton's method** [Gau97, SM03]; see also Section 10.6. The matrices occurring in Newton's method are often very sparse and structured, which can help tremendously in performing a Newton iteration.

The second classical method is **collocation**. Again, we start with a uniform mesh Π as given in (10.21). In addition, define points between t_k and t_{k+1} given by

$$t_{kl} = t_k + h_k \rho_l,$$

where $k \in \{1, \dots, M\}$, $l \in \{1, \dots, L\}$, and

$$0 \leq \rho_1 < \rho_2 < \dots < \rho_L = 1.$$

The points t_{kl} are called **collocation points**. The number and spacing of the collocation points are defined via L and h_k . It turns out that the best choice of collocation points will often be the **Gauss points**, which are chosen as the zeros of a Legendre polynomial [AMR87, Doe07]. Regardless of this choice, one may define a numerical method to solve (10.17) as follows. Let z_Π be defined as a piecewise polynomial function that reduces to a polynomial of degree at most L on each mesh subinterval $[t_k, t_{k+1}]$. We require that

$$z'_\Pi(t_{kl}) = F(z_\Pi(t_{kl})) \tag{10.23}$$

for $k \in \{1, 2, \dots, M\}$ and $l \in \{1, 2, \dots, L\}$, where z_Π is understood as a vector in this case. One also says that the conditions (10.23) are **collocation conditions**, i.e., the numerical approximation z_Π satisfies the ODE at the collocation points. This yields $L \times N \times M$ algebraic equations. Requiring continuity of z_Π at $z_\Pi(t_k)$ for $k \in \{2, \dots, M\}$ yields $(M-1) \times N$ conditions. The boundary conditions give

another N algebraic equations. On each subinterval, the polynomial is of degree at most L , so that it has $L + 1$ undetermined coefficients. Hence, it follows that

$$\begin{aligned} \text{equations} &= L \times N \times M + (M - 1) \times N + N = L \times M \times N + M \times N, \\ \text{variables} &= (L + 1) \times M \times N = L \times M \times N + M \times N. \end{aligned}$$

The resulting system of nonlinear algebraic equations can again be solved by Newton's method. In practice, many two-point boundary value solvers use a collocation method. Typical choices are between three and five collocation points, and the crucial numerical parameter is the mesh size h (as for the finite difference method). Note also very carefully that for finite differences and collocation, we solve the entire BVP at once. There is no time-stepping necessary, since we have discretized the entire problem and converted it into algebraic equations.

Exercise/Project 10.4.1. Consider Example 10.3.3 and implement the periodic orbit calculation of canard orbits using finite differences as well as collocation schemes. Compare the performance of both approaches. ◇

Another important issue for BVP methods, as well as numerics for multiscale problems in general, is **mesh adaptation**. Some references to the literature on adaptive meshes is provided in Section 10.9. Here we only mention a basic practical principle usually referred to as the **error equidistribution principle**. This principle works by simply computing an error estimator on each mesh element and then refining the mesh in those places where the error is largest so that each element roughly contributes the same local error to the global error. In many practical contexts, this principle has worked extremely well for multiple time scale problems.

10.5 Conditioning

Certain problems are difficult to solve as a pure initial value problem (IVP) problem, regardless of the numerical method used. However, the same problem can be easy to solve numerically if reformulated as a boundary value problem (BVP). We have already seen in Example 10.3.3 that canards in the van der Pol equation fall into this category. The key concept that helps us to decide when an IVP should be reformulated for numerical solution is **conditioning**.

Definition 10.5.1. A problem is called **ill conditioned** if a small error in the given data yields a much larger error in the result. If the error is only of small/moderate size, we say that the problem is **well conditioned**.

Although the definition is frequently used, it is unfortunately rather vague. We are going to discuss ill-conditioning for BVPs and IVPs together, since we can always view IVPs as a special case of BVPs. Consider the inhomogeneous nonautonomous linear BVP

$$\begin{aligned} \frac{dz}{dt} &= z' = A(t)z + q(t), \\ B_0 z(0) + B_1 z(1) &= \beta, \end{aligned} \tag{10.24}$$

where $B_0, B_1, A(t)$ are $N \times N$ matrices and $z = z(t), \beta, q(t) \in \mathbb{R}^N$. We view (10.24) as the linearized BVP for a general nonlinear BVP (10.17). Note that we can always scale the equation for the boundary conditions by a constant, which makes it natural to assume a normalization

$$\max\{\|B_0\|, \|B_1\|\} = 1$$

for some matrix norm $\|\cdot\|$.

Definition 10.5.2. A solution Z to the ODE $Z' = A(t)Z$ is called a **fundamental solution (or fundamental matrix)**. We say that $Z(t, t_0) \in \mathbb{R}^{N \times N}$ is the **principal solution** (or principal fundamental solution) if it solves the ODE

$$Z' = A(t)Z, \quad Z(t_0, t_0) = \text{Id}.$$

The terminology of fundamental and principal solutions is often used interchangeably, or the term fundamental solution is used for both terms simultaneously. Furthermore, the matrix $Z(t, t_0)$ is sometimes called the **propagator** or **evolution operator**.

Theorem 10.5.3 ([AMR87]). *The BVP (10.24) has a unique solution if and only if the matrix*

$$Q := B_0Z(0) + B_1Z(1)$$

is nonsingular/invertible, where $Z(t)$ denotes a fundamental solution to $Z' = A(t)Z$. Define $\Phi(t) := Z(t)Q^{-1}$. Then the solution of (10.24) can be written as

$$z(t) = \Phi(t)\beta + \int_0^t G(t, s)q(s) \, ds, \quad (10.25)$$

*where the **Green's function (matrix)** is given by*

$$G(t, s) = \begin{cases} \Phi(t)B_0\Phi(s)^{-1} & \text{for } s \leq t, \\ -\Phi(t)B_1\Phi(s)^{-1} & \text{for } s > t. \end{cases}$$

We shall not prove Theorem 10.5.3, but we note that (10.25) can be recognized as “particular solution + homogeneous solution = general solution.” Indeed, for an initial value problem

$$z' = A(t)z + q(t), \quad z(t_0) = z_0,$$

the solution (10.25) simplifies to the well-known formula

$$z(t) = Z(t, t_0)z_0 + \int_{t_0}^t Z(t, s)q(s) \, ds$$

involving the **principal solution** $Z(t, t_0)$, i.e., $Z' = A(t)Z$ with $Z(t_0, t_0) = \text{Id}$. Recall that we interpret (10.25) as the solution to a variational problem that

measures the growth of perturbations to a given general BVP. To estimate this growth, we take norms in (10.25) and obtain

$$\|z\|_\infty \leq \kappa_1 \|\beta\|_\infty + \kappa_2 \|q\|_p, \quad (10.26)$$

where $\|\cdot\|_p$ denotes the L^p -norm, $\|\cdot\|_\infty$ denotes the sup-norm, Hölder's inequality has been used [Fol99], and $\kappa_{1,2}$ are given by

$$\kappa_1 = \|ZQ^{-1}\|_\infty, \quad \kappa_2 = \sup_{t \in [0,1]} \left\{ \left[\int_0^1 \|G(t,s)\|^q ds \right]^{1/q} \right\}, \quad \frac{1}{p} + \frac{1}{q} = 1.$$

Note that κ_2 depends on the choice of p , which makes the following definition depend on p as well.

Definition 10.5.4. The **conditioning constant** of the BVP (10.24) is

$$\kappa := \max\{\kappa_1, \kappa_2\}.$$

The conditioning constant can be used as a bound on the amplification of perturbations. Definition 10.5.1 views a BVP as **well conditioned** if κ is a constant of “moderate” size. We shall not begin a discussion here of what moderate means, but instead show that the situation is clear for a fast–slow systems example.

Example 10.5.5. Consider a $(2, 1)$ -fast–slow system in Fenichel normal form near a saddle-type slow manifold

$$\begin{aligned} \varepsilon \dot{x}_1 &= x_1, \\ \varepsilon \dot{x}_2 &= -x_2, \\ \dot{y} &= 1. \end{aligned} \quad (10.27)$$

The critical manifold C_0 of (10.27) is the y -axis. Solving (10.27), we get

$$(x_1(\tau), x_2(\tau), y(\tau)) = (x_1(0)e^{\tau/\varepsilon}, x_2(0)e^{-\tau/\varepsilon}, \tau + y(0)).$$

Let us view (10.27) as an initial value problem with $z = (x_1, x_2, y)$ and initial condition

$$z(0) = (x_1(0), x_2(0), y(0))^\top = (\delta, k, 0)^\top \quad (10.28)$$

for $0 < \delta \ll 1$ and $k = \mathcal{O}(1)$. From the fast–slow decomposition, we observe that trajectories that are near C_0 for a long time have an exponentially small $\delta = \mathcal{O}(e^{-K/\varepsilon})$ in the initial condition. We also know that if $\delta = 0$, then trajectories remain in the stable manifold $W^s(C_0) = \{x_1 = 0\}$; see Figure 10.4.

Let us calculate the conditioning constant κ for this problem under the assumption that we are interested in a trajectory segment with initial time $\tau_0 = 0$ and final time $\tau = 1$. Using the definitions in this section yields

$$Z(\tau) = \begin{pmatrix} e^{\tau/\varepsilon} & 0 & 0 \\ 0 & e^{-\tau/\varepsilon} & 0 \\ 0 & 0 & 1 \end{pmatrix}, \quad q = q(\tau) = \begin{pmatrix} 0 \\ 0 \\ 1 \end{pmatrix},$$

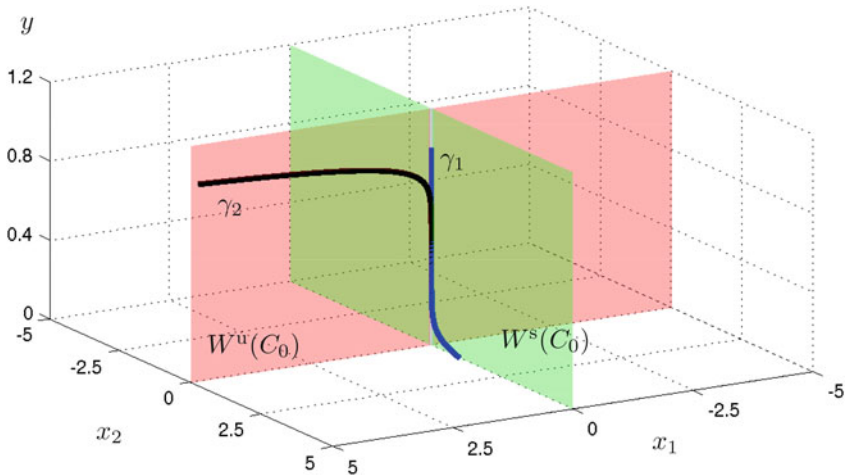


Figure 10.4: Two trajectory segments $\gamma_{1,2}$ for equation (10.27) with $\varepsilon = 0.05$ are shown. For both, we fixed initial conditions according to (10.28) with $k = 1$. The first trajectory γ_1 (blue) has $\delta = 0$ and stays near the critical manifold. The second trajectory γ_2 (black) has $\delta = 10^{-8}$ and escapes from a neighborhood of C_0 after some time.

$B_0 = \text{Id}$, $B_1 = 0$, and $\beta = z(0)$. Therefore, it follows that $Q = \text{Id}$, $\Phi(\tau) = Z(\tau)$, and

$$G(\tau, s) = \begin{cases} Z(\tau)Z(s)^{-1} & \text{for } s \leq \tau, \\ 0 & \text{for } s > \tau. \end{cases}$$

For sufficiently small $0 < \varepsilon \ll 1$, we get

$$\kappa_1 = \|Z(\tau)Q^{-1}\|_\infty = \|Z(\tau)\|_\infty = e^{1/\varepsilon}.$$

For the other constant, κ_2 , the calculation is

$$\kappa_2 = \sup_{t \in [0, 1]} \left\{ \left[\int_0^1 \|G(t, s)\|^q ds \right]^{1/q} \right\} \sim \mathcal{O}(\varepsilon e^{K/\varepsilon})$$

as $\varepsilon \rightarrow 0$. However, one should notice that the last estimate provided by κ_2 is far too crude, since

$$\int_0^\tau G(\tau, s) \begin{pmatrix} 0 \\ 0 \\ 1 \end{pmatrix} ds = \int_0^\tau \begin{pmatrix} 0 \\ 0 \\ 1 \end{pmatrix} ds, \quad (10.29)$$

so that (10.26) can provide a bound of $\mathcal{O}(1)$ for the integral term. In any case, we obtain that

$$\kappa = \max\{\kappa_1, \kappa_2\} = \kappa_1 = e^{1/\varepsilon}$$

as $\varepsilon \rightarrow 0$. Hence, a small error in the initial condition can produce an exponential error in the result. Basic fast-slow decomposition theory and our knowledge

of the exchange lemma setup from Chapter 6 provide further viewpoints on this result; see also Figure 10.4. Hence, the IVP problem for (10.27) is very ill conditioned. To compare it to a BVP formulation, we change the initial conditions (10.28) to boundary conditions

$$(x_1(1), x_2(0), y(0))^\top = (\delta, k, 0)^\top. \quad (10.30)$$

Again applying the definitions, we see that $Z(\tau)$, q , and β remain unchanged, but we now have

$$B_0 = \begin{pmatrix} 0 & 0 & 0 \\ 0 & 1 & 0 \\ 0 & 0 & 1 \end{pmatrix}, \quad B_1 = \begin{pmatrix} 1 & 0 & 0 \\ 0 & 0 & 0 \\ 0 & 0 & 0 \end{pmatrix}$$

and

$$Q = B_0 Z(0) + B_1 Z(1) = \begin{pmatrix} e^{\tau/\varepsilon} & 0 & 0 \\ 0 & 1 & 0 \\ 0 & 0 & 1 \end{pmatrix}.$$

It is relatively easy to check with direct calculation that the integral involving Green's function can again be bounded by $\mathcal{O}(1)$ as in (10.29). Hence we can again get an improved bound that replaces κ_2 by $\mathcal{O}(1)$. The key observation is that we also obtain

$$\kappa_1 = \|Z(\tau)Q^{-1}\|_\infty = \left\| \begin{pmatrix} e^{\tau/\varepsilon} & 0 & 0 \\ 0 & e^{-\tau/\varepsilon} & 0 \\ 0 & 0 & 1 \end{pmatrix} \begin{pmatrix} e^{-\tau/\varepsilon} & 0 & 0 \\ 0 & 1 & 0 \\ 0 & 0 & 1 \end{pmatrix} \right\|_\infty = 1$$

as $\varepsilon \rightarrow 0$. Therefore, the conditioning constant is $\kappa = \mathcal{O}(1)$, which certainly indicates a well-conditioned problem. Note, however, that if we increase the final time $\tau = 1$, then the conditioning constant is going to increase. ♦

Exercise/Project 10.5.6. Continue with Exercise 10.4.1 and estimate the conditioning constant for finite differences and collocation. ◇

10.6 Continuation

In addition to, and in combination with, boundary value solvers, another powerful idea is to use **numerical continuation** for fast–slow systems. We shall only briefly present the main idea, starting from a general ODE

$$x' = f(x, \lambda), \quad \text{for } x \in \mathbb{R}^m, \quad (10.31)$$

where $\lambda \in \mathbb{R}$ is viewed as a parameter; for example, one may think of an $(m, 1)$ -fast–slow system with fast subsystem (10.31), $\varepsilon = 0$, and slow variable $y = \lambda$. Suppose (10.31) has an equilibrium point (x_0, λ_0) , so that $f(x_0, \lambda_0) = 0$. The implicit function theorem gives that if $D_x f(x_0, \lambda_0)$ has rank m , then (x_0, λ_0) is part of a locally unique solution curve $(x(\lambda), \lambda)$ to the algebraic problem

$$f(x, \lambda) = 0. \quad (10.32)$$

Considering the $(m, 1)$ -fast–slow systems case again, we immediately notice that it is useful to find the curve $(x(\lambda), \lambda)$, since (10.32) is the equation for the critical manifold. An efficient method to numerically trace out the curve $(x(\lambda), \lambda)$ is provided by numerical continuation. However, the framework is much more general than computing equilibria of ODEs.

Definition 10.6.1. Let $F : \mathbb{R}^{m+1} \rightarrow \mathbb{R}^m$. The (one-dimensional) **continuation problem** is to find a solution curve $z = z(s) \in \mathbb{R}^{m+1}$ to the m equations $F(z) = 0$.

Remark: The continuation problem can even be generalized to maps $F : \mathbb{R}^{m+k} \rightarrow \mathbb{R}^m$ for $k \geq 1$, where one has to determine a k -dimensional manifold. We shall not discuss this extension in this book and refer to Section 10.9.

The equilibrium point problem (10.32) is recognized as one incarnation of the continuation problem by setting $z = (x, \lambda)$ and $F(z) = f(x, \lambda)$. The numerical result should consist of a sequence of points z_0, z_1, z_2, \dots approximating the curve $z : \mathcal{I} \rightarrow \mathbb{R}^{n+1}$ on some given interval \mathcal{I} that specifies the parameterization. Suppose we know z_0 such that $F(z_0) = 0$. The basic approach to the continuation problem is a **predictor–corrector algorithm**.

1. **Predict:** Knowing z_k , predict a new point \tilde{z}_{k+1} near the curve.
2. **Correct:** Use an iterative method $\tilde{z}_{k+1} \mapsto \dots \mapsto z_{k+1}$ s.t. $F(z_{k+1}) = 0$.

Of course, one applies step-size control and adaptivity ideas as necessary. We just illustrate here the basic steps how one may implement such an idea in practice; for more advanced details, see Section 10.9. Suppose the local parameterization of the solution curve $z = z(s)$ is chosen such that $z(s_k) = z_k$. For the prediction step, let v_k denote a suitably normalized tangent vector to the curve $z(s)$ at z_k . Define the **tangent prediction** by

$$\tilde{z}_{k+1} = z_k + h_k v_k \quad h_k = \text{step size at step } k.$$

The tangent vector at z_k can be computed by solving an algebraic system. Indeed, differentiating $F(z(s)) = 0$ at $s = s_k$ yields $D_z F(z_k) z'(s_k) = D_z F(z_k) v_k = 0$. Using the tangent vector v_{k-1} from the previous step and imposing the normalization condition $v_{k-1} \cdot v_k = v_{k-1}^\top v_k = 1$ leads to a linear system

$$\begin{pmatrix} DF \\ v_{k-1}^\top \end{pmatrix} v_k = \begin{pmatrix} 0 \\ 1 \end{pmatrix}.$$

We shall assume from now on that v_k has been found. The equation $F(\tilde{z}_{k+1}) = F(z_k + h_k v_k) = 0$ will usually not be satisfied exactly, but \tilde{z}_{k+1} might be close enough that Newton's method can be applied as a correction step. Note that

$$F(z) = 0 \quad \text{for } F : \mathbb{R}^{m+1} \rightarrow \mathbb{R}^m$$

is not directly amenable to Newton's method, since we have only m equations but $m + 1$ unknowns. Hence, an extra equation $g_k(z) = 0$ has to be added.

The **natural continuation** method specifies the Newton iterates to lie in a coordinate hyperplane containing \tilde{z}_{k+1} . The coordinate i chosen is usually the one with the largest absolute value in \tilde{z}_{k+1} ; denote this coordinate by z^i and let

$$g_k(z) := g_k(z^1, z^2, \dots, z^{m+1}) = z^i - \tilde{z}_{k+1}^i.$$

There are other important, and often more practical, choices of $g_k(z)$, such as **pseudo-arc-length continuation** and **Moore–Penrose continuation**; see Section 10.9. In any case, one may try to apply Newton’s method to the system

$$\begin{aligned} F(y) &= 0, \\ g_k(y) &= 0. \end{aligned} \tag{10.33}$$

The basic (one-dimensional) continuation problem is extremely flexible: all one needs is to formulate the computational problem as $F(z) = 0$ for a map $F : \mathbb{R}^{m+1} \rightarrow \mathbb{R}^m$. Hence, there are many different applications, e.g., the computation of steady states, bifurcation points and curves, global orbits (periodic, homoclinic, etc.), canard orbits, isochrons, spectra, and various other invariant sets (stable/unstable manifolds, slow manifolds, etc.).

To illustrate the main point of why one may apply the technique in various contexts, consider the case of a periodic orbit. The computational problem is a BVP with periodic boundary conditions as discussed in Section 10.3. It may be discretized using standard methods such as collocation, as described in Section 10.4. The resulting problem is an algebraic system, and if a free system parameter (“frozen slow variable”) is present in the system, one may apply continuation. Note that for fast–slow problems, there is always at least one relevant parameter: the time scale separation ε .

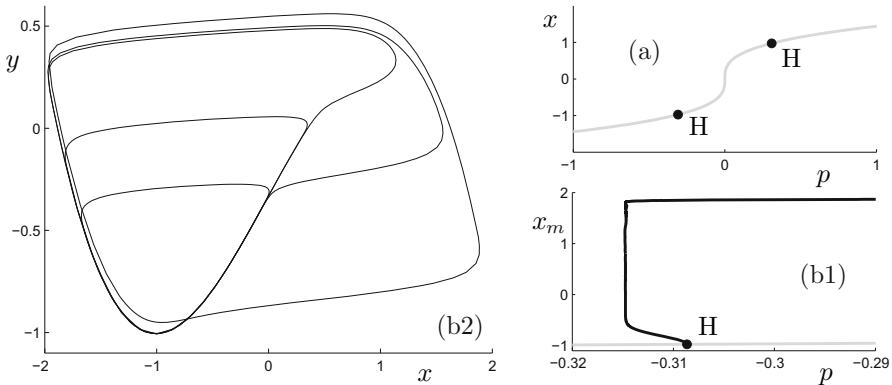


Figure 10.5: Continuation results for the FitzHugh–Nagumo equation (10.34).

Example 10.6.2. Consider the classical 2D FitzHugh–Nagumo ODE

$$\begin{aligned} x' &= x - \frac{x^3}{3} - y + p, \\ y' &= \varepsilon(x - y), \end{aligned} \tag{10.34}$$

where we fix $\varepsilon = 0.05$ and view p as the main bifurcation parameter. The values $(x, y, p) = (0, 0, 0)$ are used as a starting point for the equilibrium point continuation in Figure 10.5(a). As expected, there are two Hopf bifurcation points that occur near the passage of the global equilibrium point of (10.34) through the two fold points $(x, y) = (\pm 1, \pm 2/3 + p)$. Figure 10.5(b) shows a periodic orbit continuation in the parameters p and the period of the orbit. In Figure 10.5(b1), we recognize the diagram as a typical canard explosion near a (subcritical) singular Hopf bifurcation; cf. Section 8.4, Theorem 8.4.2, and Figure 8.3. Note that the scale for p is very small for the numerical continuation of periodic orbits, as expected from the theoretical parameter scaling region $\mathcal{O}(e^{-K/\varepsilon})$ for a canard explosion. Figure 10.5(b2) shows several periodic orbits obtained during the continuation. ♦

Exercise 10.6.3. Use a continuation software package to continue equilibrium points and periodic orbits for (10.34) in the parameter ε . Try to use starting solutions for (I) $\varepsilon = 0$ and (II) $\varepsilon = \mathcal{O}(1)$ for the equilibrium and periodic orbit continuations. ◇

Exercise 10.6.3 implicitly contains a trick that is helpful for virtually all singularly perturbed problems. For a starting solution, it is often helpful to start with a very moderate $\varepsilon = \mathcal{O}(1)$ and then use continuation to decrease the singular perturbation parameter. If the continuation code and the numerical discretization code of the problem (e.g., collocation for BVPs) have good step-size control, it is quite remarkable how many problems with small parameters one can reliably compute; see Section 10.9.

10.7 Heterogeneous Multiscale Methods

The topic of **heterogeneous multiscale methods** (HMM) is quite wide. HMM should not be interpreted as a single numerical method but rather as a general idea about how one may design a numerical multiscale scheme. Here we shall just briefly present three examples considered in [EEL⁺07] that illustrate the philosophy behind HMM nicely. Consider a fast–slow system of the form

$$\begin{aligned} \varepsilon \frac{dx}{d\tau} &= \varepsilon \dot{x} = -x + h(y), \\ \frac{dy}{d\tau} &= \dot{y} = g(x, y), \end{aligned} \tag{10.35}$$

where we can think of $(x, y) \in \mathbb{R}^2$ for simplicity, but none of our future considerations will depend on the particular dimensions. The attracting critical manifold and the associated slow flow are

$$C_0 = \{(x, y) \in \mathbb{R}^2 | x = h(y)\}, \quad \dot{y} = g(h(y), y) =: G(y).$$

Implementing a numerical method for the slow flow is no problem, but one is, of course, also interested in the numerical solution of the full system (10.35) for $0 < \varepsilon \ll 1$. In HMM, we think of the slow variables y as **macroscopic**

variables that determine the effective part of the dynamics. The name hints at the fact that a similar approach exists for problems with multiple spatial scales; see Section 10.9. The fast variables x are viewed as the **microscopic variables**. For example, one may think of x as describing molecular reactions, while y is the effective temperature or pressure of the system. Usually, one is interested in the macroscopic variables, so that the starting point is a numerical method for macroscopic (slow) variables, called the **macro solver**. A simple choice is the explicit Euler method (see Section 10.1)

$$y_{n+1} = y_n + (\delta\tau)\tilde{G}_n(y_n), \quad (10.36)$$

where $(\delta\tau) > 0$ is the time step; we shall always assume that we are working with fixed equal time steps for simplicity. The function $\tilde{G}(y_n)$ should describe the influence of the microscopic (fast) variables, where we essentially would like to use the slow manifold value for x at y_n . One way to compute this value is to consider the fast subsystem for (10.35) on the time scale $t = \tau/\varepsilon$:

$$\frac{dx}{dt} = -x + h(y_n). \quad (10.37)$$

Obviously, one may solve (10.37) numerically, say using explicit Euler again,

$$x_{n,k+1} = x_{n,k} - (\delta t)(x_{n,k} - h(y_n)), \quad (10.38)$$

where $(\delta t) > 0$ is the time step, $k = 0, 1, \dots, K$, and (10.38) is called the **micro solver**. The idea is that if K is sufficiently large, then $x_{n,K}$ lies on the slow manifold, since this manifold is normally hyperbolic and attracting. Then setting

$$\tilde{G}_n(y_n) := g(x_{n,K}, y_n)$$

yields a formula from which the macro solver can determine y_{n+1} . Effectively, what we just described is just a decomposition of the numerical integration into fast and slow dynamics. An important point to notice is that one can expect to choose K independent of ε , which is expected, since neither the slow subsystem nor the fast subsystem contains ε .

As a second example, consider a planar **Hamiltonian fast–slow system**

$$\begin{aligned} \varepsilon \frac{d\varphi}{d\tau} &= \varepsilon \dot{\varphi} = \omega(I) + \varepsilon f(I, \varphi,) \\ \frac{dI}{d\tau} &= \dot{I} = g(I, \varphi), \end{aligned} \quad (10.39)$$

where $(\varphi, I) \in S^1 \times \mathbb{R}$ are **action-angle variables** as discussed in Section 9.7, and f, g are assumed to be 2π -periodic in φ , i.e., we view the circle as $S^1 \equiv \mathbb{R}/2\pi\mathbb{Z}$. Under suitable assumptions, the averaging method from Section 9.6 applies, so that the effective slow dynamics can be expressed as

$$\dot{I} = G(I), \quad \text{where } G(I) := \frac{1}{2\pi} \int_0^{2\pi} g(I, \varphi) d\varphi. \quad (10.40)$$

Now a HMM numerical scheme can be derived almost as before. The macro solver for the slow action variables is

$$I_{n+1} = I_n + (\delta\tau)\tilde{G}_n(I_n) \quad (10.41)$$

when we use explicit Euler again for simplicity. To determine the correct function \tilde{G}_n , one needs an average over the evolution of the fast variables as suggested by (10.40). Forward Euler on the fast time scale reads

$$\varphi_{n,k+1} = \varphi_{n,k} + (\delta t)[\omega(I_n) + \varepsilon f(I_n, \varphi_{n,k})] \quad (10.42)$$

for $k = 1, \dots, K$. Stationary behavior of the numerical solution can no longer be expected, and periodic solutions have to be taken into account. This suggests that we perform an explicit time-averaging

$$\tilde{G}_n(I_n) := \frac{1}{K} \sum_{k=1}^K w_{k,K} g(I_n, \varphi_{n,k}),$$

where the weights $w_{k,K}$ are assumed to satisfy

$$\frac{1}{K} \sum_{k=1}^K w_{k,K} = 1.$$

Using the definition of \tilde{G}_n , the macro solver can be used to determine I_{n+1} . Notice that different choices of weights will also lead to different numerical schemes, which naturally leads to the question of finding the “best” weights.

As a third example, we consider stochastic differential equations (SDEs); for a more detailed introduction to fast–slow SDEs, see Chapter 15. Consider the $(n, 1)$ -fast–slow SDE

$$\begin{aligned} dx_\tau &= \frac{1}{\varepsilon} f(x_\tau, y_\tau) d\tau + \frac{\sigma}{\sqrt{\varepsilon}} F(x_\tau, y_\tau) dW_\tau, \\ dy_\tau &= g(x_\tau, y_\tau) d\tau, \end{aligned} \quad (10.43)$$

where $0 < \varepsilon \ll 1$, $W_t = (W_t^{(1)}, \dots, W_t^{(j)})^\top$ is a vector consisting of j independent Brownian motions, $f : \mathbb{R}^m \times \mathbb{R} \rightarrow \mathbb{R}^m$, $g : \mathbb{R}^m \times \mathbb{R} \rightarrow \mathbb{R}$, $F : \mathbb{R}^m \times \mathbb{R} \rightarrow \mathbb{R}^{m \times j}$ is a matrix-valued function, and $\sigma > 0$ is a parameter controlling the noise level.

Exercise 10.7.1. Show that a time rescaling $\tau = t\varepsilon$ removes the ε -dependence from the fast variables. ◇

Suppose we want to extract the effective slow dynamics of (10.43). In direct analogy to the averaging procedure above, assume that the fast variables for fixed y have an invariant probability measure $\mu_\varepsilon^y(dx)$ and consider

$$\bar{g}(y) = \lim_{\varepsilon \rightarrow 0} \int_{\mathbb{R}^m} g(x, y) \mu_\varepsilon^y(dx).$$

Then the natural candidate for the slow flow is the averaged dynamics

$$\frac{dY}{d\tau} = \bar{g}(Y). \quad (10.44)$$

We shall not discuss in detail what assumptions suffice so that (10.44) and (10.43) hold; see Section 10.9 for detailed references. From the viewpoint of HMM, it should now be clear how to construct a numerical method. One may view (10.44) as the macroscale equation and the fast subsystem as the microscale equation. For example, using forward Euler for (10.44) yields

$$Y_{n+1} = Y_n + (\delta\tau)a_n,$$

where $\delta\tau$ is the time step at time n , and the coefficient a_n is to be determined. Let $X_{n,k}$ denote the solution at time step k of the microsolver. To obtain $X_{n,k}$, one can basically use any standard numerical scheme for SDEs [KP10]. For example, using Euler–Maruyama as a microsolver, we get

$$X_{n,k+1} = X_{n,k} + \frac{(\delta\tau)}{\varepsilon} f(X_{n,k}, Y_n) + \frac{\sigma}{\sqrt{\varepsilon}} F(X_{n,k}, Y_n)(\Delta W_k), \quad (10.45)$$

where $(\delta\tau)$ is the time step and ΔW_k are independent normal random variables with mean zero and variance $(\delta\tau)$, which means that the standard deviation is $\sqrt{(\delta\tau)}$. Therefore, the last two summands in (10.45) scale like (δt) and $\sqrt{\delta t}$, where $t = \tau/\varepsilon$ is the fast time, so that we really solve a microscopic equation not depending on ε . From the microsolver results, one possibility to define a_n is

$$a_n = \frac{1}{PK} \sum_{j=1}^P \sum_{k=k_T}^K g(X_{n,k}, Y_n),$$

where P is the number of different **sample paths** (or **replicas**) used, i.e., one calculates P copies of $\{X_{n,k}\}_{k=1}^K$ for different realizations of the random variables ΔW_k . The index k_T is chosen large enough to eliminate transients in the convergence to the invariant measure.

Example 10.7.2. As a very simple test case for (10.43), consider the SDEs

$$\begin{aligned} dx_{1,t} &= y_t x_{1,t} - x_{2,t} - x_{1,t}(x_{1,t}^2 + x_{2,t}^2) dt + \sigma_1 dW_t^{(1)}, \\ dx_{2,t} &= x_{1,t} + y_t x_{2,t} - x_{2,t}(x_{1,t}^2 + x_{2,t}^2) dt + \sigma_2 dW_t^{(2)}, \\ dy_t &= \varepsilon(1 - y_t(x_{1,t}^2 + x_{2,t}^2)) dt, \end{aligned} \quad (10.46)$$

where $\sigma_1, \sigma_2 > 0$. The deterministic fast subsystem of (10.46) is the normal form for a supercritical Hopf bifurcation, and the slow variable y_t acts as a slow increasing drift in the vicinity of the deterministic Hopf bifurcation point at $(x_1, x_2, y) = (0, 0, 0)$. Figure 10.6(a) shows a simulation of (10.45) with Euler–Maruyama for the variable y_t in comparison to the HMM approach. Figure 10.6(b) shows the mean $\bar{x}_{1,t} = \mathbb{E}[x_{1,t}]$ obtained from the microsolver. Beyond the fact that the HMM approach correctly shows the slow variable, we also

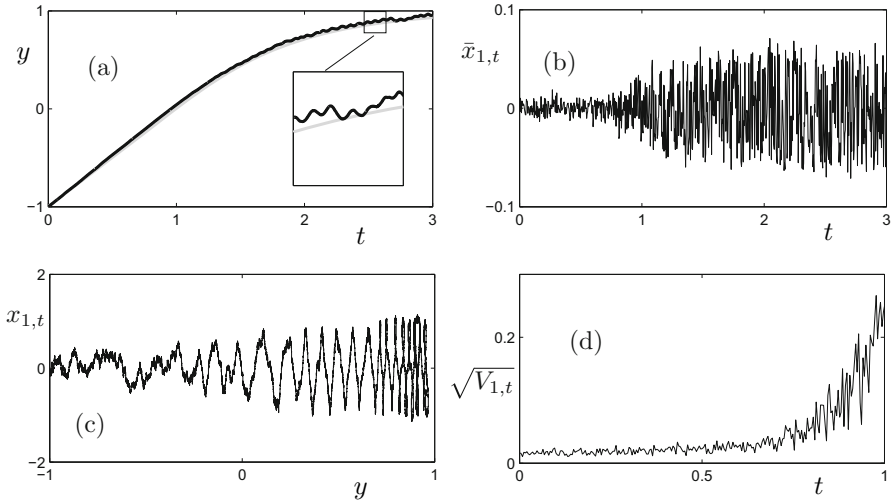


Figure 10.6: HMM method for the test problem (10.46) with parameters $\sigma_1 = 0.2$, $\sigma_2 = 0.3$. (a) Time series for the HMM method (gray) in comparison to a single sample paths calculated via Euler–Maruyama (black). (b) Mean for the variable $x_{1,t}$ at each microsolver iteration step. (c) Phase space projection onto (x_1, y) for the single sample path from (a). (d) Standard deviation for the variable $x_{1,t}$ at each microsolver iteration step up to time $t = 1$.

observe in Figure 10.6(d) that the standard deviation $\sqrt{V_{1,t}} = \mathbb{E}[(x_{1,t} - \bar{x}_1)^2]^{1/2}$ for the microsolver variable shows a clear increase before the deterministic bifurcation point is reached. This observation directly relates to the concept of early-warning signs for critical transitions discussed in Section 19.9. ♦

Exercise/Project 10.7.3. Implement an HMM solver for the system (10.43). Experiment with the macro- and micro-solver step sizes. For (10.46) as well as

$$\begin{aligned} dx_t &= -(x_t + x_t^3 - y_t) dt + \sigma dW_t, \\ dy_t &= \varepsilon(-x_t - x_t^3 + \cos(\pi t) + \sin(\sqrt{2}\pi t)) dt, \end{aligned} \quad (10.47)$$

experiment with the time step sizes for the micro- and macro-solvers, the noise level σ , and ε . For what values do you get reasonable/correct solutions? ◇

10.8 Error Analysis for HMM

As in the previous section, we are also going to focus on simple example systems to illustrate the error analysis for heterogeneous multiscale methods (HMM). Consider the $(m, 1)$ -fast–slow system

$$\begin{aligned} \varepsilon \frac{dx}{d\tau} &= \varepsilon \dot{x} = -x + h(y), \\ \frac{dy}{d\tau} &= \dot{y} = g(x, y), \end{aligned} \quad (10.48)$$

for $(x, y) \in \mathbb{R}^m \times \mathbb{R}$, and functions $h : \mathbb{R} \rightarrow \mathbb{R}^m$, $g : \mathbb{R}^{m+1} \rightarrow \mathbb{R}$. The critical manifold $C_0 = \{x = h(y)\}$ is attracting. As an HMM macrosolver we just use forward Euler again for illustration purposes,

$$y_{n+1} = y_n + (\delta\tau)\bar{g}(y_n),$$

where $(\delta\tau)$ is the slow time step, $n \in 0, 1, \dots, N$ is the time step index, and y_n denotes the numerical approximation at time $n(\delta\tau)$. The function \bar{g} is approximated via a microsolver

$$x_{n,k+1} = x_{n,k} - (\delta t)(x_{n,k} - h(y_n)), \quad (10.49)$$

where $(\delta t) = (\delta\tau)/\varepsilon$ is the fast time step, and we let

$$\bar{g}(y_n) = g(x_{n,K}, y_n), \quad \text{for some fixed } K \in \mathbb{N}. \quad (10.50)$$

The slow flow of (10.48) on C_0 is

$$\dot{Y} = g(h(Y), Y) =: G(Y), \quad (10.51)$$

and $Y = Y(\tau)$ denotes the solution of the slow flow. Then we know from Fenichel's theorem that if a trajectory $y(\tau)$ of the full system (10.48) starts near C_0 at $Y(0) = y(0)$, then it will exponentially fast approach the attracting slow manifold C_ε , so that

$$|y(\tau) - Y(\tau)| \leq k_1 \exp\left(-\frac{\tau}{\varepsilon}\right) + k_2 \varepsilon, \quad (10.52)$$

where $k_{1,2}$ are positive constants independent of ε . We decide to neglect the order- $\mathcal{O}(\varepsilon)$ -error in (10.52) from now on. However, this assumption is restrictive, since we are effectively going to operate on the singular limit level for the error analysis. If we accept this step, it is reasonable to compare the numerical solution y_n with the slow flow $Y(\tau)$. Consider the **global error**, which describes the difference between the numerical solution of the full system via HMM and the true slow flow

$$E_n = y_n - Y(n(\delta\tau)) = y_n - Y_n,$$

where Y_n is a shorthand notation for the value of the slow flow at time $n(\delta\tau)$.

Proposition 10.8.1. *Suppose that G has Lipschitz constant L_G . Then*

$$|E_n| \leq [E_{\text{mac},N} + E_{\text{mic},N}] \left(e^{L_G n(\delta\tau)} - 1 \right)$$

for $n = 0, 1, \dots, N$, where

$$E_{\text{mac},N} := \max_{0 \leq n \leq N-1} |T_n| \quad \text{and} \quad E_{\text{mic},N} := \max_{0 \leq n \leq N-1} |\bar{g}(y_n) - G(y_n)|,$$

where T_n denotes the local truncation error as defined below.

Proof. Using the definition of the global error and direct calculations, we obtain

$$\begin{aligned} \frac{E_{n+1} - E_n}{\delta\tau} &= \frac{y_{n+1} - Y_{n+1} - y_n + Y_n}{\delta\tau} = \frac{y_n + (\delta\tau)\bar{g}(y_n) - y_n - [Y_{n+1} - Y_n]}{\delta\tau} \\ &= \bar{g}(y_n) - G(Y_n) - \underbrace{\left[\frac{Y_{n+1} - Y_n}{\delta\tau} - G(Y_n) \right]}_{=:T_n} \\ &= \bar{g}(y_n) - G(y_n) + G(y_n) - G(Y_n) - T_n, \end{aligned}$$

where T_n is a **local truncation error** similar to the definition in Exercise 10.1.1. Rearranging, taking norms, and using the Lipschitz condition, we get

$$\begin{aligned} |E_{n+1}| &= |E_n + (\delta\tau)[G(y_n) - G(Y_n)] + (\delta\tau)[\bar{g}(y_n) - G(y_n)] - (\delta\tau)T_n| \\ &\leq (1 + (\delta\tau)L_G)|E_n| + (\delta\tau)|T_n| + (\delta\tau)|\bar{g}(y_n) - G(y_n)|, \end{aligned}$$

for $n = 0, 1, \dots, N-1$. Observe that the first two terms on the right-hand side appear in the usual error analysis for the forward Euler scheme on the macro (or slow) scale and that error on the micro (or fast) scale is contained in the last term. Using the last inequality and induction shows that

$$|E_n| \leq \left[\max_{0 \leq n \leq N-1} |T_n| + \max_{0 \leq n \leq N-1} |\bar{g}(y_n) - G(y_n)| \right] ((1 + (\delta\tau)L_G)^n - 1)$$

for $n = 0, 1, \dots, N$. The result follows, since $1 + (\delta\tau)L_G \leq \exp((\delta\tau)L_G)$. \square

Proposition 10.8.1 and its proof demonstrate that the error analysis techniques for the macroscale solver for HMM differ from classical methods due to the additional error term in the microsolver approximation. Indeed, we know from Section 10.1 that $E_{\text{mac},N} = \mathcal{O}(\delta\tau)$ for Euler's method. It remains to bound $E_{\text{mic},N}$.

Proposition 10.8.2. *Suppose $g = g(x, y)$ is Lipschitz in $x \in \mathbb{R}^m$ with Lipschitz constant L_g . Then*

$$E_{\text{mic},N} \leq \kappa_1 |1 - \delta t|^K = \kappa_1 \left| 1 - \frac{\delta\tau}{\varepsilon} \right|^K, \quad \text{with } \kappa_1 = L_g \max_{0 \leq n \leq N} \|x_{n,0} - h(y_n)\|,$$

where K is defined in (10.50).

Proof. We have to estimate $|\bar{g}(y_n) - G(y_n)|$. Using the definitions and applying the Lipschitz condition yields

$$|\bar{g}(y_n) - G(y_n)| = |g(x_{n,K}, y_n) - g(h(y_n), y_n)| \leq L_g \|x_{n,K} - h(y_n)\|. \quad (10.53)$$

Define $e_{n,k} := x_{n,k} - h(y_n)$ and notice that

$$e_{n,k+1} = x_{n,k+1} - h(y_n) = x_{n,k} - (\delta t)(x_{n,k} - h(y_n)) - h(y_n) = (1 - (\delta t))e_{n,k},$$

where we have applied the microsolver definition (10.49). Iterating the last argument gives that $e_{n,K} = (1 - (\delta t))^K e_{n,0}$. Using this result in (10.53) yields

$$L_g \|x_{n,K} - h(y_n)\| = \|(1 - (\delta t))^K e_{n,0}\| \leq L_g \|e_{n,0}\| |1 - (\delta t)|^K,$$

and the result follows by taking the maximum over n . \square

Combining Propositions 10.8.1 and 10.8.2, we see that the global error for HMM with Euler micro- and macrosolvers applied to the fast–slow system (10.48) is

$$|E_n| \leq \left[\kappa_0(\delta\tau) + \kappa_1 \left| 1 - \frac{\delta\tau}{\varepsilon} \right|^K \right] \left(e^{L_G n(\delta\tau)} - 1 \right), \quad (10.54)$$

where we have used that the maximum over the local truncation errors $|T_n|$ is of order $\mathcal{O}((\delta\tau))$, as shown in Exercise 10.1.1. The error $|E_n|$ consists of one term for the macrosolver, which can be made small using $0 < (\delta\tau) \ll 1$. The microsolver error can be made small by choosing $(\delta t) < 1$ and making K sufficiently large. Note that the decoupling of the dynamics that is intrinsic to HMM makes it possible to pick two different step sizes, which stabilizes the method. In fact, the same considerations also apply to other, higher-order, methods.

Theorem 10.8.3 ([E03]). *Assume that the macrosolver for (10.48) is stable of order r . Let $A(\lambda(\delta\tau)) = |x_{k+1}/x_k|$ be the **amplification factor** of the microsolver for $\dot{x} = -\lambda x$. Then there exist a constant κ_2 independent of the time steps, ε , and K such that*

$$|E_n| \leq \kappa_2 \left((\delta\tau)^r + \left| A \left(\frac{\delta\tau}{\varepsilon} \right) \right|^K \right).$$

In summary, we have discussed a very general strategy for calculating the error for HMM: (1) error analysis for the macrosolver, (2) splitting into classical error term and the contribution from the microsolver, (3) error analysis for the microsolver. This framework applies to HMM in a much wider setup than just forward Euler or Theorem 10.8.3; see Section 10.9.

10.9 References

Section 10.1: This section and the next are based mainly on [Ise96, SM03]. There are many standard textbooks on numerical solutions of ODEs, but probably none are more detailed than the two volumes [HW91a, HW91b]. Numerical integration for stiff equations has a long history [Asc85, CH52, Il'69, Mir81, PR74]. By now, many algorithms for stiff ODEs have also found their way as standard functions into large-scale software projects [SR97a], into literature surveys [KP02], as well as into numerical methods source books [PTVF07]. Numerics for stiff equations provides not only many practical but also serious theoretical problems [Lub90, Nip91, Nip02, NS95,

[NS96](#). A standard test problem is due to Carrier/Pearson [[Car54](#), [Rob86](#)]. Some other interesting directions are asymptotics-based methods [[FO77](#), [FO84](#)], backward error analysis [[KCMM03](#)], Chebyshev methods for stiff SDEs [[Abd12](#)], collocation [[VAR07](#)], comparison between methods [[EHL75](#), [SG79](#)], composite methods [[Ise84](#)], exponentials in FEM spaces [[Gro81](#), [GH79](#)], extrapolation [[EL97](#), [HL88](#)], functional fitting schemes [[Ise77](#)], implicit methods for stiff SDEs [[LAE08](#)], integrals involving kernels with multiple time scales [[Lub88](#)], avoiding Jacobian calculations [[SW79](#)], multistep methods [[Enr74](#)], quadrature-based methods [[Ise81](#), [Wei84](#)], RK methods [[HLR88](#), [LNS95](#), [Lub93](#)], ROCK methods [[AHL10](#)], step size control [[MP94](#)], and S-ROCK/Chebyshev methods [[AC08](#), [AL08](#)].

Section 10.2: The stability issues for forward integration multistep methods were laid out in [[Dah63](#)]; for $A(\alpha)$ -stability, we refer to [[Wid67](#)]. For other interesting classes beyond linear multistep schemes, we just mention implicit Runge–Kutta methods [[Ale77](#), [But64](#), [But76](#), [Ehl68](#), [Ehl73](#)], block-implicit methods [[WS72](#)], and deferred correction schemes [[Cas88](#), [DGR00](#), [Ske82](#)]. Various versions of these methods achieve A -stability and higher order, usually at increased computational cost in comparison to linear multistep schemes. There are other concepts related to A -stability such as algebraic stability [[BB80](#)], B-stability [[BB79](#), [But75](#)], D-stability [[vV83](#)], S-stability [[Ver76](#)], and stiff stability [[BJ78](#)]; for D-stability, see also Section 4.6. For a survey and relations between differential-algebraic equations and stiff initial value problems, we refer to [[Cas03](#)]. The literature on stability and stiff methods is very large [[KR12](#)], and we have not covered topics such as modern explicit time-steppers [[EJL03](#)], mesh selection [[LP77](#), [Rus79](#)], and exponential time differencing [[CM02](#)]. For a book dedicated to stability of Runge–Kutta methods, see [[DV84](#)]. Although it is very obvious, let us mention anyway that the problems of stiffness and (A -)stability reappear for time-dependent spatial problems [[HV03](#), [KT05](#)], e.g., in dealing with operator splitting [[Spo00b](#)], reaction–diffusion PDEs [[SSV06](#)], Runge–Kutta–Galerkin methods [[VMMM09](#)], and viscous wave equations [[Ver09](#)]. Of course, a similar remark about the persistence of stiffness issues also applies to other classes generalizing ODEs such as delay equations [[SWC89](#)].

Section 10.3: The main reference for this as well as the next section is [[AMR87](#)]. For a theoretical approach to classical BVPs involving ODEs, we refer to the book [[HM12](#)]. The idea to compute canards via BVPs can be found in [[MD13](#), [GL07](#), [GHW00](#), [SK07](#)]. Even in very applied contexts, it has been quite clear for a long time that computing unstable solutions via forward integration is often not a good idea [[RM80](#)]. We mention that there are techniques available to reformulate BVPs into standard form [[AR81](#)]. In general, it is far from trivial to set up BVPs properly for singular perturbation problems [[FR11](#)]. Even the existence of solutions for fast–slow BVPs for ODEs is a highly nontrivial problem [[Cha76](#), [MS13](#)].

Section 10.4: For more on collocation at Gaussian points, we refer to [[AB86](#), [BS73](#)]. Finite differences and collocation for two-point BVPs are compared in [[Rus77](#)]. Finite differences can be applied to stiff BVPs [[AKK74](#), [Kre84](#), [Kel74](#)]. The approach via collocation methods is probably one of the best ways to tackle hard singularly perturbed BVPs for ODEs [[AW83](#), [AW84a](#), [AW84b](#), [AJ89](#)]. There are many interesting topics we have not covered here, such as B-spline collocation [[DS09a](#)], Chebyshev collocation [[KPK11](#)], cross-validation between analysis and numerics [[BKVD12](#), [Bos96](#)], multiple shooting [[AM88](#)], quasilinear problems [[Rin84](#)], special methods for linear problems [[FM80](#)], and turning points [[Lin91](#)]. Furthermore, there is the ex-

tremely vast area of mesh adaptation, which is not only relevant for BVP multiple time scale problems but also for many multiscale numerics problems; see, e.g., [BO84, MNS02, RC78, Ver96, Ver94]. For the error equidistribution principle, see, e.g., [And87, RR92, Che94, HRR94]. There are also several software implementations of adaptive mesh strategies in BVP solvers, which work well for multiple time scale ODEs [ACR79, ACR81, Doe97, DCD⁺07].

Section 10.5: This section is motivated by numerics of saddle-type slow manifolds [GK09a, GK10b]. The issue of conditioning for BVPs and the associated mesh can be crucial for high accuracy and good practical performance [BT97b, CMST06, CCM07, CM05a, MT04]. It was realized quite early on that loss of normal hyperbolicity may require special numerical methods [BL87, KK81, KNB86]. Other key issues are the a priori choice of a mesh [BHR01, Roo94, Sty05], which leads to so-called Shishkin meshes [MN11b, OQ11, Shi91, Shi97], as well as the error equidistribution principle [MN11a, WCM94]. For books on adapted meshes, see [MOS96, RST96]. Other related topics for adapted meshes are advection–diffusion in fluids [HMOS95], convection–diffusion problems [FHM⁺04, FHS96, LS01a, Roo98, Shi05, SO97b], coupled ODEs [MOS02], finite-difference schemes for elliptic PDE [FMOS96], finite element methods (FEM) [LS01b, OS91, ST03, vV78], fourth-order problems [SS95], parabolic PDE [HSS00, HSS97], Richardson extrapolation [NS03], and upwind schemes [KS01a, LRV00, RL99, SR97b]. However, even on nicely adapted meshes, the resulting linear systems are far from trivial to solve [MM13a].

Section 10.6: This section uses material from [Kuz04] and [KOGV07]. For some classical references on continuation, we refer to [DK81, Gov87b, Kel83]. A general technique to redistribute the mesh points during continuation is to use the principle of error equidistribution [Cas85, DCD⁺07]. The application to fast–slow systems by continuing in the time scale separation is now a standard trick [AMPS91, CMW95]. One may use continuation methods for various local bifurcations [DKK91a, DKK91b], homoclinic orbits [CK94, CKS96], and in combination with Lin’s method [KR08, Lin90b, OCK03]. One difficulty that arises frequently is to keep track of eigenvalues or Floquet multipliers [FJ91, Lus01] to track stability of invariant sets. Some current practical software packages are AUTO [Doe97, Doe00, DCD⁺07, Doe07, DH83] and MatCont [DGK03]. There are many application areas where continuation is now a standard tool, e.g., engineering [SH87] and neuroscience [Shi12].

Section 10.7: This section is based mostly on a review of HMM in [EEL⁺07], but there are other good sources available [E11, E03, EE03a, ET05, AEEVE12]. One may also implement the HMM approach in a “seamless” way [ERVE09] based on two concurrent clocks. For HMM with a focus on stochastic systems, we refer to [ELVE05a, VE03], while modeling is the main theme in [EEH03]. The HMM view appears in many contexts [JJL05], but the idea always is to use a micro–macro algorithm [Abr12a, Abr13a]. The idea of using a special coupling between variables of different speeds seems to have been around for quite some time [CGSR78, LW70]. Some interesting HMM topics are averaging-type methods [CMSS10, CMSS12], discontinuous Galerkin methods [CES05], relations to FEM [Abd05], finite-difference schemes [AE03], high oscillations applications [CSS10], multiscale SPDEs [AP12, Bré13b], and various homogenization problems [EE05, EMZ05]. For a nice illustration via an inverted pendulum, see [STE05].

Section 10.8: The error analysis was adapted from [E03]. The philosophy of HMM is very closely related [GKK06] to so-called coarse-grained equation-free meth-

ods [EKA06, MMK02], which make the assumption that the macro-level equations are not available in closed form [KGH⁺03, GKT02]. For nice surveys on equation-free numerics, see [KS09, KGH04]. Implicit methods for stiff problems have recently been developed in this context [MSB⁺13]. Sometimes, the same framework of ideas is also headlined by so-called projective integration methods [GK03, MG13a]. Another immediately related keyword is the gap-tooth scheme [GLK03], which can be applied to homogenization-type problems [SKR06, SKR04, SRK05]. The equation-free approach can also be applied to PDEs [SKR07] and in conjunction with numerical continuation [TQK00]. Applications include liquid crystalline polymers [SGK03] and pattern formation [RTK02].

The literature on numerical multiscale methods is vast, and we can give only a very brief glimpse of topics not covered. Domain decomposition techniques are frequently applied to singularly perturbed BVPs [GK97] and have become a standard approach for many classes of elliptic PDEs [SB04]. Another natural approach to dealing with scale separation in spatial problems is that of multigrid methods [Rob09]. There are many approaches to adapting finite element methods to singular perturbation problems such as hp-FEM [Mei03, MXO13] and various types of FEM approaches to singularly perturbed problems [AAF95]. A recent overview can be found in [EH09]. Coupling micro–macro-scale problems is also the main focus of the quasicontinuum method [DLO10b, DLO10a, ELY06, Lin03, LO09, MY09], which relates to homogenization [ALS12] and the general question of numerical transition from quantum to classical mechanics [Lub08]; see also [LO13b] for a very detailed survey. Other topics we have not covered are boosting algorithms [HAL12], multitime methods [CS13, Kir03, MRC⁺05], parareal time integration [LLS13], slow-time acceleration [HNMM10], and wavelet methods [GS12a]. On the stochastic side, we have not considered nested simulation algorithms [ELVE05b, ELVE07], with typical application areas in chemical reaction networks [AK12] and molecular dynamics [SZB96]; see Section 15.10 for further references.

Highly oscillatory problems have also not been covered [PY97], with topics such as adiabatic numerical methods [LJL05], error analysis [Ise02], expansion–transformation schemes [Jah04, JL03a], Fourier expansions [CHL03], highly oscillatory forcing applied to vdP [CDI10a, CDI10b, CDI09], mollified impulse methods [SS08a], and WKB-based schemes for high oscillation Schrödinger-type equations [AAN11, AP06, Neg08]. For an overview book on highly oscillatory problems, we also refer to [EFHI09], while [HL00b] shows that the familiar second-order problems are good benchmarks in this context. There is a direct relation to integration schemes for Hamiltonian fast–slow systems [JL06, JL03b, LR01]; a book on simulation of Hamiltonian systems involving some highly oscillatory problems is [LR04a]. A related topic is preserving adiabatic invariants in Hamiltonian systems [Rei99b].

Chapter 11

Computing Manifolds

We have extensively discussed the properties of invariant manifolds and their relevance for fast–slow systems in previous chapters. However, we usually used explicit algebraic expressions or asymptotic expansions to deal with critical and slow manifolds. For a general multiple time scale system, there are several complications. They may not be in standard form, and even if they are, then calculating a slow manifold analytically may be intractable. This chapter deals with algorithms to find and compute invariant manifolds for fast–slow systems numerically.

Section 11.1 recalls the invariance equation, which can be used as a basis for computing a slow manifold. Furthermore, the use and limitations of forward integration are discussed. Section 11.2 covers the CSP method, which is a local iterative procedure to determine the slow manifold to arbitrary order. The next two sections, Sections 11.3 and 11.4, discuss various other alternatives, all of which, like CSP, have different advantages and disadvantages. In Section 11.5, we illustrate the computation of saddle-type slow manifolds via boundary value problems; in fact, saddle-type manifolds really show the problems with direct numerical integration approaches. In Section 11.6, the idea of combining boundary value problems and continuation for computing manifolds is discussed.

Background: As for Chapter 10, some programming experience would be helpful to try the different methods on practical problems.

11.1 Basic Techniques

In this section, we discuss the basic techniques for obtaining an analytical or numerical representation of a slow manifold. The first obvious idea is to use Fenichel’s theorem. Consider a general fast–slow system

$$\begin{aligned}\frac{dx}{dt} &= x' = f(x, y, \varepsilon), \\ \frac{dy}{dt} &= y' = \varepsilon g(x, y, \varepsilon),\end{aligned}\tag{11.1}$$

for $(x, y) \in \mathbb{R}^m \times \mathbb{R}^n$, $0 \leq \varepsilon \ll 1$ and f, g sufficiently smooth maps. Let C_0 denote the critical manifold of (11.1). We restate a version of Fenichel's theorem (cf. Theorem 3.1.4) that suggests a computational strategy.

Theorem 11.1.1 ([Fen79]). *Let S_0 be a compact normally hyperbolic manifold of C_0 , i.e., the matrix $D_x f(p) \in \mathbb{R}^{m \times m}$ has no eigenvalues with zero real parts for each $p \in S_0$. Then there exists a slow manifold S_ε that is $\mathcal{O}(\varepsilon)$ -close to S_0 for $\varepsilon > 0$ sufficiently small. Locally, S_ε is represented as a graph*

$$S_\varepsilon = \{(x, y) \in \mathbb{R}^{m+n} : x = h_\varepsilon(y)\},$$

where the map $h_\varepsilon : \mathbb{R}^n \rightarrow \mathbb{R}^m$ has a regular asymptotic expansion

$$h_\varepsilon(y) = h_0(y) + \varepsilon h_1(y) + \varepsilon^2 h_2(y) + \dots\tag{11.2}$$

The dynamics on S_ε are given by $\frac{dy}{d\tau} = \dot{y} = g(h_\varepsilon(y), y, \varepsilon)$, where $\tau = \varepsilon t$.

Theorem 11.1.1 shows that one way to compute the slow manifold and the dynamics on it is to calculate the maps $h_j(y)$ up to a sufficiently high order. Differentiating $x = h_\varepsilon(y)$ with respect to t yields

$$x' = Dh_\varepsilon(y)y'.$$

Therefore, we can use (11.1) to conclude that the following equation must hold:

$$f(h_\varepsilon(y), y, \varepsilon) - \varepsilon Dh_\varepsilon(y)g(h_\varepsilon(y), y, \varepsilon) = 0.\tag{11.3}$$

One refers to (11.3) as the **invariance equation**. Formally, one may write f and g as a Taylor expansion near $\varepsilon = 0$:

$$f(\cdot, h_\varepsilon, \varepsilon) = \sum_{q=0}^{\infty} f_q \varepsilon^q,\tag{11.4}$$

$$g(\cdot, h_\varepsilon, \varepsilon) = \sum_{q=0}^{\infty} g_q \varepsilon^q.\tag{11.5}$$

The rather cumbersome general form of the coefficients is

$$f_q = \sum_{k=0}^{q-1} \sum_{j=1}^{q-k} \frac{1}{k! j!} (D_x^j D_\varepsilon^k f)_0 \sum_{|\alpha|=q-k} h_\alpha + \frac{1}{q!} (D_\varepsilon^q f)_0,$$

$$g_q = \sum_{k=0}^{q-1} \sum_{j=1}^{q-k} \frac{1}{k! j!} (D_x^j D_\varepsilon^k g)_0 \sum_{|\alpha|=q-k} h_\alpha + \frac{1}{q!} (D_\varepsilon^q g)_0,$$

where $(\cdot)_0$ indicates evaluation on C_0 , i.e., at $(h_0(y), y, 0)$, and $\alpha = (\alpha_1, \dots, \alpha_j)$ is a multi-index such that $h_\alpha = (h_{\alpha_1}, \dots, h_{\alpha_j})$. Substituting (11.4) into (11.3) and setting the coefficient of ε^q equal to zero for each q leads to a sequence of equations:

$$f_q - \sum_{l=0}^{q-1} (\mathrm{D}h_l) g_{q-1-l} = 0, \quad \text{for } q = 0, 1, 2, \dots \quad (11.6)$$

The first two equations for (11.6) are

$$0 = f_0, \quad (11.7)$$

$$0 = (\mathrm{D}_x f)_0 h_1 + (\mathrm{D}_\varepsilon f)_0 - (\mathrm{D}h_0)(g)_0. \quad (11.8)$$

It should be no surprise that the critical manifold appears in (11.7) as the zeroth-order approximation to the slow manifold.

Exercise/Project 11.1.2. Show that the equation

$$\begin{aligned} &(\mathrm{D}_x f)h_2 + \frac{1}{2}(\mathrm{D}_x^2 f)_0(h_1, h_1) + (\mathrm{D}_x \mathrm{D}_\varepsilon f)_0 h_1 + \frac{1}{2}(\mathrm{D}_\varepsilon^2 f)_0 \\ &- (\mathrm{D}h_1)(g)_0 - (\mathrm{D}h_0)((\mathrm{D}_x g)_0 h_1 - (\mathrm{D}_\varepsilon g)_0) = 0 \end{aligned} \quad (11.9)$$

is obtained for $q = 2$ from (11.6). \diamond

Example 11.1.3. Consider the following planar fast–slow system:

$$\begin{aligned} x' &= y^2 - x, \\ y' &= -\varepsilon y. \end{aligned} \quad (11.10)$$

The critical manifold is $C_0 = \{(x, y) \in \mathbb{R}^2 : x = y^2\}$. The first-order correction to the slow manifold C_ε can be found from (11.8) as

$$(\mathrm{D}_x f)_0 h_1 + (\mathrm{D}_\varepsilon f)_0 - (\mathrm{D}h_0)(g)_0 = -h_1(y) + 0 - 2y(-y) \stackrel{!}{=} 0.$$

It is not difficult to see from (11.9) that $h_2(y) = 4y^2$. Therefore, it follows that

$$C_\varepsilon = \{(x, y) \in \mathbb{R}^2 : x = h_\varepsilon(y) = (1 + 2\varepsilon + 4\varepsilon^2 + \dots)y^2\}.$$

To see that the rather opaque formulas (11.7)–(11.9) really work, we now calculate the slow manifold explicitly. Observe that (11.10) is solved by

$$(x(t), y(t)) = \left(\left[x(0) - \frac{y(0)^2}{1 - 2\varepsilon} \right] e^{-t} + \frac{y(0)^2}{1 - 2\varepsilon} e^{-2\varepsilon t}, y(0)e^{-\varepsilon t} \right). \quad (11.11)$$

If $x(0) = \frac{y(0)^2}{1 - 2\varepsilon}$, then the solution (11.11) evolves only on the slow time scale $\tau = \varepsilon t$,

$$(x(t), y(t)) = \left(\frac{y(0)^2}{1 - 2\varepsilon} e^{-2\varepsilon t}, y(0)e^{-\varepsilon t} \right).$$

In particular, notice that in this case,

$$x(t) = \frac{y(t)^2}{1 - 2\varepsilon} \quad \text{for all } t \geq 0.$$

Hence, the slow manifold must be given by

$$C_\varepsilon = \left\{ (x, y) \in \mathbb{R}^2 : x = \frac{y^2}{1 - 2\varepsilon} \right\}.$$

A Taylor expansion of $1/(1 - 2\varepsilon)$ at $\varepsilon = 0$ confirms the earlier result

$$C_\varepsilon = \{(x, y) \in \mathbb{R}^2 : x = (1 + 2\varepsilon + 4\varepsilon^2 + 8\varepsilon^3 + \dots)y^2 = h_\varepsilon(y)\}.$$

Although the asymptotic approach to slow manifold calculations looks very helpful at first glance, it should be noted that the explicit formulas can quickly grow to epic proportions for realistic systems. ♦

Assume from now on that C_0 is normally hyperbolic and attracting; more precisely, all eigenvalues of $(D_x f)(p)$ for $p \in C_0$ have negative real parts. In this case, a direct numerical approach using just initial value solvers can be feasible, especially in low dimensions:

- (N1) Consider initial conditions $(x_j(0), y_j(0)) \in C_0$ for j in some index set.
- (N2) Integrate forward for some time $t > 0$ and observe that trajectories γ_j will approach C_ε during a short transient exponentially fast and then track C_ε up to an error of order $\mathcal{O}(e^{-K/\varepsilon})$ for some $K > 0$.
- (N3) Truncate the initial transient and collect the points from discrete representations of the trajectories $\gamma_j(t_k)$ for k in some index set.
- (N4) Use this cloud of points to interpolate/visualize C_ε .

Observe that the same procedure also works for repelling slow manifolds, i.e., when all eigenvalues of $(D_x f)(p)$ for $p \in C_0$ have positive real parts. In this case, one may reverse time $t \mapsto -t$ to return to the previous attracting slow manifold situation.

Example 11.1.4. As a toy example for the numerical approach using forward/backward integration, consider the (unforced) van der Pol equation

$$\begin{aligned} x' &= y - \frac{1}{3}x^3 + x \\ y' &= -\varepsilon x. \end{aligned}$$

The critical manifold is $C = \{y = \frac{1}{3}x^3 + x\}$ with two fold points at $x = \pm 1$ that separate the critical manifold into three branches:

$$C_0^{a-} = C \cap \{x < -1\}, \quad C_0^r = C \cap \{-1 < x < 1\}, \quad C_0^{a+} = C \cap \{x > 1\}.$$

The branches $C_0^{a\pm}$ are attracting, while C_0^r is repelling. Figure 11.1 shows the associated slow manifolds computed from forward and backward integration; note that the initial transients have not been truncated in this figure. ♦

The direct numerical technique often works well to get a first idea for the slow dynamics. However, the method has significant problems, such as choosing good starting points for higher-dimensional problems, which is crucial to obtaining a good mesh for the step (N4). Furthermore, it does not work adequately for saddle-type slow manifolds; see Section 11.5.

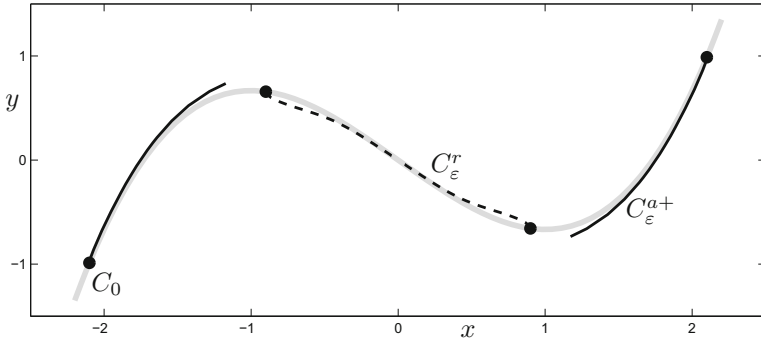


Figure 11.1: Initial conditions for four trajectories are marked by dots (black). The critical manifold C_0 (gray) and parts of the attracting (solid black) and repelling (dashed black) slow manifolds are shown.

11.2 The CSP Method

The **computational singular perturbation (CSP) method** was developed in the context of chemical reactions and combustion. In this application area, one often deals with high-dimensional fast–slow systems with attracting slow manifolds. As a starting point, consider a general fast–slow system for $z = (y, x) \in \mathbb{R}^n \times \mathbb{R}^m$:

$$\frac{dz}{dt} = z' = G(z) \quad \text{where } G = \begin{pmatrix} \varepsilon G_1 \\ G_2 \end{pmatrix} : \mathbb{R}^{n+m} \rightarrow \mathbb{R}^{n+m}. \quad (11.12)$$

We assume that $G = (\varepsilon G_1, G_2)^\top$ is sufficiently smooth and $G_{1,2}$ might implicitly depend on ε as well, e.g., $G_1 = G_1(y, x, \varepsilon)$, but we will not display this in the notation.

Henceforth, assume that the critical manifold C_0 for (11.12) is normally hyperbolic and attracting, namely that all eigenvalues of $(D_x G_2)_0$, i.e., of $D_x G_2$ evaluated on C_0 , have negative real parts. Assume also that C_0 is compact or that we have chosen a compact subset of C_0 for which we will use the same notation for simplicity. CSP is an iterative method to compute the slow manifold C_ε .

Remark: In this section, we will not obey our standard ordering of the variables and naming convention for the vector field $z' = (f, \varepsilon g)^\top$. The notation $z' = (\varepsilon G_1, G_2)^\top = G(z)$ for the CSP method emphasizes that slow variables with derivatives given by G_1 will eventually determine the dynamics; see also Chapter 2. Furthermore, the notation already indicates that CSP can also be applied to systems not given in standard form.

After q iterations of the CSP method, the approximation $K_\varepsilon^{(q)}$ of the slow manifold is $\mathcal{O}(\varepsilon^q)$ -close to C_ε . If $K_\varepsilon^{(q)}$ can be expressed as a graph $x = \psi_q(y, \varepsilon)$, then the slow dynamics are given by

$$\frac{dy}{d\tau} = \dot{y} = G_1(y, \psi_q(y, \varepsilon)), \quad \text{for } \tau = \varepsilon t.$$

There are two versions of the CSP method. The **one-step CSP method** finds the slow manifold, i.e., it expresses the fast variables in terms of the slow ones. The **two-step CSP method** also computes the flow in the direction transverse to the slow manifold. The basic idea for both methods is to use a suitable coordinate change to decouple the fast and slow variables.

Let $\mathcal{M}^{r \times c}$ denote the space of matrices with r rows and c columns. Let $A \in \mathcal{M}^{(n+m) \times (n+m)}$ be a matrix with full rank whose entries may depend on z . The columns of A form a basis, and G can be expressed in this basis as

$$G = AF \quad \text{where } F = \begin{pmatrix} F^1 \\ F^2 \end{pmatrix} : \mathbb{R}^{n+m} \rightarrow \mathbb{R}^{n+m}. \quad (11.13)$$

Let B be the left inverse to A , so that $BA = \text{Id}_{n+m}$, where $\text{Id}_{n+m} \in \mathcal{M}^{(n+m) \times (n+m)}$ is the $(n+m) \times (n+m)$ identity matrix. Hence, one finds that

$$F = BG. \quad (11.14)$$

Since F and G naturally split into two classes, it follows that one should also consider the corresponding splittings for A and B ,

$$A = (A_1, A_2) \quad \text{where } A_1 \in \mathcal{M}^{(n+m) \times m}, A_2 \in \mathcal{M}^{(n+m) \times n}, \quad (11.15)$$

$$B = \begin{pmatrix} B^1 \\ B^2 \end{pmatrix} \quad \text{where } B^1 \in \mathcal{M}^{m \times (n+m)}, B^2 \in \mathcal{M}^{n \times (n+m)}. \quad (11.16)$$

This notation implies, e.g., $F^1 = B^1 G$ and $F^2 = B^2 G$. Furthermore, we have

$$B^1 A_1 = \text{Id}_m, \quad B^2 A_1 = 0, \quad B^2 A_2 = \text{Id}_n \quad \text{and} \quad B^1 A_2 = 0.$$

Observe that differentiating the relation $BA = \text{Id}_{n+m}$ with respect to time yields

$$\frac{dB}{dt} A + B \frac{dA}{dt} = 0, \quad (11.17)$$

since Id_{n+m} is independent of time and A, B may depend on $z = z(t)$. Next, differentiating (11.14) and using the chain rule leads to

$$\begin{aligned} \frac{dF}{dt} &= B \frac{dG}{dt} + \frac{dB}{dt} G \\ &= B(DG)G + \frac{dB}{dt} G \\ &\stackrel{\text{by (11.13)}}{=} B(DG)AF + \frac{dB}{dt} AF \\ &\stackrel{\text{by (11.17)}}{=} B \left((DG)A - \frac{dA}{dt} \right) F \\ &= B((DG)A - (DA)G)F, \end{aligned}$$

where $DG \in \mathcal{M}^{(n+m) \times (n+m)}$ is the usual Jacobian matrix of G representing the total derivative. Therefore, F satisfies an ODE

$$\frac{dF}{dt} = \Lambda F \quad \text{with } \Lambda = B((DG)A - (DA)G) = B[A, G], \quad (11.18)$$

where $[\cdot, \cdot]$ denotes the **Lie bracket** defined by $[V, W] = (\mathrm{D}W)V - (\mathrm{D}V)W$.

Remark: Note that we also have $(\mathrm{ad } V)W = [V, W]$, where ad is the **adjoint representation**. These are standard notions in Lie Theory [Kna04, Hal03] linking nicely to differential geometry [Lee06] and also to the theory of normal forms [GH83].

Usually, the operator Λ is not block-diagonal. The goal of the CSP method is to bring Λ closer to block-diagonal form with each iteration. Then F^1 and F^2 will decouple, and the slow manifold is given by the equation $F^1 = 0$. The main idea is to improve the matrices A and B at each step. The algorithm is initialized with a constant matrix

$$A^{(0)} = \begin{pmatrix} A_1^{(0)}, A_2^{(0)} \end{pmatrix} = \begin{pmatrix} A_{11}^{(0)} & A_{12}^{(0)} \\ A_{21}^{(0)} & A_{22}^{(0)} \end{pmatrix},$$

where the submatrices have the following sizes:

$$A_{11}^{(0)} \in \mathcal{M}^{n \times m}, \quad A_{12}^{(0)} \in \mathcal{M}^{n \times n}, \quad A_{21}^{(0)} \in \mathcal{M}^{m \times m}, \quad A_{22}^{(0)} \in \mathcal{M}^{m \times n}.$$

A standard (but not the only) choice is $A_{11}^{(0)} = 0$. We adopt this convention so that

$$A^{(0)} = \begin{pmatrix} A_1^{(0)}, A_2^{(0)} \end{pmatrix} = \begin{pmatrix} 0 & A_{12}^{(0)} \\ A_{21}^{(0)} & A_{22}^{(0)} \end{pmatrix}.$$

The left inverse $B_{(0)}$ of $A^{(0)}$ can be calculated:

$$\begin{aligned} B_{(0)} &= \begin{pmatrix} B_1^{(0)} \\ B_2^{(0)} \end{pmatrix} = \begin{pmatrix} B_{(0)}^{11} & B_{(0)}^{12} \\ B_{(0)}^{21} & B_{(0)}^{22} \end{pmatrix} \\ &= \begin{pmatrix} -(A_{21}^{(0)})^{-1} A_{22}^{(0)} (A_{12}^{(0)})^{-1} & (A_{21}^{(0)})^{-1} \\ (A_{12}^{(0)})^{-1} & 0 \end{pmatrix}. \end{aligned}$$

As already indicated earlier, the algorithm is iterative. Let $q = 0, 1, 2, \dots$ be the iteration index. Based on (11.18), one defines a matrix

$$\begin{aligned} \Lambda_{(q)} &:= B_{(q)}(\mathrm{D}G)A^{(q)} - B_{(q)}(\mathrm{D}A^{(q)})G \\ &= \begin{pmatrix} B_{(q)}^1[A_1^{(q)}, G] & B_{(q)}^1[A_2^{(q)}, G] \\ B_{(q)}^2[A_1^{(q)}, G] & B_{(q)}^2[A_2^{(q)}, G] \end{pmatrix} = \begin{pmatrix} \Lambda_{(0)}^{11} & \Lambda_{(0)}^{12} \\ \Lambda_{(0)}^{21} & \Lambda_{(0)}^{22} \end{pmatrix}. \end{aligned} \quad (11.19)$$

Furthermore, define the matrices $U_{(q)}$ and $L_{(q)}$ as

$$U_{(q)} = \begin{pmatrix} 0 & (\Lambda_{(q)}^{11})^{-1} \Lambda_{(q)}^{12} \\ 0 & 0 \end{pmatrix}, \quad L_{(q)} = \begin{pmatrix} 0 & 0 \\ \Lambda_{(q)}^{21}(\Lambda_{(q)}^{11})^{-1} & 0 \end{pmatrix}. \quad (11.20)$$

The iterative update rules for $A^{(q)}$ and $B^{(q)}$ are

$$A^{(q+1)} = A^{(q)}(\mathrm{Id}_{n+m} - U_{(q)})(\mathrm{Id}_{n+m} + L_{(q)}), \quad (11.21)$$

$$B_{(q+1)} = (\mathrm{Id}_{n+m} - L_{(q)})(\mathrm{Id}_{n+m} + U_{(q)})B_{(q)}. \quad (11.22)$$

From an implementation viewpoint, one has to initialize all objects and then follow the rules given by (11.19), (11.21), and (11.22), which define the **two-step CSP method**. At each iteration step q , the approximate slow manifold $K_\varepsilon^{(q)}$ is given by the equation $F^1 = 0$, which indicates that the fast variables do not change. In our notation, this means that

$$B_{(q)}^1 G = 0. \quad (11.23)$$

Equation (11.23) is sometimes also called the **CSP condition**. Note carefully that $B_{(q)}^1$ for $q \geq 1$ will usually be a function evaluated on the slow manifold approximation for $q - 1$, i.e., (11.23) reads

$$B_{(q)}^1(y, \psi_{(q-1)}(y, \varepsilon))G(x, y) = 0. \quad (11.24)$$

By normal hyperbolicity, at least locally, there exists a function $\psi_{(q)}(y, \varepsilon) = x$ satisfying (11.24), and the approximate slow manifold is given by

$$K_\varepsilon^{(q)} = \{(y, x) : x = \psi_{(q)}(y, \varepsilon)\}.$$

Consider a true/correct slow manifold C_ε given by a function $h_\varepsilon(y) = x$ with asymptotic expansion

$$h_\varepsilon(y) = h_0(y) + \varepsilon h_1(y) + \varepsilon^2 h_2(y) + \dots$$

The fundamental theorem for the CSP method is that it reproduces h_ε .

Theorem 11.2.1 ([ZKK04a]). *At an iteration step $q \in \{0, 1, 2, \dots\}$, the CSP manifold $K_\varepsilon^{(q)}$ agrees with the slow manifold C_ε up to and including order $\mathcal{O}(\varepsilon^q)$. More precisely, we have that $\psi_{(q)}$ has an asymptotic expansion of the form*

$$\psi_{(q)}(y, \varepsilon) = \sum_{j=0}^q h_j(y) \varepsilon^j + \mathcal{O}(\varepsilon^{q+1}).$$

One key conclusion from Theorem 11.2.1 is that the successive coordinate changes improve the slow manifold asymptotic approximation at each order. This means that the coordinate change at iteration q does not affect terms of order $\mathcal{O}(\varepsilon^{q-1})$. This is analogous to the situation of computing a normal form at a bifurcation point [GH83]. In fact, the CSP method basically computes the Fenichel normal form of a system. However, note carefully that Theorem 11.2.1 makes an asymptotic statement and does not make any claims about convergence of approximations.

We do not prove Theorem 11.2.1 here. Instead, we are going to focus on the **one-step CSP method** and prove a similar result to Theorem 11.2.1. The main difference between the two methods is as follows:

1. The one-step CSP method reduces Λ to lower block-triangular form.
2. The two-step CSP method reduces Λ to block-diagonal form.

Remark: The last observation is the most important from a practical point of view if the equations are not already given in a fast–slow system standard form. In this case, one has to monitor the matrix Λ and check which ordering of the coordinates makes it block-diagonal. This checking procedure can be automated at each iteration step by checking the absolute values of elements of Λ .

The one-step method is very similar to the two-step version and is initialized with the same matrices $\tilde{A}^{(0)} = A^{(0)}$ and $\tilde{B}_{(0)} = B_{(0)}$. Throughout, the tilde $\tilde{}$ will be used to distinguish the matrices appearing in the two different methods. The update rules (11.21)–(11.22) are replaced by

$$\tilde{A}^{(q+1)} = \tilde{A}^{(q)}(\text{Id}_{n+m} - \tilde{U}_{(q)}), \quad (11.25)$$

$$\tilde{B}_{(q+1)} = (\text{Id}_{n+m} + \tilde{U}_{(q)})\tilde{B}_{(q)}. \quad (11.26)$$

Basically, (11.25)–(11.26) differ from (11.21)–(11.22) by one matrix multiplication each, whence the name one-step method. Note that $\tilde{U}_{(q)}$ is defined as in (11.20) with Λ replaced by $\tilde{\Lambda}$.

Exercise 11.2.2. Let $C \in \mathcal{M}^{(n+m) \times (n+m)}$ be invertible and represent a coordinate change. Set $\hat{A} = AC$ and $\hat{B} = C^{-1}B$, which represents the coordinate changes on the matrices A and B . Show that

$$\hat{\Lambda} = C^{-1}\Lambda C - C^{-1}\frac{dC}{dt}, \quad (11.27)$$

where $(DC)G = \frac{dC}{dt}$. Use (11.27) and (11.19)–(11.20) to show that the new update rule for $\tilde{\Lambda}$ is given by (11.28). \diamond

From Exercise 11.2.2, one finds that the new update rule for $\tilde{\Lambda}$ is

$$\tilde{\Lambda}_{(q+1)} = (\text{Id}_{n+m} + \tilde{U}_{(q)})\tilde{\Lambda}_{(q)}(\text{Id}_{n+m} - \tilde{U}_{(q)}) + (\text{Id}_{n+m} + \tilde{U}_{(q)})\frac{d\tilde{U}_{(q)}}{dt}. \quad (11.28)$$

Since $\tilde{A}^{(0)} = A^{(0)}$ and $\tilde{B}_{(0)} = B_{(0)}$, we also have $\tilde{\Lambda}_{(0)} = \Lambda_{(0)}$. Observe that $\tilde{U}_{(q)}$ and its time derivative have the same block structure, which implies that

$$\tilde{U}_{(q)} \frac{d\tilde{U}_{(q)}}{dt} = 0.$$

Using this fact, the rule (11.28) reduces to

$$\tilde{\Lambda}_{(q+1)} = (\text{Id}_{n+m} + \tilde{U}_{(q)})\tilde{\Lambda}_{(q)}(\text{Id}_{n+m} - \tilde{U}_{(q)}) + \frac{d\tilde{U}_{(q)}}{dt}. \quad (11.29)$$

We can rewrite (11.29) in terms of the block structure of $\tilde{\Lambda}$:

$$\begin{aligned} \tilde{\Lambda}_{(q+1)}^{11} &= \tilde{\Lambda}_{(q)}^{11} + \tilde{U}_{(q)}\tilde{\Lambda}_{(q)}^{21}, \\ \tilde{\Lambda}_{(q+1)}^{12} &= \tilde{U}_{(q)}\tilde{\Lambda}_{(q)}^{22} - \tilde{U}_{(q)}\tilde{\Lambda}_{(q)}^{21}\tilde{U}_{(q)} + \frac{d\tilde{U}_{(q)}}{dt}, \\ \tilde{\Lambda}_{(q+1)}^{21} &= \tilde{\Lambda}_{(q)}^{21}, \\ \tilde{\Lambda}_{(q+1)}^{22} &= \tilde{\Lambda}_{(q)}^{22} - \tilde{\Lambda}_{(q)}^{21}\tilde{U}_{(q)}, \end{aligned}$$

where $\tilde{U}_{(q)}$ is used as the full matrix and also as its restriction to \mathbb{R}^n represented by the matrix $(\tilde{\Lambda}_{(q)}^{11})^{-1}\tilde{\Lambda}_{(q)}^{12}$. One can still use the same condition for the one-step method to get the slow manifold

$$\tilde{B}_{(q)}^1 G = 0, \quad \text{for } q = 0, 1, 2, \dots \quad (11.30)$$

If a function $\tilde{\psi}_{(q)}$ satisfies (11.30), then the approximate slow manifold $\tilde{K}_\varepsilon^{(q)}$ is

$$\tilde{K}_\varepsilon^{(q)} = \left\{ (x, y) : x = \tilde{\psi}_{(q)}(y, \varepsilon) \right\}.$$

Theorem 11.2.3 ([ZKK04a]). *At an iteration step $q \in \{0, 1, 2, \dots\}$, the CSP manifold $\tilde{K}_\varepsilon^{(q)}$ agrees with the slow manifold C_ε up to and including order $\mathcal{O}(\varepsilon^q)$. More precisely, we have that $\tilde{\psi}_{(q)}$ has an asymptotic expansion of the form*

$$\tilde{\psi}_{(q)}(y, \varepsilon) = \sum_{j=0}^q h_j(y) \varepsilon^j + \mathcal{O}(\varepsilon^{q+1}). \quad (11.31)$$

Proof. (Sketch, [ZKK04a]) We shall show only some of the steps to set up the argument. Note that the coefficients $h_j(y)$ as defined in (11.31) are determined by the CSP condition (11.30). Hence, the goal is to express (11.30) in terms of the invariance equation (11.3), which, in the current notation, is given by

$$G_2(y, h_\varepsilon(y), \varepsilon) - \varepsilon D h_\varepsilon(y) G_1(y, h_\varepsilon(y), \varepsilon) = 0. \quad (11.32)$$

As a first step, note that using a recurrence argument and the fact that $\tilde{A}^{(0)} = A^{(0)}$, one finds that

$$\tilde{A}^{(q+1)} = A^{(0)} \prod_{j=0}^q (\text{Id}_{n+m} - \tilde{U}_{(j)}). \quad (11.33)$$

The structure of the matrix $\tilde{U}_{(j)}$ implies that $\tilde{U}_{(j)} \tilde{U}_{(j)} = 0$, so $\tilde{U}_{(j)}$ is nilpotent, which simplifies (11.33) to

$$\tilde{A}^{(q+1)} = A^{(0)} (\text{Id}_{n+m} - \tilde{P}_{(q)}), \quad (11.34)$$

where

$$\tilde{P}_{(q)} = \sum_{j=0}^q \tilde{U}_{(j)} = \begin{pmatrix} 0 & \sum_{l=0}^q (\tilde{\Lambda}_{(l)}^{11})^{-1} \tilde{\Lambda}_{(l)}^{12} \\ 0 & 0 \end{pmatrix}.$$

In the same way, one finds that

$$\tilde{B}_{(q+1)} = (\text{Id}_{n+m} + \tilde{P}_{(q)}) B_{(0)}. \quad (11.35)$$

Now one may use (11.34)–(11.35) in the transformation formula (11.27). Using that $\tilde{P}_{(q)} \frac{d\tilde{P}_{(q)}}{dt} = 0$ as well as $\tilde{\Lambda}_{(0)} = \Lambda_{(0)}$ leads to

$$\tilde{\Lambda}_{(q+1)} = (\text{Id}_{n+m} + \tilde{P}_{(q)}) \Lambda_{(0)} (\text{Id}_{n+m} - \tilde{P}_{(q)}) + \frac{d\tilde{P}_{(q)}}{dt}.$$

The CSP condition $\tilde{B}_{(q)}^1 G = 0$ can now be rewritten using the previous expressions; note that we always have $B_{(0)}^{22} = 0$. The result is

$$B_{(0)}^{12} G_2 + \varepsilon (\tilde{P}_{(q-1)} B_{(0)}^{21} + B_{(0)}^{11}) G_1 = 0.$$

Recall that $B_{(0)}^{12} = (A_{21}^{(0)})^{-1}$, which yields

$$G_2 + \varepsilon A_{21}^{(0)} (\tilde{P}_{(q-1)} B_{(0)}^{21} + B_{(0)}^{11}) G_1 = 0. \quad (11.36)$$

Observe that (11.36) has the same form as the invariance equation (11.36). In fact, (11.36) defines the map describing the approximate slow manifold $\tilde{K}_\varepsilon^{(q)}$,

$$x = \tilde{\psi}_{(q)}(y, \varepsilon) = \sum_{j=0}^{\infty} \varepsilon^j \tilde{\psi}_{q,j}(y). \quad (11.37)$$

The idea is to analyze (11.36) order by order, up to and including $\mathcal{O}(\varepsilon^q)$. The goal is to see that the coefficients $\tilde{\psi}_{q,j}(y)$ coincide with $h_j(y)$, which are the coefficients for the map defining the actual slow manifold $C_\varepsilon = \{x = h_\varepsilon(y)\}$. Substituting (11.37) into (11.36) and setting the coefficients of $1, \varepsilon, \dots, \varepsilon^q$ equal to zero produces the hierarchy of equations

$$\begin{aligned} 0 &= G_{2,j} + A_{21}^{(0)} (\tilde{P}_{(q-1,0)} B_{(0)}^{21} + B_{(0)}^{11}) G_{1,j-1} \\ &\quad + \sum_{l=1}^{j-1} A_{21}^{(0)} \tilde{P}_{(q-1,l)} B_{(0)}^{21} G_{1,j-l-1} \end{aligned} \quad (11.38)$$

for $j = 0, 1, \dots, q$, and $\tilde{P}_{(q-1,l)}$ denotes the $\mathcal{O}(\varepsilon^l)$ -coefficient in the asymptotic expansion of $\tilde{P}_{(q-1)}$. The coefficients $\tilde{\psi}_{q,j}(y)$ are defined by (11.38). The leading order $j = 0$ is the same for all q ,

$$G_2(y, \tilde{\psi}_{(q,0)}(y)) = 0 \quad \text{for } q = 0, 1, 2, \dots$$

Hence, one may already identify $\tilde{\psi}_{(q,0)}(y) = h_0(y)$. Therefore, for the zeroth-order approximation, one obtains $\tilde{K}_\varepsilon^{(0)} = C_0$, and the approximate slow manifold from the CSP method coincides with the critical manifold. The next step is to show that

$$\tilde{\psi}_{(q,j)}(y) = h_j \quad \text{for } j = 1, 2, \dots, q.$$

The equations (11.32) and (11.38) coincide if and only if

$$A_{21}^{(0)} (\tilde{P}_{(q-1,0)} B_{(0)}^{21} + B_{(0)}^{11}) = -Dh_0, \quad (11.39)$$

$$A_{21}^{(0)} \tilde{P}_{(q-1,l)} B_{(0)}^{21} = -Dh_l \quad \text{for } l = 1, 2, \dots, j-1. \quad (11.40)$$

Observe that (11.39)–(11.40) are independent of j . Hence, we can prove (11.39)–(11.40) using induction on q . We shall not carry out the, quite lengthy, induction argument here but just mention that it proceeds along the same lines as the proof so far, i.e., keeping careful track of definitions and notation and using suitable matrix identities; see [ZKK04a] for details. \square

Before discussing the relations of the CSP method to the fast dynamics, it will help to compute the details of a simple example to illustrate the method.

Example 11.2.4. The **Michaelis-Menten-Henri (MMH)** mechanism of enzyme kinetics can be described by a planar fast-slow system

$$\begin{aligned} y' &= \varepsilon G_1(y, x) = \varepsilon(-y + (y + \kappa - \lambda)x), \\ x' &= G_2(y, x) = y - (y + \kappa)x. \end{aligned} \quad (11.41)$$

It is assumed that $\kappa > \lambda > 0$ and $(x, y) \in \mathbb{R}^+ \times \mathbb{R}^+$. In this case, $(D_x G_2) = -(y + \kappa) < 0$, so that the critical manifold C_0 is normally hyperbolic and attracting,

$$C_0 = \left\{ (y, x) \in \mathbb{R}^+ \times \mathbb{R}^+ : x = \frac{y}{y + \kappa} = h_0(y) \right\}.$$

By Fenichel's theorem (see, e.g., Theorem 11.1.1), there exists a slow manifold $C_\varepsilon = \{(y, x) : x = h_\varepsilon(y) = h_0 + \varepsilon h_1 + \varepsilon^2 h_2 + \dots\}$. Using the invariance equation (11.3), we can derive the coefficients h_j of the asymptotic expansion for h_ε .

Exercise 11.2.5. Show that the coefficients h_1 and h_2 are given by

$$h_1(y) = \frac{\kappa \lambda y}{(y + \kappa)^4}, \quad h_2(y) = \frac{\kappa \lambda y (2\kappa \lambda - 3\lambda y - \kappa y - \kappa^2)}{(y + \kappa)^7}. \quad \diamond$$

We are going to apply the one-step CSP method. For the transformation matrices, the standard unit basis vectors can be used for the initialization

$$A^{(0)} = \left(A_1^{(0)}, A_2^{(0)} \right) = \begin{pmatrix} 0 & 1 \\ 1 & 0 \end{pmatrix}, \quad B_{(0)} = \begin{pmatrix} B_{(0)}^1 \\ B_{(0)}^2 \end{pmatrix} = \begin{pmatrix} 0 & 1 \\ 1 & 0 \end{pmatrix}.$$

The approximate slow manifold $\tilde{K}_\varepsilon^{(0)}$ is defined by $B_{(0)}^1 G = 0$, which yields $x = h_0(y)$, as expected. For the next order, one has to calculate

$$\Lambda_{(0)} = B_{(0)} (DG) A^{(0)} = \begin{pmatrix} -(y + \kappa) & 1 - x \\ \varepsilon(y + \kappa - \lambda) & \varepsilon(x - 1) \end{pmatrix}.$$

Therefore, it follows from the update rules (11.25)–(11.26) that

$$\tilde{A}^{(1)} = \begin{pmatrix} 0 & 1 \\ 1 & \frac{1-x}{y+\kappa} \end{pmatrix}, \quad \tilde{B}_{(1)} = \begin{pmatrix} \frac{x-1}{y+\kappa} & 1 \\ 1 & 0 \end{pmatrix}.$$

Evaluating these matrices on $\tilde{K}_\varepsilon^{(0)}$ yields

$$\tilde{A}^{(1)} = \begin{pmatrix} 0 & 1 \\ 1 & \frac{\kappa}{(y+\kappa)^2} \end{pmatrix}, \quad \tilde{B}_{(1)} = \begin{pmatrix} \frac{-\kappa}{(y+\kappa)^2} & 1 \\ 1 & 0 \end{pmatrix}.$$

The CSP condition for the first-order approximation is

$$\tilde{B}_{(1)}^1 G = y - (y + \kappa)x - \varepsilon \frac{\kappa(x(y + \kappa - \lambda) - y)}{(y + \kappa)^2} = 0. \quad (11.42)$$

After a bit of algebraic manipulation, it follows that (11.42) is satisfied if and only if

$$x = \frac{y}{y + \kappa} + \varepsilon \frac{\kappa \lambda y}{(y + \kappa)^4} - \varepsilon^2 \frac{\kappa^2 \lambda y(y + \kappa - \lambda)}{(y + \kappa)^7} + \mathcal{O}(\varepsilon^3).$$

Hence, the approximate slow manifold $\tilde{K}_\varepsilon^{(1)}$ coincides with C_ε up to order $\mathcal{O}(\varepsilon)$, as predicted by Theorem 11.2.3. However, there is still an error in the $\mathcal{O}(\varepsilon^2)$ terms. Computing the slow manifold C_ε using the one-step CSP method allows us to consider a one-dimensional ODE given by the slow dynamics on C_ε . ♦

Exercise/Project 11.2.6. Compute the manifold $\tilde{K}_\varepsilon^{(2)}$ for the MMH reaction (11.41) applying the next iteration of the one-step CSP method. Then apply the 2-step CSP method to compute the slow manifold up to order $\mathcal{O}(\varepsilon^2)$. A computer algebra package is recommended for this calculation. Can you go to higher-order expansions? ◇

The fast dynamics can be found using the 2-step CSP method. Let $p = (y, h_0(y)) \in C_0$ and denote the associated fast fiber by \mathcal{F}_0^p , i.e.,

$$\mathcal{F}_0^p = \{(y, x) \in \mathbb{R}^{m+n} : x \in \mathbb{R}^n\}.$$

Note that we still assume that for $(D_x G_2)(p)$, all eigenvalues have negative real parts. Therefore, solutions starting in \mathcal{F}_0^p will all contract toward C_ε . Fenichel's theorem provides an invariant family of fibers

$$\mathcal{F}_\varepsilon = \bigcup_{p \in C_\varepsilon} \mathcal{F}_\varepsilon^p,$$

where each fiber $\mathcal{F}_\varepsilon^p$ is $\mathcal{O}(\varepsilon)$ -close to \mathcal{F}_0^p ; see also Chapters 2 and 3. Denote by $T_p \mathcal{F}_\varepsilon$ and $T_p C_\varepsilon$ the tangent spaces to the fast fibers and the slow manifold at p . Due to the normal hyperbolicity assumption, these spaces intersect transversally at p and provide a splitting

$$\mathbb{R}^{m+n} = T_p \mathcal{F}_\varepsilon \oplus T_p C_\varepsilon.$$

Again, the idea is to compute an approximation to the fast fibers iteratively using linear algebra. Let A_f be an $(n+m) \times m$ matrix whose columns form a basis for $T_p \mathcal{F}_\varepsilon$. Similarly, let A_s be an $(n+m) \times n$ matrix whose columns form a basis of $T_p C_\varepsilon$ and set $A = (A_f, A_s)$. Then $A = A(p)$ is a point-dependent basis of \mathbb{R}^{n+m} along C_ε .

Remark: Consider a trajectory in C_ε , say $\gamma_\varepsilon(t)$. From the viewpoint of differential geometry, $A(\gamma_\varepsilon(t))$ is a **moving frame** providing a linear approximation of how initial conditions near C_ε approach and track the slow manifold.

The goal is to approximate the columns of $A_f(y, h_\varepsilon(y))$, since they provide a basis for the fast fiber at a point p . Recall that in the CSP method, one considers a matrix $A^{(q)}$, see equation (11.15), which has a part $A_1^{(q)}$ associated with the fast variables. This suggests the definition

$$\mathcal{L}_\varepsilon^{(q)}(y) := \text{span} \left(\text{cols} \left(A_1^{(q)}(y, \psi_{(q)}(y, \varepsilon)) \right) \right),$$

which is called the **CSP fast fiber** of order q at p . The next theorem shows that the name for $\mathcal{L}_\varepsilon^{(q)}(y)$ is justified.

Theorem 11.2.7 ([ZKK04b]). *The asymptotic expansions of $\mathcal{L}_\varepsilon^{(q)}(y)$ and $T_p\mathcal{F}_\varepsilon$, where $(y, h_\varepsilon(y)) = p \in C_\varepsilon$, agree up to and including terms of order $\mathcal{O}(\varepsilon^q)$ for $q = 0, 1, 2, \dots$. In particular, $\mathcal{L}_\varepsilon^{(q)} = \bigcup_{p \in C_\varepsilon} (p, \mathcal{L}_\varepsilon^{(q)}(y))$ is an $\mathcal{O}(\varepsilon^q)$ -approximation to the tangent bundle $T\mathcal{F}_\varepsilon$.*

The proof of Theorem 11.2.7 uses similar techniques to those used in the proof of Theorem 11.2.3. The goal is to show that the projection of $A_1^{(q)}$ onto TC_ε becomes smaller and smaller with each iteration step in the two-step CSP method; this requires a careful tracking of the linear algebra involved using an induction argument [ZKK04b].

Example 11.2.8. We continue with Example 11.2.4. First, it is possible to compute the asymptotic approximations to the fast fibers analytically up to and including order $\mathcal{O}(\varepsilon)$ using the asymptotic ansatz

$$y(t; \varepsilon) = \sum_j \varepsilon^j y_j(t), \quad x(t; \varepsilon) = \sum_j \varepsilon^j x_j(t). \quad (11.43)$$

Let $\mathcal{F}_\varepsilon^p$ be a fast fiber with base point $p = (y, h_\varepsilon(y))$. Denote by (y^A, x^A) and (y^B, x^B) two points on it. Define

$$\Delta y(t) = y^B(t) - y^A(t) \quad \text{and} \quad \Delta x(t) = x^B(t) - x^A(t).$$

Recall from Chapter 3 that two points in the same fast fiber contract exponentially fast toward each other with an $\mathcal{O}(1)$ exponent on the fast time scale, i.e., the points have the same **asymptotic phase**. Introducing the difference notation in the asymptotic expansions yields

$$\Delta y(t; \varepsilon) = \sum_j \varepsilon^j \Delta y_j(t), \quad \Delta x(t; \varepsilon) = \sum_j \varepsilon^j \Delta x_j(t),$$

where $\Delta y_j(t) = y_j^B(t) - y_j^A(t)$ and $\Delta x_j(t) = x_j^B(t) - x_j^A(t)$. Then the condition on exponential decay becomes

$$\Delta y_j(t) = \mathcal{O}(e^{-K_y t}) \quad \text{and} \quad \Delta x_j(t) = \mathcal{O}(e^{-K_x t})$$

as $t \rightarrow \infty$ for positive constants K_y, K_x .

Since one is interested in tangent vectors to the fast fibers, it helps to view Δy_j and Δx_j as coordinates of the vector between A and B when A and B are “infinitesimally close.” Formally, we would have to consider the limit $A \rightarrow B$ and look at $\Delta x/\Delta y$ (or $\Delta y/\Delta x$) to obtain the line approximating the fast fiber at the base point. Since the CSP method will immediately give us the tangent vectors, the formal calculation presented here will be preferable.

The standard regular perturbation approach can be carried through; it begins by substituting (11.43) into the MMH equations (11.41). For the $\mathcal{O}(1)$ terms, we get

$$\begin{aligned} y'_0 &= 0, \\ x'_0 &= y_0 - (y_0 + \kappa)x_0. \end{aligned}$$

The equations can be solved explicitly:

$$y_0(t) = y_0(0) =: y_0, \quad (11.44)$$

$$x_0(t) = \frac{y_0}{y_0 + \kappa} + \left(x_0(0) - \frac{y_0}{y_0 + \kappa} \right) e^{-(y_0 + \kappa)t}. \quad (11.45)$$

Therefore, it follows that $\Delta y_0(t) = \Delta y_0(0)$, which implies that A and B can lie in the same fast fiber only if

$$\Delta y_0(0) = 0. \quad (11.46)$$

From this fact and (11.45), it follows that

$$\Delta x_0(t) = \Delta x_0(0)e^{-(y_0 + \kappa)t}.$$

As long as $\kappa \neq -y_0$, we always have that $\Delta x_0(t)$ decays to zero exponentially. Hence, the tangent vectors to the fast fibers for order $\mathcal{O}(1)$ are of the form $(0, \alpha)^\top$ for $\alpha \neq 0$ at the base point. Note that this is not a surprising result, since the variable x in the second coordinate is fast, so we verified only the result that in the singular limit, the fast fibers are $\{y = \text{constant}\}$. For order $\mathcal{O}(\varepsilon)$, a far more detailed calculation is necessary. The $\mathcal{O}(\varepsilon)$ equations are

$$y'_1 = -y_0 + (y_0 + \kappa - \lambda)x_0, \quad (11.47)$$

$$x'_1 = y_1 - (y_0 + \kappa)x_1 - y_1x_0. \quad (11.48)$$

Substituting in the solutions for the zeroth order, (11.44)–(11.45), we see that it is possible to integrate (11.47) to obtain

$$y_1(t) = y_1(0) - \frac{\lambda y_0}{y_0 + \kappa} t + \frac{y_0 + \kappa - \lambda}{y_0 + \kappa} \left(x_0(0) - \frac{y_0}{y_0 + \kappa} \right) (1 - e^{-(y_0 + \kappa)t}).$$

Since $\Delta y_0 = 0$, it follows that

$$\Delta y_1(t) = \Delta y_1(0) + \frac{y_0 + \kappa - \lambda}{y_0 + \kappa} \Delta x_0(0) (1 - e^{-(y_0 + \kappa)t}).$$

Again, we apply the asymptotic phase condition $\lim_{t \rightarrow \infty} \Delta y_1(t) = 0$, which is satisfied if and only if

$$\Delta y_1(0) = -\frac{y_0 + \kappa - \lambda}{y_0 + \kappa} \Delta x_0(0). \quad (11.49)$$

Exercise 11.2.9. Integrate (11.48) explicitly, e.g., using a computer algebra system, and use this result to prove that there are no extra conditions on $\Delta x_1(0)$, making it a free parameter. ◇

Hence, the only conditions for order $\mathcal{O}(\varepsilon)$ are (11.46) and (11.49). This means that at the base point of each fast fiber, the following vector is tangent up to and including order $\mathcal{O}(\varepsilon)$:

$$\begin{pmatrix} 0 \\ \alpha \end{pmatrix} + \varepsilon \begin{pmatrix} -\left(1 - \frac{\lambda}{y_0 + \kappa}\right)\alpha \\ \beta \end{pmatrix} \quad (11.50)$$

for some constant β . The vector (11.50) depends on y_0 , and hence in its most general form, we should replace y_0 by some arbitrary y .

The next step is to check whether the result from the CSP method coincides with the analytical calculation. It is straightforward to check that the two-step CSP method generates at the first iteration step

$$A_1^{(1)} = \begin{pmatrix} 0 \\ 1 \end{pmatrix} + \varepsilon \frac{y + \kappa - \lambda}{y + \kappa} \begin{pmatrix} -1 \\ \frac{1-x}{y+\kappa} \end{pmatrix}. \quad (11.51)$$

Recall that we always have to evaluate results of the CSP method at each step at the current best approximation of the slow manifold. In this case, we know from Example 11.2.4 that $K_\varepsilon^{(1)}$ is described by

$$x = \frac{y}{y + \kappa} + \varepsilon \frac{\kappa \lambda y}{(y + \kappa)^4} + \mathcal{O}(\varepsilon^2).$$

Using this expansion in (11.51) yields

$$A_1^{(1)} = \begin{pmatrix} 0 \\ 1 \end{pmatrix} - \varepsilon \begin{pmatrix} 1 - \frac{\lambda}{y+\kappa} \\ \frac{\kappa}{y+\kappa} \end{pmatrix}. \quad (11.52)$$

Hence, (11.52) and (11.50) coincide with $\alpha = 1$ and $\beta = -\kappa/(y + \kappa)$. Therefore, the approximation of the two-step CSP method for the fast fibers is correct up to and including terms of order $\mathcal{O}(\varepsilon)$, as predicted by Theorem 11.2.7. ♦

11.3 The ZDP Method

In addition to the CSP method, described in the previous section, many other ideas for computing slow manifolds have been developed. Here we shall consider the so-called **zero-derivative principle**, or **ZDP**, method. A comparison between CSP and ZDP will also give a perhaps more intuitive viewpoint on why the CSP method works. We begin with a general system for $z \in \mathbb{R}^N$:

$$\frac{dz}{dt} = z' = G(z) \quad \text{where } G = \begin{pmatrix} \varepsilon G_1 \\ G_2 \end{pmatrix} : \mathbb{R}^{n+m} \rightarrow \mathbb{R}^{n+m}. \quad (11.53)$$

First, we consider the case that a known splitting into slow and fast variables exists, $z = (y, x) \in \mathbb{R}^{n+m}$ and $(G_1(y, x, \varepsilon), G_2(y, x, \varepsilon)) = (\varepsilon g(y, x, \varepsilon), f(y, x, \varepsilon))$, to introduce the idea of the method. The critical manifold is given by

$$C_0 = \{(y, x) \in \mathbb{R}^{n+m} : f(y, x, 0) = 0\} = \left\{ (y, x) \in \mathbb{R}^{n+m} : \frac{dx}{dt} = 0 \right\}.$$

The last equality seems redundant, since it is obvious from the definition that $f = 0$ corresponds to the vanishing of the first derivative of the fast variables, but it contains the basic idea. Furthermore, solutions in the slow manifold C_ε have $\mathcal{O}(1)$ derivatives for the fast variables for all higher-order derivatives. Instead of dealing with unknown bounded constants for the derivatives, we may, for example, just consider a point $p = (y_\varepsilon, x) \in C_\varepsilon$ and impose the condition

$$L^{(j)}(y_\varepsilon, x) := \left(\frac{d^{j+1}x}{dt^{j+1}} \right) (y_\varepsilon, x) = 0 \quad (11.54)$$

for $j \in \{1, 2, \dots\}$, whence the name “zero-derivative principle.” Observe that at each point $p = (y_\varepsilon, x) \in C_\varepsilon$, the j th-order variables x can be determined by the iteration of a map $\mathcal{Z}_{(j)} : \mathbb{R}^m \rightarrow \mathbb{R}^m$ given by

$$\mathcal{Z}_{(j)}(x) = x - (-H)^{j+1} \left(\frac{d^{j+1}x}{dt^{j+1}} \right) (y_\varepsilon, x) = x - (-H)^{j+1} L^{(j)}(y_\varepsilon, x), \quad (11.55)$$

where H is a positive scalar that is chosen as $H = \mathcal{O}(\varepsilon)$ for stability purposes. Observe that iterating (11.55) should converge to a fixed point at which the ZDP condition (11.54) holds. Let $h^{(j)} : \mathbb{R}^n \rightarrow \mathbb{R}^m$ denote the solution obtained by the ZDP method satisfying $L^{(j)}(y_\varepsilon, h^{(j)}(y_\varepsilon)) = 0$. The question is how the map $h^{(j)}$ relates to the map $h : \mathbb{R}^n \rightarrow \mathbb{R}^m$ that describes the true slow manifold

$$C_\varepsilon = \{(y, x) \in \mathbb{R}^{n+m} : x = h(y)\}.$$

Theorem 11.3.1 ([ZGKK09]). *Fix any $j \in \{0, 1, 2, \dots\}$. Then there is an ε_j such that for $0 < \varepsilon \leq \varepsilon_j$, the condition (11.54) can be solved locally for a given y_ε . The asymptotic expansions of h and $h^{(j)}$ agree up to and including order $\mathcal{O}(\varepsilon^j)$:*

$$h^{(j)}(y) = \sum_k h_k^{(j)}(y) \varepsilon^k = \sum_{k=0}^j h_k(y) \varepsilon^k + \mathcal{O}(\varepsilon^{j+1}).$$

Remark: The iteration (11.55) has a fixed point, which is close to the slow manifold up to a specified order. However, it can be shown that direct iteration may be problematic, since the desired fixed point might not be attracting for the map \mathcal{Z}_j . One needs a special stabilization procedure to achieve convergence [ZGKK09, SK93a, ZVG⁺12].

The proof of Theorem 11.3.1 uses the invariance equation (11.3) and induction similar to that used in the proof for the CSP method. Instead of outlining the proof, we shall compare the ZDP method with the CSP method. Recall from Section 11.2 that the two-step CSP method generates a sequence of matrices $A^{(j)}$ that allow us to obtain the splitting of the tangent space into fast and slow components at a point $p \in \mathbb{R}^N = \mathbb{R}^{n+m}$. The columns of these matrices form a basis at p for $T_p \mathbb{R}^N$. Hence, CSP generates a sequence of coordinate systems, and if one wants to compare it to ZDP, one must reinterpret the ZDP method as generating coordinates.

Let $v^{(0)}(z) = z$ be the standard coordinate system in $\mathbb{R}^N = \mathbb{R}^{n+m}$ at the initialization of the ZDP algorithm. Denote by

$$\{v^{(j)}(z) : j = 0, 1, \dots\}$$

a sequence of coordinates based on the update rule

$$v^{(j+1)}(z) = \begin{pmatrix} v_1^{(j+1)}(z) \\ v_2^{(j+2)}(z) \end{pmatrix} = \begin{pmatrix} L^{(j)}(z) \\ z_2 \end{pmatrix}, \quad (11.56)$$

where $L^{(j)}$ is defined as in (11.54). Let $A^{(0)} = \text{Id}$ be the matrix consisting of standard basis vectors, and let $A^{(j)}$ denote the matrix consisting of basis vectors for the coordinates $v^{(j)}$. This yields an update rule $A^{(j)} \rightarrow A^{(j+1)}$, which can be calculated from (11.56). The approximation of the slow manifold for the ZDP method is

$$K_\varepsilon^{(j)} = \{z \in \mathbb{R}^N : v_1^{(j+1)}(z) = L^{(j)}(z) = 0\}.$$

This observation shows a direct analogy to CSP. In fact, the notation is overloaded, since $K_\varepsilon^{(j)}$ is already used for the approximate slow manifold computed by the CSP method. The next theorem shows why this notation still makes sense.

Theorem 11.3.2 ([ZKK05]). *The update rules of local bases for the CSP and ZDP methods differ only by a scaling factor, i.e., the bases induced in the tangent space at a point $p \in C_\varepsilon$ are identical up to rescaling and permutation at a fixed iteration step j for both methods.*

Theorem 11.3.2 also gives a reinterpretation of the CSP method. One situation in which ZDP is of particular interest is that in which the differential equations are not explicitly given (**equation-free modeling**), i.e., the model is available only via a simulator; see Section 11.7.

Exercise/Project 11.3.3. Use the ZDP method to calculate an approximation to the slow manifolds in the forced van der Pol equation (8.56). Extend the slow manifolds under the fast–slow system by numerical forward integration (see Sections 10.1 and 10.2) and use the results to determine an approximation to the period of relaxation oscillations depending on the parameters $a, \omega, \varepsilon > 0$. ◇

11.4 Other Reduction Methods

The number of different methods for finding the slow manifold for a fast–slow system is very large. Here we briefly present two more methods. To simplify the situation, we assume an explicit time scale separation

$$\begin{aligned} \varepsilon \dot{x} &= f(x, y, \varepsilon), \\ \dot{y} &= g(x, y, \varepsilon), \end{aligned} \quad (11.57)$$

where $z = (x, y) \in \mathbb{R}^{m+n}$. Denote the critical manifold of (11.57) by C_0 , assume that it is normally hyperbolic and attracting, and denote the associated slow manifold by C_ε . Locally, there exists a map $h : \mathbb{R}^n \rightarrow \mathbb{R}^m$ describing C_ε as a graph with a well-defined asymptotic expansion

$$x = h(y) = \sum_j h_k(y) \varepsilon^k.$$

The zeroth-order term h_0 yields the critical manifold $C_0 = \{x = h_0(y)\}$.

The first method we are going to introduce is called **ILDM**, for **intrinsic low-dimensional manifolds** following Maas and Pope [MP92a, MP92b]. Consider the vector field (11.57) and its linearization

$$G = \begin{pmatrix} \frac{1}{\varepsilon} f \\ g \end{pmatrix}, \quad J = \begin{pmatrix} \frac{1}{\varepsilon} D_x f & \frac{1}{\varepsilon} D_y f \\ D_x g & D_y g \end{pmatrix}$$

where, e.g., $D_y g$ is an $n \times n$ matrix of partial derivatives $\partial g_i / \partial y_j$, and the other submatrices are defined similarly with appropriate dimensions. The eigenvalues of J must split into two groups, n eigenvalues with $\mathcal{O}(1)$ real parts and m eigenvalues with $\mathcal{O}(\varepsilon^{-1})$ negative real parts. This holds because the system (11.57) can be transformed, at least theoretically, to Fenichel normal form; see Section 4.1. The span of the eigenvectors of J associated with the $\mathcal{O}(1)$ eigenvalues is called the **slow subspace**, and the remaining eigenvectors span the **fast subspace**.

Definition 11.4.1. The **intrinsic low-dimensional manifold** (or **ILDM**) of (11.57) is defined as the locus of points $(x, y) \in \mathbb{R}^{m+n}$ where G lies entirely in the slow subspace.

To calculate the ILDM, one possibility is to use a **Schur decomposition** of the linearization J given by

$$J = Q N Q^\top, \tag{11.58}$$

where Q is unitary ($Q Q^\top = Q^\top Q = \text{Id}$) and N is lower triangular. The matrices have the following structure:

$$Q = (Q_1, Q_2), \quad N = \begin{pmatrix} N_{11} & 0 \\ N_{21} & N_{22} \end{pmatrix}$$

where Q_1 is an $(m+n) \times m$ matrix, Q_2 is an $(m+n) \times n$ matrix, N_{11} and N_{22} are lower triangular of size $m \times m$ and $n \times n$, and N_{21} is of size $n \times m$. The columns of Q are also called **Schur vectors**, and they form a basis for \mathbb{R}^{m+n} . The standard Schur decomposition can be modified so that the eigenvalues of J appear on the diagonal of N in descending order of their real parts.

Remark: For details on this modification, consider [MP92b], where the standard Schur algorithm [Ste73] is modified, or consider [Maa98], where the standard Schur decomposition is followed by a suitable sequence of Givens rotations [GvL96].

The n columns in Q_2 form an orthogonal basis for the slow subspace, while the m vectors in Q_1 form an orthogonal basis of the orthogonal complement. The vector field G lies entirely in the slow subspace if and only if it is orthogonal to the orthogonal complement of the slow subspace, i.e.,

$$Q_1^\top G = 0. \quad (11.59)$$

The condition (11.59) defines the ILDM and provides an approximation to the slow manifold C_ε . Since the whole method is based on a coordinate change for the linearization J , one expects that the ILDM is a linear approximation to C_ε , which is confirmed by the next result.

Theorem 11.4.2 ([KK02]). *The equation for the ILDM (11.59) admits an asymptotic solution of the form*

$$x = \psi(y, \varepsilon) = \psi_0(y) + \psi_1(y)\varepsilon + \psi_2(y)\varepsilon^2 + \dots$$

as $\varepsilon \rightarrow 0$. The terms $\psi_0 = h_0$ and $\psi_1 = h_1$ coincide with the slow manifold asymptotic expansion, so that the ILDM is an $\mathcal{O}(\varepsilon)$ -approximation to the true slow manifold C_ε . In general, $\psi_2 \neq h_2$, so that the error of the approximation is of order $\mathcal{O}(\varepsilon^2)$. More precisely, we have

$$h_2 - \psi_2 = (\mathrm{D}_x f)^{-2}(\mathrm{D}^2 h_0)(g, g),$$

where the bilinear form $(\mathrm{D}^2 h_0)(g, g) = ((\mathrm{D}^2 h_0)g)g$ and all other expression are evaluated at $(y, h_0(y), \varepsilon = 0)$. Hence, the error is directly related to the curvature of the slow manifold C_ε .

The second method we describe here is an iterative approach due to Fraser and Russel [Fra88b, RF91b]. The method is based on the invariance equation (11.3) given by

$$\varepsilon \mathrm{D}h(y)g(h(y), y, \varepsilon) = f(h(y), y, \varepsilon). \quad (11.60)$$

The idea is that to find the map $h : \mathbb{R}^n \rightarrow \mathbb{R}^m$ that defines the slow manifold, one begins with any map $\varphi^{(0)}$ and computes a sequence of functions $\{\varphi^{(j)} : j = 1, 2, \dots\}$ by solving

$$\varepsilon \mathrm{D}\varphi^{(j-1)}(y)g(\varphi^{(j)}(y), y, \varepsilon) = f(\varphi^{(j)}(y), y, \varepsilon). \quad (11.61)$$

The equation (11.61) defines $\varphi^{(j)}$ implicitly and usually is a nonlinear equation. Hence, it might be difficult to solve.

Theorem 11.4.3 ([KK02]). *If we begin with $\varphi^{(0)} = h_0$, then the iterative method of Fraser and Roussel gives an approximation of order up to and including $\mathcal{O}(\varepsilon^j)$ of the slow manifold, i.e.,*

$$\varphi^{(j)}(y) = \sum_{k=0}^j h_k(y)\varepsilon^k + \mathcal{O}(\varepsilon^{j+1}).$$

Note that the scheme proposed by Fraser and Russel is essentially a version of the graph transform discussed in Section 2.2. To illustrate the two schemes presented in this section, it helps to consider a simple example.

Example 11.4.4. We return to Example 11.1.3, discussing the toy model

$$\begin{aligned}\varepsilon \dot{x} &= y^2 - x, \\ \dot{y} &= -y,\end{aligned}\tag{11.62}$$

Recall that we have already computed the asymptotics of the slow manifold C_ε :

$$C_\varepsilon = \{(x, y) \in \mathbb{R}^2 : x = h(y) = (1 + 2\varepsilon + 4\varepsilon^2 + \dots)y^2\}.$$

The Jacobian of the vector field defined by (11.62) is

$$J = \begin{pmatrix} -\frac{1}{\varepsilon} & \frac{2y}{\varepsilon} \\ 0 & -1 \end{pmatrix}.$$

The eigenvalues are $\lambda_1 = -\frac{1}{\varepsilon}$ and $\lambda_2 = -1$ with associated eigenvectors

$$v_1 = \begin{pmatrix} 1 \\ 0 \end{pmatrix}, \quad v_2 = \begin{pmatrix} 1 \\ \frac{1-\varepsilon}{2y} \end{pmatrix}.$$

To find the ILDM, we have to determine when the vector field is entirely contained in the subspace spanned by v_2 . The orthogonal complement of v_2 is $v_2^\perp = ((\varepsilon - 1)/(2y), 1)^\top$, and the ILDM condition (11.59) becomes

$$0 = v_2^\perp \cdot \begin{pmatrix} \frac{y^2-x}{\varepsilon} \\ -y \end{pmatrix} = -y + \frac{(\varepsilon - 1)(y^2 - x)}{2y\varepsilon}.$$

Hence, it follows that the ILDM is given by

$$\text{ILDM} = \left\{ (x, y) \in \mathbb{R}^2 : x = \psi(y) = y^2 \frac{1+\varepsilon}{1-\varepsilon} = y^2(1 + 2\varepsilon + 2\varepsilon^2 + \dots) \right\}.$$

As expected from Theorem 11.4.2, the error occurs at order $\mathcal{O}(\varepsilon^2)$.

For the iterative method of Fraser and Roussel, we begin with the approximation $x = h_0(y) = \varphi^{(0)}(y) = y^2$. Then the invariance equation (11.61) yields

$$-2\varepsilon y^2 = y^2 - \varphi^{(1)}(y) \quad \Rightarrow \quad \varphi^{(1)}(y) = y^2(1 + 2\varepsilon).$$

At the next iteration, we obtain

$$-2y^2(\varepsilon + 2\varepsilon^2) = y^2 - \varphi^{(2)}(y) \quad \Rightarrow \quad \varphi^{(2)}(y) = y^2(1 + 2\varepsilon + 4\varepsilon^2).$$

This result is expected from Theorem 11.4.3, since the iterative method produces the correct j th-order approximation at the j th iteration step. ♦

Exercise/Project 11.4.5. Apply the ILDM, ZDP, and Fraser–Roussel methods to the MMH reaction (11.41). Compare the accuracy and practical implementation of the three methods with CSP. Can you explain how this comparison changes if the dimension of the fast–slow system is large? ◇

11.5 Saddle-Type Slow Manifolds

As usual, we begin with a fast–slow system in the following general form:

$$\begin{aligned}\frac{dx}{dt} &= x' = f(x, y, \varepsilon), \\ \frac{dy}{dt} &= y' = \varepsilon g(x, y, \varepsilon),\end{aligned}\tag{11.63}$$

where $z = (x, y) \in \mathbb{R}^{m+n}$ and f, g are sufficiently smooth, and we set $N = m+n$. Denote the critical manifold of (11.63) by C_0 , and the associated slow manifold by C_ε . We recall what it means for C_0 to be normally hyperbolic of saddle-type.

Definition 11.5.1. C_0 is of **saddle-type** for $p \in C_0$ if $(D_x f)(p, 0)$ has eigenvalues with positive as well as negative real parts and no eigenvalue with zero real part.

Fenichel’s Theorem provides an associated saddle-type slow manifold C_ε as a perturbation of C_0 . The problem with saddle-type slow manifolds is that they are difficult to compute. Indeed, direct numerical integration fails since C_ε is repelling with respect to forward-in-time and backward-in-time integration. We are going to describe a boundary value approach to compute trajectories near slow manifolds of saddle type. The method is appropriately called the **slow manifold of saddle type (SMST) algorithm**. Let

$$\gamma : [a, b] \rightarrow \mathbb{R}^{m+n}$$

denote the trajectory segment we are trying to compute. The basic idea of the method is that trajectories very close to C_ε must approach it close to $W^s(C_\varepsilon)$ and then leave it close to $W^u(C_\varepsilon)$. We are going to set up a well-defined boundary value problem to find such a trajectory. Truncating the initial and final transients yields an approximation of C_ε ; see also Figure 11.2. Let

$$\begin{aligned}m_s &:= \dim W^s(C_0) - \dim(C_0) = \dim W^s(C_\varepsilon) - \dim(C_\varepsilon), \\ m_u &:= \dim W^u(C_0) - \dim(C_0) = \dim W^u(C_\varepsilon) - \dim(C_\varepsilon),\end{aligned}$$

Observe that normal hyperbolicity implies $m_u + m_s = m$. The simplest non-trivial case occurs when $m = 2$, $n = 1$, $\dim(C_0) = 1$ in dimension $N = 3$, as shown in Figure 11.2, which implies $m_u = 1$ and $m_s = 1$.

We need a total of $m + n$ boundary conditions to define the trajectory γ completely. From the theoretical viewpoint, we want the following:

$$\gamma(a) \in B_a \text{ and } B_a \text{ transverse to } W^s(C_\varepsilon), \quad m_s \leq \dim(B_a) \leq m_s + n, \tag{11.64}$$

$$\gamma(b) \in B_b \text{ and } B_b \text{ transverse to } W^u(C_\varepsilon), \quad m_u \leq \dim(B_b) \leq m_u + n, \tag{11.65}$$

with $\dim(B_a) + \dim(B_b) = m + n$, since counting boundary conditions requires

$$(m + n) - \dim(B_a) + (m + n) - \dim(B_b) \stackrel{!}{=} m + n.$$

The boundary condition (11.64) means that the initial point of γ can vary transversely to the stable manifold $W^s(C_\varepsilon)$, i.e., the algorithm will eventually

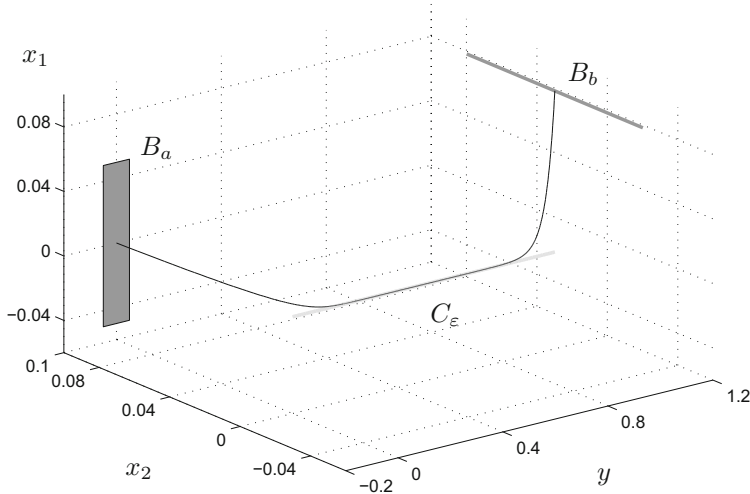


Figure 11.2: Simple example of the SMST algorithm in dimension 3. The boundary conditions are shown in dark gray, the piece of the slow manifold C_ε is light gray, and the computed trajectory γ is the thin black curve.

satisfy this condition by converging at $\gamma(a)$ to a point that is exponentially close to $W^s(C_\varepsilon)$. With reversed directions, the same explanation applies to (11.65). But we know from Fenichel's theorem that near the critical manifold,

$$W^s(C_\varepsilon) \approx E^s(C_0) \quad \text{and} \quad W^u(C_\varepsilon) \approx E^u(C_0),$$

where $E^{s,u}(C_0)$ denote the stable and unstable eigenspaces of the system linearized around C_0 . By normally hyperbolic splitting, a transverse subspace to $E^s(C_0)$ is $E^u(C_0)$, and conversely. If we denote the full vector field by $F := (f, \varepsilon g)$, we obtain the boundary value problem

$$z' = F(z) \quad \text{with } z(a) \in B_a \subseteq E_{p_a}^u(C_0) \text{ and } z(b) \in B_b \subseteq E_{p_b}^s(C_0) \quad (11.66)$$

with $\dim(B_a) + \dim(B_b) = m + n$, and the two base points $p_a, p_b \in C_0$ are chosen to mark the region between which we want to compute the trajectory γ near C_ε ; see Figure 11.2, where we have chosen $\dim(B_a) = 2$ and $\dim(B_b) = 1$. Different types of boundary value solvers, e.g., as described in Sections 10.3 and 10.4, can now be used to solve (11.66). As a starting solution for the boundary value problem there are two common choices:

- (M1) Begin with a trajectory $\gamma_0 \subset C_0$ of the slow flow.
- (M2) Rewrite the boundary value problem as

$$z' = TF(z) \quad \text{with } z(0) \in B_a \subseteq E_{p_a}^u(C_0) \text{ and } z(1) \in B_b \subseteq E_{p_b}^s(C_0), \quad (11.67)$$

where $T = b - a$ to pose it for $t \in [0, 1]$; in (11.67), a prime denotes differentiation with respect to the shifted and scaled new time variable, which we still denote by t . We then declare T a free parameter and make B_b parameter-dependent, say $B_b(\alpha)$, and add one boundary condition. This formulates the problem as a two-parameter continuation boundary value problem; see Section 10.6. Begin with the constant solution $\gamma_0 \equiv p_a$ at one endpoint and continue in α , moving $B_b(\alpha)$ from p_a to p_b in α . The situation is illustrated in Figure 11.3.

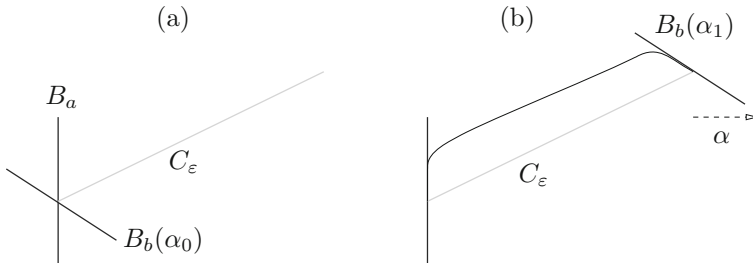


Figure 11.3: Sketch of the second way to run the SMST algorithm by starting with the zero solution. (a) We begin with $\gamma_0 \equiv p_a$ with $\alpha = \alpha_0$. (b) Then continuing in (α, T) pushes (or “drags”) the trajectory near C_0 .

Note carefully that both methods require knowledge about the critical manifold C_0 . For (M1), we need the slow flow defined on C_0 , and for (M2), the definition of $B_b(\alpha)$ requires us to move $B_b(\alpha)$ along C_0 in a suitable way. To demonstrate how the SMST algorithm can be used, we consider an example.

Example 11.5.2. Recall from Section 1.4 and Chapter 6 that the FitzHugh–Nagumo equation with diffusion can be written in a traveling wave frame as

$$\begin{aligned} \varepsilon \dot{x}_1 &= x_2, \\ \varepsilon \dot{x}_2 &= \frac{1}{5}(sx_2 - c(x_1) + y), \\ \dot{y} &= \frac{1}{s}(x_1 - y), \end{aligned} \tag{11.68}$$

where p, s are parameters and we fix $c(x_1) = x_1(x_1 - 1)(1/10 - x_1)$. Our goal is to use the SMST algorithm to compute a homoclinic orbit of (11.68). The critical manifold C_0 of the FitzHugh–Nagumo equation is the cubic curve

$$C_0 = \{(x_1, x_2, y) \in \mathbb{R}^3 : x_2 = 0, y = c(x_1)\}. \tag{11.69}$$

The two local nondegenerate extrema of $c(x_1)$ yield the fold points of C_0 . Denote the local minimum by $x_{1,-}$ and the local maximum by $x_{1,+}$. The critical manifold C_0 has three normally hyperbolic components:

$$C_0^{a-} = \{x_1 < x_{1,-}\} \cap C_0, \quad C_0^r = \{x_{1,-} < x_1 < x_{1,+}\} \cap C_0, \quad C_0^{a+} = \{x_{1,+} < x_1\} \cap C_0.$$

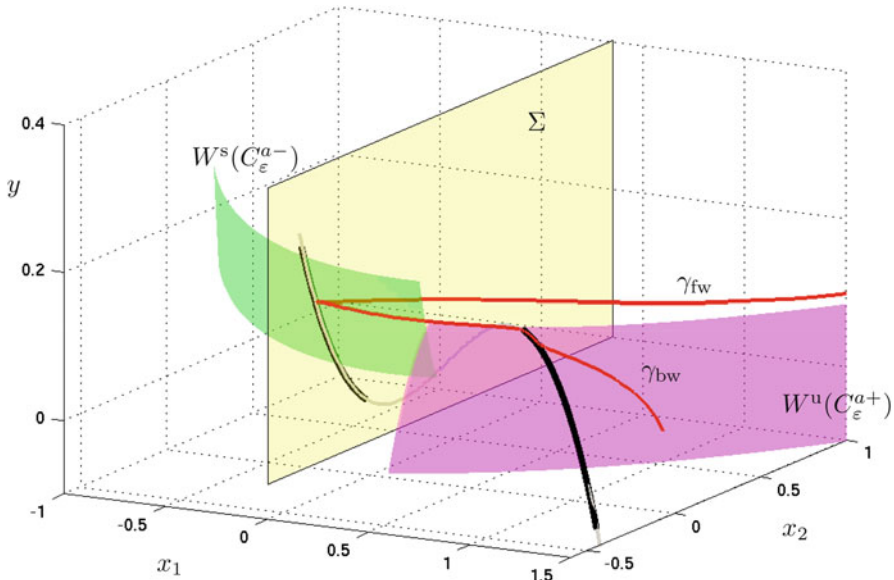


Figure 11.4: The slow manifolds $C_\varepsilon^{a\pm}$ are shown in black, and the critical manifold C_0 is shown in gray. We illustrate the transversal intersection of stable and unstable manifolds of the slow manifolds $W^s(C_\varepsilon^{a-})$ (green) and $W^u(C_\varepsilon^{a+})$ (magenta). The manifolds are truncated at the yellow section Σ , and the trajectory $\gamma_{fw} \cup \gamma_{bw}$ begun on Σ at the transversal intersection point x_{su} is shown in red. Parameter values are $\varepsilon = 0.001$ and $s = s_{\text{fast}} \approx 1.2463$.

Fenichel's theorem provides associated slow manifolds $C_\varepsilon^{a\pm}$ and C_ε^r outside neighborhoods of the fold points. The manifolds $C_\varepsilon^{a\pm}$ are of saddle type for ε sufficiently small. The middle branch C_ε^r is completely unstable in the fast directions. It can be shown that (11.68) has a unique equilibrium point, which we denote by

$$q := (0, 0, 0).$$

The unstable manifold $W^u(q)$ is one-dimensional, and the stable manifold $W^s(q)$ is two-dimensional. Homoclinic orbits exist if $W^u(q) \subset W^s(q)$. It is known that two homoclinic orbits exist at values $s = s_{\text{fast}}$ and $s = s_{\text{slow}}$ with $s_{\text{fast}} > s_{\text{slow}}$. Here we focus on the orbit consisting of two fast segments and two slow segments at $s = s_{\text{fast}}$, as discussed in Section 6.5, which is also referred to as a fast wave. Recall that the existence proof of this homoclinic orbit uses a perturbation of a singular trajectory consisting of four segments: a fast subsystem heteroclinic connection from q to C_0^{a+} at $y = 0$, a slow segment on C_0^{a+} , a fast subsystem heteroclinic from C_0^{a+} to C_0^{a-} at $y = k$ for some constant $k = k(s) > 0$, and a slow segment on C_0^{a-} connecting back to q . We aim to compute the homoclinic orbit numerically by a similar procedure for a given small $\varepsilon > 0$ in several steps:

- (S0) Find the parameter value s_{fast} at which the homoclinic orbit exists. This can be achieved by a splitting algorithm without computing the homoclinic orbit, even for very small values of ε ; see Section 11.7. Fix $s = s_{\text{fast}}$.
- (S1) Compute the slow manifolds $C_{\varepsilon}^{a\pm}$ using the SMST algorithm.
- (S2) Compute the unstable manifold of the equilibrium $W^u(q)$ by forward integration.
- (S3) Define a section $\Sigma = \{x_1 = \kappa\}$, where the constant κ is chosen between $x_{1,-}$ and $x_{1,+}$, e.g., $\kappa = (x_{1,-} + x_{1,+})/2$. Compute the transversal intersection of $W^s(C_{\varepsilon}^{a-})$ and $W^u(C_{\varepsilon}^{a+})$ on Σ , and call the intersection point $x_{su} = (\kappa, x_{2,su}, y_{su})$; see Figure 11.4. Integrate forward and backward starting at x_{su} to obtain trajectories γ_{fw} and γ_{bw} .
- (S4) The homoclinic orbit is approximated by a concatenation of the trajectory segments on $W^u(q)$, C_{ε}^{a+} , $W^u(C_{\varepsilon}^{a+}) \cap W^s(C_{\varepsilon}^{a-})$, and C_{ε}^{a-} computed in steps (S1)–(S4). The endpoints of these trajectory segments are exponentially close to one another and therefore indistinguishable numerically.

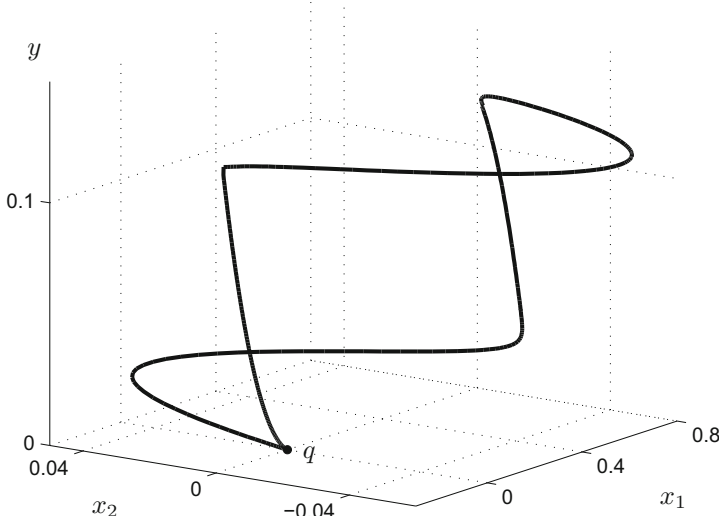


Figure 11.5: Homoclinic orbit of the FitzHugh–Nagumo equation representing a fast wave. The equilibrium point q at the origin, where the homoclinic orbit starts and ends, is shown as well.

All figures for this example are computed for $\varepsilon = 10^{-3}$, $s_0 \approx 1.2463$. The final output of the algorithm after interpolation near the truncation points is shown in Figure 11.5. Note that the red trajectory segment in Figure 11.4 illustrates very well why forward or backward integration would be hopeless. There is no way direct integration can track the two saddle-type slow manifolds

for a sufficient distance. Hence, we have demonstrated how to find an initial homoclinic orbit. This orbit can now, e.g., be used as a starting point for a continuation strategy described in Section 10.6. ♦

The computation of slow manifolds of saddle type in the three-dimensional FitzHugh–Nagumo equation turns out to be key to understanding the interaction between various classes of traveling waves; see Section 19.8.

11.6 Manifolds and Singularities

One problem with the methods presented so far is that they assume normal hyperbolicity of the slow manifold. In this section, we discuss techniques to compute slow manifolds past fold points and to continue maximal canard trajectories. To simplify the presentation, we focus on the case of one fast and two slow variables:

$$\begin{aligned}\frac{dx}{dt} &= x' = f(x, y, \varepsilon), \\ \frac{dy_1}{dt} &= y'_1 = \varepsilon g_1(x, y, \varepsilon), \\ \frac{dy_2}{dt} &= y'_2 = \varepsilon g_2(x, y, \varepsilon),\end{aligned}\tag{11.70}$$

where $z := (x, y)^\top \in \mathbb{R}^3$ and $0 < \varepsilon \ll 1$. In this section, let $S = S_0$ denote a compact subset of the critical manifold of (11.70). Suppose S_0 contains a fold curve F with a folded node; see Section 8.5. Denote the associated stable and unstable parts of the critical manifold by S_0^a and S_0^r . One possibility to compute trajectories past the fold curve is to frame the computations in terms of a two-point boundary value problem,

$$\frac{du}{d\tilde{t}} = u' = TF(u, \nu), \quad u(0) \in L, \quad u(1) \in \Sigma,\tag{11.71}$$

where $u = (x, y_1, y_2)$, $F = (f, \varepsilon g)$, $\nu \in \mathbb{R}^p$ represents system parameters, L and Σ are suitable subsets of \mathbb{R}^{m+n} , and $\tilde{t} = t/T$ is a rescaled time so that the problem is posed on the standard unit interval; see also Sections 10.3 and 10.4. Recall from Section 10.6 that (11.71) is solvable in a continuation-boundary-value setting if

$$\# \text{ free parameters} = (n + m) - \# \text{ boundary conditions} + 1,$$

where $n = 1$ and $m = 2$ in our context. For example, if we fix all the ν parameters and allow the integration time T to vary, then we must have

$$\dim(L) + \dim(\Sigma) = 3.$$

Consider the problem of computing S_ε^a . Let L be a curve in S_0^a well separated from F , and choose Σ as a plane transverse to F ; see Figure 11.6. A trajectory starting on L will rapidly approach S_ε^a and have a nonzero component parallel to Σ by the theory on folded nodes, discussed in Section 8.5. Hence, (11.71) is well posed in this context. Similarly, one computes S_ε^r up to F . A one-parameter continuation in T will now fill an open region in each part of the slow manifold.

The only remaining problem is to find an initial solution of (11.71). In the next example, a **homotopy method** is used to find this initial solution, i.e., a trivial solution is deformed into a suitable initial solution.

Example 11.6.1. Consider the **Koper model** in the following version:

$$\begin{aligned}\varepsilon_1 \dot{x} &= ky - x^3 + 3x - \lambda, \\ \dot{y} &= x - 2y + z, \\ \dot{z} &= \varepsilon_2(y - z).\end{aligned}\tag{11.72}$$

Formally, (11.72) is a three-time-scale system when ε_1 and ε_2 are both small. Here we shall consider only the case of two scales and fix the following parameters:

$$\varepsilon_1 = 0.1, \quad \varepsilon_2 = 1, \quad k = -10, \quad \lambda = 7,$$

so that (11.72) is a $(1, 2)$ -fast–slow system. The critical manifold is

$$C_0 = \left\{ (x, y, z) \in \mathbb{R}^3 : y = -\frac{1}{10}(x^3 - 3x + 7) =: c(x) \right\}.$$

Direct computation yields that there are two fold curves defined by $c'(x) = 0$ located at $x = \pm 1$. We shall focus on the folded node $p_{fn} = (-1, -0.9, -0.8)$ contained in the fold curve at $x = -1$. The goal is to compute $S_{\varepsilon_1}^a$ and $S_{\varepsilon_1}^r$. Choose boundary conditions

$$\begin{aligned}L^a &:= C_0 \cap \{(x, y, z) \in \mathbb{R}^3 : x = -1.5\}, \\ L^r &:= C_0 \cap \{(x, y, z) \in \mathbb{R}^3 : x = -0.2\}, \\ \Sigma_{fn} &:= \{(x, y, z) \in \mathbb{R}^3 : z = -0.8\},\end{aligned}$$

as shown in Figure 11.6. Consider the problem of computing $S_{\varepsilon_1}^a$. Start with a trivial solution to (11.71) given by

$$u(t) \equiv p_{fn} \quad \text{for } T = 0.$$

Fix one boundary condition of the solution to lie on the fold line $F = \{x = -1\}$. The first homotopy step is to employ numerical continuation in T until we reach

$$u(0) \in \tilde{\Sigma}^a := \{(x, y, z) \in \mathbb{R}^3 : z = -0.76\}.$$

The second homotopy step moves $u(0) \in S_0$ away from the fold curve approximately parallel to Σ_{fn} . To achieve this, consider the boundary condition defined by

$$u(0) \in \tilde{L}^a := C_0 \cap \tilde{\Sigma}^a.$$

Then we stop the continuation when L^a is reached. A similar approach can be applied for $S_{\varepsilon_1}^r$. The homotopy steps are illustrated in Figure 11.6(a)–(b). Once $S_{\varepsilon_1}^a$ and $S_{\varepsilon_1}^r$ are computed, it is possible to identify maximal canard trajectories as intersection points in Σ_{fn} . Two possible further calculations can then be easily implemented once the initial continuation-boundary-value framework has been set up:

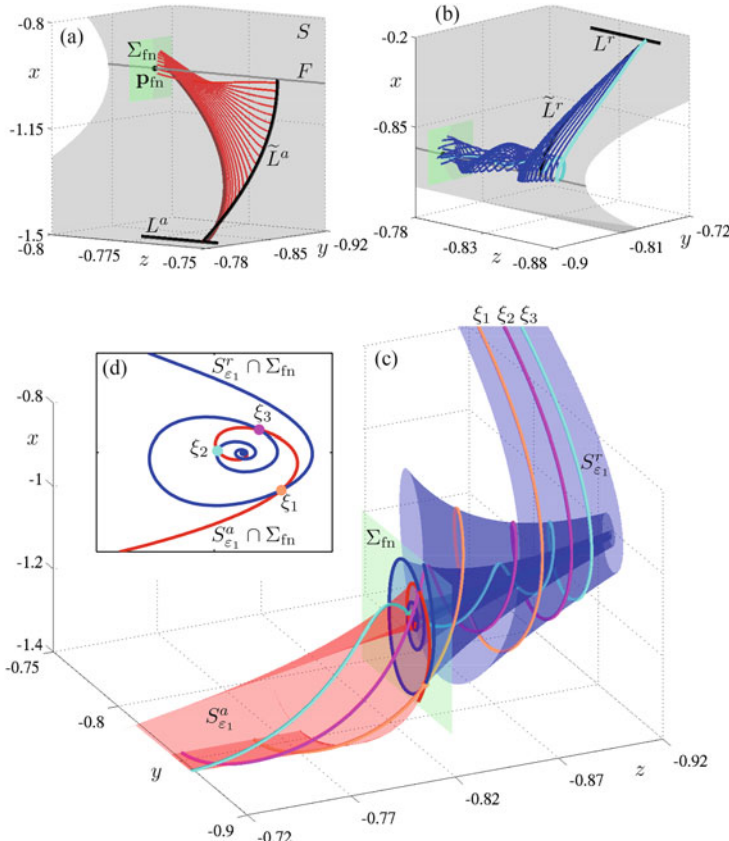


Figure 11.6: (a) and (b) show the homotopy steps to construct a suitable orbit segment to compute attracting (red) and repelling (blue) slow manifolds, respectively; also shown are a compact subset $S = S_0$ of the critical manifold and its fold curve F . The dark red orbit segment in panel (a) and the cyan orbit segment in panel (b) are obtained in the first homotopy step and connect L^a and L^r , respectively, with the section Σ_{fn} . The red and blue orbit segments are generated during the second homotopy step. Panel (c) shows the slow manifolds $S_{\varepsilon_1}^a$ and $S_{\varepsilon_1}^r$ of (11.72) computed up to the section Σ_{fn} . Furthermore, three secondary canards ξ_1 to ξ_3 are shown. Panel (d) shows the intersection curves of $S_{\varepsilon_1}^a$ and $S_{\varepsilon_1}^r$ in Σ_{fn} that are used to detect canard orbits. *Reprinted with permission from [DGK⁺12]. (Copyright 2012, Society for Industrial and Applied Mathematics)*

- (F1) Computing $S_{\varepsilon_1}^a$ and $S_{\varepsilon_1}^r$ beyond the fold point amounts to moving the section Σ_{fn} away from the fold.
- (F2) Maximal canards can be continued in parameter space as follows: Pick a maximal canard by finding an intersection point $S_{\varepsilon_1}^a \cap \Sigma_{fn} \cap S_{\varepsilon_1}^r$. Remove the boundary condition Σ_{fn} and rescale time along this orbit

to get a boundary value problem on $[0, 1]$. Then continue in suitable parameters, say (T, ε_1) with boundary conditions $u(0) \in L^a \subset S_0^a$ and $u(1) \in L^r \subset S_0^r$.

The techniques (F1) and (F2) will be used in Section 13.5 to analyze mixed-mode oscillations in the Koper model. ♦

Exercise/Project 11.6.2. Investigate secondary canards and their bifurcations discussed in Section 8.6 using (F1) and (F2). ◇

11.7 References

Section 11.1: There are two basic goals one might want to achieve by computing a slow manifold. The first is to reduce the system to the slow manifold, and the second is to understand the geometry of the manifold. These two aims provide insights into the system dynamics. For partial surveys and references on reduction methods with a focus slightly different from the presentation here, we refer to [GKS04, GKZ04, HMKS01]. The most classical reduction method is the quasi-steady-state assumption [BBS96, RSS11, RF91b, SS89, Sti98a], which has been applied to metabolic systems [KSG⁺98] and the Michaelis–Menten–Henri (MMH) reaction [BH25, Mei78]. Direct numerical integration is the first natural, but sometimes flawed, computational approach [Chi12] to obtaining the slow manifold.

Section 11.2: The section is based on the series of papers [ZKK04a, ZKK04b, ZKK05]. More details on the CSP method and its applications can be found in [Mea95, VCG⁺06, VGCN05]. If the fast fibers [BG13c] are computed as well, then one may bring the system into Fenichel normal form, which may be desirable [LO10]. CSP is essentially an iterative projection procedure, which is a common theme for slow manifold computation [ASST12, KAWC80]. It is an equally common theme to analyze a method by comparing its result to the invariance equation [GV06]. For a modern application of CSP to glycotic pathways, one may consider [KSG10]. A related method is G-scheme reduction, which also builds a local basis [VP09].

Section 11.3: The section is based on [GKKZ05, ZGKK09], but see also [ZVG⁺12]. ZDP has been applied, e.g., to enzyme kinetics [HZKW09]. Particularly in chemical systems, the reduction aspect of slow manifold computations is of primary importance [Jan89, HR02, Mas02, SFMH05]. Related topic headings in this direction are biochemical reaction networks [LL09b, LL10, RGZL08], enzymatic reactions [KJ11], stochastic networks [KK13, RA03], and various topics in systems biology [RF91c, RF91a, ZNK13]. A main application area for reduction methods is chemical combustion problems [ACGV07, ACC⁺07, DR96a]. Standard test problems for most methods are provided by the Michaelis–Menten–Henri (MMH) reaction [KKK⁺07], the Davis–Skodje example [DS99b, NF13], and the Lindemann mechanism [CS11].

Section 11.4: The section is based mainly on [KK02]; for another comparative study, we refer to [DS99b]. There are various applications in which Fraser’s method has been used [NF89, RF01]. The ILDM approach is considered in [MP92a, MP92b], and more on iterative methods can be found in [Fra88b, KBS12]. Even more details for ILDM [Maa98, MP92a, BGM08] and modified versions [BM07b, BGGM06, GGM04] have been considered. The papers [FH06, RMW99] show that one actually might be

tempted to prove stronger results than actually possible [BGG08]. ILDM can also be rephrased in the context of reaction–diffusion systems [BM07a]. In fact, it is a recent theme how one might push finite-dimensional ODE techniques to PDEs [MP13].

Section 11.5: This section is based on [GK09a, GK10b]. The boundary-value viewpoint and continuation have already been discussed and referenced in more detail in Section 10.9.

Section 11.6: This section is based mostly on [DKO10, DKO08a, DGK⁺12], but see also [EKO07]. Again, we refer to Section 10.9 for more references.

There is a variety of other methods available to compute invariant manifolds in low-dimensional systems [KOD⁺05], where the initial focus has been stable and unstable manifolds of equilibrium points. For example, one may use arc-length parameterization including remeshing [JKJ97], fat trajectories [Hen03], geodesic circles in combination with direct integration [GW93], geodesic circles together with a continuation-boundary-value approach [DCD⁺07, KO99, KO03], graph-transform methods [BHV07], PDE solvers for the invariance equation [GV04, Kaz00a, KG02], and set-oriented methods [DH96, DH97]. Although many methods are known, there is comparatively little extensive software development yet [CRK05].

Alternative approaches to reduction and invariant manifolds, which we have not discussed here, are curvature-based approaches [BYS10], diffusion maps to identify slow variables [BCGFS13, NLCK06], the ICE-PIC method [RPVG07], parameterization via stochastic terms [Abr13b], singular PDE methods [Kaz00a, KKS10, KG02], sloppy models [CTS12], transformation to fast–slow form [GDH04], and variational /optimization methods [Leb04, LS13, LSU11]. One may also compute a rigorous enclosure of slow manifolds [GJM12]. Similarly, interval arithmetic methods can be used for normally hyperbolic invariant manifolds of maps [CS12] to facilitate proofs.

Chapter 12

Scaling and Delay

This chapter has two major goals. The first is to analyze delayed loss of stability near fast subsystem bifurcation points with a focus on Hopf bifurcation. The second goal is to introduce several algebraic-combinatorial flavored tools, which turn out to be very helpful for multiscale systems.

Section 12.1 briefly recalls the fold singularity and the (small) delayed loss of stability of trajectories transitioning from slow to fast motion. A fundamental theorem on (large) delayed stability loss near a fast subsystem Hopf bifurcation is stated and proved in Section 12.2; a variation on this theme and the application of asymptotic analysis to it are covered in Section 12.3. Section 12.4 introduces the Newton polygon as a combinatorial tool. It appears in various parts of mathematics but also has quite interesting uses for fast–slow dynamics, which are covered in Sections 12.5–12.8. In fact, the Newton polygon can be used as an auxiliary tool to compute critical manifolds, to find blowup coefficients, and to compute the scaling laws of delay times and slow manifolds.

Background: No additional background is required. However, there are deep relations to Chapters 7–9, so skipping those chapters and starting here is possible, but it is probably not the optimal reading order.

12.1 The Fold Revisited

We have already encountered the loss of normal hyperbolicity in a fast–slow system in many circumstances. In this chapter, we are going to deal with this problem by focusing on scaling laws and delay times. To illustrate the basic problem, we are very briefly going to revisit the fold singularity. A normal form of the generic planar fold singularity is given by

$$\begin{aligned}\varepsilon \dot{x} &= \varepsilon \frac{dx}{d\tau} = -y - x^2, \\ \dot{y} &= \frac{dy}{d\tau} = 1.\end{aligned}\tag{12.1}$$

The critical manifold $C_0 = \{(x, y) \in \mathbb{R}^2 : y = -x^2\}$ is normally hyperbolic away from the fold bifurcation point $(x, y) = (0, 0)$ of the fast subsystem. The curve $C_0^a := C_0 \cap \{x > 0\}$ consists of attracting equilibrium points for the fast subsystem, while points on $C_0^r := C_0 \cap \{x < 0\}$ are repelling.

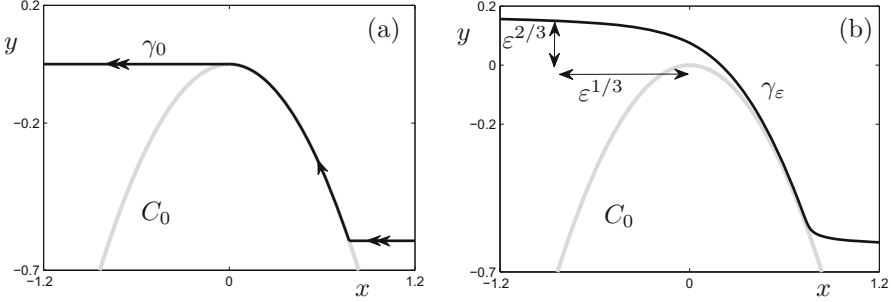


Figure 12.1: Illustration for (12.1). (a) Singular limit $\varepsilon = 0$ with a candidate trajectory γ_0 consisting of two fast and one slow segment is shown. (b) Trajectory γ_ε for (12.1) with $\varepsilon = 0.02$ and initial condition $(x(0), y(0)) = (1.2, -0.6)$.

Figure 12.1 illustrates the geometry of the fold point. The trajectory γ_0 in Figure 12.1(a) is a candidate trajectory that first approaches C_0^a , then follows the slow flow on C_0^a , and finally jumps off at the fold point. Figure 12.1(b) shows the perturbation γ_ε of the candidate for $\varepsilon = 0.02$. For every $0 < \varepsilon \ll 1$, a trajectory near the slow manifold C_ε^a will still approach the region near the fold at $(0, 0)$, but it passes through this region with a nontrivial scaling behavior. In particular, we have shown in Section 5.4 using asymptotics and in Section 7.4 using the blowup method that the correct scaling near $(0, 0)$ is given by

$$(x, y) \sim (\varepsilon^{1/3}, \varepsilon^{2/3}) \quad \text{as } \varepsilon \rightarrow 0,$$

as shown in Figure 12.1(b). This **scaling law** defines a neighborhood of the fold point

$$\mathcal{N}_\varepsilon := \{(x, y) \in \mathbb{R}^2 : |x| < k_1 \varepsilon^{1/3}, |y| < k_2 \varepsilon^{2/3}\}$$

for some positive constants $k_{1,2} = \mathcal{O}(1)$. The set \mathcal{N}_ε shrinks to the fold point itself as $\varepsilon \rightarrow 0$. Furthermore, we could say that γ_ε has a short **delay** of order $\mathcal{O}(\varepsilon^{2/3})$ in its y -coordinate before the jump. Note that near a canard point of a fold singularity (see Section 8.1), there exist maximal canard trajectories with an arbitrarily long delay. Our goal in this chapter is to quantify the scaling and delay effects in fast-slow systems. In particular, we are going to introduce several new techniques that complement the blowup method and direct asymptotics.

12.2 Delayed Hopf Bifurcation

Consider a Hopf bifurcation in a fast–slow system with two fast variables and one slow variable with the Hopf bifurcation occurring in the fast subsystem. We begin with an example to illustrate the main dynamical properties.

Example 12.2.1. Consider the $(2, 1)$ -fast–slow system

$$\begin{aligned}\varepsilon \frac{dx_1}{d\tau} &= \varepsilon \dot{x}_1 = yx_1 - x_2 - x_1(x_1^2 + x_2^2), \\ \varepsilon \frac{dx_2}{d\tau} &= \varepsilon \dot{x}_2 = x_1 + yx_2 - x_2(x_1^2 + x_2^2), \\ \frac{dy}{d\tau} &= \dot{y} = 1.\end{aligned}\tag{12.2}$$

On the fast time scale $t = \tau/\varepsilon$, equation (12.2) becomes

$$\begin{aligned}\frac{dx_1}{dt} &= x'_1 = yx_1 - x_2 - x_1(x_1^2 + x_2^2), \\ \frac{dx_2}{dt} &= x'_2 = x_1 + yx_2 - x_2(x_1^2 + x_2^2), \\ \frac{dy}{dt} &= y' = \varepsilon.\end{aligned}\tag{12.3}$$

The critical manifold of (12.2)–(12.3) is $C_0 = \{(x_1, x_2, y) \in \mathbb{R}^3 | x_1 = 0 = x_2\}$, which is just the y -axis. Setting $\varepsilon = 0$ in (12.3) yields the fast subsystem, which is identical to a (supercritical) **Hopf bifurcation normal form**. Hence, one should think of (12.3) as a Hopf normal form with y as a slowly varying parameter that drives the fast variables through the Hopf bifurcation point at $y = 0$. Using cylindrical coordinates $(x_1, x_2, y) = (r \cos \theta, r \sin \theta, y)$, it follows that (12.2) can be rewritten as

$$\begin{aligned}\varepsilon \dot{r} &= r(y - r^2), \\ \varepsilon \dot{\theta} &= 1, \\ \dot{y} &= 1.\end{aligned}\tag{12.4}$$

Assume that we start with $y(0) < 0$. From (12.4), we see that if $y < 0$, then $\dot{r} < 0$, and hence solutions decay toward the origin. Taking into account that $y(\tau) = \tau + y(0)$, we see that there is a Hopf bifurcation in the fast subsystem at $\tau = -y(0)$. For $y > 0$, solutions starting slightly perturbed from the origin are going to spiral away from it. Basically, this is the standard supercritical Hopf bifurcation scenario that yields a transition from stationary solutions for $y < 0$ to periodic solutions for $y > 0$, which are given by $r = \pm\sqrt{y}$.

The question is how the slow movement in the y -component interacts with the fast directions. Figure 12.2 shows a numerical solution γ_ε of (12.3). For $y < 0$, the trajectory γ_ε moves toward the attracting part of the critical manifold $C_0^a = C_0 \cap \{y < 0\}$. Thereafter, the Hopf bifurcation γ_ε is close to the repelling critical manifold $C_0^r = C_0 \cap \{y > 0\}$ for a substantial time after the bifurcation point at $y = 0$. This delay effect, which causes γ_ε to stay close to the repelling part of slow manifold, is the key feature of delayed Hopf bifurcation. In fact, γ_ε can also be viewed as a canard in the sense of Definition 8.1.5. ♦

Definition 12.2.2. A Hopf bifurcation in a fast subsystem of a fast–slow system in which a slow variable acts as a Hopf bifurcation parameter is called a **delayed Hopf bifurcation**.

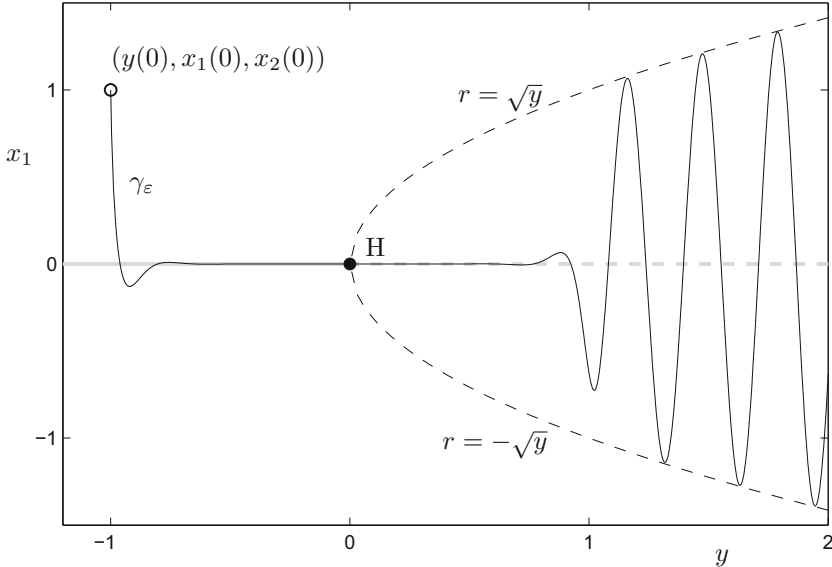


Figure 12.2: Projection onto (y, x_1) -space of a numerical solution γ_ε (thin black curve) for the delayed Hopf equations (12.3) with $\varepsilon = 10^{-3}$. The initial condition $(x_1(0), x_2(0), y(0)) = (1, 1, -1)$ is marked by a circle, the Hopf bifurcation point H at the origin by a dot. The attracting critical manifold C_0^a (thick solid gray) and the repelling critical manifold C_0^r (thick dashed gray) are shown, and the periodic orbits for the static Hopf bifurcation ($\varepsilon = 0$, thin dashed black curves) for $r = \pm\sqrt{y}$ show the effect of the delay; note that $r^2 = (x_1)^2 + (x_2)^2$ using cylindrical coordinates.

Our next goal is to quantify the delay. We consider a general $(2, 1)$ -fast–slow system

$$\begin{aligned} x'_1 &= f_1(x_1, x_2, y, \varepsilon), \\ x'_2 &= f_2(x_1, x_2, y, \varepsilon), \\ y' &= \varepsilon g(x_1, x_2, y, \varepsilon), \end{aligned} \tag{12.5}$$

and employ the notation $f := (f_1, f_2)^\top$. Throughout this section, we make the following assumptions:

- (A1) The critical set $C_0 = \{f_1 = 0, f_2 = 0\}$ of (12.5) is a smooth manifold.
- (A2) A preliminary coordinate change has been applied to rectify C_0 along the y -axis so that $C_0 = \{(x_1, x_2, y) \in \mathbb{R}^3 | x_1 = 0 = x_2\}$.
- (A3) C_0 is normally hyperbolic except at $0 = (0, 0, 0)$; C_0 is attracting for $y < 0$ and repelling for $y > 0$.
- (A4) The fast subsystem of (12.5) has a nondegenerate supercritical Hopf bifurcation for $y = 0$, i.e., a complex conjugate pair of eigenvalues $\lambda_{1,2}(y) \neq 0$ for $(D_x f)(y)$ crosses the imaginary axis at nonzero speed $v := \frac{d}{dy} \operatorname{Re}(\lambda_{1,2})|_{y=0}$.

The assumptions (A1)–(A4) yield a generic supercritical delayed Hopf bifurcation. Regarding (A1)–(A2), note that C_0 is generically not an invariant manifold for the full system ($\varepsilon > 0$) i.e., the assumptions are more general than (12.2), where we have the special case that $\{x_1 = 0 = x_2\}$ is also invariant for $\varepsilon > 0$. Regarding (A4), one may also prove the results stated below for the subcritical Hopf bifurcation, and we restrict attention to a single scenario to simplify the exposition. Furthermore, one could try to take into account additional fast variables, say $x \in \mathbb{R}^m$ for $m > 2$, but that leads to additional technical complications that we do not discuss here.

Consider the slow flow of (12.5) given by $\dot{y} = g(0, 0, y, 0)$ and denote its solution starting at $y_0 = y(0) < 0$ by $y^0(\tau)$. Define τ_* by $y^0(\tau_*) = 0$; the slow time τ_* is precisely the time of Hopf bifurcation for the fast subsystem.

Theorem 12.2.3 ([Nei87b, Nei88]). *Suppose the assumptions (A1)–(A4) for (12.5) hold and $0 < \varepsilon \ll 1$ is sufficiently small. Consider a solution $\gamma(\tau) = \gamma(\varepsilon t)$ of (12.5) starting at some $(x_1(0), x_2(0), y(0))$ that is $\mathcal{O}(\varepsilon)$ -close to C_0 . Assume that $y(0)$ is negative and bounded away from zero. Then it will be in an $\mathcal{O}(\varepsilon)$ -neighborhood of C_0 for some delay time beyond the bifurcation point $y = 0$. Several cases can occur:*

- Analytic case: Suppose f, g are real analytic and have complex analytic continuations in the (x, y) -variables in a neighborhood of the origin, remaining smooth with respect to ε . Then γ has a delay time $\tau_* + \tau_K$, where $\tau_K > 0$ is bounded away from zero, i.e., we have “ $\mathcal{O}(1)$ -delay.”
- Smooth case: Suppose $f, g \in C^\infty$. Then the generic delay time is given by $\tau_* + \sqrt{M(\varepsilon)\varepsilon|\ln \varepsilon|}$, where $M(\varepsilon) \rightarrow \infty$ monotonically as $\varepsilon \rightarrow 0$.
- Finite smoothness case: Suppose $f, g \in C^l$ for some $l < \infty$. Then the generic delay time is $\tau_* + \sqrt{2/v(l-3/2)\varepsilon|\ln \varepsilon|}$, or asymptotically, $\tau_* + \mathcal{O}(\sqrt{\varepsilon|\ln \varepsilon|})$.

Remark: In the analytic case, we get a canard orbit. For background on complex analysis and analytic continuation, see [Gam01]. Note that in the nonanalytic cases, the delay can be very short for ε sufficiently small, and in such cases, we have to avoid the situation that C_0 is also an invariant manifold for the full system ($0 < \varepsilon \ll 1$), i.e., generic higher-order perturbation terms are required to obtain a “short” delay.

Proof. (Sketch; [Nei87b, Nei88, Arn94]) We begin with the analytic case for (12.5). The equations for the fast variables $x = (x_1, x_2)$ can be written as

$$x' = A(y, \varepsilon)x + \varepsilon h(y, \varepsilon) + \mathcal{O}(\|x\|^2), \quad (12.6)$$

where $A = A(y, \varepsilon)$ is a matrix-valued function. Then we apply a change of variable to (12.6) given by

$$\tilde{x} = x + \varepsilon A^{-1}h. \quad (12.7)$$

This change of variables is well defined in a suitable neighborhood of the Hopf bifurcation at $y = 0$, since the eigenvalues of A are nonzero by assumption (A4). Calculating the system for \tilde{x} yields

$$\begin{aligned} x' &= \tilde{x}' - \varepsilon y'[(DA^{-1})h + A^{-1}\nabla h]h = A[\tilde{x} - \varepsilon A^{-1}h] + \varepsilon h + \mathcal{O}(\|x\|^2) \\ \Rightarrow \tilde{x}' &= A\tilde{x} + \varepsilon \underbrace{(\varepsilon g[(DA^{-1})h + A^{-1}\nabla h])}_{=: \tilde{h}(y, \varepsilon)} + \mathcal{O}(\|x\|^2). \end{aligned}$$

Hence, we note that the new function $\tilde{h}(y, \varepsilon)$ has order $\mathcal{O}(\varepsilon)$. This process can be continued to achieve $\mathcal{O}(\varepsilon^2)$, $\mathcal{O}(\varepsilon^3)$, etc. The sequence of coordinate changes will usually diverge, but direct estimates show that an $\mathcal{O}(1/\varepsilon)$ number of them makes the h -function exponentially small, i.e., $\mathcal{O}(e^{-K/\varepsilon})$ for some $K > 0$. This finite sequence of coordinate changes controls the influence of the slow drift in the fast variables. Next, consider a trajectory $\gamma(t) = (x(t), y(t))$ starting at

$$(x_1(0), x_2(0), y(0)) =: (x_0, y_0)$$

with y_0 chosen such that γ reaches $y = 0$ in a fast time t of order $\mathcal{O}(1/\varepsilon)$, which corresponds to a slow time τ of order $\mathcal{O}(1)$. This means that $\|x(t)\|$ will quickly decrease up to being exponentially close to the slow manifold C_ε ; this observation uses the fact that h is exponentially small, and we have

$$\|x(\tau_*/\varepsilon) - p_\varepsilon\| = \mathcal{O}(e^{-K/\varepsilon}) \quad \text{for some } p_\varepsilon \in C_\varepsilon.$$

For times $\varepsilon t = \tau > \tau_*$, there is a delay effect, since $x(t)$ has to leave an $\mathcal{O}(\varepsilon)$ -neighborhood of the slow manifold C_ε . This repulsion phase takes a fast time of order $\mathcal{O}(1/\varepsilon)$, i.e., a slow time, bounded below by a constant $\tau_K > 0$, $\tau_K = \mathcal{O}(1)$. This shows that the delay time is $\tau_* + \tau_K$ on the slow time scale, and that concludes the analytic case.

Similar arguments can be used for the other two cases. In fact, the key point is that if $f, g \in C^l$, then the sequence of coordinate changes (12.7) terminates when $h = \mathcal{O}(\varepsilon^l)$. Therefore, when γ reaches $y = 0$, we have $\|x(\tau_*/\varepsilon) + p_\varepsilon\| = \mathcal{O}(\varepsilon^{l+1})$. For the x -coordinate to grow from an $\mathcal{O}(\varepsilon^{l+1})$ -neighborhood of C_ε to leave an $\mathcal{O}(\varepsilon)$ -neighborhood of C_ε requires a slow time of order $\mathcal{O}(\sqrt{\varepsilon |\ln \varepsilon|})$. \square

Exercise 12.2.4. Explicitly check the statements about decay/growth of the x -coordinate in the proof of Theorem 12.2.3. Assume for simplicity that the fast variables have no terms of order $\mathcal{O}(\|x\|^2)$. \diamond

As a next step, one would like to calculate explicitly the time when a trajectory leaves the neighborhood of the critical manifold C_0 in the analytic case. Again, we consider only trajectories $\gamma(\tau)$ that start $\mathcal{O}(1)$ away from C_0 with $y(0) = y_0 < 0$.

Definition 12.2.5. A slow time τ is called an **asymptotic moment of jumping** of a trajectory if in an $\mathcal{O}(\varepsilon |\ln \varepsilon|)$ -neighborhood of τ , there is an interval $[\tau_a, \tau_b]$ such that $\gamma(\tau_a)$ is $\mathcal{O}(\varepsilon)$ -close to C_0 and $\gamma(\tau_b)$ is $\mathcal{O}(1)$ separated from C_0 . A time is called an **asymptotic moment of falling** if it is an asymptotic moment of jumping on reversing time.

Remark: In addition to asymptotic moments of jumping or falling, the terminology of **separation time** and **collapse time** are sometimes used.

The asymptotic moment of jumping is precisely the time when a trajectory leaves the vicinity of C_0 and the delay stops. Recall that $\lambda_{1,2}(y)$ denote the eigenvalues of the linearized fast subsystem, and $y^0(\tau)$ denotes the slow-flow solution. Assume without loss of generality that $\text{Im}(\lambda_1) < 0$. Define the **complex phase** as

$$\Psi(\tau) := \int_{\tau_*}^{\tau} \lambda_1(y^0(s)) \, ds.$$

Observe that $\text{Re}(\Psi(\tau))$ has a nondegenerate minimum for $\tau = \tau_*$. Hence, for times τ sufficiently close to τ_* , one can define a function Π that maps a time $\tau < \tau_*$ to a time $\Pi(\tau) > \tau_*$ by the condition

$$\text{Re}[\Psi(\tau)] = \text{Re}[\Psi(\Pi(\tau))]. \quad (12.8)$$

The function Π is often referred to as a **way-in/way-out map** or **input–output function**. The key idea for making use of (12.8) is to extend the time variable τ to the complex plane, i.e., $\tau \in \mathbb{C}$. In doing this, it is possible to connect pairs τ and $\Pi(\tau)$ by an arc in the complex plane given by

$$L = \{\tau \in \mathbb{C} \mid \text{Re}[\Psi(\tau)] = \text{const}\}.$$

Exercise 12.2.6. Show that for points on the real axis with vertical tangents to L , we may conclude that λ_1 is real (and hence so is λ_2 , by the assumption that we have a conjugate pair of eigenvalues). \diamond

See also Figure 12.3. The arcs L are level sets of the function $\text{Re}[\Psi(\tau)]$. Obviously, one may also consider the complex conjugate \bar{L} of the arc L . Near $\tau = \tau_*$, the following conditions hold:

- (C1) The slow-flow solution is analytic, and f, g are analytic at points of the slow-flow solution.
- (C2) $\lambda_{1,2}(y(\tau)) \neq 0$ and $\lambda_1(y(\tau)) \neq \lambda_2(y(\tau))$.
- (C3) No tangent to the curves L is vertical.

Observe that (C1)–(C3) follow from the assumptions (A1)–(A4) near $\tau = \tau_*$. However, (C1)–(C3) might eventually fail once the trajectory is far away from the Hopf point of the fast subsystem. Let τ^- and τ^+ be the lower and upper bounds of endpoints of arcs L for which (C1)–(C3) hold. Let Γ be the arc starting at τ^- and ending at τ^+ on which $\text{Re}(\Psi(\tau))$ is constant. Denote the domain in the complex z -plane bounded by Γ and its conjugate arc $\bar{\Gamma}$ by \mathcal{K} ; see Figure 12.3.

Theorem 12.2.7 ([Nei87b, Nei88]). *Suppose $\tau_0 \in (\tau^-, \tau^+)$ is an asymptotic moment of falling. Then $\Pi(\tau_0)$ is an asymptotic moment of jumping. On the interval*

$$(\tau_0 + K\varepsilon|\ln \varepsilon|, \Pi(\tau_0) - K\varepsilon|\ln \varepsilon|), \quad \text{for some fixed constant } K > 0,$$

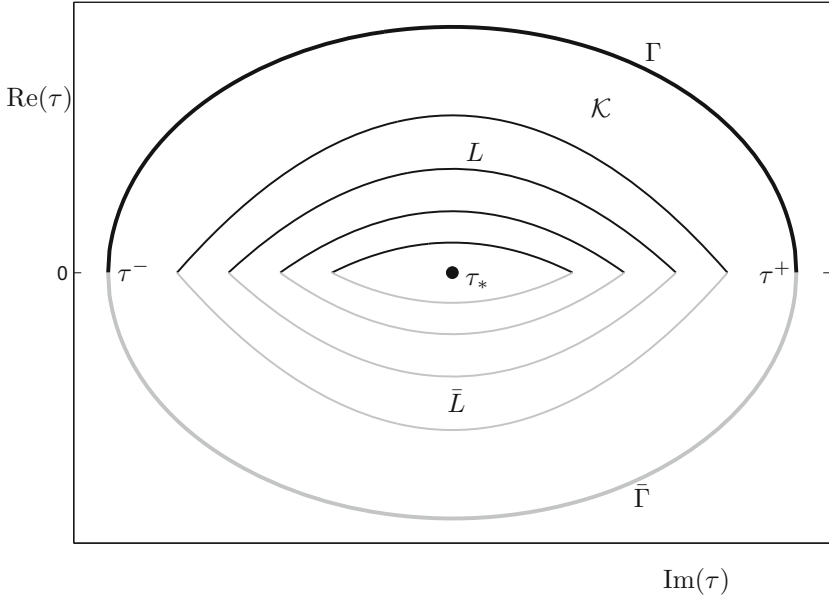


Figure 12.3: Sketch to illustrate the definitions associated with the way-in/way-out map (12.8). Arcs connecting to real time points are shown (upper half-plane in black, complex conjugate arc in gray). The region \mathcal{K} is bounded by a level curve $\Gamma \cup \bar{\Gamma}$ where the conditions (C2)–(C3) fail. Indeed, (C3) obviously fails, since there are vertical tangents at τ^\pm , while the failure of (C2) is discussed in Exercise 12.2.6.

the solution is $\mathcal{O}(\varepsilon)$ -close to C_0 . If $\tau_0 < \tau^-$ holds for the moment of falling, then the solution remains near C_0 until $\tau < \tau^+ - \delta(\varepsilon)$, where $\delta(\varepsilon) \rightarrow 0$ as $\varepsilon \rightarrow 0$.

Basically, Theorem 12.2.7 allows us to compute the asymptotic moment of jumping using the way-in/way-out map if we know where the trajectory enters a neighborhood of C_0 . We are only going to outline the main steps of the proof.

Proof. (Sketch, [Nei88]) Consider a trajectory $\gamma = \gamma(t) = (x(t), y(t))$ of the full system (12.5) before it enters an $\mathcal{O}(\varepsilon)$ -neighborhood of C_0 . Using the same technique as in the proof of Theorem 12.2.3, it is not difficult to show that the (2, 1)-fast–slow system can be written as

$$\begin{aligned} z' &= \Lambda(y)z + \mathcal{O}(|z|^2) + \mathcal{O}(\varepsilon^3), \\ y' &= \varepsilon G(y) + \varepsilon \mathcal{O}(|z|^2) + \mathcal{O}(\varepsilon^3), \end{aligned} \tag{12.9}$$

where $z = x_1 + ix_2$ is the standard change to complex coordinates for the fast subsystem and $\Lambda(y), G(y)$ denote the leading-order terms as $|z|, \varepsilon \rightarrow 0$; we note that $\Lambda(y), G(y)$ may also depend upon ε , but we do not display this dependence in the notation. Define t_1 as the first fast time when $|z(t)| = \varepsilon$ for the trajectory

γ . Let $y^\varepsilon(\tau)$ denote the solution to the truncated slow equation $y' = \varepsilon G(y)$. Consider the perturbed phase

$$\Psi_\varepsilon(\tau) = \int_{\tau_*}^{\tau} \Lambda(y^\varepsilon(s)) \, ds.$$

The perturbed version of the phase also has level curves $\{\text{Re}(\Psi_\varepsilon(\tau)) = \text{const}\}$ in the upper half of the complex τ -plane. Let Γ_ε denote the arc with left endpoint εt_1 and denote the right endpoint by $\Pi_\varepsilon(\varepsilon t_1)$. One may view Π_ε as the perturbation of the way-in/way-out map, so that

$$\Pi_\varepsilon(\varepsilon t_1) = \Pi(\tau_0) + \mathcal{O}(\varepsilon |\ln \varepsilon|).$$

Let \mathcal{K}_ε denote the domain bounded by Γ_ε and $\overline{\Gamma_\varepsilon}$. Define $S(T)$ as the part of \mathcal{K}_ε to the left of the vertical line $\text{Re}(\tau) = T$. Continue the solution $\gamma = (z, y)$ analytically into some disk with center at t_1 . If T is sufficiently close to t_1 in the complex plane, then the following inequalities hold:

$$|z(t)| < \kappa_1 \varepsilon \quad \text{and} \quad |y(t) - y^\varepsilon(\varepsilon t)| < \varepsilon. \quad (12.10)$$

Let T_1 be the value of T for which the inequalities (12.10) fail to hold in $S(T_1) =: S_1$ on analytic continuation of the solution. The goal is then to prove that

$$\varepsilon T_1 = \Pi_\varepsilon(\varepsilon t_1) = \Pi(\tau_0) + \mathcal{O}(\varepsilon |\ln \varepsilon|). \quad (12.11)$$

To prove (12.11), one has to estimate the solution components y and z . Since $|z| < \kappa_1 \varepsilon$, it follows that $y' = \varepsilon G(y) + \mathcal{O}(\varepsilon^3)$. Therefore, $y(t)$ will stay sufficiently close to the slow solution y^ε as long as $|z|$ is small. Hence, the main problem is to estimate the fast variables $z = (x_1, x_2)$; of course, this is not surprising, since we are interested in when we jump off in the fast directions. The bounds (12.10) imply that

$$z' = \Lambda(y^\varepsilon(\varepsilon t)) z + \mathcal{O}(\alpha) \quad (12.12)$$

for $t \in S_1$, where $\alpha = \varepsilon^2$ for $\text{Re}(t) < t_1 + \mathcal{O}(|\ln \varepsilon|)$ and $\alpha = \varepsilon^3$ for $\text{Re}(t) \geq t_1 + \mathcal{O}(|\ln \varepsilon|)$. Each point in S_1 can be reached by moving along Γ_ε (or using the conjugate arc) and then moving along the line $\{\text{Re}(t) = \text{const}\}$. Observe that on Γ_ε , the differential equation (12.12) becomes

$$\frac{dz}{d\sigma} = i\omega(\varepsilon\sigma)z + \mathcal{O}(\alpha), \quad (12.13)$$

where σ is a variable parameterizing Γ_ε by arc length. A major observation of the proof is that the function $\omega(\cdot)$ is real-valued on Γ_ε , since as $\text{Re}(\Psi_\varepsilon)$ is constant on the level curve. Dropping the higher-order term $\mathcal{O}(\alpha)$ from (12.13) shows that $|z(t)|$ is constant for $t \in \Gamma_\varepsilon$ (check: $d|z|/dt = 0$). Hence, for the equation with the higher-order term, it is not difficult to prove that

$$|z(t)| = |z(t_1)| + \mathcal{O}(\varepsilon^2 |\ln \varepsilon|) < \frac{3}{2} \varepsilon.$$

Once we are moving on a vertical line, the equation (12.12) becomes

$$\frac{dz}{ds} = -i\Lambda(y^\varepsilon(\varepsilon t))z + \mathcal{O}(\alpha).$$

By condition (C3), the vertical line in S_1 intersects $\{\operatorname{Re}(\Psi_\varepsilon) = \text{const}\}$ transversally. Hence, $\operatorname{Re}(\Psi_\varepsilon)$ is decreasing along this line, and this implies that the function $-i\Lambda(y^\varepsilon(\varepsilon t))$ has a nonzero negative real part. Therefore, $|z(t)|$ can only decrease on this part, and we conclude that $|z(t)| < \frac{3}{2}\varepsilon$ for $t \in S_1$. As long as we can analytically continue and (C1)–(C3) hold, the inequalities (12.10) are preserved, so that (12.11) must also be true. \square

From a practical point of view, the problem is how to calculate the way-in/way-out map $\Pi(\cdot)$. This problem often reduces, at least in principle, to dealing with the integral

$$\Psi(\tau) = \int_{\tau_*}^{\tau} \lambda_1(y^0(s)) \, ds,$$

which is used to define $\Pi(\cdot)$. To understand the problems involved, it helps to work through an example.

Example 12.2.8. We return to a slightly modified version of Example 12.2.1, which coupled the planar Hopf normal form with a slowly varying parameter. Now we consider

$$\begin{aligned} x'_1 &= yx_1 - x_2 - x_1(x_1^2 + x_2^2) + \mathcal{O}(\varepsilon), \\ x'_2 &= x_1 + yx_2 - x_2(x_1^2 + x_2^2) + \mathcal{O}(\varepsilon), \\ y' &= \varepsilon, \end{aligned} \tag{12.14}$$

where the $\mathcal{O}(\varepsilon)$ terms are assumed to be generic in the sense that they destroy the invariance of the critical manifold $C_0 = \{x_1 = 0 = x_2\}$ for $\varepsilon > 0$. The eigenvalues of the Jacobian at the origin are $\lambda_{1,2} = y \pm i$. The slow-flow solution is $y^0(\tau) = \tau + y^0(0)$. The Hopf bifurcation of the fast subsystem occurs for $\tau_* = -y^0(0)$. Therefore, we get

$$\Psi(\tau) = \int_{-y^0(0)}^{\tau} [y^0(s) - i] \, ds = \int_{-y^0(0)}^{\tau} [s + y^0(0) - i] \, ds.$$

To work out the level curves $\{\operatorname{Re}(\Psi(\tau)) = \text{const}\}$, it suffices to consider the case $y^0(0) = 0$ and $\tau_* = 0$. Substituting some complex time $\tau = a + bi$ for $a, b \in \mathbb{R}$, it follows that

$$\Psi(\tau) = \int_0^{a+bi} [s - i] \, ds = \frac{1}{2}(a + bi)^2 - i(a + bi) = \frac{1}{2}(a^2 - b^2) + abi - ia + b.$$

Therefore, an explicit formula for the level curves is

$$\operatorname{Re}(\Psi(\tau)) = \frac{1}{2}(a^2 - b^2) + b.$$

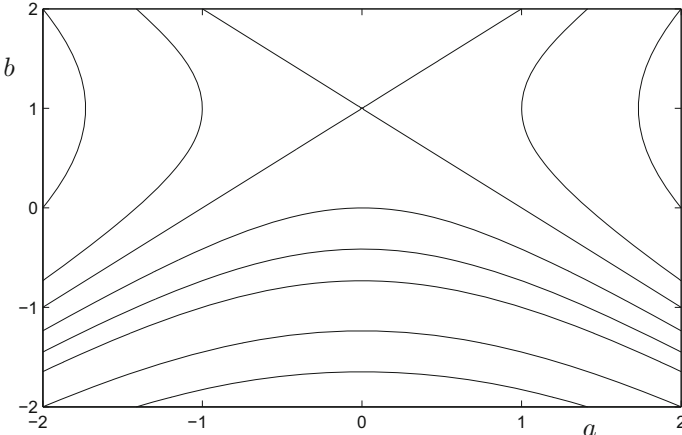


Figure 12.4: Level curves $\{\operatorname{Re}(\Psi(\tau)) = c\}$ in the complex τ -plane ($\tau = a + bi$) for $c = \pm\frac{1}{2}, \pm 1, \pm 2, -3$ are shown.

Some of the level curves $\{\operatorname{Re}(\Psi(\tau)) = \text{const}\}$ are shown in Figure 12.4. Observe that the eigenvalue $\lambda_1 = \tau - i$ becomes zero when $\tau = i$ and (C2) fails. Therefore, a natural guess for the relevant region \mathcal{K} is that it is bounded by the two line segments from $\tau = \pm 1$ to $\tau = i$ and the respective conjugate lines. Indeed, (C1) is clearly satisfied inside \mathcal{K} . To check condition (C3), we simply differentiate with respect to b :

$$\frac{\partial}{\partial b} \operatorname{Re}(\Psi(a + bi)) = -b + 1.$$

Hence, vertical tangents occur at $b = 1$. It follows that \mathcal{K} is indeed bounded by the two line segments from $\tau = \pm 1$ to $\tau = i$ and the respective conjugate lines. Furthermore, this yields $\tau^- = -1$ and $\tau^+ = 1$. Theorem 12.2.7 implies that for falling moments $\tau_0 \in (\tau^-, \tau_*)$, the delay is $\tau_* + \tau_0$. In fact, one may show that τ^+ is also an asymptotic moment of jumping for $\tau_0 < \tau^-$, but we omit the details of this calculation here. ♦

Exercise/Project 12.2.9. The delayed Hopf phenomenon appears in the context of other fast–slow singularities. Consider the singular Hopf normal form (13.7), which exhibits a folded saddle node of type II according to the classification in Lemma 8.5.7. Find a rescaling such that near a folded saddle node of type II, the system (13.7) becomes a $(2, 1)$ -fast–slow system, and determine the points of delayed Hopf bifurcation in this system. ◇

Exercise 12.2.10. Use averaging from Section 9.6 to calculate the effective slow flow on the family of periodic orbits in (12.2). ◇

12.3 Delayed Bifurcation and WKB

In the last section, we presented the main concepts of delayed Hopf bifurcation for fast–slow systems. In this section, we shall describe a slightly different approach to the problem. The main differences are that we are going to express the asymptotic moment of jumping in terms of the slow variable, and the result will be established only on a formal asymptotic level without using complex time.

As before, consider a $(2, 1)$ -fast–slow system of the form (12.5). Suppose the slow equation has an explicit solution of the form $y(\varepsilon t)$, so that

$$x' = f(x, y(\varepsilon t)). \quad (12.15)$$

Equation (12.15) focuses on the viewpoint that we are dealing with an ODE that has a slowly varying parameter in it. Again, we need several assumptions:

- (A1) For $\varepsilon = 0$, equation (12.15) has a nondegenerate Hopf bifurcation for $y = y_H$ involving an equilibrium point $x = x_s$. In particular, we point out that none of the eigenvalues $\lambda_{1,2}$ of the Jacobian $J = (D_x f)(x_s)$ are zero.
- (A2) Assume for simplicity that the bifurcation is supercritical and x_s is a stable hyperbolic focus for $y < y_H$.
- (A3) The parameter (slow variable) y is explicitly given by

$$y(\varepsilon t) = y(0) + h(\varepsilon t) = y_0 + h(\varepsilon t) \quad (12.16)$$

with $h(0) = 0$, and h is a strictly monotonically increasing function.

- (A4) The vector field $f = (f_1, f_2)^\top : \mathbb{R}^2 \rightarrow \mathbb{R}^2$ is analytic. Furthermore, f is sufficiently “generic” so that the critical manifold for $\varepsilon = 0$ is not invariant for $0 < \varepsilon \ll 1$, as discussed in the remark after Theorem 12.2.3.
- (A5) The initial condition of the trajectory under consideration (x_0, y_0) is given so that the asymptotic moment of falling τ_0 is larger than τ^- (see Section 12.2 for the relevant definitions).

Definition 12.3.1. In the context of delayed Hopf bifurcation, the function h defined by (12.16) is called a **ramp**.

In the simple case that the slow equation is $y' = \varepsilon$, it follows that $y(\varepsilon t) = y_0 + \varepsilon t$ and $h(s) = s$ is a simple linear ramp. It is helpful to keep this example in mind in what follows. Let y_f denote the parameter value at which the delay induced by the Hopf bifurcation ends, i.e., it is the slow-variable phase-space coordinate corresponding to the asymptotic moment of jumping.

Theorem 12.3.2 ([BG08a]). *Suppose (A1)–(A5) hold. Then a formal asymptotic onset condition for oscillations in (12.15) is given by*

$$0 = \int_{y_0}^{y_f} [h^{-1}(y - y_0)]' \max_k (\operatorname{Re}(\lambda_k(y))) \, dy, \quad (12.17)$$

where the eigenvalues λ_k are computed from the Jacobian $J = (\mathrm{D}_x f)(x_s)$ at the equilibrium.

Note that for $h(s) = s$, the inverse is $h^{-1}(s) = s$, and so the derivative of the inverse function $[h^{-1}(y - y_0)]'$ in (12.17) equals 1.

Proof. (Sketch; [BG08a]) By assumption, there exists an equilibrium point $x_s = x_s(y(\tau))$ for $\varepsilon = 0$ that undergoes a static Hopf bifurcation. In particular, the two eigenvalues $\lambda_{1,2}$ of the Jacobian $J = (\mathrm{D}_x f)(x_s)$ satisfy the equation

$$\det(J - \lambda_k \mathrm{Id}) = 0. \quad (12.18)$$

Now make the ansatz that the slowly varying solution x_{sv} , which undergoes the delay, has a regular perturbation expansion

$$x_{sv}(\tau) \sim x_0(\tau) + \varepsilon x_1(\tau) + \dots \quad \text{as } \varepsilon \rightarrow 0, \quad (12.19)$$

where $\tau = h(\varepsilon t)$; note that here, the slow time is adapted to the functional form of the slowly varying parameter. Substitute (12.19) into $x' = f(x, y(\varepsilon t))$. Up to leading order, we obtain $x_0(\tau) = x_s(y(\tau))$, so that

$$x_{sv}(\tau) = x_s(y(\tau)) + \mathcal{O}(\varepsilon).$$

To investigate when the slowly varying solution becomes unstable, one should solve the stability problem involving the Jacobian $J_{sv} = (\mathrm{D}_x f)(x_s(y(\tau)))$, i.e., the matrix slowly varies as well. In particular, we consider the stability for the linear variational equation

$$X' = J_{sv} X. \quad (12.20)$$

For this linear problem, one may employ the WKB method, as described in Section 9.4, with ansatz

$$X(t; \varepsilon) \sim e^{\sigma(\tau)/\varepsilon} (X_0(\tau) + \varepsilon X_1(\tau) + \dots) \quad \text{as } \varepsilon \rightarrow 0.$$

The leading-order terms yield the algebraic problem

$$(J_{sv} - \sigma'(\tau)h'(\varepsilon t)\mathrm{Id})X_0 = 0, \quad X_0 \neq 0. \quad (12.21)$$

The system (12.21) has nontrivial solutions if

$$\det(J_{sv} - \sigma'(\tau)h'(\varepsilon t)\mathrm{Id}) = 0. \quad (12.22)$$

Observe that (12.22) is in the same form as (12.18), and therefore

$$\lambda = \sigma'(\tau)h'(\varepsilon t) = \frac{\sigma'(\tau)}{(h^{-1}(\tau))'}. \quad (12.23)$$

To estimate the jump time to first order, we have to find the time τ_j when $\mathrm{Re}(\sigma) = 0$ in the WKB ansatz. Using (12.23) leads to the onset condition

$$\int_0^{\tau_j} (h^{-1}(\tau))' \max_k \mathrm{Re}(\lambda_k(y(\tau))) \, d\tau = 0. \quad (12.24)$$

Using the change of variable $y = y_0 + \tau$ in (12.24) yields

$$0 = \int_{y_0}^{y_j} [h^{-1}(y - y_0)]' \max_k(\operatorname{Re}(\lambda_k(y))) \, dy, \quad (12.25)$$

which is precisely what we set out to prove. \square

Note that Theorem 12.15 can be applied to situations in which the slowly varying equation is more general than $y' = \varepsilon$, as shown in the next example.

Example 12.3.3. Consider the planar FitzHugh–Nagumo equation with an applied current I given by

$$\begin{aligned} x'_1 &= -x_1(x_1 - a)(x_1 - 1) - x_2 + I, \\ x'_2 &= b(x_1 - \gamma x_2), \end{aligned} \quad (12.26)$$

where a, b, γ are fixed parameters. It is easy to check that there exists a Hopf bifurcation for $I = I_H$ in the system for suitable parameter values. Suppose we know that the current I is varying slowly and is of the form $I(\varepsilon t) = I_0 + (\varepsilon t)^p$. In this case, the ramp $h(s) = s^p$ is called a **power ramp**. To solve the FitzHugh–Nagumo problem with a power ramp, observe that

$$\max_k \operatorname{Re}(\lambda_k(I)) \approx v \cdot (I - I_H), \quad (12.27)$$

where v denotes the crossing speed of the real part of the complex conjugate pair at the Hopf bifurcation, i.e.,

$$v = \left[\frac{d}{dI} \max_k \operatorname{Re}(\lambda_k(I)) \right]_{I=I_H}.$$

Using the approximation (12.27), one can substitute everything into the onset condition (12.17) and integrate by parts:

$$(I_j - I_H) h^{-1}(I_j - I_0) = \int_{I_0}^{I_j} h^{-1}(I - I_0) \, dI. \quad (12.28)$$

For $h(s) = s^p$, we have $h^{-1} = s^{1/p}$, so that after a bit of algebraic manipulation, it follows that

$$I_j - I_H = p(I_H - I_0) \quad \text{for } p > 0. \quad (12.29)$$

On the one hand, (12.29) is a surprisingly simple condition. On the other hand, it is a first-order approximation and hence expected to be reasonably simple. ♦

Exercise/Project 12.3.4. Determine, analytically or numerically, a Hopf bifurcation point $I = I_H$ for the FitzHugh–Nagumo equation (12.26) and check via the first Lyapunov coefficient whether the Hopf bifurcation is sub- or supercritical. ◇

Exercise 12.3.5. Check the calculation for getting from (12.17) to (12.28). ◇

12.4 The Newton Polygon

The Newton polygon is a combinatorial tool that can be used in many different areas of mathematics including algebra, algebraic geometry, singularity theory, ordinary and partial differential equations, as well as bifurcation theory and asymptotic analysis. We are going to give the main definitions and provide a few fast–slow system examples in this section; more details can be found in the references in Section 12.9.

Consider vectors $Q = (q_1, q_2)$ in the integral lattice \mathbb{Z}^2 . Let $\mathcal{D} \subset (\mathbb{Z}^2)^+$, where $(\mathbb{Z}^2)^+$ denotes the integer lattice in the first quadrant with nonnegative entries, i.e., $Q \in (\mathbb{Z}^2)^+$ if and only if $q_1 \geq 0$ and $q_2 \geq 0$. Unfortunately, there seems to be no agreement in the literature on a unique definition of the Newton polygon of the set \mathcal{D} . Before we list three possibilities in the next definition, recall (in the sense of the remark before Proposition 2.2.3) that the **convex hull** $\text{conv}(\mathcal{D})$ of \mathcal{D} is defined as the smallest convex set in \mathbb{R}^2 containing \mathcal{D} .

Definition 12.4.1. The **Newton polygon** Γ of \mathcal{D} can be defined in the following different ways:

- (N1) Just the convex hull of \mathcal{D} .
- (N2) The convex hull of $\text{conv}(\mathcal{D}) \oplus (\mathbb{Z}^2)^+$, where \oplus denotes the **Minkowski sum** of two sets (the Minkowski sum is given by adding elements pairwise).
- (N3) The convex hull of $[\mathcal{D} \cup \{(0, k), (k, 0)\}] \oplus (\mathbb{Z}^2)^+$, where $k := \max_{Q \in \mathcal{D}}(q_1 + q_2)$.

The problem of terminology does not stop here, but before we proceed, we should try to understand (N1)–(N3) in an example.

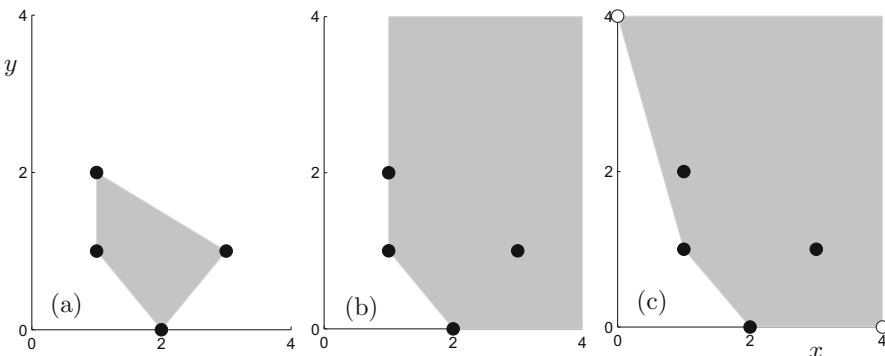


Figure 12.5: Illustration of the different definitions of Newton's polygon Γ . The set \mathcal{D} of four points is given by (12.30). The points in \mathcal{D} are marked in black; in (c) we have also marked $(0, k)$ and $(k, 0)$ as open circles according to Definition 12.4.1 (N3).

Example 12.4.2. Let \mathcal{D} be given by four vectors as follows:

$$\mathcal{D} := \{Q_1 = (2, 0), Q_2 = (1, 1), Q_3 = (1, 2), Q_4 = (3, 1)\}. \quad (12.30)$$

Figure 12.5 illustrates the different versions (N1)–(N3) of Definition 12.4.1. The convex hull $\text{conv}(\mathcal{D})$ is the bounded polygon shown in Figure 12.5(a) that defines the Newton polygon according to (N1). Figure 12.5(b) shows (N2), where taking the Minkowski sum with $(\mathbb{Z}^2)^+$ produces an unbounded Newton polygon. Figure 12.5(c) shows the situation for (N3), where we easily calculate $k = 4$ as the sum of entries for the vector Q_4 . Obviously, all three definitions produce different results. However, note carefully that all three versions of the Newton polygon Γ have the edge from $Q_1 = (2, 0)$ to $Q_2 = (1, 1)$ as part of their boundary. ♦

Exercise/Project 12.4.3. Can you prove which properties of the Newton polygon are the same for all three definitions (N1)–(N3)? ◇

We introduce some additional notation. For $j \in \{1, 2, \dots, N\}$, let $\Gamma_j^{(0)}$ denote the vertices of Newton's polygon contained in $\partial\Gamma$, and denote by $\Gamma_{j_1 j_2}^{(1)}$ the finite edges in $\partial\Gamma$ between $\Gamma_{j_1}^{(0)}$ and $\Gamma_{j_2}^{(0)}$. Note that we can also consider an outer normal vector $n_{j_1 j_2}$ associated with an edge $\Gamma_{j_1 j_2}^{(1)}$; obviously, there are infinitely many choices for the outer normal vector, and we shall only restrict the vector to have integer coefficients.

Example 12.4.4 (Example 12.4.2, continued.). Let us just write down the vertices and edges for Definition 12.4.1 (N3); note that the order of labels is arbitrary, but it helps to choose one starting vertex and then agree on clockwise labels. We have

$$\Gamma_1^{(0)} = (4, 0), \quad \Gamma_2^{(0)} = (2, 0), \quad \Gamma_3^{(0)} = (1, 1), \quad \Gamma_4^{(0)} = (0, 4).$$

There are three associated edges $\Gamma_{12}^{(1)}, \Gamma_{23}^{(1)}, \Gamma_{34}^{(1)}$ with normal vectors

$$n_{12} = (0, -1), \quad n_{23} = (-1, -1), \quad n_{34} = (-3, -1).$$

In a similar way, we can just write down the vertex and edge data for the definitions (N1) and (N2). ♦

The most interesting part of the Newton polygon for calculations is a certain part of its boundary. Unfortunately, there is again no agreement in the literature, but the following definition seems to be the most convenient.

Definition 12.4.5. Let Γ be the Newton polygon of a set $\mathcal{D} \subset (\mathbb{Z}^2)^+$ given by Definition 12.4.1 (N1), (N2), or (N3). Let $\Gamma^{(1)}$ denote a finite edge in $\partial\Gamma$, and denote by $n = (n_1, n_2) \in \mathbb{Z}^2$ an associated outer normal vector. Define the **Newton diagram** $\hat{\Gamma}$ as the subset of $\partial\Gamma$ consisting of all edges with $n_1, n_2 \leq 0$ and the vertices associated with those edges. Let $\hat{\Gamma}^- \subseteq \hat{\Gamma}$ denote the subset of the Newton diagram given by all edges that have outer unit normal vectors with negative entries, i.e., $n_1 < 0$ and $n_2 < 0$.

Definition 12.4.5 just collects all edges that have outer unit normal vectors contained in the third quadrant and does not depend on the choice of outer normal vector for each edge. Sometimes, the Newton diagram is also referred to as **Newton's open polygon**.

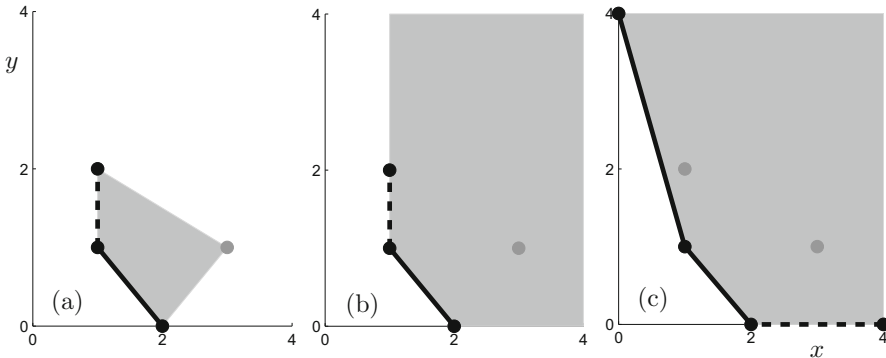


Figure 12.6: Illustration of the different definitions of Newton's diagram $\hat{\Gamma}$. The diagram is shown in black (thick lines and dots) for each case in Definition 12.4.1. The solid black line indicates $\hat{\Gamma}^-$.

Example 12.4.6 (Example 12.4.2 continued.). Figure 12.6 shows the Newton diagram for the set $\mathcal{D} \subset (\mathbb{Z}^2)^+$ given by (12.30). In each part of the Figure, the Newton diagram is marked in black; observe again that all three versions of the Newton diagram contain the edge from $(2,0)$ to $(1,1)$; $\hat{\Gamma}^-$ coincides for the Definitions (N1) and (N2), while for (N3), just one additional edge is contained in $\hat{\Gamma}^-$. ♦

Originally, Newton's polygon was developed to find the local zeros of an analytic function $f : \mathbb{R}^2 \rightarrow \mathbb{R}$. Focusing on solutions near the origin $(x,y) = (0,0)$, we can consider the Taylor expansion

$$f(x,y) = \sum_{q_1, q_2 \geq 0} f_{q_1 q_2} x^{q_1} y^{q_2},$$

which converges absolutely on some set $\mathcal{U} = \{(x,y) \in \mathbb{R}^2 : |x| < \delta, |y| < \delta\}$ for some $\delta > 0$. The Newton polygon $\Gamma(f)$ associated with f is constructed from the set

$$\mathcal{D} = \{(q_1, q_2) \in \mathbb{Z}^2 : f_{q_1 q_2} \neq 0\}.$$

The problem of describing the zeros of a function occurs naturally in fast–slow systems, as demonstrated by the next example.

Example 12.4.7. Consider the planar fast–slow system given by

$$\begin{aligned} \varepsilon \dot{x} &= x^3 + y^3 - 2xy, \\ \dot{y} &= g(x,y). \end{aligned} \tag{12.31}$$

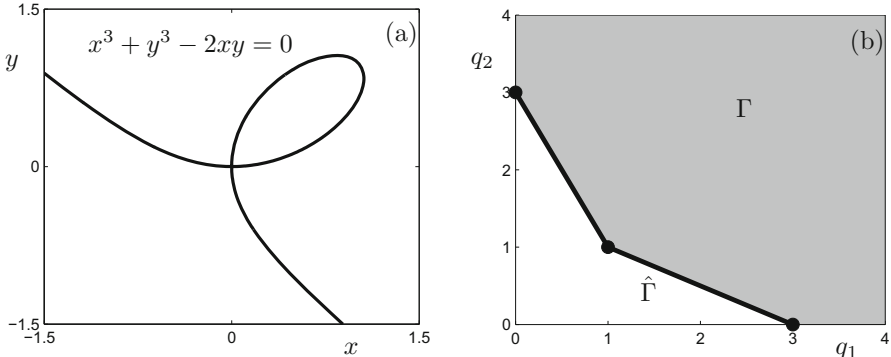


Figure 12.7: (a) Critical set $C_0 = \{f(x,y) = x^3 + y^3 - 2xy = 0\}$ for the planar fast–slow system (12.31). (b) Newton’s polygon Γ and Newton’s diagram $\hat{\Gamma}$ for the map f .

We can easily write down a formal expression for the critical set

$$C_0 = \{(x,y) \in \mathbb{R}^2 : x^3 + y^3 - 2xy = 0\}$$

and also plot it numerically; see Figure 12.7(a). Note that C_0 is not a manifold, since it has a self-intersection at the origin. The main problem in analyzing (12.31) is that we do not even have a local description of the critical manifold near the origin, i.e., a parameterization or a series expansion. Although we have not developed all the necessary tools to find a nice parameterization for C_0 , we show the Newton polygon Γ and the Newton diagram $\hat{\Gamma}$ for the map $f(x,y) = x^3 + y^3 - 2xy$ in Figure 12.7(b). Observe that all three versions (N1)–(N3) of Definition 12.4.1 coincide in this example, since

$$\mathcal{D} = \{(q_1, q_2) \in \mathbb{Z}^2 : f_{q_1 q_2} \neq 0\} = \{(3,0), (1,1), (0,3)\}. \quad \blacklozenge$$

Remark: The curve C_0 from Example 12.4.7 is known as the **folium of Descartes**.

Newton’s polygon can be used not only to find nice representations for a critical manifold (see Section 12.6); it also has a myriad other connections to fast–slow systems (see Section 12.8). Before we can outline these connections, another technical tool is needed.

12.5 Power Transformations

The method of power transformations is very similar to the blowup method. In particular, power transformations have likely motivated and influenced the blowup geometric desingularization technique. Consider a matrix

$$A = \begin{pmatrix} a_{11} & a_{12} \\ a_{21} & a_{22} \end{pmatrix}$$

with real elements $a_{ij} \in \mathbb{R}$ and $\det(A) \neq 0$. Let $B = (b_{ij})$ denote the inverse of A , so that $AB = \text{Id}$. As in the previous section, let $(x, y) \in \mathbb{R}^2$ denote the planar coordinates.

Definition 12.5.1. A **power transformation** on \mathbb{R}^2 given by the matrix A is defined by the following map:

$$(x_1, y_1) := (x^{a_{11}} y^{a_{12}}, x^{a_{21}} y^{a_{22}}), \quad (12.32)$$

with inverse given by

$$(x, y) := (x_1^{b_{11}} y_1^{b_{12}}, x_1^{b_{21}} y_1^{b_{22}}), \quad (12.33)$$

where B is the inverse of A .

Exercise 12.5.2. Verify that (12.33) is the inverse to (12.32). \diamond

Note that a power transformation can also be viewed as a usual linear map on the logarithm of the coordinates $(\ln x, \ln y)$ and $(\ln x_1, \ln y_1)$. We view power transformations as acting on the space of exponents for monomials $x^{q_1} y^{q_2}$ as follows:

$$x^{q_1} y^{q_2} = (x_1^{b_{11}} y_1^{b_{12}})^{q_1} (x_1^{b_{21}} y_1^{b_{22}})^{q_2} = x_1^{b_{11}q_1 + b_{21}q_2} y_1^{b_{12}q_1 + b_{22}q_2}. \quad (12.34)$$

The calculation (12.34) shows that if we consider the **vector exponent** (or **multi-index**) $Q = (q_1, q_2)$ as a column vector, then a power transformation induces a linear map on the space of vector exponents given by

$$Q_1 = B^\top Q, \quad (12.35)$$

where $Q_1 = (b_{11}q_1 + b_{21}q_2, b_{12}q_1 + b_{22}q_2)$. For general matrices $A, B \in \mathbb{R}^{2 \times 2}$ or $A, B \in \mathbb{C}^{2 \times 2}$, the analysis of power transformations is rather complicated. We shall restrict ourselves to **unimodular** power transformations with integer coefficients:

$$A, B \in \text{SL}^\pm(2, \mathbb{Z}),$$

where $\text{SL}(2, \mathbb{Z})$ denotes the **special linear group** with \mathbb{Z} -coefficients that are just 2×2 matrices with determinant ± 1 . For power transformation in $\text{SL}^\pm(2, \mathbb{Z})$, a few nice properties are summarized in the next result.

Proposition 12.5.3. If $A \in \text{SL}^\pm(2, \mathbb{Z})$, then the power transformation associated with A is injective away from the coordinate axes. Furthermore, if $Q \in \mathbb{Z}^2$, then $AQ \in \mathbb{Z}^2$, and A is injective on \mathbb{Z}^2 , i.e., the transformation A maps the integral lattice to itself and is a one-to-one map on the integral lattice.

Proposition 12.5.3 is relatively easy to check by a direct calculation. Equation (12.35) and Proposition 12.5.3 show that the most convenient viewpoint for power transformations is to think of them as acting on the space of vector exponents or multi-indices \mathbb{Z}^2 . If we consider an edge $\Gamma_{j_1 j_2}^{(1)}$ of the Newton polygon/diagram, we get another edge $B^\top \Gamma_{j_1 j_2}^{(1)}$ between vertices $B^\top \Gamma_{j_1}^{(0)}$ and $B^\top \Gamma_{j_2}^{(0)}$. In Section 12.6, we are going to face the problem whether there exists a power transformation that maps a given edge of the Newton diagram to an edge parallel to one of the coordinate axes.

Example 12.5.4 (Example 12.4.7 continued). Recall that the map $f(x, y) = x^3 + y^3 - 2xy$ defines the set

$$\mathcal{D} = \{(q_1, q_2) \in \mathbb{Z}^2 : f_{q_1 q_2} \neq 0\} = \{(3, 0), (1, 1), (0, 3)\}. \quad (12.36)$$

The associated Newton diagram $\hat{\Gamma}(f)$ for \mathcal{D} is shown in Figure 12.8(a). It consists of three vertices,

$$\Gamma_1^{(0)} = (3, 0), \quad \Gamma_2^{(0)} = (1, 1), \quad \Gamma_3^{(0)} = (0, 3),$$

and two edges, $\Gamma_{12}^{(1)}$ and $\Gamma_{23}^{(1)}$, between the vertices that can also be viewed as vectors

$$\Gamma_{12}^{(1)} = \Gamma_2^{(0)} - \Gamma_1^{(0)} = (-2, 1), \quad \Gamma_{23}^{(1)} = \Gamma_3^{(0)} - \Gamma_2^{(0)} = (-1, 2).$$

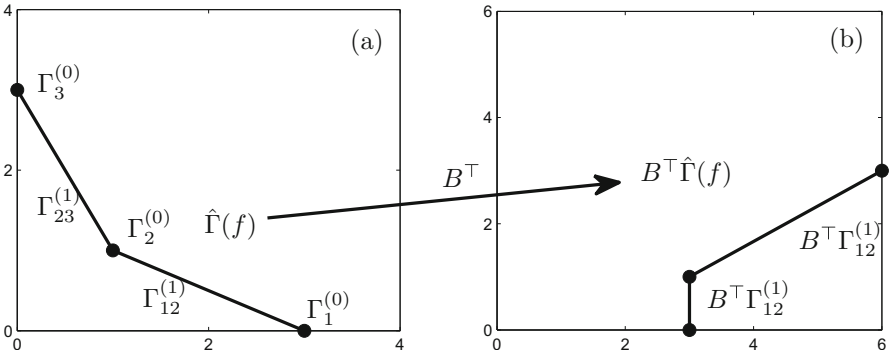


Figure 12.8: (a) Newton's diagram $\hat{\Gamma}(f)$ for the set \mathcal{D} given by (12.36). (b) Transformation of the Newton diagram under the power transformation given by the unimodular matrices A and B ; see equation (12.37).

Consider the edge $\Gamma_{12}^{(1)} = (-2, 1)$; we ask whether there is a unimodular transformation A with inverse B such that $B^\top(-2, 1)^\top$ is parallel to a coordinate axis. Consider the matrix

$$A := \begin{pmatrix} 1 & 0 \\ -2 & 1 \end{pmatrix}, \quad B = A^{-1} = \begin{pmatrix} 1 & 0 \\ 2 & 1 \end{pmatrix}. \quad (12.37)$$

It is straightforward to calculate that

$$B^\top(-2, 1)^\top = \begin{pmatrix} 1 & 2 \\ 0 & 1 \end{pmatrix} \begin{pmatrix} -2 \\ 1 \end{pmatrix} = \begin{pmatrix} 0 \\ 1 \end{pmatrix}.$$

The transformation of Newton's diagram $B^\top \hat{\Gamma}(f)$ is shown in Figure 12.8(b). Observe that the edge $B^\top \Gamma_{12}^{(1)} = B^\top(-2, 1)$ is indeed parallel to the vertical coordinate axis. ♦

It will become apparent in Section 12.6 why a power transformation that maps an edge parallel to a coordinate axis is very useful. For now, we consider the question whether the formula for the matrix A in Example 12.5.4 was just a “good guess.” A priori, it is unclear whether one can always map any nonzero vector in \mathbb{R}^2 via a unimodular matrix to a given coordinate axis.

Lemma 12.5.5. *Let $v \in \mathbb{Z}^2$. Then there exists a matrix $C = (c_{ij}) \in \mathrm{SL}^\pm(2, \mathbb{Z})$ such that $Cv \in \mathbb{Z}^2$ is a vector along one of the coordinate axes.*

Proof. (Sketch; [Bru89]) We may assume that $v_1 v_2 \neq 0$, since for $v_2 = 0$ or $v_1 = 0$, there is nothing to prove. Let $d := \gcd(v_1, v_2)$ denote the greatest common divisor of v_1 and v_2 . We require that $Cv = (d, 0)^\top$, and from solving the three algebraic equations

$$\begin{aligned} Cv - (d, 0)^\top &= 0, \\ \det(C) - 1 &= 0, \end{aligned}$$

it follows that

$$C = \begin{pmatrix} \frac{d - c_{12}v_2}{v_1} & c_{12} \\ -\frac{v_2}{d} & \frac{v_1}{d} \end{pmatrix}.$$

By definition of d , it is clear that $v_1/d \in \mathbb{Z}$ and $v_2/d \in \mathbb{Z}$. Using Bézout’s identity (also known as Bézout’s lemma; see [EW05], p. 37) one obtains c_{12} , so that $(d - c_{12}v_2)/v_1 \in \mathbb{Z}$. This concludes the proof. \square

Observe that the proof of Lemma 12.5.5 also provides an algorithm for finding the matrix C , since we can just pick an integer $k \in \mathbb{Z} - \{0\}$ and solve the **Diophantine equation**

$$d = kv_1 + c_{12}v_2. \quad (12.38)$$

From a theoretical viewpoint, equation (12.38) is solvable using Bézout’s lemma, and the equation can be solved algorithmically using the division algorithm [EW05, Bru89]; often, a solution is also easy to guess, as shown in Example 12.5.4.

Corollary 12.5.6. *There exists a power transformation A with inverse B that maps a given edge of Newton’s diagram to an edge parallel to one of the coordinate axes.*

Proof. Just use Lemma 12.5.5 and set $B^\top := C$, which yields $B = C^\top$ and $A = (C^\top)^{-1}$. \square

12.6 Parameterizing Critical Manifolds

Finally, we return to the analysis of the zeros of an analytic function $f : \mathbb{R}^2 \rightarrow \mathbb{R}$ first described in Section 12.4. Focusing on solutions near the origin $(x, y) = (0, 0)$, let us consider the Taylor expansion

$$f(x, y) = \sum_{q_1, q_2 \geq 0} f_{q_1 q_2} x^{q_1} y^{q_2}, \quad (12.39)$$

which converges absolutely on some set $\mathcal{U} = \{(x, y) \in \mathbb{R}^2 : |x| < \delta, |y| < \delta\}$ for some $\delta > 0$. The Newton diagram $\hat{\Gamma}(f)$ associated with f is constructed from the set

$$\mathcal{D} = \{(q_1, q_2) \in \mathbb{Z}^2 : f_{q_1 q_2} \neq 0\}.$$

We are interested in finding a good description of the solutions of $f(x, y) = 0$ that also define a critical manifold for a $(1, 1)$ -fast–slow system with fast vector field f . We are always going to assume that $f(0, 0) = 0$. Note that if

$$\frac{\partial f}{\partial x}(0, 0) \neq 0 \quad \text{and/or} \quad \frac{\partial f}{\partial y}(0, 0) \neq 0, \quad (12.40)$$

then the implicit function theorem yields functions $x = x(y)$ and/or $y = y(x)$ such that

$$f(x(y), y) = 0 \quad \text{and/or} \quad f(x, y(x)) = 0$$

hold locally near the origin. Since we can expand the functions $x(y)$ and $y(x)$ as Taylor series, there is really nothing to do in this scenario. Hence, assume that $(x, y) = (0, 0)$ is a singular point at which both partial derivatives (12.40) vanish. In this case, the goal is to find the zeros of $f(x, y) = 0$ as series of the form

$$\begin{aligned} x &= a_1\delta + a_2\delta^2 + \dots, \\ y &= b_1\delta + b_2\delta^2 + \dots, \end{aligned}$$

for $0 < |\delta| \ll 1$; note that (12.6) can be viewed as asymptotic series with respect to $\delta \rightarrow 0$. One more definition is required before we give an explanation of the main method.

Definition 12.6.1. Let $\Gamma_{j_1 j_2}^{(1)}$ be an edge in Newton's diagram with vertices

$$\Gamma_{j_1}^{(0)} = Q_1 = (q_{11}, q_{12}) \quad \text{and} \quad \Gamma_{j_2}^{(0)} = Q_2 = (q_{21}, q_{22}).$$

Then we define the **truncation** \hat{f} of (12.39) with respect to $\Gamma_{j_1 j_2}^{(1)}$ by

$$\hat{f}(x, y) := f_{q_{11} q_{12}} x^{q_{11}} y^{q_{12}} + f_{q_{21} q_{22}} x^{q_{21}} y^{q_{22}}.$$

The truncation of the Taylor series for f with respect to an edge keeps only those two terms that are associated with the vertices of the edge.

Example 12.6.2 (Example 12.5.4, continued). The Newton polygon for $f(x, y) = x^3 + y^3 - 2xy$ is shown in Figure 12.8(a). It has three vertices,

$$\Gamma_1^{(0)} = (3, 0), \quad \Gamma_2^{(0)} = (1, 1), \quad \Gamma_3^{(0)} = (0, 3).$$

Truncating f with respect to the edge $\Gamma_{12}^{(1)}$, we get $\hat{f}(x, y) = x^3 - 2xy$. ♦

The full details of the Newton polygon method are beyond the scope of this book. The basic steps of the method are as follows:

- (S1) Find the Newton diagram $\hat{\Gamma}(f)$.

- (S2) Choose an edge of $\hat{\Gamma}(f)$ and find a power transformation that maps this edge to an edge parallel to one of the coordinate axes.
- (S3) Rewrite the equation $f(x, y) = 0$ in this new coordinate system and rescale it in this coordinate system to reduce the order of the polynomial equation.
- (S4) Find the truncation of the resulting equation and compute its zeros explicitly (if possible).
- (S5) It can be proved that a repetitive application of the steps (S1)–(S4) will reduce the problem in a finite number of steps to a problem that is solvable explicitly.
- (S6) Changing back to the original coordinates will provide asymptotic expansions for some of the zeros of $f(x, y) = 0$.
- (S7) Repeat (S1)–(S6) for each edge of the Newton diagram to compute all curves of solutions.

We are going to limit ourselves to calculating the series (12.6) expansions in an example. However, the method presented here applies in full generality to determining series expansions near zeros of analytic functions.

Example 12.6.3. We consider the problem

$$f(x, y) = x^3 + y^3 - 2xy = 0$$

as in all previous examples in Sections 12.4 and 12.5. The Newton diagram $\hat{\Gamma}(f)$ has vertices

$$\hat{\Gamma}(f) = \{Q_1 = (3, 0), Q_2 = (1, 1), Q_3 = (0, 3)\}$$

and edges

$$\Gamma_{12}^{(1)} = (-2, 1) \quad \text{and} \quad \Gamma_{23}^{(1)} = (-1, 2).$$

Figure 12.8 illustrates the diagram. Starting with the edge $(-2, 1)$, we know from Example 12.5.4 that the power transformation given by the matrices

$$A = \begin{pmatrix} 1 & 0 \\ -2 & 1 \end{pmatrix}, \quad B = A^{-1} = \begin{pmatrix} 1 & 0 \\ 2 & 1 \end{pmatrix} \quad (12.41)$$

maps $(-2, 1)$ to $(0, 1)$ with vertices $(3, 0)$ and $(3, 1)$; see Figure 12.8(b). The power transformation for A is

$$\begin{aligned} x_1 &= x, \\ y_1 &= x^{-2}y, \end{aligned} \quad (12.42)$$

with inverse

$$\begin{aligned} x &= x_1, \\ y &= x_1^2 y_1. \end{aligned} \quad (12.43)$$

In the new coordinates, the map f is transformed to

$$f(x, y) = f(x_1, x_1^2 y_1) = x_1^3 + x_1^6 y_1^3 - 2x_1^3 y_1 =: f^{(1)}(x_1, y_1). \quad (12.44)$$

Note carefully that $f^{(1)}$ is divisible by $x_1^3 =: x_1^r$. The exponent $r = 3$ for this division is no coincidence, and it can be calculated as follows. Consider the outer normal vector $n_{12} = (-1, -2)$ for the edge $(-2, 1)$ obtained by interchanging its coordinates and multiplying the first coordinate by -1 . Then it turns out that

$$r = -\max_{Q_j \in \hat{\Gamma}(f)^{(0)}} n_{12} \cdot Q_j^\top = -\max\{-3, -6, -3\} = 3, \quad (12.45)$$

i.e., one has to maximize an inner product to find r . Note also that the two vertices associated with the edge $(-2, 1)$ both produce the correct exponent in (12.45). We rescale (12.46) as planned:

$$f^{(1,r)}(x_1, y_1) := x_1^{-3} f^{(1)}(x_1, y_1) = 1 - 2y_1 + x_1^3 y_1^3.$$

The effect of the rescaling is to shift the transformed Newton diagram $B^\top \hat{\Gamma}(f)$ by $r = 3$ units to the left. The next step is to truncate $f^{(1,r)}$ using the transformed edge $B^\top(-2, -1)^\top = (0, 1)^\top$, which amounts to dropping the term $x_1^3 y_1^3$. This leaves us with the problem

$$\hat{f}^{(1,r)}(x_1, y_1) = 1 - 2y_1 = 0.$$

The last equation has one root $y_1^0 = \frac{1}{2}$. It turns out that the unique root is equivalent to the fact that the curve of zeros we are trying to compute is locally isolated. Using the substitution

$$y_1 = y_1^0 + z = \frac{1}{2} + z \quad (12.46)$$

yields

$$f^{(1,r)}(x_1, 1/2 + z) = -2z + x_1^3 (1/2 + z)^3 = -2z + \frac{1}{8} x_1^3 + \dots.$$

The lowest-order approximation for this equation is

$$-2z + \frac{1}{8} x_1^3$$

with a root $z = \frac{1}{16} x_1^3$. This implies that $z = \frac{1}{16} x_1^3 + \dots$, where the dots denote higher-order terms in x_1 . Reverting from z to y_1 via (12.46), it follows that

$$y_1 = \frac{1}{2} + \frac{1}{16} x_1^3 + \dots.$$

As a last step, one has to use the power transformation (12.42) to return to the original coordinates

$$\begin{aligned} x &= x_1, \\ y &= \frac{1}{2} x_1^2 + \frac{1}{16} x_1^5 + \dots, \end{aligned} \quad (12.47)$$

where $x_1 = \delta$ plays the role of the small expansion parameter. Observe from (12.47) that by writing x as a function of y , we obtain the leading-order

approximation $x \sim \pm y^{1/2}$ and that the exponent $1/2$ is precisely the slope of the first edge $\Gamma_{12}^{(1)} = (-2, 1)$ multiplied by -1 . This concludes the analysis for the first edge of the Newton diagram. The second edge $\Gamma_{23}^{(1)} = (-1, 2)$ can be treated similarly, and the details of the calculations are developed in the guided Exercise 12.6.4 below. That exercise yields a second curve of solutions to $f(x, y) = 0$ given by

$$\begin{aligned} x &= 2x_1^2 - 2x_1^5 + \dots, \\ y &= 2x_1 - 2x_1^4 + \dots. \end{aligned} \quad (12.48)$$

Observe again that by writing x as a function of y , we get to leading order $x \sim y^2$, which is the slope of the edge $(-1, 2)$ multiplied by -1 .

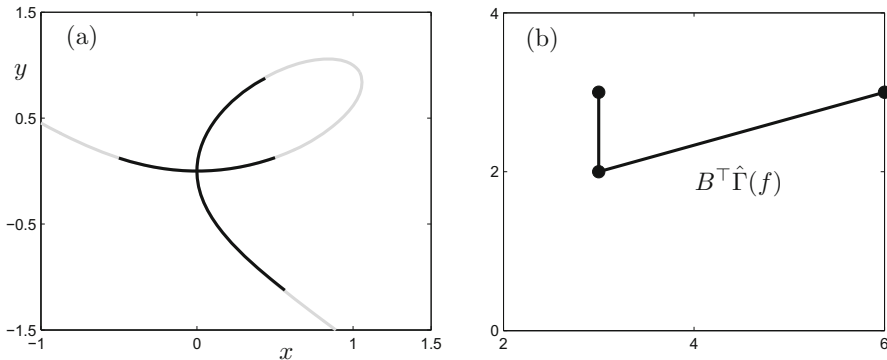


Figure 12.9: (a) The folium of Descartes $x^3 + y^3 - 2xy = 0$ is shown in gray, and the local approximations (12.47) and (12.48) are shown in black for $|x_1| \leq 0.5$. (b) Transformation of the Newton diagram under the power transformation given by the unimodular matrix A from equation (12.49); see also Exercise 12.6.4(E1)–(E2).

The two curves (12.47) and (12.48) are shown in Figure 12.9(a). Observe that the local approximation near $(x, y) = (0, 0)$ is excellent. ♦

Exercise/Project 12.6.4. This exercise develops a step-by-step solution to finding the curve of zeros (12.48) from Example 12.6.3. The remaining part is to analyze the edge $\Gamma_{23}^{(1)} = (-1, 2)$.

(E1) Show that the power transformation given by

$$A = \begin{pmatrix} 1 & -1 \\ -1 & 2 \end{pmatrix} \quad (12.49)$$

maps the edge $(-1, 2)$ parallel to one of the coordinate axes by computing $B = A^{-1}$ and B^T .

(E2) Calculate the transformed Newton diagram $B^T \hat{\Gamma}(f)$ and compare your results with Figure 12.9(b).

(E3) Apply the power transformation defined by A to get the coordinate change $(x, y) \mapsto (x_1, y_1)$.

(E4) Show that in these coordinates, we have transformed $f = 0$ to

$$x_1^3 y_1^2 (x_1^3 y_1 + y_1 - 2) = 0. \quad (12.50)$$

(E5) Prove that the truncated version of equation (12.50) is

$$y_1^2 (y_1 - 2) = 0$$

with isolated root $y_1^0 = 2$.

(E6) Deduce the formula (12.48) by returning to the original coordinates. \diamond

The next natural question is whether the algorithm we have applied in Example 12.6.3 works in more generality.

Theorem 12.6.5 ([Bru89]). *Consider a map $f : \mathbb{R}^2 \rightarrow \mathbb{R}$ analytic in a neighborhood of zero with*

$$f(0, 0) = 0, \quad \frac{\partial f}{\partial x}(0, 0) = 0, \quad \frac{\partial f}{\partial y}(0, 0) = 0.$$

Then the algorithm given by the steps (S1)–(S7) above provides asymptotic series for curves that solve the problem $f(x, y) = 0$.

We shall not discuss the proof, but we point out that the major technical step is to show that the coordinate change induced by power transformation will eventually yield a solvable problem. This is analogous to Theorem 7.1.13, where it was shown that any nonhyperbolic equilibrium point for a planar ODE can be desingularized using a finite number of blowups. The crucial point in both cases is finiteness of the transformation procedure.

Definition 12.6.6. Let $\Gamma_{j_1 j_2}^{(1)}$ be an edge of Newton's diagram $\hat{\Gamma}(f)$. Define the **height of** $\Gamma_{j_1 j_2}^{(1)}$ as the number of integral points on this edge. Define the **height of the Newton diagram** as the sum of the heights of all its edges.

The crucial observation in proving Theorem 12.6.5 is that the height of an edge decreases if we apply the rescaling in step (S3) by dividing an equation by a monomial with power $r > 0$. Eventually, the height will be 1. At this point, it is not too difficult to see that equations of height 1 are solvable.

12.7 Slowly Time-Dependent Systems

In Sections 12.4–12.6, we familiarized ourselves with the concept of the Newton polygon. In this context, the static problem of finding a series expansion for a critical manifold in planar systems has been solved. Although this is an essential

part of the scaling and delay analysis near a singularity, we would like to extend the analysis to dynamic scaling laws depending on ε . Again the Newton polygon will be used as a combinatorial tool in this analysis.

In this section we restrict ourselves to $(1, 1)$ -fast–slow systems of the form

$$\begin{aligned}\varepsilon \frac{dx}{d\tau} &= \varepsilon \dot{x} = f(x, y), \\ \frac{dy}{d\tau} &= \dot{y} = 1.\end{aligned}\tag{12.51}$$

One may interpret y as the slow time variable τ , since $y(\tau) = (\tau - \tau_0) + y(0)$. Alternatively, we can view the slow variable y as a bifurcation parameter for the one-dimensional ODE

$$\varepsilon \dot{x} = f(x, y).$$

The critical manifold of (12.51) is given by $C_0 = \{(x, y) \in \mathbb{R}^2 : f(x, y) = 0\}$. We shall deal with different branches $C_{0,j}$ of the critical manifold separately; see, for example, Figure 12.9(a). For notational convenience, the subscript j will be dropped, since we are going to consider only a single branch of the critical manifold at a time. Assume that C_0 is normally hyperbolic, so that there exists a function $h_0 : \mathcal{U}_y \subset \mathbb{R} \rightarrow \mathbb{R}$ such that $f(h_0(y), y) = 0$ and

$$C_0 = \{(x, y) \in \mathcal{U}_x \times \mathcal{U}_y \subset \mathbb{R}^2 : x = h_0(y)\},$$

where $\mathcal{U} = \mathcal{U}_x \times \mathcal{U}_y$ is a suitable domain. Fenichel's theorem provides a slow manifold C_ε given by

$$C_\varepsilon = \{(x, y) \in \mathcal{U} : x = h_\varepsilon(y) = h_0(y) + \mathcal{O}(\varepsilon)\}.$$

The variational equation around the critical manifold can be derived from the change of coordinates $x = h_0(y) + X$:

$$\varepsilon \dot{X} = f(h_0(y) + X, y) - \varepsilon h'_0(y) = a(y)X + b(X, y) - \varepsilon h'_0(y),\tag{12.52}$$

where

$$\begin{aligned}a(y) &= \frac{\partial f}{\partial x}(h_0(y), y), \\ b(X, y) &= f(h_0(y) + X, y) - a(y)X = \mathcal{O}(X^2).\end{aligned}$$

It will be more intuitive to exchange the parameter y with τ , so that the variational equation (12.52) becomes

$$\varepsilon \dot{X} = a(\tau)X + b(X, \tau) - \varepsilon h'_0(\tau),\tag{12.53}$$

which emphasizes that we are dealing with a one-dimensional nonautonomous ODE. Consider the case $a(\tau) < 0$, so that the critical manifold is attracting and $(x, \tau) = (0, 0)$ is a bifurcation point at which normal hyperbolicity is lost, so that $a(\tau) \rightarrow 0$ as $\tau \rightarrow 0$. Without loss of generality, we may assume that $-\tau_0 \leq \tau \leq 0$ for some $\tau_0 > 0$. The goal is to understand what happens to the scaling of the slow manifold C_ε near the bifurcation point.

Example 12.7.1. Consider the classical fold point scenario

$$\varepsilon \dot{x} = -\tau - x^2. \quad (12.54)$$

Here the bifurcation occurs at $(x, \tau) = (0, 0)$, and an attracting branch of the critical manifold for $\tau < 0$ is given by $x = \sqrt{-\tau}$. From Section 12.1, we already know what happens to the slow manifold, but let us pretend for now that we do not have the answer; see Figure 12.10(a). ♦

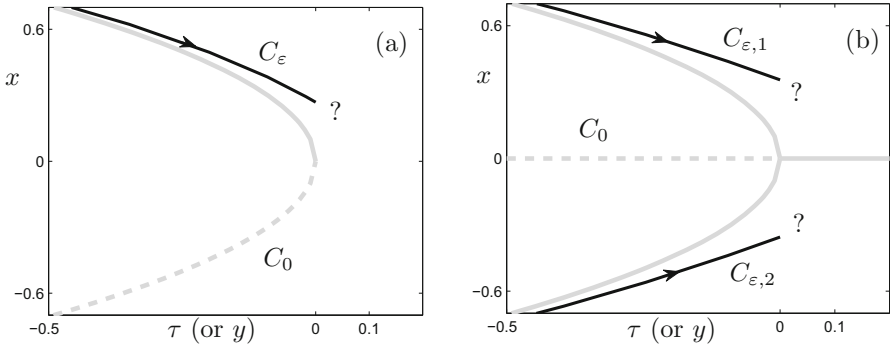


Figure 12.10: As parameter value for the computations, we fixed $\varepsilon = 0.05$. (a) Part of the slow manifold C_ε for (12.54) as it approaches the fold bifurcation point at $(x, \tau) = (0, 0)$ is shown. (b) Parts of two branches $C_{\varepsilon,1}$ and $C_{\varepsilon,2}$ of attracting slow manifolds are shown as they approach a pitchfork bifurcation (12.55).

Example 12.7.2. Obviously, we can replace the fold bifurcation normal form (12.54) by other one-dimensional bifurcations. A normal form for the **pitchfork bifurcation** with slow time-dependence is

$$\varepsilon \dot{x} = -\tau x - x^3. \quad (12.55)$$

The bifurcation occurs again at $(x, \tau) = (0, 0)$, and attracting branches of the critical manifold for $\tau < 0$ are given by $x = \pm\sqrt{-\tau}$; see Figure 12.10(b). As in Example 12.7.1, observe that the distance of the slow manifolds to C_0 seems to scale differently away from the bifurcation in comparison to a neighborhood of the bifurcation point. ♦

Suppose that the asymptotics for the singular limit are

$$h_0(\tau) \sim |\tau|^c \quad \text{and} \quad a(\tau) = \frac{\partial f}{\partial x}(h_0(\tau), \tau) \sim |\tau|^d$$

as $\tau \rightarrow 0$, where the naming conventions c and d remind us of the critical manifold and the partial derivative. To determine c , the Newton polygon can be

used as discussed in Section 12.6, where we calculated the asymptotic expansions for the solutions of

$$f(x, \tau) = 0.$$

Observe that since $h_0(\tau) \sim |\tau|^c$, it follows that $h'_0(\tau) \sim |\tau|^{c-1}$. To calculate d , we assume again for simplicity that f is analytic, so that

$$\frac{\partial f}{\partial x}(x, \tau) = \sum_{q_x \geq 1, q_\tau \geq 0} q_x f_{q_x q_\tau} x^{q_x-1} \tau^{q_\tau}.$$

Substitution of $x = \tau^c$ leads to

$$\frac{\partial f}{\partial x} = \sum_{q_x \geq 1, q_\tau \geq 0} q_x f_{q_x q_\tau} \tau^{c(q_x-1)} \tau^{q_\tau} = \sum_{q_x \geq 1, q_\tau \geq 0} q_x f_{q_x q_\tau} \tau^{c(q_x-1)+q_\tau}. \quad (12.56)$$

Cancellations in the series (12.56) are possible, as shown in the next example.

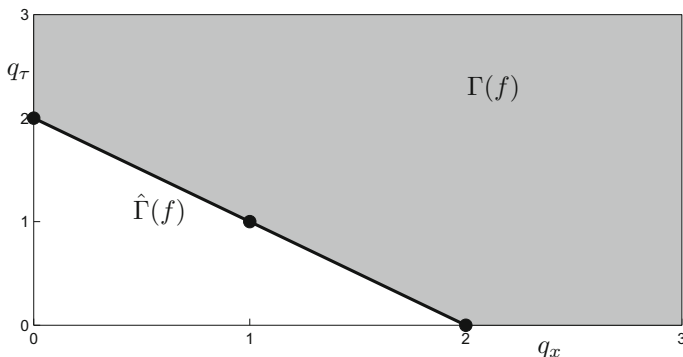


Figure 12.11: Newton polygon $\Gamma(f)$ (gray) and Newton diagram $\hat{\Gamma}(f)$ (black) for $f(x, \tau) = -(x - \tau)^2$.

Example 12.7.3. Suppose that $f(x, \tau) = -(x - \tau)^2$. Then $x = \tau$ describes the critical manifold, so that $c = 1$. The series (12.56) is

$$\frac{\partial f}{\partial x}(x, \tau) = -(2\tau - 2\tau + \tau^2) = -\tau^2,$$

so that the leading-order term of $a(\tau)$ is not of order $|\tau|$ but of order $|\tau|^2$, so that $d = 2$. However, this example is rather pathological, since the critical manifold is found as a double zero. The Newton diagram shows this, since it has two parallel edges, which implies that there are two solutions to $f(x, \tau) = 0$ that are tangent at the origin; see Figure 12.11. ♦

We would like to avoid the cancellation problem in the leading-order term of the series (12.56).

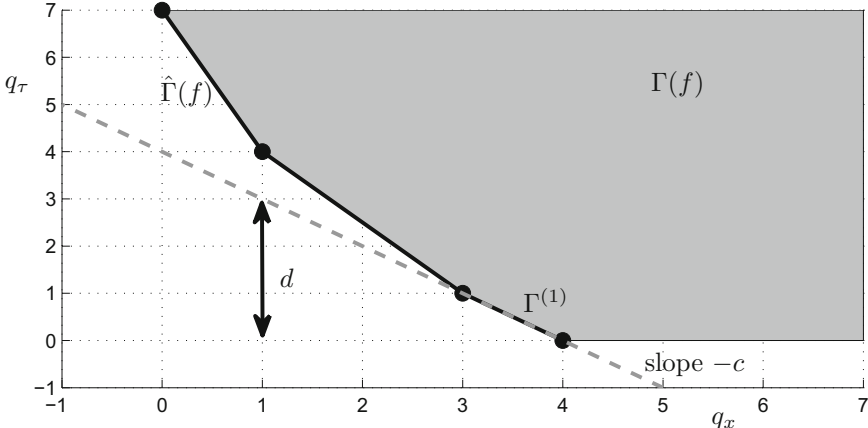


Figure 12.12: Sketch of a Newton polygon $\Gamma(f)$ (gray) and Newton diagram $\hat{\Gamma}(f)$ (black). The setup illustrates how to find the scaling for $a(\tau) = \frac{\partial f}{\partial x}(h_0(\tau), \tau) \sim |\tau|^d$ for a tame branch of the critical manifold; the branch is associated with the edge $\Gamma^{(1)}$ between $(4, 0)$ and $(3, 1)$ with slope -1 , so that $c = 1$. The scaling $d = 3$ is given by the ordinate at $q_x = 1$ for the line through $\Gamma^{(1)}$.

Definition 12.7.4. Define the scaling exponent

$$d^* := \min_{q_x, q_\tau \in \mathbb{Z}} \{c(q_x - 1) + q_\tau : f_{q_x q_\tau} \neq 0, q_x \geq 1, q_\tau \geq 0\}. \quad (12.57)$$

The branch of the critical manifold is **tame** if $d^* = d$, i.e., there are no cancellations in (12.56) that could yield the case $d > d^*$.

Proposition 12.7.5. Consider a tame branch of the critical manifold associated with an edge $\Gamma^{(1)}$ with slope $-c$ of the Newton diagram. Then the scaling exponent d is given by the ordinate at $q_x = 1$ of the line through $\Gamma^{(1)}$; see also Figure 12.12.

Proof. (Sketch) Observe that (12.57) is a linear integer programming problem over a convex domain. Therefore, standard optimization theory [BT97a] shows that the optimal solution must lie on a vertex of the Newton diagram. Evaluating $c(q_x - 1) + q_\tau$ on any vertex of $\Gamma^{(1)}$ yields the same value, since the edge has slope $-c$. Evaluating $c(q_x - 1) + q_\tau$ on another vertex of the Newton diagram increases the function value at least to $d + 1$, since the line through $\Gamma^{(1)}$ shifts further into the first quadrant; see Figure 12.12. Hence, the minimum $d^* = d$ for (12.57) is attained by evaluating $c(q_x - 1) + q_\tau$ on a vertex of $\Gamma^{(1)}$, say (v_1, v_2) , which gives

$$d = c(v_1 - 1) + v_2.$$

The line of slope $-c$ through (v_1, v_2) is given in the (q_x, q_τ) -plane by

$$q_\tau = -cq_x + v_2 + cv_1,$$

which can be evaluated at $q_x = 1$ to obtain the ordinate $-c + v_2 + cv_1 = c(1 - v_1) + v_2$, completing the proof. \square

Finally, we can state a classification theorem for one-dimensional slowly time-dependent systems. It describes the scaling of a critical manifold approaching a fast subsystem bifurcation point.

Theorem 12.7.6 ([Ber98b]). *Assume that for $-\tau \leq \tau < 0$, the function $h_0(\tau)$ is a tame branch for the critical manifold such that*

$$h_0(\tau) \sim |\tau|^c \quad \text{and} \quad \frac{\partial f}{\partial x}(h_0(\tau), \tau) \sim |\tau|^d$$

as $\tau \rightarrow 0$. Then the equation $\varepsilon \dot{x} = f(x, \tau)$ admits a slow manifold solution of the form $h_\varepsilon(\tau) = h_0(\tau) + X(\tau)$ with the following asymptotic properties as $\varepsilon \rightarrow 0$:

- (1) There exists a constant $k_1 > 0$, $k_1 = \mathcal{O}(1)$, such that

$$X(\tau) \sim \frac{\varepsilon}{\tau^{d+1-c}} \quad \text{for } -\tau_0 \leq \tau \leq -k_1 \varepsilon^{1/(c+1)}.$$

- (2) Either $X(\tau)$ diverges at $\tau = -k_1 \varepsilon^{1/(c+1)}$ or there exists a constant $k_2 > 0$, $k_2 = \mathcal{O}(1)$, such that

$$X(\tau) \geq k_2 \varepsilon^{d/(c+1)} \quad \text{for } -k_1 \varepsilon^{1/(c+1)} \leq \tau \leq 0.$$

- (3) If $f(h_0(\tau) + X(\tau), \tau) < 0$ for $0 < X < X(\tau_0)$ and $-\tau_0 \leq \tau \leq 0$, then $X(\tau)$ exists and

$$X(\tau) \sim \varepsilon^{d/(c+1)} \quad \text{for } -k_1 \varepsilon^{1/(c+1)} \leq \tau \leq 0.$$

Basically, parts (1) and (3) of Theorem 12.7.6 provide us with two different regimes for the slow manifold C_ε . Let $(x(\tau), y(\tau))$ denote the solution in the slow manifold. First, it is $\mathcal{O}(\varepsilon)$ -away from the critical manifold, and when it comes closer to the bifurcation point, it is expected to scale as

$$(x, y) \sim \left(\varepsilon^{d/(c+1)}, \varepsilon^{1/(c+1)} \right)$$

as $\varepsilon \rightarrow 0$. We shall not prove Theorem 12.7.6 but just briefly mention the main idea. We reconsider the main variational equation

$$\varepsilon \dot{X} = a(\tau)X + b(X, \tau) - \varepsilon h'_0(\tau) \tag{12.58}$$

and replace the linear terms by their scalings $a(\tau) = -A_0|\tau|^d$ and $h'_0(\tau) = H_0|\tau|^{c-1}$. Neglecting the quadratic term $b(X, \tau) = \mathcal{O}(X^2)$, we get from (12.58) that

$$\varepsilon \dot{X} = A_0|\tau|^d - \varepsilon H_0|\tau|^{c-1}. \tag{12.59}$$

The nonautonomous ODE (12.59) is linear and has an integral solution formula that can be analyzed explicitly. The analysis of this representation formula essentially gives the scalings of Theorem 12.7.6, and one is left with showing that the higher-order term $b(X, \tau)$ does not change the result of the linear calculation.

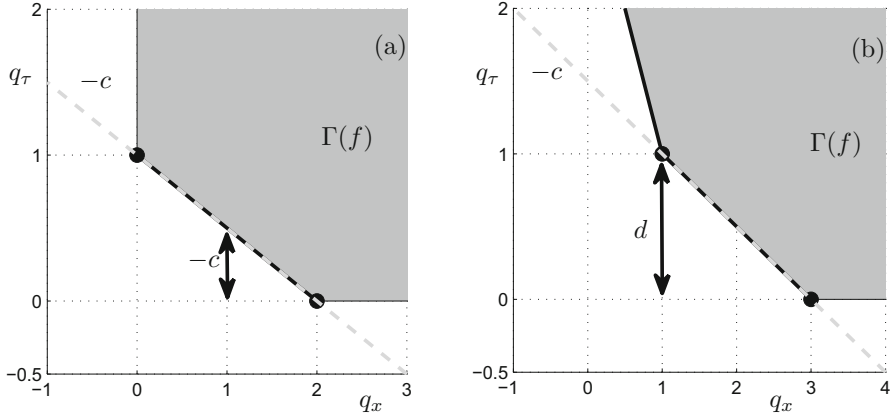


Figure 12.13: The following objects are shown: Newton polygon $\Gamma(f)$ (gray), Newton diagram $\hat{\Gamma}(f)$ (black), line with slope $-c$ through an edge of $\hat{\Gamma}(f)$ (dashed, light gray) corresponding to branch with scaling exponent c and scaling exponent d for $a(\tau)$. (a) Fold bifurcation with slow time given by $f(x, \tau) = -\tau - x^2$. (b) Pitchfork bifurcation with slow time given by $f(x, \tau) = -\tau x - x^3$; Definition 12.4.1(N3) has been used for the Newton polygon for this figure, but all three definitions give the same scaling laws.

Example 12.7.7. Using Theorem 12.7.6, we can now compute the scalings for the fold and pitchfork bifurcations with slow time from Examples 12.7.1 and 12.7.2. For the fold bifurcation, we have

$$f(x, \tau) = -\tau - x^2 \quad \Rightarrow \quad x = (-\tau)^{1/2}$$

for the attracting branch of the critical manifold C_0 . Therefore, $c = 1/2$, which would also follow from using the Newton polygon shown in Figure 12.13(a). We can immediately see from Figure 12.13(a) that $d = 1/2$, which is also confirmed by direct computation:

$$\frac{\partial f}{\partial x}(\sqrt{-\tau}, \tau) = -2\sqrt{-\tau} \sim |\tau|^{1/2}.$$

Parts (1) and (3) of Theorem 12.7.6 apply, since

$$f(h_0(\tau) + X, \tau) = -\tau - (\sqrt{-\tau} + X)^2 = -\tau + \tau - X\sqrt{-\tau} - X^2 < 0$$

for $0 < X < X(\tau_0)$ and $-\tau_0 \leq \tau \leq 0$. Therefore, near the fold bifurcation point $(x, y) = (0, 0)$ of the fast subsystem, the solution in the attracting slow manifold C_ε scales like

$$(x(\tau), y(\tau)) \sim \left(\varepsilon^{d/(c+1)}, \varepsilon^{1/(c+1)} \right) = \left(\varepsilon^{1/3}, \varepsilon^{2/3} \right)$$

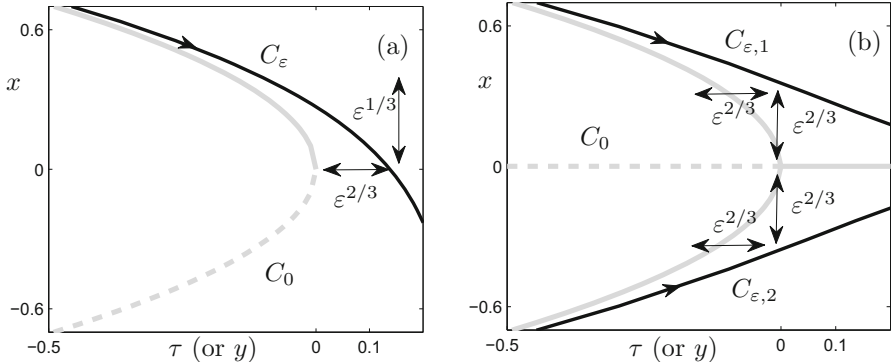


Figure 12.14: As parameter value for the computations, we fixed $\varepsilon = 0.05$; the scaling laws of the slow manifolds near the bifurcation point $(x, \tau) = (0, 0)$ are illustrated by two-headed arrows. (a) Part of the slow manifold C_ε for (12.54) as it approaches the fold bifurcation point is shown. (b) Parts of two branches $C_{\varepsilon,1}$ and $C_{\varepsilon,2}$ of attracting slow manifolds are shown as they approach a pitchfork bifurcation (12.55).

as $\varepsilon \rightarrow 0$. This is precisely the same result we found using ad hoc asymptotic methods or the blowup method. For the pitchfork bifurcation, we have

$$f(x, \tau) = -\tau x - x^3 \quad \Rightarrow \quad x = \pm(-\tau)^{1/2}$$

for the two stable branches of the critical manifold $C_{0,1}$ and $C_{0,2}$ with $\tau < 0$. From the Newton polygon in Figure 12.13(b), we see that $c = 1/2$ and $d = 1$. It is easy to check that parts (1) and (3) of Theorem 12.7.6 can again be applied. Hence, the solutions in the attracting slow manifolds $C_{\varepsilon,1}$ and $C_{\varepsilon,2}$ scale like

$$(x(\tau), y(\tau)) \sim \left(\varepsilon^{d/(c+1)}, \varepsilon^{1/(c+1)} \right) = \left(\varepsilon^{2/3}, \varepsilon^{2/3} \right)$$

as $\varepsilon \rightarrow 0$. The results are illustrated in Figure 12.14. ♦

The results from Theorem 12.7.6 cover only the approach toward the bifurcation. The dynamics near the bifurcation point, where normal hyperbolicity is lost, must be analyzed separately. However, the analysis already shows the size of the neighborhood we have to analyze and anticipates the correct blowup coefficients via the Newton polygon; see Section 12.8. Although Example 12.7.7 computes the scaling for the normal forms of two bifurcations, we should recall that normal forms have only qualitatively similar dynamics for all bifurcation points with the same normal form. In particular, the quantitative scaling laws are not universal, as the next exercise shows.

Exercise 12.7.8. Consider a pitchfork bifurcation with slow drift given by

$$\varepsilon \dot{x} = -(\tau + 2x)(\tau + x^2).$$

Show that the scaling law near the bifurcation is $(x(\tau), y(\tau)) \sim (\varepsilon^{1/4}, \varepsilon^{1/2})$. ◇

12.8 Other Newton Polygon Applications

In this section, we are going to connect the Newton polygon to the blowup method and to asymptotic analysis. First, note that the Newton polygon construction can also be applied to general planar vector fields

$$\begin{aligned} x' &= F_1(x, y), \\ y' &= F_2(x, y). \end{aligned} \tag{12.60}$$

Suppose that $(x, y) = (0, 0)$ is an equilibrium point and that $F = (F_1, F_2)$ is analytic,

$$F_1(x, y) = \sum_{q_x, q_y \geq 1} F_{1, q_x q_y} x^{q_x} y^{q_y}, \quad F_2(x, y) = \sum_{q_x, q_y \geq 1} F_{2, q_x q_y} x^{q_y} y^{q_y}.$$

Define the following subset of the integral lattice:

$$\mathcal{D}(F) := \{(q_x, q_y) \in \mathbb{Z}^2 : |F_{1, q_x q_y}| + |F_{2, q_x q_y}| > 0\}.$$

Observe that $\mathcal{D}(F)$ is located in the first quadrant, since all its points have non-negative entries. We can again associate the Newton polygon and the Newton diagram with $\mathcal{D}(F)$ as in Definitions 12.4.1 and 12.4.5. It can be shown that the solutions near nonhyperbolic equilibrium points of (12.60) can be described using the same techniques as in Section 12.6, except that we also have to analyze the vertices of the Newton diagram [Bru89].

A definite treatment of all relations between blowing up, power transformations, and Newton polygon combinatorics in arbitrary dimension N is not available at the time of writing of this book. Hence, we shall restrict ourselves to examples. We are going to assume definitions and familiarity of Chapter 7 on the blowup method for the rest of this section.

Example 12.8.1. Consider the planar vector field

$$\begin{aligned} x' &= xy + y^2 = F_1(x, y), \\ y' &= x^4 = F_2(x, y). \end{aligned} \tag{12.61}$$

It is relatively easy to find the Newton diagram, which has just two edges (see Figure 12.15):

$$\Gamma_1^{(1)} = (-3, 1) \quad \text{and} \quad \Gamma_2^{(1)} = (-1, 1).$$

Observe that the vector field $F = (F_1, F_2)$ given by (12.61) is not (α_1, α_2) -quasihomogeneous of degree k according to Definition 7.3.2; this can be checked by direct computation, since the quasihomogeneity conditions

$$\begin{aligned} r^{\alpha_1 + \alpha_2} xy + r^{2\alpha_2} y^2 &= F_1(r^{\alpha_1} x, r^{\alpha_2} y) \stackrel{!}{=} r^{\alpha_1 + k} F_1(x, y) = r^{\alpha_1 + k} (xy + y^2), \\ r^{4\alpha_1} x^4 &= F_2(r^{\alpha_1} x, r^{\alpha_2} y) \stackrel{!}{=} r^{\alpha_2 + k} F_2(x, y) = r^{\alpha_2 + k} x^4, \end{aligned}$$

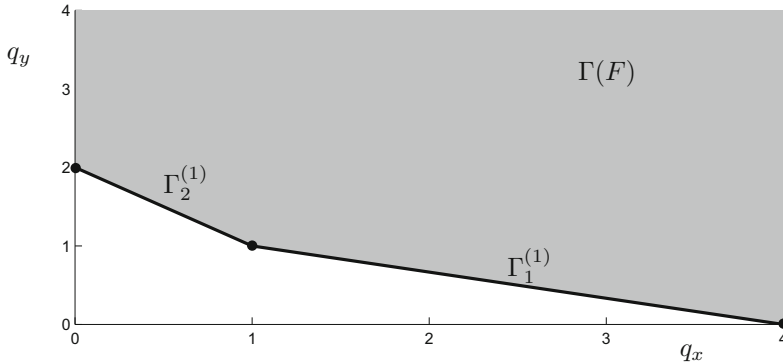


Figure 12.15: Newton polygon $\Gamma(F)$ for equation (12.61).

imply that $\alpha_1 = \alpha_2$ but also that $2\alpha_2 = 4\alpha_1$, which is a contradiction. But if we consider the truncation with respect to an edge of the Newton diagram, say $\Gamma_1^{(1)}$, we find that

$$\hat{F}(x, y) = (xy, x^4)^\top,$$

which is quasihomogeneous of type $(2k, k)$ and degree k for every $k \in \mathbb{N}$. Similarly, the truncation with respect to the edge $\Gamma_2^{(1)}$,

$$\hat{F}(x, y) = (xy, y^2),$$

is quasihomogeneous. Recall from Section 7.3 that the blowup method simplifies significantly if we consider a quasihomogeneous vector field or a component of a vector field that is quasihomogeneous. The Newton diagram now allows us to find quasihomogeneous components. ♦

Exercise/Project 12.8.2. Consider each weighted (or quasihomogeneous) blowup in Chapters 7 and 8. Calculate the Newton polygon for each case as well as the weighted blowup exponents. ◇

Another application of the Newton polygon is asymptotic analysis. Consider a two-point boundary value problem

$$F\left(\frac{d^n y}{d\tau^n}, \dots, \frac{d^2 y}{d\tau^2}, \frac{dy}{d\tau}, y, \tau; \varepsilon\right) = 0 \quad (12.62)$$

with boundary conditions at $\tau = 0$ and/or $\tau = 1$. We have seen in Sections 9.1 and 9.2 that (12.62) can have boundary layers or interior layers where a transition from fast to slow motion (or vice versa) occurs. The classical technique to find boundary layers, say at $\tau = 0$, is to consider a rescaling

$$\frac{\tau}{\varepsilon^a} = t, \quad (12.63)$$

so that two or more leading-order terms in (12.62) have the same order, i.e., the goal is to determine a dominant balance. Two or more terms for (12.62)

will dominate if they have the same lowest power in ε , which yields a potential boundary layer of thickness $\tau = \mathcal{O}(\varepsilon^a)$. Observe that the scaling (12.63) transforms monomials as follows:

$$\varepsilon^l \tau^m \frac{d^n}{d\tau^n} = \varepsilon^{l+(m-n)a} t^m \frac{d^n}{dt^n}.$$

To find the right value of a , one has to analyze the plane of powers of (τ, ε) . Hence, we put the point $Q = (q_\tau, q_\varepsilon) = (m - n, l)$ into correspondence with the monomial $\varepsilon^l \tau^m \frac{d^n}{d\tau^n}$. Observe that the point Q lies in the lattice \mathbb{Z}^2 but that it could have negative entries. In this case, we agree to define the Newton polygon as the convex hull of the given lattice points, i.e., we consider Definition 12.4.1(N1).

Example 12.8.3. Consider the second-order boundary value problem

$$\varepsilon \frac{d^2y}{d\tau^2} + (1 + \varepsilon) \frac{dy}{d\tau} + y = 0 \quad (12.64)$$

for $\tau \in [0, 1]$. We shall not spell out the boundary conditions in detail here. The set \mathcal{D} that defines the Newton polygon is given by the points

$$\mathcal{D} = \{Q_1 = (-2, 1), Q_2 = (-1, 0), Q_3 = (-1, 1), Q_4 = (0, 0)\}.$$

The Newton polygon is shown in Figure 12.16(a). Directly applying the rescaling $\tau = \varepsilon^a t$ to (12.64) yields

$$\frac{d^2y}{d\tau^2} + (1 + \varepsilon) \frac{dy}{d\tau} + \varepsilon y = 0. \quad (12.65)$$

This suggests the dominant balance of the terms $\frac{d^2y}{d\tau^2}$ and $\frac{dy}{d\tau}$ with a boundary layer of size $\tau = \mathcal{O}(\varepsilon)$. Observe that the two dominant terms correspond to the points Q_1 and Q_2 . So let us consider the edge $\Gamma^{(1)} = (Q_2 - Q_1) = (-1, 1)$. From our previous uses of the Newton polygon, we know that the outer normal vector to $\Gamma^{(1)}$ has a special significance. It turns out that one has to look at the outer normal vector

$$(-1, -a) =: P.$$

For the edge $\Gamma^{(1)} = (-1, 1)$, this means that $P = (-1, -1)$. Therefore, the boundary layer can be inferred from P as $\tau = \mathcal{O}(\varepsilon^a)$. ♦

Example 12.8.4. Consider the second-order boundary value problem

$$\varepsilon^3 \tau \frac{d^2y}{d\tau^2} - \tau^2 \frac{dy}{d\tau} - (\tau^3 + \varepsilon)y = 0 \quad (12.66)$$

for $\tau \in [0, 1]$. The Newton polygon is found from the set

$$\mathcal{D} = \{Q_1 = (-1, 3), Q_2 = (1, 0), Q_3 = (3, 0), Q_4 = (0, 1)\}.$$

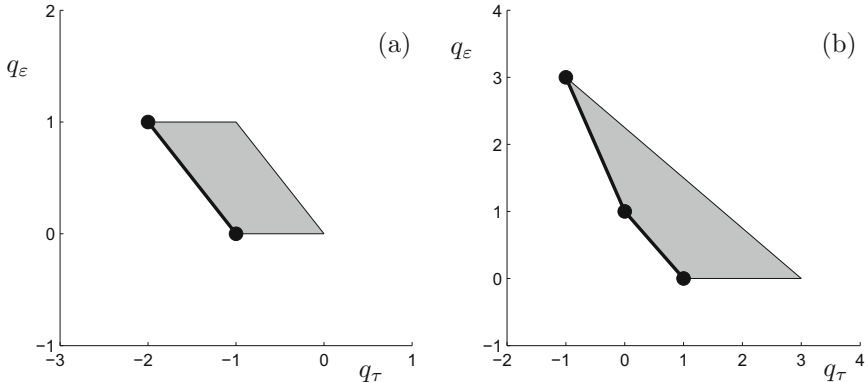


Figure 12.16: Newton polygons Γ for singularly perturbed boundary value problems. (a) Equation (12.64) and (b) equation (12.66).

Figure 12.16(b) shows that there are two edges with outer normal vectors in the third quadrant (i.e., with negative component entries). These edges are

$$\Gamma_1^{(1)} = Q_4 - Q_2 = (-1, 1), \quad \Gamma_1^{(2)} = Q_1 - Q_4 = (-1, 2).$$

The associated normal vectors are $P_1 = (-1, -1)$ and $P_2 = (-1, -1/2)$. Therefore, we conjecture that there are two boundary layers at $\tau = 0$ with size $\tau = \mathcal{O}(\varepsilon)$ and $\tau = \mathcal{O}(\varepsilon^{1/2})$. It can be shown that these two nested boundary layers exist (check it or look at [BO99]). ♦

The examples show that the Newton polygon can also be a useful combinatorial device for classical singularly perturbed boundary value problems.

12.9 References

Section 12.1: This is just a summarized quick review of certain relevant parts from Section 5.4 and Section 7.4 to introduce the main problems of scaling and delay.

Section 12.2: The section was built on the groundbreaking papers [Nei87b, Nei88], which were motivated by the so-called Shishkova example [Shi73]. There is considerable classical work on bifurcation problems with slowly varying parameters [Hab79, Kev71] and delayed-Hopf bifurcation [HE93a]. Recent surveys on the topic [FS09, Nei09, Su01] are available as well. The bifurcation-delay effect near Hopf bifurcation is a theme that has been taken further in various directions such as degenerate linear terms [RS03], delay differential equations [ZW10a], difference equations [Fru91, FS03b], effects of forcing [Su97, Su96a], Gevrey asymptotics [Bae95], imperfect bifurcations [EM86], period-doubling cascades [Bae91a, Bae91b], persistent oscillations [Su96b], saddle-center bifurcations [DH00a, DH02b], subharmonic resonance [BH98a, BH98b], and various applications [AFR13, HE93b].

Section 12.3: The section is based on the papers [BG08a, BER89] with a neuroscience application considered in [RB88]. Delayed bifurcation also occurs in applications e.g., in the Belousov–Zhabotinskii reaction [SM96], in lasers [AGMR89, CMA90, EM91, Man87, ME84, SSB⁺87], as well as in the Olsen model for the peroxidase–oxidase reaction [DKO09]. There are other references for asymptotics [ERHG91] and ramping [PDL11] available. The nonstandard analysis viewpoint on the topic is developed in [Ben09, Ben91b, Ben91a] with a detailed overview in [Lob91]. For more on fast subsystem Hopf bifurcations, we refer to [Abe85b, GO12, Sti98b, ZKSW11]. Interestingly, there are also direct relations of delayed Hopf bifurcation to the analysis of folded nodes [BGK12, KW10] via rescaling.

Section 12.4: This section aims to introduce and compare the various definitions of the Newton polygon found in the literature [Bru89, Ber98b, Dum93]. The Newton polygon appears not only in multiple time scale dynamical systems; it also has applications to a diverse set of mathematical topics, including approximation theory [BHS87], Bergman kernels [Kam04], differential operators [DMV98, DSS08], finite fields [Bom78], group theory [Oor00], Hodge polynomials [Maz73], and multiplier ideals [How01]. As usual for other topics, the number of applications is obviously much wider than we can reference here.

Section 12.5: The main reference for this and the next section is the book [Bru89]; see also [Mik08]. There could potentially be further deep links between multiscale dynamics and abstract algebraic theory via the Newton Polygon.

Section 12.6: One may also use the Newton polygon to find expansions for slow manifolds [Sam91]. The insight that the Newton polygon is very useful in understanding singularities of algebraic curves can be found already in the work of Hironaka [Hir67] and probably goes back much further.

Section 12.7: The application of the Newton polygon to bifurcation delay and scaling of slow manifolds is adapted from [Ber98b, Ber00, BK99]. A slow passage through a pitchfork bifurcation is considered in [ME87], to which one could apply the theory of Newton polygons.

Section 12.8: We refer to [Dum93] for relating blowup and the Newton polygon, while the asymptotics for the second-order equations can be found in [Mik08]. Other nice uses of the Newton polygon related to fast–slow systems are multisummability [BRS91], order reduction [IS63], and oscillatory integrals [CKN13, DNS05, Gre10, Var76].

Chapter 13

Oscillations

Many multiple time scale systems are capable of generating intricate patterns. In this chapter, we are going to focus on periodic oscillations where the fast–slow structure plays a crucial role in the generating mechanism. Let us point out that we do not aim at a complete classification. The focus is on examples and prototype mechanisms. There are two main keywords associated with this area that we want to explore: mixed-mode oscillations (MMOs) and bursting.

Section 13.1 introduces the problem and gives some basic viewpoints on the structure of oscillation patterns. We have already encountered one key mechanism for oscillations in which folded singularities play a key role. Section 13.2 covers the folded node case in quite some detail, while Section 13.3 considers the three-dimensional singular Hopf bifurcation. Section 13.4 is a brief remark on the local/global interplay and tourbillon-type small oscillations. Section 13.5 explores the folded node and singular Hopf oscillation mechanisms in the Koper model, which is an elegant, practical, and concrete example. Bursting is dealt with in the next two sections. Section 13.6 examines square-wave bursters, which are a nice example of how the relatively simple interaction of global and local bifurcations in fast–slow systems yields bursting patterns. Section 13.7 is an introduction to the class of elliptic bursters, in which two other bifurcations play the important roles. Section 13.8 shows that a three-time-scale structure can be beneficial to building explicit proofs for various types of MMOs that are generated via a canard-explosion phenomenon.

Background: No additional background is required, but the chapter is deeply cross-linked with many results discussed in previous chapters. In fact, this chapter really shows how many of the tools and results we have developed so far can be applied in classifying patterns. Hence, it is recommended to refer to previous material when it is mentioned.

13.1 Overview

Mixed-mode oscillations (MMOs) can briefly be described as periodic orbits with time series having peaks of substantially different amplitudes; see Figure 13.1(a). They form one of the major direct links of multiple time scale dynamics to physical, chemical, and biological models in the applied sciences. A famous example of MMOs arises from the Belousov–Zhabotinskii (BZ) reaction. Since this discovery and several experimental studies of the BZ reaction in the 1960s and 1970s, it was realized that quite a large variety of other chemical systems can exhibit MMOs. The next definition provides a nonrigorous working definition of MMOs.

Definition 13.1.1. A system exhibits **mixed-mode oscillations** (MMOs) if it has a periodic orbit γ and the time series (in at least one phase space variable and in some coordinate scale) of γ has oscillations differing by at least one order of magnitude.

The second important type of pattern we are going to discuss is bursting oscillations. Roughly speaking, bursting oscillations are time series patterns alternating between near steady-state and rapid oscillatory phases; see Figure 13.1(b). The main application context for bursting is neuroscience, but there is no need to restrict the terminology to this particular context. Again, we will give only a very vague definition as a first orientation.

Definition 13.1.2. A system exhibits **bursting oscillations** if it has a periodic orbit γ and the time series (in at least one fast phase space variable and in some coordinate scale) of γ alternates between rapid oscillations and near steady-state behavior.

Obviously, the distinction between MMOs and bursting is not ideal, since the two definitions are not precise and can also overlap. Figure 13.1(c) shows an example that can be classified as MMOs and bursting.

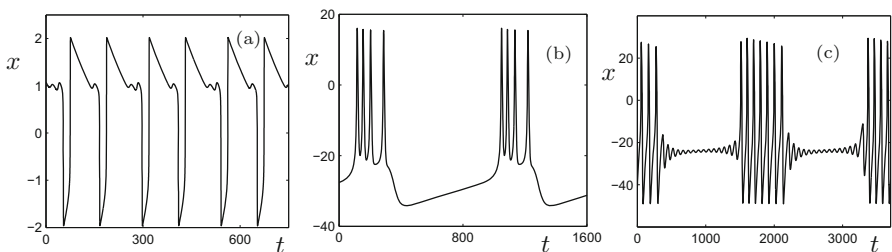


Figure 13.1: Examples of complex oscillations in multiple time scale systems. (a) MMOs of type 1¹ 2¹ in the Koper model; see Section 13.5. (b) Square-wave bursting of type 0⁴ in the 3D Morris–Lecar model; see Section 13.6. (c) Elliptic bursting, or MMOs, in the 3D Morris–Lecar model of type 7¹⁵; see Section 13.7.

A common notation to simplify the description of oscillations is to code patterns in a time series by symbol sequences

$$\cdots L_{j-1}^{s_{j-1}} L_j^{s_j} L_{j+1}^{s_{j+1}} \cdots, \quad (13.1)$$

where L^s means that we encountered L **large-amplitude oscillations (LAOs)** in the time series followed by s **small-amplitude oscillations (SAOs)**. As a shorthand notation, one writes only the periodic part of (13.1), for example $\cdots 2^3 1^2 2^3 1^2 2^3 1^2 \cdots$ would be simply denoted as an oscillation of type $2^3 1^2$. Some typical MMO patterns are 1^s , with $s \gg 1$ describing one large loop followed by s small loops, and 2^1 or 2^2 , describing alternating sequences with few small and large loops. Many bursting patterns are L^0 with $L \gg 1$, which we also refer to as **spiking**. Some typical bursting models also generate L^s patterns with $L, s \gg 1$. The principles ones seeks aim at explaining the source of small local, as well as large global, oscillations from the multiple time scales structure.

Example 13.1.3. To understand why fast–slow systems play such an important role in the description of oscillations, we will describe one of the toy models of the BZ reaction. The following equations are due to Gaspard and Nicolis:

$$\begin{aligned} \varepsilon \dot{x} &= y_1 - 0.5x^3 + 3x^2 - 5x, \\ \dot{y}_1 &= y_1(\kappa y_1 - 0.5y_2 - x + 0.6), \\ \dot{y}_2 &= y_2(y_1 + 0.3x - 1.3), \end{aligned} \quad (13.2)$$

where κ is the main bifurcation parameter. Here we simply take $\kappa = 0.49$ to illustrate some of the MMOs in the model. The idea for the interpretation of (13.2) in the context of MMOs is due to Rössler. Hence, we shall refer to (13.2) as the **Gaspard–Nicolis–Rössler (GNR)** model. The critical manifold is

$$C_0 = \{(x, y_1, y_2) \in \mathbb{R}^3 : y_1 = 0.5x^3 - 3x^2 + 5x =: c(x)\}.$$

The two fold curves are found by solving $c'(x) = 0$, which yields $L_{\pm} = \{(x, y_1, y_2) \in \mathbb{R}^3 : x_{\pm} = 2 \pm \sqrt{2/3}\}$. The fold lines split C_0 into three parts:

$$C_0^{a-} = C_0 \cap \{x < x_{-}\}, \quad C_0^r = C_0 \cap \{x_{-} < x < x_{+}\}, \quad C_0^{a+} = C_0 \cap \{x > x_{+}\},$$

where the branches $C_0^{a\pm}$ are attracting and C_0^r is repelling; see Figure 13.2(a). Fenichel's theorem implies that each piece perturbs away from the fold curves to an associated slow manifold, which we denote, e.g., by C_{ε}^{a-} . It is easy to calculate that one particular equilibrium point of the full system (13.2) is given by $q \approx (0.29, 1.21, 1.81) \in C_{\varepsilon}^{a-}$. The calculation of the linearization at q shows that q is a saddle focus with two complex conjugate eigenvalues with positive real parts. Therefore, the spiraling directions are unstable. Since the remaining direction is stable, it is a fast direction, since $q \in C_{\varepsilon}^{a-}$.

Figure 13.2 shows a periodic orbit that exhibits complex oscillations. We start following the orbit near C_{ε}^{a+} . It follows the stable branch C_{ε}^{a+} until it reaches the vicinity of the (lower) fold line L^+ . Then it jumps to a neighborhood of C_{ε}^{a-} near q . The slow evolution is dominated by the weak unstable spiraling generating small loops. Eventually, one of the small loops reaches the vicinity of the (upper) fold line L^- , and after a fast jump, the process repeats. ♦

Exercise/Project 13.1.4. Use geometric singular perturbation theory from Chapters 3 and 7 to show that one may change several constants in the Gaspard–Nicolis models (13.2) to obtain a homoclinic orbit that has a relaxation oscillation structure. ◇

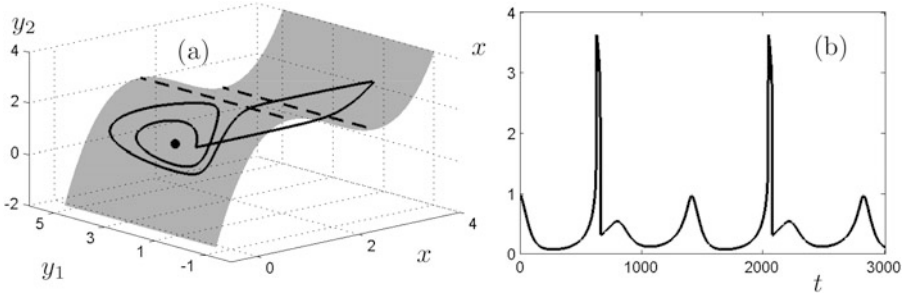


Figure 13.2: Gaspard–Nicolis–Rössler model. (a) Phase space with critical manifold C_0 (gray), fold lines L_{\pm} (dashed black) and saddle focus equilibrium point q (black dot). A 1^2 mixed-mode oscillation (solid black) is shown as well. (b) Time series (t, x) for the orbit from (a).

Figure 13.2 is a good illustration of how MMs can be explained using fast–slow systems and simple geometric insight. However, the 1^2 MMs observed in the GNR model are generated by a mechanism that cannot explain many types of bursting oscillations and MMs. The rest of this chapter describes several other mechanisms that can explain a surprisingly large variety of patterns encountered in applications.

13.2 Folded Nodes

One of the best-understood fast–slow mechanisms for the generation of small-amplitude oscillations (SAOs) is folded nodes, which we already discussed in Sections 8.5 and 8.6. We briefly recall the definitions and major results with a focus on oscillatory behavior. Consider a general $(1, 2)$ -fast–slow system

$$\begin{aligned} \varepsilon \frac{dx}{d\tau} &= \varepsilon \dot{x} = f(x, y), \\ \frac{dy_i}{d\tau} &= \dot{y}_i = g_i(x, y), \end{aligned} \quad \text{for } i = 1, 2. \quad (13.3)$$

The critical manifold is $C_0 = \{(x, y) \in \mathbb{R}^3 : f(x, y) = 0\}$ with desingularized slow flow

$$\begin{aligned} \dot{x} &= f_{y_1}g_1 + f_{y_2}g_2, \\ \dot{y}_2 &= -f_xg_2. \end{aligned} \quad (13.4)$$

Locally, we assume that C_0 is normally hyperbolic with the exception of points on a fold curve $L = \{(x, y) \in \mathbb{R}^3 : f_x(x, y) = 0, f_{xx}(x, y) \neq 0\}$. Equilibrium points of (13.4) that lie on the fold curve L are called folded singularities, and we are interested in the case that the equilibrium point of (13.4) is a node. As discussed in Sections 4.3, 8.5, and 8.6, it is convenient to consider a normal form for the analysis. Two equivalent normal forms for a folded node are

$$\begin{aligned}\varepsilon \dot{x} &= y_1 - x^2, \\ \dot{y}_1 &= -(\mu + 1)x - y_2, \\ \dot{y}_2 &= \frac{1}{2}\mu,\end{aligned}\tag{13.5}$$

and

$$\begin{aligned}\varepsilon \dot{x} &= y_1 - x^2, \\ \dot{y}_1 &= y_2 - x, \\ \dot{y}_2 &= -\nu.\end{aligned}\tag{13.6}$$

Denote the eigenvalues of (13.4) by λ_w and λ_s , and assume that $0 > \lambda_w > \lambda_s$ to obtain a folded node. The associated eigendirections ϕ_w and ϕ_s are singular primary canards. The slow flow for (13.5) is shown in Figure 13.3(a), and the desingularized slow flow in Figure 13.3(b) together with the singular canards. We denote the ratio of the eigenvalues by

$$\mu := \frac{\lambda_w}{\lambda_s} \in (0, 1).$$

It can be shown (see Exercise 13.2.1) that this definition is consistent with the use of μ in (13.5). Near the origin, the critical manifold splits into three parts, $C_0 = C_0^a \cup L \cup C_0^r$, where C_0^a is the attracting sheet with $f_x < 0$, and C_0^r the repelling sheet with $f_x > 0$. As usual, the associated slow manifolds will be denoted by C_ε^a and C_ε^r .

Exercise 13.2.1. Consider the two normal forms (13.5) and (13.6).

- (a) Replace (x, y_1, y_2, τ) in (13.6) by $(u, v_1, v_2, \tilde{\tau})$ and use the coordinate change
$$x = (1+\mu)^{1/2}u, \quad y_1 = (1+\mu)v_1, \quad y_2 = -(1+\mu)^{3/2}v_2, \quad \tau = (1+\mu)^{-1/2}\tilde{\tau}$$
to show that the normal forms are equivalent.
- (b) What is the relation between μ and ν ? Show that $\mu \approx 2\nu$ for $0 < \mu \ll 1$.
- (c) Calculate the desingularized slow flow for (13.5) and (13.6).
- (d) Show that the eigenvalue ratio for the desingularized slow flow of (13.5) is μ . \diamond

The main point is that folded nodes provide a mechanism for small oscillations in an MMO. To describe how these oscillations arise, we shall restrict attention to the case $n - 1 < \mu^{-1} < n$ for $n \in \mathbb{N}$. We also restrict μ far enough away from special transcritical and pitchfork bifurcations of canards arising near the resonances $\mu \in \mathbb{N}$; cf. Figure 8.12.

Theorem 13.2.2 (cf. Theorem 8.5.12). *For a folded node with $n - 1 < \mu^{-1} < n$, the slow manifolds C_ε^a and C_ε^r twist $n - 1$ times around the primary maximal canard solution associated with the weak eigendirection. A **twist** corresponds to a rotation by 180° .*

Theorem 13.2.3 (cf. Theorem 8.6.8 and Figure 8.12). *For a folded node, assume that $2k + 1 < \mu^{-1} < 2k + 3$ and that μ^{-1} is suitably bounded away from $2k + 2$. Then there are the two primary maximal canards, $\xi_{w,\varepsilon}$ and $\xi_{s,\varepsilon}$, obtained from perturbation of ξ_w and ξ_s . Furthermore, there are k secondary maximal canards $\xi_{j,\varepsilon}$ for $j \in \{1, 2, \dots, k\}$.*

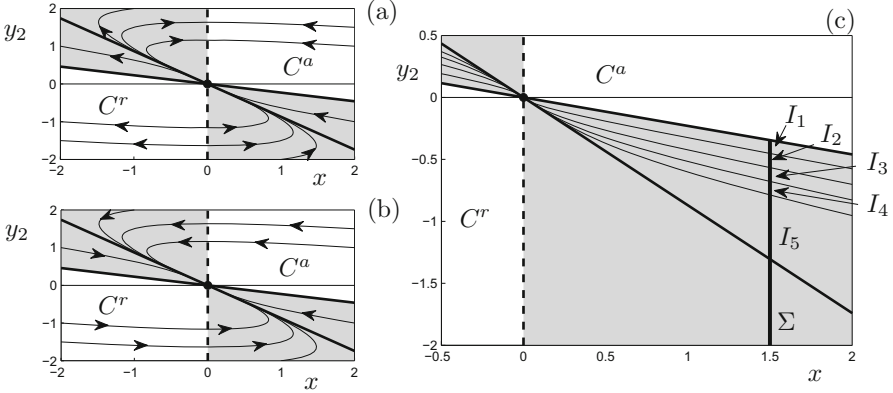


Figure 13.3: The slow flow on the critical manifold C_0 for $\mu = 0.1$. Thick black lines represent the canard orbits; the strong canard and the z -axis bound the funnel regions (gray). (a) Slow flow for (13.5). (b) Desingularized slow flow for (13.5). (c) Zoom near a cross section Σ (here placed at $x = 1.5$). The intersection of Σ with the funnel region yields the sectors of rotation I_k . Note carefully that the sectors I_1, I_2, I_3, I_4 do not exist for $\varepsilon = 0$. Here we have superimposed a sketch of these sectors onto the singular limit by inserting trajectories of the slow flow that are equally spaced with spacing $\varepsilon = 0.01$ on Σ . In the limit $\varepsilon \rightarrow 0$, all these orbits converge onto the strong canard!

The geometry of SAOs can be derived from Theorems 13.2.2 and 13.2.3. Suppose a trajectory approaches $0 := (0, 0, 0)$ via C_ε^a lying between two secondary canards. It will twist around the weak primary canard $\xi_{w,\varepsilon}$ by Theorem 13.2.2. After a certain number of SAOs, it leaves the vicinity of the folded node. A visualization of this effect is shown in Section 8.6. Here we want to understand the structure of the SAOs starting from the singular limit $\varepsilon = 0$. Every singular limit of an SAO has to lie inside the funnel \mathcal{F} , as illustrated in Figure 13.3. The question is how trajectories are organized inside the funnel in relation to the singular maximal canards and what their twisting is. Suppose we have k secondary canards as provided by Theorem 13.2.3. Define a section

$$\Sigma = \{(x, y_1, y_2) \in \mathbb{R}^3 : x = \sigma\},$$

where $\sigma > 0$ is chosen such that Σ is $\mathcal{O}(1)$ away from the folded node. Therefore, Fenichel's theorem still applies up to Σ . The situation is shown as a projection onto the (x, y_2) -coordinates in Figure 13.3(c). For $0 < \varepsilon \ll 1$, we can consider the attracting slow manifold C_ε^a . The intersection

$$\Sigma \cap C_\varepsilon^a = I_1 \cup I_2 \cup \dots \cup I_k \cup I_{k+1}$$

is subdivided by the maximal canards, i.e., I_1 has endpoints given by $\xi_{w,\varepsilon}$ and $\xi_{w,1}$, I_2 endpoints given by $\xi_{1,\varepsilon}$ and $\xi_{2,\varepsilon}$, and so on. In Figure 13.3, we have sketched where these maximal canards would lie when we project them onto the

critical manifold and into the funnel region. The next result provides us with the precise twisting of the canards.

Theorem 13.2.4 ([BKW06]). *The primary strong canard $\xi_{s,\varepsilon}$ twists once around $\xi_{w,\varepsilon}$. The j th secondary canard twists $(2j + 1)$ times around $\xi_{w,\varepsilon}$. Hence, the primary strong canard and the secondary canards are separated by a full rotation of 360° . Trajectories following C_ε^a exponentially close are separated into different rotation classes by the partitioning I_j .*

The proof of Theorem 13.2.4 follows basically from Theorem 13.2.2.

Definition 13.2.5. Suppose we can partition the phase space or a lower-dimensional subspace into regions of different numbers of small oscillations for an MMO. The different pieces of the partition are called **sectors of rotation**.

For a folded node, we can estimate the size of the sectors of rotation defined by the two primary and k secondary canards; we will use the notation I_j for $j \in \{1, 2, \dots, k, k+1\}$ as in Theorem 13.2.4 and give an estimate for the size of the intervals.

Theorem 13.2.6 ([BKW06]). *The size of the sectors I_j on Σ for $1 \leq j \leq k$ is $\mathcal{O}(\varepsilon^{(1-\mu)/2})$, where $\mu = \lambda_w/\lambda_s$ is the ratio of the strong and weak eigenvalues of the desingularized slow flow. The size of the sector I_{k+1} is $\mathcal{O}(1)$.*

Theorem 13.2.6 is harder to prove and requires a careful analysis in blowup coordinates. The most important point in Theorem 13.2.6 is how the size of the sectors depends on ε . From Theorem 13.2.6, it follows that in Figure 13.3, the indicated sectors I_1 to I_4 converge onto the strong canard as $\varepsilon \rightarrow 0$.

Corollary 13.2.7. ([BKW06]) *The secondary canards $\xi_{j,\varepsilon}$ generated by a folded node converge to the primary strong canard as $\varepsilon \rightarrow 0$.*

We expect to be able to tune a system with a folded node to exhibit different types of MMOs using a control parameter, say β . This parameter should adjust the global returns so that orbits land in different sectors. Often, the distance of orbits γ landing in Σ to the strong canard is denoted by

$$\delta = c_\gamma d(\gamma \cap \Sigma, (\xi_{w,\varepsilon}) \cap \Sigma),$$

where d denotes the usual Euclidean distance on Σ , $c_\gamma = 1$ if γ lies inside the funnel region, and $c_\gamma = -1$ otherwise. So $\delta = \delta(\varepsilon, \beta) > 0$ is the case in which γ undergoes SAOs. Small values of $\delta > 0$ indicate closeness to the strong canard, which implies a small number of twists. Larger values indicate many rotations up to the maximal number, which is achieved by orbits lying in I_{k+1} ; see also Section 13.5 as well as Section 13.9.

13.3 Singular Hopf and Hyperbolic Equilibria

The SAOs induced by a folded node described in the last section are created by twisting of slow invariant manifolds near a fold point. In particular, all invariant sets creating the rotations were only locally invariant. It is natural to consider

the case in which also an invariant set is involved. Near folded nodes, an interesting situation of this type occurs when an equilibrium point near a folded node is present. A possible normal form for this case was considered by Guckenheimer [Guc08b] by extending the last equation in (13.6) with linear terms

$$\begin{aligned}\varepsilon \dot{x} &= y_1 - x^2, \\ \dot{y}_1 &= y_2 - x, \\ \dot{y}_2 &= -\nu - ax - by_1 - cy_2,\end{aligned}\tag{13.7}$$

where (ν, a, b, c) are parameters. Observe that (13.7) has the family of global equilibrium points $p = (x_*, y_1^*, y_2^*) \in \mathbb{R}^3$ for $-\nu = ax_* + bx_*^2 + cx_*$. More explicitly, we get

$$x_* = \frac{-a - c \pm \sqrt{a^2 + 2ac + c^2 - 4b\nu}}{2b},\tag{13.8}$$

from which conditions on the parameters can be derived so that x_* is close to the folded node at $(x, y_1, y_2) = (0, 0, 0)$. For example, if $\nu = \mathcal{O}(\varepsilon^{1/2})$ and $a \neq -c$, then one of the solutions (13.8) satisfies $x_* = \mathcal{O}(\varepsilon^{1/2})$. This implies that the associated equilibrium p is $\mathcal{O}(\varepsilon)$ -close to the folded node. In analogy to the singular Hopf bifurcation in \mathbb{R}^2 , as discussed in Section 8.2, we expect a singular Hopf bifurcation of p under parameter variation of ν .

Exercise 13.3.1. Singular Hopf bifurcation in \mathbb{R}^3 is related to the existence of folded saddle nodes of type II (FSN II) as defined in Section 8.5. Consider the normal form (13.7) and compute for which parameter values it has FSN II singularities. ◇

In comparison to the two-dimensional case, the analysis of singular Hopf bifurcation for (13.7) is substantially more complicated, since a full unfolding includes at least five parameters; see Section 13.9. Here we shall discuss only the shape of SAOs. Suppose p is a saddle focus with one eigenvalue $\lambda_1 < 0$ and a pair of complex conjugate eigenvalues $\lambda_{2,3} \in \mathbb{C}$, so that

$$\lambda_1 < 0 < \operatorname{Re}(\lambda_{2,3}).$$

Let $W^s(p)$ and $W^u(p)$ denote the associated 1-dimensional stable and 2-dimensional unstable manifolds. Consider a trajectory γ such that the distance between $W^s(p)$ and γ is small,

$$\min_{p \in \gamma} \|p - q\| < \delta \quad \text{with } 0 < \delta \ll 1.\tag{13.9}$$

In this case, the trajectory γ is funneled toward $W^u(p)$ and is expected to spiral, due to the complex eigenvalues $\lambda_{2,3}$; see Figure 13.4(a) and also the Koper model in Section 13.5. The funneling for the singular Hopf bifurcation is provided by the fast–slow structure involving the folded node. Note carefully that the basic features of the SAO mechanism we have just described can already be explained using linearized dynamics near the saddle focus. As an illustration, consider the linear system

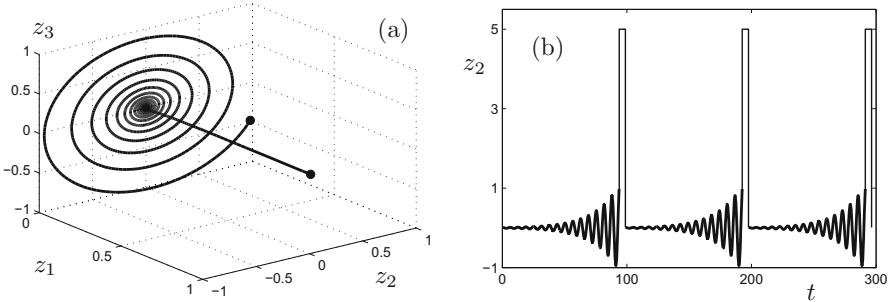


Figure 13.4: SAOs near a saddle focus for (13.10). (a) Phase space near the saddle focus at $(0, 0, 0) = p$. The stable manifold $W^s(p)$ is the z_1 -axis, and the unstable manifold $W^u(p)$ is the (z_2, z_3) -plane. (b) Time series for the local orbit from (a), where a large excursion has been inserted when $z_2 = 1$ and the orbit is returned to the initial condition $(z_1(0), z_2(0), z_3(0)) = (1, 0.01, 0)$; note that $\delta = 0.01$ as defined in (13.9).

$$z' = \begin{pmatrix} -1 & 0 & 0 \\ 0 & 0.05 & -1 \\ 0 & 1 & 0.05 \end{pmatrix} z, \quad (13.10)$$

where $\lambda_1 = -1$ and $\lambda_{2,3} = 0.05 \pm i$. Obviously, (13.10) can be solved explicitly, so that $z(t) = e^{tA}z(0)$. Figure 13.4(a) shows the local behavior near the saddle focus. Figure 13.4(b) shows a time series in which global returns have been triggered once $z_2 = 1$. The SAOs can be identified as oscillations with growing amplitude. Furthermore, their maximum amplitude can be $\mathcal{O}(1)$, independent of a time scale separation parameter, which is in contrast to the folded node case, in which oscillations occur in an $\mathcal{O}(\sqrt{\varepsilon})$ -neighborhood of the folded node. This implies that SAOs near a singular Hopf bifurcation are often easier to observe in applications. In parameter space, a singular Hopf bifurcation generically has a nearby folded node. Therefore, it is often possible to observe both phenomena—as well as the transition between them—in the same model; see also Section 13.5.

The oscillation mechanism near the hyperbolic equilibrium p is also interesting in the context of global bifurcations. Consider the general ODE

$$z' = F(z, \mu) \quad \text{for } z \in \mathbb{R}^3 \text{ and } \mu \in \mathbb{R}. \quad (13.11)$$

Suppose (13.11) has a hyperbolic saddle-focus equilibrium point at $z = 0$ for all $\mu \in \mathbb{R}$ with one real eigenvalue $\lambda_1 < 0$ and a pair of complex conjugate eigenvalues with $\operatorname{Re}(\lambda_{2,3}) > 0$ as before. Assume that for $\mu = 0$, the unstable manifold $W^u(0)$ intersects the stable manifold $W^s(0)$ in a single trajectory, forming a **homoclinic orbit**. It is known [Kuz04] that on parameter variation, either a unique orbit or infinitely many periodic orbits will bifurcate from a homoclinic orbit to a saddle focus. Suppose we have a periodic orbit for some $0 < |\mu_0| \ll 1$. Locally, this is precisely the situation shown in Figure 13.4(a). Globally, homoclinic bifurcation theory implies that the orbits lie inside a tubular neighborhood of the original homoclinic orbit.

Example 13.3.2. To illustrate the MMs near a homoclinic orbit, we consider the FitzHugh–Nagumo equation with an applied current (see also Section 1.4)

$$\begin{aligned}\varepsilon \dot{x}_1 &= x_2 \\ \varepsilon \dot{x}_2 &= 0.2(sx_2 - x_1(x_1 - 1)(0.1 - x_1) + y - p), \\ \dot{y} &= (x_1 - y)/s,\end{aligned}\quad (13.12)$$

where (p, s) are parameters. It can be shown that (13.12) has a unique equilibrium point, which we denote by q . Fixing a particular value of the applied current p , one can employ several different techniques to prove the existence of a homoclinic orbit; see, e.g., Section 6.5. In (p, s) -parameter space, there exists a curve of homoclinic bifurcations; see Section 19.8. For suitable values of ε , one finds that q is a saddle focus.

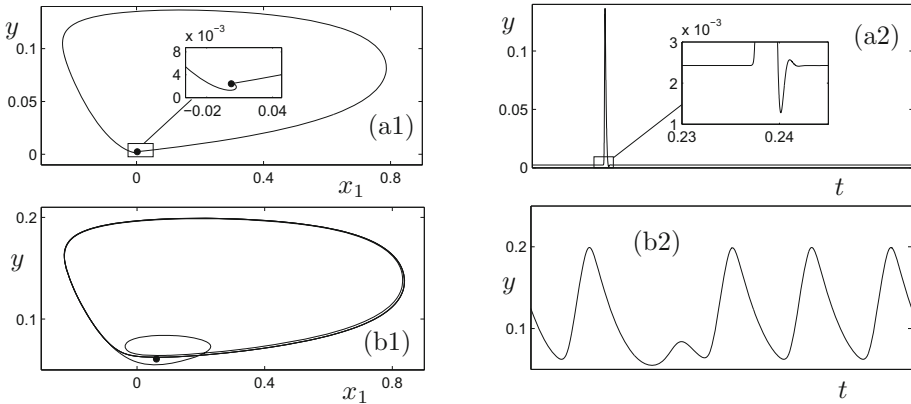


Figure 13.5: Periodic MMs in the FitzHugh–Nagumo equation (13.12) for $(s, \varepsilon) = (1, 0.01)$. (a1) Projection of a 1^1 MMO into (x_1, y) -space for $p \approx 0.00266172$. The saddle focus equilibrium q is marked with a dot, and the inset shows a zoom near the SAO. (a2) Time series for (a1) with a zoom near the SAO. (b1) Projection of a 4^1 MMO into (x_1, y) -space for $p \approx 0.0628718$; the saddle focus is marked by a dot. (b2) Time series for (b1).

Figure 13.5 shows two examples of MMs for which the global returns lie in the tubular neighborhood of a homoclinic orbit. The MMs were constructed by continuation methods as described in Section 10.6. The MMs have large periods and can be continued up to a homoclinic bifurcation point, where shifting onto a curve of homoclinic bifurcations is possible. We note that the FitzHugh–Nagumo equation supports much more complicated homoclinic orbits if the Shilnikov bifurcation conditions are satisfied [Kuz04]. ♦

Exercise 13.3.3. Show that (13.12) has a unique equilibrium point for all values of (p, s, ε) . Find the region where the equilibrium is of saddle-focus type. ◇

A theorem about MMs near a homoclinic bifurcation can be stated now, since it follows immediately from the structure of the homoclinic orbit.

Theorem 13.3.4. Suppose an (13.11) has an MMO of type L^s inside a tubular neighborhood of a homoclinic orbit for a parameter value μ near the homoclinic bifurcation at $\mu = 0$. Then $s \rightarrow \infty$ as $\mu \rightarrow 0$.

If the Shilnikov conditions are satisfied, then **n -homoclinic orbits**, i.e., orbits with n large excursions away from the saddle focus, exist. This implies that in the tubular neighborhood of this orbit, we can find MMOs with symbol sequences of the form L^s for $L = n$ under parameter variation.

13.4 Tourbillon

In this section only a very brief remark is made considering the influence of global returns on SAOs. In many applications, the global dynamics for an MMO are very complicated, whereas we usually have a good understanding of the local dynamics. However, the initial value for which we analyze the global dynamics can be crucial for the SAO mechanism. We have already seen an example in the context of folded nodes in Section 13.2, where it is important how a global orbit gets returned relative to the weak primary canard. A similar effect occurs for SAO mechanisms.

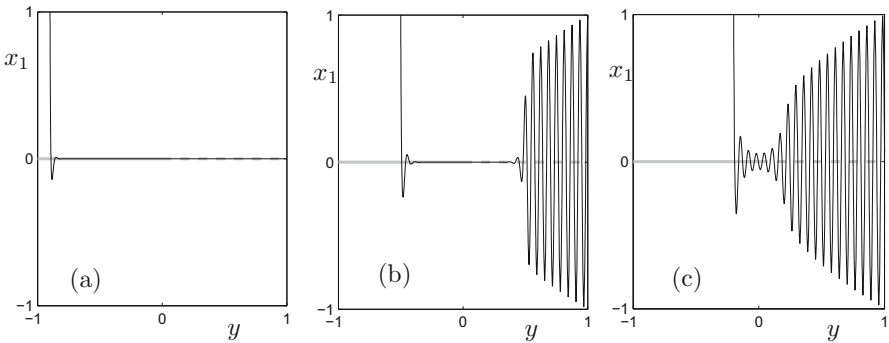


Figure 13.6: Illustration of oscillations near a delayed Hopf bifurcation in (13.13) with $l_1 = -1$ and $\varepsilon = 0.01$. The critical manifold C_0 is shown in gray (solid line = attracting part, dashed line = repelling part). The initial value for the trajectory segment is chosen as $(x_1(0), x_2(0), y(0)) = (1, 1, y_0)$, and $y_0 < 0$ is varied. (a) $y_0 = -0.9$. (b) $y_0 = -0.5$. (b) $y_0 = -0.2$.

Here we shall illustrate how global returns can influence SAOs in the context of delayed Hopf bifurcation as discussed in Section 12.2. As a simple example, consider the $(2, 1)$ -fast-slow system

$$\begin{aligned} \frac{dx_1}{dt} &= x'_1 = yx_1 - x_2 + l_1 x_1(x_1^2 + x_2^2), \\ \frac{dx_2}{dt} &= x'_2 = x_1 + yx_2 + l_1 x_2(x_1^2 + x_2^2), \\ \frac{dy}{dt} &= y' = \varepsilon, \end{aligned} \tag{13.13}$$

adapted from Example 12.2.1. The critical manifold of (13.13) is given by $C_0 = \{x_1 = 0 = x_2\}$. It splits into two parts,

$$C_0^a = \{(x_1, x_2, y) \in \mathbb{R}^3 : y < 0\} \cap C_0, \quad C_0^r = \{(x_1, x_2, y) \in \mathbb{R}^3 : y > 0\} \cap C_0,$$

separated by a nonhyperbolic fast subsystem Hopf bifurcation point at the origin $(x_1, x_2, y) = (0, 0, 0)$. If the first Lyapunov coefficient l_1 (see also Section 8.3) is negative, then the Hopf bifurcation is supercritical, while $l_1 > 0$ leads to a subcritical Hopf bifurcation of the fast subsystem. Figure 13.6 shows oscillations near the Hopf bifurcation in the supercritical case, where we vary the initial value $y(0) = y_0$. In Figure 13.6(a), there are many SAOs, but they are beyond the visible scale due to the exponentially strong contraction toward C_0^a . Indeed, the variational equation of (13.13) around C_0 for the fast directions is given by

$$\begin{pmatrix} X'_1 \\ X'_2 \end{pmatrix} = \begin{pmatrix} y & -1 \\ 1 & y \end{pmatrix} \begin{pmatrix} X_1 \\ X_2 \end{pmatrix} \quad \Rightarrow \quad \begin{pmatrix} X_1(t) \\ X_2(t) \end{pmatrix} = \begin{pmatrix} e^{yt} \cos t \\ e^{yt} \sin t \end{pmatrix}.$$

Therefore, if $y = \mathcal{O}(1)$ and $t = \mathcal{O}(1)$, the exponential term dominates strongly near C_0 , and the oscillations occur on a subexponential scale. Figure 13.6(b) shows that if y is closer to the fast subsystem Hopf bifurcation, then the SAOs are somewhat more visible. In Figure 13.6(c), the trajectory segment starts to enter a vicinity of the critical manifold only close to the fast subsystem Hopf bifurcation point, and the SAOs become visible on an $\mathcal{O}(1)$ scale, since $y(t)$ is sufficiently close to zero. This shows the crucial effect a global return mechanism might have on the practical observability of SAOs. The effect shown in Figure 13.6(c) is sometimes referred to as a **tourbillon**.

Exercise/Project 13.4.1. Consider (13.13) and give a heuristic description of what should happen for very small oscillations near C_0^r in the presence of small noise. For further investigations, you may want to consider Chapter 15. \diamond

13.5 The Koper Model

In this section, we are going to use the Koper model [Kop95] to illustrate MMOs due to folded nodes and singular Hopf bifurcation. We start from the original **Koper model**

$$\begin{aligned} \varepsilon_1 \dot{x} &= ky - x^3 + 3x - \lambda, \\ \dot{y} &= x - 2y + z, \\ \dot{z} &= \varepsilon_2(y - z), \end{aligned} \tag{13.14}$$

where λ and k are the main bifurcation parameters. Here we are going to study the Koper model as a (1, 2)-fast-slow system with $\varepsilon_2 = 1$ and $0 < \varepsilon_1 \ll 1$. For the analysis, it will be convenient to apply a coordinate change to (13.14). Replacing (x, y, z) in system (13.14) by (u, v, w) and applying the coordinate change $x = u$, $y = k v - \lambda$, and $z = k w$, we get the system

$$\begin{aligned} \varepsilon_1 \dot{x} &= y - x^3 + 3x, \\ \dot{y} &= kx - 2(y + \lambda) + z, \\ \dot{z} &= \lambda + y - z, \end{aligned} \tag{13.15}$$

which will be called the **symmetric Koper model**, because it has the symmetry

$$(x, y, z, \lambda, k, \tau) \rightarrow (-x, -y, -z, -\lambda, k, \tau). \quad (13.16)$$

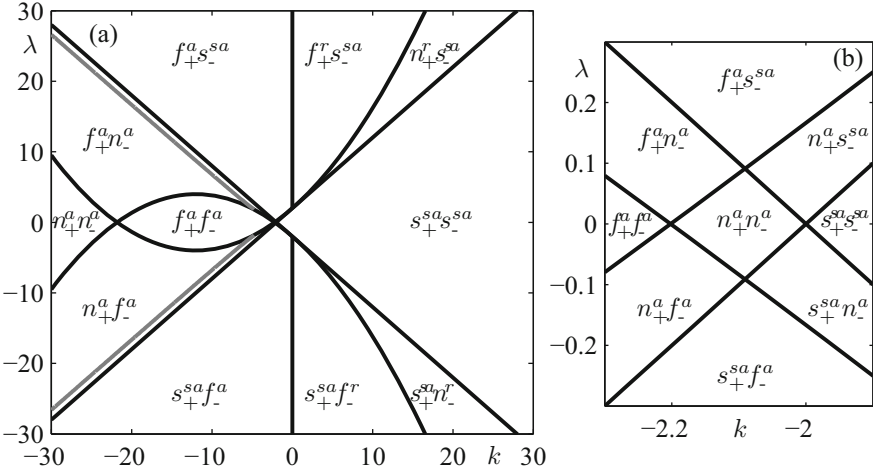


Figure 13.7: The singular bifurcation diagram (see also Section 19.8) in the (k, λ) -plane of the desingularized slow flow (13.17). Shown are the folded saddle node of type II (straight lines), the transition from a folded node to a folded focus (parabolas), and the curve (gray) indicating where the candidate orbit (see Figure 13.8) starting at the folded node returns precisely on the strong canard, so that $\delta = 0$. The gray curve is not shown in (b), where a zoom is provided. The types of folded equilibria in each parameter region are indicated as follows: f = folded focus, n = folded node, and s = folded saddle. The subscripts indicate whether the equilibrium lies on L^+ or L^- . The superscripts a , r , and sa stand for attractor, repeller, and saddle, respectively.

Note that the bifurcation diagrams in (λ, k) -parameter space are the same for (13.14) and (13.15). We may also restrict the parameter regime to $\lambda \leq 0$, say, and obtain the remaining part of the bifurcation diagram by applying the symmetry. Another advantage of the symmetric Koper model is that the critical manifold of (13.15) is given by

$$C_0 = \{(x, y, z) \in \mathbb{R}^3 | y = x^3 - 3x =: c(x)\},$$

so it does not depend on k and λ . This critical manifold C_0 has the classical cubic shape with two fold curves $L^\pm = \{(x, y, z) \in \mathbb{R}^3 | x = \pm 1, y = \mp 2\}$, which gives the usual decomposition

$$C_0 = C_0^{a,-} \cup L^- \cup C_0^r \cup L^+ \cup C_0^{a,+},$$

where $C_0^{a,-} = C_0 \cap \{x < -1\}$, $C_0^r = C_0 \cap \{-1 < x < 1\}$, and $C_0^{a,+} = C_0 \cap \{1 < x\}$ are normally hyperbolic. Note that $C_0^{a,\pm}$ are attracting, and C_0^r is repelling.

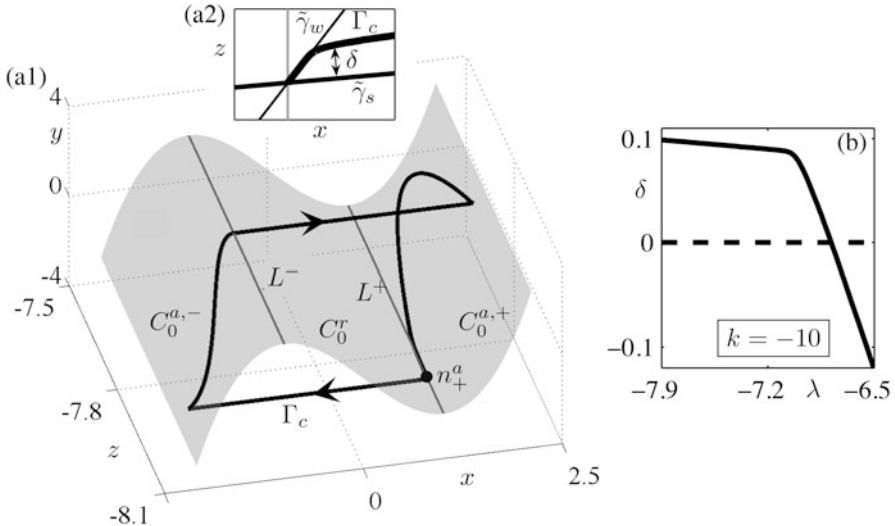


Figure 13.8: The candidate periodic orbit Γ_c of the folded node n_+^a of (13.15) with $(\varepsilon_1, \varepsilon_2, \lambda, k) = (0, 1, -7, -10)$ returns at a distance δ from the strong singular canard $\tilde{\gamma}_s$. (a1) shows all of Γ_c , while (a2) shows a zoom near n_+^a to illustrate the definition of δ . (b) Distance δ as a function of λ .

Near the fold curves, the algebraic form of (13.14) is very close to the singular Hopf normal form (13.7) as well as to the folded node normal forms (13.5)–(13.6) with a locally parabolic critical manifold and linear differential equations for the slow variables. The desingularized slow flow is easily found as

$$\begin{aligned}\dot{x} &= kx - 2(c(x) + \lambda) + z, \\ \dot{z} &= (3x^2 - 3)(\lambda + c(x) - z).\end{aligned}\tag{13.17}$$

The only equilibrium point of (13.17) on L^+ is $(x, z) = (1, 2\lambda - 4 - k)$, and the only one on L^- is $(x, z) = (-1, 2\lambda + 4 + k)$. Stability of these equilibria is determined by the associated Jacobian matrices

$$A_{\pm} = \begin{pmatrix} k & 1 \\ 6(2 + k \mp \lambda) & 0 \end{pmatrix}.\tag{13.18}$$

By classifying the folded singularities according to their type and stability, we obtain a singular bifurcation diagram, shown in Figure 13.7; see Section 19.8 for more details on singular bifurcation diagrams. The diagram indicates where folded node and singular Hopf MMOs are expected to occur in parameter space. Folded saddle nodes of type II occur when $\det(A_{\pm}) = 0 \Leftrightarrow \lambda = \pm(k + 2)$. The eigenvalues of A_{\pm} change from real to complex conjugate along the parabolic curves $\text{tr}(A_{\pm})^2 - 4\det(A_{\pm}) = k^2 + 24(k \mp \lambda) + 48 = 0$.

Figure 13.8 shows a candidate orbit that illustrates how trajectories arriving at a folded node can return to the funnel region of the folded node n_+^a . As

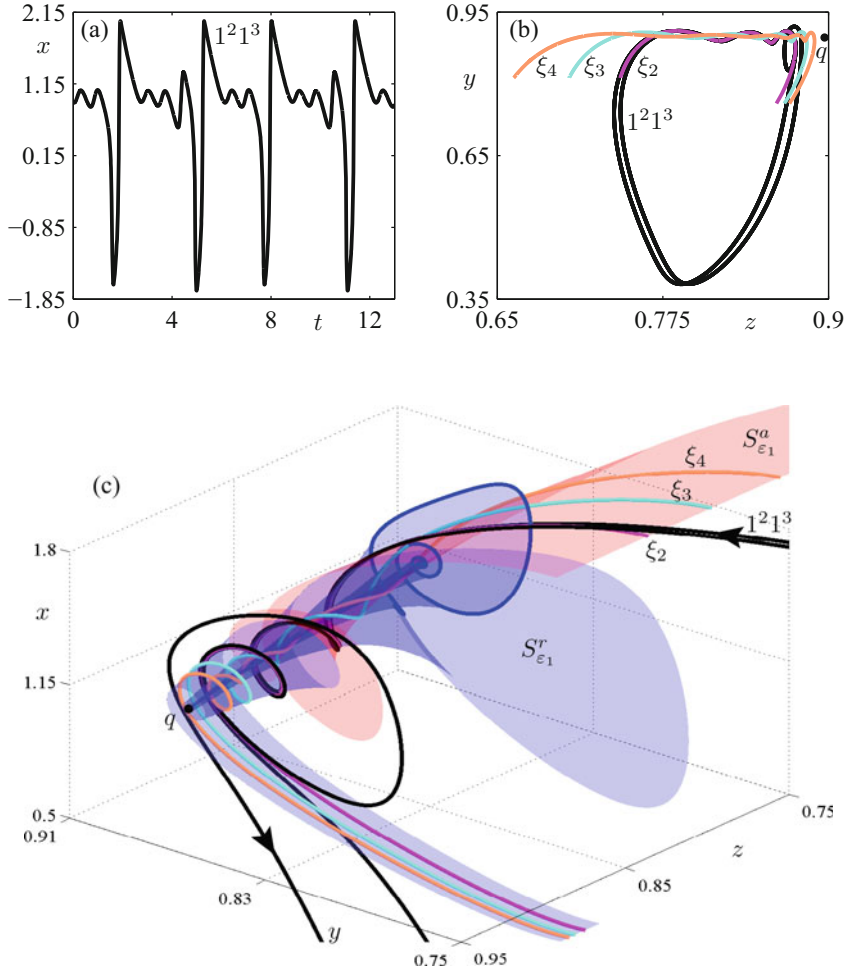


Figure 13.9: An 1^21^3 MMO (black) generated by a folded-node singularity of (13.14) for $(\varepsilon_1, \varepsilon_2, \lambda, k) = (0.1, 1, -7, -10)$. (a) Time series of x . (b) Projection onto the (z, y) -plane including nearby secondary canards ξ_2 , ξ_3 , and ξ_4 . (c) Phase space with the attracting and repelling slow manifolds $S_{\varepsilon_1}^a$ (red) and $S_{\varepsilon_1}^r$ (blue); note that the computation has been carried out for the original (asymmetric) Koper model, and we use S to denote the relevant manifolds in this model. *Reprinted with permission from [DGK⁺12]. (Copyright 2012, Society for Industrial and Applied Mathematics)*

defined in Section 13.2, we can measure the distance δ to the strong singular canard, which we denote here by $\tilde{\gamma}_s$. In Figure 13.8(b), we have fixed $k = -10$ and varied λ , showing that there is a transition from starting inside the funnel to landing outside the funnel under parameter variation. As long as $\delta > 0$, the candidate Γ_c gives rise to periodic MMOs for $\varepsilon_1 > 0$. Hence, the curve in the

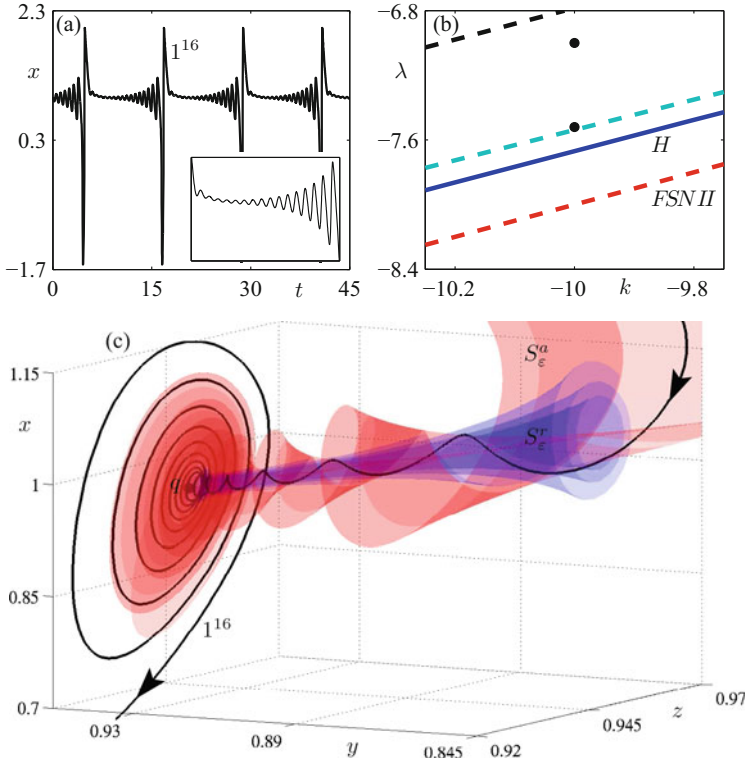


Figure 13.10: MIMO near a singular Hopf bifurcation for (13.14) with $(\varepsilon_1, \varepsilon_2, \lambda, k) = (0.1, 1, -7.52, -10)$. (a) Time series for x . (b) Bifurcation diagram to illustrate how close the parameters are to a tangency between $W^u(q)$ and S_ε^r (dashed cyan); the Hopf H (solid blue), folded saddle node of type II $FSN II$ (dashed red), and $\delta = 0$ (dashed black) curves are shown as well. The lower black dot marks the parameter values for (a) and (c). The second upper black dot is another typical example parameter set explained in [DGK⁺12]; it yields MIMOs with fewer SAOs. (c) Phase space with slow manifolds $S_\varepsilon^a = S_{\varepsilon_1}^a$ and $S_\varepsilon^r = S_{\varepsilon_1}^r$, which guide the MIMO toward the equilibrium $q \approx (0.951, 0.951, 0.951)$, after which $W^u(q)$ organizes the SAOs; note that the computation has been carried for the original (asymmetric) Koper model, and we use S to denote the relevant manifolds in this model. *Reprinted with permission from [DGK⁺12]. (Copyright 2012, Society for Industrial and Applied Mathematics)*

(k, λ) -plane along which $\delta = 0$ marks the start of the MIMO regime. The curve is shown in Figure 13.7. The two (symmetric) parameter regions bounded by the lines of folded saddle nodes of type II, where s_\pm^{sa} changes to n_\pm^a , and the curves where $\delta = 0$ are the regimes where MIMOs are predicted to exist.

Exercise 13.5.1. Consider the full symmetric Koper model (13.15).

- (a) Prove that saddle-node bifurcations occur for $\lambda = \pm 2(1 + k/3)^{3/2}$.
- (b) Prove that Hopf bifurcations occur for $\lambda = \pm (2 + k - \frac{k}{3}\varepsilon_1 + \mathcal{O}(\varepsilon_1^2))$.

Relate (a) and (b) to the singular bifurcation diagram in Figure 13.7. \diamond

Observe that the Hopf bifurcation curve from Exercise 13.5.1(b) lies $\mathcal{O}(\varepsilon_1)$ -close to the curves of folded saddle nodes of type II, as expected. Figure 13.9 shows a stable $1^{21}3$ for $(k, \lambda) = (-10, -7)$. The attracting and repelling slow manifolds $S_{\varepsilon_1}^a$, $S_{\varepsilon_1}^r$ and several canards have been computed as described in Section 11.6. The SAOs of the MMO in Figure 13.9 are mainly induced by the folded node mechanism, since the global equilibrium point, denoted by q , does not yet play a role. Note that the global return mechanism allows the MMO trajectory to alternate between two sectors of rotation that are bounded by secondary canards.

As a next step, we again fix $k = -10$ and consider a variation of λ so that the equilibrium q is moved closer to the fold curve. A singular Hopf bifurcation occurs for $\lambda = \lambda_H \approx -7.67$. If we decrease λ closer to the value λ_H , SAOs generated by a singular Hopf bifurcation occur with the characteristic increasing-amplitude pattern described in Section 13.2. It is important to note that since the Hopf bifurcation is supercritical, we have to stay above the value of λ for which there is a **tangency** between the unstable manifold $W^u(q)$ of q and the repelling slow manifold $S_{\varepsilon_1}^r$. Before the tangency occurs, small stable periodic orbits generated in the Hopf bifurcation are observed. After the tangency, orbits can escape from the region of the equilibrium past the unstable branch $S_{\varepsilon_1}^r$ to form LAOs.

The bifurcation diagram in Figure 13.10(b) shows the situation near the supercritical singular Hopf bifurcation. If we fix k and increase λ , we observe the following typical sequence of events. For small enough λ , there are no MMOs, and the attractor is an equilibrium q . This equilibrium crosses a fold of the critical manifold at a folded saddle node of type II, but it remains stable until the supercritical singular Hopf bifurcation occurs, which gives rise to small periodic orbits. The transition to MMOs starts after a tangency between $W^u(q)$ and $S_{\varepsilon_1}^r$. For λ -values just past this tangency, the MMOs have many SAOs that all lie near $W^u(q)$. As λ increases further, the MMOs exhibit SAOs organized by the folded node. Finally, a crossing of the curve $\delta = 0$ corresponds to a transition to relaxation oscillations.

13.6 Square-Wave / Fold-Homoclinic Bursting

In this section and the next one, two basic examples for bursting are discussed. Originally, bursting oscillations were studied in the context of neuroscience, but there is no reason to limit the discussion to this context. The ODEs we are going to use to illustrate bursting are a modification of the **Morris–Lecar model**

$$\begin{aligned} c \frac{dx_1}{dt} &= I - I_{ca} - \left(g_k x_2 + g_{kca} \frac{y}{y+y_0} \right) (x_1 - V_k) - g_l (x_1 - V_l), \\ \frac{dx_2}{dt} &= \phi \tau_w (w_\infty - x_2), \\ \frac{dy}{dt} &= \varepsilon (-\mu I_{ca} - y), \end{aligned} \tag{13.19}$$

where $0 < \varepsilon \ll 1$, the four auxiliary functions are given by

$$\begin{aligned} m_\infty &= 0.5(1 + \tanh((x_1 - V_1)/V_2)), & \tau_w &= \cosh((x_1 - V_3)/(2V_4)), \\ w_\infty &= 0.5(1 + \tanh((x_1 - V_3)/V_4)), & I_{ca} &= g_{ca}m_\infty(x_1 - V_{ca}), \end{aligned}$$

and the remaining terms are scalar parameters. In the neuroscience context, x_1 denotes the membrane potential difference V between the inside and outside of the neuron (or nerve cell), x_2 is a recovery, or gating, variable w , and y represents the calcium concentration [Ca] near the cell membrane; see also Section 13.9. We fix several parameters throughout the following analysis

$$\begin{aligned} V_k &= -84, & V_l &= -60, & V_{ca} &= 120, & V_1 &= -1.2, & V_2 &= 18, \\ g_k &= 8, & g_l &= 2, & c &= 20. \end{aligned} \quad (13.20)$$

Since $1/c$ is of moderate size and we assume that $0 < \varepsilon \ll 1$, it follows that the Morris–Lecar equations (13.19) may be viewed as a $(2, 1)$ -fast–slow system. Although the system (13.19) is three-dimensional, an analytical treatment of the problem is rather unwieldy, due to the dependence of the critical manifold on multiple parameters and due to the functions occurring in the vector field. Hence, we are going to use numerical techniques as described in Chapter 10, starting with the fast subsystem

$$\begin{aligned} c \frac{dx_1}{dt} &= I - I_{ca} - \left(g_k x_2 + g_{kca} \frac{y}{y+y_0} \right) (x_1 - V_k) - g_l (x_1 - V_l), \\ \frac{dx_2}{dt} &= \phi \tau_w (w_\infty - x_2), \end{aligned} \quad (13.21)$$

where y will be viewed as the main bifurcation parameter. Figure 13.11(b) shows the bifurcation diagram for equilibrium points of (13.21) for the parameter set

$$\begin{aligned} V_3 &= 12, & V_4 &= 17.4, & g_{ca} &= 4, & g_{kca} &= 0.25, \\ y_0 &= 10, & \phi &= 0.23, & \mu &= 0.2, & I &= 45. \end{aligned} \quad (13.22)$$

There are two branches of equilibria that are part of the critical manifold C_0 of the full system (13.19). The branches of the critical manifold are labeled in Figures 13.11(a)–(b), where C_0^b is the bottom, C_0^m the middle, and C_0^t the top branch. Observe that C_0^b is normally hyperbolic attracting, i.e., it consists of stable hyperbolic equilibria of the fast subsystem; C_0^b connects to the normally hyperbolic saddle-type branch C_0^m at a fold point located at $y = y_{LP} \approx 5.8017$. The upper branch C_0^t is attracting up to a value $y = y_H \approx 9.2682$, where the fast subsystem undergoes a subcritical Hopf bifurcation. The normally hyperbolic repelling family of limit cycles generated at y_H undergoes a fold bifurcation (or limit point) at some $y = y_{LPC} \approx 3.5167$, as shown in Figure 13.11(a). This means that there exists a y -dependent family of normally hyperbolic attracting limit cycles $\gamma_0^a(y)$ of the fast subsystem for $y > y_{LPC}$ in the regime where C_0^t is repelling and where the fold y_{LP} occurs. It can be shown, see Exercise 13.6.1, that the period of γ_0^a increases as the family is continued for increasing y , eventually terminating at a homoclinic bifurcation $y = y_{hom}$ to a saddle point located on C_0^m .

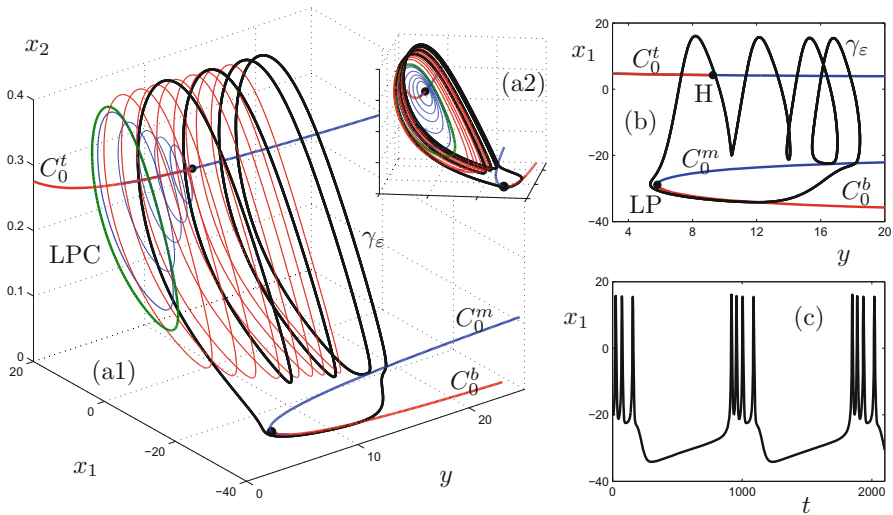


Figure 13.11: Square-wave bursting for the modified Morris–Lecar model (13.19) with parameter values (13.20) and (13.22). (a1) Phase space with periodic bursting orbit γ_ε (black) for $\varepsilon = 0.005$, stable/unstable (red/blue) equilibria, and periodic orbits of the fast subsystem (13.21). In the fast subsystem, a saddle-node (limit point = LP, black dot) and a Hopf bifurcation (H, black dot) as well as a saddle-node bifurcation (or limit point of cycles = LPC, green) occur. (a2) Viewpoint toward the subcritical Hopf bifurcation. (b) Fast subsystem bifurcation diagram for equilibria with a projection of γ_ε superimposed. (c) Time series for γ_ε .

Exercise/Project 13.6.1. Use numerical continuation to compute the family of periodic orbits γ_0^a and find the homoclinic bifurcation point for parameter values (13.20) and (13.22). Prove analytically that a homoclinic orbit to the saddle branch C_0^m exists for (13.19), where you can choose/modify the parameter set to simplify the calculations. \diamond

Building on the skeleton provided by the fast subsystem dynamics, we can now explain the bursting orbit γ_ε as shown in Figure 13.11. Fenichel’s theorem provides the slow manifold C_ε^b , near which we follow γ_ε starting with a decreasing slow variable y . Near the fold point y_{LP} , a fast jump occurs; see also Sections 4.2 and 7.4. Then γ_ε reaches the vicinity of the slow manifold Γ_ε , which is obtained by Fenichel’s theorem as a perturbation of

$$\Gamma_0 = \{\gamma_0^a(y) \subset \mathbb{R}^3 : y_{LPC} < y < y_{\text{hom}}\}$$

formed by the attracting limit cycles for $\varepsilon = 0$. A numerical calculation, or using an averaging technique, shows that the slow flow on Γ_0 has an increasing slow variable y . The bursting orbit γ_ε is attracted toward Γ_ε and spirals around it, and the y -coordinate increases. Then it reaches the vicinity of the homoclinic bifurcation of the fast subsystem $y \approx y_{\text{hom}}$, where the orbit γ_ε leaves the neighborhood of Γ_ε and is returned to a neighborhood of the attracting slow manifold

C_ε^b . The result is a limit cycle with bursting behavior switching between the steady-state behavior near C_ε^b and the oscillations around Γ_ε . The oscillations look like a square wave, which explains the name **square-wave** bursting.

Two key ingredients of the previous analysis were the mechanisms describing the transition from steady state to oscillation, the **burst initiation**, and the mechanism to return from oscillation to steady-state, the **burst termination**. This explains the name **fold-homoclinic bursting**. Another classical example for different initiation and termination mechanisms is discussed in the next section.

13.7 Elliptic / subHopf–Foldcycle Bursting

For the next example, we continue to work with the modified Morris–Lecar equation (13.19) with parameters (13.20). However, we are going to change the remaining parameters to

$$\begin{aligned} V_3 &= 2, \quad V_4 = 30, \quad g_{ca} = 4.4, \quad g_{kca} = 0.75, \\ y_0 &= 18, \quad \phi = 0.04, \quad \mu = 0.3, \quad I = 120. \end{aligned} \quad (13.23)$$

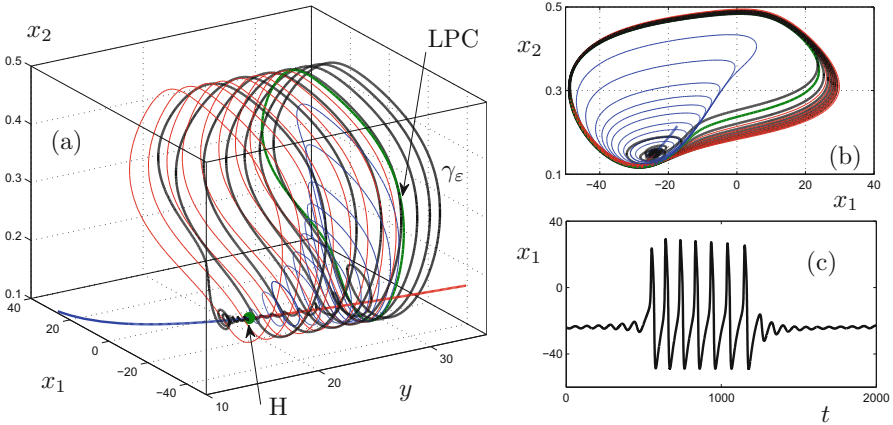


Figure 13.12: Elliptic bursting for the modified Morris–Lecar model (13.19) with parameter values (13.20) and (13.23). (a) Phase space with periodic bursting orbit γ_ε (black) for $\varepsilon = 0.002$, stable/unstable (red/blue) equilibria and periodic orbits of the fast subsystem (13.21). In the fast subsystem, a subcritical Hopf bifurcation (H , green dot) and a saddle-node bifurcation (or limit point of cycles = LPC, green) occur. (b) Projection of (a) onto the fast variables. (c) Time series for γ_ε .

Figure 13.12(c) shows a time series for a bursting periodic orbit with $\varepsilon = 0.002$. Figure 13.12(a) shows the fast subsystem bifurcations, which include a subcritical Hopf bifurcation at $y = y_H \approx 18.32$ as well as a fold bifurcation

(or limit point of cycles, LPC) at $y = y_{LPC} \approx 27.88$ of the family of limit cycles. From the bifurcation structure, we can, as explained in Section 13.6, understand the geometry of the bursting orbit γ_ε . The Hopf bifurcation divides the critical manifold into two parts:

$$C_0^a = \{(x, y) \in C_0 \subset \mathbb{R}^3 | y > y_H\} \quad \text{and} \quad C_0^r = \{(x, y) \in C_0 \subset \mathbb{R}^3 | y < y_H\},$$

both of which are of focus type with complex eigenvalues in the range of interest. We start to follow the limit cycle γ_ε near C_ε^a , toward which it spirals. The slow variable decreases, and the subcritical Hopf bifurcation occurs, which is a delayed Hopf bifurcation for the full system with $0 < \varepsilon \ll 1$; see Sections 12.2 and 12.3. Then γ_ε is repelled from C_ε^r , and it reaches an attracting normally hyperbolic family of limit cycles of the fast subsystem, which we call Γ_ε . Spikes (or LAOs) around Γ_ε and a decreasing slow variable occur until a fold bifurcation of cycles for the fast subsystem is reached beyond which the bursting orbit γ_ε spirals back toward C_ε^a . The envelope of the spikes is “elliptical,” which led to the name **elliptic bursting**. Since the burst initiation is via a subcritical Hopf bifurcation and the burst termination via a fold of cycles, the characterization as **subHopf-foldcycle bursting** is also used.

The geometric explanation of elliptic bursting was reached in a very similar way to the square-wave bursting in Section 13.6. However, there are crucial quantitative differences between the two bursting types. For example, in the elliptic case, the subcritical Hopf bifurcation allows small amplitude oscillations (SAOs). Therefore, we could also view the bursting trajectory in Figure 13.12 as an MMO, which highlights the role of delayed Hopf bifurcation as another mechanism to generate SAOs; see also Sections 12.2 and 12.3.

Izhikevich [Izh00a, Izh07] has suggested that all bursting mechanisms be classified according to the bifurcations for initiation and termination occurring in the fast subsystem. Once the two examples we presented here are understood, it is not too difficult to write down the general classification based on geometric arguments.

Exercise/Project 13.7.1. Consider a general $(2, 1)$ -fast–slow system and restrict the fast-subsystem bifurcations that can occur to all the possible codimension-one bifurcations [Kuz04]. Which types of bursting can occur? Draw a sketch of the bifurcation diagram for each type. ◇

Exercise/Project 13.7.2. Consider a general $(2, 2)$ -fast–slow system and restrict the fast-subsystem bifurcations that can occur to all the possible codimension-one bifurcations [Kuz04]. How many different bursting types can occur? ◇

13.8 Three Time-Scale Systems

A general **three-time-scale** system can be written on the slow time scale τ as

$$\begin{aligned} \varepsilon \dot{x} &= \varepsilon \frac{dx}{d\tau} = f(x, y, z), \\ \dot{y} &= \frac{dy}{d\tau} = g(x, y, z), \\ \dot{z} &= \frac{dz}{d\tau} = \varepsilon h(x, y, z), \end{aligned} \tag{13.24}$$

where we start with the simplest case that $(x, y, z) \in \mathbb{R}^3$. One may rewrite (13.24) on two other possible scales, where $\tau' = \tau\varepsilon$ is the slowest, or **superslow**, scale, and $t = \tau/\varepsilon$ is the fast scale. MMOs have been observed in several three-time-scale systems. To describe one basic idea regarding how to analyze some of these MMOs, we shall consider a particular example:

$$\begin{aligned}\frac{dx}{dt} &= x' = -y + c_2x^2 + c_3x^3, \\ \frac{dy}{dt} &= y' = \varepsilon(x - z), \\ \frac{dz}{dt} &= z' = \varepsilon^2(\mu - c_1y),\end{aligned}\tag{13.25}$$

where c_i with $i = 1, 2, 3$ are given constants with $c_1 > 0$, $c_2 > 0$, and $c_3 < 0$; μ is the primary bifurcation parameter.

Exercise 13.8.1. Prove that (13.25), near its fold points, is a subset of the singular Hopf normal form (13.7). Modify (13.7) by adding a cubic term to the fast variable and compute the explicit coordinate transformation of (13.25) to the modified singular Hopf normal form. \diamond

Observe that if we formally set $\varepsilon^2 = 0$ and assume $\varepsilon \neq 0$ in (13.25), then a familiar type of (1, 1)-fast–slow system (see, e.g., Sections 1.3 and 1.4) is obtained:

$$\begin{aligned}x' &= -y + c_2x^2 + c_3x^3, \\ y' &= \varepsilon(x - z),\end{aligned}\tag{13.26}$$

where the slowest variable z acts as a parameter. The critical manifold $\{y = c_2x^2 + c_3x^3\}$ of (13.26) has the classical cubic (or S-shaped) structure. We shall focus on the fold point at $(x, y) = (0, 0)$. We know from the analysis of canard points for the (1, 1)-fast–slow systems from Sections 8.1–8.4 that (13.26) will undergo a canard explosion. In particular, when $z = 0$, the origin becomes a canard point. The small orbits born in the associated Hopf bifurcation at $z = 0$ will grow rapidly in an exponentially small interval of z to a relaxation oscillation. Hence, one may expect that the three-dimensional system (13.25) exhibits MMOs, where the small oscillations arise due to the canard explosion in (13.26); see Figure 13.13. To show that this is indeed the case, it is natural to analyze (13.25) as a perturbation of (13.26) using special techniques near the fold point $(x, y, z) = (0, 0, 0)$.

The main goal is to define a suitable section and characterize the observed MMOs by constructing a return map to this section. Consider (13.25) on the slow time scale

$$\begin{aligned}\varepsilon\dot{x} &= -y + c_2x^2 + c_3x^3, \\ \dot{y} &= x - z, \\ \dot{z} &= \varepsilon(\mu - c_1y).\end{aligned}\tag{13.27}$$

The critical manifold is given by $C_0 = \{(x, y, z) \in \mathbb{R}^3 : y = c_2x^2 + c_3x^3\}$. It naturally breaks into three normally hyperbolic parts (as seen already several

times, e.g., Sections 7.6, 14.4–14.7, 13.5):

$$\begin{aligned} C_0^{a-} &= C_0 \cap \{x < 0\}, \\ C_0^r &= C_0 \cap \left\{0 < x < -\frac{2c_2}{3c_3}\right\}, \\ C_0^{a+} &= C_0 \cap \left\{-\frac{2c_2}{3c_3} < x\right\}. \end{aligned}$$

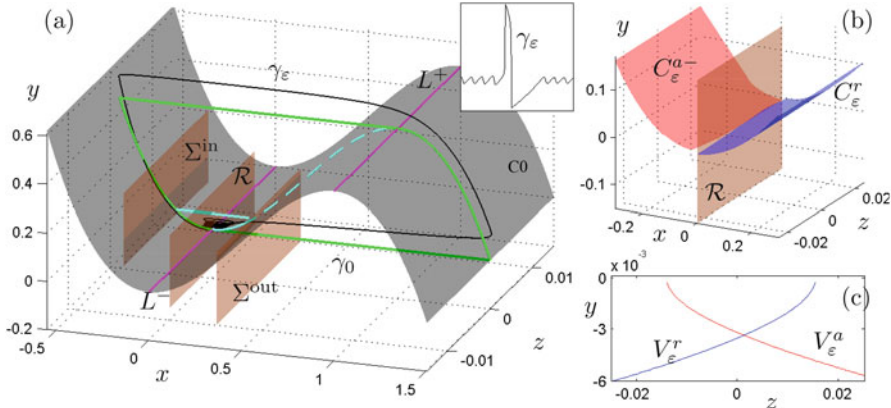


Figure 13.13: (a) Phase space for (13.25) with constants $c_1 = 0.5$, $c_2 = 1.5$, $c_3 = -1$. For $\varepsilon = 0$, we show the critical manifold C_0 (gray), the two fold lines L^\pm (magenta), and the three cross sections (brown). Furthermore, γ_0 indicates orbits for the 2D singular limit (13.26), where the green periodic orbit indicates a relaxation oscillation, the dashed cyan a maximal canard in $C_0^{a-} \cap C_0^r$, and the solid cyan segment an SAO occurring during a canard explosion. For comparison, there is also an orbit of the full system for $\varepsilon = 0.01$ and $\mu = 0.04$ (thin black curve) superimposed in the picture with the inset showing the time series in x . (b) Computation of the slow manifolds C_ε^{a-} (red) and C_ε^r (blue), which meet at the section \mathcal{R} . (c) Projection of (b) onto (z, y) -space indicating the relevant domains for the return map defined in (13.28).

The two fold curves are given by

$$\begin{aligned} L^- &= \{(x, y, z) \in \mathbb{R}^3 : x = 0, y = 0\}, \\ L^+ &= \left\{(x, y, z) \in \mathbb{R}^3 : x = -\frac{2c_2}{3c_3}, y = 0\right\}. \end{aligned}$$

We shall focus on the region near the fold line L^- . It can be shown that for $0 < \varepsilon \ll 1$, the slow manifolds C_ε^{a-} and C_ε^r , when extended by the flow beyond the fold region, intersect transversally in a maximal canard $\Gamma_{0,\varepsilon}$. Locally, this maximal canard lies close to the plane $\{z = 0\}$ and will form the organizing center of the analysis. In fact, a helpful way to think of the situation is to

view the three-scale system (13.27) as a folded node system as in Section 13.2, where the global returns can be approximated asymptotically due to the slow z -dependence; see also Figure 13.13.

Definition 13.8.2. Auxiliary canards $\Gamma_{k,\varepsilon}$ are trajectories that make k small loops near L^- before staying $\mathcal{O}(\varepsilon)$ -close to C_0^r until they reach an $\mathcal{O}(\varepsilon^{1/3})$ -neighborhood of L^+ .

Definition 13.8.2 will be made more precise when a suitable return map has been constructed. Some of the canards $\Gamma_{k,\varepsilon}$ can also be called **secondary canards**. Recall that we usually called any canard beyond the strong and weak canards near a folded node a secondary canard; see Section 8.6. Here there is only one primary canard in the singular limit $\varepsilon = 0$ available. The auxiliary canards in three-time-scale systems will be used to distinguish MMOs with different numbers of small oscillations.

To study the flow near L^- , it is helpful to introduce three cross sections; see Figure 13.13. The section Σ^{in} cuts across the part C_0^{a-} and is given by $\{x = -\delta_1\}$ for $\delta_1 > 0$ sufficiently small with bounded $|y|$ and $|z|$. The section \mathcal{R} contains the fold line L^- and is given by $\{x = 0\}$ with bounded $|y|$ and $|z|$. And Σ^{out} is transverse to the fast fibers. It is given by $\{x = \delta_2\}$ for $\delta_2 > 0$ sufficiently small and with bounded $|y|$ and $|z|$. The most important map to be defined on the sections will be a return map

$$\Pi : \mathcal{R} \rightarrow \mathcal{R}.$$

The major geometric objects to consider on \mathcal{R} are its intersections with two slow manifolds

$$V_\varepsilon^a := \mathcal{R} \cap C_\varepsilon^{a-} \quad \text{and} \quad V_\varepsilon^r := \mathcal{R} \cap C_\varepsilon^r, \quad (13.28)$$

where we implicitly assume that only the first intersection is considered; see Figure 13.13(b)–(c). Formally, we have that the curves V_ε^a and V_ε^r are unique only up to exponentially small terms, since the slow manifolds are not unique and defined only up to exponentially small terms. This nonuniqueness will not matter in the asymptotic analysis to follow.

The main reason for the generation of small oscillations is shown in Figure 13.13. Trajectories that get returned to C_ε^{a-} can lie above V_ε^r when it arrives at \mathcal{R} , in which case the repelling slow manifold C_ε^r acts as a barrier and forces them to return to C_ε^{a-} , generating a small oscillation in the process. These small oscillations can be viewed as perturbations of small periodic orbits in the canard explosion of the planar system (13.26). Trajectories lying below V_ε^r on \mathcal{R} must jump to the attracting sheet C_ε^{a+} far away. Then they get returned to C_ε^{a+} via the global return mechanism involving the fold line L^+ . This process can generate MMOs. The natural map to consider is a return map to \mathcal{R} , which should restrict to an almost one-dimensional map on V_ε^a due to the exponential contraction along C_ε^{a+} .

The main point of the three-time-scale system (13.25) is that the calculations can be carried out explicitly, giving an asymptotic expansion of the return map. An asymptotic description of the return map $\Pi : \mathcal{R} \rightarrow \mathcal{R}$ can be given in blowup coordinates. The description of the map can be made explicit for the first ε -dependent correction term. We shall outline some of the major ideas from [KPK08]. The first important step in analyzing (13.25) is to consider a rescaling that focuses on the singularity at the origin

$$x = \sqrt{\varepsilon} \bar{x}, \quad y = \varepsilon \bar{y}, \quad z = \sqrt{\varepsilon} \bar{z}, \quad t = \frac{\bar{t}}{\sqrt{\varepsilon}}. \quad (13.29)$$

For the rescaled equations, we still use a prime to denote differentiation with respect to the new time \bar{t} :

$$\begin{aligned} \bar{x}' &= -\bar{y} + c_2 \bar{x}^2 + \sqrt{\varepsilon} c_3 \bar{x}^3, \\ \bar{y}' &= \bar{x} - \bar{z}, \\ \bar{z}' &= \varepsilon(\mu - c_1 \varepsilon \bar{y}). \end{aligned} \quad (13.30)$$

Observe that (13.30) is a $(2, 1)$ -fast–slow system in which the time scale separation between x and y has disappeared. This outcome is expected, since we have defined \bar{t} as an intermediate scale between the fast time t and the slow time $\tau = \varepsilon t$. Setting $\varepsilon = 0$ in (13.30) yields

$$\begin{aligned} \bar{x}' &= -\bar{y} + c_2 \bar{x}^2, \\ \bar{y}' &= \bar{x} - \bar{z}, \\ \bar{z}' &= 0. \end{aligned} \quad (13.31)$$

Equation (13.30) is in the normal form for a $(1, 1)$ -fast–slow system with a parameter \bar{z} . As stated above, we are still interested in the behavior near the origin $(\bar{x}, \bar{y}, \bar{z}) = (0, 0, 0)$. Since \bar{z} does not change in the singular limit $\varepsilon = 0$ in (13.30) and \bar{z} is the slowest variable in the full system, a perturbation analysis starting with $\bar{z} \approx 0$ is natural. If $\bar{z} = 0$, one observes that (13.30) has a first integral

$$H(\bar{x}, \bar{y}) = \frac{1}{2} e^{-2c_2 \bar{y}} \left(-\bar{x}^2 + \frac{\bar{y}}{c_2} + \frac{1}{2c_2^2} \right), \quad (13.32)$$

since we may either refer to Proposition 8.1.9 or check directly that

$$\bar{x}' H_{\bar{x}}(\bar{x}, \bar{y}) + \bar{y}' H_{\bar{y}}(\bar{x}, \bar{y}) = 0.$$

The level curves $H(\bar{x}, \bar{y}) = h$ for some constant h are illustrated in Figure 13.14. Therefore, an equilibrium point of (13.30) with $\bar{w} = 0$ is located at $(\bar{x}, \bar{y}) = (0, 0)$ with $H(0, 0) = \frac{1}{4c_2^2} =: h_0 > 0$.

A special trajectory is obtained for $H(\bar{x}, \bar{y}) = 0$, giving a parabola

$$\bar{\gamma}_0(t) = \left(\frac{1}{2c_2} t, \frac{1}{4c_2} t^2 - \frac{1}{c_2} \right),$$

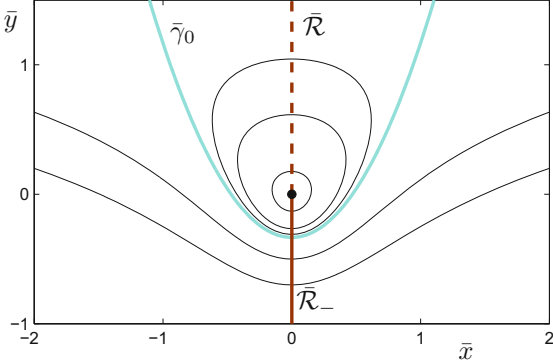


Figure 13.14: Level curves (black) for (13.32) with $c_2 = 1.5$ and values $h = -1, -0.25, 0.02, 0.05, 0.1$. The parabola γ_0 (cyan, level curve for $h = 0$) separating open and closed level curves can be clearly identified. Furthermore, we show the rescaled version of the section \mathcal{R} (brown).

which we recognize as the singular limit of the maximal canard $\Gamma_{0,\varepsilon}$ in the full system. It is also evident from Figure 13.14 that $\bar{\gamma}_0$ separates level curves of H . The level curves are open for $h < 0$ and closed for $h > 0$. Note that the section $\mathcal{R} = \{x = 0\}$ has simply been transformed to $\{\bar{x} = 0\} =: \bar{\mathcal{R}}$ in the rescaled coordinates. Define a subset of $\bar{\mathcal{R}}$ as

$$\bar{\mathcal{R}}_- := \bar{\mathcal{R}} \cap \{\bar{y} < 0\},$$

which corresponds to the part of the section below the equilibrium point. A perturbation calculation for equation (13.30) allows one to describe a map $\bar{\Pi} : \bar{\mathcal{R}}_- \rightarrow \bar{\mathcal{R}}_-$ giving asymptotic estimates of trajectories that return after they have made a small loop. The small loops take place for $h > 0$, as suggested by Figure 13.14. For $h < 0$, a large loop occurs, and hence it is a good idea not to parameterize the return map $\Pi : \mathcal{R} \rightarrow \mathcal{R}$ in (\bar{y}, \bar{z}) -coordinates but to replace \bar{y} by h . The structure of the return map is

$$\Pi(h, \bar{z}) = \begin{cases} \bar{\Pi}(h, \bar{z}) & \text{if } h > 0, \\ \Pi^{\text{in}} \circ \Pi^{\text{ret}} \circ \Pi^{\text{out}}(h, \bar{z}) & \text{if } h < 0, \end{cases} \quad (13.33)$$

where the maps Π^{in} , Π^{ret} , and Π^{out} describe the global returns of trajectories (see also Figure 13.13)

$$\Pi^{\text{in}} : \Sigma^{\text{in}} \rightarrow \bar{\mathcal{R}}_-, \quad \Pi^{\text{ret}} : \Sigma^{\text{out}} \rightarrow \Sigma^{\text{in}}, \quad \Pi^{\text{out}} : \bar{\mathcal{R}}_- \rightarrow \Sigma^{\text{out}}.$$

The maps Π^{in} and Π^{out} can be analyzed near the fold region, and two different rescalings of the original equations 13.25 will be necessary. When these two rescalings, which can be thought of as two additional charts in a blowup framework, are chosen correctly, we can obtain the maps from a perturbation of the slow flows on C_0^{a-} and C_0^r respectively. The global return map Π^{ret} can be

obtained using Fenichel's theorem and the fact that relevant trajectories stay very close to a global singular trajectory defined by the singular maximal canard γ_0 , as indicated in Figure 13.13. Observe that the return map (13.33) is composed of several maps. For each map, we can calculate the first correction term involving ε , similarly to the two-dimensional case; see, e.g., Chapter 5.

The next step is to reduce the map $\Pi : \mathcal{R} \rightarrow \mathcal{R}$ to a (nearly) one-dimensional map on the curve V_ε^a . To carry out this reduction, we will make use of definitions and notational conventions used already in this section. In particular, the blown-up system (13.30) and its associated coordinates will be used to describe the map on \mathcal{R} . Hence, it helps to think of objects such as $\bar{\mathcal{R}}$ and \mathcal{R} just as a different coordinate representation of the same object.

The main idea is to divide V_ε^a into different segments corresponding to different numbers of small oscillations. Before dividing V_ε^a , we restrict the map Π from $\bar{\mathcal{R}}_-$ to a special set of curves

$$V_\varepsilon^0 := V_\varepsilon^a \quad V_\varepsilon^j := \bar{\Pi}(\{(h, \bar{z}) \in V_\varepsilon^{j-1} : h > 0\}) \quad (13.34)$$

for $j \in \{1, 2, \dots, k\}$, where k is the maximum number of small oscillations a trajectory can make. It is not hard to show that each curve can be described by a graph of a function. To simplify the situation, a coordinate change can be used to move the intersection of the repelling slow manifold with \mathcal{R} to the set $\{h = 0\}$, i.e., so that

$$V_\varepsilon^r = \mathcal{R} \cap C_\varepsilon^r = \{(h, \bar{z}) : h = 0\} \subset \bar{\mathcal{R}}.$$

In this scenario, the functions describing V_ε^j are defined over the variable \bar{z} ,

$$V_\varepsilon^j = \{(h^j(\bar{z}), \bar{z}) \in \mathcal{R}_-\}.$$

The situation is shown in Figure 13.15(a). Due to the exponential contraction along C_ε^{a+} , the system of curves V_ε^j is expected to suffice as the domain of Π up to an exponentially small error.

Theorem 13.8.3 ([KPK08]). *Let $(h, \bar{z}) \in \bar{\mathcal{R}}_-$ and assume that $\varepsilon > 0$ is sufficiently small. Then there is an upper bound k on the number of small oscillations for each fixed set of parameters. Furthermore, for $1 \leq j \leq k$, it follows that $\Pi^j(h, \bar{z})$ is exponentially (in ε) close to $\cup_{j=1}^k V_\varepsilon^j$.*

The intersections $V_\varepsilon^j \cap V_\varepsilon^r$ are points on auxiliary canard orbits. Due to the recursive definition (13.34), it follows that to each intersection point, one can find a point in $V_\varepsilon^0 = V_\varepsilon^a = \mathcal{R} \cap C_\varepsilon^{a+}$, say p_j , such that

$$\bar{\Pi}(p_j) \in V_\varepsilon^r.$$

The situation is illustrated in Figure 13.15(a). Each p_j has an associated \bar{z} -coordinate on the graph h^0 describing the curve V_ε^0 . Using the projection onto the h -coordinate P_h , this can formally be found by requiring

$$P_h \bar{\Pi}^j(h^0(\bar{z}), \bar{z}) = 0. \quad (13.35)$$

Denote the points on the \bar{z} -axis determined by (13.35) by \bar{z}^j for $0 \leq j \leq k$.

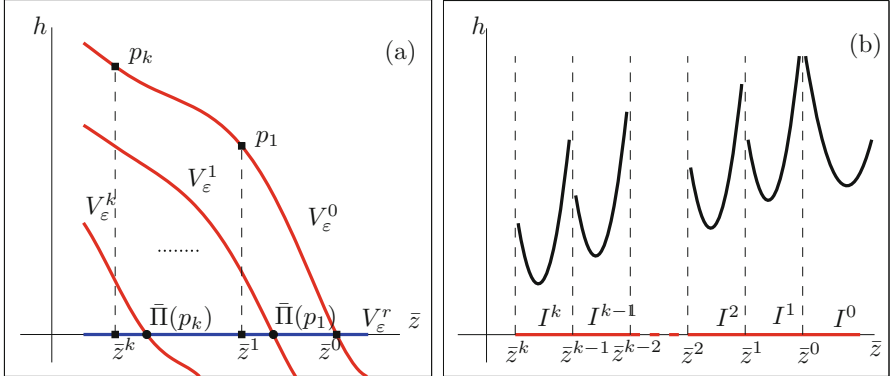


Figure 13.15: (a) A sketch of the system of curves V_ε^j (red) in the section $\bar{\mathcal{R}}$ is shown. Here the curve V_ε^r (blue) corresponding to the repelling slow manifold is rectified along the \bar{z} -axis. The points p_j are the auxiliary canards as given in Definition 13.8.2. (b) Sketch of a return map $\Phi : V_\varepsilon^a \rightarrow V_\varepsilon^a$. The sectors of rotation partition its domain into regions of different numbers of small oscillations. Near the auxiliary canards \bar{z}^j , the number of small loops changes, and more complicated dynamics occur; see also Section 8.6.

Theorem 13.8.4 ([KPK08]). *The distances between the points \bar{z}^j satisfy*

$$\bar{z}^{j-1} - \bar{z}^j = \mathcal{O}(2\varepsilon\mu\sqrt{-2\ln\varepsilon}),$$

independent of j . In the original (not blown-up) coordinates, this means

$$z^{j-1} - z^j = \sqrt{\varepsilon}(\bar{z}^{j-1} - \bar{z}^j) = \mathcal{O}(2\varepsilon^{3/2}\mu\sqrt{-2\ln\varepsilon}).$$

Next, we can define the **sectors of rotation** that partition the curve $V_\varepsilon^a = V_\varepsilon^0$ (see Figure 13.15(b)):

$$I_\varepsilon^j = \{(h^0(\bar{z}), \bar{z}) \in V_\varepsilon^a : \bar{z}^j \leq \bar{z} < \bar{z}^{j-1}\}.$$

The generation of MMs can now be analyzed by keeping track of the points landing in different sectors. For example, a trajectory starting near C_ε^{a+} and landing in sector I^3 on \mathcal{R} will make three small loops and then make a large excursion before it returns to the vicinity of C_ε^{a+} . Then it might make some more sequences of small and large loops, but it definitely will have a symbolic sequence given by $\dots 1^3 \dots$. This suggests that $\Pi : \mathcal{R} \rightarrow \mathcal{R}$ should be reducible to a map

$$\Phi : V_\varepsilon^a \rightarrow V_\varepsilon^a.$$

This map is not a Poincaré map on \mathcal{R} for the differential equation, since we have cut out several points of return of trajectories to \mathcal{R} (the small loops). The number of small loops is encoded in the partition of the domain of Φ . It is difficult to describe the map Φ near the partitioning points p_j , since trajectories

close to those points are canards. A sketch of a typical return map Φ is given in Figure 13.15(b). A detailed study of the one-dimensional map Φ can now be used to study the dynamics of MMOs. For example, restrictions on the possible symbol sequences can be found.

Theorem 13.8.5 ([KPK08]). *Assume that $k \geq 2$. Then a periodic orbit can occur if its sequence consists of segments of the form 1^k (some number of times in succession), 1^{k-1} (some number of times in succession), and 1^{k-2} (preceded by 1^k and followed by 1^{k-1} or 1^k).*

Theorem 13.8.5 can be refined in various ways. However, note carefully that the type of MMOs described in Theorem 13.8.5 is a specific example, which applies only to the particular model problem (13.25). Nevertheless, the elegant aspect of the three-scale structure is that we may explicitly control the local and global dynamics, yielding a completely analytic result; cf. Sections 14.4 and 14.5, where parts of the global returns require interval arithmetic.

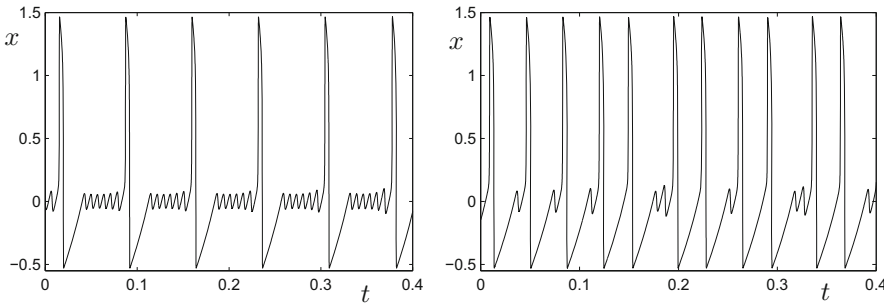


Figure 13.16: Mixed-mode oscillations for (13.25) with $c_1 = 0.5$, $c_2 = 1.5$, $c_3 = -1$, and $\varepsilon = 0.01$. The initial transients have been truncated. We observe quite different types of MMOs for different values of μ . The time series on the left has been computed for $\mu = 0.04$: there are sequences containing 1^6 and 1^5 . The time series on the right is for $\mu = 0.08$: sequences containing 1^1 , 2^1 , and 2^2 are observed.

Exercise/Project 13.8.6. Two simulations of the model problem (13.25) are shown in Figure 13.16. (a) Explore the parameter space for the c_i and μ to find other MMO patterns. (b) Consider a grid of points $\{(0, -y_0, z_l)\}_{l=1}^L \subset \mathcal{R}$ for some fixed $y_0 > 0$ and use forward integration to plot the return map to \mathcal{R} . Can you explain its structure? ◇

13.9 References

Here we shall group various approaches to an overview on the literature in addition to the short literature survey for each section. Basically, this approach follows up on the survey paper [DGK⁺12] as well as [Izh00a] and extends the references therein. We note that several models have been grouped together despite various differences in their formulation, e.g., many bursting models are of Hodgkin–Huxley type, but we

have made subgroups for specific classes only in certain cases and left the remaining models grouped under “Hodgkin–Huxley type.” Furthermore, a model may also fit into several classes simultaneously, but we have cited each work only once. Hence, Tables 13.1–13.2 and 13.3 provide a basic orientation to the literature but no detailed classification.

System / Reaction	References
Anterior burster neuron	[HWF87]
Belousov–Zhabotinsky reaction	[Bel59, Zha64, Zha85]
- Virginia group	[GHS76, HHM79, HMML81, HM81, SGH77]
- Texas group	[MS85, MS86b, MS86c, RSS83, RS81]
- Bordeaux group	[AARR87, AR85, PRR ⁺ 81, RRBV81]
- Other groups	[VRBR80] [JS90, Mas80, RK99, RK01, SG03, SK95b]
beta cells	[KDSS99]
BSFA system	[KLVE09]
Bray–Liebhafsky reaction	[Fur85, LV02, VAKA00]
Briggs–Rauscher reaction	[BR73, Fur85, OH98, VSH96]
calcium buffering	[RESG06]
CO oxidation	[EE86, EKE90, KEE92]
combustion oscillations	[GGHL81]
copper/phosphoric acid	[ARS89, SA89]
cortical neurons	[GYS95, HMP96, LGY91]
dusty plasmas	[MCC ⁺ 08]
HPTCu reaction	[BSSH08, KLE ⁺ 93, OE87, OKCRE00] [vVK95]
indium/thiocyanate reaction	[KGS92, KS91b]
light-emitting diodes	[MCA ⁺ 11]
neostriatal spiny neurons	[WK96]
neural network (PreBötC)	[NWB ⁺ 02]
p-CuInSe ₂ /H ₂ O ₂ -system	[NPT95, PNT94]
peroxidase–oxidase reaction	[GSLO92, HS93, HS94, HO96, HOBS97] [HSR95, OD78, SGL93]
pituitary cells	[TTV ⁺ 11, vGZMFS01, VBTW10, VBW12] [VTBW13]
Purkinje cells	[JK94a, LS80]
pyramidal cells	[GYY06]
spin-wave experiment	[dARAR99]
stellate cells	[DMS ⁺ 00, DMS ⁺ 06, EM08]
stomatogastric ganglion	[SOAM93]
semiconductor lasers	[ANMC ⁺ 09, GHR ⁺ 07]
trigeminal neurons	[NHCG98]

Table 13.1: Partial references for experiments involving MMOs and bursting.

Section 13.1: Initially, the occurrence of oscillations in chemical reactions was doubted [Sco94, Win84], but the Belousov–Zhabotinsky reaction [Bel59, Zha64] changed this view fundamentally. For a detailed background on chemical oscillations, we refer to [ES96, Fe85, Sco94, VP81]. The example of the Gaspard–Nicolis–Rössler

Mathematical Model	References
autocatalator(s)	[GS11, MS01b, MSLG98, PSS92, Tra94]
Barkley model	[Bar88]
Belousov–Zhabotinskii reaction	
- Field–Koros–Noyes (FKN)	[RJ72, GTF90, RRAA87]
- Geiseler–Föllner oregonator	[GF77, Tys85]
- Györgyi–Field	[GS13, GFR91, GF91]
- IUator (Indiana University)	[SO81, Tys85]
- (Minimal) Oregonator	[Abo97, FN74, HM75, PGS91, Tro85, Tys81] [RT82b]
- Model K (Kyoto)	[TIO77, Tys85]
- Showalter–Noyes–Bar–Eli	[SNBE78, Bar88, CF81, LTB90, RS84]
- Zhabotinsky–Korzuhkin	[Zha85]
Boissonade–DeKepper	[BD80, KB85, Kop95]
Boissonade–De Kepper–Strizhak	[BD80, GSK97, KHS02]
BR reaction	[KE82, NF82, OH98, Tur91, VSH96] [KLS02, KSL04, VSH96]
BSFA system	[KLVE09]
Butera model	[BBR ⁺ 05, BCB96, BCB97, BRS99a] [BRS99b] [DR10, MMR10, PDL13, TB11]
β -cell/calcium	[Cha96, Cha90a, Cha90b]
Chay–Keizer model	[AC91, Cha85, CK83a, CR85, GM12a] [Rin85] [STR93, SRS93, SR93, TAZBS06]
Chua circuit	[MT10]
CO oxidation	[EKE90, KEE92]
combustion oscillations	[GW87, GGHL81]
coupled models	[HMS85, KARG92, KAAA13, LKMH94] [Per00, RF92, Rub06, SRV95]
dopamine neurons	[ACC99, KPKR08, LBR96, MC04]
dual oscillator model	[BSZ ⁺ 04, GS09a, WB04, YWDZ12] [ZGB ⁺ 03]
Erisir model	[ELRL99, EW09]
FHN equation(s)	[DKO08b, DBFP03, GK09b, GK10b] [KVDC12, Wec05, WS11]
Hayashi model	[Hay00]
heart interneuron	[CCS07, CCS05, CGMC02, HLM ⁺ 01] [MSC11, SCC05]
Hindmarsh–Rose model	[AC91, BS11a, DKK13, FP05, GM07] [HR84, LCDS12, OTA10, OSTA12] [SG10, SLdL08, TAORS10, Wan93]
Hodgkin–Huxley type	[ACDG84, DIK04, DRSE04, RW07] [RW08, RR95, RR94, SW00b, XCKA08]

Table 13.2: Partial references for mathematical models of MMOs and bursting.

Mathematical Model	References
Hopf-hysteresis normal form	[Bar88, RRAA87]
IT reaction	[KG91, KG92, KGS92, KS91c]
Kawczynski–Strizhak	[KKS00b, KS00a, RK99, RK01]
Koper model	[KB85, Kop95, KG91, KG92, KGS92] [KS91b, KS91c, Kue11b, RWJWZ13, Z11]
LP neuron	[GHW PW97, GGH W93]
map-based models	[CNV07, Vri01, IH04, RA05, Rul02, SR04]
Morris–Lecar type	[GE98, HKK95, Izh04, ML81]
p-CuInSe ₂ /H ₂ O ₂ -system	[NPT95, PNT94]
Pernarowski model	[Vri98, Per94b, Per98, Per01b]
phantom burster	[BS04a, BS04b, BPH ⁺ 00, BSP ⁺ 07, NBS ⁺ 06]
pituitary cells	[NM ⁺ 10, SOLS08, TTFB07, VBTW10, VBTW13]
Plant’s model	[Pla81, RL87]
plastic instability model	[RA00b, RA00a]
Plenge model	[BK08a]
PO reaction	
- Olsen / DOP models	[ALC89, DOP79, DKO09, LBLA87, LS91] [LSA88, OD78, SL91]
- BFSO model, Urbanalator	[BFSO95, BSO01, HO96, LH96, OWS95, SBO01]
- Yokota-Yamazaki model	[FAB88, SOW ⁺ 97, YY77]
- FAB model	[FAB84, SOW ⁺ 97]
- Model A, Model C	[AC87, AL91]
- Model C-HSR	[HSR95]
pyramidal neurons	[DLLM02, NOB ⁺ 11, NOTA12, PR94, Wan98]
R15 neuron	[Ber93, But98, BCC ⁺ 95, CBCB93, CCB91]
Rubin–Hayes model	[DNR11, RHMN09]
self-replicating dimer	[PLRF97, PVK05]
semiconductor lasers	[ANMC ⁺ 09, KSS ⁺ 03, KW02, Pan96]
Sherman–Rinzel–Keizer	[PMK92, PMK91, SRK88, SR91]
stellate cells	[AKW03, ROWK06, WW09a, JKR10, KWR10] [RWK08, WW09b]
thalamic neuron	[RH89a, RH85, RH89b, RH89c, HR94]

Table 13.3: Partial references for mathematical models of MMOs and bursting.

(GNR) model can be found in [Bar88, GN83]. Similar to the mechanism in the GNR model, there has also been the idea that torus bifurcations could be the cause of oscillatory phenomena [BB12b], but it seems to be that the interaction of low-codimension local bifurcations and regular global returns is much more frequent than special global mechanisms. Therefore, most of this section has focused on the local mechanisms for small-amplitude oscillations.

Section 13.2: This section is based mainly on [BKW06, DGK⁺12], where the folded node oscillation mechanism is presented. One may also induce global returns in an ad hoc way by adding a cubic term to the folded-node normal form [BKW06]. More detailed references on the theoretical aspects can be found in Section 8.9.

Section 13.3: A combined analytical–numerical analysis for the multiparameter space of singular Hopf bifurcations in three dimensions is presented in [Guc08b, GM12b]; note that smaller subsets of parameter space may be easier to understand [LV13]. It is also apparent that there are “typical” sequences of MMOs occurring near a singular Hopf bifurcation, which is discussed in more detail in Section 13.5. Experimental observations also led to conjectures that certain tree structures such as Farey trees and Stern–Brocot trees [FG11a, FG11b] could potentially be used to classify MMO sequences. However, one has to be aware that the local–global interplay for the generation of oscillatory patterns could be extremely complicated, which makes small-and-simple combinatorial structures less likely.

Section 13.4: It is rarely clear when tourbillon-type dynamics really occur in practice [ČIŠA⁺13], since the boundaries between a clear entry point close to the singularity and a point far away are not really well defined. Pioneering work on the tourbillon mechanism, as well as the suggestion of its name, can be found in [Wal86].

Section 13.5: The Koper model [Kop95] is an excellent playground to test various tools for MMOs; it has been discussed in various contexts [KB85, KG91, KG92, KGS92, KS91b, KS91c]. A global view on MMO generation in the Koper model from a return map perspective is considered in [Kue11b]; see also [Pik81, PR81] for an early view on MMOs and return maps. Of course, one may also use the return map as a key tool in bursting models [GP06].

Section 13.6: In this and the next section, we have relied mainly on [ET10]. The link between fast–slow systems and bursting oscillations has been pointed out in a series of fundamental papers [Rin86, Rin87, RE89, RL86]. Since then, bifurcation theory and fast–slow systems have always played a crucial role in the analysis of bursting patterns [BBKS95, GTW05]. An abstract analysis of square-wave bursting is considered in [LT99, Ter91, Ter92], where the role of canards was later clarified [GK09a]; however, the general importance of canard-induced delay was noticed quite early for square-wave bursters [ECB97]. The coupling of square-wave bursters is discussed in [MZ12].

Section 13.7: Instead of relying on a particular model, one may also abstract the situation. For example, [BRC95, KE86, STKW96, EK86a] consider parabolic bursting, and [GJK01] outlines a general bifurcation-theoretic approach. There are also variations on the theme such as Bautin-type elliptic bursting [Izh00c]. Synchronization of elliptic bursters is an important direction toward understanding coherent neural dynamics [Izh01, LSB11]. Another natural question to ask is how one would incorporate data to fit parameters of models [TG08], which is a special task discussed in the broad field of data assimilation. Of course, one should also mention that although the fast subsystem bifurcation mechanisms explain many classes of bursting oscillations, they do not explain all of them [SSP95].

Section 13.8: The analysis presented is based on [KPK08, KPKR08]. There are more results on three-scale systems available, e.g., on asymptotic analysis [CWS83a, O'M71b], averaging [Yad13], various bursting effects [YL11], coupled systems [BKT00], machine models [DQKP94], reduction from a 6D model [JKR10, ROWK06], and surface-catalyzed reactions [CA84]. Obviously, three-time-scale dynamics is a special case of singularly perturbed problems with multiple small parameters, which has been discussed e.g., in the context of control theory [Gru79, Kha81, KK79a, KK79b] and stochastic fast–slow systems (see Chapter 15). However, there is clearly much more to do in the direction of multiple small parameters [KS11, LR04b, MS03a, RU03].

An important further direction that we have not discussed here is how the bursting mechanisms [CB05] in small models interact and synchronize on a larger-scale network level [BC98, VS01, DJD04, FBT⁺06, GSCE06, WGR95, WLL⁺12]. Unsurprisingly, multiple time scale dynamics is again employed as a key tool to analyze network dynamics; see Section 20.11.

Chapter 14

Chaos in Fast-Slow Systems

Similar to Chapter 13, the current chapter uses the theory previously discussed in parts of this book to gain substantial insight into nonlinear dynamics.

Section 14.1 begins with a geometric picture and motivation why we would expect chaotic dynamics in fast–slow systems. Sections 14.2 and 14.3 are a mini-introduction to some principles of chaotic dynamics and the Smale horseshoe as a prototypical model. In Section 14.4, we begin the discussion of the forced van der Pol equation and illuminate the geometric picture that explains why the splitting of orbits near folded singularities with canards may induce a Smale horseshoe structure in the return map. The proof is sketched in Section 14.5. Then we proceed with another short interlude, this time on Hénon-type maps, in Section 14.6. In fact, Hénon-type return maps can also appear in models of forced oscillations. Section 14.7 studies this relation in more detail; in this case, the tangency of the fast flow projection onto the critical manifold is the key mechanism. Section 14.8 shows that chaotic dynamics of the Lorenz equations can be rebuilt using fast–slow systems with an embedded double-homoclinic loop near a cusp of the critical manifold. Section 14.9 provides a glimpse at the relation between chaotic fast subsystem dynamics and the sense in which we may view it as a white-noise perturbation to slow variables.

Background: There are no additional prerequisites. However, some very elementary experience with discrete-time dynamical systems (iterated maps) would be useful. Just having simulated the logistic map for various parameters would help considerably; the books [ASY96, Hol00] contain much more material than we need here. If you would like to delve even more extensively into dynamical systems, then there are options available at all different levels, from the introductory compressed textbook to the extensive monograph [BS02, BT10, KH95, Rob03].

14.1 A Basic Idea

In many classical mathematical models involving chaotic behavior, the dynamics can be reduced to the analysis of a (nearly) one-dimensional map. We shall illustrate how this same reduction idea arises naturally in fast–slow systems. Consider the $(1, 2)$ -fast–slow system

$$\begin{aligned}\varepsilon \frac{dx}{d\tau} &= \varepsilon \dot{x} = f(x, y), \\ \frac{dy}{d\tau} &= \dot{y} = g(x, y),\end{aligned}\tag{14.1}$$

where $x \in \mathbb{R}$ and $y = (y_1, y_2)^\top \in \mathbb{R}^2$. Suppose the critical manifold C_0 of (14.1) decomposes into two attracting surfaces $C_0^{a,1}$, $C_0^{a,2}$ and a repelling surface C_0^r , and that these surfaces are separated by two fold lines L^1 and L^2 . Hence, we have

$$C_0 = C_0^{a,1} \cup L^1 \cup C_0^r \cup L^2 \cup C_0^{a,2}.$$

It is helpful to think of the periodically forced van der Pol equation as a prime example for this situation; see Section 1.3 as well as Examples 7.6.1 and 8.5.13. Furthermore, assume that all points in $L^{1,2}$ are nondegenerate fold points and the normal switching condition

$$\left(\begin{array}{c} f_{y_1} \\ f_{y_2} \end{array} \right) \cdot \left(\begin{array}{c} g_1 \\ g_2 \end{array} \right) \Big|_{(x,y) \in L_{1,2}} \neq 0\tag{14.2}$$

is satisfied for all fold points. Consider a plane H cutting $C_0^{a,1}$ transversally. We are interested in only a compact subset of the intersection $H \cap C_0^{a,2}$, which is a line segment l that can be parameterized without loss of generality by $l(s)$ with $s \in [0, 1]$. Assume that singular trajectories starting in l return to l ; more precisely, we consider the slow and fast subsystems and concatenate trajectories to obtain candidate trajectories that return to the line segment l . The situation is illustrated in Figure 14.1.

Denote the one-dimensional return map for $s \in [0, 1]$ obtained from the previous construction by $F_0 : [0, 1] \rightarrow [0, 1]$. Note that this is a singular return map, since it was obtained for the case $\varepsilon = 0$. It is not difficult to show that F is C^1 , but we shall simply take this as a given fact for now. Let $C_\varepsilon^{a,2}$ denote the slow manifold associated with $C_0^{a,2}$ obtained by Fenichel's theorem. Consider a plane H_ε such that $C_\varepsilon^{a,2} \cap H_\varepsilon = l$ and H_ε intersects $C_\varepsilon^{a,2}$ transversally. Define $l_\varepsilon(s) := H_\varepsilon \cap C_\varepsilon^{a,2}$, and let σ denote the coordinate along a generic line m contained in H_ε intersecting l_ε transversally in $m(0)$.

Exercise 14.1.1. Sketch the situation involving the plane H_ε using Figure 14.1 as a starting point. ◇

It is clear that the Poincaré return map Π on $(s, \sigma) \in l_\varepsilon \times m$ is well defined for $\sigma \in [-\sigma_1, \sigma_2]$ and $0 < \sigma_i$ sufficiently small. From the asymptotic expansion of trajectories undergoing jumps near nondegenerate fold points satisfying (14.2) and from the exponential contraction toward $C_\varepsilon^{a,2}$, we can conclude the following theorem (c.f. Section 7.6):

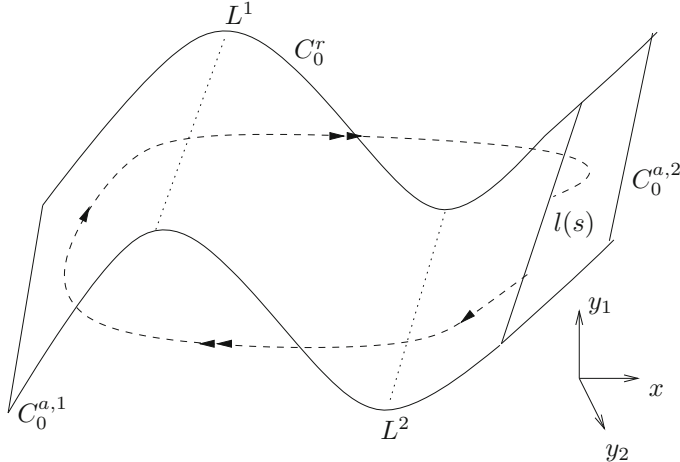


Figure 14.1: Sketch of the assumptions. A trajectory starting on the line segment $l(s)$ is shown by a broken line.

Theorem 14.1.2 ([MKKR94]). *The return map Π is well defined and nearly one-dimensional. More precisely,*

$$\Pi(s, \sigma) = (F_\varepsilon(s, \sigma; \varepsilon), C(s, \sigma; \varepsilon)e^{-\alpha/\varepsilon})$$

for some constant $\alpha > 0$. The functions C and F_ε are C^1 , and $F_\varepsilon(s, 0; \varepsilon)$ differs from $F_0(s)$ in the C^1 -norm by $\mathcal{O}(\varepsilon^{2/3})$.

The natural question to ask is what types of one-dimensional maps F_0 could occur. We shall look only at Figure 14.2 in this section. The slow flow in Figure 14.2(b) has a “folding” or “turning” mechanism, which can yield a one-dimensional map $F_0(s)$ with a unique maximum, as shown in Figure 14.2(a).

One-dimensional maps have been analyzed in detail. The return map $F_0(s)$ shown in Figure 14.2(a) belongs to an especially well understood class of maps.

Definition 14.1.3. Let $f : [0, 1] \rightarrow [0, 1]$ be continuous and satisfy $f(0) = 0 = f(1)$. Then f is called a (standard) **unimodal** map if f is increasing on $[0, c)$ and decreasing on $(c, 1]$ for some fixed $c \in (0, 1)$.

In fact, combinatorial kneading theory can be used to describe the dynamics of f under iteration; see Section 14.10. A typical example is the **logistic family**

$$f_\mu(x) = \mu x(1 - x). \quad (14.3)$$

Many introductory courses on chaotic theory of dynamical systems will describe what happens for the logistic family under variation of μ . In this context, a key result is Sharkovsky’s Theorem.

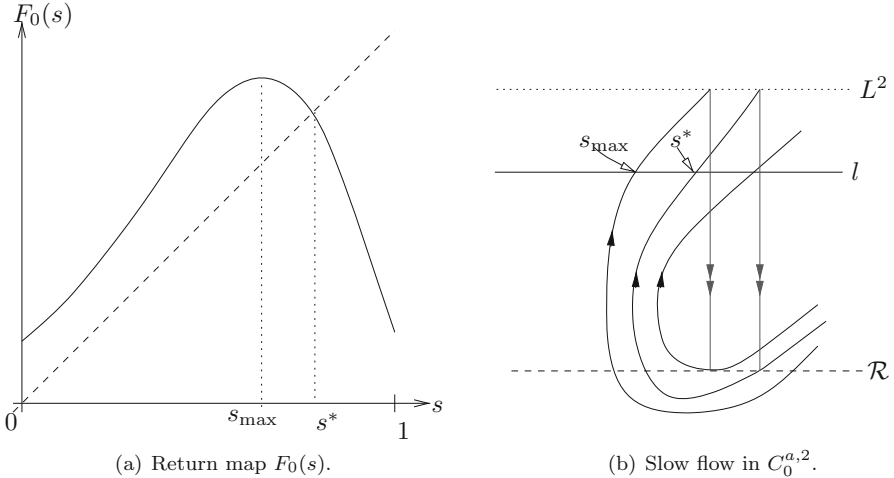


Figure 14.2: An example of a possible one-dimensional return map. The double-arrow lines indicate the global return mechanism to a subset \mathcal{R} of $C_0^{a,2}$ after a global excursion. Recall that \mathcal{R} is sometimes also called a **drop curve**.

Theorem 14.1.4 ([ASY96, Sha64a]). *Order the positive integers by the Sharkovsky ordering*

$$\begin{aligned} 1 &\triangleleft 2 \triangleleft 4 \triangleleft \cdots \triangleleft 2^k \triangleleft 2^k + 1 \triangleleft \cdots \\ &\quad \cdots \\ &\quad \cdots \triangleleft 2^2 \cdot 7 \triangleleft 2^2 \cdot 5 \triangleleft 2^2 \cdot 3 \triangleleft \\ &\quad \cdots \triangleleft 2^1 \cdot 7 \triangleleft 2^1 \cdot 5 \triangleleft 2^1 \cdot 3 \triangleleft \\ &\quad \cdots \triangleleft 7 \triangleleft 5 \triangleleft 3. \end{aligned}$$

If f is a continuous map of an interval to itself with a periodic point of period p and $q \triangleleft p$, then f has a periodic point with minimal period q . In particular, if f has a periodic point of order 3, then f has periodic points of all orders.

The Sharkovsky theorem applies to the logistic family on varying $\mu \in [2, 4]$. The behavior for a map with a periodic point of order 3 can hence be described as “chaotic,” since it has periodic orbits of all periods. Since the singular return map for a $(1, 2)$ -fast–slow system can also be unimodal, as shown in Figure 14.2(a), one expects that certain fast–slow systems should be good examples for chaotic behavior. Before we analyze several cases, it helps to discuss the notion of **chaos** in a bit more detail.

14.2 Chaotic Dynamics

We cannot provide a comprehensive theory of chaotic dynamics here. Instead, we aim to outline some basic definitions and results. For simplicity, we restrict attention to dynamical systems defined by maps; all following definitions can

be defined similarly for flows. Let

$$F : \mathbb{R}^N \rightarrow \mathbb{R}^N, \quad F(z_k) = z_{k+1}$$

be a smooth map. Fix an initial condition $z = z_0$ and let $E^0 = \partial B(z_0, 1)$ denote the unit sphere centered at z_0 . Note that

$$E^k := (\mathrm{DF}^k(z_0))E^0$$

is an ellipsoid generated by the mapping of the linearized map DF . Let r_j^k denote the length of the j th-longest orthogonal axis of E^k .

Definition 14.2.1. The j th **Lyapunov number** of z_0 is defined by

$$L_j(z_0) := \lim_{k \rightarrow \infty} (r_j^k)^{1/k}.$$

The j th **Lyapunov exponent** of z_0 is $l_j(z_0) = \ln L_j(z_0)$.

Note that Definition 14.2.1 implies the following ordering:

$$L_1 \geq L_2 \geq \cdots \geq L_N \quad \text{and} \quad l_1 \geq l_2 \geq \cdots \geq l_N.$$

The Lyapunov numbers/exponents represent expansion and contraction rates of the dynamics of the map F . Sometimes, the largest Lyapunov exponent l_1 is called the **first Lyapunov exponent**. Observe that a positive first Lyapunov exponent implies that the map F has at least one expanding direction.

Definition 14.2.2. A dynamical system (defined by a map) has **sensitive dependence on initial conditions** if it has a positive Lyapunov exponent.

Definition 14.2.3. Let $F : \mathbb{R}^m \rightarrow \mathbb{R}^m$ be a map with a bounded orbit

$$\Gamma := \{z_0, F(z_0) = z_1, F^2(z_0) = z_2, \dots\}.$$

Then we call Γ **chaotic** if the following conditions hold:

1. Γ is not asymptotically periodic,
2. no Lyapunov exponent is exactly zero,
3. $l_1(z_0) > 0$.

Roughly speaking, Definition 14.2.3 characterizes chaos as long-term behavior that has sensitive dependence on initial conditions. As an example, it can be verified that there are parameter values μ for which the logistic map (14.3) has chaotic orbits. In addition, one would like to define the term “chaos” for more general subsets $\Lambda \subset \mathbb{R}^N$ of phase space, not only single orbits. This raises several questions:

- (Q1) Preferably, Γ should be the “attractor” for the dynamical system encapsulating its long-term dynamics. There are many different definitions of **attractors**, which complicates the task of giving a single definition for a “chaotic attractor.” One definition commonly used is the maximal attractor. Suppose the map F has a compact invariant set B . Then the **maximal attractor** for B is

$$\Lambda_{\max} = \bigcap_{k>0} F^k(B).$$

However, other reasonable definitions for an attractor Λ are certainly possible [GI96, Mil85, PS89].

- (Q2) It might be desirable to have some topological properties on an attractor Λ . For example, the map F is **topologically transitive** on Λ if for all open sets $U, V \subset \mathbb{R}^N$ with $U \cap \Lambda \neq \emptyset$ and $V \cap \Lambda \neq \emptyset$, we have $F^k(U) \cap V \neq \emptyset$ for some $k \in \mathbb{N}_0$.
- (Q3) Another option is to consider F together with a measure μ and insist on **mixing**, i.e., $\lim_{k \rightarrow \infty} \mu(A \cap F^{-k}(B)) = \mu(A)\mu(B)$ for all measurable sets A, B .
- (Q4) Directly prescribing a complicated orbit structure turns out to be helpful as well, e.g., one could require that periodic orbits be dense in Λ .

Obviously, there are many other questions that should be raised. For example, the term **strange attractor** arises in this context. Originally, an attractor was called strange if it had nonintegral dimension, but some authors like to use “strange attractor” for an attractor with sensitive dependence on initial conditions, which brings us back to (Q1)–(Q4).

In this book, we take a rather pragmatic route with respect to chaotic dynamical systems. We are going to introduce several famous examples that have been proved to be chaotic systems under suitable hypotheses and are widely accepted as exhibiting chaos. Then we shall try to show that certain fast–slow systems are “equivalent” to these systems. The two main constructions we are going to use are Smale horseshoes and Hénon-type maps.

14.3 Smale Horseshoes

We are going to give a very brief introduction to Smale horseshoe maps. No proofs of results will be given, but they can be found in [IL99]. The simplest version of this map can be introduced as follows. Let $B = [0, 1] \times [0, 1]$ denote the unit square. Divide the square into five equal horizontal rectangles and call the second and fourth rectangles from the bottom \mathcal{D}_0 and \mathcal{D}_1 . Similarly, divide the square into five vertical rectangles and call the second and fourth rectangles from the left \mathcal{D}'_0 and \mathcal{D}'_1 ; see Figure 14.3.

Define a rotation map $f_0 : \mathcal{D}_0 \rightarrow \mathcal{D}'_0$ with respect to the point $(1/4, 1/4)$ contracting by a factor of $1/5$ in the horizontal direction and expanding by a factor 5 in the vertical direction. In formulas, this reads as

$$(x, y) \mapsto \left(\frac{1}{5} \left(x - \frac{1}{4} \right) + \frac{1}{4}, 5 \left(y - \frac{1}{4} \right) + \frac{1}{4} \right).$$

Note that in the reference frame of $(1/4, 1/4)$, we simply have

$$(u, v) \mapsto \left(\frac{u}{5}, 5v \right).$$

The last two formulas clearly show that the map f_0 is hyperbolic everywhere, since the linearization Df_0 has **multipliers** (i.e., eigenvalues of the linearized map) $1/5$ and 5 . Therefore, one direction is strongly contracting, while the other direction is strongly expanding. Similarly, define a map $f_1 : \mathcal{D}_1 \rightarrow \mathcal{D}'_1$ with respect to the point $(3/4, 3/4)$. Then we consider (a simple version of) the **Smale horseshoe map**

$$f : B \rightarrow B, \quad f(x, y) = \begin{cases} f_0(x, y) & \text{if } (x, y) \in \mathcal{D}_0 \\ f_1(x, y) & \text{if } (x, y) \in \mathcal{D}_1 \\ \text{undefined} & \text{otherwise} \end{cases} \quad (14.4)$$

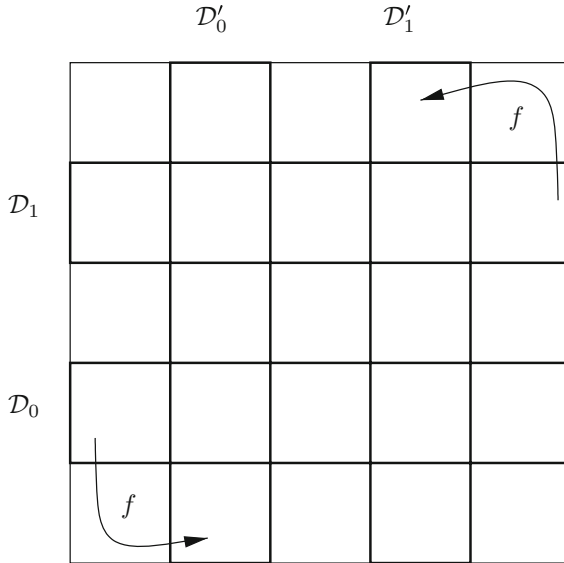


Figure 14.3: Sketch of the simple horseshoe-type map on the unit square.

Remark: We shall explain below why the map f is equivalent to a more classical version of the horseshoe map.

Let \mathcal{D}^* denote the domain on which the map f is defined for all forward iterates and backward iterates. An orbit in \mathcal{D}^* is called **complete**. Hence, \mathcal{D}^*

consists of the union of all complete orbits; it can be shown that this union is a product of nowhere-dense Cantor sets. Although \mathcal{D}^* seems to be very small, the dynamics on \mathcal{D}^* are incredibly rich. Suppose $z = (x, y) \in \mathcal{D}^*$ and define

$$\omega(z) = \{\omega_n(z) : n \in \mathbb{Z}\}, \quad \omega_n(z) = \begin{cases} 0 & \text{if } f^n(z) \in \mathcal{D}_0, \\ 1 & \text{if } f^n(z) \in \mathcal{D}_1. \end{cases}$$

The sequences $\omega(z)$ of zeros and ones encode the orbit of a point z **symbolically**. Usually, we denote the set of all two-sided sequences by Σ^2 .

Theorem 14.3.1 ([IL99]; see also [Sma63, Sma67, Sma00a]). *There exists a one-to-one correspondence between complete orbits and two-sided sequences, i.e., every two-sided sequence is realized by precisely one and only one point $z \in \mathcal{D}^*$.*

It turns out that the correspondence between \mathcal{D}^* and Σ^2 not only is true on a static bookkeeping level but holds dynamically as well. Define the **Bernoulli shift** σ on Σ^2 by

$$\omega \mapsto \sigma(\omega) =: \omega', \quad \omega'_j = \omega_{j+1},$$

i.e., σ shifts every entry of a bi-infinite sequence one place to the left. Then Σ^2 can be turned into a metric space by deriving a metric from the following norm:

$$\|\omega\|_\Sigma := \sum_{n=-\infty}^{\infty} \frac{|\omega_n|}{2^n}.$$

Then the metric is $d_\Sigma(\omega, \gamma) = \|\omega - \gamma\|_\Sigma$, and two sequences are close if they agree for many places around the index 0, i.e., $\omega_j = \gamma_j$ for some $|j| \leq N$.

Theorem 14.3.2 ([IL99]; see also [Sma63, Sma67, Sma00a]). *The Smale horseshoe map f is topologically conjugate to the Bernoulli shift. More precisely, the map $\omega : \mathcal{D}^* \rightarrow \Sigma^2$ is a homeomorphism, and*

$$\omega \circ f = \sigma \circ \omega,$$

where \circ denotes composition of maps, e.g., $\omega \circ f : \mathcal{D}^* \rightarrow \Sigma^2$.

Many extremely interesting consequences follow almost immediately from the last theorem.

Theorem 14.3.3 ([IL99]; see also [Sma63, Sma67, Sma00a]). *The following properties of the map f hold:*

- f has infinitely many periodic orbits.
- f has infinitely many homoclinic orbits to each of its fixed points.
- f has infinitely many heteroclinic orbits.

Exercise 14.3.4. Prove Theorem 14.3.3 using Theorem 14.3.2. ◇

In view of Theorem 14.3.3, it seems reasonable to classify the Smale horseshoe map f as chaotic, and it is not difficult to see that it has chaotic orbits. The name “horseshoe” comes from the original geometric construction of the map by Smale. He mapped the initial square/rectangle as one continuous object, stretching it by a factor horizontally and then compressing it vertically. Then one can fold this rectangle into a horseshoe and consider the map illustrated in Figure 14.4.

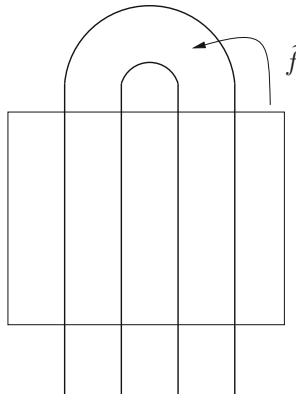


Figure 14.4: Sketch of the original geometric horseshoe-type map \tilde{f} .

The idea of stretching, folding, and returning to the initial domain is still one of the key concepts in recognizing chaotic dynamical systems from an intuitive standpoint. From a rigorous viewpoint, the map f is sometimes insufficient for more complicated applications. The reason is that we usually want to analyze the Poincaré return map of a flow. In that case, we are rarely given this map in the nice format of f , but we have to develop more general conditions under which we can recognize that a map is of horseshoe type.

Here we describe how to generalize the standard horseshoe construction to take into account nonlinear maps, domains without straight boundaries, and shift maps on more symbols. We begin by introducing several important definitions.

Definition 14.3.5. Consider a splitting

$$\mathbb{R}^{n+m} = \mathbb{R}^n \oplus \mathbb{R}^m.$$

Let $\mathcal{D}_h \subset \mathbb{R}^n$ and $\mathcal{D}_v \subset \mathbb{R}^m$ be compact connected manifolds diffeomorphic to n - and m -dimensional unit balls. A **standard rectangle** B is the Cartesian product of these domains $B = \mathcal{D}_h \times \mathcal{D}_v$. We also use the following terminology:

$\partial_h B = \mathcal{D}_h \times \partial \mathcal{D}_v$ is called the **horizontal part** of the boundary of B ,
 $\partial_v B = \partial \mathcal{D}_h \times \mathcal{D}_v$ is called the **vertical part** of the boundary of B .

Definition 14.3.6. The splitting of \mathbb{R}^{n+m} also provides a splitting of the associated tangent spaces. Let ξ and η denote tangent vectors, split into components

$$\xi = (\xi^-, \xi^+) \quad \text{and} \quad \eta = (\eta^-, \eta^+).$$

Let $\mu_h, \mu_v > 0$ be constant such that $\mu_h \mu_v < 1$. At $p \in \mathbb{R}^{n+m}$, define (μ_h, μ_v) -families of cones:

$$\begin{aligned} K_p^+ &:= \{\xi \in T_p B : |\xi^-| \leq \mu_v |\xi^+|\}, \\ K_p^- &:= \{\xi \in T_p B : |\xi^+| \leq \mu_h |\xi^-|\}. \end{aligned}$$

See Figure 14.5 for an illustration of the cones.

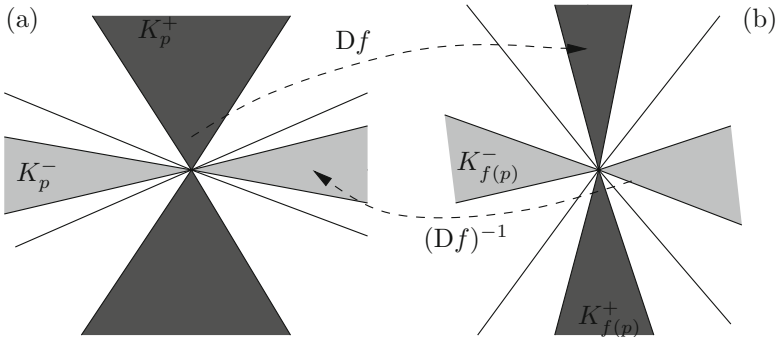


Figure 14.5: Illustration of the cone families and cone condition. (a) Cones centered at p . (b) Cones centered at $f(p)$.

Definition 14.3.7. A map $f : \mathcal{D} \rightarrow \mathcal{D}' \subset \mathbb{R}^{n+m}$ satisfies the (μ_h, μ_v) -cone condition on \mathcal{D} if for every p in the domain of f , the following conditions hold:

$$(a) (Df)K_p^+ \subset K_{f(p)}^+;$$

$$(b) (Df)^{-1}K_{f(p)}^- \subset K_p^-.$$

For $\xi \in T_p \mathbb{R}^{n+m}$, let $\eta = (Df(p))\xi$. Then

$$(c) |\xi^+| \leq \mu_v |\eta^+| \text{ for every } \xi \in K_p^+;$$

$$(d) \mu_h |\xi^-| \geq |\eta^-| \text{ for every } \eta \in K_p^-.$$

See Figure 14.5 for an illustration of the cone condition.

One way to think of the cone condition is as a condition similar to a hyperbolic splitting, e.g., at a hyperbolic fixed point of a map, the cone condition clearly holds.

Definition 14.3.8. Consider a standard rectangle $B = \mathcal{D}_h \times \mathcal{D}_v$, two constants $\mu_h, \mu_v > 0$ such that $\mu_h \mu_v < 1$, and let $G \subset \mathcal{D}_h$ be a domain with boundary. The graph of a Lipschitz map $g : G \rightarrow \mathcal{D}_v$ with Lipschitz constant μ_h is called a μ_h -horizontal surface. Similarly, we can define a μ_v -vertical surface.

The surfaces just defined are the generalizations of edges of a rectangle. Next, we have to define the corresponding generalized rectangles.

Definition 14.3.9. Let B^N denote the unit ball in \mathbb{R}^N . A (μ_h, μ_v) -rectangle $\mathcal{D} \subset \mathbb{R}^n \oplus \mathbb{R}^m$ is a domain of the form

$$\mathcal{D} = H(B^n \times B^m),$$

where $H : B^n \times B^m \rightarrow \mathbb{R}^n \oplus \mathbb{R}^m$ is a homeomorphism and the surfaces $H(B^n \times \{y\})$ and $H(\{x\} \times B^m)$ are μ_h -horizontal and μ_v -vertical respectively for every $y \in B^m$ and $x \in B^n$. The **horizontal** and **vertical parts** of the boundary of \mathcal{D} are defined as the respective images under H of the horizontal and vertical parts of the boundary of $B^n \times B^m$:

$$\partial_h \mathcal{D} := H(B^n \times \partial B^m), \quad \partial_v \mathcal{D} := H(\partial B^n \times B^m).$$

Definition 14.3.10. A (μ_h, μ_v) -rectangle is called **vertically cylindric** in a standard rectangle B if

$$\mathcal{D} \subset B \quad \text{and} \quad \partial_v \mathcal{D} \subset \partial_v B.$$

A (μ_h, μ_v) -rectangle is called **horizontally cylindric** in a standard rectangle B if

$$\mathcal{D} \subset B \quad \text{and} \quad \partial_h \mathcal{D} \subset \partial_h B.$$

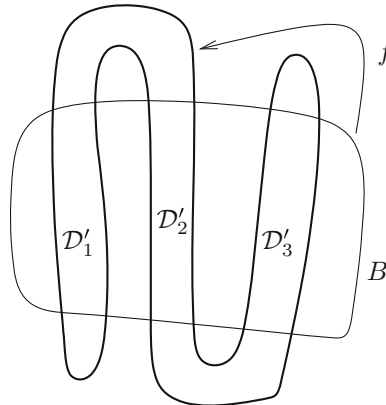


Figure 14.6: Sketch of the generalized geometric horseshoe-type map f from Theorem 14.3.11 with $N = 3$.

Having all the generalized terminology in hand, we can finally state the **Smale horseshoe existence theorem**.

Theorem 14.3.11 ([IL99]). Consider $\mu_h, \mu_v > 0$ such that $\mu_h \mu_v < 1$ and let B be a standard rectangle. Denote by $\mathcal{D}_i \subset \mathbb{R}^n \oplus \mathbb{R}^m$ for $i \in \{1, 2, \dots, N\}$ pairwise

disjoint (μ_h, μ_v) -rectangles. Let

$$f : \mathcal{D} = \bigcup_{i=1}^N \mathcal{D}_i \rightarrow f(\mathcal{D}) \subset B$$

be a diffeomorphism of the domain \mathcal{D} onto its image. Assume that f satisfies the following assumptions:

- (a) The (μ_h, μ_v) -cone condition holds for f in \mathcal{D} .
- (b) The domains \mathcal{D}_i are vertically cylindric in B , and the domains $\mathcal{D}'_i = f(\mathcal{D}_i)$ are horizontally cylindric in B .

Then the set

$$\mathcal{D}^* := \bigcap_{j=-\infty}^{\infty} f^j(\mathcal{D})$$

is an invariant Cantor set. The restriction of f to \mathcal{D}^* is topologically conjugate to the Bernoulli shift σ on Σ^N , the space of N -symbol bi-infinite sequences.

Although the technical machinery seems rather significant, Theorem 14.3.11 is a rather straightforward generalization of the classical Smale horseshoe map to the case of N “topological rectangles.” Figure 14.6 shows an illustration of the situation for $N = 3$.

14.4 Chaos in van der Pol’s Equation I

Consider the periodically forced van der Pol equation as a $(1, 2)$ -fast–slow system

$$\begin{aligned} \varepsilon \dot{x} &= y - \frac{x^3}{3} + x, \\ \dot{y} &= -x + a \sin(2\pi\theta), \\ \dot{\theta} &= \omega, \end{aligned} \tag{14.5}$$

where $a, \omega > 0$ are bifurcation parameters, $(x, y, \theta) \in \mathbb{R} \times \mathbb{R} \times S^1$, and $0 < \varepsilon \ll 1$; here we regard the circle as $S^1 = \mathbb{R}/\mathbb{Z}$.

Due to the importance of van der Pol’s equation from a historical perspective, we review some of the important milestones in its analysis. Originally, the equation was introduced by van der Pol in the 1920s [vdP20, vdP26] in the form

$$x'' + \mu(x^2 - 1)x' + x = a \sin(2\pi\nu t) \tag{14.6}$$

as a nonautonomous system of second order. We showed in Section 1.3 that it is an easy exercise to convert (14.6) into (14.5). The unforced van der Pol equation ($\omega = 0 = a$ or $\nu = 0 = a$) is a planar ODE that cannot exhibit any chaotic behavior due to the Poincaré–Bendixson theorem [HSD03].

The first key observation on the effect of the forcing was provided by van der Pol and van der Mark [vdPvdM27, vdPvdM28], who observed “irregular

noise” in an electric circuit they had built for (14.6). In the 1940s and 1950s, Cartwright and Littlewood continued van der Pol’s studies from a more detailed mathematical perspective [Car52, CL45, CL47, Lit57a, Lit57b]. They showed that (14.6) has parameter regimes with two periodic orbits of different periods and also argued that the boundary between the basins of attraction between the two orbits is not smooth. On the basis of those results, an argument can be made to consider their work the birth of chaotic dynamics [GHW03, Sma00b]. Levinson studied a modified version of (14.6), replacing the term $(x^2 - 1)$ with a piecewise constant one [Lev49, Lev50]. In the 1960s, Smale began working in dynamical systems [Sma00c], and motivated by the work of Cartwright, Littlewood, and Levinson, he developed his horseshoe map [Sma00b, Sma00a]. Essentially, Smale abstracted a geometric picture from Levinson’s paper [Sma00c] and turned it into the classical horseshoe picture; see Figure 14.4. Smale writes [Sma00b, Sma00a], “The horseshoe is a natural consequence of a geometrical way of looking at the equations of Cartwright–Littlewood and Levinson.”

At the beginning of the 1980s, Levi gave a complete qualitative description of Levinson’s equation and showed that a horseshoe exists [Lev81, Lev80]. The bifurcation analysis of (14.5) from a fast–slow systems viewpoint was carried out by Guckenheimer et al. [GHW03, BEG⁺03]. In 2005, Haiduc [Hai05, Hai09] proved in his thesis that (14.5) has a Poincaré return map that contains a Smale horseshoe for suitable parameter values. Among the major developments that made the proof of this result possible is the theory of fast–slow systems, continuing a mathematical story that began with van der Pol in the 1920s.

Theorem 14.4.1 ([Hai05, Hai09]). *There exists an open set of parameters (a, ω) such that for $\varepsilon > 0$ sufficiently small, the following properties of the periodically forced van der Pol equation (14.5) hold:*

- (a) *There exists a cross section Σ to the flow such that every trajectory intersects Σ . The return map $f_\varepsilon : \Sigma \rightarrow \Sigma$ is well defined and can be decomposed as $f_\varepsilon = F_\varepsilon \circ f_\varepsilon$, where $F_\varepsilon : \Sigma \rightarrow \Sigma$ is a diffeomorphism.*
- (b) *The nonwandering set of F_ε decomposes into two basic sets, a sink and a Cantor set Λ_ε^* . The restriction of F_ε to Λ_ε^* is topologically conjugate to the Bernoulli shift on the space Σ^3 of three symbols.*
- (c) *F_ε is C^1 -structurally stable.*

Remark: Regarding (b), p is in the **wandering set** of F_ε if there exist a neighborhood \mathcal{U} of p and some N_0 such that for all $n > N_0$, we have $F_\varepsilon^n(\mathcal{U}) \cap \mathcal{U} = \emptyset$; if p is not in the wandering set, then it is in the **nonwandering set**. We shall not consider (c) in any detail. However, we note that **C^1 -structural stability**, loosely speaking, means that every sufficiently small C^1 -perturbation of a map (or a vector field) is topologically conjugate to the unperturbed map (or vector field).

Although the decomposition in (a) looks strange at first glance, it will become clear during the analysis that a symmetry can be used to decompose the

map f_ε . We shall not discuss the complete proof of Theorem 14.4.1 but shall focus on some of the most important ideas used in proving parts (a) and (b). In fact, we are going to show only a weaker version of (a) and (b).

Theorem 14.4.2 ([Hai05, Hai09]). *For $\varepsilon > 0$ sufficiently small, there exists a compact set Λ_ε such that F_ε restricted to Λ_ε is conjugate to the Bernoulli shift on the space Σ^2 of bi-infinite two-symbol sequences.*

Although Theorem 14.4.2 omits one twist of the actual horseshoe (see Theorem 14.4.1 and Figure 14.6), it is completely sufficient to demonstrate that chaotic dynamics exist in the periodically forced van der Pol equation. The main steps are as follows:

- (S1) Carry out a basic fast–slow systems analysis focusing on the slow flow.
- (S2) Describe a horseshoe-type mapping in the singular limit $\varepsilon = 0$.
- (S3) Check that the perturbed version of this mapping satisfies Theorem 14.3.11, i.e., verify that
 - (S3a) the map has the horseshoe geometry and
 - (S3b) the cone condition is satisfied on a suitable domain.

The main step is to transition from (S2) to (S3); it requires that we combine knowledge about the fast and slow subsystems with Fenichel theory and the analysis of a folded saddle singularity. The critical manifold of (14.5) is

$$C_0 = \left\{ (x, y, \theta) \in \mathbb{R}^2 \times S^1 : y = \frac{x^3}{3} - x =: c(x) \right\}.$$

There are two critical points solving $c'(x) = 0$ defining the fold lines:

$$\begin{aligned} L^- &= \left\{ (x, y, \theta) \in \mathbb{R}^2 \times S^1 : x = -1, y = \frac{2}{3} \right\}, \\ L^+ &= \left\{ (x, y, \theta) \in \mathbb{R}^2 \times S^1 : x = 1, y = -\frac{2}{3} \right\}. \end{aligned}$$

The fold lines L^\pm divide C_0 into three parts, $C_0 = C_0^{a,-} \cup L^- \cup C_0^r \cup L^+ \cup C_0^{a,+}$. The submanifolds $C_0^{a,\pm}$ and C_0^r are normally hyperbolic and are given by

$$C_0^{a,-} = C_0 \cap \{x < -1\}, \quad C_0^r = C_0 \cap \{-1 < x < 1\}, \quad C_0^{a,+} = C_0 \cap \{x > 1\}.$$

Note that $C_0^{a,\pm}$ are attracting, while C_0^r is repelling with respect to the fast direction. We can easily compute the desingularized slow flow on C_0 as

$$\begin{aligned} \dot{x} &= -x + a \sin(2\pi\theta), \\ \dot{\theta} &= \omega(x^2 - 1). \end{aligned} \tag{14.7}$$

To find folded singularities, one has to consider $x = \pm 1$ and try to solve

$$0 = \mp 1 + a \sin(2\pi\theta).$$

This equation has no solutions for $a < 1$; we are interested only in the case $a > 1$. In this case, there are four equilibria for the desingularized slow flow: two on L^- ,

$$\left(-1, 1 - \frac{1}{2\pi} \arcsin\left(\frac{1}{a}\right)\right), \quad \left(-1, \frac{1}{2} + \frac{1}{2\pi} \arcsin\left(\frac{1}{a}\right)\right),$$

and two on L^+ ,

$$\left(1, \frac{1}{2\pi} \arcsin\left(\frac{1}{a}\right)\right), \quad \left(1, \frac{1}{2} - \frac{1}{2\pi} \arcsin\left(\frac{1}{a}\right)\right),$$

where $\arcsin : [-1, 1] \rightarrow [-\pi/2, \pi/2]$ is the inverse sin restricted to the interval $[-\pi/2, \pi/2]$. The Jacobian of (14.7) is

$$\begin{pmatrix} 0 & 2\omega x \\ 2\pi a \cos(2\pi\theta) & -1 \end{pmatrix}.$$

From this Jacobian, a direct calculation shows that on each fold line, there is always one folded saddle, whereas the other equilibrium is either a folded focus or a folded node. We shall assume that parameters are chosen such that we always have a folded saddle and a folded focus. Consider the fold line L^- and denote the two folded singularities by

$$(-1, \theta_s) = \text{folded saddle} \quad \text{and} \quad (-1, \theta_n) = \text{folded focus}.$$

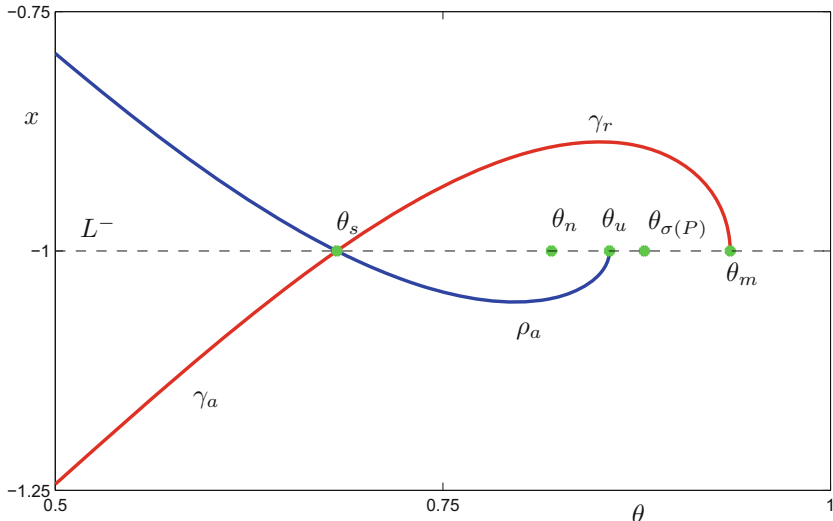


Figure 14.7: Parts of the stable (red) and unstable (blue) manifolds of the folded saddle. Also, several special points (green) that are necessary for the horseshoe construction are shown. Parameter values are $a = 1.1$ and $\omega = 1.57$.

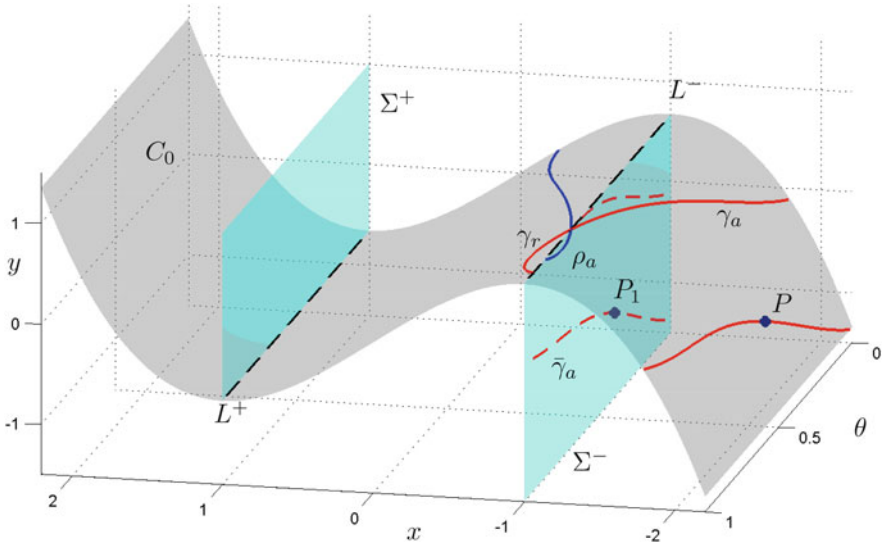


Figure 14.8: Overview of the 3D geometry for the periodically forced van der Pol equation (14.5). Parameter values are $a = 1.1$ and $\omega = 1.57$.

From the explicit formulas, it can be checked that $\theta_s < \theta_n$ holds. The folded saddle has one-dimensional stable and unstable manifolds contained in C_0 . Parts of these manifolds will play important roles in the analysis:

$$\begin{aligned}\gamma_a &:= W^s(-1, \theta_s) \cap C_0^{a,-}, \\ \gamma_r &:= W^s(-1, \theta_s) \cap C_0^r, \\ \rho_a &:= W^u(-1, \theta_s) \cap C_0^{a,-}.\end{aligned}$$

Figure 14.7 shows the manifolds and indicates already that we are going to assume that γ_r and ρ_a return to the fold line L^- . Denote the θ -coordinates of the return points by θ_u and θ_m respectively for γ_r and ρ_a ; see Figure 14.7. In the following analysis, several assumptions have to be made; we shall list all the assumptions and comment on how to prove them below. We require that γ_a intersect the circle $\{x = -2\}$ and that at the first intersection point $P := (-2, -2/3, \theta_P)$, the intersection be transverse, i.e.,

$$2 + a \sin(2\pi\theta_P) \neq 0.$$

Define two cross sections, as shown in Figure 14.8, by

$$\begin{aligned}\Sigma^- &:= \{(x, y, \theta) \in \mathbb{R}^2 \times S^1 : y < 2/3, x = -1\}, \\ \Sigma^+ &:= \{(x, y, \theta) \in \mathbb{R}^2 \times S^1 : y > -2/3, x = 1\}.\end{aligned}$$

Denote by $\bar{\gamma}_a$ the projection along the fast direction to Σ^- . Let $P_1 = (-1, -2/3, \theta_P)$ be the projection of P to Σ^- along the fast direction. Define a standard

rectangle $R \subset \Sigma^-$ as

$$R := \left\{ (-1, y, \theta) \in \mathbb{R}^2 \times S^1 : -\delta'_y \leq y + \frac{2}{3} \leq \delta''_y, \left| \theta - \frac{y}{\alpha} - \theta_P \right| \leq \delta_\theta \right\}$$

for some $\delta'_y, \delta''_y, \delta_\theta, \alpha > 0$ to be determined later. Hence, R is a parallelogram centered at P_1 with two sides parallel to the θ -axis and two sides crossing the y -axis with slope α ; see Figure 14.9. Define a map to R ,

$$\Pi_\varepsilon : R \rightarrow \Sigma^+,$$

by the flow, i.e., if $p \in R$, then $\Pi_\varepsilon(p)$ is the first intersection of the trajectory starting at p with Σ^+ . As long as one can show that Π_ε is well defined, it will follow that it is a diffeomorphism onto its image for $0 < \varepsilon \ll 1$. Next, observe that the periodically forced van der Pol equation (14.5) has the symmetry

$$\sigma(x, y, \theta) = \left(-x, -y, \theta + \frac{1}{2} \right).$$

Using this symmetry, it follows that the return map f_ε from R to Σ^- can be decomposed as a square,

$$f_\varepsilon = (\sigma \circ \Pi_\varepsilon) \circ (\sigma \circ \Pi_\varepsilon) =: (F_\varepsilon) \circ (F_\varepsilon).$$

The map $F_\varepsilon = \sigma \circ \Pi_\varepsilon$ is called the **half-return map**, and we can restrict our analysis to this map. We require that $\theta_u < \theta_{\sigma(P)} < \theta_m$, where $\theta_{\sigma(P)} = \theta_P + 1/2 \pmod{1}$. Furthermore, R should be thin enough: $\delta_\theta < \theta_{\sigma(P)} - \theta_u$ and $\delta_\theta < \theta_m - \theta_{\sigma(P)}$. The last two conditions are geometric and will guarantee that the image $F_\varepsilon(R)$ intersects R in a horseshoe-type fashion; see Figure 14.9.

The θ -direction will be horizontal for Π_ε , and the y -direction will be vertical for Π_ε . In the singular limit, the projection $\bar{\gamma}_a$ can be viewed as the basic vertical component of the horseshoe intersecting R only in the top and bottom edges. We can also consider $\bar{\gamma}_r$ to be the projection of γ_r to Σ^+ and use the symmetry to return it to Σ^- . Then $\sigma(\bar{\gamma}_r)$ represents part of the basic horizontal component of the horseshoe intersecting only the left and right edges of R ; see Figure 14.9. Note that a horizontal segment will become vertical and vice versa under the symmetry σ ; so one always has to think of interchanged horizontal and vertical labels in comparison to Section 14.3 when just analyzing Π_ε .

Figures 14.7, 14.8, and 14.9 summarize the basic assumptions for the singular limit. Before we outline the proof of Theorem 14.4.2, it will help to describe on an intuitive level how the horseshoe is generated in the full system for $0 < \varepsilon \ll 1$.

Consider a trajectory of the full system starting in R near $\bar{\gamma}_a$. It will first jump to the attracting slow manifold $C_\varepsilon^{a,-}$ and then flow close to the folded saddle. Due to the folded saddle, canard orbits occur. Hence, trajectories will follow C_ε^r and either jump back to $C_\varepsilon^{a,-}$ or jump away to $C_\varepsilon^{a,+}$. The trajectories that jump back will reach the fold line L^- and then jump to Σ^+ ; Figure 14.9 denotes the singular return of these trajectories as $\sigma(\bar{L}^-)$. For $\varepsilon > 0$, this gives one horizontal rectangle; see Figure 14.9. The trajectories that jump away

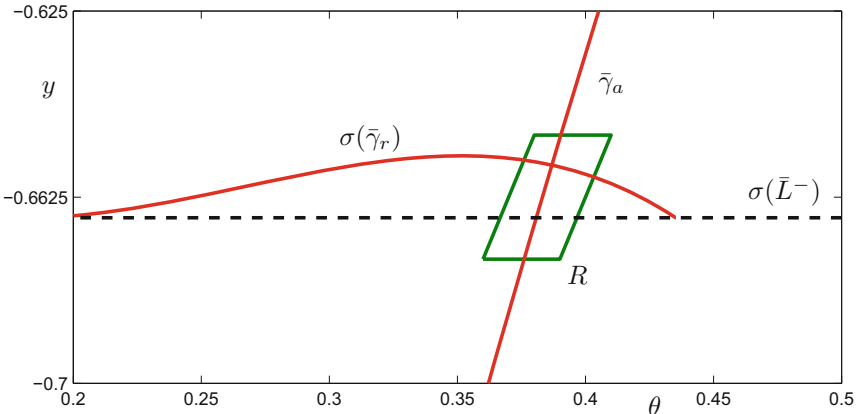


Figure 14.9: Domain $R \subset \Sigma^-$ for the return map and the singular horseshoe; besides $\bar{\gamma}_a$ and $\sigma(\bar{\gamma}_r)$ (red curves), we also show points (dashed black line, denoted by $\sigma(\bar{L}^-)$) that jumped on the fold line L^- to Σ^+ , returning them to R via the symmetry σ . Parameter values are $a = 1.1$ and $\omega = 1.57$.

immediately to Σ^+ return as $\sigma(\bar{\gamma}_r)$ and form the second horizontal rectangle; see Figure 14.9. Therefore, one expects a horseshoe, i.e., for $0 < \varepsilon \ll 1$, the stable manifold projection $\bar{\gamma}_a$ splits into two vertical rectangles that produce two horizontal rectangles due to the canard-induced splitting of trajectories flowing near the folded saddle.

14.5 Chaos in van der Pol's Equation II

In this section, we are going to describe the proof of Theorem 14.4.2. Note that the detailed steps are quite technical, and the reader should make sure to understand the geometry of the singular horseshoe in the last section. In fact, it is highly recommended to follow the next exercise to understand the technical steps of the proof.

Exercise 14.5.1. For each step that is carried out below in this section, make a sketch that relates it to Figures 14.7, 14.8, and 14.9. ◇

As a first step, we list all the conditions that we merely indicated geometrically in the last section:

- (H1) Equilibria of the slow subsystem consist only of folded saddles and foci.
- (H2) θ_s and θ_n satisfy $\frac{1}{2} < \theta_s < \frac{3}{4} < \theta_n < 1$.
- (H3) ρ_a returns to L^- with coordinate θ_u such that $\theta_n < \theta_u < \theta_s + 1$.
- (H4) γ_a intersects the circle $\{x = -2\}$ transversally.

- (H5) γ_r returns to L^- at a point with coordinate θ_m such that $\theta_m < \theta_s + \frac{1}{2}$.
- (H6) $\theta_n < \theta_u < \theta_m < \theta_s + \frac{1}{2}$.
- (H7) $\theta_u < \frac{1}{2} + \theta_P \pmod{1} < \theta_m$.
- (H8) The projection $\tilde{\gamma}_r$ of γ_r along the fast direction to $C_0^{a,-}$ does not intersect γ_a except at the folded saddle. Furthermore, the projection is transversal to the slow flow.
- (H9) $\sigma(\bar{\gamma}_r)$ intersects $\bar{\gamma}_a$ at a point $P_0 \in \Sigma^-$.
- Define d_0^u and d_0^s as the directions tangent to $\sigma(\bar{\gamma}_r)$ and $\bar{\gamma}_a$ at P_0 . Let d_1^u and d_1^s denote the tangent directions to $\{y = -2/3\}$ and $\bar{\gamma}_a$ at P_1 . The geometric idea is that d_i^u are horizontal, while d_i^s is vertical for $i = \{0, 1\}$. Let $s(d)$ denote the slope of a direction. Let (θ_i, y_i) denote the coordinates of P_i for $i = \{0, 1\}$.
- (H10) $|s(d_0^u)| < \min\{s(d_0^s), s(d_1^s)\}$.
- (H11) Choose δ_y'' so that $y_0 - y_1 < \delta_y'' < y_0 - y_1 + 0.01$.
- (H12) Choose δ_θ such that $\theta_u < \frac{1}{2} + \theta_1 \pmod{1} - \delta_\theta$ and $\frac{1}{2} + \theta_1 \pmod{1} + \delta_\theta < \theta_m$.
- (H13) Choose α such that $|\theta_P + \delta_\theta + \delta_y''/\alpha - \theta_s| < 1$.

Despite the rather complicated notation, all conditions just reflect the geometric properties displayed in Figures 14.7, 14.8, and 14.9. It turns out that the conditions are not independent. Instead of presenting a minimal version of the assumptions, we are trying to show here a strategy to prove the existence of a Smale horseshoe for a fast–slow system. We identify the relevant objects in the singular limit and then impose conditions (H1)–(H13) that reflect the geometric properties we want. Some of the properties are easy to prove.

Exercise 14.5.2. Show that if $a > \sqrt{1 + \frac{1}{(16\pi\omega)^2}}$, then conditions (H1)–(H4) hold. \diamond

The question is whether there exist parameter values (a, ω) such that all conditions hold.

Proposition 14.5.3 ([Hai05, Hai09]). *There exists an open set in (a, ω) parameter space such that (H1)–(H13) hold.*

The proof, as developed by Haiduc, requires computational assistance. Rigorous numerical computation employing interval arithmetic [Moo66] was used to rigorously verify some of the slow-flow properties that are contained in (H1)–(H13). We shall not detail the method here, but the next two exercises are very instructive for understanding much better what each condition above means.

Exercise/Project 14.5.4. Check numerically, using nonrigorous methods, that for $a = 1.1$ and $\omega = 1.57$, the conditions (H1)–(H9) hold. Find values δ_y'' , δ_θ , and α such that (H10)–(H13) hold; compute $d_{0,1}^{s,u}$ for your values. Compare your values with [Hai05, Hai09] and explain the differences/similarities. \diamond

Exercise/Project 14.5.5. Find a software package that allows for interval arithmetic computation and use it to compute a finite trajectory segment of the slow flow up to a prespecified accuracy. \diamond

Based on (H1)–(H13), we can now begin the main part of the proof. As a first step, we show that the map $\Pi_\varepsilon : R \rightarrow \Sigma^+$ is well defined for small enough $\varepsilon > 0$. Define the set $Q_0 \subset \Sigma^+$:

$$Q_0 := \{(1, 2/3, \theta) : \theta_* \leq \theta \leq \theta_s \text{ or } \theta_u \leq \theta \leq \theta^*\} \cup \bar{\gamma}_r$$

for some θ_*, θ^* with $\theta_* < \theta_s$ and $\theta^* > \theta_u$. The set Q_0 consists of one-dimensional pieces representing all points that start in R and jump from L^- and all points reaching Σ^+ via the singular canard γ_r .

Lemma 14.5.6. *For all sets $Q_0 \subset A \subset \Sigma^+$ with A relatively open in Σ^+ , there exists $\varepsilon_0 > 0$ such that for all $\varepsilon \in (0, \varepsilon_0]$, the map Π_ε is well defined and $\Pi_\varepsilon(R) \subset A$.*

Proof. Choosing ε sufficiently small, we know from the analysis near a folded saddle (see Section 8.5) that all trajectories of the full system will converge as $\varepsilon \rightarrow 0$ to candidates that have a landing point in Q_0 . Since A is relatively open and contains Q_0 , the result follows. \square

The step is to show that the singular horseshoe structure is preserved for $0 < \varepsilon \ll 1$. Consider the following points:

$$q_s^0 := \left(1, \frac{2}{3}, \theta_s\right), \quad q_u^0 := \left(1, \frac{2}{3}, \theta_u\right), \quad q_m^0 := \left(1, \frac{2}{3}, \theta_m\right).$$

Let $p^0 \in \bar{\gamma}_a$ be such that p^0 is in the relative interior of R . Define three candidate trajectories $\Gamma_s, \Gamma_u, \Gamma_m$ all starting at p^0 and ending up at q_s^0, q_u^0, q_m^0 . All three candidates jump to γ_a and follow it to the folded saddle. From there, Γ_s immediately jumps to q_s^0 , Γ_u follows the unstable manifold of the saddle and then jumps to q_u^0 , while Γ_m is the maximal canard following the stable manifold of the saddle γ_r and then Γ_m jumps to q_m^0 .

Let $Q_\varepsilon := \Pi_\varepsilon(R)$. The set Q_0 consists of one-dimensional components and perturbs to Q_ε . Standard theory of trajectories near a folded saddle yields that there are three trajectory segments from Σ^- to Σ^+ such that

$$\gamma_s^\varepsilon \rightarrow \Gamma_s, \quad \gamma_u^\varepsilon \rightarrow \Gamma_u, \quad \gamma_m^\varepsilon \rightarrow \Gamma_m$$

as $\varepsilon \rightarrow 0$. Let $p_s^\varepsilon, p_u^\varepsilon, p_m^\varepsilon$ be the starting points and $q_s^\varepsilon, q_u^\varepsilon, q_m^\varepsilon$ the endpoints of $\gamma_s^\varepsilon, \gamma_u^\varepsilon, \gamma_m^\varepsilon$ respectively. Since p^0 is in the relative interior of R , it follows that for $\varepsilon > 0$ sufficiently small, $p_s^\varepsilon, p_u^\varepsilon, p_m^\varepsilon$ are in the relative interior of R , and $q_s^\varepsilon, q_u^\varepsilon, q_m^\varepsilon$ are in the relative interior of Q_ε .

Observe that the slow manifold $C_\varepsilon^{a,-}$ is foliated by trajectories that have corresponding two-dimensional stable manifolds. These stable manifolds are

$\mathcal{O}(\varepsilon)$ -close to the singular limit fast fibers and foliate R ; denote this foliation by \mathcal{F}_ε . For example, one of the leaves of this foliation is $\bar{\gamma}_a^\varepsilon$, which is obtained as the perturbation of $\bar{\gamma}_a$. Let R_s^ε , R_u^ε , R_m^ε be the leaves \mathcal{F}_ε of the foliation containing p_s^ε , p_u^ε , p_m^ε . Furthermore, define the sets

$$Q_s^\varepsilon := \Pi_\varepsilon(R_s^\varepsilon), \quad Q_u^\varepsilon := \Pi_\varepsilon(R_u^\varepsilon), \quad Q_m^\varepsilon := \Pi_\varepsilon(R_m^\varepsilon).$$

The next lemma is an important result that provides a contracting direction for the cone condition. It will also be used to characterize how the leaves R^ε change under the map Π_ε .

Lemma 14.5.7. *Let R^ε be a leaf of the foliation \mathcal{F}_ε . Let $p \in R^\varepsilon$ and let $\eta \in T_p R^\varepsilon$. Then the vector η is exponentially contracted under the linearization of Π_ε . More precisely,*

$$\|D\Pi_\varepsilon(p)(\eta)\| \leq e^{-c/\varepsilon} \|\eta\|$$

for some $c > 0$.

Proof. (Sketch; [Hai05, Hai09]) It is not difficult to see that it suffices to consider $p \in \bar{\gamma}_a$ and the associated tangent space $T_p \bar{\gamma}_a$, i.e., we consider the leaf given by the stable manifold to γ_a . The vector η will be transported via the linearized flow $D\Pi_0$ to γ_a and will be exponentially contracted due to the fast attraction to $C_0^{a,-}$. At the folded saddle, an immediate jump can occur, which would conclude the proof, or the vector can be transported along the singular canard $\gamma_r \subset C_0^r$. Along the last part, exponential expansion in the fast direction occurs. The maximal expansion is found along the complete maximal canard segment γ_r . We shall show that the contraction dominates the expansion by integrating the variational equation along $\gamma_a \cup \gamma_r$. The fast equation is

$$\varepsilon \dot{x} = \varepsilon \frac{dx}{d\tau} = y - \frac{x^3}{3} + x.$$

Suppose the time required to flow to the end of γ_r from p is τ_1 . Then the solution of the variational (linearized) equation for the fast flow is

$$\xi(\tau_1) = e^{\frac{1}{\varepsilon} \int_0^{\tau_1} [1-x(\tau)^2] d\tau} \xi(0).$$

To obtain contraction, we have only to check whether the following integral is negative:

$$\int_0^{\tau_1} [1 - x(\tau)^2] d\tau.$$

Since $x(t) \in (-1, 1)$ only for the part along γ_r , it follows that the only expansion occurs in this part. We aim to show that this expansion is dominated already by part of the integral along γ_a . Set $h(t) = 1 - x(t)^2$ and make the change of variable $\theta = \omega\tau + \theta_0$. Then the integral becomes

$$\frac{1}{\omega} \int h(\theta) d\theta. \tag{14.8}$$

Property (H13) implies that the attracting stable manifold γ_a traverses $[\theta_s, \theta_m] \times \mathbb{R}$ twice before reaching the folded saddle. Suppose the last traversal is given by a function $h_1(\theta)$. Let $h_2(\theta)$ give $\tilde{\gamma}_r$ as a graph describing the projection of γ_r to $C_0^{a,-}$. Observe that if we can show that

$$\int_{\theta_s}^{\theta_m} h_1(\theta) \, d\theta - \int_{\theta_s}^{\theta_m} h_2(\theta) \, d\theta \leq 0, \quad (14.9)$$

then we will have established that the integral (14.8) is strictly negative, since (14.9) dominates the positive term along γ_r and contains only some contributions along γ_a . The key observation is that by (H8), we find that $h_1(\theta) - h_2(\theta) \leq 0$ for all $\theta \in [\theta_s, \theta_m]$, i.e., $\tilde{\gamma}_r$ lies closer to L^- than γ_a in this interval of angles θ . This concludes the proof. \square

Note that although the last proof omits some details, the idea should be clear why we also get an exponential contraction in the direction close to the tangent to γ_a in R . Indeed, the contraction along γ_a in the fast direction is accumulated. The geometry of the invariant manifolds for the slow flow shows that this contraction is not compensated by repulsion near C_ε^r , since γ_r is rather short, and it returns to L^- rather quickly.

Lemma 14.5.8. (a) The segments Q_s^ε , Q_u^ε , Q_m^ε have lengths $\mathcal{O}(e^{-c/\varepsilon})$, and

$$Q_s^\varepsilon \rightarrow q_s^0, \quad Q_u^\varepsilon \rightarrow q_u^0, \quad Q_m^\varepsilon \rightarrow q_m^0 \quad \text{for } \varepsilon \rightarrow 0.$$

(b) The segments R_s^ε , R_u^ε , R_m^ε are distinct and of length $\mathcal{O}(1)$, and each of them converges in the Hausdorff distance to $\bar{\gamma}_a \cap R$; R_m^ε is in between the other two.

Proof. (a) follows directly from the definitions of the segments/points and Lemma 14.5.7. Regarding (b), each leaf R^ε converges to the stable manifold of a trajectory of the slow flow on $C_0^{a,-}$. Hence, the length of R^ε is $\mathcal{O}(1)$. Suppose $R_s^\varepsilon = R_m^\varepsilon$. Then Q_s^ε and Q_m^ε converge to the same point as $\varepsilon \rightarrow 0$, and this is false, since $q_s^0 \neq q_m^0$; similar arguments for other pairs of segments shows that R_s^ε , R_u^ε , R_m^ε are distinct. Furthermore, R_m^ε is between the other two by (H6), which implies by symmetry σ that the point $\sigma(q_m^0)$ is between the points $\sigma(q_u^0)$ and $\sigma(q_s^0)$. \square

The strip of R between R_s^ε and R_m^ε is mapped by Π_ε onto the strip between Q_s^ε and Q_m^ε . Let H_0^ε be the intersection of $\sigma(R)$ with this image strip. Similarly, the strip of R between R_m^ε and R_u^ε is mapped by Π_ε onto the strip between Q_m^ε and Q_u^ε . Let H_1^ε be the intersection of $\sigma(R)$ with this image strip. It follows from our previous discussion that $H_0^\varepsilon \cap H_1^\varepsilon = \emptyset$. Therefore, we find that

$$\sigma(H_0^\varepsilon) \cap \sigma(H_1^\varepsilon) = \emptyset.$$

The sets $\sigma(H_j^\varepsilon)$ for $j = \{0, 1\}$ are going to be the horizontal strips of the horseshoe, and so we define the vertical strips as

$$V_j^\varepsilon := \Pi_\varepsilon^{-1}(H_j^\varepsilon), \quad \text{for } j = \{0, 1\}.$$

Obviously, the vertical strips are disjoint as well: V_0^ε is between R_s^ε and R_m^ε , while V_1^ε is between R_m^ε and R_u^ε . Note that one can apply (H10) to see that the sides of the vertical and horizontal strips are not parallel. This completes the main construction, and we must now work toward verifying the conditions of the horseshoe existence theorem, Theorem 14.3.11.

The map $\Pi_\varepsilon : R \rightarrow \Sigma^+$ can be decomposed into two parts. Consider an intermediate cross section

$$\Sigma := \{(x, y, \theta) \in \mathbb{R}^2 \times S^1 : x = -1\}.$$

Let Π_1^ε be the transition map induced by the flow from R via $C_0^{a,-}$ to Σ . Let $\Pi_2^\varepsilon : \Sigma \rightarrow \Sigma^+$ denote the second part of the map, so that $\Pi_\varepsilon = \Pi_2^\varepsilon \circ \Pi_1^\varepsilon$. The two-dimensional unstable manifolds of trajectories in C_ε^r will foliate $\Pi_1^\varepsilon(V_0^\varepsilon \cup V_1^\varepsilon)$. Denote the image of this foliation under Π_2^ε by \mathcal{G}_ε ; observe that \mathcal{G}_ε is a foliation of $H_0^\varepsilon \cup H_1^\varepsilon$. Lemma 14.5.7 showed that there is a contracting direction, and the next lemma shows that there is an expanding direction as well; this provides the basis for satisfying the cone condition.

Lemma 14.5.9. *For $\varepsilon > 0$ sufficiently small, the following conclusions hold:*

- (a) *There exists a constant $c > 0$ such that for every R^ε leaf of \mathcal{F}_ε with $p \in R^\varepsilon$, we have*

$$\|\mathrm{D}\Pi_1^\varepsilon(p)(\eta)\| \leq e^{-c/\varepsilon} \|\eta\|, \quad \text{for all } \eta \in T_p R^\varepsilon.$$

- (b) *There exists a constant $d > 0$ such that for every Q^ε leaf of \mathcal{G}_ε with $q \in Q^\varepsilon$, we have*

$$\|\mathrm{D}\Pi_2^\varepsilon(q)(\varsigma)\| \geq e^{d/\varepsilon} \|\varsigma\|, \quad \text{for all } \varsigma \in T_q Q^\varepsilon.$$

Proof. (Sketch, [Hai05, Hai09]) Part (a) is an easier version of Lemma 14.5.7. For part (b), we start by choosing any $q \in H_0^\varepsilon \cup H_1^\varepsilon$. Let γ_ε be a trajectory through q , and denote by Γ a candidate to which γ_ε converges as $\varepsilon \rightarrow 0$. If $q \in H_0^\varepsilon$, then Γ consists of a slow-flow segment on C_0^r and a jump away to Σ^+ . In this case, Fenichel theory provides the required expansion, since along C_0^r , there is expansion in the fast directions. The main observation that causes technical difficulty is that if $q \in H_1^\varepsilon$, then the candidate Γ will follow C_0^r and then jump back toward $C_0^{a,-}$ before flowing into the fold line L^- and jumping to Σ^+ . In this case, there is also contraction near $C_0^{a,-}$. Hence, one must show that the accumulated expansion dominates the accumulated contraction. We will prove that the directions of expansion and contraction are transverse in this scenario with an angle $\mathcal{O}(1)$ as $\varepsilon \rightarrow 0$; if this holds, then (b) follows. To see this transversality, consider a vector $v \in T_p Q^\varepsilon$. This vector is tangent to the projection of γ_r to $C_0^{a,-}$. Now recall that the last projection is transverse to the slow flow by (H8). This implies that the expanding direction v is uniformly separated from the contracting direction on $C_0^{a,-}$. \square

We summarize that the key idea of the last proof is to use the fast-slow decomposition to prove a cone condition. In particular, the geometry of the

slow flow in relation to the fast directions converts the transversality hypothesis (H8) into a splitting condition of attracting and repelling directions. Most of the major work is complete. Due to the geometry of the horizontal and vertical strips defined above, we have the following result.

Lemma 14.5.10. *There exist numbers $\nu_h, \nu_v > 0$ such that $\nu_h \nu_v < 1$, so that d_i^u are ν_h -horizontal directions and d_i^s are ν_v -vertical directions for $i \in \{0, 1\}$. Therefore, we may consider the following cones:*

$$\begin{aligned} K_h &= \{(\theta, y) \in \mathbb{R} \times S^1 : |\theta| \leq \nu_h |y|\}, \\ K_v &= \{(\theta, y) \in \mathbb{R} \times S^1 : |y| \leq \nu_v |\theta|\}. \end{aligned}$$

With a little bit of extra work, we can extend Lemma 14.5.9 to prove the cone condition.

Lemma 14.5.11. *For sufficiently small $\varepsilon > 0$, consider any*

$$p \in (V_0^\varepsilon \cup V_1^\varepsilon) \cap (\sigma(H_0^\varepsilon) \cup \sigma(H_1^\varepsilon)) \quad \text{and} \quad q = \Pi_\varepsilon(p).$$

Then we have

$$\mathrm{D}\Pi_\varepsilon(p)(K_h) \subset K_h, \quad \mathrm{D}\Pi_\varepsilon^{-1}(q)(K_v) \subset K_v.$$

Furthermore, there exist constants $c, d > 0$ chosen independently of ε and p such that for every $(\varsigma_\theta, \varsigma_y) = \mathrm{D}\Pi_\varepsilon(p)(\eta_\theta, \eta_y)$, we get

$$\begin{aligned} |\varsigma_\theta| &\geq e^{d/\varepsilon} |\eta_\theta|, \quad \text{for all } (\eta_\theta, \eta_y) \in K_h, \\ |\varsigma_y| &\leq e^{-c/\varepsilon} |\eta_y|, \quad \text{for all } (\varsigma_\theta, \varsigma_y) \in K_v. \end{aligned}$$

Proof. (Sketch; [Hai05, Hai09]) The direction defined by the foliation \mathcal{F}_ε is approximately aligned in R , with $\bar{\gamma}_a$ representing the vertical contracting cone K_v . The foliation \mathcal{G}_ε can be mapped to Σ^- via the symmetry σ , and it provides the directions for the horizontal expanding cone K_h . The expansion and contraction results follow basically from Lemma 14.5.9. The only problem is to show that at each point, the cones intersect at only a single point. This holds using the analysis near a folded saddle from Section 8.5; in particular, the intersection of the stable and unstable slow manifolds $C_\varepsilon^{a,-} \cap C_\varepsilon^r$ is transverse with an exact asymptotic order $\varepsilon^{1/2}$. Therefore, the contracting and expanding directions are still separated for every $\varepsilon > 0$, and the cones intersect in only one point. \square

As a last step, we have only to apply the horseshoe existence theorem and Lemma 14.5.11 to prove Theorem 14.4.2; note that the vertical and horizontal directions have to be exchanged to match the classical statement of Theorem 14.3.11.

Revisiting the steps of the proof, we emphasize that the Smale horseshoe generated in the periodically forced van der Pol equation can be viewed as generated by canard orbits. In particular, the organizing centers are given by the folded saddle and the associated maximal canard. In the next two sections, we shall show that we can also find fast–slow systems without canards that produce chaos.

14.6 Hénon-Type Maps

The main goal in this section and the next is to revisit the idea of approximating a Poincaré map of certain fast–slow systems by a nearly one-dimensional map.

Example 14.6.1. The classical Hénon map is a two-parameter family of maps on \mathbb{R}^2 defined by

$$H(u, v) = (v + 1 - au^2, bu). \quad (14.10)$$

Figure 14.10 shows points in the maximal attractor Λ_{\max}^H of the map for the canonical parameter values $a = 1.4$ and $b = 0.3$; Figure 14.10 was generated by simply plotting $H^k(0, 0)$ (the k th iterate of the origin) for $500 \leq k \leq 4500$.

Remark: Whenever we consider a discrete-time map such as H , we shall agree on the convention that $H^k = \underbrace{H \circ H \circ \cdots \circ H}_{k\text{-times}}$ denotes the k th iterate.

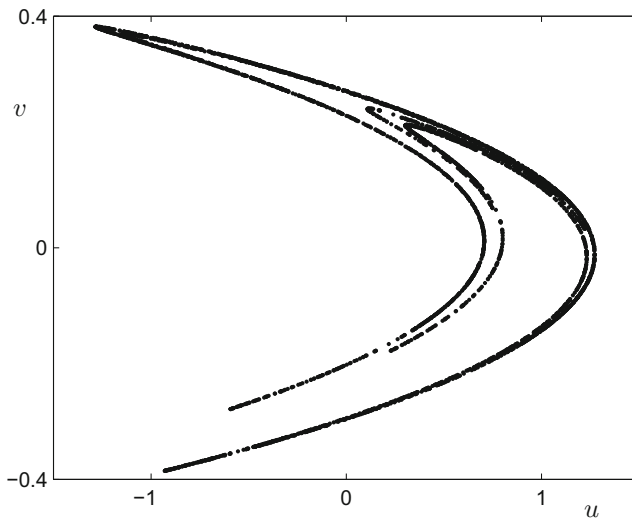


Figure 14.10: Hénon attractor for the map (14.10) with $a = 1.4$ and $b = 0.3$.

This numerical exploration suggests that the Hénon map can produce chaotic dynamics and a strange attractor. Benedicks and Carleson [BC91] investigated parameter values different from the classical ones and considered H as a perturbation of the one-dimensional unimodal map

$$x \mapsto 1 - ax^2$$

for $a = 2$ and $0 < b \ll 1$. Note that this viewpoint describes the Hénon map as a singularly perturbed map

$$\begin{pmatrix} x \\ y \end{pmatrix} \mapsto \begin{pmatrix} 1 - 2x^2 + y \\ \varepsilon x \end{pmatrix}, \quad (14.11)$$

where $\varepsilon := b$ and we set $z = (x, y)$. Observe that (14.11) has a fixed point $z_f = (x_f, y_f)$ with $x_f > 0$ that approaches $(0, 1/2)$ as $\varepsilon \rightarrow 0$. The eigenvalues of the linearization at z_f approach -2 and 0 as $\varepsilon \rightarrow 0$.

Theorem 14.6.2 ([BC91]). *Let W^u be the unstable manifold of z_f in $x, y > 0$. Then for all $c < \log 2$, there is an $\varepsilon_0 > 0$ such that for all $\varepsilon \in (0, \varepsilon_0)$, there is a set of positive one-dimensional Lebesgue measure $E(\varepsilon)$ such that for all $a \in E(\varepsilon)$, the following hold:*

- (i) *There is an open set $U = U(a, \varepsilon) \subset \mathbb{R}^2$ such that for all $z \in U$,*

$$d_H(H^k(z), \overline{W^u}) \rightarrow 0, \quad \text{as } k \rightarrow \infty,$$

where d_H denotes the Hausdorff distance, and $\overline{W^u}$ the closure of W^u .

- (ii) *There is a point $z_0 = z_0(a, \varepsilon) \in W^u$ such that*

- (a) $\{H^k(z_0)\}_{k=0}^\infty$ is dense in W^u ;
- (b) $\left\| D H^k(z_0) \begin{pmatrix} 1 \\ 0 \end{pmatrix} \right\| \geq e^{ck}$.

Theorem 14.6.2 describes the dynamics of the singularly perturbed unimodal map (14.11) as accumulating on the unstable manifold with sensitive dependence on initial conditions, i.e., as chaotic. The proof of Theorem 14.6.2 is extremely complicated and applies only to the Hénon map (14.11). ♦

Wang and Young [WY01, WY02] developed a more general theory of **Hénon-type maps** that replaces the explicit formula (14.11) by a list of geometric properties that are sufficient to prove the existence of a chaotic attractor. Our goal here is to explain how to apply this theory to fast-slow systems similar to the forced van der Pol equation; hence we shall now outline a special version of Wang–Young theory. Suppose $M = S^1 \times I$, where $I \subset \mathbb{R}$ is a closed interval. Denote the coordinates in M by (θ, y) . Consider the family of parameterized maps

$$H_{a,\varepsilon} : M \rightarrow M \quad \text{for } a \in [a_0, a_1] \subset \mathbb{R}.$$

The next two conditions, (C0) and (C1), require that $H_{a,\varepsilon}$ be a perturbation of a **rank-one map**; a map is of rank one if its image is one-dimensional.

- (C0) *Regularity conditions:* For each $\varepsilon > 0$, the map $(\theta, y, a) \mapsto H_{a,\varepsilon}(\theta, y)$ is C^3 . Furthermore, each $H_{a,\varepsilon}$ is an **embedding** of M into itself, i.e., $H_{a,\varepsilon}$ is a homeomorphism between M and $H_{a,\varepsilon}(M)$.
- (C1) *The singular limit:* There exist rank-one maps $H_{a,0} : M \rightarrow M$ such that as functions of (θ, y, a) , we have

$$\|H_{a,\varepsilon} - H_{a,0}\|_{C^3} \rightarrow 0, \quad \text{as } \varepsilon \rightarrow 0,$$

where $\|\cdot\|_{C^3}$ indicates the usual sup-norm on C^3 functions. Furthermore, we assume that $H_{a,0}(M)$ is diffeomorphic to S^1 .

Small (parameterized) changes of coordinates can make $H_{a,0}(M)$ independent of a , and we denote the resulting set by Γ . Hence, one may view $H_{a,0}$ as a map from S^1 onto itself, denoted by h_a . It is also reasonable to assume that after a suitable translation in y , the domain of h_a is embedded as $S^1 \times \{y = 0\}$ in M , i.e.,

$$\Gamma = S^1 \times \{y = 0\},$$

as shown in Figure 14.11. The next conditions, (C2)–(C5), involve only the singular limit.

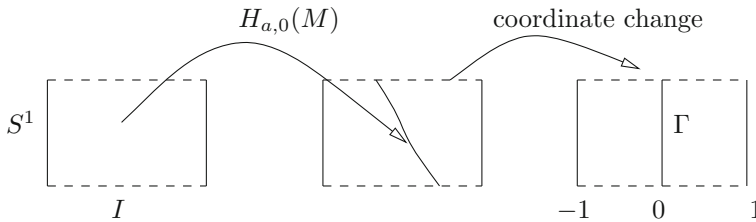


Figure 14.11: Sketch of the construction and domain for the singular Hénon-type map $H_{a,0} = h_a$. The dashed lines are identified to get $M = S^1 \times I$ as a half-open finite cylinder.

- (C2) *Expansion in one-dimensional maps:* There exists $a^* \in [a_0, a_1]$ such that $h_{a^*} =: h$ satisfies the following properties. There exist $c > 1$ and a neighborhood J of the **critical set** (the set where $h' = 0$) in Γ such that:

- if $\xi, h(\xi), \dots, h^{k-1}(\xi) \in J$, then $(h^k)'(\xi) \geq c^k$;
- $\exists N \in \mathbb{N}$ such that if $\xi, h(\xi), \dots, h^{k-1}(\xi) \in J$, then $(h^k)'(\xi) \geq c^k \forall k \geq N$;
- if $\xi \in J$ is not a critical point, then $\exists k = k(\xi)$
s.t. $h(\xi), \dots, h^{k-1}(\xi) \notin J$ and $(h^k)'(\xi) \geq c^k$;
- $\min(|h''|) > 0$ on J ;
- if ξ is a critical point, then $h^k(\xi) \notin J$ for $k > 0$.

Note that (C2) includes the assumption that the critical points are all nondegenerate, since the second derivative is bounded away from zero. Hence, critical points of h_{a^*} vary smoothly with a and have unique continuations. Unique continuation also holds for points p that have h_{a^*} orbits avoiding J .

- (C3) *Parameter transversality:* For each critical point ξ of h_{a^*} , let $p = h_{a^*}(\xi)$, and denote by ξ_a and p_a the respective parameter continuations. We require the following:

$$\frac{d}{da} h_a(\xi_a) \neq \frac{d}{da} p_a \quad \text{at } a = a^*.$$

(C4) *Nondegeneracy at turns:* At each critical point ξ of h_{a^*} ,

$$\frac{\partial H_{a^*,0}}{\partial y}(\xi, 0) \neq 0.$$

The last condition, (C5), is not strictly necessary for deriving chaos for the perturbed map, but it implies additional mixing properties.

(C5) *Mixing:* The constant c in (C2) is larger than 2. Furthermore, let J_1, \dots, J_r be intervals of monotonicity of h_{a^*} , and let $P = (p_{ij})$ be the 0–1 matrix with $p_{ij} = 1$ if and only if $J_j \subset h_{a^*}(J_i)$. Then P is **power positive**, i.e., there exists n such that all entries of P^n are positive.

It can be shown that families of maps satisfying (C0)–(C4) satisfy a key condition for deterministic chaos.

Theorem 14.6.3 ([WY01, WY02]). *Assume that the family $H_{a,\varepsilon}$ satisfies (C0)–(C4). Then for sufficiently small $\varepsilon > 0$, there is a set $A_{a,\varepsilon} \subset M$ of positive Lebesgue measure and a set of positive Lebesgue measure in parameter space with respect to a such that for every $z \in A_{a,\varepsilon}$, we have that the orbit with initial condition z has a positive Lyapunov exponent.*

If we look at measure-zero sets as negligible or unobservable, then Theorem 14.6.3 says that the set of chaotic orbits is observable in phase space as well as parameter space. The statistics of orbits can be made more precise. In particular, if (C5) is satisfied, then further strong measure-theoretic properties hold. Before we can state the detailed version of Theorem 14.6.3, we have to introduce several concepts from measure-theoretic dynamics. Since there is little extra effort involved, we assume for this introduction that we are dealing with a general C^2 -diffeomorphism

$$F : M \rightarrow M,$$

where M is a compact subset of \mathbb{R}^N with $F(z_k) =: z_{k+1}$. Let μ be an **F -invariant measure**, i.e., $\mu(F^{-1}(A)) = \mu(A)$ for all sets measurable with respect to μ . Assume that the Lyapunov exponents $l_i(z)$ for F are all nonzero μ -almost everywhere (μ -a.e.) in M . Then one may define generalizations of the usual stable and unstable manifolds at μ -almost every (μ -a.e.) point z :

$$W^u(z) := \left\{ w \in M : \limsup_{k \rightarrow \infty} \frac{1}{k} \|F^{-k}(z) - F^{-k}(w)\| = 0 \right\},$$

$$W^s(z) := \left\{ w \in M : \limsup_{k \rightarrow \infty} \frac{1}{k} \|F^k(z) - F^k(w)\| = 0 \right\}.$$

A measurable partition ς of M is called **subordinate** to W^u if for μ -a.e. z , the partition element $\varsigma(z)$ containing z is contained in $W^u(z)$. Next, consider two families of measures defined on the elements of ς : μ_x^ς denotes the **conditional measures** [Bog07] of μ , and m_z^ς is Lebesgue measure on $W^u(z)$ restricted to $\varsigma(z)$.

Definition 14.6.4. An F -invariant Borel probability measure μ is said to have **absolutely continuous conditional measures on unstable manifolds** if F has a positive Lyapunov exponent a.e. and for every measurable partition ς subordinate to W^u , we have the absolute continuity condition

$$\mu_z^\varsigma \ll m_z^\varsigma \quad \text{at } \mu\text{-a.e. } z \quad (14.12)$$

with respect to Lebesgue measure.

Recall that the **absolute continuity** condition (14.12) means that $m_z^\varsigma(B) = 0$ implies $\mu_z^\varsigma(B) = 0$ for all measurable sets B . In particular, we get a **Radon–Nikodym derivative** of μ_z with respect to m_z , which is just the probability density of μ_z . Hence, we think of Definition 14.6.4 as simply requiring that the conditional measures on unstable manifolds have densities.

Definition 14.6.5. An F -invariant measure μ is called a **Sinai–Ruelle–Bowen (SRB) measure** if F has positive Lyapunov exponents a.e. and μ has absolutely continuous conditional invariant measures on unstable manifolds.

The relevance of SRB measures is by no means obvious from their definition. To understand why these measures are extremely useful, we first have to accept the fact that in many cases, chaotic attractors have Lebesgue measure zero. Hence, from the Lebesgue measure viewpoint, these attractors are not “visible” or “physically relevant.”

Definition 14.6.6. Let $F : M \rightarrow M$ be an arbitrary map with invariant probability measure μ . Then μ is called a **physical measure** if there is a positive Lebesgue measure set $V \subset M$ such that for every continuous function $\varphi : M \rightarrow \mathbb{R}$,

$$\frac{1}{n} \sum_{k=0}^{n-1} \varphi(F^k(z)) \rightarrow \int \varphi \, d\mu \quad \text{for every } z \in V. \quad (14.13)$$

Theorem 14.6.7 ([Pes77, KS86, PS89, You02]). *Assume that F has a negative Lyapunov exponent a.e.. Then every ergodic SRB measure with no zero Lyapunov exponents is a physical measure.*

Hence, SRB measure can be used to capture the asymptotic distribution properties of orbits via equation (14.13). Now we are ready to state a more general version of Theorem 14.6.3.

Theorem 14.6.8 ([WY01, WY02]). *Assume that the family $H_{a,\varepsilon} : S^1 \times I \rightarrow S^1 \times I$ satisfies (C0)–(C4). Then for sufficiently small $\varepsilon > 0$, there is a set of positive measure of parameters a for which $H_{a,\varepsilon}$ has an SRB measure $\mu_{a,\varepsilon}$. As a consequence, there is a set of positive Lebesgue measure $A_{a,\varepsilon} \subset M$ such that for every $z \in A_{a,\varepsilon}$,*

- the orbit with initial condition z has a positive Lyapunov exponent;
- the asymptotic distribution of the orbit with initial condition z is given by $\mu_{a,\varepsilon}$, i.e., formula (14.13) holds.

If (C5) is also satisfied, then with respect to $\mu_{a,\varepsilon}$, the map $H_{a,\varepsilon}$ is mixing.

It should be noted that the theory of SRB measures presented here is rather general, since Hénon-type maps do not satisfy nice uniform hyperbolicity conditions. In particular, singularly perturbed maps arising as Poincaré maps in fast–slow systems usually do not satisfy uniform hyperbolicity conditions. Hence, we shall briefly outline what these conditions are and why they are, at least intuitively, not satisfied.

Definition 14.6.9. A compact invariant set Λ is called an **Axiom A attractor** if it has a neighborhood U such that $F^k(z) \rightarrow \Lambda$ for all $z \in U$ and if the tangent bundle over Λ has a uniformly hyperbolic splitting. More precisely, at every $z \in \Lambda$, we have a splitting

$$T_z M = E^u(z) \oplus E^s(z),$$

where E^u and E^s are DF -invariant and $DF|_{E^u}$ ($DF|_{E^s}$) is uniformly expanding (contracting); in this case, uniformly expanding means that there is a constant $\lambda > 1$ such that $\|DF(v)\| \geq \lambda\|v\|$ for every $v \in E^u$, and a similar definition applies for uniformly contracting.

For Axiom A attractors, the machinery of SRB measures simplifies considerably [You02]. It is an easy consequence of Definition 14.6.9 that the spaces E^u and E^s depend continuously on the point z . Now consider a Poincaré map for a fast–slow system that has a return mechanism via a folded critical manifold. In this case, Definition 14.6.9 will usually fail, since the return map will inherit the nonuniform hyperbolic structure from the flow, which contains passages near folded singularities.

14.7 Chaotic Forced Oscillations

In this section, we apply Wang–Young theory to a class of $(1, 2)$ -fast–slow systems that describe forced oscillations. The canonical example is a version of the periodically forced van der Pol equation.

Example 14.7.1. A modified version of the periodically forced van der Pol equation can be written as a $(1, 2)$ -fast–slow system

$$\begin{aligned} \varepsilon \dot{x} &= y + x - \frac{1}{3}x^3, \\ \dot{y} &= -x + a(x^2 - 1) \sin(2\pi\theta), \\ \dot{\theta} &= \omega, \end{aligned} \tag{14.14}$$

where $(x, y, \theta) \in \mathbb{R}^2 \times S^1$, (a, ω) are the main bifurcation parameters, $0 < \varepsilon \ll 1$, and we view S^1 as \mathbb{R}/\mathbb{Z} . ♦

In the following, we shall generalize the situation of van der Pol's equation slightly. Nevertheless, it will be helpful to keep the concrete case from Example 14.7.1 in mind at every step. Consider the following class of forced relaxation oscillators:

$$\begin{aligned}\varepsilon \dot{x} &= f(x, y, \theta), \\ \dot{y} &= g(x, y, \theta), \\ \dot{\theta} &= \omega.\end{aligned}\tag{14.15}$$

for $(x, y, \theta) \in \mathbb{R}^2 \times S^1$, $0 < \varepsilon \ll 1$, and $\omega > 0$ is the slow driving frequency. The functions f, g are assumed to be smooth. In the same spirit as Wang–Young theory, we shall prescribe several geometric assumptions on (14.15). Essentially, these assumptions are going to lead to the situation discussed in Section 14.1.

- (A0) *Geometry of the critical manifold:* The critical manifold $C = \{(x, y, \theta) \in \mathbb{R}^2 \times S^1 : f(x, y, \theta) = 0\}$ splits into three parts separated by fold curves (circles)

$$C_0 = C_0^{a,-} \cup L^- \cup C_0^r \cup L^+ \cup C_0^{a,+}.$$

The respective parts are defined as usual by

$$\begin{aligned}C_0^{a,\pm} &= \{(x, y, \theta) \in \mathbb{R}^2 \times S^1 : f_x(x, y, \theta) < 0\}, \\ C_0^r &= \{(x, y, \theta) \in \mathbb{R}^2 \times S^1 : f_x(x, y, \theta) > 0\}, \\ L^\pm &= \{(x, y, \theta) \in \mathbb{R}^2 \times S^1 : f_x(x, y, \theta) = 0, f_{xx}(x, y, \theta) \neq 0\}.\end{aligned}$$

Furthermore, we assume that $f_y(x, y, \theta) \neq 0$ on C_0 .

The assumption (A0) guarantees that C_0 is an S-shaped (or cubic-shaped) critical manifold; see Figure 14.12.

- (A2) *No folded singularities:* All points $p \in L^\pm$ are jump points, i.e., the normal switching condition

$$(f_y g + f_\theta \omega)|_{p \in L^\pm} \neq 0\tag{14.16}$$

is satisfied, and the slow flow near the fold curves L^\pm is directed toward the fold curves L^\pm .

For details on the normal switching condition and the relevance of jump points for relaxation oscillations, consider Section 7.6.

Note that the fast flow is parallel to the x -axis. Hence, it is natural to define a projection map along the x -axis describing this flow,

$$P : (\mathbb{R}^2 \times S^1 - C_0) \rightarrow C_0^a := C_0^{a,+} \cup C_0^{a,-}.$$

Then P can be described geometrically for every point $z \in (\mathbb{R}^2 \times S^1 - C_0)$. If the line parallel to the x -axis through z intersects C_0^a only once, then we define this intersection point as $P(z)$. If it intersects C_0^a twice, then $P(z)$ is defined by requiring that the segment between z and $P(z)$ not meet C_0^r ; see Figure 14.12.

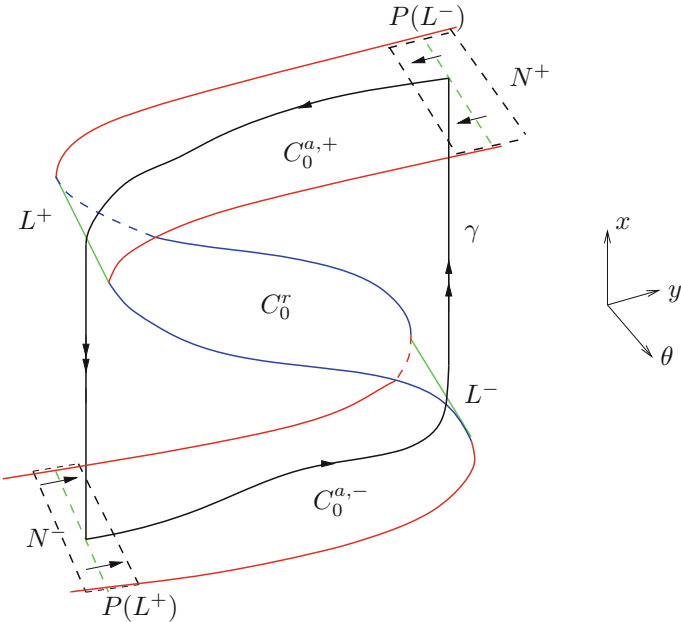


Figure 14.12: Sketch of the basic geometric assumptions on the critical manifold for equation (14.15). A candidate trajectory γ that perturbs to a relaxation oscillation is shown as well.

Exercise 14.7.2. Write down the slow flow for (14.15) in (x, θ) -coordinates on C_0 . \diamond

- (A3) *Regular slow flow:* There exist neighborhoods $N^\pm \subset C_0^{a,\pm}$ of $P(L^\mp)$ such that all trajectories of the slow flow with initial conditions in N^\pm reach the fold curve L^\pm in finite time. The associated maps $P(L^\mp) \rightarrow L^\pm$ are well defined and surjective.

Basically, (A3) requires that there be no invariant sets, for example equilibrium points, for the slow flow on C_0^a where trajectories can get trapped before they reach a fold curve and jump again. Obviously, one can construct the usual candidate trajectories of the singular system $\varepsilon = 0$ as concatenations of fast- and slow-flow solutions; see Figure 14.12. To analyze the relation between the full system and the singular limit, let us introduce cross sections at distance $\mathcal{O}(1)$ from C_0 through which the flow is transverse for $0 \leq \varepsilon \ll 1$. Let Σ^\pm be orthogonal to the x -axis, so that for sufficiently small ε , all trajectories leaving near L^\pm reach Σ^\pm ; see Figure 14.13. Then define transition maps

$$H_\varepsilon^+ : \Sigma^+ \rightarrow \Sigma^- \quad \text{and} \quad H_\varepsilon^- : \Sigma^- \rightarrow \Sigma^+$$

induced by the flow of (14.15) for $\varepsilon > 0$ and defined via candidate trajectories for $\varepsilon = 0$. We also refer to H_ε^\pm as **half-return maps**. The main map we are

going to analyze is the Poincaré map

$$H_\varepsilon := H_\varepsilon^- \circ H_\varepsilon^+ : \Sigma^- \rightarrow \Sigma^-. \quad (14.17)$$

Note that Wang–Young theory works with a family of maps $H_{a,\varepsilon}$, but we shall not display the parameter dependence explicitly at the moment and silently assume that we are working at a value $a = a^*$.

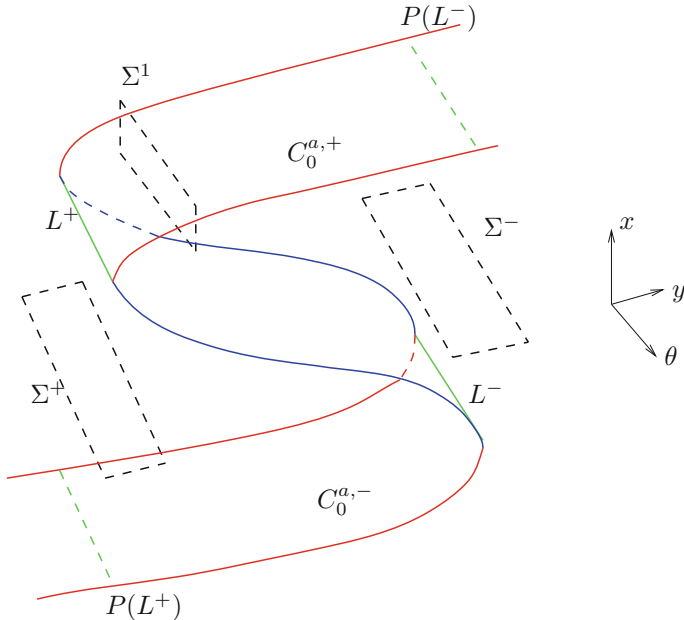


Figure 14.13: Poincaré section Σ^- for H_ε and auxiliary sections Σ^+ and Σ^1 .

If (A1)–(A3) are satisfied, then Theorem 14.1.2 implies that the return map H_ε is well defined and close to the singular map Π_0 . Note also that in this case, the fold curves can be represented as graphs

$$L^\pm = \{(x, y, \theta) \in \mathbb{R}^2 \times S^1 \cap C_0 : x = \psi^\pm(\theta)\}.$$

The slow flow is transverse to the projected curves (also called **drop curves**) $P(L^\pm)$ if

$$l^*(p) := \begin{pmatrix} 1 \\ \psi' \end{pmatrix} \cdot \left(\begin{pmatrix} f_y g + \omega f_\theta \\ -\omega \end{pmatrix} \right) \Big|_{p \in P(L^\pm)} \neq 0. \quad (14.18)$$

Proposition 14.7.3 ([GWY06]). *Suppose (A1)–(A3) hold for system (14.15). If the transversality condition (14.18) holds at all points of $P(L^\pm)$, then there exists a unique invariant torus for (14.15).*

Hence, in the case of Proposition 14.7.3, the dynamics of H_ε can be described by a circle diffeomorphism obtained in the singular limit $\varepsilon = 0$. This situation

occurs for the periodically forced van der Pol equation in Example 14.7.1 when $a < 1$. In Section 14.1, we saw that tangencies at $P(L^\pm)$ are likely to induce much more complicated dynamics. This is the situation in which we are interested.

(A4) *Tangencies:* There exists a finite number of isolated critical points $p_i^* \in P(L^\pm)$ with $i \geq 1$ that violate the transversality condition (14.18), i.e.,

$$l^*(p_i^*) = 0.$$

The critical points p_i^* also satisfy a nondegeneracy assumption:

$$(l^*)'(p_i^*) := \frac{d}{d\theta} l^*(p_i^*) \neq 0.$$

The slow flow is tangent to $P(L^\pm)$ at the critical points p_i^* , as shown in Figure 14.2. Hence, we expect the return map H_ε to have a folding mechanism. In combination with the strong contraction toward the attracting slow manifolds, one may already guess that the theory of Hénon-type maps will be applicable. Therefore, the strategy will be to show that if (A1)–(A4) hold, then the map H_ε given in (14.17) satisfies the assumptions (C1)–(C5) of Wang–Young theory in Section 14.6.

Proposition 14.7.4 ([GWY06]). *If (A1)–(A4) hold, then (C0) holds for H_ε .*

Proof. This follows immediately from existence, uniqueness, and smooth dependence of solutions for ODEs; in particular, we have assumed that the maps f, g defining the vector field are smooth (i.e., C^∞), which is more than sufficient. \square

Proposition 14.7.5 ([GWY06]). *If (A1)–(A4) hold then (C4) holds for H_ε .*

Proof. (Sketch) First note that in the current context, the domain of $h = H_0$ in Σ^- is the image of L^- in Σ^- under the projection map P along the x -axis. This corresponds to the set Γ for Wang–Young theory, and clearly, Γ is diffeomorphic to S^1 in our case, as required. Furthermore, let ξ be a critical point of h . Consider a line segment Ω through ξ parallel to the y -axis, i.e., this line segment is perpendicular to Γ . We will show below that H_0^- maps Ω diffeomorphically to a segment in Σ^+ ; similar arguments then yield an analogous result for H_0^+ . Then the derivative condition (C4) will follow by invertibility of diffeomorphisms.

The map H_0^- essentially consists of three parts. First, the projection P sends Ω to $C_0^{a,+}$, which, by the choice of Σ^- , is a diffeomorphism. Since ξ is a critical point, it follows that $P(\Omega)$ is transverse to the slow flow; note that $P(\Gamma)$ is tangent to the slow flow. Since the slow flow along $C_0^{a,+}$ is regular by (A3) up to L^+ , we conclude that the second part of H_0^- is also a diffeomorphism on Ω . Finally, P maps L^+ diffeomorphically to Σ^+ . Similar arguments apply to H_0^+ , which concludes the proof. \square

Exercise 14.7.6. Sketch the mapping of the segment Ω introduced in the proof of Proposition 14.7.5 under H_0^- in $\mathbb{R}^2 \times S^1$. \diamond

Proposition 14.7.7 ([GWY06]). *If (A1)–(A4) hold, then (C1) holds for H_ε .*

Proof. (Sketch) It is straightforward to show that $H_\varepsilon(\Sigma^-)$ is diffeomorphic to S^1 . The problem is to show that

$$H_\varepsilon \rightarrow H_0 \quad \text{as } \varepsilon \rightarrow 0$$

in the C^3 -topology of maps on Σ^- ; since we assumed that the vector field is smooth, it is actually possible to prove C^k -convergence for every finite $k \in \mathbb{N}$. Obviously, it suffices to prove this convergence only for H_ε^- or H_ε^+ and then apply similar arguments to the other half-return map. We focus on H_ε^- and decompose it into four parts:

- (M1) Let Σ^1 be a cross section intersecting and transverse to $C_0^{a,+}$ a fixed small distance $\delta = \mathcal{O}(1)$ away from L^+ ; see Figure 14.13. Then there is a well-defined map $H_\varepsilon^{-,1} : \Sigma^- \rightarrow \Sigma^1$ describing a flow toward and near a normally hyperbolic slow manifold.
- (M2) Let Σ^2 be an ε -dependent cross section before the jump at L^+ at distance $\mathcal{O}(\varepsilon^{2/3})$ from L^+ and parallel to Σ^1 . Then a map $H_\varepsilon^{-,2} : \Sigma^1 \rightarrow \Sigma^2$ describes the flow immediately before the jump.
- (M3) Let Σ^3 be an ε -dependent cross section right after the jump at L^+ at distance $\mathcal{O}(\varepsilon^{1/3})$ from L^+ and parallel to Σ^+ . Then a map $H_\varepsilon^{-,3} : \Sigma^2 \rightarrow \Sigma^3$ describes the flow near the fold curve.
- (M4) The last map, $H_\varepsilon^{-,4} : \Sigma^3 \rightarrow \Sigma^+$, captures the fast phase after the jump.

Although the C^k -convergence of $H_\varepsilon^{-,1} \rightarrow H_0^{-,1}$ is not immediate, it follows rather quickly using the normal hyperbolicity of $C_0^{a,+}$ between Σ^- and Σ^1 , which makes Fenichel's theorem applicable. In [GWY06], this argument is carried out in detail in the context of forced oscillations; however, it might be easier just to use Fenichel normal form in this context.

The proof of $H_\varepsilon^{-,j} \rightarrow H_0^{-,j}$ for $j = 2, 3, 4$ requires suitable blowup coordinate changes. Essentially, the argument carries out the blowup analysis that we outlined in the context of relaxation oscillations in \mathbb{R}^3 in Section 7.6 with the added focus on C^k -convergence of the three maps involved. One idea of proof is to choose a sequence $\varepsilon_n \rightarrow 0$ as $n \rightarrow \infty$ and then show that the derivative of $H_{\varepsilon_n}^{-,j}$ is uniformly bounded and uniformly equicontinuous. Since $H_{\varepsilon_n}^{-,j}$ is clearly a pointwise bounded sequence, the Arzelà–Ascoli theorem provides a C^1 -convergent subsequence. It is then not difficult to show that this limit for $H_{\varepsilon_n}^{-,j}$ is unique and must equal $H_0^{-,j}$. Now repeat the same procedure for the second derivative, and so on. The key step is to get the boundedness of C^k -derivatives in the respective blowup charts, and it is this longer technical step that we omit here. \square

The conditions (C2), (C3), and (C5) do not necessarily hold under the very general assumptions (A1)–(A4). This means that we have to check (C2), (C3), and (C5) in each particular example in the class of forced relaxation oscillators. As already discussed in Section 14.5, these calculations can often be carried out only numerically, and interval arithmetic has to be used to verify the computations rigorously. We are going to demonstrate in an example how the different conditions can be explored numerically.

Example 14.7.8. We return to the periodically forced van der Pol equation from Example 14.7.1 and observe that there is a symmetry

$$\sigma(x, y, \theta) = (-x, -y, \theta + 1/2)$$

that leaves 14.7.1 invariant. We shall make use of this symmetry throughout this example. As a first step, we have to show that the assumptions (A1)–(A4) actually hold for (14.14). The critical manifold is

$$C_0 = \left\{ (x, y, \theta) \in \mathbb{R}^2 \times S^1 : y = \frac{x^3}{3} - x \right\}.$$

The fold curves are easily found as

$$\begin{aligned} L^+ &:= \left\{ (x, y, \theta) \in \mathbb{R}^2 \times S^1 : x = 1, y = -\frac{2}{3} \right\}, \\ L^- &:= \left\{ (x, y, \theta) \in \mathbb{R}^2 \times S^1 : x = -1, y = \frac{2}{3} \right\}. \end{aligned}$$

On the fold curves, we have $\dot{y} \neq 0$. Hence, the normal switching condition (14.16) for (14.14) is satisfied:

$$(f_y g + f_\theta \omega)|_{p \in L^\pm} = 1 \cdot \dot{y} + 0 \cdot \omega \neq 0.$$

Therefore, the assumptions (A1)–(A2) hold. The desingularized slow subsystem is

$$\begin{aligned} \dot{x} &= -x + a(x^2 - 1) \sin(2\pi\theta), \\ \dot{\theta} &= (x^2 - 1)\omega. \end{aligned} \tag{14.19}$$

Since $\dot{\theta} \neq 0$ for points outside L^\pm , there are no equilibria outside the fold curves for the slow subsystem. The images of the fold curves $P(L^\pm)$ under the fast flow are given by

$$P(L^\pm) = \left\{ (x, y, \theta) \in \mathbb{R}^2 \times S^1 : x = \mp 2, y = \mp \frac{2}{3} \right\}.$$

The tangencies of the slow vector field to these curves occur at points where

$$0 \stackrel{!}{=} \pm 2 + 3a \sin(2\pi\theta). \tag{14.20}$$

Equation (14.20) has a pair of solutions for $a > 2/3$; these points will correspond to critical points of the return map. The tangencies are clearly nondegenerate,

and so (A4) holds. Verifying (A3) is nontrivial analytically, since we are asking for a global behavior that involves estimating solutions for the nonlinear slow subsystem (14.19). Numerically, (A3) is easy to check if as parameter values, specific (a, ω) are given.

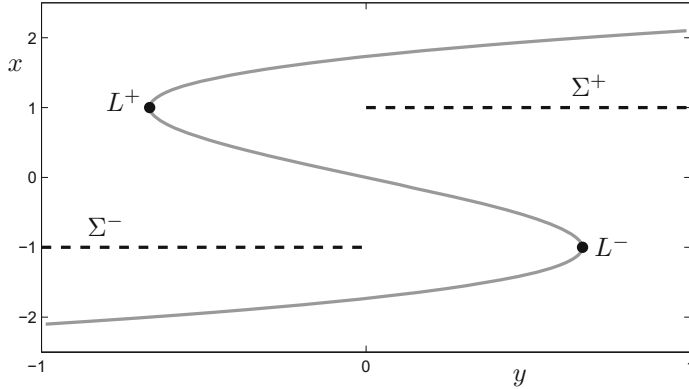


Figure 14.14: Projection onto the (y, x) -coordinates showing the S-shaped critical manifold C_0 , the fold curves L^\pm , and the cross sections Σ^\pm ; H_ε^+ maps from Σ^+ to Σ^- .

Next, we give a more precise definition of the cross sections (see Figure 14.14)

$$\begin{aligned}\Sigma^+ &:= \{(x, y, \theta) \in \mathbb{R}^2 \times S^1 : x = 1, y > 0\}, \\ \Sigma^- &:= \{(x, y, \theta) \in \mathbb{R}^2 \times S^1 : x = -1, y < 0\}.\end{aligned}$$

Observe that the symmetry σ exchanges Σ^+ and Σ^- . Let $H_\varepsilon^- : \Sigma^- \rightarrow \Sigma^+$ and $H_\varepsilon^+ : \Sigma^+ \rightarrow \Sigma^-$ be the half-return maps, and observe that it suffices to consider

$$H_\varepsilon := \sigma \circ H_\varepsilon^+ : \Sigma^+ \rightarrow \Sigma^+,$$

since the symmetry of the equations implies that the full Poincaré map on Σ^+ is given by $\Pi_\varepsilon = H_\varepsilon \circ H_\varepsilon$. Fixed points of H_ε correspond to symmetric periodic orbits. Figure 14.15(a) shows the computed return map H_0 for

$$(a, \omega) = (11.5090088860044, 41.8581499911231),$$

as suggested in [GWY06]. The initial conditions were chosen as 10 000 points equally spaced on a circle $\{x = 1, y = 2/3\}$. It is clearly visible that there are two critical points that get mapped extremely close to a fixed point p . Having these computational results, we can compute the derivatives using finite differences to verify (C2), (C3), and (C5) numerically.

The derivative H'_0 is shown in Figure 14.15(b) and clearly displays the desired expansion properties of (C2) respectively (C5); for detailed number-crunching, see [GWY06]. Therefore, the computations provide strong evidence that the periodically forced van der Pol equation has parameter regions where the Poincaré return map is a nearly Hénon-type map that exhibits chaos. ♦

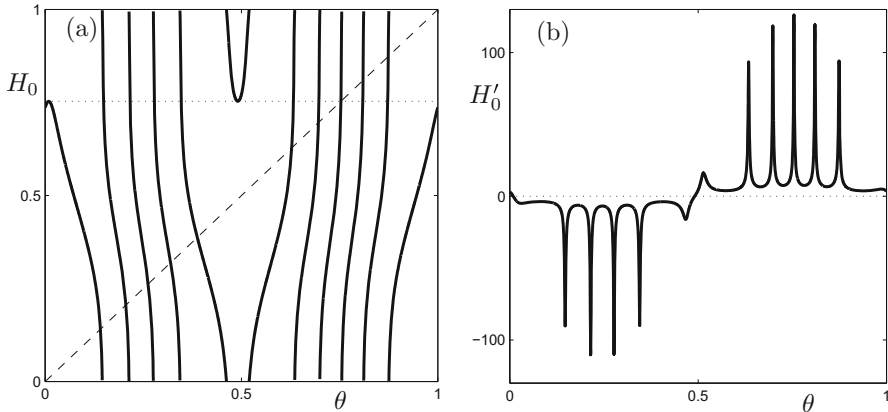


Figure 14.15: (a) Return map H_0 for the periodically forced van der Pol equation (14.14). Note that the map has two critical points with critical value $p \approx 0.7531$ and that p appears to be a fixed point $H_0(p) = p$. (b) Derivative H'_0 showing the strong expansion properties of the derivative and the nondegeneracy of the critical points.

Exercise/Project 14.7.9. (a) Look at the conditions of (C2), (C3), and (C5) and explain why Figure 14.15 is a first indication that the conditions are satisfied.

- (b) Use your favorite mathematical software to reproduce Figure 14.15 and check (C2), (C3), and (C5) numerically.
- (c) Can you find a good numerical test to determine whether (A4) holds, i.e., whether trajectories of the slow flow starting near the drop curves reach a fold curve? Hint: For which parameter values does $x(0) - x(\tau)$ decrease or increase with $[\theta(0), \theta(\tau)] = [0, 1]$. \diamond

14.8 Constructing Chaotic Attractors

So far, we have been concerned to use multiple time scales to prove the existence of chaotic attractors. Certainly, one can also ask whether we can use fast–slow systems to build or design particular attractors. The most intriguing candidate from a historical perspective is the **Lorenz attractor** generated by

$$\begin{aligned} x' &= \sigma(y - x), \\ y' &= \rho x - y - xz, \\ z' &= xy - \beta z, \end{aligned} \tag{14.21}$$

where the standard parameter values are given by $\sigma = 10$, $\rho = 28$, and $\beta = 8/3$; see also Figure 14.16.

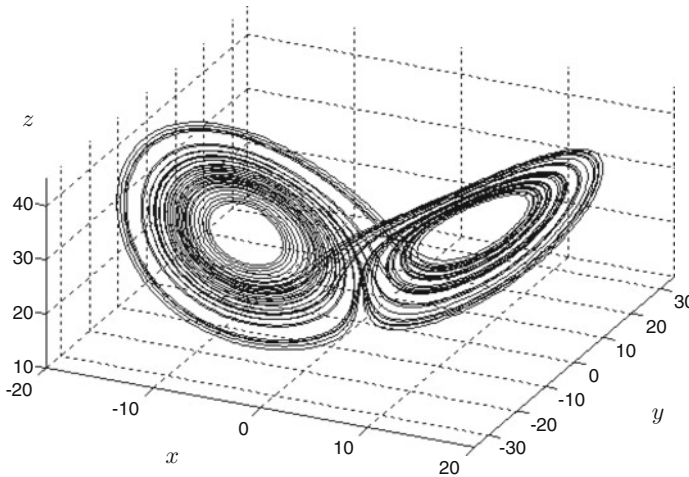


Figure 14.16: Numerical integration for the Lorenz equation (14.21) with $\sigma = 10$, $\rho = 28$, and $\beta = 8/3$ showing part of the Lorenz attractor.

Exercise/Project 14.8.1. Use numerical integration for (14.21) and visualize the Lorenz attractor for various parameter sets. Can you describe how the “butterfly” structure breaks down on parameter variation? ◇

A natural attempt to construct a Lorenz-type attractor is to start with a three-dimensional fast–slow system

$$\begin{aligned} \varepsilon \frac{dx}{d\tau} &= \varepsilon \dot{x} = y_1 - 5(x^3 - (y_2 - q)x) =: f(x, y), \\ \frac{dy_1}{d\tau} &= \dot{y}_1 = g_1(x, y), \\ \frac{dy_2}{d\tau} &= \dot{y}_2 = g_2(x, y), \end{aligned} \tag{14.22}$$

where the fast variable equation has already been chosen, $q > 0$ is a parameter, and the slow variables still have to be constructed. The critical manifold

$$C_0 = \{(x, y) \in \mathbb{R}^3 : y_1 = 5(x^3 - (y_2 - q)x)\}$$

is normally hyperbolic except at two fold curves

$$L_{\pm} = \left\{ (x, y) \in C_0 : x = \pm \sqrt{(y_2 - q)/3} \right\};$$

see also Figure 14.17(a).

Observe that L_{\pm} coincide at the point $(x, y_1, y_2) = (0, 0, q)$, which is a **cusp point** or **cusp singularity**; see also Sections 3.3 and 14.10. The fold curves divide the critical manifold into an attracting and a repelling part:

$$\begin{aligned} C_0^r &= \left\{ (x, y) \in C_0 : |x| < \sqrt{(y_2 - q)/3}, y_2 > q \right\}, \\ C_0^a &= \left\{ (x, y) \in C_0 : \sqrt{(y_2 - q)/3} < |x| \text{ or } y_2 < q \right\}. \end{aligned}$$

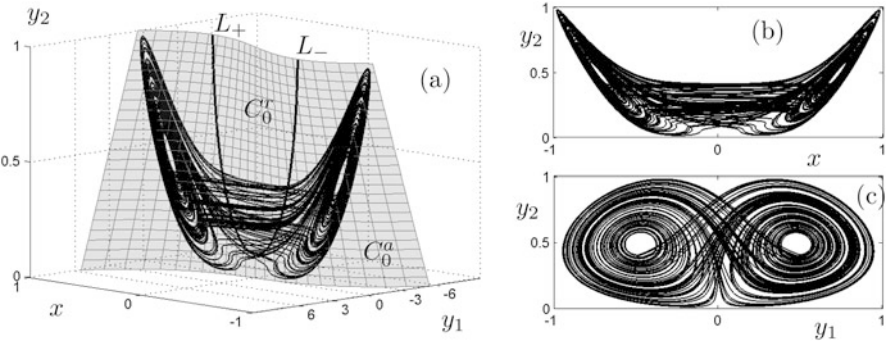


Figure 14.17: Numerical integration for (14.22) with $\kappa = -0.2$, $\varepsilon = 0.05$, and $q = 0.1$. (a) Phase space with chaotic attractor, critical manifold C_0 (gray surface), and fold curves L_{\pm} (thick black curves). (b)–(c) Projections of the chaotic attractor that show its similarity with the Lorenz attractor.

The analogues of the two “wings” of the Lorenz attractor are different parts of C_0^a given by $\{\sqrt{(y_2 - q)/3} < x\}$ and $\{x < -\sqrt{(y_2 - q)/3}\}$. To get the spiraling on the wings, the slow flow has to be chosen appropriately. The idea is to consider

$$\begin{aligned} g_1(x, y) &:= \frac{(x+1)^2}{4}g_1^+(y) + \frac{(x-1)^2}{4}g_1^-(y), \\ g_2(x, y) &:= \frac{(x+1)^2}{4}g_2^+(y) + \frac{(x-1)^2}{4}g_2^-(y), \end{aligned}$$

which essentially gives a homotopy between a flow at $x = 1$ to a different flow at $x = -1$. To simplify the construction, the functions g_1^- and g_2^- are constructed by a symmetry with respect to the y_2 -axis:

$$g_1^-(y_1, y_2) = -g_1^+(-y_1, y_2) \quad \text{and} \quad g_2^-(y_1, y_2) = g_2^+(-y_1, y_2).$$

The functions $g_1^+(y)$ and $g_2^+(y)$ are going to be used to define a vector field on \mathbb{R}^2 in two steps. First, consider the ODE

$$\begin{aligned} y'_1 &= -2y_2 &=: w_1(y_1, y_2, \kappa), \\ y'_2 &= -2y_1 + 3y_1^2 + y_2(y_1^3 - y_1^2 + y_2^2 - \kappa) &=: w_2(y_1, y_2, \kappa), \end{aligned} \tag{14.23}$$

with $w := (w_1, w_2)^\top$ and where $\kappa \in \mathbb{R}$ is a parameter. Phase portraits for three different values of κ are shown in Figure 14.18. At $\kappa = 0$, there exists a homoclinic orbit to the origin that breaks in a homoclinic bifurcation for $\kappa \neq 0$. There is also considerable spiraling of trajectories for $\kappa \neq 0$ that enter a region that was enclosed by the homoclinic orbit.

Exercise/Project 14.8.2. The goal of this exercise is a partial bifurcation analysis of (14.23). Find the equilibria, and calculate the eigenvalues and eigendirections. Prove that for $\kappa = 0$, the curve $\{y_1^3 - y_1^2 + y_2^2 = 0\}$ is a homoclinic orbit to $(0, 0)$. \diamond

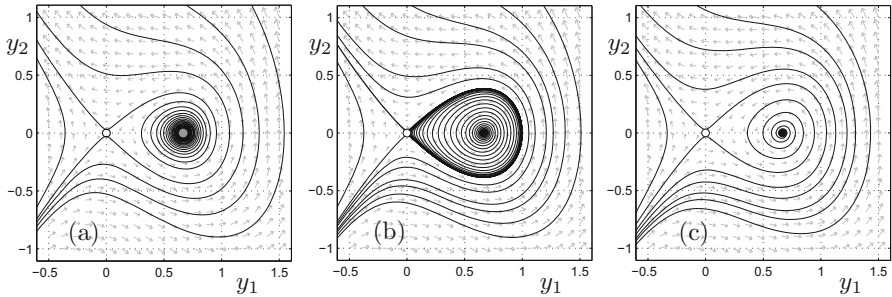


Figure 14.18: Phase portraits and trajectories for (14.23). (a) $\kappa = -0.2$: Saddle point (black circle) and unstable focus (gray dot) are shown. (b) $\kappa = 0$: Homoclinic orbit to saddle point, stable focus (black dot). To find the change of stability in parameter space of the focus located at $(y_1, y_2) = (0, 2/3)$ is part of Exercise 14.8.2. (c) $\kappa = 0.2$: Saddle point (black circle) and stable focus (black dot).

The bifurcation analysis in Exercise 14.8.2 shows that we have a homoclinic orbit. Mapping two copies of (14.23) in a suitable way on the wings of C_0^a should provide many features, such as a double homoclinic loop, similar to the Lorenz attractor; see also Section 14.10. The second step in constructing $g_1^+(y)$ and $g_2^+(y)$ is to rotate (14.23) by an angle θ in a suitable way,

$$\begin{pmatrix} g_1^+(y) \\ g_2^+(y) \end{pmatrix} = A(\theta)w(A(\theta)^\top y), \quad \text{where } A(\theta) := \begin{pmatrix} \cos \theta & -\sin \theta \\ \sin \theta & \cos \theta \end{pmatrix}.$$

Having finished the definitions, we now see that Figure 14.17 shows simulations of the full system (14.22). It is quite remarkable that many features of the chaotic attractor look very similar to the Lorenz system as shown in Figure 14.16. Obviously, the basic strategy is not limited to the Lorenz system, and multiple time scale systems are an excellent tool for devising different types of chaotic attractors.

14.9 Stochastic Replacement

In this chapter, we have been interested in identifying mechanisms for chaos, proving its existence, or constructing it. However, one may also ask whether we can avoid chaos in fast–slow systems or simplify chaotic systems. Here we shall briefly state, on a formal level, an idea that relates chaos to noise, which is already an appetizer for the deep interplay between noise and fast–slow systems considered in Chapter 15.

Consider a general (m, n) -fast–slow system with $m \geq 3$,

$$\begin{aligned} \varepsilon \frac{dx}{d\tau} &= \varepsilon \dot{x} = f(x, y), \\ \frac{dy}{d\tau} &= \dot{y} = g(x, y). \end{aligned} \tag{14.24}$$

For $\tau = \varepsilon t$ and $\varepsilon \rightarrow 0$, assume that the fast subsystem

$$\begin{aligned}\frac{dx}{dt} &= x' = f(x, y), \\ \frac{dy}{dt} &= y' = 0,\end{aligned}\tag{14.25}$$

has a chaotic attractor for each fixed y from a compact domain $y \in \mathcal{D} \subset \mathbb{R}^n$. The main idea is to replace the chaotic fast dynamics by a **white noise** stochastic process ξ_τ and to derive an effective equation for the slow variables

$$\dot{y} = G(y, \xi_\tau).\tag{14.26}$$

The intuitive idea why such a procedure may work is that on certain spatial scales and long enough temporal scales, the fast subsystem chaotic dynamics “look like” white noise, so that an effective equation for the slow variables depending on ξ_τ has some hope of being a good approximation for the slow variables in the full system (14.24). Instead of looking at trajectories of (14.24), we can also consider the evolution of a phase space density $\rho_\tau(x, y)$ of orbits that satisfies the **Liouville** partial differential equation

$$\frac{\partial \rho_\tau}{\partial \tau} = -\frac{1}{\varepsilon} \frac{\partial}{\partial x} [f \rho_\tau] - \frac{\partial}{\partial y} [g \rho_\tau].$$

The distribution of the slow variables is formally given by

$$\bar{\rho}_\tau(y) = \int \rho_\tau(x, y) dx.$$

How one may derive a closed approximate evolution equation for $\bar{\rho}_\tau(y)$ is illustrated in Section 15.5 via projection techniques. In this section, we shall only state the formal results. Let $x_y(\tau; x)$ denote the solution of the fast subsystem (14.25) with fixed value y and initial condition x written on the slow time scale. Let $\rho_y(x)$ denote the invariant density associated with the chaotic attractor and assume that a stationary density $\bar{\rho}_*(y)$ for the slow variables exists. Consider some function $h : \mathbb{R}^m \times \mathbb{R}^n \rightarrow \mathbb{R}$ and define

$$\mathbb{E}_x[h] := \int h(x, y) \rho_y(x) dx = \lim_{T \rightarrow \infty} \frac{1}{T} \int_0^T h(x_y(\tau; x), y) d\tau,$$

where the last equality holds under suitable ergodicity assumptions. Then it can be shown that the evolution equation for $\bar{\rho}_\tau(y)$, to lowest order, is

$$\frac{\partial \bar{\rho}_\tau}{\partial \tau} = -\frac{\partial}{\partial y} [\mathbb{E}_x[g] \bar{\rho}_\tau] + \frac{\partial}{\partial y} \left[D(y) \bar{\rho}_*(y) \frac{\partial}{\partial y} \frac{\bar{\rho}_\tau(y)}{\bar{\rho}_*(y)} \right],\tag{14.27}$$

where the $n \times n$ **diffusion matrix** $D(y)$ is computed via the fluctuation of the slow variable vector field

$$\delta g(x, y) := g(x, y) - \mathbb{E}_x[g]$$

and by using a formula for the autocorrelation function, which leads to

$$D(y) = \int_0^\infty \mathbb{E}_x[\delta g(x_y(\tau; x), y)\delta g(x, y)] d\tau.$$

It is now very important to note that (14.27) is a **Fokker–Planck equation**. Hence, there exists a stochastic differential equation of the form (14.26) just for the slow variables; see also Chapter 15 or [Gar09]. The second-order derivative in (14.27) basically represents the white noise contribution, and it may be substantially easier to deal with the Fokker–Planck equation or the associated SDE than to keep track of a y -dependent family of chaotic attractors. In fact, such a tracking will often be unavoidable if there is no time scale separation.

14.10 References

Section 14.1: The presented idea can be found in [MKKR94] and is detailed further in Section 14.7; to utilize one-dimensional maps to understand chaos in relaxation oscillations has been an idea for quite some time [Guc80b]. The same idea, i.e., to recognize chaotic dynamics by reduction to a one-dimensional map, has been used in other systems, such as epidemic models [SK85b], excitable cells systems [Cha85], the Lorenz equations [GW79], and the Rössler system [FK82]. Initially, a great deal of interest in chaotic dynamics of unimodal maps had been sparked by the 1975 result of “period-three implies chaos” [LY75], which had been established in more generality in [Sha64a] and is now known as Sharkovsky’s (or Sharkovskii’s) theorem. In fact, Sharkovsky had studied one-dimensional iterations extremely intensively at the beginning of the 1960s [Sha65, Sha61, Sha64b, Sha66].

Section 14.2: The section is based mainly on [ASY96], but the material can be found, in various forms and flavors, in several other sources as well [BT10, KG98, Rob13, Str00]; in fact, we have only very briefly reviewed some of the definitions to show why it is sometimes convenient to work with some concrete models of chaos. Several overviews on the origins of chaotic dynamics illuminate some of the history [Guc13, LG09]. There is also a very nice recent discussion on the problems of a definition of chaos [KR09] including a historical perspective.

Section 14.3: This section is based mostly on [IL99], but there are many different expositions on the Smale horseshoe available [GH83]. The history of the horseshoe map can be found in [Sma00c, Sma00b, Sma00a]. The geometric horseshoe map has also motivated many other related constructions of chaotic behavior, see, e.g., [GP83], and it is a long-standing debate how horseshoe-type structures appear in turbulence of fluids [CRO86]. A beautiful connection to knot theory via suspension has also been discovered [Hol86, HW85], which also relates to forced oscillations. Furthermore, we note that the Smale horseshoe is directly linked [Bro95, Hol84] to the Hénon-type maps discussed in Section 14.6. In this context, it should be noted that the Smale horseshoe is a paradigmatic case of uniformly hyperbolic dynamics, whereas Hénon maps also exhibit nonuniformly hyperbolic behavior; an excellent starting point for understanding this general viewpoint of dynamical systems, with many relevant references to uniformly and nonuniformly hyperbolic dynamics, is the book [BDV04].

Section 14.4: This section as well as the next is based on [Hai05, Hai09]. For a detailed fast–slow bifurcation analysis of the forced van der Pol (vdP) equation, see [BEG⁺03, Guc03, GHW03]. The first detailed mathematical analysis of the vdP equation can be found in [Car52, CL45, CL47, Lit57a, Lit57b], with a piecewise linear version covered afterward [Lev81, Lev49, Lev50]. It was noticed only recently that there is an interplay between chaos and canards in the forced vdP equation [IM94]. Periodic perturbations (respectively certain types of more general forcing) may cause chaos under various conditions for relaxation oscillators [AS86, BG93, CAL90, DFGRL02, DK05, GVW76, Guc80b, Lev98, PL87, RL88, SST⁺11]. Taking into account the results of Section 14.7, as well as classical Melnikov-type approaches [Hol80], chaotic phenomena are no longer surprising. Indeed, we have discussed two different mechanisms for chaos generation, and perturbed homoclinics provide a third [GH83, Hol80], while there are potentially even more [KKR96].

Section 14.5: There are many other fast–slow systems that exhibit chaotic dynamics, such as various bursting models [CCB90, CFL95, CAA09, Med06, NDL⁺11, Ter91], Chua’s circuit [Ros93, Ros89], circuits with a tunnel diode [PR81], various coupled systems [FK03a, OT94, VM06], excitable cell models [FC94], food chain models involving canards [Den04, Den01, DH02a], the Hodgkin–Huxley (HH) model [AM86, Car79, DIK04, GO02], the Hindmarsh–Rose model [WS12], laser systems [RRCL00], a leech neuron model [CS05], and predator–prey systems [KC09].

Section 14.6: The results on Hénon-type maps can be found in [WY01, WY02], with a short focused review in [GWY06]. One of the main mathematical breakthroughs in the theory was the analysis in [BC91]. However, Hénon maps have attracted attention from a variety of different research communities [BPPV85, EKR87, Gal93, GKM89]. SRB measures are a powerful tool [You02] in understanding chaotic dynamics; it is likely that measure-theoretic tools have not been used to their full potential in multiple time scale dynamics at the time of writing this book.

Section 14.7: This section follows [GWY06]. For more on chaotic relaxation oscillators, see [CO00, Guc80a, PS02, RY12] and the references above for Section 14.4. Of course, one may search for forced FHN-type systems to discover more literature on chaos in forced oscillators [CEAM13]. There is also a chaotic variation of the classical forced vdP with a third-order term [GR89]. For a study of the Lyapunov exponents of the forced vdP equation, consider [GVS05].

Section 14.8: We followed Deng [Den95a, Den94]. For more on cusp singularities, see [BKK13]. The discovery of the Lorenz attractor is documented in the famous paper [Lor63]. For some further details on chaotic dynamics in the Lorenz model, we refer to [BS09a, GW79, LMP05, Spa82, Tuc99] and references therein.

Section 14.9: We mainly followed [KJB⁺04], and there is related work in [AK13d, dWF09, dWK07, dW11, JKRH01, JGB⁺03]. There are also rigorous convergence results for skew-product flows with fast subsystem chaos to SDEs [GM13, MS11]. Another idea is to replace neglected degrees of freedom in fast–slow nonlinear Hamiltonian systems by noise using maximum entropy closure [SPKP13]. Of course, one may also ask the opposite question, as to which slow variables have an influence on noisy fast processes [LM13].

We have not covered homoclinic chaos [Shi65], which can be found in discretized perturbed NLS using fast–slow arguments [Hal98, LM97a, LM97b]. Other omitted

topics are chaos in fast–slow experimental systems [HBC⁺91, KC86], chaos in map models [SN03, SR03], correlation analysis [FK03b], inverse period-doubling cascades [Den99], limitations of asymptotics [Mur94], on–off intermittency [KR03], relations to PDEs [KRS04, Nis94], quantum mechanics [BR93], slowly varying Hamiltonian systems [GT08], suppression of slow variable chaos [Abr12b], the synchronization of chaotic systems [Jos00, Jos98], and transversal homoclinic points [Pal84].

Chapter 15

Stochastic Systems

The interaction between noise and multiscale dynamics is already a large area, and it is still a field of intensive research. This chapter aims to provide a number of diverse and interlinked techniques that reflect some recent developments.

Section 15.1 provides an introduction to the two major viewpoints we shall take on stochastic processes, i.e., either to focus on their pathwise properties or on their distribution; an example of noise-induced resonance is given as well. Section 15.2 introduces the basics of stochastic fast–slow systems and states a path-wise extension to the classical Fenichel’s theorem for normally hyperbolic invariant manifolds. In Sections 15.3 and 15.4, the fold singularity with noise is analyzed using pathwise and asymptotic approaches that demonstrate how the stochastic theory intertwines with the deterministic methods from previous chapters. Section 15.5 switches to the probability density viewpoint and illustrates a formal procedure of stochastic reduction via the Fokker–Planck equation. An abstract geometric version of Fenichel’s theorem is stated in an interlude on random dynamical systems in Section 15.6. Time-scale separation can also be formalized in the discrete-state-space continuous-time Markov chain case, which is the focus of Section 15.7. Sections 15.8 and 15.9 cover large deviation theory for stochastic differential equations. Large deviations are shown to occur on an exponential time scale due to noise-induced excursions and may be analyzed using the rate function formalism, sometimes called Wentzell–Freidlin theory, as presented in Section 15.8, while asymptotic analysis is used in Section 15.9.

Background: Although we shall introduce some basic ideas and concepts of stochastic analysis along the way, it is necessary to have a good grasp of elementary probability theory [Dur94, Ros06]. Some very basic first steps into measure-theoretic probability [Dur10a, JP04, Wil91], stochastic differential equations [Arn74, Fri06b, Øks03, Pro05], and Markov chains [Res92, Nor06] would be helpful at certain points. A rather quick, albeit less rigorous, way to get started is to focus on stochastic methods [Gar09, vK07].

15.1 Motivation and Viewpoints

In this section, we shall outline why stochastic fast–slow systems are of particular interest and which new phenomena one might expect to appear, and we shall highlight two viewpoints for analyzing them. We begin with an example that conveys a key idea.

Example 15.1.1. Beginning with Section 1.3, we have discussed the classical forced van der Pol equation many times,

$$\begin{aligned} \varepsilon \frac{dx}{d\tau} &= \varepsilon \dot{x} = y - \left(\frac{x^3}{3} - x \right), \\ \frac{dy}{d\tau} &= \dot{y} = a - x, \end{aligned} \quad (15.1)$$

where a is the forcing amplitude parameter. We know that (15.1) displays several interesting phenomena that motivated the deterministic theory of fast–slow systems. Hence, we just try to “add noise” to the system

$$\begin{cases} dx = \frac{1}{\varepsilon} \left(y - \frac{x^3}{3} + x \right) d\tau + \sigma_1 dW^1, \\ dy = (a - x) d\tau + \sigma_2 dW^2, \end{cases} \quad (15.2)$$

$$\begin{cases} \dot{x} = \frac{1}{\varepsilon} \left(y - \frac{x^3}{3} + x \right) + \sigma_1 \xi^1, \\ \dot{y} = (a - x) + \sigma_2 \xi^2. \end{cases} \quad (15.3)$$

Intuitively, a reader unfamiliar with the details of stochastic analysis may just think of solutions to the two equivalent formulations of the stochastic van der Pol equation (15.2)–(15.3) as perturbed trajectories of (15.1) under the influence of a random force with a normal distribution.

More precisely, $W^j = W^j(\tau)$ for $j \in \{1, 2\}$ are independent **Brownian motions**, and $\xi^j = \xi^j(\tau)$ are **white noise** processes, which formally may be viewed as $\dot{W}^j = \xi^j$. The formulation (15.2) is the standard mathematical notation, and $W(\tau)$ is a (continuous) stochastic process with $W(0) = 0$ and normally distributed independent increments $W(\eta) - W(\tau) \sim \mathcal{N}(0, \eta - \tau)$ for $0 \leq \tau \leq \eta$. The differential notation has to be interpreted as an integral equation (integrate both sides from 0 to some final time), which requires the notion of a stochastic integral; see also Section 15.10 for more detailed references. The formulation (15.3) is usually employed in physics and several other application areas, where ξ_τ is defined as a zero-mean delta-correlated process via $\mathbb{E}[\xi(\tau)] = 0$ and $\mathbb{E}[\xi(\tau)\xi(\eta)] = \delta(\tau - \eta)$, where $\delta(\cdot)$ denotes the δ -distribution.

Remark: The formal relation $\dot{W}(\tau) = \xi(\tau)$, or $dW = \xi(\tau)d\tau$, between Brownian motion and white noise can be made precise using the theory of generalized stochastic processes [Arn74]. This makes the two symbolic formulations (15.2)–(15.3) equivalent.

To build some intuition as to what dynamical phenomena may occur, we consider a direct numerical simulation via the Euler–Maruyama method for **stochastic differential equations (SDEs)**.

Remark: We shall not describe numerical methods for SDEs in this book. It will suffice for the purposes here to be able to generate **sample paths** $\tau \mapsto (x(\tau; \omega), y(\tau; \omega))$,

where ω indicates the noise dependence, i.e., to simulate the noise by a (pseudo)random number generator and combine it in a suitable way with classical ideas for solving ODEs numerically; see [Hig01] for an excellent introduction in which basic computer code is given so that one may start out with numerical experiments.

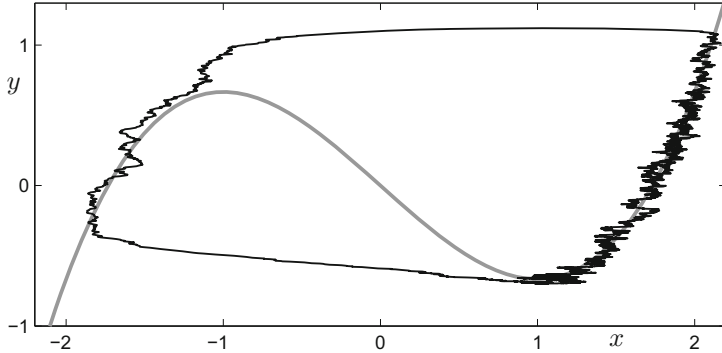


Figure 15.1: Single sample path (black) for equation (15.2) with parameter values $(\varepsilon, a, \sigma_1) = (0.05, 1.05, 0.1)$. The critical manifold C_0 (gray) is also shown. The path was started at $(x(0), y(0)) = (2, 2/3)$ and stopped at $\tau = 2400$.

Figure 15.1 shows one sample path for parameter values $(\varepsilon, a, \sigma_1) = (0.05, 1.05, 0.1)$. The figure also shows the critical manifold $C_0 = \{y = 1/3x^3 - x =: c(x)\}$. Observe that for $a = 1.05$, the deterministic system (15.1) has a stable steady state, say q , which is the only attractor. For the SDE version, Figure 15.1 shows a sample path that resembles a relaxation oscillation. The intuitive explanation is that the deterministic drift moves the path toward q , and since $q = (a, c(a))$ for $a = 1.05$ is close to the fold at $x = 1$, the noise is strong enough to kick the trajectory beyond the repelling part of the critical manifold $C_0^r = C_0 \cap \{-1 < x < 1\}$, after which it is attracted toward $C_0^{a-} = C_0 \cap \{x < -1\}$. ♦

The last example shows that new dynamical phenomena can occur for stochastic fast–slow systems. The next concept is slightly imprecise, but it provides a good term for distinguishing deterministic dynamics from stochastic effects.

Definition 15.1.2. If a stochastic dynamical system exhibits a feature not present in its deterministic limit (i.e., for zero noise), then we say that this feature is a **noise-induced effect**.

For the van der Pol equation (forced or unforced), many relevant noise-induced phenomena appear with buzzwords such as **stochastic resonance**, **coherence resonance**, and **noise-induced transitions**. Our goal in this chapter is to discuss some helpful techniques for analyzing these situations. Therefore, let us take a step back and consider the approaches that we could take to understand stochastic fast–slow systems.

The starting point is to fix a probability space $(\Omega, \mathcal{F}, \mathbb{P})$ and consider an N -dimensional **diffusion process** $z = z(t)$ associated with the SDE

$$dz = a(z) dt + \sigma A(z) dW, \quad (15.4)$$

where $a : \mathbb{R}^N \rightarrow \mathbb{R}^N$ is also called the **drift term**, $W = W(t)$ is a standard K -dimensional Brownian motion, $A = A(z) \in \mathbb{R}^{N \times K}$ is a matrix, and $\sigma \geq 0$ is the noise intensity parameter; we also refer to $\sigma A(z)$ as the **diffusion term**. The reader may think of $z = (x, y) \in \mathbb{R}^{m+n}$ with $N = n + m$, $\varepsilon t = \tau$, and $a = (f/\varepsilon, g)$ to stay inside the framework of fast–slow systems. We also note that (15.4) is understood as an integral equation

$$z(t) = z(0) + \int_0^t a(z(s)) ds + \sigma \int_0^t A(z(s)) dW(s), \quad (15.5)$$

where we shall make the assumption that stochastic integrals with respect to W , such as in (15.5), are always understood as **Itô integrals** [Pro05, Øks03]. As usual, the maps a, A are sufficiently smooth and are restricted via bounds to guarantee existence and pathwise uniqueness of solutions for SDEs. In this case, there is a continuous version for each path $t \mapsto z(t; \omega)$. The initial condition $z(0) = z_0$ is assumed to be deterministic.

Exercise 15.1.3. This exercise gives a heuristic derivation of **Itô’s formula** in the simplest case. Consider (15.4) for $z \in \mathbb{R}$ and let $v(t) := u(z(t), t)$. Show that

$$dv = \left[\frac{\partial u}{\partial t} + \frac{\partial u}{\partial z} a(z) + \frac{1}{2} \frac{\partial^2 u}{\partial z^2} A(z)^2 \right] dt + \frac{\partial u}{\partial z} A(z) dW \quad (15.6)$$

using the formal substitution formulas $(dt)(dt) = 0$, $(dW)(dt) = 0$, $(dt)(dW) = 0$, and $(dW)(dW) = dt$. Note that the second-order partial derivative with respect to z arises due to the noise term and makes (15.6) different from the result obtained by a standard chain rule. Furthermore, formulate a generalization to $z \in \mathbb{R}^N$ using $(dW^i)(dW^j) = \delta_{ij} dt$, where δ_{ij} is the **Kronecker delta**. \diamond

The notation $z(t; \omega)$ for the stochastic process indicates already the dependence on the time t and the realization of the noise ω . Hence, there are two approaches:

- (V1) Emphasize the sample path $t \mapsto z(t; \omega)$ for each given ω . This viewpoint focuses on an individual sample path and its properties, particularly bounds on its location.
- (V2) Emphasize the random variable $\omega \mapsto z(t; \omega)$ and its **probability distribution**, i.e., one focuses first on computing the **probability density** $p(z, t|z_0, 0)$, which describes the probability of being at position z at time t starting from $z(0) = z_0$ at time $t = 0$.

Of course, one may often translate results between the two approaches. We shall outline/recall some of the key techniques and components of each viewpoint.

- (V1) The focus for the sample paths approach lies in quantifying the time-dependent properties from a geometric viewpoint. Let \mathcal{D} be a bounded open subset in \mathbb{R}^N and fix $z(0) \in \mathcal{D}$. A typical case of interest arises when \mathcal{D} is positively invariant for the deterministic dynamics; for example, we could choose \mathcal{D} as a sufficiently small neighborhood of the attracting fixed point in Example 15.1.1. In the stochastic case, sample paths might leave \mathcal{D} with some probability, so that deterministically stable states in \mathcal{D} become **metastable**. A major problem is to determine the **first exit time**

$$t_{\mathcal{D}} = t_{\mathcal{D}}(\omega) = \inf \{t > 0 : z(t; \omega) \notin \mathcal{D}\}.$$

Metastability refers to the fact that $t_{\mathcal{D}}$ might be extremely large for certain domains; in this case, asking for the exit-time distribution is a typical question that can be answered by the theory of **large deviations**; see Sections 15.8 and 15.9. The overall viewpoint is that we are concerned with concentration results of sample paths. The goal is to compute how long a path stays inside a given domain.

- (V2) The **(infinitesimal) generator** of the diffusion process (15.4) (see Exercise 15.1.4) is given by

$$L := \sum_{i=1}^N a_i(z) \frac{\partial}{\partial z_i} + \frac{\sigma^2}{2} \sum_{i,j=1}^N \mathfrak{D}_{ij}(z) \frac{\partial^2}{\partial z_i \partial z_j}, \quad (15.7)$$

where $\mathfrak{D}_{ij}(z)$ are elements of the **diffusion matrix** $\mathfrak{D}(z) = A(z)A(z)^\top$. Consider the **transition probabilities** $p(x, t|y, s)$ of the diffusion of going from state y at time s to state x at time t . The function $u : (w, s) \mapsto p(z, t|w, s)$ satisfies **Kolmogorov's backward equation**

$$\frac{\partial u}{\partial s} = -Lu. \quad (15.8)$$

If we consider the map $v : (z, t) \mapsto p(z, t|w, s)$, then v satisfies **Kolmogorov's forward equation**, or **Fokker–Planck equation**,

$$\frac{\partial v}{\partial t} = L^*v, \quad (15.9)$$

where L^* denotes the adjoint operator to L . Therefore, information about the diffusion process can be obtained by considering the eigenvalues and eigenvectors of L . In particular, a spectral gap condition for the eigenvalues can be interpreted as a scale separation condition.

Exercise 15.1.4. Let $\phi \in C_b(\mathbb{R}^N, \mathbb{R})$ denote a bounded continuous function. Fix an initial condition $z_0 = z(0)$ for (15.4). Show that the linear operators

$$S(t)\phi := \mathbb{E}^{0, z_0}[\phi(z(t))] = \mathbb{E}[\phi(z(t)) | z(0) = z_0],$$

given by solving (15.4), define a continuous semiflow on $X = C_b(\mathbb{R}^N, \mathbb{R})$ (see Section 18.1). Prove that the **infinitesimal generator**

$$L\phi := \lim_{t \rightarrow 0^+} \frac{S(t)\phi - \phi}{t}$$

is indeed given by (15.7). \diamond

We shall begin with the viewpoint (V1) in the next section and pick up (V2) again in Sections 15.5 and 15.9; a third, more abstract, aspect will be considered in Section 15.6.

15.2 Fenichel Theory for SDEs

A natural first goal is to develop an analogue to Fenichel's theorem for stochastic systems. Our starting point is to modify a general fast-slow system

$$\begin{aligned} \frac{dx}{d\tau} &= \varepsilon \dot{x} = f(x, y), \\ \frac{dy}{d\tau} &= \dot{y} = g(x, y), \end{aligned} \tag{15.10}$$

where $(x, y) \in \mathbb{R}^m \times \mathbb{R}^n$. There are several choices for turning (15.10) into a stochastic differential equation (SDE). Similar to Example 15.1.1, one common choice is

$$\begin{aligned} dx &= \frac{1}{\varepsilon} f(x, y) d\tau + \frac{\sigma_f}{\sqrt{\varepsilon}} F(x, y) dW, \\ dy &= g(x, y) d\tau + \sigma_g G(x, y) dW, \end{aligned} \tag{15.11}$$

where $W = W(\tau) = (W^1(\tau), W^2(\tau), \dots, W^k(\tau))^\top$ is a k -dimensional vector of independent Brownian motions, $F : \mathbb{R}^{m+n} \rightarrow \mathbb{R}^{m \times k}$ and $G : \mathbb{R}^{m+n} \rightarrow \mathbb{R}^{n \times k}$ are matrix-valued maps, and $\sigma_f, \sigma_g \in \mathbb{R}$ control the noise level. We will always think of $\sigma_f = \sigma_f(\varepsilon)$ and $\sigma_g = \sigma_g(\varepsilon)$ as functions of ε . The scaling by $1/\sqrt{\varepsilon}$ is chosen because if $W(\tau)$ is a standard Brownian motion, then so is $\lambda^{-1/2}W(\lambda\tau)$ for every $\lambda > 0$, i.e., the two processes have the same distribution; this relation is also referred to as the **scaling law of Brownian motion**.

Exercise 15.2.1. Show that under a time rescaling $\tau = \varepsilon t$, the ratio of the scalar prefactors multiplying $F dW$ and $G dW$ remains invariant. \diamond

Remark: On an abstract level, one may also view (15.11) as a three-time-scale system. Indeed, using Brownian motion, we have the inherent assumption that there is a noise process fluctuating at a very fast temporal scale, and then there are the two scales of (x, y) ; see Example 15.5.1 for more details.

We impose several standard conditions that (15.11) has to satisfy.

- (C1) All maps f, g, F, G are sufficiently smooth on a domain $\mathcal{D} = \mathcal{D}_x \times \mathcal{D}_y \subset \mathbb{R}^{m+n}$; for example, $f, g \in C^2$ and $F, G \in C^1$ will usually suffice.
- (C2) The noise acting on the slow variable does not dominate the noise on the fast variable:

$$\rho(\varepsilon) := \frac{\sigma_g(\varepsilon)}{\sigma_f(\varepsilon)} \quad \text{is bounded above as } \varepsilon \rightarrow 0.$$

- (C3) We fix a compact normally hyperbolic attracting submanifold S_0 of the critical manifold $C_0 \subset \mathcal{D}$. Assume that S_0 and the associated slow manifold S_ε are given as graphs

$$\begin{aligned} S_0 &= \{(x, y) \in \mathcal{D} : x = h_0(y), y \in \mathcal{D}_y\}, \\ S_\varepsilon &= \{(x, y) \in \mathcal{D} : x = h_\varepsilon(y), y \in \mathcal{D}_y\}. \end{aligned}$$

We are going to need another assumption, (C4), that will be described below. The main strategy is to construct a suitable neighborhood $\mathcal{B}(s)$ for S_ε , where $s > 0$ will control the size of $\mathcal{B}(s)$. The analogue of Fenichel's theorem for the SDE (15.11) is going to provide us with bounds on the distribution of exit times from $\mathcal{B}(s)$. For the construction, it is helpful to rectify coordinates along the slow manifold and define

$$\xi = x - h_\varepsilon(y). \quad (15.12)$$

The variable $\xi = \xi(\tau)$ measures the deviation of the fast components $x = x(\tau)$ from the deterministic slow manifold. Applying Itô's formula (see (15.6) for the one-dimensional version and [Øks03, Pro05] for the general case used here) to (15.12) yields

$$\begin{aligned} d\xi &= dx - (\mathbf{D}_y h_\varepsilon)(y) dy + \mathcal{O}(\sigma_g^2) d\tau \\ &= \frac{1}{\varepsilon} (f(h_\varepsilon(y) + \xi, y) - \varepsilon(\mathbf{D}_y h_\varepsilon)(y)g(h_\varepsilon(y) + \xi, y) + \mathcal{O}(\varepsilon\sigma_g^2)) d\tau \quad (15.13) \\ &\quad + \frac{\sigma_f}{\sqrt{\varepsilon}} (F(h_\varepsilon(y) + \xi, y) - \rho\sqrt{\varepsilon}(\mathbf{D}_y h_\varepsilon)(y)G(h_\varepsilon(y) + \xi, y)) dW. \end{aligned}$$

We can consider the linear approximation of (15.12) in ξ , neglect the Itô term $\mathcal{O}(\varepsilon\sigma_g^2)$, and replace y by its deterministic version y^{det} to obtain

$$\begin{aligned} d\xi^0 &= \frac{1}{\varepsilon} A_\varepsilon(y^{\text{det}})\xi^0 d\tau + \frac{\sigma_f}{\sqrt{\varepsilon}} F_\varepsilon^0(y^{\text{det}}) dW, \\ dy^{\text{det}} &= g(h_\varepsilon(y^{\text{det}}), y^{\text{det}}) d\tau, \end{aligned} \quad (15.14)$$

where the two matrices A_ε and F_ε^0 are

$$\begin{aligned} A_\varepsilon(y) &= (\mathbf{D}_x f)(h_\varepsilon(y), y) - \varepsilon(\mathbf{D}_y h_\varepsilon)(y)(\mathbf{D}_x g)(h_\varepsilon(y), y), \\ F_\varepsilon^0(y) &= F(h_\varepsilon(y), y) - \rho\sqrt{\varepsilon}(\mathbf{D}_y h_\varepsilon)(y)G(h_\varepsilon(y), y). \end{aligned}$$

Observe that $A_0(y) = (\mathbf{D}_x f)(h_0(y), y)$ and $F_0^0(y) = F(h_0(y), y)$. To solve (15.14), one has to choose an initial condition. Suppose we start on the slow manifold of the deterministic system. Then we should choose $(\xi^0(0), y^{\text{det}}(0)) = (0, y^{\text{det}}(0))$. With this reasonable choice having been made, the solution of (15.14) is the Itô integral

$$\xi^0(\tau) = \frac{\sigma_f}{\sqrt{\varepsilon}} \int_0^\tau U(\tau, s) F_\varepsilon^0(y^{\text{det}}(s)) dW(s), \quad (15.15)$$

where $U(\tau, s)$ denotes the **principal solution** of the homogeneous linear system $\varepsilon\dot{\nu} = A_\varepsilon(y^{\text{det}}(\tau))\nu$. More precisely, this means that $\nu(\tau) = U(\tau, s_0)\nu(s_0)$; see

also Section 10.5. In fact, the fast variable (15.14) can be viewed as a nonautonomous **Ornstein–Uhlenbeck process**, which is solved in (15.15) using a variation of constants (or Duhamel’s principle). For a fixed time τ , it follows by properties of the Ornstein–Uhlenbeck process that $\xi^0(\tau)$ is a Gaussian random variable with mean zero and covariance matrix

$$\text{Cov}(\xi^0(\tau)) = \frac{\sigma_f^2}{\varepsilon} \int_0^\tau U(\tau, s) F_\varepsilon^0(y^{\det}(s)) F_\varepsilon^0(y^{\det}(s))^\top U(\tau, s)^\top ds.$$

This result is important but not unexpected. It is more crucial to note that $X(\tau) := \sigma_f^{-2} \text{Cov}(\xi^0(\tau))$ satisfies a fast–slow ODE given by

$$\begin{aligned} \varepsilon \dot{X} &= A_\varepsilon(y)X + XA_\varepsilon(y)^\top + F_\varepsilon^0(y)F_\varepsilon^0(y)^\top, \\ \dot{y} &= g(h_\varepsilon(y), y). \end{aligned} \quad (15.16)$$

Exercise 15.2.2. Verify by direct substitution that $X(\tau)$ satisfies (15.16). ◇

The system (15.16) has a critical manifold S_0^ξ given by solving the equation

$$A_0(y)X + XA_0(y)^\top + F_0^0(y)F_0^0(y)^\top = 0, \quad (15.17)$$

where we use the assumption (C2) for the limit $\varepsilon = 0$ and note that (15.17) is an algebraic **Lyapunov equation** for each fixed y . Unraveling the notation yields that (15.17) can be written as

$$(D_x f)(h_0(y), y)X + X(D_x f)(h_0(y), y)^\top + F(h_0(y), y)F(h_0(y), y)^\top = 0. \quad (15.18)$$

As in (C3), it is natural to view the critical manifold as a graph

$$S_0^\xi = \{(X, y) \in \mathcal{D} \subset \mathbb{R}^{m+n} : X = H_0(y), y \in \mathcal{D}_y\}.$$

The next lemma shows that S_0^ξ is normally hyperbolic and attracting.

Lemma 15.2.3 ([BG06, Bel60]). *Let A_1 and A_2 be square matrices of dimensions m with eigenvalues $\lambda_{1,1}, \dots, \lambda_{1,m}$ and $\lambda_{2,1}, \dots, \lambda_{2,m}$ respectively. Then the linear map $L : \mathbb{R}^{m \times m} \rightarrow \mathbb{R}^{m \times m}$ defined by*

$$L(X) = A_1X + XA_2$$

has m^2 eigenvalues given by $\{\lambda_{1,i} + \lambda_{2,j}\}$ for $i, j \in \{1, 2, \dots, m\}$.

Therefore, Fenichel theory provides us with a slow manifold

$$S_\varepsilon^\xi = \{(X, y) \in \mathcal{D} \subset \mathbb{R}^{m+n} : X = H_\varepsilon(y) = H_0(y) + \mathcal{O}(\varepsilon)\}. \quad (15.19)$$

Basically, S_ε^ξ is an attracting slow manifold for the covariance. Now we can state the last assumption, which expresses the nondegeneracy of the noise term.

(C4) The norms $\|H_\varepsilon(y)\|$ and $\|H_\varepsilon^{-1}(y)\|$ are uniformly bounded for $y \in \mathcal{D}_y$.

Finally, the neighborhood $\mathcal{B}(r)$ around the deterministic slow manifold is defined by

$$\mathcal{B}(r) := \{(x, y) \in \mathcal{D} : |[x - h_\varepsilon(y)] \cdot [H_\varepsilon^{-1}(y)(x - h_\varepsilon(y))]| < r^2\}.$$

The neighborhood $\mathcal{B}(r)$ is a union of **covariance ellipsoids** centered at S_ε with shape matrix $H_\varepsilon^{-1}(y)$. The stochastic effects are captured by adapting to the first nontrivial moment (here the covariance) of the deviation from the deterministic trajectory. The next example contains an illustration of $\mathcal{B}(r)$ for the case of a $(2, 1)$ -fast–slow system.

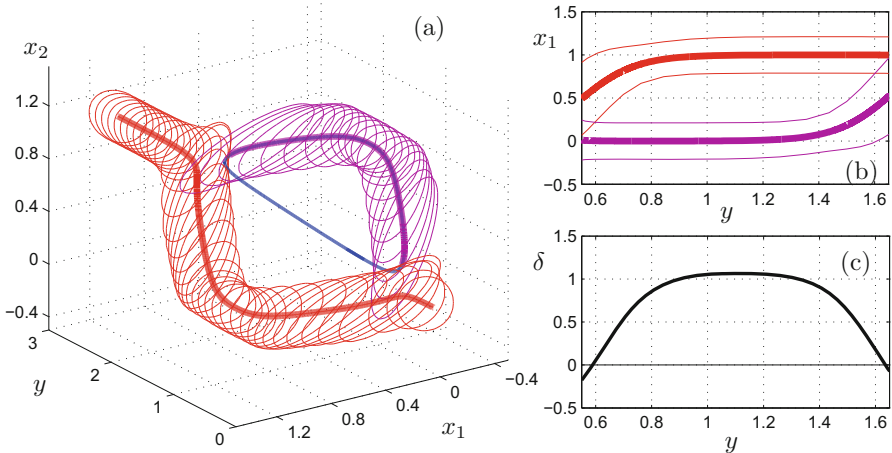


Figure 15.2: Numerical results for (15.20). The noise terms are given in (15.21). (a) The thick curves (red and violet) show the attracting parts of the critical manifold here. There are fold points on the isolated fast subsystem bifurcation curve (**isola**) from a stable node (violet, thick curve) to a saddle (blue, thin curve). We also show some of the covariance ellipsoids computed for the fixed slow variable y and embedded in (x_1, x_2, y) -coordinates; here we use $r = 1$ as the confidence parameter in the definition of $\mathcal{B}(r)$. (b) Calculation of the distance δ between the ellipsoids in the bistable regime. (c) Projection of (a) onto (y, x_1) where the x_1 maxima and minima of the ellipsoids have been connected to form tubes around the stable equilibrium branches.

Example 15.2.4. The following SDEs arise as a simplified model for competition between two neural populations x_1 and x_2 :

$$\begin{pmatrix} dx_1 \\ dx_2 \\ dy \end{pmatrix} = \begin{pmatrix} -x_1 + R(y - 1.1 x_2 - 0.35) \\ -x_2 + R(y - 1.1 x_1 - 0.375) \\ \varepsilon g(x, y) \end{pmatrix} dt + \sigma^2 F(x) dW_t, \quad (15.20)$$

where $R(u) := \frac{1}{1+\exp(-10(u-0.2))}$. Suppose we consider only the fast subsystem

in the singular limit $\varepsilon = 0$ and the noise term

$$\sigma^2 F(x^*) F(x^*)^\top = \sigma^2 \begin{pmatrix} 1 & 0.4 \\ 0.4 & 1 \end{pmatrix} \quad \text{for } \sigma = 0.3. \quad (15.21)$$

Figure 15.2 shows a computation of the one-dimensional critical manifold as well as the corresponding covariance ellipsoids at each fixed value of the slow variable. Note that the covariance ellipsoids grow as the two fold points are approached. The behavior of fast–slow SDEs near folds will be discussed in more detail in Sections 15.3 and 15.4. Furthermore, the scaling of the ellipsoid growth near fast subsystem bifurcation points will be discussed in Section 19.9. ♦

It turns out that employing covariance ellipsoids allows us to find good bounds for the first-exit problem. Define

$$\tau_{\mathcal{B}(r)} := \inf\{\tau > 0 : (x(\tau), y(\tau)) \notin \mathcal{B}(r)\}, \quad \tau_{\mathcal{D}_y} := \inf\{\tau > 0 : y(\tau) \notin \mathcal{D}_y\}.$$

The two first-exit times describe the two situations that can happen to a sample path: either we leave $\mathcal{B}(s)$, or we approach an outflow boundary of S_ε . As a notation for the next result we shall use $\mathbb{P}^{x_0, y_0}(\cdot)$, where the superscript indicates that the sample path under consideration has been started at $(x(0), y(0)) = (x_0, y_0)$.

Theorem 15.2.5 ([BG06, BG03]). *Suppose (C1)–(C4) hold and $\varepsilon > 0$ is sufficiently small. Then there exist constants $v_0, r_0, c, c_1, L > 0$ such that for all $0 < r \leq r_0$, $0 < v \leq v_0$, $\gamma \in (0, 1)$, and $\tau \geq 0$, the following hold:*

- *Upper bound: Let $x_0 = h_\varepsilon(y_0)$. Then*

$$\mathbb{P}^{x_0, y_0}(\tau_{\mathcal{B}(r)} < \min(\tau, \tau_{\mathcal{D}_y})) \leq K_\varepsilon^+(\tau) e^{-\kappa_+ r^2 / \sigma_f^2},$$

where $\kappa_+ = \gamma \left[1 - c_1 \left(r + v + n\varepsilon \rho^2 \sigma_f^2 / r^2 + e^{-c/\varepsilon} / (1 - \gamma) \right) \right]$ is uniform in time and the prefactor is

$$K_\varepsilon^+(\tau) = L \frac{1 + \tau^2}{v\varepsilon} \left[(1 - \gamma)^{-m} + e^{m/4} + e^{n/4} \right] \left(1 + \frac{\sigma_f^2}{r^2} \right).$$

- *Lower bound: There exists a time $\tau_0 > 0$ independent of ε such that for all $\tau > 0$, we have*

$$\mathbb{P}^{x_0, y_0}(\tau_{\mathcal{B}(r)} < \tau) \geq K_\varepsilon^-(\tau) e^{-\kappa_- r^2 / \sigma_f^2},$$

where $\kappa_- = 1 + c_1 (r + e^{c \min(\tau, \tau_0) / \varepsilon})$ is uniform in time for $\tau > \tau_0$, and the prefactor is

$$K_\varepsilon^-(\tau) = \frac{1}{L} \left[1 - \left(e^{m/4} + \frac{e^{n/4}}{v\varepsilon} \right) e^{-r^2 / (4\sigma_f^2)} \right].$$

It is instructive to understand Theorem 15.2.5 in more detail. Suppose we consider $\varepsilon \rightarrow 0$ with all other parameters fixed at $\mathcal{O}(1)$. Then we find that $K_\varepsilon^+(\tau) = \mathcal{O}(1/\varepsilon)$ and $\kappa_+ = \mathcal{O}(1)$; in this case, sample paths are expected to stay in $\mathcal{B}(r)$ with high probability for a long time that is slightly below an exponential time scale. Hence, roughly speaking, Theorem 15.2.5 says that sample paths are concentrated with high probability near attracting slow manifolds for $0 < \varepsilon \ll 1$ for quite long times. It is important to note that if some assumptions are dropped, such as the assumption (C2) that $\rho = \sigma_g/\sigma_f$ is bounded, or even longer time scales are considered, then different dynamical regimes arise, as discussed in Sections 15.8 and 15.9.

Exercise/Project 15.2.6. Use a numerical method to integrate the SDE (15.20) from Example 15.2.4 starting with an initial condition on C_0 . Describe what happens for different noise intensities. \diamond

The main idea to prove Theorem 15.2.5, as well as similar pathwise results, is to use a subdivision procedure for the time interval along a path. Consider a sample path $(x(\tau), y(\tau))$ with $(x(0), y(0)) \in S_\varepsilon \subset \mathcal{B}(r) \subset \mathcal{D}$ and $y(0) \in \mathcal{D}_y$. Let $T > 0$ denote a time such that the y -coordinates of the deterministic slow flow have not left \mathcal{D}_y , i.e., we look only for the event that the first-exit time of the fast variables x from $\mathcal{B}(r)$ has been reached. For a small time interval of length $\varepsilon_r > 0$, consider the probability

$$p_j := \mathbb{P}(\text{"the path has not left } \mathcal{B}(r) \text{ within time } j\varepsilon_r < \tau < (j+1)\varepsilon_r\text{"}).$$

Restarting the process on each time interval using the Markov property, one has $p_j \simeq p$. Suppose we can divide the total time the path needs to reach a certain point into N time steps of length ε_r . Then the probability of not leaving $\mathcal{B}(s)$ is

$$\begin{aligned} p^N &= e^{-N \log(1/p)} \\ \Rightarrow \mathbb{P}(\text{"the path has left } \mathcal{B}(r) \text{ within time } 0 < \tau < N\varepsilon_r\text{"}) &= 1 - e^{-N \log(1/p)}. \end{aligned}$$

It is nontrivial to make this idea precise, and the art is to choose the subdivision process correctly. If we assume that the subdivision step can be carried out, then it remains to estimate p on a given small subinterval. The main approximation using the covariance to define $\mathcal{B}(r)$ was made in equation (15.14), where the fast variables are given by

$$d\xi^0 = \frac{1}{\varepsilon} A_\varepsilon(y^{\det}) \xi^0 d\tau + \frac{\sigma_f}{\sqrt{\varepsilon}} F_\varepsilon^0(y^{\det}) dW,$$

but the full nonlinear system for $\xi = \xi(\tau)$ is given by

$$d\xi = \frac{1}{\varepsilon} [A_\varepsilon(y^{\det}) \xi + b(\xi, \eta, \tau)] d\tau + \frac{\sigma_f}{\sqrt{\varepsilon}} [F_\varepsilon^0(y^{\det}) + F^1(\xi, \eta, \tau)] dW, \quad (15.22)$$

where $\eta(\tau) = y^{\det}(\tau) + y(\tau)$ and the nonleading (nonlinear) terms have been denoted by b and F^1 . Applying Duhamel's principle to the full nonlinear system yields

$$\begin{aligned}\xi(\tau) = & U(\tau, 0)\xi(0) + \frac{1}{\varepsilon} \int_0^\tau U(\tau, s)b(\xi(s), \eta(s), s) \, ds \\ & + \frac{\sigma}{\sqrt{\varepsilon}} \int_0^\tau U(\tau, s)F_\varepsilon^0(y^{\text{det}}(s)) \, dW(s) \\ & + \frac{\sigma}{\sqrt{\varepsilon}} \int_0^\tau U(\tau, s)F^1(\xi(s), \eta(s), s) \, dW(s).\end{aligned}$$

The first term on the right-hand side is the linearized flow around S_0 , and we know from Fenichel's theorem that this term will dominate the second term coming from the deterministic nonlinear term b as long as we stay close to S_ε . The remaining two terms describe the fluctuations, which can be dealt with using methods from stochastic analysis. Abstractly, consider a stochastic process of the form

$$Z_t = \int_0^t \vartheta(\xi(s), \eta(s), s) \, dW(s),$$

which turns out to be a **martingale** [Dur10a] under rather mild assumptions. If we have growth bounds on the map $\vartheta(\xi, \eta, s)$, then we may prove a **Bernstein-type** inequality of the form

$$\mathbb{P} \left(\sup_{0 \leq s \leq \tau} \|Z_s\| > r \right) \leq K e^{-r^2 V(\tau)} \quad (15.23)$$

for a constant $K > 0$ and a function $V(\tau)$ that may be related to the bounds on $\vartheta(\xi, \eta, s)$; the proof of (15.23) employs **Doob's inequality** [BG06, Øks03] and is the main step in which stochastic analysis enters the proof. It remains to ask whether we may control the growth of $\vartheta(\xi, \eta, s)$ for our case. This is indeed true, since one may bound the leading-order term $U(\tau, s)F_\varepsilon^0(y^{\text{det}}(s))$. In fact, we know that there exists an attracting slow manifold S_0^ξ for the covariance from (15.19) that will yield the required control. For the technical details and more applications of this strategy, see Section 15.10.

15.3 Noisy Fold with Slow Drift

Consider the following simple $(1, 1)$ -fast–slow system:

$$\begin{aligned}\frac{dx}{dt} &= x' = f(x, y), \\ \frac{dy}{dt} &= y' = \varepsilon.\end{aligned} \quad (15.24)$$

In this case, the explicit solution for the slow variable is $y = y(0) + \varepsilon t$, so y can be viewed as a slowly drifting parameter. On changing to the slow time scale $\tau = \varepsilon t$, it follows that $y = y(0) + \tau$; since we can always translate the time variable, it suffices to consider $y(0) = 0$. Therefore, the fast variable evolves according to the nonautonomous system

$$\varepsilon \frac{dx}{d\tau} = \varepsilon \dot{x} = f(x, \tau) \quad \text{or} \quad x' = f(x, \varepsilon t). \quad (15.25)$$

Our goal is to understand a fold point of the critical manifold for (15.24) under the influence of noise; see also Sections 5.4, 7.4, 11.1 for the deterministic case. The SDE version of (15.25) that we consider is

$$dx = \frac{1}{\varepsilon} f(x, \tau) d\tau + \frac{\sigma}{\sqrt{\varepsilon}} F(x, \tau) dW, \quad (15.26)$$

where $W = W(\tau)$ is standard 1-dimensional Brownian motion. We assume the usual generic fold point conditions for the deterministic part

$$f(0, 0) = 0 = \frac{\partial f}{\partial x}(0, 0), \quad \frac{\partial f}{\partial \tau}(0, 0) < 0, \quad \frac{\partial^2 f}{\partial x^2}(0, 0) < 0.$$

For simplicity, we consider only the case with a noise intensity bounded from below, so that there exists $F_- > 0$ such that

$$F(x, \tau) \geq F_-, \quad \text{for all } (x, \tau) \in \mathbb{R} \times \mathbb{R}.$$

Using transformations as in Section 4.2 and Itô's formula, it can be shown, after a bit of work, that there exists a change of variables that reduces the analysis of the problem to the following standard form:

$$dx = \frac{1}{\varepsilon} (-\tau - x^2) d\tau + \frac{\sigma}{\sqrt{\varepsilon}} dW, \quad (15.27)$$

with $f(x, \tau) = -\tau - x^2$ and $F(x, \tau) = 1$. If x is positive and bounded away from zero, then sample paths stay close to $\tau = -x^2$, as described in Section 15.2. We fix a compact set near the fold point in which we work for the rest of this section:

$$\mathcal{D} := \{(x, \tau) \in \mathbb{R}^2 : |\tau| \leq T \text{ and } |x| \leq d\}.$$

The results of Section 15.2 can actually be improved. The main idea still is to construct an adapted neighborhood of the deterministic slow manifold $C_\varepsilon = \{(x, \tau) \in \mathbb{R}^2 : x = h_\varepsilon(\tau)\}$ and consider the leading linear term

$$a(\tau) := (\mathrm{D}_x f)(h_\varepsilon(\tau), \tau) = -2h_\varepsilon(\tau).$$

The asymptotic analysis of the deterministic slow manifold $x = h_\varepsilon(\tau)$ in Section 7.4 implies that the leading-order scaling of $a(\tau)$ is

$$a(\tau) = \mathcal{O}(-\max(|\tau|^{1/2}, \varepsilon^{1/3})) \quad \text{for } -T \leq \tau \leq \tau_1 = \mathcal{O}(\varepsilon^{2/3}).$$

Figure 15.3 illustrates this scaling property for the deterministic system. The trajectory shown in Figure 15.3 starts exponentially close to the attracting right-hand branch $C_0 \cap \{x > 0\}$ of the critical manifold and has leading-order approximation given by $h_0(\tau) = x$, where $h_0(\tau) = |\tau|^{1/2}$. Once it reaches the vicinity of the fold, the asymptotic scalings are $\mathcal{O}(\varepsilon^{1/3})$ in the x -direction and $\mathcal{O}(\varepsilon^{2/3})$ in the τ -direction (which is also the y -direction).

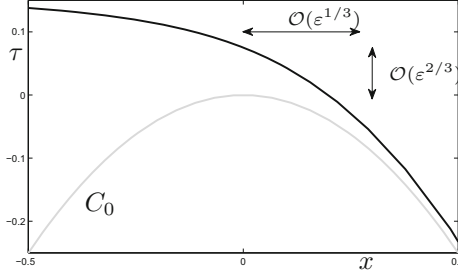


Figure 15.3: A single trajectory (black, slow manifold perturbation of right-hand stable branch) is shown for equation (15.24) with $f(x, y) = -y - x^2$ and $\varepsilon = 0.02$. It shows the behavior of the slow manifold near a fold of the critical manifold C_0 .

As in Section 15.2, we introduce an adapted neighborhood of the deterministic slow manifold

$$\mathcal{B}(r) := \{(x, \tau) \in \mathcal{D} : -T \leq \tau \leq \tau_1, |x - h_\varepsilon(\tau)| \leq r\sqrt{\varsigma(\tau)}\},$$

where $\varsigma(\tau)$ is again related to the variance of the linearization of (15.27) and has the explicit formula

$$\varsigma(\tau) = \varsigma(-T) \exp\left(\frac{2\alpha(\tau, -T)}{\varepsilon}\right) + \frac{1}{\varepsilon} \int_{-T}^{\tau} \exp\left(\frac{2\alpha(\tau, s)}{\varepsilon}\right) ds, \quad (15.28)$$

where $\alpha(\tau, s) := \int_s^\tau a(v) dv$ and $\varsigma(-T) = 1/(2|a(-T)|) + \mathcal{O}(\varepsilon)$. The formula (15.28) is basically just the solution of an inhomogeneous time-dependent linear system, as already discussed in Section 15.2. We need a few results in order to understand the asymptotics of $\varsigma(\tau)$.

Exercise/Project 15.3.1. (a) Show that $\varsigma(\tau) = 1/(2|a(\tau)|) + \mathcal{O}(\varepsilon)$ for negative τ bounded away from 0 .

(b) Prove the following integral asymptotics using **Laplace's method** [BO99, Mil06]. Fix constants $y_0 < 0$ and $\varsigma_0, c, p, q > 0$. Then the function

$$\varsigma(y, \varepsilon) = e^{c|y|^{p+1}/\varepsilon} \left(\varepsilon \varsigma_0 e^{-c|y_0|^{p+1}/\varepsilon} + \int_{y_0}^y |s|^{q+1} e^{-c|s|^{p+1}/\varepsilon} ds \right)$$

has the following asymptotics as $\varepsilon \rightarrow 0$:

$$\varsigma(y, \varepsilon) \sim \begin{cases} \varepsilon|y|^{q-p-1} & \text{for } y_0 \leq y \leq -\varepsilon^{1/(p+1)} \\ \varepsilon^{q/(p+1)} & \text{for } -\varepsilon^{1/(p+1)} \leq y \leq 0 \end{cases}$$

(c) Using (b) and integration by parts, verify that for some positive constants c_1, c_2 ,

$$\begin{aligned} \varsigma(\tau) &\sim \frac{1}{2|a(\tau)|} + \frac{\varepsilon}{\tau^2} & \text{for } T \leq -\tau \leq -c_0\varepsilon^{2/3}, \\ \varsigma(\tau) &\sim \varepsilon^{-1/3} & \text{for } -c_0\varepsilon^{2/3} \leq \tau \leq \tau_1 = c_1\varepsilon^{2/3}. \end{aligned}$$

The results (a)–(c) already provide the key estimates for obtaining exponential bounds on the escape probabilities from $\mathcal{B}(r)$. \diamond

From Exercise 15.3.1, we conclude the following key relation:

$$\varsigma(\tau) \sim \frac{1}{\max(|t|^{1/2}, \varepsilon^{1/3})} \sim \frac{1}{|a(\tau)|} \quad (15.29)$$

for all $\tau \in [-T, \tau_1]$ as $\varepsilon \rightarrow 0$. Therefore, the neighborhood $\mathcal{B}(r)$ grows as τ approaches the bifurcation value 0 and remains of constant order $\mathcal{O}(r/\sqrt{\varepsilon^{1/3}}) = \mathcal{O}(r/\varepsilon^{1/6})$ near $\tau = 0$. We also define

$$\hat{\varsigma}(\tau) := \sup_{-T \leq u \leq \tau} \varsigma(u).$$

Note that $\hat{\varsigma}(\tau) \sim \varsigma(\tau)$ for $\tau \leq \tau_1$. The next result is an improvement of Theorem 15.2.5 for the one-dimensional situation with a slow drift; it is rather technical, but we are going to sort out the detailed asymptotics after stating the result. It describes the initial attracting phase near a fold point.

Theorem 15.3.2 ([BG06]). *Let $\tau_0 \in [-T, 0)$ be fixed and set $x_0 := h_\varepsilon(\tau_0)$. Then there exist constants $r_0, v_0, c, \tilde{c} > 0$ such that for all $r \leq r_0 \hat{\varsigma}(\tau)^{-3/2}$ and $\tau_0 \leq \tau \leq \tau_1 = \mathcal{O}(\varepsilon^{2/3})$ satisfying*

$$v(r/\sigma, \varepsilon) := \frac{\sigma}{r} + \frac{e^{-cr^2/\sigma^2}}{\varepsilon} \leq r_0, \quad (15.30)$$

the following probability estimate for the first-exit time from $\mathcal{B}(r)$ holds:

$$C_{r/\sigma}(\tau, \varepsilon) e^{-\kappa_- r^2/(2\sigma^2)} \leq \mathbb{P}^{\tau_0, x_0}(\tau_{\mathcal{B}(r)} < \tau) \leq C_{r/\sigma}(\tau, \varepsilon) e^{-\kappa_+ r^2/(2\sigma^2)},$$

where the exponents are $\kappa_\pm = \mp \tilde{c} r \hat{\varsigma}(\tau)^{3/2}$. The prefactor $C_{r/\sigma}(\tau, \varepsilon)$ satisfies

$$C_{r/\sigma}(\tau, \varepsilon) = K \left[1 + \mathcal{O} \left(\frac{\varepsilon (|\log \varepsilon| + \log(1+r/\sigma))}{|\alpha(\tau, \tau_0)|} + v(r/\sigma, \varepsilon) + r \hat{\varsigma}(\tau)^{3/2} \right) \right],$$

where $K = \sqrt{\frac{2}{\pi}} \frac{|\alpha(\tau, \tau_0)| r}{\varepsilon \sigma}$.

Theorem 15.3.2 is very precise with all detailed constants, but it is now a bit of work to understand what the important consequences are. One assumption of the theorem is $r \sim \hat{\varsigma}(\tau)^{-3/2}$. Since r_0 has to exist as a bound, we must also have from (15.30) that

$$\hat{\varsigma}(\tau)^{3/2} \ll \frac{1}{\sigma}.$$

In this case, we see that $r \sim \sigma$, and so paths are concentrated in a neighborhood of the deterministic slow manifold of size

$$\sigma \sqrt{\varsigma(\tau)} \sim \frac{\sigma}{\max(|\tau|^{1/4}, \varepsilon^{1/6})}.$$

We also know from the previous discussion that $\sqrt{\varsigma(\tau)} \sim 1/|a(\tau)|$ and $a(\tau) \sim -(\max(|\tau|^{1/2}, \varepsilon^{1/3}))$. Therefore, two cases must be considered:

- *Case 1, Weak Noise:* $\sigma < \sigma_c = \sqrt{\varepsilon}$. In this case, trajectories behave essentially deterministically. Theorem 15.3.2 can be applied up to a time $\tau_1 = \mathcal{O}(\varepsilon^{2/3})$, and the spreading of paths reaches order $\sigma/\varepsilon^{1/6}$; see Figure 15.4(a).
- *Case 2, Strong Noise:* $\sigma \geq \sigma_c = \sqrt{\varepsilon}$. Theorem 15.3.2 applies only up to a time $-\sigma^{4/3}$ when the paths have spread to order $\sigma^{2/3}$. Hence, a sample path can reach the τ -axis with appreciable probability and jump across the repelling part of the slow manifold before it reaches the fold region; see Figure 15.4(b).

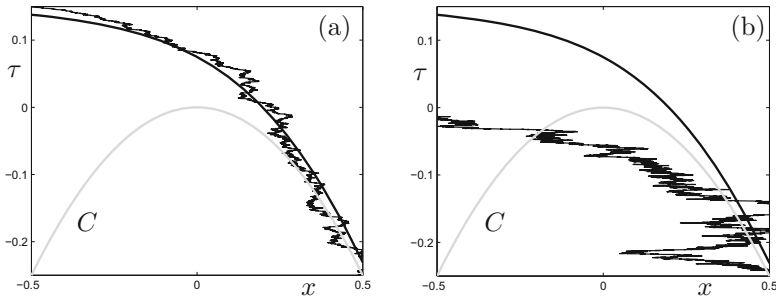


Figure 15.4: Illustration of weak and strong noise regimes near a fold. Computations are for equation (15.27) with $\varepsilon = 0.02$. (a) Weak noise with $\sigma = 0.05 < \sqrt{\varepsilon} \approx 0.1414$; the sample path tracks the deterministic trajectory (i.e., the slow manifold of the right-hand branch and its extension) very well. (b) Strong noise regime with $\sigma = 0.2$; the sample path jumps and reaches the τ -axis well before the deterministic solution passes by the fold.

Both noise regimes can be analyzed, and estimates on the relevant probabilities can be derived. We begin with the weak noise regime $\sigma \ll \sqrt{\varepsilon}$. Recall that we work in a fixed compact set

$$\mathcal{D} = \{(x, \tau) \in \mathbb{R}^2 : |\tau| \leq T \text{ and } |x| \leq d\}$$

under the assumption that $d = \mathcal{O}(1)$ as $\varepsilon \rightarrow 0$. Then we know already that the deterministic solution will reach $x = -d$ at a time $\tau_1 = \mathcal{O}(\varepsilon^{2/3})$; see Section 7.4. For weak noise, the stochastic system has sample paths that will essentially behave like deterministic solutions.

Theorem 15.3.3 ([BG06]). *The probability that a sample path has not reached $x = -d$ at time τ becomes “small” as soon as*

$$\tau - \tau_1 \gg \varepsilon^{2/3} |\log \varepsilon|,$$

i.e., shortly after the deterministic solution, most sample paths will reach the boundary of \mathcal{D} .

As in Theorem 15.3.2, one may make ‘‘small’’ precise with exponential-time escape probabilities from $\mathcal{B}(r)$. Another interesting case is the strong noise regime. Preferably, we want an estimate on the probability that a sample path has jumped across the repelling branch of the slow manifold before the saddle-node bifurcation. The next result summarizes several detailed estimates in a simple statement.

Theorem 15.3.4 ([BG06]). *The probability that a sample path crosses the repelling slow manifold and reaches $x = -d$ before the saddle-node bifurcation is*

$$1 - \mathcal{O}\left(e^{-\kappa \max\left(\frac{\sigma^2}{\varepsilon |\log \sigma|}, \frac{1}{\sigma^{4/3}}\right)}\right)$$

for some constant $\kappa > 0$ of order $\mathcal{O}(1)$. In particular, this probability is close to 1 as soon as $\sigma \gg \sqrt{\varepsilon |\log \sigma|}$.

The main idea for proving Theorems 15.3.3–15.3.4 is use a similar subdivision procedure as for Theorem 15.3.2 sketched in Section 15.2. We also remark that the methods developed here can be extended to explain the noise-induced phenomenon we observed in Example 15.1.1; see Section 15.10.

15.4 Direct Asymptotics

Instead of pathwise analysis, one may also use asymptotic techniques. The most classical use of asymptotic expansions for SDEs occurs for the case of small noise

$$dz = a(z) d\tau + \sigma A(z) dW, \quad (15.31)$$

where $W = W(\tau)$ is Brownian motion, $0 < \sigma \ll 1$ controls the noise level, and a, A are assumed to be sufficiently smooth. To find an asymptotic solution to (15.31), one makes the usual ansatz

$$x(\tau) = x_0(\tau) + \sigma x_1(\tau) + \sigma^2 x_2(\tau) + \dots \quad (15.32)$$

and expands a and A as asymptotic series in σ . In the theory of **small noise expansions**, one faces similar issues as asymptotic expansions for singularly perturbed ODEs; for example, the resulting series will often not converge. For a fast–slow system, we set $z = (x, y)^\top$, $a = (\frac{1}{\varepsilon} f, g)^\top$, $A = (\frac{\sigma}{\sqrt{\varepsilon}} F, G)^\top$ and consider the SDE

$$\begin{aligned} dx &= \frac{1}{\varepsilon} f(x, y) d\tau + \frac{\sigma_f(\varepsilon)}{\sqrt{\varepsilon}} F(x, y) dW^1, \\ dy &= g(x, y) d\tau + \sigma_g(\varepsilon) G(x, y) dW^2, \end{aligned}$$

for $(x, y) \in \mathbb{R}^2$; see Section 15.2 for more background. We also define $\sigma := \sqrt{\sigma_f^2 + \sigma_g^2}$ as the overall **noise level**. The problem is that no matter what scaling we choose for a small noise, we are always facing a limit that involves

$$(\sigma, \varepsilon) \rightarrow (0, 0),$$

i.e., a double limit. We encountered this problem earlier, in Section 15.3, for the generic fold point, where $\sigma \ll \sqrt{\varepsilon}$ and $\sigma \gg \sqrt{\varepsilon}$ lead to two dynamically different regimes. However, many other asymptotic functional relationships between the two singular quantities σ and ε arise in different problems. Formal asymptotic methods can often be used to determine the different scaling relationships that are relevant for $(\sigma, \varepsilon) \rightarrow (0, 0)$. We shall illustrate this in an example. Consider the following stochastic version of van der Pol's equation with constant forcing:

$$\begin{aligned} dx &= \frac{1}{\varepsilon} (x - \frac{1}{3}x^3 - y) d\tau + \frac{\sigma_f}{\sqrt{\varepsilon}} dW^1, \\ dy &= (x + a) d\tau + \sigma_g dW^2, \end{aligned} \quad (15.33)$$

where $W^1 = W^1(\tau)$ and $W^2 = W^2(\tau)$ are independent Brownian motions and $(\varepsilon, \sigma_f, \sigma_g)$ are parameters. We assume that we are dealing with a small noise limit

$$0 < \sigma = \sqrt{\sigma_f^2 + \sigma_g^2} \ll 1.$$

The deterministic dynamics of (15.33) for $\sigma = 0$ can be understood with the tools we have developed already in this book. The critical manifold is

$$C_0 = \left\{ (x, y) \in \mathbb{R}^2 : y = x - \frac{1}{3}x^3 \right\},$$

which is divided by two fold points at $(\pm 1, \pm 2/3)$ into a repelling branch $C_0^r = C_0 \cap \{-1 < x < 1\}$ and two attracting branches $C_0^{a,-} = C_0 \cap \{x < 1\}$ and $C_0^{a,+} = C_0 \cap \{x > 1\}$. Supercritical singular Hopf bifurcations occur when the equilibrium point at $(x_0, y_0) = (-a, -a + 1/3a^3)$ passes through the fold points

$$a_{\text{Hopf}} = \mp 1 + \mathcal{O}(\varepsilon).$$

Exercise 15.4.1. Verify the statements about the deterministic version ($\sigma = 0$) of (15.33); the relevant methods are found in Sections 8.2 and 8.3. Furthermore, show that the deterministic version has a symmetry that interchanges the fold points. \diamond

We shall focus on the case $a_{H1} = 1 + \mathcal{O}(\varepsilon)$ when the equilibrium is near the local minimum of C_0 at $x = -1$. We know that before the Hopf bifurcation for $a > a_{H1}$, there is a stable equilibrium point $(x^*, y^*) \in C_0^{a,-}$. After the bifurcation, a canard explosion to relaxation oscillations occurs. The goal is to understand the formal asymptotics for the stochastic case (15.33). Suppose we start with the standard scaling transformation that moves (x^*, y^*, a_{H1}) to the origin and provides a blowup near this point:

$$\begin{aligned} X &= \varepsilon^{-1/2}(x - x^*), & Y &= \varepsilon^{-1}(y - y^*), \\ t &= \varepsilon^{-1/2}\tau, & A &= \varepsilon^{-1}(1 - a). \end{aligned} \quad (15.34)$$

The scaling calculation of (15.33) is rather simple, since (15.34) is affine and therefore the second-order term in Itô's formula vanishes (i.e., ordinary calculus applies). For example, we get

$$\varepsilon dY = dy = (\varepsilon^{1/2}X + x^* + a)\varepsilon^{1/2} dt + \sigma_g dW^2(\varepsilon^{1/2}t).$$

Since $x^* = -a$, by the scaling law of Brownian motion we obtain

$$dY = X dt + \frac{\sigma_g}{\varepsilon^{3/4}} dW^2(t).$$

After a bit of algebraic manipulation, it follows that

$$\begin{aligned} dX &= \left(X^2 - Y + \sqrt{\varepsilon} \left(2AX - \frac{1}{3}X^3 \right) - \varepsilon AX^2 - \varepsilon^{3/2} A^2 X \right) dt + \frac{\sigma_f}{\varepsilon^{3/4}} dW^1(t), \\ dY &= X dt + \frac{\sigma_g}{\varepsilon^{3/4}} dW^2(t). \end{aligned}$$

Formally disregarding all ε -dependent terms of order higher than $\mathcal{O}(\sqrt{\varepsilon})$ yields

$$\begin{aligned} dX &= \left(X^2 - Y + \sqrt{\varepsilon} \left(2AX - \frac{1}{3}X^3 \right) \right) dt + \frac{\sigma_f}{\varepsilon^{3/4}} dW^1(t), \\ dY &= X dt + \frac{\sigma_g}{\varepsilon^{3/4}} dW^2(t). \end{aligned} \quad (15.35)$$

The limit $\varepsilon \rightarrow 0$, $\varepsilon^{-3/4}\sigma_{f,g} \rightarrow 0$ leads to the leading-order approximation by a familiar planar ODE:

$$\begin{aligned} \frac{d\bar{X}}{dt} &= \bar{X}^2 - \bar{Y}, \\ \frac{d\bar{Y}}{dt} &= \bar{X}. \end{aligned} \quad (15.36)$$

We know from Proposition 8.1.9 that (15.36) admits a first integral

$$H(X, Y) = e^{-2Y} (1 + 2Y - 2X^2),$$

since $(d/dt)H(\bar{X}, \bar{Y}) = 0$. Therefore, level curves of H are solution curves of (15.36). For $0 < H < 1$, all levels curves of H are closed circles giving periodic orbits of (15.36); cf. Figure 13.14. The behavior of trajectories is split into two classes by the separatrix

$$H(\bar{X}, \bar{Y}) = 0 \quad \text{i.e.,} \quad \bar{Y} = \bar{X}^2 - \frac{1}{2},$$

so that $H(\bar{X}, \bar{Y}) = 1$ corresponds to the equilibrium point $(\bar{X}, \bar{Y}) = (0, 0)$. For $0 < H < 1$, all trajectories of (15.36) are periodic orbits located above the separatrix, and for $H < 0$, trajectories are unbounded, flowing from $\bar{X} = -\infty$ to $\bar{X} = +\infty$ below the separatrix; cf. Figure 13.14. The key idea is that instead of aiming for a full description of the dynamics, we restrict ourselves to the change in H . Indeed, for $0 < \varepsilon \ll 1$ and $0 < \varepsilon^{-3/4}\sigma_{f,g} \ll 1$, we observe from (15.35) that H will be slowly varying. Applying Itô's formula to $H(X, Y)$ yields

$$\begin{aligned} dH &= -2\varepsilon^{1/2}e^{-2Y} \left[X^2 \left(4A - \frac{2}{3}X^2 \right) + \varepsilon^{-2} \left(\sigma_f^2 + \sigma_g^2(2X^2 - 2Y + 1) \right) \right] dt, \\ &\quad + 4\varepsilon^{-3/4}e^{-2Y} \sqrt{\sigma_f^2 X^2 + \sigma_g^2(X^2 - Y)^2} dW(t) + \dots, \end{aligned}$$

where we have omitted some higher-order terms indicated by \dots . Denote the leading-order approximation to H by \bar{H} and observe that for $0 < H < 1$, we could try to average over the slowly varying H , since it is periodic to lowest order (see Section 9.6). This averaging procedure over one period $T = T(\bar{H})$ yields the averaged system

$$d\bar{H} = b(\bar{H}) dt + c(\bar{H}) dW(t), \quad (15.37)$$

with drift and diffusion coefficients given by

$$b = -\frac{2\varepsilon^{1/2}}{T} \int_0^T e^{-2\bar{Y}} \left[\bar{X}^2 \left(4A - \frac{2}{3}\bar{X}^2 \right) + \varepsilon^{-2} (\sigma_f^2 + \sigma_g^2(2\bar{X}^2 - 2\bar{Y} + 1)) \right] dt,$$

$$c^2 = \frac{16\varepsilon^{-3/2}}{T} \int_0^T e^{-4\bar{Y}} (\sigma_f^2 \bar{X}^2 + \sigma_g^2(\bar{X}^2 - \bar{Y})^2) dt.$$

The SDE (15.37) describes the dynamics of small oscillations near the equilibrium very well. Let us look at the period $T = T(\bar{H})$ introduced above more explicitly. From (15.36), we see, by just separating variables $dt = 1/\bar{X}d\bar{Y}$, that the period is given by

$$T = 2 \int_{Y_{\min}(\bar{H})}^{Y_{\max}(\bar{H})} \frac{1}{|\bar{X}|} d\bar{Y}, \quad \text{where } \bar{X} = \pm \sqrt{\frac{1 + 2\bar{Y} - \bar{H}e^{2\bar{Y}}}{2}}. \quad (15.38)$$

If we are interested in escapes from the region of small periodic orbits near the equilibrium point, we must focus on $0 < \bar{H} \ll 1$, so that orbits are near the separatrix, and we must choose initial conditions such that orbits start for $\bar{H} > 0$. After a bit of calculation, we obtain from (15.38) that

$$T \sim 4\sqrt{\ln \bar{H}^{-1/2}} \quad \text{as } \bar{H} \rightarrow 0. \quad (15.39)$$

Note that T increases only very slowly as $\bar{H} \rightarrow 0$, and therefore, we are sometimes going to make the ad hoc assumption that T is constant.

Exercise/Project 15.4.2. Justify (15.39) on the level of formal asymptotics. ◇

We also know that trajectories will spend most of their time near the separatrix $\bar{Y} = \bar{X}^2 - \frac{1}{2}$, which, in conjunction with (15.39), $T \gg 1$, and $0 < \bar{H} \ll 1$, provides more explicit formulas for the drift and diffusion coefficients

$$b \sim \sqrt{\frac{\pi e^2}{2\varepsilon^3 \ln \bar{H}^{-1/2}}} (\varepsilon^2(A^* - A) - \sigma_f^2 - 2\sigma_g^2),$$

$$c^2 \sim \sqrt{\frac{\pi e^4}{4\varepsilon^3 \ln \bar{H}^{-1/2}}} (\sigma_f^2 + 2\sigma_g^2),$$

where $A^* = \frac{1}{8}$ turns out to be the coefficient that determines the $\mathcal{O}(\varepsilon)$ -approximation to the parameter value at which the maximal canard is generated near the deterministic fold, i.e., the value for the canard explosion is displaced by magnitude $\varepsilon/8 + \mathcal{O}(\varepsilon^{3/2})$ from $a = 1$; see also Sections 8.2 and 8.3.

The next important trick, which we learned about in Section 15.2, is to consider a sequence of times $t_n = nT$ splitting the dynamics up into n discrete intervals. Here we assume that T is constant, so that the t_n are equally spaced. The next goal is to estimate the probability density $p_n(H)$ that a trajectory

remains in the vicinity of the fixed point so that $H(t_n) > 0$ is above the separatrix after n turns around the fixed point. Note that this means that we are dealing with a discretized version of (15.4). As long as we are above $H = 0$ and $H \ll 1$, the averaging procedure works, and the dynamics of H are asymptotically given by a Gaussian random variable with mean bT and diffusion c^2T . From this, one can actually write down an asymptotic formula for $p_n(\bar{H})$; see [MVE08] for details. Let r_n denote the probability that the trajectory escapes during the n th cycle. Then we have

$$r_n \sim \int_{-\infty}^0 p_n(\bar{H}) d\bar{H},$$

since everything that happens for $\bar{H} < 0$ should be counted as an escape. The total probability r for escape after any number of cycles is then simply given by summation:

$$r = \sum_{n=1}^{\infty} r_n.$$

It can be shown that r is not necessarily equal to 1. Further formal asymptotic analysis of r reveals several scaling regimes for the parameters $\sigma_{f,g} \rightarrow 0$ and $\varepsilon \rightarrow 0$; see Section 15.10 for various different approaches to this problem.

The three important messages from the previous analysis are (I) formal asymptotic methods can be used to derive scaling laws quite quickly; (II) the deterministic asymptotic analysis techniques of fast–slow systems can often be reused in a probabilistic context; and (III) estimates of probabilities are often easier to obtain when the time and phase space are suitably subdivided.

15.5 Stochastic Reduction

So far, we have not considered how to construct a stochastic slow flow on a stochastic critical manifold. We begin by illustrating the problem with a famous example from probability theory.

Example 15.5.1. The first mathematical foundation of Brownian motion was developed by Einstein [Ein05] in 1905. A few years later, Langevin [Lan08] proposed another approach to the theory. He considered a (spherical) particle with position $y(\tau) \in \mathbb{R}$ and velocity $v(\tau) \in \mathbb{R}$ governed by the following model:

$$\begin{aligned} \frac{dy}{d\tau} &= v, \\ m \frac{dv}{d\tau} &= -\beta v + \sqrt{2k\beta T} \xi(\tau), \end{aligned} \tag{15.40}$$

where m is the mass of the particle, T is the surrounding temperature, k is Boltzmann's constant, and β incorporates viscosity and particle diameter. Equation (15.40) is now referred to as the **Langevin equation**. The first equation states that velocity is the derivative of position, and the second is just Newton's law with an additional $\xi(\tau)$ -term. Langevin modeled the collisions with other

particles via the function $\xi(\tau)$, which represents a rapidly varying noise term with zero mean value. Langevin's equation can also be motivated by the original description of the botanist Brown [Bro28], who observed the erratic movement of pollen grains in a liquid. As already indicated in Example 15.1.1, it is possible to make the mathematical concepts precise by constructing Brownian motion $W(\tau)$ with the intuition that

$$\int_0^\tau \xi(s) \, ds = W(\tau) \quad \text{or} \quad dW(\tau) = \xi(\tau) \, d\tau.$$

There is also a very nice formal fast–slow systems derivation for this construction. Let us assume that the mass of the particle is very small. Setting $0 < \varepsilon := m \ll 1$, relabeling $v = x$, and defining $\sigma = \sqrt{2k\beta T}/\beta$, we transform (15.40) to

$$\begin{aligned} \varepsilon \frac{dx}{d\tau} &= -\beta x + \sigma \beta \xi(\tau), \\ \frac{dy}{d\tau} &= x. \end{aligned} \tag{15.41}$$

Clearly, the differential equation (15.41) looks like a normal fast–slow system apart from the—as yet undefined—noise $\xi(\tau)$. Setting $\varepsilon = 0$ immediately leads to a critical manifold

$$C_0 = \{(x, y) : x = \sigma \xi(\tau)\}.$$

Substituting $x = \sigma \xi(\tau)$ into the equation for the slow variable in (15.41) gives the slow subsystem

$$\dot{y} = \frac{dy}{d\tau} = \sigma \xi(\tau) \quad \leftrightarrow \quad dy = \sigma \xi(\tau) \, d\tau = \sigma \, dW.$$

Hence, the evolution of $y(\tau)$ in the singular limit is given by a Brownian motion with noise level σ . It is quite intriguing to think about the purely formal interpretation we have given, which immediately reveals that there is a multiple time scale structure hidden in the Brownian motion W . ♦

The open question remains how we can put the ad hoc approach presented in Example 15.5.1 into a more systematic reduction approach. Several different ideas could be employed such as the pathwise approach from Sections 15.2–15.4. Here we are going to outline a method that uses the Fokker–Planck equation, i.e., the viewpoint (V2) outlined in Section 15.1, and illustrate a formal reduction method by an example. Consider the fast–slow SDE

$$\begin{aligned} dx &= -\frac{x}{\varepsilon} \, d\tau + \frac{\sigma}{\sqrt{\varepsilon}} \, dW, \\ dy &= (x - y) \, d\tau, \end{aligned} \tag{15.42}$$

where $\sigma > 0$ is the noise level and $W = W(\tau)$ is a standard Brownian motion. The scaling of the noise term by $1/\sqrt{\varepsilon}$ is chosen for convenience, and usually, we also assume that $\sigma = \sigma(\varepsilon)$ depends on the time scale separation in some form; see also Section 15.2. The deterministic critical manifold $C_0 = \{x = 0\}$ of (15.42) is attracting, so one would like to reduce the equation to a stochastic slow subsystem.

Recall from Section 15.1 that there is a general correspondence between an SDE $dz = a(z)d\tau + A(z)dW$ and the Fokker–Planck equation

$$\frac{\partial p}{\partial \tau} = - \sum_{i=1}^n \frac{\partial}{\partial z_i} (a_i(z)p) + \frac{\sigma^2}{2} \sum_{i,j=1}^n \frac{\partial^2}{\partial z_i \partial z_j} (\mathfrak{D}_{ij}(z)p), \quad \mathfrak{D}(z) = A(z)A(z)^\top,$$

where $p = p(z, \tau | z_0, \tau_0)$ is the transition probability density from $z(\tau_0) = z_0$ to $z(\tau)$. Therefore, the Fokker–Planck equation for (15.42) is given by

$$\frac{\partial p}{\partial \tau} = - \frac{\partial}{\partial x} \left(\frac{x}{\varepsilon} p \right) - \frac{\partial}{\partial y} ((x - y)p) + \frac{\sigma^2}{2\varepsilon} \frac{\partial^2 p}{\partial x^2}. \quad (15.43)$$

It is tempting simply to multiply (15.43) by ε and then consider $\varepsilon \rightarrow 0$, but the resulting Fokker–Planck equation is degenerate and just recovers the deterministic critical manifold. To take the noise term into account, we have to do some additional work. The aim is derive a Fokker–Planck equation for

$$\hat{p} = \hat{p}(y, t) := \int_{\mathbb{R}} p(x, y, t) dx,$$

i.e., for the marginal density of the slow variable y with the fast variable x eliminated. Rescaling $y \mapsto \sqrt{\varepsilon}y$ and regrouping the terms in (15.43) yields

$$\frac{\partial p}{\partial \tau} = \underbrace{\frac{1}{\varepsilon} \left(\frac{\partial}{\partial x} (-xp) + \frac{\sigma^2}{2} \frac{\partial^2 p}{\partial x^2} \right)}_{=: L_1 p} + \underbrace{\frac{1}{\sqrt{\varepsilon}} \frac{\partial}{\partial y} (-xp)}_{=: L_2 p} + \underbrace{\frac{\partial}{\partial y} (yp)}_{=: L_3 p}, \quad (15.44)$$

and so we can write the Fokker–Planck equation in operator notation as

$$\frac{\partial p}{\partial \tau} = (\gamma^2 L_1 + \gamma L_2 + L_3) p, \quad (15.45)$$

where we have set $\gamma := \frac{1}{\sqrt{\varepsilon}}$, which avoids writing too many fractions; the limit of interest then becomes $\gamma \rightarrow \infty$. The major steps in deriving a reduced Fokker–Planck equation for \hat{p} are as follows:

- (S1) Define a projection operator onto the y -variables using the stationary distribution of x .
- (S2) Use the Laplace transform to simplify the Fokker–Planck equation and apply the projection.
- (S3) The correlation function for x will provide another auxiliary tool.
- (S4) Derive the reduced equation for \hat{p} from the results in Steps (S1)–(S3).

It is important to note that when we carry out the steps (S1)–(S4) below, this is a formal reduction procedure. In particular, rigorous results for a general Fokker–Planck equation associated with a fully nonlinear fast–slow SDE seem to be difficult to obtain.

Step (S1): The idea is to eliminate the variable x , since it will quickly decay toward a stationary distribution. Therefore, we define

$$(Pf)(x, y) := p_s(x) \int_{\mathbb{R}} f(\tilde{x}, y) d\tilde{x} = \left(p_s(x) \int_{\mathbb{R}} d\tilde{x} \right) f(\tilde{x}, y), \quad (15.46)$$

where $p_s(x)$ is the stationary distribution of x , which solves the stationary Fokker–Planck equation $L_1 p_s(x) = 0$. The second equality in (15.46) is just a different notation for the same object; P projects onto the null space of L_1 and satisfies the following properties:

$$P^2 = P \circ P = P, \quad (15.47)$$

$$PL_1 = L_1 P = 0, \quad (15.48)$$

$$P = \lim_{\tau \rightarrow \infty} \exp(\tau L_1), \quad (15.49)$$

$$PL_2 P = 0, \quad (15.50)$$

$$PL_3 = L_3 P. \quad (15.51)$$

It is not difficult to see that (15.47) holds, since $\int p_s(x) dx = 1$, and (15.48) follows from a direct calculation. For (15.49), recall that $\exp(\tau L_1)$ represents the semigroup solving the Fokker–Planck equation

$$\frac{\partial p}{\partial \tau} = L_1 p,$$

and so it approaches the stationary solution $p_s(x)$ in the limit $\tau \rightarrow \infty$. The least obvious property is (15.50), for which we first have to observe that $x(\tau)$ has stationary mean zero. This can be seen as follows:

$$\frac{d}{d\tau} \mathbb{E}[x(\tau)] = \mathbb{E}[x'(\tau)] = -\frac{1}{\varepsilon} \mathbb{E}[x(\tau)] + \frac{\sigma}{\sqrt{\varepsilon}} \mathbb{E}[\xi(\tau)] = -\frac{1}{\varepsilon} \mathbb{E}[x(\tau)], \quad (15.52)$$

where we have used the white noise $\xi(\tau)d\tau = dW(\tau)$ as in Examples 15.1.1 and 15.5.1 using the property that it has mean zero. Therefore, it follows from (15.52) that the mean of $x(\tau)$ decays to zero as $\tau \rightarrow 0$.

Remark: The calculation indicating that $x(\tau)$ has zero mean in its stationary state is a key ingredient of the stochastic reduction method, i.e., it reflects that the fast variable(s) form a stationary Markov process with zero mean. In our case, this is nicely linked to the fact that the critical manifold is normally hyperbolic and attracting. As an aside, we also mention that common notation for the mean (or expected value) of the stationary distribution is $\langle x \rangle_s := \int x p_s(x) dx$ in the physics literature and $\mathbb{E}_s[x] := \int x p_s(x) dx$ in the mathematics literature.

Now we can justify (15.50) by the a direct calculation:

$$\begin{aligned} (PL_2 P f)(x, y) &= \left(p_s(x) \int_{\mathbb{R}} dx \right) \left(-\frac{\partial}{\partial y} x \right) \left(p_s(x) \int_{\mathbb{R}} dX \right) f(X, y) \\ &= -p_s(x) \underbrace{\left(\int_{\mathbb{R}} x p_s(x) dx \right)}_{=0} \left(\frac{\partial}{\partial y} \right) \left(\int_{\mathbb{R}} dX \right) f(X, y) = 0. \end{aligned}$$

The last property (15.51) follows directly by noticing that L_3 is independent of x .

Step (S2): We could try to apply the projection P directly to the Fokker–Planck equation (15.45), but that would involve rather unpleasant computations involving the time derivative $\frac{\partial p}{\partial \tau}$. Since the Fokker–Planck equation is linear, it is possible to use the Laplace transform to our advantage. The **Laplace transform** of a function f is defined by

$$\tilde{f}(s) := \int_0^\infty e^{-st} f(t) dt.$$

A basic property of the Laplace transform is

$$\int_0^\infty e^{-st} f'(t) dt = s\tilde{f}(s) - f(0),$$

which follows using integration by parts if $f(t) \rightarrow 0$ as $t \rightarrow \infty$; since we are going to apply the Laplace transform only to probability densities, this decay at infinity automatically holds. Writing $p(x, y, t) = p(t)$ and applying the Laplace transform to (15.45) gives

$$s\tilde{p}(s) - p(0) = (\gamma^2 L_1 + \gamma L_2 + L_3)\tilde{p}(s).$$

We introduce additional notation for the operator $Q := \text{Id} - P$ and the projected functions

$$\tilde{v}(s) := P\tilde{p}(s), \quad v(s) := Pp(s), \quad \tilde{w}(s) := Q\tilde{p}(s), \quad w(s) := Qp(s).$$

Finally, we can apply our projection P to (15.45), which yields

$$\begin{aligned} s\tilde{v}(s) &= P(\gamma^2 L_1 + \gamma L_2 + L_3)\tilde{p}(s) + v(0) \\ &= \gamma PL_2(P\tilde{p}(s) + Q\tilde{p}(s)) + L_3P\tilde{p}(s) + v(0) \\ &= \gamma PL_2\tilde{w}(s) + L_3\tilde{v}(s) + v(0), \end{aligned} \tag{15.53}$$

where we have used $PL_1 = 0$, $PL_2P = 0$, and $PL_3 = L_3P$. We can also apply Q to (15.45), which gives

$$\begin{aligned} s\tilde{w}(s) &= Q(\gamma^2 L_1 + \gamma L_2 + L_3)\tilde{p}(s) + w(0) \\ &= \gamma^2 L_1 Q\tilde{p}(s) + \gamma QL_2(P\tilde{p}(s) + Q\tilde{p}(s)) + L_3Q\tilde{p}(s) + w(0) \\ &= (\gamma^2 L_1 + \gamma QL_2 + L_3)\tilde{w}(s) + \gamma L_2\tilde{v}(s) + w(0). \end{aligned} \tag{15.54}$$

We will assume that $w(0) = 0$, which means that the initial condition of the Fokker–Planck equation is a product of densities, where the stationary distribution of $p_s(x)$ is used for the fast variables, i.e.,

$$w(0) = 0 \quad \Leftrightarrow \quad p(x, y, \tau = 0) = p_s(x)\tilde{p}(y, \tau = 0).$$

From the viewpoint of fast–slow systems, this means that we basically start with a product distribution of fast and slow variables. Then we find from (15.54) that

$$-\tilde{w}(s) = [-s + \gamma^2 L_1 + \gamma Q L_2 + L_3]^{-1} \gamma L_2 \tilde{v}(s).$$

Plugging this result into (15.53) yields

$$s\tilde{v}(s) = L_3 \tilde{v}(s) - \gamma^2 P L_2 [-s + \gamma^2 L_1 + \gamma Q L_2 + L_3]^{-1} L_2 \tilde{v}(s) + v(0).$$

Factoring out γ^{-2} from the inverted operator term and letting $\gamma \rightarrow \infty$ gives the limit

$$s\tilde{v}(s) = (L_3 - P L_2 L_1^{-1} L_2) \tilde{v}(s) + v(0). \quad (15.55)$$

Since this result is not in a nice explicit form, we must compute $P L_2 L_1^{-1} L_2 \tilde{v}$.

Step (S3): Before we can see why we need the correlation function in this step, we recall that

$$\begin{aligned} \tilde{v}(s) &= \tilde{p}(y) p_s(x), \\ P L_2 L_1^{-1} L_2 \tilde{v} &= p_s(x) \int dX \left(-\frac{\partial}{\partial y} X \right) L_1^{-1} \left(-\frac{\partial}{\partial y} X \right) p_s(X) \tilde{p}(y). \end{aligned}$$

This shows that we must compute

$$\int dx x L_1^{-1} x p_s(x) =: -\Xi.$$

The obstacle is to deal with L_1^{-1} , but using $P = \lim_{\tau \rightarrow \infty} \exp(\tau L_1)$ from (15.49) above, we obtain

$$\int_0^\infty \exp(\tau L_1) d\tau = L_1^{-1} \left(\lim_{\tau \rightarrow \infty} \exp(\tau L_1) - 1 \right) = -L_1^{-1} Q. \quad (15.56)$$

Furthermore, a direct computation shows that

$$P x p_s(x) = p_s(X) \mathbb{E}_s[x] = 0. \quad (15.57)$$

Using (15.56)–(15.57), it follows that

$$\Xi = \int dx x \int_0^\infty \exp(\tau L_1) x p_s(x) d\tau. \quad (15.58)$$

Now observe that $\exp(\tau L_1) x p_s(x)$ is the solution of the Fokker–Planck equation $\partial_\tau f = L_1 f$ with initial condition $f(x, 0) = x p_s(x)$. This implies

$$\exp(\tau L_1) x p_s(x) = \int dX p(x, \tau | X, 0) X p_s(X),$$

which follows from the theory of solutions for the Fokker–Planck equation (see, e.g., [Ris96]). Substituting the last result into (15.58) then shows that

$$\Xi = \int_0^\infty d\tau \int dx dX x X p(x, \tau | x, 0) p_s(x) = \int_0^\infty d\tau \mathbb{E}_s[x(\tau)x(0)],$$

and we recognize the last term $\mathbb{E}_s[x(\tau)x(0)]$ as the **stationary correlation function** for x . We could just proceed with this result, since Ξ is now expressed as a very simple formula. Recall that for our model problem, we have

$$dx = -\frac{x}{\varepsilon} d\tau + \frac{\sigma}{\sqrt{\varepsilon}} dW,$$

which is just a special case of the more general **Ornstein–Uhlenbeck** process given by

$$dx = -kx d\tau + D^* dW, \quad (15.59)$$

so that we have $k = 1/\varepsilon$ and $D^* = \sigma^2/\varepsilon$. In this case, it is known that the stationary correlation function is

$$\mathbb{E}_s[x(\tau)x(0)] = \frac{D^*}{2k} e^{-k\tau} = \frac{\sigma^2}{2} e^{-\tau/\varepsilon} = \frac{\sigma^2}{2} e^{-\gamma^2 \tau}. \quad (15.60)$$

The next exercise will guide us through the calculations that lead to (15.60).

Exercise 15.5.2. Make the ansatz $y = e^{k\tau}$ for (15.59) and use Itô's formula to derive an equation for y . Solve the equation for y by integration and transform back to x to obtain

$$x(\tau) = x(0)e^{-k\tau} + \sqrt{D^*} \int_0^\tau e^{-k(\tau-t')} dW(t'). \quad (15.61)$$

Use (15.61) to calculate the mean and variance of $x(\tau)$. Calculate the **correlation function** $\mathbb{E}[x(\tau)x(s)]$ and let $s = 0$ to deduce (15.60). \diamond

Observe that if we consider any finite time τ in (15.60) and consider the limit $\varepsilon \rightarrow 0$ (or alternatively $\gamma \rightarrow \infty$), then it follows that

$$\mathbb{E}_s[x(\tau)x(0)] = \frac{\sigma^2}{2} \cdot 0 = 0.$$

Therefore, the term $PL_2L_1^{-1}L_2\tilde{v}$ vanishes from (15.55), so that we are left with

$$s\tilde{v}(s) = L_3\tilde{v}(s) + v(0), \quad (15.62)$$

or in a different notation, $sP\tilde{p}(s) - Pp(0) = L_3P\tilde{p}(s)$. Transforming back via the Laplace transform properties, we get

$$\frac{\partial \hat{p}}{\partial \tau} = L_3\hat{p} = \frac{\partial}{\partial y}(\hat{y}\hat{p}), \quad (15.63)$$

where $\hat{p}(y, \tau) = \int dx p(x, y, \tau)$ is the desired marginal density. Formally, the Fokker–Planck equation (15.63) corresponds to the SDE given by

$$dy = -y d\tau + 0 dW,$$

which is just the deterministic equation $\dot{y} = -y$; note that we still would have to undo the rescaling $y \mapsto \sqrt{\varepsilon}y$ introduced above before we took the limit $\varepsilon \rightarrow 0$, but that would not change the result, since L_3 is invariant under this scaling.

Since we already know the approximation $\dot{y} = -y$ from the deterministic equations, we have carried out all the complicated calculations above without any result! Or have we? In fact, the method introduced is a general procedure for reducing (linear) fast–slow stochastic SDEs. For our model problem (15.42), the zeroth-order approximation $\varepsilon = 0$ is not stochastic, and the noise can then be viewed as a higher-order effect. Crucially, we have assumed that $\sigma = \mathcal{O}(1)$ and that the noise is given by $\sigma/\sqrt{\varepsilon}$, and Section 15.3 showed already that other scalings of $\sigma(\varepsilon) = \sigma$ can drastically change the system dynamics.

Before we conclude this section, we give another example that can be analyzed using the same techniques but that gives a more surprising result, i.e., the noise shows up in the lowest order.

Example 15.5.3. The following $(1, 1)$ -fast–slow system [Gar09] describes a simplified chemical reaction:

$$\begin{aligned}\varepsilon \frac{dx}{d\tau} &= -2x + y + a, \\ \frac{dy}{d\tau} &= -y + x.\end{aligned}\tag{15.64}$$

The critical manifold is $C_0 = \{(x, y) \in \mathbb{R}^2 : y = 2x - a \text{ or } x = \frac{y+a}{2}\}$, which is normally hyperbolic attracting everywhere. Therefore, the effective dynamics are described by the slow flow

$$\dot{y} = \frac{a - y}{2}.\tag{15.65}$$

Consider the stochastic version of (15.64) given by the SDE

$$\begin{pmatrix} dx \\ dy \end{pmatrix} = \begin{pmatrix} -\frac{2}{\varepsilon}x + y + a \\ -y + \frac{x}{\varepsilon} \end{pmatrix} d\tau + \sigma B \begin{pmatrix} dW^1 \\ dW^2 \end{pmatrix},\tag{15.66}$$

where we have scaled the fast variable $x \mapsto x/\varepsilon$, $B = (B_{ij}) \in \mathbb{R}^{2 \times 2}$ is a matrix, $\sigma > 0$ is a constant noise level, and $W^1 = W^1(\tau)$, $W^2 = W^2(\tau)$ are independent Brownian motions. We assume that the matrix B satisfies

$$BB^\top = \begin{pmatrix} 4a & -2a \\ -2a & 2a \end{pmatrix}.$$

Observe carefully that the structure of the equations (15.66) means that the noise terms for the x - and y -variables are **correlated**; this makes the problem more complicated and provides an example for correlated noise, which we have ignored so far. The Fokker–Planck equation for (15.66) is

$$\begin{aligned}\frac{\partial p}{\partial \tau} &= \left[-\frac{\partial}{\partial x} \left(-\frac{2}{\varepsilon}x + y + a \right) - \frac{\partial}{\partial y} \left(\frac{x}{\varepsilon} - y \right) \right. \\ &\quad \left. + 2a\sigma^2 \frac{\partial^2}{\partial x^2} + a\sigma^2 \frac{\partial^2}{\partial y^2} - 2a\sigma^2 \frac{\partial^2}{\partial x \partial y} \right] p,\end{aligned}\tag{15.67}$$

where $p = p(x, y, t)$. Finding the correct Fokker–Planck equation for the marginal density $\hat{p}(y) = \hat{p}$ is quite substantial work. The result is

$$\frac{\partial \hat{p}}{\partial \tau} = \frac{\partial}{\partial y} \frac{y - a}{2} \hat{p} + \frac{a\sigma^2}{2} \frac{\partial^2 \hat{p}}{\partial y^2}. \quad (15.68)$$

It has an extra diffusive term that is not predicted by the deterministic approximation (15.65). The SDE associated with (15.68) is

$$dy = \frac{a - y}{2} d\tau + \sqrt{a}\sigma dW. \quad (15.69)$$

Hence, the reduced equation contains a noise term that is not immediately obvious from the original SDE. ♦

The following exercise is quite lengthy but instructive in helping to understand the reduction procedure for correlated noise.

Exercise/Project 15.5.4. (a) Prove the result (15.68). (b) Consider the SDE from Example 15.5.3 without the rescaling of the fast variable

$$\begin{pmatrix} \varepsilon dx \\ dy \end{pmatrix} = \begin{pmatrix} -2x + y + a \\ -y + x \end{pmatrix} d\tau + \sigma \tilde{B} \begin{pmatrix} dW^1 \\ dW^2 \end{pmatrix} \quad (15.70)$$

and a diagonal diffusion matrix

$$\tilde{B} \tilde{B}^\top = \begin{pmatrix} 2a^2 & 0 \\ 0 & 2a^2 \end{pmatrix}.$$

Formally use $\xi_j(\tau) d\tau = dW_j$ and the usual direct fast–slow reduction to a critical manifold to obtain a reduced SDE for y from (15.70). Can you prove your result from (b) using Fokker–Planck equation techniques? ◊

15.6 Random Dynamical Systems

So far, we have always considered a fast–slow system of SDEs as our main object of study. For example, in the case of purely additive noise, we have

$$\begin{aligned} d\tilde{x} &= \frac{1}{\varepsilon} f(\tilde{x}, \tilde{y}) d\tau + \frac{\sigma_f}{\sqrt{\varepsilon}} dW^1, \\ d\tilde{y} &= g(\tilde{x}, \tilde{y}) d\tau + \sigma_g dW^2, \end{aligned} \quad (15.71)$$

for $(\tilde{x}, \tilde{y}) \in \mathbb{R}^{m+n}$ and Brownian motions $W^1 \in \mathbb{R}^m$, $W^2 \in \mathbb{R}^n$. Studying sample paths and probability densities has provided substantial insight into fast–slow stochastic systems. However, one may also ask for some abstract stochastic analogues of the geometric objects arising in deterministic invariant manifold theory. The goal of this section is to approach (15.71) as a random dynamical system and state a theorem on the existence of random slow manifolds. This viewpoint is going to show that on an abstract level, there is still a familiar-looking invariant manifold theory.

As a first step, we have to reinterpret Brownian motion as a dynamical system. Let $W = W(\tau)$ be standard Brownian motion in \mathbb{R}^N . Define the following space of continuous paths:

$$\Omega := \{\omega \in C^0(\mathbb{R}, \mathbb{R}^N) : \omega(0) = 0\}.$$

Observe that if we formally write $W(\tau)(\omega) = \omega(\tau)$, then this views Brownian motion as a path. Let \mathcal{F} be the Borel σ -algebra of Ω and denote by \mathbb{P} the **Wiener measure** on \mathcal{F} induced by $W(\tau)$, i.e., for every sequence of times $0 < \tau_1 < \tau_2 < \dots < \tau_j$ and Borel-measurable sets $A_1, A_2, \dots, A_j \subset \mathbb{R}^N$, we have $\mathbb{P}(\{\omega : \omega(\tau_1) \in A_1, \dots, \omega(\tau_j) \in A_j\}) =$

$$\int_{A_1} \int_{A_2} \cdots \int_{A_j} p(0, z_1, \tau_1) p(z_1, z_2, \tau_2 - \tau_1) \cdots p(z_{j-1}, z_j, \tau_j - \tau_{j-1}) dz_1 dz_2 \cdots dz_j,$$

where $p(z, w, \tau) = \frac{1}{\sqrt{(2\pi)^N \tau}} \exp\left(-\frac{\|z-w\|^2}{2\tau}\right)$. The Wiener measure is directly related to the definition of Brownian motion, and we also call $(\Omega, \mathcal{F}, \mathbb{P})$ the **Wiener space**. Define the shift

$$\theta_\tau \omega(\cdot) := \omega(\tau + \cdot) - \omega(\tau).$$

Exercise 15.6.1. Show that

$$\Theta := (\Omega, \mathcal{F}, \mathbb{P}, \{\theta_\tau\}_{\tau \in \mathbb{R}})$$

generates a **metric dynamical system**, i.e., show that (a) $(\tau, \omega) \mapsto \theta_\tau \omega$ is measurable, and $\theta_\tau \mathbb{P} = \mathbb{P}$ holds, which means that θ is measure-preserving. \diamond

The metric dynamical system $(\Omega, \mathcal{F}, \mathbb{P}, \{\theta_\tau\}_{\tau \in \mathbb{R}})$ just models Brownian motion as a flow on path space. The following definition of a random dynamical system works for every metric dynamical system (not only Brownian motion), but for our purposes, it suffices to think of the concrete example.

Definition 15.6.2. Consider \mathbb{R}^N with Borel σ -algebra $\mathcal{B}(\mathbb{R}^N)$. A **random dynamical system (RDS)** is a measurable mapping

$$\varphi : \mathbb{R}^+ \times \Omega \times \mathbb{R}^N \rightarrow \mathbb{R}^N, \quad (\tau, \omega, z) \mapsto \varphi_\tau(\omega)z$$

such that (a) $\varphi_0(\omega) = \text{Id}_{\mathbb{R}^N}$ and (b) for all $s, \tau \geq 0$ and all $\omega \in \Omega$, the **cocycle property** holds:

$$\varphi_{\tau+s}(\omega) = \varphi_\tau(\theta_s \omega) \circ \varphi_s(\omega).$$

Remark: There are some natural modifications and generalizations for the RDS concept. We could require two-sided time \mathbb{R} instead of \mathbb{R}^+ or consider discrete time \mathbb{Z} . Furthermore, one might try to require that φ be continuous, which is quite reasonable, or even that φ be C^k -smooth, which is often a bit too strong as a requirement.

Observe that omitting the randomness/noise ω in Definition 15.6.2 gives a usual semiflow; see Section 18.1. However, it is often nontrivial to check whether

the cocycle property is satisfied; interlinking the metric dynamical system θ , which advances the noise with an underlying flow, produces a quite abstract mathematical object. It is important to note that we can also view θ and φ as a **skew-product flow**

$$(\omega, z) \mapsto (\theta_\tau \omega, \varphi_\tau(\omega)z)$$

on $\Omega \times \mathbb{R}^N$. One natural way to generate an RDS is to consider a **random differential equation (RDE)**

$$\dot{z} = F(\theta_\tau \omega, z) \quad (15.72)$$

for $z \in \mathbb{R}^N$ with ω fixed for each solution path. Dealing with random objects (e.g., sets, maps) geometrically is often much simpler in the case of RDEs.

Definition 15.6.3. Let Θ^1 and Θ^2 be two independent metric dynamical systems representing Brownian motions on the slow time scale τ . A **fast–slow random differential equation** is given by

$$\begin{aligned} \varepsilon \frac{dx}{d\tau} &= \varepsilon \dot{x} = f(\theta_t^1 \omega_1, \theta_\tau^2 \omega_2, x, y), \\ \frac{dy}{d\tau} &= \dot{y} = g(\theta_t^1 \omega_1, \theta_\tau^2 \omega_2, x, y), \end{aligned} \quad (15.73)$$

where $t = \tau/\varepsilon$ is the fast time scale, $(x, y) \in \mathbb{R}^{m+n}$, and $\omega := (\omega_1, \omega_2)$.

Note that the class of fast–slow RDEs (15.73) does not immediately match the more familiar fast–slow SDEs (15.71); however, it turns out to be sometimes possible to transform one into the other under suitable conditions, as we shall see later on. The next goal is to introduce random invariant manifolds. The starting point is to define random sets for a given RDS.

Definition 15.6.4. A family of nonempty closed sets $S = \{S(\omega)\}_{\omega \in \Omega}$ is called a **random set** if for every $z \in \mathbb{R}^N$, the mapping

$$\omega \mapsto \inf_{\tilde{z} \in S(\omega)} \|\tilde{z} - z\|$$

is measurable. The set S is called **positively invariant with respect to the RDS φ** if

$$\varphi_\tau(\omega, S(\omega)) \subseteq S(\theta_\tau \omega)$$

for $t \geq 0$ and every $\omega \in \Omega$.

The definition of positive invariance is very similar to the deterministic definition; see Section 2.3. When dealing with RDS, one often just adds the additional requirement that all objects depend on the chosen noise ω ; in our case, we should think of choosing a sample path for Brownian motion when we choose ω . Consider a map

$$\gamma : \Omega \times \mathbb{R}^n \rightarrow \mathbb{R}^m, \quad \gamma(\omega, y) \in \mathbb{R}^m$$

that is globally Lipschitz in y for all $\omega \in \Omega$. It is not difficult to see that the graph of γ is a random set. Hence, we can finally define the random invariant manifold.

Definition 15.6.5. The random set $S(\omega) := \{(\gamma(\omega, y), y) \in \mathbb{R}^{m+n}\}$ is a **random invariant manifold** for the fast–slow RDE (15.73) if it is positively invariant under the RDS generated by (15.73).

We can also require that for all $z = (x, y) \in \mathbb{R}^{m+n}$,

$$\lim_{\tau \rightarrow \infty} d_H(\varphi_\tau(\omega)z, S(\theta_\tau \omega)) = 0, \quad (15.74)$$

where d_H is the usual Hausdorff distance; if (15.74) holds, we say that S is an **attracting** random invariant manifold. We are going to make several assumptions on (15.73) that will allow us to prove the existence of a suitable attracting random invariant manifold.

- (A1) The maps f, g are given as a decomposition of linear parts A, B and non-linear parts F, G :

$$\begin{aligned} f(\theta_t^1 \omega_1, \theta_\tau^2 \omega_2, x, y) &= A(\theta_t^1 \omega_1, \theta_\tau^2 \omega_2)x + F(\theta_t^1 \omega_1, \theta_\tau^2 \omega_2, x, y), \\ g(\theta_t^1 \omega_1, \theta_\tau^2 \omega_2, x, y) &= B(\theta_t^1 \omega_1, \theta_\tau^2 \omega_2)y + G(\theta_t^1 \omega_1, \theta_\tau^2 \omega_2, x, y). \end{aligned}$$

- (A2) The maps $(\omega_1, \omega_2) \mapsto A(\omega_1, \omega_2)$ and $(\omega_1, \omega_2) \mapsto B(\omega_1, \omega_2)$ are measurable with their norms $\|\cdot\|$ contained in $L^1(\Omega, \mathcal{F}, \mathbb{P})$.

- (A3) There are constants $c_A > 0$ and $c_B \geq 0$ such that

$$x^\top A^\top(\omega_1, \omega_2)x \leq -c_A \|x\|^2 \quad \text{and} \quad \|B(\omega_1, \omega_2)\| \leq c_B$$

for all (ω_1, ω_2) .

- (A4) The maps F and G are measurable with respect to the arguments (ω_1, ω_2) , and they satisfy a Lipschitz condition with Lipschitz constant L with respect to the variables (x, y) .
- (A5) $c_A > aL$ for some constant $a \geq 1$ that can be determined from the linearized system. This gives a **spectral gap** condition, i.e., the fast linear part contracts sufficiently fast.
- (A6) There exist $c_F \geq 0$ and $c_G \geq 0$ such that

$$\sup_{(\omega_1, \omega_2, x, y)} \|F(\omega_1, \omega_2, x, y)\| =: c_F \quad \text{and} \quad \sup_{(\omega_1, \omega_2, x, y)} \|G(\omega_1, \omega_2, x, y)\| =: c_G.$$

Remark: To determine the constant $a \geq 1$ more precisely, let $U_{\varepsilon, \tau}^A(\omega)$ denote the solution of the linear random differential equation $\dot{x} = A(\theta_{\tau/\varepsilon} \omega)x$. It is not too difficult to see that $U_{\varepsilon, \tau}^A$ defines a random dynamical system. Furthermore, we can use (A3) to show that $\|U_{\varepsilon, \tau}^A(\tau - s, \omega)\| \leq ae^{-c_A(\tau-s)}$. This provides a way to compute/define the constant a . Similarly, we can also get a constant $b \geq 1$ such that $\|U_{\varepsilon, \tau}^B(\tau - s, \omega)\| \leq be^{c_B(\tau-s)}$.

The proof of the existence of an attracting invariant manifold uses a random version of the classical graph transform technique; see Chapter 2 for the classical graph transform. Let G_Γ denote the metric space of all Lipschitz random maps $\gamma : \Omega \times \mathbb{R}^n \rightarrow \mathbb{R}^m$ with Lipschitz constant at most Γ .

Theorem 15.6.6 ([SS08b]). *Under the assumptions (A1)–(A6) and for $\varepsilon > 0$ sufficiently small, there exists an attracting random invariant manifold S_ε for (15.73). The manifold is defined by the graph of a map*

$$\gamma_\varepsilon : \Omega \times \mathbb{R}^n \rightarrow \mathbb{R}^m, \quad \text{with } \gamma_\varepsilon \in G_\Gamma, \quad \Gamma = \frac{2b(c_A - \alpha)}{c_A - \alpha - aL},$$

and $\alpha > 0$ satisfies $c_A - \alpha > aL$. Furthermore, there exists a bound on the graph of the map

$$\sup_{\omega \in \Omega} \sup_{y \in \mathbb{R}^n} \|\gamma_\varepsilon(\omega, y)\| \leq K \frac{c_F}{c_A},$$

where K is any real number greater than 1.

Theorem 15.6.6 is another stochastic generalization of deterministic Fenichel theory for attracting normally hyperbolic manifolds; cf. Theorem 15.2.5. In addition to Theorem 15.6.6, it can be shown that the limit $S_\varepsilon \rightarrow S_0$ as $\varepsilon \rightarrow 0$ makes sense.

Theorem 15.6.7 ([SS08b]). *Under the hypotheses (A1)–(A6), there exists an attracting random invariant critical manifold S_0 .*

The points for a deterministic critical manifold S_0 are equilibrium points for the fast subsystem. In the RDS case, they are **random equilibrium points** parameterized by the slow variables y and the noise ω_2 associated with the slow variable Brownian motions.

Exercise 15.6.8. Try to make a reasonable definition of a random equilibrium point for a general RDS. Compare your ideas with [Arn03]. \diamond

Theorems 15.6.6–15.6.7 can be related to the solutions of the general fast–slow SDE (15.71). Since the methods to achieve this correspondence are not within the main theme of this book, we only sketch the idea. As a first step, we linearize the SDE (15.71). Linear SDEs with constant noise are solved by an Ornstein–Uhlenbeck process, say $z_\tau^{\text{lin}} = (x_\tau^{\text{lin}}, y_\tau^{\text{lin}})$. Using this solution, we change variables by $\tilde{z}_\tau = z_\tau - z_\tau^{\text{lin}}$. It turns out that this transformation removes the original Brownian motion from the SDE, and we end up with an RDE.

Theorem 15.6.9 ([SS08b]). *There exists a random (i.e., ω -dependent) transformation $(x, y) = V_\varepsilon(\omega, \tilde{x}, \tilde{y})$ such that the fast–slow SDE (15.71) can be mapped to a fast–slow RDE (15.73).*

Under a suitable notion of equivalence, we can then indeed show that the attracting invariant manifold for a fast–slow RDE also exists for the corresponding fast–slow SDE; for details, see [SS08b, Arn01].

15.7 Markov Chains

So far, we have focused in this chapter on fast–slow stochastic differential equations (SDEs). Clearly, this is not the only class of stochastic multiple time scale systems. In this section, we consider continuous-time **Markov chains** $X = X(\tau)$ ($\tau \in \mathbb{R}$). First, we outline some basic notation and results from standard Markov chain theory; see Section 15.10 for more background. For simplicity, assume that the states of the Markov chain form a finite set I , so that we may index each state by some $i \in \mathbb{N}$ and we have $X(\tau) = i$ at time τ . The basic data of a continuous-time Markov chain are given by its **infinitesimal generator**, or **Q-matrix** $Q = (q_{ij})$, which satisfies the following conditions:

- (1) $0 \leq -q_{ii} < \infty$ for all i ;
- (2) $q_{ij} \geq 0$ for all $i \neq j$;
- (3) $\sum_{j \in I} q_{ij} = 0$ for all i .

One may interpret the q_{ij} as rates; this can be seen nicely by considering the associated **jump matrix** $\Pi = (\Pi_{ij})$ to Q . It is obtained by considering each row of Q , scaling the off-diagonal entries to sum to 1, and then putting a 0 on the diagonal. If the off-diagonal entries are all zeros, we leave them and put a 1 on the diagonal.

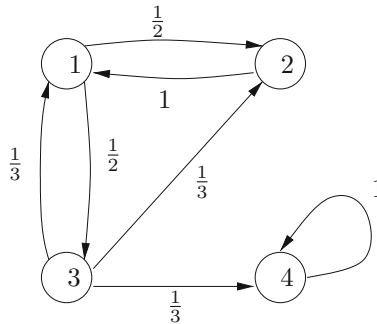


Figure 15.5: Illustration of basic Markov chain defined by (15.75).

Example 15.7.1. Consider the generator Q with jump matrix Π given by

$$Q = \begin{pmatrix} -2 & 1 & 1 & 0 \\ 1 & -1 & 0 & 0 \\ 1 & 1 & -3 & 1 \\ 0 & 0 & 0 & 0 \end{pmatrix}, \quad \Pi = \begin{pmatrix} 0 & \frac{1}{2} & \frac{1}{2} & 0 \\ \frac{1}{2} & 0 & 0 & 0 \\ \frac{1}{3} & \frac{1}{3} & 0 & \frac{1}{3} \\ 0 & 0 & 0 & 1 \end{pmatrix}, \quad (15.75)$$

where the entries of Π can be viewed as probabilities. For example, $\Pi_{13} = \frac{1}{2}$ means that we jump with probability $\frac{1}{2}$ from state 1 to state 3; see Figure 15.5. Note that state 4 is **absorbing** and that the chain will end up in this state eventually. ♦

In general, we are most interested in the **transition probabilities** of the chain

$$p_{ij}(\tau) := \mathbb{P}(X(\tau) = j | X_0 = i).$$

It is known that $P(\tau) = (p_{ij}(\tau))$ satisfies the following forward equation:

$$\frac{dP}{d\tau} = \dot{P}(\tau) = P(\tau)Q, \quad P(0) = \text{Id}, \quad (15.76)$$

which is a system of ODEs of size $(\#|I|)^2$, i.e., there is one equation for each transition probability $p_{ij}(\tau)$. Obviously, (15.76) is the analogue to the Fokker–Planck equation (or Kolmogorov forward equation) for SDEs; see Section 15.1.

Remark: Although we are not going to consider this case, we remark that the generator $Q = Q(\tau)$ might also depend on time, which leads to additional complications of the theory, producing a nonautonomous ODE (15.76).

One link between Markov chain theory and multiple time scale systems arises if the generator is decomposed as

$$Q^\varepsilon = \frac{1}{\varepsilon} \tilde{Q} + \hat{Q},$$

where we assume that \tilde{Q} and \hat{Q} are constant matrices that are themselves generators. If we return to the rate interpretation of the entries of Q , then \tilde{Q}/ε represents fast motion, and \hat{Q} the slow motion, of the system corresponding to the ODE

$$\varepsilon \dot{P} = P \left[\tilde{Q} + \varepsilon \hat{Q} \right], \quad P(0) = \text{Id}.$$

Instead of developing the general theory, we restrict the discussion to a very simple example of a **fast–slow (or singularly perturbed) Markov chain**.

Example 15.7.2. Consider the fast–slow Markov chain defined by

$$\tilde{Q} = \begin{pmatrix} -1 & 1 & 0 \\ 1 & -1 & 0 \\ 0 & 0 & 0 \end{pmatrix}, \quad \hat{Q} = \begin{pmatrix} -1 & 0 & 1 \\ 0 & -1 & 1 \\ 1 & 2 & -3 \end{pmatrix}.$$

Therefore, the associated nine-dimensional system of ODEs is

$$\begin{aligned} \varepsilon \dot{p}_{i1} &= -p_{i1}(1 + \varepsilon) + p_{i2} + \varepsilon p_{i3}, \\ \varepsilon \dot{p}_{i2} &= p_{i1} - p_{i2}(1 + \varepsilon) + 2\varepsilon p_{i3}, \\ \dot{p}_{i3} &= p_{i1} + p_{i2} - 3p_{i3}, \end{aligned} \quad (15.77)$$

for $i = 1, 2, 3$. Then (15.77) is a $(6, 3)$ -fast–slow system. The fast subsystem is given by

$$\begin{aligned} p'_{i1} &= -p_{i1} + p_{i2}, \\ p'_{i2} &= p_{i1} - p_{i2}, \end{aligned} \quad (15.78)$$

and it decouples from the slow variables p_{i3} ; the system (15.78) can also be viewed as the forward equation for a two-state Markov chain

$$\tilde{P}' = \tilde{P}(t) \begin{pmatrix} -1 & 1 \\ 1 & -1 \end{pmatrix} =: \tilde{P}(t)Q_f, \quad (15.79)$$

which has the generator Q_f . It is relatively easy to see that Q_f is the generator for a Markov chain that just cycles between two states such that the stationary probability distribution for \tilde{P} has equal probability in each state $i = 1$ and $i = 2$; this distribution is also called the **quasistationary distribution**. Indeed, for $0 < \varepsilon \ll 1$, there is a positive probability of being in the state $i = 3$, so the quasistationary distribution does not coincide with the stationary one. The critical manifold of (15.77)

$$C_0 = \{p_{ij} \in \mathbb{R}^9 : p_{i1} = p_{i2}, \text{ for } i = 1, 2, 3\},$$

and the slow flow $\dot{p}_{i3} = 2p_{i1} - 3p_{i3}$ are actually quite degenerate, since C_0 is six-dimensional, i.e., it does not have the generic dimension three expected for a $(6, 3)$ -fast–slow system. ♦

Exercise 15.7.3. Find the jump matrix associated with Example 15.7.2. Draw the diagram associated with this jump matrix, similar to Figure 15.5. ◇

From Exercise 15.7.3, it follows that the Markov chain from Example 15.7.2 is expected to fluctuate between two states with some, quite rare, transitions to the third state. The distinction between frequent and infrequent transitions between various states is a classical topic in statistical physics. The next section covers a crucial mathematical building block in understanding rare transitions.

15.8 Large Deviations

Essentially, the theory of large deviations aims to describe events that occur with low probability over a given time interval. The next example illustrates one of the simplest situations.

Example 15.8.1. Consider the classical **double-well potential**

$$U : \mathbb{R} \rightarrow \mathbb{R}, \quad U(z) := \frac{1}{4}z^4 - \frac{1}{2}z^2. \quad (15.80)$$

The potential generates a **gradient system**

$$\frac{dz}{dt} = z' = -U'(z) = z - z^3. \quad (15.81)$$

The system has two stable equilibria at $z = \pm 1$ and an unstable equilibrium at $z = 0$; see Figure 15.6(a). Perturbing (15.81) by additive noise yields the SDE

$$dz = [z - z^3] dt + \sigma dW, \quad (15.82)$$

where $W = W(t)$ is one-dimensional Brownian motion and $\sigma > 0$ controls the noise level. Figure 15.6(b) shows a time series for the SDE (15.82) that illustrates that the process $z(t)$ spends most of the time oscillating near a stable equilibrium. However, there is one large deviation where $z(t)$ switches from $z = -1$ to $z = 1$. Of course, a large deviation can also occur as a transition

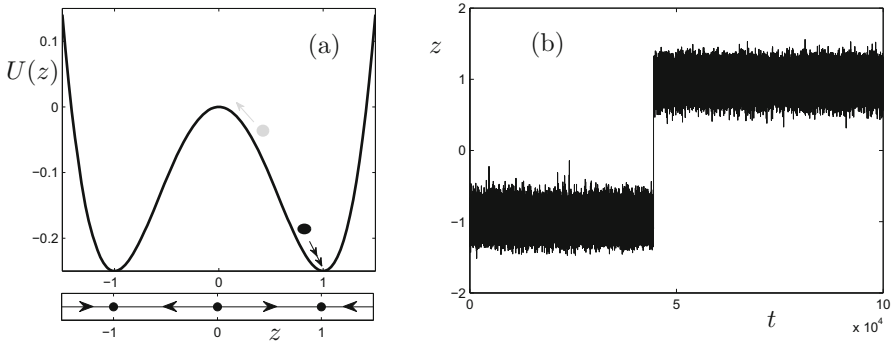


Figure 15.6: Gradient system for a double-well potential. (a) In the top part, the potential (15.80) is shown, and a particle illustrates the two different time scales: fast/frequent attraction to the equilibrium due to the deterministic attraction (black) and slow/rare excursions to the alternative stable state induced by a large deviation of the noise (gray). The bottom part of the figure illustrates the stability of the three equilibria for (15.81). (b) A typical time series of the SDE (15.82) obtained for $\sigma = 0.2$, $z(0) = 1$, and final time $T = 10^5$.

from $z = 1$ to $z = -1$, as sketched in Figure 15.6(a). There are two time scales in the problem for $\sigma > 0$ sufficiently small. On the short time scale, one sees only small fluctuations, while on the long time scale, large deviations can occur. ♦

Example 15.8.2. We briefly return to the stochastic van der Pol equation (15.2) introduced in Section 15.1 in a slightly simpler form,

$$\begin{aligned} dx &= \left(y - \frac{x^3}{3} + x \right) dt + \sigma dW, \\ dy &= \varepsilon(a - x) dt. \end{aligned} \quad (15.83)$$

Considering the fast subsystem singular limit ($\varepsilon = 0$), we obtain a gradient system

$$dx = -\frac{\partial U}{\partial x}(x; y) dt + \sigma dW, \quad U(x; y) = -xy - \frac{1}{2}x^2 + \frac{1}{12}x^4.$$

In particular, the classical double-well large-deviations problem from Example 15.8.1 reappears in context of the vdP equation with noise if the slow variable is frozen. ♦

Consider a more general SDE given by

$$dz = a(z) dt + \sigma A(z) dW, \quad (15.84)$$

where $z = z(t) \in \mathbb{R}^N$, $W(t)$ is a vector of k independent Brownian motions, and $A(z) \in \mathbb{R}^{N \times k}$ is a matrix. Throughout this section, it is assumed that the

diffusion matrix

$$\mathfrak{D}(z) := A(z)A(z)^\top \quad \text{is positive definite.}$$

As a thought experiment, suppose that $z(0)$ starts near a stable equilibrium $z^* \in \mathcal{D} \subset \mathbb{R}^N$ where \mathcal{D} is a bounded domain, e.g., it lies inside the **basin of attraction** of z^* , so that $z(t) \rightarrow z^*$ as $t \rightarrow \infty$. If $\sigma > 0$ is small, then one may hope to calculate the distribution of the **first-exit time**

$$\tau = \tau_{\mathcal{D}} := \inf\{t > 0 : z(t) \notin \mathcal{D}\} \quad (15.85)$$

asymptotically as $\sigma \rightarrow 0$. In fact, the probability of escape vanishes when $\sigma = 0$, and it should be small for $0 < \sigma \ll 1$. As usual, it helps to subdivide the time interval $[0, \infty)$ into pieces, e.g., $\mathcal{I}_j = [j, j+1]$ for $j \in \mathbb{N}_0$. If the escape events from \mathcal{D} on each \mathcal{I}_j could be approximated as independent events, then a natural guess is that the exit from \mathcal{D} is governed by some exponential distribution that depends on f , F , and σ . **Large deviation theory** provides a quantitative way to estimate this exponential distribution.

Consider the space $\mathcal{X} = C_0([0, T], \mathbb{R}^N)$ of continuous functions ϕ with $\phi(0) = 0$. This space contains the sample paths for (15.84) starting at $z(0) = 0$; note that we may always translate the initial condition, such as $z(0) = z^*$, to $z = 0$ if necessary. Observe that $\{z(t)\}$ induces a natural probability measure μ on \mathcal{X} . We also write $\mu^\sigma = \mu$ to emphasize that the measure depends on the noise level.

Definition 15.8.3. A mapping $I : \mathcal{X} \rightarrow [0, \infty]$ is called a **good rate function** if it is lower semicontinuous [Fol99] and the level set $\{h : I(h) \leq \alpha\}$ is compact for each $\alpha \in [0, \infty)$.

Sometimes the term **action functional** is used instead of rate function.

Definition 15.8.4. The measures $\{\mu^\sigma\}$ satisfy a **large deviation principle (LDP)** with good rate function I if

$$-\inf_{\Gamma^\circ} I \leq \liminf_{\sigma \rightarrow 0} \sigma^2 \ln \mu^\sigma(\Gamma) \leq \limsup_{\sigma \rightarrow 0} \sigma^2 \ln \mu^\sigma(\Gamma) \leq -\inf_{\bar{\Gamma}} I \quad (15.86)$$

holds for every measurable set of paths $\Gamma \subset \mathcal{X}$.

Remark: Although a specific choice of \mathcal{X} has been made to focus on SDEs, observe that Definitions 15.8.3–15.8.4 naturally extend to every topological space \mathcal{X} , Borel measurable sets $\mathcal{B}_{\mathcal{X}}$, and a suitable family of measures. In particular, LDPs and the associated time-scale separation of the stochastic process appear in a much wider context in probability theory; see Section 15.10.

In the context of the SDE (15.84), one may write (15.86) as

$$-\inf_{\Gamma^\circ} I \leq \liminf_{\sigma \rightarrow 0} \sigma^2 \ln \mathbb{P}(z(t) \in \Gamma) \leq \limsup_{\sigma \rightarrow 0} \sigma^2 \ln \mathbb{P}(z(t) \in \Gamma) \leq -\inf_{\bar{\Gamma}} I. \quad (15.87)$$

Furthermore, the infima over the interior Γ^o and closure $\bar{\Gamma}$ often coincide, so that the two limits in (15.87) are equal. To state the result on the form of the rate function for (15.84), consider the Sobolev space

$$H_1 := \{\phi : [0, T] \rightarrow \mathbb{R}^m : \phi \text{ absolutely continuous, } \phi' \in L^2, \phi(0) = 0\}.$$

For more on Sobolev spaces in PDEs, see [Eva02], and for the abstract theory, see [AF03].

Theorem 15.8.5 ([FW98b, DZ98]). *The processes $\{z(t)\}$, parameterized by σ , satisfy an LDP with good rate function*

$$I(\phi) = \begin{cases} \frac{1}{2} \int_0^T [\phi'(t) - f(\phi(t))]^\top \mathfrak{D}(\phi(t))^{-1} [\phi'(t) - f(\phi(t))] dt, & \text{if } \phi \in z(0) + H_1, \\ 0 & \text{otherwise.} \end{cases}$$

Example 15.8.6. A simple example occurs for $f = 0$, $F = \text{Id}$, $z(0) = 0$, so that $z(t) = \sigma W(t)$ is a scaled standard Brownian motion. The rate function is

$$I(\phi) = \begin{cases} \frac{1}{2} \int_0^T \|\phi'(t)\|^2 dt, & \text{if } \phi \in H_1, \\ 0 & \text{otherwise,} \end{cases} \quad (15.88)$$

which is also known as **Schilder's theorem**. To apply the LDP (15.87), one has to compute $\inf I(\phi)$. From the calculus of variations [Eva02], it follows that minimizing a functional

$$\phi \mapsto \int_0^T Q(t, \phi(t), \phi'(t)) dt, \quad Q := Q(t, \chi, \xi),$$

is equivalent to solving the **Euler–Lagrange equations**

$$\frac{\partial Q}{\partial \chi}(t, \phi(t), \phi'(t)) - \frac{\partial}{\partial t} \left[\frac{\partial Q}{\partial \xi}(t, \phi(t), \phi'(t)) \right] = 0.$$

Therefore, the minimizer of the rate function (15.88) is determined by $\phi''(t) = 0$ with straight lines $\phi(t) = ct$ as solutions. If we choose the subset Γ in Definition 15.8.4 as

$$\Gamma := \left\{ \phi \in \mathcal{X} : \sup_{0 \leq t \leq T} \phi(t) > L \right\},$$

then the minimizer is $\phi^*(t) = Lt/T$, and $I(\phi^*(t)) = L^2/(2T)$. This implies an LDP given by

$$\lim_{\sigma \rightarrow 0} \sigma^2 \ln \mathbb{P} \left(\sup_{0 \leq t \leq T} \sigma W(t) > L \right) = -\frac{L^2}{2T}. \quad (15.89)$$

Although (15.89) is only a **logarithmic equivalence**, one is always tempted to rewrite the LDP more succinctly as

$$\mathbb{P} \left(\sup_{0 \leq t \leq T} \sigma W(t) > L \right) \sim \kappa e^{-\frac{L^2}{2T\sigma^2}} \quad \text{as } \sigma \rightarrow 0$$

for some constant $\kappa > 0$ to emphasize the exponential time scale dependence on σ . The intuitive interpretation of the result (15.89) is that it is unlikely for a (scaled) Brownian motion to reach very large values on short time intervals. On long time scales, the large excursions become more and more likely. ♦

We return to the first-exit time (15.85) for (15.84). To understand $\tau_{\mathcal{D}}$, it helps to define

$$V(\tilde{z}, \chi; s) := \inf\{I(\phi) : \phi \in C([0, s], \mathbb{R}^N), \phi(0) = \tilde{z}, \phi(s) = \chi\}, \quad (15.90)$$

which is the **cost** for a path starting at \tilde{z} to reach $\chi \in \mathbb{R}^N$ in time s . By Theorem 15.8.5, it follows that

$$\lim_{\sigma \rightarrow 0} \sigma^2 \ln \mathbb{P}(\tau_{\mathcal{D}} \leq t | z(0) = \tilde{z}) = \inf\{V(\tilde{z}, \chi; s) : s \in [0, t], \chi \notin \mathcal{D}\}. \quad (15.91)$$

For the case of a stable deterministic equilibrium $z^* \in \mathcal{D}$, where $\bar{\mathcal{D}}$ is inside the basin of attraction of z^* , the function

$$V(z^*, \chi) = \inf_{s>0} V(z^*, \chi; s)$$

is called the **quasipotential**. Since we are interested in the first-exit time from \mathcal{D} , it is natural to minimize the quasipotential over $\partial\mathcal{D}$,

$$\bar{V} := \inf_{\chi \in \partial\mathcal{D}} V(z^*, \chi).$$

Theorem 15.8.7 ([FW98b]). *For all initial conditions $\tilde{z} \in \mathcal{D}$ and all $\delta > 0$, the following two limits hold:*

$$\lim_{\sigma \rightarrow 0} \mathbb{P}\left(e^{(\bar{V}-\delta)/\sigma^2} < \tau_{\mathcal{D}} < e^{(\bar{V}+\delta)/\sigma^2} | z(0) = \tilde{z}\right) = 1, \quad (15.92)$$

$$\lim_{\sigma \rightarrow 0} \sigma^2 \ln \mathbb{E}[\tau_{\mathcal{D}} | z(0) = \tilde{z}] = \bar{V}. \quad (15.93)$$

Remark: Theorem 15.8.7 can be extended to determine the precise exit location if the map $u \mapsto V(z^*, u)$ has a unique minimum $\chi^* \in \partial\mathcal{D}$. In this case, paths are going to exit with high probability near χ^* ; see Section 15.10.

Theorem 15.8.7 shows that it is important to compute the quasipotential. If the SDE (15.84) has a gradient structure with additive noise, i.e., $A(z) = \text{Id}$ and $a(z) = -\nabla U(z)$ for $U : \mathbb{R}^N \rightarrow \mathbb{R}$, it can be proved that for a nondegenerate, unique global minimum of the potential z^* , the quasipotential is given by

$$V(z^*, \chi) = 2(U(\chi) - U(z^*)).$$

Shifting the potential, we may achieve $U(z^*) = 0$, so that the quasipotential V differs from the actual potential U by only a multiplicative constant, which explains the name. From Theorem 15.8.7, it follows that the first exit time has expected value

$$\mathbb{E}[\tau_{\mathcal{D}} | z(0) = \tilde{z}] \sim \kappa e^{2(U(\chi) - U(z^*))/\sigma^2} \quad \text{as } \sigma \rightarrow 0$$

for some constant $\kappa > 0$.

Example 15.8.8. We continue with Example 15.8.1, where $U(z) := \frac{1}{4}z^4 - \frac{1}{2}z^2$. Suppose we start near the stable equilibrium $z^* = 1$ and define $\mathcal{D} := [0, \infty)$, so that the point of escape $\chi = 0$ is the local maximum of the potential at the origin. It follows that

$$V(z^*, \chi) = 2(U(\chi) - U(z^*)) = \frac{1}{2} \quad \Rightarrow \quad \mathbb{E}[\tau_{\mathcal{D}}] \sim \kappa e^{\frac{1}{2\sigma^2}} \text{ as } \sigma \rightarrow 0.$$

Therefore, the time scale to escape from one stable equilibrium to the other stable equilibrium is exponentially large for small noise. One should note that for quite general gradient systems with additive noise and a saddle point u of the potential, one may also compute the prefactor κ using the **Arrhenius–Eyring–Kramers law**; see Section 15.10. ♦

Exercise/Project 15.8.9. Consider the van der Pol equation (15.83) for $\varepsilon = 0$. Examine large deviation principles for different values of the slow variable y . Do large deviations explain the dynamics in Figure 15.1? ◇

15.9 Dynkin's Equation and WKB

We keep the notation introduced in the last section,

$$dz = a(z) dt + \sigma A(z) dW, \quad z(t) \in \mathbb{R}^N, \quad \mathfrak{D}(z) = A(z)A(z)^\top, \quad (15.94)$$

where $W(t)$ is a vector of k independent Brownian motions; we also let $\tau_{\mathcal{D}}$ denote the first-exit time from a domain $\mathcal{D} \subset \mathbb{R}^N$. The goal is to illustrate an alternative approach to tackling the first exit problem. Recall from Section 15.1 that associated to an SDE there are PDEs (backward Kolmogorov and forward Kolmogorov / Fokker–Planck) that contain the full information of the probability density.

Theorem 15.9.1 ([FW98b]). *Let $z \in \mathcal{D}$, $\psi : \partial\mathcal{D} \rightarrow \mathbb{R}$, and $\rho : \mathcal{D} \rightarrow \mathbb{R}$ continuous, and define*

$$\begin{aligned} u(z) &= \mathbb{E} \left[\psi(z(\tau_{\mathcal{D}})) - \int_0^{\tau_{\mathcal{D}}} \rho(z(s)) ds \middle| z(0) = z \right] \\ &= \mathbb{E}^{0,z} \left[\psi(z(\tau_{\mathcal{D}})) - \int_0^{\tau_{\mathcal{D}}} \rho(z(s)) ds \right]. \end{aligned}$$

Then $u(z)$ is the unique solution of the Kolmogorov backward equation

$$\begin{cases} \rho(z) = \frac{\sigma^2}{2} \sum_{i,j=1}^N \mathfrak{D}_{ij}(z) \frac{\partial^2 u}{\partial z_i \partial z_j} + \sum_{i=1}^N a_i(z) \frac{\partial u}{\partial z_i}, & \text{for } z \in \mathcal{D}, \\ \psi(z) = u(z), & \text{for } z \in \partial\mathcal{D}. \end{cases} \quad (15.95)$$

If we let $\psi(z) \equiv 0$, $\rho(z) \equiv -1$, then $u(z) = \mathbb{E}[\tau_{\mathcal{D}}]|z(0) = z] = \mathbb{E}^{0,z}[\tau_{\mathcal{D}}]$ is the mean first exit time from a domain \mathcal{D} starting at z , and it solves

$$\begin{cases} -1 = \frac{\sigma^2}{2} \sum_{i,j=1}^N \mathfrak{D}_{ij}(z) \frac{\partial^2 u}{\partial z_i \partial z_j} + \sum_{i=1}^N a_i(z) \frac{\partial u}{\partial z_i}, & \text{for } z \in \mathcal{D}, \\ 0 = u(z), & \text{for } z \in \partial\mathcal{D}. \end{cases} \quad (15.96)$$

Sometimes, one also refers to (15.96) as **Dynkin's equation**. Therefore, Theorem 15.9.1 shows that we may also analyze an elliptic PDE with Dirichlet boundary conditions to understand the first-exit problem. The next example illustrates the simplest case.

Example 15.9.2. Returning to Example 15.8.1, where $a(z) = z - z^3$, $\mathfrak{D} = 1$, and $\mathcal{D} = [0, b]$ for some large fixed $b \gg 1$, we want to focus on the escape past the saddle at $z = 0$. It follows that (15.95) is given by

$$\frac{\sigma^2}{2} u''(z) + u'(z)(z - z^3) = -1, \quad u(0) = 0 = u(b). \quad (15.97)$$

Although an explicit formula for the solution of this ODE exists, it is much more important to notice that (15.97) is again a singularly perturbed problem for $\sigma \rightarrow 0$. In this one-dimensional case, one may even recognize a fast–slow system for $\varepsilon := \sigma^2/2$ and $u'(z) =: v(z)$, so that

$$\begin{aligned} \varepsilon \dot{v} &= -(z - z^3)v - 1, \\ \dot{u} &= v, \\ \dot{z} &= 1. \end{aligned} \quad (15.98)$$

Alternatively, the substitutions $\varepsilon := \sigma/\sqrt{2}$ and $\varepsilon u'(z) =: v(z)$ yield

$$\begin{aligned} \varepsilon \dot{v} &= -(z - z^3)v - 1, \\ \varepsilon \dot{u} &= v, \\ \dot{z} &= 1. \end{aligned} \quad (15.99)$$

Note that (15.99) has no critical manifold, since $v = 0$ implies $0 \cdot (z - z^3) = 1$, while the critical manifold for (15.98) is given by

$$C_0 = \{(v, u, z) \in \mathbb{R}^3 : (z^3 - z)v = 1\}. \quad (15.100)$$

Since there is a singularity at $z = 0$ and we also have a boundary condition at $z = 0$, we already see that the singular perturbation analysis of the exit-time problem is not straightforward. ♦

Example 15.9.2 shows already that working out the singularly perturbed Dynkin PDE (15.95) for small noise directly is not the best strategy. In fact, the same problem persists for every dimension. However, we already know from Section 15.8 that the mean exit time has an exponential scaling e^{K/σ^2} , so a natural approach is to use a WKB-type ansatz (see Section 9.4)

$$\tilde{u}(z) = e^{-K/\sigma^2} u(z), \quad \text{for some constant } K > 0, K = \mathcal{O}(1) \text{ as } \sigma \rightarrow 0, \quad (15.101)$$

so that $\tilde{u}(z) \sim \mathcal{O}(1)$ as $\sigma \rightarrow 0$. The resulting problem is

$$-e^{-K/\sigma^2} = \frac{\sigma^2}{2} \sum_{i,j=1}^N \mathfrak{D}_{ij}(z) \frac{\partial^2 \tilde{u}}{\partial z_i \partial z_j} + \sum_{i=1}^N a_i(z) \frac{\partial \tilde{u}}{\partial z_i} \quad (15.102)$$

with the Dirichlet boundary condition $e^{-K/\sigma^2} \tilde{u}(z) = 0$ for $z \in \partial\mathcal{D}$. To illustrate the calculation of the leading-order term $\tilde{u}_0(z)$ in the asymptotic expansion

$$\tilde{u}(z) = \tilde{u}_0(z) + \varepsilon \tilde{u}_1(z) + \dots,$$

we shall consider the simple planar situation of an attracting equilibrium point and noise-induced escape from the unit disk. More precisely, we consider

$$N = 2 = k, \quad a(0) = 0, \quad A(z) \equiv \text{Id}, \quad \mathcal{D} = \{z \in \mathbb{R}^2 : \|z\| \leq 1\}$$

with a vector field a pointing inward on $\partial\mathcal{D}$. We also assume that $z^* = 0$ is the only invariant set in \mathcal{D} and that z^* is stable. Then the formal leading-order PDE from (15.101) is just

$$0 = \sum_{i=1}^2 a_i(z) \frac{\partial \tilde{u}}{\partial z_i} = a(z)^\top \nabla \tilde{u},$$

which can be solved using the method of characteristics; see Section 17.3. But the characteristics are just flow lines of the planar vector field $z' = a(z)$. Using the dynamical assumptions on $z' = a(z)$, it follows that all characteristics meet at $z^* = 0$. Let us make the assumption, which one has to verify eventually, that \tilde{u}_0 is continuous. By continuity at $z^* = 0$ and the fact that $\tilde{u}_0(z)$ is also constant on characteristics, it follows that $\tilde{u}_0(z) \equiv \kappa_0$ for some constant κ_0 to be computed.

However, we have not derived a solution that satisfies the boundary condition, i.e., $\tilde{u}_0 = \kappa_0$ is the leading-order term in an outer expansion, as discussed in Section 9.1. Near the boundary $\partial\mathcal{D} = S^1$, an inner expansion has to be developed, and we focus on the point $(z_1, z_2) = (0, 1)$ without loss of generality. Consider a small neighborhood $\mathcal{B} \subset \mathbb{R}^2$ of $(0, 1)^\top$ and define the mapping

$$\tilde{v} = \zeta(z) := \frac{z_1^2 + z_2^2 - 1}{2}. \quad (15.103)$$

The transformation (15.103) locally straightens the boundary, so that the inside of \mathcal{D} corresponds to $\tilde{v} < 0$, and $\partial\mathcal{D}$ to $\tilde{v} = 0$. Furthermore, the point $(0, 1)$ is moved to $(0, 0)$. Observe that the outer unit normal vector $\vec{n} = (0, 1)^\top$ can also be expressed as $\vec{n} = \nabla \zeta$. In the new coordinates (z_1, \tilde{v}) , we aim for a dominant balance argument (see Sections 9.1 and 9.2) and define $v := \tilde{v}/\sigma^2$.

Exercise 15.9.3. Carry out the change-of-variable (15.103) and the scaling $v = \tilde{v}/\sigma^2$ for (15.102). Substitute $\tilde{u} \sim \sum_j \tilde{U}_j(z_1, v)\sigma^j$ into the resulting equation to derive that the leading-order term satisfies the ODE

$$\frac{1}{2} \frac{\partial^2 \tilde{U}_0}{\partial v^2} + a_2(0, 1) \frac{\partial \tilde{U}_0}{\partial v} = 0$$

for $v \in (-\infty, 0)$ and boundary condition $\tilde{U}_0(0, 1) = 0$. Hence, prove that $\tilde{U}_0 = \kappa^*(z_1)(1 - \exp(-\frac{v}{2\alpha}))$, where $\alpha = a_2(0, 1) < 0$ and $\kappa^*(z_1)$ is some function of z_1 . \diamond

Using the insight from Exercise 15.9.3, it follows that the general leading-order approximation term near $\partial\mathcal{D}$ is given by

$$\tilde{U}_0 = \kappa(z) \left[1 - \exp \left(-\frac{\alpha(z)}{2\sigma^2} \right) \right],$$

where $\alpha(z), \kappa(z)$ can be computed from the vector field $a = a(z)$ near $\partial\mathcal{D}$. However, using asymptotic matching, we must have that \tilde{U}_0 and \tilde{u}_0 agree on an overlap region, which is possible only if $\kappa(z) \equiv \kappa_0$. The resulting leading-order composite expansion is

$$u(z) \sim \kappa_0 \exp \left(\frac{K}{\sigma^2} \right) \left[1 - \exp \left(-\frac{\alpha(z)}{2\sigma^2} \right) \right] + \dots \quad \text{as } \sigma \rightarrow 0. \quad (15.104)$$

Hence, if we fix all quantities except $\sigma \rightarrow 0$ then the first-exit time increases exponentially. However, if we fix $0 < \sigma \ll 1$ and vary the initial point z , then the mean exit time decays as $z \rightarrow \partial\mathcal{D}$, since $\alpha(z) < 0$.

There is a large literature on singular perturbation techniques for first-exit problems. The formula (15.104) can also be quantified in much more detail, e.g., by computing the prefactor κ as a function of σ ; see Section 15.10 for more details.

15.10 References

Section 15.1: The material presented in this section can be found in many different background sources [Fre96]. There are many good motivations to consider noisy dynamics, for example in neuroscience [DRL12, Fox97]. Clearly, noise-induced phenomena such as stochastic resonance [BSV81, JH91, NN81, PK97, Tal99, WSB04] and related effects [DDEM05, GHJM98, GMSS99, GMS95, Gam95, GMSS⁺89, HJZM93] are among the most spectacular aspects of stochastic multiscale systems, since they yield new nondeterministic dynamical effects. The simplest classes of examples for stochastic resonance and the potential regularizing effect of noise on the interspike interval distribution are those of FitzHugh–Nagumo type and of van der Pol type [Lin04, LGONSG04, LSG99, LSG00, KPLM13, LC98]. However, the noise-induced resonance effects appear in many applications, such as biological information processing [Hän02], climate science [BPSV82, BPSV83], ecology [SMSG07], epidemics [KGG07, YKL06], information theory [GH00, SGH01], networks [Kue12b], neuroscience [HE05, Lon97], nucleation [MGB95], and optics [BHJ94]. Also in other contexts, van der Pol-type equations provide a playground for understanding fast–slow SDEs [Che82, Nar93, Nar91, Nar87], so our choice of example is quite standard. It is clear from the setup that multiple small parameters should play a key role in the field [FS99a, Hel02, Spi13a].

Section 15.2: The main sources for this section are [BG06, BG03]. The idea to use the covariance to control a stochastic process is used quite frequently [CMR13]. For a direct asymptotics approach to stochastic Fenichel theory, see [KP92, Per94a, KPS91]. The neuroscience example is considered in [CSRR08, Kue12a]. The pathwise theory can also be applied to the noise-induced passage through fast subsystem periodic

orbits [BG04, BG13a], to neuroscience models [BG09, LL09a], and to climate models [BG02d, Kwa13]. The estimates are also directly related to fluctuation–dissipation theorems [Abr10, MAG05] and linear response theory [AK13a, HM10], which we do not cover.

Section 15.3: This section was compiled from [BG06]. Various other bifurcation phenomena can be treated similarly [BG02e, BG02a, BG02c, BG02b], including the small noisy oscillations near a folded node in \mathbb{R}^3 [BGK12]; see also [BGK13, BKLC10, KB02, KB09a, SK11b, TKD13, YKL08] for more on noisy MMOs and [CFNS09, CK88, VS00, HM09c, JZLZ13, SRT04, WSGR11] for noisy bursting oscillations. We have not discussed canards $\mathcal{O}(1)$ -away from a singular Hopf bifurcation, since they are usually destroyed by noise except in the exponentially small noise case [Sow08]. This effect of noise-induced shortening of bifurcation delay has been known for quite some time [TM88, dBM87, VMS00, ZMD89]. Note that it can have a positive regularizing or optimizing effect [Kue12b]. One may also apply probability-density-based methods to understand fast subsystem delayed bifurcations [Kus99, Kus00], i.e., dynamic bifurcations in the presence of noise [JL98, Kus03, ZGO13]. The effect also carries over to stochastic partial differential equations (SPDEs) [Lyt95].

Section 15.4: The asymptotics were derived in the works [MVE08, MVEE05]. They help in understanding the substochastic Markov chain [Num84] of spikes in the noisy FitzHugh–Nagumo equation [BL12, GX01, NBK13]. In fact, firing patterns on stochastic input is a key topic in applications [BFF99]. Singular perturbation methods can be applied to a wide variety of stochastic problems [Hop95, KP03a, Pap77, Pap76], and the existence of boundary-layer-type solutions for SDEs has been known for some time [BS79]. In fact, other classical methods that we discussed are applicable to stochastic problems such as matched asymptotic expansions [WK93, WHK93] and the boundary function method [Bob07]. Of course, one may also apply asymptotic methods for the probability density [GH99, KY05, KY96b, KY96c]; see also the references for Section 15.9 below.

Section 15.5: Operator-theoretic reduction [Gar09] and the general need for stochastic reduction methods [Raz78] are quite well known and have many applications [GMG07, Mun79]. Regarding the first example, the multiscale nature of Brownian motion is still a key topic in stochastic analysis [CD09]. Nice application examples in which the reduction of stochastic models is required include climate models [FMVE05, MTVE03, MTVE01, MTVE06, MTVE99, MTVE02] and general fluid dynamics problems [KM03b, KM03a]. There are other reduction techniques. For a path-integral formulation of stochastic reduction, see [SM11], and for linear-noise approximation, consider [TGS12, TSG11]. The philosophy also carries over to kinetic Fokker–Planck equations [WB87a, WB87b, WB87c]. One may also consider reduction ideas for other stochastic models such as jump-Markov processes [LMYZ12, Yvi13] and various versions of the master equation [BKWL12].

Section 15.6: This section is based mainly on [SS08b]; see also [FLD13]. For general background on random dynamical systems, consider [Arn95, Arn03]. A quite general approach to persistence of normally hyperbolic invariant manifolds for random dynamical systems can be found in [LLB13]. One may also look into the dynamics on a random attracting slow manifold and ask about random attractors [CF94, SH98]. Another task is to approximate random slow manifolds numerically [RDJ12]. There is also a relation to parameter estimation [RD13]. Furthermore, we note that the skew-product viewpoint of RDS can also be applied to deterministic fast–slow systems

[Art99b]. Furthermore, one may ask for the extension of random slow manifolds for RDS generated by SPDEs [DLS03, DLS04, DD07].

Section 15.7: Basic background on Markov chains can be found in [Nor06, Res92]. This section was based on a very small subset of the book [YZ98]. For the discrete-time case, see [YZ05, YZ03], and for a detailed analysis of various singularly perturbed Markov chains, consider [YZB00a, YZB00c, YZ00, ZY96, ZY04]; for another view, see [AFH13]. Multiscale Markov chains arise in many situations [DVE06, NY10] and have crucial applications such as chemical reaction networks [BKPR06, PP13]. The topic has been of interest for quite a long time in applied mathematics [CWS83b, Del83, RW88], and asymptotic methods have often been the core technique [KY97, KY96a]. Perturbed Markov chains also arise frequently in control theory [AF92, AF95, AFB90, BF91, ZY99, Zha96, YZ97, YZ94, YYYZ02, ZYB97] and have interesting applications such as consensus formation [KTY09], economic market models [ZYL05], filtering [YD03, WZY06, ZYM07], hybrid systems [YZ02b], network traffic [GKT97, TGT95], queueing theory [YZ04b, YZ08, YZ07, YZ02a], and time-dependent parameter estimation [YK05]. Another interesting direction is fast–slow Markov chains and phase transitions [DG93b, DG93a].

Section 15.8: This section is based mostly on [FW98b, DZ98]. The presented theory is now commonly known as Wentzell–Freidlin theory [WF70, WF73, Fre73] or large deviation principles (LDPs) [DV75a, DV75b, DV76, DV83a] due to Donsker and Varadhan [DV89, KOV89, Var08]. There are several variations available for fast–slow systems [KP95, Lip96, Puh13]. LDPs are covered extensively in the literature [dH08, DS89a, Var84]. They also hold for many graph-related models [FW93, FW06, Fre00a, FW98a, FW99, FW04], Markov chains [OS95, OS96], percolation-type problems [DP96], and SPDEs [BG13b, CR05, CR04, CR03, KORVE07, WRD12]. LDPs can also be applied to deterministic PDEs [Fre85, Fre91] and to understanding stochastic resonance [Fre00b, Fre01, HI05, HI02], which was previously studied via spectral power amplification [IP02, IP01]. The Arrhenius–Eyring–Kramers law [Arr89, Eyr35, Kra40] is one of the classical topics of statistical physics [Ber13, HTB90a, HIP08]. The exact prefactor was proved recently using potential theory [BEGK04, BGK05], but it can also be obtained using semiclassical analysis [HN04, HN05]. There are many different generalizations and extensions available, e.g., to discrete-time systems [Kif90], exit-time distributions [Dur85, Dur92, MOS89], moderate deviation principles (MDPs) [GL05], and Markov chains [Bak00, Bak03]. One may also aim for a much finer estimate involving so-called characteristic boundaries [MS01a, MS92, MS96a]. The associated exit laws [Day83, Day87, Day89, Day94, Day90, Day92, Day95, Day84] from a domain [Kif81, MS97, MS93b, MS93a] may also be viewed as a control problem [PZ92, Fle77, Fle71] connecting it to Hamilton–Jacobi equations. The exit problem for Lévy processes has also generated interest [IP06a, IP06b, IPW09]. A recent direction in the spirit of large deviations is to develop transition path theory (TPT) [EVE06, EVE10, EVE04], since the link between metastability and transition paths has a long history in statistical physics [CGOV84, OV05]; see [MSVE06, MSVE09] for example applications of TPT. It is also natural to ask for reduced models for transitions between states [GOV87a, LL13, SS11b].

Section 15.9: The basis for this section was the book [Sch09b], where singular perturbations for SDEs are a focus [Sch80]. The material is quite classical by now, building on the series of works [MS77, MS79, MS82, MSBJ82, MST83, NKMS90]. One may extend many of the results to colored noise [KDMS88, KDMS89, MS88].

There are several interesting applications of singular perturbation theory to large deviations and mean-first passage times [BS82, DEF74]. In fact, the WKB method reappears quite frequently for various noisy multiscale problems [BJBMS82, BM11, BN13, FJ92, MS96b]. Extensions of large deviation principles exist in certain situations, e.g., for escape from a domain via a narrow hole [HS04, SSH07], other narrow-escape-type models [CWS10, PWPK10, SSHE06, SSH06a, SSH06b, SSH08], Markov jump processes [MSK⁺84, KMZT85, KMZT86c], and even non-Markovian processes [DMS86a, DMS86b]. Furthermore, it should be noted that there are further links to deterministic elliptic boundary value problems [EF90, EF93], semiclassical analysis [HS84, HHS08, Sim83, Sim84], and spectral theory [HMS04, Mat95, Sug95]. For links to evolution equations for measures, see [PSV12, PSV10]. Last but not least, we shall mention that LDPs generally do not apply to rugged energy landscapes in which many small jumps occur [SN13].

As expected, stochastic averaging works for many SDEs, similar to the deterministic case [BK04, Fre78, KK01, KY04, Kif01b, LS00, Wai11, WF70], and it can be carried through to various other situations such as conditional averages [SWHH04, WS06a], discrete time [Bak96], energy projection methods [BKM12], stochastic Hamiltonian systems [Li08], hybrid systems [KMS04], jump processes [GT12a, GT12b], Lévy noise [XDX11], Markov chains [YZB00b], random differential equations [Gem79], random impulsive systems [SS11a], in connection to slow manifolds [WR13], stochastic control systems [BG07a, Kus90], stochastic partial differential equations [Bré12a, Cer09, Cer11, CF09, FD11, WR12], stochastic reaction networks [PS06], stratified spaces [Sow02], and tangent flows [Sow01].

There are many other nice interactions between noise and fast–slow systems such as blinking systems [HBB13a, HBB13b], Brownian particle interactions [BPH94], filtering [MK93a], Fleming–Viot processes [Gup12], Glauber dynamics [BdHS10, CFM12, dH04], noisy Hamiltonian systems [O'B03], hidden Markov models [HDFS06], integrodifferential equations [IKY99], the Isaacs equation [Zha95], jump diffusions [BY02, KY99, Yin01, YK99, YZ10, YY04], Kawasaki dynamics [BdHN06], mixed discrete–continuous equations [GK04], random matrix theory [Dys62, ESY11, GMGW98], ratchets [RMSaSL12], stochastic approximation algorithms [Bor97, MP11], superprocesses [MT12], three-wave resonance [LP93], and variational principles [NN13].

Since we have given only an introduction, we had to skip spatially extended systems and fast–slow dynamics that occur, e.g., in Allen–Cahn-type/Nagumo equations [HL00a, TR98], the Cahn–Hilliard model [ABK12, BGW10], the Ginzburg–Landau equation [Lyt96, Ste04], the Kuramoto–Sivashinsky equation [PTK⁺11], various SPDE amplitude equations [Blö07, Blö03, BH04, BHP07, BHP05, BM09], SPDEs with fast boundary conditions [WD09, FW92], SPDEs in perforated domains [WDD07, WD07], and the Swift–Hohenberg equation [MBK13]. A similar remark applies to the less developed field of stochastic delay equations [Kus10, KK05].

Also, the statistical direction has not been covered appropriately; for example, sampling of multiscale processes is extremely important [DSW12, Spi13b] as well as parameter estimation [BC94b, KPK13, PS07a, PPS09]. Stochasticity and multiple time scales in chemical systems is another interesting direction to consider [KGN98]; another nice application area is lasers [CDG⁺98]. Queuing systems is a topic that we have omitted here as well [KMZT86a, KMZT86b, KMZT87b, KMZT87c, KMZT87a]. Another challenging task is to push stochastic methods further in the context of climate models [FG13]. Furthermore, there are connections to homogenization and classical

Langevin equations [[PS05b](#), [PSZ07](#), [PS05a](#), [Pav05](#), [OP11](#), [PK75](#)] and various second-order problems [[CF06a](#), [CF06b](#), [Fre04](#), [PV01](#)]. On the numerical side, there are several topics that we have omitted as well, such as stochastic sampling algorithms [[CL11](#), [BLP12](#), [LSR07](#), [LSR10](#)] and the string method for rare events [[ERVE02](#), [ERVE05](#)]; see also Section 10.9. A general challenging question is to determine what really constitutes a “stochastic bifurcation” [[Nam90](#), [HL06](#), [SH96](#)].

Chapter 16

Topological Methods

All methods to understand multiple time scale systems we have presented so far needed some kind of mathematical analysis. In particular, for any geometric construction, asymptotic calculation, or numerical method, we needed tools such as transversality arguments, asymptotic comparison, and error estimates. But what if we are primarily interested in existence statements such as, does a given fast–slow system have a periodic orbit? In this chapter, we shall use a different approach, based on (algebraic) topology, to answer existence questions using only a minimal amount of analytic information.

The main tool is the Conley index, which is introduced in Sections 16.1 and 16.2. It has been used successfully in a variety of dynamical systems to prove the existence of invariant sets. The case of connecting orbits between equilibria is considered in Section 16.3. Since our focus is on the main ideas for fast–slow systems, Section 16.4 deals with the translation of the multiple time scale geometry into topological objects utilizing singular index pairs. Section 16.4 illustrates how this approach can be taken further, i.e., how the natural fast–slow decomposition also translates into a topological decomposition.

Background: In this chapter, we assume that the reader either has, or is willing to acquire, a solid background in algebraic topology; otherwise, one has to accept many statements on faith. A highly recommended textbook is [Hat02]. Other interesting alternatives are [Ful97, Mun96, Wal07b, Wal07a], while one could also stay more with the geometric viewpoint via [Bre97] or aim for a really ambitious “introduction” with [Spa66].

16.1 Decomposition of Invariant Sets

Instead of analyzing trajectories of dynamical systems directly, another possibility is to capture regions of interest in phase space by suitable sets, prove topological/algebraic statements about those sets, and then draw conclusions

about the dynamics from this information. We begin with the general case without time scale separation. Let $\phi : \mathbb{R}^N \times \mathbb{R} \rightarrow \mathbb{R}^N$ denote a flow, $(z, t) \in \mathbb{R}^N \times \mathbb{R}$ the space and time coordinates, e.g., $\{\phi(z, t) \in \mathbb{R}^N : t \in [0, \infty)\}$ is the forward orbit starting at z .

Definition 16.1.1. A compact set $\mathcal{N} \subset \mathbb{R}^N$ is called an **isolating neighborhood** if

$$\text{Inv}(\mathcal{N}, \phi) := \{z \in \mathcal{N} : \phi(z, \mathbb{R}) \subset \mathcal{N}\} \subset \mathcal{N}^\circ,$$

where \mathcal{N}° denotes the interior of \mathcal{N} .

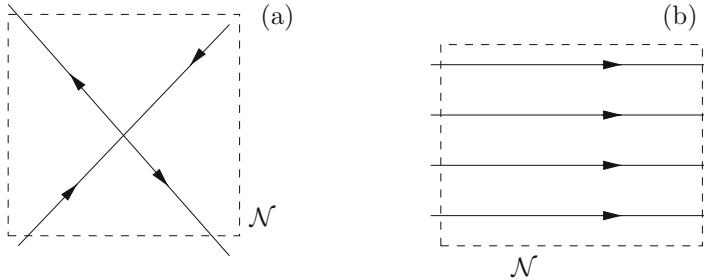


Figure 16.1: (a) Saddle equilibrium, any nondegenerate disk or rectangle easily gives an isolating neighborhood. (b) Regular flow; the set $\text{Inv}(\mathcal{N}, \phi)$ is empty.

The requirement for an isolating neighborhood is rather weak; two examples are shown in Figure 16.1. For example, if we consider the saddle equilibrium in Figure 16.1(a), it is clear that an open neighborhood of the equilibrium gives an isolating neighborhood and that $\text{Inv}(\mathcal{N}, \phi)$ consists of the equilibrium itself. It is not difficult to show that isolating neighborhoods are “stable” under perturbation, i.e., consider a continuously parameterized flow

$$\phi_\lambda : \mathbb{R}^N \times \mathbb{R} \rightarrow \mathbb{R}^N \quad \text{for } \lambda \in [-1, 1].$$

Proposition 16.1.2. Let \mathcal{N} be an isolating neighborhood for ϕ_0 . Then for $|\lambda| < \delta$ with $\delta > 0$ sufficiently small, \mathcal{N} is an isolating invariant neighborhood for ϕ_λ .

Definition 16.1.3. Let $\mathcal{N} \subset \mathbb{R}^N$ be a compact set and let $S_\lambda := \text{Inv}(\mathcal{N}, \phi_\lambda)$. Two isolated invariant sets $S_{\lambda_0}, S_{\lambda_1}$ are **related by continuation** if \mathcal{N} is an isolating neighborhood for all ϕ_λ with $\lambda \in [\lambda_0, \lambda_1]$.

Consider Figure 16.1(a) again and perturb the flow. Then the saddle equilibrium point generically will move slightly. Hence, the two equilibria are related by continuation if we choose an isolated neighborhood of suitable size. Note that the main statement in Definition 16.1.3 is about the isolating neighborhood \mathcal{N} , not about the invariant sets. The next step is to try to deduce some of the structure of the invariant set by studying \mathcal{N} .

Example 16.1.4. Consider a planar flow ϕ_λ with two hyperbolic saddle equilibrium points p_1 and p_2 . Suppose there exists a **heteroclinic orbit** S for the parameter $\lambda = 0$, i.e., if $z \in \gamma \subset \mathbb{R}^2$, then

$$p_1 = \lim_{t \rightarrow -\infty} \phi_0(z, t) \quad \text{and} \quad p_2 = \lim_{t \rightarrow \infty} \phi_0(z, t),$$

as shown in Figure 16.2. Alternatively, we can also write the condition for a heteroclinic connection in terms of α - and ω -limit sets

$$\begin{aligned} p_1 &= \alpha(z) = \alpha(\gamma, \phi) = \bigcap_{s \in \mathbb{R}} \overline{\{\phi(z, t) : t < s\}}, \\ p_2 &= \omega(z) = \omega(\gamma, \phi) = \bigcap_{s \in \mathbb{R}} \overline{\{\phi(z, t) : t > s\}}, \end{aligned}$$

where we have recalled alternative notation and the definitions of α - and ω -limit sets in the last equation.

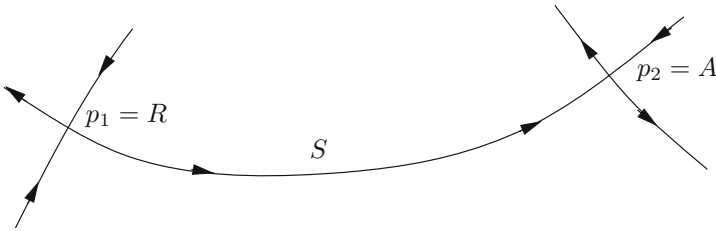


Figure 16.2: Heteroclinic connection between two saddle equilibrium points.

The heteroclinic connection S can be decomposed into the two saddles—one attracting for points in S and the other repelling—and the remaining part of the connection. Instead of studying the detailed flow between p_1 and p_2 , a goal of this chapter is to introduce an algebraic-topological method to determine for what values of λ the heteroclinic connection exists. ♦

The following definition provides a general framework for decomposing invariant sets.

Definition 16.1.5. Let $S \subset \mathbb{R}^N$ be a compact invariant set. We say that $A \subset S$ is an **attractor** in S if there exists a neighborhood U of A such that

$$\omega(U \cap S) = A.$$

The corresponding **dual repeller** of A in S is

$$R := \{z \in S : \omega(z) \cap A = \emptyset\}.$$

The pair (A, R) is called an **attractor–repeller pair decomposition** of S .

It is not difficult to see that the definition of attractors and repellers in Definition 16.1.5 entails that A and R are isolated invariant sets. In the case of the heteroclinic connection in Example 16.1.4, we simply have $(A, R) = (p_2, p_1)$. Traditionally, the next observation is stated in the form of a theorem.

Theorem 16.1.6 ([MM02]; see also [Con78, McC88, Sal85]). *Let (A, R) be an attractor–repeller decomposition of an invariant set S . Define the **connecting orbits** by*

$$C(R, A; S) := \{z \in S : \omega(z) \subset A, \alpha(z) \subset R\}.$$

Then S decomposes as $S = A \cup R \cup C(R, A; S)$.

Exercise 16.1.7. Show that attractor–repeller decompositions continue under small parameter variations. More precisely, given an attractor–repeller pair (A_λ, R_λ) in S_λ for $\lambda = 0$, there is an interval $I = [-\lambda_*, \lambda_*]$ with $\lambda_* > 0$ such that (A_λ, R_λ) is an attractor–repeller pair for $\lambda \in I$. Furthermore, A , R , and S continue; for example, A_{λ_1} continues to A_{λ_2} for $\lambda_{1,2} \in I$. \diamond

Having understood how to trace the definitions introduced so far, we proceed to more-concrete examples.

Example 16.1.8. Suppose we are given the following planar ODE for $z = (x, y) \in \mathbb{R}^2$:

$$\begin{aligned} x' &= y, \\ y' &= cy + \lambda - x^2, \end{aligned} \tag{16.1}$$

for $c \in \mathbb{R}$ and $\lambda \in [-1, 1]$. The goal is to establish a suitable attractor–repeller decomposition for (16.1). It is easy to see that the rectangle $\mathcal{N} = [-k, k]^2 \subset \mathbb{R}^2$ is an isolating neighborhood as long as $k > 0$ is chosen sufficiently large; see also the phase portrait for the system in Figure 16.3.

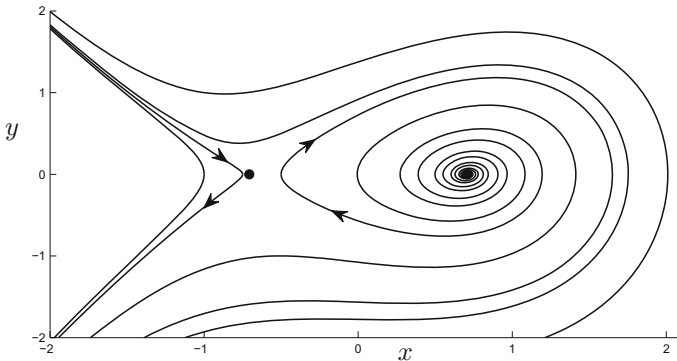


Figure 16.3: Phase portrait for (16.1) with $c = \frac{1}{4}$ and $\lambda = \frac{1}{2}$ the two equilibria $(\pm 1/\sqrt{2}, 0)$ are marked with black dots.

Define $S_{c,\lambda} = \text{Inv}(\mathcal{N})$ and consider the case $c > 0$ and $\lambda \in (0, 1)$. Then (16.1) has two equilibrium points $(\pm\sqrt{\lambda}, 0)$. It is not difficult to check that $((-\sqrt{\lambda}, 0), (\sqrt{\lambda}, 0))$ is an attractor–repeller pair; see Figure 16.3. And $S_{c,\lambda}$ can be decomposed into the two equilibria and a connecting orbit between them. Of course, the nice attractor–repeller decomposition breaks down for $\lambda = 0$ and also for $c = 0$ if $\lambda > 0$. \blacklozenge

Example 16.1.9. Another natural problem occurs when we have more than two invariant sets. Consider

$$\begin{aligned} x' &= y, \\ y' &= cy + (x^2 - 1) \left(x + \frac{1}{2} \right). \end{aligned} \quad (16.2)$$

System (16.2) has three equilibrium points, $(-1, 0)$, $(-1/2, 0)$, and $(1, 0)$. For an attractor–repeller pair, we can easily define an order on the sets, e.g., we could agree on $R > A$, but it is not so clear how to proceed for more complicated invariant sets such as a set with many equilibrium points. ♦

A relation $<$ on a set \mathcal{P} is called a **partial order** if $p > p$ never holds for $p \in \mathcal{P}$ and if $p > q$ and $q > r$ implies $p > r$. If, in addition, we have for all $p, q \in \mathcal{P}$ that either $p > q$ or $q > p$, then $>$ is a **total order**. Ordering attractor–repeller pairs can easily be done by a total order (“from the repeller, to the attractor”), but for more complicated invariant sets, one might not be able to compare the points in two sets. Hence, we must use a partial order.

Definition 16.1.10. A finite collection $\mathcal{M}(S) = \{M(p) : p \in \mathcal{P}\}$ of disjoint compact invariant subsets of S is called a **Morse decomposition** if there exists a partial order $>$ on the index set \mathcal{P} such that for every

$$z \in S - \bigcup_{p \in \mathcal{P}} M(p),$$

there exist $p, q \in \mathcal{P}$ such that $p > q$ and

$$\omega(z) \subset M(q) \quad \text{and} \quad \alpha(z) \subset M(p).$$

A subset $I \subset \mathcal{P}$ is called an **interval** if $p, q \in I$ and $p > r > q$ implies $r \in I$. The set of intervals on $(\mathcal{P}, >)$ will be denoted by $\mathcal{I}(\mathcal{P}, >)$.

Example 16.1.11. Consider Example 16.1.9 again. Let $\mathcal{N} = [-k, k]^2$ be chosen with $k > 0$ such that all three equilibria of (16.2) are contained in \mathcal{N} , and set $S_c := \text{Inv}(\mathcal{N})$. Figure 16.4 shows a typical phase portrait for $c > 0$.

We want to construct a Morse decomposition for S_c . First, one defines

$$M(1) := (1, 0), \quad M(2) := (-1, 0), \quad M(3) := (-1/2, 0).$$

One possible partial ordering $>$ that gives a Morse decomposition is $3 > 2 > 1$, so that

$$\mathcal{M}(S_c) = \{M(i) : i = 1, 2, 3 \text{ with } 3 > 2 > 1\}. \quad \blacklozenge$$

Unfortunately, just decomposing some invariant sets is not sufficient. We have not yet learned enough about connecting orbits or nontrivial invariant sets such as periodic orbits.

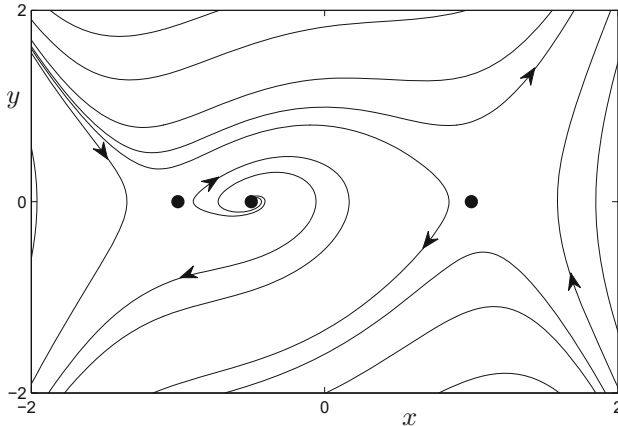


Figure 16.4: Phase portrait for (16.2) with $c = \frac{1}{2}$; the three equilibria are marked with black dots.

16.2 Conley Index

The Conley index allows us to attach an algebraic invariant to a certain set. Sometimes, this is an invariant that allows us to exclude only certain dynamical behavior. In other situations, it can be powerful enough to locate complicated invariant sets explicitly. The following definition is of fundamental importance in all results and ideas to follow.

Definition 16.2.1. Let S be an isolated invariant set. A pair of compact sets (\mathcal{N}, L) with $L \subset \mathcal{N}$ is called an **index pair** for S if the following conditions hold:

- (a) $S = \text{Inv}(\overline{\mathcal{N}} - L)$ (where $\overline{\mathcal{N}} - L$ is the closure of $\mathcal{N} - L$) and $\mathcal{N} - L$ is a neighborhood of S ;
- (b) L is positively invariant in \mathcal{N} , i.e., for every $z \in L$ and $\phi(z, [0, t]) \subset \mathcal{N}$, we have $\phi(z, [0, t]) \subset L$;
- (c) L is an **exit set** for \mathcal{N} , i.e., for every $z \in \mathcal{N}$ and $t_1 > 0$ such that $\phi(z, t_1) \notin \mathcal{N}$, there exists $t_0 \in [0, t_1]$ for which $\phi(z, [0, t_0]) \subset \mathcal{N}$ and $\phi(z, t_0) \in L$.

Example 16.2.2. Consider the following very simple ODE $z' = z$ for $z = (z_1, z_2) \in \mathbb{R}^2$. Obviously, the origin $0 = (0, 0)$ is an unstable node. Define

$$\mathcal{N} = B(0, r) \quad \text{and} \quad L = \partial B(0, r),$$

where $B(0, r)$ denotes the closed ball centered at 0 of radius $r > 0$. Then it is not difficult to check that (\mathcal{N}, L) is an index pair for $S = \text{Inv}(\mathcal{N}) = \{0\}$. Indeed, conditions (a) and (b) of Definition 16.2.1 hold, and all trajectories leave through the boundary L , so that L is an exit set. ♦

A stricter concept than isolating neighborhoods and index pairs is that of isolating blocks.

Definition 16.2.3. A compact set \mathcal{B} is called an **isolating block** if

$$\mathcal{B}^- := \{z \in \mathcal{B} : \phi(z, [0, T)) \not\subset \mathcal{B}, \forall T > 0\} \quad (16.3)$$

is closed and for all $T > 0$, and we require

$$\text{Inv}_T(\mathcal{B}, \phi) := \{z \in \mathcal{B} : \phi(z, [-T, T]) \subset \mathcal{B}\} \subset \mathcal{B}^o,$$

where \mathcal{B}^o denotes the interior of \mathcal{B} .

Example 16.2.4. Returning to Example 16.2.2 and the ODE $z' = z$ for $z \in \mathbb{R}^2$, we again consider a closed ball $B(0, r)$ and let

$$\mathcal{B} = B(0, r) \quad \text{and therefore} \quad \mathcal{B}^- = \partial B(0, r).$$

Obviously, \mathcal{B} is compact and \mathcal{B}^- is closed. Also it is not difficult to see that for every $T > 0$, we have $\text{Inv}_T(\mathcal{B}, \phi) \subset \mathcal{B}^o$. Note that $(\mathcal{B}, \mathcal{B}^-)$ is an index pair, as shown in Example 16.2.2. ♦

Hence, Example 16.2.4 suggests that there is a close connection between index pairs and isolating blocks. The next theorem makes this connection more precise.

Theorem 16.2.5 ([MM02]; see also [Con78, CE71]). *Let S be an isolated invariant set. Then there exists an isolating block \mathcal{B} such that $S = \text{Inv}(\mathcal{B})$. In addition, $(\mathcal{B}, \mathcal{B}^-)$ is an index pair for S .*

Our main object of interest will be index pairs, but many classical results use isolating blocks as well, and hence we have mentioned them here. Finally, we are ready to define two versions of the Conley index. The next definition assumes basic familiarity with the concepts of algebraic topology; see Section 16.6 for suitable background reading.

Definition 16.2.6. Let (\mathcal{N}, L) be an index pair for an isolated invariant set S . The **(homological) Conley index** of S is

$$CH_*(S) := H_*(\mathcal{N}, L),$$

where $H_*(X, A)$ denotes the homology of a space X relative to a subspace A [Hat02]. We can also define the **(cohomological) Conley index** as

$$CH^*(S) := H^*(\mathcal{N}, L).$$

Note that coefficients in \mathbb{Z} are usually understood for homology and cohomology if we do not specify them explicitly. A homotopy version of the Conley index exists as well but is often not very suitable for computations. The next result is required to show that Definition 16.2.6 actually makes sense.

Proposition 16.2.7. *The Conley index is well defined, i.e., given two different index pairs (\mathcal{N}, L) and (\mathcal{N}', L') for an invariant set S , the homology and cohomology are isomorphic:*

$$CH_*(\mathcal{N}, L) \cong CH_*(\mathcal{N}', L') \quad \text{and} \quad CH^*(\mathcal{N}, L) \cong CH^*(\mathcal{N}', L').$$

Therefore, we shall sometimes also write $CH_*(S)$ or $CH^*(S)$.

In practice, we shall use both the homological and cohomological versions. It is understood that most general theorems we state, say for CH_* , have a suitable analogue for CH^* .

Theorem 16.2.8 (Continuation property, [MM02]; see also [Con78, Sal85]). *The Conley index is constant under continuation. More precisely, let S_{λ_1} and S_{λ_2} be invariant sets that are related by continuation. Then*

$$CH_*(S_{\lambda_1}) = CH_*(S_{\lambda_2}).$$

It is also not unexpected that the algebraic summation property of relative homology carries over nicely.

Theorem 16.2.9 (Summation property, [MM02]; see also [Con78, Sal85]). *Assume that $S = S_1 \cup S_2$ is an isolated invariant set with S_1 and S_2 disjoint isolated invariant sets as well. Then it follows that*

$$CH_*(S) = CH_*(S_1) \oplus CH_*(S_2).$$

Proof. Since S_i for $i = 1, 2$ are disjoint invariant sets, we can find disjoint isolating neighborhoods \mathcal{N}_i with index pairs (N_i, L_i) . A direct calculation then yields

$$\begin{aligned} CH_*(S) &= H_*(\mathcal{N}_1 \cup \mathcal{N}_2, L_1 \cup L_2) = H_*(\mathcal{N}_1, L_1) \oplus H_*(\mathcal{N}_2, L_2) \\ &= CH_*(S_1) \oplus CH_*(S_2), \end{aligned}$$

where the summation property of relative homology [Hat02] was used in the second equality. \square

It is not difficult to see that $CH_*(\emptyset) = 0$, and the easy converse of this statement is surprisingly useful.

Theorem 16.2.10 (Wazewski property, [MM02]; see also [Con78, Sal85]). *Let \mathcal{N} be an isolating neighborhood and assume that $CH_*(Inv(\mathcal{N})) \neq 0$. Then $Inv(\mathcal{N}) \neq \emptyset$.*

The easiest way to apply Theorem 16.2.10 is to choose an isolating neighborhood where one suspects to find interesting dynamics, then compute that the Conley index is nontrivial (i.e., not zero) and conclude that there is some interesting invariant set. Frequently, one may want something a bit more refined than the last argument, and for certain invariant sets this is possible.

Theorem 16.2.11 ([MM02]; see also [Con78, Sal85]). *Let S be a hyperbolic equilibrium point for an ODE with unstable manifold of dimension n . Then*

$$CH_k(S) = \begin{cases} \mathbb{Z} & \text{if } k = n, \\ 0 & \text{otherwise.} \end{cases}$$

Proof. (Sketch; [MM02]) Moving the equilibrium S to the origin and applying the Hartman–Grobman theorem, we can consider the topologically equivalent linear system

$$\begin{aligned} z'_1 &= Az_1, \\ z'_2 &= Bz_2, \end{aligned}$$

for $z \in \mathbb{R}^{m+n}$, where A is an $m \times m$ matrix with eigenvalues that have negative real part and B is an $n \times n$ matrix with eigenvalues having positive real part. An isolating neighborhood of the origin is

$$\mathcal{N} = [-1, 1]^m \times [-1, 1]^n \quad \text{with exit set } L = [-1, 1]^m \times \partial([-1, 1]^n).$$

Using techniques from algebraic topology (see, e.g., Section 2.1 in [Hat02]), one may compute the relative homology $H_*(\mathcal{N}, L)$ explicitly, and the result follows. \square

Understanding local dynamics near hyperbolic equilibria from the Conley index viewpoint is relatively straightforward, but the same also holds for the analytic viewpoint. The challenging problem lies in the case of global dynamics. To understand global dynamics, we need to rephrase the concept of Poincaré section in the current context.

Definition 16.2.12. Let \mathcal{N} be an isolating neighborhood for an invariant set $S \subset \mathbb{R}^N$. Then $\Sigma \subset \mathbb{R}^N$ is called a **Poincaré section** with respect to \mathcal{N} for the flow ϕ if it is transversal to the flow, $\Sigma \cap \mathcal{N}$ is closed, and for every $z \in \mathcal{N}$, there exists a time $t_z > 0$ such that $\phi(z, t_z) \in \Sigma$.

Note that Σ is not necessarily a subset of \mathcal{N} . We shall see in Example 16.2.14 that it is possible to prove the existence of a Poincaré section in a practical problem. The next theorem shows that the key idea in applying the Conley index is to combine it with some (hopefully minimal and obtainable) knowledge about the dynamics to conclude the existence of an interesting invariant set.

Theorem 16.2.13 ([MM02]; see also [Con78, Mis95]). *If \mathcal{N} is an isolating neighborhood that admits a Poincaré section, and for all $j \in \mathbb{Z}$ either*

$$\dim CH_{2j}(\text{Inv}(\mathcal{N})) = \dim CH_{2j+1}(\text{Inv}(\mathcal{N}))$$

or

$$\dim CH_{2j}(\text{Inv}(\mathcal{N})) = \dim CH_{2j-1}(\text{Inv}(\mathcal{N})),$$

where not all of the above dimensions are zero, then $\text{Inv}(\mathcal{N})$ contains a periodic trajectory.

Example 16.2.14. We again consider the $(2, 1)$ -fast–slow FitzHugh–Nagumo equation

$$\begin{aligned} x'_1 &= x_2, \\ x'_2 &= sx_2 - c(x_1) + y, \\ y' &= \frac{\varepsilon}{s}(x_1 - y), \end{aligned} \tag{16.4}$$

where c is a cubic polynomial with $c(0) = 0$ chosen such that (16.4) has a unique equilibrium point at $(x_1, x_2, y) = (0, 0, 0) = 0$. Let ϕ_ε denote the flow induced by (16.4). Recall that we have seen in Chapter 6 that (16.4) has an orbit homoclinic to 0 and ε sufficiently small. Now we shall prove that there exists a periodic orbit for $0 < \varepsilon \ll 1$. The critical manifold is

$$C_0 = \{(x_1, x_2, y) \in \mathbb{R}^3 : x_2 = 0, y = c(x_1)\}.$$

Let $x_{1,-}$ denote the x_1 -coordinate of the local minimum of the cubic c , and let $x_{1,+}$ be the x_1 -coordinate of the local maximum. The points $(x_{1,\pm}, 0, c(x_{1,\pm}))$ are the two fold points, and the critical manifold splits into three parts,

$$C_0^{a-} = \{x_1 < x_{1,-}\} \cap C_0, \quad C_0^r = \{x_{1,-} \leq x_1 \leq x_{1,+}\} \cap C_0, \quad C_0^{a+} = \{x_{1,+} < x_1\} \cap C_0,$$

as shown already in Figures 6.5 and 11.5. The fast subsystem is given by

$$\begin{aligned} x'_1 &= x_2, \\ x'_2 &= sx_2 - c(x_1) + y. \end{aligned} \tag{16.5}$$

We focus on the case in which $y \in (c(x_{1,-}), c(x_{1,+}))$, so that the fast subsystem has three equilibrium points. It is easy to check that fast subsystem equilibria on $C_0^{a\pm}$ are saddle points. Suppose we make the following assumption:

- (F1) In the parameterized family of fast subsystems, there exist a heteroclinic connection γ_* for $y = y_*$ from C_0^{a-} to C_0^{a+} and another heteroclinic connection γ^* from C_0^{a+} to C_0^{a-} for $y = y^*$ with $0 < y_* < y^* < c(x_{1,+})$; cf. Figure 11.5, where the lower heteroclinic connection now is supposed to exist “above” the equilibrium point y -value, since we assumed $0 < y_*$.

Note that the statement (F1) can actually be proved by Conley index techniques introduced in Section 16.3 applied to the fast subsystem (16.5). If (F1) holds, we conjecture the existence of a periodic orbit obtained as a perturbation of the candidate orbit obtained by concatenating four singular limit trajectories. The two fast subsystem trajectories are γ_* and γ^* , and the slow subsystem trajectories lie on the manifolds

$$\begin{aligned} S_l &:= \{c(x_{1,-}) < y < c(x_{1,+})\} \cap C_0^{a-}, \\ S_r &:= \{c(x_{1,-}) < y < c(x_{1,+})\} \cap C_0^{a+}. \end{aligned}$$

Consider tubular neighborhoods T_l and T_r around S_l and S_r as well as tubular neighborhoods T_* and T^* around γ_* and γ^* . Define

$$\mathcal{N} = T_* \cup T_r \cup T^* \cup T_l.$$

We make two more assumptions (which actually turn out to be facts):

(F2) \mathcal{N} is an isolating neighborhood for $0 < \varepsilon \ll 1$.

(F3) Let $S_\varepsilon = \text{Inv}(\mathcal{N}, \phi_\varepsilon)$. Then the Conley index, computed with \mathbb{Z}_2 -coefficients, is

$$CH_k(S_\varepsilon) = \begin{cases} \mathbb{Z}_2 & \text{if } k = 1, 2, \\ 0 & \text{otherwise.} \end{cases}$$

We will actually see in Section 16.4 how to use the fast–slow structure of the FitzHugh–Nagumo equation to prove (F2)–(F3). Then we have the following theorem.

Theorem 16.2.15 ([MM02]; see also [Sal85]). *For $0 < \varepsilon \ll 1$, there exists a periodic orbit lying in \mathcal{N} .*

Proof. (Sketch; [MM02, Sal85]) The goal is to apply Theorem 16.2.13, and since (F1)–(F3) hold, it remains to show that there is a Poincaré section. Using Theorem 16.2.5, we can find an isolating block \mathcal{B} within an arbitrarily small neighborhood of S_ε such that $\text{Inv}(\mathcal{B}, \phi_\varepsilon) = S_\varepsilon$. For $\delta > 0$ sufficiently small, define

$$K := \{z = (x_1, x_2, y) \in \mathcal{B} \cap T_l : (y_* + y^*)/2 - \delta < y < (y_* + y^*)/2 + \delta\},$$

$$K_0 := \{z = (x_1, x_2, y) \in \mathcal{B} \cap T_l : y = (y_* + y^*)/2\}.$$

For the slow flow on $C_0^{a-} \cap \{y > 0\}$, we have $\dot{y} < 0$. Therefore, choosing \mathcal{B} within a sufficiently small neighborhood of S_ε implies that K_0 is a local section. Note that

$$\mathcal{B}^- = \{z \in \mathcal{B} : \phi_\varepsilon(z, [0, s)) \not\subset \mathcal{B}, \forall s > 0\}$$

is a local section to the flow. Define $\Sigma := (\mathcal{B}^- - K) \cup K_0$ and observe that with a bit of further work, one can show that Σ is the required Poincaré section; we note that this requires finding a further isolating block E contained in \mathcal{B}^o , and we would have to apply Theorem 16.2.13, showing that Σ is a Poincaré section to $\text{Inv}(E)$. We shall omit these technical details here. \square

Apart from the technical difficulties showing the existence of a Poincaré section, Example 16.2.14 posed two major problems. Firstly, we have to show that a nonlinear ODE has a heteroclinic orbit (see assumption/fact (F1)), and secondly, we have to find index pairs for fast–slow systems (see assumptions (F2)–(F3)). Section 16.4 will deal with the problem of index pairs, and the next section deals with connecting orbits on a more general level. ♦

16.3 Connecting Orbits

To investigate connecting orbits, we begin with the case of an invariant set S with attractor–repeller pair decomposition (A, R) . Before we can state a result about the existence of a connecting orbit from R to A , more technical tools are needed.

Definition 16.3.1. An **index triple** for (A, R) is a collection of compact sets $\mathcal{N}_0 \subset \mathcal{N}_1 \subset \mathcal{N}_2$ such that

- $(\mathcal{N}_2, \mathcal{N}_0)$ is an index pair for S ,
- $(\mathcal{N}_2, \mathcal{N}_1)$ is an index pair for R ,
- $(\mathcal{N}_1, \mathcal{N}_0)$ is an index pair for A .

Theorem 16.3.2 ([MM02]; see also [Con78, McC88]). *Let S be an isolated invariant set and let (A, R) be an attractor–repeller pair decomposition for S . Then there exists an index triple.*

Exercise/Project 16.3.3. Prove Theorem 16.3.2. \diamond

Since $\mathcal{N}_0 \subset \mathcal{N}_1 \subset \mathcal{N}_2$, there also exists a short exact sequence of chain complexes

$$0 \rightarrow C_*(\mathcal{N}_1, \mathcal{N}_0) \rightarrow C_*(\mathcal{N}_2, \mathcal{N}_0) \rightarrow C_*(\mathcal{N}_1, \mathcal{N}_0) \rightarrow 0.$$

Elementary algebraic topology [Hat02] shows that a short exact sequence of chains gives rise to a long exact sequence in homology,

$$\cdots \rightarrow H_j(\mathcal{N}_1, \mathcal{N}_0) \rightarrow H_j(\mathcal{N}_2, \mathcal{N}_0) \rightarrow H_j(\mathcal{N}_1, \mathcal{N}_0) \xrightarrow{\partial_j} H_{j-1}(\mathcal{N}_2, \mathcal{N}_1) \rightarrow \cdots.$$

By the definition of the Conley index, the long exact sequence is equivalent to

$$\cdots \rightarrow CH_j(A) \rightarrow CH_j(S) \rightarrow CH_j(R) \xrightarrow{\partial_j} CH_{j-1}(A) \rightarrow \cdots. \quad (16.6)$$

One should focus in (16.6) on the **boundary map**, or **connecting homomorphism**, ∂_j . The map ∂_j is of degree -1 and sends j -level homology to $j-1$ -level homology.

Theorem 16.3.4 ([MM02]; see also [Con78, Mis95]). *Let (A, R) be the attractor–repeller pair decomposition of an isolated invariant set S . If $S = A \cup R$, then $\partial_j = 0$.*

As a direct corollary, the last theorem can actually be applied to the connecting orbit problem.

Corollary 16.3.5. *If $\partial_j \neq 0$, then $S \neq A \cup R$. In particular, there exists a connecting orbit between A and R , i.e., $C(R, A; S) \neq \emptyset$.*

Example 16.3.6. We return to the vector field discussed in Example 16.1.8 given by

$$\begin{aligned} x' &= y, \\ y' &= cy + \lambda - x^2, \end{aligned}$$

for $c \in \mathbb{R}$ and $\lambda \in [-1, 1]$. The aim is to show that for $c > 0$ and $\lambda \in (0, 1]$, there exists a connecting orbit from the spiral source $R = (\sqrt{\lambda}, 0)$ to the saddle point $A = (-\sqrt{\lambda}, 0)$. Note that this looks “obvious” from the phase portrait in

Figure 16.3, but let us use the Conley index to give a rigorous proof. For the computations, \mathbb{Z}_2 coefficients will be used. Then it follows that

$$CH_k(R) = \begin{cases} \mathbb{Z}_2 & \text{if } k = 2, \\ 0 & \text{otherwise,} \end{cases} \quad CH_k(A) = \begin{cases} \mathbb{Z}_2 & \text{if } k = 1, \\ 0 & \text{otherwise.} \end{cases}$$

Recall that $\mathcal{N} = [-k, k]^2$ for $k > 0$ sufficiently large is an isolating neighborhood, and set $S = \text{Inv}(\mathcal{N})$. We claim that $CH_*(S) = 0$ for our choice of parameter values $c > 0$ and $\lambda \in (0, 1]$. The trick to see this is to consider the case $\lambda = -1$, which gives $S = \emptyset$, so that $CH_*(S) = 0$; next, observe that $S_{c, \lambda=-1}$ and $S_{c, \lambda \in (0, 1]}$ are related by continuation. Applying the continuation property of the Conley index from Theorem 16.2.8 yields $CH_*(S) = 0$. Finally, we consider part of the exact sequence (16.6):

$$\cdots \rightarrow CH_2(S) \rightarrow CH_2(R) \xrightarrow{\partial_2} CH_1(A) \rightarrow CH_1(S) \rightarrow \cdots.$$

Knowing $CH_*(R)$, $CH_*(A)$, and $CH_*(S)$, we see that this part of the sequence reduces to

$$\cdots \rightarrow 0 \rightarrow \mathbb{Z}_2 \xrightarrow{\partial_2} \mathbb{Z}_2 \rightarrow 0 \rightarrow \cdots.$$

But by exactness, it follows that $\partial_2(A, R) \neq 0$. Now simply apply Corollary 16.3.5 to conclude that there is a heteroclinic connection from R to A . ♦

Example 16.3.6 demonstrates that the easiest way to understand the map ∂_j is to assume that we calculate homology with field coefficients; computationally, the simplest case is that of \mathbb{Z}_2 coefficients. Hence, we shall assume for now that homology is calculated with coefficients in a field. Note that in this case, $CH_*(A) \oplus CH_*(R)$ and $CH_*(S)$ are graded vector spaces, and the related map ∂_* , consisting of the ∂_j maps, acts as $\partial_*(A, R) : CH_*(R) \rightarrow CH_*(A)$. Next, it is helpful to view $CH_*(A) \oplus CH_*(R)$ as a chain complex with some boundary operator Ξ . One natural question to ask is whether we can choose Ξ to get

$$CH_j(S) = H\Xi_j := \frac{\text{nullspace}(\Xi_j)}{\text{image}(\Xi_{j+1})} \tag{16.7}$$

for all $j = 0, 1, 2, \dots$. The summation property implies that if $S = A \cup R$, then $CH_*(S) = CH_*(A) \oplus CH_*(R)$. Therefore, the (too simple) choice $\Xi = 0$ would guarantee that (16.7) holds. Fortunately, there is a better way to choose Ξ ; observe that since we are dealing with vector spaces here, Ξ will just be a matrix.

Theorem 16.3.7 ([MM02]; see also [Con78, Mis95, Sal85]). *Define the boundary operator by*

$$\Xi := \begin{pmatrix} 0 & \partial_j(A, R) \\ 0 & 0 \end{pmatrix} : CH_*(A) \oplus CH_*(R) \rightarrow CH_*(A) \oplus CH_*(R). \tag{16.8}$$

Then it follows that $H\Xi_ = CH_*(S)$.*

The map Ξ is a special case of a connection matrix in the case of an attractor–repeller decomposition. Unfortunately, the general construction of connection matrices is technically involved. The idea is to find an analogue to (16.8) for Morse decompositions. We shall avoid the precise definition of connection matrices, and only list some of their properties and describe the general setup. Let $\mathcal{M}(S) = \{M(p) : p \in (\mathcal{P}, >)\}$ be a Morse decomposition. Since each Morse set $M(p)$ is an isolated invariant set, it has a Conley index $CH_*(M(p))$. Define Ξ as a linear operator

$$\Xi : \bigoplus_{p \in \mathcal{P}} CH_*(M(p)) \rightarrow \bigoplus_{p \in \mathcal{P}} CH_*(M(p)).$$

The homology groups involved are vector spaces, since field coefficients are assumed, so one may write Ξ as a matrix $\Xi = (\Xi(p, q))$. Furthermore, define a version of Ξ for an interval $I \in \mathcal{I}(\mathcal{P}, >)$:

$$\Xi(I) = (\Xi(p, q))_{p, q \in I} : \bigoplus_{p \in I} CH_*(M(q)) \rightarrow \bigoplus_{p \in I} CH_*(M(p)).$$

If Ξ is a **connection matrix**, then it must satisfy at least the following properties:

- (a) Ξ is upper triangular;
- (b) Ξ is a boundary operator;
- (c) for every interval $I \in \mathcal{I}(\mathcal{P}, >)$, we have $H_*\Xi(I) := \frac{\ker \Xi(I)}{\text{image } \Xi(I)} = CH_*(M(I))$;
- (d) for two adjacent Morse sets $M(p)$ and $M(q)$ (i.e., no points in the interior of an interval between them), we have

$$\Xi(p, q) = \begin{pmatrix} 0 & \partial_*(M(p), M(q)) \\ 0 & 0 \end{pmatrix}.$$

Although (a)–(d) do not define a connection matrix, they are the immediate analogues of statements we have already seen to hold for the attractor–repeller decomposition case. One might ask whether it is even possible to satisfy (a)–(d) with any matrix.

Theorem 16.3.8 ([MM02]; see also [Fra88a]). *Given any isolated invariant set S with Morse decomposition $\mathcal{M}(S)$, there is at least one connection matrix.*

Connection matrices can be used in a similar way to that shown in Example 16.3.6. In many applications, the existence statement for a particular orbit at given parameters is insufficient, since we also want to know about the bifurcations of a problem. Next, we are going to use connection matrices to investigate global bifurcations for general parameterized ODEs of the form

$$x' = f(x, y) \quad \text{for } x \in \mathbb{R}^n \text{ and } y \in \mathbb{R},$$

where we regard y as a parameter for now. Assume that \mathcal{N} is an isolating neighborhood for all $y \in \mathbb{R}$ and set $S_y = \text{Inv}(\mathcal{N})$. Furthermore, assume that the Morse decomposition

$$\mathcal{M}(S_y) := \{M_y(p) : p \in (\mathcal{P}, >)\}$$

continues as well. Choosing $\lambda = \pm 1$ yields two connection matrices Ξ_{\pm} that are boundary operators on the complexes $\bigoplus CH_*(M_{\pm}(p))$. **Transition matrices** are chain maps between these two complexes and can often be used to detect bifurcations for some $y \in [-1, 1]$. The interesting point is that transition matrices can be defined using fast-slow systems. Consider the following equations:

$$\begin{aligned} x' &= f(x, \lambda), \\ y' &= \varepsilon(y^2 - 1). \end{aligned} \tag{16.9}$$

Note that $\mathcal{N} \times [-2, 2]$ is an isolating neighborhood for (16.9) for every $\varepsilon > 0$. Set $K_{\varepsilon} = \text{Inv}(\mathcal{N} \times [-2, 2])$ and define

$$M(p^+) := M_1(p) \quad \text{and} \quad M(p^-) := M_{-1}(p).$$

Observe that $\mathcal{M}(K_{\varepsilon}) = \{M(p^{\pm}) : p \in \mathcal{P}\}$ is a Morse decomposition. An admissible ordering $>>$ is given by

$$q^+ >> p^-, \quad q^- >> p^- \Leftrightarrow q > p, \quad q^+ >> p^+ \Leftrightarrow q > p.$$

Since $\mathcal{M}(K_{\varepsilon})$ is a Morse decomposition, there is a connection matrix Ξ_{ε} . In fact, $y = \pm 1$ gives two invariant manifolds with flows $x' = f(x, \pm 1)$,

$$\Xi : \bigoplus_{p \in \mathcal{P}} CH_*(M(p^-)) \bigoplus_{p \in \mathcal{P}} CH_*(M(p^+)) \rightarrow \bigoplus_{p \in \mathcal{P}} CH_*(M(p^-)) \bigoplus_{p \in \mathcal{P}} CH_*(M(p^+)),$$

and so the connection matrix takes the form

$$\Xi_{\varepsilon} = \begin{pmatrix} \Xi_- & T_{\varepsilon} \\ 0 & \Xi_+ \end{pmatrix}, \tag{16.10}$$

where T_{ε} is given by

$$T_{\varepsilon} : \bigoplus_{p \in \mathcal{P}} CH_{*+1}(M(p^+)) \rightarrow \bigoplus_{p \in \mathcal{P}} CH_*(M(p^+))$$

with matrix entries

$$T_{\varepsilon}(q^-, p^+) : CH_{*+1}(M(p^+)) \rightarrow CH_*(M(q^-)).$$

Formally, the expression (16.10) can be justified despite the elements of Ξ being defined on different spaces.

Definition 16.3.9. It can also be shown that there exists a sequence $\varepsilon_j \rightarrow 0$ along which T_{ε_j} is constant. The set of matrices obtained by this limiting process is called the set of **singular transition matrices** $\mathcal{T}_{-1,1}^{\text{sing}}$.

Theorem 16.3.10 ([MM02]; see also [Con78, Mis95]). Suppose $T \in \mathcal{T}_{-1,1}^{sing}$ and assume that p, q are adjacent elements with respect to the ordering $>$ and $T(q^-, p^+) \neq 0$. Then there exists a connecting orbit from $M_y(p)$ to $M_y(q)$ for some $y \in [-1, 1]$.

Proof. There exists a sequence $\varepsilon_j \rightarrow 0$ for which $T_{\varepsilon_j} \neq 0$. Therefore, there exists a connecting orbit Λ_{ε_j} from $M_1(p)$ to $M_{-1}(q)$ for each ε_j . The limit of Λ_{ε_j} as $\varepsilon_j \rightarrow 0$ gives the desired connecting orbit from $M_y(p)$ to $M_y(q)$. \square

Hence, the matrices T_ε respectively Ξ_ε provide a link between the geometric theory of fast–slow systems and purely algebraic properties. We end this section by mentioning a very nice application of connection and singular transition matrices.

Example 16.3.11. Consider the following fast–slow system:

$$\begin{aligned} x'_1 &= x_2, \\ x'_2 &= x_2 y - x_1(x_1 - 1), \\ y' &= \varepsilon(1 - y^2). \end{aligned} \tag{16.11}$$

Observe that (16.11) has exactly four equilibria,

$$B^\pm := (0, 0, \pm 1) \quad \text{and} \quad A^\pm := (1, 0, \pm).$$

We shall not explain the rather long and involved proof but just mention that using connection matrices, one may show that there are infinitely many connecting orbits from B^- to B^+ for every $\varepsilon > 0$; see Section 16.6. ♦

16.4 Singular Index Pairs

The next natural question regarding the Conley index is whether its application can be simplified in the context of a general (m, n) -fast–slow system

$$\begin{aligned} \frac{dx}{dt} &= x' = f(x, y, \varepsilon), \\ \frac{dy}{dt} &= y' = \varepsilon g(x, y, \varepsilon), \end{aligned} \tag{16.12}$$

for $z = (x, y) \in \mathbb{R}^m \times \mathbb{R}^n$. We can also rewrite (16.12) in a different, sometimes more convenient, form,

$$z' = F_0(z) + \sum_{i=1}^j \varepsilon^i F_i(z) + o(\varepsilon^j). \tag{16.13}$$

We denote the flow of (16.12), respectively of (16.13), by $\phi_\varepsilon : \mathbb{R}^{m+n} \times \mathbb{R} \rightarrow \mathbb{R}^{m+n}$. Observe that ϕ_0 is the flow of the fast subsystem. Recall that $\mathcal{N} \subset \mathbb{R}^{m+n}$ is an isolating neighborhood for ϕ_ε if

$$\text{Inv}(\mathcal{N}, \phi_\varepsilon) = \{z \in N : \phi_\varepsilon(z, \mathbb{R}) \subset \mathcal{N}\} \subset \mathcal{N}^o,$$

where \mathcal{N}^o denotes the interior of \mathcal{N} . It is easy to see that if \mathcal{N} is an isolating neighborhood for ϕ_0 , then it is also an isolating neighborhood for ϕ_ε .

Example 16.4.1. To see the problem with this approach in finding isolating neighborhoods, consider van der Pol's equation as an example:

$$\begin{aligned} x' &= y - \frac{1}{3}x^3 + x, \\ y' &= -\varepsilon x. \end{aligned} \quad (16.14)$$

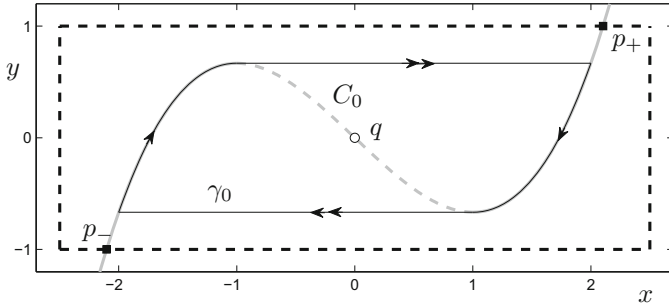


Figure 16.5: Critical manifold C_0 (gray), equilibrium point $q = (0,0)$ (black circle), singular periodic orbit γ_0 (black), and isolating neighborhood \mathcal{N} (dashed black) for van der Pol's equation (16.14). The two problematic points in $C_0 \cap \partial \mathcal{N}$ are also shown (solid black squares).

The critical manifold is given by $C_0 = \{y = \frac{1}{3}x^3 - x\}$, and the two fold points are located at $(\pm 1, \mp 2/3)$. So if we consider the rectangle $\mathcal{N} = [-2.5, 2.5] \times [-1, 1]$, we expect that it is a nice isolating neighborhood for $0 < \varepsilon \ll 1$, since (16.14) has an equilibrium point at $(0,0)$ and a classical relaxation limit cycle contained in \mathcal{N}° that is attracting; see Figure 16.5. The problem is that for $\varepsilon = 0$, one may check that

$$\text{Inv}(\mathcal{N}, \phi_0) = C_0 \cap \mathcal{N},$$

and two points $p_\pm \in C_0 \cap \mathcal{N}$ do not lie in the interior \mathcal{N}° ; in particular, they are contained in $\partial \mathcal{N}$, as shown in Figure 16.5. ♦

Example 16.4.1 implies that the direct singular limit approach $\varepsilon = 0$ to isolating neighborhoods does not work. This motivates the next definition.

Definition 16.4.2. A compact set $\mathcal{N} \subset \mathbb{R}^{m+n}$ is called a **singular isolating neighborhood** if \mathcal{N} is not an isolating neighborhood for ϕ_0 but there exists $\bar{\varepsilon}$ such that \mathcal{N} is an isolating neighborhood for ϕ_ε with $\varepsilon \in (0, \bar{\varepsilon}]$.

To check whether a compact set is a singular isolating neighborhood, one may temporarily decide to define the complications away.

Definition 16.4.3. Let \mathcal{N} be a compact set and let $z \in \text{Inv}(\mathcal{N}, \phi_0) =: S$. We say that z is a **slow exit (entrance) point** if there exist a neighborhood

U of z and an $\bar{\varepsilon} > 0$ such that for all $\varepsilon \in (0, \bar{\varepsilon}]$, there is a time $T(\varepsilon, U) > 0$ ($T(\varepsilon, U) < 0$) such that

$$\phi_\varepsilon(T(\varepsilon, U), U) \cap U = \emptyset.$$

Let S^- (S^+) denote the set of slow exit (entrance) points. Furthermore, define the following sets:

$$S_\partial := S \cap \partial\mathcal{N} \quad \text{and} \quad S_\partial^\pm := S_\partial \cap S^\pm.$$

Definition 16.4.3 imposes quite strong requirements, so that the next result is relatively easy to prove.

Theorem 16.4.4 ([MMR99]). *If $\text{Inv}(\mathcal{N}, \phi_0) \cap \partial\mathcal{N}$ consists of slow exit and entrance points, then \mathcal{N} is a singular isolating neighborhood, i.e., it is an isolating neighborhood for the full fast–slow system for sufficiently small $\varepsilon > 0$.*

Proof. It has to be shown that $\text{Inv}(\mathcal{N}, \phi_\varepsilon) \subset \mathcal{N}^\circ$, where \mathcal{N}° denotes the interior of \mathcal{N} . In particular, this means that there is an $\bar{\varepsilon} > 0$ such that if $z \in \partial\mathcal{N}$ and $\varepsilon \in (0, \bar{\varepsilon}]$, then $\phi_\varepsilon(z, \mathbb{R}) \not\subset \mathcal{N}$. But for each $z \in \text{Inv}(\mathcal{N}, \phi_0) \cap \partial\mathcal{N}$, Definition 16.4.3 provides a neighborhood U of z , some $\varepsilon > 0$, and a time $T(\varepsilon, U)$ such that

$$\phi_\varepsilon(T(\varepsilon, U), U) \cap U = \emptyset.$$

Since $\text{Inv}(\mathcal{N}, \phi_0) \cap \partial\mathcal{N}$ is compact, this argument can be extended uniformly over all points of interest using a finite cover. \square

Hence, we have reduced the problem to characterizing slow exit/entrance points in a more computable way. The next definition provides a technical notion that will be necessary for this task.

Definition 16.4.5. The **average** of a function h on $S \subset \mathbb{R}^{m+n}$, denoted by $\text{Avg}(h, S)$, is the limit as $T \rightarrow \infty$ of the set of numbers

$$\left\{ \frac{1}{T} \int_0^T h(\phi_0(z, s)) \, ds : z \in S \right\}.$$

We say that h has **strictly positive averages** on S if $\text{Avg}(h, S) \subset (0, \infty)$.

Before stating the next theorem, recall (in the sense of the remark before Proposition 2.2.3) that a point is **chain recurrent**, loosely speaking, if it becomes periodic under a small perturbation of the flow. This definition naturally extends to **chain recurrent sets** by requiring that all points in the set be chain recurrent; see [GH83] for a precise definition.

Theorem 16.4.6 ([Con80]). *A point $z \in S$ is a slow exit point if there exist a compact set $K_z \subset S$ invariant under ϕ_0 , a neighborhood U_z of the chain recurrent set $\mathcal{R}(K_z)$ of K_z , an $\bar{\varepsilon} > 0$, and a function $l : \overline{U_z} \times [0, \bar{\varepsilon}] \rightarrow \mathbb{R}$ such that the following conditions are satisfied:*

- (a) $\omega(z, \phi_0) \subset K_z$.
- (b) l is of the form $l(w, \varepsilon) = l_0(w) + \varepsilon l_1(w) + \dots + \varepsilon^j l_j(w)$.
- (c) If $L_0 = \{w : l_0(w) = 0\}$, then $K_z \cap \overline{U_z} = S \cap L_0 \cap \overline{U_z}$ and $l_0|_{S \cap \overline{U_z}} \leq 0$.
- (d) Let $g_j(w) = \nabla_z l_0(w) \cdot F_j(w) + \nabla_z l_1(w) \cdot F_{j-1}(w) + \dots + \nabla_z l_j(w) \cdot F_0(w)$. Then for some k , $g_k = 0$ if $k < j$ and g_j has strictly positive averages on $\mathcal{R}(K_z)$.

A point is a slow entrance point if the same conditions hold under reversal of time. Points that satisfy (a)–(d) (satisfy the conditions under time reversal) will be denoted by S^- (S^+) and will be called **C-slow exit (entrance) points**. The compact set K_z will be called a **slow exit guide**.

As a simple example, we consider the $(1, 1)$ -fast–slow system

$$\begin{aligned} x' &= -x, \\ y' &= \varepsilon. \end{aligned} \tag{16.15}$$

Consider the set $\mathcal{N} = [-a, a] \times [-b, 0]$ for some $a, b > 0$. We aim to show that $z_0 = (0, 0)$ is a C-slow exit point. Note that $S = \text{Inv}(\mathcal{N}, \phi_0) = \{(0, y) \in \mathbb{R}^2 : y \in [-b, 0]\}$. Let $K_{z_0} = \{(0, 0)\}$ and $U_{z_0} = B(0, \delta)$ for sufficiently small $\delta > 0$. Furthermore, define the function

$$l(x, y) := y - x^2.$$

Now we can check the different conditions in Theorem 16.4.6. One can easily see that (a) holds, since $\omega(z_0, \phi_0) = \{z_0\}$, and (b) holds by construction. For (c), observe that $L_0 = \{y = x^2\}$ and that

$$\{z_0\} = K_{z_0} \cap \overline{U_{z_0}} = S \cap L_0 \cap \overline{U_{z_0}} = \{z_0\}.$$

The second part of (c) $l_0|_{S \cap \overline{U_{z_0}}} \leq 0$ holds, since $l_0(x, y) = y - x^2 \leq 0$ for $y \leq x^2$. The last condition (d) gives that

$$\begin{aligned} g_0(x, y) &= \nabla_z l_0(x, y) \cdot F_0(x, y) = (-2x, 1)^\top \cdot (y - x^2, 0)^\top = 2x^3 - 2xy, \\ g_1(x, y) &= \nabla_z l_0(x, y) \cdot F_1(x, y) = (-2x, 1)^\top \cdot (0, 1)^\top = 1. \end{aligned}$$

Since $g_0 \equiv 0$ on $\mathcal{R}(K_{z_0}) = z_0 = (0, 0)$ and g_1 obviously has positive average, we see that $z_0 = (0, 0)$ is a C-slow exit point.

An important observation is that the slow flow on $C_0 = \{x = 0\}$ is given by $\frac{dy}{d\tau} = 1$ for $\tau = \varepsilon t$, and this flow is transverse to the boundary $\partial\mathcal{N}$ at $(0, 0)$. Hence, we may link a geometric/dynamical property (transversality) to the algebraic/topological view (singular isolating neighborhood). Intuitively, it is best to think of general slow exit and entry points as points where the slow flow is transverse to $\partial\mathcal{N}$; see also Section 16.6.

Example 16.4.7. In van der Pol's equation from Example 16.4.1, we can use a similar argument as for equation (16.15). Hence, the two points p_{\pm} contained in $S \cap \partial\mathcal{N}$ are slow entrance points for van der Pol's equation (16.14); see Figure 16.5. Therefore, we conclude that $\mathcal{N} = [-2.5, 2.5] \times [-1, 1]$ is a singular isolating neighborhood by Theorem 16.4.4. ♦

Having dealt with isolating neighborhoods, we see that the next natural step is to ask how to compute the Conley index using information about the singular limit systems. We shall follow the same strategy as above and simply define the notion of interest.

Definition 16.4.8. A pair of compact sets (\mathcal{N}, L) with $L \subset \mathcal{N}$ is called a **singular index pair** if $\overline{\mathcal{N} - L}$ is a singular isolating neighborhood and there exists an $\bar{\varepsilon} > 0$ such that for all $\varepsilon \in (0, \bar{\varepsilon}]$,

$$H_*(\mathcal{N}, L) = CH_*(\text{Inv}(\overline{\mathcal{N} - L}, \phi_\varepsilon)).$$

Recall that the Conley index enjoys the continuation property and is therefore stable under perturbation, so that

$$CH_*(\text{Inv}(\mathcal{N}, \phi_0)) = CH_*(\text{Inv}(\mathcal{N}, \phi_\varepsilon))$$

for $\varepsilon > 0$ sufficiently small. Again, we are looking for computable/testable conditions that characterize singular index pairs. Recall that if S is an isolated invariant set, then a pair of compact sets (\mathcal{N}, L) is an index pair if the following three conditions hold (see Definition 16.2.1):

- (1) $S = \text{Inv}(\overline{\mathcal{N} - L})$, and $\mathcal{N} - L$ is a neighborhood of S .
- (2) L is positively invariant in \mathcal{N} , i.e., for every $z \in L$ and $\phi(z, [0, t]) \subset \mathcal{N}$, we have $\phi(z, [0, t]) \subset L$.
- (3) L is an exit set for \mathcal{N} , i.e., for every $z \in \mathcal{N}$ and $t_1 > 0$ such that $\phi(z, t_1) \notin \mathcal{N}$, there exists $t_0 \in [0, t_1]$ for which $\phi(z, [0, t_0]) \subset \mathcal{N}$ and $\phi(z, t_0) \in L$.

If we search for an index pair for the full system, then the singular index pair should be characterized by conditions similar to (1)–(3). From the exit set requirement, it follows that L has to contain the **immediate exit set** of \mathcal{N} ,

$$\mathcal{N}^- := \{z \in \partial\mathcal{N} : \phi_0(z, (0, t)) \not\subset \mathcal{N} \text{ for all } t > 0\}.$$

Regarding positive invariance, it turns out that given $Y \subset \mathcal{N}$, one has to consider the **pushforward set** in \mathcal{N} under the flow ϕ_0 defined by

$$\rho(Y, \mathcal{N}, \phi_0) := \{z \in \mathcal{N} : \exists w \in Y, t \geq 0 \text{ s.t. } \phi_0(w, [0, t]) \subset \mathcal{N}, \phi_0(w, t) = z\}.$$

Basically, $\rho(Y, \mathcal{N}, \phi_0)$ consists of points in \mathcal{N} that can be reached from Y by a forward orbit in \mathcal{N} ; observe that by construction, we must have $Y \subset \rho(Y, \mathcal{N}, \phi_0)$.

In addition, we also must consider a special version of the unstable manifold of a point lying in \mathcal{N} :

$$W_{\mathcal{N}}^u(Y) := \{z \in \mathcal{N} : \phi_0(z, (-\infty, 0)) \subset \mathcal{N} \text{ and } \alpha(z, \phi_0) \subset Y\}.$$

Again we observe that $Y \subset W_{\mathcal{N}}^u(Y)$. Before we can state a theorem about characterizing singular index pairs, one last definition is needed.

Definition 16.4.9. A slow entrance point z is called a **strict slow entrance point** if there exist a neighborhood V of z and an $\bar{\varepsilon} > 0$ such that if $v \in V \cap \mathcal{N}$ and $\varepsilon \in (0, \bar{\varepsilon}]$, then there exists a time $t_v(\varepsilon)$ such that

$$\phi_\varepsilon(v, [0, t_v(\varepsilon)]) \subset \mathcal{N}.$$

The set of strict slow entrance points will be denoted by S_∂^{++} .

Theorem 16.4.10 ([MMR99]). *Let \mathcal{N} be a singular isolating neighborhood. Assume the following:*

- (A) S_∂^- consists of C -slow exit points.
- (B) $S_\partial \subset S_\partial^{++} \cup S_\partial^-$.
- (C) $(S_\partial^{++} - S_\partial^-) \cap \overline{N^-} = \emptyset$.

For each $z \in S_\partial^-$, let K_z be a slow exit guide for z . Define

$$L := \rho(\overline{N^-}, \mathcal{N}, \phi_0) \cup W_{\mathcal{N}}^u \left(\bigcup_{z \in S_\partial^-} \mathcal{R}(K_z) \right).$$

If L is closed, then (\mathcal{N}, L) is a singular index pair.

Example 16.4.11. To see how Theorem 16.4.10 can be applied, we continue with van der Pol's equation (with time reversed; see also Examples 16.4.1 and 16.4.7)

$$\begin{aligned} x' &= -y + x^3/3 - x, \\ y' &= \varepsilon x. \end{aligned} \tag{16.16}$$

We already know that $\mathcal{N} = [-2.5, 2.5] \times [-1, 1]$ is a singular isolating neighborhood and that the two points $p_\pm \in \partial\mathcal{N} \cap S$ are slow exit points for (16.16). Observe that the two slow exit points lie on the left and right branches of the critical manifold:

$$\begin{aligned} C_0^{r-} &= \left\{ (x, y) \in \mathbb{R}^2 : y = \frac{1}{3}x^3 - x, x < -1 \right\}, \\ C_0^{r+} &= \left\{ (x, y) \in \mathbb{R}^2 : y = \frac{1}{3}x^3 - x, x > 1 \right\}. \end{aligned}$$

For equation (16.16), the manifolds $C_0^{r\pm}$ are repelling, and therefore, the unstable manifolds of the two slow exits points are given by the top and bottom edges

of \mathcal{N} . Since the immediate exit set of \mathcal{N} consists of the left and right edges of \mathcal{N} , we conclude that $L = \partial\mathcal{N}$. Conditions (A)–(C) of Theorem 16.4.10 hold, since $S_\partial^+ = \emptyset$; see also Figure 16.5. Therefore, the Conley index of (\mathcal{N}, L) is

$$CH_k(S) = \begin{cases} \mathbb{Z} & \text{if } k = 2, \\ 0 & \text{otherwise.} \end{cases}$$

But the origin $(x, y) = (0, 0)$ is an attracting fixed point for (16.16) and has a zero Conley index. This means that there must be another invariant set in \mathcal{N} . Since there are no other equilibria in \mathcal{N} , the Poincaré–Bendixson theorem implies that there must be a periodic orbit in \mathcal{N} . ♦

Exercise/Project 16.4.12. Show that (16.16) has a (repelling) periodic orbit that is a relaxation oscillation γ_ε , i.e., it lies in a small tubular neighborhood of the singular periodic orbit γ_0 constructed from two fast and two slow segments; see Figure 16.5. This exercise requires a different choice of isolating neighborhood (which should be obvious from the tubular neighborhood requirement) as well as computations similar to those in Example 16.4.11 and Theorem 16.2.13. ◇

16.5 Further Techniques

Having applied Conley index theory for fast–slow systems to some low-dimensional examples, it is a natural goal to make the theory more computable for higher-dimensional problems. Unfortunately, a rigorous approach entails a lengthy development of notation and some additional, relatively advanced, algebraic topology. Here we shall restrict ourselves to an outline of the main ideas. The following results all hold for $(m, 1)$ -fast–slow systems:

$$\begin{aligned} \frac{dx}{dt} &= x' = f(x, y, \varepsilon), \\ \frac{dy}{dt} &= y' = \varepsilon g(x, y, \varepsilon), \end{aligned} \tag{16.17}$$

where $(x, y) \in \mathbb{R}^m \times \mathbb{R}$. We denote the critical manifold of (16.17) by C_0 . A typical example is the three-dimensional FitzHugh–Nagumo equation (16.4). A central goal is to prove the existence of periodic and heteroclinic orbits by an algorithmic approach. This requires the following three concepts:

1. A set $T \subset \mathbb{R}^m \times \mathbb{R}$ will be called a **tube** if it is an isolating invariant neighborhood for the fast subsystem, and the slow flow inside T satisfies a technical condition; see Figure 16.6(a). Intuitively, we think of tubes as neighborhoods of the critical manifold where the slow flow is simple and has no invariant sets.
2. A set $B \subset \mathbb{R}^m \times \mathbb{R}$ will be called a **box** if (1) it is an isolating invariant neighborhood for the fast flow ϕ_0 , (2) there exists a Morse decomposition of $\text{Inv}(B, \phi_0)$, and (3) the slow flow inside B satisfies a technical

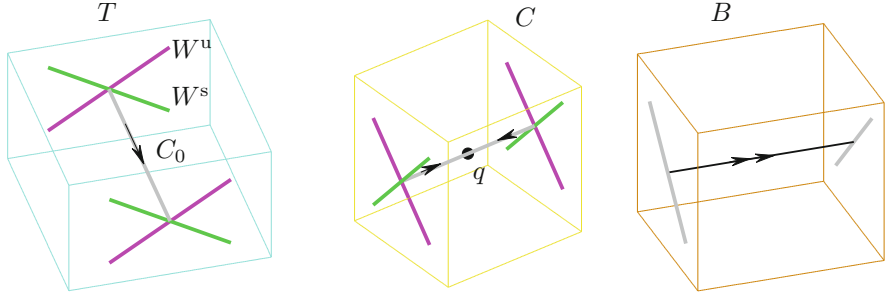


Figure 16.6: Tube T (cyan) with slow flow (black) on the critical manifold C_0 (gray), which has associated fast stable (green) and unstable (magenta) directions. Cap C (yellow) with slow flow (black) and fast stable (green) and unstable (magenta) directions. Note that inside the cap, there is an equilibrium point q (black dot). Box B (brown) with two parts of C_0 (gray) and a fast flow trajectory (black) connecting the two parts of C_0 .

condition; see Figure 16.6(c). We can interpret boxes as enclosing heteroclinic connections in the fast subsystem between different parts of the critical manifold.

3. A set $C \subset \mathbb{R}^m \times \mathbb{R}$ will be called a **cap** if it is an isolating invariant neighborhood for the fast subsystem and the slow flow inside C satisfies a technical condition; see Figure 16.6(b). Caps formalize the concept of beginning and end points of heteroclinic connections and can be interpreted as isolating blocks for the slow flow on the critical manifold.

The detailed construction of tubes, boxes, and caps can be found in [GKM⁺99]. We shall restrict ourselves to stating two results that use the construction.

Theorem 16.5.1 ([GKM⁺99]). *Consider a collection of tubes and boxes. Denote their union by \mathcal{N} . Assume that the slow and fast flows on the intersections of a tube and a box satisfy suitable technical conditions. Then \mathcal{N} is an isolating invariant neighborhood for $\varepsilon > 0$ sufficiently small.*

Using Theorem 16.5.1, a Poincaré section to the flow, and a Conley index computation, one can use the ideas presented in the previous sections to prove the existence of a periodic orbit in \mathcal{N} . A sketch of the tubes and boxes for the FitzHugh–Nagumo equation is shown in Figure 16.7.

Theorem 16.5.2 ([GKM⁺99]). *Consider a collection of tubes, boxes, and caps. Denote their union by \mathcal{N} . Assume that the slow and fast flows on the intersections of a tube and a box satisfy the same conditions as in Theorem 16.5.1. Furthermore, on the intersections of caps and tubes, additional technical assumptions hold. Then \mathcal{N} is an isolating invariant neighborhood for $\varepsilon > 0$ sufficiently small.*

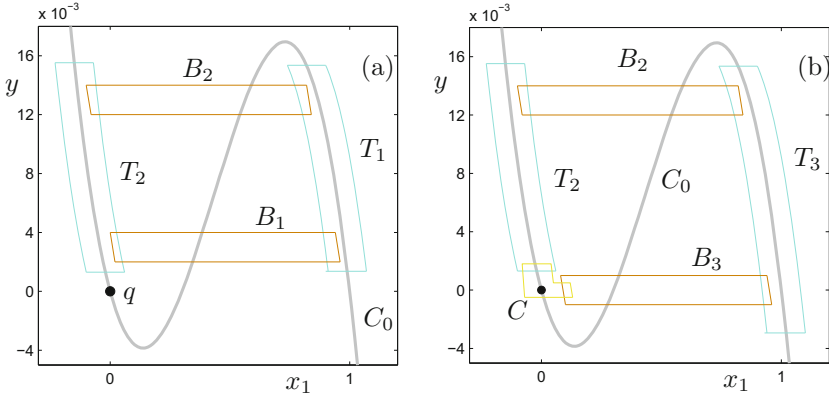


Figure 16.7: Possible topological decomposition for orbits of the FitzHugh–Nagumo equation (16.4), plotted for the cubic $c(x) = \frac{1}{5}x_1(1-x_1)(x_1-0.3)$, which defines the critical manifold $C_0 = \{y = c(x_1), x_2 = 0\}$. (a) Projection of tubes T_i (cyan) and boxes B_i (brown) for $i = 1, 2$ onto the (x_1, y) -plane. $\mathcal{N} = T_1 \cup B_1 \cup T_2 \cup B_2$ perturbs to an isolating invariant neighborhood by Theorem 16.5.1, which could potentially enclose a periodic orbit. (b) Modified version of (a) where a cap C is added. T_1 and B_1 are modified to T_3 and B_3 . $\mathcal{N} = T_3 \cup B_3 \cup T_2 \cup B_2 \cup C$ perturbs to an isolating invariant neighborhood by Theorem 16.5.2, which could potentially enclose a homoclinic orbit, to the global saddle equilibrium $q = (0, 0, 0)$.

Although Theorems 16.5.1 and 16.5.2 apply in a wide variety of applications, they do not claim anything about systems with multiple slow variables, i.e., (16.17) with $(x, y) \in \mathbb{R}^m \times \mathbb{R}^n$. The main observation will be that for such systems, the cohomological Conley index has a nice product structure that reflects the splitting (16.17) into fast and slow variables. We begin with an example.

Example 16.5.3. Consider the following $(1, 1)$ -fast–slow system in polar coordinates:

$$\begin{aligned} r' &= r(1-r), \\ \theta' &= \varepsilon, \end{aligned} \tag{16.18}$$

with $(r, \theta) \in (0, \infty) \times [0, 2\pi)$. The critical manifold is given by the unit circle $C_0 = \{r = 1\}$, since we do not consider $r = 0$ as part of the domain. Now consider

$$\mathcal{N} = \left\{ (r, \theta) : \frac{1}{2} \leq r \leq \frac{3}{2} \right\} \quad \text{and} \quad L = \left\{ (r, \theta) : r = \frac{1}{2} \text{ or } r = \frac{3}{2} \right\},$$

as sketched in Figure 16.8. It is easy to check that (\mathcal{N}, L) defines an index pair for all $\varepsilon \geq 0$. We also have

$$CH^k(\text{Inv}(\mathcal{N}, \phi_\varepsilon); \mathbb{Z}_2) = \begin{cases} \mathbb{Z}_2 & \text{if } k = 1, 2, \\ 0 & \text{otherwise.} \end{cases}$$

It is not difficult to prove the existence of a Poincaré section, and hence Theorem 16.2.13 implies that (16.18) has a periodic orbit.

Remark: Observe that this fact can also be deduced directly, since the critical manifold equals the slow manifold $C_0 = C_\varepsilon$ for $\varepsilon > 0$, and the circle has a flow with no fixed points on it.

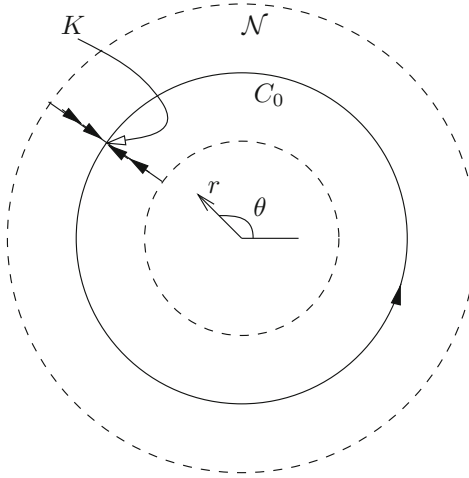


Figure 16.8: Sketch of the situation for the toy model (16.18).

Unfortunately, the fast–slow structure of the system (16.18) is not reflected in the last Conley index calculation. To show how it can be used, consider the fast flow ϕ_0 and fix a point $K = (1, \theta_0)$ on C_0 that is a hyperbolic equilibrium in the fast subsystem it defines; see Figure 16.8. A direct Conley index calculation yields

$$CH^k(K; \mathbb{Z}_2) = \begin{cases} \mathbb{Z}_2 & \text{if } k = 1, \\ 0 & \text{otherwise.} \end{cases}$$

Note that the isolating invariant neighborhood N can be expressed as a product $N = C_0 \times [\frac{1}{2}, \frac{3}{2}]$, so that N can be viewed as a bundle with base C_0 and intervals as fibers. We remark that in other situations, it is also possible to construct isolating invariant neighborhoods as other types of fiber bundles. For the particular case discussed here, one may apply the Thom isomorphism theorem [Spa66, MS74] to conclude that

$$CH^*(\text{Inv}(N, \phi_\varepsilon); \mathbb{Z}_2) = CH^*(K; \mathbb{Z}_2) \smile H^*(C_0, \mathbb{Z}_2),$$

where \smile denotes the cup product [Hat02, Spa66]. Therefore, the Conley index decomposes as the Conley index for the fast flow and a part capturing the topology of the critical manifold. ♦

Unfortunately, the simple idea in the previous example often fails, since the critical manifold might be unbounded. To salvage the situation, more advanced machinery is required.

Definition 16.5.4. A pair of compact sets (\mathcal{N}, L) with a continuous surjection $p : \mathcal{N} \rightarrow A$ forms an **index bundle** over the base space A if there exists an open cover $\{U\}$ of A such that for every $a \in A$ and an element U_a of the cover containing a , the inclusion map

$$j_{U_a} : (\mathcal{N}(a), L(a)) \rightarrow (\mathcal{N}(U_a), L(U_a))$$

induces an isomorphism

$$j_{U_a}^* : H^*(\mathcal{N}(a), L(a)) \rightarrow H^*(\mathcal{N}(U_a), L(U_a)),$$

where $\mathcal{N}(a) = p^{-1}(a)$, $\mathcal{N}(U) = p^{-1}(U)$, and $L(a) = L \cap \mathcal{N}(a)$.

It turns out that index bundles can be used to calculate the Conley index for fast–slow systems. The base space A will be a singular trajectory for the slow flow on the critical manifold. Concatenating this singular solution with a singular trajectory of the fast subsystem gives an associated index bundle. In fact, using the same collections of tubes, boxes, and caps as previously, one can establish theorems similar to Theorems 16.5.1–16.5.2; see also Section 16.6.

16.6 References

Section 16.1: Most of this section and parts of the rest of the chapter are based on extracting the relevant fast–slow tools for the Conley index from the general survey [MM02]; other good references on the Conley index are [Jos06, Sal85]. Probably the first work on index theory for singularly perturbed systems is that due to Conley [Con80] with a focus on isolating blocks [CE71]. One of the most relevant early applications of isolating blocks was to establish the existence of waves in the FitzHugh–Nagumo (FHN) equation [Car77, CS76]. There is another nice application to stationary solutions of the FHN equation [CS86].

Section 16.2: The basics for fast–slow Conley index theory are laid out in [GKM⁺99, GKMO06]. One might expect that there are infinite-dimensional versions of the fast–slow theory [Ryb87]. Working with the homological version usually turns out to be more convenient, but see [Kur86]. The applications range up to very applied systems such as bursting oscillations [Kin00, Kin08] and cell cycle models [Ged10]. The continuation idea of the Conley index can be refined to control invariant sets [Flo87] and to prove persistence of invariant manifolds [Flo90]; and it can be related to averaging [Pri05].

Section 16.3: Several important connecting orbits are related directly to traveling waves [GS83, Mil97a]. Not only can one investigate connecting orbits for waves using the Conley index, but even chaotic dynamics can be treated [GGK⁺07, GKMO02]. For traveling waves in a phase field model, we refer to [GJ90], and for shock waves, to [Kla12].

Section 16.4: This section is built on the groundwork on singular index pairs in [MMR99] as well as the recent work on relating geometric and topological definitions of singular index pairs [Kue10a]. We note that one also may apply the Conley index to classical second-order singularly perturbed problems [GM06], which have a natural fast–slow structure.

Section 16.5: More details and precise statements can be found in [GKMO06]. For the case of infinitely many connecting orbits, see [KMO96]. Topological degree theory has also been applied to the analysis of canards [PRSZ11] and chaos [PZ08] in fast–slow systems.

One may also relate the so-called Brouwer degree to averaging [BL04]. Another interesting recent direction of more algebraic flavor is the relationship among Morse theory, homology, and adiabatic limits [SX12]. In a similar spirit, we mention the connection to Morse–Bott homology [BH13, Hur13]. Even more on the algebraic side are approximately group invariant solutions for systems with small parameters [BI00]. However, there is relatively little hope that one may use algebraic techniques to express particular trajectories explicitly for many fast–slow systems [Oda95].

Chapter 17

Spatial Dynamics

In this chapter, the main topic is traveling waves for time-dependent spatially extended systems in one space dimension. Note that we have already extensively discussed various techniques to prove the existence of waves for partial differential equations (PDEs); see, e.g., Chapter 6. Hence, we focus here on further topics beyond the existence of waves in PDEs.

Section 17.1 provides the background for stability analysis of structures in spatially extended system, with a focus on the Evans function. In Section 17.2, the methods are applied to a fast–slow predator–prey system with diffusion. We also consider the splitting of the Evans function via fast–slow decomposition. Section 17.3 moves to hyperbolic conservation laws and various so-called diffusive, or viscous, regularizations. Geometric singular perturbation theory turns out to be helpful in analyzing shocks and rarefaction solutions in this context. Section 17.4 deals with the FitzHugh–Nagumo equation on a lattice and under what conditions the existence of the classical fast pulse carries over to the discrete-space setting. Finally, we conclude the chapter in Section 17.5 with waves in neural field equations, which are partial integrodifferential equations closely related to reaction–diffusion systems.

Background: No additional prerequisites are necessary. Of course, any experience with various classes of PDEs would be helpful, either via an introductory textbook [Str08, ZT88], a graduate-level text [Eva02, RR04], motivated by applications [OHLMO3], or using a more specialized monograph [Daf10, Fri92, LeV92, Smo94].

17.1 Stability of Traveling Waves I

We discussed the exchange lemma in Chapter 6 and used it in Section 6.5 to establish the existence of traveling waves for the FitzHugh–Nagumo (FHN) PDE consisting of two fast and two slow segments. We have not discussed stability

of this wave as a solution to the FHN PDE. The stability analysis of traveling waves and more general patterns in PDEs is an extremely large area of research. Therefore, in this section, we shall only touch on some basic definitions and results that will be needed in Section 17.2; for more detailed references, see Section 17.6. We restrict ourselves to systems of reaction–diffusion equations of the form

$$\frac{\partial u}{\partial t} = \frac{\partial^2 u}{\partial x^2} + f(u), \quad (17.1)$$

where $x \in \mathbb{R}$, $u = u(x, t) \in \mathbb{R}^N$, $u(\cdot, t) \in X$ for a suitable Banach space X , and $f : \mathbb{R}^N \rightarrow \mathbb{R}^N$ is a (nonlinear) sufficiently smooth function representing the reaction terms. The usual traveling-wave ansatz is to consider a **moving frame** $\xi = x - st$, where s is the **wave speed**. Using this formulation for (17.1), we get an equation for $v(\xi, t) := u(x - st, t)$ given by

$$\frac{\partial v}{\partial t} = \frac{\partial^2 v}{\partial \xi^2} + s \frac{\partial v}{\partial \xi} + f(v). \quad (17.2)$$

Traveling wave solutions are stationary solutions $q(\xi)$ of (17.2), so one has to solve

$$0 = \frac{d^2 v}{d \xi^2} + s \frac{d v}{d \xi} + f(v), \quad (17.3)$$

where a suggestive notation has been employed to emphasize that the problem has been reduced to a system of second-order ODEs. The first approach to analyzing the stability of the steady state $q(\xi)$ is to linearize (17.2) around this solution, which gives

$$\frac{\partial V}{\partial t} = \frac{\partial^2 V}{\partial \xi^2} + s \frac{\partial V}{\partial \xi} + (\mathbf{D}_v f)(q(\xi))V. \quad (17.4)$$

Basically, the nonlinear terms $f(v)$ have been replaced with their linear approximation near q . The right-hand side of (17.4) can also be written in operator notation as

$$\mathcal{L}V := \left[\frac{\partial^2}{\partial \xi^2} + s \frac{\partial}{\partial \xi} + (\mathbf{D}_v f)(q(\xi)) \right] V.$$

One may hope that studying the **spectral** (or **eigenvalue**) **problem**

$$\lambda V = \mathcal{L}V \quad (17.5)$$

for the linear operator \mathcal{L} will provide stability results of the traveling wave; to complete the problem formulation (17.5), choose the Banach space $X = C_{\text{unif}}^0(\mathbb{R}, \mathbb{R}^N)$ of uniformly continuous maps and observe that \mathcal{L} is a densely defined operator on this space.

Definition 17.1.1. The values λ for which (17.5) has a nonzero solution $V \in X$ are called **eigenvalues** of \mathcal{L} . The values λ for which $(\mathcal{L} - \lambda \text{ Id})$ does not have a bounded inverse form the **spectrum** $\sigma(\mathcal{L})$. The spectrum decomposes as

$$\sigma(\mathcal{L}) = \sigma_p(\mathcal{L}) \cup \sigma_e(\mathcal{L}),$$

where $\sigma_p(\mathcal{L}) := \{\lambda \in \sigma(\mathcal{L}) : \lambda \text{ is an isolated eigenvalue with finite multiplicity}\}$, is the **point spectrum**, and $\sigma_e(\mathcal{L}) := \sigma(\mathcal{L}) - \sigma_p(\mathcal{L})$ is the **essential spectrum**.

If $q(\xi)$ is not a constant function, one observes that $\lambda = 0$ is an eigenvalue. It follows from differentiating (17.3) that the associated eigenfunction is $q_\xi(\xi) = dq/d\xi$, since

$$0 = \frac{d^2 q_\xi}{d\xi^2} + s \frac{dq_\xi}{d\xi} + (\mathbf{D}_v f)(q) q_\xi. \quad (17.6)$$

Essentially, the eigenvalue $\lambda = 0$ is generated by the **translation invariance** with respect to t , i.e., solutions are formally one-parameter families in the traveling frames $x + t^* - st$ with parameter $t^* \in \mathbb{R}$. The eigenvalue associated with q_ξ is sometimes also called the **trivial eigenvalue**.

Definition 17.1.2. A traveling wave $q(\xi)$ is **(strictly) spectrally stable** if for some fixed $\beta > 0$, we have that $\operatorname{Re}(\lambda) < -\beta$ for all nontrivial λ in the spectrum $\sigma(\mathcal{L})$.

Definition 17.1.3. A traveling wave $q(\xi)$ is **nonlinearly stable** if every solution of (17.1) with initial condition sufficiently close to $q(\xi)$ tends to some translate $q(\xi + \xi_0)$ (for some $\xi_0 \in \mathbb{R}$) of the wave as $t \rightarrow \infty$.

For reaction–diffusion systems, it is not too difficult to show that strict spectral stability implies nonlinear stability [Hen81] under relatively mild assumptions. However, Definitions 17.1.2 and 17.1.3 apply to more general evolution PDEs, in which case the distinctions are vital. Regarding linear stability, one may sometimes show that the essential spectrum for reaction–diffusion equations of the form (17.1) is properly contained in the left complex half-plane $\sigma_e \subset \{\lambda \in \mathbb{C} : \operatorname{Re}(\lambda) < -\beta\}$ for some fixed $\beta > 0$; see Figure 17.1(a).

In this case, we know that a potential instability of the traveling wave can be caused only by the point spectrum. Let $\Omega \subset \mathbb{C}$ denote the connected component of $\mathbb{C} - \sigma_e$ that contains the right half-plane $\{\lambda : \operatorname{Re}(\lambda) > 0\}$. An important tool for calculating the point spectrum is the **Evans function** $E(\lambda)$, which is defined on Ω . To construct the Evans function, let us return to the spectral problem

$$\frac{d^2 V}{d\xi^2} + c \frac{dV}{d\xi} + (\mathbf{D}_v f)(q(\xi)) V = \lambda V. \quad (17.7)$$

The system of second-order ODEs (17.7) can be written as a first-order system by setting $dV/d\xi = W$, which yields

$$\begin{aligned} \begin{pmatrix} \frac{dV}{d\xi} \\ \frac{dW}{d\xi} \end{pmatrix} &= \begin{pmatrix} W \\ \lambda V - cW - (\mathbf{D}_v f)(q(\xi))V \end{pmatrix} \\ &= \underbrace{\begin{pmatrix} 0 & \operatorname{Id} \\ \lambda \operatorname{Id} - (\mathbf{D}_v f)(q(\xi)) & -c \operatorname{Id} \end{pmatrix}}_{=:A(\xi; \lambda)} \begin{pmatrix} V \\ W \end{pmatrix}. \end{aligned}$$

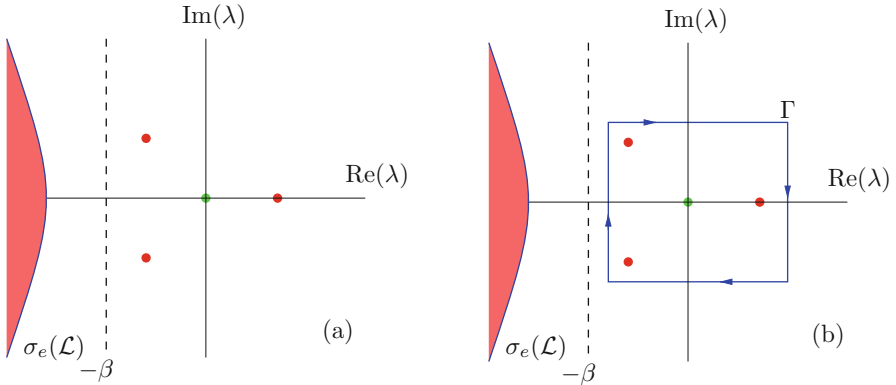


Figure 17.1: (a) Sketch of the spectrum for the linear operator \mathcal{L} . The essential spectrum $\sigma_e(\mathcal{L})$ (red, blue boundary) lies in the left half-plane, and the point spectrum (dots) consists of one trivial eigenvalue (green dot) at $\lambda = 0$ and three other nontrivial eigenvalues (red dots). (b) Spectrum from (a), indicating that the essential spectrum is bounded away from the imaginary axis and also showing a closed contour Γ (blue) around the point spectrum.

Observe that the problem for $(V, W) =: Z$ is now posed in \mathbb{R}^{2N} and can be written in the concise form

$$\frac{dZ}{d\xi} = A(\xi; \lambda)Z. \quad (17.8)$$

Denote by $\Phi(\xi, \xi_0; \lambda)$ the **principal matrix solution** of (17.8), i.e., $\Phi(\xi, \xi_0; \lambda)$ is a matrix-valued function satisfying (17.8) and $\Phi(\xi_0, \xi_0; \lambda) = \text{Id}$. It can be shown [San01, KKS04] that under suitable technical conditions, there exist continuous projection operators $P_s(\xi; \lambda)$ and $P_u(\xi; \lambda)$ for $\xi \in \mathbb{R}$, defined on \mathbb{R}^{2N} and depending analytically on λ , as well as constants $\kappa_s < 0 < \kappa_u$, $K \geq 1$, such that

$$\begin{aligned} \|\Phi(\xi, \zeta; \lambda)P_u(\zeta; \lambda)\| &\leq Ke^{\kappa_u(\xi-\zeta)}, & \text{for } \xi \leq \zeta \text{ and } \xi, \zeta \in \mathbb{R}, \\ \|\Phi(\xi, \zeta; \lambda)P_s(\zeta; \lambda)\| &\leq Ke^{\kappa_s(\xi-\zeta)}, & \text{for } \xi \geq \eta \text{ and } \xi, \zeta \in \mathbb{R}. \end{aligned} \quad (17.9)$$

One usually refers to (17.9) as an **exponential dichotomy**. From the formulation (17.9), it is apparent that exponential dichotomies generalize the classical splitting into stable and unstable eigenspaces for linear autonomous systems to the nonautonomous linear system (17.8).

Furthermore, let $\mathcal{N}(\cdot)$ denote the null space and $\mathcal{R}(\cdot)$ the range of an operator, and suppose $\lambda \notin \sigma_e(\mathcal{L})$. The values $\dim(\mathcal{N}(P_s(0; \lambda)))$ and $\dim(\mathcal{N}(P_u(0; \lambda)))$ are also called the **Morse indices** of P_s and P_u , and $\dim(\mathcal{N}(P_s(0; \lambda)))$ is also called the Morse index associated with an exponential dichotomy. Since the projections depend analytically on λ , there are analytic bases [Kat80] for

$\mathcal{R}(P_s(0; \lambda))$ and $\mathcal{R}(P_u(0; \lambda))$. We denote these bases by

$$\{b_1(\lambda), \dots, b_k(\lambda)\} \quad \text{and} \quad \{b_{k+1}(\lambda), \dots, b_{2N}(\lambda)\}.$$

Then we define a $2N \times 2N$ complex matrix

$$B(\lambda) := (b_1(\lambda) \cdots b_k(\lambda) b_{k+1}(\lambda) \cdots b_{2N}(\lambda)).$$

One way to think of the matrix $B(\lambda)$ is that it just collects the exponentially growing and decaying directions as $|\xi| \rightarrow \infty$.

Definition 17.1.4. The **Evans function** is $E(\lambda) := \det(B(\lambda))$.

Note that we have not defined the Evans function uniquely, since its definition involves a choice of bases. All the different versions of the Evans function differ by multiplication by an analytic function that does not vanish on Ω . The remarkable properties of the Evans function are summarized in the next theorem.

Theorem 17.1.5 ([Eva72, AGJ90]). *The Evans function $E(\lambda)$ has the following properties:*

- $E(\lambda)$ is analytic for $\lambda \in \Omega$.
- $E(\lambda) \in \mathbb{R}$ if $\lambda \in \mathbb{R} \cap \Omega$.
- $E(\lambda) = 0$ if and only if λ is an eigenvalue.
- The order of a zero of $E(\lambda)$ is equal to the algebraic multiplicity if we view the zero as an eigenvalue.

Unfortunately, Definition 17.1.4 does not immediately reveal why the properties in Theorem 17.1.5 should follow. There is another, slightly simpler, way to define the Evans function if we assume that all eigenvalues are simple. It turns out that Theorem 17.1.5 is a natural result if one works through the different possible definitions; in this regard, [Kap05] provides an introduction, and [San01] provides a survey as well as further details; see also the book [KP13]. One interesting consequence of Theorem 17.1.5 is that we can count the number of eigenvalues by the argument principle

$$\#\{\text{eigenvalues enclosed by a curve } \Gamma\} = \frac{1}{2\pi i} \oint_{\Gamma} \frac{E'(\lambda)}{E(\lambda)} d\lambda, \quad (17.10)$$

where $\#\{\cdot\}$ indicates the cardinality of a set, and we have assumed that Γ is a simple closed curve contained in $\mathbb{C} - \Omega$ and that eigenvalues are counted using algebraic multiplicity. Formula (17.10) is illustrated in Figure 17.1(b). If we can find only the trivial eigenvalue inside a sufficiently large curve Γ , then we may conclude that the traveling wave is stable. The drawback of the Evans function is that it is difficult to compute analytically as well as numerically. Therefore, our next natural question is to consider what happens if the traveling-wave problem has a multiple time scale structure as illustrated in Section 6.5? Does the calculation simplify?

17.2 Stability of Traveling Waves II

In this section, we indicate how the fast–slow structure of the equations can be utilized for stability analysis and how such an analysis interacts with topological methods. In particular, we show that the fast–slow structure induces a decomposition of the eigenvalues in the point spectrum. As a concrete example, consider two coupled reaction–diffusion equations

$$\begin{aligned}\frac{\partial u_1}{\partial t} &= \varepsilon^2 \frac{\partial^2 u_1}{\partial x^2} + u_1 f_1(u), \\ \frac{\partial u_2}{\partial t} &= \frac{\partial^2 u_2}{\partial x^2} + u_2 f_2(u),\end{aligned}\quad (17.11)$$

where $u = (u_1, u_2)$ is restricted to the nonnegative quadrant $\{u_{1,2} \geq 0\}$. The main assumptions for (17.11) are these:

- (A1) $\frac{\partial f_1}{\partial u_2} < 0$ and $\frac{\partial f_2}{\partial u_1} > 0$.
- (A2) The nullclines $\{f_1 = 0\}$ and $\{f_2 = 0\}$ are as shown in Figure 17.2.

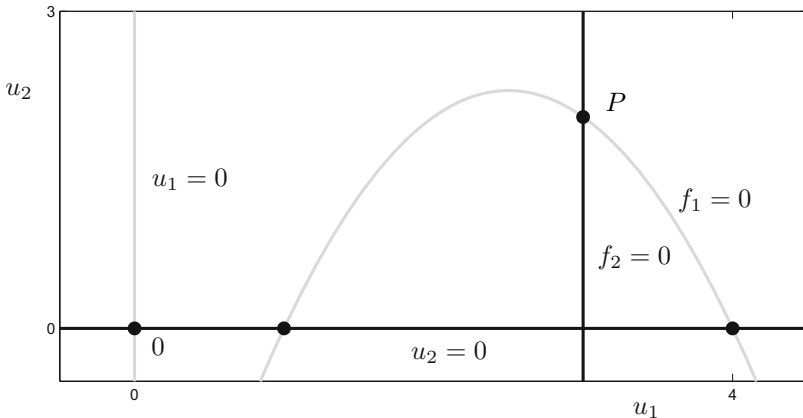


Figure 17.2: Geometry of the nullclines for (17.11) without diffusion for the specific model (17.13). The four steady states are marked by dots; the traveling-front solution connects from $0 = (0, 0)$ to $P = \{f_1 = 0\} \cap \{f_2 = 0\}$. We note that the nullcline $\{f_2 = 0\}$ is not required to be vertical for assumption (A2), but we require only that the steady state P lie on the right branch of $\{f_1 = 0\}$.

The reaction–diffusion equations (17.11) are mainly motivated by predator–prey models from ecology. For example, if we add diffusion to a **Rosenzweig–MacArthur**–type ODE model for $u = (u_1, u_2)$ and positive parameters p_i given by

$$\begin{aligned}u'_1 &= u_1(a(u_1) - u_2 b(u_1)) = u_1 f_1(u), \\ u'_2 &= u_2(p_1 u_1 b(u_1) - p_2) = u_2 f_2(u),\end{aligned}\quad (17.12)$$

then we get reaction–diffusion equations of the form (17.11). The condition (A1) is given by $-b(u_1) < 0$ and $b(u_1) + u_1 b'(u_1) > 0$. From a modeling

standpoint, $u_1 a(u_1)$ represents the growth rate of the prey u_1 with no predator. The **functional response** for predator-prey interaction $b(u_1)$ is always positive, e.g., a Holling type-II response $b(u_1) = 1/(p_3 + u_1)$ is chosen for the classical Rosenzweig-MacArthur model, so that $b(u_1) > 0$ always holds. A similar remark applies to the second condition $b(u_1) + u_1 b'(u_1) > 0$.

To make (A2) even more concrete, consider a specific version of (17.12) with $b(u_1) = 1$, $p_1 = 1$, $p_2 = 3$, and $a(u_1) = (u_1 - 1)(4 - u_1)$, so that the growth term for the prey exhibits an **Allee effect**. In this case, we have that

$$f_1(u) = -u_2 + (u_1 - 1)(4 - u_1) \quad f_2(u) = u_1 - 3, \quad (17.13)$$

so that the assumptions (A1)–(A2) are both satisfied; see Figure 17.2. From now on, the reader may think either of the concrete example (17.13) or the abstract conditions (A1)–(A2).

There are four steady-state solutions, and we are interested in traveling-front solutions that connect $0 = (0, 0)$ to $P = \{f_1 = 0\} \cap \{f_2 = 0\}$. We look for traveling-wave solutions of the form $v(\tau) := u(x - \varepsilon s t)$ of (17.11) and find the associated ODEs

$$\begin{aligned} \varepsilon \frac{dv_1}{d\tau} &= \varepsilon \dot{v}_1 = w_1, \\ \varepsilon \frac{dw_1}{d\tau} &= \varepsilon \dot{w}_1 = -sw_1 - v_1 f_1(v), \\ \frac{dv_2}{d\tau} &= \dot{v}_2 = w_2, \\ \frac{dw_2}{d\tau} &= \dot{w}_2 = -\varepsilon sw_2 - v_2 f_2(v). \end{aligned} \quad (17.14)$$

Obviously, (17.14) has four equilibrium points associated with the steady states of the PDE. By slight abuse of notation, we again use the notation $P = \{f_1(v) = 0 = f_2(v)\}$ and $0 = (0, 0, 0, 0)$. It is easy to check that P and 0 are saddle points. The critical manifold of (17.14) is

$$C_0 = \{(v_1, w_1, v_2, w_2) \in \mathbb{R}^4 : w_1 = 0, v_1 = 0 \text{ or } w_1 = 0, f_1(v) = 0\}.$$

We can put the two parts of C_0 in direct correspondence with the two gray curves in Figure 17.2; we refer to the left part of the parabolic-shaped curve up to the maximum as C_0^l and the right part as C_0^r . The interesting aspect of the traveling-wave problem is that we are dealing with a (2, 2)-fast-slow system (17.14). Therefore, the both the slow flow and the fast flow give rise to nontrivial connecting orbits. Despite this additional difficulty, the well-known fast-slow decomposition strategy (see, e.g., Section 6.5) still yields the existence of a traveling wave. In fact, the fast part of the orbit of the wave connects $\{v_1 = 0, w_1 = 0\} \subset C_0$ to $C_0^r \subset C_0$.

Theorem 17.2.1 ([Gar84, GJ91]). *Under the assumptions (A1)–(A2) and for $\varepsilon > 0$ sufficiently small, there exists a wave speed $s = s(\varepsilon)$ such that (17.14) has a heteroclinic connection. Therefore, the PDE (17.11) has a traveling-front solution for $\varepsilon > 0$ sufficiently small.*

Exercise/Project 17.2.2. Use geometric singular perturbation theory similar to that presented in Chapter 6 and/or Conley index theory from Chapter 16 to prove Theorem 17.2.1. Furthermore, compute the heteroclinic connection numerically using any combination of methods from Chapters 10 and 11. ◇

Regarding stability of the wave in Theorem 17.2.1, it can be shown that the essential spectrum σ_e^ε is contained in the left half of the complex plane, where we use the superscript ε to indicate the dependence of the spectrum on ε . We focus again on the point spectrum σ_p^ε and let Ω be the connected component of $\mathbb{C} - \sigma_e^\varepsilon$ that contains the right half-plane $\{\lambda \in \mathbb{C} : \operatorname{Re}(\lambda) > 0\}$. Computing the point spectrum σ_p^ε for (17.11) directly is difficult. To understand the problem, we begin with the usual approach and linearize (17.11) around a traveling wave v existing at a wave speed $s = s(\varepsilon)$, where $\tau = x - \varepsilon st$. We get the eigenvalue problem

$$\begin{aligned}\lambda V_1 &= \varepsilon^2 \frac{d^2 V_1}{d\tau^2} + \varepsilon s \frac{dV_1}{d\tau} + \frac{\partial}{\partial v_1} [v_1 f_1(v)] V_1 + \frac{\partial}{\partial v_2} [v_1 f_1(v)] V_2, \\ \lambda V_2 &= \frac{d^2 V_2}{d\tau^2} + \varepsilon s \frac{dV_2}{d\tau} + \frac{\partial}{\partial v_1} [v_2 f_2(v)] V_1 + \frac{\partial}{\partial v_2} [v_2 f_2(v)] V_2,\end{aligned}\quad (17.15)$$

where the partial derivatives with respect to $v_{1,2}$ are evaluated at the traveling wave $(v_1, v_2) = q$. To simplify the notation, we define

$$A_{ij}(\tau; \varepsilon) := \frac{\partial}{\partial_j} [v_i f_i(v)], \quad \text{evaluated at } v = q(\tau; \varepsilon).$$

Setting $(\varepsilon \dot{V}_1, \dot{V}_2) = (W_1, W_2)$, we end up with the $(2, 2)$ -fast–slow nonautonomous system

$$\begin{aligned}\varepsilon \dot{V}_1 &= W_1, \\ \varepsilon \dot{W}_1 &= -sW_1 - (A_{11}(\tau; \varepsilon) - \lambda)V_1 - A_{12}(\tau; \varepsilon)V_2, \\ \dot{V}_2 &= W_2, \\ \dot{W}_2 &= -\varepsilon sW_2 - A_{21}(\tau; \varepsilon)V_1 - (A_{22}(\tau; \varepsilon) - \lambda)V_2.\end{aligned}\quad (17.16)$$

This suggests that we split the linearized problem (17.16) into fast and slow subsystems. The slow subsystem is given by

$$\begin{aligned}\dot{V}_2 &= W_2, \\ \dot{W}_2 &= -A_{21}(\tau; 0)V_1 - (A_{22}(\tau; 0) - \lambda)V_2,\end{aligned}\quad (17.17)$$

and is defined on the critical manifold

$$\tilde{C}_0 = \{(V, W) \in \mathbb{R}^4 : W_1 = 0, (A_{11}(\tau; 0) - \lambda)V_1 + A_{12}(\tau; 0)V_2 = 0\}.$$

The fast subsystem of (17.16) is

$$\begin{aligned}V'_1 &= W_1, \\ W'_1 &= -sW_1 - (A_{11}(\tau; 0) - \lambda)V_1 - A_{12}(\tau; 0)V_2.\end{aligned}\quad (17.18)$$

Obviously, we can search for eigenvalues λ based on the subsystems (17.17) and (17.18). This yields a point spectrum for the reduced problem

$$\sigma_p^0 = \sigma_p^{0,f} \cup \sigma_p^{0,s},$$

where $\sigma_p^{0,f}$ and $\sigma_p^{0,s}$ are the point spectra of the fast and slow subsystems. Although this approach is appealing, we have to answer two major questions:

(Q1) How can we calculate $\sigma_p^{0,f}$ and $\sigma_p^{0,s}$?

(Q2) How can we prove that $\sigma_p^0 = \sigma_p^\varepsilon$ for $0 < \varepsilon \ll 1$?

Proposition 17.2.3. *The fast subsystem has associated point spectrum given by $\sigma_p^f = \{0\}$. The eigenvalue $\lambda = 0$ is a trivial eigenvalue with multiplicity 1.*

Proof. (Sketch, [GJ91]) Observe that the fast subsystem (17.18) can be viewed as a linearization for the traveling-wave problem

$$\frac{\partial u_1}{\partial t} = \frac{\partial^2 u_1}{\partial x^2} + u_1 f_1(u). \quad (17.19)$$

It can be shown that there is a traveling-front solution to (17.19) that can be identified with the fast transition connection in (17.14). However, for this problem, a result by Fife and McLeod [FM77] implies that the traveling-front solution of (17.19) has only the trivial eigenvalue $\lambda = 0$ in the point spectrum. \square

The result for the slow subsystem cannot be obtained by applying a previous theorem but requires a more detailed calculation.

Proposition 17.2.4 ([GJ91]). *Let S_R denote the subset of the right branch of C_0^r with $v_2 \geq 0$. Suppose that*

$$\max_{v \in S_R} \frac{|A_{12}(v)A_{21}(v)|}{A_{11}(v)^2} < 1,$$

where A_{ij} are the entries of the Jacobian matrix of $(v_1 f_1, v_2 f_2)$. Then $\sigma_p^s = \emptyset$.

Hence, we are left with the question (Q2). Alexander, Gardner, and Jones [AGJ90] developed a very interesting relationship of the point spectrum to topology to address this problem. To develop the complete theory is beyond the scope of this book, but we shall outline the basic idea. The required background from topology can be found in [MS74].

Theorem 17.2.5 ([AGJ90, GJ91]). *Consider a curve Γ as illustrated in Figure 17.1(b) in Ω such that no eigenvalues lie on Γ . Then there exists a complex 2-plane bundle $\mathcal{E}(\varepsilon)$ over the real two-sphere S^2 ,*

$$\mathcal{E}(\varepsilon) : E \xrightarrow{\Pi} S^2, \quad E \subset S^2 \times \mathbb{C}^2,$$

associated with Γ , where Π is the bundle projection map. Furthermore, we have that

$$\#\{\text{eigenvalues enclosed by } \Gamma\} = c_1(\mathcal{E}(\varepsilon)),$$

where $c_1(\mathcal{E}(\varepsilon))$ is the first Chern number of the bundle.

Therefore, a topological invariant is attached to the number of eigenvalues. Since we also know that the Evans function $E(\lambda)$ can be used to count the number of eigenvalues, we have the elegant formula

$$\frac{1}{2\pi i} \oint_{\Gamma} \frac{E'(\lambda)}{E(\lambda)} d\lambda = c_1(\mathcal{E}(\varepsilon)).$$

The key ingredient in using Theorem 17.2.5 in the context of the diffusive predator-prey system (17.11) is to show that the fast-slow structure induces a splitting of the bundle $\mathcal{E}(\varepsilon)$ into a Whitney sum

$$\mathcal{E}(\varepsilon) = \mathcal{E}_f(\varepsilon) \oplus \mathcal{E}_s(\varepsilon) \quad (17.20)$$

of complex line bundles $\mathcal{E}_f(\varepsilon)$ and $\mathcal{E}_s(\varepsilon)$. A fact from topology implies that the Chern number behaves additively under this decomposition,

$$c_1(\mathcal{E}(\varepsilon)) = c_1(\mathcal{E}_f(\varepsilon)) + c_1(\mathcal{E}_s(\varepsilon)).$$

From Propositions 17.2.3–17.2.4, we can conclude that

$$c_1(\mathcal{E}(0)) = c_1(\mathcal{E}_f(0)) + c_1(\mathcal{E}_s(0)) = 1 + 0 = 1,$$

which means that for the singular limit $\varepsilon = 0$, we have only the trivial eigenvalue. The advantage of the topological construction is that a homotopy/continuation argument (see also Chapter 16) can be used to show that

$$c_1(\mathcal{E}_f(\varepsilon)) = c_1(\mathcal{E}_f(0)) \quad \text{and} \quad c_1(\mathcal{E}_s(\varepsilon)) = c_1(\mathcal{E}_s(0))$$

for $\varepsilon > 0$ sufficiently small. Therefore, only the trivial eigenvalue is in the point spectrum.

Theorem 17.2.6 ([GJ91]). *Consider a traveling front for (17.11) as described in Theorem 17.2.1. Let S_R denote be the subset of the right branch of C_0^r with $v_2 \geq 0$. Suppose that*

$$\max_{v \in S_R} \frac{|A_{12}(v)A_{21}(v)|}{A_{11}(v)^2} < 1,$$

where A_{ij} are the entries of the Jacobian matrix of $(v_1 f_1, v_2 f_2)$. Then the traveling wave is stable.

Theorem 17.2.6 demonstrates that the fast-slow decomposition can also be useful in analyzing the stability of traveling-wave solutions. The splitting of vector bundles (17.20) again illustrates how the multiscale structure of fast-slow systems is naturally inherited across mathematical disciplines.

17.3 Conservation Laws

Another connection between fast-slow systems and partial differential equations is the existence of (regularized) **conservation laws**. We shall consider only the simplest **conservation law** in one spatial dimension,

$$\frac{\partial u}{\partial t} + \frac{\partial}{\partial x} F(u) = u_t + F(u)_x = 0, \quad (17.21)$$

where $t \geq 0$, $x \in \mathbb{R}$, $u = u(x, t) \in \mathbb{R}$, and $F : \mathbb{R} \rightarrow \mathbb{R}$ is sufficiently smooth. Augmenting (17.21) with initial conditions yields the problem

$$\begin{cases} u_t + F(u)_x = 0 & \text{for } (x, t) \in \mathbb{R} \times (0, \infty), \\ u = G & \text{for } x \in \mathbb{R} \text{ and } t = 0, \end{cases} \quad (17.22)$$

where $G : \mathbb{R} \rightarrow \mathbb{R}$. It is well known that classical smooth solutions to (17.22) may not exist. To illustrate this problem, we briefly review some of the main concepts of solutions in the next two examples.

Example 17.3.1. First, consider **Burgers' equation**

$$\begin{cases} u_t + \left(\frac{u}{2}\right)_x = u_t + uu_x = 0 & \text{for } (x, t) \in \mathbb{R} \times (0, \infty) =: \Gamma, \\ u = G & \text{for } (x, t) \in \mathbb{R} \times \{t = 0\} = \partial\Gamma, \end{cases} \quad (17.23)$$

where

$$G = G(x) = \begin{cases} 1 & \text{for } x \leq 0, \\ 1 - x & \text{for } x \in (0, 1), \\ 0 & \text{for } x \geq 1. \end{cases} \quad (17.24)$$

Note that the PDE (17.23) can also be rewritten in the general form

$$a(x, t, u)u_t + b(x, t, u)u_x = c(x, t, u) \quad (17.25)$$

with $a(x, t, u) = 1$, $b(x, t, u) = u$, and $c(x, t, u) = 0$. Therefore, we can attempt to use the **method of characteristics** to find a solution [LeV92, Eva02]. The method tries to infer the solution in the interior of the domain Γ from the boundary value on $\partial\Gamma$. Indeed, suppose $u = u(x, t)$ solves the PDE (17.25). Then $z = u(x, t)$ describes a surface S , and (17.25) can be interpreted as

$$(a(x, t, u), b(x, t, u), c(x, t, u)) \cdot (u_t, u_x, -1)^\top = 0.$$

Since the normal vector to $S = \{(x, t, u(x, t))\}$ is given by $(u_t, u_x, -1)$, one observes that the vector $(a(x, t, u), b(x, t, u), c(x, t, u))$ must be tangent to S . So we set $z(s) := u(x(s), t(s))$ and search for **characteristic curves** (or simply **characteristics**)

$$(x(s), t(s)) \quad \text{through } \partial\Omega$$

that satisfy the **characteristic ODEs**

$$\begin{aligned} \frac{dx}{ds} &= b(x, t, z) = z, \\ \frac{dt}{ds} &= a(x, t, z) = 1, \\ \frac{dz}{ds} &= c(x, t, z) = 0, \end{aligned} \quad (17.26)$$

with initial conditions $(x(0), t(0), z(0)) = (x_0, 0, G(x_0))$; see Figure 17.3. It is straightforward to solve (17.26), which gives

$$(x(s), t(s), z(s)) = (G(x_0)s + x_0, s, G(x_0)).$$

This implies that the characteristics are straight lines and $u(x(s), t(s)) = z(s) = G(x_0)$ is constant on each characteristic. We have

$$u(x, t) = \begin{cases} 1 & \text{if } x \leq t \quad \text{and } t \in [0, 1], \\ \frac{1-x}{1-t} & \text{if } t \leq x \leq 1 \quad \text{and } t \in [0, 1], \\ 0 & \text{if } x \geq 1 \quad \text{and } t \in [0, 1]. \end{cases} \quad (17.27)$$

The situation is illustrated in Figure 17.3.

Exercise 17.3.2. Derive the formula (17.27) from the characteristics. \diamond

Observe that the method of characteristics breaks down at $t = 1$. In particular, the characteristics begin to cross, which generates the major problem. From a geometric viewpoint, one still would like to piece the characteristics together in a sensible way for $t > 1$. We introduce another curve (see Figure 17.3),

$$s(t) := \frac{1+t}{2}, \quad (17.28)$$

and propose a solution

$$u(x, t) = \begin{cases} 1 & \text{if } x < s(t) \text{ and } t > 1, \\ 0 & \text{if } x > s(t) \text{ and } t > 1. \end{cases} \quad (17.29)$$

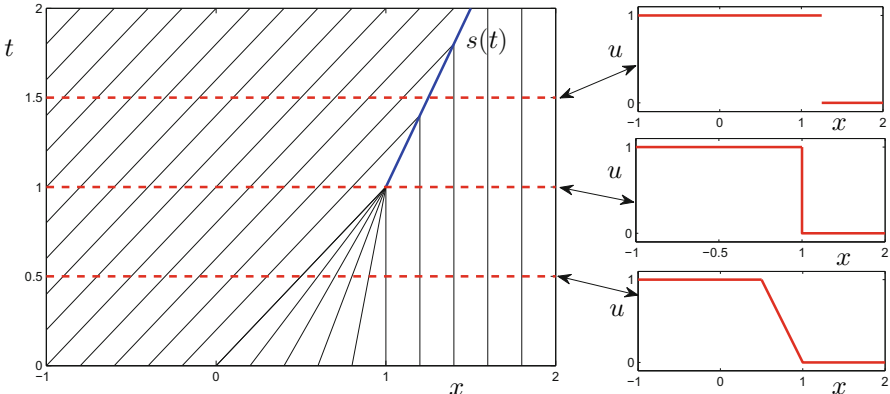


Figure 17.3: On the left-hand side, we show the (x, t) -plane together with the characteristic curves (lines) in black for Burgers' equation; the initial condition is (17.24). The shock curve $s(t) = \frac{1+t}{2}$ is shown in blue, and red dashed lines mark slices of the solution at fixed time snapshots $t = t^*$ for $t^* \in \{0.5, 1, 1.5\}$; these snapshots are shown on the right-hand side in (x, u) -plots with $(x, u) = (x, u(x, t^*))$.

The formula (17.27) describes a solution with a jump discontinuity along $s(t)$; this solution is called a **shock wave** or simply a **shock**. Notice that the shock travels in x -space toward $+\infty$ as t increases. The choice of $s(t)$ seems

arbitrary, but it can be justified using weak solutions, i.e., by multiplying the PDE $u_t + F(u)_x = 0$ by a **test function**

$$v : \mathbb{R} \times [0, \infty) \rightarrow \mathbb{R}, \quad v \text{ smooth, with compact support} \quad (17.30)$$

and formally integrating by parts as follows:

$$\begin{aligned} 0 &= \int_0^\infty \int_{-\infty}^\infty (u_t + F(u)_x)v \, dx \, dt \\ &= - \int_0^\infty \int_{-\infty}^\infty uv_t \, dx \, dt - \int_{-\infty}^\infty uv \, dx|_{t=0} - \int_0^\infty \int_{-\infty}^\infty F(u)v_x \, dx \, dt. \end{aligned}$$

From the last equation and the initial condition $u = G$ on $\partial\Gamma$, it follows that

$$\int_0^\infty \int_{-\infty}^\infty (uv_t + F(u)v_x) \, dx \, dt + \int_{-\infty}^\infty vG \, dx|_{t=0} = 0. \quad (17.31)$$

A solution $u \in L^\infty(\mathbb{R} \times (0, \infty))$ that satisfies (17.31) for all test functions (17.30) is called a **weak solution** for the conservation law. Using this ansatz, it is not too difficult to derive a condition that curves $s(t)$ have to satisfy so that solutions like (17.29) are weak solutions.

Exercise 17.3.3. Use the weak formulation of the conservation law $u_t + F(u)_x = 0$ to derive the **Rankine–Hugoniot** condition

$$F(u_+) - F(u_-) - s'(t)(u_+ - u_-) = 0 \quad (17.32)$$

for shocks that have a jump discontinuity between two constants u_- to u_+ along a curve $s(t)$. ◇

It is easy to check that the curve $s(t) = (1+t)/2$ defined for solving Burgers' equation satisfies the Rankine–Hugoniot condition with $u_- = 1$ and $u_+ = 0$:

$$F(0) - F(1) - s'(t)(0 - 1) = \frac{0^2}{2} - \frac{1^2}{2} + \frac{1}{2} = 0.$$

To conclude the example, we note that often, it is required that shock solutions satisfy not only the Rankine–Hugoniot condition but also an entropy condition [Eva02], which we are not going to discuss here. ◆

Example 17.3.4. As a second example, we consider Burgers' equation (17.23) again but with another initial condition

$$G = G(x) = \begin{cases} 0 & \text{for } x < 0, \\ 1 & \text{for } x > 0. \end{cases} \quad (17.33)$$

The method of characteristics works again (see Figure 17.4) and yields two types of characteristics,

$$\begin{aligned} (x(s), t(s), z(s)) &= (x_0, s, 0) & \text{for } x_0 < 0, \\ (x(s), t(s), z(s)) &= (s + x_0, s, 1) & \text{for } x_0 > 0. \end{aligned}$$

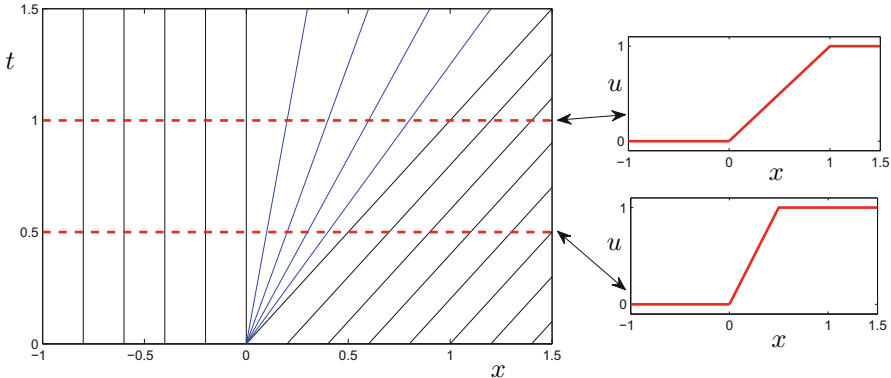


Figure 17.4: On the left-hand side, we show the (x, t) -plane together with the characteristic curves (lines) in black for Burgers' equation; the initial condition is (17.33). The rarefaction is shown in blue, and red dashed lines mark slices of the solution at fixed time snapshots $t = t^*$ for $t^* \in \{0.5, 1\}$; these snapshots are shown on the right-hand side in (x, u) -plots with $(x, u) = (x, u(x, t^*))$.

However, these characteristics fail to fill the entire cone given by

$$\{(x, t) \in \mathbb{R} \times [0, \infty) : x > 0, t > x\}, \quad (17.34)$$

as indicated in Figure 17.4. Although we know the solution outside the cone,

$$u_1(x, t) = \begin{cases} 0 & \text{if } x < 0, \\ 1 & \text{if } x > t, \end{cases} \quad (17.35)$$

we could try to generate a solution inside the cone (17.34) that interpolates continuously between the two different states $u = 0$ and $u = 1$. One possibility is to consider

$$u_2(x, t) = \begin{cases} 0 & \text{if } x < 0, \\ \frac{x}{t} & \text{if } 0 \leq x \leq t, \\ 1 & \text{if } x > t, \end{cases} \quad (17.36)$$

as shown in Figure 17.4. The solution (17.36) is an example of a **rarefaction wave**, or simply a **rarefaction**. ♦

Linking special solutions of conservation laws such as shocks and rarefactions to multiple time scale dynamics is not obvious. Nevertheless, one might already guess from Examples 17.3.1, 17.3.4 that shocks could correspond to fast jumps in the singular limit $\varepsilon = 0$ and that rarefactions might be interpreted as slowly changing parts of a solution. To develop this viewpoint, let us return to the general scalar conservation law

$$u_t + F(u)_x = 0. \quad (17.37)$$

Definition 17.3.5. The **Riemann problem** for (17.37) considers the piecewise constant initial condition

$$u(x, 0) = G(x) = \begin{cases} u_L & \text{for } x < 0, \\ u_R & \text{for } x > 0, \end{cases}$$

where u_L and u_R are constants. We refer to solutions of the Riemann problem as **Riemann solutions**.

The Riemann problem is a natural starting point. Let us assume that a part of the solution consists of a shock of the form

$$u(x, t) = \begin{cases} u_- & \text{for } x < ct, \\ u_+ & \text{for } x > ct, \end{cases} \quad (17.38)$$

where u_- and u_+ are constants, and the shock curve is $s(t) = ct$. The Rankine–Hugoniot condition is always assumed to hold for this shock. We have already observed in Examples 17.3.1, 17.3.4 that shocks and rarefactions can be viewed as moving profiles in time. The standard way to obtain smooth moving profiles is to regularize (17.37) and augment it with a diffusion term u_{xx} , so that we get

$$u_t + F(u)_x = u_{xx}. \quad (17.39)$$

In the theory of conservation laws, it is common to call (17.39) the **viscous regularization**. We consider a traveling-wave ansatz $u = u(x - ct)$ for (17.39) and look for stationary solutions that satisfy

$$u(-\infty) = u_- \quad \text{and} \quad u(+\infty) = u_+.$$

A direct calculation shows that such solutions exist only if the ODE

$$u' = F(u) - F(u_-) - c(u - u_-) \quad (17.40)$$

has an equilibrium at u_+ and a heteroclinic connection from u_- to u_+ ; observe that (17.40) always has an equilibrium at u_- and that the equilibrium condition on u_+ is equivalent to the Rankine–Hugoniot condition

$$0 = F(u_+) - F(u_-) - c(u_+ - u_-).$$

We shall always assume that the heteroclinic orbit exists, and we encode this condition in the next definition.

Definition 17.3.6. If for a shock (17.38), there exists a traveling-wave solution of (17.39) with the same speed and the same left and right end states, then we say that the shock satisfies the **viscous profile criterion**.

Sometimes, the viscous regularization (17.39) is also written as

$$u_t + F(u)_x = \varepsilon u_{xx}. \quad (17.41)$$

However, note that one may remove ε from (17.41) by scaling to obtain (17.39). On a formal level, it is intuitive look at traveling waves of (17.41) and consider the limit $\varepsilon \rightarrow 0$ to recover shock solutions.

Another possible, though less standard, choice for a regularization is stated in the next definition.

Definition 17.3.7. The **Dafermos regularization** of a conservation law is given by

$$u_t + F(u)_x = \varepsilon t u_{xx}. \quad (17.42)$$

To bring rarefaction waves into consideration as well, let us look for **scale-invariant solutions**

$$v(\xi) = u(x, t), \quad \text{for } \xi = \frac{x}{t}, \quad (17.43)$$

where the terminology derives from the fact that the scaling $(x, t) \mapsto (\alpha x, \alpha t)$ for $\alpha \neq 0$ leaves the solution invariant. Another direct computation shows that the scale-invariance assumption transforms (17.42) into the second-order nonautonomous ODE

$$\varepsilon \frac{d^2 v}{d\xi^2} - ((DF)(v) - \xi) \frac{dv}{d\xi} = 0, \quad (17.44)$$

where we could also write the total derivative as $DF = F'$ as $F : \mathbb{R} \rightarrow \mathbb{R}$. The boundary conditions

$$v(-\infty) = u_L \quad \text{and} \quad v(+\infty) = u_R \quad (17.45)$$

can be derived from the initial condition of the Riemann problem. Solutions of (17.44)–(17.45) are called **Riemann–Dafermos solutions**.

Exercise 17.3.8. Check that substituting (17.43) into the Dafermos regularization yields (17.44). Furthermore, show that the ODE (17.44) can be rewritten as an autonomous first-order system using the ansatz $\xi = \xi(0) + \varepsilon t$,

$$\begin{aligned} \frac{dv}{dt} &= v' = w, \\ \frac{dw}{dt} &= w' = (A(v) - \xi)w, \\ \frac{d\xi}{dt} &= \xi' = \varepsilon, \end{aligned} \quad (17.46)$$

with boundary conditions

$$(v, w, \xi)(-\infty) = (u_L, 0, -\infty) \quad \text{and} \quad (v, w, \xi) = (u_R, 0, \infty) \quad (17.47)$$

and where $A(v) := (DF)(v)$. \diamond

The system (17.46) is a $(2, 1)$ -fast–slow system in standard form. It turns out that Riemann–Dafermos solutions correspond to solutions of (17.46)–(17.47) with $\varepsilon > 0$. To understand the geometry of the problem better, we consider a concrete example.

Example 17.3.9. Consider the Riemann problem for the scalar conservation law (17.37) with

$$F(u) = u^2(u+1) \quad \text{and} \quad G(x) = \begin{cases} -1 & \text{for } x < 0, \\ \frac{4}{9} & \text{for } x > 0, \end{cases} \quad (17.48)$$

where it should be noted that $F(u)$ is not convex, which complicates the problem. The setup gives two types of characteristics:

$$\begin{aligned} (x, t, z) &= ([3G(x_0)^2 + 2G(x_0)]s + x_0, s, -1) = (s + x_0, s, -1) \quad \text{for } x_0 < 0, \\ (x, t, z) &= ([3G(x_0)^2 + 2G(x_0)]s + x_0, s, \frac{4}{9}) = (\frac{40}{27}s + x_0, s, \frac{4}{9}) \quad \text{for } x_0 > 0. \end{aligned}$$

Hence, we find that in (x, t) -space, the characteristics are shown as in Figure 17.5. In particular, already at $(x, t) = (0, 0)$ the characteristics cross, and a shock is formed. Since $F(u) = u^2(u+1)$, the jump occurs from $u_L = -1$ to $u_M = 0$. To determine the shock curve $s(t)$, we look at the Rankine–Hugoniot condition

$$0 = F(0) - F(-1) - s'(t)(0 - (-1)) = -s'(t).$$

Therefore, the speed of the shock curve is zero, and it is a vertical line in the (x, t) -plane. Between the shock curve and the characteristic $t = \frac{27}{40}x$, there is a cone that does not have a defined solution, i.e., directly after the shock wave, there is a rarefaction wave. Hence, we have to find a self-similar rarefaction fan solution $v^*(\xi)$ with $\xi = x/t$ that changes smoothly between $u_M = 0$ and $u_R = \frac{4}{9}$ and that satisfies the ODEs (17.46) with $\varepsilon = 0$. Let us look at those ODEs,

$$\begin{aligned} v' &= w, \\ w' &= (3v^2 + 2v - \xi)w, \\ \xi' &= \varepsilon, \end{aligned} \quad (17.49)$$

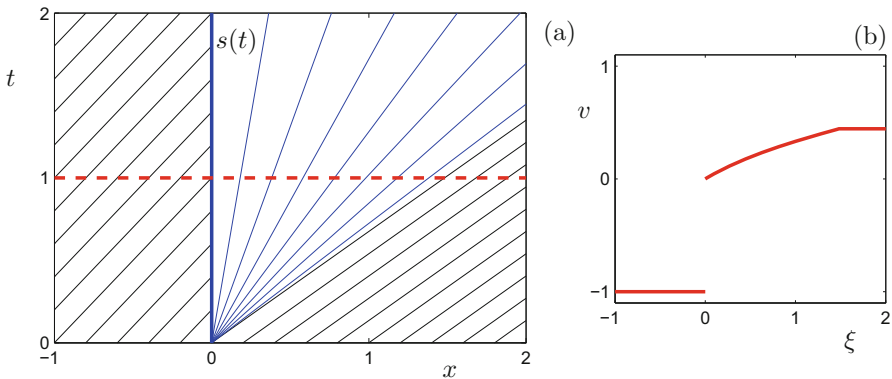


Figure 17.5: In (a), we show the (x, t) -plane together with the characteristic curves (lines) in black for a conservation law with data (17.48). The rarefaction is indicated by light blue lines and the shock $s(t)$ by a thickened vertical blue line at $x = 0$, and the red dashed line marks a slice of the solution at the fixed time $t = 1$. In (b) we show the solution (17.50).

for $\varepsilon \geq 0$ from the viewpoint of fast–slow systems. The critical manifold is given by the plane

$$C_0 = \{(v, w, \xi) \in \mathbb{R}^3 : w = 0\}.$$

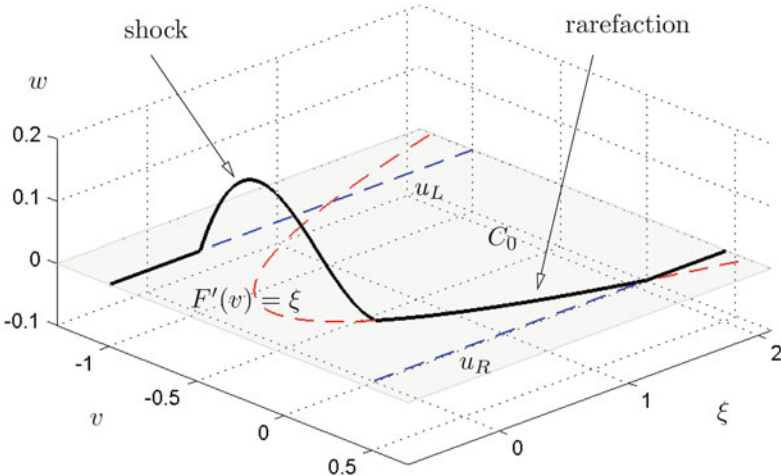


Figure 17.6: We show the representation of the Riemann solution for $\varepsilon = 0$ in the fast–slow system (17.49). The critical manifold is the transparent plane $\{w = 0\}$; the red dashed curve represents $F'(v) = \xi$, where the fast subsystem equilibria have two zero eigenvalues; the blue dashed lines are the asymptotic states of the Riemann initial condition; and the thickened black curve represents the Riemann solution.

Observe carefully that C_0 is two-dimensional despite the fact that we have a $(2, 1)$ -fast–slow system; these systems usually lead to one-dimensional critical manifolds, since two algebraic constraints have to be satisfied simultaneously. The linearization in the fast variables around C_0 is given by

$$\begin{pmatrix} 0 & 1 \\ 0 & 3v^2 + 2v - \xi \end{pmatrix},$$

which has eigenvalues 0 and $3v^2 + 2v - \xi$, so that C_0 is not normally hyperbolic, but it has an unstable fast direction for $3v^2 + 2v > \xi$ and a stable fast direction for $3v^2 + 2v < \xi$. The curve

$$\xi = 3v^2 + 2v = F'(v)$$

separates these two possibilities. Note also that the planes $\{\xi = \text{const}\}$ are invariant for $\varepsilon = 0$. Therefore, one might conjecture how the fast–slow geometry relates to the solution of the Riemann problem and to the Riemann–Dafermos problem; see Figure 17.6. The Riemann solution consists of four different sets, as shown in Figure 17.6:

1. the asymptotic state $v = u_L$ given by $\{(v, w, \xi) : v = u_L, w = 0, \xi \leq 0\}$;
2. a heteroclinic orbit from $v = u_L$ to $v = 0$ of the fast subsystem representing the shock;
3. a slow segment along $\{\xi = F'(v)\}$ given by $\{(v, w, \xi) : 0 \leq v \leq u_L, w = 0, \xi \leq 0, \xi = F'(v)\}$;
4. the asymptotic state $v = u_R$ given by $\{(v, w, \xi) : v = u_R, w = 0, F'(v) < \xi\}$;

We can write the solution of the Riemann problem for this setup as

$$v(\xi) = \begin{cases} -1 & \text{for } \xi < 0, \\ v^*(\xi) & \text{for } 0 \leq \xi \leq \frac{40}{27}, \\ \frac{4}{9} & \text{for } \xi > \frac{40}{27}, \end{cases} \quad (17.50)$$

where $v^*(\xi) = (F')^{-1}(\xi)$; see also Figure 17.5. The next natural question to ask is whether there is a Riemann–Dafermos solution to the conservation law that is a perturbation of the singular orbit shown in Figure 17.6. ♦

Theorem 17.3.10 ([SS04b]). *Consider a scalar conservation law $u_t + F(u)_x = 0$ and suppose that the associated Riemann problem has a solution $u(x, t) = v_0(x/t)$ given by a composition of an asymptotic state, a shock wave, a rarefaction, and an asymptotic state. Suppose the shock satisfies the Rankine–Hugoniot condition and the viscous profile criterion. Then for $\varepsilon > 0$ sufficiently small, there exists a Riemann–Dafermos solution v_ε that converges to v_0 as $\varepsilon \rightarrow 0$.*

Theorem 17.3.10 can be extended to cover more-general conservation laws. Consider a system of conservation laws in one space dimension,

$$u_t + F(u)_x = 0, \quad (17.51)$$

where $u(x, t) : \mathbb{R} \times [0, \infty) \rightarrow \mathbb{R}^N$ and $F : \mathbb{R}^N \rightarrow \mathbb{R}^N$ may have a higher-dimensional range for some $N \geq 1$. We can again consider the associated Riemann problem for the Dafermos regularization. The ODEs obtained from assuming self-similar solutions $u(x, t) = v(x/t)$ given by (17.46) basically remain the same:

$$\begin{aligned} \frac{dv}{dt} &= v' = w, \\ \frac{dw}{dt} &= w' = (A(v) - \xi)w, \\ \frac{d\xi}{dt} &= \xi' = \varepsilon, \end{aligned} \quad (17.52)$$

where $A(v) := (\mathrm{DF})(v)$ and $(v, w) \in \mathbb{R}^N \times \mathbb{R}^N$. To make the same ideas work as for the one-dimensional case in Theorem 17.3.10 requires some modified assumptions:

(H1) The matrix $A(v)$ has real distinct eigenvalues; when this assumption is satisfied, we say that the conservation law (17.51) is (**strictly**) **hyperbolic**.

- (H2) There exists a solution $v_0(x/t)$ consisting of an **n -wave Riemann solution**, that is, there are n -waves consisting of shocks and/or rarefactions.
- (H3) Shock solutions satisfy the Rankine–Hugoniot condition and the viscous profile criterion.
- (H4) The Riemann solution v_0 is structurally stable; basically, this condition requires that if we perturb the asymptotic states slightly then there must still be an n -wave Riemann solution with the same structure as in (H2).

Theorem 17.3.11 ([SS09]). *Under the assumptions (H1)–(H4) and for $\varepsilon > 0$ sufficiently small, a Riemann solution perturbs to a Riemann–Dafermos solution.*

A really interesting aspect of Theorem 17.3.11 is that its proof requires the blowup method and a strengthened version of the classical exchange lemma; see Chapters 6 and 7.

We already alluded to the possibility of using the standard viscous regularization with a small parameter instead of using the Dafermos regularization, leading to

$$u_t + F(u)_x = \varepsilon u_{xx}. \quad (17.53)$$

As mentioned previously, ε can be scaled out in (17.53), which makes the general situation for singular perturbation theory very difficult. However, the next example shows a situation in which the standard viscous regularization interacts with fast–slow techniques in a nice way for studying traveling waves.

Example 17.3.12. Consider **advection–reaction–diffusion (ARD)** equations of the form

$$u_t + F(u)_x = S(u) + \varepsilon u_{xx}, \quad (17.54)$$

where $u \in \mathbb{R}^3$. The terms $S(u)$ are reaction (or source) terms, and εu_{xx} is the usual viscous perturbation of a conservation law; in principle, the source terms could also be small, so that conservation law effects are expected to be relevant. Equations of the form (17.54) appear, for example, in the modeling of cell migration. Mathematical modeling of cell migration motivates one possible choice for the unknown functions:

$$F(w) = \begin{pmatrix} 0 \\ -f_2(u_1, u_3) \\ f_3(u_1, u_3)u_2 \end{pmatrix}, \quad S(w) = \begin{pmatrix} f_2(u_1, u_3) \\ 0 \\ f_1(u_1, u_3) \end{pmatrix}, \quad (17.55)$$

where f_1, f_2, f_3 are smooth functions of two variables.

Exercise/Project 17.3.13. Use a traveling-wave ansatz $\tau = x - ct$ and convert (17.54)–(17.55) to a system of three second-order ODEs. As a second step, prove

that this system can be transformed to five first-order ODEs given by

$$\begin{aligned}\dot{w}_1 &= -f_2(u_1, u_3), \\ \dot{w}_2 &= -f_1(u_1, u_3), \\ \varepsilon\dot{u}_1 &= w_1 - cu_1, \\ \varepsilon\dot{u}_2 &= -cu_2 - f_2(u_1, u_3), \\ \varepsilon\dot{u}_3 &= w_2 - cu_3 + f_3(u_1, u_3)u_2,\end{aligned}\tag{17.56}$$

where $\cdot = d/d\tau$. Hint: If you cannot find a solution to the second step, consider a **Liénard transformation** similar to the derivation of the van der Pol equation in Section 1.3. \diamond

The resulting ODEs (17.56) in the traveling-wave frame form a $(3, 2)$ -fast–slow system in standard form. Therefore, the critical manifold is generically two-dimensional and normally hyperbolic with the usual generic folded singularities such as folded saddles or folded nodes; see Section 8.5. In particular, if we look for heteroclinic connections between equilibria on the critical manifold, then the connecting orbits can pass near these singularities; see Section 17.6. However, note carefully that (17.56) becomes quite degenerate if the source terms vanish, since this implies $\dot{w}_1 = 0 = \dot{w}_2$. \blacklozenge

17.4 Lattice Dynamical Systems

In this section, we consider the following fast–slow **lattice differential equations (LDEs)**:

$$\begin{aligned}\frac{du_i}{dt} &= u'_i = \alpha[u_{i+1} + u_{i-1} - 2u_i] + g(u_i) - w_i, \\ \frac{dw_i}{dt} &= w'_i = \varepsilon(u_i - \gamma w_i),\end{aligned}\tag{17.57}$$

where $w_i, u_i \in \mathbb{R}$, $i \in \mathbb{Z}$, $g : \mathbb{R} \rightarrow \mathbb{R}$, $\gamma, \alpha > 0$ are parameters, and $0 < \varepsilon \ll 1$. Choosing a cubic nonlinearity

$$g(u) = u(1-u)(u-a)$$

for $0 < a < 1/2$, we immediately realize the similarities between (17.57) and the classical FitzHugh–Nagumo (FHN) PDE

$$\begin{aligned}\frac{\partial u}{\partial t} &= D \frac{\partial^2 u}{\partial x^2} + u(1-u)(u-a) - w, \\ \frac{\partial w}{\partial t} &= \varepsilon(u - \gamma w),\end{aligned}\tag{17.58}$$

as discussed in Section 1.4, where $D > 0$ is a parameter controlling the diffusion, and $u = u(x, t)$ and $w = w(x, t)$ are unknown functions. Indeed, if we consider a finite difference discretization of the Laplacian on a regular grid with step length $h > 0$, we get

$$\frac{\partial^2 u}{\partial x^2} \approx \frac{u_{i+1} + u_{i-1} - 2u_i}{h^2}.$$

Therefore, one may view the LDE (17.57) as an approximation to (17.58) if $\frac{D}{h^2} \approx \alpha$.

Another motivation to consider (17.57) instead of (17.58) is that a neuronal axon is surrounded by an insulating myelin coating that has gaps; see Section 17.6. These gaps are a motivation to model the propagation of signals in neurons with a discrete version of the FHN PDE. Continuing with the analysis of (17.57), we are always going to assume that $\gamma > 0$ is chosen such that

$$g(\gamma w) = \gamma w(1 - \gamma w)(\gamma w - a) \neq w$$

for all $w \neq 0$. This implies that $\{(u_i, w_i)\}_{i \in \mathbb{Z}} = (0, 0)$ is the only i -independent equilibrium point of (17.57). We have already seen that the FHN PDE (17.58) admits so-called fast-traveling-pulse solutions; see Section 6.5. Recall that the traveling-wave ansatz to find these solutions is

$$(u, w)(\xi) = (u, w)(x + st), \quad (17.59)$$

where $s > 0$ is the wave speed. Substituting (17.59) into (17.58) leads to the $(2, 1)$ -fast-slow system

$$\begin{aligned} u' &= v, \\ v' &= \frac{1}{D}(sv - g(u) + w), \\ w' &= \frac{\varepsilon}{s}(u - \gamma w). \end{aligned} \quad (17.60)$$

In (17.60), homoclinic orbits to the equilibrium at the origin correspond to traveling pulse solutions. For the LDE-version of the FHN, it is natural to modify (17.59) and consider

$$(u, w)(\xi) = (u, w)(i + st), \quad (17.61)$$

since the space variable x corresponds to discrete lattice sites at index i . Substituting (17.61) into (17.57) (and dropping the star subscript again) yields

$$\begin{aligned} s \frac{du}{d\xi} &= \alpha[u(\xi + 1) + u(\xi - 1) - 2u(\xi)] + g(u(\xi)) - w(\xi), \\ s \frac{dw}{d\xi} &= \varepsilon(u(\xi) - \gamma w(\xi)). \end{aligned} \quad (17.62)$$

Observe that (17.62) has a retarded (or delay) term $u(\xi - 1)$ and also an advanced term $u(\xi + 1)$, which makes it a **mixed functional differential equation (MFDE)**. Hence, we have to consider an infinite-dimensional phase space, and the following choice is convenient:

$$X := C([-1, 1], \mathbb{R}) \times \mathbb{R} =: X_1 \times X_2.$$

Considering the fact that many delay equations (i.e., with no advance terms; see also Section 18.4) are already difficult to analyze, it is not unexpected that the detailed analysis of (17.62) is rather lengthy. Here we shall confine ourselves to stating results about homoclinic orbits to the origin,

$$(u, w)(\xi) \rightarrow (0, 0) \quad \text{as } |\xi| \rightarrow \infty.$$

We are also going to point out briefly the difficulties that arise in the proofs. Recall from Section 6.5 that the fast-pulse homoclinic orbits of (17.60) consist of two fast segments and two slow segments. The first fast segment for (17.60) is a fast subsystem heteroclinic connection at $w = 0$ from $(u, v) = (0, 0)$ to $(u, v) = (1, 0)$; see also Figure 17.7. In trying a similar approach for the MFDE (17.62), one has to study heteroclinic orbits (i.e., traveling fronts) of

$$s \frac{du}{d\xi} = \alpha[u(\xi + 1) + u(\xi - 1) - 2u(\xi)] + g(u(\xi)). \quad (17.63)$$

It is tempting to conjecture that (17.63) admits a heteroclinic solution between $u = 0$ and $u = 1$ for every $a \in (0, 1/2)$ as in the case of FHN PDE analysis. The next result shows that the lattice structure yields a new effect.

Theorem 17.4.1 ([HS10c, Kee87, MP99]). *For each sufficiently small $\alpha > 0$, there exists $a_0 \in (0, 1/2)$ such that for each $a \in [a_0, 1/2]$, a heteroclinic solution of (17.63) connecting $u = 0$ and $u = 1$ exists if and only if $s = 0$.*

Theorem 17.4.1 implies that if $a > 0$ is too large, then only a standing front exists. In this case, we say that (17.63) exhibits **propagation failure**. If $a > 0$ is sufficiently small, then propagation failure can be avoided. To state this result more precisely, we recall the basic structure of the critical manifold of (17.60) given by

$$C_0 := \{(u, v, w) \in \mathbb{R}^3 : w = g(u), v = 0\}$$

with fold points at $u = u_{\pm}$ that satisfy $g'(u_{\pm}) = 0$ and $u_- < u_+$; see Figure 17.7. The fold points split the critical manifold into three parts,

$$C_0^- := C_0 \cap \{u \leq u_-\}, \quad C_0^m := C_0 \cap \{u_- < u < u_+\}, \quad C_0^+ := C_0 \cap \{u \geq u_+\}.$$

We write each part as a graph of a function and introduce the notation $C_0^{\pm} := \{u = h_{\pm}(w), v = 0\}$.

Lemma 17.4.2 ([HS10c, MP99]). *Suppose $a > 0$ is sufficiently small and $\varepsilon = 0$. Then there are constants $w^* \in (0, g(u_+))$ and $s^* > 0$ such that the MFDE (17.62) with $s = s^*$ admits two heteroclinic solutions $(q_f, 0)$ and (q_b, w^*) with*

- (a) $\lim_{\xi \rightarrow -\infty} q_f(\xi) = 0$ and $\lim_{\xi \rightarrow \infty} q_f(\xi) = 1$,
- (b) $\lim_{\xi \rightarrow -\infty} q_b(\xi) = h_+(w^*)$ and $\lim_{\xi \rightarrow \infty} q_b(\xi) = h_-(w^*)$.

The solution in Lemma 17.4.2(a) is the traveling front from the equilibrium to the right branch C_0^+ of the critical manifold, while the solution in (b) is the traveling back from the right branch C_0^+ to the left branch C_0^- ; see Figure 17.7. Therefore, the restriction to sufficiently small $a > 0$ allows us to conclude the same existence result for the two fast heteroclinic segments as in the ODE case. We write γ_0 for the singular homoclinic orbit that can be represented by the following sequence of transitions:

$$(0, 0) \xrightarrow{q_f} (1, 0) \xrightarrow{C_0^+} (h_+(w^*), w^*) \xrightarrow{q_b} (h_-(w^*), w^*) \xrightarrow{C_0^-} (0, 0).$$

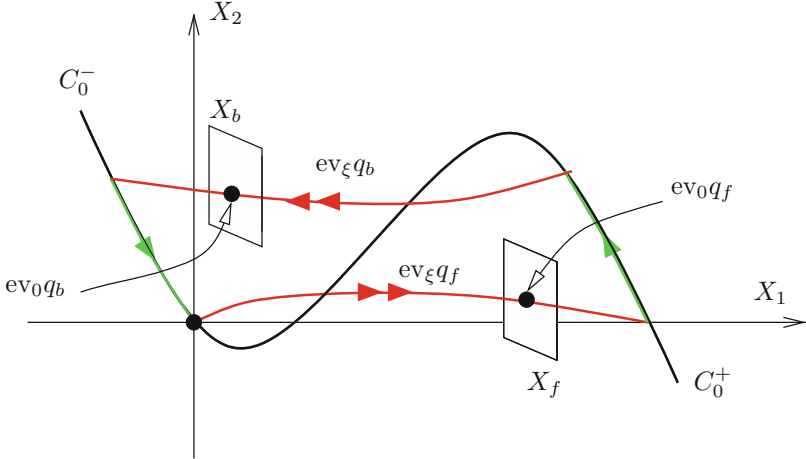


Figure 17.7: Sketch of the singular homoclinic orbit γ_0 in the FitzHugh–Nagumo MFDE (17.62). The orbit γ_0 consists of two fast segments (red) given by a traveling front $\text{ev}_\xi q_f$ and a traveling back $\text{ev}_\xi q_b$, and two slow segments (green) on C_0^\pm ; the fold points $(u_\pm, g(u_\pm))$ are the local maximum and minimum of the cubic curve $C_0 = C_0^- \cup C_0^m \cup C_0^+$. The phase space is $X = X_1 \times X_2$, where $u \in X_1 = C([-1, 1], \mathbb{R})$ and $X_2 = \mathbb{R}$. This figure also illustrates Definition 17.4.3.

To make the notion of homoclinic solution for the full MFDE (17.62) with $\varepsilon > 0$ more precise, we return to the phase space $X = X_1 \times X_2$ with $u \in X_1 = C([-1, 1], \mathbb{R})$ and $w \in X_2 = \mathbb{R}$. The goal is to define a precise meaning for the statement that the singular orbit γ_0 perturbs to a unique single-pulse homoclinic orbit in X . The state of a function $u \in C(\mathbb{R}, \mathbb{R})$ at “time” ξ will be denoted by $\text{ev}_\xi u \in X_1$; it is given by

$$(\text{ev}_\xi u)(\theta) := u(\xi + \theta), \quad \text{for } \theta \in (-1, 1).$$

Therefore, the “evaluation operator” $\text{ev}_\xi u$ produces a slice of the function u between $\xi - 1$ and $\xi + 1$ with a new domain given by $[-1, 1]$. As a next step, pick two subspaces X_f and X_b of X such that

$$X_1 = \text{span}\{\text{ev}_0 q'_f\} \oplus X_f \quad \text{and} \quad X_1 = \text{span}\{\text{ev}_0 q'_b\} \oplus X_b.$$

We can think of X_f and X_b as spaces transverse to the front and back solutions, i.e., they are Poincaré sections when viewed as $X_f \times X_2$ and $X_b \times X_2$; see Figure 17.7. Finally, a perturbed homoclinic solution for the MFDE case can be defined.

Definition 17.4.3. For each $0 < \delta \ll 1$ and $\xi_* \gg 1$, we say that a pair $(u, w) \in C(\mathbb{R}, \mathbb{R}^2)$ is a (δ, ξ_*) -homoclinic solution if for all $\xi \in \mathbb{R}$, the following conditions hold:

- (C1) [“solution property”] (u, w) satisfies the MFDE (17.62);
- (C2) [“homoclinic property”] $\lim_{|\xi| \rightarrow \infty} (u(\xi), w(\xi)) = (0, 0)$;

(C3) [“unique front passage”] there exists a unique $\xi_f \in \mathbb{R}$ such that

$$\|\text{ev}_{\xi_f} u - \text{ev}_0 q_f\| < \delta, \quad |w(\xi_f)| < \delta, \quad \text{and} \quad \text{ev}_{\xi_f} u \in \text{ev}_{\xi_f} q_f + X_f;$$

(C4) [“unique back passage”] there exists a unique $\xi_b \in \mathbb{R}$ such that

$$\|\text{ev}_{\xi_b} u - \text{ev}_0 q_b\| < \delta, \quad |w(\xi_b) - w^*| < \delta, \quad \text{and} \quad \text{ev}_{\xi_b} u \in \text{ev}_{\xi_b} q_b + X_b;$$

(C5) [“close to singular orbit”] the solution (u, w) is close to γ_0 , i.e.,

$$\begin{aligned} |u(\xi) - q_f(\xi - \xi_f)| &< \delta \quad \text{and} \quad |w(\xi)| < \delta & \text{for } \xi \leq \xi_f + \xi_*, \\ |u(\xi) - h_+(w(\xi))| &< \delta & \text{for } \xi_f + \xi_* \leq \xi \leq \xi_b - \xi_*, \\ |u(\xi) - q_b(\xi - \xi_b)| &< \delta \quad \text{and} \quad |w(\xi) - w^*| < \delta & \text{for } \xi_b - \xi_* \leq \xi \leq \xi_b + \xi_*, \\ |u(\xi) - h_-(w(\xi))| &< \delta & \text{for } \xi_b + \xi_* \leq \xi. \end{aligned}$$

Theorem 17.4.4 ([HS10c]). *Consider the MFDE (17.62) for $0 < a \ll 1$ sufficiently small. Then there exist constants $0 < \delta \ll 1$ and $\xi_* \gg 1$ such that for a wave speed s sufficiently close to the singular limit wave speed s_* with $s < s_*$, there exists $\varepsilon = \varepsilon(c) > 0$ for which (17.62) has a (δ, ξ_*) -homoclinic solution. The pair (u, w) is $\mathcal{O}(c - c_*)$ -close to the singular homoclinic orbit γ_0 and is unique up to translations.*

Basically, Theorem 17.4.4 allows us to conclude that we have only to avoid the propagation failure case to obtain a complete analogue of the FHN PDE existence result for the FHN LDE given by (17.57). However, the proof of Theorem 17.4.4 presents several novel challenges:

- Fenichel theory is not directly available for MFDEs of the form (17.62). Hence, one has to identify which of the different proofs of Fenichel’s theorem (see Section 2.5) can be carried over to MFDE. Proving a Fenichel’s theorem analogue yields slow manifolds $C_\varepsilon^\pm = \{(h_\pm(w), w)\}$; see also Section 18.2.
- Another step is to establish transversal intersections between $W^u(C_\varepsilon^-)$ and $W^s(C_\varepsilon^+)$ for $w \approx 0$ and between $W^u(C_\varepsilon^+)$ and $W^s(C_\varepsilon^-)$ for $w \approx w^*$. This can be achieved for MFDEs using a Lin’s method argument and Melnikov integrals; see also Sections 10.9, 19.8, and 6.1.
- The third difficulty is to generalize the exchange lemma which, allows a passage near C_ε^+ ; see also Chapter 6.

The additional reward from generalizing the exchange lemma is that stability of the fast pulse solutions can be proven as well.

Theorem 17.4.5 ([HS13]). *Under the same assumptions as in Theorem 17.4.4, the fast-pulse solution (u, w) is stable, i.e., each solution that starts sufficiently close to it at $t = 0$ will remain in a small neighborhood and converge to a translate of the fast pulse as $t \rightarrow \infty$.*

Theorem 17.4.5 is analogous to the fast-pulse stability for the FHN PDE.

Exercise/Project 17.4.6. Use the methods sketched in Sections 17.1 and 17.2 to prove the stability for the fast pulse in the FHN PDE from Section 6.5. ◇

For LDEs, the technical difficulties in the proof are more substantial, since classical Evans function techniques are not available. From a general point of view, the analysis of the fast–slow FHN LDE model has shown that we should expect many results from continuous systems to have strong relations to the corresponding lattice models.

17.5 Adaptive Neural Fields

Viewing electrical activity in the brain on a macroscopic level, one is naturally led to consider so-called **neural fields** $u = u(x, t)$, which represent the local activity of a population of neurons at a position x and time t . Usually, one takes $x \in \mathbb{R}$ if one is interested only in radial activity patterns $x \in \mathbb{R}^2$ for cortex models and $x \in \mathbb{R}^3$ for a full spatial model. For simplicity, we shall discuss only the case $(x, t) \in \mathbb{R} \times [0, \infty)$ in this section. A classical model for the evolution of u is given by an **integrodifferential equation**

$$\frac{\partial u}{\partial t}(x, t) = -u(x, t) + \int_{\mathbb{R}} w(x - y)F(u(y, t) - \kappa) dy, \quad (17.64)$$

where w is the interaction kernel between neurons, F is a function modeling the firing rate, and κ is the firing threshold. A typical concrete choice for F is a sigmoid shape, and for w , an exponential interaction function, e.g.,

$$F(u - \kappa) = \frac{1}{1 + e^{-\eta(u - \kappa)}} \quad \text{and} \quad w(x) = \frac{1}{2\sigma}e^{-|x|/\sigma}, \quad (17.65)$$

where η is the gain, and σ controls the range of synaptic connections. In the large-gain limit $\eta \rightarrow +\infty$, the firing rate function becomes a **Heaviside function**

$$F(u - \kappa) = H(u - \kappa) = \begin{cases} 1 & \text{if } u > \kappa, \\ 0 & \text{if } u < \kappa, \end{cases} \quad (17.66)$$

shifted by κ . For the case (17.66), one observes that $u = 0$ is a homogeneous steady state if $H(-\kappa) = 0$ or $\kappa > 0$. Another homogeneous steady state $u = u_+ > 0$ is obtained from the condition

$$u_+ = \int_{\mathbb{R}} w(y) dy.$$

One may look for traveling-front solutions $u(\xi) = u(x - st) = u(x, t)$ of (17.64) for $F(u - \kappa) = H(u - \kappa)$ between the two steady states, which requires

$$\lim_{\xi \rightarrow -\infty} u(\xi) = u_+ \quad \text{and} \quad \lim_{\xi \rightarrow +\infty} u(\xi) = 0. \quad (17.67)$$

Suppose the threshold $u = \kappa$ is crossed only once and that the threshold crossing is located at $\xi = 0$, so that $u(0) = \kappa$; note that the second assumption about the crossing location is not restrictive, since (17.64) is translation-invariant. Now the spatial dynamics ansatz $\xi = x - st$ leads to the equation

$$-s \frac{du}{d\xi} + u = \int_{-\infty}^0 w(\xi - \tilde{\xi}) d\tilde{\xi} = \int_{\xi}^{\infty} w(y) dy =: W(\xi). \quad (17.68)$$

Exercise/Project 17.5.1. Multiply (17.68) by $e^{-\xi/s}$ and derive a solution formula. Compute the condition that κ has to satisfy based on the conditions (17.67). \diamond

Exercise 17.5.1 shows that a representation formula for traveling-wave solutions can be derived for a Heaviside firing rate function. One may then use this solution as the starting point for a continuation-argument to deform the Heaviside function. This yields a traveling-front solution for smooth firing rate functions such as (17.65); see also Section 17.6.

However, traveling fronts are often not realistic for neural fields, since neurons usually do not stay in an active state for all times. Traveling pulses, which represent localized activity, are usually more reasonable from a biophysics viewpoint. This motivated the consideration of adaptive neural fields models such as

$$\begin{aligned} \frac{\partial u}{\partial t}(x, t) &= -u(x, t) + \int_{\mathbb{R}} w(x - y) F(u(y, t) - \kappa) dy - \beta v, \\ \frac{\partial v}{\partial t}(x, t) &= \varepsilon(u - v), \end{aligned} \quad (17.69)$$

where the parameters β and ε control the adaptation. Obviously, we shall assume $0 < \varepsilon \ll 1$, which models a slow adaptation process. The traveling-wave ansatz $\xi = x - st$ leads to

$$\begin{aligned} -su' &= -u + \int_{\mathbb{R}} w(\xi - \tilde{\xi}) F(u(\tilde{\xi}) - \kappa) d\tilde{\xi} - \beta v, \\ -sv' &= \varepsilon(u - v), \end{aligned} \quad (17.70)$$

where $' = d/d\xi$. The next step is to analyze the fast-slow integrodifferential equation (17.70). The fast subsystem is given by

$$-su' = -u + \int_{\mathbb{R}} w(\xi - \tilde{\xi}) F(u(\tilde{\xi}) - \kappa) d\tilde{\xi} - \beta v_0 \quad (17.71)$$

for a constant v_0 . Using the coordinate shift $u(\xi) \rightarrow u(\xi) + \beta v_0$, it is possible to convert (17.71) to the scalar neural field traveling-wave equation (17.68). We already know that this equation can exhibit heteroclinic connections representing traveling-front solutions. In particular, it is very important to notice the direct analogy to the situation of heteroclinic connections in the FitzHugh–Nagumo equation presented in Section 6.5 (Figure 6.5) and the discrete FitzHugh–Nagumo equation in Section 17.4 (Figure 17.7). Changing to the slow time scale $\zeta = \varepsilon\xi$ in (17.70) yields

$$\begin{aligned} -s\varepsilon \frac{du}{d\zeta} &= -s\varepsilon \dot{u} = -u + \int_{\mathbb{R}} \frac{1}{\varepsilon} w((\zeta - \tilde{\zeta})/\varepsilon) F(u(\tilde{\zeta}) - \kappa) d\tilde{\zeta} - \beta v, \\ -s \frac{dv}{d\zeta} &= -s\dot{v} = u - v. \end{aligned} \quad (17.72)$$

In principle, the system (17.72) is difficult to analyze, since one has to make sense of the limit $\varepsilon \rightarrow 0$ on the slow time scale. However, if we assume that

$$w \in L^1(\mathbb{R}), \quad w(x) \geq 0, \quad \forall x \in \mathbb{R}, \quad \int_{\mathbb{R}} w(x) \, dx = 1,$$

then the situation simplifies substantially, since $w_\varepsilon(x) = \frac{1}{\varepsilon}w(x/\varepsilon)$ is an **approximation to the identity**, and it converges in the limit $\varepsilon \rightarrow 0$ to the **δ -distribution**, $\lim_{\varepsilon \rightarrow 0} w_\varepsilon(x) = \delta(x)$, which entails that

$$\lim_{\varepsilon \rightarrow 0} \int_{\mathbb{R}} \frac{1}{\varepsilon} w((\zeta - \tilde{\zeta})/\varepsilon) F(u(\tilde{\zeta}) - \kappa) \, d\tilde{\zeta} = \int_{\mathbb{R}} \delta(\zeta - \tilde{\zeta}) F(u(\tilde{\zeta}) - \kappa) \, d\tilde{\zeta} = F(u(\zeta) - \kappa).$$

Therefore, taking the (formal) limit $\varepsilon \rightarrow 0$ in (17.72) leads to the slow subsystem

$$\begin{aligned} 0 &= -u + F(u(\zeta) - \kappa) - \beta v, \\ -sv &= u - v. \end{aligned} \tag{17.73}$$

As for the FitzHugh–Nagumo equation, there are choices for the nonlinearity F and the parameter β such that there is only one global equilibrium point of the full system (17.70) with $\varepsilon > 0$. Starting from this equilibrium point, one may use the heteroclinic orbits in two fast subsystems together with two parts of the slow subsystem (17.73) to construct a pulse solution consisting of four segments under certain conditions on the firing rate function:

- (H1) $F(u)$ is defined on $[0, 1]$, smooth and monotonically increasing;
- (H2) $F'(0) < 1$, $F'(1) < 1$;
- (H3) the function $f(u) := -u + F(u)$ has precisely three zeros at $u = 0, u_*, 1$ with $0 < u^* < 1$.

The hypothesis (H3) yields the cubic (or S-shaped) critical manifold structure with which we are familiar for the FitzHugh–Nagumo equation.

Theorem 17.5.2 ([PE01a]). *Assuming (H1)–(H3), there exists a traveling pulse solution for the adaptive neural field integrodifferential equation (17.69). The pulse consists of two fast and two slow segments.*

Obviously, one may relax certain assumptions, but the important message is that the principle of constructing the fast FitzHugh–Nagumo pulse, as discussed in Sections 6.5 and 17.4, also applies to adaptive neural fields and several other classes of integral equations. In fact, many results known for reaction–diffusion equations can be recovered in the case of neural fields or, more generally, in certain classes of integrodifferential equations; see Section 17.6.

17.6 References

Section 17.1: Many basic results about stability of waves can be found in [San01], on which the section is based. For a nice Evans function introduction, we also refer to [Kap05]. A textbook that nicely details many further stability results is [KP13].

We have not covered other related approaches to traveling-wave stability, e.g., the SLEP method [Nis94, NF87] and the NLEP method [DGK01, DvHK13]. For stability results of the FHN pulse that we have investigated in Chapter 6, one may consider [Flo91, Jon84, Mag78, Mag85, Mag80, Nii97]. For classical results on stability of waves in Hodgkin–Huxley-type systems, see [EF77]. For the related Ginzburg–Landau equation (GLE), see [Doe93, DHV04, DHV07, Doe96, DSSS09, HV07, KR00]. Background on the analysis of traveling waves can be found in many books, e.g., [Kno00, VVV94].

Section 17.2: This section is based on the main works [AGJ90, GJ91, Eva72]. There are many other models in which fast–slow techniques, such as the exchange lemma, blowup, and Evans function splitting, are relevant in analyzing stability. For example, we refer the reader to bifurcations in semiconductor models [KKS00a, Szm89b, Szm89a], cardiac tissue waves in Karma’s model [BJSW08, MS03e, Kar93], combustion waves [Gha09a, Gha09b, Gha10, GHL13, GSS13], the generalized Korteweg de Vries (KdV) equation [ST97], layer solutions in reaction–diffusion systems [NF87], multiple small parameters [NMIF90], the Ostrovsky equation [MCJS09, CMJ09], pulses and spikes in Gierer–Meinhardt [KSWW06, VD13, DKP07] and quasi-linear relaxation systems [WWL11].

Section 17.3: The section is based mainly on basics from [Eva02] and the Dafermos regularization analysis in [SS09, SS04b]; for more work in this direction, we refer to [Sch04, Sch02, Sch06, SPM04, KT12]. The ARD equation approach we mentioned in an example is described in [WP10]. Other interesting related topics are coupling hyperbolic and elliptic equations [Man06], Dafermos regularization and stability [LS03, Lin06], magnetohydrodynamics shocks [FS95], saddle-node bifurcations of the spectrum [AS12], slow manifolds for viscous regularizations [BW11], slow motion of viscous shock layers [GK01, GK98, LO93, RW95b, WR95, Wol94], stability of small-amplitude shock waves [FS02a, FS10a], and waves for systems of conservation laws [Liu04].

Section 17.4: Traveling waves for the lattice FHN model are considered in [HS10c, HPS11, HS13], on which this section is based. Propagation failure in lattice equations is a well-known phenomenon [BE95, EN93, Kee87, LE92, RP12]. As general references in lattice equations, see [Cho03, MP99]. Other lattice models also exhibit very interesting waves, e.g., relaxation oscillations and chaos [Vak10]. Of course, one may use asymptotic analysis for lattice problems such as the two-timing approach [CL10, MLR11]. Other relevant models are chains of coupled oscillators [HM09a, VH08], the discrete cubic nonlinear Schrödinger (NLS) equation [Li03], the discretized KdV–Burgers’ equation [AGK⁺11], and general excitable cell models [CB02, EV05].

Section 17.5: For general background on neural fields, see [Coo05, LT03, LTGE02]. The construction we outlined in the section for traveling waves is due to [PE01a, PE01b] and the exposition in [Bre12b]. For some of the first works on neural fields, see [EM93, WC73]. We have already seen waves in the FHN equation, but there are even further examples in which traveling waves appear in neuroscience, particularly in neural networks [Jal04, YTE01]. Other nonlocal equations such as delay equations [Gou00, ZP08, GC02, GR03], integrodifferential FKPP-type models with delay [ABBG02], nonlocal reaction–diffusion models [Bos00], and various other integrodifferential equations [RX04] can also be analyzed using fast–slow tools; see also Section 18.7 for the delay case. Multiple-time-scale behavior frequently occurs in stochastic neural field equations [WB13] and may even be induced directly by trace-class noise [KR14].

An equation that we have not discussed in this book, but which also is very important for singular perturbation theory, is the Fisher–Kolmogorov–Petrovskii–Piscounov (FKPP) equation [Fis37, KPP91], whereby one often focuses on pushed or pulled front solutions. Detailed surveys about FKPP dynamics can be found in [EvS00, vS03]; see also [AMPP87, HN01, Kin13] and references therein. There are also relations to stochastic dynamics [DMS03] and links to delayed models [Ai07]. An interesting version is the FKPP equation with cutoff [BD97], which can be treated using a blowup procedure [MP12, DPK10, DPK07b, DPK07a, Pop11, PK06], and the method can be extended to the Nagumo equation [Pop12]; see [HS12] for another related direction considering Lotka–Volterra systems. One may also add a fourth-order term to the FKPP equation [RW01], change to an arbitrary power nonlinearity [KB09b], or consider nonlocal singular perturbations [AK13b].

A similar remark as for the FKPP model applies to the Gray–Scott model, where pulse solutions play a key role [DEK00, DEK06, HPT00, MDK00, SWR05]. A very detailed Gray–Scott analysis is contained in [DGK02]. One may also focus on sharp interfaces as singular perturbation problems [TN94], which we have not covered here but which appear, e.g., in the Allen–Cahn equation [AHM08]. Also, the nonlinear Schrödinger equation [CML02, Hal99], the perturbed sine–Gordon equation [DDvGV03], the Landau–Lifshitz–Gilbert equation [MR13], and the Cahn–Hilliard equation [RW95a, SW00c] are not even mentioned, despite their relations to fast–slow systems.

The interaction of various traveling-wave structures is also almost absent from this book, but it is a highly interesting topic, occurring in many reaction–diffusion systems [Hek01, DK03]. We refer to work on three-component systems [DvHK09, vHDK08, vHDKP10, vHDK⁺11, vHS11], semistrong sharp fronts [Rad13], and interactions in the Brusselator model [KEW06]. Other topics omitted are stationary layer-type solutions [Lin01, HL99] and special standing waves [FL12].

Further ideas directly relevant for fast–slow systems are activator–inhibitor-type systems [Doc92], asymptotic methods [Fif88, Kee80, OR75], various biological models [ACY03, Ai10, BDK06, LW10b, WW07], bioreactor models [SZ04], combustion waves [BNS85, MS06], crime hotspot modeling [LO13a], cross-diffusion systems [WZ05], destabilization of fronts [DIN04], detonation waves [RV98], dissipative–dispersive equations [Man09a, Man09b, Man13], fourth-order diffusion equations [KBB05], the freezing method for numerical wave calculations [BST08], pulses and fronts in porous media [GGJ07, MS03b, SM01], reaction–diffusion mechanics problems [HDK13], singular diffusion [ADD12], swarming [MKK00], thin liquid films [MS09], traffic flow waves [HHH13], and waves in hyperbolic systems [Bar84, Bar83].

Chapter 18

Infinite Dimensions

Generalizing the geometric viewpoint of fast–slow ODEs to truly infinite-dimensional dynamical systems is notoriously difficult. However, there has been quite a bit of progress in recent years.

Section 18.1 begins with a brief tutorial on semiflows, which are a natural framework in which to phrase many partial and delay differential equations. In Section 18.2, we state a generalization of Fenichel’s theorem for semiflows and discuss two examples to illustrate its uses and limitations. Section 18.3 discusses “homogenization” for elliptic PDEs using the method of multiple scales (or two-timing). Section 18.4 considers delay differential equations (DDEs) with small delay. In this case, the small delay time becomes a natural singular perturbation parameter, and one may identify invariant manifolds. Section 18.5 is an interlude on set-valued differential equations, which frequently arise in control theory and for which an analogue of Fenichel’s theorem is again available. We conclude this chapter with Section 18.6, where amplitude equations are outlined. These equations arise near the onset of instability for spatially extended systems and have an intrinsic multiple time scales structure, which is exploited using an asymptotic technique.

Background: Some basic functional analysis is required such as rudimentary elements of Banach space theory, which, among many other topics, can be found in [Con90, Fol99, Lax02, Rud91]. Although not necessary, any familiarity with ways in which one may view PDEs and DDEs as infinite-dimensional dynamical systems is obviously helpful [CFNT89, HL93, HMO83, Rob01, Tem97].

18.1 Semigroups

In this section, we briefly outline the basic definitions of semigroup theory and motivate why semigroups are a natural starting point in looking for generalizations of the finite-dimensional theory of normally hyperbolic invariant manifolds. As a simple starting point, consider the familiar finite-dimensional ODE

$$\frac{dx}{dt} = x' = f(x)$$

with $x \in \mathbb{R}^m$. For this system we know from standard ODE theory that as long as f is at least Lipschitz, then we can find a solution (at least locally in forward and in backward time) for a given initial value $x(0) = x_0$. Hence, we have a (local) **flow**

$$\phi(x, t) : \mathbb{R}^m \times \mathbb{R} \rightarrow \mathbb{R}^m \quad \text{with } \frac{d\phi}{dt} = f(\phi).$$

Furthermore, ϕ satisfies the initial condition, so that

$$(i) \quad \phi(x_0, 0) = x_0.$$

We shall often suppress the dependence of ϕ on the initial condition and just write $\phi(t)$. Further standard uniqueness and continuity results for ODEs imply that ϕ satisfies

$$(ii) \quad \phi(t+s) = \phi(t)\phi(s) \text{ for all } t, s \in \mathbb{R},$$

$$(iii) \quad \phi \text{ is a continuous map in } x \text{ and } t.$$

The idea is to abstract the properties (i)–(iii), and this leads to the definition of a semigroup.

Definition 18.1.1. Let X be Banach space. We call a map $S : X \times [0, \infty) \rightarrow X$ a **C^0 -semigroup** (or continuous **semiflow**) if it satisfies

$$(I) \quad S(0) = \text{Id};$$

$$(II) \quad S(t+s) = S(t)S(s) \text{ for all } t, s \in [0, \infty);$$

$$(III) \quad \text{the map } (x, t) \mapsto S(t)x \text{ is continuous in } x \text{ and } t \text{ for } (x, t) \in X \times [0, \infty).$$

Remark: We shall drop the C^0 -quantifier for a semigroup, since all semigroups we consider will be C^0 . In some parts of the literature, the alternative notation $S(t) = S_t$ is used for semigroups to limit the notational complexity, but since we eventually want to talk about a semigroup $S_0(t)$ and its perturbation $S_\varepsilon(t)$, we shall avoid this notation.

Obviously, a flow $\phi(t)$ for an ODE forms a semigroup with $X = \mathbb{R}^m$. However, the main difference between (i)–(iii) and (I)–(III) is that a semiflow is often not defined in backward time for $t \in (-\infty, 0)$ or even for $t \in (-T, 0)$ for any $T > 0$. In fact, the main motivation for Definition 18.1.1 comes from the fact that many infinite-dimensional systems do not satisfy the definition of a flow but do generate semiflows.

It is helpful to think of many semigroups as solutions to an ODE on a Banach space X of the form

$$u'(t) = f(u(t)) \quad \text{with given initial condition } u(0)$$

for $u = u(t) \in X$ and $t \geq 0$. Although we are now looking at the evolution in an infinite-dimensional function space, the analogies to finite-dimensional ODEs are large enough that one may hope to develop a geometric singular perturbation theory in this context. We begin with several important classes of semiflows arising in applications that one would like to cover with such a theory.

Example 18.1.2 (Linear second-order parabolic PDE). Let Ω be an open bounded subset of \mathbb{R}^n with smooth boundary. Consider the partial differential equation (PDE)

$$\begin{cases} \frac{\partial u}{\partial t} + Lu = f & \text{in } \Omega \times (0, T] \\ u = 0 & \text{on } \partial\Omega \times [0, T] \\ u = g & \text{on } \Omega \times \{t = 0\}, \end{cases} \quad (18.1)$$

where $f : \Omega \times (0, T] \rightarrow \mathbb{R}$ and $g : \Omega \rightarrow \mathbb{R}$ are given sufficiently smooth functions. The unknown function of the initial boundary value problem (18.1) is $u = u(x, t)$. By L we denote a second-order linear differential operator of the form

$$Lu := - \sum_{i,j=1}^n a^{ij}(x) \frac{\partial^2 u}{\partial x_i \partial x_j} + \sum_{i=1}^m b^i(x) \frac{\partial u}{\partial x_i} + c(x)u,$$

for given sufficiently smooth coefficients $a^{ij}, b^i, c : \mathbb{R}^n \rightarrow \mathbb{R}$ that are independent of time. From a physical point of view, the terms involving a^{ij} represent diffusion; those involving b^i , transport; and the one with c is associated with creation/deletion. We assume that the differential operator $\frac{\partial}{\partial t} + L$ is **parabolic**, i.e., there exists a positive constant $K > 0$ such that

$$\sum_{i,j=1}^n a^{ij}(x) \xi_i \xi_j \geq K \|\xi\|^2, \quad (18.2)$$

for all $x \in \Omega$ and $\xi \in \mathbb{R}^n$. Note that (18.2) is equivalent to requiring positive definiteness of the symmetric matrix (a^{ij}) . It can be shown that the PDE (18.1) generates a semiflow on $X = L^2(\Omega)$. A simple example of a parabolic differential operator is $\frac{\partial}{\partial t} - \Delta$, where Δ denotes the Laplacian, so that

$$Lu = -\Delta u = - \sum_{i=1}^n \frac{\partial^2 u}{\partial x_i^2}.$$

Note that the PDE $u_t - \Delta u = 0$ is the classical **heat equation**, which gives a good physical intuition why one does not want to require a semiflow to be defined in backward time, since one would have to “invert” a diffusion process. ♦

Although many techniques for semiflows are developed with parabolic PDEs in mind, the next example shows that the semigroup framework is much wider.

Example 18.1.3 (Retarded functional differential equations). Suppose $\tau > 0$, and let $X = C^0([-\tau, 0], \mathbb{R}^n)$ with the supremum norm. Consider the equation

$$x'(t) = F(x_t), \quad (18.3)$$

where $F : X \rightarrow \mathbb{R}^n$ is at least C^1 , and we define $x_t(s)$ as a function in X given by $x_t(s) = x(t + s)$ for $s \in [-\tau, 0]$. Equation (18.3) is an example of a retarded functional differential equation. Often, (18.1.3) is also referred to as a **delay equation** with **delay** τ . Let $u \in X$ be a given function, which we are going to view as the initial condition. Consider a function

$$x : [-\tau, T] \rightarrow \mathbb{R}^n$$

defined for some $T > 0$. To define a solution of the retarded functional differential equation (RFDE) (18.3), we have to take into account an initial condition $u \in X$; we are going to attach this information to x by writing $x(u)(t)$ or $x(u, t)$. We call x a solution to the RFDE (18.3) if

- $x_0(u, \cdot) = x(u, 0 + \cdot) = u$ for a given $u \in X$ as an initial condition;
- $x(u, t)$ is C^1 for $t \in (0, T)$;
- the right-hand derivative of $x(u, t)$ approaches a limit as $t \rightarrow 0$;
- $x(u, t)$ satisfies (18.3) on $[0, T]$.

Existence and uniqueness of $x(u, t)$ can be proven; see Section 18.7. Now let

$$S(t)u := x_t(u, \cdot) = x(u, t + \cdot).$$

If solutions are defined for all time $t \geq 0$, then $S(t)$ defines a semigroup on X . A very simple example of an RFDE is

$$x'(t) = x(t) - x(t - \tau), \quad x(t) = u(t) \text{ for } t \in [-\tau, 0]. \quad (18.4)$$

Observe that (18.4) is a special case of (18.3) in which $F(x_t) = x(t) - x(t - \tau)$. ♦

Returning to PDEs, we note that Example 18.1.2 will often be insufficient for modeling complex phenomena, since the function u appears only in linear terms. One of the most tractable types of nonlinear parabolic PDEs is **reaction–diffusion equations**, which model many important nonlinear phenomena in physics, biology, chemistry, and engineering.

Example 18.1.4 (Reaction–diffusion equations). Let Ω be an open bounded set in \mathbb{R}^n with smooth boundary, $f : \mathbb{R}^n \rightarrow \mathbb{R}^n$ a sufficiently smooth map. Let $u = u(x, t)$, and consider the following equation:

$$u_t - \Delta u = f(u) \quad \text{on } \Omega \times [0, \infty). \quad (18.5)$$

In addition to (18.5), we consider suitable boundary conditions such as a Dirichlet condition $u = 0$ on $\partial\Omega$ or a Neumann condition $\frac{\partial u}{\partial n} = \vec{n} \cdot \mathbf{D}u = 0$ on $\partial\Omega$, where \vec{n} is the outer unit normal vector to $\partial\Omega$. Furthermore, one also has to prescribe the initial value $u_0 = u(x, 0)$. Also of interest is the case in which Ω is unbounded, e.g., $\Omega = \mathbb{R}^n$, in which case (18.5) can be considered as a pure initial value problem.

To prove existence, uniqueness, and smoothness results for reaction–diffusion equations, one has to restrict the class of nonlinear terms $f(u)$ and/or the size of the initial data. We shall assume that sufficient assumptions are made that a solution exists for all $t \geq 0$. Then $S(t)u_0 = u(x, t)$ defines a semiflow on a suitable Banach space X . It is often useful to choose a **Lebesgue space** $L^p(\Omega) = X$, a Sobolev space $W^{k,p}(\Omega) = X$, or some variant thereof; see [Eva02] for details on basic function spaces for PDEs. ♦

The general definition of invariant sets for semiflows is directly adapted from the case of flows.

Definition 18.1.5. Let $S(t)$ be a semiflow on X . We say that a set $M \subset X$ is **invariant** if

$$S(t)M = M \quad \text{for all } t \geq 0.$$

We call $M \subset X$ **positively invariant** if

$$S(t)M \subset M \quad \text{for all } t \geq 0.$$

In a similar way, we may also generalize definitions of invariant manifolds, attractors, limit sets, and so on; see also Section 18.7. It is natural to ask whether Fenichel's theorems on invariant manifolds from Chapters 2 and 3 carry over to the infinite-dimensional semigroup setting. This provides the first step for a geometric singular perturbation theory for infinite-dimensional fast–slow systems.

18.2 Invariant Manifolds

Our goal in this section is to describe an extension of Fenichel's theorem for invariant manifolds for semiflows. It is recommended that the reader frequently compares the results presented here with the more intuitive finite-dimensional case presented in Chapter 2. Let X be a Banach space with norm $\|\cdot\|$, i.e., instead of our usual convention that no subindex for the norm implies the Euclidean norm, we now allow $\|\cdot\|$ to be any norm, since we will be dealing with a general Banach space X . Consider a linear operator L on X . Then we overload the notation and also use $\|\cdot\|$ for the **operator norm**

$$\|L\| := \sup\{\|Lx\| : x \in X, \|x\| = 1\}.$$

For a sufficiently smooth nonlinear mapping F on a bounded subset $B \subset X$, one may introduce the C^k -norms

$$\begin{aligned} \|F\|_0 &= \sup\{\|Fx\| : x \in B\}, \\ \|F\|_k &= \|F\|_0 + \sum_{j=1}^k \sup\{\|\mathbf{D}^j F(x)\| : x \in B\}, \end{aligned}$$

where D denotes the **Fréchet derivative** of F . As in Section 18.1, let $S_0(t)$ denote a semiflow on X ; recall that we always assume that $S_0 : X \times [0, \infty) \rightarrow X$ is continuous. For the rest of this section, we also make the following assumptions:

- (H1) for each $t \geq 0$, $S_0(t) : X \rightarrow X$ is C^1 ;
- (H2) for $S_0(t)$, there exists a C^2 compact connected positively invariant manifold $M_0 \subset X$;
- (H3) M_0 is normally hyperbolic.

Note that the manifold $M_0 \subset X$ is now considered a **Banach manifold**, i.e., it is locally homeomorphic to an open subset of some Banach space Y . The definitions of tangent space, tangent bundle, and vector bundle carry over in a similar way. However, for the definition of normal hyperbolicity, we encounter the problem of $S_0(t)$ not being defined for $t < 0$. Instead, **normal hyperbolicity** of M_0 under the semiflow is defined as follows:

- (i) For each $p \in M_0$, there is a decomposition of X into closed subspaces

$$X = X_{0,p}^u \oplus T_p M_0 \oplus X_{0,p}^s, \quad (18.6)$$

where we also write $X_{0,p}^c = T_p M_0$ for the tangent space to M_0 at p . We require that the splitting is invariant under the linearized flow $DS_0(t)$.

- (ii) For $p \in M_0$, $t \geq 0$, and $q = S_0(t)p$, consider the linearizations

$$DS_t(p)|_{X_{0,p}^\alpha} : X_{0,p}^\alpha \rightarrow X_{0,q}^\alpha \quad \text{for } \alpha = c, u, s.$$

We require that $DS_0(t)(p)$ is an isomorphism from $X_{0,p}^u$ onto $X_{0,q}^u$.

- (iii) There exist $t_0 \geq 0$ and $\lambda < 1$ such that for all $t \geq t_0$,

$$\begin{aligned} \lambda \cdot \inf\{\|DS_0(t)(p)x^u\| : x^u \in X_{0,p}^u, \|x^u\| = 1\} &> \max\{1, \|DS_0(t)(p)|_{T_p M_0}\|\}, \\ \lambda \cdot \inf\{\|DS_0(t)(p)x^c\| : x^c \in T_p M_0, \|x^c\| = 1\} &> \|DS_0(t)(p)|_{X_{0,p}^s}\|. \end{aligned}$$

Note that the key condition is (iii), which gives meaning to the intuitive notion that the flow in the directions normal to M_0 dominates the flow in the tangent directions.

Theorem 18.2.1 ([BLZ98]). *Suppose $S_0(t)$ is a semiflow on X , and M_0 is a C^1 compact connected invariant manifold for which the conditions (H1)–(H3) hold. Fix $t_1 > t_0$ (see (iii) above) and let N_0 be a sufficiently small tubular neighborhood of M_0 . For each small $\varepsilon > 0$, there exists $\vartheta = \vartheta(\varepsilon) > 0$ such that if $S_\varepsilon(t)$ is a C^1 -semiflow satisfying*

$$\|S_\varepsilon(t_1) - S_0(t_1)\|_1 \leq \vartheta(\varepsilon) \quad \text{and} \quad \|S_\varepsilon(t) - S_0(t)\|_0 \leq \vartheta(\varepsilon), \quad \text{for } 0 \leq t \leq t_1, \quad (18.7)$$

where the norm in (18.7) is taken with respect to a small neighborhood B of $M_0 \subset X$ such that $N_0 \subset B$, then the following hold:

- *Persistence:* The semiflow $S_\varepsilon(t)$ has a C^1 compact connected normally hyperbolic invariant manifold M_ε near M_0 .
- *Convergence:* M_ε converges to M_0 in the C^1 -topology as $\|S_\varepsilon(t_1) - S_0(t_1)\| \rightarrow 0$.
- *Existence:* $S_\varepsilon(t)$ has C^1 invariant manifolds W_ε^{cs} and W_ε^{cu} defined in a tubular neighborhood N_ε of M_ε that are tangent to the center-stable vector bundle $TM_\varepsilon \oplus X_\varepsilon^s$ and the center-unstable vector bundle $TM_\varepsilon \oplus X_\varepsilon^u$.
- *Characterization:* $W_\varepsilon^{cs} \cap W_\varepsilon^{cu} = M_\varepsilon$ and
$$W_\varepsilon^{cs} = \{p \in N_\varepsilon : S_\varepsilon(t_1)^k p \in N_\varepsilon, \text{ for } k \geq 1, S_\varepsilon(t_1)^k p \rightarrow M_\varepsilon \text{ as } k \rightarrow \infty\},$$

$$W_\varepsilon^{cu} = \{p \in N_\varepsilon : \exists \{p_k\}_{k \geq 0} \subset N_\varepsilon \text{ s.t.}$$

$$S_\varepsilon(t_1)p_k = p_{k-1} \text{ for } k \geq 1 \text{ and } p_k \rightarrow M_\varepsilon \text{ as } k \rightarrow \infty\};$$

W_ε^{cs} and W_ε^{cu} are called the **center-stable** and **center-unstable manifolds** respectively.

Proof. (Outline; see [BLZ98] for all details) We shall not give the long technical proof but instead point out the main steps and outline the difficulties in order to compare the strategy with the techniques from Chapter 2. The main problem to overcome is that semiflows are not defined in backward time, so there is a problem to define backward orbits for $t \leq 0$. Further technical problems arise. For example, a Banach space might not be locally compact, and since M_0 is a Banach manifold, some results from finite-dimensional differential geometry do not hold. The good news is that the general strategy of defining a suitable graph transform, as discussed in Chapter 2, works. There are several main steps:

1. Construct local coordinate systems for a tubular neighborhood of M .
2. Consider cones with vertex M_0 and axes X_0^s and X_0^u obtained from the splitting (18.6). Establish suitable invariance properties of these cones.
3. View the normal bundle $X_0^u \oplus X_0^s$ as a bundle over X_0^u . Consider Lipschitz sections/graphs Λ^u of this bundle.
4. Use the cones to get a well-defined graph transform on $\{\Lambda^u\}$. This yields existence of the center-unstable manifold.
5. Time cannot be reversed to get the center-stable manifold. Look at the bundle $X_0^u \oplus X_0^s$ over X_0^s and graphs Λ^s .
6. More-detailed analysis shows that flowing a graph Λ^s backward can yield no preimage or multiple preimages, but a well-defined graph transform still exists; this is a major step, since one basically has to operate with preimages instead of a well-defined backward flow.
7. M_ε is the intersection of the center-stable and center-unstable manifolds.

These steps complete the main construction of M_ε . To prove the smoothness and normal hyperbolicity of M_ε requires further technical work. \square

Instead of delving into the proof, we shall consider two examples to illustrate Theorem 18.2.1.

Example 18.2.2. Let $\Omega := [0, 1] \subset \mathbb{R}$ model the longitudinal direction of a semiconductor laser; see also Sections 20.4 and 20.12. Consider $\psi(z, t) \in \mathbb{C}^2$, $\eta(z, t) \in \mathbb{C}^2$ for $(z, t) \in \Omega \times [0, T]$ for some positive time $T > 0$; the vector $E = (\psi, \eta)^\top \in \mathbb{C}^4$ represents the light amplitude for the laser, and $y = y(t) \in \mathbb{R}$ the carrier density. The initial boundary value problem for $u(t) := (\psi, \eta, y)(\cdot, t)$ is given by

$$\begin{cases} \frac{\partial \psi_1}{\partial t} = -\frac{\partial \psi_1}{\partial z} + [(1 + 5i)(y - 1) - c_2] \psi_1 + \rho(y)[\eta_1 - \psi_1], \\ \frac{\partial \psi_2}{\partial t} = \frac{\partial \psi_2}{\partial z} + [(1 + 5i)(y - 1) - c_2] \psi_2 + \rho(y)[\eta_2 - \psi_2], \\ \frac{\partial \eta_1}{\partial t} = [iF_1(y) - F_2(y)]\eta_1 + F_2(y)\psi_1, \\ \frac{\partial \eta_2}{\partial t} = [iF_1(y) - F_2(y)]\eta_2 + F_2(y)\psi_2, \\ \frac{\partial y}{\partial t} = I_0 - \frac{y}{\tau_0} - \delta_0 \int_0^1 E^* G(y)E \, dz, \end{cases} \quad (18.8)$$

$$\begin{cases} \psi_1(0, t) = c_0 \psi_2(0, t), & \psi_1(1, t) = c_1 \psi_2(1, t), \\ \psi(z, 0) = \psi_0, & \eta(z, 0) = \eta_0, & y(0) = y_0, \end{cases} \quad (18.9)$$

where (18.8) should hold for $(z, t) \in \Omega \times [0, T]$, (18.8) should hold for $(z, t) \in \partial(\Omega \times [0, T])$, E^* denotes the **Hermitian conjugate** (i.e., complex conjugate transpose) of E , and $G(y) \in \mathbb{R}^{4 \times 4}$ is a matrix-valued map given by

$$G(y) = \begin{pmatrix} [y - 1 - \rho(y)] \text{Id} & \frac{1}{2}\rho(y) \text{Id} \\ \frac{1}{2}\rho(y) \text{Id} & 0 \end{pmatrix},$$

where Id denotes the 2×2 identity matrix, and 0 the 2×2 zero matrix in the last expression. We shall rewrite (18.8)–(18.9) in a simpler notation below. First, some physically reasonable specifications on the parameters and functions are made,

$$\begin{aligned} c_{0,1,2} \in \mathbb{C}, \quad \text{Re}(c_2) > 0, \quad |c_{0,1}| < 1, \quad I_0 \in \mathbb{R}, \quad 0 < I_0 \ll 1, \\ \tau_0 \in \mathbb{R}, \quad \tau_0 \gg 1, \quad \delta_0 \in \mathbb{R}, \quad 0 < \delta_0 \ll 1. \end{aligned}$$

Basically, I_0 represents an input current, and $1/\tau_0$ a decay rate of relaxation time. The real-valued functions F_1, F_2 are assumed to be sufficiently smooth, Lipschitz, and globally bounded. The real-valued function ρ is also sufficiently smooth and Lipschitz; furthermore, $\rho(y)$ is bounded for $y \rightarrow -\infty$, $\rho(y) > 0$ for $y > 1$, and $\rho(y)/(y - 1) \rightarrow 0$ as $y \rightarrow \infty$. Observe that the differential equation (18.8) is a linear hyperbolic system for the variable E , which is coupled to an ordinary integrodifferential equation for y , where all terms are multiplied by small parameters. Hence, we may abstractly write (18.8) as an evolution equation

$$\begin{aligned} E' &= H(y)E, \\ y' &= \varepsilon g(E, y), \end{aligned} \quad (18.10)$$

where $g(E, y) := \frac{1}{\varepsilon} \left[I_0 - \frac{y}{\tau_0} - \delta_0 \int_0^1 E^* G(y) E \, dz \right]$, and the linear operator $H(y)$ is given by

$$\begin{aligned} H(y) &:= \begin{pmatrix} \begin{bmatrix} -\frac{\partial}{\partial z} + \beta(y) & 0 \\ 0 & \frac{\partial}{\partial z} + \beta(y) \end{bmatrix} & \rho(y) \operatorname{Id} \\ F_2(y) \operatorname{Id} & [\mathrm{i}F_1(y) - F_2(y)] \operatorname{Id} \end{pmatrix} \quad (18.11) \\ &= H_0(y) + \begin{pmatrix} 0 & \rho(y) \operatorname{Id} \\ F_2(y) \operatorname{Id} & 0 \end{pmatrix}, \end{aligned}$$

where $\beta(y) = (1+5i)(u-1) - c_2 - \rho(y)$ and $H_0(y)$ is a diagonal operator. We shall assume that $0 < \varepsilon \ll 1$ is chosen such that all terms in g are of order $\mathcal{O}(1)$. From the notation (18.10) and the assumptions on the parameters, it follows immediately that it is a good idea to view the evolution equation as a fast–slow system on a function space X . Consider the space

$$X_0 := L^2([0, 1], \mathbb{C}^2) \times L^2([0, 1], \mathbb{C}^2), \quad X := X_0 \times \mathbb{R},$$

so that we may view (18.10) as the abstract evolution equation on X with $(\psi, \eta) \in X_0$ and $y \in \mathbb{R}$. Given a sufficiently smooth initial condition $u(0)$, we shall accept the fact here that the solution operator for (18.10) given by $S_\varepsilon(t)u(0) = u(t)$ yields a well-defined semiflow for $\varepsilon \geq 0$ that is strongly continuous in t and C^1 in u . In this case, the solution $u(t)$ turns out to be a classical solution that satisfies quite strong a priori bounds.

Exercise 18.2.3. Suppose $u(0) \in X$. Prove that there exists a constant $\kappa > 0$ such that $\|S_\varepsilon(t)u(0)\| < \kappa$ for all $t \geq 0$. ◇

Observe that $S_0(t)$ is the semiflow associated with the fast subsystem

$$\begin{aligned} E' &= H(y)E, \\ y' &= 0, \end{aligned} \quad (18.12)$$

which is generated by a linear operator $H(y)$ for each fixed y . The linearity, as well as the structure of $H(y)$, can be exploited to show the next result.

Lemma 18.2.4 ([Sie13]). *Suppose $c_0c_1 \neq 0$ and $\rho(y) > 0$. Then there exists an open set $\mathcal{I} \subset \mathbb{R}$ of carrier densities y such that if $y \in \mathcal{I}$; there exists a splitting of X_0 into two $H(y)$ -invariant subspaces X_0^s and X_0^c , which depend continuously on y , such that $X_0 = X_0^s \oplus X_0^c$; X_0^c is finite-dimensional and $H(y)|_{X_0^c}$ has all eigenvalues on the imaginary axis; and*

$$\|S_0(t)|_{X_0^s}\| \leq M e^{-\alpha t} \quad \text{for some } M > 0, \alpha > 0, \text{ and all } t \geq 0.$$

The proof of Lemma 18.2.4 exploits the fact that the linear operator $H(y)$ is a compact perturbation of a diagonal operator H_0 , and for the diagonal operator, one may estimate the relevant eigenvalues; see Section 18.7. The next step is to observe that a relevant invariant (critical) manifold of (18.10) for $\varepsilon = 0$ is given by

$$C_0 := \{(E, y) \in X : y \in \mathcal{I}, P^s(y)E = 0\},$$

where \mathcal{I} is an open interval provided by Lemma 18.2.4, and $P^s(y) : X_0 \rightarrow X_0^s$ denotes the continuous family of projections onto X_0^s , i.e., the null space of $P^s(y)$ is X_0^c . Essentially, we are interested in dynamics on C_0 , since it contains the slow variable y as well as all slow parts of the variable E . These are all the components that do not decay exponentially fast. The main problems are now the following:

- (P1) *C_0 is not compact:* To find a suitable compact submanifold $M_0 \subset C_0$, one may use a cutoff procedure. Since X_0^c is finite-dimensional, it follows that M_0 is finite-dimensional as well.
- (P2) *Check the normal hyperbolicity for M_0 :* The splitting from Lemma 18.2.4 is the main ingredient in checking normal hyperbolicity. In fact, the situation is simplified by the fact that the semiflow $S_0(t)$ for $\varepsilon = 0$ is already linear for each y .
- (P3) *Check the closeness of semigroups:* More precisely, one has to check the condition (18.7), which requires that the operator norms of $S_0(t)$ and $S_\varepsilon(t)$ be close for some time interval in the C^1 -topology in a neighborhood of M_0 .

The details for (P1)–(P2) can be found in [Sie13]. Here we shall just sketch some ideas for (P3) to illustrate an important point of Theorem 18.2.1. Let $v = (E_v, y_v) \in X$ be a fixed initial condition, independent of ε and satisfying the boundary conditions, and denote the solution of (18.10) at time t by $u_\varepsilon(t)$. Then we have

$$\begin{aligned} \|S_\varepsilon(t)v - S_0(t)v\| &= \|u_\varepsilon(t) - u_0(t)\| = \left\| \int_0^t u'_\varepsilon(s) - u'_0(s) \, ds \right\| \\ &= \left\| \int_0^t \left(\begin{array}{l} E'_\varepsilon(s) - E'_0(s) \\ \varepsilon g(E_\varepsilon(s), y_\varepsilon(s)) \end{array} \right) ds \right\|. \end{aligned}$$

It is important that the function $g : X \rightarrow \mathbb{R}$ can be bounded, since it is given by an integral term, a smooth function $\rho(y)$, and globally bounded arguments $E_\varepsilon(s), y_\varepsilon(s)$ (by Exercise 18.2.3). In particular, there exists a constant σ such that

$$\varepsilon g(E_\varepsilon(s), y_\varepsilon(s)) \leq \varepsilon \sigma, \quad \text{for } 0 \leq s \leq t,$$

which deals with the second component. For the first component, we use that on a bounded time interval, $y_\varepsilon(s) = y_0(s) + \mathcal{O}(\varepsilon)$, which implies

$$\begin{aligned} E'_\varepsilon(s) - E'_0(s) &= H(y_\varepsilon(s))E_\varepsilon(s) - H(y_0(s))E_0(s), \\ &= H(y_0(s))E_\varepsilon(s) - H(y_0(s))E_0(s) + \mathcal{O}(\varepsilon), \end{aligned}$$

since y does not enter into the differential operator part of $H(y)$ given by the partial derivatives $-\frac{\partial}{\partial z}$ and $\frac{\partial}{\partial z}$. By Lemma 18.2.4 applied to the difference $v(s) := E_\varepsilon(s) - E_0(s)$, we may also bound the first component. Note that the

argument to bound various terms would not work if the slow equation were of the form

$$\frac{\partial y}{\partial t} = \varepsilon Ly + \varepsilon g(E, y), \quad (18.13)$$

where L is a general differential operator. We would not immediately know how to bound εL , since the differential operator could be unbounded; see Example 18.2.6. After a bit of additional work for (P3) to get the required C^1 -closeness estimate and by checking (P1)–(P2), one arrives at the following result:

Theorem 18.2.5 ([Sie13]). *There exists a locally invariant manifold M_ε obtained as a perturbation of $M_0 \subset C_0$ that is locally exponentially attracting. Furthermore, the dynamics on M_ε are given by a finite-dimensional system of ODEs.*

It turns out that the ODEs on M_ε are quite low-dimensional, which makes them amenable to further analytical and numerical treatment. ♦

Example 18.2.2 illustrates a case in which Theorem 18.2.1 applies. Example 18.2.6 is going to show that even if we cannot apply Theorem 18.2.1 directly, a slow manifold may still exist. The next example also discusses an equation arising in laser dynamics for the case of two-level lasers.

Example 18.2.6. Consider a periodic domain $S^1 = [0, 1]/(0 \sim 1)$ (i.e., S^1 is the circle parameterized by $[0, 1]$ with 0 and 1 identified) with spatial variable $z \in S^1$ and unknown functions $(v(z, t), w(z, t), y(z, t)) \in \mathbb{C} \times \mathbb{R} \times \mathbb{C}$. A special version of the **Maxwell–Bloch equations** is given by

$$\begin{aligned} \frac{\partial v}{\partial t} &= yw - (1 + i\delta)v, \\ \frac{\partial w}{\partial t} &= 2 - w - \frac{1}{2}(y^*v + yv^*), \\ \frac{\partial y}{\partial t} &= \varepsilon \left(-\frac{\partial y}{\partial z} + v - y \right), \end{aligned} \quad (18.14)$$

where $\delta \in \mathbb{R}$ is a parameter and $(\cdot)^*$ denotes complex conjugate. As for Example 18.2.2, we could have included many other free parameters in the equations and specified their ranges, but we shall not do so for this example; but see Section 18.7. The main observation is that (18.14) has a slow variable of the form (18.13) with unbounded operator $L = -\frac{\partial}{\partial z}$. As function spaces, one may consider suitable spaces of continuous functions with their natural sup-norms

$$X_0 := \left\{ (v, w) \in C(S^1, \mathbb{C} \times \mathbb{R}) : \|(v, w)\| := \sup_{z \in S^1} (|v(z)|^2 + |w(z)|^2)^{1/2} < \infty \right\},$$

$$X_1 := \left\{ y \in C(S^1, \mathbb{C}) : \|y\| := \sup_{z \in S^1} |y(z)| < \infty \right\},$$

$$X := X_0 \times X_1.$$

Ideally, we would like to view (18.14) as a fast–slow system with slow variable y and analyze the perturbation of the equilibria of the fast subsystem, which are given as a graph $h_0 : X_1 \rightarrow X_2$ by

$$C_0 = \left\{ (v, w, y) \in X : v(z) = \frac{2(1 - i\delta)y(z)}{1 + \delta^2 + |y(z)|^2} \text{ and } w(z) = \frac{2(1 + \delta^2)}{1 + \delta^2 + |y(z)|^2} \right\},$$

where the two equations are understood to hold for each $z \in S^1$. As previously, one has to use a cutoff procedure to consider a compact submanifold $M_0 \subset C_0$. Instead of classical solutions, we shall consider **mild solutions** in $X := X_0 \times X_1$,

$$\begin{aligned} v(t) &= e^{-(1+i\delta)t}v(0) + \int_0^t e^{-(1+i\delta)(t-s)}y(s)w(s) \, ds, \\ w(t) &= e^{-t}w(0) + 2(1 - e^{-t}) - \int_0^t e^{-(t-s)}\operatorname{Re}(y(s)^*v(s)) \, ds, \\ y(t) &= e^{-\varepsilon t}e^{-\varepsilon t\partial_z}y(0) + \varepsilon \int_0^t e^{-\varepsilon(t-s)}e^{-\varepsilon(t-s)\partial_z}v(s) \, ds, \end{aligned}$$

where $e^{-\varepsilon t\partial_z}$, $t \in \mathbb{R}$, denotes the one-parameter linear flow on $C(S^1, \mathbb{C})$ generated by the **transport equation** $\frac{\partial y}{\partial t} + \varepsilon \frac{\partial y}{\partial z} = 0$ and explicitly given by $e^{-\varepsilon t\partial_z}y(z) = y(z - \varepsilon t)$. The solutions (18.2.6) are associated with (18.14) via the **variation-of-constants formula** (or **Duhamel's principle**); see [Hal09, Joh82] for more details on Duhamel's principle. The next result is quite surprising; it makes use of the special structure of (18.14).

Lemma 18.2.7 ([MH01, CFG89]). *For $u(t) := (v(\cdot, t), w(\cdot, t), y(\cdot, t)) \in X$, the laser equations (18.14) generate a C^∞ global flow $\phi : X \times (-\infty, \infty) \rightarrow X$, $\phi(u(0), t) = u(t)$ in the sense of mild solutions.*

It is a key point that the flow is global in time and defined for $t \in (-\infty, \infty)$. A key ingredient for Lemma 18.2.7, as for the laser equations in Example 18.2.2, is a priori estimates.

Exercise/Project 18.2.8. Fix $\varepsilon > 0$. Show that there exist constants $K, \kappa > 0$ such that

$$\|(v, w)(t)\|^2 \leq e^{-\kappa t} \|(v, w)(0)\|^2 + K(1 - e^{-2\kappa t}). \quad (18.15)$$

Can you also find an a priori estimate for the slow variable? ◇

Using estimates such as (18.15), one can show that the solutions remain globally bounded inside a large enough ball for all $t \geq 0$. Instead of working to meet the requirements of Theorem 18.2.1, one may also set up a graph transform directly to perturb M_0 to M_ε , which is one possible strategy for proving the next result.

Theorem 18.2.9 ([MH01]). *For every $r \in \mathbb{N}_0$, there exists $\varepsilon_0 > 0$ such that for each $\varepsilon \in (0, \varepsilon_0(r)]$, there is a positively invariant C^r -smooth globally attracting manifold M_ε given as a graph over the slow variables $M_\varepsilon = \{(h_\varepsilon(y), y) \in X\}$ where $h_\varepsilon : X_1 \rightarrow X_0$. Furthermore, $\|h_\varepsilon(y) - h_0(y)\| \rightarrow 0$ uniformly on compact sets.*

Although it is possible to write a formal set of reduced equations on M_ε , there are variants of (18.14) with additional parameters where the singular limit $\varepsilon = 0$ does not represent the dynamics for $\varepsilon > 0$; see Section 18.7. ♦

Instead of considering first-order equations, such as the laser equations from Examples 18.2.2 and 18.2.6, it is possible to find slow manifolds for other types of PDEs such as reaction-diffusion equations or retarded function differential equations; see, e.g., Section 18.4. It is important to note that the topic of invariant manifolds for infinite-dimensional dynamical systems is frequently discussed using the terminology of inertial manifolds.

Definition 18.2.10. Let X be a Banach space with a semiflow ϕ . A manifold $M \subset X$ is an **inertial manifold** if it is a finite-dimensional smooth invariant manifold that attracts all solutions of ϕ exponentially fast in forward time.

An inertial manifold contains the global attractor of the dynamical system; see also Section 18.7 for detailed references and Section 18.4 for inertial manifolds in the context of delay equations.

18.3 Homogenization

Topics considered under the heading **homogenization** form an extremely vast area. Here we shall focus on the classical case for elliptic PDEs to illustrate a typical result in the area. Furthermore, we shall link the one-dimensional case to the fast–slow systems theory developed so far in this book; more detailed references on homogenization can be found in Section 18.7.

Consider the following PDE for $u_\varepsilon = u_\varepsilon(y)$ with $y \in \mathbb{R}^N$:

$$\begin{cases} -\nabla \cdot (A_\varepsilon \nabla u_\varepsilon) = f & \text{for } y \in \Omega, \\ u_\varepsilon = 0 & \text{for } y \in \partial\Omega, \end{cases} \quad (18.16)$$

where $\Omega \subset \mathbb{R}^N$ is a smooth bounded domain, $A_\varepsilon = A(y/\varepsilon)$ is an $\mathbb{R}^{N \times N}$ -matrix, $f : \mathbb{R}^N \rightarrow \mathbb{R}$, and $0 < \varepsilon \ll 1$ is a small parameter. Note that (18.16) is a time-independent PDE, so that we formally cannot interpret ε as a time scale separation. However, we can already spot two different spatial scales in (18.16) given by

$$y \quad \text{and} \quad x := \frac{y}{\varepsilon},$$

and we can think of y as a macroscopic spatial scale associated with a “slow time τ ” and of $x = y/\varepsilon$ as a microscopic spatial scale associated with a “fast time $t = \tau/\varepsilon$.” We are going to make the following assumptions on $A(x)$:

- (A1) (periodicity and smoothness) $A(x) \in C^\infty(\mathbb{T}^N, \mathbb{R}^{N \times N})$, where we view \mathbb{T}^N as the unit torus in N dimensions, so that $A(y/\varepsilon)$ is ε -periodic in all N directions of \mathbb{R}^N ;
- (A2) (positive definiteness) there exists $\alpha > 0$ such that $z^\top A(x) z \geq \alpha \|z\|^2$ for all $z \in \mathbb{R}^N$, $x \in \mathbb{T}^N$.

The assumptions on $A(x)$ imply that the differential operator in (18.16) is **uniformly elliptic**, which makes all the classical existence and uniqueness theory of elliptic PDEs applicable; see, e.g., [Eva02] for details. To explain the name “homogenization,” it helps to view (18.16) as the stationary problem associated with

$$\begin{cases} \frac{\partial v}{\partial t} - \nabla \cdot (A_\varepsilon \nabla v_\varepsilon) = f & \text{for } y \in \Omega, \\ v_\varepsilon = 0 & \text{for } y \in \partial\Omega, \end{cases} \quad (18.17)$$

where $v_\varepsilon = v_\varepsilon(y, t)$, and we recognize (18.17) as a heat equation with source/sink term f . In this context, one interprets $A_\varepsilon = A(y/\varepsilon)$ as the **thermal conductivity tensor** of the material. The coefficients of $A(y/\varepsilon)$ vary rapidly on the

microscopic scale, so that the material is **heterogeneous**. The singular limit $\varepsilon \rightarrow 0$ physically corresponds to heterogeneities vanishing. We may hope that for sufficiently small ε , the heterogeneous material tensor $A(y/\varepsilon)$ can be replaced by a **homogenized material tensor** $\bar{A} \in \mathbb{R}^{N \times N}$, where \bar{A} has constant coefficients. The replacement of $A(y/\varepsilon)$ by \bar{A} is called **homogenization**.

We are going to discuss a formal asymptotic derivation of the constant-coefficient matrix \bar{A} . One interesting aspect of this derivation is that it is motivated by classical multiple time scales asymptotics using the ansatz

$$\begin{aligned} u_\varepsilon(y) &= u_0(y/\varepsilon, y) + \varepsilon u_1(y/\varepsilon, y) + \varepsilon^2 u_2(y/\varepsilon, y) + \dots \\ &= u_0(x, y) + \varepsilon u_1(x, y) + \varepsilon u_2(x, y) + \dots, \end{aligned} \quad (18.18)$$

where $u_l : \mathbb{T}^N \times \Omega \rightarrow \mathbb{R}$ are to be determined for $l \in \mathcal{N}_0$. Taking into account Section 9.8, we recognize (18.18) immediately as the method of multiple scales (or two-timing). If we assume that

$$u_\varepsilon \rightarrow u_0 =: u \quad \text{as } \varepsilon \rightarrow 0,$$

then the main goal is to derive an equation that u has to satisfy. The standard plan is to plug (18.18) into (18.16) and to work at different orders of ε . Before carrying out this plan, we remind the reader (see Section 9.8) that the partial derivatives of functions of the form $w(x, y) = w(y/\varepsilon, y) =: \tilde{w}(y)$ are needed and are given by

$$\frac{\partial w}{\partial y_i} = \frac{\partial w}{\partial y_i} + \frac{1}{\varepsilon} \frac{\partial w}{\partial x_i}$$

for $i \in \{1, \dots, N\}$. Using these partial derivatives, we can rewrite the differential operator

$$L\tilde{w} := - \sum_{i,j=1}^N \frac{\partial}{\partial y_j} \left(a_{ij}(y/\varepsilon) \frac{\partial \tilde{w}}{\partial y_i} \right)$$

from equation (18.16) as

$$L = \frac{1}{\varepsilon^2} L_1 + \frac{1}{\varepsilon} L_2 + L_3, \quad (18.19)$$

where

$$L_1 w := - \sum_{i,j=1}^N \frac{\partial}{\partial x_j} \left(a_{ij}(x) \frac{\partial w}{\partial x_i} \right), \quad (18.20)$$

$$L_2 w := - \sum_{i,j=1}^N \frac{\partial}{\partial x_j} \left(a_{ij}(x) \frac{\partial w}{\partial y_i} \right) + \frac{\partial}{\partial y_j} \left(a_{ij}(x) \frac{\partial w}{\partial x_i} \right), \quad (18.21)$$

$$L_3 w := - \sum_{i,j=1}^N \frac{\partial}{\partial y_j} \left(a_{ij}(x) \frac{\partial w}{\partial y_i} \right). \quad (18.22)$$

Now one can just plug the expansion $u_\varepsilon = u_0 + \varepsilon u_1 + \varepsilon^2 u_2 + \dots$ into $L u_\varepsilon = f$. Using the differential operator notation from (18.19)–(18.22), we obtain

$$\frac{1}{\varepsilon^2} L_1 u_0 + \frac{1}{\varepsilon} (L_1 u_1 + L_2 u_0) + (L_1 u_2 + L_2 u_1 + L_3 u_0) + \mathcal{O}(\varepsilon) = f.$$

Considering different orders of ε yields three PDEs,

$$0 = L_1 u_0, , \quad (18.23)$$

$$0 = L_1 u_1 + L_2 u_0, , \quad (18.24)$$

$$f = L_1 u_2 + L_2 u_1 + L_3 u_0. \quad (18.25)$$

Looking at (18.20), we see that $L_1 u_0 = 0$ involves only derivatives with respect to x . Therefore, $u_0 = u(x, y)$ solves $L_1 u_0 = 0$ for each fixed y . Recall that $x \in \mathbb{T}^N$, so that all solutions u_0 are 1-periodic in x .

Exercise 18.3.1. Using the previous observations, show that all solutions $u_0(x, y)$ to $L_1 u_0 = 0$ are constant in x and depend only on y . \diamond

By Exercise 18.3.1, we know that $u_0 = u(y)$. Note that this result should definitely motivate us to move on, since our final goal was to derive an equation for u in y -space. Using $u_0 = u(y)$, (18.21), and (18.24), we get

$$L_1 u_1 = -L_2 u_0 = \sum_{i,j=1}^N \frac{\partial a_{ij}}{\partial x_j} \frac{\partial u}{\partial y_i},$$

where $a_{ij} = a_{ij}(x)$ and $u = u(y)$. The next step involves a trick that gives a good representation formula for $u_1 = u_1(x, y)$ with separated variables. To get this formula, consider the PDE

$$\begin{cases} L_1 \chi_i = -\sum_{j=1}^N a_{ij}(x)_{x_j} & \text{on } \mathbb{T}^N \\ \chi_i \text{ is 1-periodic} \end{cases} \quad (18.26)$$

for $i = 1, \dots, N$. It can be shown that (18.26) has a solution χ_i , which is unique up to a constant.

Exercise/Project 18.3.2. Prove the last claim about the existence and uniqueness (up to a constant) of χ_i . Hints: (1) Integrate the right-hand side of (18.26) over \mathbb{T}^N and show that the result is zero. (2) You might want to use the Fredholm alternative at some point. \diamond

With a solution to (18.26), we notice that $u_1(x, y)$ can be written as follows:

$$u_1(x, y) = - \sum_{i=1}^N \chi_i(x) \frac{\partial u}{\partial y_i}(y) + \tilde{u}_1(y), \quad (18.27)$$

where \tilde{u}_1 is an arbitrary function of y ; the validity of (18.27) is easily checked by applying L_1 to both sides. The last PDE we have to consider is (18.25), which can be written as

$$L_1 u_2 = f - L_2 u_1 - L_3 u_0. \quad (18.28)$$

As for the PDE (18.26), we will need that the right-hand side of (18.28) integrates to zero over $x \in \mathbb{T}^N$, so that the problem has a solution u_2 that is 1-periodic in x . Therefore, we require

$$\int_{\mathbb{T}^N} L_2 u_1 + L_3 u_0 \, dx = \int_{\mathbb{T}^N} f \, dy = f(y). \quad (18.29)$$

The integral condition can be simplified; the definition of L_2 implies

$$\int_{\mathbb{T}^N} L_2 u_1 \, dx = - \sum_{j,k=1}^N \int_{\mathbb{T}^N} \frac{\partial}{\partial x_k} \left(a_{j,k}(x) \frac{\partial u_1}{\partial y_j} \right) \, dx + \frac{\partial}{\partial y_j} \left(\int_{\mathbb{T}^N} a_{jk}(x) \frac{\partial u_1}{\partial x_k} \, dx \right).$$

The first term on the right-hand side vanishes after application of the divergence theorem and using periodicity of the remaining integrand in x . Using the representation formula (18.27) for u_1 , it follows that

$$\begin{aligned} \int_{\mathbb{T}^N} L_2 u_1 \, dx &= - \sum_{j,k=1}^N \frac{\partial}{\partial y_j} \left(\int_{\mathbb{T}^N} a_{jk}(x) \frac{\partial u_1}{\partial x_k} \, dx \right) \\ &= \sum_{i,j,k=1}^N \left(\int_{\mathbb{T}^N} a_{jk}(x) \frac{\partial \chi_i}{\partial x_k} \, dx \right) \frac{\partial^2 u}{\partial y_i \partial y_j}. \end{aligned}$$

Recalling that $u = u_0$ and using the PDE integral condition (18.29), we can further simplify the last result and obtain

$$- \sum_{i,j=1}^N \left(\int_{\mathbb{T}^N} a_{ij}(x) - \sum_{k=1}^N a_{jk}(x) \frac{\partial \chi_i}{\partial x_k} \, dx \right) \frac{\partial^2 u}{\partial y_i \partial y_j} = f. \quad (18.30)$$

Note carefully that equation (18.30) is indeed a PDE for $u = u_0$ given by

$$\begin{cases} - \sum_{i,j=1}^N \bar{a}_{ij} \frac{\partial^2 u}{\partial y_i \partial y_j} = f & \text{in } \Omega \\ u = 0 & \text{on } \partial\Omega, \end{cases} \quad (18.31)$$

where the **homogenized coefficients** \bar{a}_{ij} are given explicitly by

$$\bar{a}_{ij} := \int_{\mathbb{T}^N} a_{ij}(x) - \sum_{k=1}^N a_{jk}(x) \frac{\partial \chi_i}{\partial x_k} \, dx, \quad (18.32)$$

and χ_i for $i = 1, \dots, N$ solves the so-called **cell problem** (18.26); we remark that the cell problem is sometimes also called the **corrector problem**, and χ is referred to as the **first-order corrector**. Hence, we have succeeded in deriving a PDE for $u_0 = u$ with constant-coefficient matrix $\bar{A} = \{\bar{a}_{ij}\}_{i,j=1}^N$ for the differential operator. We also expect from our formal calculation that $u_\varepsilon \rightarrow u$ as $\varepsilon \rightarrow 0$. This idea can be made rigorous, and the following theorem is one example of various results that can be obtained.

Theorem 18.3.3 ([PS08]; see also [All92, BLP11, Ngu89]). Consider the PDE (18.16) for u_ε . Assume that $f \in L^2(\Omega)$ and that A satisfies the periodicity, smoothness, and positive definiteness conditions (A1)–(A2) stated above. Then $\|u_\varepsilon - u\|_{L^2(\Omega)} \rightarrow 0$ as $\varepsilon \rightarrow 0$, where u solves the homogenized PDE (18.31)–(18.32).

Stronger results than L^2 -convergence can be obtained if we add another correction term to $u = u_0$ [PS08]. We shall not discuss the proof of Theorem 18.3.3 here, but we are going to mention one of the main tools for the proof.

Definition 18.3.4. Let $u_\varepsilon(y) = u_\varepsilon$ be a sequence of functions in $L^2(\Omega)$. We say that $u_\varepsilon(y)$ **two-scale converges** to $u_0(x, y) \in L^2(\mathbb{T}^N \times \Omega)$ if for every $h \in L^2(\Omega, C_{per}(\mathbb{T}^N))$, we have

$$\lim_{\varepsilon \rightarrow 0} \int_{\Omega} u_\varepsilon(y) h(y/\varepsilon, y) \, dy = \int_{\Omega} \int_{\mathbb{T}^N} u_0(x, y) h(x, y) \, dx \, dy.$$

A bit of familiarity with weak solutions of PDEs (see, e.g., [Eva02]) suffices to see that the periodic functions h can be viewed as test functions, so that two-scale convergence can be viewed as a type of weak convergence on two different scales. It can be shown that if a sequence u_ε is bounded in $L^2(\Omega)$, then we can find a convergent subsequence. These observations provide the main strategy to proving Theorem 18.3.3. The idea is to make the asymptotic approach rigorous by combining it with weak convergence and two-scale convergence arguments; see Section 18.7.

As a last step, we illustrate homogenization for elliptic PDEs for one of the simplest possible examples and to illustrate that there exists a link to fast–slow systems in this case.

Example 18.3.5. Consider the one-dimensional case

$$\begin{cases} -\frac{d}{dy} \left(a(y/\varepsilon) \frac{du_\varepsilon}{dy} \right) = f, & \text{for } y \in (0, L), \\ u(y) = 0, & \text{for } y = 0 \text{ and } y = L, \end{cases} \quad (18.33)$$

where $a(x)$ is smooth and 1-periodic. It is not too difficult to derive the homogenized problem (18.31)–(18.32) associated with (18.33), since the cell problem is solvable explicitly.

Exercise 18.3.6. Show that the homogenized coefficient (18.32) is given by $\bar{a} = \frac{1}{\int_0^1 a(x)^{-1} \, dx}$. \diamond

Note that \bar{a} is not simply the average over one period, but the so-called **harmonic average**, which is formed by inverting the average of the inverse. The interesting aspect of (18.33) is that we can view it directly as a (2, 1)-fast–slow system. Indeed, $v_\varepsilon := a(y/\varepsilon) \frac{du_\varepsilon}{dy}$, so that (18.33) yields

$$\begin{aligned} a(x) \frac{dv_\varepsilon}{dt} &= v_\varepsilon, \\ \frac{dv_\varepsilon}{dt} &= -f, \\ \varepsilon \frac{dx}{dt} &= 1. \end{aligned} \quad (18.34)$$

Changing to the time scale $s = t/\varepsilon$ and viewing (18.34) as a nonautonomous system leads to

$$\begin{aligned}\frac{du_\varepsilon}{ds} &= \varepsilon \frac{v_\varepsilon}{a(s)}, \\ \frac{dv_\varepsilon}{ds} &= -\varepsilon f,\end{aligned}\tag{18.35}$$

which is in the standard form for averaging. The averaged equations are

$$\begin{aligned}\frac{du_0}{ds} &= v_0 \int_0^1 (a(s))^{-1} ds, \\ \frac{dv_0}{ds} &= -f,\end{aligned}\tag{18.36}$$

since a was assumed to be 1-periodic. Converting (18.36) back to a second-order ODE gives

$$-\frac{d}{dx} \left(\frac{1}{\int_0^1 (a(x))^{-1} dx} \frac{du_0}{dx} \right) = f,$$

as desired (and expected from the abstract homogenization theory). ♦

The last example showed that in one dimension, the simplest case of homogenization theory for periodic coefficients is directly related to averaging. However, we already know that averaging is expected to work for other invariant sets in the fast subsystem, not only periodic orbits (see, e.g., Sections 9.6, 9.11, 10.7, 14.9, 13.6). For the fast–slow systems case, one replaces the fast variables by an integral over a suitable ergodic invariant measure in the fast subsystem. Hence, one may hope that there are results for “homogenization” of PDEs or other infinite-dimensional differential equations, where one is allowed to replace periodicity by more general assumptions; see Section 18.7.

However, homogenization procedures may also fail in several cases. In fact, averaging may already fail for finite-dimensional ODEs, e.g., when a fast subsystem periodic orbit is not normally hyperbolic or a fast subsystem invariant measure is not ergodic.

18.4 Delay Equations with Small Delay

In this section, we are going to develop a link between delay equations with small delay and fast–slow systems. As a starting point, we briefly recall and slightly generalize some definitions from Example 18.1.3. Consider a delay $\tau > 0$ and let $X = C^0([-\tau, 0], \mathbb{R}^n)$ denote the space of continuous functions on $[-\tau, 0]$ to \mathbb{R}^n .

Remark: The notation τ for the delay is standard in the literature on delay differential equations. Usually, we use τ as our slow time scale, but sometimes, there is no way of avoiding notational problems; hence we introduce s as another time scale to have t and s available as time scales.

A **retarded functional differential equation** (RFDE) is given by

$$\dot{y}(s) = \frac{dy}{ds} = F(y_s),\tag{18.37}$$

where $F : X \rightarrow \mathbb{R}^n$ is at least C^1 , and we define $y_s(r)$ as a function in X given by $y_s(r) = y(s + r)$ for $r \in [-\tau, 0]$; see also Example 18.1.3. Equation (18.37) will also be referred to as a delay equation with delay τ . Let $u \in X$ be a given function as the initial condition. Consider a function

$$y : [\sigma - \tau, \sigma + T] \rightarrow \mathbb{R}^n$$

depending on the final time $T > 0$ and the initial time $\sigma \in \mathbb{R}$. To define a solution of the RFDE (18.37), we also have to be given an initial solution function $u \in X$. A solution $y(\sigma, u, s)$ (we sometimes write $y(\sigma, u)(s)$ or just $y(s)$) to (18.37) is a C^1 function on $[\sigma - \tau, \sigma + T]$ that satisfies the initial condition u at σ , so that $y_\sigma(u, \cdot) = u(\cdot)$, and that satisfies the RFDE for $s \in [\sigma, \sigma + T]$,

$$\dot{y}(s) = F(y_s) = F(y(\sigma, u, s + \cdot)).$$

If we assume a small delay $0 < \tau \ll 1$, then one might hope that the solutions of the RFDE (18.37) are “close to” or “determined by” an ordinary differential equation. The initial condition $u \in X$ belongs to an infinite-dimensional function space, but the domain of definition of the functions is small, since the delay τ is small. To make this idea precise, we have to introduce a subclass of solutions to RFDEs.

Definition 18.4.1. A solution y to the RFDE (18.37) is called a **special solution** if it is defined for all times $s \in \mathbb{R}$ and

$$\sup_{s \in \mathbb{R}} e^{-|s|/\tau} \|y(s)\| < \infty.$$

Suppose that $\eta : \mathbb{R}^n \times \mathbb{R} \rightarrow \mathbb{R}^n$ is a continuous function such that for each $\xi \in \mathbb{R}^n$, the function $s \mapsto \eta(\xi, s)$ is a special solution. Then we call η a **special flow** for the RFDE (18.37) if for all $s, r \in \mathbb{R}$ and $\xi \in \mathbb{R}^n$, we have

$$\eta(\xi, 0) = \xi \quad \text{and} \quad \eta(\eta(\xi, s), r) = \eta(\xi, s + r).$$

Note carefully that the initial conditions for the special flow η are in \mathbb{R}^n and not in the infinite-dimensional space X . We will see that it can sometimes be possible to describe the RFDE dynamics just using a finite-dimensional special flow. Consider the map

$$\xi \mapsto \eta(\xi, \cdot)$$

from $\mathbb{R}^n \rightarrow X$. Let $M \subset X$ denote the image of this map. If all solutions of the RFDE (18.37) were attracted exponentially fast to M as $s \rightarrow \infty$, then the finite-dimensional special flow would indeed describe the asymptotic dynamics of the system. Recall from Section 18.2 that M is called an inertial manifold in this case. For an inertial manifold, one may just write the vector field \tilde{F} on M as

$$\tilde{F}(\xi) = \frac{d}{ds} \eta(\xi, s) \Big|_{s=0} = F(\eta(\xi, \cdot)), \tag{18.38}$$

which defines a finite-dimensional ODE on M . We are particularly interested in carrying out this reduction for **delay equations** that commonly occur in applications of the form

$$\dot{y}(s) = f(y(s), y(s - \tau)) \quad (18.39)$$

for $f : \mathbb{R}^n \times \mathbb{R}^n \rightarrow \mathbb{R}^n$. We restrict our analysis to (18.39) from now on. Since τ is small, we are tempted just to expand the vector field in a series in τ . This process is sometimes called **post-Newtonian expansion**, since forces act instantaneously in Newton's laws, while in Maxwell's or Einstein's field theories, they propagate at the speed of light, i.e., there is a delay until they act from some distance. Just expanding (18.39) up to order $\mathcal{O}(\tau)$ yields

$$\dot{y}(s) = f(y(s), y(s)) + \tau D_2 f(y(s), y(s))\dot{y}(s) + \mathcal{O}(\tau^2), \quad \text{as } \tau \rightarrow 0, \quad (18.40)$$

where $D_2 f$ denotes the derivative of f with respect to the second argument. Therefore, we could try to replace the delay equation with a first-order ODE by dropping the order- $\mathcal{O}(\tau^2)$ term. This equation has a one-dimensional solution space. It turns out that the solutions of the first-order ODE indeed formally agree with the flow on the inertial manifold up to order $N = 1$. The problem arises at higher orders. We shall see below that the post-Newtonian expansion produces vector fields that have dimension nN . Clearly, there is some analysis required to see how these higher-dimensional solutions relate to the inertial manifold.

Let us assume that there is a special flow η for (18.39) and denote it by $\eta(\xi, s; \tau)$, since it depends on the delay τ as a parameter. Then the vector field (18.38) can be written as

$$\tilde{F}(\xi; \tau) = f(\xi, \eta(\xi, -\tau; \tau)). \quad (18.41)$$

The vector field (18.41) defines an ODE on M . We will show that a finite-order post-Newtonian expansion produces a fast–slow system and that this system has a slow manifold. The vector field on the slow manifold agrees with the vector field on the inertial manifold up to the order at which we truncate the series expansions. We are going to focus on the fast–slow systems aspect of the construction and just state existence theorems for special flows and inertial manifolds.

Theorem 18.4.2 ([Chi03]). *Suppose $f : \mathbb{R}^n \times \mathbb{R}^n \rightarrow \mathbb{R}^n$ is a C^1 Lipschitz map with Lipschitz constant $K > 0$ and $0 \leq 8Kb < 1$. Then the delay equation (18.39) has a C^1 -family of special flows $\eta : \mathbb{R}^n \times \mathbb{R} \times [0, b] \rightarrow \mathbb{R}^n$ for delays $\tau \in [0, b]$.*

Theorem 18.4.3 ([Dri68, Dri76, JK75]). *Suppose $f : \mathbb{R}^n \times \mathbb{R}^n \rightarrow \mathbb{R}^n$ is a C^1 Lipschitz map with Lipschitz constant $K > 0$, and let p be the least positive root of the equation $p = Ke^{p\tau}$, $K\tau e^{1+K\tau+p\tau} < 1$. Then every solution to the RFDE (18.39) is attracted exponentially fast to the manifold of special solutions.*

Theorem 18.4.3 also applies to more general RFDEs of the form (18.37); see [Dri68, Dri76]. Theorem 18.4.2 partially applies to (18.37) without the smoothness conclusion. However, we need smoothness to find a vector field on the inertial manifold M , which is another reason to focus on (18.39). Note that Theorem 18.4.2 gives an explicit estimate on the size of the delay depending on the Lipschitz constant K . From now on, we always assume that this estimate is satisfied, and we have a C^1 -family of special flows. The strategy to showing the equivalence of vector fields on the inertial and slow manifolds is as follows:

- (S1) Determine the expansion of the vector field on the inertial manifold by an invariance equation.
- (S2) Directly expand the map $f(y(s), y(s - \tau))$ in τ near $\tau = 0$ using a post-Newtonian expansion.
- (S3) Use assumptions on the fast–slow system from (S2) to get a normally hyperbolic slow manifold.
- (S4) Determine the expansion of the vector field on the slow manifold using an invariance equation.
- (S5) Observe that the vector fields from (S1) and (S4) coincide.

Calculating the asymptotic expansions up to a general order N is very tedious and not very illuminating. Therefore, we restrict ourselves to order $N = 2$. We start by using the special flow to reduce the RFDE (18.39) to the inertial manifold. Let

$$\tilde{F}(\xi; \tau) = f(\xi, \eta(\xi, -\tau; \tau)), \quad (18.42)$$

as suggested by equation (18.41). Formally, one may expand \tilde{F} in τ to obtain

$$\tilde{F}(\xi; \tau) = \tilde{F}(\xi; 0) + \tau \tilde{F}_\tau(\xi; 0) + \frac{\tau^2}{2} \tilde{F}_{\tau\tau}(\xi; 0) + \mathcal{O}(\tau^3), \quad (18.43)$$

where the subscript τ for \tilde{F} denotes the partial derivative.

Proposition 18.4.4. *The reduction of the vector field to the inertial manifold for the RFDE (18.39) is given by*

$$\begin{aligned} \tilde{F}(\xi; \tau) = f(\xi, \xi) - \tau D_2 f(\xi, \xi) + \frac{\tau^2}{2} & [D_2^2 f(\xi, \xi)(f(\xi, \xi), f(\xi, \xi)) + \\ & D_2 f(\xi, \xi)(D_1 f(\xi, \xi) + 3D_2 f(\xi, \xi))f(\xi, \xi)] + \mathcal{O}(\tau)^3. \end{aligned} \quad (18.44)$$

Proof. To prove (18.44), we look at the formal result (18.43) term by term. For the zeroth order, we have

$$\tilde{F}(\xi; 0) = f(\xi, \eta(\xi, 0; 0)) = f(\xi, \xi).$$

Before looking at the next order, recall that the special flow has to satisfy the RFDE (18.39), so that

$$\frac{d\eta}{ds}(\xi, s; \tau) = \dot{\eta}(\xi, s; \tau) = f(\eta(\xi, s; \tau), \eta(\xi, s - \tau; \tau)) \quad \text{and} \quad \eta(\xi, 0; \tau) = \xi,$$

which is the classical invariance condition. Therefore, we get

$$\begin{aligned}\tilde{F}_\tau(\xi; \tau) &= D_2 f(\xi, \eta(\xi, -\tau; \tau)) [\eta_\tau(\xi, -\tau; \tau) - \dot{\eta}(\xi, -\tau; \tau)] \\ &= D_2 f(\xi, \eta(\xi, -\tau; \tau)) [\eta_\tau(\xi, -\tau; \tau) - f(\eta(\xi, -\tau; \tau), \eta(\xi, -2\tau; \tau))].\end{aligned}$$

Observe that since $\eta(\xi, 0; \tau) = \xi$, all derivatives of the map $\tau \mapsto \eta(\xi, 0; \tau)$ vanish. It follows that

$$\tilde{F}_\tau(\xi; \tau) = -D_2 f(\xi, \xi) f(\xi, \xi),$$

which proves the order- $\mathcal{O}(\tau)$ term. By a similar direct argument, we get the result for $\mathcal{O}(\tau^2)$. \square

Proposition 18.4.4 completes step (S1) of the strategy. The next step brings fast–slow systems into play. We want to compute the post-Newtonian expansion of

$$\tau \mapsto f(y(t), y(t - \tau)),$$

which just amounts to expanding in τ around $\tau = 0$. We can directly compute the expansion

$$\begin{aligned}f(y(s), y(s - \tau)) &= f(y(s), y(s)) - \tau D_2 f(y(s), y(s)) \dot{y}(s) \\ &\quad + \frac{\tau^2}{2} [D_2 f(y(s), y(s)) \ddot{y}(s) + D_2^2 f(y(s), y(s)) (\dot{y}(s), \dot{y}(s))] + \mathcal{O}(\tau^3)\end{aligned}$$

up to and including order two. Truncating the expansion at this order and looking at the resulting ODE

$$\begin{aligned}\dot{y}(s) &= f(y(s), y(s)) - \tau D_2 f(y(s), y(s)) \dot{y}(s) \\ &\quad + \frac{\tau^2}{2} [D_2 f(y(s), y(s)) \ddot{y}(s) + D_2^2 f(y(s), y(s)) (\dot{y}(s), \dot{y}(s))]\end{aligned}$$

reveals a second-order singularly perturbed equation. In particular, if we convert it to a first-order system by setting $y' = x$, we get

$$\begin{aligned}\frac{\tau^2}{2} D_2 f(y, y) \frac{dx}{ds} &= x - f(y, y) + \tau D_2 f(y, y) x - \frac{\tau^2}{2} D_2^2 f(y, y)(x, x). \\ \frac{dy}{ds} &= x.\end{aligned}\tag{18.45}$$

Using the relabeling $\sqrt{\varepsilon} = \tau$ and assuming that $D_2 f(y, y)$ is invertible, we can transform (18.45) into an (n, n) -fast–slow system

$$\begin{aligned}\varepsilon \dot{x} &= 2D_2 f(y, y)^{-1} [x - f(y, y) + \sqrt{\varepsilon} D_2 f(y, y) x - \frac{\varepsilon}{2} D_2^2 f(y, y)(x, x)], \\ \dot{y} &= x.\end{aligned}\tag{18.46}$$

In (18.46), the time s plays the role of the slow time. From (18.46), we can immediately see that the normal hyperbolicity assumption we would like to assume is that $D_2 f(y, y)^{-1}$ has no eigenvalues on the imaginary axis, i.e., it should be a hyperbolic matrix. In this case, the n -dimensional critical manifold

$$C_0 = \{(x, y) \in \mathbb{R}^{2n} : x = f(y, y)\}$$

is normally hyperbolic. Recall from linear algebra that λ is an eigenvalue of an invertible square matrix A if and only if λ^{-1} is an eigenvalue of A^{-1} . This fact implies that the hyperbolicity of $D_2 f(y, y)^{-1}$ is equivalent to the hyperbolicity of $D_2 f(y, y)$. Finally, we can state the main result on the formal equivalence of asymptotic expansions for the two vector fields under consideration.

Theorem 18.4.5 ([Chi03, Chi04]). Suppose the matrix $D_2 f(y, y)$ is hyperbolic for all $y \in \mathbb{R}^n$. Then there exists a slow manifold C_ε for (18.46), and the vector field on C_ε agrees with the flow on the inertial manifold up to and including order N for a given $N \in \mathbb{N}$.

Proof. (Sketch, [Chi03, Chi04]) Again we only consider the first interesting case $N = 2$. The existence result for the slow manifold C_ε follows immediately from Fenichel's theorem. A bit of work is required to show that the slow manifold of (18.45) can locally be given as a graph with asymptotic expansion

$$x = h_\varepsilon(y) = f(y, y) + \tau h_1(y) + \tau^2 h_2(y) \quad (18.47)$$

up to order $\mathcal{O}(\tau^2)$. Substituting (18.47) into (18.45) and equating terms of equal powers in τ , we are going to find that the functions h_1 and h_2 precisely coincide with the terms for the vector field on the inertial manifold given in (18.44). \square

Exercise/Project 18.4.6. Suppose that $n = 1$, so that we are dealing with a delay equation on \mathbb{R} . Substitute the ansatz (18.47) into (18.45) and verify that $h_1(y) = -D_2 f(y, y)$. Do you have the patience to check $h_2(y)$ and higher orders? \diamond

18.5 Differential Inclusions

Another interesting type of differential equation that we have not treated yet is **differential inclusions**

$$\frac{dz}{dt} = z' \in F(z(t)), \quad \text{for } t \in [0, T], \quad (18.48)$$

where $F : \mathbb{R}^N \rightarrow \mathbb{R}^N$ is a **set-valued map**, i.e., the range of F consists of subsets of \mathbb{R}^N . Obviously, all classical ODEs are differential inclusions. It is not too difficult to find examples beyond ODEs.

Example 18.5.1. A simple example of a differential inclusion is

$$z' \in \begin{cases} 1, & \text{if } z < 0, \\ [-1, 1], & \text{if } z = 0, \\ -1, & \text{if } z > 0, \end{cases} \quad (18.49)$$

with initial condition $z(0) = z_0$. Solving (18.49) yields

$$z(t) = \begin{cases} t + z_0, & \text{if } z_0 < 0 \text{ and } t < |z_0|, \\ -t + z_0, & \text{if } z_0 > 0 \text{ and } t < |z_0|, \\ 0, & \text{otherwise.} \end{cases} \quad (18.50)$$

The solution is not continuously differentiable. Therefore, the classical space of solutions for ODEs is necessarily too small for differential inclusions. New concepts of solutions are required. \blacklozenge

Definition 18.5.2. The set of **solutions** for (18.48) with initial condition $z(0) = z_0$ and $t \in [0, T]$ consists of absolutely continuous functions $z(\cdot) \in \text{AC}([0, T], \mathbb{R}^N)$ that satisfy (18.48) almost everywhere $t \in [0, T]$.

Usually, we will need some additional assumptions on the set-valued map F to allow for an analysis of differential inclusions.

(A1) The sets $F(z)$ are nonempty, compact, and convex for all $z \in \mathbb{R}^N$.

(A2) The map F is **Lipschitz** in z , i.e., there exists $L \geq 0$ such that

$$F(z_1) \subset F(z_2) + L\|z_1 - z_2\|B_1, \quad \text{for all } z_1, z_2 \in \mathbb{R}^N,$$

where $B_1 = \{z \in \mathbb{R}^N : \|z\| \leq 1\}$ is the unit ball.

We always assume (A1), since nonconvex set-valued maps are often very difficult to deal with analytically. The assumption (A2) is more natural, because even for ODEs, we must assume a Lipschitz condition to prove the classical existence and uniqueness results.

Theorem 18.5.3 ([Smi02]). *Under the assumptions (A1)–(A2), there exists a solution to the differential inclusion (18.48). Furthermore, the set of solutions is arcwise connected.*

Before proceeding to fast–slow differential inclusions, we briefly mention two very important applications of differential inclusions.

Example 18.5.4. Consider a parameterized differential equation

$$z' = f(z, u), \tag{18.51}$$

where $z \in \mathbb{R}^N$, and $u \in U \subset \mathbb{R}^p$ is viewed as a control parameter or more generally as a function $u : [0, T] \rightarrow \mathbb{R}^p$ depending on time that controls the dynamics of (18.51). If $u(t) \in U$ for $t \in [0, T]$, we say that u is an **admissible** (or **feasible**) **control**. In this case, (18.51) is a nonautonomous ODE,

$$.z' = f(z, u(t)). \tag{18.52}$$

Finding trajectories of (18.52) using admissible controls is equivalent to solving the differential inclusion $z' \in \bigcup_{u \in U} f(z, u)$. ♦

Control theory is one of the major application areas in which differential inclusions appear. Another prominent example is nonsmooth electrical and mechanical systems.

Example 18.5.5. Fillipov systems model a wide variety of nonsmooth systems; more details of Fillipov systems are defined in Section 19.3. It is interesting to note that every two-zone Fillipov system can be written as a differential inclusion,

$$z' \in F(z) := \begin{cases} \{F_1(z)\}, & \text{if } H(z) > 0, \\ \{F_1(z) + \alpha(F_2(z) - F_1(z)); \alpha \in [0, 1]\}, & \text{if } H(z) = 0, \\ \{F_2(z)\}, & \text{if } H(z) < 0. \end{cases} \tag{18.53}$$

The function $H : \mathbb{R}^N \rightarrow \mathbb{R}$ is usually assumed to be smooth, and its zero set defines the boundary between two smooth vector fields $F_{1,2}(z)$. A typical example for (18.53) is the **bilinear oscillator**

$$u'' + 2au' + k_i^2 u = b + c \cos(t), \quad (18.54)$$

where the parameters (a, b, c) are fixed, but the stiffness k_i^2 with $i \in \{1, 2\}$ changes depending on the phase-space region. If we let $(u, u', t) = (z_1, z_2, z_3)$, we can define $F_{1,2}(z)$ by (18.54) depending on the value of k_i^2 . Considering a function $H(z)$, for example $H(z) = z_1$, the bilinear oscillator can be written as a differential inclusion (18.53). ♦

Exercise/Project 18.5.6. Draw a (z_1, z_2) -phase portrait of the bilinear oscillator (18.54) for $c = 0$. Can you explain any of the dynamical phenomena and bifurcations for $c > 0$? ◇

We proceed to specialize to multiple time scale differential inclusions. A **fast–slow differential inclusion** is given by

$$\begin{pmatrix} \varepsilon \frac{dx}{d\tau} \\ \frac{dy}{d\tau} \end{pmatrix} = \begin{pmatrix} \varepsilon \dot{x} \\ \dot{y} \end{pmatrix} \in F(x, y), \quad (18.55)$$

where F is a set-valued map from \mathbb{R}^{m+n} into \mathbb{R}^{m+n} . We shall view the differential inclusion (18.55) as an initial value problem with $(x(0), y(0)) = (x_0, y_0)$ on a time interval $\tau \in [0, T]$ for some fixed $T > 0$. Taking the singular limit $\varepsilon \rightarrow 0$ in (18.55) provides the analogue of the classical slow subsystem

$$\begin{pmatrix} 0 \\ \dot{y} \end{pmatrix} \in F(x, y). \quad (18.56)$$

In addition to the usual solution concept in Definition 18.5.2, we shall assume that solutions of (18.56) also satisfy that y is measurable on $[0, T]$. When we want to indicate the dependence of solutions on ε , we write

$$z(\tau; \varepsilon) = (x(\tau; \varepsilon), y(\tau; \varepsilon)),$$

where $z(\tau; \varepsilon)$ solves (18.55) and $z(\tau; 0)$ solves the singular limit (18.56). The sets of all solutions will be denoted by $Z(\varepsilon)$ and $Z(0)$ respectively.

Example 18.5.7. As an example of a singularly perturbed differential inclusion, we start with a linear nonautonomous system on a fixed time interval $[0, T]$,

$$\begin{pmatrix} \varepsilon \dot{x} \\ \dot{y} \end{pmatrix} = A(\tau) \begin{pmatrix} x \\ y \end{pmatrix} + B(\tau)u(\tau) =: F(x, y, u, \tau),$$

where $(x, y) \in \mathbb{R}^{m+n}$ with $N := m + n$, $A : \mathbb{R} \rightarrow \mathbb{R}^{N \times N}$, and $B : \mathbb{R} \rightarrow \mathbb{R}^{N \times N}$ are matrix-valued maps, and $u(\tau)$ is the control as in Example 18.5.4. Let U be the set of admissible controls, and define the attainable set

$$K_\varepsilon := \{w \in \mathbb{R}^N : \exists u(\cdot) \in U, w = (x(T), y(T))\},$$

where $(x(\tau; \varepsilon), y(\tau; \varepsilon)) \in Z(\varepsilon)$ is a solution to the differential inclusion

$$\begin{pmatrix} \varepsilon \dot{x} \\ \dot{y} \end{pmatrix} \in \bigcup_{u \in U} F(x, y, u, \tau).$$

In optimal control theory, we would like to study the problem

$$\inf_{w \in K_\varepsilon} \{\kappa(w)\},$$

where $\kappa : \mathbb{R}^N \rightarrow \mathbb{R}$ is a given function. For example, we could choose κ as a cost function or energy that we are trying to minimize. Hence, we must ask how K_ε and K_0 are related if we want to use the singular limit $\varepsilon = 0$ as an approximation. ♦

A first step to relating the attainable sets in Example 18.5.7 is to analyze how $Z(\varepsilon)$ and $Z(0)$ are related. For ODEs, we can rely on Fenichel's theorem; we illustrate this situation with a simple $(1, 1)$ -fast–slow system,

$$\begin{aligned} \varepsilon \dot{x} &= -x, \\ \dot{y} &= 1 + \varepsilon. \end{aligned} \tag{18.57}$$

The solution of (18.57) is given by $x(\tau; \varepsilon) = x_0 e^{-\tau/\varepsilon}$ and $y(\tau; \varepsilon) = (1 + \varepsilon)\tau + y_0$ with singular limit solutions $x(\tau; 0) \equiv 0$ and $y(\tau; 0) = \tau + y_0$. Clearly, we have

$$\sup_{\tau \in [0, T]} |y(\tau; \varepsilon) - y(\tau; 0)| = \|y(\tau; \varepsilon) - y(\tau; 0)\|_\infty \rightarrow 0, \quad \text{as } \varepsilon \rightarrow 0.$$

This means that $y(\tau; \varepsilon) \rightarrow y(\tau; 0)$ in the space $C([0, T], \mathbb{R}^m)$ with the supremum norm. For convergence of $x(\tau; \varepsilon)$, we fix any $\delta > 0$ and observe that

$$\sup_{\tau \in [\delta, T]} |x(\tau; \varepsilon) - x(\tau; 0)| = |x_0 e^{-\tau/\varepsilon}| \rightarrow 0$$

as $\varepsilon \rightarrow 0$. Hence, $x(\tau; \varepsilon) \rightarrow x(\tau; 0)$ in the space of continuous maps $C([\delta, T], \mathbb{R}^n)$ with the supremum norm for any $\delta > 0$. Obviously, we can extend this result to more general normally hyperbolic fast–slow systems and other norms; for example, when the vector field is sufficiently smooth, we can consider C^r -spaces with their associated norms. However, for differential inclusions, it is unclear whether even the simplest convergence of (x, y) in $C([\delta, T], \mathbb{R}^m) \times C([0, T], \mathbb{R}^n)$ still holds.

Before we state a convergence result analogous to Fenichel's theorem for differential inclusions, we need a few definitions. We say that a set-valued map $F : \mathbb{R}^N \rightarrow \mathbb{R}^N$ is **upper semicontinuous** at a point in its domain $z_0 \in \mathbb{R}^N$ if for every open set V containing $F(z_0)$, there exists a neighborhood U of z_0 such that $F(U) \subset V$.

Exercise 18.5.8. Compare the definition of upper semicontinuity for set-valued maps to upper semicontinuity for functions. Note: A function $F : \mathbb{R}^N \rightarrow \mathbb{R} \cup \{+\infty\}$ is **upper semicontinuous** at $z_0 \in \mathbb{R}^N$ if $\limsup_{z \rightarrow z_0} F(z) \leq F(z_0)$. ♦

Consider a set $A \subset \mathbb{R}^N$ and define the **support function** to A as $\sigma(z, A) := \sup_{w \in A} w^\top z$.

Exercise 18.5.9. Let $A \subset \mathbb{R}^N$ be compact and convex, and fix $w \in \mathbb{R}^N$. Show that if $z^\top w \leq \sigma(z, A)$ for all $z \in \mathbb{R}^N$, then $w \in A$. \diamond

We also have to consider a crucial refinement to the solution set $Z(\varepsilon)$ of the fast–slow differential inclusion (18.55) defined by

$$Z_L(\varepsilon) := \{(x, y) : (x, y) \text{ is Lipschitz in } [\delta(\varepsilon), 1] \times [0, 1] \text{ with Lipschitz constant } L\},$$

where $\delta(\varepsilon) \rightarrow 0$ as $\varepsilon \rightarrow 0$ and $\delta(\varepsilon) \gg \varepsilon \ln(1/\varepsilon)$. Considering the restricted solution set $Z_L(\varepsilon)$ and the map $\varepsilon \rightarrow Z_L(\varepsilon)$, one can prove an analogue to Fenichel’s theorem.

Theorem 18.5.10 ([DDS96]). *Suppose (A1)–(A2), as previously stated in this section, hold for (18.55), and assume without loss of generality that the final time is $T = 1$. Suppose that $\varepsilon \in [0, \varepsilon_0]$ and $\varepsilon_0 > 0$ is sufficiently small. Furthermore, assume that the following conditions hold:*

(A3) $F(x, y)$ is upper semicontinuous and measurable.

(A4) There exist constants $\mu_x > 0$, $\mu_y > 0$ such that for every $(x_i, y_i) \in \mathbb{R}^{m+n}$, $i \in \{1, 2\}$,

$$\begin{aligned} \sigma(x_1 - x_2, F^{(x)}(x_1, y_1)) - \sigma(x_1 - x_2, F^{(x)}(x_2, y_2)) \\ \leq -\mu_x \|x_1 - x_2\|^2 + \mu_y \|y_1 - y_2\|^2, \end{aligned} \quad (18.58)$$

where $F^{(x)}(x_i, y_i) := \{x \in \mathbb{R}^m : (x, y) \in F(x_i, y_i)\}$ is the x -part of $F(x_i, y_i)$.

Then there exists a constant $L > 0$ such that $\varepsilon \mapsto Z_L(\varepsilon)$ is nonempty-valued for $\varepsilon \in [0, \varepsilon_0]$ and upper semicontinuous at $\varepsilon = 0^+$ in $C[\delta, 1] \times C[0, 1]$ for every $\delta \in (0, 1]$.

Before we outline the proof of Theorem 18.5.10, we examine the main technical condition (18.58). Consider the simple $(1, 1)$ -fast–slow system

$$\begin{aligned} \varepsilon \dot{x} &= sx, \\ \dot{y} &= 1, \end{aligned} \quad (18.59)$$

where $s = \pm 1$, and we have $F(x, y) = (sx, 1)^\top$ in the notation of (18.55). The condition (18.58) for the simple model problem (18.59) is given by

$$s(x_1 - x_2)^2 \leq -\mu_x |x_1 - x_2|^2 + \mu_y |y_1 - y_2|^2.$$

Setting $y_1 = y_2$, we see that $s = -1$ is required for (18.58) to hold. Therefore, we can interpret the main technical condition (A4) of Theorem 18.5.10 as a stability condition for the critical manifold. The main part in the proof of Theorem 18.5.10 is to establish the following auxiliary estimates.

Lemma 18.5.11 ([DDS96]). *Suppose the same conditions as in Theorem 18.5.10 hold. Given $\varepsilon_0 > 0$ sufficiently small, there exists a constant K such that for every $\varepsilon \in (0, \varepsilon_0]$, there is a solution $(x(\tau; \varepsilon), y(\tau; \varepsilon))$ of the fast–slow differential inclusion (18.55) such that for every $\tau \in [0, 1]$ and for every $s \in [0, 1 - \tau]$,*

$$\begin{aligned} \|x(s + \tau; \varepsilon) - x(s; \varepsilon)\| &\leq K\tau \left[1 + \frac{1}{\varepsilon} \exp(-\mu_x s/\varepsilon) \right], \\ \|y(s + \tau; \varepsilon) - y(s; \varepsilon)\| &\leq K\tau. \end{aligned} \quad (18.60)$$

We shall not prove Lemma 18.5.11; the proof requires careful applications of techniques from functional, convex, and set-valued analysis to obtain a situation whereby the key estimates can be obtained by an application of Gronwall’s lemma. The following outline of the proof of Theorem 18.5.10 shows some of the techniques that are also involved in proving Lemma 18.5.11.

Proof. (of Theorem 18.5.10, sketch; [DDS96]) From Lemma 18.5.11, we know that solutions to the fast–slow differential inclusion (18.55) exist for $\varepsilon \in (0, \varepsilon_0]$. Furthermore, these solutions satisfy the estimates (18.60), and it is not too difficult to see that this implies that $Z_L(\varepsilon)$ is nonempty for $\varepsilon > 0$. To extend this result to the singular limit $\varepsilon = 0$, we pick a sequence $\varepsilon_k \in (0, \varepsilon_0]$ with $\varepsilon_k \rightarrow 0$ and solutions

$$(x_k, y_k) := (x(\tau; \varepsilon_k), y(\tau; \varepsilon_k))$$

that are provided by Lemma 18.5.11. We extend x_k from $(0, 1)$ to the interval $[-1, 2]$ by assuming that it is constant outside of $(0, 1)$. Then we define for $\tau \in [-1, 2]$,

$$\tilde{x}_k(\tau) := \begin{cases} x_k(\tau) & \text{for } \delta(\varepsilon_k) \leq \tau \leq 2, \\ x_k(\delta(\varepsilon_k)) & \text{otherwise.} \end{cases}$$

Observe that (18.60) implies that for every s and τ in $[0, 1]$, we have

$$\|\tilde{x}_k(s + \tau) - \tilde{x}_k(s)\| \leq K\tau \left(1 + \frac{1}{\varepsilon_k} \exp \left(-\mu_x \frac{\delta(\varepsilon_k)}{\varepsilon_k} \right) \right) \leq 2K\tau, \quad (18.61)$$

where the last inequality follows from the assumption that $\delta(\varepsilon) \gg \varepsilon \ln(1/\varepsilon)$. From (18.61), we conclude that (\tilde{x}_k, y_k) is uniformly bounded and equicontinuous. Therefore, the Arzelà–Ascoli theorem, Theorem [Fol99], implies that there exists a subsequence of (\tilde{x}_k, y_k) that converges in $C[0, 1] \times C[0, 1]$ to some (x_0, y_0) . It is easy to see that from (18.60) and (18.61), it follows that (x_0, y_0) must also be Lipschitz continuous.

It remains to show that (x_0, y_0) is a solution to the singular limit fast–slow differential inclusion, i.e., we have to show that $(x_0, y_0) \in Z(0)$. Observe that $\{\dot{y}_k\}_{k=1}^\infty$ is bounded in $L^\infty[0, 1]$, and therefore, it is sequentially compact in $L^1[0, 1]$ -weak. Hence, we may assume that $(\tilde{x}_k, y_k) \rightarrow (x_0, y_0)$ in $C[0, 1] \times C[0, 1]$ and $\dot{y}_k \rightarrow \dot{y}_0$ in $L^1[0, 1]$ -weak as $k \rightarrow \infty$. Choose an arbitrary point $(p, q) \in \mathbb{R}^{m+n}$ and a measurable subset $S \subset [0, 1]$. Then

$$\begin{aligned} \int_{S-[0, \delta(\varepsilon_k)]} p^\top (\varepsilon_k \dot{x}_k) + q^\top \dot{y}_k \, d\tau &\leq \int_{S-[0, \delta(\varepsilon_k)]} \sigma((p, q), F(x_k, y_k)) \, d\tau = \dots \\ \dots &= \int_S \sigma((p, q), F(\tilde{x}_k, y_k)) \, d\tau - \int_{S \cap [0, \delta(\varepsilon_k)]} \sigma((p, q), F(\tilde{x}_k, y_k)) \, d\tau. \end{aligned}$$

We want to consider a limit as $k \rightarrow \infty$ in the last inequality. Observe that (18.61) implies that $\dot{\tilde{x}}_k$ is bounded in $L^\infty[0, 1]$, and so $\varepsilon_k \dot{\tilde{x}}_k \rightarrow 0$ in $L^\infty[0, 1]$ as $k \rightarrow \infty$. Therefore, we get

$$\begin{aligned} \int_S q^\top \dot{y}_0 \, d\tau &= \lim_{k \rightarrow \infty} \int_{S - [0, \delta(\varepsilon_k)]} q^\top \dot{y}_k \, d\tau \\ &\leq \limsup_{k \rightarrow \infty} \int_S \sigma((p, q), F(\tilde{x}_k, y_k)) \, d\tau \\ &\quad - \lim_{k \rightarrow \infty} \int_{S \cap [0, \delta(\varepsilon_k)]} \sigma((p, q), F(\tilde{x}_k, y_k)) \, d\tau \\ &\leq \int_S \sigma((p, q), F(x_0, y_0)) \, d\tau, \end{aligned}$$

where the last inequality follows, after a bit of work, from the boundedness of (\tilde{x}_k, y_k) in $C[0, 1] \times C[0, 1]$ and the assumptions (A1)–(A3) on F . Now we can apply Exercise 18.5.9 to conclude that $(x_0, y_0) \in Z_L(0)$. It remains to prove the upper semicontinuity of the map $\varepsilon \rightarrow Z_L(\varepsilon)$ at $\varepsilon = 0^+$ in $C[\delta, 1] \times C[0, 1]$. We argue by contradiction and assume that there exists a sequence $z_k \in Z_L(\varepsilon_k)$ such that the $C[\delta, 1] \times C[0, 1]$ -distance to $Z_L(0)$ is always bigger than a fixed constant. However, using the same argument as in the first part of the proof, we can extract a subsequence of z_k that converges in $C[\delta, 1] \times C[0, 1]$ to an element in $Z_L(0)$. This provides the desired contradiction and finishes the proof. \square

The outline of the proof of Theorem 18.5.10 illustrates that many geometric arguments are more difficult to formalize in the context of differential inclusions. Rather subtle points regarding modes of convergence and different function spaces start to play a more important role. The references in Section 18.7 provide further examples and results for fast–slow differential inclusions.

18.6 Amplitude Equations

Pattern-formation in spatially extended systems is closely related to phenomena observed in finite-dimensional dynamics. However, it turns out that new technical tools are required, and we shall briefly outline one of the methods that relates to fast–slow systems.

A classical model for pattern-formation is the **Swift–Hohenberg equation**

$$\frac{\partial u}{\partial t} = \mu u - u^3 - (\Delta + k_c^2)^2 u =: F(u; \mu), \quad (18.62)$$

where $u = u(x, y, t) \in \mathbb{R}$, $z = (x, y)^\top \in \mathbb{R}^2$, Δ denotes the Laplacian with respect to z , $\mu \in \mathbb{R}$ is a parameter, and we are going to assume that $k_c = 1$ for simplicity. In particular, we will be interested in the stability and bifurcations of the trivial solution $u \equiv 0$. It is important that the domain be unbounded. The case $(x, y) \in \Omega$ for some bounded domain Ω can be reduced, in many cases, to a finite-dimensional problem via center manifold reduction. For the spatially extended system, novel techniques are required. Linearizing (18.62) around the trivial solution yields

$$\frac{\partial U}{\partial t} = \left(\frac{\partial F}{\partial u}(0; \mu) \right) U = \mu U - (\Delta + k_c^2)^2 U. \quad (18.63)$$

Consider a **wave vector** $(k_x, k_y)^\top = \vec{k} \in \mathbb{R}^2$ and the solution ansatz

$$U(x, y, t) = v e^{\sigma t + i \vec{k} \cdot \vec{z}} + \text{c.c.} \quad (18.64)$$

for (18.63) with a constant $v \in \mathbb{C}$, $|v| \ll 1$, and c.c. denotes the complex conjugate of the first term. The eigenvalue σ determines the growth or decay properties of the solutions (18.64). Substituting (18.64) into (18.63) yields

$$\sigma = \mu - (k^2 - 1)^2, \quad (18.65)$$

where $k = \|\vec{k}\|$ is the **wavenumber**. Note that $\sigma < 0$ as long as $\mu < 0$. At $\mu = 0$, modes with $k^2 = 1$ are neutrally stable, and for $\mu > 0$, instability occurs. The linear analysis already suggests that the trivial solution $u = 0$ of (18.62) destabilizes for $\mu > 0$.

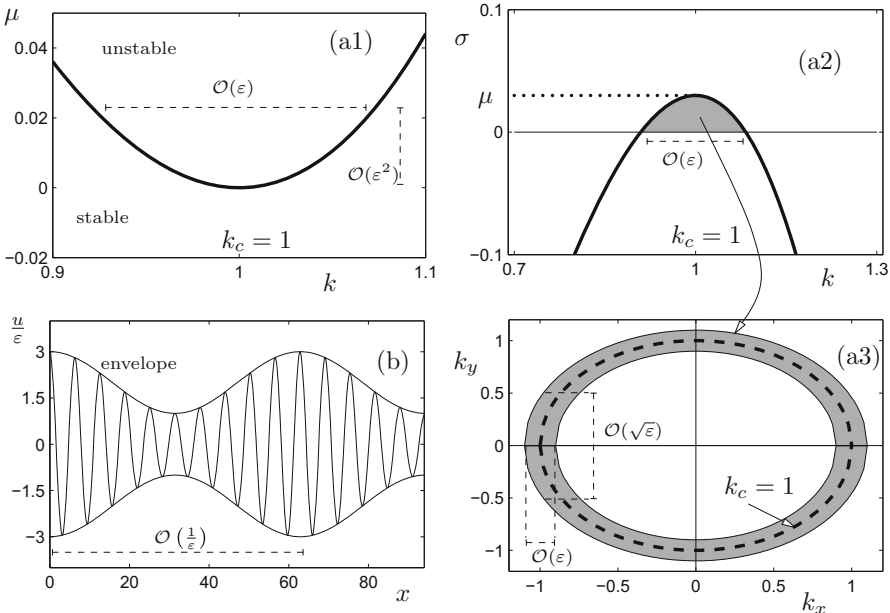


Figure 18.1: Illustration of scalings for amplitude equations arising from the Swift–Hohenberg equation (18.62). (a1) Curve of neutral stability $\mu = (k^2 - 1)^2$ delimiting the regions of stable and unstable modes. (a2) Eigenvalues σ for $\mu = 0.03$ fixed. The shaded areas are unstable modes that are presented in (a3) in the space of wave vectors. (b) Sketch of a potential pattern $u = \varepsilon A(X, Y, T) e^{ix} + \text{c.c.}$ with envelope $2\varepsilon A(X, Y, T)$ depending on x for fixed Y and T .

Figure 18.1(a1) shows the neutral stability curve $\mu = (k^2 - 1)^2$. Figures 18.1(a2)–(a3) illustrate that a continuous band of modes becomes

unstable for $\mu > 0$. To capture what happens after the instability arises, we restrict, for simplicity, to the case of two Fourier modes

$$u(x) = \varepsilon A e^{ix} + \varepsilon \bar{A} e^{-ix} \quad (18.66)$$

at the instability $\mu = 0$ with wave vectors $\vec{k} = (1, 0)^\top$, $\vec{k} = (-1, 0)^\top$, and $0 < |\varepsilon| \ll 1$. Geometrically, the ansatz (18.66) corresponds to small-amplitude roll or stripe patterns. The important reasoning from the viewpoint of multiple time scale dynamics is to start considering various scalings. Assume that

$$\mu = \varepsilon^2 \hat{\mu}.$$

Perturbing away from the critical wave number leads one to consider a wave vector

$$\vec{k} = \begin{pmatrix} 1 + k_x \\ 0 \end{pmatrix} + \begin{pmatrix} 0 \\ k_y \end{pmatrix} \quad (18.67)$$

for small k_x and k_y and to insert (18.67) into (18.65), which yields

$$\sigma = \varepsilon^2 \hat{\mu} - (2k_x + k_x^2 + k_y^2)^2. \quad (18.68)$$

Imposing the requirements $k_x = \mathcal{O}(\varepsilon)$, $k_y = \mathcal{O}(\sqrt{\varepsilon})$, and $\sigma = \mathcal{O}(\varepsilon^2)$ ensures that each term in (18.68) contributes to the leading order at the instability; see also Figures 18.1(a1)–(a3).

The **carrier wave** e^{ix} contained in (18.66) is modulated by the amplitude A , which gives the **envelope**; see Figure 18.1(b). The scalings derived from equation (18.68) suggest that A should vary slowly in space and time. In this case, a time scale separation exists between carrier wave and the envelope wave. Furthermore, the scalings in the perturbed wave vector lead to natural new variables

$$X := \varepsilon x, \quad Y := \sqrt{\varepsilon} y, \quad T := \varepsilon^2 T,$$

on which a method of multiple scales analysis can be based, as described in Section 9.8 and Section 18.3. So one formally considers the guess

$$u = u(x; X, Y, T) = \varepsilon A(X, Y, T) e^{ix} + \text{c.c.}, \quad (18.69)$$

where u depends on several independent variables. As before, it is highly non-trivial to make the independent variable assumption of the method of multiple scales rigorous; also, guessing that the correct order of u is $\mathcal{O}(\varepsilon)$ is not obvious a priori. The partial derivatives are now replaced as follows:

$$\frac{\partial}{\partial x} \rightarrow \frac{\partial}{\partial x} + \varepsilon \frac{\partial}{\partial X}, \quad \frac{\partial}{\partial y} \rightarrow \frac{\partial}{\partial y} + \sqrt{\varepsilon} \frac{\partial}{\partial Y}, \quad \frac{\partial}{\partial t} \rightarrow \frac{\partial}{\partial t} + \varepsilon^2 \frac{\partial}{\partial T}. \quad (18.70)$$

Using (18.70) in the Swift–Hohenberg equation (18.62) yields

$$\begin{aligned} \varepsilon^2 \frac{\partial u}{\partial T} &= \varepsilon^2 \hat{\mu} - \left[\left(\frac{\partial^2}{\partial x^2} + 1 \right)^2 + 2\varepsilon \left(\frac{\partial^2}{\partial x^2} + 1 \right) \left(2 \frac{\partial^2}{\partial x \partial X} + \frac{\partial^2}{\partial Y^2} \right) \right. \\ &\quad \left. + \varepsilon^2 \left(2 \frac{\partial^2}{\partial X^2} \left(\frac{\partial^2}{\partial x^2} + 1 \right) + \left(2 \frac{\partial^2}{\partial x \partial X} + \frac{\partial^2}{\partial Y^2} \right)^2 \right) + \dots \right] u - u^3, \end{aligned}$$

where we have used that u does not depend on y . The asymptotic expansion for the solution u is then inserted into the last result under the assumption

$$u = \varepsilon u_1 + \varepsilon^2 u_2 + \varepsilon^3 u_3,$$

where $u_j = u_j(x; X, Y, T)$, $u_j = \mathcal{O}(1)$ for $j = 1, 2, 3$, and $u_0 \equiv 0$, since (18.69) requires that $u = \mathcal{O}(\varepsilon)$. Collecting terms of equal orders in the Swift–Hohenberg equations gives at leading order $\mathcal{O}(\varepsilon)$ that

$$L(u_1) := \left(1 + \frac{\partial^2}{\partial x^2}\right)^2 u_1 = 0. \quad (18.71)$$

The only nontrivial solutions to (18.71) that remain bounded as $|x| \rightarrow \infty$ are

$$u_1 = A(X, Y, T)e^{ix} + \text{c.c.}, \quad (18.72)$$

which is in accordance with (18.69). At $\mathcal{O}(\varepsilon^2)$, we obtain

$$L(u_2) = -2 \left(2 \frac{\partial^2}{\partial x \partial X} + \frac{\partial^2}{\partial Y^2}\right) \left(\frac{\partial^2}{\partial x^2} + 1\right) u_1,$$

which holds automatically by (18.71) and if we assume $L(u_2) = 0$. The interesting effect occurs at order $\mathcal{O}(\varepsilon^3)$, which yields, if we assume $L(u_3) = 0$, that

$$0 = -\frac{\partial u_1}{\partial T} + \hat{\mu} u_1 - \left(2 \frac{\partial^2}{\partial X^2} \left(\frac{\partial^2}{\partial x^2} + 1\right) + \left(2 \frac{\partial^2}{\partial x \partial X} + \frac{\partial^2}{\partial Y^2}\right)^2\right) u_1 - u_1^3. \quad (18.73)$$

Inserting (18.72) into (18.73) and collecting terms for different exponentials, one observes that the coefficient for e^{ix} is

$$-\frac{\partial A}{\partial T} + \hat{\mu} A - 3|A|^2 A + 4 \left(\frac{\partial}{\partial X} - \frac{i}{2} \frac{\partial^2}{\partial Y^2}\right)^2 A \quad (18.74)$$

and that (18.74) is the complex conjugate of the coefficient of e^{-ix} . Satisfying (18.73) certainly requires (18.74) to vanish. Setting (18.74) equal to zero and scaling the variables $\hat{A} = \sqrt{3}A$, $\hat{X} = X/2$, $\hat{Y} = Y/\sqrt{2}$ gives

$$\frac{\partial A}{\partial T} = \mu A - |A|^2 A + \left(\frac{\partial}{\partial X} - \frac{i}{2} \frac{\partial^2}{\partial Y^2}\right)^2 A, \quad (18.75)$$

where the hats have been removed from all transformed quantities. The PDE (18.75) is called the **Newell–Whitehead–Segel equation**. It is a particular form of an **amplitude equation**; alternative terms for this type of PDE are **envelope** and **modulation equation**.

Exercise/Project 18.6.1. Instead of a two-timing-type argument, try to adapt the RG method from Sections 9.9 and 9.10 to derive (18.75). \diamond

Another important case occurs when there is no Y -dependence in the solution ansatz, so that $A = A(X, T)$. This reduces (18.75) to

$$\frac{\partial A}{\partial T} = \mu A - |A|^2 A + \frac{\partial^2 A}{\partial X^2}, \quad (18.76)$$

which is the (real) **Ginzburg–Landau equation**. One can think of (18.75) and (18.76) as slow reduced flows that describe the amplitude variation of solutions near instability. Another interpretation views the PDEs (18.75) and (18.76) as analogues of finite-dimensional normal forms that can be obtained near a bifurcation point; see Section 18.7 for further details.

18.7 References

Section 18.1: The basic background from semigroup theory can be found in [EN00, Paz83] with a more dynamics-oriented view in [Hen81]. We also point out that there is a long history of singular perturbation techniques for PDEs and semiflows [BK82, KP03b], often in tandem with classical techniques such as the maximum principle [DPS73], asymptotic analysis [CHM77, Hop70], and operator theory [BF71, BF70]. For a dedicated book on the topic, see [MB95]. There are several works on invariant manifolds for PDEs, e.g., see [BJ89, CCLCP13]. A particular focus has been on inertial manifolds [FST88, FST89, JS95, MPS88], their applications [IBS98, SIB01], as well as their numerical computation [FJK⁺88, GANT98]. Inertial manifolds are relevant for diverse topics such as blowup in NLS [KL95, RK02, RK03], chains of FHN oscillators [MK01], coupled noisy Kuramoto oscillators [GPP12, GPPP12], FHN PDE dynamics [AF09], Kuramoto–Shivashinsky dynamics [JKT90], and numerical methods for PDEs [FT91, Tem90]. For surveys and textbooks on inertial manifolds, we refer to [Con89, Rob01, Zel13].

Section 18.2: The main result for semigroups can be found in [BLZ00, BLZ98]. For a related result, consider [PS01]. The two examples are taken from [Sie13, MH01] with relevant background in [Kat80, NRL86]. There are books and surveys available on the general attractor theory of evolution equations [BV92, MZ08, Vis93].

Section 18.3: The results were adapted from the exposition in [PS08]. Some basic results on homogenization for elliptic problems and two-scale convergence can be found in [All92], with broad overviews in [BLP11, Tar09]; see also [Lio73]. One of the most important application areas of homogenization techniques is materials science [BP89]. There are also relations of homogenization techniques to the Bellman–Isaacs equation [ABM07], discrete stochastic elliptic equations [GO11], elasticity [OSY92], Hamiltonian systems [BS97, SB97], hyperbolic conservation laws [EE93, E06], propagation failure of waves [Kee00a, Kee00b], speed of traveling waves [DS09b], transport equations [E92], variational problems [E91], and Wasserstein flows [AMP⁺12]. Of course, as we have shown, there is the immediate relation to averaging problems [FV03, MSU07, VC01].

Section 18.4: This section is based mainly on [Chi03, Chi04], where it should be noted that we could also have tried to apply the theory from Section 18.2 directly. The small-delay slow manifold methods have been applied to acoustics [CH08], delay-induced canards [CSE09], and radiation damping [CKMR01]. Small-delay problems

can be considered in many different directions [Dri68, Dri76], including differential–difference equations [Fri02a, O'M71a]. Another perturbation strategy is to consider large-delay problems [GPEK00]. As expected, averaging works also for many delay equations [Hal66, Leh02, LW99b, LW99a], while other singular perturbation methods can be very intricate in this context [Fow05]. There are many different links between singular perturbations and delay equations [AS01, GRMP10], such as bursting in the Hindmarsh–Rose model [ZW12b], control theory [Fri02d, Gli01b, Gli04, Gli98, Gli07, Gli03c, Gli03a, Gli00a, Gli03b, Gli01a, Gli08, SR73], dimension reduction [WH01], ecological models [KR11], delay-coupled vdP oscillators [WR02], differential–difference equations [GKR13], electrooptic oscillators [PJC⁺09, WEJ⁺12, WED⁺13], gene regulatory networks with delay [SP10], laser dynamics [HGEK99, YW10, ZW10b], lattice equations [GKR11a, GKR11b, GKR12], linear delay equations [Cam80a], multiresonance [HYL12], the Oregonator model [SB08], period-doubling bifurcations [ACM08b], relaxation oscillations [FM02, KK93, ZW12a], state-dependent delay [MPN11], and waves in delayed PDEs [LWW12]. Distributed delays also interface well with singular perturbation methods, e.g., in the vdP equation [Lin07], for delay solitary waves in KdV [Zha08], and for various traveling wave problems [LY05, LY06b, LY06a, PS07b].

Section 18.5: Some of the main results on fast–slow differential inclusions can be found in [AKN00, DS95a, DV83b, DDS96, Vel97], on which this section has been built; for the background in differential inclusions, the results can be found in [DS90, Smi02]. Differential inclusions can be averaged under suitable conditions [DD03, DS99c, FK90, Gra96, KN03], and several results extend to infinite intervals [Wat05]. A frequent application of these methods is to control theory [GL99, Gru81]. Techniques based on Young measures [Art99a, AKST07, Art98] and variational inequalities [MPM08] have been considered as well. Naturally, differential inclusions can also exhibit dynamical patterns such as oscillations [Kha93].

Section 18.6: This section is based mainly on [Hoy06, CH93]. For more details on patterns in the Swift–Hohenberg equation, we refer to [KP05, LSAC08, MS10, MSZ00, MS95] as well as to the surveys on pattern-formation mentioned below. Amplitude equations are one of the main tools for capturing pattern-formation near bifurcation points [DSSS03, Sch01]. The Ginzburg–Landau equation [KSM92, Mie02, Sch96], the Newell–Whitehead equation [Sch95a], and the NLS equation [Sch98] can all be viewed as amplitude equations. Amplitude equation techniques can also be applied in the context of slowly varying parameters [KE97] and evaporation patterns [HM13].

Pattern-formation in infinite-dimensional spatiotemporal dynamics [FS03a, Gri91] has been covered only very tangentially. For surveys on the asymptotic analysis approach, see [War06, War05], and for applications, see, e.g., [EA91]. Some interesting patterns are spiral/rotating waves [Kee86, PE94], scroll waves [Kee88, KT92], and slow-motion fronts [War94, BK90]. The Cahn–Hilliard equation [Peg89] is a main source of singularly perturbed multiscale patterns such as coarsening [BF90, BH92, CP89, CP90, Che92, CNO06, FH89, Gra95, KO02, WORD03], bubble solutions [ABF91, ABF97, AF98, AF94], metastable patterns on slow manifolds [BX98, BX95], multispike stationary solutions [BDS99, BF00], and nucleation [BF93, RW05].

A particularly interesting case of singularly perturbed problems is that of spike (or layer) solutions [AM06, Ni98, Ni04] for elliptic problems [CK99, dPMP05, Fif73, LN05, LNT88, LNW07, Mal05, MP07, SWW05, Wan92], where small diffusion often plays the key role [KS12]. Bifurcation phenomena occur naturally for singularly perturbed elliptic equations [But07, BNS01, JK86, Kee74, KK73, NM89]. For early work with a

focus on asymptotics and references, see [[Com71a](#), [Com71b](#), [Eck72](#), [Gre69](#), [How79b](#)]. Of course, one may also study the associated parabolic problem, e.g., using slow manifolds [[BLZ08](#)]. Related topics are aggregation phenomena [[SO97a](#)] and dynamics of the Keller–Segel model [[WX13](#)].

Singularly perturbed Hamilton–Jacobi equations in relation to viscosity solutions [[AB02](#), [AB03](#), [BCD08](#)] as well as homogenization [[DBL13](#)] provide another avenue to explore. There are many other relevant topics we have not covered, such as coupled Ginzburg–Landau equations [[LL03a](#)], drift–diffusion semiconductor models [[GLMS01](#), [Jün09](#)], gradient flows [[OR07](#)], harmonic maps and curvature [[RSK89](#)], mode approximation [[MR71](#)], Nash–Moser iteration [[TZ11](#)], renormalization [[EFK00](#)], the vdP equation with diffusion [[KMR98](#)], and wave equations with viscous terms [[AMR02](#)].

Chapter 19

Other Topics

This chapter collects various topics that did not fit immediately within the main flow of the book. Nevertheless, they have been included here due to their general importance and interaction with fast–slow systems.

Differential-algebraic equations (DAEs) arise as the singular limit slow subsystem. DAEs are discussed in Section 19.1, with a focus on linear systems, and in Section 19.2, centered on numerical methods. Section 19.3 covers regularization of certain classes of nonsmooth planar systems, which naturally lead to fast–slow systems after the regularization procedure. Section 19.4 is a brief exposition of hysteresis operators to demonstrate that the resulting trajectories in these dynamical systems can often be closely linked to multiple time scales. In Sections 19.5 and 19.6, we make a tour through nonstandard analysis, which can be employed to dissect the classical infinite time scale separation case using hyperreal numbers. An application to canard orbits in the van der Pol equation is given. Section 19.7 treats the classical topic of adiabatic invariants for multiple time scale systems, which are quantities that deviate only very slowly from the singular limit. One may certainly argue that this topic should occupy a more prominent role than it currently does in this book. Section 19.8 raises the issue of how much of a bifurcation diagram we may construct in parameter space just from the fast and slow subsystems. Section 19.9 introduces a very recent topic of active research that aims to compute early-warning signs before trajectories arrive near a fast subsystem bifurcation point or cross a repelling slow manifold.

Background: No additional prerequisites are necessary. However, it is necessary to refer back to some material presented earlier in this book at several places; for example, the early-warning sign discussion will make relatively little sense if one has not read parts of Chapter 15, on fast–slow stochastic systems.

19.1 Differential-Algebraic Equations I

In this section, we briefly explain the terminology and some basic analytic properties of differential-algebraic equations. To motivate the results, recall that the singular limit form of a fast–slow system on the slow time scale τ ,

$$\begin{aligned} \varepsilon \frac{dx}{d\tau} &= \varepsilon \dot{x} = f(x, y), & \xrightarrow{\varepsilon \rightarrow 0} \quad 0 &= f(x, y), \\ \frac{dy}{d\tau} &= \dot{y} = g(x, y), & \dot{y} &= g(x, y), \end{aligned} \quad (19.1)$$

is a **differential-algebraic equation (DAE)** defined by the slow-flow dynamics restricted to the critical manifold $C_0 := \{(x, y) \in \mathbb{R}^{m+n} : f(x, y) = 0\}$. So far, we have not considered a systematic theory of differential-algebraic equations, and we have often assumed that we have a good understanding of the DAE in (19.1) either analytically or numerically. However, there is a tremendous amount of theory that has been developed for DAEs. In the DAE literature, one often refers to the singular limit (19.1) as a **semiexplicit system** of DAEs or as a **constrained ODE**. The form

$$0 = F(z, \dot{z}) \quad (19.2)$$

for $z \in \mathbb{R}^N$ represents the general case of a DAE. Let us point out that we will always assume that the initial and/or boundary conditions of a DAE are chosen such that they are consistent with the DAE; for example, for the slow subsystem, it does not make sense to choose an initial condition outside of C_0 . It is also evident that a semiexplicit DAE is just a special case of (19.2) with $z = (x, y)$ and

$$F((x, y), (\dot{x}, \dot{y})) = \begin{pmatrix} f(x, y) \\ \dot{y} - g(x, y) \end{pmatrix}.$$

However, note also that we can write every DAE (19.2) in a semiexplicit form by introducing N additional variables by the standard trick $z' = w$, which yields

$$\begin{aligned} 0 &= F(z, w), \\ z' &= w. \end{aligned} \quad (19.3)$$

The next definition is a building block of DAE theory; several examples follow the definition to illustrate it.

Definition 19.1.1. Consider (19.2). Then the **(differentiation) index** along a solution z is the minimum number of time derivatives that are required to solve for \dot{z} in terms of z (i.e., to define an ODE for z). Hence, the index is defined in terms of the overdetermined system

$$\begin{aligned} 0 &= F(z, \dot{z}), \\ 0 &= \frac{dF}{d\tau}(z, \dot{z}, \ddot{z}), \\ &\vdots \\ 0 &= \frac{d^p F}{d\tau^p}(z, \dot{z}, \dots, z^{(p+1)}), \end{aligned} \quad (19.4)$$

where p is the smallest integer such that \dot{z} can be solved for in terms of z by algebraic manipulations of (19.4).

Observe that we agreed to the convention that differentiating a vector-valued function once with respect to time counts as one derivative.

Example 19.1.2. Consider the DAE

$$0 = F((x, y), (\dot{x}, \dot{y})) = \begin{pmatrix} y - x \\ \dot{y} - 1 \end{pmatrix}, \quad (19.5)$$

which arises from a simple $(1, 1)$ -fast–slow system with $(f(x, y), g(x, y)) = (y - x, 1)$; see Figure 19.1(a). Differentiating (19.5) gives

$$0 = \frac{dF}{d\tau}((x, y), (\dot{x}, \dot{y})) = \begin{pmatrix} \dot{y} - \dot{x} \\ \ddot{y} \end{pmatrix}. \quad (19.6)$$

Since we obtained an ODE for (\dot{x}, \dot{y}) by combining (19.5) and (19.6), the DAE (19.5) is of index 1. ♦

The last example suggests a generalization to (m, n) -dimensional fast–slow systems with the associated singular limit slow subsystem

$$0 = F((x, y), (\dot{x}, \dot{y})) = \begin{pmatrix} f(x, y) \\ \dot{y} - g(x, y) \end{pmatrix}. \quad (19.7)$$

Differentiating (19.5) gives

$$0 = \frac{dF}{d\tau}((x, y), (\dot{x}, \dot{y})) = \begin{pmatrix} (\mathrm{D}_x f)\dot{x} + (\mathrm{D}_y f)\dot{y} \\ \ddot{y} - (\mathrm{D}_x g)\dot{x} + (\mathrm{D}_y g)\dot{y} \end{pmatrix}. \quad (19.8)$$

We already have an ODE for \dot{y} using (19.7). Hence, we want to use (19.8) to get an ODE for \dot{x} . Let us assume that $\mathrm{D}_x f$ is invertible. Then we obtain

$$\dot{x} = -(\mathrm{D}_x f)^{-1}(\mathrm{D}_y f)\dot{y}. \quad (19.9)$$

Note carefully that the derivation of the ODE for \dot{x} is precisely one of the standard approaches we always used to derive a slow flow on the critical manifold; see Section 3.2. We conclude from (19.9) that invertibility of $\mathrm{D}_x f$ leads to a DAE of index 1. Invertibility of $\mathrm{D}_x f$ also implies that the critical manifold consists of regular points and is obviously weaker than normal hyperbolicity. DAEs of the form (19.7) with invertible $\mathrm{D}_x f$ are also referred to as **Hessenberg index 1** systems. Therefore, we have proven the following simple result.

Proposition 19.1.3. *Consider a fast–slow system with a critical manifold C_0 that consists only of regular points (e.g., a manifold C_0 that is normally hyperbolic). Then the slow subsystem is a DAE of index 1.*

Example 19.1.4. Consider the DAE

$$\begin{aligned} 0 &= f(y), \\ \dot{y} &= g(x, y), \end{aligned} \quad (19.10)$$

where the algebraic constraint defining the critical manifold C_0 depends only on the slow variable. Differentiating $0 = f(y)$ yields

$$0 = (\mathbf{D}_y f)\dot{y} = (\mathbf{D}_y f)g(x, y). \quad (19.11)$$

The algebraic equation $0 = (\mathbf{D}_y f)g(x, y)$ derived from (19.11) is also called a **hidden constraint**, since it appears only after differentiation. Differentiating (19.11) once more, we obtain

$$(\mathbf{D}_y f)[(\mathbf{D}_x g)\dot{x} + (\mathbf{D}_y g)\dot{y}] + (\mathbf{D}_{yx} f)(\dot{x}, \dot{y}) + (\mathbf{D}_{yy} f)(\dot{y}, \dot{y}) = 0.$$

If this equation can be solved for \dot{x} , then (19.10) is a DAE with index 2; see also Figure 19.1(b). Observe also that our calculation has shown that

$$\begin{aligned} 0 &= (\mathbf{D}_y f)g(x, y), \\ \dot{y} &= g(x, y). \end{aligned} \quad (19.12)$$

So the hidden constraint and the slow dynamics describe another DAE. ♦

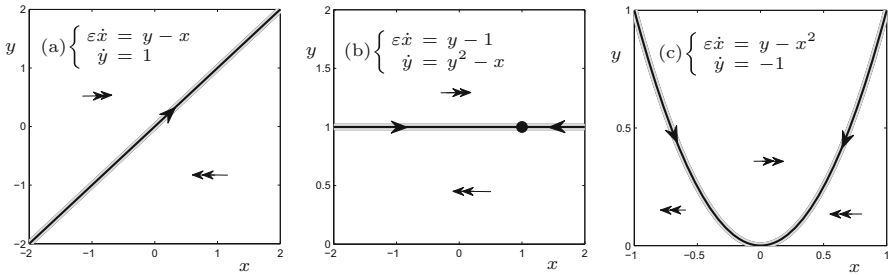


Figure 19.1: Examples of DAEs with different indices arising from fast–slow systems as slow subsystems ($\varepsilon = 0$). The slow subsystem flow (black curves) is constrained to the critical manifold C_0 (thick gray curves). We also indicate the fast subsystem flow by double arrows, as usual. (a) Example of an index-1 DAE from Example 19.1.2. (b) Index-2 DAE for the class of equations in Example 19.1.4. (c) Classical fold point from Exercise 19.1.5(B).

The manipulation of DAEs and their indices is an important concept for their analysis and numerical solution. It can often be beneficial to apply preliminary manipulations to reduce the index of a DAE and work with only the standard semiexplicit index-1 form; see Section 19.2.

Exercise 19.1.5. Determine the index of the following two DAEs:

$$(A) \begin{cases} 0 = f(y), \\ \dot{y} = g(y, z), \\ \dot{z} = h(x, y, z), \end{cases} \quad (B) \begin{cases} 0 = y - x^2, \\ \dot{y} = g(x, y). \end{cases}$$

See also Figure 19.1(c) for an illustration. ♦

It is also helpful to know when a DAE can be solved explicitly. In particular, for large fast–slow systems, where a simple calculation of the ODEs defining the slow flow may not be easy, it is helpful to have solution formulas. Consider a **linear DAE** given by

$$E\dot{z} = Az, \quad (19.13)$$

where E, A are $N \times N$ matrices. As in the theory of linear ODEs, it is convenient to assume that the coefficients of E and A are complex numbers. In fact, the solutions of (19.13) can be constructed using only algebraic methods. Before we can write down a solution formula, a few definitions are needed. The pair (E, A) is called **regular** if the characteristic polynomial

$$p(\lambda) = \det(\lambda E - A)$$

is not the zero polynomial. Under the regularity assumptions, we can transform the pair (E, A) into a canonical form.

Theorem 19.1.6 ([KM06b]). *Suppose $(E, A) \in (\mathbb{C}^{N \times N}, \mathbb{C}^{N \times N})$ is a regular matrix pair. Then there exist invertible matrices $P, Q \in \mathbb{C}^{N \times N}$ such that*

$$PEQ = \begin{pmatrix} \text{Id} & 0 \\ 0 & \mathcal{N} \end{pmatrix} \quad \text{and} \quad PAQ = \begin{pmatrix} \mathcal{J} & 0 \\ 0 & \text{Id} \end{pmatrix}, \quad (19.14)$$

where \mathcal{N} is nilpotent and \mathcal{J} is in Jordan canonical form. The canonical form (19.14) obtained after simultaneous transformation of E and A is also called **Weierstrass canonical form**.

We define the **index of nilpotency** $\nu \in \mathbb{N}$ of the pair (E, A) as the smallest integer such that $\mathcal{N}^\nu = 0$ and $\mathcal{N}^{\nu-1} \neq 0$. Note that we refer to the index of (E, Id) simply as the index of E .

Remark: For our purposes here, we can think of the index of nilpotency and the differentiation index as equal. However, there are many more definitions of an “index” that play a role for DAEs; see Section 19.10.

Definition 19.1.7. Let ν be the index of $E \in \mathbb{C}^{N \times N}$. A matrix $X \in \mathbb{C}^{N \times N}$ that satisfies

$$EX = XE, \quad XEX = X, \quad XE^{\nu+1} = E^\nu$$

is called the **Drazin inverse** of E . The Drazin inverse is also denoted by $X = E^D$.

It can be shown that a Drazin inverse exists and is unique. It can also be checked that for an invertible matrix E , we get $E^{-1} = E^D$, so that E^D is a generalized matrix inverse.

Theorem 19.1.8 ([KM06b]). *Consider the DAE (19.13) and suppose*

$$EA = AE \quad \text{and} \quad \text{nullspace}(A) \cap \text{nullspace}(E) = \{0\}.$$

Then every solution of the DAE (19.13) has the form

$$z(\tau) = \exp((\tau - \tau_0)E^D A)E^D E v \quad (19.15)$$

for some vector $v \in \mathbb{C}^N$ and initial time $\tau_0 \in \mathbb{R}$. Furthermore, the DAE (19.13) has a solution if and only if there exists v such that $z(\tau_0) = E^D E v$.

The result (19.15) is immediately recognized as a generalization of the usual solution formula for linear ODEs, where $E = \text{Id}$. For the application of Theorem 19.1.8, the biggest restriction seems to be that E and A have to commute. However, if (E, A) is a regular matrix pair, we can choose $\lambda^* \in \mathbb{C}$ such that $(\lambda^* E - A)$ is nonsingular and define (see [Cam80b])

$$E^* := (\lambda^* E - A)^{-1} E \quad \text{and} \quad A^* := (\lambda^* E - A)^{-1} A.$$

Then E^* and A^* commute. As for ODEs, there are very few nonlinear DAEs that are solvable analytically. Hence, it is very helpful to have efficient numerical methods for nonlinear systems of DAEs.

19.2 Differential-Algebraic Equations II

In this section we briefly describe a few techniques for the numerical solution of DAEs of the form (19.2). We shall focus on those numerical methods that have a direct relation to fast–slow systems and their numerical solution. We will always assume that the DAE for $(x, y) \in \mathbb{R}^{m+n}$ is in semiexplicit form

$$0 = f(x, y) \quad (19.16)$$

$$\dot{y} = g(x, y) \quad (19.17)$$

and that $D_x f$ is invertible (i.e., the critical manifold of the associated fast–slow system consists of only regular points). So far, we have often avoided solving (19.16)–(19.17) numerically, since most slow subsystems have been low-dimensional. For high-dimensional nonlinear fast–slow systems, we have already indicated in Chapters 10 and 11 that numerical methods are necessary and extremely important.

There are two natural ways that one could approach the numerical solution of (19.16)–(19.17). One possibility is to use the following steps:

- (E1) Consider (19.16)–(19.17) as a fast–slow system with $\varepsilon > 0$ replacing (19.16) by $\varepsilon \dot{x} = f(x, y)$.
- (E2) Apply a numerical method to the fast–slow system.
- (E3) Set $\varepsilon = 0$ to obtain a numerical method for the DAE problem.

Definition 19.2.1. Steps (E1)–(E3) are called the **ε -embedding method**.

We already know from Section 10.1 how to apply (implicit) multistep methods to fast–slow systems. For a linear k -step method, the steps (E1)–(E2) yield

$$\begin{aligned}\varepsilon \sum_{j=0}^k a_j x_{n+j} &= h \sum_{j=0}^k b_j f(x_{n+j}, y_{n+j}), \\ \sum_{j=0}^k a_j y_{n+j} &= h \sum_{j=0}^k b_j g(x_{n+j}, y_{n+j}),\end{aligned}\quad (19.18)$$

where h is the step size and a_j , b_j are the coefficients of the method. Setting $\varepsilon = 0$ in (19.18) gives

$$\begin{aligned}0 &= h \sum_{j=0}^k b_j f(x_{n+j}, y_{n+j}), \\ \sum_{j=0}^k a_j y_{n+j} &= h \sum_{j=0}^k b_j g(x_{n+j}, y_{n+j}).\end{aligned}\quad (19.19)$$

Convergence and accuracy for methods defined by (19.19) essentially follow from the results for multistep methods for ODEs using our assumption on invertibility of $D_x f$. The second approach to solving (19.16)–(19.17) converts the DAE to an ODE directly:

(S1) By the implicit function theorem, we can write (19.16)–(19.17) as

$$\dot{y} = g(H_0(y), y) \quad (19.20)$$

for some function $H_0 : \mathbb{R}^n \rightarrow \mathbb{R}^m$.

(S2) Apply a numerical method to (19.20).

(S3) Replace the implicit function with a numerical algebraic constraint.

Definition 19.2.2. The steps (S1)–(S3) are called the **state space form method**.

Carrying out (S1)–(S3) for a linear k -step method gives

$$\begin{aligned}0 &= f(x_{n+k}, y_{n+k}), \\ \sum_{j=0}^k a_j y_{n+j} &= h \sum_{j=0}^k b_j g(x_{n+j}, y_{n+j}),\end{aligned}\quad (19.21)$$

where the condition $0 = f(x_{n+k}, y_{n+k})$ ensures that the numerical solution satisfies the algebraic constraint at each step. Note carefully that both numerical approaches for DAEs that we discussed here are natural ideas from the viewpoint of fast–slow systems. The ε -embedding method calculates the leading- (or zeroth-) order solution to a trajectory near a critical manifold, while the state space form approach just solves the slow flow. Error analysis for ε -embedding and state space form methods are beyond the scope of this book, but detailed references are given in Section 19.10. Instead, we shall look at an example.

Example 19.2.3. As a test problem we consider the **Stommel flow** (see also Section 20.9), given by

$$\begin{aligned}\varepsilon \dot{x}_1 &= -x_1 + \sin y_1 \cos y_2, \\ \varepsilon \dot{x}_2 &= -x_2 - p - \cos y_1 \sin y_2, \\ \dot{y}_1 &= x_1, \\ \dot{y}_2 &= x_2,\end{aligned}\quad (19.22)$$

which is a $(2, 2)$ -fast–slow system describing the settling of particles with small inertia under the influence of a fluid flow, and $p \in (0, 1)$ is a parameter representing the (scaled) settling velocity. The velocity of the particle is given by the fast variables (x_1, x_2) , and the positions are the slow variables (y_1, y_2) . From the fast–slow systems analysis, it is easily seen that the critical manifold

$$C_0 = \{(x, y) \in \mathbb{R}^4 : x_1 = \sin y_1 \cos y_2, x_2 = -p_1 - \cos y_1 \sin y_2\} \quad (19.23)$$

is normally hyperbolic, since linearizing with respect to the fast variables yields

$$\mathbf{D}_x f = \begin{pmatrix} -1 & 0 \\ 0 & -1 \end{pmatrix}.$$

Since both eigenvalues of $\mathbf{D}_x f$ are -1 , it follows that C_0 is attracting, so that Fenichel’s theorem dictates that we should already understand much of the dynamics by just looking at the slow subsystem

$$\begin{aligned} 0 &= -x_1 + \sin y_1 \cos y_2, \\ 0 &= -x_2 - p - \cos y_1 \sin y_2, \\ \dot{y}_1 &= x_1, \\ \dot{y}_2 &= x_2. \end{aligned} \quad (19.24)$$

It is easy in this case to write the slow subsystem explicitly in terms of the variables (y_1, y_2) , so that we have a test problem where we can use the numerical solution of

$$\begin{aligned} \dot{y}_1 &= \sin y_1 \cos y_2, \\ \dot{y}_2 &= -p - \cos y_1 \sin y_2, \end{aligned} \quad (19.25)$$

as the “true” reference solution for a DAE solution of (19.24). As a DAE solver, we will use a backward differentiation formula (BDF) k -step method (see also Section 10.1) for (19.19) with $k = 2$ and

$$a_0 = 1, \quad a_1 = -4, \quad a_2 = 3, \quad \text{and} \quad b_0 = 0 = b_1, \quad b_2 = 2. \quad (19.26)$$

Observe that backward differentiation formulas give the same numerical scheme for ε -embedding and state space form approaches. The method (19.26) is obviously implicit, and we use Newton’s method to solve the resulting algebraic equations at each iteration step; the step size $h = 0.05$ and the parameter $p = 0.6$ were fixed. Figure 19.2 shows the result of the computations, displaying excellent agreement between the “exact” solution of (19.25) and the DAE solution. We can draw several physical conclusions from the results in Figure 19.2. The periodic orbits of the slow flow on C_0 show that particles may potentially get trapped in a single flow cell without settling. In this case, the position of the particle oscillates, and the colored contour plot of the critical manifold nicely illustrates the switching sign of the velocity. Therefore, one may also conjecture from Figure 19.2 that the region of periodic solutions might be bounded by a heteroclinic orbit. ♦

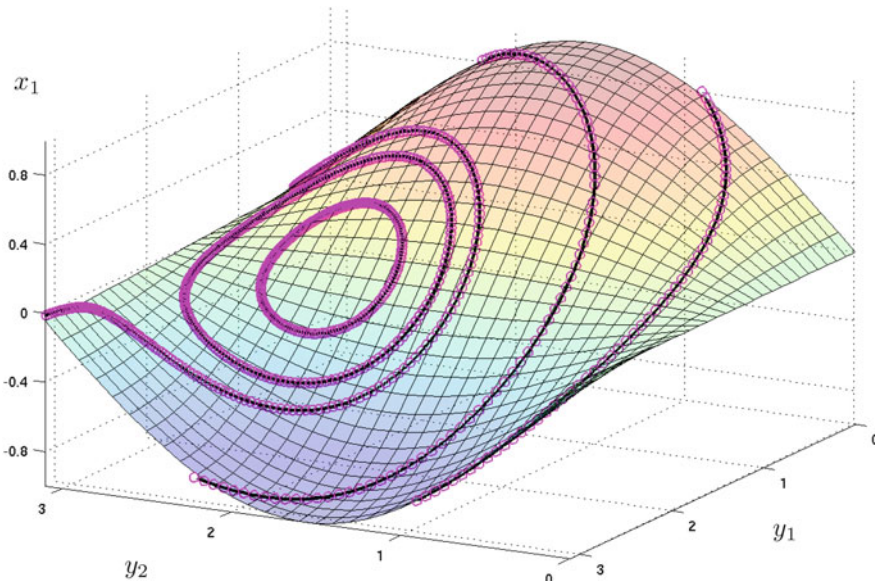


Figure 19.2: Numerical solution of the DAE (19.24) with $p = 0.6$ in a single cell of the flow with $y_i \in [0, \pi]$ for $i = 1, 2$. The critical manifold (algebraic constraint) C_0 is also plotted, colored with a height function that interpolates from blue (low) to high (red) values. The “exact” solutions are plotted as solid black curves using a high-accuracy numerical scheme for (19.25) and then using the algebraic constraint given by C_0 in (19.23). The DAE solution with a second-order BDF method is indicated by circles (magenta); the step size was fixed at $h = 0.05$.

Exercise/Project 19.2.4. Consider Figure 19.3, which shows a numerical solution of the slow subsystem (19.25). Can you prove the existence of heteroclinic solutions? What happens for $\varepsilon > 0$? ◇

We have seen in this section that a direct numerical approach to DAEs is possible. For the Stommel flow problem, this strategy may not be necessary, but for higher-dimensional problems or critical manifolds without an easy parameterization, a DAE solver is often a good option for understanding the slow dynamics. An advantage is that computing the slow flow via a DAE solver also computes part of the critical manifold C_0 .

19.3 Nonsmooth Dynamical Systems

To explain how fast–slow systems naturally appear in the theory of nonsmooth dynamical systems, we begin with an example. Consider a function $H : \mathbb{R}^2 \rightarrow \mathbb{R}$ given by $H(x, y) = x$. The zero set

$$\Sigma := \{H^{-1}(0)\} = \{(x, y) \in \mathbb{R}^2 : x = 0\}$$

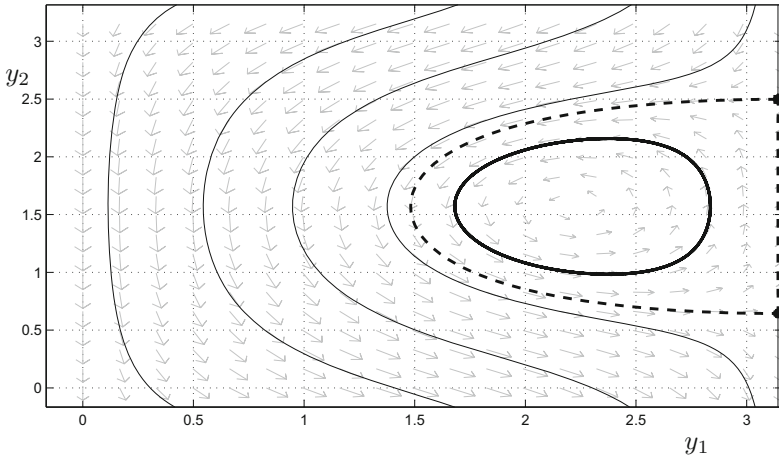


Figure 19.3: Numerical solution of the slow flow (19.25) for a single cell $y_i \in [0, \pi]$ with $i = 1, 2$. There are two equilibrium points on the boundary that are saddles with two heteroclinic connections between them (a **heteroclinic cycle**). Several other trajectories are shown, and also a periodic orbit (solid thick curve) trapped inside the heteroclinic cycle.

represents discontinuities occurring in the vector field. More concretely, we consider the vector field

$$\begin{pmatrix} \frac{dx}{dt} \\ \frac{dy}{dt} \end{pmatrix} = \begin{pmatrix} x' \\ y' \end{pmatrix} = \begin{cases} F_1(x, y) = \begin{pmatrix} -1 \\ 1 \end{pmatrix} & \text{if } x > 0, \\ F_2(x, y) = \begin{pmatrix} 1 \\ 1 \end{pmatrix} & \text{if } x < 0, \end{cases} \quad (19.27)$$

which is shown in Figure 19.4. The vector field (19.27) is one of the simplest examples of a **discontinuous vector field**; for more detailed references on the theory of nonsmooth and hybrid dynamical systems, see Section 19.10. A standard way to extend the flow of (19.27) to Σ is to consider the **Filippov convex method**. One just considers a convex combination

$$\lambda \begin{pmatrix} -1 \\ 1 \end{pmatrix} + (1 - \lambda) \begin{pmatrix} 1 \\ 1 \end{pmatrix}, \quad (19.28)$$

where the parameter λ is chosen as

$$\lambda := \frac{\nabla H \cdot F_2}{\nabla H \cdot (F_2 - F_1)}.$$

The next exercise shows that the choice (19.28) is natural for describing a **sliding vector field** along the set Σ .

Exercise/Project 19.3.1. (a) Describe the geometric interpretation of (19.28). (b) Show that the flow on Σ is indeed tangent to Σ . (c) Can you generalize the previous observations to more general nonsmooth differential equations? \diamond

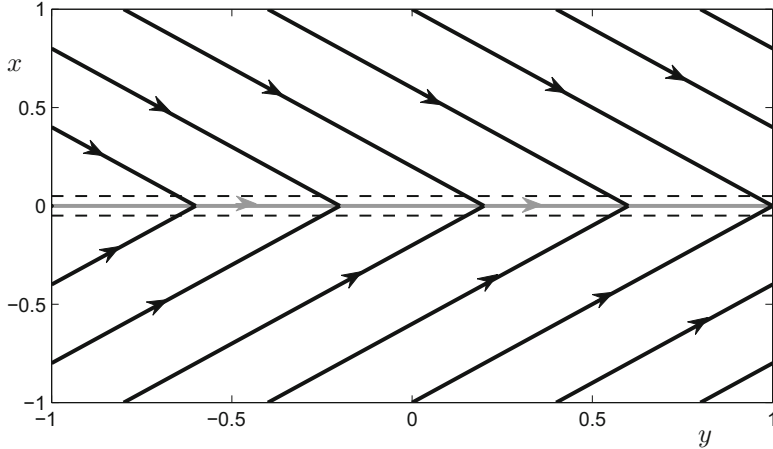


Figure 19.4: Flow of the nonsmooth vector field (19.27). The gray line $\Sigma = \{x = 0\}$ is the set on which the flow is not smooth; the thin dashed lines indicate a small neighborhood of Σ .

Figure 19.4 shows the flow induced by (19.28) on Σ . Clearly, we can define trajectories as concatenations of solutions to the flow on $\mathbb{R}^2 - \Sigma$ and the **sliding flow** on Σ . For example, if we choose the initial condition $(x(0), y(0)) = (1, -1)$, then

$$\gamma_0 = \{x = -y, y \in [-1, 0]\} \cup \{x = 0, y \geq 0\}$$

represents a solution in phase space. Analyzing Filippov systems can be technically difficult. Furthermore, it is nontrivial to think of a generic perturbation of a nonsmooth system or to define what we mean by a generic bifurcation in the nonsmooth context. Therefore, we might want to consider a smooth version of the Filippov system. For example, in Figure 19.4, a neighborhood of Σ is shown (dashed thin lines); we can think of removing the nonsmooth flow in this neighborhood and replacing it by a smooth flow. Viewing Σ as the critical manifold, we are trying to find a slow manifold and the nearby flow to replace the neighborhood of Σ .

We generalize the previous example. Let $K \subset \mathbb{R}^2$ be a compact set and consider a smooth function $H : K \rightarrow \mathbb{R}$, and suppose that H has a regular value at 0. Then define

$$\Sigma := \{(x, y) \in H^{-1}(0) \subset \mathbb{R}^2\}$$

and a vector field

$$\begin{pmatrix} x' \\ y' \end{pmatrix} = \begin{cases} F_1(x, y) & \text{if } H(x, y) > 0, \\ F_2(x, y) & \text{if } H(x, y) < 0, \end{cases} \quad (19.29)$$

where F_1 and F_2 are assumed to be sufficiently smooth. The vector field (19.29) is extended as a Filippov system to Σ by (19.28) where possible, i.e., when $\lambda \in \mathbb{R}$ is well-defined.

Definition 19.3.2. A C^∞ function $\varphi : \mathbb{R} \rightarrow \mathbb{R}$ is called a **transition function** if

$$\varphi(w) = \begin{cases} -1 & \text{if } w \leq -1, \\ 1 & \text{if } w \geq 1, \end{cases}$$

and $\varphi'(w) > 0$ for $w \in (-1, 1)$. The **φ -regularization** of the nonsmooth vector field $F = (F_1, F_2)$ is the 1-parameter family F_ε of vector fields

$$F_\varepsilon(x, y) = \left(\frac{1}{2} + \frac{\varphi(H(x, y)/\varepsilon)}{2} \right) F_1(x, y) + \left(\frac{1}{2} - \frac{\varphi(H(x, y)/\varepsilon)}{2} \right) F_2(x, y).$$

Remark: Note that the smoothing procedure of Definition 19.3.2 is just one possible choice. The definition is motivated primarily by mathematical aspects to make the analysis convenient and sufficiently general.

Suppose we apply the smoothing technique to our simple problem (19.27). Using $\varphi(w) = w$ near $w = 0$ we obtain

$$F_\varepsilon(x, y) = \left(\frac{1}{2} + \frac{x}{2\varepsilon} \right) \begin{pmatrix} -1 \\ 1 \end{pmatrix} + \left(\frac{1}{2} - \frac{x}{2\varepsilon} \right) \begin{pmatrix} 1 \\ 1 \end{pmatrix} = \begin{pmatrix} -x/\varepsilon \\ 1 \end{pmatrix}.$$

Therefore, the fast–slow system replacing the Filippov sliding vector field near Σ is

$$\begin{aligned} \varepsilon \frac{dx}{d\tau} &= \varepsilon \dot{x} = -x, \\ \frac{dy}{d\tau} &= \dot{y} = 1. \end{aligned}$$

Obviously, the example we have considered is rather simple, and we have to ask whether the smoothing from Definition 19.3.2 always gives a fast–slow system in the transition region.

Theorem 19.3.3 ([BdST06]). *Consider a planar Filippov system given by (19.29). Suppose that φ is a polynomial of degree k in a sufficiently small interval $I \subset (-1, 1)$ with $0 \in I$. Then the trajectories of the φ -regularization F_ε in $V_\varepsilon = \{z \in K : H(z)/\varepsilon \in I\}$ are in one-to-one correspondence with an ODE $z' = \kappa(z, \varepsilon)$ and $\kappa(z, 0) = 0$ for every $z \in \Sigma$. Furthermore, suppose $(x^*, y^*) \in \Sigma$ and*

$$(\nabla H^k)(x^*, y^*) \cdot (F_1 - F_2)(x^*, y^*) \neq 0. \quad (19.30)$$

Then there exists a coordinate change that transforms the φ -regularization into a standard $(1, 1)$ -fast–slow system near (x^, y^*) .*

Before we prove Theorem 19.3.3, we remark that it provides only an existence result and does not show how the promised coordinate change can be found explicitly. Condition (19.30) is essentially a normal hyperbolicity condition, as the following proof will show.

Proof. (of Theorem 19.3.3) Suppose the discontinuous vector field $F = (F_1, F_2)$ is given by $F_1 = (f_1, g_1) \in \mathbb{R}^2$ and $F_2 = (f_2, g_2) \in \mathbb{R}^2$ and let

$$a_1 w + \cdots + a_k w^k \quad (19.31)$$

be the polynomial expression of φ on $I \subset \mathbb{R}$ with $0 \in I$. Then the trajectories of the vector field F_ε on V_ε satisfy the following ODE:

$$\begin{aligned} x' &= \frac{1}{2}(f_1 + f_2) + \frac{1}{2}\varphi(H/\varepsilon)(f_1 - f_2), \\ y' &= \frac{1}{2}(g_1 + g_2) + \frac{1}{2}\varphi(H/\varepsilon)(g_1 - g_2). \end{aligned}$$

Using (19.31) and the time rescaling $\varepsilon^k t =: \tau$, we get

$$\begin{aligned} \frac{dx}{d\tau} &= \frac{\varepsilon^k}{2}(f_1 + f_2) + \frac{1}{2}(a_1 H \varepsilon^{k-1} + \cdots + a_k H^k)(f_1 - f_2) =: \kappa_1, \\ \frac{dy}{d\tau} &= \frac{\varepsilon^k}{2}(g_1 + g_2) + \frac{1}{2}(a_1 H \varepsilon^{k-1} + \cdots + a_k H^k)(g_1 - g_2) =: \kappa_2. \end{aligned} \quad (19.32)$$

We can take $\kappa(x, y, \varepsilon) = (\kappa_1(x, y, \varepsilon), \kappa_2(x, y, \varepsilon))$ and observe that $\kappa(x, y, 0) = 0$ for every $(x, y) \in \Sigma$. Linearizing (19.32) at $(x^*, y^*) \in \Sigma$ with $\varepsilon = 0$, one observes that the eigenvalues of $(D_{(x,y)}\kappa)(x^*, y^*, 0)$ are given by solving

$$\lambda^2 - \frac{a_k \lambda}{2}(\nabla H^k)(x^*, y^*) \cdot (F_1 - F_2)(x^*, y^*) = 0.$$

Therefore, $\lambda = 0$ is always an eigenvalue with multiplicity at least one; note that this zero eigenvalue is expected as the zero eigenvalue from the slow direction. By our assumption (19.30), we find that the zero eigenvalue has multiplicity exactly one and Σ is normally hyperbolic near (x^*, y^*) . Now apply Fenichel's normal form theorem (see Section 4.1) to get the result. \square

Unfortunately, Theorem 19.3.3 is not very explicit, since the Fenichel normal form transformation is usually not trivial to compute. The next theorem provides a condition to classify those discontinuous vector fields that are more directly related to the standard fast–slow form.

Theorem 19.3.4 ([BdST06]). *Let $F = (F_1, F_2)$ be a Filippov system. Suppose there exists a smooth function $\xi : K \subset \mathbb{R}^2 \rightarrow \mathbb{R}$ with $(D\xi)(0, 0) = 0$ that satisfies the partial differential equation (PDE)*

$$(\nabla \xi) \cdot (F_1 - F_2) = \Pi_j(F_1 - F_2) \quad (19.33)$$

for $j = 1$ or $j = 2$, where Π_j is the canonical projection onto x for $j = 1$ and onto y for $j = 2$. Assume that φ is a polynomial of degree k in a small interval $I \subset \mathbb{R}$ with $0 \in I$. Then the φ -regularization F_ε can be transformed into standard fast–slow form by an explicit coordinate transformation involving ξ .

We shall not prove Theorem 19.3.4 but consider an example instead to demonstrate how to interpret and carry out the coordinate transformation.

Example 19.3.5. Let us consider $H(x, y) = y$ such that the solutions of the vector field are smooth except on the x -axis $\Sigma = \{y = 0\}$. Now we look at

$$F_1(x, y) = (1, x) \quad \text{and} \quad F_2(x, y) = (-1, -3x). \quad (19.34)$$

The vector field is illustrated in Figure 19.5. We immediately see that there is a special singularity at the origin $(x, y) = (0, 0)$, since the vector field is tangent to Σ at that point. Furthermore, the sliding seems to point in opposite directions near the singularity.

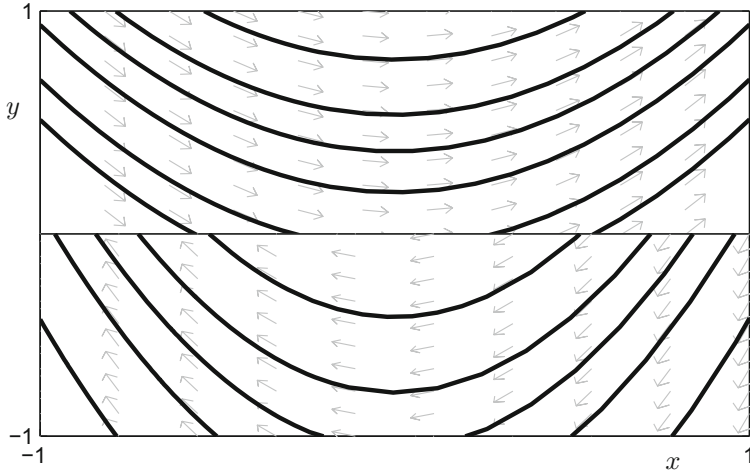


Figure 19.5: Flow (gray arrows) of the nonsmooth vector field defined by (19.34) including some trajectories (thick curves).

The last few observations suggest that the outcome of the φ -regularization is not difficult to guess, since the resulting fast–slow system should have a fold point. Let us consider the case $\varphi(z) = z$ near $z = 0$. Then we get

$$F_\varepsilon = \begin{pmatrix} \frac{y}{\varepsilon} \\ \frac{2xy}{\varepsilon} - x \end{pmatrix}. \quad (19.35)$$

The PDE (19.33) for $j = 2$ is easily shown to be

$$2 \frac{\partial \xi}{\partial x} + 4x \frac{\partial \xi}{\partial y} = 4x. \quad (19.36)$$

It does not require too much ingenuity to spot that $\xi(x, y) = x^2$ solves (19.36) and satisfies $(D\xi)(0, 0) = 0$. Then we can consider the coordinate change

$$(X, Y) = (x, y - x^2)$$

to the new variables $(X, Y) \in \mathbb{R}^2$. Plugging this transformation into (19.35), we find that

$$\begin{aligned} \varepsilon \dot{X} &= Y + X^2, \\ \dot{Y} &= -X. \end{aligned}$$

Hence, we have obtained not only a fold point but a canard point; see Section 8.1. In principle, we can view (19.33) as an invariance equation that can be used to find the correct coordinate transformation for the regularized vector field. ♦

There are more connections between fast–slow systems and Filippov vector fields that we do not present here. For example, it is not difficult to see that the Filippov sliding flow is related to the slow flow on the critical manifold. Furthermore, one can also use the blowup technique to analyze singularities of the regularized vector field and apply those results in the nonsmooth context. Generalizations to higher-dimensional nonsmooth systems exist as well; see Section 19.10 for detailed references.

19.4 Hysteresis

The basic idea of hysteresis is to consider the dynamics of a variable $x(t)$ that depends on a time-dependent given input $y(t)$ where the system has a certain memory property. The details of the memory of the system will be illustrated below.

Remark: Frequently, the terminology **hysteresis** is also used for certain types of relaxation oscillations. Unfortunately, this may lead to confusion, since hysteresis operators, as described in this section, may not produce relaxation oscillations. Even worse, in some cases, hysteresis operators may lead to systems that produce time series very similar to relaxation oscillations.

The goal in this section is to show how certain hysteretic systems can be viewed as fast–slow systems and conversely. We begin with a simple example to illustrate the theory of hysteresis.

Example 19.4.1. Figure 19.6(a) illustrates a mechanical system with a bead on a string inside a movable frame of width h . We assume that the system is one-dimensional and that the frame position is the input $y(t)$ measured by the position of the right edge. The bead position is denoted by $x(t)$. The bead position changes if the bead is at the left or right edge of the frame. If $x(t)$ is at the left edge, the frame pushes the bead to the right; if $x(t)$ is at the right edge, the bead is pushed to the left. In particular, the volume of the bead, friction, etc., are all to be neglected here. The state of the system depends on the input $y(t)$ and on the initial position of the bead $x(0) = x_0$. If the initial position x_0 is outside of the frame, we will set it instantaneously to the nearest edge of the frame. Formally, we can write

$$x(t) = P[x_0]y(t) \quad (19.37)$$

for an operator P called the **play operator**. Figure 19.6(b) shows an example of the output of the play operator for

$$h = 1, \quad x_0 = 1/4 \quad \text{and} \quad y(t) = 1 + \sin t.$$

The output is shown up to time $t = 2\pi$, and we clearly see that a loop emerges. Such loops often occur for hysteresis operators, and characterizing the loop structure is an important task.

The play operator $P[x_0]y(t) = x(t)$ may also be described by its action on certain classes of input functions. Suppose $y : [0, T] \rightarrow \mathbb{R}$ is a piecewise

The Play Operator

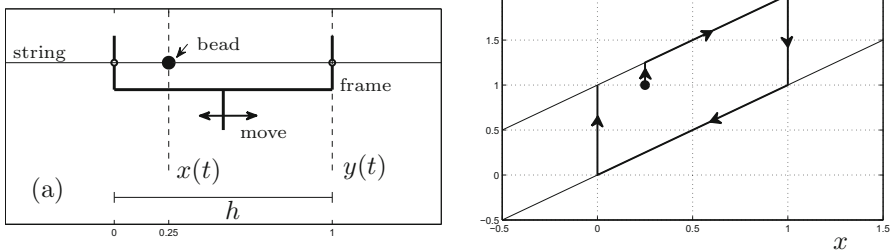


Figure 19.6: (a) Mechanical system to illustrate the play operator. The input $y(t)$ moves the frame, and the bead position $x(t)$ is moved once it is at the edges of the frame. (b) Example of the play operator in $(x, y) = (x(t), y(t))$ -space with $h = 1$, $y(t) = 1 + \sin t$, and initial position $x(0) = (1/4, 1)$ up to time $t = 2\pi$. The arrows indicate the time direction; a part of the hysteresis loop is shown.

monotone function with monotonic behavior on time intervals $[t_i, t_{i+1}] \subset [0, T]$ for $i \in \{0, 1, 2, \dots\}$. Then we can define the play operator inductively as follows:

$$\begin{aligned} x(0) &= p_h(x_0, y(0)) && \text{if } t = 0, \\ x(t) &= p_h(x(t_i), y(t)) && \text{for } t \in (t_i, t_{i+1}], \end{aligned} \quad (19.38)$$

where the map p_h is given by

$$p_h(x, y) := \max\{y - h, \min\{x, y\}\}. \quad (19.39)$$

The construction (19.38)–(19.39) is not immediately intuitive. First, note that every starting point outside the region delimited by the two lines (see Figure 19.6(b))

$$y = x \quad \text{and} \quad y = x + h$$

is projected horizontally onto the lines instantaneously at the start time. Consider starting at $(x, y) = (1.5, 1)$. Then we get

$$x(t_0) = \max\{1 - 1, \min\{1.5, 1\}\} = 1,$$

which is the correct instantaneous reset we have prescribed. The map p_h in (19.39) allows for three different types of outputs of the hysteresis operator. The input-independent mode $p_h(x, y) = x$ means that the bead is inside the frame and away from the edges, while there are two input-dependent modes $p_h(x, y) = y - h$ and $p_h(x, y) = y$ corresponding to the edge positions. An important fact that also immediately follows from the definition (19.38)–(19.39) is that the play operator satisfies

$$x(\phi(t)) = P[x_0]y(\phi(t)) \quad (19.40)$$

for every continuous increasing $\phi : [0, T] \rightarrow [0, T]$ with $\phi(0) = 0$ and $\phi(T) = T$. ♦

The property (19.40) that we observed for the play operator is called **rate-independence**, and it characterizes general hysteresis operators.

Definition 19.4.2. An operator H acting on functions $y : [0, T] \rightarrow \mathbb{R}$ via $(Hy)(t) = x(t)$ is called a **hysteresis operator** if

$$x(\phi(t)) = (Hy)(\phi(t)) \quad (19.41)$$

for every continuous increasing **admissible time change** $\phi : [0, T] \rightarrow [0, T]$ with $\phi(0) = 0$ and $\phi(T) = T$. The property (19.41) is also called **rate-independent memory**.

In Definition (19.4.2), we have suppressed the dependence of H on the initial value $x(0)$. Furthermore, to be precise, one would also have to provide a definite function space on which H acts. For example, one can choose

$$H : M_{pm}[0, T] \rightarrow \text{Map}[0, T]$$

such that H takes a piecewise monotone real-valued map $y \in M_{pm}[0, T]$ to a real-valued map $x \in \text{Map}[0, T]$. This choice of function spaces is often sufficient for hysteresis operators arising in applications.

The definitions of hysteresis operators and their algebraic descriptions (see, e.g., (19.38)–(19.39)) can be very complicated to analyze. Hence, it is natural to ask whether we can find an ODE for $(x, y) = (x(t), y(t))$ that represents a hysteresis operator H . The first attempt is to consider

$$\begin{aligned} \frac{dx}{dt} &= x' = f(x(t), y(t)), \\ \frac{dy}{dt} &= y' = g(y(t)), \end{aligned} \quad (19.42)$$

for suitable smooth maps f and g . Applying a differentiable admissible time change $\phi(t) =: s$ to (19.42) gives, using $\frac{ds}{dt} = \phi'(t) = \phi'(\phi^{-1}(s))$, that

$$\begin{aligned} \frac{dx}{ds} &= \frac{1}{\phi'(\phi^{-1}(s))} f(x(s), y(s)), \\ \frac{dy}{ds} &= \frac{1}{\phi'(\phi^{-1}(s))} g(y(s)). \end{aligned} \quad (19.43)$$

We cannot expect that the output $x(t)$ defined by (19.42) will be rate-independent. Furthermore, we have already seen for the play operator in Example 19.4.1 that the hysteresis loop is not smooth at discrete points. Therefore, classical ODEs will usually fail to represent hysteresis operators. It is an idea attributed to Netushil [MOP05, Net68, Net70] to use singular limits of fast–slow systems to represent hysteresis operators. **Netushil's principle** is summarized (in an imprecise format) in the following result.

Proposition 19.4.3. Suppose we are given a hysteresis operator $(Hy)(t) = x(t)$ with $x \in C(\mathbb{R}, \mathbb{R}^m)$ and $y \in C(\mathbb{R}, \mathbb{R}^n)$. Consider the ODE

$$\varepsilon \dot{x} = \varepsilon \frac{dx}{d\tau} = f(x, y(\tau)). \quad (19.44)$$

Then many hysteresis operators H admit a function $f : \mathbb{R}^{m+n} \rightarrow \mathbb{R}^m$ such that the singular limit $\varepsilon = 0$ of (19.44) represents the dynamics of H .

It is not entirely clear how to make Proposition 19.4.3 precise, i.e., to clarify what “many hysteresis operators” means, how one can constructively obtain the map f , or what we mean by “represents the dynamics.” We shall not consider these questions here and only illustrate the Netushil representation for the play operator; detailed references can be found in Section 19.10.

Example 19.4.4 (Example 19.4.1, continued). To construct the singularly perturbed ODE associated with the play operator, we first consider the function

$$F(u) := \begin{cases} -u & \text{if } u \geq 0, \\ 0 & \text{if } u \in (-h, 0), \\ -(u + h) & \text{if } u \leq -h, \end{cases} \quad (19.45)$$

where we recall that h is the parameter for the play operator describing the width of the moving frame; see also Figure 19.7. Then we define the vector field for (19.44) by

$$\varepsilon \dot{x} = f(x, y(\tau)) := F(x - y(\tau)). \quad (19.46)$$

If the input $y(\tau)$ is differentiable, we can also view it as a solution of a differential equation $\dot{y} = g(y)$ and interpret y as the slow variable. The critical manifold of the associated $(1, 1)$ -fast–slow system is

$$C_0 = \{(x, y) \in \mathbb{R}^2 : F(x - y) = 0\}.$$

The definition of F implies that C_0 is attracting and two-dimensional; C_0 represents the domain of the play operator for positive times, i.e., after an initial transient phase, the dynamics occur near C_0 . If $\varepsilon = 0$, the initial transient is instantaneous, and the relevant dynamics occur inside C_0 . The boundary

$$\partial C_0 = \{(x, y) \in \mathbb{R}^2 : y = x \text{ or } y = x + h\}$$

represents the situation whereby the bead is at the edges of the frame. The interior $C_0 - \partial C_0$ corresponds to the case in which the bead is not moving inside the frame. Figure 19.7 shows the forward evolution of the singularly perturbed ODE (19.46) with parameters

$$h = 1, \quad \varepsilon = 0.1, \quad (x(0), y(0)) = (0.25, 1), \quad y(t) = 1 + \sin t.$$

One can clearly observe that the ODE solutions from Netushil’s representation of the play operator will converge to the dynamics of the play operator as $\varepsilon \rightarrow 0$. ♦

Exercise 19.4.5. Denote the solution of Netushil’s representation (19.46) of the play operator by $x = x(\tau; \varepsilon)$. Show that $x(\tau; \varepsilon)$ converges (pointwise) to the solution of the play operator defined by (19.37) as $\varepsilon \rightarrow 0$. Hint: You have to “smooth the corners” of $F(u)$ to apply standard fast–slow systems theory. ◇

We have seen that for the play operator, it is rather straightforward to use Netushil’s idea to link fast–slow systems to hysteresis operators. Sometimes, one may need a slight extension or different interpretation of Proposition 19.4.3

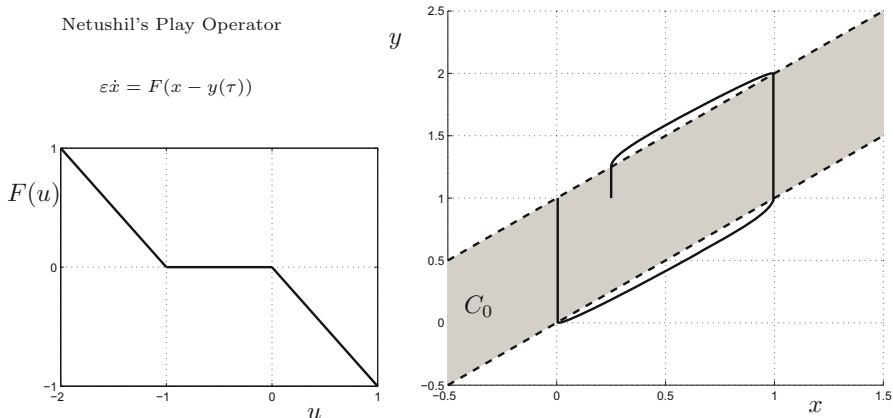


Figure 19.7: Netushil representation of the play operator via the singularly perturbed ODE (19.46); the parameter for the play operator is $h = 1$. The left panel shows the function $F(u)$ given by (19.45) that defines the vector field for the (fast) variable x . The input is $y(\tau) = 1 + \sin \tau$ with initial condition $(x(0), y(0)) = (0.25, 1)$. The phase space result is shown on the right for $\varepsilon = 0.1$; cf. Figure 19.6(b).

to establish this link for more general hysteresis operators; see Section 19.10. Of course, we can also apply Netushil's idea in the reverse direction. Given a singularly perturbed problem

$$\begin{aligned}\varepsilon \dot{x} &= f(x, y), \\ \dot{y} &= g(x, y),\end{aligned}$$

it has been suggested that one might try to represent the slow subsystem singular limit $\varepsilon = 0$ with

$$\begin{aligned}x(t) &= G[x_0]y(t), \\ \dot{y} &= g(x, y),\end{aligned}$$

where G is a suitable hysteresis operator. This strategy could make methods from hysteresis theory available for some fast-slow systems.

Exercise/Project 19.4.6. Suppose we do not measure the position of the bead as in Example 19.4.1 but define $x(t)$ as the distance between the bead and the right edge of the frame. The associated hysteresis operator is called a **stop operator** (or **stop nonlinearity**). Establish analogous results and interpretations obtained above for the play operator for the stop operator. ◇

19.5 Nonstandard Analysis: Introduction

In this section, we provide a very brief introduction to nonstandard analysis. One of the main ideas of the theory is to provide a rigorous notion of infinitesimal numbers. Our goal here is to provide a short overview of the main technical terms; for a completely rigorous construction of infinitesimals, see Section 19.10.

The idea of considering “infinitesimals” is at least as old as calculus itself and can be found in the works of Newton and Leibniz. However, Dedekind, Weierstrass, and Cantor showed that we can construct number systems such as \mathbb{Q} and \mathbb{R} and the entire framework of calculus and analysis without appealing to any intuitive concepts of “very small numbers.” For example, if we work with the real numbers \mathbb{R} , the statement

$$|\varepsilon| < \frac{1}{n} \quad \text{for all } n \in \mathbb{N} \quad (19.47)$$

immediately implies that $\varepsilon = 0$. A priori, such a result makes no statement whether it is a good or a bad idea to try to enlarge \mathbb{R} . In nonstandard analysis, a number ε satisfying (19.47) is **infinitesimal** or **infinitely small** and may be different from $0 \in \mathbb{R}$.

For multiple time scale dynamics, the existence of an ε that is neither 0 nor in \mathbb{R} seems to be appealing. Usually, we have assumed that the time scale separation ε is sufficiently small, $0 < \varepsilon \ll 1$, or that $\varepsilon = 0$ in the singular limit

$$\begin{array}{lll} \varepsilon \in \mathbb{R}, 0 < \varepsilon \ll 1 & \varepsilon \notin \mathbb{R}, 0 < \varepsilon < \frac{1}{n} & \varepsilon \in \mathbb{R}, \varepsilon = 0 \\ \left\{ \begin{array}{l} \varepsilon \dot{x} = f(x, y) \\ \dot{y} = g(x, y) \end{array} \right. & \left\{ \begin{array}{l} \varepsilon \dot{x} = f(x, y) \\ \dot{y} = g(x, y) \end{array} \right. & \left\{ \begin{array}{l} 0 = f(x, y) \\ \dot{y} = g(x, y) \end{array} \right. \\ \text{“full system”} & \text{“nonstandard”} & \text{“singular limit”} \end{array}$$

where the second ODE could potentially provide a nice way to move from the singular limit to results for the full system. The existence of infinitesimals also seems to require us to introduce **infinitely large** or **infinite** numbers such as $\omega := \frac{1}{\varepsilon}$, where

$$|\omega| > n \quad \text{for all } n \in \mathbb{N}.$$

It is possible to include infinitesimals and infinite numbers into an ordered field ${}^*\mathbb{R}$, which contains \mathbb{R} as a proper subfield, so that $\omega, \varepsilon \in {}^*\mathbb{R}$, $\mathbb{R} \subset {}^*\mathbb{R}$, and $\mathbb{R} \neq {}^*\mathbb{R}$. The algebraic operations of addition, multiplication, and inversion all carry over to ${}^*\mathbb{R}$.

Definition 19.5.1. The field ${}^*\mathbb{R}$ is called the **hyperreal numbers**.

Definition 19.5.1 is obviously incomplete, since we have not given an explicit construction of ${}^*\mathbb{R}$, nor provided a sufficient set of axioms that it has to satisfy. We shall only motivate the construction instead of giving full details, which are technically involved. One possibility for constructing \mathbb{R} from \mathbb{Q} is to consider Cauchy sequences

$$r = (r_1, r_2, r_3, \dots), \quad r_j \in \mathbb{Q}, \quad \lim_{m,n \rightarrow \infty} |r_m - r_n| = 0.$$

Two Cauchy sequences r and s are identified via an equivalence relation if

$$\lim_{n \rightarrow \infty} |r_n - s_n| = 0. \quad (19.48)$$

Using this equivalence, one can construct \mathbb{R} from \mathbb{Q} . Note that the construction identifies the sequences

$$(0, 0, 0, \dots) \quad \text{and} \quad \left(1, \frac{1}{2}, \frac{1}{3}, \dots\right),$$

which is precisely what we do not want to happen to get an enlargement ${}^*\mathbb{R}$ of \mathbb{R} . Instead of starting with rational sequences r , we can use \mathbb{R} as a basis to construct ${}^*\mathbb{R}$. Just applying the previous Cauchy sequence equivalence relation (19.48) will not produce infinitely large or small numbers, and we will replace it by the (admittedly rather vague) statement that

$$s = r \quad \text{if and only if} \quad s_n = r_n \text{ for almost every } n, \quad (19.49)$$

i.e., we will call sequences equivalent if they agree at a sufficiently large number of places. To make this idea precise requires some technical tools built around a so-called “ultrafilter”; see Section 19.10 for references. Although we do not present the details here, it is clear that

$$(0, 0, 0, \dots) \neq \left(1, \frac{1}{2}, \frac{1}{3}, \dots\right) \quad (19.50)$$

under the relation (19.49), since the two sequences in (19.50) do not agree on any element. Once the hyperreals ${}^*\mathbb{R}$ are constructed, it is a relatively straightforward procedure to extend the usual arithmetic operations, identify \mathbb{R} , identify the hypernatural numbers ${}^*\mathbb{N} \subset {}^*\mathbb{R}$, and so on. A particularly important operation is to extend real-valued functions to hyperreal-valued ones. Suppose we are given $f : \mathbb{R} \rightarrow \mathbb{R}$. Let $r \in {}^*\mathbb{R}$ be a hyperreal number defined via a sequence $\{r_n\}_{n \in \mathbb{N}}$. Then define

$${}^*f(r) = (f(r_1), f(r_2), f(r_3), \dots),$$

which yields a hyperreal-valued function ${}^*f : {}^*\mathbb{R} \rightarrow {}^*\mathbb{R}$; we shall often omit the star in the notation and simply write ${}^*f = f$ when the automatic extension of f is understood from the context. One of the most important goals of nonstandard analysis is to simplify many proofs. But what happens when we want to prove a result about \mathbb{R} and we obtain a result only in the framework of ${}^*\mathbb{R}$ or conversely? The key tool is called the **transfer principle**, which can be expressed heuristically in the following two parts:

- **universal transfer:** If a standard property holds for all real numbers, then it holds for all hyperreal numbers.
- **existential transfer:** If there exists a hyperreal number satisfying a (nonstandard) property, then there exists a real number that satisfies the corresponding (standard) property.

For both statements, the term “property” is very vague, and the technical conditions have to be made much more precise. To make the statement

rigorous, one can use tools from mathematical logic that distinguish statements/properties that are formulated in such a way that they can be transferred. Consider as an example the following statement:

$$\forall x \in \mathbb{R} \quad \sin(x) = -\sin(-x).$$

Universal transfer then provides the statement

$$\forall x \in {}^*\mathbb{R} \quad \sin(x) = -\sin(-x).$$

On a superficial level, we have just applied a “*-transform” to the real number statement. A similar principle works in the reverse direction. Suppose we are given a sequence $s = \{s_n\}_{n \in \mathbb{N}}$ of real numbers; it is not too difficult to see that viewing the sequence as a map $s : \mathbb{N} \rightarrow \mathbb{R}$, we get a hyperreal sequence *s_n defined also for infinitely large values $n \in {}^*\mathbb{N}$. Suppose we can prove that

$$\exists y \in {}^*\mathbb{R} \quad \forall n \in {}^*\mathbb{N} \quad |{}^*s_n| < y,$$

which means that all terms of a sequence of hyperreals $\{{}^*s_n\} \subset {}^*\mathbb{R}$ are bounded in absolute value by some hyperreal y . Existential transfer then yields the corresponding statement

$$\exists y \in \mathbb{R} \quad \forall n \in \mathbb{N} \quad |s_n| < y,$$

so that we can indeed conclude that boundedness of a hyperreal sequence gives boundedness of the corresponding real-valued sequence. Existential transfer is a key tool for the nonstandard analysis of multiple time scale systems, since proving an existence result for some infinitesimal ε can potentially lead immediately to an existence result for a real $0 \leq \varepsilon \ll 1$. Before we can proceed to an application, we have to introduce quite a bit of terminology that is frequently used in nonstandard analysis.

Definition 19.5.2. A hyperreal number $r \in {}^*\mathbb{R}$ is called

- **limited** if $|r| < n$ for some $n \in \mathbb{N}$;
- **unlimited** if $|r| > n$ for all $n \in \mathbb{N}$;
- **infinitesimal** if $|r| < \frac{1}{n}$ for all $n \in \mathbb{N}$;
- **appreciable** if $\frac{1}{n} < |r| < n$ for some $n \in \mathbb{N}$.

Another part of terminology and notation that is absolutely necessary considers comparisons of hyperreals.

Definition 19.5.3. Hyperreal numbers $r, s \in {}^*\mathbb{R}$ are **of limited distance apart**, denoted by $r \sim s$, if $r - s$ is limited. It can be shown that \sim is an equivalence relation, and the corresponding equivalence class is called the **galaxy**

$$\text{gal}(r) = \{s \in {}^*\mathbb{R} : r \sim s\}.$$

Using the last definition, we can characterize the limited hyperreal numbers as $\text{gal}(0)$.

Definition 19.5.4. A hyperreal $r \in {}^*\mathbb{R}$ is **infinitely close** to $s \in {}^*\mathbb{R}$, denoted by $r \simeq s$, if $r - s$ is infinitesimal. It can be shown that \simeq is an equivalence relation, and the corresponding equivalence class is called the **halo**

$$\text{hal}(r) = \{s \in {}^*\mathbb{R} : r \simeq s\}.$$

Exercise 19.5.5. Prove that \sim from Definition 19.5.3 and \simeq from Definition 19.5.4 are equivalence relations. \diamond

Observe that $\text{hal}(r)$ for some $r \in \mathbb{R}$ consists of r itself and all numbers of the form $r + \varepsilon$, where ε is infinitesimal. Hence, we can also think of $\text{hal}(r)$ as an “infinitesimal neighborhood” of a real number. However, we may also ask, what is the “real neighborhood” of a hyperreal number?

Theorem 19.5.6 ([Gol98]). *Every limited hyperreal r is infinitely close to precisely one real number, called the **shadow** of r , denoted by $\text{sh}(r)$ or ${}^o r$.*

Sometimes, one also refers to ${}^o r$ as the **standard part** of r . It is clear that we can also take the shadow (or standard part) of functions defined on the hyperreals by just evaluating them on the shadows of hyperreal numbers.

Exercise 19.5.7. Show that if $s, r \in {}^*\mathbb{R}$ are limited, then $\text{sh}(s + r) = \text{sh}(s) + \text{sh}(r)$ and $\text{sh}(s \cdot r) = \text{sh}(s) \cdot \text{sh}(r)$. \diamond

Before we proceed to a multiple time scale application of nonstandard analysis, it will be of interest to briefly reconsider some elementary calculus over the hyperreal numbers. For example, an intuitive statement about continuity is that a function is continuous if an infinitely small change in the argument produces an infinitely small change in the function value. This can now be made precise using nonstandard language.

Theorem 19.5.8 ([Gol98]). *A function f is continuous at $c \in \mathbb{R}$ if and only if $f(x) \simeq f(c)$ for all $x \in {}^*\mathbb{R}$ with $x \simeq c$.*

The proof of Theorem 19.5.8 is based on applying universal transfer to a suitably stated classical definition of continuity, which will show that classical continuity implies $f(x) \simeq f(c)$ for all $x \in {}^*\mathbb{R}$ with $x \simeq c$. The converse is then treated using existential transfer. It will be instructive to consider a very simple application of Theorem 19.5.8.

Example 19.5.9. Consider the function $f(x) = \sin x$, which can easily be extended to a hyperreal function ${}^*f : {}^*\mathbb{R} \rightarrow {}^*\mathbb{R}$, which we will also denote by $\sin x$. To show that $\sin x$ is continuous, fix $c \in \mathbb{R}$ and consider $y \in {}^*\mathbb{R}$ such that $y \simeq c$. Then we know that $y = c + \varepsilon$ for some infinitesimal ε , so that

$$\begin{aligned}\sin y - \sin c &= \sin(c + \varepsilon) - \sin c \\ &= \sin c \cos \varepsilon + \cos c \sin \varepsilon - \sin c \\ &= \sin c (\cos \varepsilon - 1) + \cos c \sin \varepsilon,\end{aligned}$$

where the last expression on the right-hand side is easily seen to be an infinitesimal, since $\cos \varepsilon \simeq 1$ and $\sin \varepsilon \simeq 0$. Therefore, it follows that $\sin y \simeq \sin c$, which shows by Theorem 19.5.8 that $f(x) = \sin(x)$ is continuous at every point in \mathbb{R} . ♦

Essentially, one can reconstruct calculus and real analysis entirely using non-standard terminology and proofs. Besides continuity, another striking example is derivatives, which can be defined on a very intuitive basis.

Definition 19.5.10. Consider $f : \mathbb{R} \rightarrow \mathbb{R}$. Then a real number $f'(x)$ is called the derivative of f at $x \in \mathbb{R}$ if for every infinitesimal ε , we have that $f(x + \varepsilon)$ is defined and

$$f'(x) \simeq \frac{f(x + \varepsilon) - f(x)}{\varepsilon}.$$

Therefore, we can indeed view the derivative as an infinitesimal rate of change. Using transfer, it can again be shown that the nonstandard derivative coincides with our well-known definition of differentiation:

$$\lim_{h \rightarrow 0} \frac{f(x + h) - f(x)}{h} =: f'(x).$$

Example 19.5.11. Consider $f(x) = \sin x$ and use Definition 19.5.10 to show that $f'(x) = \cos x$. ♦

The applications of nonstandard analysis go beyond basic real analysis and extend to many branches of pure and applied mathematics; see references in Section 19.10. As a last reassuring note, we mention that it can be shown, under certain assumptions on the construction of nonstandard analysis, that we do not obtain logically new theorems. One often refers to this approach as a conservative extension to standard methods, which means that it is always possible to use standard methods to prove a theorem. However, this does not mean that the hyperreals are superfluous. For example, the definitions of continuity and differentiability show that nonstandard analysis has the potential to provide interesting ways to discover and prove results.

19.6 Nonstandard Analysis: An Application

In this section, we are going to discuss an example of nonstandard analysis applied to fast-slow systems of the form

$$\begin{aligned} \frac{dx}{d\tau} &= \dot{x} = \frac{1}{\varepsilon} f(x, y), \\ \frac{dy}{d\tau} &= \dot{y} = g(x, y), \end{aligned} \tag{19.51}$$

where $\varepsilon \in {}^*\mathbb{R}$ is infinitely small. The main goal is to get used to the reasoning and terminology. Therefore, we focus on the well-known van der Pol equation with constant forcing

$$\begin{aligned} \dot{x} &= \frac{1}{\varepsilon} \left(y - \frac{x^3}{3} + x \right), \\ \dot{y} &= \mu - x, \end{aligned} \tag{19.52}$$

where μ is the main bifurcation parameter. The fast–slow decomposition gives the critical manifold

$$C = \{(x, y) \in \mathbb{R}^2 : y = x^3/3 - x =: h(x)\}$$

with fold points at $(x_{\pm}, y_{\pm}) = (\pm 1, \mp 2/3)$. A parameter variation from $\mu > 1$ to $\mu < 1$ moves the unique equilibrium given by $C \cap \{\mu = x\}$ from the attracting branch of the critical manifold $C^{a,+} = C \cap \{x > 1\}$ to the repelling branch $C^r = C \cap \{-1 < x < 1\}$; see also Figure 19.8(a). We have shown in Section 8.2 using standard analysis that this parameter variation is an example of a singular Hopf bifurcation, and that canard orbits exist in some exponentially small neighborhood of a parameter value $\mu_c(\varepsilon) = \mu_c$. Here we aim to present a “nonstandard proof” of the existence of canards, which historically preceded the standard argument.

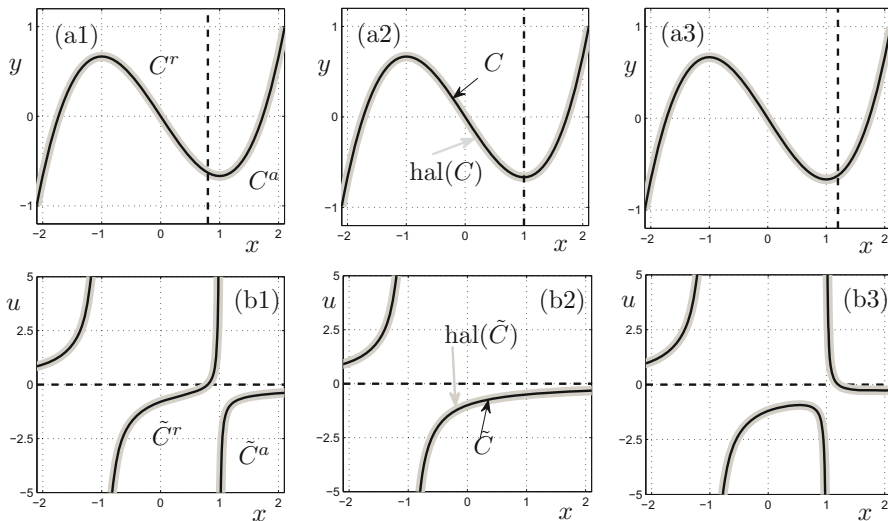


Figure 19.8: (a) Fast–slow decomposition of (19.52). (b) Fast–slow decomposition of (19.54). The parameter values are $\mu = 0.8$ for (a1)/(b1), $\mu = 1$ for (a2)/(b2), and $\mu = 1.2$ for (a3)/(b3). The critical manifolds are shown in black, the halos of the critical manifolds are schematically indicated in gray, and the slow variable nullclines are shown as dashed black lines.

Since ε is infinitely small, we see that \dot{x} is infinitely large as long as we are not infinitely close to C , i.e., as long as we are not in the halo of the critical manifold $\text{hal}(C)$. The derivative \dot{y} is limited regardless of the location in phase space. We are interested in canard trajectories of (19.52) that start in $\text{hal}(C^{a,+})$ and continue into $\text{hal}(C^r)$. Consider the change of coordinates

$$u := \frac{y - h(x)}{\varepsilon}, \quad (19.53)$$

which standard terminology would view as a blowup or rescaling transformation near the critical manifold. Since we want to assume that $\varepsilon \in {}^*\mathbb{R} - \mathbb{R}$, the standard terminology is not quite appropriate. In nonstandard analysis, one refers to transformations of the form (19.53) as **magnifying glass** transformations. Implicit differentiation of (19.53) with respect to the time τ yields

$$\varepsilon \dot{u} = \dot{y} - h'(x)\dot{x} = \mu - x - (x^2 - 1)\dot{x} = \mu - x - u(x^2 - 1),$$

since $\dot{x} = u$ by the definition (19.53). Therefore, we have obtained another $(1, 1)$ -fast–slow system

$$\begin{aligned}\dot{u} &= \frac{1}{\varepsilon} (\mu - x - (x^2 - 1)u), \\ \dot{x} &= u,\end{aligned}\tag{19.54}$$

where u is now the fast variable and x the slow variable; see also Figure 19.8(b). The critical manifold of (19.54) is

$$\tilde{C} = \left\{ (u, x) \in \mathbb{R}^2 : u = \frac{{}^o\mu - x}{x^2 - 1} \right\},$$

where ${}^o\mu$ is the standard part (or shadow $\text{sh}(\mu) = {}^o\mu$) of μ . Observe that \tilde{C} is repelling for $x \in (-1, 1)$ and attracting for $x < -1$ and $x > 1$. Note carefully that if we are infinitely close to \tilde{C} , then the dynamics of (19.54) are given by

$$\dot{x} \simeq \frac{{}^o\mu - x}{x^2 - 1},\tag{19.55}$$

which recovers our usual slow flow on the critical manifold C .

To study the dynamics of (19.54), we observe that trajectories of (19.54) can be viewed as graphs of solutions to the 1-dimensional differential equation

$$\frac{du}{dx} = \frac{1}{\varepsilon} \left(\frac{\mu - x}{u} - (x^2 - 1) \right),\tag{19.56}$$

which is defined over \mathbb{R} only for $u \neq 0$. Denote the solution of (19.56) by $u(x; \mu)$. We will always consider an initial value $(x_0, u(x_0; \mu))$ with $x_0 \gg 1$. If $\frac{{}^o\mu - x_0}{u(x_0; \mu)} - (x_0^2 - 1)$ is not infinitely close to 0, i.e.,

$$\frac{{}^o\mu - x_0}{u(x_0; \mu)} - (x_0^2 - 1) \not\simeq 0,$$

then du/dx is infinitely large. This implies that the solution of (19.56) will reach the halo of $\tilde{C}^{a,+} := \tilde{C} \cap \{x > 1\}$ infinitely fast, since the right branch $\tilde{C}^{a,+}$ of the critical manifold is attracting. Suppose that $\mu > 1$ and $\mu \not\simeq 1$. Then solutions inside $\text{hal}(\tilde{C}^{a,+})$ obey

$$\dot{x} \simeq \frac{{}^o\mu - x}{x^2 - 1}.\tag{19.57}$$

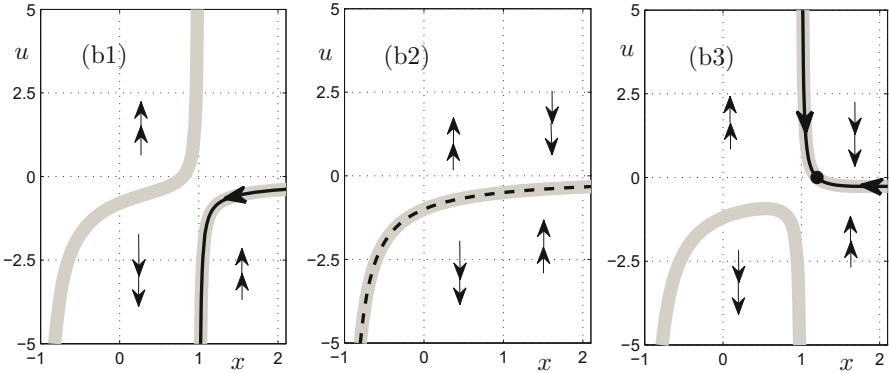


Figure 19.9: Illustration for the nonstandard proof of canard orbits for (19.54). Parameter values are (b1) $\mu = 0.8$, (b2) $\mu = 1$, and (b3) $\mu = 1.2$. The halos of the critical manifold are indicated in gray. In (b1) and (b3), we show two trajectories (solid black) that lie in the halos. In (b2), the canard trajectory is indicated (dashed black).

When $x \simeq 1$, we get that u is infinitely large and positive; see Figure 19.9(b3). By a similar argument, we find that for ${}^o\mu < 1$, u is infinitely large and negative when $x \simeq 1$. Now applying continuity of solutions to (19.55) gives that there exists $\mu^* \simeq 1$ such that u is limited as $x \simeq 1$ and also for $x < 1$. For $\mu^* \simeq 1$, we have

$$\dot{x} \simeq \frac{1-x}{x^2-1} = \frac{-1}{x+1},$$

which implies that solutions for $x \simeq 1$ must pass from $\text{hal}(\tilde{C}^{a,+})$ to $\text{hal}(\tilde{C}^r)$, where $\tilde{C}^r = \tilde{C} \cap \{-1 < x < 1\}$. Hence, we have obtained a result on canards in a nonstandard form.

Proposition 19.6.1 ([DD95]). *There exists $\mu^* \simeq 1$ such that (19.55) has a canard orbit lying in $\text{hal}(\tilde{C}^{a,+}) \cup \text{hal}(\tilde{C}^r)$. Therefore, the van der Pol equation (19.52) also has such a canard orbit lying in $\text{hal}(C^{a,+}) \cup \text{hal}(C^r)$.*

The proof of Proposition 19.6.1 presented above is not entirely rigorous at each step, since the continuity argument needs a bit more detail. However, it shows that the intuitive framework for nonstandard analysis can provide a possible tool for understanding the dynamics of canard orbits. The last step required to recover our well-known results on canards is to apply existential transfer to Proposition 19.6.1, since we have shown the existence of canard orbits only for

$$0 \simeq \varepsilon \quad \text{and} \quad \mu^* \simeq 1,$$

which are hyperreal numbers. A rigorous transfer of Proposition 19.6.1 into a result that replaces an infinitesimal ε by a sufficiently small real $0 < \varepsilon \ll 1$ and that computes the associated $\mu^* = \mu^*(\varepsilon)$ is far beyond the scope of this book and will not be considered here.

19.7 Averaging and Adiabatic Invariants

In this section, we provide a brief introduction to the theory of planar Hamiltonian systems with slowly changing parameters, and we are going to define what “adiabatic invariants” are. Consider the Hamiltonian function $H : \mathbb{R}^2 \rightarrow \mathbb{R}$ and the associated **Hamiltonian system**

$$\frac{dp}{dt} = -\frac{\partial H}{\partial q}, \quad \frac{dq}{dt} = \frac{\partial H}{\partial p} \quad (19.58)$$

for $(p, q) \in \mathbb{R}^2$. Recall that H is always a first integral, since $\frac{d}{dt}H(p(t), q(t)) = 0$. Hence, the level curves $H(p, q) = h$, for suitable $h \in \mathbb{R}$, are also trajectories of (19.58).

Example 19.7.1. The Hamiltonian $H = \frac{1}{2}a^2p^2 + \frac{1}{2}b^2q^2$ defines the dynamics of a **harmonic oscillator**. The classical case is $a = 1 = b$ with

$$p' = -q, \quad q' = p.$$

Nonconstant trajectories are circles $M_h := \{(p, q) \in \mathbb{R}^2 | H(p, q) = h\}$ for $h > 0$. ♦

In essence, we always want to think of the harmonic oscillator, but we can generalize easily by assuming that (19.58) has trajectories $M_h := \{(p, q) \in \mathbb{R}^2 | H(p, q) = h\}$, where each trajectory is diffeomorphic to a circle $S^1 \cong \mathbb{R}/(2\pi\mathbb{Z})$. Classical theory [Arn97, AKN06] provides a canonical transformation

$$K : (p, q) \rightarrow (I, \varphi) \in \mathbb{R} \times S^1,$$

where I is the **action** and $\varphi \in S^1$ is the **angle**, so that in these new **action–angle coordinates**, the dynamics of (19.58) are given by

$$\frac{dI}{dt} = 0, \quad \frac{d\varphi}{dt} = \omega(I), \quad (19.59)$$

where H_0 is the new Hamiltonian function, $\omega(I) := \frac{\partial H_0}{\partial I}$, $I = I(h)$ depends only on h , and $\int_{M_h} d\varphi = 2\pi$. The transformation is called **canonical** if it preserves the underlying symplectic 2-form [Lee06]

$$\Omega = dp \wedge dq \quad \text{i.e., we have } K^*\Omega = \Omega,$$

where K^* denotes the usual pullback of a differential form [Lee06].

Example 19.7.2. For the harmonic oscillator from Exercise 19.7.1 with $a = 1 = b$, we can simply introduce polar coordinates (r, φ) and note that

$$dp \wedge dq = r \, dr \wedge d\varphi = d\left(\frac{r^2}{2}\right) \wedge d\varphi.$$

This shows that $I := \frac{1}{2}p^2 + \frac{1}{2}q^2$ and φ are action–angle coordinates. ♦

A canonical transformation K is always related to a so-called **generating function** $K_g = K_g(I, q)$ such that

$$p = \frac{\partial K_g(I, q)}{\partial q}, \quad \varphi = \frac{\partial K_g(I, q)}{\partial q}, \quad H\left(\frac{\partial K_g(I, q)}{\partial q}, q\right) = h(I).$$

Theorem 19.7.3 ([Arn97, AKN06]). *Set $K_g(I, q) = \int_{q_0}^q p \, dq|_{H=h(I)}$, where the integral is restricted along a level curve $\{H = h(I)\}$ of the Hamiltonian. Then K_g is the generating function for a canonical transformation, so that the Hamiltonian system (19.58) simplifies to (19.59).*

Furthermore, it turns out that the correct action variable is

$$I = I(h) = \frac{A(h)}{2\pi},$$

where $A(h)$ is the area enclosed by the curve $M_h = \{H(p, q) = h\}$. Indeed, for the harmonic oscillator, we precisely have that $A(h) = 2\pi h = \pi(p^2 + q^2) = 2\pi I$. With these preparations, we can now look at perturbations of a Hamiltonian system in action-angle coordinates

$$\begin{aligned} \varphi' &= \omega(I) + \varepsilon f(I, \varphi), \\ I' &= \varepsilon g(I, \varphi), \end{aligned} \tag{19.60}$$

where $0 < \varepsilon \ll 1$ and f, g are assumed to be 2π -periodic in φ . We immediately recognize that (19.60) is a $(1, 1)$ -fast–slow system in which the angle is the fast (“rapidly rotating”) variable, while the action is the slow (“drifting”) variable. We want to apply the averaging theorem from Section 9.6 in this context, which should yield the effective slow variable drift, since

$$J' = \varepsilon \bar{g}(J), \quad \text{where } \bar{g}(J) = \frac{1}{2\pi} \int_0^{2\pi} g(J, \varphi) \, d\varphi.$$

Theorem 19.7.4 ([Arn97, AKN06]). *Suppose that f, g, ω are sufficiently smooth for I in some bounded region $\mathcal{B} \subset \mathbb{R}$ and that $\omega(I) > 0$ for $I \in \mathcal{B}$. Then for $0 < \varepsilon \ll 1$, we have*

$$|I(t) - J(t)| = \mathcal{O}(\varepsilon), \quad \text{for all } t \text{ such that } 0 \leq t \leq \mathcal{O}(1/\varepsilon).$$

Hence, the averaging theorem allows us to say that the averaged action J will deviate only slightly for long times of order $\mathcal{O}(1/\varepsilon)$ from the true action I .

As a second application of fast–slow theory to Hamiltonian systems, we are going to consider slowly changing quantities that are of particular interest in physics. For example, in the context of the harmonic oscillator $H = \frac{1}{2}a^2p^2 + \frac{1}{2}b^2q^2$, we may ask what happens when the parameters a, b change slowly in time. In general, this makes a Hamiltonian a slowly time-dependent function with a slow time $\tau = \varepsilon t$ yielding a nonautonomous Hamiltonian system

$$\frac{dp}{dt} = -\frac{\partial H}{\partial q}, \quad \frac{dq}{dt} = \frac{\partial H}{\partial p}, \quad H = H(p, q; \tau). \tag{19.61}$$

Definition 19.7.5. A quantity $I_a(p, q; \tau)$ is called an **adiabatic invariant** for (19.61) if for every $\kappa > 0$, there exists $\varepsilon_0 > 0$ such that if $\varepsilon \in (0, \varepsilon_0)$ and $0 < t < 1/\varepsilon$, then

$$|I_a(p(t), q(t); \tau) - I_a(p(0), q(0); 0)| \leq \kappa.$$

Definition 19.7.5 already suggests that the action is a very natural candidate for an adiabatic invariant.

Theorem 19.7.6 ([Arn97, AKN06]). *Suppose the frequency $\omega(I)$ in action-angle coordinates for (19.61) is nonzero. Then the action is an adiabatic invariant.*

Proof. (Sketch; [Arn97, AKN06]) For each time t , there exists a canonical transformation $K(t) : (p, q) \rightarrow (I, \varphi)$ transforming the Hamiltonian system (19.61) into action-angle coordinates. Let K_g be the associated generating function of this transformation. It can be shown by a calculation, which we skip here, that the transformed time-dependent Hamiltonian is given by

$$H_K(I, \varphi; \tau) = H_0(I, \varphi) + \frac{\partial K_g}{\partial \tau} = H_0(I, \varphi) + \varepsilon \frac{\partial K_g}{\partial t}.$$

This means that the resulting Hamiltonian system is

$$\begin{aligned} \varphi' &= \omega(I; \tau) + \varepsilon f(I, \varphi; \tau), & f &= \frac{\partial^2 K_g}{\partial I \partial \tau}, \\ I' &= \varepsilon g(I, \varphi; \tau), & g &= -\frac{\partial^2 K_g}{\partial \varphi \partial \tau}, \\ \tau' &= \varepsilon, \end{aligned} \tag{19.62}$$

which is a $(1, 2)$ -fast-slow system. The averaging theorem 19.7.4 applies, since we have $\omega \neq 0$ by assumption. The averaged equation for the action I is

$$J' = \varepsilon \bar{g}, \quad \bar{g} = \frac{1}{2\pi} \int g \, d\varphi = -\frac{1}{2\pi} \int \frac{\partial}{\partial \varphi} \frac{\partial K_g}{\partial \tau} \, d\varphi.$$

Observing that $\frac{\partial K_g}{\partial \tau}$ is independent of φ yields that the last integral vanishes. Hence $\bar{g} \equiv 0$, which implies $J(t) = J(0)$. Then the conclusion of the averaging theorem provides the estimate $|I(t) - I(0)| = \mathcal{O}(\varepsilon)$ for times t with $0 \leq t \leq \mathcal{O}(1/\varepsilon)$. Therefore, the action is an adiabatic invariant. \square

Example 19.7.7. As an example, we consider the harmonic oscillator $H = \frac{1}{2}a^2 p^2 + \frac{1}{2}b^2 q^2$ again. The action is given by

$$I = I(h) = \frac{A(h)}{2\pi} = \frac{1}{2\pi} \pi \frac{\sqrt{2h}}{a} \frac{\sqrt{2h}}{b} = \frac{h}{ab}.$$

Figure 19.10(a) shows a plot of the trajectories of the Hamiltonian system

$$p' = -b^2 q, \quad q' = a^2 p,$$

with $b = 1$ and $a = 1 + \varepsilon t$ for $\varepsilon = 0$ and $\varepsilon = 0.02$. Observe that the adiabatic action $I = h/(ab)$ can be interpreted as the ratio of the energy in the system h and the oscillation frequency $ab = \omega$. ♦

There are many further interesting applications of fast–slow systems theory to Hamiltonian dynamics, and we refer to Section 19.10 for more detailed references.

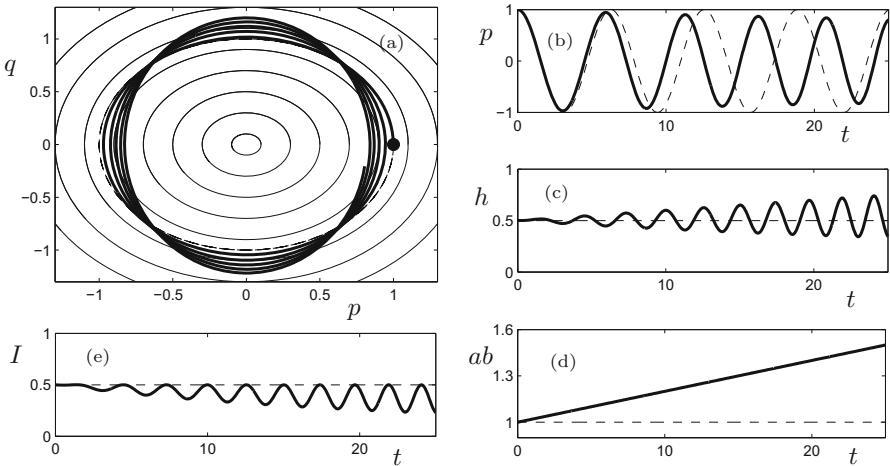


Figure 19.10: The slowly time-dependent harmonic oscillator. (a) Momentum–position (p, q) phase space. Thin curves are for $a = b = 1$, and the thick curve γ_ε is for $a = 1, b = 1 + \varepsilon t$ with starting point $(1, 0)$ (black dot) and $\varepsilon = 0.02$. (b)–(e) Times series for quantities associated with $\varepsilon = 0$ (thin dashed curves) and $\varepsilon = 0.02$ (thick curves).

19.8 Singular Bifurcation Diagrams

Most of the theory we have developed for multiple time scale systems focused on understanding the geometry, asymptotics, and numerics for solutions in phase space by relating results for $\varepsilon = 0$ to the case $0 < \varepsilon \ll 1$. However, one may also ask how the multiple time scale structure affects parameter space and bifurcation diagrams.

Definition 19.8.1. A **singular bifurcation diagram** is a subdivision of parameter space distinguishing regions of qualitatively different dynamics for $\varepsilon = 0$, i.e., only information about fast and slow subsystems is used.

Definition 19.8.1 may look slightly strange at first glance, but we are going to give a detailed example to show why the concept is useful. Consider the FitzHugh–Nagumo PDE (see also Section 1.4)

$$\begin{cases} u_\tau = \delta u_{xx} + f_a(u) - w + p, \\ w_\tau = \varepsilon(u - \gamma w), \end{cases} \quad (19.63)$$

where $f_a(u) = u(u - a)(1 - u)$ and p, γ, δ, a are parameters. Consider traveling wave solutions to (19.63) and set $u(x, \tau) = u(x + s\tau) = u(t)$ and $w(x, \tau) = w$

$(x + s\tau) = w(t)$, where s represents the wave speed. By the chain rule, it follows that $u_\tau = su'$, $u_{xx} = u''$, and $w_\tau = sw'$. Set $u = x_1$, $w = y$, and $x_2 = x'_1$ and substitute into (19.63) to obtain the system

$$\begin{aligned} x'_1 &= x_2, \\ x'_2 &= \frac{1}{\delta}(sx_2 - f_a(x_1) + y - p), \\ y' &= \frac{\varepsilon}{s}(x_1 - \gamma y). \end{aligned} \quad (19.64)$$

We are going to fix the parameter values

$$\gamma = 1, \quad a = \frac{1}{10}, \quad \delta = 5, \quad (19.65)$$

and focus on the (singular) bifurcation diagram in (p, s) -parameter space. Note that (19.64) has the symmetry

$$x_1 \rightarrow \frac{11}{15} - x_1, \quad x_2 \rightarrow \frac{11}{15} - x_2, \quad y \rightarrow -y, \quad p \rightarrow \frac{11}{15} \left(1 - \frac{33}{225}\right) - p, \quad (19.66)$$

which will be helpful in reducing the number of calculations. Homoclinic orbits of (19.64) correspond to traveling pulse solutions of (19.63). Periodic orbits of (19.64) correspond to traveling wave trains of (19.63). We are going to focus on these two types of solution here; see also Chapter 6. Observe that (19.64) is a $(1, 2)$ -fast–slow system with critical manifold

$$C_0 = \left\{ (x_1, x_2, y) \in \mathbb{R}^3 : x_2 = 0 \quad y = x_1(x_1 - 1) \left(\frac{1}{10} - x_1\right) + p =: c(x_1) \right\}.$$

The parameter p moves the cubic curve C_0 up and down. There are two fold points with x_1 -coordinates

$$x_{1,\pm} = \frac{1}{30} (11 \pm \sqrt{91}) \quad \text{or numerically: } x_{1,+} \approx 0.6846, \quad x_{1,-} \approx 0.0487.$$

The fold points divide C_0 into three curve segments,

$$C_0^{a-} = \{x_1 < x_{1,-}\} \cap C_0, \quad C_0^r = \{x_{1,-} \leq x_1 \leq x_{1,+}\} \cap C_0, \quad C_0^{a+} = \{x_{1,+} < x_1\} \cap C_0,$$

where $C_0^{a\pm}$ are of saddle type with one attracting and one repelling direction, while C_0^r is repelling. The slow flow is obtained by differentiation $d/d\tau$ of $y = c(x_1)$, which yields

$$\frac{1}{s}(x_1 - y) = \dot{x}_1 c'(x_1) \quad \Rightarrow \quad \dot{x}_1 = \frac{1}{sc'(x_1)}(x_1 - c(x_1)). \quad (19.67)$$

The fixed-point problem $x_1 = c(x_1)$ has only a single real solution x_1^* , which is the unique equilibrium of the slow flow (19.67). Furthermore, the point $(x_1^*, 0, x_1^*) =: q$ is the unique equilibrium of the full system (19.64). Note that q depends on p . Increasing p moves the equilibrium from left to right on the critical manifold. The bifurcations of the slow flow occur when x_1^* passes through the fold points at which the folds become canard points. This occurs when $p = p_- \approx 0.0511$ and $p = p_+ \approx 0.5584$, where the subscripts indicate the fold point at which each equilibrium is located.

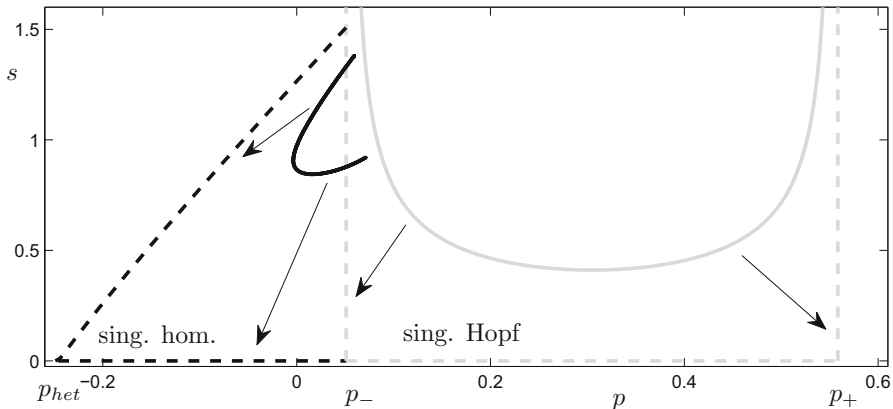


Figure 19.11: Bifurcation diagram for the three-dimensional FitzHugh–Nagumo equation (19.64) with parameters (19.65). The singular bifurcation diagram for $\varepsilon = 0$ is given by the dashed curves and is obtained from the fast and slow flows. The solid curves are computed by numerical continuation for $\varepsilon = 0.01$. Hopf bifurcations are shown in gray, and homoclinic bifurcations in black. The arrows indicate convergence as $\varepsilon \rightarrow 0$ of the U-shaped Hopf curve and the C-shaped homoclinic curve.

Exercise 19.8.2. Check some of the previous computations (analytically or numerically); draw C_0 and the slow flow for different parameter values p . \diamond

By the previous calculation, we expect that the canard point gives rise to a singular Hopf bifurcation, as described in Section 8.2. This results in periodic orbits (or wave trains) that should appear near $p = p_{\pm}$ if ε is sufficiently small; see Figure 19.11.

Exercise/Project 19.8.3. Compute, either numerically or analytically, the Hopf bifurcations for (19.64) in (p, s) -parameter space. The resulting U-shaped curve is shown in Figure 19.11. Prove that this curve converges to the set $\{p = p_{-}\} \cup \{s = 0, p_{-} < p < p_{+}\} \cup \{p = p_{+}\}$ as $\varepsilon \rightarrow 0$. \diamond

Analyzing the singular Hopf bifurcations was relatively simple, since the slow subsystem is one-dimensional. However, the fast subsystem is two-dimensional,

$$\begin{aligned} x'_1 &= x_2, \\ x'_2 &= \frac{1}{5} (sx_2 - x_1(x_1 - 1)) \left(\frac{1}{10} - x_1 \right) + y - p. \end{aligned} \quad (19.68)$$

Since y and p have the same effect as bifurcation parameters, we set $p - y = \bar{p}$. There are three equilibria for (19.68) for approximately $\bar{p}_l = -0.1262 < \bar{p} < 0.0024 = \bar{p}_r$, two equilibria on the boundary of this interval, and one equilibrium otherwise. Observe that \bar{p}_l and \bar{p}_r correspond to the fold points of C_0 .

The next goal is to investigate global bifurcations of the fast subsystem (19.68). For $s = 0$, it is easy to see that (19.68) is a Hamiltonian system

$$\begin{aligned} x'_1 &= \frac{\partial H}{\partial x_2} = x_2, \\ x'_2 &= -\frac{\partial H}{\partial x_1} = \frac{1}{5} (-x_1(x_1 - 1)(\frac{1}{10} - x_1) - \bar{p}), \end{aligned} \quad (19.69)$$

with Hamiltonian function

$$H(x_1, x_2) = \frac{1}{2}x_2^2 - \frac{1}{100}x_1^2 + \frac{11}{150}x_1^3 - \frac{1}{20}x_1^4 + \frac{\bar{p}}{5}x_1. \quad (19.70)$$

Note that if we fix $y = x_1^*$, then the equilibrium $q = (x_1^*, 0, x_1^*)$ of the full system is also an equilibrium for (19.69). Figure 19.12 shows the level set $\{H(x_1^*, 0) = \text{const}\}$ for three different values of p . We observe that there exist homoclinic orbits to $q \in C_0^{a-}$ for an interval $(p, s) \in [-0.246, p_-] \times \{0\}$. At $p \approx -0.246$, a double heteroclinic orbit exists between the two saddle points on C_0^{a-} and C_0^{a+} . When $q \in C_0^{a+}$, a similar analysis applies to yield homoclinic orbits in a second parameter interval with $s = 0$ using the reflection symmetry for p given by (19.66). These parameter space intervals within which singular homoclinic orbits exist form another part of the singular bifurcation diagram shown in Figure 19.11. The singular homoclinic orbits perturb to homoclinic orbits, so-called slow waves, for the full system when $0 < \varepsilon \ll 1$; see Section 6.1.

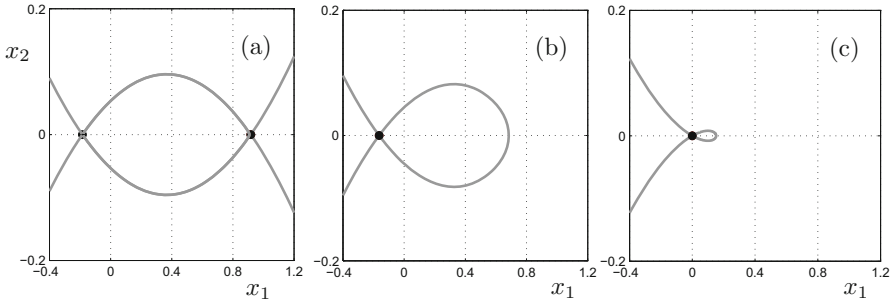


Figure 19.12: Level curves at the equilibrium $y = x_1^*$ for (19.69). (a) $p = -0.246$. Double heteroclinic between the two saddle points. (b) $p = -0.2$. Homoclinic orbit to the saddle q on C_0^{a-} . (c) $p = 0$. Small homoclinic orbit that is going to disappear when $p = p_- > 0$.

The remaining global bifurcations for the singular limit have to be obtained by combining heteroclinic orbits of the fast subsystem with slow flow on C_0^{a-} and C_0^{a+} . For example, if the equilibrium q of the full system is on C_0^{a-} , then we can construct candidates as follows (see e.g., Figure 6.5):

$$\begin{array}{ccc} C_0^{a-} & \leftarrow \{ \text{fast } C_0^{a+} \rightarrow C_0^{a-} \} \leftarrow & C_0^{a+} \\ \downarrow & & \uparrow \\ \{ \text{slow on } C_0^{a-} \} & & \{ \text{slow on } C_0^{a+} \} \\ \downarrow & & \uparrow \\ q & \rightarrow \{ \text{fast } C_0^{a-} \rightarrow C_0^{a+} \} \rightarrow & C_0^{a+} \end{array} \quad (19.71)$$

The construction, geometry, and perturbation of these fast waves is discussed at length in Chapter 6 using the exchange lemma. From the singular bifurcation diagram viewpoint, we have only to verify at which points in (p, s) -parameter space two heteroclinic orbits occur. These form the fast subsystem connections for a candidate homoclinic orbit consisting of four segments; see Section 18.3. We shall outline a numerical strategy to compute heteroclinics.

Suppose that $\bar{p} \in (\bar{p}_l, \bar{p}_r)$, so that (19.68) has three hyperbolic equilibrium points x_l , x_m , and x_r . We denote by $W^u(x_l)$ the unstable manifold of x_l , and by $W^s(x_l)$ the stable manifold of x_l . The same notation is also used for x_r , and tangent spaces to $W^s(\cdot)$ and $W^u(\cdot)$ are denoted by $T^s(\cdot)$ and $T^u(\cdot)$. Recall that x_m is a source and not of interest regarding heteroclinic orbits. We start with the orbits from C_0^{a-} to C_0^{a+} and fix $y = x_1^*$. Define the cross section Σ by

$$\Sigma = \left\{ (x_1, x_2) \in \mathbb{R}^2 : x_1 = \frac{x_l + x_r}{2} \right\}.$$

One may use forward integration of initial conditions in $T^u(x_l)$ and backward integration of initial conditions in $T^s(x_r)$ to obtain trajectories γ^+ and γ^- respectively. Then we calculate their intersection with Σ and define

$$\gamma_l(p, s) := \gamma^+ \cap \Sigma, \quad \gamma_r(p, s) := \gamma^- \cap \Sigma.$$

Heteroclinic connections occur at zeros of the function

$$h(p, s) := \gamma_l(p, s) - \gamma_r(p, s).$$

This approach of finding heteroclinic orbits is the simplest version of **Lin's method**; see Section 10.9.

Exercise/Project 19.8.4. Implement Lin's method for the fast subsystem (19.68). Fix $s = 1$ for simplicity and compute the value p at which a candidate orbit of the form (19.71) exists. \diamond

Once we find a parameter pair (p_0, s_0) such that $h(p_0, s_0) = 0$, these parameters can be continued along a curve of heteroclinic connections in (p, s) parameter space; see also Section 10.6. One has to employ the same procedure to ensure that on this curve in parameter space, we can find $y > x_1^*$, so that a heteroclinic orbit exists from C_0^{a+} to C_0^{a-} for (19.68). The result of this computation is the line of singular homoclinic orbits for $s > 0$ shown in Figure 19.11.

In summary, we have obtained the major bifurcation structure for traveling waves and pulses when $\varepsilon = 0$ without ever having to analyze the full system (19.64). The main curves are a half-open triangle that corresponds to a C-shaped curve of homoclinic bifurcations for $\varepsilon > 0$ and the half-open cylinder that corresponds to a U-shaped curve of Hopf bifurcations for $\varepsilon > 0$. Convergence of this **CU-system** of curves when $\varepsilon \rightarrow 0$ can be examined as well; see Section 19.10.

19.9 Critical Transitions

Bifurcations can cause dynamical systems with slowly varying parameters to transition to far-away attractors. The terms **critical transition** and **tipping point** have been used to describe this situation. We shall demonstrate here that the theory of (stochastic) fast–slow systems can be applied to enhance our understanding of large classes of critical transitions. The focus will be on the question whether **early-warning signs** can be developed to predict a critical transition before it occurs.

A nonmathematical working definition of a critical transition is an abrupt drastic change in a dynamical system. There are many examples in applications. In ecosystems, rapid changes to desertification or extinctions of species can occur. Medical conditions can quickly change from regular to irregular behavior; examples are asthma attacks and epileptic seizures. Financial markets can transition from a balanced market to a financial crisis. Changes in the climate and its constituent subsystems may occur abruptly.

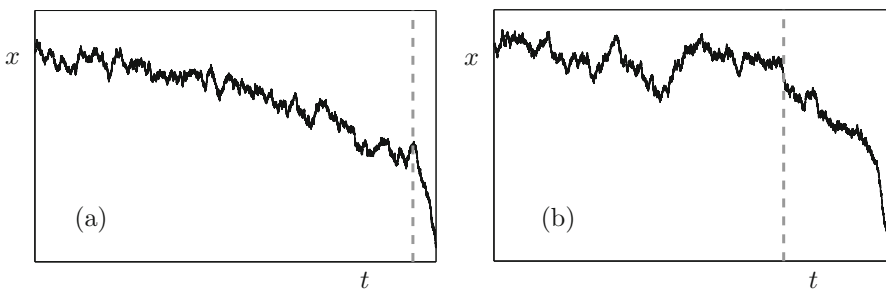


Figure 19.13: Two time series with critical transitions. The gray dashed vertical lines have been added to indicate where one might argue that a visual change in the time series behavior appears; both series were generated using fast–slow stochastic dynamical systems: (a) fast subsystem fold bifurcation and (b) fast subsystem transcritical bifurcation.

Typical time series of critical transitions are shown in Figure 19.13. It has been suggested that all these apparently different critical transitions share several attributes [Sch09a, SBB⁺09]:

- (A1) An abrupt qualitative change in the dynamical system occurs.
- (A2) The change occurs rapidly in comparison to the regular dynamics.
- (A3) The system crosses a special threshold near a transition.
- (A4) The new state of the system is far away from its previous state.
- (A5) There is small noise in the system, i.e., the data have a major deterministic component with small random fluctuations.

It is essentially obvious that the genericity of bifurcations in parameterized vector fields explains why critical transitions in distinct application areas share different features such as (A1)–(A5). Using fast–slow systems, we can make this statement more formal. Starting from a general (m, n) -fast–slow system

$$\begin{aligned}\frac{dx}{dt} &= x' = f(x, y), \\ \frac{dy}{dt} &= y' = \varepsilon g(x, y),\end{aligned}\tag{19.72}$$

where f, g are sufficiently smooth, $(x, y) \in \mathbb{R}^m \times \mathbb{R}^n$, we interpret the variables y as slowly varying parameters and the slow flow on an attracting critical manifold $C_0 = \{f = 0\}$ as the regular dynamics from (A2). Then we recall the definition of a **candidate orbit** as a homeomorphic image $\gamma_0(t)$ of a real interval (a, b) with $a < b$, where

- the interval is partitioned as $a = t_0 < t_1 < \dots < t_m = b$;
- the image of each subinterval $\gamma_0(t_{j-1}, t_j)$ is a trajectory of either the fast or the slow subsystem;
- the image $\gamma_0(a, b)$ has an orientation that is consistent with the orientations on each subinterval $\gamma_0(t_{j-1}, t_j)$ induced by the fast and slow flows.

If consecutive images $\gamma_0(t_{j-1}, t_j)$ and $\gamma_0(t_j, t_{j+1})$ are trajectories for different subsystems, i.e., there is a transition at t_j from fast to slow or from slow to fast, then we say that $\gamma_0(t_j)$ is a **transition point**. Using candidates and transition points, we can give one possible definition of a large class of critical transitions.

Definition 19.9.1. Let $p = (x_p, y_p) \in C_0$ be a point where the critical manifold C_0 is not normally hyperbolic. We say that a **critical transition** occurs at p if there is a candidate γ_0 such that

- (C1) $\gamma_0(t_{j-1}, t_j)$ is a normally hyperbolic attracting submanifold of C_0 ;
- (C2) $p = \gamma_0(t_j)$ is a transition point;
- (C3) $\gamma_0(t_{j-1}, t_j)$ is oriented from $\gamma_0(t_{j-1})$ to $\gamma_0(t_j)$.

From a fast–slow systems perspective, a critical transition occurs at a bifurcation point $y = y_p$ of the fast subsystem that induces switching from a stable slow motion to a fast motion. Definition 19.9.1 can easily be generalized to more complicated invariant sets of the fast subsystem. Note that Definition 19.9.1 just expresses (A1)–(A4) in the terminology of fast–slow systems, where the fast subsystem bifurcation point represents the special transition point from (A3).

Remark: To distinguish the concept in Definition 19.9.1 from several other phenomena, it has been suggested that one emphasizes the fast subsystem bifurcation point and refers to the situation as a bifurcation-induced critical transition or **B-tipping**.

For simplicity, we shall restrict ourselves to two-dimensional fast and slow subsystems, so that $0 \leq m, n \leq 2$ from now on. Consider the fast subsystem of (19.72) given by

$$\begin{aligned}x' &= f(x, y), \\ y' &= 0,\end{aligned}\tag{19.73}$$

and suppose that $x' = f(x, y)$ has a bifurcation, where the number of slow variables $y \in \mathbb{R}^n$ is chosen as the codimension of the bifurcation. Assume that all the necessary genericity conditions (nondegeneracy and transversality) for the bifurcation are satisfied [Kuz04].

Proposition 19.9.2 ([Kue11a, Kue13a]). *Under the previous assumptions and suitable assumptions on the slow flow, the following fast subsystem codimension-one bifurcations are critical transitions:*

(B1) fold, subcritical Hopf,

(B2) (transcritical, subcritical pitchfork).

Under added suitable assumptions on the normal form coefficients, the following fast subsystem codimension-two bifurcations can yield critical transitions:

(B3) cusp, Bautin, Bogdanov–Takens, Gavrilov–Guckenheimer, Hopf–Hopf.

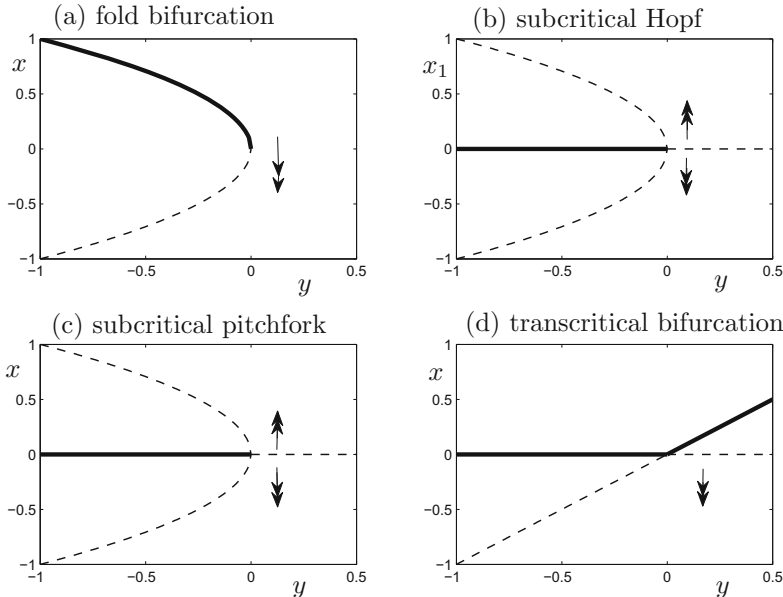


Figure 19.14: Fast subsystem bifurcation diagrams for four bifurcations that are critical transitions. Solid curves indicate stability, dashed curves instability. For the Hopf bifurcation in (b), only the projection onto (x_1, y) is shown. Double arrows indicate the flow of the fast subsystem.

Note that the cases in (B2) are not generic within general smooth vector fields but are often also found in applications due to symmetry or positivity assumptions. The proof of 19.9.2 is straightforward, and the case (B1) is illustrated in Figure 19.14. One has to make sure that the slow flow satisfies a

transversal crossing condition from an attracting to a repelling critical manifold. In addition, a fast subsystem jump at the bifurcation point has to be possible. For example, this excludes the supercritical Hopf bifurcation as a critical transition. Note that the transcritical bifurcation is still included, since there are candidates that jump on reaching the transcritical point.

Within this formal framework, the interesting question now is whether we can predict a critical transition from time series data before it occurs. This requires us to use the last assumption (A5), and we shall see that we can take advantage of stochastic effects for prediction. The intuitive idea is as follows: When a trajectory of the slow flow approaches a fast subsystem bifurcation point, perturbations in the fast directions tend to decay much more slowly back toward the slow manifold. This is the well-known **slowing down** effect near bifurcation points. The stochastic component of a fast variable in a time series allows us to measure this decay, and we may hope to use this information to predict the point where normal hyperbolicity is completely lost.

Hence, we are led to consider stochastic fast–slow systems as discussed in Chapter 15; we shall also adopt the notation from Chapter 15 here. Consider the fast–slow SDE

$$\begin{aligned} dx &= \frac{1}{\varepsilon} f(x, y) d\tau + \frac{\sigma}{\sqrt{\varepsilon}} F(x, y) dW, \\ dy &= g(x, y) d\tau. \end{aligned} \quad (19.74)$$

To illustrate the main idea for finding early-warning signs, recall from Section 15.3 the case in which the deterministic system ($\sigma = 0$) has a fold bifurcation with a slowly drifting parameter,

$$\begin{aligned} dx &= \frac{1}{\varepsilon} (-y - x^2) d\tau + \frac{\sigma}{\sqrt{\varepsilon}} dW, \\ dy &= 1 d\tau. \end{aligned} \quad (19.75)$$

Fix some $x(0) > 0$. A sample path starting for some $x(0) \approx \sqrt{-y(0)}$ is expected to stay with high probability near the stable equilibrium of the deterministic system at $x = \sqrt{-y}$ if σ is sufficiently small; see Theorem 15.2.5. The main arguments to see what happens when we begin to approach the critical transition point at $(x, y) = (0, 0)$ were discussed in Sections 15.2 and 15.3, and we recast the essence of this analysis here. Let us focus on the attracting slow manifold

$$C_\varepsilon = \{x = \sqrt{-y} + \mathcal{O}(\varepsilon) = h_0(y) + \mathcal{O}(\varepsilon) = h_\varepsilon(y)\}.$$

The coordinate change $(\xi, y) := (x - h_\varepsilon(y), y)$ transforms (19.75) to

$$d\xi = \frac{1}{\varepsilon} (-2h_0(y)\xi - \xi^2 + \mathcal{O}(\varepsilon)) d\tau + \frac{\sigma}{\sqrt{\varepsilon}} dW. \quad (19.76)$$

The variational equation for (19.76) around $\xi = 0$ is

$$d\xi^l = \frac{1}{\varepsilon} (-2h_0(y)\xi^l) d\tau + \frac{\sigma}{\sqrt{\varepsilon}} dW, \quad (19.77)$$

which captures, on a linearized level, the fluctuations around the slow manifold. Define $X(\tau) := \sigma^{-2}\text{Var}(\xi^l(\tau))$ and observe that the scaled variance $X = X(\tau)$ satisfies the fast–slow system

$$\begin{aligned}\varepsilon \dot{X} &= -4h_0(y)X + 1, \\ \dot{y} &= 1,\end{aligned}\tag{19.78}$$

as shown in Section 15.2. In Section 15.2, we also discussed that X is a fast variable for (19.78) with attracting critical manifold

$$S_0 = \left\{ (X, y) \in \mathbb{R}^2 : X = \frac{1}{4h_0(y)} = \frac{1}{4\sqrt{-y}} \right\}.$$

Hence, we can conclude (up to leading order and neglecting error terms) that

$$\text{Var}(x) \sim \frac{\sigma^2}{4\sqrt{-y}} = \mathcal{O}\left(\frac{1}{\sqrt{-y}}\right)\tag{19.79}$$

as $y \rightarrow 0^-$ with $\sigma > 0$ fixed. A **scaling law** of the form (19.79) is the crucial reason why one may hope to find early-warning signs near bifurcations for stochastic fast–slow systems.

Knowing a partial time series

$$(x(\tau_0), y(\tau_0)), (x(\tau_1), y(\tau_1)), \dots, (x(\tau_j), y(\tau_j))$$

approaching a general fold critical transition, we can estimate the variance, for example by considering a **moving/sliding window** of fixed length M , and compute the sample variance for M consecutive points. Then we use the scaling law (19.79) in the form

$$\text{Var}(x(\tau)) \sim \frac{A}{\sqrt{y(\tau_c) - y(\tau)}} \quad \text{as } y(\tau) \rightarrow y(\tau_c),\tag{19.80}$$

and fit it to the sample variance using A and $y(\tau_c)$ as fitting parameters. As a result, we can use $y(\tau_c)$ as the predictor, where the rapid jump near the fold critical transitions of the underlying dynamical system will occur. Note that the procedure simplifies near the fold if the parameter is linearly related to time,

$$y(\tau) = \kappa_y \tau + y(0) \Rightarrow \text{Var}(x(\tau)) \sim \frac{\tilde{A}}{\sqrt{\tau_c - \tau}} \quad \text{as } \tau \rightarrow \tau_c,\tag{19.81}$$

so that we may estimate the time of the critical transition. The linear relation is generic near a fold, so one often refers to (19.81) and does not measure a time series of the parameter.

Example 19.9.3. We consider a model for the **North Atlantic thermohaline circulation** given by two boxes B_1 and B_2 representing low and high latitudes respectively. An atmospheric freshwater flux and differences in insulation can induce temperature and salinity differences $\Delta T = T_1 - T_2$ and

$\Delta S = S_1 - S_2$. The resulting system has an Atlantic northward surface current and an Atlantic southward bottom current. For a version of this model, it can be shown that $(\Delta T, \Delta S)$ obey a two-dimensional fast–slow system in which the temperature difference represents the fast variable. After reduction to an attracting slow manifold and a rescaling of the variables, the dynamics reduce to the **Stommel–Cessi** model

$$\dot{Y} = \mu - Y (1 + \eta^2(1 - Y)^2), \quad (19.82)$$

where Y represents the salinity difference, we fix $\eta^2 = 7.5$, and μ is a parameter proportional to the atmospheric freshwater flux. Obviously, the freshwater flux can also be viewed as a dynamical variable, and we assume that it changes more slowly than Y . Furthermore, assume that (19.82) is subject to small stochastic perturbations, which is reasonable if we decide not to model the system in more detail. Setting $x := Y$ and $y := \mu$, we get another two-dimensional fast–slow system

$$\begin{aligned} dx &= \frac{1}{\varepsilon} [y - x(1 + 7.5(1 - x)^2)] d\tau + \frac{\sigma}{\sqrt{\varepsilon}} F(y) dW, \\ dy &= g(x, y) d\tau. \end{aligned} \quad (19.83)$$

The deterministic critical manifold is

$$C_0 = \{(x, y) \in \mathbb{R}^2 : y = x(1 + 7.5(1 - x)^2) =: h_0(x)\},$$

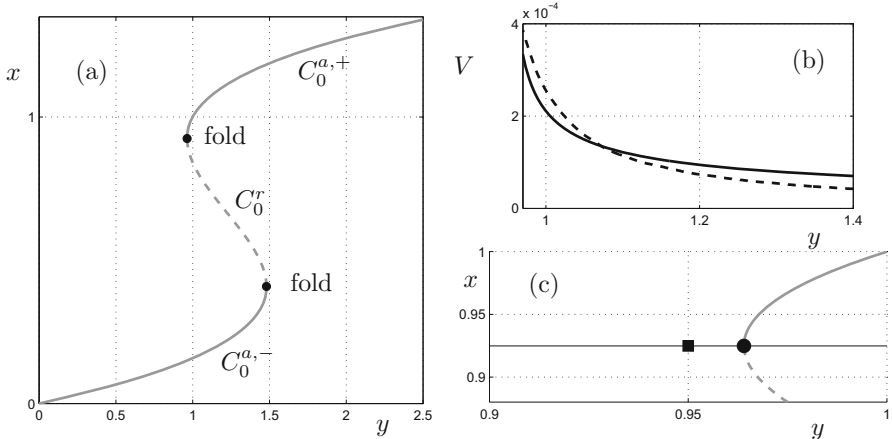


Figure 19.15: Stommel–Cessi model (19.83) with parameters given in (19.84). (a) Standard fast–slow decomposition in phase space. (b) The dashed curve shows the variance $V = \text{Var}(x(y))$ averaged over 1000 sample paths. The solid curve is a least-squares fit of (19.85). (c) Zoom near the fold point (black dot). The square marker indicates the estimator for y_c from the least-squares fit of (19.85) plotted at the same x -value as the fold point. (b) Time series of the trajectory shown in (a).

which is immediately recognized as a classical S-shaped (or cubic) fast subsystem nonlinearity. There are two fold points; see Figure 19.15(a).

The critical manifold splits into three parts, $C_0^{a,-} := C_0 \cap \{x < x_-\}$, $C_0^r := C_0 \cap \{x^- < x < x^+\}$, and $C_0^{a,+} := C_0 \cap \{x > x^+\}$, where $C_0^{a,\pm}$ are attracting and C_0^r is repelling. The lower branch $C_0^{a,-}$ represents a small salinity difference that corresponds to a weak circulation. The upper branch $C_0^{a,+}$ corresponds to a strong circulation, which can be viewed as the present state of the climate. A critical transition from a strong to a weak regime would mean a significant cooling of the mild European climate. Therefore, we shall focus on the critical transition (x^+, y^+) with initial conditions on $C_0^{a,+}$. We fix the initial condition at $(x_0, y_0) = (x_0, 3/2) \in C_0^{a,+}$, which roughly corresponds to the drop point on the upper attracting critical manifold after a transition at (x^-, y^-) . We simulate (19.83) with parameters

$$\varepsilon = 0.01, \quad \sigma = 0.01, \quad F(y) \equiv 1, \quad g(x, y) \equiv -1, \quad (19.84)$$

where the assumptions on g mean that we can also interpret y as a time variable. We stop the sample path at a final value $x = 0.95$. We want to estimate the variance $\text{Var}(y)$ from a time series

$$x_0 = x(\tau_0), x(\tau_1), \dots, x(\tau_N) = 0.95, \quad y(\tau_0) = y(0), y(\tau_1), \dots, y(\tau_N).$$

We can view the values $x(\tau_j) =: x_j$ as functions of y , since $y(\tau) = (\tau - \tau_0) + y(0)$, and we can also indicate this by writing $\text{Var}(x(y))$ for the variance we are trying to estimate. Figure 19.15(b) provides the variance estimate for a simple sliding window technique together with a least-squares fit of

$$\text{Var}(x(y)) = \frac{A}{\sqrt{y - y_c}} \quad (19.85)$$

with fitting parameters A and y_c . The results in Figure 19.15 show that the variance increase is as predicted by the theory. By fitting (19.85), we also obtain an estimate for the critical transition point y_c , which is slightly delayed due to positive ε and seems to be a very good prediction compared to direct simulations. Obviously, we do not make any claims about the real North Atlantic circulation with our calculations, since that would require the analysis of a real data set, which raises many new issues. ♦

Exercise/Project 19.9.4. Figure 19.15 was computed as an average over many paths of the stochastic process. Repeat the calculation with a single time series obtained from direct numerical simulation of (19.83). What can you say about the variance indicator obtained from a single time series? ◇

Along similar lines as for the fold bifurcation, all other codimension-two bifurcations have been analyzed. The scaling laws for the variance, respectively the covariances, in the approach phase to the fast subsystem bifurcation have been computed; see Section 19.10 for more details. Note also that Definition 19.9.1 does not apply if the noise is large and noise-induced jumps are more likely than reaching the bifurcation point. However, in this scenario, we can bring large deviation theory into play; see Sections 15.8 and 15.9.

19.10 References

Section 19.1: The two main references for DAEs we used are [CG95a, KM06b]. The Drazin inverse is also covered in more detail for singular problems in [CJR76]. Sometimes, DAEs are also referred to as constrained equations following the classical paper [Tak76]. We know already that fast–slow systems exhibit generically various singularities, and DAEs do so as well [Cam80b] with associated canonical/normal forms [CP83, KM94]. For the differentiation trick, we refer to [CL91]. There are many books available on DAEs that focus on other aspects, such as electrical circuits [Ria08], mechanics [RR00], numerical methods [BCP87], optimal control [Ger12], and projections to resolve singularities [LMT13].

Section 19.2: In this section, we mainly followed [CG95a]. The example of the Stommel flow follows [Jon95, RJM95]. It is very important to highlight that one may regularize DAEs to obtain fast–slow systems [Han95, KO96, OK94, OK96]. Of course, DAEs are a wide field, particularly on the computational side [CG95b, KM98], and we have barely scratched the surface. A few relevant numerical topics are high-index DAEs [CM95], ODE methods [GP84], regularization [Kno92, WS01], and singular problems [Cam77].

Section 19.3: The basic references we followed are [ST96, BdST06]. For many more details on nonsmooth desingularization, we refer to the series of papers [BdST05, BdST12, LdST09, LdST08, LdST07, TdS12, TdC11]. Canards in nonsmooth systems have been considered as well [BdCdS10]. Impulsive differential equations with a small parameter are actually quite classical [BC94a]. Further relevant topics are boundary bifurcations [KG11], chattering [Fri02b], coupled oscillators [SL13], fast–slow perturbations [SK10], gene networks [MEvdD13], impacting systems with one-sided fast–slow behavior [BF13], and piecewise-linear systems [RCG12]. Sometimes, fast–slow systems have been approximated by nonsmooth ones [JCdB10, DJ11a]. There are many general references on nonsmooth systems available [dBBC08, LN04, SJLS05], although a unified theory has not emerged yet.

Section 19.4: The correspondence between hysteresis and fast–slow systems follows [MOPS05], but see also [Kre05]. The background from hysteresis operators is extracted from [BS96]. There are several monographs available [KP89, Kre96, May03, Vis94] with varying focal points around hysteresis operators. Classical references on hysteresis operators are the papers [Net68, Net70]. Singular perturbation methods can be used to analyze hysteresis [BGS97].

Section 19.5: This section mostly follows the textbook [Gol98]. There is also a link between asymptotics analysis and nonstandard methods [Bla91, vdB87]. The Fenichel–Tikhonov theorem can be discussed from a nonstandard viewpoint [LST98].

Section 19.6: The analysis of canards in a nonstandard setup can be found in [Die84, DD95, DD91]. Even within nonstandard analysis, there are different techniques and approaches to understanding relaxation oscillations [Bor04a, Bor04b, Kon09]. For a review of canards with nonstandard analysis, we highlight [ZS84]. There are various other applications of nonstandard analysis to fast–slow systems [SY04], including delayed bifurcation problems [Cal93].

Section 19.7: This section follows the basic references [Arn97, AKN06], with adiabatic invariants discussed in more detail in the second reference [AKN06]. The literature on adiabatic invariants in fast–slow systems is vast [ANZ11, ANZV10,

[ACVV13](#), [Gar59](#), [Nei00](#), [Nei81](#), [NV06](#), [Su12](#), [VNAZ12](#)], since it is a classical topic in mechanics [[Hen93](#)]. Common themes in Hamiltonian fast–slow systems are averaging [[AKN06](#), [BK92](#), [BK91](#), [Nei76](#)], billiard-type models [[GRKT12](#), [IN12](#), [NA12](#)], separatrix crossing problems [[CET86](#), [Nei91](#), [Nei87a](#), [NST97](#), [NV05](#), [TCE86](#)], and various applications [[ILNV02](#)]. Multiscale ideas also appear very frequently in the context of Arnold diffusion [[DH11](#), [GGM00](#), [Pro03](#)]. There are many other interesting topics we have not covered in fast–slow Hamiltonian dynamics, such as constrained systems [[SZ02](#)], energy transfer [[DL11](#)], ghost separatrix loops [[LG05](#)], Hamiltonian/conservative reduced problems [[AP98a](#), [BYB10](#)], heteroclinic orbits [[SS10](#)], more on invariant manifolds [[GL02](#)], KAM tori [[GL03](#), [Tre04](#)], lobe areas [[KW91](#)], numerical methods [[TOM11](#), [TOM10](#)], resonance phenomena [[Hal95](#), [Hen82](#), [IVKS07](#), [NS12](#), [NS13a](#)], separatrix splitting [[GS12b](#), [NSTV08](#)], shadowing [[BG08b](#), [BSG10](#)], strongly containing potentials [[Rei00](#)], and volume-preserving systems [[NV99](#), [VNM06](#)]. One may also go one step further and look at completely integrable systems [[BMN10](#)].

Section 19.8: This section is based on the singular bifurcation diagram computation in the FHN equation [[GK09b](#), [GK09a](#), [GK10b](#)]. The original motivation arose from numerical continuation results [[CKK⁺07](#)]. The lower left-hand corner of the triangle is treated rigorously in [[KSS97](#)]. The CU structure also appears in various other systems [[TZKS12](#)], and one may focus on heteroclinic connections for a different set of parameters [[ZFM⁺97](#)].

Section 19.9: This section is based mainly on [[Kue11a](#), [Kue13a](#)], where fast subsystem bifurcation-induced transitions and their warning signs are discussed, based on the motivation from applications in [[Sch09a](#), [SBB⁺09](#)]; see also the seminal paper [[Wie85](#)]. The simple box model is due to Stommel–Cessi [[Sto49](#), [Sto61](#), [Ces94](#), [BG02d](#)]. For a distinction between noise-induced and bifurcation-induced effects, we refer to [[AWVC12](#), [Kue13a](#)]. There are many areas in which warning signs for critical transitions have been considered, such as biomechanics [[VGVC07](#), [Kue13a](#)], climate [[AMN⁺03](#), [BLH⁺09](#), [DSvN⁺08](#), [DJ10](#), [LHK⁺08](#), [LL07](#), [TS11b](#), [TS10](#), [TS11a](#), [WALC11](#)], ecology [[CB06](#), [CCP⁺11](#), [CCB⁺01](#), [GJ08](#), [HW10](#), [HHvNS11](#), [SC03](#), [SCF⁺01](#), [vNS07](#)], engineering [[CBT⁺11](#), [CSHD12](#)], finance [[MLS08](#)], medicine [[VWM⁺05](#), [MST03](#), [MK12b](#), [MAEL07](#), [Ric11](#)], and social networks [[KMR14](#)].

It is important to point out that critical transitions and associated warning signs have also been observed in experiments [[DG10](#), [VFD⁺12](#)]. Interesting recent directions are to move toward spatially extended systems [[DvND⁺09](#), [DKR⁺11](#), [DFD⁺10](#), [GJ09](#), [KRA⁺07](#), [RDdRvdK04](#)], to use generalized models [[LG12](#), [KG13](#), [KSG13](#)], and to consider traveling waves [[Kue13b](#)]. Also, warning signs for nonsmooth systems are expected to be drastically different from those in the smooth case [[Kue09](#)].

Since the topic is mostly related to multiscale spatial dynamics, wavelets have not been considered in this book. For textbooks on wavelets, see [[Chu92](#), [Dau92](#), [PW00](#), [Wal01](#), [Woj97](#)]. Of course, wavelets have proved to be tremendously useful in various multiscale spatial problems. It was also tempting to venture further into multiscale spatial dynamics including topics such as the Cauchy–Born rule [[EM07](#), [TOP96](#), [YE06](#)] and Car–Parrinello molecular dynamics [[BS98](#), [TB91a](#), [TB91b](#), [TBM91](#), [TBM94](#), [TBR91](#), [TMB90](#), [TP94a](#), [TP94b](#)]. The Berry phase from quantum dynamics and adiabatic change [[Ber84](#), [Ber85](#), [Ber87](#)] could have been included as well. The method of multiple scales can be applied in this context [[And92](#)], and we refer to [[BM72](#)] for a review in which the relationship to WKB and turning points

is discussed. Other issues that could have been discussed from a fast–slow viewpoint are convergence rates to invariant sets [Art04], coupled cell systems [RT12], differential games [FS80, SF84], filtering [GM08, GM10], finite-time Lyapunov exponents [MG12, Mea05, MTA08], integral transform techniques [LK85b], monotone systems [WS06b, WS08], particle filters [GSW09], and relaxation times in glassy dynamics [Bil10, GFZ11].

Chapter 20

Applications

In this chapter we touch on several application areas in which time scale separation arises naturally. As you can guess from the rather diverse set of section headings, it is quite reasonable to conjecture that most quantitative sciences that employ mathematical modeling may eventually encounter various multi-scale problems. Each section centers on one or two key examples in which one can clearly identify the time scale separation parameter as well as apply many of the methods discussed in this book.

20.1 Engineering

We begin with a **feedback system** example that applies to many engineering subdisciplines. Figure 20.1(a) shows a block diagram of a feedback system with two variables $(x, y) \in \mathbb{R}^2$ and an input $u \in \mathbb{R}$. The blocks correspond to standard dynamical operations

Nonlinear function	\xrightarrow{v}		$\xrightarrow{N(v)}$
Gain block	\xrightarrow{v}		\xrightarrow{Kv}
Integrator	\xrightarrow{v}		$\xrightarrow{\int_0^s v(s) ds}$

where $K > 0$ is a positive constant. We are going to assume that the nonlinear function $N : \mathbb{R} \rightarrow \mathbb{R}$ in Figure 20.1(a) is strictly increasing; an example is given by

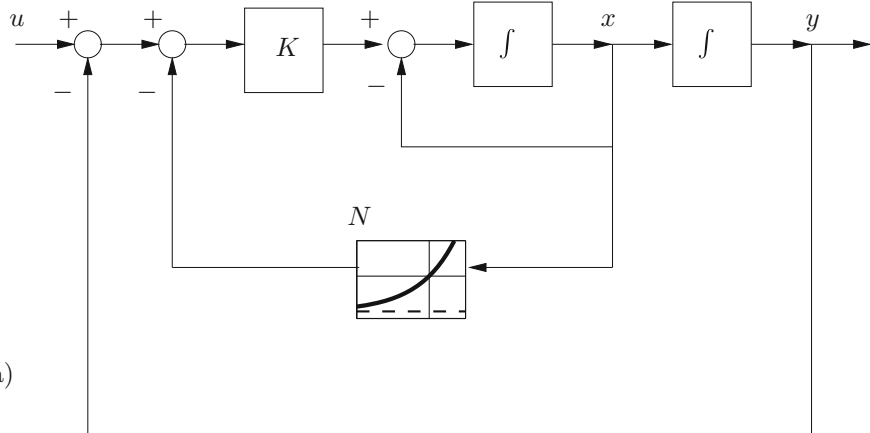
$$N(v) = e^v - 1.$$

The block diagram in Figure 20.1(a) can be translated into a system of ODEs

$$\begin{aligned} \frac{dx}{d\tau} &= \dot{x} = -x - Ky - KN(x) + Ku, \\ \frac{dy}{d\tau} &= \dot{y} = x. \end{aligned} \tag{20.1}$$

It is common to consider the case of a **high-gain amplifier**, where $K \gg 1$. Setting $\varepsilon := 1/K$, it follows that (20.1) can be written as a $(1, 1)$ -fast–slow system in standard form:

$$\begin{aligned}\varepsilon \dot{x} &= -y - \varepsilon x - N(x) + u, \\ \dot{y} &= x.\end{aligned}\tag{20.2}$$



(a)

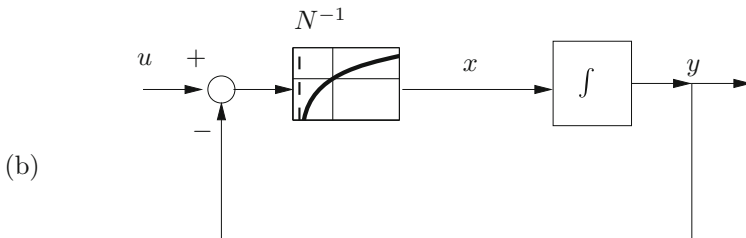


Figure 20.1: Block diagrams of a feedback system with a high-gain amplifier. (a) Block diagram for the full system associated with the $(1, 1)$ -fast–slow system (20.2). (b) Block diagram for the reduced system described by the slow flow (20.3).

The critical manifold is given by

$$C_0 = \{(x, y) \in \mathbb{R}^2 : y = u - N(x) \text{ or } x = N^{-1}(u - y)\};$$

C_0 is attracting, since $N'(x) > 0$ by assumption. For $N(x) = e^x - 1$, a direct calculation gives the slow flow

$$x = N^{-1}(u - y) = \ln(u - y + 1) \quad \Rightarrow \quad \dot{y} = \ln(u - y + 1),\tag{20.3}$$

which is defined for $y < u + 1$. The **reduced block diagram** associated with the slow flow is given in Figure 20.1(b). Therefore, fast–slow systems ideas can provide a direct application to reducing engineering systems. Obviously, we cannot always expect to encounter such a nice situation in every system.

As a second example, we consider a model for the behavior of metals at very low temperatures. At these temperatures, it is observed in tensile tests that the stress can oscillate instead of reaching equilibrium. This behavior is referred to as **discontinuous plastic deformation**. Estrin and Kubin [EK80] proposed a two-variable model valid at low temperature and given in dimensionless form by

$$\begin{aligned}\frac{d\theta}{dt} &= \theta' = \frac{1}{(1+\theta)^3} \left[-\theta + \mu \Sigma_0 \sigma \exp\left(\frac{\beta\theta+\alpha(\sigma-1)}{1+\theta}\right) \right], \\ \frac{d\sigma}{dt} &= \sigma' = \Sigma_0 \left[1 - \exp\left(\frac{\beta\theta+\alpha(\sigma-1)}{1+\theta}\right) \right],\end{aligned}\quad (20.4)$$

where θ represents the temperature and σ the average stress of the material. The other unknowns in (20.4) are viewed as parameters, α is the equilibrium stress, β the equilibrium activation enthalpy for the plastic flow, Σ_0 the nominal shear strain rate, and μ the ratio of elastic and caloric energies. The transition to the plastic deformation state in (20.4) occurs via a Hopf bifurcation.

Considering the small strain rate case $0 < \Sigma_0 =: \varepsilon \ll 1$, together with a large ratio μ so that $\mu\Sigma_0 =: \nu$ is of order one, the system (20.4) can be recast as a $(1, 1)$ -fast–slow system,

$$\begin{aligned}x' &= \frac{1}{(1+x)^3} \left[-x + \nu y \exp\left(\frac{\beta x + \alpha(y-1)}{1+x}\right) \right] =: f(x, y), \\ y' &= \varepsilon \left[1 - \exp\left(\frac{\beta x + \alpha(y-1)}{1+x}\right) \right] =: g(x, y),\end{aligned}\quad (20.5)$$

where we have introduced the standard variables $(\theta, \sigma) =: (x, y)$. The critical manifold is

$$C_0 = \left\{ (x, y) \in \mathbb{R}^2 : 0 = x - \nu y \exp\left(\frac{\beta x + \alpha(y-1)}{1+x}\right) \right\},$$

and direct differentiation shows that

$$\begin{aligned}\left. \frac{\partial f}{\partial x} \right|_{C_0} &= \frac{2(x-2)(1+x) - e^{\frac{(y-1)\alpha+x\beta}{1+x}} y \nu (3+3x+(y-1)\alpha-\beta)}{(1+x)^5} \\ &= \frac{2(x-2)(1+x) - x(3+3x+(y-1)\alpha-\beta)}{(1+x)^5}.\end{aligned}\quad (20.6)$$

Hence, it is easy to observe that normal hyperbolicity can be lost, since (20.6) can vanish for certain parameter values. A more detailed analysis shows that near a fold point, the Hopf bifurcation is singular, and a canard explosion to relaxation oscillation occurs in the model [Brø05].

Exercise/Project 20.1.1. Calculate the singular points for (20.5) and determine the parameter values for which a maximal canard exists using the techniques of Chapter 8 or Chapter 10. For simplicity, you may fix $(\alpha, \mu) = (150, 28)$ and determine the relevant quantities in (ε, β) parameter space. ◇

The important practical conclusion from the analysis of the Estrin–Kubin model is that the transition to discontinuous plastic deformation can occur extremely rapidly under a small parameter variation and that the “discontinuity” in the oscillations may originate from the rapid fast segments during a relaxation oscillation cycle. Further references to models in engineering with multiple time scales can be found in Section 20.12.

20.2 Neuroscience

A cornerstone of mathematical neuroscience is dynamical models for individual neurons. Although we certainly cannot give a detailed neurophysiological introduction to the subject of single-neuron models, we shall briefly present some principles. The basic elements of electrical activity of neurons arise due to currents through the cell membrane. Usually, there are four main ions involved in this process:

calcium Ca^{2+} , potassium K^+ , sodium Na^+ , and chloride Cl^- .

Since the cell membrane has ion channels, there is the possibility of ion transport between the extracellular and the intracellular media. Skipping several details of the biochemical processes, we may say that these ion transport mechanisms lead to electrochemical gradients. At this point, mathematical modeling can be used with a focus on dynamics of the **(trans)membrane potential**

$$V = V_{\text{interior}} - V_{\text{exterior}} \quad (\text{measured in mV})$$

representing the voltage difference between the interior and exterior parts of the cell. The different ionic current densities I_{Ca} , I_K , I_{Na} , and I_{Cl} (measured in $\mu\text{A}/\text{cm}^2$) certainly depend on the potential difference V . For example, a direct proportionality relation between I_K and V can be expressed as

$$I_K = g_K(V - E_K), \tag{20.7}$$

where g_K (in mS/cm^2) is the K^+ conductance, and E_K is the K^+ **equilibrium** (or **Nernst**) **potential**. Kirchhoff's law gives total current I across a patch of the cell membrane as

$$I = C \frac{dV}{dt} + I_{\text{Ca}} + I_K + I_{\text{Na}} + I_{\text{Cl}}, \tag{20.8}$$

where C (in $\mu\text{F}/\text{cm}^2$) is the capacitance density and t (in ms) denotes the time. Rewriting equation (20.8) slightly yields

$$C \frac{dV}{dt} = I - I_{\text{Ca}} - I_K - I_{\text{Na}} - I_{\text{Cl}}, \tag{20.9}$$

where we can interpret I as a source or sink term, i.e., $I = 0$ represents no external current. The differential equation (20.8) is a cornerstone of single-neuron modeling. Often, direct proportionality assumptions like (20.7) are too

simple, and one has to take into account that the gates through the membrane can be activated or deactivated. This leads to additional dynamical **gating variables**. For example, the famous **Hodgkin–Huxley equations** [HH52d] are given by

$$\begin{aligned} CV' &= I - I_{\text{Na}} - I_{\text{K}} - I_{\text{L}}, \\ m' &= \alpha_m(V)(1-m) - \beta_m(V)m, \\ h' &= \alpha_h(V)(1-h) - \beta_h(V)h, \\ n' &= \alpha_n(V)(1-n) - \beta_n(V)n, \end{aligned} \quad (20.10)$$

where the so-called leak current I_{L} is mostly carried by Cl^- ions, and (n, m, h) are the gating variables. The ionic currents are modeled as

$$I_{\text{K}} = g_{\text{K}}n^4(V - E_{\text{K}}), \quad I_{\text{Na}} = g_{\text{Na}}m^3h(V - E_{\text{Na}}), \quad I_{\text{L}} = g_{\text{L}}(V - E_{\text{L}}).$$

The functions $\alpha_{m,h,n}$ and $\beta_{m,h,n}$ are given by

$$\begin{aligned} \alpha_m(V) &= \frac{(V + 40)/10}{1 - \exp(-(V + 40)/10)}, \\ \alpha_h(V) &= 0.07 \exp(-(V + 65)/20), \\ \alpha_n(V) &= \frac{(V + 55)/100}{1 - \exp(-(V + 55)/10)}, \\ \beta_m(V) &= 4 \exp(-(V + 65)/18), \\ \beta_h(V) &= \frac{1}{1 + \exp(-(V + 35)/10)}, \\ \beta_n(V) &= 0.125 \exp(-(V + 65)/80). \end{aligned}$$

The gating variables (m, h, n) are dimensionless, and each function α_x and β_x for $x = m, h, n$ is expressed in units of $(\text{ms})^{-1}$. It should be noted that there are different conventions for writing the Hodgkin–Huxley equations, e.g., in the formulation used in [RW07] and in this book, the voltage V is shifted from the original Hodgkin–Huxley voltage $V_{\text{HH}} = V + 65$ used in [HH52d, KS08a].

Exercise/Project 20.2.1. Investigate the Hodgkin–Huxley model numerically with a technique of your choice from Chapter 10 and/or Chapter 11. In particular, try to find parameters that yield more complex spiking behavior than just a single spike. ◇

The classical parameter values for the Hodgkin–Huxley equations are

$$\begin{aligned} g_{\text{Na}} &= 120, \quad g_{\text{K}} = 36, \quad g_{\text{L}} = 0.3, \\ E_{\text{Na}} &= 50, \quad E_{\text{K}} = -77, \quad E_{\text{L}} = -54.4, \quad C = 1. \end{aligned} \quad (20.11)$$

It is not immediately apparent from the ODEs (20.10) whether there is a time scale separation. Figure 20.2 shows a numerical simulation displaying a rapid change in the voltage variable, which is also referred to as a **spike** of the neuron. FitzHugh [Fit60] observed that the variables (V, m) change rapidly in comparison to (h, n) during spikes. Another argument to identify slow and fast variables

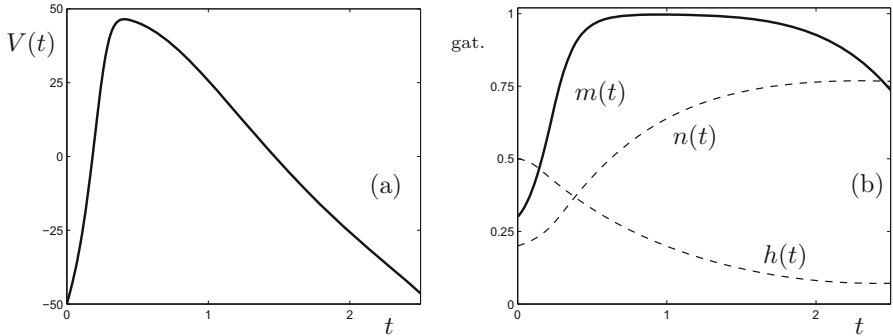


Figure 20.2: Numerical simulation of the Hodgkin–Huxley model (20.10) with parameter values (20.11) and $I = 9.6$. The starting point is $(V(0), m(0), h(0), n(0)) = (-50, 0.3, 0.5, 0.2)$. (a) Voltage, (b) gating variables. The two variables (V, m) (thick solid curves) display clear fast transitions during the spike, while (h, n) (dashed thin curves) vary slowly.

relies on biophysical considerations, which show that the activation of sodium channels m is a much faster process than activation of potassium and leak currents (h, n) . These observations suggest that the Hodgkin–Huxley equations are a $(2, 2)$ -fast–slow system.

It is clear that a fast–slow systems analysis would be easier if one could bring the Hodgkin–Huxley equations into a more standard form. It is instructive to show how this process actually works in practice [RW07]. The main strategy we will adopt is to nondimensionalize the system. We begin by focusing on the voltage variable V and try to normalize it so that it is comparable with the gating variables. Define

$$v := \frac{V}{k_v} \quad \text{and} \quad \tau := \frac{t}{k_t},$$

where k_v has the unit mV, and k_t the unit ms, so that v and τ are dimensionless. Then the Hodgkin–Huxley equations (20.10) can be rewritten as

$$\begin{aligned} \frac{dv}{d\tau} &= \frac{g}{C} k_t [\bar{I} - \bar{g}_{\text{Na}} m^3 h(v - \bar{E}_{\text{Na}}) - \bar{g}_{\text{K}} n^4 (v - \bar{E}_{\text{K}}) - \bar{g}_{\text{L}} (v - \bar{E}_{\text{L}})], \\ \frac{dm}{d\tau} &= k_t [\alpha_m(v)(1 - m) - \beta_m(v)m], \\ \frac{dh}{d\tau} &= k_t [\alpha_h(v)(1 - h) - \beta_h(v)h], \\ \frac{dn}{d\tau} &= k_t [\alpha_n(v)(1 - n) - \beta_n(v)n], \end{aligned} \tag{20.12}$$

where $\bar{I} := \frac{I}{k_v g}$, $\bar{E}_x := E_x/k_v$, and $\bar{g}_x := g_x/g$ for $x = m, h, n$ are dimensionless, and g is a reference conductance to be chosen. The Nernst potentials form

natural limits for the voltage

$$E_K \leq V \leq E_{Na}, \quad (20.13)$$

which gives a maximum variation of $E_{Na} - E_K = 127$ mV using the classical values (20.11). Hence, we can choose a typical scale as $k_v = 100$ mV. Using $g = g_{Na}$ ensures that all terms in the voltage equation inside square brackets have absolute values bounded by 1. These two choices are very important, since they incorporate an assumption about the units and magnitude of the phase space variables into the differential equations. Therefore, the characteristic time scale of the voltage equation can be identified as

$$\frac{1}{\varepsilon} := \frac{g_{Na}}{C} k_t.$$

If we assume a typical time scale as $k_t = 1$ ms, then $0 < \varepsilon \ll 1$ is indeed a small parameter, since $(g_{Na} k_t)/C = 120 \gg 1$. Now we still have to justify the choice of k_t and deal with the gating variables.

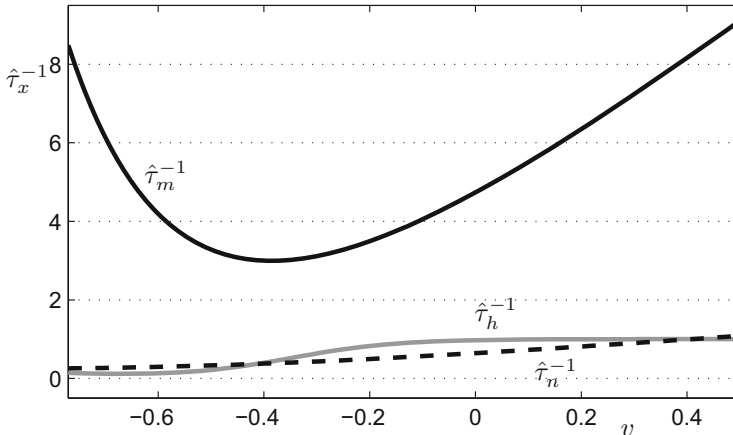


Figure 20.3: Plot of the characteristic time scale $1/\hat{\tau}_x(v) = \alpha_x(v) + \beta_x(v)$ for $x = m$ (solid black), $x = h$ (solid gray), and $x = n$ (dashed black). The domain on the horizontal axis is given by $v \in [-0.77, 0.5]$, which is physiologically prescribed by (20.13).

To simplify the notation, we are going to adopt the variable x as a placeholder for m, h, n . Then the ODEs for the gating variables are of the form

$$\frac{dx}{d\tau} = \frac{k_t}{\hat{\tau}_x(v)} [x_\infty(v) - x], \quad (20.14)$$

where the functions $\hat{\tau}$ and x_∞ are defined by

$$\hat{\tau}_x(v) := \frac{1}{\alpha_x(v) + \beta_x(v)}, \quad x_\infty(v) := \frac{\alpha_x(v)}{\alpha_x(v) + \beta_x(v)},$$

for $x = m, h, n$. Note that $0 \leq x \leq 1$ and $0 \leq x_\infty(v) \leq 1$ imply that the dimensionless term in square brackets in (20.14) satisfies

$$|x_\infty(v) - x| \leq 1.$$

Since $\hat{\tau}_x(v)$ has units of ms , the prefactor signals the characteristic time scales of the channel mechanisms. Figure 20.3 shows a plot of $1/\hat{\tau}_x(v)$ for the three different gating variables for a physiologically reasonable range of $v \in [-0.77, 0.5]$ (recall that the Nernst potentials bound the voltage by (20.13) and that we rescaled V by $k_v = 100$ mV). Figure 20.3 shows that the slowest time scale is approximately $1\ ms$, so that we are certainly justified taking $k_t = 1\ ms$ if we want to write the system on the slow time scale. Furthermore, Figure 20.3 suggests to consider a rescaling

$$\frac{1}{\tau_x(v)} := \frac{1}{T_x \hat{\tau}_x(v)}, \quad \text{where } T_x = \max_{v \in [-0.77, 0.5]} (1/\hat{\tau}_x(v))$$

to normalize the scaling prefactors $1/\hat{\tau}_x(v)$ to the same order. Observe carefully that $T_m \approx 10\ (ms)^{-1}$, while $T_h \approx T_n \approx 1\ (ms)^{-1}$, so that m is indeed a faster variable than (h, n) . The Hodgkin–Huxley equations now read

$$\begin{aligned} \varepsilon \frac{dv}{d\tau} &= [\bar{I} - \bar{g}_{Na}m^3h(v - \bar{E}_{Na}) - \bar{g}_K n^4(v - \bar{E}_K) - \bar{g}_L(v - \bar{E}_L)], \\ \frac{1}{T_m} \frac{dm}{d\tau} &= \frac{1}{\tau_m(v)}[m_\infty(v) - m], \\ \frac{1}{T_h} \frac{dh}{d\tau} &= \frac{1}{\tau_h(v)}[h_\infty(v) - h], \\ \frac{1}{T_n} \frac{dn}{d\tau} &= \frac{1}{\tau_n(v)}[n_\infty(v) - n]. \end{aligned} \tag{20.15}$$

If we define $\tilde{\varepsilon} := \frac{1}{T_m} \ll 1$, we can also observe that $\tilde{\varepsilon} \approx 1/10 \approx \sqrt{\varepsilon}$, since $\varepsilon \approx 1/100$. Using the approximation $T_h = T_n = 1$, we get

$$\begin{aligned} \varepsilon \frac{dv}{d\tau} &= [\bar{I} - \bar{g}_{Na}m^3h(v - \bar{E}_{Na}) - \bar{g}_K n^4(v - \bar{E}_K) - \bar{g}_L(v - \bar{E}_L)], \\ \sqrt{\varepsilon} \frac{dm}{d\tau} &= \frac{1}{\tau_m(v)}[m_\infty(v) - m], \\ \frac{dh}{d\tau} &= \frac{1}{\tau_h(v)}[h_\infty(v) - h], \\ \frac{dn}{d\tau} &= \frac{1}{\tau_n(v)}[n_\infty(v) - n], \end{aligned} \tag{20.16}$$

which is a three-time-scale system in standard form, where the voltage is the fastest variable, sodium activation m a fast variable, and the other two gating variables (h, n) are slow variables.

Exercise/Project 20.2.2. Investigate under which assumptions the Hodgkin–Huxley equations can be reduced to a $(1, 2)$ -fast–slow system. There are two natural choices to consider:

- (a) $1/T_m = \varepsilon$ in (20.15), so that we get a $(2, 2)$ -fast–slow system,
- (b) $1/T_m = \sqrt{\varepsilon}$, so that we get a three-scale system (20.16). \diamond

The upshot of the transformation of the Hodgkin–Huxley equations into a standard form is that we have used several assumptions about the biophysics of the system to derive relevant magnitudes of the vector field. Subsequently, suitable normalization procedures have been applied to identify the relevant time scales.

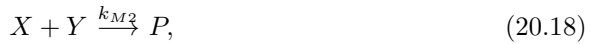
Obviously, neuroscience has evolved far beyond the original groundbreaking discovery of the Hodgkin–Huxley equations. On a very basic classification level, large classes of single-neuron models are (m, n) -fast–slow systems of the form

$$\begin{aligned} & \text{(fast voltage/spiking variables)} & \dot{x} &= \frac{1}{\varepsilon} f(x, y), \\ & \text{(slow gating/modulation variables)} & \dot{y} &= g(x, y), \end{aligned}$$

where we usually have $m \ll n$. In fact, multiple time scale dynamics has become a major paradigm in the analysis of neuronal systems in models ranging from the cellular and subcellular scale to complex networks. Networks of neurons naturally produce another multiple time scale problem, which is discussed in Section 20.11.

20.3 Chemical Oscillations

For a long time, it was suggested that chemical reactions could not display oscillations. This belief was challenged in striking fashion by experiments. A reaction playing a key role in this context is the **Belousov–Zhabotinsky reaction**, or simply **BZ reaction**. Experimental studies of the BZ reaction have shown that it exhibits mixed-mode oscillations (MMOs); see Chapter 13. Various reaction mechanisms have been proposed to model the BZ reaction. Here we shall focus only on a simplification of the **Field–Körös–Noyes (FKN) mechanism**. The chemical reactions are given by [FN74]



where (X, Y, Z) are the main chemical species to be considered, and $k_{(\cdot)} > 0$ are reaction rates. Roughly speaking, X corresponds to bromous acid, Y to bromide, Z to cerium oxide, and A, B to bromate ions. This relates the model (20.17)–(20.21) to the full FKN mechanism [R.J72]. Turning (20.17)–(20.21) into ODEs for the concentrations (x, y, z) of (X, Y, Z) , assuming constant values for A and B given by a and b , can be achieved by standard mass

action kinetics. For example, the derivative dx/dt has gain terms from (20.17) and (20.19), while the reactions (20.18) and (20.20) translate into loss terms, so that

$$x' = \frac{dx}{dt} = k_{M1}ay - k_{M2}xy + k_{M3}bx - 2k_{M4}x^2,$$

where the concentration rates become prefactors, and the polynomial terms follow directly from the reactions (20.17)–(20.20). Similar observations for y' and z' lead to the so-called **Oregonator** model

$$\begin{aligned} x' &= k_{M1}ay - k_{M2}xy + k_{M3}bx - 2k_{M4}x^2, \\ y' &= -k_{M1}ay - k_{M2}xy + k_{M5}z, \\ z' &= k_{M3}bx - k_{M5}z. \end{aligned} \quad (20.22)$$

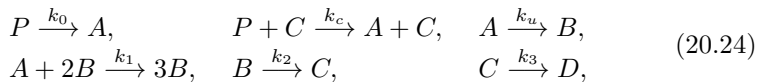
Numerical computations and a nondimensionalization of (20.22) by Field and Noyes [FN74] suggest that the Oregonator is indeed a multiple time scales system. The main ingredients for the time scale separation are the widely disparate reaction rates, e.g., reasonable choices are

$$\begin{aligned} k_{M1} &= \mathcal{O}(1), & k_{M2} &= \mathcal{O}(10^9), & k_{M3} &= \mathcal{O}(10^3), \\ k_{M4} &= \mathcal{O}(10^7), & k_{M5} &= \mathcal{O}(1), \end{aligned} \quad (20.23)$$

where suitable units are implicitly understood. A priori, it is not clear how to nondimensionalize the ODEs (20.22) or any other chemical reaction with disparate reaction time scales; see also Chapter 13. It is an excellent open-ended and application-oriented project to understand the BZ reaction mechanisms better.

Exercise/Project 20.3.1. (a) Numerically integrate (20.22) for different values of a, b and concentrations of order of magnitudes given by (20.23). Can you find a periodic solution? What about a periodic orbit with MMOs? (b) Compare the different models for the BZ reaction; see Sections 13.9 and 19.10 to get started. Do you find similar solutions for the same set of physical parameters in the different models? ◇

Another interesting fast–slow chemical system is the **autocatalator** model proposed by Petrov, Scott, and Showalter [PSS92] as a prototypical chemical system exhibiting mixed-mode oscillations. The reactions are given by



where $k_{(.)}$ are reaction rates and P is treated as a constant initial reactant making it a parameter. A direct calculation (see Exercise 20.3.2) yields three ODEs for $(x, y_1, y_2) \in (\mathbb{R}^+)^3$:

$$\begin{aligned} \varepsilon \frac{dx}{d\tau} &= y_1 x^2 + y_1 - x, \\ \frac{dy_1}{d\tau} &= \mu(\kappa + y_2) - y_1 x^2 - y_1, \\ \delta \frac{dy_2}{d\tau} &= x - y_2, \end{aligned} \quad (20.25)$$

where (μ, κ) are the main bifurcation parameters, $0 < \varepsilon \ll 1$, and we shall assume from now on that $\delta = 1$. Figure 20.4 shows a phase-space projection together with a typical MMO time series of (20.25); see also Chapter 13.

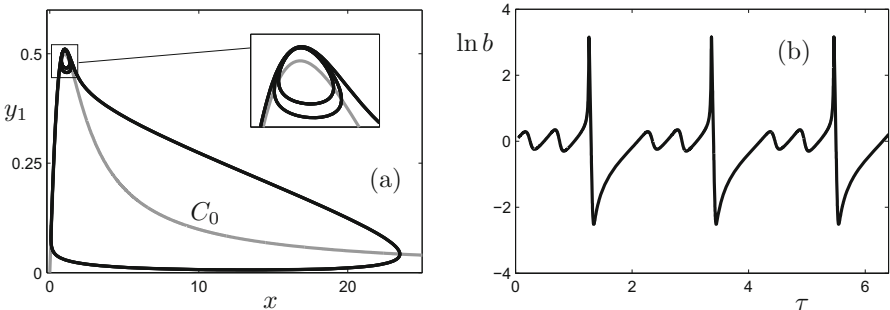


Figure 20.4: Simulation of (20.25) for $(\mu, \kappa, \varepsilon) = (0.2965, 2.5, 0.01)$ and $\delta = 1$. (a) Projection onto (x, y_1) -coordinates; in addition to the attracting MMO orbit (black), we also show the critical manifold C_0 . (b) Time series associated with the orbit in (a) displaying a 1^2 MMO.

Exercise 20.3.2. Let (a, b, c) denote the chemical concentrations of (A, B, C) . Using the laws of mass action and a nondimensionalization given by a phase-space and time scaling

$$y_1 = \left(\frac{k_1 k_u}{k_2^2} \right)^{1/2} a, \quad x = \left(\frac{k_1}{k_u} \right)^{1/2} b, \quad y_2 = \left(\frac{k_1 k_3^2}{k_u k_2^2} \right)^{1/2} c, \quad k_u t = \tau,$$

and a parameter scaling

$$\mu = \frac{k_c p}{k_3}, \quad \kappa = \frac{k_0 k_3}{k_2 k_c} \left(\frac{k_1}{k_u} \right)^{1/2}, \quad \delta = \frac{k_u}{k_3}, \quad \varepsilon = \frac{k_u}{k_2},$$

show that the reactions (20.24) yield the ODEs (20.25). \diamond

The critical manifold of (20.25) is $C_0 = \{(x, y) \in \mathbb{R}^3 : y_1 = x/(1 + x^2)\}$. Figure 20.4(a) shows that C_0 has a single fold point and that it becomes tangent to the fast direction as $x \rightarrow \infty$. These two features are the main problems to be addressed in the mathematical analysis of the autocatalator model. To analyze the loss of normal hyperbolicity, it has been suggested to focus on a $(1, 1)$ -fast–slow system given by

$$\begin{aligned} \varepsilon \dot{x} &= y - x + yx^2, \\ \dot{y} &= \bar{\mu} - y - yx^2, \end{aligned} \tag{20.26}$$

where the parameter $\bar{\mu}$ mimics some of the effects caused by c , μ , and κ in the autocatalator (20.25). The various versions of the autocatalator have led to several interesting studies with different methods; see Section 19.10. Some viewpoints are sketched in the next exercise.

Exercise/Project 20.3.3. (a) Study the models (20.25) and/or (20.26) numerically using integration, numerical continuation, and computing invariant manifolds; see Chapters 10 and 11.

- (b) Prove that the planar autocatalator (20.26) has a periodic orbit for every $\bar{\mu} > 1$ and $\varepsilon > 0$ sufficiently small. Hint: Using a blowup analysis is suitable in this context but highly nontrivial; see Chapters 7 and 8. \diamond

20.4 Lasers

The basic physical mechanism of a **laser** (an acronym for light amplification by stimulated emission of radiation) depends crucially on different time scales. The basic idea is to consider a gain (or amplifying) medium that is supplied with additional energy (“pumping”). Free photons are absorbed in the laser until their number in an excited state exceeds the number in some lower-energy state, which is called **population inversion**. In this case, emission of photons is larger than absorption, and light passing through the medium is amplified. Using the correct medium, geometrical setup, etc., this principle suffices to construct a laser [Sil04]. For our fast–slow viewpoint, the important observation is that the dynamics of laser intensity or photon density may act on a different—often faster—time scale than that of the gain medium and the carrier density. Here we shall only present two ODE models for lasers that make use of this principle.

Al-Naimee et al. [ANMC⁺09] considered a semiconductor laser in a closed-loop optical system with a nonlinear alternating current (AC) feedback loop. In an experiment, they observed a wide variety of oscillations as parameters for the feedback loop were varied. As a model, they considered standard laser rate equations [CKS94] for the photon density S and carrier density N together with a variable I for the feedback current,

$$\begin{aligned}\frac{dS}{ds} &= [g(N - N_t) - \gamma_0]S, \\ \frac{dN}{ds} &= \frac{I_0 + f_F(I)}{eV} - \gamma_c N - g(N - N_t)S, \\ \frac{dI}{ds} &= -\gamma_f I + k[g(N - N_t) - \gamma_0]S,\end{aligned}\tag{20.27}$$

where I_0 , e , V , g , N_t , γ_0 , γ_c , γ_f , k are parameters, and the function

$$f_F(I) := \frac{AI}{1 + s'I}$$

models the nonlinear amplifier feedback with parameters A and s' . A helpful affine coordinate change is given by

$$x = \frac{g}{\gamma_c}S, \quad y = \frac{g}{\gamma_0}(N - N_t), \quad z = \frac{g}{k\gamma_c}I - \frac{g}{\gamma_c}S, \quad t = \gamma_0 s.\tag{20.28}$$

Inserting (20.28) into (20.27) yields the simplified three-dimensional system

$$\begin{aligned}\frac{dx}{dt} &= x(y - 1), \\ \frac{dy}{dt} &= \gamma \left(\delta_0 - y + \alpha \frac{z+x}{1+\sigma(z+x)} - xy \right), \\ \frac{dz}{dt} &= -\varepsilon(z + x),\end{aligned}\quad (20.29)$$

where γ , δ_0 , α , σ , and ε are parameters.

Exercise/Project 20.4.1. (a) Compute the parameters in (20.29) in terms of the parameters for (20.27). (b) The parameter γ_0 represents the photon damping rate, γ_f the cutoff frequency of the high-pass filter, and γ_c the population/carrier relaxation rate. Search in the laser science literature to determine realistic values for these parameters. \diamond

Based on Exercise 20.4.1(b) and our previous description of the physical mechanisms for a laser, it is reasonable to assume that $0 < \gamma \ll 1$, so that the scaled photon density is a much faster variable than the variable y representing the gain. Typically, the AC feedback is even slower than y , so that z is a superslow variable and $0 < \varepsilon \ll \gamma \ll 1$. Numerical integration in Figure 20.5 shows a trajectory with complicated oscillatory behavior. We may hope that a multiple time scale decomposition allows us to understand these oscillations.

Rescaling time in (20.29) by $\tau := \varepsilon t$ and then considering the singular limit $\varepsilon \rightarrow 0$, we find that the 1-dimensional critical manifold C_0 is given by

$$C_0 = \left\{ (x, y, z) \in \mathbb{R}^3 : (x = 0 \text{ or } y = 1), \delta_0 + \alpha \frac{z+x}{1+\sigma(z+x)} = y(1+x) \right\}.$$

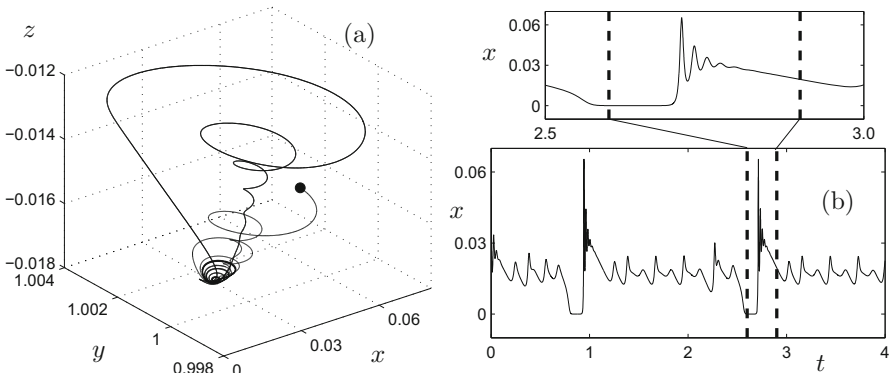


Figure 20.5: Numerical simulation of (20.29) with parameter values $\sigma = 11$, $\alpha = 1$, $\delta_0 = 1.017$, and time scale separation parameters $(\gamma, \varepsilon) = (10^{-3}, 10^{-5})$. (a) Trajectory in phase space. The initial condition is marked by a dot. (b) Time series for x of the trajectory from (a); the time axis is scaled by a factor of 10^{-5} .

The fast subsystem for $\varepsilon \rightarrow 0$ with $z' = 0$ is given by

$$\begin{aligned} x' &= x(y - 1), \\ y' &= \gamma \left(\delta_0 - y + \alpha \frac{z+x}{1+\sigma(z+x)} - xy \right), \end{aligned} \quad (20.30)$$

which is again a fast–slow system with $0 < \gamma \ll 1$ and critical manifold

$$\tilde{C}_{\gamma=0} = \tilde{C}_0 = \{(x, y) \in \mathbb{R}^2 : x(y - 1) = 0\} = \{x = 0\} \cup \{y = 1\} =: \tilde{C}_{x0} \cup \tilde{C}_{y1}.$$

The next exercise provides a guide to how to continue the dynamical analysis.

Exercise/Project 20.4.2. Consider the parameter values $(\sigma, \alpha, \delta_0) = (11, 1, 1.017)$ for (20.29) and assume that $0 < \varepsilon \ll \gamma \ll 1$.

- (a) Determine the stability of C_0 and split it into normally hyperbolic attracting, repelling, and saddle-type branches.
- (b) Find the types of the singularities where C_0 is not normally hyperbolic.
- (c) Use the fast subsystem (20.30) and its critical manifold \tilde{C}_0 to determine the switching between different branches of C_0 computed in (a)–(b).

Furthermore, reproduce Figure 20.5(a) and visualize your results from this exercise, including possible candidate orbits, in the plot. ◇

Another example of fast–slow laser dynamics is the **Yamada model** [Yam93, DK99, DKL99] of a laser with a saturable absorber. In this case, it is interesting to consider the dynamics via the population density $y_1 \geq 0$ in the absorbing medium as well as the population density $y_2 \geq 0$ in the amplifying medium. Physical principles suggest, as above, that the dynamics of $y = (y_1, y_2)$ should be slower than the laser intensity variable $x \geq 0$. The Yamada model considers the following rate equations for the interaction of x and y :

$$\begin{aligned} x' &= (y_1 - y_2 - 1)x \\ y'_1 &= \varepsilon(A - y_1 - y_1 x), \\ y'_2 &= \varepsilon(B - y_2 - ay_2 x), \end{aligned} \quad (20.31)$$

where (A, B, a) are parameters and $0 < \varepsilon \ll 1$ is the time scale separation (with typical values of order $\mathcal{O}(10^{-3})$, as for the previous laser model). A detailed analysis of (20.31) is beyond the scope of this book. However, it is of interest to note that numerical bifurcation analysis [DK99, DKL99], geometric methods [HS05, KE03], as well as asymptotic matching [Ern88, EGPS99] have been applied to analyzing (20.31). It would certainly be an interesting, and open-ended, project to study differences, similarities, and interactions among the different methods.

20.5 Ecology

Among the most famous models of mathematical ecology are various versions of **predator–prey** models. The simplest forms involve two species, a prey X and a predator Y . A classical model describing evolution of the associated population densities (x, y) is the **Rosenzweig–MacArthur model** [RM63]. There is also a fast–slow version of this model considered by Rinaldi and Muratori [RM92],

$$\begin{aligned}\frac{dx}{dt} &= x' = x \left(1 - \frac{x}{K} - \frac{ay}{x+d}\right), \\ \frac{dy}{dt} &= y' = \varepsilon y \left(\frac{ax}{x+d} - \kappa\right),\end{aligned}\tag{20.32}$$

where (a, d, K, κ) are positive parameters and it is a natural ecological assumption that the densities (x, y) are nonnegative; for now, we shall always assume for simplicity that

$$K = 1 \quad \text{and} \quad \kappa = 1.\tag{20.33}$$

The parameter $\varepsilon > 0$ can be interpreted as the ratio between the linear death rate of the predator and the linear growth rate of the prey. If predators live very long and encounter many different generations of prey, it is a natural assumption that $0 < \varepsilon \ll 1$. For example, hares and squirrels reproduce much faster than their predators, such as lynx and coyotes. Obviously, not all predator–prey systems satisfy this assumption, and the predator variable could be fast in comparison to the prey variable; a standard example for this scenario is the spruce–budworm system [LJH78]. The critical set C_0 and y -nullcline \mathcal{L}_y of (20.32) are

$$\begin{aligned}C_0 &= \{(x, y) \in (\mathbb{R}_0^+)^2 : x = 0 \text{ or } y = (1/a)(x + d)(1 - x) =: c_0(x)\}, \\ \mathcal{L}_y &= \{(x, y) \in (\mathbb{R}_0^+)^2 : y = 0 \text{ or } ax = x + d\}.\end{aligned}$$

Note that the sets $\{x \geq 0\} \subset C_0$ and $\{y \geq 0\} \subset \mathcal{L}_y$ guarantee that the population densities remain nonnegative. However, they also present a typical challenge for fast–slow ecological systems, since some of the relevant invariant manifolds lie exactly at the domain boundary. Figure 20.6 shows a numerical integration toward an attracting periodic orbit for (20.32) and $(\varepsilon, a, d, K, \kappa) = (0.01, 4, 0.5, 1, 1)$. A candidate for $\varepsilon = 0$ is shown as well, together with a fold point $(x, y) = (1/4, c_0(1/4))$ and a transcritical point $(x, y) = (0, c_0(0))$. Observe that the candidate orbits pass through both points.

Exercise/Project 20.5.1. Fix $(a, d) = (4, 0.5)$ and consider (20.32).

- (a) Use methods for scaling/delay (Chapter 12) to analyze the transcritical point.
- (b) Use blowup (Chapters 7 and 8) to prove existence of a periodic orbit.
- (c) Use the Conley index (Chapter 16) to prove existence of a periodic orbit.

Now drop the assumption $(a, d) = (4, 0.5)$ and try to generalize your results from (a)–(c). Consider numerical continuation to analyze the (a, d) -parameter space. ◇

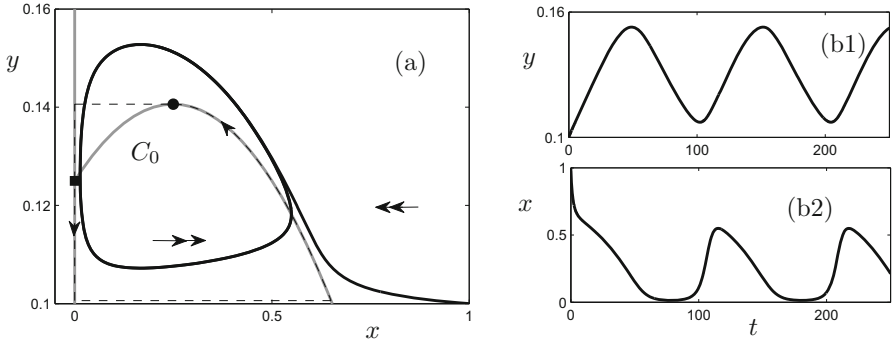


Figure 20.6: Numerical simulation of (20.32) starting at $(x(0), y(0)) = (1, 0.1)$ with parameter values $(\varepsilon, a, d, K, \kappa) = (0.01, 4, 0.5, 1, 1)$. (a) Phase space: the trajectory is shown in black, the critical set C_0 in gray. A possible candidate orbit is shown as a dashed curve. The fold point (black dot) and transcritical point (black square) are marked as well.

Another important origin of time scale separation in ecology arises if one wants to study population and **evolutionary dynamics** simultaneously. We briefly outline some standard modeling techniques for evolutionary dynamics under the assumptions of rare mutations [MGM⁺91, DL96]. Let u be a **trait** of some species X with per capita birth rate β and assume that the associated population density x is at equilibrium $x = x^*$. Denote the mutant trait by \bar{u} and the instantaneous per capita rate of increase by R . Then the **canonical equation of adaptive dynamics** is

$$\frac{du}{dt} = u' = k(\beta x^*) \left(\frac{r}{\beta} \right), \quad \text{with } r := \left. \frac{\partial R}{\partial \bar{u}} \right|_{\bar{u}=u}, \quad (20.34)$$

where $k > 0$ is a constant proportional to the probability that an offspring is a mutant. We shall not be concerned here with the reasoning to derive (20.34) from biological modeling but only make the important observation that $k > 0$ is another time scale. Therefore, under the assumptions of modeling trait dynamics by (20.34), a natural multiple time scale structure arises by the inclusion of evolution.

Furthermore, it is quite remarkable that fast–slow systems can be used to improve the modeling ansatz (20.34) and to weaken the assumption $x = x^*$. Suppose the population dynamics have an attracting limit cycle $x = x^*(s)$ with $x^*(s) = x^*(s + T)$. Then it has been suggested to replace (20.34) by

$$u' = k \langle \beta x^* \rangle \left\langle \frac{r}{\beta} \right\rangle, \quad (20.35)$$

where the angle brackets denote temporal averaging over the limit cycle

$$\langle \cdot \rangle := 1/T \int_0^T (\cdot) \, ds.$$

To get a closed-form ODE from (20.35), one has to calculate the temporal average. If the limit cycle arises from a singular limit candidate solution—see, for example, Figure 20.6—then the candidate can be used as an approximation that simplifies the temporal averaging. This idea has been worked out by Dercole et al. [DFGR06]. Consider fast–slow predator–prey dynamics given by the Rosenzweig–MacArthur model (20.32) and associate to each population (X, Y) a single trait (u, v) . The interaction between population and evolutionary dynamics is modeled by considering

$$\begin{aligned} K = K(u) &= 2K_0 \left[\left(\frac{u}{u_0} \right)^2 + \left(\frac{u_0}{u} \right)^2 \right]^{-1}, \\ \kappa = \kappa(v) &= 2\kappa_0 \left[\left(\frac{v}{v_0} \right)^2 + \left(\frac{v_0}{v} \right)^2 \right]^{-1}, \\ d = d(u, v) &= d_0 + d_1(u - v)^2, \end{aligned}$$

where subscripts indicate parameters. The resulting four-variable system is

$$\begin{aligned} x' &= x \left(1 - \frac{x}{K} - \frac{ay}{x+d} \right), \\ y' &= \varepsilon_1 y \left(\frac{ax}{x+d} - \kappa \right), \\ u' &= \varepsilon_2 \langle x^* \rangle \langle r^u \rangle, \\ v' &= \varepsilon_3 \left\langle \frac{ax}{d+x} x^* \right\rangle \left\langle \frac{r^v}{\frac{ax}{d+x}} \right\rangle, \end{aligned} \tag{20.36}$$

where the superscripts indicate the different traits for r , and $\varepsilon_{1,2,3}$ are time scales. An analysis of (20.36) is beyond our goals here, but the next exercise sketches some directions.

- Exercise/Project 20.5.2.** (a) Perform a (partial) bifurcation analysis of (20.36) and prove that there exist parameter regions with a globally stable equilibrium point and regions with a globally stable limit cycle (cf. Exercise 20.5.1).
- (b) Choose one primary bifurcation parameter and investigate (20.36) in the stable equilibrium regime for different multiple scale structures, e.g., consider $0 < \varepsilon_2 \approx \varepsilon_3 \ll \varepsilon_1 \ll 1$ or other reasonable biological scalings.
- (c) Use the singular candidate orbit from Exercise 20.5.1 to compute the time averages in (20.36) to get ODEs for (u, v) . \diamond

20.6 Pattern Formation

A fascinating example of pattern formation occurs for hydras (a fresh-water polyp). Morphogenesis allows hydras to regenerate. For example, if its original head is removed, a new one is automatically grown. One suggested mechanism

for this phenomenon consists in a slowly diffusing activator initiating the growth of a head coupled to a rapidly diffusing inhibitor, which prevents the formation of a second head. Based on these assumptions, Gierer and Meinhardt [GM72] proposed a reaction–diffusion system for $u = u(z, s)$, $v = v(z, s)$ with $(z, s) \in \mathbb{R} \times \mathbb{R}_0^+$ given by

$$\begin{cases} \varepsilon^2 \frac{\partial u}{\partial s} = \frac{\partial^2 u}{\partial z^2} - \varepsilon^2 \mu u + v^2, \\ \frac{\partial v}{\partial s} = \varepsilon^2 \frac{\partial^2 v}{\partial z^2} - v + \frac{v^2}{u}, \end{cases} \quad (20.37)$$

which is now also known as the **Gierer–Meinhardt equation**. Obviously, we shall assume that $0 < \varepsilon \ll 1$ and note that the small parameter arises due to the considered difference in diffusion time scales; for biological reasons, we are also going to assume that $u, v \geq 0$. A first step in the analysis of (20.37) is to integrate the PDE, say with Neumann boundary conditions on a fixed interval

$$x \in [0, L], \quad \frac{\partial u}{\partial z}(0, 0) = 0 = \frac{\partial u}{\partial z}(L, 0), \quad \frac{\partial v}{\partial z}(0, 0) = 0 = \frac{\partial v}{\partial z}(L, 0).$$

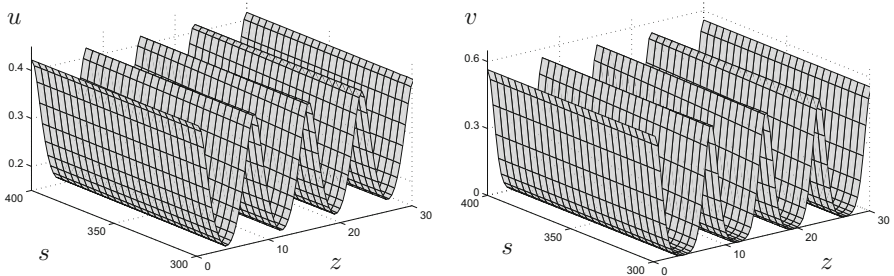


Figure 20.7: Integration of the Gierer–Meinhardt PDE (20.37) with $(\mu, \varepsilon) = (1, 0.5)$ for $(z, s) \in [0, 30] \times [0, 400]$ on a coarse mesh with initial condition $u(z, 0) \equiv 1 \equiv v(z, 0)$.

Figure 20.7 shows the results of numerical integration. After an initial transient, solutions seem to decay toward a stationary, spatially periodic pattern. This motivates studying the stationary version of (20.37) with $u_s = 0 = v_s$ and to look for periodic orbits in the resulting ODEs. Using the notation

$$x_1 := v, \quad x_2 := \varepsilon \frac{dv}{dz}, \quad y_1 := u, \quad y_2 := \frac{du}{dz},$$

we get, after a short calculation, the $(2, 2)$ -fast–slow system

$$\begin{aligned} \varepsilon \dot{x}_1 &= x_2, \\ \varepsilon \dot{x}_2 &= x_1 - \frac{x_1^2}{y_1}, \\ \dot{y}_1 &= y_2, \\ \dot{y}_2 &= -x_1^2 + \varepsilon^2 \mu y_1, \end{aligned} \quad (20.38)$$

where we have set $\frac{d}{dz} = \cdot = \frac{d}{d\tau}$. The critical set of (20.38) is

$$C_0 = \{(x_1, x_2, y_1, y_2) \in \mathbb{R}^+ \times \mathbb{R} \times \mathbb{R}^+ \times \mathbb{R} : x_2 = 0, x_1 = 0 \text{ or } x_2 = 0, x_1 = y_1\}.$$

Consider a compact 2-dimensional submanifold $M_0 \subset \{x_1 = 0 = x_2, y_1 > 0\} \subset C_0$ and observe that M_0 is a normally hyperbolic manifold of saddle type. The slow and fast subsystems are

$$\begin{cases} \dot{y}_1 = y_2, \\ \dot{y}_2 = 0, \end{cases} \quad \text{and} \quad \begin{cases} x'_1 = x_2, \\ x'_2 = x_1 - \frac{x_1^2}{y_1}, \end{cases} \quad (20.39)$$

where $' = \frac{d}{dt}$ for $\varepsilon t = \tau$. Figure 20.8 shows the phase portraits of the fast and slow subsystems. The slow flow has a degenerate line of equilibria. For $y_1 = 1$, the fast flow has a homoclinic orbit to a saddle point at the origin that is expected to break under perturbation.

Exercise/Project 20.6.1. (a) Prove that the fast subsystem has a homoclinic orbit for $y_1 = 1$. Then generalize the result to $y_1 \neq 1$. (b) Prove that the three-dimensional manifolds $W^s(M_0)$ and $W^u(M_0)$ coincide. \diamond

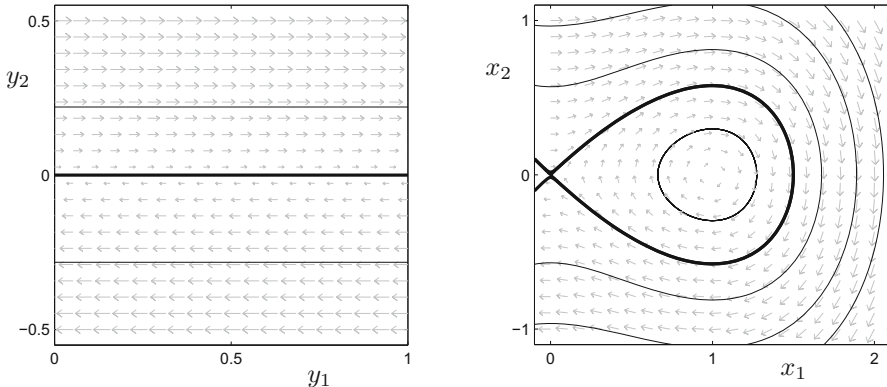


Figure 20.8: Phase flows for the slow and fast subsystems (20.39) of the Gierer–Meinhardt model. The slow flow (left) has a line of equilibrium points $\{y_2 = 0\}$. The fast flow (right) is shown for $y_1 = 1$.

The previous observations and Exercise 20.6.1 show that the situation is quite degenerate for $\varepsilon = 0$. A special feature of the Gierer–Meinhardt model is that there is an elegant way to analyze the situation for $\varepsilon > 0$ directly [Hek10]. First, observe that M_0 is invariant not only for the slow flow but also for the full system (20.38) for every $\varepsilon > 0$. This implies that the slow manifold M_ε is equal to the critical manifold M_0 . Moreover, the flow on M_ε is

$$\begin{aligned} \dot{y}_1 &= y_2, \\ \dot{y}_2 &= \varepsilon^2 \mu y_1. \end{aligned} \quad (20.40)$$

It is instructive to sketch the flow (20.40) as a perturbation to the slow flow shown in Figure 20.8. The line of equilibria for the slow flow is reduced to an equilibrium at $(0,0)$. It is also expected that the stable and unstable manifolds $W^s(M_\varepsilon)$ and $W^u(M_\varepsilon)$ no longer coincide.

Exercise/Project 20.6.2. (a) Prove that $W^s(M_\varepsilon) \cap W^u(M_\varepsilon)$ is a two-dimensional set. Hint: Use Melnikov theory. Therefore, $W^s(M_\varepsilon) \cap W^u(M_\varepsilon)$ consists of a 1-parameter family of orbits that are biasymptotic to M_ε in forward and backward time.

- (b) Use a trajectory segment of the flow (20.40), which is a perturbation of the slow flow, and a biasymptotic orbit from (a) to sketch a possible periodic orbit for (20.38).

What other types of orbits can be constructed? \diamond

Another important example for a pattern-forming system is the **Barkley model** [Bar91]

$$\begin{cases} \frac{\partial u}{\partial s} = \kappa \Delta_{zz} u + \frac{1}{\varepsilon} u(1-u)(u-(v+b)/a), \\ \frac{\partial v}{\partial s} = u - v, \end{cases} \quad (20.41)$$

where $z \in \mathbb{R}^2$, Δ_{zz} is the Laplacian, (a, b, κ) are parameters, $0 < \varepsilon \ll 1$, and $u = u(z, s)$, $v = v(z, s)$ are the unknown functions. The PDE (20.41) is a toy model for a reaction–diffusion model of an excitable system; in many respects, it is similar to the FitzHugh–Nagumo equation. In the case of no diffusion, $\kappa = 0$, the Barkley model is a $(1, 1)$ -fast–slow system

$$\begin{cases} \varepsilon \dot{u} = u(1-u)(u-(v+b)/a) =: f(u, v), \\ \dot{v} = u - v =: g(u, v), \end{cases} \quad (20.42)$$

with critical set C_0 given by

$$C_0 = \{(u, v) \in \mathbb{R}^2 : u = 0 \text{ or } u = 1 \text{ or } v = au - b\}.$$

The critical set C_0 is a normally hyperbolic manifold away from two transcritical points $(0, -b)$ and $(1, a - b)$; see Figure 20.9(b). Let us consider the parameter set

$$a = 0.75, \quad b = 0.02, \quad \varepsilon = 0.05. \quad (20.43)$$

Then the only global equilibrium point $(u^*, v^*) = (0, 0)$ of (20.42) is a stable node. The fast–slow structure suggests that all bounded orbits of (20.42) tend to (u^*, v^*) . However, the stable node is very close to an unstable branch of the critical manifold given by $C_m := C_0 \cap \{0 < u < 1\}$. Therefore, it is conceivable that the PDE (20.41), with $\kappa > 0$, generates nonstationary solutions due to diffusion. That this is indeed the case is shown in Figure 20.9, where a time snapshot of $v(z, s)$ shows a **spiral wave pattern**.

Exercise/Project 20.6.3. (a) Integrate numerically the PDE (20.41) and plot the time series $u(z, s)$ and $v(z, s)$ for some fixed spatial point.

- (b) Now consider a one-dimensional cut in (z_1, z_2) and plot the values of u and v on this cut for different time points.

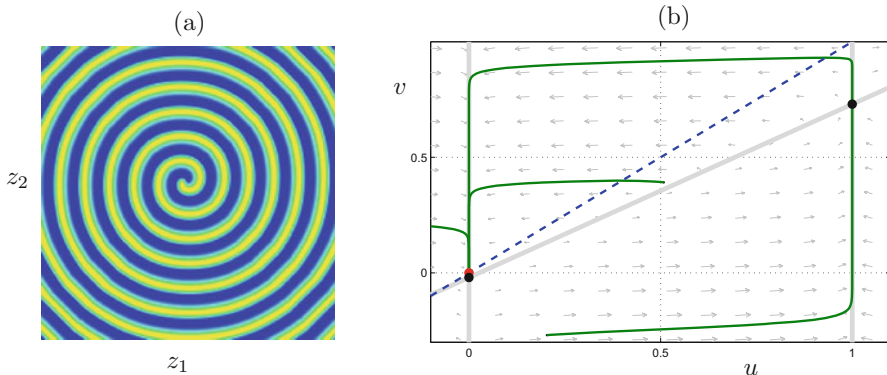


Figure 20.9: The Barkley model for parameter values (20.43). (a) Spiral wave pattern for $\kappa = 1$ of the PDE (20.41). The colors indicate different values of the function $v(z, s)$ for a fixed time s ; computations were carried out using software developed by Barkley [Bar91, Bar97]. (b) Fast–slow decomposition of the ODE (20.42). The critical manifold C_0 (gray), the v -nullcline (dashed blue), the two transcritical points (black), the equilibrium point (red), and several forward-integration trajectories (green) are shown.

- (c) How do the observed patterns in (a)–(b) relate to the fast–slow structure of the ODE (20.42)? Simulate the PDE for larger values of ε and also for larger values of b so that the fast–slow excitable system structure is no longer present. Can you find nonstationary patterns in this case?
- (d) Replace the functions $f(u, v)$ and $g(u, v)$ in (20.41) by FitzHugh–Nagumo-type functions (see Section 1.4) to obtain a cubic critical manifold. Compare numerical results for this system to the Barkley model. ◇

20.7 Celestial Mechanics

The motion of a single planet around the sun, the **two-body problem**, is one of the most basic systems of planetary motion. Neglecting the influence of all other planets, consider the motion in a plane in polar coordinates (r, θ) with the sun at the center; see Figure 20.10(a). A straightforward calculation (see Exercise 20.7.1) yields that the radial and transverse components of the planet’s acceleration are

$$a_r = \frac{d^2 r}{dt^2} - r \left(\frac{d\theta}{dt} \right)^2 \quad \text{and} \quad a_\theta = \frac{1}{r} \frac{d}{dt} \left(r^2 \frac{d\theta}{dt} \right). \quad (20.44)$$

Exercise 20.7.1. Define radial and transverse vectors $v_r = (\cos \theta, \sin \theta)^\top$ and $v_\theta = (-\sin \theta, \cos \theta)^\top$. Note that the position is rv_r , where $r \in [0, \infty)$ is the radius and $\theta = \theta(t)$, $r = r(t)$ are time-dependent. Now calculate the velocities and accelerations in the radial and transverse directions. ◇

Newton's law of universal gravitation states that $F = G \frac{Mm}{r^2}$, where F is the attractive force, G the gravitational constant, and M, m the masses of the sun and the planet. Combining this law with (20.44) gives

$$-G \frac{Mm}{r^2} = \frac{d^2r}{dt^2} - r \left(\frac{d\theta}{dt} \right)^2, \quad (20.45)$$

$$0 = \frac{1}{r} \frac{d}{dt} \left(r^2 \frac{d\theta}{dt} \right). \quad (20.46)$$

Integrating (20.46) once yields **Kepler's second law**

$$r^2 \frac{d\theta}{dt} = \text{constant} =: \nu.$$

To determine the actual trajectory $r(\theta)$, a helpful definition is $u(\theta) := 1/r(\theta)$. We get via direct differentiation that

$$\frac{du}{d\theta} = \frac{\frac{du}{dt}}{\frac{d\theta}{dt}} = -\frac{1}{r^2} \frac{\frac{dr}{dt}}{\frac{d\theta}{dt}} = -\frac{1}{\nu} \frac{dr}{dt},$$

using Kepler's second law. Hence, differentiating again yields

$$\frac{d^2u}{d\theta^2} = \frac{d}{dt} \frac{\frac{du}{d\theta}}{\frac{d\theta}{dt}} = -\frac{r^2}{\nu^2} \frac{d^2r}{dt^2}.$$

Finally, we can also use (20.45) in the last equation to obtain

$$\frac{d^2u}{d\theta^2} + u = G \frac{Mm}{\nu^2},$$

which can be simplified by introducing a characteristic distance \bar{r} via $w = \bar{r}u$, so that

$$\frac{d^2w}{d\theta^2} + w = K, \quad (20.47)$$

where $K = G \frac{Mm\bar{r}}{\nu^2}$ is a constant. Obviously, the equation (20.47), say with initial conditions $w(0) = p_0$ and $dw/dt(0) = v_0$, can be solved explicitly via variation of constants, giving the expected classical ellipsoidal solutions for the planet. However, we have actually made a “mistake” in the derivation of (20.47), since Newton's law of gravitation is not quite as universal as the name suggests. In fact, general relativity predicts [JF96, Ber60] that equation (20.47) has to be modified to

$$\frac{d^2w}{d\theta^2} + w = K + \varepsilon w^2, \quad \text{where } 0 < \varepsilon \ll 1. \quad (20.48)$$

Remark: It is important to point out that the situation we have just encountered is not special to celestial mechanics. When we model any system, we frequently neglect the influence of certain effects that usually have slowly varying or “small” contributions. This means that a fast–slow systems approach is very natural for including such effects into a model.

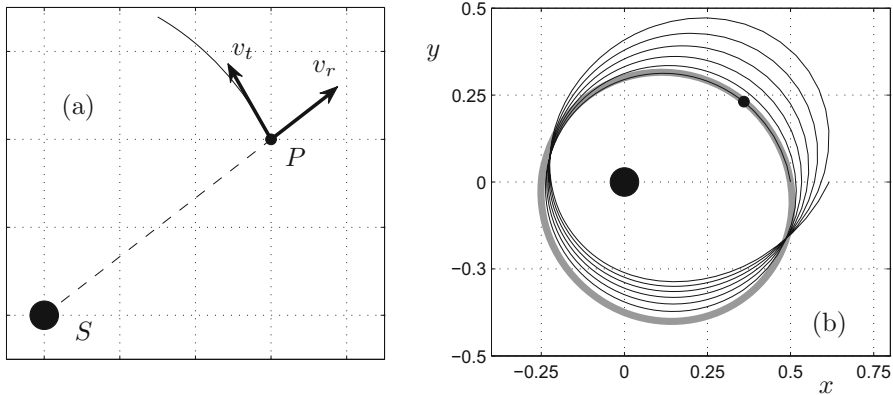


Figure 20.10: Two-body problem. (a) Sketch of the sun (S) and planet (P) two-body problem with transverse and radial component vectors v_t and v_r for the planet's movement. (b) Solution (gray) of (20.48) for $\varepsilon = 0$ and $w(0) = 2$, $dw/dt(0) = \frac{1}{3}$, and $K = 3$ and naive approximation (black) from (20.50) with $\varepsilon = 0.01$ for $\theta \in [0, 12\pi]$.

A first step in approximating the solution of (20.48) is to assume that

$$w(\theta) = w_0(\theta) + \varepsilon w_1(\theta) + \mathcal{O}(\varepsilon^2) \quad (20.49)$$

and to insert this formal expansion into (20.48).

Exercise 20.7.2. Prove that the first two terms in (20.49) are given by

$$\begin{aligned} w_0(\theta) &= K + (p_0 - K) \cos \theta + v_0 \sin \theta, \\ w_1(\theta) &= K(p_0 - K)\theta \sin \theta - Kv_0\theta \cos \theta + \dots, \end{aligned} \quad (20.50)$$

and note carefully that $w_1(\theta)$ contains terms that grow in θ . \diamond

The result (20.50) shows that the naive asymptotic series approach produces terms growing in θ , so-called **secular terms**. We already encountered secular terms in Section 9.8. Now we can explain the terminology as originating from celestial mechanics.

Exercise 20.7.3. Consider the ODE (20.48) with $w(0) = 2$, $dw/dt(0) = \frac{1}{3}$ for $0 < \varepsilon \ll 1$, and $K = 3$. Figure 20.10(b) shows a plot of the naive asymptotic expansion from Exercise 20.7.2 containing secular terms as well as the solutions for $\varepsilon = 0$.

- (a) Use the method of multiple scales (or two-timing) from Section 9.8 to derive an asymptotic solution that is uniformly valid up to $\theta = \mathcal{O}(1/\varepsilon)$.
- (b) Numerically integrate the problem for $\varepsilon = 0.01$ with schemes from Chapter 10 for different step sizes.

Compare your results from (a) and (b). \diamond

20.8 Systems Biology

In contrast to many classical approaches in biology, systems biology aims at an integrated or networks perspective of organisms and biological processes. Usually, several coupled processes are studied. The goal is to infer global functioning mechanisms from the interaction of genes, enzymes, proteins, metabolites, and many other biological components. Due to the variety of components, it is natural to expect that multiple time scales will arise. Furthermore, the neuroscience models discussed in Section 20.2 as well as the networks approach in Section 20.11 deeply link with systems biology. Here we shall look at only two models that provide a flavor of the subject.

The first system we discuss is due to Goldbeter [Gol91, Gol97]; it models **mitotic oscillations** in eukaryotes. Omitting the biological details, Goldbeter considers three variables (X, M, C) that are involved in triggering mitosis; C models a protein called cyclin, which beyond a threshold, causes the activation of the enzyme cdc2 kinase. The variable M is the fraction of active cdc2 kinase. The remaining variable X models the fraction of active cyclin protease, another enzyme. Goldbeter proposed a minimal model for mitosis given by the ODEs

$$\begin{aligned}\frac{dX}{dt} &= X' = V_3(M) \frac{1-X}{K_3+1-X} - V_4 \frac{X}{K_4+X}, \\ \frac{dM}{dt} &= M' = V_1(C) \frac{1-M}{K_1+1-M} - V_2 \frac{M}{K_2+M}, \\ \frac{dC}{dt} &= C' = v_i - v_d X \frac{C}{K_d+C} - k_d C,\end{aligned}\tag{20.51}$$

where $V_1(C) = V_{M1}C/(K_c+C)$, $V_3(M) = V_{M3}M$, and all subscripted quantities in (20.51) are parameters. The most common terms in (20.51) are fractions representing **Michaelis–Menten-type** kinetics. The parameters K_i for $i \in \{1, 2, 3, 4\}$ are also called Michaelis constants, which are often taken as small parameters, so let us set $\varepsilon := K_1 = K_2 = K_3 = K_4$. Figure 20.11(a) shows a time series of (20.51) with fast–slow behavior. Hence, it is natural to consider the limit $K_i = \varepsilon \rightarrow 0$ in (20.51), which yields

$$\begin{aligned}X' &= V_3(M) - V_4, \\ M' &= V_1(C) - V_2, \\ C' &= v_i - v_d X \frac{C}{K_d+C} - k_d C.\end{aligned}\tag{20.52}$$

All three variables in (20.52) have nontrivial dynamics. In particular, the original equation (20.51), despite being intrinsically a fast–slow system, is not in standard form. Figure 20.11(b) shows the approach of a trajectory toward a periodic orbit. Parts of the periodic orbit are slow segments that seem to transition through four planes,

$$\dots \xrightarrow{\text{fast}} \{M = 0\} \xrightarrow{\text{slow}} \{X = 0\} \xrightarrow{\text{fast}} \{M = 1\} \xrightarrow{\text{slow}} \{X = 1\} \xrightarrow{\text{fast}} \dots,$$

where transitions can be either fast jumps between planes or slow sliding near the edges $\{X = 0 = M\}$ and $\{X = 1 = M\}$, and the movement on the planes is slow. Kosiuk and Szmolyan analyzed (20.51) with GSPT techniques [KS13],

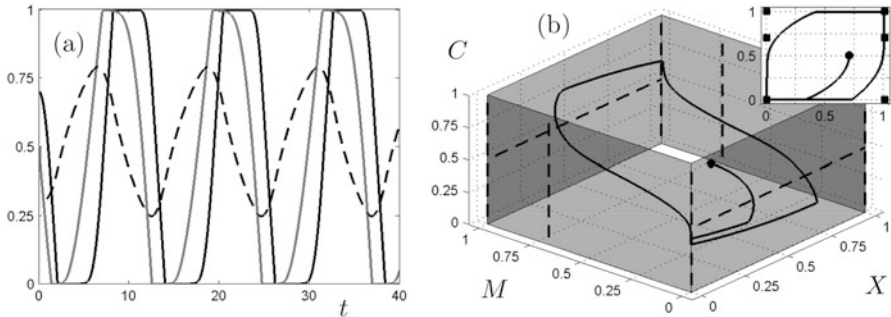


Figure 20.11: Mitotic oscillator (20.51) for parameters $\varepsilon = 0.001$, $V_{M1} = 3$, $V_2 = 1.5$, $V_{M3} = 1$, $V_4 = 0.5$, $v_i = 0.25$, $v_d = 0.25$, $K_c = 0.5$, $K_d = 0$, and $k_d = 0.25$. (a) Time series of X (solid black), M (solid gray), and C (dashed black). (b) Phase space with trajectory (black) starting at $(0.7, 0.5, 0.3)$ (black dot) and approaching a periodic orbit. The critical manifolds/planes (gray) and several nonhyperbolic lines (dashed black) are shown as well. The inset shows a projection onto (X, M) -space, where the squares (black) mark projections of the vertical nonhyperbolic lines.

building on the intuitive idea of jumps and slides we just described. The next project will guide you through the first few steps of the analysis in [KS13]. The calculations are going to show that although the mitotic oscillator is not in standard form, the methods of GSPT can still be applied.

Exercise/Project 20.8.1. Consider the mitotic oscillator (20.51) with standard parameters as given in Figure 20.11 but with $0 < \varepsilon \ll 1$ as a free timescale parameter.

- Apply a time rescaling $t = s(\varepsilon + 1 - M)(\varepsilon + 1 - X)(\varepsilon + M)(\varepsilon + X)$ to (20.51) and compute the resulting polynomial vector field.
- Starting from the result in (a), consider $\varepsilon = 0$ and view the resulting equations as the fast subsystem.
- Compute the critical sets (manifolds) as equilibrium points of the fast subsystem; see Figure 20.11(b). Compute where the manifolds are normally hyperbolic attracting or repelling.
- Can you construct a candidate orbit for a limit cycle? \diamond

Another interesting topic within the realm of systems biology is to understand the **sleep–wake cycle**, particularly in the context of the circadian rhythm. We consider a model proposed in [RBT10]. It aims at modeling the switching between sleep and wake phases as well as REM and NREM sleep phases. Experimental evidence suggests that the four phases are associated with different neuronal populations that are modeled by a single **Morris–Lecar equation**, each

$$\begin{aligned}\delta_i \dot{x}_i &= \sigma_i [f(x_i, y_i) + h_i(X, t) + I_i], \\ \dot{y}_i &= \sigma_i [g_i(x_i, y_i)],\end{aligned}\quad \text{for } i \in \{1, 2, 3, 4\}, \quad (20.53)$$

with parameters $\sigma_i, \delta_i, I_i > 0$, where (x_i, y_i) are voltage and gating variables respectively; the vector X is defined below. The functions $f, g_i : \mathbb{R}^2 \rightarrow \mathbb{R}$ are given by

$$f(x, y) = 3x - x^3 + 2 - y \quad \text{and} \quad g_i(x, y) = \frac{\varepsilon_i}{\tau_i(x)} (\gamma_i H_\infty(x) - y), \quad (20.54)$$

where $H_\infty(x) = \frac{1}{2} \tanh(x/0.01)$ is a smoothed Heaviside function, $\varepsilon_i, \gamma_i > 0$ are parameters, and $\tau_i(x) = \tau_{i,1} - (\tau_{2,i} - \tau_{i,1})H_\infty(x)$. The functions h_i basically represent input currents and will be discussed later. Notice carefully that the timescale separation in (20.54) is assumed to be state-dependent due to the functions $\tau_i(x)$. Disregarding this state-dependence and the influence of h_i , the fast–slow structure of the Morris–Lecar model is quite classical, with a cubic critical manifold and a monotone y -nullcline; see Figure 20.12(a). Therefore, each uncoupled population (x_i, y_i) can act as a relaxation oscillator—or switch—representing the two states of the four phases.

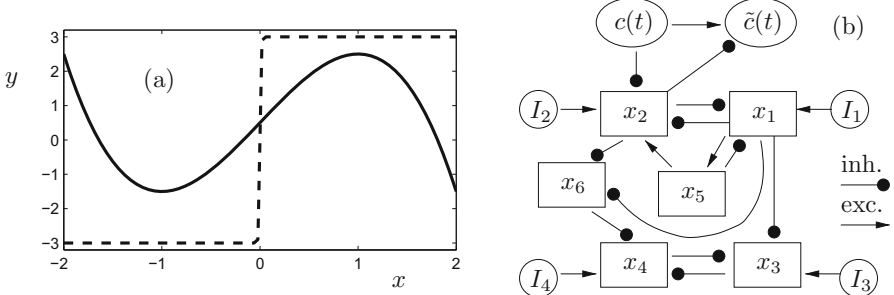


Figure 20.12: Sleep/wake cycle model. (a) Morris–Lecar model (20.53)–(20.54) geometry: critical manifold (solid) and y -nullcline (dashed) are shown. (b) System diagram for the sleep/wake model showing the interaction between the four neuron groups (x_i, y_i) , represented by the voltage variables, and the two auxiliary variables $x_{5,6}$. Also shown are background cortical activities $I_{1,2}$, the influence of the circadian rhythm $c(t)$, and orexin neurons $\tilde{c}(t)$. Inhibition and excitation are indicated via dots and arrows, respectively.

The key modeling task is to specify the interactions. Two auxiliary variables (x_5, x_6) are introduced to model a “special” portion of the (x_1, y_1) -population and the homeostat of the sleep/wake cycle respectively; we let $X = (x_1, \dots, x_6)$. The circadian rhythm is introduced via a time-periodic function $c(t)$ with 24-hour period, which explains why h_i is nonautonomous. Hence, the total model is a 10-dimensional nonautonomous multiple time scale system with additional input current parameters I , which we do not discuss here. To visualize the interactions $h_i(X, t) + I_i$, it is common practice in systems biology to represent

interactions in a network diagram as shown in Figure 20.12(b). **Inhibitory** connections indicate a counteracting process, e.g., the wake-promoting cells (x_1, y_1) inhibit the sleep-promoting cells (x_2, y_2) and vice versa, thereby creating a switch. **Excitatory** connections increase the processes that they influence. For example, the background cortical activities I_i are assumed to provide external excitation, appearing as positive (or additive) factors.

Exercise/Project 20.8.2. Consider a medium-to-large-scale systems biology model, say differential equations with at least five variables, from a recent research paper of your choice; denote this paper by (*). For example, you could begin with the detailed version of the model we sketched here [RBT10].

- (a) Implement a numerical integrator for the parameter sets given in (*).
- (b) Reproduce/check the behavior described in (*) numerically. What about dependence on initial conditions?
- (c) Use the reduction methods from Chapter 11 to determine fast and slow variables and find slow manifolds. ◇

20.9 Fluid Dynamics

Problems arising in fluid dynamics have played a pivotal role in recognizing the importance of small parameters and singularly perturbed problems. Starting from the original work of Prandtl [Pra05] in 1905, there has been great high interest in asymptotic solutions for fluid dynamics ever since. An extensive number of problems in the area involve multiple time or multiple spatial scales and often even both. Here we shall just present a few fluid dynamics examples in which a clear multiple time scale structure emerges; for some further references, see Section 19.10.

The first problem we consider is radially symmetric flow in a wedge of angle α with plane walls, also called **Jeffrey–Hamel flow**, with constant flow rate per unit width; see Figure 20.13(a). Center the vertex at the origin and consider polar coordinates (r, θ) . Since the flow was assumed to be radial, the tangential velocities are zero, and we have only to consider the radial velocity $v_r = \tilde{f}(r, \theta)$. From conservation of mass, it can be concluded (see, e.g., [Pan05]) that $\tilde{f}(r, \theta) = f(\theta)/r$ for some function f . It will be convenient to normalize the velocity by the centerline velocity $f(r, 0)$ and to scale the angle to lie in the unit interval

$$F(\theta) := \frac{f(\theta)}{f(0)}, \quad \eta := \frac{\theta}{\alpha}. \quad (20.55)$$

Then it can be shown (see, e.g. [Pan05], pp. 336–338 or [Bat67], pp. 294–296) that the Navier–Stokes PDE reduces to an ODE given by

$$\frac{d^3 F}{d\eta^3} + 2\alpha \operatorname{Re} F \frac{dF}{d\eta} + 4\alpha^2 \frac{dF}{d\eta} = 0, \quad (20.56)$$

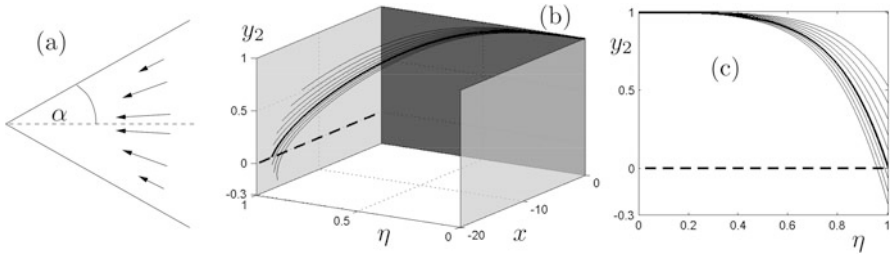


Figure 20.13: (a) Sketch of the wedge with inflow and opening angle α ; we consider only solutions that are reflection-symmetric about the centerline (dashed). (b) (x, η, y_2) -coordinates for (20.59). The gray planes indicate $\eta = 0, 1$, and the dark plane $\{x = 0\}$ is a critical manifold. Several trajectories are shown that satisfy the initial conditions at $\eta = 0$, but only one orbit (thick black curve) satisfies the boundary condition at $\eta = 1$. (c) Flow profiles associated with the trajectories in (b).

where $\text{Re} = \alpha f(0)/\nu$ is the dimensionless **Reynolds number** defined via the **kinematic viscosity** ν of the fluid. If $f(0) < 0$, we have inflow toward the apex of the wedge, while $f(0) > 0$ represents outflow at the center line. We restrict ourselves to inflow along the entire profile for now and require $f(0) < 0$ as well as $F(\eta) \geq 0$ for $\eta \in [0, 1]$. Reasonable boundary conditions for (20.56) that describe symmetric solutions around $\theta = 0$ are

$$F(0) = 1, \quad F'(0) = 0, \quad F(1) = 0, \quad (20.57)$$

which also enforce no-slip conditions at the walls. In fluid dynamics, one is often interested in the limiting cases of $\text{Re} \rightarrow 0$ (low viscosity) and $|\text{Re}| \rightarrow \infty$ (high viscosity), so that the Reynolds number becomes a crucial singular perturbation parameter for fluid dynamics. For (20.56), we set $\varepsilon := -1/\text{Re}$.

Exercise/Project 20.9.1. Apply dominant balance and matched asymptotic expansions to (20.56)–(20.57) to derive a two-layer asymptotic solution for $\varepsilon \rightarrow 0$. What about $\varepsilon \rightarrow \infty$? \diamond

An alternative to the direct asymptotic approach is to rewrite (20.56) as

$$\varepsilon \dot{H} - 2\alpha FG + 4\alpha^2 \varepsilon G = 0, \quad \dot{G} = H, \quad \dot{F} = G. \quad (20.58)$$

The system (20.58) can be viewed as a multiple time scale system in standard form with $(H, G, F) = (x, y_1, y_2)$:

$$\begin{cases} \varepsilon \dot{x} = 2\alpha y_2 y_1 - 4\varepsilon \alpha^2 y_1, \\ \dot{y}_1 = x, \\ \dot{y}_2 = y_1, \end{cases} \xrightarrow{\varepsilon Y_1 = y_1} \begin{cases} \dot{x} = 2\alpha y_2 Y_1 - 4\varepsilon \alpha^2 Y_1, \\ \varepsilon \dot{Y}_1 = x, \\ \dot{y}_2 = \varepsilon Y_1, \end{cases} \quad (20.59)$$

with boundary conditions $y_2(0) = 1$, $y_2(1) = 0$, and $y_1(0) = 0$, where “time” is the coordinate η . Trajectories of (20.59) for fixed α basically correspond

to velocity profiles for the flow. Figure 20.13(b) shows various trajectories in (x, η, y_2) -space for initial conditions $y_2(0) = 1$ and $y_1(0) = 0$. Note that the second formulation of the system (20.59) as a three-time-scale system seems to capture the boundary layer effect near the critical manifold $C := \{(x, y) \in \mathbb{R}^3 : x = 0\}$, since the correct solution stays close to $y_2 \approx 1$ and $x \approx 0$ for a considerable amount of time. Figure 20.13(c) shows the relevant flow profiles $y_2 = F$. The flow is nearly of equal strength up the angle $\alpha/4$ and develops a sharper layer toward the wall when $\eta = 1$, where there is no flow due to the no-slip boundary condition.

Exercise/Project 20.9.2. Consider the case $\text{Re} \rightarrow 0^+$ and study outflow solutions for $\alpha = 10^\circ$. Identify a critical manifold and an associated boundary layer where the flow leaves the vicinity of the associated slow manifold. ◇

The Jeffrey–Hamel flow already shows the variety of possible scalings and multiple time scale problems that can arise from a simple fluid dynamics problem. Once the full Navier–Stokes PDEs are considered in slightly more complicated geometries, for example flow past a sphere, the asymptotics become quickly involved.

As a second fluid dynamics example, we consider aerosol particles in a flow. The long-time behavior and possible settling of these particles in a flow is an important problem in meteorology and oceanography. One possibility to study the interesting effects for various flows is to prescribe a flow field and consider a **Lagrangian viewpoint** to track a particle via its position and velocity in the flow. To model a stationary homogeneous turbulent flow, Maxey and Corrsin [MC86] consider a periodic/cellular flow field

$$\left(U_0 \sin\left(\frac{w_1}{L}\right) \cos\left(\frac{w_2}{L}\right), -U_0 \cos\left(\frac{w_1}{L}\right) \sin\left(\frac{w_2}{L}\right) \right),$$

where (w_1, w_2) are coordinates, L is the length, and U_0 the velocity scale of the flow. After a suitable rescaling [MC86], the motion of a particle with position $x = (x_1, x_2)$ and velocity $y = (y_1, y_2)$ in the flow is described by

$$\begin{aligned} \varepsilon \frac{dx_1}{d\tau} + x_1 &= \sin y_1 \cos y_2 &=: f_1(x, y), \\ \varepsilon \frac{dx_2}{d\tau} + x_2 &= -p_1 - \cos y_1 \sin y_2 &=: f_2(x, y), \\ \frac{dy_1}{d\tau} &= x_1 &=: g_1(x, y), \\ \frac{dy_2}{d\tau} &= x_2 &=: g_2(x, y), \end{aligned} \tag{20.60}$$

where $p_1 \in [0, 1]$ is a nondimensional parameter describing the settling/terminal velocity of the particle, and ε is a nondimensional parameter, also called the **Stokes number** in this context, describing inertial effects. For $0 \leq \varepsilon \ll 1$, the physical interpretation is that particles basically follow the streamlines of the flow. Rubin, Jones, and Maxey [RJM95] (see also [Jon95]) recognized that (20.60) is a $(2, 2)$ -fast–slow system and studied it from the multiple time scale perspective; they also refer to it as the **Stommel flow** based on the work [Sto49]. It is easily seen from (20.60) that the critical manifold

$$C_0 = \{(x, y) \in \mathbb{R}^4 : x_1 = \sin y_1 \cos y_2, x_2 = -p_1 - \cos y_1 \sin y_2\}$$

is normally hyperbolic and attracting, since $D_x f = -\text{Id} \in \mathbb{R}^{2 \times 2}$ for $f = (f_1, f_2)^\top$. Note that C_0 can also be viewed as a torus due to the periodicity in (y_1, y_2) : see Section 19.2 for associated visualizations and the slow flow.

Exercise 20.9.3. Compute an asymptotic expansion for the slow manifold C_ε using a regular perturbation ansatz up to first order in ε . Calculate an asymptotic flow on C_ε up to first order in ε . \diamond

Using the results from Exercise 20.9.3, one can show [RJM95] that for arbitrarily small inertia $\varepsilon > 0$, almost all particles must eventually settle.

20.10 Quantum Mechanics

One of the most fundamental equations in quantum mechanics is the linear **Schrödinger equation** governing dynamics in a potential $V(x)$ of a single particle

$$i\hbar \frac{\partial \psi}{\partial t} = -\hbar^2 \Delta \psi + V(x)\psi, \quad (20.61)$$

where \hbar is **Planck's constant**, $(t, x) \in \mathbb{R} \times \mathbb{R}^n$, and $\psi(t, x)$ is the complex-valued **wave function** describing the quantum (or probabilistic) state of the particle, and Δ denotes the Laplacian. A typical assumption for understanding (20.61) is to look for **stationary** (or **standing**) **waves** with the ansatz

$$\psi(t, x) = e^{-i\hbar^{-1}Et} u(x), \quad u(x) \in \mathbb{R}, \quad u > 0, \quad (20.62)$$

where E represents an energy level. Substituting (20.62) into (20.61) yields

$$-\hbar^2 \Delta u + \underbrace{(V(x) - E)}_{=:Q(x)} u = 0. \quad (20.63)$$

Planck's constant is extremely small, and we certainly have $0 < \varepsilon := \hbar \ll 1$. In the one-dimensional case ($x \in \mathbb{R}$), this implies that (20.63) is a singularly perturbed ODE

$$\varepsilon^2 \frac{d^2 u}{dx^2} = Q(x)u. \quad (20.64)$$

Recall that problems of the form (20.64) are precisely of the form we discussed using WKB asymptotics in Section 9.4. Note that (20.64) still needs boundary and/or initial conditions. A particularly interesting set of boundary conditions is used to model **tunneling**, the classically forbidden, but quantum-mechanically allowed, possibility of a particle tunneling through a potential barrier. Suppose the smooth potential $V(x)$ has a unique global maximum at $x = 0$ with $V(0) > E$ and

$$\lim_{x \rightarrow \pm\infty} V(x) = 0, \quad V'(x) > 0 \text{ for } x < 0, \quad V'(x) < 0 \text{ for } x > 0.$$

Classically, the particle can only be in a state where $E < V(x)$, so that the region $[x_l, x_r]$ with $V(x_l) = E = V(x_r)$ is forbidden from this view. The idea is to place boundary conditions on $u(x)$ at $x = \pm\infty$ that represent solutions obtained from tunneling. Suppose the basic dynamic for $x \ll 0$ is a right-moving wave $\exp(-ix\sqrt{E}/\varepsilon)$ with unit amplitude. Then reflection at the barrier also produces a left-moving wave $A \exp(ix\sqrt{E}/\varepsilon)$ with amplitude A visible for $x \ll 0$. Tunneling should produce another right-moving wave $B \exp(-ix\sqrt{E}/\varepsilon)$ visible for $x \gg 0$. This suggests that we consider the boundary conditions

$$\begin{aligned} u(x) &\sim e^{-ix\sqrt{E}/\varepsilon} + Ae^{ix\sqrt{E}/\varepsilon}, & \text{as } x \rightarrow -\infty, \\ u(x) &\sim Be^{-ix\sqrt{E}/\varepsilon}, & \text{as } x \rightarrow \infty. \end{aligned} \quad (20.65)$$

The terms $|A|^2 = R$ and $|B|^2 = T$ with $R + T = 1$ are called **reflection** and **transmission coefficients**, respectively. WKB theory can now be used to try to determine the unknown amplitudes A and B . The major problem is that the boundary between classical and quantum regions are **turning points**, i.e., $Q(x_l) = 0 = Q(x_r)$. The next exercise provides a guide how to use the “physical optics approximation” of WKB theory in this context; a detailed solution can be found in [BO99].

- Exercise/Project 20.10.1.** (a) For simplicity, try to solve the Schrödinger-type problem (20.64) for one simple turning at $x = 0$, where $Q(x) = 0$, $Q(x) \sim kx$ as $x \rightarrow 0$ with $k < 0$. The goal is to consider a WKB solution $u_{WKB}(x)$ for $x > 0$, and then compute how it should behave for $x < 0$.
- (b) Now consider the tunneling problem. Assume that $V(x) \ll 1/x$ as $x \rightarrow \pm\infty$ and compute the WKB asymptotics in the regions $x < x_l$ and $x > x_r$.
- (c) Use (a) and (b) to determine the WKB solution $u_{WKB}(x)$ for $x \in [x_l, x_r]$.
- (d) Prove that $R \sim 1$ and $T \sim e^{-1/\varepsilon}$ as $\varepsilon \rightarrow 0$. \diamond

The main result of Exercise 20.10.1 is that the transmission probability for tunneling is not zero, but it is exponentially small. In fact, the solution exhibits a two-time -scale behavior due to the exponentially long scale for tunneling in comparison to the regular $\mathcal{O}(1)$ reflection time scale.

Obviously, quantum mechanics covers much more than the single-particle problem (20.61). A much more general form of the **Schrödinger equation** is

$$i\varepsilon \frac{\partial \psi}{\partial t} = H(t, \varepsilon)\psi, \quad (20.66)$$

where $0 < \varepsilon \ll 1$, $\psi = \psi(t, x) \in X$, $(t, x) \in \mathbb{R}_0^+ \times \mathbb{R}^n$, and $H(t, \varepsilon)$ is a time-dependent operator on a suitable complex Banach space X , called the **(quantum) Hamiltonian**. One of the most fundamental results about (20.66) is the **(quantum) adiabatic theorem** due to Born and Fock [BF28] as well as Kato [Kat50]. Here we state only a brief nontechnical version of this result [BG05]. Consider a time interval $t \in [0, T] =: \mathcal{I}$ and assume that the operator $H(t, \varepsilon)$ is given by

$$H(t, \varepsilon) = H_0(t) + \varepsilon H_1(t, \varepsilon),$$

where H_0, H_1 are linear operators and $H_1(t, \varepsilon)$ is uniformly bounded in ε . Notice carefully that a time-rescaling $t = \varepsilon\tau$ in the Schrödinger equation (20.66) reveals that $H(t, \varepsilon) = H(\varepsilon\tau, \varepsilon)$ is a slowly varying Hamiltonian. Suppose the spectrum $\sigma(t)$ for $H_0(t)$ splits into two parts $\sigma_1(t), \sigma_2(t)$ with a **spectral gap**

$$\text{dist}(\sigma_1(t), \sigma_2(t)) \geq \alpha > 0, \quad \forall t \in \mathcal{I}.$$

Denote by $P_1(t)$ and $P_2(t)$ the time-dependent spectral projection operators associated with $\sigma_1(t)$ and $\sigma_2(t)$. Let $U(t, s, \varepsilon) : X \rightarrow X$ be the principal solution, so that

$$i\varepsilon \frac{\partial U(t, s, \varepsilon)}{\partial t} = H(t, \varepsilon)U(t, s, \varepsilon), \quad U(s, s, \varepsilon) = \text{Id}.$$

Then a basic version of the quantum adiabatic theorem states that

$$(\text{Id} - P_j(t))U(t, s, \varepsilon)P_j(s) = \mathcal{O}(\varepsilon), \quad \text{as } \varepsilon \rightarrow 0. \quad (20.67)$$

From a dynamical systems standpoint, the result implies, for example, that if $\psi(0, x) \in P_j(0)X$, then the solution $\psi(t, x)$ for $t \in \mathcal{I}$ remains close to the subspace $P_j(t)X$. In the limit of infinite time scale separation $\varepsilon \rightarrow 0$, the Hamiltonian varies infinitely slowly, and the correspondence between initial eigenspace $P_j(0)X$ and final eigenspace $P_j(t)X$ is exact. This is the colloquial statement of the quantum adiabatic theorem: infinitely slow Hamiltonian variation implies “adiabatic” tracing or following of the energy level selected at the beginning. The quantum adiabatic theorem is also one of the motivations for the study of fast–slow systems in which the only slow variable is time,

$$\begin{aligned} \varepsilon \dot{x} &= f(x, y, \varepsilon). \\ \dot{y} &= 1. \end{aligned}$$

Exercise/Project 20.10.2. Prove the quantum adiabatic theorem in the finite-dimensional case when $H(t, \varepsilon)$ is a family of matrices. \diamond

20.11 Networks

Networks are a cornerstone in the description of complex systems. Many scientific disciplines make use of elements of network theory; see Section 19.10. In fact, multiple time scale ideas form—at least implicitly—one of the major building blocks of network theory. To explain this point, let us consider a general **network (or graph)** G consisting of a set of **vertices (or nodes)** V and a set of **edges (or links)** E between the vertices. Figure 20.14 explains two basic viewpoints:

- (P1) Assume that vertices have a fixed type such as different economic agents or types of neurons. Furthermore, assume that certain fixed types of edges are considered, such as undirected, directed, and weighted edges. It is often even assumed that the entire network consists of only one type of

vertices and one type of edges. Then we are interested in studying the formation, combinatorics, and complexity of networks that we can build or observe. This means that we study the **dynamics of networks**; see Figure 20.14(a).

- (P2) Assume a given fixed network with a fixed topology. In this case, the connections between economic agents or within the neural wiring are static. However, one allows the individual dynamics of vertices to change. A typical example from dynamical systems is classical models of coupled oscillators where the coupling (or adjacency) is fixed and each oscillator obeys a differential equation. Therefore, this viewpoint studies **dynamics on networks**; see Figure 20.14(b).

Remark: In the statistical physics literature, one would sometimes refer to (P1) as the **annealed network** case, while (P2) is called the static network case.

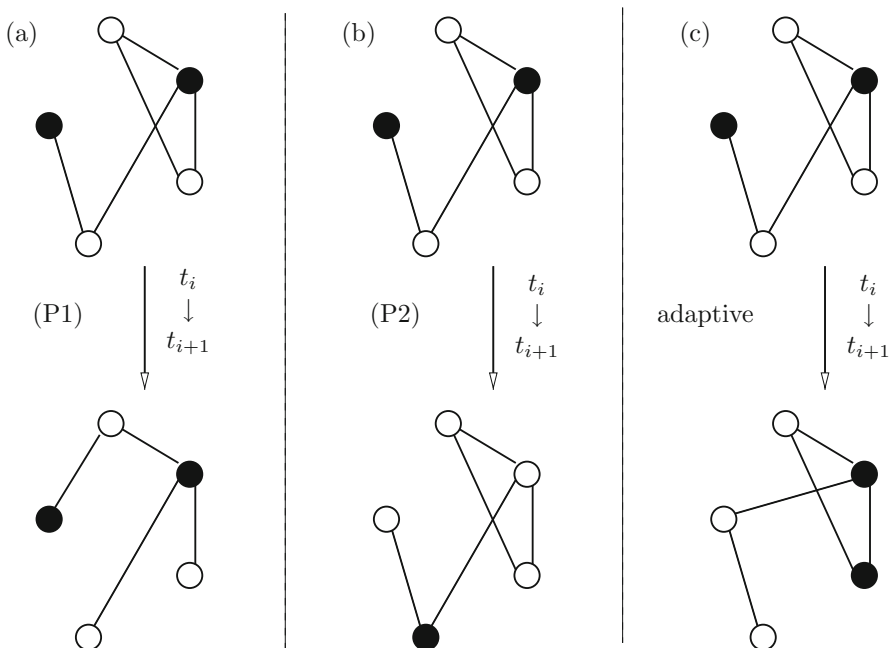


Figure 20.14: The different approaches in network science. The transition from the top to the bottom row represents a time step $t_{i+1} > t_i$. (a) Dynamics of networks according to paradigm (P1); the vertices have fixed colors corresponding to static (or frozen) dynamics, while the topology changes. (b) Dynamics of networks according to paradigm (P2); the topology is fixed, but the vertices change their dynamical state. (c) Fully adaptive network where both dynamics, and also their interaction, are time-dependent.

In real networks, it is frequently the case that (P1) and (P2) are “singular limits.” Indeed, we expect that the network is **coevolutionary (or adaptive)**,

so that the topology of the network and the dynamics of the nodes interact; see Figure 20.14(c). The main reason why one should still study (P1) and (P2) in isolation is the assumption of a time scale separation. One either assumes that individual dynamics change so slowly that only the topological aspects become important, or, more commonly in dynamical systems, one assumes that the topology is invariant and individual dynamics constitute a fast process. Although the time scale separation assumption is rarely mentioned explicitly, it clearly forms a major component of network science.

Even when the network is adaptive, we can still use fast–slow systems. Observe that (P1)–(P2) correspond to the case of a singular limit $\varepsilon = 0$ with infinite time scale separation. If topological and individual dynamics interact, there still may be a finite time scale separation with $0 < \varepsilon \ll 1$. As an example, we will consider an adaptive network proposed by Bornholdt and Röhl [BR00].

Consider a directed graph $G = G(V, E, v, e)$ with vertex set V , edge set E , vertex values $v_i(t) \in \{-1, +1\}$, and edge weights $e_{ij}(t) \in \{-1, 0, +1\}$. Assume that the cardinality $|V|$ of V is fixed to some $N \gg 1$. A nonzero edge weight $|e_{ij}(t)| = 1$ indicates a directed edge from vertex j to vertex i . Loops will not be allowed, so that $e_{ii}(t) = 0$ for all $i \in \{1, 2, \dots, N\}$. Double edges will also not be allowed, which is indicated by the requirement that nonzero edge weights be ± 1 . However, the number of edges can change with time. The dynamics on the vertices from time t to time $t + 1$ are given by

$$v_i(t+1) = \begin{cases} \operatorname{sgn}[f_i(t)] & \text{if } f_i(t) \neq 0, \\ v_i(t) & \text{if } f_i(t) = 0, \end{cases} \quad (20.68)$$

where

$$f_i(t) = \sum_{j=1, j \neq i}^N e_{ij}(t) v_j(t). \quad (20.69)$$

The rules (20.68)–(20.69) describe the dynamics on the graph G . The functions $f_i(t)$ can be viewed as the inputs to vertex i . Node i is going to adopt the majority “opinion” of its neighbors. Note carefully that at each time step, all nodes are updated in parallel. It is assumed that a certain number of vertex updates $T_{\max} \gg 1$ are performed, for example $T_{\max} = 1000$. Then the average activity of each node over the last $T_a := \lfloor T_{\max}/2 \rfloor$ updates is measured,

$$A(i) = \frac{1}{T_{\max} - T_a} \sum_{t=T_a}^{T_{\max}} v_i(t). \quad (20.70)$$

Based on (20.70), the topology of the graph is updated as follows: Vertices with $|A(i)| = 1$ indicate **frozen nodes** that did not change their value for a long time, while $|A(i)| < 1$ are **active nodes**. The intuition is that frozen nodes should receive new connections to activate them, and active nodes should lose links to reduce activity. More precisely, the complete algorithm can be summarized as follows:

- (A0) Start with a random directed graph [Dur10b] with given **average connectivity** $K_{ini} = |E|/|V|$. Choose a random initial vertex state vector $v(0) = (v_1(0), \dots, v_N(0))^\top$.
- (A1) Apply the update rule (20.68)–(20.69).
- (A2) Choose a site i at random and calculate the average activity $A(i)$ using (20.70).
- (A3) If $|A(i)| = 1$, then i receives a new (nonexistent) edge e_{ij} from a node j chosen at random. The edge weight is chosen with equal probability from $\{\pm 1\}$. If $|A(i)| < 1$, then one of the existing nonzero edges is deleted by setting the associated edge weight to zero.
- (A4) Go back to step (A1).

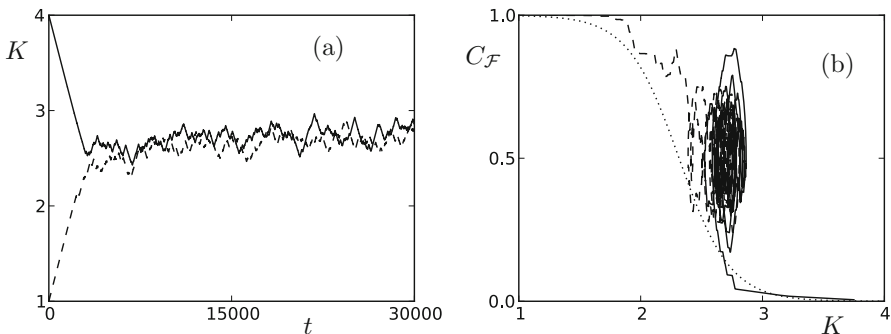


Figure 20.15: Simulation of the Bornholdt–Rohlf model (A0)–(A4) with $N = 1000$ nodes and parameter values (20.71). (a) Time series of the average connectivity K for two different initial conditions $K_{ini} = 1$ (dashed curve) and $K_{ini} = 4$ (solid curve). (b) 1000 time points (topological updates) moving-average plot for the two trajectories in (K, C_F) -space, where C_F is the frozen component size (20.72). The dotted curve indicates a “phase transition” obtained from additional numerical simulations by Bornholdt and Rohlf; see equation 20.73.

Remark: It is important to note that random sampling in (A1)–(A3) always means random with respect to a uniform distribution. Of course, one could try other distributions as well, but we shall not attempt this here.

From a multiple time scales viewpoint, we observe that the dynamics of the graph defined by topological update rule (A2)–(A3) are much slower than the dynamics on the graph via the iteration (A1). Basically, we have a time scale separation described by

$$0 < \frac{T_{\text{top}}}{T_{\max}} = \frac{1}{T_{\max}} \ll 1.$$

Figure 20.15 shows simulation results for the full network with $N = 1000$ nodes and parameter values

$$K_{\text{ini}} \in \{1, 4\}, \quad T_{\text{max}} = 1000, \quad T_a = 500, \quad (20.71)$$

for a total number of 30 000 topological updates (A2)–(A3). It can be observed from the time series in Figure 20.15(a) that random graphs with different initial connectivities seem to converge rapidly toward a special connectivity value. Figure 20.15 shows a plot of the average network connectivity K against the so-called **frozen component size**

$$C_{\mathcal{F}} := \frac{1}{N} |\{i \in \{1, \dots, N\} : v_i(t) = v_i(t+1) \forall t \in [T_a, T_{\text{max}}]\}|, \quad (20.72)$$

which is computed after the completion of T_{max} applications of the dynamical update (A1). The network seems to organize itself toward a “critical connectivity” between the completely frozen state $C_{\mathcal{F}} = 1$ and a disordered state $C_{\mathcal{F}} = 0$. This phenomenon has been termed **adaptive self-organized criticality**; see Section 19.10 for references.

Remark: It is often natural to view the dynamical variable $C_{\mathcal{F}}$ as fast and the topological variable K as slow. Then one may interpret the transition in Figure 20.15 as a fast subsystem bifurcation. Since the system converges near the fast subsystem bifurcation point, there should exist a global equilibrium near this value on an attracting part of the critical manifold. In fact, this shows that on an abstract mathematical level, self-organized criticality has similarities to excitable systems where we also have a global equilibrium close to a fast subsystem bifurcation.

Bornholdt–Rohlf used numerical simulations to suggest that the frozen component size depends on the connectivity K and the system size as

$$C_{\mathcal{F}}(K, N) = \frac{1}{2} [1 + \tanh(-\alpha(N)(K - K_0(N)))] , \quad (20.73)$$

where the functions $K_0(N)$ and $\alpha(N)$ are given by

$$K_0(N) = 2 + aN^{-\beta}, \quad \text{and} \quad \alpha(N) = bN^{\gamma}$$

with $a \approx 3.3$, $\beta \approx 0.34$, $b \approx 0.14$, and $\gamma \approx 0.41$. The sigmoidal function (20.73) is shown in Figure 20.15(b) (dotted curve). Its parameters were fitted by fixing different values of K , sampling 1000 random graphs with the given K , and then measuring C after a long number of dynamical update steps $T_{\text{max}} \gg T_a \gg 1$, i.e., by finding $C_{\mathcal{F}}$ for the “dynamical attractor” [BR00].

20.12 References

Section 20.1: The first example is based on [KKO99], while more details for the second example can be found in [Brø05, EK80]. Other engineering-oriented problems with multiple scales are, e.g., aerospace systems [NC01, PB81], aircraft flight path optimization [Kel71], aircraft ground dynamics [RDKL11], biomolecule metastability [NHSS07],

bond graphs [DTBL85, SDT91, AG13], buck converters [MNB01], car suspension control [AS96], chattering [Nam03], decision theory [SB82], elastic pendulums [Geo99], feedback robot control [SKK87, DNCB95], fiber lay-down processes [GKMW07], modeling of foams [SS13a], gyroscopes [BS88], Josephson junctions [Hau01, KRS13, NP03], n -link manipulators [KK85, MKP97], materials science [CDD⁺03], multibody systems [GS00], multimachine systems [AKWC80, Cho91, CGAP95, CWPS90, KACW82, WCB⁺81, WCAK80], nonlinear pendulums and rods [Geo05, GS01b, GS99], nuclear reactor control [RS75a], plastic deformation [KA11], power systems [CK85, PKC82], reservoir management [HH06], robot manipulators [LL03b], rotary drilling systems [GdWNS09], satellites [KSS⁺01], control systems for space science [Cal88], structure mechanics [GBC98], and thin-beam models [Sch85b]. Canards again appear in various engineering concepts such as in an optomechanical experiment [MM13b]. There are several uses of fast–slow systems that relate more to fundamental research in physics, e.g., gas discharges [SHPC09], induction machines [HS98], Ising-type models [PCS93], lattice models [Rak00], the Lorentz–Dirac equation [Spo00a], Maxwell–Lorentz equations [KS00b], optical bistability [EM83], particles in a magnetic field [INV00], particles in a Maxwell field [KS01f], plasma physics [DBR⁺13], quasistatic paths in mechanical systems [MRS06], quenched mechanics [Dan13], spin glass models [JAB⁺01], ultrafast diffusion on heterogeneous surfaces [REG11], and viscoelasticity [Wil06]. Semiconductor theory [MS89, Mar86, MR84, OS90] and its applications [MS86a, Sch89] are another subject at the interface of physics and engineering where small parameters appear regularly; see also the book [MRS90].

Section 20.2: The Hodgkin–Huxley transformation to fast–slow systems was extracted from [RW07]. The fact that neuronal systems have many intrinsic time scales is nearly obvious [HKBS07], but it is not always clear what the fast and slow variables are [SM13]. Canards have recently emerged as a key factor in understanding neurodynamics and occur, e.g., in neuron synchronization [DRSE04]. For more background on neuroscience and mathematical physiology, we refer to the books [ET10, Izh07, KS08a, KS08b], the surveys [RVSA06, RH13, RT02a], and the motivation [Kop00]. The neuroscience view on spiking is well explained in various publications [ELRL99, GK02]. A major example arising from single-neuron models is the Hodgkin–Huxley equations, which have been studied extensively [GL93, Has78, Izh03, Tro78]. There are many other situations arising in neuroscience that exhibit fast–slow behavior, e.g., calcium dynamics [HKO⁺10, HKWS11, TSO96, Tsa12], central pattern generators [She08], coupled Hindmarsh–Rose neurons [SHX08], dendritic spine models [WB98], hippocampus interneurons [HMJ10], inferior olive neurons [LS12], integrate-and-fire models [SG13], brain lactate kinetics [LACFG13], heart neuron models [SB03, BS04c], insect locomotion [GH04b, GH04a], neurohormones [CV09], propofol anesthesia [MMKW13], reduced neuron models [LR94], somatograph models [NM⁺10], spike-time reliability [YLK13], and stimulus adaptation for auditory neurons [ULFN04]. There are also various phenomena that can be studied by fast–slow dissection such as frequency-response curves [Erm98], phase-response curves [BMH04, Erm96, LFS⁺09, OM11], and rebound spiking [MK12a]. Networks of neurons form another extremely large topic involving various aspects, e.g., fast–slow kinetics [WBPK00], coupled bursting oscillators [RRE13], and neural network modeling [Pin95].

Section 20.3: The first example is taken from [FN74]. The autocatalator model is nicely described in [PSS92]. Many more details on autocatalator(s) can be found in [GS11, GS09c, Kue14, MS01b, MSLG98, PSS92]. A primary application to chemical systems is the analysis of mixed-mode oscillations discussed in

Chapter 13. Furthermore, as already pointed out in Section 11.7, there are many links to combustion applications [GGKS99, SFH⁺01] such as combustion of dusty gases [GGZ02, GZSS96]. Other applications include exothermic reactions [GACV06] and thermal explosion in hot gases [BGGG02]. Many more references on chemical oscillations can be found in Section 13.9.

Section 20.4: The first example is adapted from [ANMC⁺09]. The variant of the Yamada model was taken from [HS05]. There is also a detailed numerical bifurcation analysis of the Yamada model [DK99, DKL99]. Furthermore, many other applications are available, such as coupled lasers [HGEK97, KBKW98, Mus06], optical feedback [EKL07, LTLE95], quantum dot lasers [EVM07], Q-switching [KNE⁺06], microchips [EPG00], noise-driven lasers [Wie09], and vertical-cavity surface emission [vdSDWE03].

Section 20.5: The predator–prey example is taken from [RM92]. There is book on adaptive dynamics and evolution available [DR08] with a multiscale focus. Although evolution is often slow in comparison to system dynamics, it is interesting to point that this situation may be reversed in some cases [CE10]. Unsurprisingly, canard periodic orbits also appear in predator–prey systems [VB07], which form a core topic in ecology [AB93, CHL09, RM92, RS00]. Canards also appear in a forest–pest model [BK10b, Rin09]. An interesting question is how and what may destabilize ecosystems [RG04]. There is a wide variety of topics related to ecology that benefit from multiple time scale methods [Has10] such as adaptive trait dynamics [BW12, BW13], chemostats [HR09], cross-migration models [Hua05], Cucker–Smale flocking [HS10a, HJS12], ecological management [Cré07], food chain systems [FR98, KPAK02], harvesting in competing populations [BS99b], logistic-type models [LD77], Lotka–Volterra systems [LQY10], migratory–demographic populations [MSdIPS09], population economics models [MP96, MPFS96], population genetics models [Hop76], Red Queen dynamics [DFGR06], and swarming models [Lee11]. A similar remark [MPdIP12] regarding applicability of multiscale methods holds for epidemiology [Sou13], with topics such as behavior changes during epidemics [PCA⁺09], discrete-time systems [NHdIPA11], environmental transmission of diseases [Bre13a], spread of malaria [FSML04, FYZ04], classical SIS models [BPL13], and tuberculosis modeling [SCCA02, McC06]. For textbooks with a broad view on mathematical biology, consider [GE06, Mur02b, Mur03].

Section 20.6: The Barkley model has been used to analyze spiral waves numerically in the series of papers [Bar92, Bar91, Bar97]. The Gierer–Meinhardt [GM72] example is taken from [Hek10]. For a more detailed analysis of the Gierer–Meinhardt model, consider [DKvdP01], since there is a wide variety of possible patterns such as pulses [DKvdP01, DGK01, vdPD05], spikes [IW02, IWW01, WW03, WMH⁺02], and stripes [DvdP02]. It is quite frequent that techniques from Gierer–Meinhardt can be carried over to pattern analysis in the Gray–Scott model [DGK98, DKZ97, KWW05b, KWW05a] and vice versa. Other interesting pattern-formation models from mathematical biology are the Keller–Segel [KS70] and phytoplankton–nutrient models [ZD11, ZDTS09]. Furthermore, pattern formation in the cubic nonlinear Schrödinger equation [RK02, RK03] and the Allen–Cahn equation [War96] are related topics. Regarding spiral waves, asymptotic matching methods are often applied under the assumption of fast reaction and slow diffusion [Ber91]. Particularly in the FHN equation, spiral waves have been studied extensively [PH93] as well as scroll waves [PK95].

Section 20.7: The two-body problem in celestial mechanics is a standard problem in many books [AKN06, KC96]. Resonances [NS04] have been a considerable topic in celestial mechanics. Of course, the two-timing method (“method multiple time scales”) is a classical approach in orbital mechanics [NE03]. A key application in celestial mechanics is the three-body problem, where singular perturbation theory yields tremendous insight [Per76]. Other applications include Arnold diffusion [Moe96], coorbital motion [SD03], elastic space tethers [KUR12], and Kepler’s problem [YPMD08]; for more on Arnold diffusion, see also Section 19.10.

Section 20.8: The mitotic oscillator example can be found in [Gol91, KS13]. The sleep–wake cycle model was considered in [RBT10]; understanding the sleep–wake cycle is a quite recent direction in fast–slow systems [BB12a, FPR08, OCA11]. A primary topic in systems biology is the occurrence of oscillations [Gol97, GK81, TCN03], particularly in connection with feedback loops [BJLM05, YTHL11]. Due to the high complexity of systems biology applications, there are many other fast–slow applications such as actin-based motility [EGF07], beta-cell dynamics [WKvdB12], biochemical networks [Gun12, MG13b, SSL⁺09, TG09], enzymatic reactions [DS89b], enzyme motion [MAP96], haplotype frequencies [WM06], melanogenic systems [OPO03], metabolic–genetic generalized models [RKS13], muscle respiration [Mur74], physiological time series [CGP02], protein dynamics [LTK⁺07], rhythmic systems [RG12, DWC⁺98], saccadic system models [ABAC05], signaling pathways [GHK08], systems biology algorithms [Mit09], and tumor models [DFAR13, FHR09]. Another challenging problem is to understand learning [GW12] via neural network models [TS95].

Section 20.9: The Jeffrey–Hamel example can be found in certain forms in [KC96, Pan05]. The aerosol particle problem is discussed in [MC86, RJM95]. It is quite common to recognize fluid dynamics as the area in which many singular perturbation methods were first pioneered. The fundamental paper of Prandtl [Pra05] undoubtedly played a crucial role in the development of the field [O’M10]. Of course, the main equations of fluid dynamics, e.g., Euler and Navier–Stokes, can be tackled using multiple time scale and singular perturbation methods [CM07, EJ10, EJM08, EJM10]. A standard buzzword in fluids is boundary layer theory [Car70, OS99, SG00], and there are various books dedicated to singular perturbation techniques in fluid dynamics, e.g., [vD64]. Other applications we could have chosen are data assimilation [C.C13], Faraday waves [HPK08], flow separation behind a cylinder [SH08], inertial particles in flows [HS08], liquid jet stability [Nay70], plane wake flow [BDM99], polymeric fluids [LVEZE04], nematic suspensions [GMCH12], nonpolar solvation in liquids [Ber98a], rotating fluids [GOT07], shallow water sloshing [HM91], shallow water waves [NT01], slow viscous flow around a cylinder [Bre62], transition to turbulence [FH03], triple deck theory [Mey83], viscoelastic fluids [MR12a], viscous compressible flow through a nozzle [HHL10b, HHL10a], and wings in subsonic flow [GVBM09]. Various fast–slow phenomena we have discussed reappear, such as canard orbits [BFS08] in the Blasius equation [HL86, HLN87]. Another natural application related to fluid dynamics is climate models [BM05, BM10, KM06a, Maj07, MB04, MK03], which often focus on atmospheric circulation [BUB10, Tuw03, WS00] as the primary example of a geophysical flow [DPS07].

Section 20.10: The WKB ansatz for the Schrödinger equation is classical [BO99]. The outline of the quantum adiabatic theorem is based on [BG05]. For more on the adiabatic theorem, we refer to [AE99, AFGG12, Kat50]. Adiabatic behavior in quantum-mechanical systems has been studied for a long time [Bor98, BG05]. Typical

results are exponentially rare transitions [JKP91], the Landau–Zener formula [Joy94], and analysis of the time-dependent Schrödinger equation [JP93, JP91a, JP91b]. However, there are also many emerging directions such as quantum feedback networks [GNW10], quantum phase transition [SKR08], and various other quantum-mechanical applications [Gin85]. One may also try to couple classical and quantum mechanics [SB99], where averaging ideas naturally come into play [Rei99a].

Section 20.11: This section is adapted from [Kue12b], where also the concept of time-scale resonance is introduced. Adaptive (or coevolutionary) networks have been considered in a vast number of different scenarios [GB08, GS09b, CDKS98, GZ06, SS08c]. For a general introduction to network science, we refer to [BBV08, BS03, New03, New11, NBW03, Str01]. For more on self-organized criticality, we refer to [CM05b]. The most classical link of networks arises when each node is a fast–slow system such as coupled FHN systems on a lattice [GH13], globally coupled FHN oscillators [BK10a], various other versions of FHN-type coupled systems [RW12, KVC13], coupled relaxation oscillators [TW95, MT11], and various other systems [TAWJ08, ASBT10]. It is quite natural that coupled oscillator networks [IH03] can also exhibit MMOs [PSSM08], chaos [Che11], and canard dynamics [RKZE03a, RK06], but there are also new phenomena, e.g., spatiotemporal patterns [RT00], synchronization [MKHC02, RT02b], and transitions between patterns [BPTW07]. For a very detailed view on some singular perturbation and fast–slow structures in neural networks, we refer to the book [HI97]. In fact, a very important aspect that occurs not only for neural nets is that one may exploit multiscale structures to reduce networks to mean-field models [BN11, EK86b, KE90], enforce closure relations [RHD11], and use averaging in an elegant way [Erm94]. Another famous use of averaging is to justify the mean-field theory for Kuramoto models [HS11]. There are many other areas that have been investigated, such as relations to combinatorics [DL13], inferring coupling structure [NRT⁺10], neural networks with slowly decaying coupling or adaptation [GR94, GR93, NBB08], opinion formation on a ring [IKKB09, IKKB11], the Ott–Antonsen ansatz [ATB⁺12], power system networks [Cho82], and time scales via graph theory [LSS13].

Other elegant applications of the techniques we have presented are bioeconomics [GH06], Boltzmann-type price formation models [BCMW13], the Frenkel equation [WK01], cardiac dynamics [SB11], Kirchhoff problems with weak dissipation [Ghi12], locomotion [HFKG06], nucleation growth [PMHC⁺10], oxidation on crystals [CHKL03], parameter estimation [RCR08], particles in varying potentials [KS06], polyhomeostatic adaptation [LG13], relationship dynamics [Rin94], target tracking [AG97a], variable reconstruction [BK96], and virus–bacteria interaction [PACNH09].

There are also relations to game theory, including algorithms converging to Nash distributions [CL03], control of differential games [Gli00b], control with several time scales [SC82, SC81, SC84], Hamilton–Jacobi equations [Sub96], H_∞ optimal control [PB93], Nash strategies in differential games [Kha80], game theory involving population dynamics [AP98c, AP98b], singularly perturbed Nash games [KK79c], and Stackelberg strategies [SC83].

Bibliography

- [AAA12] B. Ambrosio and M.A. Aziz-Alaoui. Synchronization and control of coupled reaction–diffusion systems of the FitzHugh–Nagumo type. *Comput. Math. Appl.*, 64(5):934–943, 2012.
- [AAF95] S. Adjerid, M. Aiffa, and J.E. Flaherty. High-order finite element methods for singularly perturbed elliptic and parabolic problems. *SIAM J. Appl. Math.*, 55(2):520–543, 1995.
- [AAM98] J. Awrejcewicz, I.V. Andrianov, and L.I. Manevitch. *Asymptotic Approaches in Nonlinear Dynamics*. Springer, 1998.
- [AAN11] A. Arnold, N.B. Abdallah and C. Negulescu. WKB-based schemes for the oscillatory 1D Schrödinger equation in the semi-classical limit. *SIAM J. Numer. Anal.*, 49(4):1436–1460, 2011.
- [AARR87] F. Argoul, A. Arneodo, P. Richetti, and J.C. Roux. From quasi-periodicity to chaos in the Belousov–Zhabotinskii reaction. I. Experiment. *J. Chem. Phys.*, 86(6):3325–3338, 1987.
- [AB86] U. Ascher and G. Bader. Stability of collocation at Gaussian points. *SIAM J. Numer. Anal.*, 23(2):412–422, 1986.
- [AB93] P. Auger and E. Benoit. A prey-predator model in a multi-patch environment with different time scales. *J. Biol. Syst.*, 1(2):187–197, 1993.
- [AB02] O. Alvarez and M. Bardi. Viscosity solutions methods for singular perturbations in deterministic and stochastic control. *SIAM J. Control Optim.*, 40(4):1159–1188, 2002.
- [AB03] O. Alvarez and M. Bardi. Singular perturbations of nonlinear degenerate parabolic PDEs: a general convergence result. *Arch. Rat. Mech. Anal.*, 170(1):17–61, 2003.
- [ABAC05] O.E. Akman, D.S. Broomhead, R.V. Abadi, and R.A. Clement. Eye movement instabilities and nystagmus can be predicted by a nonlinear dynamics model of the saccadic system. *J. Math. Biol.*, 51(6):661–694, 2005.
- [ABBG02] P. Ashwin, M.V. Bartuccelli, T.J. Bridges, and S.A. Gourley. Travelling fronts for the KPP equation with spatio-temporal delay. *Zeitschr. Angewand. Math. Phys.*, 53(1):103–122, 2002.
- [ABC⁺06] N.D. Alikakos, P.W. Bates, J.W. Cahn, P.C. Fife, G. Fusco, and G.B. Tanoglu. Analysis of a corner layer problem in anisotropic interfaces. *Discr. Cont. Dyn. Syst. B*, 6(2):237–266, 2006.
- [Abd05] A. Abdulle. On a priori error analysis of fully discrete heterogeneous multiscale FEM. *Multiscale Model. Simul.*, 4(2):447–459, 2005.
- [Abd12] A. Abdulle. Explicit methods for stiff stochastic differential equations. *Lecture Notes in Comput. Sci. Engineer.*, 82:1–22, 2012.
- [Abe85a] E.H. Abed. Multiparameter singular perturbation problems: iterative expansions and asymptotic stability. *Syst. Contr. Lett.*, 5(4):279–282, 1985.
- [Abe85b] E.H. Abed. Singularly perturbed Hopf bifurcation. *IEEE Transactions on Circuits and Systems*, 32(12):1270–1280, 1985.
- [Abe86a] E.H. Abed. Decomposition and stability for multiparameter singular perturbation problems. *IEEE Transactions on Automatic Control*, 31(10):925–934, 1986.
- [Abe86b] E.H. Abed. Strong D-stability. *Syst. Contr. Lett.*, 7(3):207–212, 1986.
- [ABF91] N.D. Alikakos, P.W. Bates, and G. Fusco. Slow motion for the Cahn–Hilliard equation in one space dimension. *J. Differential Equat.*, 90(1):81–135, 1991.
- [ABF97] N.D. Alikakos, L. Bronsard, and G. Fusco. Slow motion in the gradient theory of phase transitions via energy and spectrum. *Calc. Var. Partial Diff. Equat.*, 6(1):39–66, 1997.
- [ABK12] D.C. Antonopoulou, D. Blömker, and G.D. Karali. Front motion in the one-dimensional stochastic Cahn–Hilliard equation. *SIAM J. Math. Anal.*, 44(5):3242–3280, 2012.
- [ABM07] O. Alvarez, M. Bardi, and C. Marchi. Multiscale problems and homogenization for second-order Hamilton–Jacobi equations. *J. Differential Equat.*, 243(2):349–387, 2007.
- [Abo97] E.F. Abouafadel. Qualitative analysis of a singularly-perturbed system of differential equations related to the van der Pol equations. *Rocky Mountain J. Math.*, 27(2):367–385, 1997.
- [Abr10] R.V. Abramov. Approximate linear response for slow variables of dynamics with explicit time scale separation. *J. Comp. Phys.*, 229(20):7739–7746, 2010.
- [Abr12a] R.V. Abramov. A simple linear response closure approximation for slow dynamics of a multiscale system with linear coupling. *Multiscale Model. Simul.*, 10(1):28–47, 2012.
- [Abr12b] R.V. Abramov. Suppression of chaos at slow variables by rapidly mixing fast dynamics through linear energy-preserving coupling. *Comm. Math. Sci.*, 10(2):595–624, 2012.
- [Abr13a] R.V. Abramov. A simple closure approximation for slow dynamics of a multiscale system: nonlinear and multiplicative coupling. *Multiscale Model. Simul.*, 11(1):134–151, 2013.
- [Abr13b] R.V. Abramov. A simple stochastic parameterization for reduced models of multiscale dynamics. *arXiv:1302.4132v1*, pages 1–23, 2013.

- [AC87] B.D. Aguda and B.L. Clarke. Bistability in chemical reaction networks: theory and application to the peroxidase-oxidase reaction. *J. Chem. Phys.*, 87(6):3461–3470, 1987.
- [AC91] J.C. Alexander and D. Cai. On the dynamics of bursting systems. *J. Math. Biol.*, 29:405–423, 1991.
- [AC08] A. Abdulle and S. Cirilli. S-ROCK: Chebyshev methods for stiff stochastic differential equations. *SIAM J. Sci. Comput.*, 30(2):997–1014, 2008.
- [ACC99] B. Amini, J.W. Clark, and C.C. Canavier. Calcium dynamics underlying pacemaker-like and burst firing oscillations in midbrain dopaminergic neurons: a computational study. *J. Neurophysiol.*, 82(5):2249–2261, 1999.
- [ACC⁺07] A. Adrover, F. Creta, S. Cerbelli, M. Valorani, and M. Giona. The structure of slow invariant manifolds and their bifurcational routes in chemical kinetic models. *Comput. Chem. Eng.*, 31(11):1456–1474, 2007.
- [ACDG84] J. Argémi, H. Chagnieux, C. Ducreux, and M. Gola. Qualitative study of a dynamical system for metrazol-induced paroxysmal depolarization shifts. *Bull. Math. Biol.*, 46(5):903–922, 1984.
- [ACGV07] A. Adrover, F. Creta, M. Giona, and M. Valorani. Stretching-based diagnostics and reduction of chemical kinetic models with diffusion. *J. Comp. Phys.*, 225(2):1442–1471, 2007.
- [ACM08a] N. Ben Abdallah, F. Castella, and F. Méhats. Time averaging for the strongly confined nonlinear Schrödinger equation, using almost-periodicity. *J. Differential Equations*, 245(1): 154–200, 2008.
- [ACM08b] M.H. Adhikari, E.A. Coutsias, and J.K. McIver. Periodic solutions of a singularly perturbed delay differential equation. *Physica D*, 237:3307–3321, 2008.
- [ACR79] U. Ascher, J. Christiansen, and R.D. Russell. COLSYS-A collocation code for boundary-value problems. In *Codes for Boundary-Value Problems in Ordinary Differential Equations*, pages 164–185. Springer, 1979.
- [ACR81] U. Ascher, J. Christiansen, and R.D. Russell. Collocation software for boundary-value ODEs. *ACM Trans. Math. Software*, 7(2):209–222, 1981.
- [ACV13] M. Avendano-Camacho and Yu. Vorobiev. On the global structure of normal forms for slow–fast Hamiltonian systems. *Russ. J. Math. Phys.*, pages 138–148, 2013.
- [ACVV13] M. Avendano-Camacho, J.A. Vallejo, and Yu. Vorobiev. Higher order corrections to adiabatic invariants of generalized slow–fast Hamiltonian systems. *arXiv:1305.3974v1*, pages 1–22, 2013.
- [ACY03] S. Ai, S.-N. Chow, and Y. Yi. Travelling wave solutions in a tissue interaction model for skin pattern formation. *J. Dyn. Diff. Eq.*, 15(2):517–534, 2003.
- [ADD12] E.O. Alzahrani, F.A. Davidson, and N. Dodds. Reversing invasion in bistable systems. *J. Math. Biol.*, 65:1101–1124, 2012.
- [ADF90] F. Awaszus, J. Dehnhardt, and T. Funke. The singularly perturbed Hodgkin–Huxley equations as a tool for the analysis of repetitive nerve activity. *J. Math. Biol.*, 28(2):177–195, 1990.
- [AE99] J.E. Avron and A. Elgart. Adiabatic theorem without a gap condition. *Commun. Math. Phys.*, 203:445–463, 1999.
- [AE03] A. Abdulle and W. E. Finite difference heterogeneous multi-scale method for homogenization problems. *J. Comp. Phys.*, 191(1):18–39, 2003.
- [AEEVE12] A. Abdulle, W. E, B. Engquist, and E. Vanden-Eijnden. The heterogeneous multiscale method. *Acta Numerica*, 21:1–87, 2012.
- [AF92] M. Abbad and J.A. Filar. Perturbation and stability theory for Markov control problems. *IEEE Trans. Aut. Contr.*, 37(9): 1415–1420, 1992.
- [AF94] N.D. Alikakos and G. Fusco. Slow dynamics for the Cahn–Hilliard equation in higher space dimension part I: spectral estimates. *Comm. Partial Diff. Equat.*, 19(9):1387–1447, 1994.
- [AF95] M. Abbad and J.A. Filar. Algorithms for singularly perturbed Markov control problems: a survey. *Contr. Dynamic Syst.*, 73:257–287, 1995.
- [AF98] N.D. Alikakos and G. Fusco. Slow dynamics for the Cahn–Hilliard equation in higher space dimensions: the motion of bubbles. *Arch. Rat. Mech. Anal.*, 141(1):1–61, 1998.
- [AF03] R.A. Adams and J.J.F. Fournier. *Sobolev Spaces*. Elsevier, 2003.
- [AF09] B. Ambrosio and J.-P. Francoise. Propagation of bursting oscillations. *Phil. Trans. R. Soc. A*, 367:4863–4875, 2009.
- [AFB90] M. Abbad, J.A. Filar, and T.R. Bielecki. Algorithms for singularly perturbed limiting average Markov control problems. *Decision and Control: Proc. 29th IEEE Conf.*, pages 1402–1497, 1990.
- [AFFS06] N.D. Alikakos, P.C. Fife, G. Fusco, and C. Soudris. Analysis of the heteroclinic connection in a singularly perturbed system arising from the study of crystalline grain boundaries. *Interfaces & Free Boundaries*, 8(2):159–183, 2006.
- [AFGG12] J.E. Avron, M. Fraas, G.M. Graf, and P. Grech. Adiabatic theorems for generators of contracting evolutions. *Commun. Math. Phys.*, 314:163–191, 2012.
- [AFH13] K.E. Avrachenkov, J.A. Filar, and P.G. Howett. *Analytic Perturbation Theory and Its Applications*. SIAM, 2013.
- [AFR13] A.H. Abbasiyan, H. Fallah, and M.R. Razvan. Symmetric bursting behaviors in the generalized FitzHugh–Nagumo model. *Biol. Cybern.*, pages 1–12, 2013. to appear.
- [AG82] C.M. Andersen and J.F. Geer. Power series expansions for the frequency and period of the limit cycle of the van der Pol equation. *SIAM J. Appl. Math.*, 42(3):678–693, 1982.
- [AG97a] Z. Artstein and V. Gaitsgory. Linear-quadratic tracking of coupled slow and fast targets. *Math. Control Signals Systems*, 10: 1–30, 1997.
- [AG97b] Z. Artstein and V. Gaitsgory. Tracking fast trajectories along a slow dynamics: a singular perturbations approach. *SIAM J. Contr. Optim.*, 35:1487, 1997.
- [AG00] Z. Artstein and V. Gaitsgory. The value function of singularly perturbed control systems. *Appl. Math. Optim.*, 41:425–445, 2000.
- [AG13] G.G. Avalos and N.B. Gallegos. Quasi-steady state model determination for systems with singular perturbations modelled by bond graphs. *Math. Computer Mod. Dyn. Syst.*, pages 1–21, 2013. to appear.
- [AGJ90] J.C. Alexander, R.A. Gardner, and C.K.R.T. Jones. A topological invariant arising in the stability analysis of travelling waves. *J. Reine Angew. Math.*, 410:167–212, 1990.

- [AGK⁺11] Z. Artstein, C.W. Gear, I.G. Kevrekidis, M. Slemrod, and E.S. Titi. Analysis and computation of a discrete KdV-Burgers type equation with fast dispersion and slow diffusion. *SIAM J. Numer. Anal.*, 49(5):2124–2143, 2011.
- [AGMR89] F.T. Arechi, W. Gadomski, R. Meucci, and J.A. Roversi. Delayed bifurcation at the threshold of a swept gain CO₂ laser. *Optics Commun.*, 70(2):155–160, 1989.
- [AH78] D. Altshuler and A.H. Haddad. Near optimal smoothing for singularly perturbed linear systems. *Automatica*, 14:81–87, 1978.
- [AHL10] A. Abdulle, Y. Hu, and T. Li. Chebyshev methods with discrete noise: the tau-ROCK methods. *J. Comp. Math.*, 28(2):195–217, 2010.
- [AHM08] M. Alfaro, D. Hilhorst, and H. Matano. The singular limit of the Allen–Cahn equation and the FitzHugh–Nagumo system. *J. Differen. Equat.*, 245(2):505–565, 2008.
- [Ai07] S. Ai. Traveling wave fronts for generalized Fisher equations with spatio-temporal delays. *J. Differential Equat.*, 232(1):104–133, 2007.
- [Ai10] S. Ai. Traveling waves for a model of a fungal disease over a vineyard. *SIAM J. Math. Anal.*, 42(2):833–856, 2010.
- [AIT09] D. Aroraitei, M. Ilea, and M. Turnea. Boundary functions method from differential equations systems with small parameter in enzyme kinetics. *Int. J. Math. Model. Simul. Appl.*, 2:77–91, 2009.
- [AJ89] U. Ascher and S. Jacobs. On collocation implementation for singularly perturbed two-point problems. *SIAM J. Sci. Stat. Comput.*, 10(3):533–549, 1989.
- [AK00] A.N. Atassi and H.K. Khalil. Separation results for the stabilization of nonlinear systems using different high-gain observer designs. *Syst. Contr. Lett.*, 39(3):183–191, 2000.
- [AK12] D.F. Anderson and M. Koyama. Weak error analysis of approximate simulation methods for multiscale stochastic chemical kinetic systems. *Multiscale Model. Simul.*, 10(4):1493–1524, 2012.
- [AK13a] R.V. Abramov and M.P. Kjerland. The response of reduced models of multiscale dynamics to small external perturbations. *arXiv:1305.0862*, pages 1–20, 2013.
- [AK13b] F. Achleitner and C. Kuehn. On bounded positive stationary solutions for a nonlocal Fisher-KPP equation. *arXiv:1307.3480*, pages 1–20, 2013.
- [AK13c] F. Achleitner and C. Kuehn. Traveling waves for a bistable equation with nonlocal-diffusion. *arXiv:1312.6304*, pages 1–45, 2013.
- [AK13d] H. Aoki and K. Kaneko. Slow stochastic switching by collective chaos of fast elements. *Phys. Rev. Lett.*, 111(14):144102, 2013.
- [AKK74] L.R. Abrahamsson, H.B. Keller, and H.-O. Kreiss. Difference approximations for singular perturbations of systems of ordinary differential equations. *Numer. Math.*, 22:367–391, 1974.
- [aKM89] E. Yanagida and K. Maginu. Stability of double-pulse solutions in nerve axon equations. *SIAM J. Appl. Math.*, 49(4):1158–1173, 1989.
- [AKN00] A. Andreini, M. Kamenskii, and P. Nistri. A result on the singular perturbation theory for differential inclusions in Banach spaces. *Top. Meth. Nonl. Anal. J. Juliusz Schauder Center*, 15: 1–15, 2000.
- [AKN06] V.I. Arnold, V.V. Kozlov, and A.I. Neishstadt. *Mathematical Aspects of Classical and Celestial Mechanics*. Springer, 3rd edition, 2006.
- [AKST07] Z. Artstein, I.G. Kevrekidis, M. Slemrod, and E.S. Titi. Slow observables of singularly perturbed differential equations. *Nonlinearity*, 20(11):2463–2481, 2007.
- [AKW03] C.D. Acker, N. Kopell, and J.A. White. Synchronization of strongly coupled excitatory neurons: Relating network behaviour to biophysics. *J. Comput. Neurosci.*, 15:71–90, 2003.
- [AKWC80] B. Avramovic, P.V. Kokotovic, J.R. Winkelman, and J.H. Chow. Area decomposition for electromechanical models of power systems. *Automatica*, 16(6):637–648, 1980.
- [AL91] B.D. Aguda and R. Larter. Periodic-chaotic sequences in a detailed mechanism of the peroxidase-oxidase reaction. *J. Am. Chem. Soc.*, 113:7913–7916, 1991.
- [AL08] A. Abdulle and T. Li. S-ROCK methods for stiff Itô SDEs. *Comm. Math. Sci.*, 6(4):845–868, 2008.
- [ALC89] B.D. Aguda, R. Larter, and B.L. Clarke. Dynamic elements of mixed-mode oscillations and chaos in a peroxidase-oxidase network. *J. Chem. Phys.*, 90(8):4168–4175, 1989.
- [Ale77] R. Alexander. Diagonally implicit Runge–Kutta methods for stiff ODE's. *SIAM J. Numer. Anal.*, 14(6):1006–1021, 1977.
- [All92] G. Allaire. Homogenization and two-scale convergence. *SIAM J. Math. Anal.*, 23(6):1482–1518, 1992.
- [ALS12] A. Abdulle, P. Lin, and A. Shapeev. Numerical methods for multilattices. *Multiscale Model. Simul.*, 10(3):696–726, 2012.
- [ALT07] Z. Artstein, J. Linshiz, and E.S. Titi. Young measure approach to computing slowly advancing fast oscillations. *Multiscale Model. Simul.*, 243:1085–1097, 2007.
- [AM86] K. Aihara and G. Matsumoto. Chaotic oscillations and bifurcations in squid giant axons. In A. Holden, editor, *Chaos*, pages 257–269. Manchester University Press, 1986.
- [AM88] U.M. Ascher and R.M.M. Mattheij. General framework, stability and error analysis for numerical stiff boundary value methods. *Numer. Math.*, 54:355–372, 1988.
- [AM06] A. Ambrosetti and A. Malchiodi. *Perturbation Methods and Semilinear Elliptic Problems on \mathbb{R}^n* . Birkhäuser, 2006.
- [Ami84] D.J. Amit. *Field theory, the renormalization group, and critical phenomena*. World Scientific, 1984.
- [AMN⁺03] R.B. Alley, J. Marotzke, W.D. Nordhaus, J.T. Overpeck, D.M. Petet, R.A. Pielke Jr., R.T. Pierrehumbert, P.B. Rhines, T.F. Stocker, L.D. Talley, and J.M. Wallace. Abrupt climate change. *Science*, 299:2005–2010, 2003.
- [AMP⁺12] S. Arnrich, A. Mielke, M.A. Peletier, G. Savaré, and M. Veneroni. Passing to the limit in a Wasserstein gradient flow: from diffusion to reaction. *Calc. Var. Partial Differential Equat.*, 44:419–454, 2012.
- [AMPP87] S.B. Angenent, J. Mallet-Paret, and L.A. Peletier. Stable transition layers in a semilinear boundary value problem. *J. Differential Equat.*, 67(2):212–242, 1987.
- [AMPS91] U.M. Ascher, P.A. Markowich, P. Pietra, and C. Schmeiser. A phase plane analysis of transonic solutions for the hydrodynamic semiconductor model. *Math. Mod. Meth. Appl. Sci.*, 1(3):347–376, 1991.
- [AMR87] U.M. Ascher, R.M.M. Mattheij, and R.D. Russell. *Numerical Solution of Boundary Value Problems for Ordinary Differential Equations*. SIAM, 1987.
- [AMR88] R. Abraham, J.E. Marsden, and T. Ratiu. *Manifolds, Tensor Analysis and Applications*. Springer, 1988.

- [AMR02] M. De Angelis, A.M. Monte, and P. Renno. On fast and slow times in models with diffusion. *Math. Models Methods Appl. Sci.*, 12:1741–1749, 2002.
- [Ana83] K.K. Anand. On relaxation oscillations governed by a second order differential equation for a large parameter and with a piecewise linear function. *Canad. Math. Bull.*, 26(1):80–91, 1983.
- [And87] J.L. Anderson. Equidistribution schemes, Poisson generators, and adaptive grids. *Appl. Math. Comput.*, 24(3):211–227, 1987.
- [And92] J.L. Anderson. Multiple time scale methods for adiabatic systems. *Amer. J. Phys.*, 60:923–927, 1992.
- [ANMC⁺09] K. Al-Naimee, F. Marino, M. Ciszak, R. Meucci, and F.T. Arezchi. Chaotic spiking and incomplete homoclinic scenarios in semiconductor lasers with optoelectric feedback. *New Journal of Physics*, 11:073022, 2009.
- [Ano99] O.D. Anosova. On invariant manifolds in singularly perturbed systems. *J. Dyn. Contr. Syst.*, 5(4):501–507, 1999.
- [ANZ11] A.V. Artemyev, A.I. Neishtadt, and L.M. Zelenyi. Jumps of adiabatic invariant at the separatrix of a degenerate saddle point. *Chaos*, 21:043120, 2011.
- [ANZV10] A.V. Artemyev, A.I. Neishtadt, L.M. Zelenyi, and D.L. Vainchtein. Adiabatic description of capture into resonance and surfatron acceleration of charged particles by electromagnetic waves. *Chaos*, 20:043128, 2010.
- [AO70] R.C. Ackerberg and R.E. O’Malley. Boundary layer problems exhibiting resonance. *Stud. Appl. Math.*, 49:277–295, 1970.
- [AP98a] P. Auger and J.-C. Poggiale. Aggregation and emergence in systems of ordinary differential equations. *Math. Comput. Model.*, 27(4):1–21, 1998.
- [AP98b] P. Auger and D. Pontier. Fast game dynamics coupled to slow population dynamics: a single population with hawk-dove strategies. Aggregation and emergence in population dynamics. *Math. Comput. Modelling*, 27(4):81–88, 1998.
- [AP98c] P. Auger and D. Pontier. Fast game theory coupled to slow population dynamics: the case of domestic cat populations. *Math. Biosci.*, 148:65–82, 1998.
- [AP06] N. Ben Abdallah and O. Pinaud. Multiscale simulation of transport in an open quantum system: Resonances and WKB interpolation. *J. Comp. Phys.*, 213(1):288–310, 2006.
- [AP12] A. Abdulle and G. Pavliotis. Numerical methods for stochastic partial differential equations with multiple scales. *J. Comp. Phys.*, 231(6):2482–2497, 2012.
- [AR81] U. Ascher and R.D. Russell. Reformulation of boundary value problems into standard form. *SIAM Rev.*, 23(2):238–254, 1981.
- [AR85] F. Argoul and J.C. Roux. Quasiperiodicity in chemistry: an experimental path in the neighbourhood of a codimension-two bifurcation. *Phys. Lett. A*, 108(8):426–430, 1985.
- [Ard80] M.D. Ardema. Nonlinear singularly perturbed optimal control problems with singular arcs. *Automatica*, 16:99–104, 1980.
- [ARLS11] M. Assaf, E. Roberts, and Z. Luthey-Schulten. Determining the stability of genetic switches: explicitly accounting for mRNA noise. *Phys. Rev. Lett.*, 106:248102, 2011.
- [Arn73] V.I. Arnold. *Ordinary Differential Equations*. MIT Press, 1973.
- [Arn74] L. Arnold. *Stochastic Differential Equations: Theory and Applications*. Wiley, 1974.
- [Arn83] V.I. Arnold. *Geometrical Methods in the Theory of Ordinary Differential Equations*. Springer, New York, NY, 1983.
- [Arn92] V.I. Arnold. *Catastrophe Theory*. Springer, 1992.
- [Arn94] V.I. Arnold. *Encyclopedia of Mathematical Sciences: Dynamical Systems V*. Springer, 1994.
- [Arn95] L. Arnold. Random dynamical systems. In *Dynamical Systems (Montecatini Terme, 1994)*, pages 1–43. Springer, 1995.
- [Arn97] V.I. Arnold. *Mathematical Methods of Classical Mechanics*. Springer, 1997.
- [Arn01] L. Arnold. Recent progress in stochastic bifurcation theory. In *IUTAM Symposium on Nonlinearity and Stochastic Structural Dynamics*, pages 15–27. Springer, 2001.
- [Arn03] L. Arnold. *Random Dynamical Systems*. Springer, Berlin Heidelberg, Germany, 2003.
- [Arr89] S. Arrhenius. Über die Reaktionsgeschwindigkeit bei der Inversion von Rohrzucker durch Säuren. *Zeitschr. Phys. Chem.*, 4:226–248, 1889.
- [ARS95] F.N. Albahadily, J. Ringland, and M. Schell. Mixed-mode oscillations in an electrochemical system. I. A Farey sequence which does not occur on a torus. *J. Chem. Phys.*, 90:813–821, 1989.
- [Art98] Z. Artstein. Stability in the presence of singular perturbations. *Nonlinear Analysis*, 34:817–827, 1998.
- [Art99a] Z. Artstein. Invariant measures of differential inclusions applied to singular perturbations. *J. Differential Equat.*, 152:289–307, 1999.
- [Art99b] Z. Artstein. Singularly perturbed ordinary differential equations with nonautonomous fast dynamics. *J. Dyn. Diff. Eq.*, 11(2):297–318, 1999.
- [Art04] Z. Artstein. Distributional convergence in planar dynamics and singular perturbations. *J. Differential Equations*, 201:250–286, 2004.
- [Art05] Z. Artstein. Bang-bang controls in the singular perturbations limit. *Control and Cybernetics*, 34(3):645–663, 2005.
- [Art07] Z. Artstein. Averaging of time-varying differential equations revisited. *J. Differen. Equat.*, 243:146–167, 2007.
- [Art09] Z. Artstein. Pontryagin Maximum Principle for coupled slow and fast systems. *Control and Cybernetics*, 38(4):1003–1019, 2009.
- [Art10] Z. Artstein. Averaging of ordinary differential equations with slowly varying averages. *Discr. Cont. Dyn. Syst. B*, 14(2):353–360, 2010.
- [AS65] M. Abramowitz and I.A. Stegun. *Handbook of Mathematical Functions*. Dover, 1965.
- [AS86] R.H. Abraham and H.B. Stewart. A chaotic blue sky catastrophe in forced relaxation oscillations. *Physica D*, 21(2):394–400, 1986.
- [AS96] Y. Ando and M. Suzuki. Control of active suspension systems using the singular perturbation method. *Contr. Eng. Pract.*, 4(3):287–293, 1996.
- [AS01] Z. Artstein and M. Slemrod. On singularly perturbed retarded functional differential equations. *J. Differential Equat.*, 171:88–109, 2001.

- [AS12] F. Achleitner and P. Szmolyan. Saddle-node bifurcation of viscous profiles. *Physica D*, 241(20):1703–1717, 2012.
- [ASBT10] S. Ahn, B.H. Smith, A. Borisyuk, and D. Terman. Analyzing neuronal networks using discrete-time dynamics. *Physica D*, 239(9):515–528, 2010.
- [Asc85] U. Ascher. On some difference schemes for singular singularly-perturbed boundary value problems. *Numer. Math.*, 46:1–30, 1985.
- [ASS13] P. Antonelli, J.-C. Saut, and C. Sparber. Well-posedness and averaging of NLS with time-periodic dispersion management. *Adv. Differential Equations*, 18(1):49–68, 2013.
- [ASST12] G. Ariel, J.M. Sanz-Serna, and R. Tsai. A multiscale technique for finding slow manifolds of stiff mechanical systems. *Multiscale Model. Simul.*, 10(4):1180–1203, 2012.
- [ASY96] K.T. Alligood, T.D. Sauer, and J.A. Yorke. *Chaos: An Introduction to Dynamical Systems*. Springer, 1996.
- [ATB⁺12] D. Anderson, A. Tenzer, G. Barlev, M. Girvan, T.M. Antonsen, and E. Ott. Multiscale dynamics in communities of phase oscillators. *Chaos*, 22(1):013102, 2012.
- [Att11] B.S. Attili. Numerical treatment of singularly perturbed two point boundary value problems exhibiting boundary layers. *Commun. Nonlinear Sci. Numer. Simulat.*, 16:3504–3511, 2011.
- [AW74] D.G. Aronson and H.F. Weinberger. Nonlinear diffusion in population genetics, combustion, and nerve pulse propagation. In *Partial Differential Equations and Related Topics*, volume 446 of *Lecture Notes in Mathematics*, pages 5–49. Springer, 1974.
- [AW83] U. Ascher and R. Weiss. Collocation for singular perturbation problems I: first order systems with constant coefficients. *SIAM J. Numer. Anal.*, 20(3):537–557, 1983.
- [AW84a] U. Ascher and R. Weiss. Collocation for singular perturbation problems II: linear first order systems without turning points. *Mathematics of Computation*, 43(167):157–187, 1984.
- [AW84b] U. Ascher and R. Weiss. Collocation for singular perturbation problems III: nonlinear problems without turning points. *SIAM J. Sci. Stat. Comput.*, 5(4):811–829, 1984.
- [AWVC12] P. Ashwin, S. Wieczorek, R. Vitolo, and P. Cox. Tipping points in open systems: bifurcation, noise-induced and rate-dependent examples in the climate system. *Phil. Trans. R. Soc. A*, 370:1166–1184, 2012.
- [AZSPS82] S. Ahmed-Zaid, P. Sauer, M. Pai, and M. Sarioglu. Reduced order modeling of synchronous machines using singular perturbation. *IEEE Trans. Circ. Syst.*, 29(11):782–786, 1982.
- [Bae91a] C. Baesens. Noise effect on dynamic bifurcations: the case of a period-doubling cascade. In E. Benoît, editor, *Dynamic Bifurcations*, volume 1493 of *Lecture Notes in Mathematics*, pages 107–130. Springer, 1991.
- [Bae91b] C. Baesens. Slow sweep through a period-doubling cascade: delayed bifurcations and renormalisation. *Physica D*, 53(2):319–375, 1991.
- [Bae95] C. Baesens. Gevrey series and dynamic bifurcations for analytic slow–fast mappings. *Nonlinearity*, 8(2):179, 1995.
- [Bak86] V.I. Bakhtin. Averaging in multifrequency systems. *Func. Anal. Appl.*, 20(2):83–88, 1986.
- [Bak96] V.I. Bakhtin. Averaging along a Markov chain. *Funct. Anal. Appl.*, 30(1):42–44, 1996.
- [Bak00] V.I. Bakhtin. Cramér asymptotics in a system with slow and fast Markovian motions. *Theor. Prob. Appl.*, 44(1):1–17, 2000.
- [Bak03] V.I. Bakhtin. Cramér’s asymptotics in systems with fast and slow motions. *Stochastics Stoch. Rep.*, 75(5):319–341, 2003.
- [Bal77] J.M. Ball. Remarks on blow-up and nonexistence theorems for nonlinear evolution equations. *Quart. J. Math.*, 28(4):473–486, 1977.
- [Bal82] M.J. Balas. Reduced-order feedback control of distributed parameter systems via singular perturbation methods. *J. Math. Anal. Appl.*, 87:281–294, 1982.
- [Bal00] W. Balser. *Formal Power Series and Linear Systems of Meromorphic Ordinary Differential Equations*. Springer, 2000.
- [Bar83] J.W. Barker. Interactions of fast and slow waves in hyperbolic systems with two time scales. *Math. Methods Appl. Sci.*, 5(3):292–307, 1983.
- [Bar84] J.W. Barker. Interactions of fast and slow waves in problems with two time scales. *SIAM J. Math. Anal.*, 15(3):500–513, 1984.
- [Bar88] D. Barkley. Slow manifolds and mixed-mode oscillations in the Belousov–Zhabotinskii reaction. *J. Chem. Phys.*, 89(9):5547–5559, 1988.
- [Bar91] D. Barkley. A model for fast computer simulation of waves in excitable media. *Physica D*, 49:61–70, 1991.
- [Bar92] D. Barkley. Linear stability analysis of rotating spiral waves in excitable media. *Phys. Rev. Lett.*, 68(13):2090–2093, 1992.
- [Bar97] D. Barkley. Fast simulation of waves in three-dimensional excitable media. *Int. J. Bif. Chaos*, 7(11):2529–2545, 1997.
- [Bat67] G.K. Batchelor. *An Introduction to Fluid Dynamics*. CUP, 1967.
- [Bat94] F. Battelli. Heteroclinic orbits in singular systems: a unifying approach. *J. Dyn. Diff. Eq.*, 6(1):147–173, 1994.
- [BB79] K. Burrage and J.C. Butcher. Stability criteria for implicit Runge–Kutta methods. *SIAM J. Numer. Anal.*, 16(1):46–57, 1979.
- [BB80] K. Burrage and J.C. Butcher. Nonlinear stability of a general class of differential equation methods. *BIT*, 20(2):185–203, 1980.
- [BB87] A. Bensoussan and G.L. Blankenship. Singular perturbations in stochastic control. In *Singular Perturbations and Asymptotic Analysis in Control Systems*, volume 90 of *Lecture Notes in Control and Information Sciences*, pages 171–260. Springer, 1987.
- [BB12a] C.G. Diniz Behn and V. Booth. A fast–slow analysis of the dynamics of REM sleep. *SIAM J. Appl. Dyn. Syst.*, 11(1):212–242, 2012.
- [BB12b] Yu.N. Bibikov and V.R. Bukaty. Multifrequency oscillations of singularly perturbed systems. *Differential Equat.*, 48(1):19–25, 2012.
- [BB13] P. Berger and A. Bounemoura. A geometrical proof of the persistence of normally hyperbolic submanifolds. *Dynamical Systems*, pages 1–15, 2013. to appear.

- [BBE91] M. Brøns and K. Bar-Eli. Canard explosion and excitation in a model of the Belousov–Zhabotinsky reaction. *J. Phys. Chem.*, 95:8706–8713, 1991.
- [BBE94] M. Brøns and K. Bar-Eli. Asymptotic analysis of canards in the EOE equations and the role of the inflection line. *Proc. R. Soc. Lond. A*, 445:305–322, 1994.
- [BBK⁺11] G.N. Benes, A.M. Barry, T.J. Kaper, M.A. Kramer, and J. Burke. An elementary model of torus canards. *Chaos*, 21:023131, 2011.
- [BBKS95] R. Bertram, M.J. Butte, T. Kiemel, and A. Sherman. Topological and phenomenological classification of bursting oscillations. *Bull. Math. Biol.*, 57(3):413–429, 1995.
- [BBR⁺05] J. Best, A. Borisyuk, J. Rubin, D. Terman, and M. Wechselberger. The dynamic range of bursting in a model respiratory pacemaker network. *SIAM J. Appl. Dyn. Syst.*, 4(4):1107–1139, 2005.
- [BBSR91] W. Balser and B.L.J. Braaksma, J.P. Ramis and Y. Sibuya. Multisummability of formal power series solutions of linear ordinary differential equations. *Asymp. Anal.*, 5(1):27–45, 1991.
- [BBS96] J.A. Borghans, R.J. De Boer, and L.A. Segel. Extending the quasi-steady state approximation by changing variables. *Bull. Math. Biol.*, 58(1):43–63, 1996.
- [BBV08] A. Barrat, M. Barthélémy, and A. Vespignani. *Dynamical Processes on Complex Networks*. CUP, 2008.
- [BC91] M. Benedicks and L. Carleson. The dynamics of the Hénon map. *Annals of Mathematics*, 133:73–169, 1991.
- [BC94a] D. Bainov and V. Covachev. *Impulsive differential equations with a small parameter*. World Scientific, 1994.
- [BC94b] C. Berzuini and D. Clayton. Bayesian analysis of survival on multiple time scales. *Statistics in Medicine*, 13(8):823–838, 1994.
- [BC98] P.C. Bressloff and S. Coombes. Desynchronization, mode locking, and bursting in strongly coupled integrate-and-fire oscillators. *Phys. Rev. Lett.*, 81(10):2168–2171, 1998.
- [BCB96] R.J. Butera, J.W. Clark, and J.H. Byrne. Dissection and reduction of a modeled bursting neuron. *J. Comput. Neurosci.*, 3(3):199–223, 1996.
- [BCB97] R.J. Butera, J.W. Clark, and J.H. Byrne. Transient responses of a modeled bursting neuron: analysis with equilibrium and averaged nullclines. *Biol. Cybernet.*, 77(5):307–322, 1997.
- [BCC⁺95] R.J. Butera, J.W. Clark, C.C. Canavier, D.A. Baxter, and J.H. Byrne. Analysis of the effects of modulatory agents on a modeled bursting neuron: dynamic interactions between voltage and calcium dependent systems. *J. Comput. Neurosci.*, 2(1):19–44, 1995.
- [BCD08] M. Bardi and I. Capuzzo-Dolcetta. *Optimal Control and Viscosity Solutions of Hamilton–Jacobi–Bellman Equations*. Birkhäuser, 2008.
- [BCGFS13] T. Berry, J.R. Cressman, Z. Greguric-Ferencik, and T. Sauer. Time-scale separation from diffusion-mapped delay coordinates. *SIAM J. Appl. Dyn. Syst.*, 12(2):618–649, 2013.
- [BCHV93] H.W. Broer, S.N. Chow, A. Hagen, and G. Vegter. A normally elliptic Hamiltonian bifurcation. *Z. Angewand. Math. Phys.*, 44(3):389–432, 1993.
- [BCMWM13] M. Burger, L. Caffarelli, P. Markowich, and M.-T. Wolfram. On a Boltzmann type price formation model. *Proc. R. Soc. A*, 469:1–21, 2013.
- [BCPS7] K.E. Brenan, S.L. Campbell, and L.R. Petzhold. *Numerical solution of initial-value problems in differential-algebraic equations*. SIAM, 1987.
- [BD80] J. Boissonade and P. DeKepper. Transitions from bistability to limit cycle oscillations. Theoretical analysis and experimental evidence in an open chemical system. *J. Phys. Chem.*, 84:501–506, 1980.
- [BD86] S.V. Belokopytov and M.G. Dmitriev. Direct scheme in optimal control problems with fast and slow motions. *Syst. Contr. Lett.*, pages 129–135, 1986.
- [BD97] E. Brunet and B. Derrida. Shift in the velocity front due to a cutoff. *Phys. Rev. E*, 56(3):2597–2604, 1997.
- [BD02] D.C. Bell and B. Deng. Singular perturbation of n -front travelling waves in the FitzHugh–Nagumo equations. *Nonl. Anal.: Real World Appl.*, 3:515–541, 2002.
- [BDB⁺12] J. Burke, M. Desroches, A.M. Barry, T.J. Kaper, and M.A. Kramer. A showcase of torus canards in neuronal bursters. *J. Math. Neurosci.*, 2:3, 2012.
- [BdCdS10] C.A. Buzzi, T. de Carvalho, and P.R. da Silva. Canard cycles and Poincaré index of non-smooth vector fields on the plane. *arXiv:1002:4169v2*, pages 1–20, 2010.
- [BDFN92] J.J. Binney, N.J. Dowrick, A.J. Fisher, and M. Newman. *The Theory of Critical Phenomena: An Introduction to the Renormalization Group*. OUP, 1992.
- [BdHN06] A. Bovier, F. den Hollander, and F.R. Nardi. Sharp asymptotics for Kawasaki dynamics on a finite box with open boundary. *Prob. Theory Rel. Fields*, 135(2):265–310, 2006.
- [BdHS10] A. Bovier, F. den Hollander, and C. Spitoni. Homogeneous nucleation for Glauber and Kawasaki dynamics in large volumes at low temperatures. *Ann. Prob.*, 38(2):661–713, 2010.
- [BDK06] M. Beck, A. Doelman, and T.J. Kaper. A geometric construction of traveling waves in a bioremediation model. *J. Nonlinear Sci.*, 16(4):329–349, 2006.
- [BDM99] T.J. Burns, R.W. Davis, and E.F. Moore. A perturbation study of particle dynamics in a plane wake flow. *J. Fluid Mech.*, 384(1):1–26, 1999.
- [BDMNC96] J.P. Barbot, M. Djemai, S. Monaco, and D. Normand-Cyrot. Analysis and control of nonlinear singularly perturbed systems under sampling. *Control and Dynamic Systems*, 79:203–246, 1996.
- [BDS99] P.W. Bates, E.N. Dancer, and J. Shi. Multi-spike stationary solutions of the Cahn–Hilliard equation in higher-dimension and instability. *Adv. Differential Equat.*, 4(1):1–70, 1999.
- [BdST05] C.A. Buzzi, P.R. da Silva, and M.A. Teixeira. Singular perturbation problems for time-reversible systems. *Proc. Amer. Math. Soc.*, 133(11):3323–3331, 2005.
- [BdST06] C.A. Buzzi, P.R. da Silva, and M.A. Teixeira. A singular approach to discontinuous vector fields on the plane. *J. Diff. Eq.*, 231:633–655, 2006.
- [BdST12] C.A. Buzzi, P.R. da Silva, and M.A. Teixeira. Slow-fast systems on algebraic varieties bordering piecewise-smooth dynamical systems. *Bull. Sci. Math.*, 136(4):444–462, 2012.
- [BDV04] C. Bonatti, L.J. Diaz, and M. Viana. *Dynamics Beyond Uniform Hyperbolicity*. Springer, 2004.
- [BE86] S.M. Baer and T. Erneux. Singular Hopf bifurcation to relaxation oscillations I. *SIAM J. Appl. Math.*, 46(5):721–739, 1986.
- [BE92] S.M. Baer and T. Erneux. Singular Hopf bifurcation to relaxation oscillations II. *SIAM J. Appl. Math.*, 52(6):1651–1664, 1992.

- [BE95] V. Booth and T. Erneux. Understanding propagation failure as a slow capture near a limit point. *SIAM J. Appl. Math.*, 55(5):1372–1389, 1995.
- [Bea00] R.R. Beardmore. Double singularity-induced bifurcation points and singular Hopf bifurcations. *Dyn. Stab. Syst.*, 15(4):319–342, 2000.
- [BEG⁺03] K. Bold, C. Edwards, J. Guckenheimer, S. Guharay, K. Hoffman, J. Hubbard, R. Oliva, and W. Weckesser. The forced van der Pol equation II: canards in the reduced system. *SIAM Journal of Applied Dynamical Systems*, 2(4):570–608, 2003.
- [BEGK04] A. Bovier, M. Eckhoff, V. Gayrard, and M. Klein. Metastability in reversible diffusion processes. I. Sharp asymptotics for capacities and exit times. *J. Euro. Math. Soc.*, 6(4):399–424, 2004.
- [Bel59] B.P. Belousov. A periodic reaction and its mechanism (in Russian). *Collections of Abstracts on Radiation Medicine*, page 145, 1959.
- [Bel60] R. Bellman. *Introduction to Matrix Analysis*. McGraw-Hill, 1960.
- [Ben82] E. Benoît. Systèmes lents-rapides dans \mathbb{R}^3 et leurs canards. In *Third Snepfenried geometry conference*, volume 2, pages 159–191. Soc. Math. France, 1982.
- [Ben84] A. Bensussan. On some singular perturbation problems arising in stochastic control. *Stoch. Anal. Appl.*, 2:13–53, 1984.
- [Ben85] E. Benoît. Enlacements de canards. *C.R. Acad. Sc. Paris*, 300(8):225–230, 1985.
- [Ben90] E. Benoît. Canards et enlacements. *Publ. Math. IHES*, 72:63–91, 1990.
- [Ben91a] E. Benoît, editor. *Dynamic Bifurcations*, volume 1493 of *Lecture Notes in Mathematics*. Springer, 1991.
- [Ben91b] E. Benoît. Linear dynamic bifurcation with noise. In E. Benoît, editor, *Dynamic Bifurcations*, volume 1493 of *Lecture Notes in Mathematics*, pages 131–150. Springer, 1991.
- [Ben96] E. Benoît. Asymptotic expansions of canards with poles. Application to the stationary unidimensional Schrödinger equation. Nonstandard analysis. *Bull. Belg. Math. Soc.*, pages 71–90, 1996. suppl.
- [Ben01] E. Benoît. Perturbation singulière en dimension trois: canards en un point pseudo-singulier noeud. *Bull. Soc. Math. France*, 129:91–113, 2001.
- [Ben09] E. Benoît. Bifurcation delay - the case of the sequence: stable focus - unstable focus - unstable node. *Discr. Cont. Dyn. Sys. - Series S*, 2(4):911–929, 2009.
- [Ber60] P.G. Bergmann. *Introduction to the Theory of Relativity*. Prentice Hall, 1960.
- [Ber84] M.V. Berry. Quantal phase factors accompanying adiabatic changes. *Proc. R. Soc. A*, 392(1802):45–57, 1984.
- [Ber85] M.V. Berry. Classical adiabatic angles and quantal adiabatic phase. *J. Phys. A*, 18(1):15, 1985.
- [Ber87] M.V. Berry. Quantum phase corrections from adiabatic iteration. *Proc. R. Soc. A*, 414(1846):31–46, 1987.
- [BER89] S.M. Baer, T. Erneux, and J. Rinzel. The slow passage through a Hopf bifurcation: delay, memory effects, and resonance. *SIAM J. Appl. Math.*, 49(1):55–71, 1989.
- [Ber91] A.J. Bernoff. Spiral wave solutions for reaction–diffusion equations in a fast reaction/slow diffusion limit. *Physica D*, 53:125–150, 1991.
- [Ber93] R. Bertram. A computational study of the effects of serotonin on a molluscan burster neuron. *Biol. Cybern.*, 69(3):257–267, 1993.
- [Ber98a] M. Berg. Viscoelastic continuum model of nonpolar solvation. 1. Implications for multiple time scales in liquid dynamics. *J. Phys. Chem.*, 102:17–30, 1998.
- [Ber98b] N. Berglund. *Adiabatic Dynamical Systems and Hysteresis*. PhD thesis, EPFL, 1998.
- [Ber00] N. Berglund. Control of dynamic Hopf bifurcations. *Nonlinearity*, 13:225–248, 2000.
- [Ber01] N. Berglund. Perturbation theory of dynamical systems. *arXiv:math/0111178*, pages 1–111, 2001.
- [Ber13] N. Berglund. Kramers’ law: validity, derivations and generalisations. *Markov Processes Relat. Fields*, pages 1–24, 2013. to appear.
- [BF28] M. Born and V. Fock. Beweis des Adiabatensatzes. *Z. Phys.*, 51:165–169, 1928.
- [BF70] M. Berger and L. Fraenkel. On the asymptotic solution of a nonlinear Dirichlet problem. *Indiana Univ. Math. J.*, 19:553–585, 1970.
- [BF71] M. Berger and L. Fraenkel. On singular perturbations of nonlinear operator equations. *Indiana Univ. Math. J.*, 20:623–631, 1971.
- [BF90] P.W. Bates and P.C. Fife. Spectral comparison principles for the Cahn–Hilliard and phase-field equations, and time scales for coarsening. *Physica D*, 43(2):335–348, 1990.
- [BF91] T.R. Bielecki and J.A. Filar. Singularly perturbed Markov control problem: limiting average cost. *Annals of Operations Research*, 28(1):152–168, 1991.
- [BF93] P.W. Bates and P.C. Fife. The dynamics of nucleation for the Cahn–Hilliard equation. *SIAM J. Appl. Math.*, 53(4):990–1008, 1993.
- [BF96] F. Battelli and M. Fečkan. Global centre manifolds in singular systems. *Nonlinear Different. Equat. Appl.*, 3:19–34, 1996.
- [BF00] P.W. Bates and G. Fusco. Equilibria with many nuclei for the Cahn–Hilliard equation. *J. Differential Equat.*, 160(2):283–356, 2000.
- [BF13] F. Battelli and M. Fečkan. Fast–slow dynamical approximation of forced impact systems near periodic solutions. *Bound. Value Probl.*, 2013:71, 2013.
- [BFF99] D. Brown, J. Feng, and S. Feirick. Variability of firing of Hodgkin–Huxley and FitzHugh–Nagumo neurons with stochastic synaptic input. *Phys. Rev. Lett.*, 82(23):4731–4734, 1999.
- [BFM06] P. Breitenlohner, P. Forgács, and D. Maison. Classification of static, spherically symmetric solutions of the Einstein–Yang–Mills theory with positive cosmological constant. *Commun. Math. Phys.*, 261(3):569–611, 2006.
- [BFS08] B. Brighi, A. Fruchard, and T. Sari. On the Blasius problem. *Adv. Differential Equat.*, 13(5):509–600, 2008.
- [BFSO95] T.V. Bronnikova, V.R. Fed’kina, W.M. Schaffer, and L.F. Olsen. Period-doubling bifurcations and chaos in a detailed model of the peroxidase-oxidase reaction. *J. Phys. Chem.*, 99(23):9309–9312, 1995.
- [BFSW98a] E. Benoît, A. Fruchard, R. Schäfke, and G. Wallet. Overstability: towards a global study. *C. R. Acad. Sci. Paris Sér. I Math.*, 326:873–878, 1998.
- [BFSW98b] E. Benoît, A. Fruchard, R. Schäfke, and G. Wallet. Solutions surstables des équations différentielles complexes lentes-rapides à point tournant. *Ann. Fac. Sci. Toulouse Math.*, 6(7):627–658, 1998.

- [BG74] H. Bavinck and J. Grasman. The method of matched asymptotic expansions for the periodic solution of the van der Pol equation. *Int. J. Nonl. Mech.*, 9(6):421–434, 1974.
- [BG88] I. Borno and Z. Gajic. Parallel algorithms for optimal control of weakly coupled and singularly perturbed jump linear systems. *Automatica*, 31(7):985–988, 1988.
- [BG92] J.J.W. Bruce and P.J. Giblin. *Curves and Singularities: a geometrical introduction to singularity theory*. CUP, 1992.
- [BG93] B. Braaksma and J. Grasman. Critical dynamics of the Bonhoeffer–van der Pol equation and its chaotic response to periodic stimulation. *Physica D*, 68(2):265–280, 1993.
- [BG95] G. Benfatto and G. Gallavotti. *Renormalization Group*. Princeton University Press, 1995.
- [BG01] V.F. Butuzov and E.A. Gromova. A boundary value problem for a system of fast and slow second-order equations in the case of intersecting roots of the degenerate equation. *Comp. Math. Math. Phys.*, 41(8):1108–1121, 2001.
- [BG02a] N. Berglund and B. Gentz. As sample-paths approach to noise-induced synchronization: stochastic resonance in a double-well potential. *Ann. Appl. Prob.*, 12(4):1419–1470, 2002.
- [BG02b] N. Berglund and B. Gentz. Beyond the Fokker–Planck equation: pathwise control of noisy bistable systems. *J. Phys. A: Math. Gen.*, 35:2057–2091, 2002.
- [BG02c] N. Berglund and B. Gentz. The effect of additive noise on dynamical hysteresis. *Nonlinearity*, 15: 605–632, 2002.
- [BG02d] N. Berglund and B. Gentz. Metastability in simple climate models: Pathwise analysis of slowly driven Langevin equations. *Stoch. Dyn.*, 2:327–356, 2002.
- [BG02e] N. Berglund and B. Gentz. Pathwise description of dynamic pitchfork bifurcations with additive noise. *Probab. Theory Related Fields*, 3:341–388, 2002.
- [BG03] N. Berglund and B. Gentz. Geometric singular perturbation theory for stochastic differential equations. *J. Diff. Eqs.*, 191:1–54, 2003.
- [BG04] N. Berglund and B. Gentz. On the noise-induced passage through an unstable periodic orbit I: Two-level model. *J. Statist. Phys.*, 114(5):1577–1618, 2004.
- [BG05] V.S. Buslaev and E.A. Grinina. Remarks on the quantum adiabatic theorem. *St. Petersburg Math. J.*, 16(4):639–649, 2005.
- [BG06] N. Berglund and B. Gentz. *Noise-Induced Phenomena in Slow–Fast Dynamical Systems*. Springer, 2006.
- [BG07a] V.S. Borkar and V. Gaitsgory. Averaging of singularly perturbed controlled stochastic differential equations. *Appl. Math. Optim.*, 56(2):169–209, 2007.
- [BG07b] V.S. Borkar and V. Gaitsgory. Singular perturbations in ergodic control of diffusions. *SIAM J. Control Optim.*, 46:1562–1577, 2007.
- [BG08a] S.M. Baer and E.M. Gaekel. Slow acceleration and deacceleration through a Hopf bifurcation: power ramps, target nucleation, and elliptic bursting. *Phys. Rev. E*, 78:036205, 2008.
- [BG08b] N. Brännström and V. Gelfreich. Drift of slow variables in slow–fast Hamiltonian systems. *Physica D*, 237:2913–2921, 2008.
- [BG09] N. Berglund and B. Gentz. Stochastic dynamic bifurcations and excitability. In C. Laing and G. Lord, editors, *Stochastic methods in Neuroscience*, volume 2, pages 65–93. OUP, 2009.
- [BG13a] N. Berglund and B. Gentz. On the noise-induced passage through an unstable periodic orbit II: The general case. *SIAM J. Math. Anal.*, 2013, accepted, to appear.
- [BG13b] N. Berglund and B. Gentz. Sharp estimates for metastable lifetimes in parabolic SPDEs: Kramers' law and beyond. *Electronic J. Probability*, 18(24):1–58, 2013.
- [BG13c] V. Bykov and V. Gol'dshtain. Fast and slow invariant manifolds in chemical kinetics. *Comput. Math. Appl.*, 65(10):1502–1515, 2013.
- [BGG08] S. Borok, I. Goldfarb, and V. Gol'dshtain. About non-coincidence of invariant manifolds and intrinsic low dimensional manifolds (ILDM). *Comm. Nonl. Sci. Numer. Simul.*, 13(6):1029–1038, 2008.
- [BGGG02] V. Bykov, I. Goldfarb, V. Gol'dshtain, and J.B. Greenberg. Thermal explosion in a hot gas mixture with fuel droplets: a two reactant model. *Combust. Theor. Model.*, 6(2):339–359, 2002.
- [BGM06] V. Bykov, I. Goldfarb, V. Gol'dshtain, and U. Maas. On a modified version of ILDM approach: asymptotic analysis based on integral manifolds. *IMA J. Appl. Math.*, 71(3):359–382, 2006.
- [BGK05] A. Bovier, V. Gayrard, and M. Klein. Metastability in reversible diffusion processes. II. Precise estimates for small eigenvalues. *J. Euro. Math. Soc.*, 7:69–99, 2005.
- [BGK12] N. Berglund, B. Gentz, and C. Kuehn. Hunting French ducks in a noisy environment. *J. Differential Equat.*, 252(9):4786–4841, 2012.
- [BGK13] N. Berglund, B. Gentz, and C. Kuehn. From random Poincaré maps to stochastic mixed-mode-oscillation patterns. *arXiv:1312.6353*, pages 1–55, 2013.
- [BGM08] V. Bykov, V. Gol'dshtain, and U. Maas. Simple global reduction technique based on decomposition approach. *Combust. Theor. Model.*, 12(2):389–405, 2008.
- [BGS97] F. Broner, G.H. Goldsztein, and S.H. Strogatz. Dynamical hysteresis without static hysteresis: scaling laws and asymptotic expansions. *SIAM J. Appl. Math.*, 57(4):1163–1187, 1997.
- [BGW10] D. Blöümker, B. Gawron, and T. Wanner. Nucleation in the one-dimensional stochastic Cahn–Hilliard model. *Discr. Cont. Dyn. Syst. A*, 27:25–52, 2010.
- [BH25] G.E. Briggs and J.B.S. Haldane. A note on the kinetics of enzyme action. *Biochem. J.*, 19(2):338–339, 1925.
- [BH88] F.J. Bourland and R. Haberman. The modulated phase shift for strongly nonlinear, slowly varying, and weakly damped oscillators. *SIAM J. Appl. Math.*, 48(4):737–748, 1988.
- [BH90] M.V. Berry and C.J. Howls. Hyperasymptotics. *Proc. R. Soc. A*, 430(1880):653–668, 1990.
- [BH92] L. Bronsard and D. Hilhorst. On the slow dynamics for the Cahn–Hilliard equation in one space dimension. *Proc. R. Soc. A*, 439(1907):669–682, 1992.
- [BH98a] J.D. Brothers and R. Haberman. Accurate phase after slow passage through subharmonic resonance. *SIAM J. Appl. Math.*, 59(1):347–364, 1998.
- [BH98b] J.D. Brothers and R. Haberman. Slow passage through a homoclinic orbit with subharmonic resonances. *Stud. Appl. Math.*, 101(2):211–232, 1998.
- [BH04] D. Blöümker and M. Hairer. Multiscale expansion of invariant measures for SPDEs. *Comm. Math. Phys.*, 251(3):515–555, 2004.

- [BH13] A. Banyaga and D.E. Hurtubise. Cascades and perturbed Morse–Bott functions. *Algebraic Geom. Topol.*, 13:237–275, 2013.
- [BHF02] E. Benoît, A. El Hamidi, and A. Fruchard. On combined asymptotic expansions in singular perturbations. *Electron. J. Differential Equat.*, 2002(51):1–27, 2002.
- [BHQ94] R. Bartussek, P. Hägggi, and P. Jung. Stochastic resonance in optical bistable systems. *Phys. Rev. E*, 49(5):3930, 1994.
- [BHK91] F.J. Bourland, R. Haberman, and W.L. Kath. Averaging methods for the phase shift of arbitrarily perturbed strongly nonlinear oscillators with an application to capture. *SIAM J. Appl. Math.*, 51(4):1150–1167, 1991.
- [BHP05] D. Blömker, M. Hairer, and G.A. Pavliotis. Modulation equation for SPDEs on large domains. *Comm. Math. Phys.*, 258:479–512, 2005.
- [BHP07] D. Blömker, M. Hairer, and G.A. Pavliotis. Multiscale analysis for stochastic partial differential equations with quadratic nonlinearities. *Nonlinearity*, 20(7):1721–1744, 2007.
- [BHR01] C.J. Budd, H. Huang, and R.D. Russell. Mesh selection for a nearly singular boundary value problem. *J. Sci. Comput.*, 16(4):525–552, 2001.
- [BHS87] C. De Boor, K. Höllig, and M. Sabin. High accuracy geometric Hermite interpolation. *Computer Aided Geometric Design*, 4(4):269–278, 1987.
- [BHV07] H.W. Broer, A. Hagen, and G. Vegter. Numerical continuation of normally hyperbolic invariant manifolds. *Nonlinearity*, 20(6):1499–1534, 2007.
- [BI00] V.A. Baikov and N.H. Ibragimov. Continuation of approximate transformation groups via multiple time scales method. Modern group analysis. *Nonlinear Dynam.*, 22:3–13, 2000.
- [Bi04] Q. Bi. Dynamical analysis of two coupled parametrically excited van der Pol oscillators. *Int. J. Non-Linear Mech.*, 39(1):33–54, 2004.
- [Bil10] A. Billoire. Distribution of timescales in the Sherrington–Kirkpatrick model. *J. Stat. Mech.*, 11:P11034, 2010.
- [Bir08a] G.D. Birkhoff. Boundary value and expansion problems of ordinary linear differential equations. *Trans. Amer. Math. Soc.*, 9(4):373–395, 1908.
- [Bir08b] G.D. Birkhoff. On the asymptotic character of the solutions of certain linear differential equations containing a parameter. *Trans. Amer. Math. Soc.*, 9(2):219–231, 1908.
- [BJ78] T.A. Bickart and E.I. Jury. Arithmetic tests for A-stability, A[α]-stability, and stiff-stability. *BIT*, 18:9–21, 1978.
- [BJ89] P.W. Bates and C.K.R.T. Jones. Invariant manifolds for semilinear partial differential equations. In U. Kirchgraber and H.O. Walther, editors, *Dynamics Reported*, volume 2, pages 1–37. Wiley, 1989.
- [BJ12] C.M. Bender and H.F. Jones. WKB analysis of PT-symmetric Sturm–Liouville problems. *J. Phys. A*, 45(44):444004, 2012.
- [BJBMS82] E. Ben-Jacob, D.J. Bergman, B.J. Matkowsky, and Z. Schuss. Lifetime of oscillatory steady states. *Phys. Rev. A*, 26(5):2805, 1982.
- [BJLM05] O. Brandman, J.E. Ferrell Jr, R. Li, and T. Meyer. Interlinked fast and slow positive feedback loops drive reliable cell decisions. *Science*, 310:496–498, 2005.
- [BJSW08] M. Beck, C.K.R.T. Jones, D. Schaeffer, and M. Wechselberger. Electrical waves in a one-dimensional model of cardiac tissue. *SIAM J. Appl. Dyn. Syst.*, 7(4):1558–1581, 2008.
- [BK82] G.L. Browning and H.-O. Kreiss. Problems with different time scales for nonlinear partial differential equations. *SIAM J. Appl. Math.*, 42(4):704–718, 1982.
- [BK90] L. Bronsard and R.V. Kohn. On the slowness of phase boundary motion in one space dimension. *Comm. Pure Appl. Math.*, 43(8):983–997, 1990.
- [BK91] D.L. Bosley and J. Kevorkian. Sustained resonance in very slowly varying oscillatory Hamiltonian systems. *SIAM J. Appl. Math.*, 51(2):439–471, 1991.
- [BK92] D.L. Bosley and J. Kevorkian. Adiabatic invariance and transient resonance in very slowly varying oscillatory Hamiltonian systems. *SIAM J. Appl. Math.*, 52(2):494–527, 1992.
- [BK94] I.U. Bronstein and A.Ya. Kopanskii. *Smooth invariant manifolds and normal forms*. World Scientific, 1994.
- [BK96] G.L. Browning and H.-O. Kreiss. Analysis of periodic updating for systems with multiple timescales. *H. Atmos. Sci.*, 53(2):335–348, 1996.
- [BK99] N. Berglund and H. Kunz. Memory effects and scaling laws in slowly driven systems. *J. Phys. A: Math. Gen.*, 32:15–39, 1999.
- [BK04] V.I. Bakhtin and Yu. Kifer. Diffusion approximation for slow motion in fully coupled averaging. *Probab. Theory Relat. Fields*, 129:157–181, 2004.
- [BK08a] N. Baba and K. Krischer. Mixed-mode oscillations and cluster patterns in an electrochemical relaxation oscillator under galvanostatic control. *Chaos*, 18, 2008.
- [BK08b] V.I. Bakhtin and Yu. Kifer. Nonconvergence examples in averaging. *Contemp. Math.*, 469:1–17, 2008.
- [BK10a] A. Birzu and K. Krischer. Resonance tongues in a system of globally coupled FitzHugh–Nagumo oscillators with time-periodic coupling strength. *Chaos*, 20:043114, 2010.
- [BK10b] M. Brens and R. Kaasen. Canards and mixed-mode oscillations in a forest pest model. *Theor. Popul. Biol.*, 77:238–242, 2010.
- [BKK13] H.W. Broer, T.J. Kaper, and M. Krupa. Geometric desingularization of a cusp singularity in slow–fast systems with applications to Zeeman’s examples. *J. Dyn. Diff. Eq.*, 25(4):925–958, 2013.
- [BKLC10] P. Borowski, R. Kuske, X.-X. Li, and J.L. Cabrera. Characterizing mixed mode oscillations shaped by noise and bifurcation structure. *Chaos*, 20:043117, 2010.
- [BK12] L.L. Bonilla, A. Klar, and S. Martin. Higher order averaging of linear Fokker–Planck equations with periodic forcing. *SIAM J. Appl. Math.*, 72(4):1315–1342, 2012.
- [BKP06] L. Buric, A. Klic, and L. Purmova. Canard solutions and travelling waves in the spruce budworm population model. *Appl. Math. Comput.*, 183(2):1039–1051, 2006.
- [BKPR06] K. Ball, T.G. Kurtz, L. Popovic, and G. Rempala. Asymptotic analysis of multiscale approximations to reaction networks. *Ann. Appl. Prob.*, 16(4):1925–1961, 2006.
- [BKR02] A.S. Bobkov, A.Y. Kolesov, and N.K. Rozov. The “duck survival” problem in three-dimensional singularly perturbed systems with two slow variables. *Math. Notes*, 71(5):749–760, 2002.

- [BKT00] A. Bose, N. Kopell, and D. Terman. Almost-synchronous solutions for mutually coupled excitatory neurons. *Physica D*, 140(1):69–94, 2000.
- [BKVD12] T. Bakri, Y.A. Kuznetsov, F. Verhulst, and E. Doedel. Multiple solutions of a generalized singular perturbed Bratu problem. *Int. J. Bif. Chaos*, 22(4), 2012.
- [BKW06] M. Brøns, M. Krupa, and M. Wechselberger. Mixed mode oscillations due to the generalized canard phenomenon. *Fields Institute Communications*, 49:39–63, 2006.
- [BKWL12] P. Bokes, J.R. King, A.T.A. Wood, and M. Loose. Multiscale stochastic modelling of gene expression. *J. Math. Biol.*, 65:493–520, 2012.
- [BL23] G.D. Birkhoff and R.E. Langer. The boundary problems and developments associated with a system of ordinary linear differential equations of the first order. *Proc. Amer. Acad. Arts Sci.*, 58(2):51–128, 1923.
- [BL82] E. Benoît and C. Lobry. Les canards de \mathbb{R}^3 . *C.R. Acad. Sc. Paris*, 294:483–488, 1982.
- [BL87] D. Brown and J. Lorenz. A higher-order method for stiff boundary-value problems with turning points. *SIAM J. Sci. Stat. Comp.*, 8:790–805, 1987.
- [BL04] A. Buică and J. Llibre. Averaging methods for finding periodic orbits via Brouwer degree. *Bull. des Sci. Math.*, 128(1):7–22, 2004.
- [BL12] N. Berglund and D. Landau. Mixed-mode oscillations and interspike interval statistics in the stochastic FitzHugh–Nagumo model. *Nonlinearity*, 25:2303–2335, 2012.
- [Bla81] G. Blankenship. Singularly perturbed difference equations in optimal control problems. *IEEE Trans. Auto. Contr.*, 1981:911–917, 1981.
- [Bla91] F. Blais. Asymptotic expansions of rivers. In E. Benoit, editor, *Dynamic Bifurcations*, volume 1493 of *Lecture Notes in Mathematics*, pages 181–189. Springer, 1991.
- [BLH⁺09] J. Bakke, Ø. Lie, E. Heegaard, T. Dokken, G.H. Haug, H.H. Birks, P. Dulski, and T. Nilsen. Rapid oceanic and atmospheric changes during the Younger Dryas cold period. *Nature Geosci.*, 2:202–205, 2009.
- [BLM09] A. Buică, J. Llibre, and O. Makarenkov. Asymptotic stability of periodic solutions for nonsmooth differential equations with application to the nonsmooth van der Pol oscillator. *SIAM J. Math. Anal.*, 40(6):2478–2495, 2009.
- [Blö03] D. Blömker. Amplitude equations for locally cubic nonautonomous nonlinearities. *SIAM J. Appl. Dyn. Syst.*, 2(3):464–486, 2003.
- [Blö07] D. Blömker. *Amplitude Equations for Stochastic Partial Differential Equations*. World Scientific, 2007.
- [BLP11] A. Bensoussan, J.-L. Lions, and G. Papanicolaou. *Asymptotic analysis for periodic structures*. Chelsea, 2011.
- [BLP12] C. Le Bris, T. Lelièvre, and M. Perez. A mathematical formalization of the parallel replica dynamics. *Monte Carlo Meth. Appl.*, 18(2):119–146, 2012.
- [BLZ98] P.W. Bates, K. Lu, and C. Zeng. Existence and persistence of invariant manifolds for semiflows in Banach spaces. *Mem. Amer. Math. Soc.*, 135, 1998.
- [BLZ00] P.W. Bates, K. Lu, and C. Zeng. Invariant foliations near normally hyperbolic invariant manifolds for semiflows. *Transactions of the AMS*, 352(10):4641–4676, 2000.
- [BLZ08] P.W. Bates, K. Lu, and C. Zeng. Approximately invariant manifolds and global dynamics of spike states. *Invent. Math.*, 174:355–433, 2008.
- [BM61] N.N. Bogoliubov and I.A. Mitropol'skii. *Asymptotic methods in the theory of non-linear oscillations*. Gordon Breach Science Pub., 1961.
- [BM72] M.V. Berry and K.E. Mount. Semiclassical approximations in wave mechanics. *Rep. Prog. Phys.*, 35(1):315, 1972.
- [BM81] D. Bainov and S. Milusheva. Justification of the averaging method for a system of differential equations with fast and slow variables and with impulses. *Z. Angew. Math. Phys.*, 32(3):237–254, 1981.
- [BM90] M. Brunella and M. Miari. Topological equivalence of a plane vector field with its principal part defined through newton polyhedra. *J. Differential Equat.*, 85:338–366, 1990.
- [BM05] J.A. Biello and A.J. Majda. A new multiscale model for the Madden Julian oscillation. *J. Atmosph. Sci.*, 62:1694–1720, 2005.
- [BM07a] V. Bykov and U. Maas. The extension of the ILDM concept to reaction–diffusion manifolds. *Comust. Theor. Model.*, 11(6):839–862, 2007.
- [BM07b] V. Bykov and U. Maas. Extension of the ILDM method to the domain of slow chemistry. *Proceed. Comust. Inst.*, 31(1):465–472, 2007.
- [BM09] D. Blömker and W.W. Mohammed. Amplitude equation for SPDEs with quadratic nonlinearities. *Electron. J. Prob.*, 14(88):2527–2550, 2009.
- [BM10] J.A. Biello and A.J. Majda. Intraseasonal multi-scale moist dynamics of the tropical tropospheres. *Commun. Math. Sci.*, 8(2):519–540, 2010.
- [BM11] A.J. Black and A.J. McKane. WKB calculation of an epidemic outbreak distribution. *J. Stat. Mech.*, 2011:P12006, 2011.
- [BMD11] P. Bonckaert, P. De Maesschalck, and F. Dumortier. Well adapted normal linearization in singular perturbation problems. *J. Dyn. Diff. Eq.*, 23(1):115–139, 2011.
- [BMF02] W. Balser and J. Mozo-Fernandez. Multisummability of formal solutions of singular perturbation problems. *J. Differential Equat.*, 183:526–545, 2002.
- [BMH04] E. Brown, J. Moehlis, and P. Holmes. On the phase reduction and response dynamics of neural oscillator populations. *Neural Comput.*, 16(4):673–715, 2004.
- [BMN10] M. Bobieński, P. Mardesić, and D. Novikov. Pseudo-abelian integrals on slow–fast Darboux systems. *arXiv:1007.2001v1*, pages 1–11, 2010.
- [BMS08] A. Braides, M. Maslennikov, and L. Sigalotti. Homogenization by blow-up. *Applicable Analysis*, 87(12):1341–1356, 2008.
- [BN11] C.L. Buckley and T. Nowotny. Multiscale model of an inhibitory network shows optimal properties near bifurcation. *Phys. Rev. Lett.*, 106:238109, 2011.
- [BN13] P.C. Bressloff and J.M. Newby. Metastability in a stochastic neural network modeled as a velocity jump Markov process. *SIAM J. Appl. Dyn Syst.*, 12:1394–1435, 2013.

- [BNR82] H.L. Berk, W.M. Nevins, and K.V. Roberts. New Stokes line in WKB theory. *J. Math. Phys.*, 23(6):988–1002, 1982.
- [BNS85] H. Berestycki, B. Nicolaenko, and B. Scheurer. Traveling wave solutions to combustion models and their singular limits. *SIAM J. Math. Anal.*, 16(6):1207–1242, 1985.
- [BNS99] V.F. Butuzov, N.N. Nefedov, and K.R. Schneider. Singularly perturbed boundary value problems for systems of Tichonov's type in case of exchange of stabilities. *J. Differential Equat.*, 159(2):427–446, 1999.
- [BNS01] V.F. Butuzov, N.N. Nefedov, and K.R. Schneider. Singularly perturbed elliptic problems in the case of exchange of stabilities. *J. Differential Equat.*, 169(2):373–395, 2001.
- [BNS04] V.F. Butuzov, N.N. Nefedov, and K.R. Schneider. Singularly perturbed problems in case of exchange of stabilities. *J. Math. Sci.*, 121(1):1973–2079, 2004.
- [BO84] M. Berger and J. Oliger. Adaptive mesh refinement for hyperbolic partial differential equations. *J. Comput. Phys.*, 53(3):484–512, 1984.
- [BO99] C.M. Bender and S.A. Orszag. *Asymptotic Methods and Perturbation Theory*. Springer, 1999.
- [Bob07] R.V. Bobryk. Closure method and asymptotic expansions for linear stochastic systems. *J. Math. Anal. Appl.*, 329(1):703–711, 2007.
- [Bog07] V.I. Bogachev. *Measure Theory*, volume 1. Springer, 2007.
- [Bon78] E. Bombieri. On exponential sums in finite fields, II. *Invent. Math.*, 47(1):29–39, 1978.
- [Bon87] C. Bonet. Singular perturbation of relaxed periodic orbits. *J. Differential Equat.*, 66(3):301–339, 1987.
- [Bor97] V.S. Borkar. Stochastic approximation with two time scales. *Syst. Contr. Lett.*, 29(5):291–294, 1997.
- [Bor98] F. Bornemann. *Homogenization in Time of Singularly Perturbed Mechanical Systems*. Springer, 1998.
- [Bor04a] A.V. Borovskikh. Investigation of relaxation oscillations by constructive nonstandard analysis. I. *Differ. Equ.*, 40(3):309–317, 2004.
- [Bor04b] A.V. Borovskikh. Investigation of relaxation oscillations by constructive nonstandard analysis. II. *Differ. Equ.*, 40(4):491–501, 2004.
- [Bos95] A. Bose. Symmetric and antisymmetric pulses in parallel coupled nerve fibres. *SIAM J. Appl. Math.*, 55(6):1650–1674, 1995.
- [Bos96] D.L. Bosley. An improved matching procedure for transient resonance layers in weakly nonlinear oscillatory systems. *SIAM J. Appl. Math.*, 56(2):420–445, 1996.
- [Bos00] A. Bose. A geometric approach to singularly perturbed nonlocal reaction-diffusion equations. *SIAM J. Math. Anal.*, 31(2):431–454, 2000.
- [Bot95] S. Bottani. Pulse-coupled relaxation oscillators: from biological synchronization to self-organized criticality. *Phys. Rev. Lett.*, 74:4189–4192, 1995.
- [Boy99] J.P. Boyd. The devil's invention: asymptotic, superasymptotic and hyperasymptotic series. *Acta Appl. Math.*, 56:1–98, 1999.
- [Boy05] J.P. Boyd. Hyperasymptotics and the linear boundary layer problem: Why asymptotic series diverge. *SIAM Rev.*, 47:553–575, 2005.
- [BP89] N.S. Bakhvalov and G.P. Panasenko. *Homogenisation: averaging processes in periodic media: mathematical problems in the mechanics of composite materials*. Kluwer, 1989.
- [BP91] V.N. Bogaevski and A. Povzner. *Algebraic Methods in Nonlinear Perturbation Theory*. Springer, 1991.
- [BPO1] F. Battelli and K.J. Palmer. Transverse intersection of invariant manifolds in singular systems. *J. Different. Equat.*, 177:77–120, 2001.
- [BP03] F. Battelli and K.J. Palmer. Singular perturbations, transversality, and Sil'nikov saddle-focus homoclinic orbits. *J. Dynam. Different. Equat.*, 15:357–425, 2003.
- [BP08] F. Battelli and K.J. Palmer. Connections to fixed points and Sil'nikov saddle-focus homoclinic orbits in singularly perturbed systems. *Ukrainian Math. J.*, 60(1):28–55, 2008.
- [BPH⁺00] R. Bertram, J. Previte, A. Herman, T.A. Kinard, and L.S. Satin. The phantom burster model for pancreatic β -cells. *Biophys. J.*, 79(6):2880–2892, 2000.
- [BPH94] L. Bocquet and J. Piasecki and J.-P. Hansen. On the Brownian motion of a massive sphere suspended in a hard-sphere fluid. I. Multiple-time-scale analysis and microscopic expression for the friction coefficient. *J. Statist. Phys.*, 76:505–526, 1994.
- [BPL13] J. Banasiak, E.K. Phongi, and M. Lachowicz. A singularly perturbed SIS model with age structure. *Math. Biosci. Eng.*, 10(3):499–521, 2013.
- [BPPV85] R. Benzi, G. Paladin, G. Parisi, and A. Vulpiani. Characterisation of intermittency in chaotic systems. *J. Phys. A*, 18(12):2157–2165, 1985.
- [BPSV82] R. Benzi, G. Parisi, A. Sutera, and A. Vulpiani. Stochastic resonance in climatic change. *Tellus*, 34(11):10–16, 1982.
- [BPSV83] R. Benzi, G. Parisi, A. Sutera, and A. Vulpiani. A theory of stochastic resonance in climatic change. *SIAM J. Appl. Math.*, 43(3):565–578, 1983.
- [BPTW07] J. Best, C. Park, D. Terman, and C. Wilson. Transitions between irregular and rhythmic firing patterns in excitatory-inhibitory neuronal networks. *J. Comput. Neurosci.*, 23(2):217–235, 2007.
- [BR73] T.S. Briggs and W.C. Rauscher. An oscillating iodine clock. *J. Chem. Educ.*, 50:496, 1973.
- [BR93] M.V. Berry and J.M. Robbins. Chaotic classical and half-classical adiabatic reactions: geometric magnetism and deterministic friction. *Proc. R. Soc. A*, 442(1916):659–672, 1993.
- [BR00] S. Bornholdt and T. Rohlff. Topological evolution of dynamical networks: global criticality from local dynamics. *Phys. Rev. Lett.*, 84(26):6114–6117, 2000.
- [Bra92] B. Braaksma. Phantom ducks and models of excitability. *J. Dyn. Diff. Equat.*, 4(3):485–513, 1992.
- [Bra93] M. Braun. *Differential Equations and Their Applications*. Springer, 1993.
- [Bra98] B. Braaksma. Singular Hopf bifurcation in systems with fast and slow variables. *J. Nonlinear Sci.*, 8(5):457–490, 1998.
- [Bra03] P.A. Braza. The bifurcation structure of the Holling-Tanner model for predator-prey interactions using two-timing. *SIAM J. Appl. Math.*, 63(3):889–904, 2003.
- [BRC95] S.M. Baer, J. Rinzel, and H. Carrillo. Analysis of an autonomous phase model for neuronal parabolic bursting. *J. Math. Biol.*, 33(3):309–333, 1995.
- [Bre51] H. Bremmer. The WKB approximation as the first term of a geometric-optical series. *Comm. Pure. Appl. Math.*, 4(1):105–115, 1951.

- [Bre60] H. Bremmer. The scientific work of Balthasar van der Pol. *Philips Tech. Rev.*, 22:36–52, 1960.
- [Bre62] F.P. Bretherton. Slow viscous motion round a cylinder in a simple shear. *J. Fluid Mech.*, 12:591–613, 1962.
- [Bre97] G.E. Bredon. *Topology and Geometry*. Springer, 1997.
- [Bré12a] C.-E. Bréhier. Strong and weak orders in averaging for SPDEs. *Stoch. Proc. Appl.*, 122(7):2553–2593, 2012.
- [Bré12b] P.C. Bressloff. Spatiotemporal dynamics of continuum neural fields. *J. Phys. A: Math. Theor.*, 45:(033001), 2012.
- [Bre13a] R. Breban. Role of environmental persistence in pathogen transmission: a mathematical modeling approach. *J. Math. Biol.*, 66(3):535–546, 2013.
- [Bré13b] C.-E. Bréhier. Analysis of an HMM time-discretization scheme for a system of stochastic PDEs. *SIAM J. Numer. Anal.*, 51(2):1185–1210, 2013.
- [Bri26] L. Brillouin. La mécanique ondulatoire de Schrödinger: une méthode générale de résolution par approximations successives. *Comptes Rendus de l'Academie des Sciences*, 183:24–26, 1926.
- [Bri09] I. Bright. Tight estimates for general averaging applied to almost-periodic differential equations. *J. Differential Equat.*, 246(7):2922–2937, 2009.
- [Bri11] I. Bright. Moving averages of ordinary differential equations via convolution. *J. Differential Equat.*, 250(3):1267–1284, 2011.
- [Bro28] R. Brown. A brief account of microscopical observations made in the months of June, July and August, 1827, on the particles contained in the pollen of plants; and on the general existence of active molecules in organic and inorganic bodies. *Phil. Mag.*, 4:161–173, 1828.
- [Bro95] R. Brown. Horseshoes in the measure-preserving Hénon map. *Ergodic Theor. Dyn.Syst.*, 15(6):1045–1060, 1995.
- [Bro05] M. Brøns. Relaxation oscillations and canards in a nonlinear model of discontinuous plastic deformation in metals at very low temperature. *Proc. R. Soc. A*, 461:2289–2302, 2005.
- [Bro11] M. Brøns. Canard explosion of limit cycles in templator models of self-replication mechanisms. *J. Chem. Phys.*, 134(14):144105, 2011.
- [Bro12] M. Brøns. An iterative method for the canard explosion in general planar systems. *arXiv:1209.1109*, pages 1–9, 2012.
- [BRS99a] R.J. Butera, J. Rinzel, and J.C. Smith. Models of respiratory rhythm generation in the pre-Bötzinger complex. I. Bursting pacemaker neurons. *J. Neurophysiol.*, 82(1):382–397, 1999.
- [BRS99b] R.J. Butera, J. Rinzel, and J.C. Smith. Models of respiratory rhythm generation in the pre-Bötzinger complex. II. Populations of coupled pacemaker neurons. *J. Neurophysiol.*, 82(1):398–415, 1999.
- [Bru70] N.G. De Bruijn. *Asymptotic Methods in Analysis*. Dover, 1970.
- [Bru89] Alexander D. Bruno. *Local Methods in Nonlinear Differential Equations*. Springer, 1989.
- [Bru96] P. Brunovský. Tracking invariant manifolds without differential forms. *Acta Math. Univ. Comenianae*, LXV(1):23–32, 1996.
- [Bru98] P. Brunovský. S-shaped bifurcation of a singularly perturbed boundary value problem. *J. Differential Equat.*, 145(1):52–100, 1998.
- [Bru99] P. Brunovský. C^r -inclination theorems for singularly perturbed equations. *J. Differential Equat.*, 155(1):133–152, 1999.
- [BS73] C. De Boor and B. Swartz. Collocation at Gaussian points. *SIAM J. Numer. Anal.*, 10:582–606, 1973.
- [BS79] G. Blankenship and S. Sachs. Singularly perturbed linear stochastic ordinary differential equations. *SIAM J. Math. Anal.*, 1979:306–320, 1979.
- [BS82] B.Z. Bobrovsky and Z. Schuss. A singular perturbation method for the computation of the mean first passage time in a nonlinear filter. *SIAM J. Appl. Math.*, 42(1):174–187, 1982.
- [BS88] S.V. Bogolyubov and V.A. Sobolev. Separating the rapid and slow motions in the problems of the dynamics of systems of rigid bodies and gyroscopes. *J. Appl. Math. Mech.*, 52(1):41–48, 1988.
- [BS91] S.A. Belikov and S.N. Samborskii. Canard-cycles of fast–slow fields with a one-dimensional slow component. *Math. Notes*, 49(3):339–346, 1991.
- [BS96] M. Brokate and J. Sprekels. *Hysteresis and Phase Transitions*. Springer, 1996.
- [BS97] F.A. Bornemann and C. Schütte. Homogenization of Hamiltonian systems with a strong constraining potential. *Physica D*, 102(1):57–77, 1997.
- [BS98] F.A. Bornemann and C. Schütte. A mathematical investigation of the Car–Parrinello method. *Numer. Math.*, 78(3):359–376, 1998.
- [BS99a] W.-J. Beyn and M. Stiefenhofer. A direct approach to homoclinic orbits in the fast dynamics of singularly perturbed systems. *J. Dyn. Diff. Equat.*, 11(4):671–709, 1999.
- [BS99b] H. Boudjellaba and T. Sari. Stability loss delay in harvesting competing populations. *J. Differential Equat.*, 152(2):394–408, 1999.
- [BS01] M. Brøns and J. Sturis. Explosion of limit cycles and chaotic waves in a simple nonlinear chemical system. *Phys. Rev. E*, 64:026209, 2001.
- [BS02] M. Brin and G. Stuck. *Introduction to Dynamical Systems*. CUP, 2002.
- [BS03] S. Bornholdt and H.G. Schuster, editor. *Handbook of Graphs and Networks*. Wiley, 2003.
- [BS04a] R. Bertram and A. Sherman. A calcium-based phantom bursting model for pancreatic islets. *Bull. Math. Biol.*, 66(5):1313–1344, 2004.
- [BS04b] R. Bertram and A. Sherman. Filtering of calcium transients by the endoplasmic reticulum in pancreatic β -cells. *Biophys. J.*, 87(6):3775–3785, 2004.
- [BS04c] V.N. Biktašhev and R. Suckley. Non-Tikhonov asymptotic properties of cardiac excitability. *Phys. Rev. Lett.*, 93(16):169103, 2004.
- [BS09a] R. Barrio and S. Serrano. Bounds for the chaotic region in the Lorenz model. *Physica D*, 16(1):1615–1624, 2009.
- [BS09b] H. Boudjellaba and T. Sari. Dynamic transcritical bifurcations in a class of slow–fast predator–prey models. *J. Diff. Eq.*, 246:2205–2225, 2009.
- [BS10] M.V. Berry and P. Shukla. High-order classical adiabatic reaction forces: slow manifold for a spin model. *J. Phys. A: Math. Theor.*, 43(4):045102, 2010.

- [BS11a] R. Barrio and A. Shilnikov. Parameter-sweeping techniques for temporal dynamics of neuronal systems: case study of Hindmarsh–Rose model. *J. Math. Neurosci.*, 1(1):1–22, 2011.
- [BS11b] S. Bianchini and L. Spinolo. Invariant manifolds for a singular ordinary differential equation. *J. Differential Equat.*, 250(4):1788–1827, 2011.
- [BSG10] N. Brännström, E. De Simone, and V. Gelfreich. Geometric shadowing in slow–fast Hamiltonian systems. *Nonlinearity*, 23:1169, 2010.
- [BSO01] T.V. Broomkova, W.M. Schaffer, and L.F. Olsen. Nonlinear dynamics of the peroxidase-oxidase reaction. I. Bistability and bursting oscillations at low enzyme concentrations. *J. Phys. Chem. B*, 105:310–321, 2001.
- [BSP⁺07] R. Bertram, L.S. Satin, M.G. Pedersen, D.S. Luciani, and A. Sherman. Interaction of glycolysis and mitochondrial respiration in metabolic oscillations of pancreatic islets. *Biophys. J.*, 92(5):1544–1555, 2007.
- [BSSH08] D. Bakes, L. Schreiberova, I. Schreiber, and M.J.B. Hauser. Mixed-mode oscillations in a homogeneous ph-oscillatory chemical reaction system. *Chaos*, 18, 2008.
- [BSSV98] C. Bonet, D. Sauzin, T. Seara, and M. Valencia. Adiabatic invariant of the harmonic oscillator, complex matching and resurgence. *SIAM J. Math. Anal.*, 29(6):1335–1360, 1998.
- [BST08] W.-J. Beyn, S. Selle, and V. Thümmler. Freezing multipulses and multifronts. *SIAM J. Appl. Dyn. Syst.*, 7(2):577–608, 2008.
- [BSV81] R. Benzi, A. Sutera, and A. Vulpiani. The mechanism of stochastic resonance. *J. Phys. A*, 14(11):453–457, 1981.
- [BSZ⁺04] R. Bertram, L. Satin, M. Zhang, P. Smolen, and A. Sherman. Calcium and glycolysis mediate multiple bursting modes in pancreatic islets. *Biophys. J.*, 87(5):3074–3087, 2004.
- [BT97a] D. Bertsimas and J.N. Tsitsiklis. *Introduction to Linear Optimization*. Athena Scientific, 1997.
- [BT97b] L. Brugnano and D. Trigiante. A new mesh selection strategy for ODEs. *Appl. Numer. Math.*, 24:1–21, 1997.
- [BT10] H. Broer and F. Takens. *Dynamical Systems and Chaos*. Springer, 2010.
- [BU01] N. Berglund and T. Uzer. The averaged dynamics of the hydrogen atom in crossed electric and magnetic fields as perturbed Kepler problem. *Found. Phys.*, 31(2):283–326, 2001.
- [BU11] M.V. Berry and R. Uzdin. Slow non-Hermitian cycling: exact solutions and the Stokes phenomenon. *J. Phys. A: Math. Theor.*, 44:435303, 2011.
- [BUB10] C.S. Bretherton, J. Uchida, and P.N. Blossey. Slow manifolds and multiple equilibria in stratoscumulus-capped boundary layers. *J. Adv. Model. Earth Syst.*, 2(14):1–20, 2010.
- [Bud01] C.J. Budd. Asymptotics of multibump blow-up self-similar solutions of the nonlinear Schrödinger equation. *SIAM J. Appl. Math.*, 62(3):801–830, 2001.
- [Bur70] R.R. Burnside. A note on Lighthill’s method of strained coordinates. *SIAM J. Appl. Math.*, 18(2):318–321, 1970.
- [But64] J.C. Butcher. Implicit Runge–Kutta processes. *Math. Comput.*, 18(85):50–64, 1964.
- [But75] J.C. Butcher. A stability property of implicit Runge–Kutta methods. *BIT Numer. Math.*, 15(4):358–361, 1975.
- [But76] J.C. Butcher. On the implementation of implicit Runge–Kutta methods. *BIT Numer. Math.*, 16(3):237–240, 1976.
- [But98] R.J. Butera. Multirhythmic bursting. *Chaos*, 8(1):274–284, 1998.
- [But07] V.F. Butuzov. Singularly perturbed two-dimensional parabolic problem in the case of intersecting roots of the reduced equation. *Comp. Math. Math. Phys.*, 47(4):620–628, 2007.
- [BV92] A.V. Babin and M.I. Vishik. *Attractors of Evolution Equations*. North-Holland, 1992.
- [BW11] M. Beck and C.E. Wayne. Using global invariant manifolds to understand metastability in the Burgers equation with small viscosity. *SIAM Rev.*, 53(1):129–153, 2011.
- [BW12] A. Bovier and S.-D. Wang. Multi-time scales in adaptive dynamics: microscopic interpretation of a trait substitution tree model. *arXiv:1207.4690v1*, pages 1–23, 2012.
- [BW13] A. Bovier and S.-D. Wang. Trait substitution trees on two time scales analysis. *arXiv:1304.4640v1*, pages 1–28, 2013.
- [BX95] P.W. Bates and J.P. Xun. Metastable patterns for the Cahn–Hilliard equation: Part II. Layer dynamics and slow invariant manifold. *J. Differential Equat.*, 117(1):165–216, 1995.
- [BX98] P.W. Bates and J.P. Xun. Metastable patterns for the Cahn–Hilliard equation, part I. *J. Differential Equat.*, 111(2):421–457, 1998.
- [BY02] G. Badowski and G.G. Yin. Stability of hybrid dynamic systems containing singularly perturbed random processes. *IEEE Trans. Aut. Contr.*, 47(12):2021–2032, 2002.
- [BYB10] M. Benbachir, K. Yadi, and R. Bebbouchi. Slow and fast systems with Hamiltonian reduced problems. *Electr. J. Diff. Eq.*, 2010(6):1–19, 2010.
- [BYS10] E.M. Boltt, C. Yao, and I.B. Schwartz. Dimensional implications of dynamical data on manifolds to empirical KL analysis. *Physica D*, 239(23):2039–2049, 2010.
- [CA84] H.-C. Chang and M. Aluko. Multi-scale analysis of exotic dynamics in surface catalyzed reactions I: justification and preliminary model discriminations. *Chem. Engineer. Sci.*, 39(1):37–50, 1984.
- [CAA09] N. Corson and M.A. Aziz-Alaoui. Asymptotic dynamics of the slow–fast Hindmarsh–Rose neuronal system. *Dyn. Contin. Discrete Impuls. Syst. Ser. B*, 16(4):535–549, 2009.
- [CAK78] J.H. Chow, J.J. Allemon, and P.V. Kokotovic. Singular perturbation analysis of systems with sustained high frequency oscillations. *Automatica*, 14(3):271–279, 1978.
- [Cal88] A.J. Calise. Singular perturbation analysis of the atmospheric orbital plane change problem. *J. Astronaut. Sci.*, 36:35–43, 1988.
- [CAL90] B. Christiansen, P. Alstrom, and M.T. Levinsen. Routes to chaos and complete phase locking in modulated relaxation oscillators. *Phys. Rev. A*, 42(4):1891–1900, 1990.
- [Cal93] J.-L. Callot. Champs lents-rapides complexes à une dimension lente. *Ann. Sci. École Norm. Sup.*, 26(2):149–173, 1993.
- [Cam77] S.L. Campbell. Linear systems of differential equations with singular coefficients. *SIAM J. Math. Anal.*, 8(6):1057–1066, 1977.

- [Cam78] S.L. Campbell. Singular perturbation of autonomous linear systems, II. *J. Differential Equat.*, 29(3):362–373, 1978.
- [Cam80a] S.L. Campbell. Singular linear systems of differential equations with delays. *Appl. Anal.*, 11(2):129–136, 1980.
- [Cam80b] S.L. Campbell. *Singular Systems of Differential Equations I*. Pitman, 1980.
- [Car52] M.L. Cartwright. Van der Pol's equation for relaxation oscillations. In *Contributions to the Theory of Nonlinear Oscillations II*, pages 3–18. Princeton University Press, 1952.
- [Car54] G.F. Carrier. Boundary layer problems in applied mathematics. *Comm. Pure Appl. Math.*, 7:11–17, 1954.
- [Car70] G.F. Carrier. Singular perturbation theory and geophysics. *SIAM Rev.*, 12(2):175–193, 1970.
- [Car77] G.A. Carpenter. A geometric approach to singular perturbation problems with applications to nerve impulse equations. *J. Differential Equat.*, 23:335–367, 1977.
- [Car79] G.A. Carpenter. Bursting phenomena in excitable membranes. *SIAM J. Appl. Math.*, 36(2):334–372, 1979.
- [Car81] J. Carr. *Applications of Centre Manifold Theory*. Springer, 1981.
- [Car96] J. Cardy. *Scaling and Renormalization in Statistical Physics*. CUP, 1996.
- [Car08] R. Carles. *Semi-classical Analysis for Nonlinear Schrödinger Equations*. World Scientific, 2008.
- [Cas85] J.R. Cash. Adaptive Runge–Kutta methods for nonlinear two-point boundary value problems with mild boundary layers. *Comp. Maths. with Appl.*, 11(6):605–619, 1985.
- [Cas88] J.R. Cash. On the numerical integration of nonlinear two-point boundary value problems using iterated deferred corrections. Part 2: The development and analysis of highly stable deferred correction formulae. *SIAM J. Numer. Anal.*, 25(4):862–882, 1988.
- [Cas03] J.R. Cash. Efficient numerical methods for the solution of stiff initial-value problems and differential algebraic equations. *Proc. R. Soc. Lond. A*, 459:797–815, 2003.
- [CB02] A. Carpio and L.L. Bonilla. Pulse propagation in discrete systems of coupled excitable cells. *SIAM J. Appl. Math.*, 63(2):619–635, 2002.
- [CB05] S. Coombes and P.C. Bressloff, editors. *Bursting: The genesis of rhythm in the nervous system*. World Scientific, 2005.
- [CB06] S.R. Carpenter and W.A. Brock. Rising variance: a leading indicator of ecological transition. *Ecology Letters*, 9:311–318, 2006.
- [CBCB93] C.C. Canavier, D.A. Baxter, J.W. Clark, and J.H. Byrne. Nonlinear dynamics in a model neuron provide a novel mechanism for transient synaptic inputs to produce long-term alterations of postsynaptic activity. *J. Neurophysiol.*, 69(6):2252–2257, 1993.
- [CBT⁺11] M. Chertkov, S. Backhaus, K. Turzisyn, V. Chernyak, and V. Lebedev. Voltage collapse and ODE approach to power flows: analysis of a feeder line with static disorder in consumption/production. *arXiv:1106.5003v1*, pages 1–8, 2011.
- [CC69] K.W. Chang and W.A. Coppel. Singular perturbations of initial value problems over a finite interval. *Arch. Rat. Mech. Anal.*, 32(4):268–280, 1969.
- [CC96] O. Costin and R. Costin. Rigorous WKB for finite-order linear recurrence relations with smooth coefficients. *SIAM J. Math. Anal.*, 27(1):110–134, 1996.
- [CC03] H. Cai and R. Chadwick. Radial structure of traveling waves in the inner ear. *SIAM J. Appl. Math.*, 63(4):1105–1120, 2003.
- [CC12] C.-N. Chen and Y.S. Choi. Standing pulse solutions to FitzHugh–Nagumo equations. *Arch. Rational Mech. Anal.*, 206: 741–777, 2012.
- [C.C13] C. Cotter. Data assimilation on the exponentially accurate slow manifold. *Phil. Trans. R. Soc. A*, 317:(20120300), 2013.
- [CCB90] C.C. Canavier, J.W. Clark, and J.H. Byrne. Routes to chaos in a model of a bursting neuron. *Biophys. J.*, 57(6):1245–1251, 1990.
- [CCB91] C.C. Canavier, J.W. Clark, and J.H. Byrne. Simulation of the bursting activity of neuron R15 in Aplysia: role of ionic currents, calcium balance, and modulatory transmitters. *J. Neurophysiol.*, 66(6):2107–2124, 1991.
- [CCB⁺01] J.S. Clark, S.R. Carpenter, M. Barber, S. Collins, A. Dobson, J.A. Foley, D.M. Lodge, M. Pascual, R. Pielet Jr., W. Pizer, C. Pringle, W.V. Reid, K. A. Rose, O. Sala, W.H. Schlesinger, D.H. Wall, and D. Wear. Ecological forecasts: an emerging imperative. *Science*, 293:657–660, 2001.
- [CCLCP13] A.N. Carvalho, J.W. Cholewa, G. Lozada-Cruz, and M.R.T. Primo. Reduction of infinite dimensional systems to finite dimensions: compact convergence approach. *SIAM J. Math. Anal.*, 45(2):600–638, 2013.
- [CCM07] S. Capper, J. Cash, and F. Mazzia. On the development of effective algorithms for the numerical solution of singularly perturbed two-point boundary value problems. *Int. J. Comput. Sci. Math.*, 1(1):42–57, 2007.
- [CCP⁺11] S.R. Carpenter, J.J. Cole, M.L. Pace, R. Batt, W.A. Brock, T. Cline, J. Coloso, J.R. Hodgson, J.F. Kitchell, D.A. Seekell, L. Smith, and B. Weidel. Early warning signs of regime shifts: a whole-ecosystem experiment. *Science*, 332:1079–1082, 2011.
- [CCR79] B. Caroli, C. Caroli, and B. Roulet. Diffusion in a bistable potential: a systematic WKB treatment. *J. Stat. Phys.*, 21(4):415–437, 1979.
- [CCS05] G.S. Cymbalyuk, R.L. Calabrese, and A.L. Shilnikov. How a neuron model can demonstrate co-existence of tonic spiking and bursting. *Neurocomput.*, 65:869–875, 2005.
- [CCS07] P. Channell, G. Cymbalyuk, and A. Shilnikov. Origin of bursting through homoclinic spike adding in a neuron model. *Phys. Rev. Lett.*, 98(13):134101, 2007.
- [CD91] M. Canalis-Durand. Formal expansion of van der Pol equation canard solutions are Gevrey. In E. Benoit, editor, *Dynamic Bifurcations*, volume 1493 of *Lecture Notes in Mathematics*, pages 29–39. Springer, 1991.
- [CD93] M. Canalis-Durand. Solution formelle Gevrey d'une équation singulièrement perturbée: le cas multidimensionnel. *Annales de l'institut Fourier*, 43(2):469–483, 1993.
- [CD94] M. Canalis-Durand. Solution formelle Gevrey d'une équation différentielle singulièrement perturbée. *Asymptotic Anal.*, 8:185–216, 1994.

- [CD96] P.D. Christofides and P. Daoutidis. Compensation of measurable disturbances for two-time-scale nonlinear systems. *Automatica*, 32(11):1553–1573, 1996.
- [CD09] N. Chernov and D. Dolgopyat. *Brownian Brownian motion*, volume 927 of *Mem. Amer. Math. Soc.* AMS, 2009.
- [CDD⁺03] S. Conti, A. DeSimone, G. Dolzmann, S. Müller, and F. Otto. Multiscale modeling of materials - the role of analysis. In *Trends in Nonlinear Analysis*, pages 375–408. Springer, 2003.
- [CDF90] S.-N. Chow, B. Deng, and B. Fiedler. Homoclinic bifurcation at resonant eigenvalues. *J. Dyn. Diff. Eq.*, 2(2):177–244, 1990.
- [CDG⁺98] J.C. Cale, D. Dangoisse, P. Glorieux, G. Lythe, and T. Erneux. Slowly passing through resonance strongly depends on noise. *Phys. Rev. Lett.*, 81(5):975–978, 1998.
- [CDI09] M. Condon, A. Deano, and A. Iserles. On highly oscillatory problems arising in electronic engineering. *ESAIM: Math. Model. Numer. Anal.*, 43(4):785–804, 2009.
- [CDI10a] M. Condon, A. Deano, and A. Iserles. On second-order differential equations with highly oscillatory forcing terms. *Proc. R. Soc. A*, 466:1809–1828, 2010.
- [CDI10b] M. Condon, A. Deano, and A. Iserles. On systems of differential equations with extrinsic oscillation. *Discr. Cont. Dyn. Syst. A*, 28(4):1345–1367, 2010.
- [CDKS98] K. Christensen, R. Donangelo, B. Koiller, and K. Sneppen. Evolution of random networks. *Phys. Rev. Lett.*, 81(11):2380–2383, 1998.
- [CDMFS07] M. Canalis-Durand, J. Mozo-Fernández, and R. Schäffke. Monomial summability and doubly singular differential equations. *J. Differential Equat.*, 233:485–511, 2007.
- [CDP13] B. Coll, F. Dumortier, and R. Prohens. Configurations of limit cycles in Liénard equations. *J. Differential Equat.*, 255(11):4169–4184, 2013.
- [CDRSS00] M. Canalis-Durand, J.P. Ramis, R. Schäffke, and Y. Sibuya. Gevrey solutions of singularly perturbed differential equations. *J. Reine Angew. Math.*, 518:95–129, 2000.
- [CDT90] S.-N. Chow, B. Deng, and D. Terman. The bifurcation of homoclinic and periodic orbits from two heteroclinic orbits. *SIAM J. Math. Anal.*, 21(1):179–204, 1990.
- [CE71] C. Conley and R. Easton. Isolated invariant sets and isolating blocks. *Trans. AMS*, 158:35–61, 1971.
- [CEO1] R. Curtu and B. Ermentrout. Oscillations in a refractory neural net. *J. Math. Biol.*, 43(1):81–100, 2001.
- [CE10] M.H. Cortez and S.P. Ellner. Understanding rapid evolution in predator-prey interactions using the theory of fast-slow systems. *Am. Nat.*, 176(5):109–127, 2010.
- [CEAM13] M. Ciszak, S. Euzzor, T. Arechi, and R. Meucci. Experimental study of firing death in a network of chaotic FitzHugh–Nagumo neurons. *Phys. Rev. E*, 87:022919, 2013.
- [Cer09] S. Cerrai. A Khasminskii type averaging principle for stochastic reaction–diffusion equations. *Ann. Appl. Prob.*, 19(3):899–948, 2009.
- [Cer11] S. Cerrai. Averaging principle for systems of reaction–diffusion equations with polynomial nonlinearities perturbed by multiplicative noise. *SIAM J. Math. Anal.*, 43(6):2482–2518, 2011.
- [Ces94] P. Cessi. A simple box model of stochastically forced thermohaline circulation. *J. Phys. Oceanogr.*, 24:1911–1920, 1994.
- [CES05] S. Chen, W. E, and C.W. Shu. The heterogeneous multiscale method based on the discontinuous Galerkin method for hyperbolic and parabolic problems. *Multiscale Model. Simul.*, 3(4):871–894, 2005.
- [CET86] J.R. Cary, D.F. Escande, and J.L. Tennyson. Adiabatic-invariant change due to separatrix crossing. *Phys. Rev. A*, 34(5):4256–4275, 1986.
- [CF81] M.F. Crowley and R.J. Field. Electrically coupled Belousov–Zhabotinsky oscillators: a potential chaos generator. In C. Vidal and A. Pacault, editors, *Nonlinear Phenomena in Chemical Dynamics*, pages 147–153. Springer, 1981.
- [CF94] H. Crauel and F. Flandoli. Attractors for random dynamical systems. *Probab. Theory Relat. Fields*, 100(3):365–393, 1994.
- [CF06a] S. Cerrai and M. Freidlin. On the Smoluchowski–Kramers approximation for a system with an infinite number of degrees of freedom. *Probab. Theory Rel. Fields*, 135(3):363–394, 2006.
- [CF06b] S. Cerrai and M. Freidlin. Smoluchowski–Kramers approximation for a general class of SPDEs. *J. Evol. Equat.*, 6(4):657–689, 2006.
- [CF09] S. Cerrai and M. Freidlin. Averaging principle for a class of stochastic reaction–diffusion equations. *Probab. Theory Rel. Fields*, 144(1):137–177, 2009.
- [CFG89] P. Constantin, C. Foias, and J.D. Gibbon. Finite dimensional attractor for the laser equations. *Nonlinearity*, 2:241–269, 1989.
- [CFL78] D.S. Cohen, A. Fokas, and P.A. Lagerstrom. Proof of some asymptotic results for a model equation for low Reynolds number flow. *SIAM J. Appl. Math.*, 35(1):187–207, 1978.
- [CFL95] T.R. Chay, Y.S. Fan, and Y.S. Lee. Bursting, spiking, chaos, fractals, and universality in biological rhythms. *Int. J. Bif. Chaos*, 5(3):595–635, 1995.
- [CFM12] P. Chleboun, A. Faggionato, and F. Martinelli. Time scale separation and dynamic heterogeneity in the low temperature east model. *arXiv:1212.2399v1*, pages 1–40, 2012.
- [CFNS09] P. Channell, I. Wuwape, A.B. Neiman, and A. Shilnikov. Variability of bursting patterns in a neuron model in the presence of noise. *J. Comp. Neurosci.*, 27(3):527–542, 2009.
- [CFNT89] P. Constantin, C. Foias, B. Nicolaenko, and R. Temam. *Integral Manifolds and Inertial Manifolds for Dissipative Partial Differential Equations*. Springer, 1989.
- [CG92] M. Corless and L. Glielmo. On the exponential stability of singularly perturbed systems. *SIAM J. Contr. Optim.*, 30(6):1338–1360, 1992.
- [CG95a] S.L. Campbell and C.W. Gear. The index of general nonlinear DAEs. *Numer. Math.*, 72:173–196, 1995.
- [CG95b] S.L. Campbell and E. Griepentrog. Solvability of general differential algebraic equations. *SIAM J. Sci. Comput.*, 16(2):257–270, 1995.
- [CG00] C. Coumarbatch and Z. Gajic. Exact decomposition of the algebraic Riccati equation of deterministic multimodeling optimal control problems. *IEEE Trans. Aut. Contr.*, 45(4):790–794, 2000.
- [CGAP95] J.H. Chow, R. Galarza, P. Accari, and W.W. Prince. Inertial and slow coherency aggregation algorithms for power system dynamic model reduction. *IEEE Trans. Power Syst.*, 10(2):680–685, 1995.

- [CGMC02] G.S. Cymbalyuk, Q. Gaudry, M. Masino, and R.L. Calabrese. Bursting in leech heart interneurons: cell-autonomous and network-based mechanisms. *J. Neurosci.*, 22(24):10580–10592, 2002.
- [CGO94] L.Y. Chen, N. Goldenfeld, and Y. Oono. Renormalization group theory for global asymptotic analysis. *Phys. Rev. Lett.*, 73(10): 1311–1315, 1994.
- [CGO96] L.Y. Chen, N. Goldenfeld, and Y. Oono. Renormalization group and singular perturbations: multiple scales, boundary layers, and reductive perturbation theory. *Phys. Rev. E*, 54(1):376–394, 1996.
- [CGOP94] L.Y. Chen, N. Goldenfeld, Y. Oono, and G. Paquette. Selection, stability and renormalization. *Physica A*, 204(1):111–133, 1994.
- [CGOV84] M. Cassandro, A. Galves, E. Olivieri, and M.E. Vares. Metastable behavior of stochastic dynamics: a pathwise approach. *J. Stat. Phys.*, 35(5):603–634, 1984.
- [CGP02] M. Costa, A.L. Goldberger, and C.K. Peng. Multiscale entropy analysis of complex physiologic time series. *Phys. Rev. Lett.*, 89(6):068102, 2002.
- [CGSR78] R.J. Clasen, D. Garfinkel, N.Z. Shapiro, and G.C. Roman. A method for solving certain stiff differential equations. *SIAM J. Appl. Math.*, 34(4):732–742, 1978.
- [CH52] C.F. Curtiss and J. Hirschfelder. Integration of stiff equations. *Proc. Natl. Acad. Sci. USA*, 38(3): 235–243, 1952.
- [CH76] C. Comstock and G.C. Hsiao. Singular perturbations for difference equations. *Rocky Moun. J. Math.*, 6(4):561, 1976.
- [CH84] K.W. Chang and F.A. Howes. *Nonlinear Singular Perturbation Phenomena: Theory and Applications*. Springer, 1984.
- [CH93] M.C. Cross and P.C. Hohenberg. Pattern formation outside of equilibrium. *Rev. Mod. Phys.*, 65(3): 851–1112, 1993.
- [CH06] C. De Coster and P. Habets. *Two-Point Boundary Value Problems: Lower and Upper Solutions*. Elsevier, 2006.
- [CH08] C. Chicone and M.T. Heitzman. The field theory two-body problem in acoustics. *Gen. Relativ. Gravit.*, 40:1087–1107, 2008.
- [CH13] C. Chicone and M.T. Heitzman. Phase-locked loops, demodulation, and averaging approximation time-scale extensions. *SIAM J. Appl. Dyn. Syst.*, 12(2):674–721, 2013.
- [Cha69] K.W. Chang. Two problems in singular perturbations of differential equations. *J. Austral. Math. Soc.*, 10:33–50, 1969.
- [Cha76] K.W. Chang. Singular perturbations of a boundary problem for a vector second order differential equation. *SIAM J. Appl. Math.*, 30(1):42–54, 1976.
- [Cha85] T.R. Chay. Chaos in a three-variable model of an excitable cell. *Physica D*, 16(2):233–242, 1985.
- [Cha87] F. Chaplais. Averaging and deterministic optimal control. *SIAM J. Control Optim.*, 25(3):767–780, 1987.
- [Cha90a] T.R. Chay. Bursting excitable cell models by a slow Ca^{2+} current. *J. Theor. Biol.*, 142(3):305–315, 1990.
- [Cha90b] T.R. Chay. Electrical bursting and intracellular Ca^{2+} oscillations in excitable cell models. *Biol. Cybernet.*, 63(1):15–23, 1990.
- [Cha96] T.R. Chay. Electrical bursting and luminal calcium oscillation in excitable cell models. *Biol. Cybernet.*, 75(5):419–431, 1996.
- [Che49] T.M. Cherry. Uniform asymptotic expansions. *J. London Math. Soc.*, 1(2):121–130, 1949.
- [Che50] T.M. Cherry. Uniform asymptotic formulae for functions with transition points. *Trans. Amer. Math. Soc.*, 68(2):224–257, 1950.
- [Che82] N.N. Chentsova. An investigation of a certain model system of quasi-stochastic relaxation oscillations. *Russ. Math. Surv.*, 37(5):164, 1982.
- [Che92] X. Chen. Generation and propagation of interfaces for reaction–diffusion equations. *J. Differential Equat.*, 96(1):116–141, 1992.
- [Che94] K. Chen. Error equidistribution and mesh adaptation. *SIAM J. Sci. Comput.*, 15(4):798–818, 1994.
- [Che04] H. Cheng. The renormalized two-scale method. *Stud. Appl. Math.*, 113(4):381–387, 2004.
- [Che11] A. Chen. Modeling a synthetic biological chaotic system: relaxation oscillators coupled by quorum sensing. *Nonlinear Dyn.*, 63:711–718, 2011.
- [Chi03] C. Chicone. Inertial and slow manifolds for delay differential equations. *J. Differential Equat.*, 190:364–406, 2003.
- [Chi04] C. Chicone. Inertial flows, slow flows, and combinatorial identities for delay equations. *J. Dyn. Diff. Eq.*, 16(3):805–831, 2004.
- [Chi08] H. Chiba. C^1 approximation of vector fields based on the renormalization group method. *SIAM J. Appl. Dyn. Sys.*, 7(3):895–932, 2008.
- [Chi09] H. Chiba. Extension and unification of singular perturbation methods for ODEs based on the renormalization group method. *SIAM J. Appl. Dyn. Sys.*, 8(3):1066–1115, 2009.
- [Chi10] C. Chicone. *Ordinary Differential Equations with Applications*. Texts in Applied Mathematics. Springer, 2nd edition, 2010.
- [Chi12] E. Chiavazzo. Approximation of slow and fast dynamics in multiscale dynamical systems by the linearized relaxation redistribution method. *J. Comp. Phys.*, 231(4):1751–1765, 2012.
- [Chi13] H. Chiba. Reduction of weakly nonlinear parabolic partial differential equations. *J. Math. Phys.*, 54:101501, 2013.
- [CHKL03] J. Cisternas, P. Holmes, I.G. Kevrekidis, and X. Li. CO oxidation on thin Pt crystals: temperature slaving and the derivation of lumped models. *J. Chem. Phys.*, 118:3312, 2003.
- [CHL03] D. Cohen, E. Hairer, and C. Lubich. Modulated Fourier expansions of highly oscillatory differential equations. *Found. Comput. Math.*, 3(4):327–345, 2003.
- [CHL09] F. Castella, J.-P. Hoffbeck, and Y. Lagadeuc. A reduced model for spatially structured predator–prey systems with fast spatial migrations and slow demographic evolutions. *Asymptot. Anal.*, 61(3):125–175, 2009.
- [CHM77] D.S. Cohen, F.C. Hoppensteadt, and R.M. Miura. Slowly modulated oscillations in nonlinear diffusion processes. *SIAM J. Appl. Math.*, 33(2):217–229, 1977.

- [Cho77] J.H. Chow. Preservation of controllability in linear time-invariant perturbed systems. *Int. J. Contr.*, 25(5):697–704, 1977.
- [Cho78] J.H. Chow. Asymptotic stability of a class of non-linear singularly perturbed systems. *J. Frank. Inst.*, 305(5):275–281, 1978.
- [Cho79] J.H. Chow. A class of singularly perturbed, nonlinear, fixed-endpoint control problems. *J. Optim. Theor. Appl.*, 29(2):231–251, 1979.
- [Cho82] J.H. Chow, editor. *Time-Scale Modeling of Dynamic Networks with Applications to Power Systems*, volume 46 of *Lect. Notes Contr. Infor. Sci.* Springer, 1982.
- [Cho91] J.H. Chow. Aggregation properties of linearized two-time-scale power networks. *IEEE Trans. Circ. Syst.*, 38(7):720–730, 1991.
- [Cho03] S.-N. Chow. Lattice dynamical systems. In J.W. Macki and P. Zecca, editors, *Dynamical Systems*, pages 1–102. Springer, 2003.
- [Chr00] P.D. Christofides. Robust output feedback control of nonlinear singularly perturbed systems. *Automatica*, 36(1):45–52, 2000.
- [Chu92] C.K. Chu. *An Introduction to Wavelets*. Academic Press, 1992.
- [ČišA+13] Ž. Čupić, A. Ivanović-Šasić, S. Anić, B. Stanković, J. Maksimović, J. Kolar-Anić, and G. Schmitz. Tourbillion in the phase space of the Bray-Liebhafsky nonlinear oscillatory reaction and related multiple-time-scale model. *MATCH Commun. Math. Comput. Chem.*, 69:805–830, 2013.
- [CJRK98] J.M. Cline, M. Joyce, and K. Kainulainen. Supersymmetric electroweak baryogenesis in the WKB approximation. *Phys. Lett. B*, 417(1):79–86, 1998.
- [CJR76] S.L. Campbell, C.D. Meyer Jr, and N.J. Rose. Applications of the Drazin inverse to linear systems of differential equations with singular constant coefficients. *SIAM J. Appl. Math.*, 31(3):411–425, 1976.
- [CK76] J.H. Chow and P.V. Kokotovic. A decomposition of near-optimum regulators for systems with slow and fast modes. *IEEE Trans. Aut. Contr.*, 21(5):701–705, 1976.
- [CK78a] J.H. Chow and P.V. Kokotovic. Near-optimal feedback stabilization of a class of nonlinear singularly perturbed systems. *SIAM J. Contr. Optim.*, 16(5):756–770, 1978.
- [CK78b] J.H. Chow and P.V. Kokotovic. Two-time-scale feedback design of a class of nonlinear systems. *IEEE Trans. Aut. Contr.*, 23(3):438–443, 1978.
- [CK83a] T.R. Chay and J. Keizer. Minimal model for membrane oscillations in the pancreatic beta-cell. *Biophys. J.*, 42(2):181–189, 1983.
- [CK83b] R.C.Y. Chin and R.A. Krasny. A hybrid asymptotic-finite element method for stiff two-point boundary value problems. *SIAM J. Sci. Statist. Comput.*, 4(2):229–243, 1983.
- [CK85] J.H. Chow and P.V. Kokotovic. Time scale modeling of sparse dynamic networks. *IEEE Trans. Aut. Contr.*, 30(8):714–722, 1985.
- [CK88] T.R. Chay and H.S. Kang. Role of single-channel stochastic noise on bursting clusters of pancreatic beta-cells. *Biophys. J.*, 54(3):427–435, 1988.
- [CK94] A.R. Champneys and Yu.A. Kuznetsov. Numerical detection and continuation of codimension-two homoclinic bifurcations. *Int. J. Bif. Chaos*, 4(4):785–822, 1994.
- [CK98] M. Christ and A. Kiselev. Absolutely continuous spectrum for one-dimensional Schrödinger operators with slowly decaying potentials: some optimal results. *J. Amer. Math. Soc.*, 11(4):771–797, 1998.
- [CK99] D. Cao and T. Küpper. On the existence of multipeaked solutions to a semilinear Neumann problem. *Duke Math. J.*, 97(2):261–300, 1999.
- [CK11] M. Christ and A. Kiselev. WKB and spectral analysis of one-dimensional Schrödinger operators with slowly varying potentials. *Comm. Math. Phys.*, 218(2):245–262, 2011.
- [CKK+07] A.R. Champneys, V. Kirk, E. Knobloch, B.E. Oldeman, and J. Sneyd. When Shil'nikov meets Hopf in excitable systems. *SIAM J. Appl. Dyn. Syst.*, 6(4):663–693, 2007.
- [CKK+09] A.R. Champneys, V. Kirk, E. Knobloch, B.E. Oldeman, and J.D.M. Rademacher. Unfolding a tangent equilibrium-to-periodic heteroclinic cycle. *SIAM J. Appl. Dyn. Sys.*, 8(3): 1261–1304, 2009.
- [CKMR01] C. Chicone, S.M. Kopeikin, B. Mashhoon, and D.G. Retzloff. Delay equations and radiation damping. *Phys. Lett. A*, 285:17–26, 2001.
- [CKN13] K. Cho, J. Kamimoto, and T. Nose. Asymptotic analysis of oscillatory integrals via the Newton polyhedra of the phase and the amplitude. *J. Math. Soc. Japan*, 65(2):521–562, 2013.
- [CKS94] W.W. Chow, S.W. Koch, and M. Sargent. *Semiconductor Laser Physics*. Springer, 1994.
- [CKS96] A.R. Champneys, Yu.A. Kuznetsov, and B. Sandstede. A numerical toolbox for homoclinic bifurcation analysis. *Int. J. Bif. Chaos*, 6(5):867–887, 1996.
- [CL45] M.L. Cartwright and J.E. Littlewood. On non-linear differential equations of second order. I. The equation $\ddot{y} - k(1 - y^2)\dot{y} + y = b\lambda k \cos(\lambda t + a)$, k large. *J. London Math. Soc.*, 20:180–189, 1945.
- [CL47] M.L. Cartwright and J.E. Littlewood. On non-linear differential equations of second order. II. The equation $\ddot{y} - kf(y, \dot{y}) + g(y, k) = p(t)$, $k > 0$, $f(y) \geq 1$. *Ann. Math.*, 48(2):472–494, 1947.
- [CL52] E.A. Coddington and N. Levinson. A boundary value problem for a nonlinear differential equation with a small parameter. *Proc. Amer. Math. Soc.*, 3(1):73–81, 1952.
- [CL55] E.A. Coddington and N. Levinson. *Theory of Ordinary Differential Equations*. McGraw-Hill, 1955.
- [CL91] S.L. Campbell and B. Leimkuhler. Differentiation of constraints in differential-algebraic equations. *J. Struct. Mech.*, 19:19–39, 1991.
- [CL95] S.N. Chow and H. Leiva. Existence and roughness of the exponential dichotomy for skew-product semiflow in Banach spaces. *J. Differential Equat.*, 120(2):429–477, 1995.
- [CL00] C. Chicone and W. Liu. On the continuation of an invariant torus in a family with rapid oscillations. *SIAM J. Math. Anal.*, 31(2):386–415, 2000.
- [CL03] E.J. Collins and D.S. Leslie. Convergent multiple-timescales reinforcement learning algorithms in normal form games. *Ann. Appl. Probab.*, 13(4):1231–1251, 2003.
- [CL10] G.A. Cassatella, Contra and D. Levi. Discrete multiscale analysis: a biatomic lattice system. *J. Nonlinear Math. Phys.*, 17:357–377, 2010.
- [CL11] C. Chipot and T. Lelièvre. Enhanced sampling of multidimensional free-energy landscapes using adaptive biasing forces. *SIAM J. Appl. Math.*, 71(5):1673–1695, 2011.
- [CLW94] S.-N. Chow, C. Li, and D. Wang. *Normal Forms and Bifurcation of Planar Vector Fields*. CUP, 1994.
- [CM70] V.H. Chu and C.M. Mei. On slowly-varying Stokes waves. *J. Fluid Mech.*, 41(4):873–887, 1970.

- [CM95] S.L. Campbell and E. Moore. Constraint preserving integrators for general nonlinear higher index DAEs. *Numer. Math.*, 69(4):383–399, 1995.
- [CM02] S.M. Cox and P.C. Matthews. Exponential time differencing for stiff systems. *J. Comput. Phys.*, 176(2):430–455, 2002.
- [CM05a] J.R. Cash and F. Mazzia. A new mesh selection algorithm, based on conditioning, for two-point boundary value codes. *J. Comp. Appl. Math.*, 184:362–381, 2005.
- [CM05b] K. Christensen and N.R. Moloney. *Complexity and Criticality*. Imperial College Press, 2005.
- [CM07] J. Cousteix and J. Mauss. *Asymptotic Analysis and Boundary Layers*. Springer, 2007.
- [CMA90] M. Ciofini, R. Meucci, and F.T. Arecchi. Transient statistics in a CO_2 laser with a slowly swept pump. *Phys. Rev. A*, 42:482–486, 1990.
- [CMJ09] N. Costanzino, V. Manukian, and C.K.R.T. Jones. Solitary waves of the regularized short pulse and Ostrovsky equations. *SIAM J. Math. Anal.*, 41(5):2088–2106, 2009.
- [CML02] D. Cai, D.W. McLaughlin, and K.T.R. Mc Laughlin. The nonlinear Schrödinger equation as both a PDE and a dynamical system. In B. Fiedler, editor, *Handbook of Dynamical Systems 2*, pages 599–675. Elsevier, 2002.
- [CPM77] S.N. Chow and J. Mallet-Paret. Integral averaging and bifurcation. *J. Differential Equat.*, 26(1):112–159, 1977.
- [CMR13] G.W.A. Constable, A.J. McKane, and T. Rogers. Stochastic dynamics on slow manifolds. *J. Phys. A*, 46:295002, 2013.
- [CMS05] R. Carles, N.J. Mauser, and H.P. Stimming. (Semi)classical limit of the Hartree equation with harmonic potential. *SIAM J. Appl. Math.*, 66(1):29–56, 2005.
- [CMSS10] P. Chartier, A. Murua, and J.M. Sanz-Serna. Higher-order averaging, formal series and numerical integration I: B-series. *Found. Comput. Math.*, 10(6):695–727, 2010.
- [CMSS12] P. Chartier, A. Murua, and J.M. Sanz-Serna. Higher-order averaging, formal series and numerical integration II: the quasi-periodic case. *Found. Comput. Math.*, 12(4):471–508, 2012.
- [CMST06] J.R. Cash, F. Mazzia, N. Sumarti, and D. Trigiante. The role of conditioning in mesh selection algorithms for first order systems of linear two point boundary value problems. *J. Comp. Appl. Math.*, 185:212–224, 2006.
- [CMW95] J.R. Cash, G. Moore, and R.W. Wright. An automatic continuation strategy for the solution of singularly perturbed linear two-point boundary value problems. *J. Comp. Phys.*, 122:266–279, 1995.
- [CNO06] S. Conti, B. Niethammer, and F. Otto. Coarsening rates in off-critical mixtures. *SIAM J. Math. Anal.*, 37(6):1732–1741, 2006.
- [CNV07] M. Courbage, V.I. Nekorkin, and L.V. Vdovin. Chaotic oscillations in a map-based model of neural activity. *Chaos*, 17:043109, 2007.
- [CO74] J. Chen and R.E. O’Malley. On the asymptotic solution of a two-parameter boundary value problem of chemical reactor theory. *SIAM J. Appl. Math.*, 26(4):717–729, 1974.
- [CO99] J. Cronin and R.E. O’Malley, editors. *Analyzing Multiscale Phenomena Using Singular Perturbation Methods*, volume 56 of *Proc. Symp. Appl. Math.* AMS, 1999.
- [CO00] S. Coombes and A.H. Osbaldestin. Period-adding bifurcations and chaos in a periodically stimulated excitable neural relaxation oscillator. *Phys. Rev. E*, 62(3):4057–4066, 2000.
- [Com68] C. Comstock. On Lighthill’s method of strained coordinates. *SIAM J. Appl. Math.*, 16(3):596–602, 1968.
- [Com71a] C. Comstock. Singular perturbations of elliptic equations. I. *SIAM J. Appl. Math.*, 20(3):491–502, 1971.
- [Com71b] C. Comstock. Singular perturbations of elliptic equations. II. In *Analytic Theory of Differential Equations*, pages 200–206. Springer, 1971.
- [Com72] C. Comstock. The Poincaré-Lighthill perturbation technique and its generalizations. *SIAM Rev.*, 14(3):433–446, 1972.
- [Con78] C. Conley. *Isolated Invariant Sets and the Morse Index*. Amer. Math. Soc., 1978.
- [Con80] C. Conley. A qualitative singular singular perturbation theorem. In Z. Nitecki and C. Robinson, editors, *Global Theory of Dynamical Systems*, pages 65–89. Springer, 1980.
- [Con89] P. Constantin. *Integral Manifolds and Inertial Manifolds for Dissipative Partial Differential Equations*. Springer, 1989.
- [Con90] J. B. Conway. *A Course in Functional Analysis*. Springer, 1990.
- [Con04] F. Cong. The approximate decomposition of exponential order of slow–fast motions in multifrequency systems. *J. Differential Equat.*, 196(2):466–480, 2004.
- [Coo01] S. Coombes. Phase locking in networks of synaptically coupled McKean relaxation oscillators. *Physica D*, 160(3):173–188, 2001.
- [Coo05] S. Coombes. Waves, bumps, and patterns in neural field theories. *Biol. Cybern.*, 93:91–108, 2005.
- [Cop78] W.A. Copel. *Dichotomies in Stability Theory*. Springer, 1978.
- [COR12] F. Casas, J.A. Oteo, and J. Ros. Unitary transformations depending on a small parameter. *Proc. R. Soc. A*, 468:685–700, 2012.
- [Cos09] O. Costin. *Asymptotics and Borel Summability*. Chapman-Hall, 2009.
- [CPS83] S.L. Campbell and L.R. Petzhold. Canonical forms and solvable singular systems of differential equations. *SIAM J. Algebraic Discr. Meth.*, 4(4):517–521, 1983.
- [CP89] J. Carr and R.L. Pego. Metastable patterns in solutions of $u_t = \epsilon^2 u_{xx} - f(u)$. *Comm. Pure Appl. Math.*, 42(5):523–576, 1989.
- [CP90] J. Carr and R.L. Pego. Invariant manifolds for metastable patterns in $u_t = \epsilon^2 u_{xx} - f(u)$. *Proc. R. Soc. Edinburgh A*, 116(1):133–160, 1990.
- [CPS90] A.J. Calise, J.V.R. Prasad, and B. Siciliano. Design of optimal output feedback compensators in two-time scale systems. *IEEE Trans. Auto. Contr.*, 35(4):488–492, 1990.
- [CR79] S.L. Campbell and N.J. Rose. Singular perturbation of autonomous linear systems. *SIAM J. Math. Anal.*, 10(3):542–551, 1979.
- [CR85] T.R. Chay and J. Rinzel. Bursting, beating, and chaos in an excitable membrane model. *Biophys. J.*, 47(3):357–366, 1985.
- [CR88] T. Chakraborty and R.H. Rand. The transition from phase locking to drift in a system of two weakly coupled van der Pol oscillators. *Int. J. Non-Linear Mech.*, 23(5):369–376, 1988.

- [CR03] S. Cerrai and M. Röckner. Large deviations for invariant measures of general stochastic reaction-diffusion systems. *Comptes Rendus Acad. Sci. Paris S. I Math.*, 337:597–602, 2003.
- [CR04] S. Cerrai and M. Röckner. Large deviations for stochastic reaction-diffusion systems with multiplicative noise and non-Lipschitz reaction term. *Annals of Probability*, 32:1–40, 2004.
- [CR05] S. Cerrai and M. Röckner. Large deviations for invariant measures of stochastic reaction-diffusion systems with multiplicative noise and non-Lipschitz reaction term. *Annales de l'Institut Henri Poincaré (B)*, 41:69–105, 2005.
- [CR11] R. Curtu and J. Rubin. Interaction of canard and singular Hopf mechanisms in a neural model. *SIAM J. Appl. Dyn. Syst.*, 10:1443–1479, 2011.
- [Cré07] A.-S. Crépin. Using fast and slow processes to manage resources with thresholds. *Environ. Resource Econ.*, 36(2):191–213, 2007.
- [CRK05] R. Clewley, H.G. Rotstein, and N. Kopell. A computational tool for the reduction of nonlinear ODE systems possessing multiple scales. *Multiscale Model. Simul.*, 4(3):732–759, 2005.
- [CRO86] W.L. Chien, H. Rising, and J.M. Ottino. Laminar mixing and chaotic mixing in several cavity flows. *J. Fluid Mech.*, 170(1): 355–377, 1986.
- [Cro87] J. Cronin, editor. *Mathematical Aspects of Hodgkin–Huxley Neural Theory*. CUP, 1987.
- [CS76] C. Conley and Joel Smoller. Remarks on traveling wave solutions of non-linear diffusion equations. in: *Structural Stability, the Theory of Catastrophes, and Applications in the Sciences (LNM 525)*, pages 77–89, 1976.
- [CS86] C. Conley and Joel Smoller. Bifurcation and stability of stationary solutions of the FitzHugh–Nagumo equations. *J. Differential Equat.*, 63(3):389–405, 1986.
- [CS05] G.S. Cymbalyuk and A.L. Shilnikov. Coexistence of tonic spiking oscillations in a leech neuron model. *J. Comput. Neurosci.*, 18(3):255–263, 2005.
- [CS11] M.S. Calder and D. Siegel. Properties of the Lindemann mechanism in phase space. *Electron. J. Differential Equat.*, 2011(8):1–31, 2011.
- [CS12] M.J. Capinski and C. Simo. Computer assisted proof for normally hyperbolic invariant manifolds. *Nonlinearity*, 25:1997–2026, 2012.
- [CS13] E.M. Constantinescu and A. Sandu. Extrapolated multirate methods for differential equations with multiple time scales. *J. Sci. Comput.*, 56:28–44, 2013.
- [CSE09] S.A. Campbell, E. Stone, and T. Erneux. Delay induced canards in a model of high speed machining. *Dynamical Systems*, 24(3):373–392, 2009.
- [CSHD12] E. Cotilla-Sánchez, P. Hines, and C.M. Danforth. Predicting critical transitions from time series synchrophasor data. *IEEE Trans. Smart Grid*, 3(4):1832–1840, 2012.
- [CSR08] R. Curtu, A. Shpiro, N. Rubin, and J. Rinzel. Mechanisms for frequency control in neuronal competition models. *SIAM J. Appl. Dyn. Syst.*, 7(2):609–649, 2008.
- [CSS10] M.P. Calvo and J.M. Sanz-Serna. Heterogeneous multiscale methods for mechanical systems with vibrations. *SIAM J. Sci. Comput.*, 32:2029–2046, 2010.
- [CTS12] R. Chacra, M.K. Transtrum, and J.P. Sethna. Structural susceptibility and separation of time scales in the van der Pol oscillator. *Phys. Rev. E*, 86:026712, 2012.
- [Cur10] R. Curtu. Singular Hopf bifurcation and mixed-mode oscillations in a two-cell inhibitory neural network. *Physica D*, 239:504–514, 2010.
- [CV09] F. Clément and A. Vidal. Foliation-based parameter tuning in a model of the GnRH pulse and surge generator. *SIAM J. Appl. Dyn. Syst.*, 8(4):1591–1631, 2009.
- [CWPS90] J.H. Chow, J.R. Winkelman, M.A. Pai, and P.W. Sauer. Singular perturbation analysis of large-scale power systems. *Int. J. Elec. Power Energ. Syst.*, 12(2):117–126, 1990.
- [CWS83a] M. Coderch, A.S. Willsky, and S.S. Sastry. Hierarchical aggregation of linear systems with multiple time scales. *IEEE Trans. Aut. Contr.*, 28(11):1017–1030, 1983.
- [CWS83b] M. Coderch, A.S. Willsky, and S.S. Sastry. Hierarchical aggregation of singularly perturbed finite state Markov processes. *Stochastics*, 8(4):259–289, 1983.
- [CWS10] A.F. Cheviakov, M.J. Ward, and R. Straube. An asymptotic analysis of the mean first passage time for narrow escape problems: Part II: The sphere. *Multiscale Model. Simul.*, 8(3):836–870, 2010.
- [DA67] R.T. Davis and K.T. Alfriend. Solutions to van der Pol's equation using a perturbation method. *Int. J. Non-Linear Mech.*, 2(2):153–162, 1967.
- [Daf10] C.M. Dafermos. *Hyperbolic Conservation Laws in Continuum Physics*. Springer, 2010.
- [Dah63] G. Dahlquist. A special stability problem for linear multistep methods. *BIT*, 3:27–43, 1963.
- [Dan13] M.J.H. Dantas. Quenching in a class of singularly perturbed mechanical systems. *Int. J. Non-Linear Mech.*, 50:48–57, 2013.
- [dARAR99] F.M. de Aguiar, S. Rosenblatt, A. Azevedo, and S.M. Rezende. Observation of mixed-mode oscillations in spin-wave experiments. *J. Appl. Phys.*, 85(8):5086–5087, 1999.
- [Dau92] I. Daubechies. *Ten Lectures on Wavelets*. SIAM, 1992.
- [Day83] M.V. Day. On the exponential exit law in the small parameter exit problem. *Stochastics*, 8(4):297–323, 1983.
- [Day84] M.V. Day. On the asymptotic relation between equilibrium density and exit measure in the exit problem. *Stochastics*, 12(3):303–330, 1984.
- [Day87] M.V. Day. Recent progress on the small parameter exit problem. *Stochastics*, 20(2):121–150, 1987.
- [Day89] M.V. Day. Boundary local time and small parameter exit problems with characteristic boundaries. *SIAM J. Math. Anal.*, 20(1):222–248, 1989.
- [Day90] M.V. Day. Large deviations results for the exit problem with characteristic boundary. *J. Math. Anal. Appl.*, 147(1):134–153, 1990.
- [Day92] M.V. Day. Conditional exits for small noise diffusions with characteristic boundary. *Ann. Prob.*, 20(3):1385–1419, 1992.
- [Day94] M.V. Day. Cycling and skewing of exit measures for planar systems. *Stochastics*, 48(3):227–247, 1994.
- [Day95] M.V. Day. On the exit law from saddle points. *Stoch. Proc. Appl.*, 60(2):287–311, 1995.
- [dBBCK08] M. di Bernardo, C.J. Budd, A.R. Champneys, and P. Kowalczyk. *Piecewise-smooth Dynamical Systems*, volume 163 of *Applied Mathematical Sciences*. Springer, 2008.

- [DBFP03] C. Doss-Bachelet, J.-P. Francoise, and C. Piquet. Bursting oscillations in two coupled FitzHugh–Nagumo systems. *ComPlexUs*, 2:101–111, 2003.
- [DBKK12] M. Desroches, J. Burke, T.J. Kaper, and M.A. Kramer. Canards of mixed type in a neural burster. *Phys. Rev. E*, 85:021920, 2012.
- [DBL13] M. Dobson, C. Le Bris, and F. Legoll. Symplectic schemes for highly oscillatory Hamiltonian systems: the homogenization approach beyond the constant frequency case. *IMA J. Numer. Anal.*, 33:30–56, 2013.
- [dBM87] C. Van den Broeck and P. Mandel. Delayed bifurcations in the presence of noise. *Phys. Lett. A*, 122:36–38, 1987.
- [DBR⁺13] M. M. Brøns, J.J. Rasmussen, V. Naulin, and G. Xu. Bifurcation analysis and dimension reduction of a predator–prey model for the LH transition. *Physics of Plasmas*, 20:102302, 2013.
- [DCD⁺07] E.J. Doedel, A. Champneys, F. Dercole, T. Fairgrieve, Y. Kuznetsov, B. Oldeman, R. Paffenroth, B. Sandstede, X. Wang, and C. Zhang. Auto 07p: Continuation and bifurcation software for ordinary differential equations (with homcont). <http://cmvl.cs.concordia.ca/auto>, 2007.
- [DD91] F. Diener and M. Diener. Maximal delay. In E. Benoît, editor, *Dynamic Bifurcations*, volume 1493 of *Lecture Notes in Mathematics*, pages 71–86. Springer, 1991.
- [DD95] F. Diener and M. Diener. *Nonstandard Analysis in Practice*. Springer, 1995.
- [DD03] T. Donchev and A.L. Dontchev. Singular perturbations in infinite-dimensional control systems. *SIAM J. Contr. Optim.*, 42(5):1795–1812, 2003.
- [DD07] A. Du and J. Duan. Invariant manifold reduction for stochastic dynamical systems. *Dyn. Syst. Appl.*, 16:681–696, 2007.
- [DDS96] A. Dontchev, T. Donchev, and I. Slavov. A Tikhonov-type theorem for singularly perturbed differential inclusions. *Nonl. Anal., Theory, Meth. & Appl.*, 26(9):1547–1554, 1996.
- [DDvGV03] G. Derkx, A. Doelman, S.A. van Gils, and T. Visser. Travelling waves in a singularly perturbed sine-Gordon equation. *Physica D*, 180:40–70, 2003.
- [DEF74] A. Devinatz, R. Ellis, and A. Friedman. The asymptotic behavior of the first real eigenvalue of second order elliptic operators with a small parameter in the highest derivatives. II. *Ind. Univ. Math. J.*, 23(11):991–1011, 1974.
- [DEK00] A. Doelman, W. Eckhaus, and T.J. Kaper. Slowly modulated two-pulse solutions in the Gray–Scott Model I: asymptotic construction and stability. *SIAM J. Appl. Math.*, 61(3):1080–1102, 2000.
- [DEK06] A. Doelman, W. Eckhaus, and T.J. Kaper. Slowly modulated two-pulse solutions in the Gray–Scott Model II: geometric theory, bifurcations, and splitting dynamics. *SIAM J. Appl. Math.*, 61(6):2036–2062, 2006.
- [Del83] F. Delebecque. A reduction process for perturbed Markov chains. *SIAM J. Appl. Math.*, 43(2):325–350, 1983.
- [Dem10] H. Demiray. Multiple time scale formalism and its application to long water waves. *Appl. Math. Model.*, 34(5):1187–1193, 2010.
- [Den90] B. Deng. Homoclinic bifurcations with nonhyperbolic equilibria. *SIAM J. Math. Anal.*, 21(3):693–720, 1990.
- [Den91] B. Deng. The existence of infinitely many traveling front and back waves in the FitzHugh–Nagumo equations. *SIAM J. Appl. Math.*, 22(6):1631–1650, 1991.
- [Den93a] B. Deng. Homoclinic twisting bifurcations and cusp horseshoe maps. *J. Dyn. Diff. Eq.*, 5(3):417–467, 1993.
- [Den93b] B. Deng. On Silnikov’s homoclinic saddle-focus theorem. *J. Differential Equat.*, 102:305–329, 1993.
- [Den94] B. Deng. Constructing homoclinic orbits and chaotic attractors. *Int. J. Bif. Chaos*, 4(4):823–841, 1994.
- [Den95a] B. Deng. Constructing Lorenz type attractors through singular perturbations. *Int. J. Bif. Chaos*, 5(6):1633–1642, 1995.
- [Den95b] B. Deng. Sil’nikov–hopf bifurcations. *J. Differential Equat.*, 119:1–23, 1995.
- [Den99] B. Deng. Glucose-induced period-doubling cascade in the electrical activity of pancreatic β -cells. *J. Math. Biol.*, 38(1):21–78, 1999.
- [Den01] B. Deng. Food chain chaos due to junction-fold point. *Chaos*, 11(3):514–525, 2001.
- [Den04] B. Deng. Food chain chaos with canard explosion. *Chaos*, 14(4): 1083–1092, 2004.
- [Dep69] A. Deprit. Canonical transformations depending on a small parameter. *Celest. Mech.*, 1(1):12–30, 1969.
- [DEV04] H.S. Dumas, J.A. Ellison, and M. Vogt. First-order averaging principles for maps with applications to accelerator beam dynamics. *SIAM J. Appl. Dyn. Syst.*, 3(4):409–432, 2004.
- [DFAR13] C. DuBois, J. Farnham, E. Aaron, and A. Radunskaya. A multiple time-scale computational model of a tumor and its micro environment. *Math. Biosci. Eng.*, 10:121–150, 2013.
- [DFD⁺10] R. Donangelo, H. Fort, V. Dakos, M. Scheffer, and E.H. Van Nes. Early warnings for catastrophic shifts in ecosystems: comparison between spatial and temporal indicators. *Int. J. Bif. Chaos*, 20(2):315–321, 2010.
- [DFGR06] F. Dercole, R. Ferrière, A. Gragnani, and S. Rinaldi. Coevolution of slow–fast populations: evolutionary sliding, evolutionary pseudo-equilibria and complex Red Queen dynamics. *Proc. R. Soc. B*, 273:983–990, 2006.
- [DFGRL02] E. Doedel, E. Freire, E. Gamero, and A. Rodriguez-Luis. An analytical and numerical study of a modified van der Pol oscillator. *J. Sound Vibration*, 256(4):755–771, 2002.
- [DFH⁺13] M. Desroches, E. Freire, S.J. Hogan, E. Ponce, and P. Thota. Canards in piecewise-linear systems: explosions and super-explosions. *Proc. R. Soc. A*, 469:20120603, 2013.
- [DG79] A.L. Dontchev and T.R. Giocva. Convex singularly perturbed optimal control problem with fixed final state, controllability and convergence. *Optimization*, 10(3):345–355, 1979.
- [DG90] M.B. Dadfar and J. Geer. Resonances and power series solutions of the forced van der Pol oscillator. *SIAM J. Appl. Math.*, 50(5):1496–1506, 1990.
- [DG93a] D. Dawson and A. Greven. Hierarchical models of interacting diffusions: multiple time scale phenomena, phase transition and pattern of cluster-formation. *Probab. Theory Related Fields*, 96(4):435–473, 1993.
- [DG93b] D. Dawson and A. Greven. Multiple time scale analysis of interacting diffusions. *Probab. Theory Related Fields*, 95(4):467–508, 1993.

- [DG10] J.M. Drake and B.D. Griffen. Early warning signals of extinction in deteriorating environments. *Nature*, 467:456–459, 2010.
- [DGA84] M.B. Dadfar, J. Geer, and C.M. Andersen. Perturbation analysis of the limit cycle of the free van der Pol equation. *SIAM J. Appl. Math.*, 44(5):881–895, 1984.
- [DGK98] A. Doelman, R.A. Gardner, and T.J. Kaper. Stability analysis of singular patterns in the 1D Gray-Scott model: a matched asymptotics approach. *Physica D*, 122(1):1–36, 1998.
- [DGK01] A. Doelman, R.A. Gardner, and T.J. Kaper. Large stable pulse solutions in reaction-diffusion equations. *Indiana Univ. Math. J.*, 50(1):443–507, 2001.
- [DGK02] A. Doelman, R.A. Gardner, and T.J. Kaper. *A Stability Index Analysis of 1-D Patterns of the Gray-Scott Model*, volume 737 of *Mem. Amer. Math. Soc.* AMS, 2002.
- [DGK03] A. Dhooge, W. Govaerts, and Yu.A. Kuznetsov. MATCONT: A MATLAB package for numerical bifurcation analysis of ODEs. *ACM Trans. Math. Softw.*, 29:141–164, 2003.
- [DGK⁺12] M. Desroches, J. Guckenheimer, C. Kuehn, B. Krauskopf, H. Osinga, and M. Wechselberger. Mixed-mode oscillations with multiple time scales. *SIAM Rev.*, 54(2):211–288, 2012.
- [DGL94] H.S. Dumas, F. Golse, and P. Lochak. Multiphase averaging for generalized flows on manifolds. *Ergodic Theor. Dyn. Syst.*, 14(1):53–67, 1994.
- [DGR00] A. Dutt, L. Greengard, and V. Rokhlin. Spectral deferred correction methods for ordinary differential equations. *BIT Numer. Math.*, 40(2):241–266, 2000.
- [DGR13] A. Delshams, M. Gidea, and P. Roldán. Transition map and shadowing lemma for normally hyperbolic invariant manifolds. *Discrete Contin. Dyn. Syst.*, 33(3):1089–1112, 2013.
- [DH82] V. Dragan and A. Halanay. Suboptimal stabilization of linear systems with several time scales. *Int. J. Contr.*, 36:109–126, 1982.
- [DH83] E. Doedel and R.F. Heinemann. Numerical computation of periodic solution branches and oscillatory dynamics of the stirred tank reactor with $A \rightarrow B \rightarrow C$ reactions. *Chemical Engineering Science*, 38(9):1493–1499, 1983.
- [DH96] M. Dellnitz and A. Hohmann. The computation of unstable manifolds using subdivision and continuation. In H.W. Broer, S.A. Van Gils, I. Hoveijn, and F. Takens, editors, *Nonlinear Dynamical Systems and Chaos PNLD 19*, pages 449–459. Birkhäuser, 1996.
- [DH97] M. Dellnitz and A. Hohmann. A subdivision algorithm for the computation of unstable manifolds and global attractors. *Numer. Math.*, 75:293–317, 1997.
- [DH99] F. Dumortier and C. Herssens. Polynomial Liénard equations near infinity. *J. Differential Equat.*, 153(1):1–29, 1999.
- [DH00a] D.C. Diminnie and R. Haberman. Slow passage through a saddle-center bifurcation. *J. Nonlinear Sci.*, 10:197–221, 2000.
- [DH00b] A. Doelman and G. Hek. Homoclinic saddle-node bifurcations in singularly perturbed systems. *J. Dyn. Diff. Eq.*, 12(1):169–215, 2000.
- [DH02a] B. Deng and G. Hines. Food chain chaos due to Shilnikov orbit. *Chaos*, 12(3):533–538, 2002.
- [DH02b] D.C. Diminnie and R. Haberman. Slow passage through homoclinic orbits for the unfolding of a saddle-center bifurcation and the change in the adiabatic invariant. *Physica D*, 162:34–52, 2002.
- [dH04] F. den Hollander. Metastability under stochastic dynamics. *Stoch. Proc. Appl.*, 114:1–26, 2004.
- [dH08] F. den Hollander. *Large Deviations*. Amer. Math. Soc., 2008.
- [DH11] A. Delshams and G. Huguet. A geometric mechanism of diffusion: rigorous verification in a priori unstable Hamiltonian systems. *J. Differential Equat.*, 250(5):2601–2623, 2011.
- [DH^{H+}08] L. DeVille, A. Harkin, M. Holzer, K. Josić, and T.J. Kaper. Analysis of a renormalization group method and normal form theory for perturbed ordinary differential equations. *Physica D*, 237:1029–1052, 2008.
- [DHV04] A. Doelman, G. Hek, and N. Valkhoff. Stabilization by slow diffusion in a real Ginzburg–Landau system. *J. Nonlinear Sci.*, 14(3):237–278, 2004.
- [DHV07] A. Doelman, G. Hek, and N. Valkhoff. Algebraically decaying pulses in a Ginzburg–Landau system with a neutrally stable mode. *Nonlinearity*, 20:357–389, 2007.
- [Die84] M. Diener. The canard unchained or how fast/slow dynamical systems bifurcate. *The Mathematical Intelligencer*, 6:38–48, 1984.
- [Die94] M. Diener. Regularizing microscopes and rivers. *SIAM J. Math. Anal.*, 25:148–173, 1994.
- [DIK04] S. Doi, J. Inoue, and S. Kumagai. Chaotic spiking in the Hodgkin–Huxley nerve model with slow inactivation in the sodium current. *J. Integr. Neurosci.*, 3(2):207–225, 2004.
- [DIN04] A. Doelman, D. Iron, and Y. Nishiura. Destabilization of fronts in a class of bistable systems. *SIAM J. Math. Anal.*, 35(6):1420–1450, 2004.
- [DIZ97] P.A. Deift, A.R. Its, and X. Zhou. A Riemann–Hilbert approach to asymptotic problems arising in the theory of random matrix models, and also in the theory of integrable statistical mechanics. *Ann. of Math.*, 146(1):149–235, 1997.
- [DJ10] P.D. Ditlevsen and S.J. Johnsen. Tipping points: early warning and wishful thinking. *Geophys. Res. Lett.*, 37:19703, 2010.
- [DJ11a] M. Desroches and M. Jeffrey. Canards and curvature: nonsmooth approximation by pinching. *Nonlinearity*, 24:1655, 2011.
- [DJ11b] M. Desroches and M. Jeffrey. Canards and curvature: the smallness of ϵ in slow–fast dynamics. *Proc. R. Soc. A*, 467:2404–2421, 2011.
- [DJD04] M. Dhamala, V.K. Jirsa, and M. Ding. Transitions to synchrony in coupled bursting neurons. *Phys. Rev. Lett.*, 92:028101, 2004.
- [DK81] D.W. Decker and H.B. Keller. Path following near bifurcation. *Comm. Pure Appl. Math.*, 34(2):149–175, 1981.
- [DK84] M.G. Dmitriev and A.M. Klishevich. Iterative solution of optimal control problems with fast and slow motions. *Syst. Contr. Lett.*, 4(4):223–226, 1984.
- [DK99] J.L.A. Dubbeldam and B. Krauskopf. Self-pulsations of lasers with saturable absorber: dynamics and bifurcations. *Optics Communications*, 159:325–338, 1999.
- [DK03] A. Doelman and T.J. Kaper. Semistrong pulse interactions in a class of coupled reaction-diffusion equations. *SIAM J. Appl. Dyn. Syst.*, 2(1):53–96, 2003.

- [DK05] S. Doi and S. Kumagai. Generation of very slow neuronal rhythms and chaos near the Hopf bifurcation in single neuron models. *J. Comput. Neurosci.*, 19(3):325–356, 2005.
- [DK06] M.G. Dmitriev and G.A. Kurina. Singular perturbations in control problems. *Autom. Remote Contr.*, 67:1–43, 2006.
- [DK13] D. Dolgopyat and L. Koralov. Averaging of incompressible flows on two-dimensional surfaces. *J. Amer. Math. Soc.*, 26(2):427–449, 2013.
- [DKK91a] E. Doedel, H.B. Keller, and J.-P. Kernevez. Numerical analysis and control of bifurcation problems. I. Bifurcation in finite dimensions. *Internat. J. Bifur. Chaos Appl. Sci. Engrg.*, 1(3):493–520, 1991.
- [DKK91b] E. Doedel, H.B. Keller, and J.-P. Kernevez. Numerical analysis and control of bifurcation problems. II. Bifurcation in infinite dimensions. *Internat. J. Bifur. Chaos Appl. Sci. Engrg.*, 1(4):745–772, 1991.
- [DKK13] M. Desroches, T.J. Kaper, and M. Krupa. Mixed-mode bursting oscillations: dynamics created by a slow passage through spike-adding canard explosion in a square-wave burster. *Chaos*, 23:046106, 2013.
- [DKL99] J.L.A. Dubbeldam, B. Krauskopf, and D. Lenstra. Excitability and coherence resonance in lasers with saturable absorber. *Phys. Rev. E*, 59(6):6580–6588, 1999.
- [DKM02] A. Doelman, A.F. Koenderink, and L.R.M. Maas. Quasi-periodically forced nonlinear Helmholtz oscillators. *Physica D*, 164(1):1–27, 2002.
- [DKO08a] M. Desroches, B. Krauskopf, and H.M. Osinga. The geometry of slow manifolds near a folded node. *SIAM J. Appl. Dyn. Syst.*, 7(4):1131–1162, 2008.
- [DKO08b] M. Desroches, B. Krauskopf, and H.M. Osinga. Mixed-mode oscillations and slow manifolds in the self-coupled FitzHugh–Nagumo system. *Chaos*, 18:015107, 2008.
- [DKO09] M. Desroches, B. Krauskopf, and H.M. Osinga. The geometry of mixed-mode oscillations in the Olsen model for the peroxidase-oxidase reaction. *DCDS-S*, 2(4):807–827, 2009.
- [DKO10] M. Desroches, B. Krauskopf, and H.M. Osinga. Numerical continuation of canard orbits in slow–fast dynamical systems. *Nonlinearity*, 23(3):739–765, 2010.
- [DKP07] A. Doelman, T.J. Kaper, and K. Promislow. Nonlinear asymptotic stability of the semistrong pulse dynamics in a regularized Gierer–Meinhardt model. *SIAM J. Math. Anal.*, 38(6):1760–1787, 2007.
- [DKR⁺11] V. Dakos, S. Kéfi, M. Rietkerk, E.H. van Nes, and M. Scheffer. Slowing down in spatially patterned systems at the brink of collapse. *Am. Nat.*, 177(6):153–166, 2011.
- [DKR13] M. Desroches, M. Krupa, and S. Rodrigues. Inflection, canards and excitability threshold in neuronal models. *J. Math. Biol.*, 67(4):989–1017, 2013.
- [DKvdP01] A. Doelman, T.J. Kaper, and H. van der Ploeg. Spatially periodic and aperiodic multi-pulse patterns in the one-dimensional Gierer–Meinhardt equation. *Meth. Appl. Anal.*, 8(3):387–414, 2001.
- [DKZ97] A. Doelman, T.J. Kaper, and P.A. Zegeling. Pattern formation in the one-dimensional Gray–Scott model. *Nonlinearity*, 10(2):523–563, 1997.
- [DL96] U. Dieckmann and R. Law. The dynamical theory of coevolution: a derivation from stochastic ecological processes. *J. Math. Biol.*, 34:579–612, 1996.
- [DL11] D. Dolgopyat and C. Liverani. Energy transfer in fast–slow Hamiltonian systems. *Comm. Math. Phys.*, 308:201–225, 2011.
- [DL13] L. DeVille and E. Lerman. Dynamics on networks I. Modular continuous-time systems. *J. Euro. Math. Soc.*, pages 1–59, 2013. to appear.
- [DLLM02] B. Doiron, C.R. Laing, A. Longtin, and L. Maler. Ghostbursting: a novel neuronal burst mechanism. *J. Comput. Neurosci.*, 12:5–25, 2002.
- [DLO10a] M. Dobson, M. Luskin, and C. Ortner. Sharp stability estimates for the force-based quasicontinuum approximation of homogeneous tensile deformation. *Multiscale Model. Simul.*, 8(3):782–802, 2010.
- [DLO10b] M. Dobson, M. Luskin, and C. Ortner. Stability, instability, and error of the force-based quasicontinuum approximation. *Arch. Rat. Mech. Anal.*, 197:179–202, 2010.
- [DLS00] A. Delshams, R. De La Llave, and T.M. Seara. A geometric approach to the existence of orbits with unbounded energy in generic periodic perturbations by a potential of generic geodesic flows of T^2 . *Comm. Math. Phys.*, 209(2):353–392, 2000.
- [DLS03] J. Duan, K. Lu, and B. Schmalfuss. Invariant manifolds for stochastic partial differential equations. *Ann. Prob.*, 31(4):2109–2135, 2003.
- [DLS04] J. Duan, K. Lu, and B. Schmalfuss. Smooth stable and unstable manifolds for stochastic evolutionary equations. *J. Dyn. Diff. Eq.*, 16(4):949–972, 2004.
- [DLS08] A. Delshams, R. De La Llave, and T.M. Seara. Geometric properties of the scattering map of a normally hyperbolic invariant manifold. *Adv. Math.*, 217(3):1096–1153, 2008.
- [DLZ97] F. Dumortier, C. Li, and Z. Zhang. Unfolding of a quadratic integrable system with two centers and two unbounded heteroclinic loops. *J. Differential Equat.*, 139(1):146–193, 1997.
- [DM08] J. Durham and J. Moehlis. Feedback control of canards. *Chaos*, 18:015110, 2008.
- [DM10] S.Yu. Dobrokhotov and D.S. Minenkov. On various averaging methods for a nonlinear oscillator with slow time-dependent potential and a nonconservative perturbation. *Reg. & Chaotic Dynamics*, 15(2):285–299, 2010.
- [Dmi78] M.G. Dmitriev. On a class of singularly perturbed problems of optimal control. *J. Appl. Math. Mech.*, 42(2):238–242, 1978.
- [DMS⁺00] C.T. Dickson, J. Magistretti, M.H. Shalishnyk, E. Fransen, M.E. Hasselmo, and A. Alonso. Properties and role of I_h in the pacing of subthreshold oscillations in entorhinal cortex layer II neurons. *J. Neurophysiol.*, 83:2562–2579, 2000.
- [DMS03] C.R. Doering, C. Mueller, and P. Smereka. Interacting particles, the stochastic Fisher–Kolmogorov–Petrovsky–Piscounov equation, and duality. *Physica A*, 325:243–259, 2003.
- [DMS⁺06] C.T. Dickson, J. Magistretti, M.H. Shalishnyk, B. Hamam, and A. Alonso. Oscillatory activity in entorhinal neurons and circuits: mechanisms and function. *Ann. N.Y. Acad. Sci.*, 911:127–150, 2006.
- [DMS86a] M.M. Dygas, B.J. Matkowsky, and Z. Schuss. A singular perturbation approach to non-Markovian escape rate problems. *SIAM J. Appl. Math.*, 46(2):265–298, 1986.
- [DMS86b] M.M. Dygas, B.J. Matkowsky, and Z. Schuss. A singular perturbation approach to non-Markovian escape rate problems with state dependent friction. *J. Chem. Phys.*, 84:3731, 1986.

- [DMV98] R. Denk, R. Mennicken, and L. Volevich. The newton polygon and elliptic problems with parameter. *Math. Nachr.*, 192(1):125–157, 1998.
- [DNCB95] B. D'Andréa-Novel, G. Campion, and G. Bastin. Control of wheeled mobile robots not satisfying ideal velocity constraints: a singular perturbation approach. *Int. J. Robust Nonl. Contr.*, 5(4):243–267, 1995.
- [DNR11] J.R. Dunmyre, C.A. Del Negro, and J.E. Rubin. Interactions of persistent sodium and calcium-activated nonspecific cationic currents yield dynamically distinct bursting regimes in a model of respiratory neurons. *J. Comp. Neurosci.*, 31(2):305–328, 2011.
- [DNS05] J. Denef, J. Nicaise, and P. Sargos. Oscillating integrals and Newton polyhedra. *J. Anal. Math.*, 95:147–172, 2005.
- [Doc92] J.D. Dockery. Existence of standing pulse solutions for an excitable activator-inhibitory system. *J. Dyn. Diff. Eq.*, 4(2):231–257, 1992.
- [Doe93] A. Doelman. Traveling waves in the complex Ginzburg–Landau equation. *J. Nonlinear Sci.*, 3(1):225–266, 1993.
- [Doe96] A. Doelman. Breaking the hidden symmetry in the Ginzburg–Landau equation. *Physica D*, 97(4):398–428, 1996.
- [Doe97] E.J. Doedel. Auto 97: Continuation and bifurcation software for ordinary differential equations. <http://indy.cs.concordia.ca/auto>, 1997.
- [Doe00] E.J. Doedel. Auto 2000: Continuation and bifurcation software for ordinary differential equations (with homcont). <http://cmvl.cs.concordia.ca/auto>, 2000.
- [Doe07] E.J. Doedel. Lecture notes on numerical analysis of nonlinear equations. <http://cmvl.cs.concordia.ca/publications/notes.ps.gz>, 2007.
- [Don83] A.L. Dontchev. *Perturbations, Approximations and Sensitivity Analysis of Optimal Control Systems*, volume 52 of *Lect. Notes Contr. Inf. Sci.* Springer, 1983.
- [Don92] A.L. Dontchev. Time-scale decomposition of the reachable set of constrained linear systems. *Math. Contr. Sign. Syst.*, 5(3):327–340, 1992.
- [DOP79] H. Degn, L.F. Olsen, and J.W. Perram. Bistability, oscillation, and chaos in an enzyme reaction. *Annals of the New York Academy of Sciences*, 316(1):623–637, 1979.
- [Dor47] A.A. Dorodnitsyn. Asymptotic solutions of van der Pol's equation. *Prikl. Matem. i Mekhan.*, 11(3):313–328, 1947.
- [DP96] J.D. Deuschel and A. Pisztora. Surface order large deviations for high-density percolation. *Probab. Theory Rel. Fields*, 104(4):467–482, 1996.
- [DPK07a] F. Dumortier, N. Popovic, and T.J. Kaper. The asymptotic critical wave speed in a family of scalar reaction-diffusion equations. *J. Math. Anal. Appl.*, 326(2):1007–1023, 2007.
- [DPK07b] F. Dumortier, N. Popovic, and T.J. Kaper. The critical wave speed for the Fisher–Kolmogorov–Petrovskii–Piscesonov equation with cut-off. *Nonlinearity*, 20(4):855–877, 2007.
- [DPK10] F. Dumortier, N. Popovic, and T.J. Kaper. A geometric approach to bistable front propagation in scalar reaction–diffusion equations with cut-off. *Physica D*, 239(20):1984–1999, 2010.
- [dPMP05] M. del Pino, M. Musso, and A. Pistoia. Supercritical boundary bubbling in a semilinear Neumann problem. *Ann. Inst. H. Poincaré Anal. Non Linéaire*, 22(1):45–82, 2005.
- [DPS73] F.W. Dorr, S.V. Parter, and L.F. Shampine. Applications of the maximum principle to singular perturbation problems. *SIAM Rev.*, 15(1):43–88, 1973.
- [DPS07] J. Duan, C. Pötzsche, and S. Siegmund. Slow integral manifolds for Lagrangian fluid dynamics in unsteady geophysical flows. *Physica D*, 233(1):73–82, 2007.
- [DQKP94] N. Derbel, A. Quali, M.B.A. Kamoun, and M. Poloujadoff. Two step three time scale reduction of doubly fed machine models. *IEEE Trans. Energy Conv.*, 9(1):77–84, 1994.
- [DR96a] P. Duchene and P. Rouchon. Kinetic scheme reduction via geometric singular perturbation techniques. *Chem. Engineer. Sci.*, 51(20):4661–4672, 1996.
- [DR96b] F. Dumortier and R. Roussarie. *Canard Cycles and Center Manifolds*, volume 121 of *Memoirs Amer. Math. Soc.* AMS, 1996.
- [DR07] F. Dumortier and R. Roussarie. Bifurcation of relaxation oscillations in dimension two. *Discr. Cont. Dyn. Syst.*, 19(4):631–674, 2007.
- [DR08] F. Dercle and S. Rinaldi. *Analysis of Evolutionary Processes: The Adaptive Dynamics Approach and Its Applications*. Princeton University Press, 2008.
- [DR10] J.R. Dunmyre and J.E. Rubin. Optimal intrinsic dynamics for bursting in a three-cell network. *SIAM J. Appl. Dyn. Syst.*, 9(1):154–187, 2010.
- [Dri68] R.D. Driver. On Ryabov's asymptotic characterization of the solutions of quasi-linear differential equations with small delays. *SIAM Rev.*, 10(3):329–341, 1968.
- [Dri76] R.D. Driver. Linear differential systems with small delays. *J. Diff. Eq.*, 21:148–166, 1976.
- [DRL12] A. Destexhe and M. Rudolph-Lilith. *Neuronal Noise*. Springer, 2012.
- [DRR94] F. Dumortier, R. Roussarie, and C. Rousseau. Hilbert's 16th problem for quadratic vector fields. *J. Differential Equat.*, 110(1):86–133, 1994.
- [DRS97] F. Dumortier, R. Roussarie, and J. Sotomayor. Bifurcations of cuspidal loops. *Nonlinearity*, 10(6):1369–1408, 1997.
- [DRS07] E.N. Dancer, X. Ren, and S. Shusen. On multiple radial solutions of a singularly perturbed nonlinear elliptic system. *SIAM J. Math. Anal.*, 38(6):2005–2041, 2007.
- [DRSE04] J. Drover, J. Rubin, J. Su, and B. Ermentrout. Analysis of a canard mechanism by which excitatory synaptic coupling can synchronize neurons at low firing frequencies. *SIAM J. Appl. Math.*, 65(1):69–92, 2004.
- [DRW89] M.M. Dodson, B.P. Rynne, and J.A.G. Wickers. Averaging in multifrequency systems. *Nonlinearity*, 2(1):137, 1989.
- [DS49] B.R. Dudley and H.W. Swift. Frictional relaxation oscillations. *Philosophical Magazine*, 40:849–861, 1949.
- [DS88] A.L. Dontchev and J.I. Slavov. Lipschitz properties of the attainable set of singularly perturbed linear systems. *Syst. Contr. Lett.*, 11(5):385–391, 1988.
- [DS89a] J.D. Deuschel and D.W. Stroock. *Large Deviations*. Academic Press, 1989.

- [DS89b] I. Dvorak and J. Siska. Analysis of metabolic systems with complex slow and fast dynamics. *Bull. Math. Biol.*, 51(2):255–274, 1989.
- [DS90] A.L. Dontchev and J.I. Slavov. Upper semicontinuity of solutions of singularly perturbed differential inclusions. In *System Modelling and Optimization*, volume 143 of *Lect. Notes Contr. Inf. Sci.*, pages 273–280. Springer, 1990.
- [DS95a] T. Donchev and I. Slavov. Singularly perturbed functional-differential inclusions. *Set-Valued Analysis*, 3:113–128, 1995.
- [DS95b] F. Dumortier and B. Smits. Transition time analysis in singularly perturbed boundary value problems. *Trans. Amer. Math. Soc.*, 347(10):4129–4145, 1995.
- [dS99a] P.R. da Silva. Canard cycles and homoclinic bifurcation in a 3-parameter family of vector fields on the plane. *Publ. Mat.*, 43:163–189, 1999.
- [DS99b] M.J. Davis and R.T. Skodje. Geometric investigation of low-dimensional manifolds in systems approaching equilibrium. *J. Chem. Phys.*, 111:859–874, 1999.
- [DS99c] T. Donchev and I. Slavov. Averaging method for one-sided Lipschitz differential inclusions with generalized solutions. *SIAM J. Contr. Optim.*, 37(5):1600–1613, 1999.
- [DS06] E.N. Dancer and S. Shusen. Interior peak solutions for an elliptic system of FitzHugh–Nagumo type. *J. Differential Equat.*, 229(2):654–679, 2006.
- [DS09a] I. Dag and A. Sahin. Numerical solution of singularly perturbed problems. *Int. J. Nonlin. Sci.*, 8(1):32–39, 2009.
- [DS09b] F. Dkhil and A. Stevens. Traveling wave speeds in rapidly oscillating media. *Discr. Cont. Dyn. Syst. A*, 26(1):89–108, 2009.
- [DSS08] R. Denk, J. Saal, and J. Seiler. Inhomogeneous symbols, the Newton polygon, and maximal L^p -regularity. *Russ. J. Math. Phys.*, 15(2):171–191, 2008.
- [DSSS03] A. Doelman, B. Sandstede, A. Scheel, and G. Schneider. Propagation of hexagonal patterns near onset. *Euro. J. Appl. Math.*, 14(1):85–110, 2003.
- [DSSS09] A. Doelman, B. Sandstede, A. Scheel, and G. Schneider. The dynamics of modulated wavetrains. *Memoirs of the AMS*, 199(934):1–105, 2009.
- [DSvN⁺08] V. Dakos, M. Scheffer, E.H. van Nes, V. Brovkin, V. Petoukhov, and H. Held. Slowing down as an early warning signal for abrupt climate change. *Proc. Natl. Acad. Sci. USA*, 105(38):14308–14312, 2008.
- [DSW12] P. Dupuis, K. Spiliopoulos, and H. Wang. Importance sampling for multiscale diffusions. *Multiscale Model. Simul.*, 10(1):1–27, 2012.
- [DTBL85] M.J. Dauphine-Tanguy, P. Borne, and M. Lebrun. Order reduction of multi-time scale systems using bond graphs, the reciprocal system and the singular perturbation method. *J. Frank. Inst.*, 319:157–171, 1985.
- [Dum77] F. Dumortier. Singularities of vector fields on the plane. *J. Differential Equat.*, 23(1):53–106, 1977.
- [Dum78] F. Dumortier. *Singularities of Vector Fields*. IMPA, Rio de Janeiro, Brazil, 1978.
- [Dum93] F. Dumortier. Techniques in the theory of local bifurcations: Blow-up, normal forms, nilpotent bifurcations, singular perturbations. In D. Schlesinger, editor, *Bifurcations and Periodic Orbits of Vector Fields*, pages 19–73. Kluwer, Dordrecht, The Netherlands, 1993.
- [Dum11] F. Dumortier. Slow divergence integral and balanced canard solutions. *Qual. Theory Dyn. Syst.*, 10(1):65–85, 2011.
- [Dum13] F. Dumortier. Canard explosion and position curves. In *Recent Trends in Dynamical Systems*, volume 35 of *Proceed. Math. Stat.*, pages 51–78. Springer, 2013.
- [Dur85] J. Durbin. The first-passage density of a continuous Gaussian process to a general boundary. *J. Appl. Prob.*, 22:99–122, 1985.
- [Dur92] J. Durbin. The first-passage density of the Brownian motion process to a curved boundary. *J. Appl. Prob.*, 29:291–304, 1992. with an appendix by D. Williams.
- [Dur94] R. Durrett. *The Essentials of Probability*. Duxbury, 1994.
- [Dur10a] R. Durrett. *Probability: Theory and Examples - 4th edition*. CUP, 2010.
- [Dur10b] R. Durrett. *Random Graph Dynamics*. CUP, 2010.
- [DV75a] M.D. Donsker and S.R.S. Varadhan. Asymptotic evaluation of certain Markov process expectations for large time, I. *Comm. Pure Appl. Math.*, 28(1):1–47, 1975.
- [DV75b] M.D. Donsker and S.R.S. Varadhan. Asymptotic evaluation of certain Markov process expectations for large time, II. *Comm. Pure Appl. Math.*, 28(2):279–301, 1975.
- [DV76] M.D. Donsker and S.R.S. Varadhan. Asymptotic evaluation of certain Markov process expectations for large time, III. *Comm. Pure Appl. Math.*, 29(4):389–461, 1976.
- [DV83a] M.D. Donsker and S.R.S. Varadhan. Asymptotic evaluation of certain Markov process expectations for large time, IV. *Comm. Pure Appl. Math.*, 36(2):183–212, 1983.
- [DV83b] A.L. Dontchev and V. Veliov. Singular perturbation in Mayer’s problem for linear systems. *SIAM J. Control Optim.*, 21(4):566–581, 1983.
- [DV84] K. Dekker and J.G. Verwer. *Stability of Runge–Kutta Methods for Stiff Nonlinear Differential Equations*. North-Holland, 1984.
- [DV89] M.D. Donsker and S.R.S. Varadhan. Large deviations from a hydrodynamic scaling limit. *Comm. Pure Appl. Math.*, 42(3):243–270, 1989.
- [DvdP02] A. Doelman and H. van der Ploeg. Homoclinic stripe patterns. *SIAM J. Appl. Dyn. Syst.*, 1(1):65–104, 2002.
- [DVE06] L. DeVille and E. Vanden-Eijnden. A nontrivial scaling limit for multiscale Markov chains. *J. Stat. Phys.*, 126(1):75–94, 2006.
- [DVEM05] L. DeVille, E. Vanden-Eijnden, and C.B. Muratov. Two distinct mechanisms of coherence in randomly perturbed dynamical systems. *Phys. Rev. E*, 72(3):031105, 2005.
- [DvHK09] A. Doelman, P. van Heijster, and T.J. Kaper. Pulse dynamics in a three-component system: existence analysis. *J. Dyn. Diff. Eq.*, 21:73–115, 2009.
- [DvHK13] A. Doelman, P. van Heijster, and T.J. Kaper. An explicit theory for pulses in two component, singularly perturbed, reaction–diffusion equations. *J. Dyn. Diff. Eq.*, pages 1–42, 2013. accepted, to appear.

- [DvND⁺09] V. Dakos, E.H. van Nes, R. Donangelo, H. Fort, and M. Scheffer. Spatial correlation as leading indicator of catastrophic shifts. *Theor. Ecol.*, 3(3):163–174, 2009.
- [DW10] H.-H. Dai and F.-F. Wang. Asymptotic bifurcation solutions for compressions of a clamped nonlinearly elastic rectangle: transition region and barrelling to a corner-like profile. *SIAM J. Appl. Math.*, 70(7):2673–2692, 2010.
- [dW11] A.S. de Wijn. Internal degrees of freedom and transport of benzene on graphite. *Phys. Rev. E*, 84:011610, 2011.
- [DWC⁺98] M.J. Donovan, P. Wenner, N. Chub, J. Tabak, and J. Rinzel. Mechanisms of spontaneous activity in the developing spinal cord and their relevance to locomotion. *Ann. New York Acad. Sci.*, 860(1):130–141, 1998.
- [dWF09] A.S. de Wijn and A. Fasolino. Relating chaos to deterministic diffusion of a molecule adsorbed on a surface. *J. Phys.: Condens. Matter*, 21:264002, 2009.
- [dWK07] A.S. de Wijn and H. Kantz. Vertical chaos and horizontal diffusion in the bouncing-ball billiard. *Phys. Rev. E*, 75:046214, 2007.
- [Dys62] F.J. Dyson. A Brownian-motion model for the eigenvalues of a random matrix. *J. Math. Physics*, 3(6):1191, 1962.
- [DZ98] A. Dembo and O. Zeitouni. *Large Deviations Techniques and Applications*, volume 38 of *Applications of Mathematics*. Springer-Verlag, 1998.
- [E91] W. E. A class of homogenization problems in the calculus of variations. *Comm. Pure Appl. Math.*, 44(7):733–759, 1991.
- [E92] W. E. Homogenization of linear and nonlinear transport equations. *Comm. Pure Appl. Math.*, 45(3):301–326, 1992.
- [E03] W. E. Analysis of the heterogeneous multiscale method for ordinary differential equations. *Comm. Math. Sci.*, 1(3):423–426, 2003.
- [E06] W. E. Homogenization of scalar conservation laws with oscillatory forcing terms. *SIAM J. Appl. Math.*, 52(4):959–972, 2006.
- [E11] W. E. *Principles of Multiscale Modeling*. CUP, 2011.
- [EA86] H. Eyad and L. André. On the stability of multiple time-scale systems. *Int. J. Contr.*, 44:211–218, 1986.
- [EA91] J. Elezgaray and A. Arneodo. Modeling reaction-diffusion pattern formation in the Couette flow reactor. *J. Chem. Phys.*, 95:323–350, 1991.
- [ECB97] T. Erneux, T.W. Carr, and V. Booth. Near-threshold bursting is delayed by a slow passage near a limit point. *SIAM J. Appl. Math.*, 57(5):1406–1420, 1997.
- [Eck72] W. Eckhaus. Boundary layers in linear elliptic singular perturbation problem. *SIAM Rev.*, 14(2):225–270, 1972.
- [Eck73] W. Eckhaus. *Matched Asymptotic Expansions and Singular Perturbations*. North-Holland, 1973.
- [Eck77] W. Eckhaus. Matching principles and composite expansions. In *Singular Perturbations and Boundary Layer Theory*, volume 594 of *Lect. Notes Math.*, pages 146–177. Springer, 1977.
- [Eck79] W. Eckhaus. *Asymptotic Analysis of Singular Perturbations*. Elsevier, 1979.
- [Eck83] W. Eckhaus. Relaxation oscillations including a standard chase on French ducks. *Lecture Notes in Mathematics*, 985:449–494, 1983.
- [Eck92] W. Eckhaus. Singular perturbations of homoclinic orbits in \mathbb{R}^4 . *SIAM J. Math. Anal.*, 23(5):1269–1290, 1992.
- [Eck94] W. Eckhaus. Fundamental concepts of matching. *SIAM Rev.*, 36(3):431–439, 1994.
- [EdJ66] W. Eckhaus and E.M. de Jager. Asymptotic solutions of singular perturbation problems for linear differential equations of elliptic type. *Arch. Rat. Mech. Anal.*, 23(1):26–86, 1966.
- [EdJ82] W. Eckhaus and E.M. de Jager. *Theory and Applications of Singular Perturbations*. Springer, 1982.
- [Edw00] D.A. Edwards. An alternative example of the method of multiple scales. *SIAM Rev.*, 42(2):317–332, 2000.
- [EE86] M. Eiswirth and G. Ertl. Kinetic oscillations in the catalytic CO oxidation on a Pt(110) surface. *Surf. Sci.*, 177(1):90–100, 1986.
- [EE93] B. Engquist and W. E. Large time behavior and homogenization of solutions of two-dimensional conservation laws. *Comm. Pure Appl. Math.*, 46(1):1–26, 1993.
- [EE03a] W. E and B. Engquist. The heterogeneous multiscale methods. *Comm. Math. Sci.*, 1(1):87–132, 2003.
- [EE03b] W. E and B. Engquist. Multiscale modeling and computation. *Notices of the AMS*, 50(9):1063–1070, 2003.
- [EE05] W. E and B. Engquist. The heterogeneous multi-scale method for homogenization problems. In *Multiscale Methods in Science and Engineering*, volume 44 of *Lecture Notes Comput. Sci. Eng.*, pages 89–110. Springer, 2005.
- [EEH03] W. E, B. Engquist, and Z. Huang. Heterogeneous multiscale method: a general methodology for multiscale modeling. *Phys. Rev. B*, 67(9):092101, 2003.
- [EEL⁺07] W. E, B. Engquist, X. Li, W. Ren, and E. Vanden-Eijnden. Heterogeneous multiscale methods: a review. *Comm. Comp. Phys.*, 2(3):367–450, 2007.
- [EF77] J.W. Evans and J.A. Feroe. Local stability of the nerve impulse. *Math. Biosci.*, 37(1):23–50, 1977.
- [EF90] A. Eizenberg and M. Freidlin. On the Dirichlet problem for a class of second order PDE systems with small parameter. *Stoch. Stoch. Rep.*, 33(3):111–148, 1990.
- [EF93] A. Eizenberg and M. Freidlin. Large deviations for Markov processes corresponding to PDE systems. *Ann. Probab.*, 21(2): 1015–1044, 1993.
- [EFF82] J.W. Evans, N. Fenichel, and J.A. Feroe. Double impulse solutions in nerve axon equations. *SIAM J. Appl. Math.*, 42(2): 219–234, 1982.
- [EFHI09] B. Engquist, A. Fokas, E. Hairer, and A. Iserles. *Highly Oscillatory Problems*. CUP, 2009.
- [EFK00] S.-I. Ei, K. Fujii, and T. Kunihiro. Renormalization-group method for reduction of evolution equations; invariant manifolds and envelopes. *Ann. Phys.*, 280(2):236–298, 2000.
- [EGF07] M. Enculescu, A. Ghoshalami, and M. Falcke. Dynamic regimes and bifurcations in a model of actin-based motility. *Phys. Rev. E*, 78(3):031915, 2007.

- [EGPS99] T. Erneux, P. Gavrielides, P. Peterson, and M.P. Sharma. Dynamics of passively Q-switched microchip lasers. *IEEE J. Quant. Electr.*, 35:1247–1256, 1999.
- [EH09] Y.R. Efendiev and T.Y. Hou. *Multiscale Finite Element Methods. Theory and Applications*. Springer, 2009.
- [Ehl68] B.L. Ehle. High order A-stable methods for the numerical solution of systems of DE's. *BIT Numer. Math.*, 8(4):276–278, 1968.
- [Ehl73] B.L. Ehle. A-stable methods and Padé approximations to the exponential. *SIAM J. Math. Anal.*, 4(4):671–680, 1973.
- [EHL75] W.H. Enright, T.E. Hull, and B. Lindberg. Comparing numerical methods for stiff systems of ODEs. *BIT Numer. Math.*, 15(1):10–48, 1975.
- [Ein05] A. Einstein. Über die von der molekularkinetischen Theorie der Wärme geforderte Bewegung von in ruhenden Flüssigkeiten suspendierten Teilchen. *Ann. Phys.*, pages 549–560, 1905.
- [EJ10] E. Endres and H.K. Jenssen. Singularly perturbed ODEs and profiles for stationary symmetric Euler and Navier–Stokes shocks. *Discr. Cont. Dyn. Sys.*, 27(1):133–169, 2010.
- [EJL03] K. Eriksson, C. Johnson, and A. Logg. Explicit time-stepping for stiff ODEs. *SIAM J. Sci. Comput.*, 25(4):1142–1157, 2003.
- [EJM08] E. Endres, H.K. Jenssen, and M. Milliams. Symmetric Euler and Navier–Stokes shocks in stationary barotropic flow on a bounded domain. *J. Differential Equat.*, 245(10):3025–3067, 2008.
- [EJM10] E. Endres, H.K. Jenssen, and M. Milliams. Singularly perturbed ODEs and profiles for stationary symmetric Euler and Navier–Stokes shocks. *Dynamical Systems*, 27(1):133–169, 2010.
- [EK80] Y. Estrin and L. Kubin. Criterion for thermomechanical instability of low temperature plastic deformation. *Scripta Metallurgica*, 14:1359–1364, 1980.
- [EK86a] G.B. Ermentrout and N. Kopell. Parabolic bursting in an excitable system coupled with a slow oscillation. *SIAM J. Appl. Math.*, 46(2):233–253, 1986.
- [EK86b] G.B. Ermentrout and N. Kopell. Symmetry and phaselocking in chains of weakly coupled oscillators. *Comm. Pure Appl. Math.*, 39(5):623–660, 1986.
- [EK90] R. Estrada and R.P. Kanwal. A distributional theory for asymptotic expansions. *Proc. R. Soc. London A*, 428(1875):399–430, 1990.
- [EK91] G.B. Ermentrout and N. Kopell. Multiple pulse interactions and averaging in systems of coupled neural oscillators. *J. Math. Biol.*, 29:195–217, 1991.
- [EK95] R. Estrada and R.P. Kanwal. A distributional approach to the boundary layer theory. *J. Math. Anal. Appl.*, 192(3):796–812, 1995.
- [EK02] R. Estrada and R.P. Kanwal. *Asymptotics Analysis: A Distributional Approach*. Birkhäuser, 2002.
- [EKA06] R. Erban, I.G. Kevrekidis, D. Adalsteinsson, and T.C. Elston. Gene regulatory networks: a coarse-grained, equation-free approach to multiscale computation. *J. Chem. Phys.*, 124(8): 084106, 2006.
- [EKE90] M. Eiswirth, K. Krischer, and G. Ertl. Nonlinear dynamics in the CO-oxidation on Pt single crystal surfaces. *Appl. Phys. A*, 51:79–90, 1990.
- [EKL07] H. Erzgräber, B. Krauskopf, and D. Lenstra. Bifurcation analysis of a semiconductor laser with filtered optical feedback. *SIAM J. Appl. Dyn. Syst.*, 6(1):1–28, 2007.
- [EKO07] J.P. England, B. Krauskopf, and H.M. Osinga. Computing two-dimensional global invariant manifolds in slow–fast systems. *Int. J. Bif. Chaos*, 17(3):805–822, 2007.
- [EKR87] J.P. Eckmann, S.O. Kamphorst, and D. Ruelle. Recurrence plots of dynamical systems. *Europhys. Lett.*, 4(9):973–977, 1987.
- [EL97] C. Engstler and C. Lubich. Multirate extrapolation methods for differential equations with different time scales. *Computing*, 58(2):173–185, 1997.
- [EL07] B. Eisenberg and W. Liu. Poisson–Nernst–Planck systems for ion channels with permanent charges. *SIAM J. Math. Anal.*, 38(6):1932–1966, 2007.
- [Eld12] J. Elderding. Persistence of noncompact normally hyperbolic invariant manifolds in bounded geometry. *Comptes Rendus Mathématique*, 350(11):617–620, 2012.
- [Eld13] J. Elderding. *Normally Hyperbolic Invariant Manifolds: The Noncompact Case*. Atlantis Press, 2013.
- [ELRL99] A. Erisir, D. Lau, B. Rudy, and C.S. Leonard. Function of specific K^+ channels in sustained high-frequency firing of fast-spiking interneurons. *J. Neurophysiol.*, 82:2476–2489, 1999.
- [ELVE04] W. E, X. Li, and E. Vanden-Eijnden. Some recent progress in multiscale modeling. In *Multiscale Modelling and Simulation*, pages 3–21. Springer, 2004.
- [ELVE05a] W. E, D. Liu, and E. Vanden-Eijnden. Analysis of multiscale methods for stochastic differential equations. *Comm. Pure App. Math.*, 58:1544–1585, 2005.
- [ELVE05b] W. E, D. Liu, and E. Vanden-Eijnden. Nested stochastic simulation algorithm for chemical kinetic systems with disparate rates. *J. Chem. Phys.*, 123:194107, 2005.
- [ELVE07] W. E, D. Liu, and E. Vanden-Eijnden. Nested stochastic simulation algorithm for chemical kinetic systems with multiple time scales. *J. Comp. Phys.*, 221(1):158–180, 2007.
- [ELY06] W. E, J. Lu, and J.Z. Yang. Uniform accuracy of the quasicontinuum method. *Phys. Rev. B*, 74(21):214115, 2006.
- [EM83] T. Erneux and P. Mandel. Temporal aspects of absorptive optical bistability. *Phys. Rev. A*, 28(2): 896–909, 1983.
- [EM86] T. Erneux and P. Mandel. Imperfect bifurcation with a slowly-varying control parameter. *SIAM J. Appl. Math.*, 46(1):1–15, 1986.
- [EM91] T. Erneux and P. Mandel. Slow passage through the laser first threshold: influence of the initial conditions. *Optics Commun.*, 85(1):43–46, 1991.
- [EM92] S.-I. EI and M. Mimura. Relaxation oscillations in combustion models of thermal self-ignition. *J. Dyn. Diff. Eq.*, 4(1):191–229, 1992.
- [EM93] G.B. Ermentrout and J.B. McLeod. Existence and uniqueness of travelling waves for a neural network. *Proc. R. Soc. Edinburgh A*, 123(3):461–478, 1993.
- [EM07] W. E and P. Ming. Cauchy–Born rule and the stability of crystalline solids: static problems. *Arch. Rat. Mech. Anal.*, 183(2):241–297, 2007.
- [EM08] I. Erchova and D.J. McGonigle. Rhythms of the brain: an examination of mixed mode oscillation approaches to the analysis of neurophysiological data. *Chaos*, 18:015115, 2008.

- [EMZ05] W. E, P. Ming and P. Zhang. Analysis of the heterogeneous multiscale method for elliptic homogenization problems. *J. Amer. Math. Soc.*, 18(1):121–156, 2005.
- [EN93] T. Erneux and G. Nicolis. Propagating waves in discrete bistable reaction-diffusion systems. *Physica D*, 67(1):237–244, 1993.
- [EN00] K.-J. Engel and R. Nagel. *Semigroups for Linear Evolution Equations*. Springer, 2000.
- [Enr74] W.H. Enright. Second derivative multistep methods for stiff ordinary differential equations. *SIAM J. Numer. Anal.*, 11(2):321–331, 1974.
- [EP02] C.H. Edwards and D.E. Penney. *Calculus*. Prentice Hall, 2002.
- [EPG00] T. Erneux, P. Peterson, and A. Gavrielides. The pulse shape of a passively Q-switched microchip laser. *Eur. Phys. J. D*, 10(3):423–431, 2000.
- [ER03] A. El-Rabih. Canards solutions of difference equations with small step size. *J. Difference Equ. Appl.*, 9(10):911–931, 2003.
- [Erd56] A. Erdelyi. *Asymptotic Expansions*. Dover, 1956.
- [ERHG91] T. Erneux, E.L. Reiss, L.J. Holden, and M. Georgiou. Slow passage through bifurcations and limit points. Asymptotic theory and applications. In E. Benoît, editor, *Dynamic Bifurcations*, volume 1493 of *Lecture Notes in Mathematics*, pages 14–28. Springer, 1991.
- [Erm94] G.B. Ermentrout. Reduction of conductance-based models with slow synapses to neural nets. *Neural Comput.*, 6(4):679–695, 1994.
- [Erm96] G.B. Ermentrout. Type I membranes, phase resetting curves, and synchrony. *Neural Comput.*, 8(5):979–1001, 1996.
- [Erm98] G.B. Ermentrout. Linearization of FI curves by adaptation. *Neural Comput.*, 10(7):1721–1729, 1998.
- [Erm88] T. Erneux. Q-switching bifurcation in a laser with a saturable absorber. *J. Opt. Soc. Amer. B Opt. Phys.*, 5:1063–1069, 1988.
- [ERVE02] W. E., W. Ren, and E. Vanden-Eijnden. String method for the study of rare events. *Phys. Rev. B*, 66(5):052301, 2002.
- [ERVE05] W. E., W. Ren, and E. Vanden-Eijnden. Finite temperature string method for the study of rare events. *J. Phys. Chem. B*, 109(14):6688–6693, 2005.
- [ERVE09] W. E., W. Ren, and E. Vanden-Eijnden. A general strategy for designing seamless multiscale methods. *J. Comput. Phys.*, 228(15):5437–5433, 2009.
- [ES96] I.R. Epstein and K. Showalter. Nonlinear chemical dynamics: oscillations, patterns, and chaos. *J. Phys. Chem.*, 100:13132–13147, 1996.
- [ESD90] J.A. Ellison, A.W. Sáenz, and H.S. Dumas. Improved N -th order averaging theory for periodic systems. *J. Differential Equations*, 84(2):383–403, 1990.
- [ESY11] L. Erdős, B. Schlein, and H.T. Yau. Universality of random matrices and local relaxation flow. *Invent. Math.*, 185(1):75–119, 2011.
- [ET05] B. Enquist and Y.-H. Tsai. Heterogeneous multiscale methods for stiff ordinary differential equations. *Math. Comput.*, 74(252):1707–1742, 2005.
- [ET10] G.B. Ermentrout and D.H. Terman. *Mathematical Foundations of Neuroscience*. Springer, 2010.
- [EV05] C. Elmer and E.S. Van Vleck. Spatially discrete FitzHugh-Nagumo equations. *SIAM J. Appl. Math.*, 65(4):1153–1174, 2005.
- [Eva72] J. Evans. Nerve axon equations III: stability of nerve impulses. *Indiana U. Math. J.*, 22:577–594, 1972.
- [Eva02] L.C. Evans. *Partial Differential Equations*. AMS, 2002.
- [EVE04] W. E and E. Vanden-Eijnden. Metastability, conformation dynamics, and transition pathways in complex systems. In *Multiscale Modelling and Simulation*, pages 35–68. Springer, 2004.
- [EVE06] W. E and E. Vanden-Eijnden. Towards a theory of transition paths. *J. Stat. Phys.*, 123(3):503–523, 2006.
- [EVE10] W. E and E. Vanden-Eijnden. Transition-path theory and path-finding algorithms for the study of rare events. *Phys. Chem.*, 61:391–420, 2010.
- [EVM07] T. Erneux, E.A. Viktorov, and P. Mandel. Time scales and relaxation dynamics in quantum-dot lasers. *Phys. Rev. A*, 76(2):023819, 2007.
- [EvS00] U. Ebert and W. van Saarloos. Front propagation into unstable states: universal algebraic convergence towards uniformly translating pulled fronts. *Physica D*, 146:1–99, 2000.
- [EW05] G. Everest and T. Ward. *An Introduction to Number Theory*. Springer, 2005.
- [EW09] B. Ermentrout and M. Wechselberger. Canards, clusters and synchronization in a weakly coupled interneuron model. *SIAM J. Appl. Dyn. Syst.*, 8(1):253–278, 2009.
- [EY91] W. E and H. Yang. Numerical study of oscillatory solutions of the gas-dynamic equations. *Stud. Appl. Math.*, 85:29–52, 1991.
- [Eyr35] H. Eyring. The activated complex in chemical reactions. *J. Chem. Phys.*, 3:107–115, 1935.
- [FAB84] V.R. Fed'kina, F.I. Ataullakhanov, and T.V. Bronnikova. Computer simulations of sustained oscillations in the peroxidase-oxidase reaction. *Biophysical Chemistry*, 19:259–264, 1984.
- [FAB88] V.R. Fed'kina, F.I. Ataullakhanov, and T.V. Bronnikova. Stimulated regimens in the peroxidase-oxidase reaction. *Theor. Exp. Chem.*, 24(2):172–178, 1988.
- [Fat28] P. Fatou. Sur le mouvement d'un système soumis à des forces à courte période. *Bull. Soc. Math.*, 56:98–139, 1928.
- [FBT⁺06] F. Fröhlich, M. Bazhenov, I. Timofeev, M. Steriade, and T.J. Sejnowski. Slow state transitions of sustained neural oscillations by activity-dependent modulation of intrinsic excitability. *J. Neurosci.*, 26(23):6153–6162, 2006.
- [FC94] H. Fan and T.R. Chay. Generation of periodic and chaotic bursting in an excitable cell model. *Biol. Cybernet.*, 71(5):417–431, 1994.
- [FD11] H. Fu and J. Duan. An averaging principle for two time-scale stochastic partial differential equations. *Stoch. Dyn.*, 11:353–367, 2011.
- [FDS12] A. Franci, G. Drion, and R. Sepulchre. An organizing center in a planar model of neuronal excitability. *SIAM J. Appl. Dyn. Syst.*, 11(4):1698–1722, 2012.
- [FDS13] A. Franci, G. Drion, and R. Sepulchre. Modeling neuronal bursting: singularity theory meets neuropsychology. *arXiv:1305.7364*, pages 1–28, 2013.
- [Fe85] R.J. Field and M. Burger (eds.). *Oscillations and traveling waves in chemical systems*. Wiley, 1985.

- [Feč91] M. Fečkan. Discretization in the method of averaging. *Proc. Amer. Math. Soc.*, 113(4):1105–1113, 1991.
- [Feč00] M. Fečkan. Bifurcation of multi-bump homoclinics in systems with normal and slow variables. *Electron. J. Differential Equations*, 41:1–17, 2000.
- [Féj01] J. Féjoz. Averaging the planar three-body problem in the neighborhood of double inner collisions. *J. Differential Equat.*, 175(1):175–182, 2001.
- [Fen71] N. Fenichel. Persistence and smoothness of invariant manifolds for flows. *Indiana Univ. Math. J.*, 21:193–225, 1971.
- [Fen74] N. Fenichel. Asymptotic stability with rate conditions. *Indiana Univ. Math. J.*, 23:1109–1137, 1974.
- [Fen77] N. Fenichel. Asymptotic stability with rate conditions II. *Indiana Univ. Math. J.*, 26:81–93, 1977.
- [Fen79] N. Fenichel. Geometric singular perturbation theory for ordinary differential equations. *J. Differential Equat.*, 31:53–98, 1979.
- [Fen83a] N. Fenichel. Oscillatory bifurcations in singular perturbation theory, I. Slow oscillations. *SIAM J. Math. Anal.*, 14(5): 861–867, 1983.
- [Fen83b] N. Fenichel. Oscillatory bifurcations in singular perturbation theory, II. Fast oscillations. *SIAM J. Math. Anal.*, 14(5):868–874, 1983.
- [Fen85] N. Fenichel. Global uniqueness in geometric singular perturbation theory. *SIAM J. Math. Anal.*, 16(1):1–6, 1985.
- [Fer78] J.A. Feroe. Temporal stability of solitary impulse solutions of a nerve equation. *Biophys. J.*, 21(2):103–110, 1978.
- [Fer81] J.A. Feroe. Traveling waves of infinitely many pulses in nerve equations. *Math. Biosci.*, 55(3):189–203, 1981.
- [Fer82] J.A. Feroe. Existence and stability of multiple impulse solutions of a nerve equation. *SIAM J. Appl. Math.*, 42(2):235–246, 1982.
- [FFH97] A.J. Fossard, J. Foisneau, and T.H. Huynh. Approximate closed-loop optimization of nonlinear systems by singular perturbation technique. In *Nonlinear Systems*, pages 189–246. Springer, 1997.
- [FG76] M.I. Freedman and B. Granhoff. Formal asymptotic solution of a singularly perturbed nonlinear optimal control problem. *J. Optim. Theor. Appl.*, 19(2):301–325, 1976.
- [FG11a] J.G. Freire and J.A.C. Gallegas. Stern-Brocot trees in cascades of mixed-mode oscillations and canards in the extended Bonhoeffer-van der Pol and the FitzHugh-Nagumo models of excitable systems. *Phys. Lett. A*, 375:1097–1103, 2011.
- [FG11b] J.G. Freire and J.A.C. Gallegas. Stern-Brocot trees in the periodicity of mixed-mode oscillations. *Phys. Chem. Chem. Phys.*, 13:12191–12198, 2011.
- [FG13] J.E. Frank and G.A. Gottwald. Stochastic homogenization for an energy conserving multi-scale toy model of the atmosphere. *Physica D*, 254:46–56, 2013.
- [FGH01] J.A. Filar, V. Gaitsgory, and A.B. Haurie. Control of singularly perturbed hybrid stochastic systems. *IEEE Trans. Aut. Contr.*, 46(2):179–190, 2001.
- [FH89] G. Fusco and J.K. Hale. Slow-motion manifolds, dormant instability, and singular perturbations. *J. Dyn. Diff. Eq.*, 1:75–94, 1989.
- [FH03] A.C. Fowler and P.D. Howell. Intermittency in the transition to turbulence. *SIAM J. Appl. Math.*, 63(4):1184–1207, 2003.
- [FH06] D. Flockerzi and W. Heineken. Comment on: Chaos 9, 108–123 (1999). Identification of low order manifolds: validating the algorithm of Maas and Pope. *Chaos*, 16(4):048101, 2006.
- [FHM⁺04] P.A. Farrell, A.F. Hegarty, J.J.H. Miller, E. O’Riordan, and G.I. Shishkin. Singularly perturbed convection-diffusion problems with boundary and weak interior layers. *J. Comput. Appl. Math.*, 166:133–151, 2004.
- [FHR09] A. Fasano, M.A. Herrero, and M.R. Rodrigo. Slow and fast invasion waves in a model of acid-mediated tumour growth. *Math. Biosci.*, 220:45–56, 2009.
- [FHS96] P.A. Farrell, P.W. Hemker, and G.I. Shishkin. Discrete approximations for singularly perturbed boundary value problems with parabolic layers. I. *J. Comput. Math.*, 14:71–97, 1996.
- [Fif73] P.C. Fife. Semilinear elliptic boundary value problems with small parameters. *Arch. Rational Mech. Anal.*, 52(3):205–232, 1973.
- [Fif74] P.C. Fife. Transition layers in singular perturbation problems. *J. Differential Equat.*, 15:77–105, 1974.
- [Fif76] P.C. Fife. Boundary and interior transition layer phenomenon for pairs of second-order differential equations. *J. Math. Anal. Appl.*, 54:497–521, 1976.
- [Fif88] P.C. Fife. *Dynamics of internal layers and diffusive interfaces*. SIAM, 1988.
- [Fil06] D.S. Filippychev. Applying the dual operator formalism to derive the zeroth-order boundary function of the plasma-sheath equation. *Comput. Math. Model.*, 17(4):341–353, 2006.
- [Fin83] W.F. Fiden. An asymptotic approximation for singular perturbations. *SIAM J. Appl. Math.*, 43(1):107–119, 1983.
- [Fis37] R.A. Fisher. The wave of advance of advantageous genes. *Ann. Eugenics*, 7:353–369, 1937.
- [Fis74] M.E. Fisher. The renormalization group in the theory of critical behavior. *Rev. Mod. Phys.*, 46(4): 597–616, 1974.
- [Fis06] M.E. Fisher. Hyperbolic sets that are not locally maximal. *Ergodic Theory Dyn. Syst.*, 26(5):1491–1510, 2006.
- [Fit55] R. FitzHugh. Mathematical models of threshold phenomena in the nerve membrane. *Bull. Math. Biophysics*, 17:257–269, 1955.
- [Fit60] R. FitzHugh. Thresholds and plateaus in the Hodgkin-Huxley nerve equations. *J. Gen. Physiol.*, 43:867–896, 1960.
- [Fit61] R. FitzHugh. Impulses and physiological states in models of nerve membranes. *Biophys. J.*, 1:445–466, 1961.
- [FJ82] J.E. Flaherty and R.E. O’Malley Jr. Singularly perturbed boundary value problems for nonlinear systems, including a challenging problem for a nonlinear beam. In *Theory and Applications of Singular Perturbations*, volume 942 of *Lecture Notes in Mathematics*, pages 170–191. Springer, 1982.
- [FJ91] T.F. Fairgrieve and A.D. Jepson. O.K. Floquet multipliers. *SIAM J. Numer. Anal.*, 28(5):1446–1462, 1991.

- [FJ92] W.H. Fleming and M.R. James. Asymptotic series and exit time probabilities. *Ann. Probab.*, 20(3):1369–1384, 1992.
- [FJK⁺88] C. Foias, M.S. Jolly, I.G. Kevrekidis, G.R. Sell, and E.S. Titi. On the computation of inertial manifolds. *Phys. Lett. A*, 131(7):433–436, 1988.
- [FK76] M.I. Freedman and J.L. Kaplan. Singular perturbations of two-point boundary value problems arising in optimal control. *SIAM J. Contr. Optim.*, 14(2):189–215, 1976.
- [FK82] S. Fraser and R. Kapral. Analysis of flow hysteresis by a one-dimensional map. *Phys. Rev. A*, 25(6):3223–3233, 1982.
- [FK85] C.L. Frenzen and J. Kevorkian. A review of the multiple scale and reductive perturbation methods for deriving uncoupled nonlinear evolution equations. *Wave Motion*, 7:25–42, 1985.
- [FK90] O.P. Filatov and M.M. Khapaev. Averaging of differential inclusions with “fast” and “slow” variables. *Math. Notes*, 47(6):596–601, 1990.
- [FK93] P. Frankel and T. Kiemel. Relative phase behavior of two slowly coupled oscillators. *SIAM J. Appl. Math.*, 53(5):1436–1446, 1993.
- [FK96] A.C. Fowler and G. Kember. The Lorenz-Krishnamurthy slow manifold. *J. Atmospheric Sci.*, 53(10):1433–1437, 1996.
- [FK02] D.B. Forger and R.E. Kronauer. Reconciling mathematical models of biological clocks by averaging on approximate manifolds. *SIAM J. Appl. Math.*, 62(4):1281–1296, 2002.
- [FK03a] K. Fujimoto and K. Kaneko. Bifurcation cascade as chaotic itinerancy with multiple time scales. *Chaos*, 13(3):1041–1056, 2003.
- [FK03b] K. Fujimoto and K. Kaneko. How fast elements can affect slow dynamics. *Physica D*, 180:1–16, 2003.
- [FL12] H. Fan and X.-B. Lin. Standing waves for phase transitions in a spherically symmetric nozzle. *SIAM J. Math. Anal.*, 44(1):405–436, 2012.
- [FLD13] H. Fu, X. Liu, and J. Duan. Slow manifolds for multi-time-scale stochastic evolutionary systems. *Comm. Math. Sci.*, 11(1):141–162, 2013.
- [Fle71] W.H. Fleming. Stochastic control for small noise intensities. *SIAM J. Control*, 9(3):473–517, 1971.
- [Fle77] W.H. Fleming. Exit probabilities and optimal stochastic control. *Appl. Math. Optim.*, 4(1):329–346, 1977.
- [Flo87] A. Floer. A refinement of the Conley index and an application to the stability of hyperbolic invariant sets. *Ergod. Th. Dynam. Syst.*, 7:93–103, 1987.
- [Flo90] A. Floer. A topological persistence theorem for normally hyperbolic manifolds via the Conley index. *Trans. Amer. Math. Soc.*, 321(2):647–657, 1990.
- [Flo91] G. Flores. Stability analysis for the slow traveling pulse of the FitzHugh–Nagumo system. *SIAM J. Math. Anal.*, 22(2):392–399, 1991.
- [FM77] P. Fife and J.B. McLeod. The approach of solutions nonlinear diffusion equations to travelling front solutions. *Arch. Rational Mech. Anal.*, 65:335–361, 1977.
- [FM80] J.E. Flaherty and W. Mathon. Collocation with polynomial and tension splines for singularly-perturbed boundary value problems. *SIAM J. Sci. Stat. Comput.*, 1(2):260–289, 1980.
- [FM92] I. Fonseca and S. Müller. Quasiconvex integrands and lower semicontinuity in L^1 . *Bull. Belg. Math. Soc.*, 23:1081–1098, 1992.
- [FM02] A.C. Fowler and M.C. Mackey. Relaxation oscillations in a class of delay differential equations. *SIAM J. Appl. Math.*, 63(1):299–323, 2002.
- [FM05] A. Fruchard and E. Matzinger. Matching and singularities of canard values. *Contemp. Math.*, 373:317–336, 2005.
- [FM13] M. Federson and J.G. Mesquita. Non-periodic averaging principles for measure functional differential equations and functional dynamic equations on time scales involving impulses. *J. Differential Equat.*, 255(10):3098–3126, 2013.
- [FMOS96] P.A. Farrell, J.J. Miller, E. O’Riordan, and G.I. Shishkin. A uniformly convergent finite difference scheme for a singularly perturbed semilinear equation. *SIAM J. Numer. Anal.*, 33(3):1135–1149, 1996.
- [FMVE05] C. Franzke, A.J. Majda, and E. Vanden-Eijnden. Low-order stochastic mode reduction for a realistic barotropic model climate. *J. Atmos. Sci.*, 62:1722–1745, 2005.
- [FN74] R.J. Field and R.M. Noyes. Oscillations in chemical systems IV. Limit cycle behavior in a model of a real chemical reaction. *J. Chem. Phys.*, 60:1877–1884, 1974.
- [FO77] J.E. Flaherty and R.E. O’Malley. The numerical solution of boundary value problems for stiff differential equations. *Math. Comput.*, 31:66–93, 1977.
- [FO84] J.E. Flaherty and R.E. O’Malley. Numerical methods for stiff systems of two-point boundary value problems. *SIAM J. Sci. Stat. Comput.*, 5(4):865–886, 1984.
- [Fol99] G. Folland. *Real Analysis - Modern Techniques and Their Applications*. Wiley, 1999.
- [For08] T. Forget. Asymptotic study of planar canard solutions. *Bull. Belg. Math. Soc.*, 15(5):809–824, 2008.
- [Fow05] A.C. Fowler. Asymptotic methods for delay equations. *J. Engrg. Math.*, 53(3):271–290, 2005.
- [Fox97] R.F. Fox. Stochastic versions of the Hodgkin–Huxley equations. *Biophys. J.*, 72:2068–2074, 1997.
- [FP05] J.-P. Francoise and C. Piaget. Hysteresis dynamics, bursting oscillations and evolution to chaotic regimes. *Acta Biotheoretica*, 53(4):381–392, 2005.
- [FPR08] B.D. Fulcher, A.J.K. Phillips, and P.A. Robinson. Modeling the impact of impulsive stimuli on sleep-wake dynamics. *Phys. Rev. E*, 78(5):051920, 2008.
- [FPV08] J.-P. Francoise, C. Piaget, and A. Vidal. Enhanced delay to bifurcation. *Bull. Belg. Math. Soc.*, 15(5):825–831, 2008.
- [FR98] O. De Feo and S. Rinaldi. Singular homoclinic bifurcations in tritrophic food chains. *Math. Biosci.*, 148:7–20, 1998.
- [FR11] S. Franz and H.-G. Roos. The capriciousness of numerical methods for singular perturbations. *SIAM Rev.*, 53(1):157–173, 2011.
- [Fra69] L.E. Fraenkel. On the method of matched asymptotic expansions. Parts I–III. *Proc. Cambridge Phil Soc.*, 65:209–284, 1969.
- [Fra82] B.A. Francis. Convergence in the boundary layer for singularly perturbed equations. *Automatica*, 18(1):57–62, 1982.

- [Fra88a] R.D. Franzosa. The continuation theory for Morse decompositions and connection matrices. *Trans. Amer. Math. Soc.*, 310(2):781–803, 1988.
- [Fra88b] S.J. Fraser. The steady state and equilibrium approximations: a geometrical picture. *J. Chem. Phys.*, 88:4732–4738, 1988.
- [Fra98] S.J. Fraser. Double perturbation series in the differential equations of enzyme kinetics. *J. Chem. Phys.*, 109(2):411–423, 1998.
- [Fra11] T. Frankel. *The Geometry of Physics*. CUP, 2011.
- [Fra12] J.-P. Francoise. Poincaré–Andronov–Hopf bifurcation and the local Hilbert’s 16th problem. *Qualit. Theor. Dyn. Syst.*, 11(1): 61–77, 2012.
- [Fre72] D.D. Freund. A note on Kaplun limits and double asymptotics. *Proc. Amer. Math. Soc.*, 35(2):464–470, 1972.
- [Fre73] M.I. Freidlin. The action functional for a class of stochastic processes. *Theory Probab. Appl.*, 17(3): 511–515, 1973.
- [Fre78] M.I. Freidlin. The averaging principle and theorems on large deviations. *Russ. Math. Surv.*, 33(5): 117–176, 1978.
- [Fre85] M.I. Freidlin. Limit theorems for large deviations and reaction–diffusion equations. *Ann. Probab.*, 13(3):639–675, 1985.
- [Fre86] M.I. Freidlin. Geometric optics approach to reaction–diffusion equations. *SIAM J. Appl. Math.*, 46(2):222–232, 1986.
- [Fre91] M.I. Freidlin. Coupled reaction–diffusion equations. *Ann. Probab.*, 19(1):29–57, 1991.
- [Fre96] M.I. Freidlin. *Markov Processes and Differential Equations: Asymptotic Problems*. Springer, 1996.
- [Fre00a] M.I. Freidlin. Diffusion processes on graphs: stochastic differential equations, large deviation principle. *Probab. Theory Rel. Fields*, 116(2):181–220, 2000.
- [Fre00b] M.I. Freidlin. Quasi-deterministic approximation, metastability and stochastic resonance. *Physica D*, 137(3):333–352, 2000.
- [Fre01] M.I. Freidlin. On stable oscillations and equilibria induced by small noise. *J. Stat. Phys.*, 103(1):283–300, 2001.
- [Fre04] M.I. Freidlin. Some remarks on the Smoluchowski–Kramers approximation. *J. Stat. Phys.*, 117(3): 617–634, 2004.
- [Fre06] E. Frenod. Application of the averaging method to the gyrokinetic plasma. *Asymp. Anal.*, 46:1–28, 2006.
- [Fri92] A. Friedman. *Partial Differential Equations of Parabolic Type*. Dover, 1992.
- [Fri01] E. Fridman. A descriptor system approach to nonlinear singularly perturbed optimal control problem. *Automatica*, 37(4):543–549, 2001.
- [Fri02a] E. Fridman. Effects of small delays on stability of singularly perturbed systems. *Automatica*, 38(5):897–902, 2002.
- [Fri02b] E. Fridman. Singularly perturbed analysis of chattering in relay control systems. *IEEE Trans. Aut. Contr.*, 47(12):2079–2084, 2002.
- [Fri02c] E. Fridman. Slow periodic motions with internal sliding modes in variable structure systems. *Internat. J. Control.*, 75(7):524–537, 2002.
- [Fri02d] E. Fridman. Stability of singularly perturbed differential–difference systems: a LMI approach. *Dyn. Cont. Discr. Impul. Syst. B*, 9:201–212, 2002.
- [Fri06a] E. Fridman. Robust sampled-data H_∞ control of linear singularly perturbed systems. *IEEE Transactions on Automatic Control*, 51(3):470–475, 2006.
- [Fri06b] A. Friedman. *Stochastic Differential Equations and Applications*. Dover, 2006.
- [Fru88] A. Fruchard. Canards discrets. *Compt. Rend. Acad. Sci. Math.*, 307(1):41–46, 1988.
- [Fru91] A. Fruchard. Existence of bifurcation delay: the discrete case. In E. Benoît, editor, *Dynamic Bifurcations*, volume 1493 of *Lecture Notes in Mathematics*, pages 87–106. Springer, 1991.
- [Fru92] A. Fruchard. Canards et râteaux. *Ann. Inst. Fourier*, 42(4):825–855, 1992.
- [FS80] N. Farber and J. Shinar. Approximate solution of singularly perturbed nonlinear pursuit-evasion games. *J. Optim. Theor. Appl.*, 32:39–73, 1980.
- [FS95] H. Freistühler and P. Szmydyan. Existence and bifurcation of viscous profiles for all intermediate magnetohydrodynamic shock waves. *SIAM J. Math. Anal.*, 26(1):112–128, 1995.
- [FS99a] M.I. Freidlin and R.B. Sowers. A comparison of homogenization and large deviations, with applications to wavefront propagation. *Stoch. Proc. Appl.*, 82(1):23–52, 1999.
- [FS99b] A. Fruchard and R. Schäfke. Exceptional complex solutions of the forced van der Pol equation. *Funktional. Ekvacioj*, 42(2):201–223, 1999.
- [FS02a] H. Freistühler and P. Szmydyan. Spectral stability of small shock waves. *Arch. Rational Mech. Anal.*, 164:287–309, 2002.
- [FS02b] Y.B. Fu and P.M. Sanjouran. WKB method with repeated roots and its application to the buckling analysis of an everted cylindrical tube. *SIAM J. Appl. Math.*, 62(6):1856–1871, 2002.
- [FS03a] B. Fiedler and A. Scheel. Spatio-temporal dynamics of reaction–diffusion patterns. In M. Kirkilionis, S. Krömer, R. Rannacher, and F. Tomi, editors, *Trends in Nonlinear Analysis*, pages 21–150. Springer, 2003.
- [FS03b] A. Fruchard and R. Schäfke. Bifurcation delay and difference equations. *Nonlinearity*, 16:2199–2220, 2003.
- [FS03c] A. Fruchard and R. Schäfke. Overstability and resonance. *Ann. Inst. Fourier*, 53(1):227–264, 2003.
- [FS04] A. Fruchard and R. Schäfke. Classification of resonant equations. *J. Differential Equat.*, 207(2):360–391, 2004.
- [FS05] A. Fruchard and R. Schäfke. On singularities of solutions to singular perturbation problems. *J. Phys.: Conf. Series*, 22:56–66, 2005.
- [FS09] A. Fruchard and R. Schäfke. A survey of some results on overstability and bifurcation delay. *Discr. Cont. Dyn. Sys. - Series S*, 2(4):941–965, 2009.
- [FS10a] H. Freistühler and P. Szmydyan. Spectral stability of small-amplitude viscous shock waves in several space dimensions. *Arch. Rational Mech. Anal.*, 195(2):353–373, 2010.

- [FS10b] A. Fruchard and R. Schäfke. Composite asymptotic expansions and turning points of singularly perturbed ordinary differential equations. *Comptes Rendus Math.*, 348(23):1273–1277, 2010.
- [FS10c] A. Fruchard and R. Schäfke. Développements asymptotiques combinés et points tournants d'équations différentielles singulièrement perturbées. *arXiv:1003.4110v1*, pages 1–71, 2010.
- [FS13] A. Fruchard and R. Schäfke. *Composite Asymptotic Expansions*, volume 2066 of *Lect. Notes Math.* Springer, 2013.
- [FSML04] Z. Feng, D.L. Smith, F. Ellise McKenzie, and S.A. Levin. Coupling ecology and evolution: malaria and the S-gene across time scales. *Math. Biosci.*, 189(1):1–19, 2004.
- [FST88] C. Foias, G.R. Sell, and R. Temam. Inertial manifolds for nonlinear evolutionary equations. *J. Differential Equat.*, 73(2):309–353, 1988.
- [FST89] C. Foias, G.R. Sell, and E.S. Titi. Exponential tracking and approximation of inertial manifolds for dissipative nonlinear equations. *J. Dyn. Diff. Eq.*, 1(2):199–244, 1989.
- [FT91] C. Foias and E.S. Titi. Determining nodes, finite difference schemes and inertial manifolds. *Nonlinearity*, 4(1):135, 1991.
- [Ful97] W. Fulton. *Algebraic Topology*. Springer, 1997.
- [Fur85] S.D. Furrow. Chemical oscillators based on iodate ion and hydrogen peroxide. In R.J. Field and M. Burger, editors, *Oscillations and Traveling Waves in Chemical Systems*, pages 171–192. Wiley-Interscience, 1985.
- [FV03] B. Fiedler and M.I. Vishik. Quantitative homogenization of global attractors for reaction-diffusion systems with rapidly oscillating terms. *Asymp. Anal.*, 34(2):159–185, 2003.
- [FW92] M.I. Freidlin and A.D. Wentzell. Reaction-diffusion equations with randomly perturbed boundary conditions. *Ann. Probab.*, 20(2):963–986, 1992.
- [FW93] M.I. Freidlin and A.D. Wentzell. Diffusion processes on graphs and the averaging principle. *Ann. Probab.*, 21(4):2215–2245, 1993.
- [FW98a] M.I. Freidlin and M. Weber. Random perturbations of nonlinear oscillators. *Ann. Probab.*, 26(3): 925–967, 1998.
- [FW98b] M.I. Freidlin and A.D. Wentzell. *Random Perturbations of Dynamical Systems*. Springer, 1998.
- [FW99] M.I. Freidlin and M. Weber. A remark on random perturbations of the nonlinear pendulum. *Ann. Appl. Probab.*, 9(3):611–628, 1999.
- [FW04] M.I. Freidlin and A.D. Wentzell. Random perturbations of dynamical systems and diffusion processes with conservation laws. *Probab. Theory Rel. Fields*, 128(3):441–466, 2004.
- [FW06] M.I. Freidlin and A.D. Wentzell. Long-time behavior of weakly coupled oscillators. *J. Stat. Phys.*, 123(6):1311–1337, 2006.
- [FYZ04] Z. Feng, Y. Yi, and H. Zhu. Fast and slow dynamics of malaria and the S-gene frequency. *J. Dyn. Diff. Eq.*, 16(4):869–896, 2004.
- [GACV06] M. Giona, A. Adrover, F. Creta, and M. Valorani. Slow manifold structure in explosive kinetics. 2. Extension to higher dimensional systems. *J. Phys. Chem. A*, 110(50):13463–13474, 2006.
- [Gai86] V. Gaitsgory. Use of the averaging method in control problems. *Differential Equat.*, 22:1290–1299, 1986.
- [Gai92] V. Gaitsgory. Suboptimization of singularly perturbed control systems. *SIAM J. Contr. Optim.*, 30(5):1228–1249, 1992.
- [Gai04] V. Gaitsgory. On a representation of the limit occupational measures set of a control system with applications to singularly perturbed control systems. *SIAM J. Contr. Optim.*, 43(1):325–340, 2004.
- [Gaj86] Z. Gajić. Numerical fixed-point solution for near-optimum regulators of linear quadratic gaussian control problems for singularly perturbed systems. *Int. J. Contr.*, 43(2):373–387, 1986.
- [Gaj88] Z. Gajić. The existence of a unique and bounded solution of the algebraic Riccati equation of multimodel estimation and control problems. *Syst. Contr. Lett.*, 10(3):185–190, 1988.
- [Gal93] J.A. Gallas. Structure of the parameter space of the Hénon map. *Phys. Rev. Lett.*, 70(18):2714–2717, 1993.
- [Gam95] L. Gammaitoni. Stochastic resonance and the dithering effect in threshold physical systems. *Phys. Rev. E*, 52(5):4691, 1995.
- [Gam01] T.W. Gamelin. *Complex Analysis*. Springer, 2001.
- [GANT98] B. Garcia-Archilla, J. Novo, and E.S. Titi. Postprocessing the Galerkin method: a novel approach to approximate inertial manifolds. *SIAM J. Numer. Anal.*, 35(3):941–972, 1998.
- [Gar59] C.S. Gardner. Adiabatic invariants of periodic classical systems. *Phys. Rev.*, 2(115):791–794, 1959.
- [Gar84] R. Gardner. Existence of travelling wave solutions of predator-prey systems via the connection index. *SIAM J. Appl. Math.*, 44(1):56–79, 1984.
- [Gar93] R.A. Gardner. An invariant-manifold analysis of electrophoretic traveling waves. *J. Dyn. Diff. Eq.*, 5(4):599–606, 1993.
- [Gar09] C. Gardiner. *Stochastic Methods*. Springer, Berlin Heidelberg, Germany, 4th edition, 2009.
- [Gau97] Walter Gautschi. *Numerical Analysis*. Birkhäuser Boston, 1997.
- [GB08] T. Gross and B. Blasius. Adaptive coevolutionary networks: a review. *Journal of the Royal Society – Interface*, 5:259–271, 2008.
- [GB10] O.V. Gendelman and T. Bar. Bifurcations of self-excitation regimes in a van der Pol oscillator with a nonlinear energy sink. *Physica D*, 239:220–229, 2010.
- [GBC98] I.T. Georgiou, A.K. Bajaj, and M. Corless. Slow and fast invariant manifolds, and normal modes in a two degree-of-freedom structural dynamical system with multiple equilibrium states. *Int. J. Non-Linear Mech.*, 33(2):275–300, 1998.
- [GC02] S.A. Gourley and M.A.J. Chaplain. Travelling fronts in a food-limited population model with time delay. *Proc. Roy. Soc. Edinburgh Sect. A*, 132:75–89, 2002.
- [GC04] B. Guo and H. Chen. Homoclinic orbit in a six-dimensional model of a perturbed higher-order nonlinear Schrödinger equation. *Comm. Nonl. Sci. Numer. Simul.*, 9(4):431–441, 2004.
- [GDH04] Z.P. Gerdtzen, P. Daoutidis, and W.S. Hu. Non-linear reduction for kinetic models of metabolic reaction networks. *Metabolic Engineering*, 6(2):140–154, 2004.
- [GdWNS09] C. Germay, N. Van de Wouw, H. Nijmeijer, and R. Sepulchre. Nonlinear drillstring dynamics analysis. *SIAM J. Appl. Dyn. Syst.*, 8(2):527–553, 2009.

- [GE98] B.S. Gutkin and G.B. Ermentrout. Dynamics of membrane excitability determine interspike interval variability: a link between spike generation mechanisms and cortical spike train statistics. *Neural Comput.*, 10(5):1047–1065, 1998.
- [GE06] J. Guckenheimer and S. Ellner. *Dynamic Models in Biology*. Princeton University Press, 2006.
- [Ged10] T. Gedeon. Oscillations in monotone systems with a negative feedback. *SIAM J. Appl. Dyn. Syst.*, 9(1):84–112, 2010.
- [Gel89] I.M. Gel'fand. *Lectures on Linear Algebra*. Dover, 1989.
- [Gem79] S. Geman. Some averaging and stability results for random differential equations. *SIAM J. Appl. Math.*, 36(1):86–105, 1979.
- [Geo99] I. Georgiou. On the global geometric structure of the dynamics of the elastic pendulum. *Nonlinear Dyn.*, 18(1):51–68, 1999.
- [Geo05] I. Georgiou. Advanced proper orthogonal decomposition tools: using reduced order models to identify normal modes of vibration and slow invariant manifolds in the dynamics of planar nonlinear rods. *Nonlinear Dyn.*, 41(1):69–110, 2005.
- [GER78] E.D. Gilles, G. Eigenberger, and W. Ruppel. Relaxation oscillations in chemical reactors. *AICHE J.*, 24(5):912–920, 1978.
- [Ger12] M. Gerdtz. *Optimal control of ODEs and DAEs*. de Gruyter, 2012.
- [GF77] W. Geiseler and H.H. Föllner. Three steady state situation in an open chemical reaction system. I. *Bioophys. Chem.*, 6(1):107–115, 1977.
- [GF91] L. Györgyi and R.J. Field. Simple models of deterministic chaos in the Belousov–Zhabotinsky reaction. *J. Phys. Chem.*, 95:6594–6602, 1991.
- [GFZ11] I. Gholami, A. Fiege, and A. Zippelius. Slow dynamics and precursors of the glass transition in granular fluids. *Phys. Rev. E*, 84:031305, 2011.
- [GG74] M. Golubitsky and V. Guillemin. *Stable Mappings and their Singularities*. Springer, 1974.
- [GG88] T. Grodt and Z. Gajic. The recursive reduced-order numerical solution of the singularly perturbed matrix differential Riccati equation. *IEEE Trans. Aut. Contr.*, 33(8):751–754, 1988.
- [GG97] V. Gaitsgory and G. Grammel. On the construction of asymptotically optimal controls for singularly perturbed systems. *Syst. Contr. Lett.*, 30(2):139–147, 1997.
- [GGHLS1] P. Gray, J.F. Griffiths, S.M. Hasko, and P.-G. Lignola. Oscillatory ignitions and cool flames accompanying the non-isothermal oxidation of acetaldehyde in a well stirred, flow reactor. *Proc. R. Soc. Lond.*, 374(1758):313–339, 1981.
- [GGHW93] J. Guckenheimer, S. Gueron, and R. Harris-Warrick. Mapping the dynamics of a bursting neuron. *Phil. Trans. Roy. Soc. B*, 341:345–359, 1993.
- [GGJ07] A. Ghazaryan, P. Gordon, and C.K.R.T. Jones. Traveling waves in porous media combustion: uniqueness of waves for small thermal diffusivity. *J. Dyn. Diff. Eq.*, 19(4):951–966, 2007.
- [GGK⁺07] M. Gameiro, T. Gedeon, W. Kalies, H. Kokubu, K. Mischaikow, and H. Oka. Topological horseshoes of traveling waves for a fast–slow predator–prey system. *J. Dyn. Diff. Eq.*, 19(3):623–654, 2007.
- [GGKS99] I. Goldfarb, V. Gol'dshtein, G. Kuzmenko, and S. Sazhin. Thermal radiation effect on thermal explosion in gas containing fuel droplets. *Combust. Theor. Model.*, 3(4):769–787, 1999.
- [GGM00] G. Gallavotti, G. Gentile, and V. Mastropietro. Hamilton–Jacobi equation, heteroclinic chains and Arnol'd diffusion in three time scale systems. *Nonlinearity*, 13(2):323, 2000.
- [GGM04] I. Goldfarb, V. Gol'dshtein, and U. Maas. Comparative analysis of two asymptotic approaches based on integral manifolds. *IMA J. Appl. Math.*, 69(4):353–374, 2004.
- [GGZ02] I. Goldfarb, V. Gol'dshtein, and A. Zinoviev. Delayed thermal explosion in porous media: method of invariant manifolds. *IMA J. Appl. Math.*, 67(3):263–280, 2002.
- [GH79] P.P.N. De Groot and P.W. Hemker. Error bounds for exponentially fitted Galerkin methods applied to stiff two-point boundary value problems. In P.W. Hemker and J.J.H. Miller, editors, *Numerical Analysis of Singular Perturbation Problems*, pages 217–249. Academic Press, 1979.
- [GH83] J. Guckenheimer and P. Holmes. *Nonlinear Oscillations, Dynamical Systems, and Bifurcations of Vector Fields*. Springer, New York, NY, 1983.
- [GH84] B. Greenspan and P. Holmes. Repeated resonance and homoclinic bifurcation in a periodically forced family of oscillators. *SIAM J. Math. Anal.*, 15(1):69–97, 1984.
- [GH88] H. Gingold and P.F. Hsieh. Asymptotic solutions of a Hamiltonian system in intervals with several turning points. *SIAM J. Math. Anal.*, 19(5):1142–1150, 1988.
- [GH99] J. Grasman and O.A. Van Herwaarden. *Asymptotic Methods for the Fokker–Planck Equation and the Exit Problem in Applications*. Springer, 1999.
- [GH00] I. Goychuk and P. Hänggi. Stochastic resonance in ion channels characterized by information theory. *Phys. Rev. E*, 61(4):4272, 2000.
- [GH04a] R.M. Ghigliazza and P. Holmes. A minimal model of a central pattern generator and motoneurons for insect locomotion. *SIAM J. Appl. Dyn. Syst.*, 3(4):671–700, 2004.
- [GH04b] R.M. Ghigliazza and P. Holmes. Minimal models of bursting neurons: how multiple currents, conductances, and timescales affect bifurcation diagrams. *SIAM J. Appl. Dyn. Syst.*, 3(4):636–670, 2004.
- [GH05] J. Guckenheimer and R. Haiduc. Canards at folded nodes. *Mosc. Math. J.*, 5(1):91–103, 2005.
- [GH06] K.M. Grimsrud and R. Huffaker. Solving multidimensional bioeconomic problems with singular-perturbation reduction methods: Application to managing pest resistance to pesticidal crops. *J. Environ. Econ. Manag.*, 51(3):336–353, 2006.
- [GH13] M. Grace and M.-T. Hütt. Predictability of spatio-temporal patterns in a lattice of coupled FitzHugh–Nagumo oscillators. *J. R. Soc. Interface*, 10:20121016, 2013.
- [Gha09a] A. Ghazaryan. Nonlinear stability of high Lewis number combustion fronts. *Indiana Univ. Math. J.*, 58:181–212, 2009.
- [Gha09b] A. Ghazaryan. On the stability of high Lewis number combustion fronts. *Discrete Contin. Dyn. Syst. A*, 24:809–826, 2009.
- [Gha10] A. Ghazaryan. On the existence of high Lewis number combustion fronts. *Math. Comput. Simul.*, 82(6):1133–1141, 2010.
- [Ghi12] M. Ghisi. Hyperbolic-parabolic singular perturbation for mildly degenerate Kirchhoff equations with weak dissipation. *Adv. Differential Equat.*, 17(1):1–36, 2012.

- [GHJM98] L. Gammaletti, P. Hänggi, P. Jung, and F. Marchesoni. Stochastic resonance. *Rev. Mod. Phys.*, 70: 223–287, 1998.
- [GHL13] A. Ghazaryan, J. Humphreys, and J. Lytle. Spectral behavior of combustion fronts with high exothermicity. *SIAM J. Appl. Math.*, 73(1):422–437, 2013.
- [GHK08] E.A. Gaffney, J.K. Heath and M.Z. Kwiatkowska. A mass action model of a Fibroblast Growth Factor signaling pathway and its simplification. *Bull. Math. Biol.*, 70(8):2229–2263, 2008.
- [GHR⁺07] D. Goulding, S.P. Hegarty, O. Rasskazov, S. Melnik, M. Hartnett, G. Greene, J.G. McInerney, D. Rachinskii, and G. Huyet. Excitability and self-pulsations near homoclinic bifurcations in semiconductor lasers. *Phys. Rev. Lett.*, 98:153903, 2007.
- [GHS76] K.R. Graziani, J.L. Hudson, and R.A. Schmitz. The Belousov–Zhabotinskii reaction in a continuous flow reactor. *The Chemical Engineering Journal*, 12(1):9–21, 1976.
- [GHW00] J. Guckenheimer, K. Hoffman, and W. Weckesser. Numerical computation of canards. *Internat. J. Bifur. Chaos Appl. Sci. Engrg.*, 10(12):2669–2687, 2000.
- [GHW03] J. Guckenheimer, K. Hoffman, and W. Weckesser. The forced van der Pol equation I: the slow flow and its bifurcations. *SIAM J. Appl. Dyn. Syst.*, 2(1):1–35, 2003.
- [GHW05] J. Guckenheimer, K. Hoffman, and W. Weckesser. Bifurcations of relaxation oscillations near folded saddles. *Internat. J. Bifur. Chaos Appl. Sci. Engrg.*, 15(11):3411–3421, 2005.
- [GHWPW97] J. Guckenheimer, R. Harris-Warrick, J. Peck, and A.R. Willms. Bifurcation, bursting, and spike frequency adaptation. *J. Comp. Neurosci.*, 4:257–277, 1997.
- [GI91] V. Gautheron and E. Isambert. Finitely differentiable ducks and finite expansions. In E. Benoit, editor, *Dynamic Bifurcations*, volume 1493 of *Lecture Notes in Mathematics*, pages 40–56. Springer, 1991.
- [GI96] A. Gorodetski and Yu.S. Ilyashenko. Minimal and strange attractors. *Int. J. Bifur. Chaos*, 6:1177–1183, 1996.
- [GI01] J. Guckenheimer and Yu. Ilyashenko. The duck and the devil: canards on the staircase. *Mosc. Math. J.*, 1(1):27–47, 2001.
- [Gil75] D.E. Gilsinn. The method of averaging and domains of stability for integral manifolds. *SIAM J. Appl. Math.*, 29(4):628–660, 1975.
- [Gil82] D.E. Gilsinn. A high order generalized method of averaging. *SIAM J. Appl. Math.*, 42(1):113–134, 1982.
- [Gil83] A.D. MacGillivray. On the leading term of the outer asymptotic expansion of van der Pol's equation. *SIAM J. Appl. Math.*, 43(6):1221–1239, 1983.
- [Gil90] A.D. MacGillivray. Justification of matching with the transition expansion of van der Pol's equation. *SIAM J. Math. Anal.*, 21(1):221–240, 1990.
- [Gil93] R. Gilmore. *Catastrophe Theory for Scientists and Engineers*. Dover, 1993.
- [Gil97] A.D. MacGillivray. A method for incorporating transciently small terms into the method of matched asymptotic expansions. *Studies in Appl. Math.*, 99:285–310, 1997.
- [Gin85] H. Gingold. An asymptotic decomposition method applied to multi-turning point problems. *SIAM J. Math. Anal.*, 16(1):7–27, 1985.
- [Gin09] J.-M. Ginoux. *Differential Geometry Applied to Dynamical Systems*. World Scientific, 2009.
- [GJ79] J. Grasman and M.J.W. Jansen. Mutually synchronized relaxation oscillators as prototypes of oscillating systems in biology. *J. Math. Biol.*, 7(2):171–197, 1979.
- [GJ90] R. Gardner and C.K.R.T. Jones. Traveling waves of a perturbed diffusion equation arising in a phase field model. *Ind. Univ. Math. J.*, 39(4):1197–1222, 1990.
- [GJ91] R. Gardner and C.K.R.T. Jones. Stability of travelling wave solutions of diffusive predator-prey systems. *Trans. Amer. Math. Soc.*, 327(2):465–524, 1991.
- [GJ08] V. Guttal and C. Jayaprakash. Changing skewness: an early warning signal of regime shifts in ecosystems. *Ecology Letters*, 11:450–460, 2008.
- [GJ09] V. Guttal and C. Jayaprakash. Spatial variance and spatial skewness: leading indicators of regime shifts in spatial ecological systems. *Theor. Ecol.*, 2:3–12, 2009.
- [GJK01] M. Golubitsky, K. Josic, and T.J. Kaper. An unfolding theory approach to bursting in fast-slow systems. In H.W. Broer, B. Krauskopf, and G. Vegter, editors, *Global Analysis of Dynamical Systems: Festschrift dedicated to Floris Takens on the occasion of his 60th birthday*, pages 277–308. Institute of Physics Publ., 2001.
- [GJM12] J. Guckenheimer, T. Johnson, and P. Meerkamp. Rigorous enclosures of a slow manifold. *SIAM J. Appl. Dyn. Syst.*, 11(3):831–863, 2012.
- [GK81] A. Goldbeter and D.E. Koshland. An amplified sensitivity arising from covalent modification in biological systems. *Proc. Natl. Acad. Sci. USA*, 78:6840–6844, 1981.
- [GK86] Z. Gajic and H. Khalil. Multimodel strategies under random disturbances and imperfect partial observations. *Automatica*, 22(1):121–125, 1986.
- [GK91] E.V. Grigor'eva and S.A. Kashchenko. Relaxation oscillations in a system of equations describing the operation of a solid-state laser with a nonlinear element of delaying action. *Differential Equations*, 27(5):506–512, 1991.
- [GK97] M. Garbey and H.G. Kaper. Heterogeneous domain decomposition for singularly perturbed elliptic boundary value problems. *SIAM J. Numer. Anal.*, 34(4):1513–1544, 1997.
- [GK98] P.P.N. De Groen and G.E. Karadzhov. Exponentially slow travelling waves on a finite interval for Burgers'-type equation. *Electron. J. Differential Equat.*, 1980(30):1–38, 1998.
- [GK01] P.P.N. De Groen and G.E. Karadzhov. Slow travelling waves on a finite interval for Burgers'-type equations. *J. Comput. Appl. Math.*, 132:155–189, 2001.
- [GK02] W. Gerstner and W. Kistler. *Spiking Neuron Models*. Cambridge University Press, 2002.
- [GK03] C.W. Gear and I.G. Kevrekidis. Projective methods for stiff differential equations: problems with gaps in their eigenvalue spectrum. *SIAM J. Sci. Comput.*, 24(4):1091–1106, 2003.
- [GK04] D. Givon and R. Kupferman. White noise limits for discrete dynamical systems driven by fast deterministic dynamics. *Physica A*, 335(3):385–412, 2004.
- [GK09a] J. Guckenheimer and C. Kuehn. Computing slow manifolds of saddle-type. *SIAM J. Appl. Dyn. Syst.*, 8(3):854–879, 2009.
- [GK09b] J. Guckenheimer and C. Kuehn. Homoclinic orbits of the FitzHugh–Nagumo equation: The singular limit. *Discr. Cont. Dyn. Syst. S*, 2(4):851–872, 2009.

- [GK10a] D.Y. Gao and V.A. Krysko. *Introduction to Asymptotic Methods*. CRC Press, 2010.
- [GK10b] J. Guckenheimer and C. Kuehn. Homoclinic orbits of the FitzHugh–Nagumo equation: Bifurcations in the full system. *SIAM J. Appl. Dyn. Syst.*, 9:138–153, 2010.
- [GKK06] D. Givon, I.G. Kevrekidis, and R. Kupferman. Strong convergence of projective integration schemes for singularly perturbed stochastic differential systems. *Comm. Math. Sci.*, 4(4):707–729, 2006.
- [GKKZ05] C.W. Gear, T.J. Kaper, I.G. Kevrekidis, and A. Zagaris. Projecting to a slow manifold: singularly perturbed systems and legacy codes. *SIAM J. Appl. Dyn. Syst.*, 4(3):711–732, 2005.
- [GKM89] P. Grassbeger, H. Kantz, and U. Moenig. On the symbolic dynamics of the Hénon map. *J. Phys. A*, 22(24):5217–5230, 1989.
- [GKM⁺99] T. Gedeon, H. Kokubu, K. Mischaikow, H. Oka, and J.F. Reineck. The Conley index for fast–slow systems I. One-dimensional slow variable. *J. Dyn. Diff. Eq.*, 11(3):427–470, 1999.
- [GKMO02] T. Gedeon, H. Kokubu, K. Mischaikow, and H. Oka. Chaotic solutions in slowly varying perturbations of Hamiltonian systems with applications to shallow water sloshing. *J. Dyn. Diff. Eq.*, 14(1):63–84, 2002.
- [GKMO06] T. Gedeon, H. Kokubu, K. Mischaikow, and H. Oka. The Conley index for fast–slow systems II. Multidimensional slow variable. *J. Differential Equat.*, 225:242–307, 2006.
- [GKMW07] T. Götz, A. Klar, N. Marheineke, and R. Wegener. A stochastic model and associated Fokker–Planck equation for the fiber lay-down process in nonwoven production processes. *SIAM J. Appl. Math.*, 67(6):1704–1717, 2007.
- [GKR08] S.D. Glyzin, A.Yu. Kolesov, and N.Kh. Rozov. Blue sky catastrophe in relaxation systems with one fast and two slow variables. *Differential Equat.*, 44(2):161–175, 2008.
- [GKR11a] S.D. Glyzin, A.Yu. Kolesov, and N.Kh. Rozov. Relaxation self-oscillations in neuron systems: I. *Differential Equat.*, 47(7):927–941, 2011.
- [GKR11b] S.D. Glyzin, A.Yu. Kolesov, and N.Kh. Rozov. Relaxation self-oscillations in neuron systems: II. *Differential Equat.*, 47(12): 1697–1713, 2011.
- [GKR12] S.D. Glyzin, A.Yu. Kolesov, and N.Kh. Rozov. Relaxation self-oscillations in neuron systems: III. *Differential Equat.*, 48(2):159–175, 2012.
- [GKR13] S.D. Glyzin, A.Yu. Kolesov, and N.Kh. Rozov. On a method for mathematical modeling of chemical synapses. *Differential Equat.*, 49(10):1193–1210, 2013.
- [GKS04] D. Givon, R. Kupferman, and A.M. Stuart. Extracting macroscopic dynamics: model problems and algorithms. *Nonlinearity*, 17:55–127, 2004.
- [GKT97] M. Grossglauser, S. Keshav, and D.N. Tse. RCBR: a simple and efficient service for multiple time-scale traffic. *IEEE/ACM Trans. Netw.*, 5(6):741–755, 1997.
- [GKT02] C.W. Gear, I.G. Kevrekidis, and C. Theodoropoulos. Coarse-integration/bifurcation analysis via microscopic simulators micro-Galerkin methods. *Comput. Chem. Eng.*, 26(7):941–963, 2002.
- [GKZ04] A.N. Gorban, I.V. Karlin, and A.Yu. Zinov'yev. Constructive methods of invariant manifolds for kinetic problems. *Physics Reports*, 396:197–403, 2004.
- [GL93] J. Guckenheimer and I.S. Labouriau. Bifurcations of the Hodgkin and Huxley equations; a new twist. *Bull. Math. Biol.*, 55:937–952, 1993.
- [GL99] V. Gaitsgory and A. Leizarowitz. Limit occupational measures set for a control system and averaging of singularly perturbed control systems. *J. Math. Anal. Appl.*, 233(2):461–475, 1999.
- [GL01] Z. Gajić and M.-T. Lim. *Optimal Control of Singularly Perturbed Linear Systems and Applications*. Marcel Dekker, 2001.
- [GL02] V. Gelfreich and L. Lerman. Almost invariant elliptic manifold in a singularly perturbed Hamiltonian system. *Nonlinearity*, 15(2):447–457, 2002.
- [GL03] V. Gelfreich and L. Lerman. Long-periodic orbits and invariant tori in a singularly perturbed Hamiltonian system. *Physica D*, 176(3):125–146, 2003.
- [GL05] A. Guillin and R. Liptser. MDP for integral functionals of fast and slow processes with averaging. *Stochastic Process. Appl.*, 115(7):1187–1207, 2005.
- [GL07] J. Guckenheimer and D. LaMar. Periodic orbit continuation in multiple time scale systems. In *Understanding Complex Systems: Numerical continuation methods for dynamical systems*, pages 253–267. Springer, 2007.
- [GL11] J.-M. Ginoux and J. Llibre. The flow curvature method applied to canard explosion. *J. Phys. A: Math. Theor.*, 44:465203, 2011.
- [GL12] J.-M. Ginoux and C. Letellier. Van der Pol and the history of relaxation oscillations: toward the emergence of a concept. *Chaos*, 22:023120, 2012.
- [Gla77] R.T. Glassey. On the blowing up of solutions to the Cauchy problem for nonlinear Schrödinger equations. *J. Math. Phys.*, 18:1794–1797, 1977.
- [GLC13] J.-M. Ginoux, J. Llibre, and L.O. Chua. Canards from Chua's circuit. *Int. J. Bif. Chaos*, 23:1330010, 2013.
- [Gle94] P. Glendinning. *Stability, Instability and Chaos*. CUP, 1994.
- [Gli98] V.Y. Glizer. Asymptotic solution of a singularly perturbed set of functional-differential equations of Riccati type encountered in the optimal control theory. *Nonl. Diff. Eq. Appl.*, 5(4):491–515, 1998.
- [Gli00a] V.Y. Glizer. Asymptotic solution of a boundary-value problem for linear singularly-perturbed functional differential equations arising in optimal control theory. *J. Optim. Theor. Appl.*, 106(2):309–335, 2000.
- [Gli00b] V.Y. Glizer. Asymptotic solution of zero-sum linear-quadratic differential game with cheap control for minimizer. *Nonl. Diff. Eq. Appl.*, 7(2):213–258, 2000.
- [Gli01a] V.Y. Glizer. Controllability of singularly perturbed linear time-dependent systems with small state delay. *Dynamics and Control*, 11(3):261–281, 2001.
- [Gli01b] V.Y. Glizer. Euclidean space controllability of singularly perturbed linear systems with state delay. *Syst. Contr. Lett.*, 43(3):181–191, 2001.
- [Gli03a] V.Y. Glizer. Asymptotic analysis and solution of a finite-horizon H_∞ control problem for singularly-perturbed linear systems with small state delay. *J. Optim. Theor. Appl.*, 117(2):295–325, 2003.

- [Gli03b] V.Y. Glizer. Blockwise estimate of the fundamental matrix of linear singularly perturbed differential systems with small delay and its application to uniform asymptotic solution. *J. Math. Anal. Appl.*, 278(2):409–433, 2003.
- [Gli03c] V.Y. Glizer. Controllability of nonstandard singularly perturbed systems with small state delay. *IEEE Trans. Aut. Contr.*, 48(7):1280–1285, 2003.
- [Gli04] V.Y. Glizer. On stabilization of nonstandard singularly perturbed systems with small delays in state and control. *IEEE Trans. Aut. Contr.*, 49(6):1012–1016, 2004.
- [Gli07] V.Y. Glizer. Infinite horizon quadratic control of linear singularly perturbed systems with small state delays: an asymptotic solution of Riccati-type equations. *IMA J. Math. Contr. Inform.*, 24(4):435–459, 2007.
- [Gli08] V.Y. Glizer. Novel controllability conditions for a class of singularly-perturbed systems with small state delays. *J. Optim. Theor. Appl.*, 137:135–156, 2008.
- [GLK03] C.W. Gear, J. Li, and I.G. Kevrekidis. The gap-tooth method in particle simulations. *Phys. Lett. A*, 316(3):190–195, 2003.
- [GLMM00] A. Gasull, J. Llibre, V. Mañosas, and F. Mañosas. The focus-centre problem for a type of degenerate system. *Nonlinearity*, 13(3):699–729, 2000.
- [GLMS01] I. Gasser, C.D. Levermore, P.A. Markowich, and C. Schmeiser. The initial time layer problem and the quasineutral limit in the semiconductor drift-diffusion model. *Eur. J. Appl. Math.*, 12(4):497–512, 2001.
- [GM72] A. Gierer and H. Meinhardt. A theory of biological pattern formation. *Kybernetik*, 12:30–39, 1972.
- [GM77] J. Grasman and B.J. Matkowsky. A variational approach to singularly perturbed boundary value problems for ordinary and partial differential equations with turning points. *SIAM J. Appl. Math.*, 32(3):588–597, 1977.
- [GM06] T. Gedeon, , and K. Mischaikow. Singular boundary value problems via the Conley index. *Topol. Methods Nonlinear Anal.*, 28(2):263–283, 2006.
- [GM07] J.M. González-Miranda. Complex bifurcation structures in the Hindmarsh–Rose neuron model. *Int. J. Bif. Chaos*, 17(9):3071–3083, 2007.
- [GM08] B. Gershgorin and A. Majda. A nonlinear test model for filtering slow–fast systems. *Commun. Math. Sci.*, 6(3):611–649, 2008.
- [GM10] B. Gershgorin and A. Majda. Filtering a nonlinear slow–fast system with strong fast forcing. *Commun. Math. Sci.*, 8(1):67–92, 2010.
- [GM12a] J.M. González-Miranda. Nonlinear dynamics of the membrane potential of a bursting pacemaker cell. *Chaos*, 22:013123, 2012.
- [GM12b] J. Guckenheimer and P. Meerkamp. Bifurcation analysis of singular Hopf bifurcation in \mathbb{R}^3 . *SIAM J. Appl. Dyn. Syst.*, 11(4):1325–1359, 2012.
- [GM13] G. Gottwald and I. Melbourne. Homogenization for deterministic maps and multiplicative noise. *Proc. R. Soc. A*, 469:20130201, 2013.
- [GMCH12] L. Giomi, L. Mahadevan, B. Chakraborty, and M.F. Hagan. Banding, excitability and chaos in active nematic suspensions. *Nonlinearity*, 25(8):2245–2269, 2012.
- [GMG07] G. Gigante, M. Mattia, and P.D. Giudice. Diverse population-bursting modes of adapting spiking neurons. *Phys. Rev. Lett.*, 98(14):148101, 2007.
- [GMGW98] T. Guhr, A. Müller-Groeling, and H.A. Weidenmüller. Random-matrix theories in quantum physics: common concepts. *Phys. Rep.*, 299(4):189–425, 1998.
- [GMMSS89] L. Gammaconi, F. Marchesoni, E. Menichella-Saetta, and S. Santucci. Stochastic resonance in bistable systems. *Phys. Rev. Lett.*, 62(4):349–352, 1989.
- [GMS95] L. Gammaconi, F. Marchesoni, and S. Santucci. Stochastic resonance as a bona fide resonance. *Phys. Rev. Lett.*, 74(7):1052–1055, 1995.
- [GMSS+89] L. Gammaconi, E. Menichella-Saetta, S. Santucci, F. Marchesoni, and C. Presilla. Periodically time-modulated bistable systems: stochastic resonance. *Phys. Rev. A*, 40(4):2114, 1989.
- [GN83] P. Gaspard and G. Nicolis. What can we learn from homoclinic orbits in chaotic dynamics? *J. Stat. Phys.*, 31(3):499–518, 1983.
- [GN01] V. Gaitsgory and M.-T. Nguyen. Averaging of three time scale singularly perturbed control systems. *Syst. Contr. Lett.*, 42(5): 395–403, 2001.
- [GN02] V. Gaitsgory and M.-T. Nguyen. Multiscale singularly perturbed control systems: limit occupational measures sets and averaging. *SIAM J. Contr. Optim.*, 41(3):954–974, 2002.
- [GNJ89] Z.-M. Gu, N.N. Nefedov, and R.E. O’Malley Jr. On singular singularly perturbed initial value problems. *SIAM J. Appl. Math.*, 49(1):1–25, 1989.
- [GNV84] J. Grasman, H. Nijmeijer, and E.J.M. Veling. Singular perturbations and a mapping on an interval for the forced van der Pol relaxation oscillator. *Physica D*, 13(1):195–210, 1984.
- [GNW10] J.E. Gough, H.I. Nurdin, and S. Wildeuer. Commutativity of the adiabatic elimination limit of fast oscillatory components and the instantaneous feedback limit in quantum feedback networks. *J. Math. Phys.*, 51:123518, 2010.
- [GO02] J. Guckenheimer and R.A. Oliva. Chaos in the Hodgkin–Huxley model. *SIAM J. Appl. Dyn. Syst.*, 1:105–114, 2002.
- [GO10] E.V. Goncharova and A.I. Ovseevich. Asymptotic estimates for reachable sets of singularly perturbed linear systems. *Dif. Uravneniya*, 46(12):1737–1748, 2010.
- [GO11] A. Gloria and F. Otto. An optimal variance estimate in stochastic homogenization of discrete elliptic equations. *Ann. Probab.*, 39:779–856, 2011.
- [GO12] J. Guckenheimer and H.M. Osinga. The singular limit of a Hopf bifurcation. *Discr. Cont. Dyn. Syst. A*, 32:2805–2823, 2012.
- [Gol91] A. Goldbeter. A minimal cascade model for the mitotic oscillator involving cyclin and cdc2 kinase. *Proc. Natl. Acad. Sci USA*, 88:9107–9111, 1991.
- [Gol92] N. Goldenfeld. *Lectures on Phase Transitions and the Renormalization Group*. Westview Press, 1992.
- [Gol97] A. Goldbeter. *Biochemical Oscillations and Cellular Rhythms*. CUP, 1997.
- [Gol98] R. Goldblatt. *Lectures on the Hyperreals*. Springer, 1998.

- [GOT07] G. Gottwald, M. Oliver, and N. Tercu. Long-time accuracy for approximate slow manifolds in a finite dimensional model of balance. *J. Nonlinear Sci.*, 17:283–307, 2007.
- [Gou00] S.A. Gourley. Travelling fronts in the diffusive Nicholson’s blowflies equation with distributed delay. *Math. Comput. Model.*, 32(7):843–853, 2000.
- [Gou13] D.A. Goussis. The role of slow system dynamics in predicting the degeneracy of slow invariant manifolds: The case of vdP relaxation-oscillations. *Physica D*, 248:16–32, 2013.
- [GOV87a] A. Galves, E. Olivieri, and M.E. Vares. Metastability for a class of dynamical systems subject to small random perturbations. *Ann. Prob.*, 15(4):1288–1305, 1987.
- [Gov87b] W.F. Govaerts. *Numerical Methods for Bifurcations of Dynamical Equilibria*. SIAM, Philadelphia, PA, 1987.
- [GP83] P. Grassberger and I. Procaccia. Measuring the strangeness of strange attractors. *Physica D*, 9(1):189–208, 1983.
- [GP84] C.W. Gear and L.R. Petzhold. ODE methods for the solution of differential/algebraic systems. *SIAM J. Numer. Anal.*, 21(4):716–728, 1984.
- [GP87] D.L. González and O. Piro. Global bifurcations and phase portrait of an analytically solvable nonlinear oscillator: relaxation oscillations and saddle-node collisions. *Phys. Rev. A*, 36(9):4402–4410, 1987.
- [GP06] R.E. Griffiths and M. Pernarowski. Return map characterizations for a model of bursting with two slow variables. *SIAM J. Appl. Math.*, 66(6):1917–1948, 2006.
- [GPCS06] A. García, E. Pérez-Chavela, and A. Susin. A generalization of the Poincaré compactification. *Arch. Rat. Mech. Anal.*, 179(2):285–302, 2006.
- [GPEK00] A. Gavrielides, D. Pieroux, T. Erneux, and V. Kovanis. Hopf bifurcation subject to a large delay in a laser system. *SIAM J. Appl. Math.*, 61(3):966–982, 2000.
- [GPP12] G. Giacomini, K. Pakdaman, and X. Pellegrin. Global attractor and asymptotic dynamics in the Kuramoto model for coupled noisy phase oscillators. *Nonlinearity*, 25:1247–1273, 2012.
- [GPPP12] G. Giacomini, K. Pakdaman, X. Pellegrin, and C. Poquet. Transitions in active rotator systems: invariant hyperbolic manifold approach. *SIAM J. Math. Anal.*, 44(6):4165–4194, 2012.
- [GPS90] Z. Gajic, D. Petkovski, and X. Shen. *Singularly perturbed and weakly coupled linear control systems: a recursive approach*. Springer, 1990.
- [GR89] J. Grasman and J. Roerdink. Stochastic and chaotic relaxation oscillations. *J. Stat. Phys.*, 54(3):949–970, 1989.
- [GR93] D. Golomb and J. Rinzel. Dynamics of globally coupled inhibitory neurons with heterogeneity. *Phys. Rev. E*, 48(6):4810, 1993.
- [GR94] D. Golomb and J. Rinzel. Clustering in globally coupled inhibitory neurons. *Physica D*, 72(3):259–282, 1994.
- [GR03] S.A. Gourley and S. Ruan. Convergence and travelling fronts in functional differential equations with nonlocal terms: a competition model. *SIAM J. Math. Anal.*, 35(3):806–822, 2003.
- [Gra80] J. Grasman. Relaxation oscillations of a van der Pol equation with large critical forcing term. *Quart. Appl. Math.*, 38:9–16, 1980.
- [Gra84] J. Grasman. The mathematical modeling of entrained biological oscillators. *Bull. Math. Biol.*, 46(3):407–422, 1984.
- [Gra87] J. Grasman. *Asymptotic Methods for Relaxation Oscillations and Applications*. Springer, 1987.
- [Gra95] C.P. Grant. Slow motion in one-dimensional Cahn–Morral systems. *SIAM J. Math. Anal.*, 26(1):21–34, 1995.
- [Gra96] G. Grammel. Singularly perturbed differential inclusions: an averaging approach. *Set-Valued Analysis*, 4(4):361–374, 1996.
- [Gra99] G. Grammel. Limits of nonlinear discrete-time control systems with fast subsystems. *Syst. Contr. Lett.*, 36(4):277–283, 1999.
- [Gra04] G. Grammel. On nonlinear control systems with multiple time scales. *J. Dyn. Contr. Sys.*, 10(1):11–28, 2004.
- [GRC08] J.M. Ginoux, B. Rossetto, and L.O. Chua. Slow invariant manifolds as curvature of the flow of dynamical systems. *Int. J. Bif. Chaos*, 18(11):3409–3430, 2008.
- [Gre37] G. Green. On the motion of waves in a variable canal of small depth and width. *Trans. Cambridge Phil. Soc.*, 6:457–462, 1837.
- [Gre69] W.M. Greenlee. Singular perturbation of eigenvalues. *Arch. Rat. Mech. Anal.*, 34(2):143–164, 1969.
- [Gre10] M. Greenblatt. Oscillatory integral decay, sublevel set growth, and the Newton polyhedron. *Math. Ann.*, 346:857–895, 2010.
- [GRF91] L. Györgyi, S. Rempe, and R.J. Field. A novel model for the simulation of chaos in low-flow-rate CSTR experiments with the Belousov–Zhabotinskii reaction: a chemical mechanism for two-frequency oscillations. *J. Phys. Chem.*, 95:3159–3165, 1991.
- [Gri91] P. Grindrod. *Patterns and Waves: The Theory and Applications of Reaction-Diffusion Equations*. Clarendon Press, 1991.
- [GRKT12] V. Gelfreich, V. Rom-Kedar, and D. Turaev. Fermi acceleration and adiabatic invariants for non-autonomous billiards. *Chaos*, 22(3):033116, 2012.
- [GRMP10] C. Grotta-Ragazzo, C. Pereira Malta, and K. Pakdaman. Metastable periodic patterns in singularly perturbed delayed equations. *J. Dyn. Diff. Eq.*, 22(2):203–252, 2010.
- [Gro77] P.P.N. De Groen. Spectral properties of second-order singularly perturbed boundary value problems with turning points. *J. Math. Anal. Appl.*, 57(1):119–145, 1977.
- [Gro80] P.P.N. De Groen. The nature of resonance in a singular perturbation problem of turning point type. *SIAM J. Math. Anal.*, 11(1):1–22, 1980.
- [Gro81] P.P.N. De Groen. A finite element method with a large mesh-width for a stiff two-point boundary value problem. *J. Comput. Appl. Math.*, 7(1):3–15, 1981.
- [Gru79] L.T. Gruijic. Singular perturbations and large-scale systems. *Int. J. Contr.*, 29(1):159–169, 1979.
- [Gru81] L.T. Gruijic. Uniform asymptotic stability of non-linear singularly perturbed general and large-scale systems. *Int. J. Contr.*, 33(3):481–504, 1981.
- [Gru98] J. Gruendler. Homoclinic solutions and chaos in ordinary differential equations with singular perturbations. *Trans. Amer. Math. Soc.*, 350(9):3797–3814, 1998.

- [GS77] J.L. Gervais and B. Sakita. WKB wave function for systems with many degrees of freedom: a unified view of solitons and pseudoparticles. *Phys. Rev. D*, 16(12):3507–3514, 1977.
- [GS83] R. Gardner and J. Smoller. The existence of periodic travelling waves for singularly perturbed predator-prey equations via the Conley index. *J. Differential Equat.*, 47:133–161, 1983.
- [GS85] M. Golubitsky and D. Schaeffer. *Singularities and Groups in Bifurcation Theory*, volume 1. Springer, 1985.
- [GS91] G.N. Gorenov and V.A. Sobolev. Mathematical modeling of critical phenomena in thermal explosion theory. *Combust. Flame*, 87(2):203–210, 1991.
- [GS92] G.N. Gorenov and V.A. Sobolev. Duck-trajectories in a thermal explosion problem. *Appl. Math. Lett.*, 5(6):3–6, 1992.
- [GS93] I. Gasser and P. Szmolyan. A geometric singular perturbation analysis of detonation and deflagration waves. *SIAM J. Math. Anal.*, 24(4):968–986, 1993.
- [GS95] I. Gasser and P. Szmolyan. Detonation and deflagration waves with multistep reaction schemes. *SIAM J. Appl. Math.*, 55(1): 175–191, 1995.
- [GS99] I. Georgiou and I.B. Schwartz. Dynamics of large scale coupled structural/mechanical systems: a singular perturbation/proper orthogonal decomposition approach. *SIAM J. Appl. Math.*, 59(4): 1178–1207, 1999.
- [GS00] F. Ghorelb and M.W. Spong. Integral manifolds of singularly perturbed systems with application to rigid-link flexible-joint multibody systems. *Int. J. Non-Linear Mech.*, 35(1):133–155, 2000.
- [GS01a] I. Gasser and P. Szmolyan. The frozen flow and the equilibrium limits in a polyatomic gas with relaxation effects. *Math. Mod. Meth. Appl. Sci.*, 11(1):87–104, 2001.
- [GS01b] I. Georgiou and I.B. Schwartz. Invariant manifolds, nonclassical normal modes, and proper orthogonal modes in the dynamics of the flexible spherical pendulum. *Nonlinear Dyn.*, 25(1):3–31, 2001.
- [GS09a] P. Goel and A. Sherman. The geometry of bursting in the dual oscillator model of pancreatic β -cells. *SIAM J. Appl. Dyn. Syst.*, 8(4):1664–1693, 2009.
- [GS09b] T. Gross and H. Sayama, editors. *Adaptive Networks: Theory, Models and Applications*. Springer, 2009.
- [GS09c] I. Gucwa and P. Szmolyan. Geometric singular perturbation analysis of an autocatalator model. *Discr. Cont. Dyn. Syst. S*, 2(4):783–806, 2009.
- [GS11] J. Guckenheimer and C. Scheper. A geometric model for mixed-mode oscillations in a chemical system. *SIAM J. Appl. Dyn. Sys.*, 10(1):92–128, 2011.
- [GS12a] R. Gobbi and R. Spigler. Comparing Shannon to autocorrelation-based wavelets for solving singularly perturbed elliptic BV problems. *BIT Numer. Math.*, 52:21–43, 2012.
- [GS12b] M. Guardi and T.M. Seara. Exponentially and non-exponentially small splitting of separatrices for the pendulum with a fast meromorphic perturbation. *Nonlinearity*, 25:1367–1412, 2012.
- [GS13] J. Guckenheimer and C. Scheper. Multiple time scale analysis of a model Belousov–Zhabotinskii reaction. *SIAM J. Appl. Dyn. Sys.*, 12(4):1968–1996, 2013.
- [GSCE06] D. Golomb, A. Shemini, R. Curtu, and G.B. Ermentrout. Persistent synchronized bursting activity in cortical tissues with low magnesium concentration: a modeling study. *J. Neurophysiol.*, 95(2):1049–1067, 2006.
- [GSK97] A. Goryachev, P. Strizhak, and R. Kapral. Slow manifold structure and the emergence of mixed-mode oscillations. *J. Chem. Phys.*, 107(18):2881–2889, 1997.
- [GSLO92] T. Geest, C.G. Steinmetz, R. Larter, and L.F. Olsen. Period-doubling bifurcations and chaos in an enzyme reaction. *J. Phys. Chem.*, 96:5678–5680, 1992.
- [GSS85] M. Golubitsky, D. Schaeffer, and I. Stewart. *Singularities and Groups in Bifurcation Theory*, volume 2. Springer, 1985.
- [GS06] G.N. Gorenov, E.A. Shchepakina, and V.A. Sobolev. Canards and critical behavior in autocatalytic combustion models. *J. Engineer. Math.*, 56(2):143–160, 2006.
- [GSS13] A. Ghazaryan, S. Schecter, and P.L. Simon. Gasless combustion fronts with heat loss. *SIAM J. Appl. Math.*, 73(3):1303–1326, 2013.
- [GSW09] D. Givon, P. Stinis, and J. Weare. Variance reduction for particle filters of systems with time scale separation. *IEEE Trans. Signal Proc.*, 57(2):424–435, 2009.
- [GT03] M. Grossglauser and D.N. Tse. A time-scale decomposition approach to measurement-based admission control. *IEEE/ACM Trans. Netw.*, 11(4):550–563, 2003.
- [GT08] V. Gelfreich and D. Turaev. Unbounded energy growth in Hamiltonian systems with a slowly varying parameter. *Comm. Math. Phys.*, 283(3):769–794, 2008.
- [GT12a] A. Genadot and M. Thieullen. Averaging for a fully coupled piecewise-deterministic Markov process in infinite dimensions. *Adv. Appl. Probab.*, 44(3):749–773, 2012.
- [GT12b] A. Genadot and M. Thieullen. Multiscale piecewise deterministic Markov process in infinite dimension: central limit theorem and Langevin approximation. *arXiv:1211.1894v1*, pages 1–33, 2012.
- [GTF90] L. Györgyi, T. Turányi, and R.J. Field. Mechanistic details of the oscillatory Belousov–Zhabotinskii reaction. *J. Phys. Chem.*, 94:7162–7170, 1990.
- [GTGN97] S.V. Gonchenko, D.V. Turaev, P. Gaspard, and G. Nicolis. Complexity in the bifurcation structure of homoclinic loops to a saddle-focus. *Nonlinearity*, 10:409–423, 1997.
- [GTW05] J. Guckenheimer, J.H. Tien, and A.R. Willms. Bifurcations in the fast dynamics of neurons: implications for bursting. In *Bursting, The Genesis of Rhythm in the Nervous System*, pages 89–122. World Sci. Publ., 2005.
- [Gua13] H. Guan. An averaging theorem for a perturbed KdV equation. *Nonlinearity*, 26(6):1599–1621, 2013.
- [Guc80a] J. Guckenheimer. Dynamics of the van der Pol equation. *IEEE Trans. Circ. Syst.*, 27(11):983–989, 1980.
- [Guc80b] J. Guckenheimer. Symbolic dynamics and relaxation oscillations. *Physica D*, 1(2):227–235, 1980.
- [Guc84] J. Guckenheimer. Multiple bifurcation problems of codimension two. *SIAM J. Math. Anal.*, 15(1):1–49, 1984.
- [Guc96] J. Guckenheimer. Towards a global theory of singularly perturbed systems. *Progress in Nonlinear Differential Equations and Their Applications*, 19:214–225, 1996.
- [Guc02] J. Guckenheimer. Bifurcation and degenerate decomposition in multiple time scale dynamical systems. In *Nonlinear Dynamics and Chaos: Where do we go from here?*, pages 1–20. Taylor and Francis, 2002.

- [Guc03] J. Guckenheimer. Global bifurcations of periodic orbits in the forced van der Pol equation. In H.W. Broer, B. Krauskopf, and G. Vegter, editors, *Global Analysis of Dynamical Systems - Festschrift dedicated to Floris Takens*, pages 1–16. Inst. of Physics Pub., 2003.
- [Guc04] J. Guckenheimer. Bifurcations of relaxation oscillations. In *Normal Forms, Bifurcations and Finiteness Problems in Differential Equations*, volume 137 of *NATO Sci. Ser. II Math. Phys. Chem.*, pages 295–316. Springer, 2004.
- [Guc08a] J. Guckenheimer. Return maps of folded nodes and folded saddle-nodes. *Chaos*, 18:015108, 2008.
- [Guc08b] J. Guckenheimer. Singular Hopf bifurcation in systems with two slow variables. *SIAM J. Appl. Dyn. Syst.*, 7(4):1355–1377, 2008.
- [Guc13] J. Guckenheimer. The birth of chaos. In *Recent Trends in Dynamical Systems*, volume 35 of *Proceed. Math. Stat.*, pages 3–24. Springer, 2013.
- [Gun12] J. Gunawardena. A linear framework for time-scale separation in nonlinear biochemical systems. *PLOS ONE*, 7:e36321, 2012.
- [Gup12] A. Gupta. The Fleming-Viot limit of an interacting spatial population with fast density regulation. *Electronic J. Probab.*, 17(104):1–55, 2012.
- [GV73] J. Grasman and E.J.M. Veling. An asymptotic formula for the period of a Volterra-Lotka system. *Math. Biosci.*, 18(1):185–189, 1973.
- [GV04] J. Guckenheimer and A. Vladimirsky. A fast method for approximating invariant manifolds. *SIAM J. Appl. Dyn. Syst.*, 3(3):232–260, 2004.
- [GV06] D.A. Gousis and M. Valorani. An efficient iterative algorithm for the approximation of the fast and slow dynamics of stiff systems. *J. Comp. Phys.*, 214:316–346, 2006.
- [GV10] Y.A. Godin and B. Vainberg. On the determination of the boundary impedance from the far field pattern. *SIAM J. Appl. Math.*, 70(7):2273–2280, 2010.
- [GVBM09] O.V. Gendelman, A.F. Vakakis, L.A. Bergman, and D.M. McFarland. Asymptotic analysis of passive nonlinear suppression of aeroelastic instabilities of a rigid wing in subsonic flow. *SIAM J. Appl. Math.*, 70(5):1655–1677, 2009.
- [GvL96] G.H. Golub and C. van Loan. *Matrix Computations*. Johns Hopkins University Press, Baltimore, MD, 1996.
- [GVS05] J. Grasman, F. Verhulst, and S.D. Shih. The Lyapunov exponents of the van der Pol oscillator. *Math. Meth. Appl. Sci.*, 28(10):1131–1139, 2005.
- [GVW76] J. Grasman, E.J.M. Veling, and G.M. Willems. Relaxation oscillations governed by a van der Pol equation with periodic forcing term. *SIAM J. Appl. Math.*, 31(4):667–676, 1976.
- [GW79] J. Guckenheimer and R.F. Williams. Structural stability of Lorenz attractors. *Inst. Hautes Études Sci. Publ. Math.*, 50:59–72, 1979.
- [GW87] P. Gaspard and X.-J. Wang. Homoclinic orbits and mixed-mode oscillations in far-from-equilibrium systems. *Journal of Statistical Physics*, 48:151–199, 1987.
- [GW92] M. Ghil and G. Wolansky. Non-hamiltonian perturbations of integrable systems and resonance trapping. *SIAM J. Appl. Math.*, 52(4):1148–1171, 1992.
- [GW93] J. Guckenheimer and P. Wolfson. Dynamical systems: some computational problems. In D. Schlesinger, editor, *Bifurcations and Periodic Orbits of Vector Fields*, pages 241–277. Kluwer, 1993.
- [GW00] J. Guckenheimer and A.R. Williams. Asymptotic analysis of subcritical Hopf-homoclinic bifurcation. *Physica D*, 139:195–216, 2000.
- [GW12] M.N. Galtier and G. Wainrib. Multiscale analysis of slow–fast neuronal learning models with noise. *J. Math. Neurosci.*, 2:13, 2012.
- [GWY06] J. Guckenheimer, M. Wechselberger, and L.-S. Young. Chaotic attractors of relaxation oscillations. *Nonlinearity*, 19:701–720, 2006.
- [GX01] P.-L. Gong and J.-X. Xu. Global dynamics and stochastic resonance of the forced FitzHugh–Nagumo neuron model. *Phys. Rev. E*, 63(3):031906, 2001.
- [GYS95] Y. Gutfreund, Y. Yarom, and I. Segev. Subthreshold oscillations and resonant frequency in guinea-pig cortical neurons: physiology and modelling. *J. Physiol.*, 483:621–640, 1995.
- [GYY06] D. Golomb, C. Yue, and Y. Yaari. Contribution of persistent Na^+ current and M-type K^+ current to somatic bursting in CA1 pyramidal cells: combined experimental and modeling study. *J. Neurophysiol.*, 96(4):1912–1926, 2006.
- [GZ06] S. Gil and D.H. Zanette. Coevolution of agents and networks: opinion spreading and community disconnection. *Phys. Lett. A*, 356:89–94, 2006.
- [GZSS96] V. Gol'dshtain, A. Zinoviev, V. Sobolev, and E. Shchepakina. Criterion for thermal explosion with reactant consumption in a dusty gas. *Proc. R. Soc. London A*, 542(1952):2013–2119, 1996.
- [Hab78] P. Habets. On relaxation oscillations in a forced van der Pol oscillator. *Proc. Roy. Soc. Edinburgh A*, 82(1):41–49, 1978.
- [Hab79] R. Haberman. Slowly varying jump and transition phenomena associated with algebraic bifurcation problems. *SIAM J. Appl. Math.*, 37(1):69–106, 1979.
- [Hab91a] R. Haberman. Phase shift modulations for stable, oscillatory, traveling, strongly nonlinear waves. *Stud. Appl. Math.*, 84(1):57–69, 1991.
- [Hab91b] R. Haberman. Standard form and a method of averaging for strongly nonlinear oscillatory dispersive traveling waves. *SIAM J. Appl. Math.*, 51(6):1638–1652, 1991.
- [Har03] J. Härtwich. Viscous profiles for traveling waves of scalar balance laws: the canard case. *Meth. Appl. Anal.*, 10(1):97–118, 2003.
- [Hai05] R. Haiduc. Horseshoes in the forced van der Pol equation. *PhD Thesis, Cornell University*, 2005.
- [Hai09] R. Haiduc. Horseshoes in the forced van der Pol system. *Nonlinearity*, 22:213–237, 2009.
- [Hal66] J.K. Hale. Averaging methods for differential equations with retarded arguments and a small parameter. *J. Differential Equat.*, 2:57–73, 1966.
- [Hal95] G. Haller. Diffusion at intersecting resonances in Hamiltonian systems. *Phys. Lett. A*, 200(1):34–42, 1995.
- [Hal98] G. Haller. Multi-dimensional homoclinic jumping and the discretized NLS equation. *Comm. Math. Phys.*, 193(1):1–46, 1998.

- [Hal99] G. Haller. Homoclinic jumping in the perturbed nonlinear Schrödinger equation. *Comm. Pure Appl. Math.*, 152(1):1–47, 1999.
- [Hal03] B.C. Hall. *Lie Groups, Lie Algebras, and Representations*. Springer, 2003.
- [Hal09] J.K. Hale. *Ordinary Differential Equations*. Dover, New York, NY, 2009.
- [HAL12] Y. Hu, A. Abdulle, and T. Li. Boosted hybrid method for solving chemical reaction systems with multiple scales in time and population size. *Comm. Comp. Phys.*, 12:981–1005, 2012.
- [Hal13] B.C. Hall. *Quantum Theory for Mathematicians*. Springer, 2013.
- [Han95] M. Hanke. Regularizations of differential-algebraic equations revisited. *Math. Nachr.*, 174:159–183, 1995.
- [Han98] H. Hanßmann. The quasi-periodic centre-saddle bifurcation. *J. Differential Equat.*, 142(2):305–370, 1998.
- [Hän02] P. Hänggi. Stochastic resonance in biology how noise can enhance detection of weak signals and help improve biological information processing. *ChemPhysChem*, 3(3):285–290, 2002.
- [Has71] A.H. Nayfeh S.D. Hassan. The method of multiple scales and non-linear dispersive waves. *J. Fluid Mech.*, 48:463–475, 1971.
- [Has75] S.P. Hastings. Some mathematical problems from neurobiology. *The American Mathematical Monthly*, 82(9):881–895, 1975.
- [Has76a] S.P. Hastings. On the existence of homoclinic and periodic orbits in the FitzHugh–Nagumo equations. *Quart. J. Math. Oxford*, 2(27):123–134, 1976.
- [Has76b] S.P. Hastings. On travelling wave solutions of the Hodgkin–Huxley equations. *Arch. Rat. Mech. Anal.*, 60(3):229–257, 1976.
- [Has78] B. Hassard. Bifurcation of periodic solutions of the Hodgkin–Huxley model for the squid giant axon. *J. Theor. Biol.*, 71(3): 401–420, 1978.
- [Has82] S.P. Hastings. Single and multiple pulse waves for the FitzHugh–Nagumo. *SIAM J. Appl. Math.*, 42(2):247–260, 1982.
- [Has83] S.P. Hastings. Formal relaxation oscillations for a model of a catalytic particle. *Quart. Appl. Math.*, 41(4):395–405, 1983.
- [Has10] A. Hastings. Timescales, dynamics, and ecological understanding. *Ecology*, 91:3471–3480, 2010.
- [Hat02] A. Hatcher. *Algebraic Topology*. CUP, 2002.
- [Hau01] W. Hauck. Kinks and rotations in long Josephson junctions. *Math. Meth. Appl. Sci.*, 24(15):1189–1217, 2001.
- [Hay00] T. Hayashi. Mixed-mode oscillations and chaos in a glow discharge. *Phys. Rev. Lett.*, 84(15):3334–3337, 2000.
- [HB12] X. Han and Q. Bi. Slow passage through canard explosion and mixed-mode oscillations in the forced van der Pol's equation. *Nonlinear Dyn.*, 68:275–283, 2012.
- [HBB13a] M. Hasler, V. Belykh, and I. Belykh. Dynamics of stochastically blinking systems. Part I: Finite time properties. *SIAM J. Appl. Dyn. Syst.*, 12(2):1007–1030, 2013.
- [HBB13b] M. Hasler, V. Belykh, and I. Belykh. Dynamics of stochastically blinking systems. Part II: Asymptotic properties. *SIAM J. Appl. Dyn. Syst.*, 12(2):1031–1084, 2013.
- [HBC⁺91] J.J. Healey, D.S. Broomhead, K.A. Cliffe, R. Jones, and T. Mullin. The origins of chaos in a modified van der Pol oscillator. *Physica D*, 48(2):322–339, 1991.
- [HDFS06] I. Horenko, E. Dittmer, A. Fischer, and C. Schütte. Automated model reduction for complex systems exhibiting metastability. *Multiscale Model. Simul.*, 5(3):802–827, 2006.
- [HDK13] M. Holzer, A. Doelman, and T.J. Kaper. Existence and stability of traveling pulses in a reaction-diffusion-mechanics system. *J. Nonlinear Sci.*, 23(1):129–177, 2013.
- [HE93a] L. Holden and T. Erneux. Slow passage through a Hopf bifurcation: from oscillatory to steady state solutions. *SIAM J. Appl. Math.*, 53(4):1045–1058, 1993.
- [HE93b] L. Holden and T. Erneux. Understanding bursting oscillations as periodic slow passages through bifurcation and limit points. *J. Math. Biol.*, 31(4):351–365, 1993.
- [HE05] R.C. Hilborn and R.J. Erwin. Fokker–Planck analysis of stochastic coherence in models of an excitable neuron with noise in both fast and slow dynamics. *Phys. Rev. E*, 72:031112, 2005.
- [Hek01] G. Hek. Fronts and pulses in a class of reaction–diffusion equations: a geometric singular perturbation approach. *Nonlinearity*, 14(1):35–72, 2001.
- [Hek10] G. Hek. Geometric singular perturbation theory in biological practice. *J. Math. Biol.*, 60:347–386, 2010.
- [Hel02] B. Helffer. *Semiclassical Analysis, Witten Laplacians and Statistical Mechanics*. World Scientific, 2002.
- [Hen62] P. Henrici. *Discrete Variable Methods in Ordinary Differential Equations*. Wiley, 1962.
- [Hen70] J. Henrard. On a perturbation theory using Lie transforms. *Celest. Mech.*, 3(1):107–120, 1970.
- [Hen81] D. Henry. *Geometric Theory of Semilinear Parabolic Equations*. Springer, Berlin Heidelberg, Germany, 1981.
- [Hen82] J. Henrard. Capture into resonance: an extension of the use of adiabatic invariants. *Celest. Mech.*, 27(1):3–22, 1982.
- [Hen93] J. Henrard. The adiabatic invariant in classical mechanics. In *Dynamics Reported Vol. 2*, pages 117–235. Springer, 1993.
- [Hen03] M.E. Henderson. Computing invariant manifolds by integrating fat trajectories. *Technical Report RC22944*, IBM Research, 2003.
- [HFKG06] P.J. Holmes, R.J. Full, D. Koditschek, and J. Guckenheimer. The dynamics of legged locomotion: models, analyses, and challenges. *SIAM Rev.*, 48(2):207–304, 2006.
- [HGEK97] A. Hohlo, A. Gavriielides, T. Erneux, and V. Kovani. Localized synchronization in two coupled non-identical semiconductor lasers. *Phys. Rev. Lett.*, 78(25):4745–4748, 1997.
- [HGEK99] A. Hohlo, A. Gavriielides, T. Erneux, and V. Kovani. Quasiperiodic synchronization for two delay-coupled semiconductor lasers. *Phys. Rev. A*, 59(5):3941–3949, 1999.
- [HH52a] A.L. Hodgkin and A.F. Huxley. The components of membrane conductance in the giant axon of *Loligo*. *J. Physiol.*, 116:473–496, 1952.
- [HH52b] A.L. Hodgkin and A.F. Huxley. Currents carried by sodium and potassium ions through the membrane of the giant axon of *Loligo*. *J. Physiol.*, 116:449–472, 1952.

- [HH52c] A.L. Hodgkin and A.F. Huxley. Measurement of current-voltage relations in the membrane of the giant axon of *Loligo*. *J. Physiol.*, 116:424–448, 1952.
- [HH52d] A.L. Hodgkin and A.F. Huxley. A quantitative description of membrane current and its application to conduction and excitation in nerve. *J. Physiol.*, 117:500–544, 1952.
- [HH06] R. Huffaker and R. Hotchkiss. Economic dynamics of reservoir sedimentation management: optimal control with singularly perturbed equations of motion. *J. Econ. Dyn. Contr.*, 30(12):2553–2575, 2006.
- [HHH13] J.M. Hong, C.-H. Hsu, and B.-C. Huang. Geometric singular perturbation approach to the existence and instability of stationary waves for viscous traffic flow models. *Comm. Pure Appl. Anal.*, 12(3):1501–1526, 2013.
- [HHL10a] J.M. Hong, C.-H. Hsu, and W. Liu. Inviscid and viscous stationary waves of gas flow through contracting-expanding nozzles. *J. Differential Equat.*, 248(1):50–76, 2010.
- [HHL10b] J.M. Hong, C.-H. Hsu, and W. Liu. Viscous standing asymptotic states of isentropic compressible flows through a nozzle. *Arch. Rat. Mech. Anal.*, 196(2):575–597, 2010.
- [HHM79] J.L. Hudson, M. Hart, and D. Marinko. An experimental study of multiple peak periodic and non-periodic oscillations in the Belousov–Zhabotinskii reaction. *J. Chem. Phys.*, 71(4):1601–1606, 1979.
- [HHS08] F. Hérau, M. Hitrik, and J. Sjöstrand. Tunnel effect for Kramers–Fokker–Planck type operators. *Ann. Henri Poincaré*, 9(2):209–275, 2008.
- [HVNS11] M. Hirota, M. Holmgren, E.H. van Nes, and M. Scheffer. Global resilience of tropical forest and savanna to critical transitions. *Science*, 334:232–235, 2011.
- [HI97] F.C. Hoppenstaedt and E.M. Izhikevich. *Weakly Connected Neural Networks*. Springer, 1997.
- [HI02] S. Herrmann and P. Imkeller. Barrier crossings characterize stochastic resonance. *Stoch. Dyn.*, 2(3):413–436, 2002.
- [HI05] S. Herrmann and P. Imkeller. The exit problem for diffusions with time-periodic drift and stochastic resonance. *Ann. Appl. Probab.*, 15:39–68, 2005.
- [Hig01] D.J. Higham. An algorithmic introduction to numerical simulation of stochastic differential equations. *SIAM Rev.*, 43(3):525–546, 2001.
- [Hin91] E.J. Hinch. *Perturbation Methods*. CUP, 1991.
- [HIP08] S. Herrmann, P. Imkeller, and D. Peithmann. Large deviations and a Kramers type law for self-stabilizing diffusions. *Ann. Appl. Probab.*, 18(4):1379–1423, 2008.
- [Hir64a] H. Hironaka. Resolution of singularities of an algebraic variety over a field of characteristic zero: I. *Ann. of Math.*, 79(1):109–203, 1964.
- [Hir64b] H. Hironaka. Resolution of singularities of an algebraic variety over a field of characteristic zero: II. *Ann. of Math.*, 79(2):205–326, 1964.
- [Hir67] H. Hironaka. Characteristic polyhedra of singularities. *Kyoto J. Math.*, 7(3):251–293, 1967.
- [HJ01] G.A. Hagedorn and A. Joye. A time-dependent Born–Oppenheimer approximation with exponentially small error estimates. *Comm. Math. Phys.*, 223(3):583–626, 2001.
- [HJS12] S.-Y. Ha, S. Jung, and M. Slemrod. Fast-slow dynamics of planar particle models for flocking and swarming. *J. Differen. Equat.*, 252:2563–2579, 2012.
- [HJZM93] P. Hägggi, P. Jung, C. Zerbe, and F. Moss. Can colored noise improve stochastic resonance? *J. Stat. Phys.*, 70(1):25–47, 1993.
- [HK71] A. Haddad and P. Kokotovic. Note on singular perturbation of linear state regulators. *IEEE Trans. Aut. Contr.*, 16(3):279–281, 1971.
- [HK77] A. Haddad and P. Kokotovic. Stochastic control of linear singularly perturbed systems. *IEEE Trans. Aut. Contr.*, 22(5):815–821, 1977.
- [HK91] J.K. Hale and H. Kocak. *Dynamics and Bifurcations*. Springer, New York, NY, 1991.
- [HK99] H. Haario and L. Kalachev. Model reductions and identifications for multiphase phenomena. *Math. Engrg. Indust.*, 7(4):457–478, 1999.
- [HK00] A.J. Homburg and B. Krauskopf. Resonant homoclinic flip bifurcations. *J. Dyn. Diff. Eq.*, 12(4):807–850, 2000.
- [HKBS07] C.J. Honey, R. Köttner, M. Breakspear, and O. Sporns. Network structure of cerebral cortex shapes functional connectivity on multiple time scales. *Proc. Natl. Acad. Sci.*, 104(24):10240–10245, 2007.
- [HKK95] S.K. Han, C. Kurzer, and Y. Kuramoto. Dephasing and bursting in coupled neural oscillators. *Phys. Rev. Lett.*, 75(17):3190–3193, 1995.
- [KKKO98] M. Hayes, T.J. Kaper, N. Kopell, and K. Ono. On the application of geometric singular perturbation theory to some classical two point boundary value problems. *Int. J. Bif. Chaos*, 8(2): 189–209, 1998.
- [HKN01a] A. Harkin, T.J. Kaper, and A. Nadim. Coupled pulsation and translation of two gas bubbles in a liquid. *J. Fluid Mech.*, 445:377–411, 2001.
- [HKN01b] A.J. Homburg, H. Kokubu, and V. Naudot. Homoclinic-doubling cascades. *Arch. Rational Mech. Anal.*, 160:195–243, 2001.
- [HKO68] G.H. Handelman, J.B. Keller, and R.E. O’Malley. Loss of boundary conditions in the asymptotic solution of linear ordinary differential equations, I eigenvalue problems. *Comm. Pure Appl. Math.*, 21(3):243–261, 1968.
- [HKO+10] E. Harvey, V. Kirk, H.M. Osinga, J. Sneyd, and M. Wechselberger. Understanding anomalous delays in a model of intracellular calcium dynamics. *Chaos*, 20:045104, 2010.
- [HKV05] M. Higuera, E. Knobloch, and J.M. Vega. Dynamics of nearly inviscid Faraday waves in almost circular containers. *Physica D*, 201(1):83–120, 2005.
- [HKWS11] E. Harvey, V. Kirk, M. Wechselberger, and J. Sneyd. Multiple time scales, mixed-mode oscillations and canards in models of intracellular calcium dynamics. *J. Nonlinear Sci.*, 21:639–683, 2011.
- [HL55] S. Haber and N. Levinson. A boundary value problem for a singularly perturbed differential equation. *Proc. Amer. Math. Soc.*, 6(6):866–872, 1955.
- [HL86] M.Y. Hussaini and W.D. Lakin. Existence and non-uniqueness of similarity solutions of a boundary-layer problem. *Quarterly J. Mech. Appl. Math.*, 39:15–24, 1986.
- [HL88] E. Hairer and C. Lubich. Extrapolation at stiff differential equations. *Numer. Math.*, 52(4):377–400, 1988.
- [HL93] J.K. Hale and S.M. Verduyn Lunel. *Introduction to Functional Differential Equations*. Springer, New York, NY, 1993.

- [HL99] J.K. Hale and X.-B. Lin. Multiple internal layer solutions generated by spatially oscillatory perturbations. *J. Differential Equat.*, 154(2):364–418, 1999.
- [HL00a] S. Habib and G. Lythe. Dynamics of kinks: nucleation, diffusion, and annihilation. *Phys. Rev. Lett.*, 84(6):1070–1073, 2000.
- [HL00b] E. Hairer and C. Lubich. Long-time energy conservation of numerical methods for oscillatory differential equations. *SIAM J. Numer. Anal.*, 38(2):414–441, 2000.
- [HL06] W. Horsthemke and R. Lefever. *Noise-Induced Transitions*. Springer, 2006.
- [HLM92] S.P. Hastings, C. Lu, and A.D. MacGillivray. A boundary value problem with multiple solutions from the theory of laminar flow. *SIAM J. Math. Anal.*, 23(1):201–208, 1992.
- [HLM⁺01] A.A. Hill, J. Lu, M. Masino, O.H. Olsen, and R.L. Calabrese. A model of a segmental oscillator in the leech heartbeat neuronal network. *J. Comput. Neurosci.*, 10(3):281–302, 2001.
- [HLN87] M.Y. Hussaini, W.D. Lakin, and A. Nachman. On similarity solutions of a boundary layer problem with an upstream moving wall. *SIAM J. Appl. Math.*, 47(4):699–709, 1987.
- [HLR88] E. Hairer, C. Lubich, and M. Roche. Error of Runge–Kutta methods for stiff problems studied via differential algebraic equations. *BIT*, 28(3):678–700, 1988.
- [HM75] S.P. Hastings and J.D. Murray. The existence of oscillatory solutions in the Field–Noyes model for the Belousov–Zhabotinskii reaction. *SIAM J. Appl. Math.*, 28(3):678–688, 1975.
- [HM77] J. Henrard and K.R. Meyer. Averaging and bifurcations in symmetric systems. *SIAM J. Appl. Math.*, 32(1):133–145, 1977.
- [HM81] J.L. Hudson and J.C. Mankin. Chaos in the Belousov–Zhabotinskii reaction. *J. Chem. Phys.*, 74: 6171–6177, 1981.
- [HM91] S.P. Hastings and J.B. McLeod. On the periodic solutions of a forced second-order equation. *J. Nonlinear Sci.*, 1(2):225–245, 1991.
- [HM09a] M. Hairer and J.C. Mattingly. Slow energy dissipation in anharmonic oscillator chains. *Comm. Pure. Appl. Math.*, 62(8):999–1032, 2009.
- [HM09b] S.P. Hastings and J.B. McLeod. An elementary approach to a model problem of Lagerstrom. *SIAM J. Math. Anal.*, 40(6):2421–2436, 2009.
- [HM09c] P. Hitzcenk and G.S. Medvedev. Bursting oscillations induced by small noise. *SIAM J. Appl. Math.*, 69(5):1359–1392, 2009.
- [HM10] M. Hairer and A.J. Majda. A simple framework to justify linear response theory. *Nonlinearity*, 23(4):909–922, 2010.
- [HM12] S.P. Hastings and J.B. McLeod. *Classical Methods in Ordinary Differential Equations: With Applications to Boundary Value Problems*. AMS, 2012.
- [HM13] M.G. Hennessy and A. Münch. A multiple-scale analysis of evaporation induced Marangoni convection. *SIAM J. Appl. Math.*, 73(2):974–1001, 2013.
- [HMD13] R. Huszak, P. De Maesschalck, and F. Dumortier. Limit cycles in slow–fast codimension 3 saddle and elliptic bifurcations. *J. Differential Equat.*, pages 1–40, 2013. to appear.
- [HMJ10] H. Hu, M. Martina, and P. Jonas. Fast-spiking hippocampal interneurons dendritic mechanisms underlying rapid synaptic activation of fast-spiking hippocampus interneurons. *Science*, 327:52–58, 2010.
- [HMKS01] S. Handrock-Meyer, L.V. Kalachev, and K.R. Schneider. A method to determine the dimension of long-time dynamics in multi-scale systems. *J. Math. Chem.*, 30(2):133–160, 2001.
- [HMML81] J.L. Hudson, J. Mankin, J. McCullough, and P. Lamba. Experiment on chaos in a continuous stirred reactor. In C. Vidal and A. Pacault, editors, *Nonlinear Phenomena in Chemical Dynamics*, pages 44–48. Springer, 1981.
- [HMO83] J.K. Hale, L.T. Magelhaes, and W.M. Oliva. *An Introduction to Infinite Dimensional Dynamical Systems – Geometric Theory*. Springer, 1983.
- [HMOS95] A.F. Hegarty, J.J. Miller, E. O’Riordan, and G.I. Shishkin. Special meshes for finite difference approximations to an advection–diffusion equation with parabolic layers. *J. Comput. Phys.*, 117: 47–54, 1995.
- [HMP96] B. Hutcheon, R.M. Miura, and E. Puil. Subthreshold membrane resonance in neocortical neurons. *J. Neurophysiol.*, 76(2):683–697, 1996.
- [HMS85] J. Honerkamp, G. Mutschler, and R. Seitz. Coupling of a slow and a fast oscillator can generate bursting. *Bull. Math. Biol.*, 47(1):1–21, 1985.
- [HMS04] W. Huisings, S. Meyn, and C. Schütte. Phase transitions and metastability in Markovian and molecular systems. *Ann. Prob.*, 14(1):419–458, 2004.
- [HN01] F. Hamel and N. Nadirashvili. Travelling fronts and entire solutions of the Fisher–KPP equation in \mathbb{R}^N . *Arch. Ration. Mech. Anal.*, 157:91–163, 2001.
- [HN04] B. Helffer and F. Nier. Quantitative analysis of metastability in reversible diffusion processes via a Witten complex approach: the case with boundary. *Mat. Contemp.*, 26:41–85, 2004.
- [HN05] B. Helffer and F. Nier. *Hypoelliptic Estimates and Spectral Theory for Fokker–Planck Operators and Witten Laplacians*, volume 1862 of *Lect. Notes Math.* Springer, 2005.
- [HNMM10] A. Haselbacher, F.M. Najar, L. Massa, and R.D. Moser. Slow-time acceleration for modeling multiple-time-scale problems. *J. Comput. Phys.*, 229(2):325–342, 2010.
- [HO96] M.J.B. Hauser and L.F. Olsen. Mixed-mode oscillations and homoclinic chaos in an enzyme reaction. *J. Chem. Soc. Faraday Trans.*, 92(16):2857–2863, 1996.
- [HOBS97] M.J.B. Hauser, L.F. Olsen, T.V. Bronnikova, and W.M. Schaffer. Routes to chaos in the peroxydase–oxidase reaction: period-doubling and period-adding. *J. Phys. Chem. B*, 101:5075–5083, 1997.
- [Hog03] S.J. Hogan. Relaxation oscillations in a system with a piecewise smooth drag coefficient. *J. Sound Vibration*, 263(2):467–471, 2003.
- [Hol80] P.J. Holmes. Averaging and chaotic motions in forced oscillations. *SIAM J. Appl. Math.*, 38(1):65–80, 1980.
- [Hol84] P.J. Holmes. Bifurcation sequences in horseshoe maps: infinitely many routes to chaos. *Phys. Lett. A*, 104(6):299–302, 1984.
- [Hol86] P.J. Holmes. Knotted periodic orbits in suspensions of Smale’s horseshoe: period multiplying and cabled knots. *Physica D*, 21(1):7–41, 1986.

- [Hol95] M.H. Holmes. *Introduction to Perturbation Methods*. Springer, 1995.
- [Hol99] M.H. Holmes. The method of multiple scales. In *Analyzing Multiscale Phenomena using Singular Perturbation Methods*, pages 23–46. AMS, 1999.
- [Hol00] R.A. Holmgren. A first course in discrete dynamical systems. *Springer*, 2000.
- [Hop66] F.C. Hoppenstaedt. Singular perturbations on the infinite interval. *Trans. Amer. Math. Soc.*, 123(2):521–535, 1966.
- [Hop68] F.C. Hoppenstaedt. Asymptotic stability in singular perturbation problems. *J. Differential Equat.*, 4:350–358, 1968.
- [Hop70] F.C. Hoppenstaedt. Cauchy problems involving a small parameter. *Bull. Amer. Math. Soc.*, 76:142–146, 1970.
- [Hop71] F.C. Hoppenstaedt. Properties of solutions of ordinary differential equations with small parameters. *Comm. Pure Appl. Math.*, 24(6):807–840, 1971.
- [Hop74] F.C. Hoppenstaedt. Asymptotic stability in singular perturbation problems. II: Problems having matched asymptotic expansion solutions. *J. Differential Equat.*, 15(3):510–521, 1974.
- [Hop75] F.C. Hoppenstaedt. Analysis of some problems having matched asymptotic expansion solutions. *SIAM Rev.*, 17:123–135, 1975.
- [Hop76] F.C. Hoppenstaedt. A slow selection analysis of two locus, two allele traits. *Theor. Popul. Biol.*, 9: 68–81, 1976.
- [Hop95] F.C. Hoppenstaedt. Singular perturbation solutions of noisy systems. *SIAM J. Appl. Math.*, 55(2): 544–551, 1995.
- [How75] F.A. Howes. Singularly perturbed nonlinear boundary value problems with turning points. *SIAM J. Math. Anal.*, 6(4):644–660, 1975.
- [How76a] F.A. Howes. Effective characterization of the asymptotic behavior of solutions of singularly perturbed boundary value problems. *SIAM J. Appl. Math.*, 30(2):296–306, 1976.
- [How76b] F.A. Howes. *Singular perturbations and differential inequalities*, volume 5 of *Memoirs of the Amer. Math. Soc.* AMS, 1976.
- [How78a] F.A. Howes. The asymptotic solution of a class of singularly perturbed nonlinear boundary value problems via differential inequalities. *SIAM J. Math. Anal.*, 9(2):215–249, 1978.
- [How78b] F.A. Howes. *Boundary-interior layer interactions in nonlinear singular perturbation theory*, volume 203 of *Memoirs of the Amer. Math. Soc.* AMS, 1978.
- [How78c] F.A. Howes. Singularly perturbed boundary value problems with angular limiting solutions. *Trans. Amer. Math. Soc.*, 241: 155–182, 1978.
- [How78d] F.A. Howes. Singularly perturbed nonlinear boundary value problems with turning points. II. *SIAM J. Math. Anal.*, 9(2):250–271, 1978.
- [How79a] F.A. Howes. An improved boundary layer estimate for a singularly perturbed initial value problem. *Math. Zeitschr.*, 165(2):135–142, 1979.
- [How79b] F.A. Howes. Singularly perturbed semilinear elliptic boundary value problems. *Comm. Partial Diff. Eq.*, 4:1–39, 1979.
- [How01] J. Howald. Multiplier ideals of monomial ideals. *Trans. Amer. Math. Soc.*, 353(7):2665–2671, 2001.
- [How10] C.J. Howls. Exponential asymptotics and boundary-value problems: keeping both sides happy at all orders. *Proc. R. Soc. A*, 466(2121):2771–2794, 2010.
- [Hoy06] R. Hoyle. *Pattern Formation: An Introduction to Methods*. Cambridge University Press, 2006.
- [HP70] M.W. Hirsch and C.C. Pugh. Stable manifolds and hyperbolic sets. In S.-S. Chern and S. Smale, editors, *Global Analysis (Proc. Sympos. Pure Math., Vol. XIV, Berkeley, Calif., 1968)*, pages 133–163. AMS, 1970.
- [HP05] B. Hasselblatt and Y. Pesin. Partially hyperbolic dynamical systems. In *Handbook of Dynamical Systems 1B*, pages 1–55. Elsevier, 2005.
- [HPK08] M. Higuera, J. Porter, and E. Knobloch. Faraday waves, streaming flow, and relaxation oscillations in nearly circular containers. *Chaos*, 18(1):015104, 2008.
- [HPS77] M.W. Hirsch, C.C. Pugh, and M. Shub. *Invariant Manifolds*. Springer, 1977.
- [HPS11] H.J. Hupkes, D. Pelinovsky, and B. Sandstede. Propagation failure in the discrete Nagumo equation. *Proc. Amer. Math. Soc.*, 139:3537–3551, 2011.
- [HPT00] J.K. Hale, L.A. Peletier, and W.C. Troy. Exact homoclinic and heteroclinic solutions of the Gray–Scott model for autocatalysis. *SIAM J. Appl. Math.*, 61(1):102–130, 2000.
- [HR78] P.J. Holmes and D.A. Rand. Bifurcations of the forced van der Pol oscillator. *Quarterly Appl. Math.*, 35:495–509, 1978.
- [HR82] J.L. Hindmarsh and R.M. Rose. A model of the nerve impulse using two first-order differential equations. *Nature*, 296:162–164, 1982.
- [HR84] J.L. Hindmarsh and R.M. Rose. A model of neuronal bursting using three coupled first order differential equations. *Proc. Roy. Soc. London B*, 221(1222):87–102, 1984.
- [HR94] J.L. Hindmarsh and R.M. Rose. A model for rebound bursting in mammalian neurons. *Proc. Roy. Soc. London B*, 346(1316):129–150, 1994.
- [HR02] E.L. Haseltine and Rawlings. Approximate simulation of coupled fast and slow reactions for stochastic chemical kinetics. *J. Chem. Phys.*, 117(15):6959–6969, 2002.
- [HR09] M. El Hajji and A. Rapaport. Practical coexistence of two species in the chemostat - a slow–fast characterization. *Math. Biosci.*, 218(1):33–39, 2009.
- [HRR94] W. Huang, Y. Ren, and R.D. Russell. Moving mesh partial differential equations (MMPDES) based on the equidistribution principle. *SIAM J. Numer. Anal.*, 31(3):709–730, 1994.
- [HS84] B. Helffer and J. Sjostrand. Multiple wells in the semi-classical limit I. *Comm. Partial Diff. Equat.*, 9(4):337–408, 1984.
- [HS93] T. Hauck and F.W. Schneider. Mixed-mode and quasiperiodic oscillations in the peroxidase-oxidase reaction. *J. Phys. Chem.*, 97:391–397, 1993.
- [HS94] T. Hauck and F.W. Schneider. Chaos in a Farey sequence through period doubling in the peroxidase-oxidase reaction. *J. Phys. Chem.*, 98:2072–2077, 1994.
- [HS98] H. Hofmann and S.R. Sanders. Speed-sensorless vector torque control of induction machines using a two-time-scale approach. *IEEE Trans. Ind. Appl.*, 34:169–177, 1998.

- [HS99] P.-F. Hsieh and Y. Sibuya. *Basic Theory of Ordinary Differential Equations*. Springer, 1999.
- [HS04] D. Holcman and Z. Schuss. Escape through a small opening: receptor trafficking in a synaptic membrane. *J. Stat. Phys.*, 117(5):975–1014, 2004.
- [HS05] A. Huber and P. Szmolyan. Geometric singular perturbation analysis of the Yamada model. *SIAM J. Applied Dynamical Systems*, 4(3):607–648, 2005.
- [HS08] G. Haller and T. Sapsis. Where do inertial particles go in fluid flows? *Physica D*, 237(5):573–583, 2008.
- [HS09] S.-B. Hsu and J. Shi. Relaxation oscillation profile of limit cycle in predator-prey system. *Discr. Cont. Dyn. Syst. B*, 11(4):893–911, 2009.
- [HS10a] S.-Y. Ha and M. Slemrod. Flocking dynamics of singularly perturbed oscillator chain and the Cucker-Smale system. *J. Dyn. Diff. Eq.*, 22:325–330, 2010.
- [HS10b] A.J. Homburg and B. Sandstede. Homoclinic and heteroclinic bifurcations in vector fields. In H. Broer, F. Takens, and B. Hasselblatt, editors, *Handbook of Dynamical Systems III*, pages 379–524. Elsevier, 2010.
- [HS10c] H.J. Hupkes and B. Sandstede. Traveling pulse solutions for the discrete FitzHugh–Nagumo system. *SIAM J. Appl. Dyn. Sys.*, 9(3):827–882, 2010.
- [HS11] S.-Y. Ha and M. Slemrod. A fast–slow dynamical systems theory for the Kuramoto type phase model. *J. Differential Equat.*, 251(10):2685–2695, 2011.
- [HS12] M. Holzer and A. Scheel. A slow pushed front in a Lotka–Volterra competition model. *Nonlinearity*, 25(7):2151–2179, 2012.
- [HS13] H.J. Hupkes and B. Sandstede. Stability of traveling pulse solutions for the discrete FitzHugh–Nagumo system. *Trans. Amer. Math. Soc.*, 365:251–301, 2013.
- [HSD03] M.W. Hirsch, S. Smale, and R. Devaney. *Differential Equations, Dynamical Systems, and an Introduction to Chaos*. Academic Press, 2nd edition, 2003.
- [Hsi65] P.F. Hsieh. A turning point problem for a system of linear ordinary differential equations of the third order. *Arch. Rat. Mech. Anal.*, 19(2):117–148, 1965.
- [HR95] Y.-F. Hung, I. Schreiber, and J. Ross. New reaction mechanism for the oscillatory peroxidase-oxidase reaction and comparison with experiments. *J. Phys. Chem.*, 99:1980–1987, 1995.
- [HSS97] P.W. Hemker, G.I. Shishkin, and L.P. Shishkina. The use of defect correction for the solution of parabolic singular perturbation problems. *Z. Angew. Math. Mech.*, 77(1):59–74, 1997.
- [HSS00] P.W. Hemker, G.I. Shishkin, and L.P. Shishkina. ϵ -uniform schemes with high-order time-accuracy for parabolic singular perturbation problems. *IMA J. Numer. Anal.*, 20(1):99–121, 2000.
- [HT90] C. Hunter and M. Tajdari. Singular complex periodic solutions of van der Pol's equation. *SIAM J. Appl. Math.*, 50(6):1764–1779, 1990.
- [HTB90a] P. Hägggi, P. Tulkner, and M. Borkovec. Reaction-rate theory: fifty years after Kramers. *Rev. Mod. Phys.*, 62(2):251–341, 1990.
- [HTB90b] C. Hunter, M. Tajdari, and S.D. Boyer. On Lagerstrom's model of slow incompressible viscous flow. *SIAM J. Appl. Math.*, 50(1):48–63, 1990.
- [Hua05] Y. Huang. How do cross-migration models arise? *Math. Biosci.*, 195(2):127–140, 2005.
- [Hur13] D.E. Hurtubise. Three approaches to Morse–Bott homology. *arXiv:1208.5066v2*, pages 1–35, 2013.
- [HV97] R.J.A.G. Huveneers and F. Verhulst. A metaphor for adiabatic evolution to symmetry. *SIAM J. Appl. Math.*, 57(5):1421–1442, 1997.
- [HV03] W. Hundsdorfer and J.G. Verwer. *Numerical Solution of Time-dependent Advection-Diffusion-Reaction Equations*. Springer, 2003.
- [HV07] G. Hek and N. Valkhoff. Pulses in a complex Ginzburg–Landau system: persistence under coupling with slow diffusion. *Physica D*, 232(1):62–85, 2007.
- [HW85] P.J. Holmes and R.F. Williams. Knotted periodic orbits in suspensions of Smale's horseshoe: torus knots and bifurcation sequences. *Arch. Rat. Mech. Anal.*, 90(2):115–194, 1985.
- [HW91a] E. Hairer and G. Wanner. *Solving Ordinary Differential Equations I*. Springer, 1991.
- [HW91b] E. Hairer and G. Wanner. *Solving Ordinary Differential Equations II*. Springer, 1991.
- [HW93] G. Haller and S. Wiggins. Orbits homoclinic to resonances: the Hamiltonian case. *Physica D*, 66(3):298–346, 1993.
- [HW95] G. Haller and S. Wiggins. N-pulse homoclinic orbits in perturbations of resonant Hamiltonian systems. *Arch. Rat. Mach. Anal.*, 130(1):25–101, 1995.
- [HW10] A. Hastings and D.B. Wysham. Regime shifts in ecological systems can occur with no warning. *Ecol. Lett.*, 13:464–472, 2010.
- [HWF87] R.M. Harris-Warrick and R.E. Flamm. Multiple mechanisms of bursting in a conditional bursting neuron. *J. Neurosci.*, 7(7):2113–2128, 1987.
- [HYL12] D. Hu, J. Yang, and X. Liu. Delay-induced vibrational multiresonance in FitzHugh–Nagumo system. *Commun. Nonlinear Sci. Numer. Simulat.*, 17:1031–1035, 2012.
- [HYY09] C.-H. Hsu, T.-H. Yang, and C.-R. Yang. Diversity of traveling wave solutions in FitzHugh–Nagumo type equations. *J. Differential Equat.*, 247(4):1185–1205, 2009.
- [HZKW09] H.M. Hådin, A. Zagaris, K. Krab, and H.V. Westerhoff. Simplified yet highly accurate enzyme kinetics for cases of low substrate concentrations. *FEBS J.*, 276(19):5491–5506, 2009.
- [IBS98] P. Iannelli, S. Baigent, and J. Stark. Inertial manifolds for dynamics of cells coupled by gap junctions. *Dynamics and Stability of Systems*, 13(2):187–213, 1998.
- [IH03] E. Izhikevich and F. Hoppensteadt. Slowly coupled oscillators: phase dynamics and synchronization. *SIAM J. Appl. Math.*, 63(6):1935–1953, 2003.
- [IH04] E. Izhikevich and F. Hoppensteadt. Classification of bursting mappings. *Int. J. Bif. Chaos*, 14(11):3847–3854, 2004.
- [IK85] P. Ioannou and P. Kokotovic. Decentralized adaptive control of interconnected systems with reduced-order models. *Automatica*, 21(4):401–412, 1985.
- [Ike89] G. Ikegami. Singular perturbations in foliations. *Invent. Math.*, 95(2):215–246, 1989.
- [IKKB09] G. Iñiguez, J. Kertész, K.K. Kaski, and R.A. Barrio. Opinion and community formation in coevolving networks. *Phys. Rev. E*, 80(6):066119, 2009.

- [IKKB11] G. Iñiguez, J. Kertész, K.K. Kaski, and R.A. Barrio. Phase change in an opinion-dynamics model with separation of time scales. *Phys. Rev. E*, 83:016111, 2011.
- [IKY99] A.M. Il'in, R.Z. Khasminskii, and G. Yin. Asymptotic expansions of solutions of integro-differential equations for transition densities of singularly perturbed switching diffusions: rapid switchings. *J. Math. Anal. Appl.*, 238(2):516–539, 1999.
- [Il'69] A.M. Il'in. Differencing scheme for a differential equation with a small parameter affecting the highest derivative. *Math. Notes Acad. Sci. USSR*, 6(2):596–602, 1969.
- [IL99] Yu. Ilyashenko and W. Li. *Nonlocal Bifurcations*. AMS, 1999.
- [ILNV02] A.P. Itin, R. De La Llave, A.I. Neishtadt, and A.A. Vasiliev. Transport in a slowly perturbed convective cell flow. *Chaos*, 12(4):1043–1053, 2002.
- [Ily97] Yu. Ilyashenko. Embedding theorems for local maps, slow–fast systems and bifurcation from Morse–Smale to Morse–Williams. *Amer. Math. Soc. Transl.*, 180(2):127–139, 1997.
- [Ily02] Yu. Ilyashenko. Centennial history of Hilbert's 16th problem. *Bull. Amer. Math. Soc.*, 39(3):301–354, 2002.
- [IM94] M. Itoh and H. Murakami. Chaos and canards in the van der Pol equation with periodic forcing. *Int. J. Bif. Chaos*, 4(4):1023–1029, 1994.
- [IN94] T. Ikeda and Y. Nishiura. Pattern selection for two breathers. *SIAM J. Appl. Math.*, 54(1):195–230, 1994.
- [IN12] A.P. Itin and A.I. Neishtadt. Fermi acceleration in time-dependent rectangular billiards due to multiple passages through resonances. *Chaos*, 22(2):026119, 2012.
- [INV00] A.P. Itin, A.I. Neishtadt, and A.A. Vasiliev. Captures into resonance and scattering on resonance in dynamics of a charged relativistic particle in magnetic field and electrostatic wave. *Physica D*, 141(3):281–296, 2000.
- [IP01] P. Imkeller and I. Pavlyukevich. Stochastic resonance in two-state Markov chains. *Archiv Math.*, 77:107–115, 2001.
- [IP02] P. Imkeller and I. Pavlyukevich. Model reduction and stochastic resonance. *Stoch. Dyn.*, 2(4):463–506, 2002.
- [IP06a] P. Imkeller and I. Pavlyukevich. First exit times of SDEs driven by stable Lévy processes. *Stoch. Process. Appl.*, 116(4):611–642, 2006.
- [IP06b] P. Imkeller and I. Pavlyukevich. Lévy flights: transitions and meta-stability. *J. Phys. A*, 39(15):L237, 2006.
- [IPW09] P. Imkeller, I. Pavlyukevich, and T. Wetzel. First exit times for Lévy-driven diffusions with exponentially light jumps. *Ann. Probab.*, 37(2):530–564, 2009.
- [Irw70] M.C. Irwin. On the stable manifold theorem. *Bull. London Math. Soc.*, 2(2):196–198, 1970.
- [Irw80] M.C. Irwin. A new proof of the pseudostable manifold theorem. *J. London Math. Soc.*, 2(3):557–566, 1980.
- [IS63] M. Iwano and Y. Sibuya. Reduction of the order of a linear ordinary differential equation containing a small parameter. *Kodai Math. J.*, 15:1–28, 1963.
- [IS90] P. Ibison and K. Scott. Detailed bifurcation structure and new mixed-mode oscillations of the Belousov–Zhabotinskii reaction in a stirred flow reactor. *J. Chem. Soc. Faraday Trans.*, 86(22):3695–3700, 1990.
- [IS01] Yu. Ilyashenko and M. Saprykina. Embedding theorems for local families and oscillatory slow–fast systems. In *Progress in Nonlinear Science*, volume 1, pages 389–410. Inst. Appl. Phys., 2001.
- [Ise77] A. Iserles. Functional fitting - new family of schemes for integration of stiff ODE. *Math. Comput.*, 31:112–123, 1977.
- [Ise81] A. Iserles. Quadrature methods for stiff ordinary differential systems. *Math. Comput.*, 36:171–182, 1981.
- [Ise84] A. Iserles. Composite methods for numerical solution of stiff systems of ODEs. *SIAM J. Num. Anal.*, 21:340–351, 1984.
- [Ise96] A. Iserles. *A First Course in the Numerical Analysis of Differential Equations*. CUP, 1996.
- [Ise02] A. Iserles. On the global error of discretization methods for highly-oscillatory ordinary differential equations. *BIT*, 42:561–599, 2002.
- [ISKB92] A. Isidori, S.S. Sastry, P.V. Kokotovic, and C.I. Byrnes. Singularly perturbed zero dynamics of nonlinear systems. *IEEE Trans. Auto. Contr.*, 37(10):1625–1631, 1992.
- [Ito84] M. Ito. A remark on singular perturbation methods. *Hiroshima Math. J.*, 14:619–629, 1984.
- [IVKS07] A.P. Itin, A.A. Vasiliev, G. Krishna, and S.Watanabe. Change in the adiabatic invariant in a nonlinear two-mode model of Feshbach resonance passage. *Physica D*, 232:108–115, 2007.
- [IW87] S. Iyer and C.M. Will. Black-hole normal modes: A WKB approach. I. Foundations and application of a higher-order WKB analysis of potential-barrier scattering. *Phys. Rev. D*, 35(12):3621, 1987.
- [IW02] D. Iron and M.J. Ward. The dynamics of multispike solutions to the one-dimensional Gierer–Meinhardt model. *SIAM J. Appl. Math.*, 62(6):1924–1951, 2002.
- [Iwa08] M. Iwasa. Solution of reduced equations derived with singular perturbation methods. *Phys. Rev. E*, 78:066213, 2008.
- [IWW01] D. Iron, M.J. Ward, and J. Wei. The stability of spike solutions to the one-dimensional Gierer–Meinhardt model. *Physica D*, 150(1):25–62, 2001.
- [IY08] Yu. Ilyashenko and S. Yakovenko. *Lectures on Analytic Differential Equations*. AMS, 2008.
- [Izh00a] E. Izhikevich. Neural excitability, spiking, and bursting. *Int. J. Bif. Chaos*, 10:1171–1266, 2000.
- [Izh00b] E. Izhikevich. Phase equations for relaxation oscillators. *SIAM J. Appl. Math.*, 60(5):1789–1805, 2000.
- [Izh00c] E. Izhikevich. Subcritical elliptic bursting of Bautin type. *SIAM J. Appl. Math.*, 60(2):503–535, 2000.
- [Izh01] E. Izhikevich. Synchronization of elliptic bursters. *SIAM Rev.*, 43(2):315–344, 2001.
- [Izh03] E. Izhikevich. Simple model of spiking neurons. *IEEE Trans. Neural Netw.*, 14(6):1569–1572, 2003.
- [Izh04] E. Izhikevich. Which model to use for cortical spiking neurons? *IEEE Trans. Neural Netw.*, 15(5):1063–1070, 2004.
- [Izh07] E. Izhikevich. *Dynamical Systems in Neuroscience*. MIT Press, 2007.
- [JAB⁺01] G. Jongen, J. Anemüller, D. Bollé, A.C.C. Coolen, and C. Pérez-Vicente. Coupled dynamics of fast spins and slow exchange interactions in the XY spin glass. *J. Phys. A*, 34(19):3957–3984, 2001.

- [Jah04] T. Jahnke. Long-time-step integrators for almost-adiabatic quantum dynamics. *SIAM J. Sci. Comput.*, 25:2145–2164, 2004.
- [Jak13] P. Jakobsen. Introduction to the method of multiple scales. *arXiv:1312.3651*, pages 1–63, 2013.
- [Jal04] J. Jalics. Slow waves in mutually inhibitory neuronal networks. *Physica D*, 192:95–122, 2004.
- [Jan89] J.A.M. Janssen. The elimination of fast variables in complex chemical reactions. I. Macroscopic level. *J. Stat. Phys.*, 57(1):157–169, 1989.
- [Jän94] K. Jänich. *Linear Algebra*. Springer, 1994.
- [Jän01] K. Jänich. *Vector Analysis*. Springer, 2001.
- [Jan03] M. Janowicz. Method of multiple scales in quantum optics. *Phys. Rep.*, 375(5):327–410, 2003.
- [Jav78a] S.H. Javid. The time-optimal control of a class of non-linear singularly perturbed systems. *Int. J. Contr.*, 27(6):831–836, 1978.
- [Jav78b] S.H. Javid. Uniform asymptotic stability of linear time-varying singularly perturbed systems. *J. Frankl. Inst.*, 305:27–37, 1978.
- [JCdBS10] M.R. Jeffrey, A.R. Champneys, M. di Bernardo, and S.W. Shaw. Catastrophic sliding bifurcations and onset of oscillations in a superconducting resonator. *Phys. Rev. E*, 81:016213, 2010.
- [Jef24] H. Jeffreys. On certain approximate solutions of linear differential equations of the second order. *Proc. London Math. Soc.*, 23:428–436, 1924.
- [JF96] E.M. De Jager and J. Furu. *The Theory of Singular Perturbations*. North-Holland, 1996.
- [JGB⁺03] W. Just, K. Gelfert, N. Baba, A. Riepert, and H. Kantz. Elimination of fast chaotic degrees of freedom: on the accuracy of the Born approximation. *J. Stat. Phys.*, 112:277–292, 2003.
- [JH91] P. Jung and P. Hägggi. Amplification of small signals via stochastic resonance. *Phys. Rev. A*, 44(12):8032, 1991.
- [JKK97] M.E. Johnson, M.S. Jolly, and I.G. Kevrekidis. Two-dimensional invariant manifolds and global bifurcations: some approximation and visualization studies. *Num. Alg.*, 14(1):125–140, 1997.
- [J JL05] J. Jansson, C. Johnson, and A. Logg. Computational modeling of dynamical systems. *Math. Mod. Meth. Appl. Sci.*, 15(3):471, 2005.
- [JK75] J. Jarník and J. Kurzweil. Ryabov's special solutions of functional differential equations. *Boll. Un. Mat. Ital.*, (4), 11(3):198–208, 1975.
- [JK77] S.H. Javid and P.V. Kokotovic. A decomposition of time scales for iterative computation of time-optimal controls. *J. Optim. Theor. Appl.*, 21(4):459–468, 1977.
- [JK86] C.K.R.T. Jones and T. Küpper. On the infinitely many solutions of a semilinear elliptic equation. *SIAM J. Math. Anal.*, 17(4):803–835, 1986.
- [JK94a] H. JahnSEN and S. Karnup. A spectral analysis of the integration of artificial synaptic potentials in mammalian central neurons. *Brain Res.*, 666:9–20, 1994.
- [JK94b] C.K.R.T. Jones and N. Kopell. Tracking invariant manifolds with differential forms in singularly perturbed systems. *J. Differential Equat.*, 108(1):64–88, 1994.
- [JKK96] C.K.R.T. Jones, T.J. Kaper, and N. Kopell. Tracking invariant manifolds up to exponentially small errors. *SIAM J. Math. Anal.*, 27(2):558–577, 1996.
- [JKL01] C.K.R.T. Jones, N. Kopell, and R. Langer. Construction of the FitzHugh–Nagumo pulse using differential forms. In *Multiple-Time-Scale Dynamical Systems*, pages 101–113. Springer, 2001.
- [JKP91] A. Joye, H. Kunz, and C.E. Pfister. Exponential decay and geometric aspect of transition probabilities in the adiabatic limit. *Ann. Phys.*, 208(2):299–332, 1991.
- [JKR10] J. Jalics, M. Krupa, and H.G. Rotstein. Mixed-mode oscillations in a three time-scale system of ODEs motivated by a neuronal model. *Dynamical Systems*, 25(4):445–482, 2010.
- [JKRH01] W. Just, H. Kantz, C. Röderbeck, and M. Helm. Stochastic modelling: replacing fast degrees of freedom by noise. *J. Phys. A*, 34:3199–3213, 2001.
- [JKT90] M.S. Jolly, I.G. Kevrekidis, and E.S. Titi. Approximate inertial manifolds for the Kuramoto–Sivashinsky equation: analysis and computations. *Physica D*, 44(1):38–60, 1990.
- [JL92] W. Jäger and S. Luckhaus. On explosions of solutions to a system of partial differential equations modelling chemotaxis. *Trans. Amer. Math. Soc.*, 329(2):819–824, 1992.
- [JL98] K.M. Jansons and G.D. Lythe. Stochastic calculus: application to dynamic bifurcations and threshold crossings. *J. Stat. Phys.*, 90:227–251, 1998.
- [JL03a] T. Jahnke and C. Lubich. Numerical integrators for quantum dynamics close to the adiabatic limit. *Numerische Mathematik*, 94:289–314, 2003.
- [JL03b] Z. Jia and B. Leimkuhler. A parallel multiple time-scale reversible integrator for dynamics simulation. *Future Gen. Comp. Syst.*, 19:415–424, 2003.
- [JL06] Z. Jia and B. Leimkuhler. Geometric integrators for multiple timescale simulation. *J. Phys. A*, 439:5379–5403, 2006.
- [JMS11] S. Jin, P. Markowich, and C. Sparber. Mathematical and computational methods for semiclassical Schrödinger equations. *Acta Numer.*, 20:121–209, 2011.
- [Joh82] F. John. *Partial Differential Equations*. Springer, 1982.
- [John05] R.S. Johnson. *Singular Perturbation Theory*. Springer, 2005.
- [Jon84] C.K.R.T. Jones. Stability of the travelling wave solution of the FitzHugh–Nagumo system. *Trans. Amer. Math. Soc.*, 286(2): 431–469, 1984.
- [Jon95] C.K.R.T. Jones. Geometric singular perturbation theory. In *Dynamical Systems (Montecatini Terme, 1994)*, volume 1609 of *Lect. Notes Math.*, pages 44–118. Springer, 1995.
- [Jos98] K. Josic. Invariant manifolds and synchronization of coupled dynamical systems. *Phys. Rev. Lett.*, 80(14):3053–3056, 1998.
- [Jos00] K. Josic. Synchronization of chaotic systems and invariant manifolds. *Nonlinearity*, 13(4):1321–1336, 2000.
- [Jos06] J. Jost. *Partial Differential Equations*. Springer, 2006.
- [Joy94] A. Joye. Proof of the Landau-Zener formula. *Asymp. Anal.*, 9(3):209–258, 1994.
- [JP91a] A. Joye and C.E. Pfister. Exponentially small adiabatic invariant for the Schrödinger equation. *Comm. Math. Phys.*, 140(1):15–41, 1991.
- [JP91b] A. Joye and C.E. Pfister. Full asymptotic expansion of transition probabilities in the adiabatic limit. *J. Phys. A*, 24(4):753, 1991.

- [JP93] A. Joye and C.E. Pfister. Superadiabatic evolution and adiabatic transition probability between two nondegenerate levels isolated in the spectrum. *J. Math. Phys.*, 34(2):454, 1993.
- [JP04] J. Jacod and P. Protter. *Probability Essentials*. Springer, 2004.
- [Jr60] W.A. Harris Jr. Singular perturbations of two-point boundary problems for systems of ordinary differential equations. *Arch. Rat. Mech. Anal.*, 5(1):212–225, 1960.
- [Jr62] W.A. Harris Jr. Singular perturbations of a boundary value problem for a nonlinear system of differential equations. *Duke Math. J.*, 29(3):429–445, 1962.
- [JRH98] C.K.R.T. Jones and J.E. Rubin. Existence of standing pulse solutions to an inhomogeneous reaction-diffusion system. *J. Dyn. Diff. Eq.*, 10(1):1–35, 1998.
- [JS95] D.A. Jones and A.M. Stuart. Attractive invariant manifolds under approximation part I: inertial manifolds. *J. Differential Equat.*, 123(2):588–637, 1995.
- [JT09] C.K.R.T. Jones and S.-K. Tin. Generalized exchange lemmas and orbits heteroclinic to invariant manifolds. *Discr. Cont. Dyn. Syst. S*, 2(4):967–1023, 2009.
- [Jün09] A. Jüngel. *Transport Equations for Semiconductors*. Springer, 2009.
- [JZLZ13] L. Ji, J. Zhang, X. Lang, and X. Zhang. Coupling and noise induced spiking-bursting transition in a parabolic bursting model. *Chaos*, 23:013141, 2013.
- [KA11] J. Kumar and G. Ananthakrishna. Multi-scale modeling approach to acoustic emission during plastic deformation. *Phys. Rev. Lett.*, 106:106001, 2011.
- [KAAA13] M. Krupa, B. Ambrosio, and M.A. Aziz-Alaoui. Weakly coupled two slow–two fast systems, folded node and mixed mode oscillations. *arXiv:1302.1800v1*, pages 1–19, 2013.
- [KACW82] P.V. Kokotovic, B. Avramovic, J.H. Chow, and J.R. Winkelman. Coherency based decomposition and aggregation. *Automatica*, 18:47–56, 1982.
- [Kal03] V. Kaloshin. The existential Hilbert 16-th problem and an estimate for cyclicity of elementary polycycles. *Invent. Math.*, 151(3):451–512, 2003.
- [Kal13] V.I. Kalachev. On the algebraic fundamentals of singular perturbation theory. *Differential Equat.*, 49(3):397–401, 2013.
- [Kam04] J. Kamimoto. Newton polyhedra and the Bergman kernel. *Math. Z.*, 246:405–440, 2004.
- [Kap98] T. Kapitula. Bifurcating bright and dark solitary waves for the perturbed cubic-quintic nonlinear Schrödinger equation. *Proc. R. Soc. Edinburgh A*, 128(3):585–629, 1998.
- [Kap99] T.J. Kaper. An introduction to geometric methods and dynamical systems theory for singular perturbation problems. In J. Cronin and R.E. O’Malley, editors, *Analyzing Multiscale Phenomena Using Singular Perturbation Methods*, pages 85–131. Springer, 1999.
- [Kap05] T. Kapitula. Stability analysis of pulses via the Evans function: dissipative systems. In *Dissipative Solitons*, volume 661 of *Lecture Notes in Physics*, pages 407–427. Springer, 2005.
- [Kar49] G. Karreman. Some types of relaxation oscillations as models of all-or-none phenomena. *Bull. Math. Biophys.*, 11(4):311–318, 1949.
- [Kar93] A. Karma. Spiral breakup in model equations of action potential propagation in cardiac tissue. *Phys. Rev. Lett.*, 71:1103–1106, 1993.
- [KARG92] J.M. Kowalski, G.L. Albert, B.K. Rhoades, and G.W. Gross. Neuronal networks with spontaneous, correlated bursting activity: theory and simulations. *Neural Networks*, 5(5):805–822, 1992.
- [Kat50] T. Kato. On the adiabatic theorem of quantum mechanics. *J. Phys. Soc. Japan*, 5:435–439, 1950.
- [Kat80] T. Kato. *Perturbation Theory for Linear Operators*. Springer, 1980.
- [Kat83a] W.L. Kath. Conditions for sustained resonance. II. *SIAM J. Appl. Math.*, 43:579–583, 1983.
- [Kat83b] W.L. Kath. Necessary conditions for sustained re-entry roll resonance. *SIAM J. Appl. Math.*, 43:314–324, 1983.
- [KAWC80] P.V. Kokotovic, J.J. Allemong, J.R. Winkelman, and J.H. Chow. Singular perturbation and iterative separation of time scales. *Automatica*, 16:23–33, 1980.
- [Kaz58] N.D. Kazarinoff. Asymptotic theory of second order differential equations with two simple turning points. *Arch. Rat. Mech. Anal.*, 2(1):129–150, 1958.
- [Kaz00a] N. Kazantzis. Singular PDEs and the problem of finding invariant manifolds for nonlinear dynamical systems. *Phys. Lett. A*, 272(4):257–263, 2000.
- [Kaz00b] B. Kaczmarczak. Travelling waves in a system modelling laser sustained plasma. *Z. Angew. Math. Phys.*, 51(2):304–317, 2000.
- [KB37] N.M. Krylov and N.N. Bogoliubov. *Introduction to Nonlinear Mechanics*. Izd. AN UkrSSR, 1937. (in Russian).
- [KB85] P. De Kepper and J. Boissonade. From bistability to sustained oscillations in homogeneous chemical systems in flow reactor mode. In R.J. Field and M. Burger, editors, *Oscillations and Traveling Waves in Chemical Systems*, pages 223–256. Wiley-Interscience, 1985.
- [KB02] R. Kuske and S.M. Baer. Asymptotic analysis of noise sensitivity in a neuronal burster. *Bull. Math. Biol.*, 64(3):447–481, 2002.
- [KB09a] R. Kuske and R. Borowski. Survival of subthreshold oscillations: the interplay of noise, bifurcation structure, and return mechanism. *Discr. Cont. Dyn. Sys. S*, 2(4):873–895, 2009.
- [KB09b] Y.N. Kyrychko and K.B. Blyuss. Persistence of travelling waves in a generalized Fisher equation. *Phys. Lett. A*, 373(6):668–674, 2009.
- [KBB05] Y.N. Kyrychko, M.V. Bartuccelli, and K.B. Blyuss. Persistence of travelling wave solutions of a fourth order diffusion system. *J. Comp. Appl. Math.*, 176(2):433–443, 2005.
- [KBG99] V. Kecman, S. Bingulac, and Z. Gajic. Eigenvector approach for order-reduction of singularly perturbed linear-quadratic optimal control problems. *Automatica*, 35(1):151–158, 1999.
- [KBKW98] A.I. Khibnik, Y. Braiman, T.A.B. Kennedy, and K. Wiesenfeld. Phase model analysis of two lasers with injected field. *Physica D*, 111(1):295–310, 1998.
- [KBS12] K.U. Kristiansen, M. Brøns, and J. Starke. An iterative method for the approximation of fibers in slow–fast systems. *arXiv:1208.6420*, pages 1–28, 2012.
- [KC86] M. Kennedy and L. Chua. Van der Pol and chaos. *IEEE Trans. Circ. Syst.*, 33(10):974–980, 1986.
- [KC92] H.K. Khalil and F.C. Chen. H_∞ -control of two-time-scale systems. *Syst. Contr. Lett.*, 19(1):35–42, 1992.
- [KC96] J. Kevorkian and J.D. Cole. *Multiple Scale and Singular Perturbation Methods*. Springer, 1996.

- [KC09] M. Kuwamura and H. Chiba. Mixed-mode oscillations and chaos in a prey-predator system with dormancy of predators. *Chaos*, 19:043121, 2009.
- [KCD98] A. Kumar, P.D. Christofides, and P. Daoutidis. Singular perturbation modeling of nonlinear processes with nonexplicit time-scale multiplicity. *Chem. Engineer. Sci.*, 53(8):1491–1504, 1998.
- [KCG10] S. Koskie, C. Coumarbatch, and Z. Gajic. Exact slow–fast decomposition of the singularly perturbed matrix differential Riccati equation. *Appl. Math. Comput.*, 216(5):1401–1411, 2010.
- [KCMM03] D.A. Knoll, L. Chacon, L.G. Margolin, and V.A. Mousseau. On balanced approximations for time integration of multiple time scale systems. *J. Comput. Phys.*, 185(2):583–611, 2003.
- [KDMS88] M.M. Klosek-Dygas, B.J. Matkowsky, and Z. Schuss. Colored noise in dynamical systems. *SIAM J. Appl. Math.*, 48(2):425–441, 1988.
- [KDMS89] M.M. Klosek-Dygas, B.J. Matkowsky, and Z. Schuss. Colored noise in activated rate processes. *J. Stat. Phys.*, 54(5):1309–1320, 1989.
- [KDSS99] T.A. Kinard, G. DeVries, A. Sherman and L.S. Satin. Modulation of the bursting properties of single mouse pancreatic- β -cells by artificial conductances. *Biophys. J.*, 78(3):1423–1435, 1999.
- [KE82] P. De Kepper and I.R. Epstein. A mechanistic study of oscillations and bistability in the Briggs–Rauscher reaction. *J. Am. Chem. Soc.*, 104:49–55, 1982.
- [KE86] N. Kopell and G.B. Ermentrout. Subcellular oscillations and bursting. *Math. Biosci.*, 78(2):265–291, 1986.
- [KE90] N. Kopell and G.B. Ermentrout. Phase transitions and other phenomena in chains of coupled oscillators. *SIAM J. Appl. Math.*, 50(4):1014–1052, 1990.
- [KE97] R. Kuske and W. Eckhaus. Pattern formation in systems with slowly varying geometry. *SIAM J. Appl. Math.*, 57(1):112–152, 1997.
- [KE03] G. Kozyreff and T. Erneux. Singular Hopf bifurcation to strongly pulsating oscillations in lasers containing a saturable absorber. *Euro. J. Appl. Math.*, 14:407–420, 2003.
- [KE14] G. Kozyreff and T. Erneux. Singular hopf bifurcation in a differential equation with large state-dependent delay. *Proc. Roy. Soc. A*, 470(2162):20130596, 2014.
- [Kee74] J.P. Keener. Perturbed bifurcation theory at multiple eigenvalues. *Arch. Rat. Mech. Anal.*, 56(4): 348–366, 1974.
- [Kee80] J.P. Keener. Waves in excitable media. *SIAM J. Appl. Math.*, 39(3):528–548, 1980.
- [Kee86] J.P. Keener. A geometrical theory for spiral waves in excitable media. *SIAM J. Appl. Math.*, 46(6): 1039–1056, 1986.
- [Kee87] J.P. Keener. Propagation and its failure in coupled systems of discrete excitable cells. *SIAM J. Appl. Math.*, 47:556–572, 1987.
- [Kee88] J.P. Keener. The dynamics of three-dimensional scroll waves in excitable media. *Physica D*, 31(2): 269–276, 1988.
- [KEE92] K. Krischer, M. Eiswirth, and G. Ertl. Oscillatory CO oxidation on Pt(110): modeling of temporal self-organization. *J. Chem. Phys.*, 96(12):9161–9172, 1992.
- [Kee00a] J.P. Keener. Homogenization and propagation in the bistable equation. *Physica D*, 136(1):1–17, 2000.
- [Kee00b] J.P. Keener. Propagation of waves in an excitable medium with discrete release sites. *SIAM J. Appl. Math.*, 61(1):317–334, 2000.
- [Kel67] A. Kelley. The stable, center-stable, center, center-unstable, unstable manifolds. *J. Differential Equat.*, 3(4):546–570, 1967.
- [Kel71] H.J. Kelley. Flight path optimization with multiple time scales. *J. Aircraft*, 8(4):238–240, 1971.
- [Kel74] H. Keller. Accurate difference methods for nonlinear two-point boundary value problems. *SIAM J. Numer. Anal.*, 11(2): 305–320, 1974.
- [Kel83] H. Keller. The bordering algorithm and path following near singular points of higher nullity. *SIAM J. Sci. Comput.*, 4(4): 573–582, 1983.
- [Kev66] J. Kevorkian. Von Zeipel method and the two-variable expansion procedure. *Astronomical J.*, 71:878, 1966.
- [Kev71] J. Kevorkian. Passage through resonance for a one-dimensional oscillator with slowly varying frequency. *SIAM J. Appl. Math.*, 20:364–373, 1971.
- [Kev87] J. Kevorkian. Perturbation techniques for oscillatory systems with slowly varying coefficients. *SIAM Rev.*, 29(3):391–461, 1987.
- [KEW06] T. Kolokolnikov, T. Erneux, and J. Wei. Mesa-type patterns in the one-dimensional Brusselator and their stability. *Physica D*, 214(1):63–77, 2006.
- [KFR01] Yu.A. Kuznetsov, O. De Feo, and S. Rinaldi. Belyakov homoclinic bifurcations in a tritrophic food chain model. *SIAM J. Appl. Math.*, 62(2):462–487, 2001.
- [KG84] H.K. Khalil and Z. Gajic. Near-optimum regulators for stochastic linear singularly perturbed systems. *IEEE Trans. Aut. Contr.*, 29(6):531–541, 1984.
- [KG91] M.T.M. Koper and P. Gaspard. Mixed-mode and chaotic oscillations in a simple model of an electrochemical oscillator. *J. Chem. Phys.*, 95:4945–4947, 1991.
- [KG92] M.T.M. Koper and P. Gaspard. The modeling of mixed-mode and chaotic oscillations in electrochemical systems. *J. Chem. Phys.*, 96(10):7797–7813, 1992.
- [KG98] D. Kaplan and L. Glass. *Understanding Nonlinear Dynamics*. Springer, 1998.
- [KG02] N. Kazantzis and T. Good. Invariant manifolds and the calculation of the long-term asymptotic response of nonlinear processes using singular PDEs. *Comput. Chem. Engineer.*, 26(7):999–1012, 2002.
- [KG11] P. Kowalczyk and P. Glendinning. Boundary-equilibrium bifurcations in piecewise-smooth slow–fast systems. *Chaos*, 21: 023126, 2011.
- [KG13] C. Kuehn and T. Gross. Nonlocal generalized models of predator–prey systems. *Discr. Cont. Dyn. Syst. B*, 18(3): 693–720, 2013.
- [KGG07] R. Kuske, L.F. Gordillo, and P. Greenwood. Sustained oscillations via coherence resonance in SIR. *J. Theor. Biol.*, 245(3): 459–469, 2007.
- [KGH⁺03] I.G. Kevrekidis, C.W. Gear, J.M. Hyman, P.G. Kevrekidis, O. Runborg, and C. Theodoropoulos. Equation-free, coarse-grained multiscale computation: enabling macroscopic simulators to perform system-level analysis. *Comm. Math. Sci.*, 1(4):715–762, 2003.

- [KGH04] I.G. Kevrekidis, C.W. Gear, and G. Hummer. Equation-free: the computer-aided analysis of complex multiscale systems. *AICHE Journal*, 50(7):1346–1355, 2004.
- [KGN98] A.L. Kawczynski, J. Gorecki, and B. Nowakowski. Microscopic and stochastic simulations of oscillations in a simple model of chemical system. *J. Phys. Chem. A*, 102(36):7113–7122, 1998.
- [KGS92] M.T.M. Koper, P. Gaspard, and J.H. Sluyters. Mixed-mode oscillations and incomplete homoclinic scenarios to a saddle focus in the indium/thiocyanate electrochemical oscillator. *J. Chem. Phys.*, 97(11):8250–8260, 1992.
- [KH75] P.V. Kokotovic and A. Haddad. Controllability and time-optimal control of systems with slow and fast modes. *IEEE Trans. Aut. Contr.*, 20(1):111–113, 1975.
- [KHS89] H.K. Khalil and Y.N. Hu. Steering control of singularly perturbed systems: a composite control approach. *Automatica*, 25(1):65–75, 1989.
- [KH95] A. Katok and B. Hasselblatt. *Introduction to the Modern Theory of Dynamical Systems*. CUP, 1995.
- [Kha79] H.K. Khalil. Stabilization of multiparameter singularly perturbed systems. *IEEE Trans. Aut. Contr.*, 24(5):790–791, 1979.
- [Kha80] H.K. Khalil. Multimodel design of a Nash strategy. *J. Optim. Theor. Appl.*, 31(4):553–564, 1980.
- [Kha81] H.K. Khalil. Asymptotic stability of nonlinear multiparameter singularly perturbed systems. *Automatica*, 17(6):797–804, 1981.
- [Kha89] H.K. Khalil. Feedback control of nonstandard singularly perturbed systems. *IEEE Trans. Aut. Contr.*, 34(10):1052–1060, 1989.
- [Kha93] V.L. Khatskevich. Periodic solutions of monotone differential inclusions with fast and slow variables. *Ukrainian Math. J.*, 45(5):761–772, 1993.
- [Kho89] K. Khorasani. Robust stabilization of non-linear systems with unmodelled dynamics. *Int. J. Control.*, 50(3):827–844, 1989.
- [KHS02] V.O. Khavrus, H.Farkas, and P.E. Strizhak. Conditions for mixed-mode oscillations and deterministic chaos in nonlinear chemical systems. *Theoretical and Experimental Chemistry*, 38(5):301–307, 2002.
- [Kif81] Yu. Kifer. The exit problem for small random perturbations of dynamical systems with a hyperbolic fixed point. *Israel J. Math.*, 40(1):74–96, 1981.
- [Kif90] Yu. Kifer. A discrete-time version of the Wentzell–Freidlin theory. *Ann. Prob.*, 18(4):1676–1692, 1990.
- [Kif92] Yu. Kifer. Averaging in dynamical systems and large deviations. *Invent. Math.*, 110(2):337–370, 1992.
- [Kif01a] Yu. Kifer. Averaging and climate models. In *Stochastic Climate Models*, pages 171–188. Birkhäuser, 2001.
- [Kif01b] Yu. Kifer. Stochastic versions of Anosov’s and Neistadt’s theorems on averaging. *Stoch. Dyn.*, 1(1):1–21, 2001.
- [Kif03] Yu. Kifer. L^2 diffusion approximation for slow motion in averaging. *Stoch. Dyn.*, 3(2):213–246, 2003.
- [Kif04a] Yu. Kifer. Averaging principle for fully coupled dynamical systems and large deviations. *Ergodic Theory Dyn. Syst.*, 24(3): 847–871, 2004.
- [Kif04b] Yu. Kifer. Some recent advances in averaging. In *Modern Dynamical Systems and Applications*, pages 385–403. CUP, 2004.
- [Kif08] Yu. Kifer. Convergence, nonconvergence and adiabatic transitions in fully coupled averaging. *Nonlinearity*, 21(3):T27, 2008.
- [Kin00] W.M. Kinney. An application of Conley index techniques to a model of bursting in excitable membranes. *J. Differential Equat.*, 162(2):451–472, 2000.
- [Kin08] W.M. Kinney. Applying the Conley index to fast–slow systems with one slow variable and an attractor. *Rocky Mountain J. Math.*, 38(4):1177–1214, 2008.
- [Kin13] J.R. King. Wavespeed selection in the heterogeneous Fisher equation: slowly varying inhomogeneity. *Networks and Heterogeneous Media*, 8(1):343–378, 2013.
- [Kir03] R. Kirby. On the convergence of high resolution methods with multiple time scales for hyperbolic conservation laws. *Math. Comp.*, 72(243):1239–1250, 2003.
- [Kir12] E. Kirkilis. The renormalization group: a perturbation method for the graduate curriculum. *SIAM Rev.*, 54(2):374–388, 2012.
- [KJ01] T.J. Kaper and C.K.R.T. Jones. A primer on the exchange lemma for fast–slow systems. In *Multiple-Time-Scale Dynamical Systems*, pages 65–88. Springer, 2001.
- [KJ11] A. Kumar and K. Josić. Reduced models of networks of coupled enzymatic reactions. *J. Theor. Biol.*, pages 87–106, 2011.
- [KJB⁺04] H. Kantz, W. Just, N. Baba, K. Gelfert, and A. Riegert. Fast chaos versus white noise – entropy analysis and a Fokker–Planck model for the slow dynamics. *Physica D*, 187:200–213, 2004.
- [KJK00] P.G. Kevrekidis, C.K.R.T. Jones, and T. Kapitula. Exponentially small splitting of heteroclinic orbits: from the rapidly forced pendulum to discrete solitons. *Phys. Lett. A*, 269(2): 120–129, 2000.
- [KJS76] P.V. Kokotovic, R.E. O’Malley Jr, and P. Sannuti. Singular perturbations and order reduction in control theory – an overview. *Automatica*, 12(2):123–132, 1976.
- [KK62] A.I Klimushev and N.N. Krasovski. Uniform asymptotic stability of systems of differential equations with a small parameter in the derivative terms. *J. Appl. Math. Mech.*, 25:1011–1025, 1962.
- [KK73] J.P. Keener and H.B. Keller. Perturbed bifurcation theory. *Arch. Rat. Mech. Anal.*, 50(3):159–175, 1973.
- [KK79a] H.K. Khalil and P.V. Kokotovic. Control of linear systems with multiparameter singular perturbations. *Automatica*, 15(2): 197–207, 1979.
- [KK79b] H.K. Khalil and P.V. Kokotovic. D-stability and multi-parameter singular perturbation. *SIAM J. Contr. Optim.*, 17(1): 56–65, 1979.
- [KK79c] H.K. Khalil and P.V. Kokotovic. Feedback and well-posedness of singularly perturbed Nash games. *IEEE Trans. Aut. Contr.*, 24(5):699–708, 1979.
- [KK81] B. Kreiss and H.-O. Kreiss. Numerical methods for singular perturbation problems. *SIAM J. Numer. Anal.*, 18(2):262–276, 1981.
- [KK85] K. Khorasani and P.V. Kokotovic. Feedback linearization of a flexible manipulator near its rigid body manifold. *Syst. Control Lett.*, 6(3):187–192, 1985.
- [KK86] K. Khorasani and P.V. Kokotovic. A corrective feedback design for nonlinear systems with fast actuators. *IEEE Trans Aut. Contr.*, 31(1):67–69, 1986.

- [KK91] H.K. Khalil and P.V. Kokotovic. On stability properties of nonlinear systems with slowly varying inputs. *IEEE Trans. Aut. Contr.*, 36(2):229, 1991.
- [KK93] A.Yu. Kolesov and Yu.S. Kolesov. Relaxation cycles in systems with delay. *Russ. Acad. Sci. Sbor. Math.*, 76(2):507–522, 1993.
- [KK95] A.Yu. Kolesov and Yu.S. Kolesov. Relaxation oscillations in mathematical models of ecology. *Proc. Steklov Inst. Math.*, 199(1):1–126, 1995.
- [KK96] T.J. Kaper and G. Kovacic. Multi-bump orbits homoclinic to resonance bands. *Trans. Amer. Math. Soc.*, 348:3835–3888, 1996.
- [KK01] R.Z. Khasminskii and N. Krylov. On averaging principle for diffusion processes with null-recurrent fast component. *Stoch. Proc. Appl.*, 93(2):229–240, 2001.
- [KK02] H.G. Kaper and T.J. Kaper. Asymptotic analysis of two reduction methods for systems of chemical reactions. *Physica D*, 165:66–93, 2002.
- [KK05] M.M. Klosek and R. Kuske. Multiscale analysis of stochastic delay differential equations. *Multiscale Model. Simul.*, 3(3):706–729, 2005.
- [KK13] H.-W. Kang and T.G. Kurtz. Separation of time scales and model reduction for stochastic reaction networks. *Ann. Appl. Probab.*, 23(2):529–583, 2013.
- [KKK04] A. Kuznetsov, M. Kærn, and N. Kopell. Synchrony in a population of hysteresis-based genetic oscillators. *SIAM J. Appl. Math.*, 65(2):392–425, 2004.
- [KKK⁺07] L.V. Kalachev, H.G. Kaper, T.J. Kaper, N. Popovic, and A. Zagaris. Reduction for Michaelis–Menten–Henri kinetics in the presence of diffusion. *Electronic J. Diff. Eq.*, 16:155–184, 2007.
- [KKO96a] M. Kisaka, H. Kokubu, and H. Oka. Bifurcations to n -homoclinic orbits and n -periodic orbits in vector fields. *J. Dyn. Diff. Eq.*, 5(2):305–357, 1996.
- [KKO96b] H. Kokubu, M. Komuro, and H. Oka. Multiple homoclinic bifurcations from orbit-flip. I. Successive homoclinic doublings. *Int. J. Bif. Chaos*, 6(5):833–850, 1996.
- [KKO99] P. Kokotovic, H.K. Khalil, and J. O'Reilly. *Singular Perturbation Methods in Control: Analysis and Design*. SIAM, 1999.
- [KKR96] A.Yu. Kolesov, Yu.S. Kolesov, and N.Kh. Rozov. Chaos of the broken torus type in three-dimensional relaxation systems. *J. Math. Sci.*, 80(1):1533–1545, 1996.
- [KKS00a] B. Katsenberger, M. Krupa, and P. Szmolyan. Bifurcation of traveling waves in extrinsic semiconductors. *Physica D*, 144(1): 1–19, 2000.
- [KKS00b] A.L. Kawczynski, V.O. Khavrus, and P.E. Strizhak. Complex mixed-mode periodic and chaotic oscillations in a simple three-variable model of nonlinear system. *Chaos*, 10(2):299–310, 2000.
- [KKS04] T. Kapitula, J.N. Kutz, and B. Sandstede. The Evans function for nonlocal equations. *Indiana U. Math. J.*, 53(4):1095–1126, 2004.
- [KKS10] N. Kazantzis, C. Kravaris, and L. Syrou. A new model reduction method for nonlinear dynamical systems. *Nonlinear Dyn.*, 59(1):183–194, 2010.
- [KL88] H. Kurland and M. Levi. Transversal heteroclinic intersections in slowly varying systems. In *Dynamical Systems Approaches to Nonlinear Problems in Systems and Circuits*, pages 29–38. Springer, 1988.
- [KL93] B. Kreiss and J. Lorenz. Manifolds of slow solutions for highly oscillatory problems. *Indiana Univ. Math. J.*, 42(4):1169–1191, 1993.
- [KL94] B. Kreiss and J. Lorenz. On the existence of slow manifolds for problems with different timescales. *Philosophical Transactions: Physical Sciences and Engineering*, 346(1679):159–171, 1994.
- [KL95] N. Kopell and M. Landman. Spatial structure of the focusing singularity of the nonlinear Schrödinger equation: a geometrical analysis. *SIAM J. Appl. Math.*, 55(5):1297–1323, 1995.
- [Kla12] A. Klaiber. Viscous profiles for shock waves in isothermal magnetohydrodynamics. *J. Dyn. Diff. Eq.*, 24(3):663–683, 2012.
- [KLE⁺93] K. Krischer, M. Luebke, M. Eiswirth, W. Wolf, J.L. Hudson, and G. Ertl. A hierarchy of transitions to mixed mode oscillations in an electrochemical system. *Physica D*, 62:123–133, 1993.
- [Klo83] W. Klonowskii. Simplifying principles for chemical and enzyme reaction kinetics. *Biophys. Chem.*, 18(2):73–87, 1983.
- [KLS02] K.-R. Kim, D.J. Lee, and K.J. Shin. A simplified model for the Briggs–Rauscher reaction mechanism. *J. Chem. Phys.*, 117(6):2710–2717, 2002.
- [KLVE09] K. Kovacs, M. Leda, V.K. Vanag, and I.R. Epstein. Small-amplitude and mixed-mode oscillations in the Bromate–Sulfite–Ferrocyanide–Aluminium(III) system. *J. Phys. Chem.*, 113: 146–156, 2009.
- [KM89] A.Yu. Kolesov and E.F. Mishchenko. Existence and stability of the relaxation torus. *Russ. Math. Surv.*, 44(3):204–205, 1989.
- [KM91] A.Yu. Kolesov and E.F. Mishchenko. The Pontryagin delay phenomenon and stable duck trajectories for multidimensional relaxation systems with one slow variable. *Math. USSR Sbor.*, 70:1–10, 1991.
- [KM94] P. Kunkel and V. Mehrmann. Canonical forms for linear differential-algebraic equations with variable coefficients. *J. Comput. Appl. Math.*, 56(3):225–251, 1994.
- [KM98] P. Kunkel and V. Mehrmann. Regular solutions of nonlinear differential-algebraic equations and their numerical determination. *Numer. Math.*, 79(4):581–600, 1998.
- [KM03a] P. Kramer and A. Majda. Stochastic mode reduction for particle-based simulation methods for complex microfluid systems. *SIAM J. Appl. Math.*, 64(2):401–422, 2003.
- [KM03b] P. Kramer and A. Majda. Stochastic mode reduction for the immersed boundary method. *SIAM J. Appl. Math.*, 64(2):369–400, 2003.
- [KM06a] R. Klein and A.J. Majda. Systematic multiscale models for deep convection on mesoscales. *Theor. Comp. Fluid Dyn.*, 20:525–551, 2006.
- [KM06b] P. Kunkel and V. Mehrmann. *Differential-Algebraic Equations*. European Mathematical Society, 2006.
- [KMO96] H. Kokubu, K. Mischaikow, and H. Oka. Existence of infinitely many connecting orbits in a singularly perturbed ordinary differential equation. *Nonlinearity*, 9:1263–1280, 1996.
- [KMR95] Y.A. Kuznetsov, S. Muratori, and S. Rinaldi. Homoclinic bifurcations in slow–fast second order systems. *Nonl. Anal.: Theory, Methods & Appl.*, 25(7):747–767, 1995.
- [KMR98] A.Yu. Kolesov, E.F. Mishchenko, and N.Kh. Rozov. Asymptotic methods of investigation of periodic solutions of nonlinear hyperbolic equations. *Proc. Steklov Inst. Math.*, 222:1–189, 1998.

- [KMR99] A.Yu. Kolesov, E.F. Mishchenko, and N.Kh. Rozov. Solution to singularly perturbed boundary value problems by the duck hunting method. *Proc. Steklov Inst. Math.*, 224:169–188, 1999.
- [KMR08] A.Yu. Kolesov, E.F. Mishchenko, and N.Kh. Rozov. On one bifurcation in relaxation systems. *Ukr. Math. Journal*, 60(1): 63–72, 2008.
- [KMR14] C. Kuehn, E.A. Martens, and D. Romero. Critical transitions in social network activity. *J. Complex Networks*, 2(2):141–152, 2014. see also arXiv:1307.8250.
- [KMS04] M.A. Katsoulakis, A.J. Majda, and A. Sopasakis. Multiscale couplings in prototype hybrid deterministic/stochastic systems: part I, deterministic closures. *Commun. Math. Sci.*, 2(2): 255–294, 2004.
- [KMZT85] C. Knessl, B.J. Matkowsky, Z. Schuss, and C. Tier. An asymptotic theory of large deviations for Markov jump processes. *SIAM J. Appl. Math.*, 45(6):1006–1028, 1985.
- [KMZT86a] C. Knessl, B.J. Matkowsky, Z. Schuss and C. Tier. Asymptotic analysis of a state-dependent M/G/1 queueing system. *SIAM J. Appl. Math.*, 46(3):483–505, 1986.
- [KMZT86b] C. Knessl, B.J. Matkowsky, Z. Schuss and C. Tier. On the performance of state-dependent single server queues. *SIAM J. Appl. Math.*, 46(4):657–697, 1986.
- [KMZT86c] C. Knessl, B.J. Matkowsky, Z. Schuss and C. Tier. A singular perturbation approach to first passage times for Markov jump processes. *J. Stat. Phys.*, 42(1):169–184, 1986.
- [KMZT87a] C. Knessl, B.J. Matkowsky, Z. Schuss and C. Tier. Asymptotic expansions for a closed multiple access system. *SIAM J. Comput.*, 16(2):378–398, 1987.
- [KMZT87b] C. Knessl, B.J. Matkowsky, Z. Schuss and C. Tier. A Markov-modulated M/G/1 queue I: stationary distribution. *Queueing Syst.*, 1(4):355–374, 1987.
- [KMZT87c] C. Knessl, B.J. Matkowsky, Z. Schuss and C. Tier. The two repairmen problem: a finite source M/G/2 queue. *SIAM J. Appl. Math.*, 47(2):367–397, 1987.
- [KN03] M. Kamenskii and P. Nistri. An averaging method for singularly perturbed systems of semilinear differential inclusions with analytic semigroups. *Nonl. Anal.*, 53:467–480, 2003.
- [Kna04] A.W. Knapp. *Lie Groups Beyond an Introduction*. Birkhäuser, 2004.
- [KNB86] H.-O. Kreiss, N.K. Nichols, and D.L. Brown. Numerical methods for stiff two-point boundary value problems. *SIAM J. Numer. Anal.*, 18(2):325–386, 1986.
- [Kne94] C. Knessl. On the distribution of the maximum number of broken machines for the repairman problem. *SIAM J. Appl. Math.*, 54(2):508–547, 1994.
- [KNE⁺06] T. Kolokolnikov, M. Nizette, T. Erneux, N. Joly, and S. Bielawski. The Q-switching instability in passively mode-locked lasers. *Physica D*, 219(1):13–21, 2006.
- [Kno92] M. Knorrerchild. Differential/algebraic equations as stiff ordinary differential equations. *SIAM J. Numer. Anal.*, 29(6):1694–1715, 1992.
- [Kno00] R. Knobel. *An Introduction to the Mathematical Theory of Waves*. AMS, 2000.
- [KO92] L.V. Kalachev and I.A. Obukhov. Asymptotic behavior of a solution of the Poisson equation in a model of a three-dimensional semiconductor structure. *Comput. Math. Math. Phys.*, 32(9):1361–1366, 1992.
- [KO96] L.V. Kalachev and R.E. O’Malley. The regularization of linear differential-algebraic equations. *SIAM J. Math. Anal.*, 27(1):258–273, 1996.
- [KO99] B. Krauskopf and H.M. Osinga. Two-dimensional global manifolds of vector fields. *Chaos*, 9(3): 768–774, 1999.
- [KO00] B. Krauskopf and H.M. Osinga. Investigating torus bifurcations in the forced van der Pol oscillator. In *Numerical Methods for Bifurcation Problems and Large-Scale Dynamical Systems*, pages 199–208. Springer, 2000.
- [KO02] R.V. Kohn and F. Otto. Upper bounds on coarsening rates. *Comm. Math. Phys.*, 229(3):375–395, 2002.
- [KO03] B. Krauskopf and H.M. Osinga. Computing geodesic level sets on global (un)stable manifolds of vector fields. *SIAM J. Appl. Dyn. Syst.*, 4(2):546–569, 2003.
- [KOD⁺05] B. Krauskopf, H.M. Osinga, E.J. Doedel, M.E. Henderson, J. Guckenheimer, A. Vladimirsky, M. Dellnitz, and O. Junge. A survey of methods for computing (un)stable manifolds of vector fields. *Int. J. Bif. Chaos*, 15(3):763–791, 2005.
- [KOGV07] B. Krauskopf, H.M. Osinga, and J. Galán-Vique, editors. *Numerical Continuation Methods for Dynamical Systems: Path following and boundary value problems*. Springer, 2007.
- [Kok75] P.V. Kokotovic. A Riccati equation for block-diagonalization of ill-conditioned systems. *IEEE Trans. Aut. Contr.*, 20(6):812–814, 1975.
- [Kok81] P.V. Kokotovic. Subsystems, time scales and multimodeling. *Automatica*, 17(6):789–795, 1981.
- [Kok84] P.V. Kokotovic. Applications of singular perturbation techniques to control problems. *SIAM Rev.*, 26(4):501–550, 1984.
- [Kol74] F.W. Kolloet. Two-timing methods valid on expanding intervals. *SIAM J. Math. Anal.*, 5(4):613–625, 1974.
- [Kol89] A.Yu. Kolesov. On the instability of duck-cycles arising during the passage of an equilibrium of a multidimensional relaxation system through the disruption manifold. *Russ. Math. Surv.*, 44(5): 203–205, 1989.
- [Kol92] A.Yu. Kolesov. Specific relaxation cycles of systems of Lotka–Volterra type. *Math. USSR-Izvestiya*, 38(3):503–523, 1992.
- [Kol94] A.Yu. Kolesov. On the existence and stability of a two-dimensional relaxational torus. *Math. Notes*, 56(6):1238–1243, 1994.
- [Kol07] J. Kollár. *Lectures on Resolution of Singularities*. Princeton University Press, 2007.
- [Kon03] R.A. Konoplya. Quasinormal behavior of the D -dimensional Schwarzschild black hole and the higher order WKB approach. *Phys. Rev. D*, 68(2):024018, 2003.
- [Kon08] L.I. Kononenko. The influence of the integral manifold shape on the onset of relaxation oscillations. *J. Appl. Ind. Math.*, 2(4):508–512, 2008.
- [Kon09] L.I. Kononenko. Relaxation oscillations and canard solutions in singular systems on a plane. *J. Appl. Ind. Math.*, 4(2):194–199, 2009.
- [Kop79] N. Kopell. A geometric approach to boundary layer problems exhibiting resonance. *SIAM J. Appl. Math.*, 37(2):436–458, 1979.

- [Kop80] N. Kopell. The singularly perturbed turning point problem: a geometric approach. In R. Meyer, editor, *Singular Perturbations and Asymptotics*, pages 173–190. Academic Press, 1980.
- [Kop85] N. Kopell. Invariant manifolds and the initialization problem for some atmospheric equations. *Physica D*, 14(2):203–215, 1985.
- [Kop95] M.T.M. Koper. Bifurcations of mixed-mode oscillations in a three-variable autonomous van der Pol–Duffing model with a cross-shaped phase diagram. *Physica D*, 80:72–94, 1995.
- [Kop00] N. Kopell. We got rhythm: Dynamical systems of the nervous system. *Notices of the AMS*, 47(1):6–16, 2000.
- [KOPR13] A.M. Krasnosel'skii, E. O'Grady, A.V. Pokrovskii, and D.I. Rachinskii. Periodic canards trajectories with multiple segments following the unstable part of the critical manifold. *Discr. Cont. Dyn. Syst. B*, 18(2):467–482, 2013.
- [Kör04] T.W. Körner. *A Companion to Analysis: A Second First and First Second Course in Analysis*. AMS, 2004.
- [Kor06] S.A. Kordyukova. Approximate group analysis and multiple time scales method for the approximate Boussinesq equation. *Nonlinear Dynam.*, 46(1):73–85, 2006.
- [Kör12] T.W. Körner. *Vectors, Pure and Applied: A General Introduction to Linear Algebra*. CUP, 2012.
- [KORVE07] R.V. Kohn, F. Otto, M.G. Reznikoff, and E. Vanden-Eijnden. Action minimization and sharp-interface limits for the stochastic Allen–Cahn equation. *Comm. Pure Appl. Math.*, 60(3):393–438, 2007.
- [Kou97] M.A. Kouritzin. Averaging for fundamental solutions of parabolic equations. *J. Differential Equat.*, 136(1):35–75, 1997.
- [KOV89] C. Kipnis, S. Olla, and S.R.S. Varadhan. Hydrodynamics and large deviation for simple exclusion processes. *Comm. Pure. Appl. Math.*, 42(2):115–137, 1989.
- [Kov92] G. Kovacic. Dissipative dynamics of orbits homoclinic to a resonance band. *Phys. Lett. A*, 167(2):143–150, 1992.
- [Kov93] G. Kovacic. Singular perturbation theory for homoclinic orbits in a class of near-integrable Hamiltonian systems. *J. Dyn. Diff. Eq.*, 5(4):559–597, 1993.
- [Kov95] G. Kovacic. Singular perturbation theory for homoclinic orbits in a class of near-integrable dissipative systems. *SIAM J. Math. Anal.*, 26(6):1611–1643, 1995.
- [KP74] H.-O. Kreiss and S.V. Parter. Remarks on singular perturbations with turning points. *SIAM J. Math. Anal.*, 5(2):230–251, 1974.
- [KP81] N. Kopell and S.V. Parter. A complete analysis of a model nonlinear singular perturbation problem having a continuous locus of singular points. *Adv. Appl. Math.*, 2:212–238, 1981.
- [KP89] M.A. Krasnosel'skii and A.V. Pokrovskii. *Systems with Hysteresis*. Springer, 1989.
- [KP91a] Y.M. Kabanov and S.M. Pergamenshchikov. On optimal control of singularly perturbed stochastic differential equations. In *Modeling, Estimation and Control of Systems with Uncertainty*, pages 200–209. Birkhäuser, 1991.
- [KP91b] Y.M. Kabanov and S.M. Pergamenshchikov. Optimal control of singularly perturbed stochastic linear systems. *Stochastics*, 36(2):109–135, 1991.
- [KP92] Y.M. Kabanov and S.M. Pergamenshchikov. Singular perturbations of stochastic differential equations. *Math. USSR-Sbor.*, 71:15–27, 1992.
- [KP95] Y.M. Kabanov and S.M. Pergamenshchikov. Large deviations for solutions of singularly perturbed stochastic differential equations. *Russ. Math. Surv.*, 50(5):989–1013, 1995.
- [KP97] Y.M. Kabanov and S.M. Pergamenshchikov. On convergence of attainability sets for controlled two-scale stochastic linear systems. *SIAM J. Contr. Optim.*, 35(1):134–159, 1997.
- [KP02] M.K. Kadalbajoo and K.C. Patidar. A survey of numerical techniques for solving singularly perturbed ordinary differential equations. *Appl. Math. Comp.*, 130(2):457–510, 2002.
- [KP03a] Y. Kabanov and S. Pergamenshchikov. *Two-Scale Stochastic Systems*. Springer, 2003.
- [KP03b] M.K. Kadalbajoo and K.C. Patidar. Singularly perturbed problems in partial differential equations: a survey. *Appl. Math. Comp.*, 134(2):371–429, 2003.
- [KP05] R. Kuske and L.A. Peletier. A singular perturbation problem for a fourth order ordinary differential equation. *Nonlinearity*, 18(3):1189, 2005.
- [KP10] P.E. Kloeden and E. Platen. *Numerical Solution of Stochastic Differential Equations*. Springer, 2010.
- [KP13] T. Kapitula and K. Promislow. *Spectral and Dynamical Stability of Nonlinear Waves*. Springer, 2013.
- [KPAK02] B.W. Kooi, J.C. Poggiale, P. Auger, and S.A.L.M. Kooijman. Aggregation methods in food chains with nutrient recycling. *Ecol. Model.*, 157(1):69–86, 2002.
- [KPBO0] L. Kocarev, U. Parlitz, and R. Brown. Robust synchronization of chaotic systems. *Phys. Rev. E*, 61(4):3716–3720, 2000.
- [KPK08] M. Krupa, N. Popovic, and N. Kopell. Mixed-mode oscillations in three time-scale systems: a prototypical example. *SIAM J. Appl. Dyn. Syst.*, 7(2):361–420, 2008.
- [KPK11] P. Kim, X. Piao, and S.D. Kim. An error-corrected Euler method for solving stiff problems based on Chebyshev collocation. *SIAM J. Numer. Anal.*, 49(6):2211–2230, 2011.
- [KPK13] S. Krumscheid, G.A. Pavliotis and S. Kalliadasis. Semiparametric drift and diffusion estimation for multiscale diffusions. *Multiscale Model. Simul.*, 11(2):442–473, 2013.
- [KPKR08] M. Krupa, N. Popovic, N. Kopell, and H.G. Rotstein. Mixed-mode oscillations in a three time-scale model for the dopaminergic neuron. *Chaos*, 18:015106, 2008.
- [KPLM13] I.A. Khovanov, A.V. Polovinkin, D.G. Luchinsky, and P.V.E. McClintock. Noise-induced escape in an excitable system. *Phys. Rev. E*, 87:032116, 2013.
- [KPP91] A. Kolmogorov, I. Petrovskii, and N. Piscounov. A study of the diffusion equation with increase in the amount of substance, and its application to a biological problem. In V.M. Tikhomirov, editor, *Selected Works of A. N. Kolmogorov I*, pages 248–270. Kluwer, 1991. Translated by V. M. Volosov from Bull. Moscow Univ., Math. Mech. 1, 1–25, 1937.
- [KPR12] K.U. Kristiansen, P. Palmer, and R.M. Roberts. The persistence of a slow manifold with bifurcation. *SIAM J. Appl. Dyn. Syst.*, 11(2):661–683, 2012.
- [KPS91] Y.M. Kabanov, S.M. Pergamenshchikov, and J.M. Stoyanov. Asymptotic expansions for singularly perturbed stochastic differential equations. In V. Sazonov and T. Shervashidze, editors, *New Trends in Probability and Statistics - In Honor of Yu. Prohorov*, pages 413–435. VSP, 1991.

- [KR89] M.K. Kadalbajoo and Y.N. Reddy. Asymptotic and numerical analysis of singular perturbation problems: a survey. *Appl. Math. Comp.*, 30(3):223–259, 1989.
- [KR96] Y.M. Kabanov and W.J. Rungaldier. On control of two-scale stochastic systems with linear dynamics in the fast variables. *Math. Contr. Sig. Syst.*, 9(2):107–122, 1996.
- [KR99] A.Yu. Kolesov and N.Kh. Rozov. 'Buridan's ass' problem in relaxation systems with one slow variable. *Math. Notes*, 65(1): 128–131, 1999.
- [KR00] T. Kapitula and J. Rubin. Existence and stability of standing hole solutions to complex Ginzburg–Landau equations. *Nonlinearity*, 13(1):77–112, 2000.
- [KR03] A.Yu. Kolesov and N.Kh. Rozov. On-off intermittency in relaxation systems. *Differ. Equat.*, 39(1): 36–45, 2003.
- [KR08] B. Krauskopf and T. Riess. A Lin's method approach to finding and continuing heteroclinic connections involving periodic orbits. *Nonlinearity*, 21(8):1655–1690, 2008.
- [KR09] A.Yu. Kolesov and N.Kh. Rozov. On the definition of chaos. *Russian Math. Surveys*, 64(4):701–744, 2009.
- [KR11] A.Yu. Kolesov and N.Kh. Rozov. The theory of relaxation oscillations for the Hutchinson equation. *Sb. Math.*, 202(5):829–858, 2011.
- [KR12] D. Kushnir and V. Rokhlin. A highly accurate solver for stiff ordinary differential equations. *SIAM J. Sci. Comput.*, 34(3): A1296–A1315, 2012.
- [KR14] C. Kuehn and M.G. Riedler. Large deviations for nonlocal stochastic neural fields. *J. Math. Neurosci.*, 4(1):1–33, 2014.
- [Kra26] H.A. Kramers. Wellenmechanik und halbzählig Quantisierung. *Zeitschrift für Physik*, 39(10):828–840, 1926.
- [Kra40] H.A. Kramers. Brownian motion in a field of force and the diffusion model of chemical reactions. *Physica*, 7(4):284–304, 1940.
- [KRA⁺07] S. Kéfi, M. Rietkerk, C.L. Alados, Y. Peyo, V.P. Papanastasis, A. El Aich, and P.C. de Ruiter. Spatial vegetation patterns and imminent desertification in Mediterranean arid ecosystems. *Nature*, 449:213–217, 2007.
- [Kre79] H.-O. Kreiss. Problems with different time scales for ordinary differential equations. *SIAM J. Numer. Anal.*, 16(6):980–998, 1979.
- [Kre80] H.-O. Kreiss. Problems with different time scales for partial differential equations. *Comm. Pure Appl. Math.*, 33:399–439, 1980.
- [Kre81] H.-O. Kreiss. Resonance for singular perturbation problems. *SIAM J. Appl. Math.*, 41(2):331–344, 1981.
- [Kre84] H.-O. Kreiss. Central difference schemes and stiff boundary value problems. *BIT*, 24:560–567, 1984.
- [Kre96] P. Krejčí. *Hysteresis, Convexity and Dissipation in Hyperbolic Equations*. Gakkotosho, Tokyo, 1996.
- [Kre05] P. Krejčí. Hysteresis, convexity and dissipation in hyperbolic equations. *J. Phys.: Conf. Ser.*, 22(1):103–123, 2005.
- [Kri89] G.A. Kriegsmann. Bifurcation in classical bipolar transistor oscillator circuits. *SIAM J. Appl. Math.*, 49(2):390–403, 1989.
- [Kro91] M.S. Krol. On the averaging method in nearly time-periodic advection–diffusion problems. *SIAM J. Appl. Math.*, 51(6):1622–1637, 1991.
- [KRP85] P. Kokotovic, B. Riedle, and L. Praly. On a stability criterion for continuous slow adaptation. *Syst. Contr. Lett.*, 6(1):7–14, 1985.
- [KRS04] A.Yu. Kolesov, N.Kh. Rozov, and V.A. Sadovnichiy. Life on the edge of chaos. *J. Math. Sci.*, 120(3):1372–1398, 2004.
- [KRS13] V. Kelptsyn, O. Romaskevich, and I. Schurov. Josephson effect and slow–fast systems. *Nanostructures. Math. Phys. Model.*, 8(1):31–46, 2013.
- [KS68] P. Kokotovic and P. Sannuti. Singular perturbation method for reducing the model order in optimal control design. *IEEE Trans. Aut. Contr.*, 13(4):377–384, 1968.
- [KS70] E. Keller and S. Segel. Initiation of slime mold aggregation viewed as an instability. *J. Theor. Biol.*, 26:399–415, 1970.
- [KS86] A. Katok and J.-M. Strelcyn. *Invariant Manifolds, Entropy and Billiards; Smooth Maps with Singularities*, volume 1222 of *Springer Lecture Notes in Math.* Springer, 1986.
- [KS91a] T. Kapitaniak and W.H. Steeb. Transition to hyperchaos in coupled generalized van der Pol equations. *Phys. Lett. A*, 152: 33–36, 1991.
- [KS91b] M.T.M. Koper and J.H. Sluyters. Electrochemical oscillators: an experimental study of the indium/thiocyanate oscillator. *J. Electroanal. Chem.*, 303:65–72, 1991.
- [KS91c] M.T.M. Koper and J.H. Sluyters. Electrochemical oscillators: their description through a mathematical model. *J. Electroanal. Chem.*, 303:73–94, 1991.
- [KS94] L.I. Kononenko and V.A. Sobolev. Asymptotic decomposition of slow integral manifolds. *Siberian Math. J.*, 35(6):1119–1132, 1994.
- [KS95] N. Kopell and D. Somers. Anti-phase solutions in relaxation oscillators coupled through excitatory interactions. *J. Math. Biol.*, 33(3):261–280, 1995.
- [KS00a] A.L. Kawczynski and P.E. Strizhak. Period adding and broken Farey tree sequences of bifurcations for mixed-mode oscillations and chaos in the simplest three-variable nonlinear system. *J. Chem. Phys.*, 112(14):6122–6130, 2000.
- [KS00b] M. Kunze and H. Spohn. Adiabatic limit for the Maxwell-Lorentz equations. *Ann. Henri Poincaré*, 1(4):625–653, 2000.
- [KS01a] N. Kopteva and M. Stynes. A robust adaptive method for a quasi-linear one-dimensional convection–diffusion problem. *SIAM J. Numer. Anal.*, 39(4):1446–1467, 2001.
- [KS01b] M. Krupa and P. Szmolyan. Extending geometric singular perturbation theory to nonhyperbolic points – fold and canard points in two dimensions. *SIAM J. Math. Anal.*, 33(2):286–314, 2001.
- [KS01c] M. Krupa and P. Szmolyan. Extending slow manifolds near transcritical and pitchfork singularities. *Nonlinearity*, 14: 1473–1491, 2001.
- [KS01d] M. Krupa and P. Szmolyan. Geometric analysis of the singularly perturbed fold. in: *Multiple-Time-Scale Dynamical Systems*, IMA Vol. 122:89–116, 2001.

- [KS01e] M. Krupa and P. Szmolyan. Relaxation oscillation and canard explosion. *J. Differential Equat.*, 174: 312–368, 2001.
- [KS01f] M. Kunze and H. Spohn. Post-Coulombian dynamics at order $c\cdot 3$. *J. Nonlinear Sci.*, 11(5):321–396, 2001.
- [KS03] L.V. Kalachev and T.I. Seidman. Singular perturbation analysis of a stationary diffusion/reaction system whose solution exhibits a corner-type behavior in the interior of the domain. *J. Math. Anal. Appl.*, 288(2):722–743, 2003.
- [KS05] L.V. Kalachev and K.R. Schneider. Global behavior and asymptotic reduction of a chemical kinetics system with continua of equilibria. *J. Math. Chem.*, 37(1):57–74, 2005.
- [KS06] M. Kunze and H. Spohn. Radiation reaction and center manifolds. *SIAM J. Math. Anal.*, 32(1):30–53, 2006.
- [KS08a] J. Keener and J. Sneyd. *Mathematical Physiology 1: Cellular Physiology*. Springer, 2008.
- [KS08b] J. Keener and J. Sneyd. *Mathematical Physiology 2: Systems Physiology*. Springer, 2008.
- [KS09] I.G. Kevrekidis and G. Samaey. Equation-free multiscale computation: algorithms and applications. *Annu. Rev. Phys. Chem.*, 60:321–344, 2009.
- [KS11] I. Kosiuk and P. Szmolyan. Scaling in singular perturbation problems: blowing-up a relaxation oscillator. *SIAM J. Appl. Dyn. Syst.*, 10(4):1307–1343, 2011.
- [KS12] G. Karali and C. Sourdis. Radial and bifurcating non-radial solutions for a singular perturbation problem in the case of exchange of stabilities. *Ann. Inst. Henri Poincaré (C)*, 29(2): 131–170, 2012.
- [KS13] I. Kosiuk and P. Szmolyan. A new type of relaxation oscillations in a model of the mitotic oscillator. *preprint*, 2013.
- [KSG⁺98] B.N. Kholodenko, S. Schuster, J. Garcia, H.V. Westerhoff, and M. Cascante. Control analysis of metabolic systems involving quasi-equilibrium reactions. *Biochimica et Biophysica Acta*, 1379(3): 337–352, 1998.
- [KSG10] P.D. Koudris, R. Steuer, and D.A. Goussis. Physical understanding of complex multiscale biochemical models via algorithmic simplification: glycolysis in *Saccharomyces cerevisiae*. *Physica D*, 239(18):1798–1817, 2010.
- [KSG13] C. Kuehn, S. Siegmund, and T. Gross. On the analysis of evolution equations via generalized models. *IMA J. Appl. Math.*, 78(5):1051–1077, 2013.
- [KSL04] K.-R. Kim, K.J. Shin, and D.J. Lee. Complex oscillations in a simple model for the Briggs–Rauscher reaction. *J. Chem. Phys.*, 121(6):2664–2672, 2004.
- [KSM92] P. Kirrmann, G. Schneider, and A. Mielke. The validity of modulation equations for extended systems with cubic nonlinearities. *Proc. R. Soc. Edinburgh A*, 122(1):85–91, 1992.
- [KSS97] M. Krupa, B. Sandstede, and P. Szmolyan. Fast and slow waves in the FitzHugh–Nagumo equation. *J. Differential Equat.*, 133:49–97, 1997.
- [KSS⁺01] M. Krupa, M. Schagerl, A. Steinidl, P. Szmolyan, and H. Troger. Relative equilibria of tethered satellite systems and their stability for very stiff tethers. *Dynamical Systems*, 16(3):253–278, 2001.
- [KSS⁺03] B. Krauskopf, K. Schneider, J. Sieber, S. Wieczorek, and M. Wolfrum. Excitability and self-pulsations near homoclinic bifurcations in semiconductor lasers. *Optics Communications*, 215:367–379, 2003.
- [KSWW06] T. Kolokolnikov, W. Sun, M.J. Ward, and J. Wei. The stability of a stripe for the Gierer–Meinhardt model and the effect of saturation. *SIAM J. Appl. Dyn. Syst.*, 5(2):313–363, 2006.
- [KT84] G.A. Klaasen and W.C. Troy. Stationary wave solutions of a system of reaction–diffusion equations derived from the FitzHugh–Nagumo equations. *SIAM J. Appl. Math.*, 44(1):96–110, 1984.
- [KT92] J.P. Keener and J.J. Tyson. The dynamics of scroll waves in excitable media. *SIAM Rev.*, 34(1):1–39, 1992.
- [KT97] N. Kakiuchi and K. Tchizawa. On an explicit duck solution and delay in the FitzHugh–Nagumo equation. *J. Differential Equat.*, 141(2):327–339, 1997.
- [KT05] A.K. Kassam and L.N. Trefethen. Fourth-order time-stepping for stiff PDEs. *SIAM J. Sci. Comput.*, 26(4):1214–1233, 2005.
- [KT12] B.L. Keyfitz and C. Tsikkou. Conserving the wrong variables in gas dynamics: a Riemann solution with singular shocks. *Quart. Appl. Math.*, 70:407–436, 2012.
- [KTK08] M.A. Kramer, R.D. Traub, and N.J. Kopell. New dynamics in cerebellar Purkinje cells: torus canards. *Phys. Rev. Lett.*, 101(6):068103, 2008.
- [KTS11] K. Konishi, M. Takeuchi and T. Shimizu. Design of external forces for eliminating traveling wave in a piecewise linear FitzHugh–Nagumo model. *Chaos*, 21:023101, 2011.
- [KTY09] V. Krishnamurthy, K. Topley, and G. Yin. Consensus formation in a two-time-scale Markovian system. *Multiscale Model. Simul.*, 7(4):1898–1927, 2009.
- [Kue02] W. Kuehn. *Differential Geometry – Curves, Surfaces, Manifolds*. AMS, 2002.
- [Kue09] C. Kuehn. Scaling of saddle-node bifurcations: degeneracies and rapid quantitative changes. *J. Phys. A: Math. and Theor.*, 42(4):045101, 2009.
- [Kue10a] C. Kuehn. Characterizing slow exit points. *Electron. J. Differential Equations*, 2010(106):1–20, 2010.
- [Kue10b] C. Kuehn. From first Lyapunov coefficients to maximal canards. *Int. J. Bif. Chaos*, 20(5):1467–1475, 2010.
- [Kue11a] C. Kuehn. A mathematical framework for critical transitions: bifurcations, fast–slow systems and stochastic dynamics. *Physica D*, 240(12):1020–1035, 2011.
- [Kue11b] C. Kuehn. On decomposing mixed-mode oscillations and their return maps. *Chaos*, 21(3):033107, 2011.
- [Kue12a] C. Kuehn. Deterministic continuation of stochastic metastable equilibria via Lyapunov equations and ellipsoids. *SIAM J. Sci. Comp.*, 34(3):A1635–A1658, 2012.
- [Kue12b] C. Kuehn. Time-scale and noise optimality in self-organized critical adaptive networks. *Phys. Rev. E*, 85(2):026103, 2012.
- [Kue13a] C. Kuehn. A mathematical framework for critical transitions: normal forms, variance and applications. *J. Nonlinear Sci.*, 23(3):457–510, 2013.
- [Kue13b] C. Kuehn. Warning signs for wave speed transitions of noisy Fisher–KPP invasion fronts. *Theor. Ecol.*, 6(3):295–308, 2013.

- [Kue14] C. Kuehn. Normal hyperbolicity and unbounded critical manifolds. *Nonlinearity*, 27(6):1351–1366, 2014.
- [Kun76] C.F. Kung. Singular perturbation of an infinite interval linear state regulator problem in optimal control. *J. Math. Anal. Appl.*, 55(2):365–374, 1976.
- [Kur86] H.L. Kurland. Following homology in singularly perturbed systems. *J. Differential Equat.*, 62(1):1–72, 1986.
- [KUR12] K.U. Kristiansen, P.L. Uldall, and R.M. Roberts. Numerical modelling of elastic space tethers. *Celestial Mech. Dynam. Astronom.*, 113(2):235–254, 2012.
- [Kus90] H.J. Kushner. *Weak Convergence Methods and Singularly Perturbed Stochastic Control and Filtering Problems*. Birkhäuser, 1990.
- [Kus99] R. Kuske. Probability densities for noisy delay bifurcation. *J. Stat. Phys.*, 96(3):797–816, 1999.
- [Kus00] R. Kuske. Gradient-particle solutions of Fokker–Planck equations for noisy delay bifurcations. *SIAM J. Sci. Comput.*, 22(1):351–367, 2000.
- [Kus03] R. Kuske. Multi-scale analysis of noise-sensitivity near a bifurcation. In *IUTAM Symposium on Nonlinear Stochastic Dynamics*, pages 147–156. Springer, 2003.
- [Kus10] R. Kuske. Competition of noise sources in systems with delay: the role of multiple time scales. *J. Vibration and Control*, 16(7):983–1003, 2010.
- [Kuz04] Yu.A. Kuznetsov. *Elements of Applied Bifurcation Theory*. Springer, New York, NY, 3rd edition, 2004.
- [KVC13] M. Krupa, A. Vidal, and F. Clément. A network model of the periodic synchronization process in the dynamics of calcium concentration in GnRH neurons. *J. Math. Neurosci.*, 3(4):1–40, 2013.
- [KVDC12] M. Krupa, A. Vidal, M. Desroches, and F. Clément. Mixed-mode oscillations in a multiple time scale phantom bursting system. *SIAM J. Appl. Dyn. Syst.*, 11(4):1458–1498, 2012.
- [KvdGL97] B. Krauskopf, W.A. van der Graaf, and D. Lenstra. Bifurcations of relaxation oscillations in an optically injected diode laser. *Quantum Semiclass. Optics*, 9(5):797–809, 1997.
- [KW79] G.A. Kriegsmann and M. Williams. On the tracing of light rays through deformed glass rods with radially graded refractive indices. *SIAM J. Appl. Math.*, 36(2):263–272, 1979.
- [KW91] T.J. Kaper and S. Wiggins. Lobe area in adiabatic Hamiltonian systems. *Physica D*, 51(1):205–212, 1991.
- [KW02] B. Krauskopf and S.M. Wieczorek. Accumulating regions of winding periodic orbits in optically driven lasers. *Physica D*, 173:97–113, 2002.
- [KW10] M. Krupa and M. Wechselberger. Local analysis near a folded saddle-node singularity. *J. Differential Equat.*, 248(12): 2841–2888, 2010.
- [KW12] K.U. Kristiansen and C. Wulff. Exponential estimates of slow manifolds. *arXiv:1208.4219*, pages 1–31, 2012.
- [Kwa13] F. Kwasniok. Analysis and modelling of glacial climate transitions using simple dynamical systems. *Phil. Trans. R. Soc. A*, 371(1991):20110472, 2013.
- [KWR10] T. Kispersky, J.A. White, and H.G. Rotstein. The mechanism of abrupt transition between theta and hyper-excitatory spiking activity in medial entorhinal cortex layer II stellate cells. *PLoS ONE*, 5(11):e13697, 2010.
- [KWW05a] T. Kolokolnikov, M. J. Ward, and J. Wei. The existence and stability of spike equilibria in the one-dimensional Gray–Scott model: the pulse-splitting regime. *Physica D*, 202(3):258–293, 2005.
- [KWW05b] T. Kolokolnikov, M.J. Ward, and J. Wei. The existence and stability of spike equilibria in the one-dimensional Gray–Scott model: the low feed rate regime. *Stud. Appl. Math.*, 115(1):21–71, 2005.
- [KY72] P. Kokotovic and R. Yackel. Singular perturbation of linear regulators: basic theorems. *IEEE Trans. Aut. Contr.*, 17(1):29–37, 1972.
- [KY96a] R.Z. Khasminskii and G. Yin. Asymptotic expansions of singularly perturbed systems involving rapidly fluctuating Markov chains. *SIAM J. Appl. Math.*, 56(1):277–293, 1996.
- [KY96b] R.Z. Khasminskii and G. Yin. Asymptotic series for singularly perturbed Kolmogorov–Fokker–Planck equations. *SIAM J. Appl. Math.*, 56(6):1766–1793, 1996.
- [KY96c] R.Z. Khasminskii and G. Yin. On transition densities of singularly perturbed diffusions with fast and slow components. *SIAM J. Appl. Math.*, 56(6):1794–1819, 1996.
- [KY97] R.Z. Khasminskii and G. Yin. Constructing asymptotic series for probability distributions of Markov chains with weak and strong interactions. *Quart. Appl. Math.*, 55(1):177–200, 1997.
- [KY99] R.Z. Khasminskii and G. Yin. Singularly perturbed switching diffusions: rapid switchings and fast diffusions. *J. Optim. Theor. Appl.*, 102(3):555–591, 1999.
- [KY04] R.Z. Khasminskii and G. Yin. On averaging principles: an asymptotic expansion approach. *SIAM J. Math. Anal.*, 35(6):1534–1560, 2004.
- [KY05] R.Z. Khasminskii and G. Yin. Limit behavior of two-time-scale diffusions revisited. *J. Differential Equat.*, 212(1):85–113, 2005.
- [LACFG13] M. Lahutte-Auboin, R. Costalat, J.-P. Francoise, and R. Guillemin. Dip and buffering in a fast–slow system associated to brain lactate kinetics. *arXiv:1308.0486v1*, pages 1–11, 2013.
- [LAE08] T. Li, A. Abdulle, and W. E. Effectiveness of implicit methods for stiff stochastic differential equations. *Comm. Comp. Phys.*, 3(2):295–307, 2008.
- [Lag88] P.A. Lagerstrom. *Matched Asymptotic Expansions: Ideas and Techniques*. Springer, 1988.
- [Lan08] P. Langevin. Sur la théorie du mouvement brownien. *Compte-rendus des séances de l'Académie des sciences*, 146:530–534, 1908.
- [Lan49] R.E. Langer. The asymptotic solutions of ordinary linear differential equations of the second order, with special reference to a turning point. *Trans. Amer. Math. Soc.*, 67(2):461–490, 1949.
- [LaS49] J. LaSalle. Relaxation oscillations. *Quart. Appl. Math.*, 7:1–19, 1949.
- [Lax02] P.D. Lax. *Functional Analysis*. John Wiley & Sons, 2002.
- [LBLA87] R. Larter, C.L. Bush, T.R. Lonis, and B.D. Aguda. Multiple steady states, complex oscillations, and the devil's staircase in the peroxidase–oxidase reaction. *J. Chem. Phys.*, 87(10): 5765–5771, 1987.
- [LBR96] Y.X. Li, R. Bertram, and J. Rinzel. Modeling *N*-methyl-d-aspartate-induced bursting in dopamine neurons. *Neurosci.*, 71(2):397–410, 1996.
- [LC72] P.A. Lagerstrom and R.G. Casten. Basic concepts underlying singular perturbation techniques. *SIAM Rev.*, 14(1):63–120, 1972.

- [LC98] A. Longtin and D.R. Chialvo. Stochastic and deterministic resonances for excitable systems. *Phys. Rev. Lett.*, 81(18):4012–4015, 1998.
- [LCDS12] D. Llinaró, A. Champneys, M. Desroches, and M. Storace. Codimension-two homoclinic bifurcations underlying spike adding in the Hindmarsh–Rose burster. *SIAM J. Appl. Dyn. Syst.*, 11(3):939–962, 2012.
- [LD77] W.D. Lakin and P. Van Den Driessche. Time scales in population biology. *SIAM J. Appl. Math.*, 32(3):694–705, 1977.
- [LdST07] J. Llibre, P.R. da Silva, and M.A. Teixeira. Regularization of discontinuous vector fields via singular perturbation. *J. Dyn. Diff. Eq.*, 19(2):309–331, 2007.
- [LdST08] J. Llibre, P.R. da Silva, and M.A. Teixeira. Sliding vector fields via slow–fast systems. *Bull. Belg. Math. Soc.*, 15(5):851–869, 2008.
- [LdST09] J. Llibre, P.R. da Silva, and M.A. Teixeira. Study of singularities in nonsmooth dynamical systems via singular perturbation. *SIAM J. Appl. Dyn. Syst.*, 8(1):508–526, 2009.
- [LE88] S.A. Lomov and A.G. Eliseev. Asymptotic integration of singularly perturbed problems. *Russ. Math. Surv.*, 43(3):1–63, 1988.
- [LE92] J.P. Laprade and T. Erneux. Propagation failure in arrays of coupled bistable chemical reactors. *J. Phys. Chem.*, 96(12): 4931–4934, 1992.
- [Leb04] D. Lebiedz. Computing minimal entropy production trajectories: an approach to model reduction in chemical kinetics. *J. Chem. Phys.*, 120:6890–6897, 2004.
- [Lee06] J.M. Lee. *Introduction to Smooth Manifolds*. Springer, 2006.
- [Lee11] C.F. Lee. Singular perturbation analysis of a reduced model for collective motion: a renormalization group approach. *Phys. Rev. E*, 83:031127, 2011.
- [Lef57] S. Lefschetz. *Differential Equations: Geometric Theory*. Interscience Publishers, 1957.
- [Leh02] B. Lehman. The influence of delays when averaging slow and fast oscillating systems: overview. *IMA J. Math. Control Inform.*, 19:201–215, 2002.
- [Les98] A. Lesne. *Renormalization Methods: Critical Phenomena, Chaos, Fractal Structures*. Wiley, 1998.
- [Lev47] N. Levinson. Perturbations of discontinuous solutions of nonlinear systems of differential equations. *Proc. Nat. Acad. Sci. USA*, 33:214–218, 1947.
- [Lev49] N. Levinson. A second order differential equation with singular solutions. *Ann. Math.*, 50:127–153, 1949.
- [Lev50] N. Levinson. Perturbations and discontinuous solutions of non-linear systems of differential equations. *Acta. Math.*, 50:127–153, 1950.
- [Lev56] J.J. Levin. Singular perturbations of nonlinear systems of differential equations related to conditional stability. *Duke Math. J.*, 23(4):609–620, 1956.
- [Lev80] M. Levi. Periodically forced relaxation oscillations. In *Global Theory of Dynamical Systems*. Springer, 1980.
- [Lev81] M. Levi. *Qualitative analysis of the periodically forced relaxation oscillations*, volume 32 of *Mem. Amer. Math. Soc.* AMS, 1981.
- [Lev90] H.A. Levine. The role of critical exponents in blowup theorems. *SIAM Rev.*, 32(2):262–288, 1990.
- [LeV92] R.J. LeVeque. *Numerical Methods for Conservation Laws*. Birkhäuser, 1992.
- [Lev98] M. Levi. A new randomness-generating mechanism in forced relaxation oscillations. *Physica D*, 114(3):230–236, 1998.
- [Lev99] M. Levi. Geometry and physics of averaging with applications. *Physica D*, 132(1):150–164, 1999.
- [LFST⁺09] B.N. Lundstrom, M. Famulare, L.B. Sorenson, W.J. Spain, and A.L. Fairhall. Sensitivity of firing rate to input fluctuations depends on time scale separation between fast and slow variables in single neurons. *J. Comput. Neurosci.*, 27(2):277–290, 2009.
- [LG00] M.T. Lin and Z. Gajic. Reduced-order H_∞ optimal filtering for systems with slow and fast modes. *IEEE Trans. Circ. Syst.*, 47(2):250–254, 2000.
- [LG05] L. Lerman and V. Gelfreich. Fast-slow Hamiltonian dynamics near a ghost separatrix loop. *J. Math. Sci.*, 126:1445–1466, 2005.
- [LG09] C. Letellier and J.-M. Ginoux. Development of the nonlinear dynamical systems theory from radio engineering to electronics. *Int. J. Bif. Chaos*, 19:2131–2163, 2009.
- [LG12] S.J. Lade and T. Gross. Early warning signals for critical transitions: a generalized modeling approach. *PLoS Comp. Biol.*, 8:e1002360–6, 2012.
- [LG13] M. Linkerhand and C. Gros. Self-organized stochastic tipping in slow–fast dynamical systems. *Math. Mech. Complex Syst.*, pages 1–16, 2013, to appear.
- [LGONGSG04] B. Lindner, J. Garcia-Ojalvo, A. Neiman, and L. Schimansky-Geier. Effects of noise in excitable systems. *Physics Reports*, 392:321–424, 2004.
- [LGY91] R.R. Llinas, A.A. Grace, and Y. Yarom. In vitro neurons in mammalian cortical layer 4 exhibit intrinsic oscillatory activity in the 10–to 50-Hz frequency range. *Proc. Natl. Acad. Sci.*, 88(3):897–901, 1991.
- [LH96] R. Larter and S. Hemkin. Further refinements of the peroxidase-oxidase oscillator mechanism: Mixed-mode oscillations and chaos. *J. Phys. Chem.*, 100:18924–18930, 1996.
- [LHKH⁺08] T.M. Lenton, H. Held, E. Kriegler, J.W. Hall, W. Lucht, S. Rahmstorf, and H.J. Schellnhuber. Tipping elements in the Earth’s climate system. *Proc. Natl. Acad. Sci. USA*, 105(6):1786–1793, 2008.
- [Li03] Y. Li. Homoclinic tubes in discrete nonlinear Schrödinger equation under Hamiltonian perturbations. *Nonlinear Dyn.*, 31(4):393–434, 2003.
- [Li08] X.M. Li. An averaging principle for a completely integrable stochastic Hamiltonian system. *Nonlinearity*, 21(4):803–822, 2008.
- [Lic69] W. Lick. Two-variable expansions and singular perturbation problems. *SIAM J. Appl. Math.*, 17(4): 815–825, 1969.
- [Lin88] X.-B. Lin. Shadowing lemma and singularly perturbed boundary value problems. *SIAM J. Appl. Math.*, 49(1):26–54, 1988.
- [Lin90a] X.-B. Lin. Heteroclinic bifurcation and singularly perturbed boundary value problems. *J. Differential Equat.*, 84:319–382, 1990.
- [Lin90b] X.-B. Lin. Using Melnikov’s method to solve Shilnikov’s problems. *Proc. Roy. Soc. Edinburgh*, 116: 295–325, 1990.

- [Lin91] P. Lin. A numerical method for quasilinear singular perturbation problems with turning points. *Computing*, 46(2):155–164, 1991.
- [Lin01] X.-B. Lin. Construction and asymptotic stability of structurally stable internal layer solutions. *Trans. Amer. Math. Soc.*, 353:2983–3043, 2001.
- [Lin03] P. Lin. Theoretical and numerical analysis for the quasi-continuum approximation of a material particle model. *Math. Comput.*, 72(242):657–675, 2003.
- [Lin04] B. Lindner. Interspike interval statistics of neurons driven by colored noise. *Phys. Rev. E*, 69:022901, 2004.
- [Lin06] X.-B. Lin. Slow eigenvalues of self-similar solutions of the Dafermos regularization of a system of conservation laws: an analytic approach. *J. Dyn. Diff. Eq.*, 18(1):1–52, 2006.
- [Lin07] G. Lin. Periodic solutions for van der Pol equation with time delay. *Appl. Math. Comp.*, 187(2):1187–1198, 2007.
- [Lin09] X.-B. Lin. Algebraic dichotomies with an application to the stability of Riemann solutions of conservation laws. *J. Differential Equat.*, 11(1):2924–2965, 2009.
- [Lio37] J. Liouville. Sur le développement des fonctions et séries. *J. de Mathématiques Pures et Appliquées*, 1: 16–35, 1837.
- [Lip73] J.L. Lions. *Perturbations singulières dans les problèmes aux limites et en contrôle optimal*. Springer, 1973.
- [Lip96] R. Liptser. Large deviations for two scaled diffusions. *Prob. Theor. Rel. Fields*, 106:71–104, 1996.
- [Lit57a] J.E. Littlewood. On non-linear differential equations of second order: III. The equation $\ddot{y} - k(1 - y^2)\dot{y} + y = b\mu k \cos(\mu t + \alpha)$ for large k , and its generalizations. *Acta. Math.*, 97:267–308, 1957.
- [Lit57b] J.E. Littlewood. On non-linear differential equations of second order: IV. The general equation $\ddot{y} - kf(y)\dot{y} + g(y) = bkp(\varphi)$, $\varphi = t + a$ for large k and its generalizations. *Acta. Math.*, 98: 1–110, 1957.
- [Liu00] D. Liu. Exchange lemmas for singular perturbation problems with certain turning points. *J. Differential Equat.*, 167:134–180, 2000.
- [Liu04] W. Liu. Multiple viscous wave fan profiles for Riemann solutions of hyperbolic systems of conservation laws. *Discr. Cont. Dyn. Syst.*, 10(4):871–884, 2004.
- [Liu05] W. Liu. Geometric singular perturbation approach to steady-state Poisson-Nernst-Planck systems. *SIAM J. Appl. Math.*, 65(3):754–766, 2005.
- [Liu06] W. Liu. Geometric singular perturbations for multiple turning points: invariant manifolds and exchange lemmas. *J. Dyn. Diff. Eq.*, 18(3):667–691, 2006.
- [LJH78] D. Ludwig, D.D. Jones, and C.S. Holling. Qualitative analysis of insect outbreak systems: The spruce budworm and forest. *J. Animal Ecol.*, 47(1):315–332, 1978.
- [LJL05] K. Lorenz, T. Jahnke, and C. Lubich. Adiabatic integrators for highly oscillatory second-order linear differential equations with time-varying eigendecomposition. *BIT*, 45:91–115, 2005.
- [LK70] R.Y.S. Lynn and J.B. Keller. Uniform asymptotic solutions of second order linear ordinary differential equations with turning points. *Comm. Pure Appl. Math.*, 23(3):379–408, 1970.
- [LK84] B. Litkouhi and H. Khalil. Infinite-time regulators for singularly perturbed difference equations. *Int. J. Contr.*, 39(3):587–598, 1984.
- [LK85a] B. Litkouhi and H. Khalil. Multirate and composite control of two-time-scale discrete-time systems. *IEEE Trans. Aut. Contr.*, 30(7):645–651, 1985.
- [LK85b] D. Luse and H. Khalil. Frequency domain results for systems with slow and fast dynamics. *IEEE Trans. Aut. Contr.*, 30(12):1171–1179, 1985.
- [LK00] W.M. Long and L.V. Kalachev. Asymptotic analysis of dissolution of a spherical bubble (case of fast reaction outside the bubble). *Rocky Mountain J. Math.*, 30(1):293–313, 2000.
- [LKMH94] T. LoFaro, N. Kopell, E. Marder, and S.L. Hooper. Subharmonic coordination in networks of neurons with slow conductances. *Neural Comput.*, 6(1):69–84, 1994.
- [LL03a] F. Lin and T.-C. Lin. Multiple time scale dynamics in coupled Ginzburg–Landau equations. *Commun. Math. Sci.*, 1(4): 671–695, 2003.
- [LL03b] J. Lin and F.L. Lewis. Two-time scale fuzzy logic controller of flexible link robot arm. *Fuzzy Sets Syst.*, 139:125–149, 2003.
- [LL07] V.N. Livina and T.M. Lenton. A modified method for detecting incipient bifurcations in a dynamical system. *Geophysical Research Letters*, 34:L03712, 2007.
- [LL09a] C. Laing and G. Lord, editors. *Stochastic Methods in Neuroscience*. OUP, 2009.
- [LL09b] C.H. Lee and R. Lui. A reduction method for multiple time scale stochastic reaction networks. *J. Math. Chem.*, 46(4):1292–1321, 2009.
- [LL10] C.H. Lee and R. Lui. A reduction method for multiple time scale stochastic reaction networks with non-unique equilibrium probability. *J. Math. Chem.*, 47(2):750–770, 2010.
- [LL13] S. Lahbabi and F. Legoll. Effective dynamics for a kinetic Monte-Carlo model with slow and fast time scales. *arXiv:1301.0266v1*, pages 1–44, 2013.
- [LLB13] J. Li, K. Lu, and P. Bates. Normally hyperbolic invariant manifolds for random dynamical systems: Part I - persistence. *Trans. Amer. Math. Soc.*, 365(11):5933–5966, 2013.
- [LLS13] F. Legoll, T. Lelièvre, and G. Samaey. A micro-macro parareal algorithm: application to singularly perturbed ordinary differential equations. *SIAM J. Sci. Comput.*, 35(4):A1951–A1986, 2013.
- [LM88] P. Lochak and C. Meunier. *Multiphase averaging for classical systems: with applications to adiabatic theorems*. Springer, 1988.
- [LM94a] C.G. Lange and R.M. Miura. Singular perturbation analysis of boundary value problems for differential-difference equations. V. Small shifts with layer behaviour. *SIAM J. Appl. Math.*, 54(1):249–272, 1994.
- [LM94b] C.G. Lange and R.M. Miura. Singular perturbation analysis of boundary value problems for differential-difference equations. VI. Small shifts with rapid oscillations. *SIAM J. Appl. Math.*, 54(1):273–283, 1994.
- [LM97a] Y. Li and D.W. McLaughlin. Homoclinic orbits and chaos in discretized perturbed NLS systems: Part I. Homoclinic orbits. *J. Nonlinear Sci.*, 7(3):211–269, 1997.
- [LM97b] Y. Li and D.W. McLaughlin. Homoclinic orbits and chaos in discretized perturbed NLS systems: Part II. Symbolic dynamics. *J. Nonlinear Sci.*, 7(4):315–370, 1997.

- [LM13] P.S. Landa and P.V.E. McClintock. Nonlinear systems with fast and slow motions. Changes in the probability distribution for fast motions under the influence of slower ones. *Phys. Rep.*, 532(1):1–26, 2013.
- [LMH92] C. Lu, A.D. MacGillivray, and S.P. Hastings. Asymptotic behaviour of solutions of a similarity equation for laminar flows in channels with porous walls. *IMA J. Appl. Math.*, 49(2):139–162, 1992.
- [LMP05] S. Luzzatto, I. Melbourne, and F. Paccaut. The Lorenz attractor is mixing. *Comm. Math. Phys.*, 260(2):393–401, 2005.
- [LMT13] R. Lamour, R. März, and C. Tischendorf. *Differential-Algebraic Equations: A Projector Based Analysis*. Springer, 2013.
- [LMYZ12] J. Lei, M.C. Mackey, R. Yvinec, and C. Zhuge. Adiabatic reduction of a piecewise deterministic Markov model of stochastic gene expression with bursting transcription. *arXiv:1202.5411*, pages 1–39, 2012.
- [LN04] R.I. Leine and H. Nijmeijer. *Dynamics and Bifurcations of Non-Smooth Mechanical Systems*. Springer, 2004.
- [LN05] Y. Li and L. Nirenberg. The Dirichlet problem for singularly perturbed elliptic equations. *Comm. Pure Appl. Math.*, 15(6):1162–1222, 2005.
- [LN13] M.J. Luczak and J.R. Norris. Averaging over fast variables in the fluid limit for Markov chains: application to the supermarket model with memory. *Ann. Appl. Probab.*, 23(3):957–986, 2013.
- [LNS95] Ch. Lubich, K. Nipp, and D. Stoffer. Runge–Kutta solutions of stiff differential equations near stationary points. *SIAM J. Numer. Anal.*, 32(4):1296–1307, 1995.
- [LNT88] C.S. Lin, W.M. Ni, and I. Takagi. Large amplitude stationary solutions to a chemotaxis system. *J. Differential Equat.*, 72(1): 1–27, 1988.
- [LNW07] C.S. Lin, W.M. Ni, and J.C. Wei. On the number of interior peak solutions for a singularly perturbed Neumann problem. *Comm. Pure Appl. Math.*, 60:252–281, 2007.
- [LO93] J.G. Laforgue and R.E. O’Malley. Supersensitive boundary value problems. In *Asymptotic and Numerical Methods for Partial Differential Equations with Critical Parameters*, pages 215–223. Springer, 1993.
- [LO09] M. Luskin and C. Ortner. An analysis of node-based cluster summation rules in the quasicontinuum method. *SIAM J. Numer. Anal.*, 47(4):3070–3086, 2009.
- [LO10] C.H. Lee and H.G. Othmer. A multi-time-scale analysis of chemical reaction networks: I. Deterministic systems. *J. Math. Biol.*, 60:387–450, 2010.
- [LO13a] D.J.B. Lloyd and H. O’Farrell. On localised hotspots of an urban crime model. *Physica D*, 253:23–39, 2013.
- [LO13b] M. Luskin and C. Ortner. Atomistic-to-continuum coupling. *Acta Numerica*, 22:397–508, 2013.
- [Lob91] C. Lobry. Dynamic bifurcations. In E. Benoit, editor, *Dynamic Bifurcations*, volume 1493 of *Lecture Notes in Mathematics*, pages 1–13. Springer, 1991.
- [Lom92] S.A. Lomov. *Introduction to the General Theory of Singular Perturbations*. AMS, 1992.
- [Lon87] L.N. Long. Uniformly-valid asymptotic solutions to the Orr–Sommerfeld equation using multiple scales. *J. Eng. Math.*, 21(3):167–178, 1987.
- [Lon97] A. Longtin. Autonomous stochastic resonance in bursting neurons. *Phys. Rev. E*, 55(1):868–876, 1997.
- [Lop82] O. Lopes. FitzHugh–Nagumo system: boundedness and convergence to equilibrium. *J. Differential Equat.*, 44(3):400–413, 1982.
- [Lor63] E.N. Lorenz. Deterministic nonperiodic flows. *J. Atmosph. Sci.*, 20:130–141, 1963.
- [Lou59] W.S. Loud. Periodic solutions of a perturbed autonomous system. *Ann. Math.*, 70(3):490–529, 1959.
- [LP77] A.M. Lestini and V. Pereyra. An adaptive finite difference solver for nonlinear two-point boundary value problems with mild boundary layers. *SIAM J. Numer. Anal.*, 14:91–111, 1977.
- [LP93] G.D. Lythe and M.R.E. Proctor. Noise and slow–fast dynamics in a three-wave resonance problem. *Phys. Rev. E*, 47:3122–3127, 1993.
- [LP99] A. Luongo and A. Paolone. On the reconstitution problem in the multiple time-scale method. *Nonlinear Dynam.*, 19(2):133–156, 1999.
- [LQY10] Y. Li, H. Qian, and Y. Yi. Nonlinearity oscillations and multiscale dynamics in a closed chemical reaction system. *J. Dyn. Diff. Eq.*, 22:491–507, 2010.
- [LR60] C.C. Lin and A.L. Rabenstein. On the asymptotic solutions of a class of ordinary differential equations of the fourth order: I. Existence of regular formal solutions. *Trans. Amer. Math. Soc.*, 94(1):24–57, 1960.
- [LR84a] P.A. Lagerstrom and D.A. Reinelt. Note on logarithmic switchback terms in regular and singular perturbation expansions. *SIAM J. Appl. Math.*, 44(3):451–462, 1984.
- [LR84b] P. Lundberg and L. Rahm. A nonlinear convective system with oscillatory behaviour for certain parameter regimes. *J. Fluid Mech.*, 139:237–260, 1984.
- [LR94] Y.X. Li and J. Rinzel. Equations for $InSP_3$ receptor-mediated $[Ca^{2+}]_i$ oscillations derived from a detailed kinetic model: a Hodgkin–Huxley like formalism. *J. Theor. Biol.*, 166(4): 461–473, 1994.
- [LR01] B. Leimkuhler and S. Reich. A reversible averaging integrator for multiple time-scale dynamics. *J. Comput. Phys.*, 171:95–114, 2001.
- [LR04a] B. Leimkuhler and S. Reich. *Simulating Hamiltonian Dynamics*. CUP, 2004.
- [LR04b] T. Linß and H.-G. Roos. Analysis of a finite-difference scheme for a singularly perturbed problem with two small parameters. *J. Math. Anal. Appl.*, 289(2):355–366, 2004.
- [LRV00] T. Linß, H.-G. Roos, and R. Vulanovic. Uniform pointwise convergence on Shishkin-type meshes for quasi-linear convection-diffusion problems. *SIAM J. Numer. Anal.*, 38(3):897–912, 2000.
- [LS42] N. Levinson and O.K. Smith. A general equation for relaxation oscillations. *Duke Math. J.*, 9(2): 382–403, 1942.
- [LS75] N.R. Lebovitz and R.J. Schaar. Exchange of stabilities in autonomous systems I. *Stud. Appl. Math.*, 54:229–260, 1975.
- [LS77] N.R. Lebovitz and R.J. Schaar. Exchange of stabilities in autonomous systems II. *Stud. Appl. Math.*, 56:1–50, 1977.
- [LS80] R. Llinás and M. Sugimori. Electrophysiological properties of in vitro Purkinje cell dendrites in mammalian cerebellar slices. *J. Physiol.*, 305(1):197–213, 1980.
- [LS83] G.S. Ladde and D.D. Siljuk. Multiparameter singular perturbations of linear systems with multiple time scales. *Automatica*, 19(4):385–394, 1983.

- [LS86] J. Lorenz and R. Sanders. Second order nonlinear singular perturbation problems with boundary conditions of mixed type. *SIAM J. Math. Anal.*, 17(3):580–594, 1986.
- [LS91] R. Larter and C.G. Steinmetz. Chaos via mixed-mode oscillations. *Phil. Trans. R. Soc. Lond. A*, 337:291–298, 1991.
- [LS00] R. Liptser and V. Spokoiny. On estimating a dynamic function of a stochastic system with averaging. *Stat. Inf. Stoch. Proc.*, 3(3):225–249, 2000.
- [LS01a] T. Linß and M. Stynes. Asymptotic analysis and Shishkin-type decomposition for an elliptic convection–diffusion problem. *J. Math. Anal. Appl.*, 261(2):604–632, 2001.
- [LS01b] T. Linß and M. Stynes. The SDFEM on Shishkin meshes for linear convection–diffusion problems. *Numer. Math.*, 87(3):457–484, 2001.
- [LS03] X.-B. Lin and S. Schechter. Stability of self-similar solutions of the Dafermos regularization of a system of conservation laws. *SIAM J. Math. Anal.*, 35(4):884–921, 2003.
- [LS12] K.W. Lee and S.N. Singh. Bifurcation of orbits and synchrony in inferior olive neurons. *J. Math. Biol.*, 65:465–491, 2012.
- [LS13] D. Lebiedz and J. Siehr. A continuation method for the efficient solution of parametric optimization problems in kinetic model reduction. *arXiv:1301.5815*, pages 1–19, 2013.
- [LSA88] R. Larter, C.G. Steinmetz, and B.D. Aguda. Fast-slow variable analysis of the transition to mixed-mode oscillations and chaos in the peroxidase reaction. *J. Chem. Phys.*, 89(10):6506–6514, 1988.
- [LSAC08] D.J.B. Lloyd, B. Sandstede, D. Avitabile, and A.R. Champneys. Localized hexagon patterns of the planar Swift–Hohenberg equation. *SIAM J. Appl. Dyn. Syst.*, 7(3):1049–1100, 2008.
- [LSB11] G. Lajoie and E. Shea-Brown. Shared inputs, entrainment, and desynchrony in elliptic bursters: from slow passage to discontinuous circle maps. *SIAM J. Appl. Dyn. Syst.*, 10(4):1232–1271, 2011.
- [LSG99] B. Lindner and L. Schimansky-Geier. Analytical approach to the stochastic FitzHugh–Nagumo system and coherence resonance. *Phys. Rev. E*, 60(6):7270–7276, 1999.
- [LSG00] B. Lindner and L. Schimansky-Geier. Coherence and stochastic resonance in a two-state system. *Phys. Rev. E*, 61(6):6103–6110, 2000.
- [LSR07] T. Lelièvre, G. Stoltz, and M. Rousset. Computation of free energy profiles with parallel adaptive dynamics. *J. Chem. Phys.*, 126:134111, 2007.
- [LSR10] T. Lelièvre, G. Stoltz, and M. Rousset. *Free Energy Computations: A Mathematical Perspective*. World Scientific, 2010.
- [LSS13] H.K.H. Lentz, T. Selhorst, and I.M. Sokolov. Unfolding accessibility provides a macroscopic approach to temporal networks. *Phys. Rev. Lett.*, 110:118701, 2013.
- [LST98] C. Lobry, T. Sari, and S. Touhami. On Tykhonov’s theorem for convergence of solutions of slow and fast systems. *Electron. J. Differential Equat.*, 19:1–22, 1998.
- [LSU11] D. Lebiedz, J. Siehr, and J. Unger. A variational principle for computing slow invariant manifolds in dissipative dynamical systems. *SIAM J. Sci. Comput.*, 33(2):703–720, 2011.
- [LT99] E. Lee and D. Terman. Uniqueness and stability of periodic bursting solutions. *J. Differential Equat.*, 158:48–78, 1999.
- [LT03] C.R. Laing and W.C. Troy. PDE methods for nonlocal models. *SIAM J. Appl. Dyn. Syst.*, 2(3):487–516, 2003.
- [LT13] E. Lee and D. Terman. Stable antiphase oscillations in a network of electrically coupled model neurons. *SIAM J. Appl. Dyn. Syst.*, 12(1):1–27, 2013.
- [LTB90] D. Lindberg, J.S. Turner, and D. Barkley. Chaos in the Showalter–Noyes–Bar–Eli model of the Belousov–Zhabotinskii reaction. *J. Chem. Phys.*, 92(5):3238–3239, 1990.
- [LTGE02] C.R. Laing, W.C. Troy, B. Gutkin, and B. Ermentrout. Multiple bumps in a neuronal model of working memory. *SIAM J. Appl. Math.*, 63(1):62–97, 2002.
- [LTK⁺07] K. Henzler-Wildman M. Lei, V. Thai, J. Kerns, M. Karplus, and D. Kern. A hierarchy of timescales in protein dynamics is linked to enzyme catalysis. *Nature*, 450:913–918, 2007.
- [LTLE95] A.M. Levine, G.H.M. Van Tartwijk, D. Lenstra, and T. Erneux. Diode lasers with optical feedback: stability of the maximum gain mode. *Phys. Rev. A*, 52(5):3436–3439, 1995.
- [Lu76] Y.-C. Lu. *Singularity Theory and an Introduction to Catastrophe Theory*. Springer, 1976.
- [Lub88] Ch. Lubich. Convolution quadrature and discretized operational calculus. II. *Numer. Math.*, 52(4):413–415, 1988.
- [Lub90] Ch. Lubich. On the convergence of multistep methods for nonlinear stiff differential equations. *Numer. Math.*, 58(1):839–853, 1990.
- [Lub93] Ch. Lubich. Integration of stiff mechanical systems by Runge–Kutta methods. *Z. Angew. Math. Phys.*, 44(6):1022–1053, 1993.
- [Lub08] C. Lubich. *From Quantum to Classical Molecular Dynamics: Reduced Models and Numerical Analysis*. EMS, 2008.
- [Lus01] K. Lust. Improved numerical Floquet multipliers. *Int. J. Bif. Chaos*, 11:2389–2410, 2001.
- [LV02] B. Lánová and J. Vršek. Study of the Bray–Liebhafsky reaction by on-line mass spectrometry. *J. Phys. Chem. A*, 106: 1228–1232, 2002.
- [LV06] W. Liu and E. Van Vleck. Turning points and traveling waves in FitzHugh–Nagumo type equations. *J. Differential Equat.*, 225(2):381–410, 2006.
- [LV13] J. Llibre and C. Valls. Darboux integrability of polynomial differential systems in \mathbb{R}^3 . *Bull. Belg. Math. Soc.*, 20(4):603–619, 2013.
- [LVEZE04] T. Li, E. Vandewijnden, P. Zhang, and W. E. Stochastic models of polymeric fluids at small Deborah number. *J. Non-Newtonian Fluid Mech.*, 121:117–125, 2004.
- [LW70] W. Liniger and R.A. Willoughby. Efficient integration methods for stiff systems of ordinary differential equations. *SIAM J. Numer. Anal.*, 7(1):47–66, 1970.
- [LW99a] B. Lehman and S.P. Weibel. Averaging theory for delay difference equations with time-varying delays. *SIAM J. Appl. Math.*, 59(4):1487–1506, 1999.
- [LW99b] B. Lehman and S.P. Weibel. Fundamental theorems of averaging for functional-differential equations. *J. Differential Equat.*, 152:160–190, 1999.
- [LW10a] W. Liu and B. Wang. Poisson–Nernst–Planck systems for narrow tubular-like membrane channels. *J. Dyn. Diff. Eq.*, 22(3):413–437, 2010.

- [LW10b] G. Lv and M. Wang. Existence, uniqueness and asymptotic behavior of traveling wave fronts for a vector disease model. *Nonl. Anal.: Real World Appl.*, 11(3):2035–2043, 2010.
- [LWH07] X. Li, J. Wang, and W. Hu. Effects of chemical synapses on the enhancement of signal propagation in coupled neurons near the canard regime. *Phys. Rev. E*, 76(4):041902, 2007.
- [LWW12] D. Liang, P. Weng, and J. Wu. Travelling wave solutions in a delayed predator-prey diffusion PDE system point-to-periodic and point-to-point waves. *IMA J. Appl. Math.*, 77(4):516–545, 2012.
- [LXY03] W. Liu, D. Xiao, and Y. Yi. Relaxation oscillations in a class of predator-prey systems. *J. Differential Equat.*, 188(1):306–331, 2003.
- [LY75] T.-Y. Li and J.A. Yorke. Period three implies chaos. *Amer. Math. Monthly*, 82(10):985–992, 1975.
- [LY05] G. Lin and R. Yuan. Periodic solution for a predator-prey system with distributed delay. *Math. Comput. Model.*, 42(9):959–966, 2005.
- [LY06a] G. Lin and R. Yuan. Periodic solution for equations with distributed delays. *Proc. R. Soc. Edinburgh A*, 136(6):1317–1325, 2006.
- [LY06b] G. Lin and R. Yuan. Travelling waves for the population genetics model with delay. *The ANZIAM Journal*, 48(1):57–71, 2006.
- [Lya47] A.M. Lyapunov. *Problème général de la stabilité du mouvement*. Princeton University Press, 1947.
- [Lyt95] G.D. Lythe. Noise and dynamic transitions. In *Stochastic Partial Differential Equations (Edinburgh, 1994)*, pages 181–188. Springer, 1995.
- [Lyt96] G.D. Lythe. Domain formation in transitions with noise and a time-dependent bifurcation parameter. *Phys. Rev. E*, 53:4271, 1996.
- [LZ11] N. Lu and C. Zeng. Normally elliptic singular perturbations and persistence of homoclinic orbits. *J. Differential Equat.*, 250(11):4124–4176, 2011.
- [LZ13] C. Li and H. Zhu. Canard cycles for predator-prey systems with Holling types of functional response. *J. Differential Equat.*, 254:879–910, 2013.
- [LZSK12] C.R. Laing, Y. Zou, B. Smith, and I.G. Kevrekidis. Managing heterogeneity in the study of neural oscillator dynamics. *J. Math. Neurosci.*, 2:5, 2012.
- [Maa98] U. Maas. Efficient calculation of intrinsic low-dimensional manifolds for simplification of chemical kinetics. *Comp. Vis. Sci.*, 1:69–82, 1998.
- [Mac68] B.D. MacMillan. Asymptotic methods for systems of differential equations in which some variables have very short response times. *SIAM J. Appl. Math.*, 16(4):704–722, 1968.
- [Mac78] A.D. MacGillivray. On a model equation of Lagerstrom. *SIAM J. Appl. Math.*, 34(4):804–812, 1978.
- [Mac79] A.D. MacGillivray. The existence of an overlap domain for a singular perturbation problem. *SIAM J. Appl. Math.*, 36(1):106–114, 1979.
- [Mac80] A.D. MacGillivray. On the switchback term in the asymptotic expansion of a model singular perturbation problem. *J. Math. Anal. Appl.*, 77(2):612–625, 1980.
- [Mac01] A. Maccari. The response of a parametrically excited van der Pol oscillator to a time delay state feedback. *Nonlinear Dynamics*, 26(2):105–119, 2001.
- [Mac04] R.S. MacKay. Slow manifolds. In *Energy Localisation and Transfer*, pages 149–192. World Scientific, 2004.
- [Mae07a] P. De Maesschalck. Ackerberg-O’Malley resonance in boundary value problems with a turning point of any order. *Comm. Pure Appl. Anal.*, 6(2):311–333, 2007.
- [Mae07b] P. De Maesschalck. Gevrey properties of real planar singularly perturbed systems. *J. Differential Equat.*, 238:338–365, 2007.
- [MAEL07] F. Mormann, R.G. Andrzejak, C.E. Elger, and K. Lehnertz. Seizure prediction: the long and winding road. *Brain*, 130:314–333, 2007.
- [Mag78] K. Maginu. Stability of periodic travelling wave solutions of a nerve conduction equation. *J. Math. Biol.*, 6(1):49–57, 1978.
- [Mag80] K. Maginu. Existence and stability of periodic travelling wave solutions to Nagumo’s nerve equation. *J. Math. Biol.*, 10(2):133–153, 1980.
- [Mag85] K. Maginu. Geometrical characteristics associated with stability and bifurcations of periodic travelling waves in reaction-diffusion systems. *SIAM J. Appl. Math.*, 45(5):750–774, 1985.
- [MAG05] A.J. Majda, R.V. Abramov, and M.J. Grote. *Information Theory and Stochastics for Multiscale Nonlinear Systems*. AMS, 2005.
- [Mah82] M.S. Mahmoud. Structural properties of discrete systems with slow and fast modes. *Large Scale Systems*, 3(4):227–236, 1982.
- [Maj03] A.J. Majda. *Introduction to PDEs and Waves for the Atmosphere and Ocean*. AMS, 2003.
- [Maj07] A.J. Majda. New multiscale models and self-similarity in tropical convection. *J. Atmos. Sci.*, 64(4):1393–1404, 2007.
- [Mal05] A. Malchiodi. Concentration at curves for a singularly perturbed Neumann problem in three-dimensional domains. *Geom. Funct. Anal.*, 15(6):1162–1222, 2005.
- [Man78] R. Mané. Persistent manifolds are normally hyperbolic. *Trans. Amer. Math. Soc.*, 246:261–283, 1978.
- [Man87] P. Mandel. Properties of a good cavity laser with swept losses. *Optics Commun.*, 64(6):549–552, 1987.
- [Man06] M.B.A. Mansour. Existence of traveling wave solutions in a hyperbolic-elliptic system of equations. *Comm. Math. Sci.*, 4(4):731–739, 2006.
- [Man09a] M.B.A. Mansour. Existence of traveling wave solutions for a nonlinear dissipative-dispersive equation. *Appl. Math. Mech.*, 30(4):513–516, 2009.
- [Man09b] M.B.A. Mansour. Travelling wave solutions for a singularly perturbed Burgers-KdV equation. *Pramana*, 73(5):799–806, 2009.
- [Man13] M.B.A. Mansour. A geometric construction of traveling waves in a generalized nonlinear dispersive-dissipative equation. *J. Geom. Phys.*, pages 1–11, 2013. in press.
- [MAP96] A.M. Mandel, M. Akke, and A.G. Palmer. Dynamics of ribonuclease H: temperature dependence of motions on multiple time scales. *Biochem.*, 35(50):16009–16023, 1996.
- [Mar70] R.A. Marcus. Extension of the WKB method to wave functions and transition probability amplitudes (S -matrix) for inelastic or reactive collisions. *Chem. Phys. Lett.*, 7(5):525–532, 1970.
- [Mar85] R. Marino. High-gain feedback in non-linear control systems. *Int. J. Control.*, 42(6):1369–1385, 1985.
- [Mar86] P.A. Markowich. *The Stationary Semiconductor Device Equations*. Springer, 1986.

- [Mar96] G.J.M. Maree. Slow passage through a pitchfork bifurcation. *SIAM J. Appl. Math.*, 56(3):889–918, 1996.
- [Mas80] J. Maselko. Experimental studies of complicated oscillations. The system Mn^{2+} -malonic acid- $\text{KBrO}_3\text{-H}_2\text{SO}_4$. *Chem. Phys.*, 51(3):473–480, 1980.
- [Mas94] V.P. Maslov. *The Complex WKB Method for Nonlinear Equations: Linear theory*. Springer, 1994.
- [Mas02] M. Massot. Singular perturbation analysis for the reduction of complex chemistry in gaseous mixtures using the entropic structure. *Comptes Rendus Math.*, 335:93–98, 2002.
- [Mat95] P. Mathieu. Spectra, exit times and long time asymptotics in the zero-white-noise limit. *Stoch. Stoch. Rep.*, 55(1):1–20, 1995.
- [Mat00] É. Matzinger. A note on the forced van der Pol equation. *C. R. Acad. Sci. Paris Sér. I Math.*, 331(4):281–286, 2000.
- [Mat01] K. Matthies. Time-averaging under fast periodic forcing of parabolic partial differential equations: exponential estimates. *J. Differential Equat.*, 174(1):133–180, 2001.
- [Mat06] É. Matzinger. Asymptotic behaviour of solutions near a turning point: the example of the Brusselator equation. *J. Differential Equat.*, 220(2):478–510, 2006.
- [May03] I.D. Mayergoyz. *Mathematical Models of Hysteresis and their Applications*. Academic Press, 2003.
- [Maz73] B. Mazur. Frobenius and the Hodge filtration (estimates). *Ann. Math.*, 98(1):58–95, 1973.
- [MB95] J.R. Mika and J. Banasiak. *Singularly perturbed evolution equations with applications to kinetic theory*. World Scientific, 1995.
- [MB04] A.J. Majda and J.A. Biello. A multiscale model for tropical intraseasonal oscillations. *Proc. Nat. Acad. Sci. USA*, 101:4736–4741, 2004.
- [MBK13] W.W. Mohammed, D. Blöümker, and K. Klepel. Modulation equation for stochastic Swift–Hohenberg equation. *SIAM J. Math. Anal.*, 45(1):14–30, 2013.
- [MC85] D.D. Moerdler and A.J. Calise. Two-time scale stabilization of systems with output feedback. *J. Guid. Contr. Dyn.*, 8:731–736, 1985.
- [MC86] M.R. Maxey and S. Corrsin. Gravitational settling of aerosol particles in randomly oriented cellular flow fields. *J. Atmos. Sci.*, 43(11):1112–1134, 1986.
- [MC04] G.S. Medvedev and J.E. Cisternas. Multimodal regimes in a compartmental model of the dopamine neuron. *Phys. D*, 194(3–4):333–356, 2004.
- [MCA⁺11] F. Marino, M. Ciszak, S.F. Abdalah, K. Al-Naimee, R. Meucci, and F.T. Arecchi. Mixed-mode oscillations via canard explosions in light-emitting diodes with optoelectronic feedback. *Phys. Rev. E*, 84:047201, 2011.
- [McC88] C. McCord. The connection map for attractor-repeller pairs. *Trans. Amer. Math. Soc.*, 307(1):195–203, 1988.
- [McC06] C. McCluskey. Lyapunov functions for tuberculosis models with fast and slow progression. *Math. Biosci. Eng.*, 3(4):603–614, 2006.
- [MCC⁺08] M. Mikikian, M. Cavarrroc, L. Couedel, Y. Tessier, and L. Boufendi. Mixed-mode oscillations in complex plasma instabilities. *Physical Review Letters*, 100(22), 2008.
- [MCJS09] V. Manukian, N. Costanzino, C.K.R.T. Jones, and B. Sandstede. Existence of multi-pulses of the regularized short-pulse and Ostrovsky equations. *J. Dyn. Diff. Eq.*, 21:607–622, 2009.
- [McK55] R.W. McKelvey. The solutions of second order linear ordinary differential equations about a turning point of order two. *Trans. Amer. Math. Soc.*, 79(1):103–123, 1955.
- [McK70] H.P. McKean. Nagumo's equation. *Adv. Math.*, 4:209–223, 1970.
- [MCS86] M.S. Mahmoud, Y. Chen, and M.G. Singh. Discrete two-time-scale systems. *Int. J. Syst. Sci.*, 17(8):1187–1207, 1986.
- [MD10] P. De Maesschalck and F. Dumortier. Singular perturbations and vanishing passage through a turning point. *J. Differential Equat.*, 248:2294–2328, 2010.
- [MD11] P. De Maesschalck and F. Dumortier. Detectable canard cycles with singular slow dynamics of any order at the turning point. *Discr. Cont. Dyn. Syst. A*, 29(1):109–140, 2011.
- [MD13] P. De Maesschalck and M. Desroches. Numerical continuation techniques for planar slow–fast systems. *SIAM J. Appl. Dyn. Syst.*, 12(3):1159–1180, 2013.
- [MDK00] D.S. Morgan, A. Doelman, and T.J. Kaper. Stationary periodic patterns in the 1D Gray–Scott model. *Math. Appl. Anal.*, 7(1):105–150, 2000.
- [ME84] P. Mandel and T. Erneux. Laser Lorenz equations with a time-dependent parameter. *Phys. Rev. Lett.*, 53(19):1818–1821, 1984.
- [ME87] P. Mandel and T. Erneux. The slow passage through a steady bifurcation: delay and memory effects. *J. Stat. Phys.*, 48(5):1059–1070, 1987.
- [Mea95] K.D. Mease. Geometry of computational singular perturbations. *Nonlinear Contr. Syst. Design*, 2:855–861, 1995.
- [Mea05] K.D. Mease. Multiple time-scales in nonlinear flight mechanics: diagnosis and modeling. *Appl. Math. Comput.*, 164(2):627–648, 2005.
- [Med05] G.S. Medvedev. Reduction of a model of an excitable cell to a one-dimensional map. *Physica D*, 202(1):37–59, 2005.
- [Med06] G.S. Medvedev. Transition to bursting via deterministic chaos. *Phys. Rev. Lett.*, 97(4):048102, 2006.
- [Mei78] W. Meiske. An approximate solution of the Michaelis–Menten mechanism for quasi-steady and state quasi-equilibrium. *Math. Biosci.*, 42:63–71, 1978.
- [Mei07] J.D. Meiss. *Differential Dynamical Systems*. SIAM, 2007.
- [Meli03] J.M. Melenk. *hp-Finite Element Methods for Singular Perturbations*, volume 1796 of *Lecture Notes in Mathematics*. Springer, 2003.
- [MEvdD13] A. Machina, R. Edwards, and P. van den Driessche. Singular dynamics in gene network models. *SIAM J. Appl. Dyn. Syst.*, 12(1):95–125, 2013.
- [Mey67] R.E. Meyer. On the approximation of double limits by single limits and the Kaplun extension theorem. *J. Inst. Math. Appl.*, 3:245–249, 1967.
- [Mey83] R.E. Meyer. A view of the triple deck. *SIAM J. Appl. Math.*, 43(4):639–663, 1983.
- [MG53] S.C. Miller and R.H. Good. A WKB-type approximation to the Schrödinger equation. *Phys. Rev.*, 91:174, 1953.

- [MG12] L. Mitchell and G.A. Gottwald. On finite-size Lyapunov exponents in multiscale systems. *Chaos*, 22(2):023115, 2012.
- [MG13a] J. MacLean and G.A. Gottwald. On the convergence of the projective integration method for stiff ordinary differential equations. *arXiv:1301:6851v1*, pages 1–22, 2013.
- [MG13b] I. Mirzaev and J. Gunawardena. Laplacian dynamics on general graphs. *Bull. Math. Biol.*, 75(11):2118–2149, 2013.
- [MGB95] F. Marchesoni, L. Gammapponi, and A.R. Bulsara. Spatiotemporal stochastic resonance in a ϕ^4 model of kink-antikink nucleation. *Phys. Rev. Lett.*, 76(15):2609, 1995.
- [MGM⁺91] J.A.J. Metz, S.A.H. Geritz, G. Meszena, F.J.A. Jacobs, and J.S. van Heerwaarden. Adaptive dynamics: a geometrical study of the consequences of nearly faithful reproduction. In S.J. van Strien and S.M. Verduyn Lunel, editors, *Stochastic and Spatial Structures of Dynamical Systems*, pages 183–231. North-Holland, 1991.
- [MH01] G. Menon and G. Haller. Infinite dimensional geometric singular perturbation theory for the Maxwell-Bloch equations. *SIAM J. Math. Anal.*, 33(2):315–346, 2001.
- [Mic08] P.W. Michor. *Topics in Differential Geometry*. AMS, 2008.
- [Mie90] A. Mielke. Normal hyperbolicity of center manifolds and Saint-Venant's principle. *Arch. Rat. Mech. Anal.*, 110(4):353–372, 1990.
- [Mie02] A. Mielke. The Ginzburg-Landau equation in its role as a modulation equation. In *Handbook of Dynamical Systems 2*, pages 759–834. Elsevier, 2002.
- [Mik08] O. Mikitchenko. *Applications of the resolution of singularities to asymptotic analysis of differential equations*. PhD thesis, Boston University, Boston, USA, 2008.
- [Mil85] J. Milnor. On the concept of attractor. *Comm. Math. Phys.*, 99:177–195, 1985.
- [Mil97a] P.D. Miller. Nonmonotone waves in a three species reaction-diffusion model. *Meth. Appl. Anal.*, 4:261–282, 1997.
- [Mil97b] J.W. Milnor. *Topology from the Differentiable Viewpoint*. Princeton University Press, 1997.
- [Mil06] P.D. Miller. *Applied Asymptotic Analysis*. AMS, 2006.
- [Min47] N. Minorsky. *Introduction to Non-Linear Mechanics. Topological Methods. Analytical Methods. Non-Linear Resonance. Relaxation Oscillations*. Ann Arbor [Mich.]: J.W. Edwards, 1947.
- [Min62] N. Minorsky. *Nonlinear Oscillations*. Van Nostrand, 1962.
- [Mir81] W.L. Miranker. *Numerical Methods for Stiff Equations and Singular Perturbation Problems*. Kluwer, 1981.
- [Mis58] E.F. Mishchenko. Asymptotic theory of relaxation oscillations described by systems of second order. *Mat. Sb. N.S. (in Russian)*, 44(86):457–480, 1958.
- [Mis61] E.F. Mishchenko. Asymptotic calculation of periodic solutions of systems of differential equations containing small parameters in the derivatives. *AMS Transl. Ser.*, 2(18):199–230, 1961.
- [Mis95] K. Mischaikow. Conley Index Theory. In *Dynamical Systems*, pages 119–207. Springer, 1995.
- [Mit09] A. Mitrofanova. *Efficient systems biology algorithms for biological networks over multiple time-scales: from evolutionary to regulatory time*. PhD thesis, Courant Institute of Mathematical Sciences, NYU, New York, USA, 2009.
- [Miu76] R.M. Miura. The Korteweg-de Vries equation: a survey of results. *SIAM Rev.*, 18(3):412–459, 1976.
- [MK74] R.M. Miura and M.D. Kruskal. Application of a nonlinear WKB method to the Korteweg-DeVries equation. *SIAM J. Appl. Math.*, 26:376–395, 1974.
- [MK88] R. Marino and P.V. Kokotovic. A geometric approach to nonlinear singularly perturbed control systems. *Automatica*, 24(1):31–41, 1988.
- [MK93a] G.B. Di Masi and Y.M. Kabanov. The strong convergence of two-scale stochastic systems and singular perturbations of filtering equations. *J. Math. Syst. Est. Contr.*, 3:207–224, 1993.
- [MK93b] E.F. Mishchenko and A.Yu. Kolesov. Asymptotical theory of relaxation oscillations. *Proc. Steklov Inst. Math.*, 197:1–93, 1993.
- [MK01] G.S. Medvedev and N. Kopell. Synchronization and transient dynamics in the chains of electrically coupled Fitzhugh-Nagumo oscillators. *SIAM J. Appl. Math.*, 61(5):1762–1801, 2001.
- [MK03] A.J. Majda and R. Klein. Systematic multi-scale models for the tropics. *J. Atmosph. Sci.*, 60:393–408, 2003.
- [MK12a] M.M. McCarthy and N. Kopell. The effect of propofol anesthesia on rebound spiking. *SIAM J. Appl. Dyn. Syst.*, 11(4):1674–1697, 2012.
- [MK12b] C. Meisel and C. Kuehn. On spatial and temporal multilevel dynamics and scaling effects in epileptic seizures. *PLoS ONE*, 7(2):e30371, 2012.
- [MKHC02] D. McMillen, N. Kopell, J. Hasty, and J.J. Collins. Synchronizing genetic relaxation oscillators by intercell signaling. *Proc. Natl. Acad. Sci. USA*, 99(2):679–684, 2002.
- [MKK00] G.S. Medvedev, T.J. Kaper, and N. Kopell. A reaction-diffusion system with periodic front dynamics. *SIAM J. Appl. Math.*, 60(5):1601–1638, 2000.
- [MKKR94] E.F. Mishchenko, Yu.S. Kolesov, A.Yu. Kolesov, and N.Kh. Rozov. *Asymptotic Methods in Singularly Perturbed Systems*. Plenum Press, 1994.
- [MKP97] M. Moallem, K. Khorasani, and R.V. Patel. An integral manifold approach for tip-position tracking of flexible multi-link manipulators. *IEEE Trans. Robot. Aut.*, 13(6):823–837, 1997.
- [ML81] C. Morris and H. Lecar. Voltage oscillations in the barnacle giant muscle fiber. *Biophys. J.*, 35(1):193–213, 1981.
- [ML93] K. Murali and M. Lakshmanan. Transmission of signals by synchronization in a chaotic van der Pol-Duffing oscillator. *Phys. Rev. E*, 48(3):R1624–R1626, 1993.
- [MLK94] A.D. MacGillivray, B. Liu, and N.D. Kazarinoff. Asymptotic analysis of the peeling-off point of a French duck. *Methods and Applications of Analysis*, 1(4):488–509, 1994.
- [MLR11] K. Manktelow, M.J. Leamy, and M. Ruzzene. Multiple scales analysis of wave-wave interactions in a cubically nonlinear atomic chain. *Nonlinear Dyn.*, 63:193–203, 2011.
- [MLS08] R. May, S.A. Levin, and G. Sugihara. Ecology for bankers. *Nature*, 451:893–895, 2008.
- [MLSA07] R. Mankin, T. Laasa, E. Soika, and A. Ainsaar. Noise-controlled slow-fast oscillations in predator-prey models with the Beddington functional response. *Eur. Phys. J. B*, 59:259–269, 2007.
- [MM76] J. Marsden and M. McCracken. *The Hopf Bifurcation and Its Applications*. Springer, 1976.

- [MM02] K. Mischaikow and M. Mrozek. Conley Index Theory. In B. Fiedler, editor, *Handbook of Dynamical Systems*, volume 2, pages 393–460. North-Holland, 2002.
- [MM13a] S. MacLachlan and N. Madden. Robust solution of singularly perturbed problems using multigrid methods. *SIAM J. Sci. Comput.*, 35(5):A2225–A2254, 2013.
- [MM13b] F. Marino and F. Marin. Coexisting attractors and chaotic canard explosions in a slow–fast optomechanical system. *Phys. Rev. E*, 87(5):052906, 2013.
- [MMK02] A.G. Makeev, D. Maroudas, and I.G. Kevrekidis. “Coarse” stability and bifurcation analysis using stochastic simulators: kinetic Monte Carlo examples. *J. Chem. Phys.*, 116(23):10083–10091, 2002.
- [MMKW13] J. Mitry, M. McCarthy, N. Kopell, and M. Wechselberger. Excitable neurons, firing threshold manifolds and canards. *J. Math. Neurosci.*, 3:12, 2013.
- [MMR99] K. Mischaikow, M. Mrozek, and J.F. Reineck. Singular index pairs. *J. Dyn. Diff. Eq.*, 11(3):399–425, 1999.
- [MMR10] E. Manica, G.S. Medvedev, and J.E. Rubin. First return maps for the dynamics of synaptically coupled conditional bursters. *Biol. Cybernet.*, 103:87–104, 2010.
- [MN11a] J. Mohapatra and S. Natesan. Parameter-uniform numerical methods for singularly perturbed mixed boundary value problems using grid equidistribution. *J. Appl. Math. Comput.*, 37:247–265, 2011.
- [MN11b] K. Mukherjee and S. Natesan. Optimal error estimate of upwind scheme on Shishkin-type meshes for singularly perturbed parabolic problems with discontinuous convection coefficients. *BIT Numer. Math.*, 51:289–315, 2011.
- [MNB01] S.K. Mazmudar, A.H. Nayfeh, and D. Boroyevich. Theoretical and experimental investigation of the fast-and-slow-scale instabilities of a DC-DC converter. *IEEE Trans. Power Electron.*, 16(2):201–216, 2001.
- [MNS02] P. Morin, R.H. Nochetto, and K.G. Siebert. Convergence of adaptive finite element methods. *SIAM Rev.*, 44(4):631–658, 2002.
- [MO03] B. Mudavanhu and R.E. O’Malley. A new renormalization method for the asymptotic solution of weakly nonlinear vector systems. *SIAM J. Appl. Math.*, 63(2):373–397, 2003.
- [Moe96] R. Moeckel. Transition tori in the five-body problem. *J. Differential Equat.*, 129(2):290–314, 1996.
- [Moe02] J. Moehlis. Canards in a surface oxidation reaction. *J. Nonlinear Sci.*, 12:319–345, 2002.
- [Moe06] J. Moehlis. Canards for a reduction of the Hodgkin–Huxley equations. *J. Math. Biol.*, 52:141–153, 2006.
- [Mon86] J.T. Montgomery. Existence and stability of periodic motion under higher order averaging. *J. Differential Equat.*, 64(1):67–78, 1986.
- [Moo66] R.E. Moore. *Interval Analysis*. Prentice-Hall, 1966.
- [MOPSP05] M.P. Mortell, R.E. O’Malley, A. Pokrovskii, and V. Sobolev. *Singular Perturbations and Hysteresis*. SIAM, 2005.
- [Mor66] J.A. Morrison. Comparison of the modified method of averaging and the two variable expansion procedure. *SIAM Rev.*, 8:66–85, 1966.
- [Mor86] I.M. Moroz. Amplitude expansions and normal forms in a model for thermohaline convection. *Stud. Appl. Math.*, 74(2):155–170, 1986.
- [MOS89] F. Martinelli, E. Olivieri, and E. Scoppola. Small random perturbations of finite-and infinite-dimensional dynamical systems: unpredictability of exit times. *J. Stat. Phys.*, 55(3):477–504, 1989.
- [MOS96] J.J. Miller, E. O’Riordan, and G.I. Shishkin. *Fitted Numerical Methods for Singular Perturbation Problems*. World Scientific, 1996.
- [MOS02] S. Matthews, E. O’Riordan, and G.I. Shishkin. A numerical method for a system of singularly perturbed reaction–diffusion equations. *J. Comput. Appl. Math.*, 145:151–166, 2002.
- [MP92a] U. Maas and S.B. Pope. Implementation of simplified chemical kinetics based on intrinsic low-dimensional manifolds. In *Proceedings of the 24th International Symposium on Combustion*, pages 103–112. The Combustion Institute, 1992.
- [MP92b] U. Maas and S.B. Pope. Simplifying chemical kinetics: intrinsic low-dimensional manifolds in composition space. *Combust. Flame*, 88:239–264, 1992.
- [MP94] P.K. Moore and L.R. Petzold. A stepsize control strategy for stiff systems of ordinary differential equations. *Appl. Numer. Math.*, 15(4):449–463, 1994.
- [MP96] A. Milik and A. Prskawetz. Slow–fast dynamics in a model of population and resource growth. *Math. Popul. Stud.*, 6(2):155–169, 1996.
- [MP98] T.A. Mel’nikov and V.A. Plotnikov. Averaging of quasidifferential equations with fast and slow variables. *Siberian Math. J.*, 39(5):947–952, 1998.
- [MP99] J. Mallet-Paret. The global structure of traveling waves in spatially discrete dynamical systems. *J. Dyn. Diff. Eq.*, 8:49–128, 1999.
- [MP07] R. Molle and D. Passaseo. Multispike solutions of nonlinear elliptic equations with critical Sobolev exponent. *Comm. Partial Differential Equations*, 32:797–818, 2007.
- [MP08] R.O. Moore and K. Promislow. The semistrong limit of multipulse interaction in a thermally driven optical system. *J. Differential Equat.*, 245(6):1616–1655, 2008.
- [MP11] A. Mokkadem and M. Pelletier. A generalization of the averaging procedure: the use of two-time-scale algorithms. *SIAM J. Control Optim.*, 49(4):1523–1543, 2011.
- [MP12] P. De Maesschalck and N. Popovic. Gevrey properties of the asymptotic critical wave speed in a family of scalar reaction–diffusion equations. *J. Math. Anal. Appl.*, 386(2):542–558, 2012.
- [MP13] J.D. Mengers and J.M. Powers. One-dimensional slow invariant manifolds for fully coupled reaction and micro-scale diffusion. *SIAM J. Appl. Dyn. Syst.*, 12(2):560–595, 2013.
- [MPdIP12] M. Marvá, J.-C. Poggiale, and R. Bravo de la Parra. Reduction of slow–fast periodic systems with applications to population dynamics models. *Math. Models Methods Appl. Sci.*, 22(10):1250025, 2012.
- [MPFS96] A. Milik, A. Prskawetz, G. Feichtinger, and W.C. Sanderson. Slow–fast dynamics in Wonderland. *Environ. Model. Assessm.*, 1(1):3–17, 1996.
- [MPK09] P. De Maesschalck, N. Popovic, and T.J. Kaper. Canards and bifurcation delays of spatially homogeneous and inhomogeneous types in reaction–diffusion equations. *Adv. Differential Equat.*, 14(9):943–962, 2009.

- [MPL93] R. Mettin, U. Parlitz, and W. Lauterborn. Bifurcation structure of the driven van der Pol oscillator. *Int. J. Bif. Chaos*, 3(6):1529–1555, 1993.
- [MPM08] A. Mielke, A. Petrov, and J.A.C. Martins. Convergence of solutions of kinetic variational inequalities in the rate-independent quasi-static limit. *J. Math. Anal. Appl.*, 348:1012–1020, 2008.
- [MPN11] J. Mallet-Paret and R.D. Nussbaum. Superstability and rigorous asymptotics in singularly perturbed state-dependent delay-differential equations. *J. Differential Equat.*, 11(1):4037–4084, 2011.
- [MPS88] J. Mallet-Paret and G.R. Sell. Inertial manifolds for reaction diffusion equations in higher space dimensions. *J. Amer. Math. Soc.*, 1(4):805–866, 1988.
- [MPSS93] J. Mallet-Paret, G.R. Sell, and Z.D. Shao. Obstructions to the existence of normally hyperbolic inertial manifolds. *Indiana Univ. Math. J.*, 42(3):1027–1055, 1993.
- [MPY11] K.R. Meyer, J.F. Palacián, and P. Yanguas. Geometric averaging of Hamiltonian systems: periodic solutions, stability, and KAM tori. *SIAM J. Appl. Dyn. Syst.*, 10(3):817–856, 2011.
- [MR71] B.J. Matkowsky and E.L. Reiss. On the asymptotic theory of dissipative wave motion. *Arch. Rat. Mech. Anal.*, 42(3):194–212, 1971.
- [MR77] B.J. Matkowsky and E.L. Reiss. Singular perturbations of bifurcations. *SIAM J. Appl. Math.*, 33(2):230–255, 1977.
- [MR80] E.F. Mishchenko and N.Kh. Rozov. *Differential Equations with Small Parameters and Relaxation Oscillations (translated from Russian)*. Plenum Press, 1980.
- [MR83] P.A. Markowich and C.A. Ringhofer. Singular perturbation problems with a singularity of the second kind. *SIAM J. Math. Anal.*, 14(5):897–914, 1983.
- [MR84] P.A. Markowich and C.A. Ringhofer. A singularly perturbed boundary value problem modelling a semiconductor device. *SIAM J. Appl. Math.*, 44:213–256, 1984.
- [MR90] V. Moll and S.I. Rosencrans. Calculation of the threshold surface for nerve equations. *SIAM J. Appl. Math.*, 50:1419–1441, 1990.
- [MR12a] K.L. Maki and Y. Renardy. The dynamics of a viscoelastic fluid which displays thixotropic yield stress behavior. *J. Non-Newtonian Fluid Mech.*, 181:30–50, 2012.
- [MR12b] L. Mamouhdi and R. Roussarie. Canard cycles of finite codimension with two breaking parameters. *Qual. Theory Dyn. Syst.*, 11(1):167–198, 2012.
- [MR13] C. Melcher and J.D.M. Rademacher. Patterns formation in axially symmetric Landau-Lifshitz-Gilbert-Slonczewski equations. *arXiv:1309.5523*, pages 1–27, 2013.
- [MRC⁺05] T. Mei, J. Roychowdhury, T.S. Coffey, S.A. Hutchinson, and D.M. Day. Robust, stable time-domain methods for solving MPDEs of fast/slow systems. *IEEE Trans. Computer-Aided Desg. Integr. Circ. Syst.*, 24(2):226–239, 2005.
- [MRS90] P.A. Markowich, C.A. Ringhofer, and C. Schmeiser. *Semiconductor Equations*. Springer, 1990.
- [MRS06] J.A.C. Martins, N.V. Revrova, and V.A. Sobolev. On the (in)-stability of quasi-static paths of smooth systems: definitions and sufficient conditions. *Math. Meth. Appl. Sci.*, 29(6):741–750, 2006.
- [MS74] J.W. Milnor and J.D. Stasheff. *Characteristic Classes*. Princeton University Press, 1974.
- [MS77] B.J. Matkowsky and Z. Schuss. The exit problem for randomly perturbed dynamical systems. *SIAM J. Appl. Math.*, 33(2):365–382, 1977.
- [MS79] B.J. Matkowsky and Z. Schuss. The exit problem: a new approach to diffusion across potential barriers. *SIAM J. Appl. Math.*, 36(3):604–623, 1979.
- [MS82] B.J. Matkowsky and Z. Schuss. Diffusion across characteristic boundaries. *SIAM J. Appl. Math.*, 42(4):822–834, 1982.
- [MS84] R. Silva Madriz and S.S. Sastry. Input–output description of linear systems with multiple time-scales. *Int. J. Contr.*, 40(4):699–721, 1984.
- [MS85] J. Maselko and H.L. Swinney. A complex transition sequence in the Belousov–Zhabotinskii reaction. *Physica Scripta*, T9:35–39, 1985.
- [MS86a] P.A. Markowich and C. Schmeiser. Uniform asymptotic representation of solutions of the basic semiconductor-device equations. *IMA J. Appl. Math.*, 36(1):43–57, 1986.
- [MS86b] J. Maselko and H.L. Swinney. A Farey triangle in the Belousov–Zhabotinskii reaction. *Phys. Lett. A*, 119(8):403–406, 1986.
- [MS86c] J. Maselko and H.L. Swinney. Complex periodic oscillation and Farey arithmetic in the Belousov–Zhabotinskii reaction. *J. Chem. Phys.*, 85:6430–6441, 1986.
- [MS87] J. Marsden and J. Scheurle. The construction and smoothness of invariant manifolds by the deformation method. *SIAM J. Math. Anal.*, 18(5):1261–1274, 1987.
- [MS88] B.J. Matkowsky and Z. Schuss. Uniform asymptotic expansions in dynamical systems driven by colored noise. *Phys. Rev. A*, 38(5):2605, 1988.
- [MS89] P.A. Markowich and P. Szmolyan. A system of convection-diffusion equations with small diffusion-coefficient arising in semiconductor physics. *J. Differential Equat.*, 81(2):234–254, 1989.
- [MS92] R.S. Maier and D.L. Stein. Transition-rate theory for nongradient drift fields. *Phys. Rev. Lett.*, 69(26):3691, 1992.
- [MS93a] R.S. Maier and D.L. Stein. Effect of focusing and caustics on exit phenomena in systems lacking detailed balance. *Phys. Rev. Lett.*, 71(12):1783, 1993.
- [MS93b] R.S. Maier and D.L. Stein. Escape problem for irreversible systems. *Phys. Rev. E*, 48(2):931, 1993.
- [MS95] A. Mielke and G. Schneider. Attractors for modulation equations on unbounded domains-existence and comparison. *Nonlinearity*, 8(5):743, 1995.
- [MS96a] R.S. Maier and D.L. Stein. Oscillatory behavior of the rate of escape through an unstable limit cycle. *Phys. Rev. Lett.*, 77(24):4860, 1996.
- [MS96b] R.S. Maier and D.L. Stein. A scaling theory of bifurcations in the symmetric weak-noise escape problem. *J. Stat. Phys.*, 83(3):291–357, 1996.
- [MS96c] R. McGehee and E. Sander. A new proof of the stable manifold theorem. *Z. Angew. Math. Phys.*, 47(4):497–513, 1996.
- [MS96d] D. McLaughlin and J. Shatah. Melnikov analysis for PDE's. In P. Deift, C.D. Levermore, and C.E. Wayne, editors, *Dynamical systems and probabilistic methods in partial differential equations (Berkeley, CA, 1994)*, pages 51–100. AMS, 1996.

- [MS97] R.S. Maier and D.L. Stein. Limiting exit location distributions in the stochastic exit problem. *SIAM J. Appl. Math.*, 57(3):752–790, 1997.
- [MS01a] R.S. Maier and D.L. Stein. Noise-activated escape from a sloshing potential well. *Phys. Rev. Lett.*, 86(18):3942, 2001.
- [MS01b] A. Milik and P. Szmolyan. Multiple time scales and canards in a chemical oscillator. In C.K.R.T. Jones, editor, *Multiple Time Scale Dynamical Systems*, volume 122, pages 117–140. Springer, 2001.
- [MS03a] N. Madden and M. Stynes. A uniformly convergent numerical method for a coupled system of two singularly perturbed linear reaction–diffusion problems. *IMA J. Numer. Anal.*, 23(4):627–644, 2003.
- [MS03b] D. Marchesin and S. Schechter. Oxidation heat pulses in two-phase expansive flow in porous media. *Z. Angew. Math. Phys.*, 54(1):48–83, 2003.
- [MS03c] K. Matthies and A. Scheel. Exponential averaging for Hamiltonian evolution equations. *Trans. Amer. Math. Soc.*, 355:747–773, 2003.
- [MS03d] G. Métivier and S. Schochet. Averaging theorems for conservative systems and the weakly compressible Euler equations. *J. Differential Equat.*, 187(1):106–183, 2003.
- [MS03e] C.C. Mitchell and D.G. Schaeffer. A two-current model for the dynamics of cardiac membrane. *Bull. Math. Biol.*, 65:767–793, 2003.
- [MS05] C. Mira and A. Shilnikov. Slow-fast dynamics generated by noninvertible plane maps. *Int. J. Bif. Chaos*, 15(11):3509–3534, 2005.
- [MS06] J.C. Da Mota and S. Schechter. Combustion fronts in a porous medium with two layers. *J. Dyn. Diff. Eq.*, 18(3):615–665, 2006.
- [MS09] V. Manukian and S. Schechter. Travelling waves for a thin liquid film with surfactant on an inclined plane. *Nonlinearity*, 22(1):85–122, 2009.
- [MS10] S. McCalla and B. Sandstede. Snaking of radial solutions of the multi-dimensional Swift–Hohenberg equation: A numerical study. *Physica D*, 239:1581–1592, 2010.
- [MS11] I. Melbourne and A. Stuart. A note on diffusion limits of chaotic skew product flows. *Nonlinearity*, 24:1361–1367, 2011.
- [MS13] J.B. McLeod and S. Sadhu. Existence of solutions and asymptotic analysis of a class of singularly perturbed ODEs with boundary conditions. *Adv. Differential Equat.*, 18(9):825–848, 2013.
- [MSB⁺13] C. Marschler, J. Sieber, R. Berkemer, A. Kawamoto, and J. Starke. Implicit methods for equation-free analysis: convergence results and analysis of emergent waves in microscopic traffic models. *arXiv:1301.6640v1*, pages 1–30, 2013.
- [MSBJ82] B.J. Matkowsky, Z. Schuss, and E. Ben-Jacob. A singular perturbation approach to Kramers’ diffusion problem. *SIAM J. Appl. Math.*, 42(4):835–849, 1982.
- [MSC11] T. Malashchenko, K. Shilnikov, and G. Cymbalyuk. Bistability of bursting and silence regimes in a model of a leech heart interneuron. *Phys. Rev. E*, 84:041910, 2011.
- [MSdIPS09] M. Marvá, E. Sánchez, R. Bravo de la Parra, and L. Sanz. Reduction of slow–fast discrete models coupling migration and demography. *J. Theoret. Biol.*, 258(3):371–379, 2009.
- [MSK⁺84] B.J. Matkowsky, Z. Schuss, C. Knossl, C. Tier, and M. Mangel. Asymptotic solution of the Kramers–Moyal equation and first-passage times for Markov jump processes. *Phys. Rev. A*, 29(6):3359, 1984.
- [MSLG98] A. Milik, P. Szmolyan, H. Loeffelmann, and E. Groeller. Geometry of mixed-mode oscillations in the 3-d autocatalator. *Int. J. Bif. Chaos*, 8(3):505–519, 1998.
- [MST83] B.J. Matkowsky, Z. Schuss, and C. Tier. Diffusion across characteristic boundaries with critical points. *SIAM J. Appl. Math.*, 43(4):673–695, 1983.
- [MST03] P.E. McSharry, L.A. Smith, and L. Tarassenko. Prediction of epileptic seizures. *Nature Med.*, 9:241–242, 2003.
- [MSU07] K. Matthies, G. Schneider, and H. Uecker. Exponential averaging for traveling wave solutions in rapidly varying periodic media. *Math. Nachr.*, 280(4):408–422, 2007.
- [MSVE06] P. Metzner, C. Schütte, and E. Vanden-Eijnden. Illustration of transition path theory on a collection of simple examples. *J. Chem. Phys.*, 125:084110, 2006.
- [MSVE09] P. Metzner, C. Schütte, and E. Vanden-Eijnden. Transition path theory for Markov jump processes. *Multiscale Model. Simul.*, 7(3):1192–1219, 2009.
- [MSZ00] A. Mielke, G. Schneider, and A. Ziegra. Comparison of inertial manifolds and application to modulated systems. *Math. Nachr.*, 214:53–70, 2000.
- [MT04] F. Mazzià and D. Trigant. A hybrid mesh selection strategy based on conditioning for boundary value ODE problems. *Numerical Algorithms*, 36:169–187, 2004.
- [MT10] W. Marszałek and Z. Trzaska. Mixed-mode oscillations in a modified Chua’s circuit. *Circuits Syst. Signal Process.*, 29(6):1075–1087, 2010.
- [MT11] T.V. Martini and R. Toral. Synchronization induced by repulsive interactions in a system of van der Pol oscillators. *Prog. Theor. Phys.*, 126(3):353–368, 2011.
- [MT12] S. Méléard and V.C. Tran. Slow and fast scales for superprocess limits of age-structured populations. *Stochastic Process. Appl.*, 122:250–276, 2012.
- [MTA08] K.D. Mease, U. Topcu, and E. Aykutluog. Characterizing two-timescale nonlinear dynamics using finite-time Lyapunov exponents and vectors. *arXiv:0807.0239v1*, pages 1–38, 2008.
- [MTVE99] A.J. Majda, I. Timofeyev, and E. Vanden-Eijnden. Models for stochastic climate prediction. *Proc. Nat. Acad. USA*, 96:14687–14691, 1999.
- [MTVE01] A.J. Majda, I. Timofeyev, and E. Vanden-Eijnden. A mathematical framework for stochastic climate models. *Comm. Pure and Appl. Math.*, 54:891–974, 2001.
- [MTVE02] A.J. Majda, I. Timofeyev, and E. Vanden-Eijnden. A priori tests of a stochastic mode reduction strategy. *Physica D*, 170:206–252, 2002.
- [MTVE03] A.J. Majda, I. Timofeyev, and E. Vanden-Eijnden. Systematic strategies for stochastic mode reduction in climate. *J. Atmosph. Sci.*, 60:1705–1722, 2003.
- [MTVE06] A.J. Majda, I. Timofeyev, and E. Vanden-Eijnden. Stochastic models for selected slow variables in large deterministic systems. *Nonlinearity*, 19:769–794, 2006.
- [Mun79] T. Munakata. Hydrodynamic equations from Fokker–Planck equations - multiple time scale method. *J. Phys. Soc. Japan*, 46:748–755, 1979.
- [Mun96] J.R. Munkres. *Elements Of Algebraic Topology*. Westview Press, 1996.

- [Mun97] J.R. Munkres. *Analysis on Manifolds*. Westview Press, 1997.
- [Mur74] J.D. Murray. On the role of myoglobin in muscle respiration. *J. Theor. Biol.*, 47(1):115–126, 1974.
- [Mur83] J. Murdoch. Some asymptotic estimates for higher order averaging and a comparison with iterated averaging. *SIAM J. Math. Anal.*, 14(3):421–424, 1983.
- [Mur84] J.D. Murray. *Asymptotic Analysis*. Springer, 1984.
- [Mur87] J.A. Murdoch. *Perturbations: Theory and Methods*. SIAM, 1987.
- [Mur94] J. Murdoch. Some foundational issues in multiple scale theory. *Applicable Analysis*, 53(3):157–173, 1994.
- [Mur02a] J. Murdoch. *Normal Forms and Unfoldings for Local Dynamical Systems*. Springer, 2002.
- [Mur02b] J.D. Murray. *Mathematical Biology I: An Introduction*. Springer, 3rd edition, 2002.
- [Mur03] J.D. Murray. *Mathematical Biology II: Spatial Models and Biomedical Applications*. Springer, 3rd edition, 2003.
- [Mus06] A. Mustafin. Two mutually loss-coupled lasers featuring astable multivibrator. *Physica D*, 218(2):167–176, 2006.
- [MVE08] C.B. Muratov and E. Vanden-Eijnden. Noise-induced mixed-mode oscillations in a relaxation oscillator near the onset of a limit cycle. *Chaos*, 18:015111, 2008.
- [MVEE05] C.B. Muratov, E. Vanden-Eijnden, and W. E. Self-induced stochastic resonance in excitable systems. *Physica D*, 210:227–240, 2005.
- [MW96] J. Murdoch and L.C. Wang. Validity of the multiple scale method for very long intervals. *Z. Angew. Math. Phys.*, 47(5):760–789, 1996.
- [MXO13] J.M. Melenk, C. Xenophontos, and L. Oberbroeckling. Robust exponential convergence of hp FEM for singularly perturbed reaction-diffusion systems with multiple scales. *IMA J. Numer. Anal.*, 33(2):609–628, 2013.
- [MY07] G. Medvedev and Y. Yoo. Multimodal oscillations in systems with strong contraction. *Physica D*, 228:87–106, 2007.
- [MY08] G. Medvedev and Y. Yoo. Chaos at the border of criticality. *Chaos*, 18:033105, 2008.
- [MY09] P. Ming and J.Z. Yang. Analysis of a one-dimensional nonlocal quasi-continuum method. *Multiscale Model. Simul.*, 7(4):1838–1875, 2009.
- [MZ08] A. Miranville and S. Zelik. Attractors for dissipative partial differential equations in bounded and unbounded domains. In *Handbook of Differential Equations: Evolutionary Equations*, pages 103–200. Elsevier, 2008.
- [MZ12] G. Medvedev and S. Zhuravlytska. Shaping bursting by electrical coupling and noise. *Biol. Cybern.*, 106(2):67–88, 2012.
- [NA12] A.I. Neishtadt and A.V. Artemyev. Destruction of adiabatic invariance for billiards in a strong nonuniform magnetic field. *Phys. Rev. Lett.*, 108:064102, 2012.
- [Nag39] M. Nagumo. Über das Verhalten der Integrale von $\lambda y'' + f(x, y, y', \lambda) = 0$ für $\lambda \rightarrow 0$. *Proc. Phys. Math. Soc. Japan*, 21:529–534, 1939.
- [Nag93] M. Nagumo. *Mitio Nagumo Collected Papers*. Springer, 1993.
- [Nai02] D.S. Naidu. Singular perturbations and time scales in control theory and applications: an overview. *Dynamics of Continuous, Discrete and Impulsive Systems Series B: Applications & Algorithms*, 9:233–278, 2002.
- [Nak03] M. Nakahara. *Geometry, Topology and Physics*. Taylor & Francis, 2003.
- [Nam90] S. Namachchivaya. Stochastic bifurcation. *Appl. Math. Comp.*, 38:101–159, 1990.
- [Nam03] S. Namachchivaya. Spindle speed variation for the suppression of regenerative chatter. *J. Nonl. Sci.*, 13(3):265–288, 2003.
- [Nar87] K. Narita. Asymptotic analysis for interactive oscillators of the van der Pol type. *Adv. Appl. Prob.*, 19:44–80, 1987.
- [Nar91] K. Narita. Asymptotic behavior of velocity process in the Smoluchowski-Kramers approximation for stochastic differential equations. *Adv. Appl. Prob.*, 23:317–326, 1991.
- [Nar93] K. Narita. Asymptotic behavior of solutions of SDE for relaxation oscillations. *SIAM J. Math. Anal.*, 24(1):172–199, 1993.
- [NAY62] J. Nagumo, S. Arimoto, and S. Yoshizawa. An active pulse transmission line simulating nerve axon. *Proc. IRE*, 50:2061–2070, 1962.
- [Nay70] A.H. Nayfeh. Nonlinear stability of a liquid jet. *Phys. Fluids*, 13:841, 1970.
- [Nay81] A.H. Nayfeh. *Introduction to Perturbation Techniques*. Wiley, 1981.
- [Nay04] A.H. Nayfeh. *Perturbation Methods*. Wiley, 2004.
- [Nay05] A.H. Nayfeh. Resolving controversies in the application of the method of multiple scales and the generalized method of averaging. *Nonlinear Dynam.*, 40:61–102, 2005.
- [Nay11] A.H. Nayfeh. *The Method of Normal Forms*. Wiley, 2011.
- [NBB08] W.H. Nesse, A. Borisyuk, and P.C. Bressloff. Fluctuation-driven rhythmogenesis in an excitatory neuronal network with slow adaptation. *J. Comput. Neurosci.*, 25(2):317–333, 2008.
- [NBK13] J.M. Newby, P.C. Bressloff, and J.P. Keener. Breakdown of fast–slow analysis in an excitable system with channel noise. *Phys. Rev. Lett.*, 111(12):128101, 2013.
- [NBS⁺06] C.S. Nunemaker, R. Bertram, A. Sherman, K. Tsaneva-Atanasova, C.R. Daniel, and L.S. Satin. Glucose modulates $[\text{Ca}^{2+}]_i$ oscillations in pancreatic islets via ionic and glycolytic mechanisms. *Biophys. J.*, 91(6):2082–2096, 2006.
- [NBW03] M.E.J. Newman, A.-L. Barabási, and D.J. Watts. *The Structure and Dynamics of Networks*. Princeton University Press, 2003.
- [NCO01] D.S. Naidu and A.J. Calise. Singular perturbations and time scales in guidance and control of aerospace systems: a survey. *J. Guid. Contr. Dyn.*, 24(6):1057–1078, 2001.
- [NDL⁺11] A.B. Neiman, K. Dierkes, B. Lindner, L. Han, and A.L. Shilnikov. Spontaneous voltage oscillations and response dynamics of a Hodgkin-Huxley type model of sensory hair cells. *J. Math. Neurosci.*, 1:1–24, 2011.
- [NE03] W.I. Newman and M. Efroimsky. The method of variation of constants and multiple time scales in orbital mechanics. *Chaos*, 13(2):476–485, 2003.
- [Neg08] C. Negulescu. Numerical analysis of a multiscale finite element scheme for the resolution of the stationary Schrödinger equation. *Numer. Math.*, 108(4):625–652, 2008.

- [Nei76] A.I. Neishtadt. Passage through a separatrix in a resonance problem with a slowly-varying parameter. *J. Appl. Math. Mech.*, 39(4):594–605, 1976.
- [Nei81] A.I. Neishtadt. On the accuracy of conservation of the adiabatic invariant. *J. Appl. Math. Mech.*, 45(1):58–63, 1981.
- [Nei84] A.I. Neishtadt. The separation of motions in systems with rapidly rotating phase. *J. Appl. Math. Mech.*, 48(2):133–139, 1984.
- [Nei87a] A.I. Neishtadt. On the change in the adiabatic invariant on crossing a separatrix in systems with two degrees of freedom. *J. Appl. Math. Mech.*, 51(5):586–592, 1987.
- [Nei87b] A.I. Neishtadt. Persistence of stability loss for dynamical bifurcations. I. *Differential Equations Translations*, 23:1385–1391, 1987.
- [Nei88] A.I. Neishtadt. Persistence of stability loss for dynamical bifurcations. II. *Differential Equations Translations*, 24:171–176, 1988.
- [Nei91] A.I. Neishtadt. Probability phenomena due to separatrix crossing. *Chaos*, 1(1):42–48, 1991.
- [Nei00] A.I. Neishtadt. On the accuracy of persistence of adiabatic invariant in single-frequency systems. *Reg. Chaotic Dyn.*, 5(2):213–218, 2000.
- [Nei03] A.I. Neishtadt. On averaging in two-frequency systems with small Hamiltonian and much smaller non-Hamiltonian perturbations. *Mosc. Math. J.*, 3:1039–1052, 2003.
- [Nei09] A.I. Neishtadt. On the stability loss delay for dynamical bifurcations. *Discr. Cont. Dyn. Sys. S*, 2(4):897–909, 2009.
- [Nes93] A.V. Nesterov. A modification of the boundary function method for singularly perturbed partial differential equations. *Math. Notes*, 54(1):705–709, 1993.
- [Net68] A.V. Netushil. Nonlinear element of stop type. *Avtom. Telemech.*, 7:175–179, 1968. (in Russian).
- [Net70] A.V. Netushil. Self-oscillations in systems with negative hysteresis. In *Proc. 5th International Conference on Nonlinear Oscillations*, volume 4, pages 393–396. Izdatne Inst. Mat. Akad. Nauk Ukrains., 1970. (in Russian).
- [Neu83] J.C. Neu. Resonantly interacting waves. *SIAM J. Appl. Math.*, 43:141–156, 1983.
- [New03] M.E.J. Newman. The structure and function of complex networks. *SIAM Review*, 45:167–256, 2003.
- [New11] M.E.J. Newman. *Networks - An Introduction*. OUP, 2011.
- [NF82] R.M. Noyes and S.D. Furrow. The oscillatory Briggs–Rauscher reaction. 3. A skeleton mechanism for oscillations. *J. Am. Chem. Soc.*, 104:45–48, 1982.
- [NF87] Y. Nishiura and H. Fujii. Stability of singularly perturbed solutions to systems of reaction–diffusion equations. *SIAM J. Math. Anal.*, 18(6):1726–1770, 1987.
- [NF89] A.H. Nguyen and S.J. Fraser. Geometrical picture of reaction in enzyme kinetics. *J. Chem. Phys.*, 91:186, 1989.
- [NF13] P. Nicolini and D. Frezzato. Features in chemical kinetics. II. A self-emerging definition of slow manifolds. *J. Chem. Phys.*, 138:234102, 2013.
- [Ngu89] G. Nguetseng. A general convergence result for a functional related to the theory of homogenization. *SIAM J. Math. Anal.*, 20(3):608–623, 1989.
- [NHCG98] C.A. Del Negro, C.F. Hsiao, S.H. Chandler, and A. Garfinkel. Evidence for a novel bursting mechanism in rodent trigeminal neurons. *Biophysical J.*, 75:174–182, 1998.
- [NHdIPA11] T. Nguyen-Huu, R. Bravo de la Parra, and P. Auger. Approximate aggregation of linear discrete models with two time scales: re-scaling slow processes to the fast scale. *J. Difference Equ. Appl.*, 17(4):621–635, 2011.
- [NHSS07] F. Noé, I. Horenko, C. Schütte, and J.C. Smith. Hierarchical analysis of conformational dynamics in biomolecules: transition networks of metastable states. *J. Chem. Phys.*, 126:(155101), 2007.
- [Ni98] W.-M. Ni. Diffusion, cross-diffusion and their spike-layer steady states. *Notices Amer. Math. Soc.*, 45(1):9–18, 1998.
- [Ni04] W.-M. Ni. Qualitative properties of solutions to elliptic problems. In *Stationary Partial Differential Equations*, volume 1 of *Handbook of Differential Equations*, pages 157–233. North-Holland, 2004.
- [Nii96] S. Nii. N-homoclinic bifurcations for homoclinic orbits changing their twisting. *J. Dyn. Diff. Eq.*, 8(4):549–572, 1996.
- [Nii97] S. Nii. Stability of travelling multiple-front (multiple-back) wave solutions of the FitzHugh–Nagumo equations. *SIAM J. Math. Anal.*, 28(5):1094–1112, 1997.
- [Nip83] K. Nipp. An extension of Tikhonov’s theorem in singular perturbations for the planar case. *Z. Angew. Math. Phys.*, 34(3):277–290, 1983.
- [Nip85] K. Nipp. Invariant manifolds of singularly perturbed ordinary differential equations. *ZAMP*, 36: 309–320, 1985.
- [Nip86a] K. Nipp. Breakdown of stability in singularly perturbed autonomous systems I. Orbit equations. *SIAM J. Math. Anal.*, 17(5):512–532, 1986.
- [Nip86b] K. Nipp. Breakdown of stability in singularly perturbed autonomous systems II. Estimates for the solutions and application. *SIAM J. Math. Anal.*, 17(5):1068–1085, 1986.
- [Nip91] K. Nipp. Numerical integration of stiff ODE’s of singular perturbation type. *Zeitschr. Appl. Math. Phys.*, 42:54–79, 1991.
- [Nip02] K. Nipp. Numerical integration of differential algebraic systems and invariant manifolds. *BIT*, 42(2):408–439, 2002.
- [Nis94] Y. Nishiura. Coexistence of infinitely many stable solutions to reaction diffusion systems in the singular limit. In *Dynamics Reported*, pages 25–103. Springer, 1994.
- [NKMS90] T. Naeh, M.M. Klosek, B.J. Matkowsky, and Z. Schuss. A direct approach to the exit problem. *SIAM J. Appl. Math.*, 50(2):595–627, 1990.
- [NLCK06] B. Nadler, S. Lafon, R.R. Coifman, and I.G. Kevrekidis. Diffusion maps, spectral clustering and reaction coordinates of dynamical systems. *Appl. Comput. Harmonic Anal.*, 21(1):113–127, 2006.
- [NM89] Y. Nishiura and M. Mimura. Layer oscillations in reaction–diffusion systems. *SIAM J. Appl. Math.*, 49(2):481–514, 1989.
- [NM95] A.H. Nayfeh and D.T. Mook. *Nonlinear Oscillations*. Wiley, 1995.

- [NM⁺10] J. Nowacki, , S.H. Mazlan, H.M. Osinga, and K.T. Tsaneva-Atanasova. The role of large-conductance Calcium-activated K^+ (BK) channels in shaping bursting oscillations of a somatotroph cell model. *Physica D*, 239(9):485–493, 2010.
- [NMIF90] Y. Nishiura, M. Mimura, H. Ikeda, and H. Fujii. Singular limit analysis of stability of traveling wave solutions in bistable reaction-diffusion systems. *SIAM J. Math. Anal.*, 21(1):85–122, 1990.
- [NN81] C. Nicolis and G. Nicolis. Stochastic aspects of climatic transitions—additive fluctuations. *Tellus*, 33(3):225–234, 1981.
- [NN13] F. Noé and F. Nüske. A variational approach to modeling slow processes in stochastic dynamical systems. *Multiscale Model. Simul.*, 11(2):635–655, 2013.
- [NOB⁺11] J. Nowacki, H.M. Osinga, J.T. Brown, A.D. Randall, and K.T. Tsaneva-Atanasova. A unified model of CA1/3 pyramidal cells: an investigation into excitability. *Progress in Biophysics and Molecular Biology*, 105:34–48, 2011.
- [Nor06] J.R. Norris. *Markov Chains*. Cambridge University Press, 2006.
- [NOTA12] J. Nowacki, H.M. Osinga, and K.T. Tsaneva-Atanasova. Dynamical systems analysis of spike-adding mechanisms in transient bursts. *J. Math. Neurosci.*, 2:7, 2012.
- [NP87] D.S. Naidu and D.B. Price. Time-scale synthesis of a closed-loop discrete optimal control system. *J. Guid. Contr. Dyn.*, 10(5):417–421, 1987.
- [NP88] D.S. Naidu and D.B. Price. Singular perturbation and time scale approaches in discrete control systems. *J. Guid. Contr. Dyn.*, 11(6):592–594, 1988.
- [NP03] E. Neumann and A. Pikovsky. Slow-fast dynamics in Josephson junctions. *Eur. Phys. J. B*, 34:293–303, 2003.
- [NPT95] G. Neher, L. Pohlmann, and H. Tributsch. Mixed-mode oscillations self-similarity and time-transient chaotic behaviour in the (photo-) electrochemical system $p - CuInSe_2/H_2O_2$. *J. Phys. Chem.*, 99:17763–17771, 1995.
- [NR85] D.S. Naidu and A.K. Rao. *Singular Perturbation Analysis of Discrete Control Systems*. Springer, 1985.
- [NRL86] A. Neves, H. Ribeiro, and O. Lopes. On the spectrum of evolution operators generated by hyperbolic systems. *J. Funct. Anal.*, 67:320–344, 1986.
- [NRT⁺10] J. Nawrath, M.C. Romano, M. Thiel, I. Kiss, M. Wickramasinghe, J. Timmer, J. Kurths, and B. Schelter. Distinguishing direct from indirect interactions in oscillatory networks with multiple time scales. *Phys. Rev. Lett.*, 104:038701, 2010.
- [NS95] K. Nipp and D. Stoffer. Invariant manifolds and global error estimates of numerical integration schemes applied to stiff systems of singular perturbation type - Part I: RK-methods. *Numer. Math.*, 70:245–257, 1995.
- [NS96] K. Nipp and D. Stoffer. Invariant manifolds and global error estimates of numerical integration schemes applied to stiff systems of singular perturbation type - Part II: Linear multistep methods. *Numer. Math.*, 74:305–323, 1996.
- [NS98] J.A. Nohel and D.H. Sattinger, editors. *Selected Papers of Norman Levinson Volume 1*. Springer, 1998.
- [NS99] N.N. Nefedov and K.R. Schneider. Immediate exchange of stabilities in singularly perturbed systems. *Differential and Integral Equat.*, 12:583–600, 1999.
- [NS03] M.C. Natividad and M. Stynes. Richardson extrapolation for a convection-diffusion problem using a Shishkin mesh. *Appl. Numer. Math.*, 45(2):315–329, 2003.
- [NS04] A.I. Neishtadt and V.V. Sidorenko. Wisdom system: dynamics in the adiabatic approximation. *Celestial Mechanics and Dynamical Astronomy*, 90(3):307–330, 2004.
- [NS08] N.N. Nefedov and K.R. Schneider. On immediate-delayed exchange of stabilities and periodic forced canards. *Comput. Math. Math. Phys.*, 48(1):43–58, 2008.
- [NS12] A.I. Neishtadt and T. Su. On phenomenon of scattering on resonances associated with discretisation of systems with fast rotating phase. *Regular & Chaotic Dyn.*, 17(3):359–366, 2012.
- [NS13a] A.I. Neishtadt and T. Su. On asymptotic description of passage through a resonance in quasilinear Hamiltonian systems. *SIAM J. Appl. Dyn. Syst.*, 12(3):1436–1473, 2013.
- [NS13b] K. Nipp and D. Stoffer. *Invariant Manifolds in Discrete and Continuous Dynamical Systems*. EMS, 2013.
- [NST97] A.I. Neishtadt, V.V. Sidorenko, and D.V. Treschev. Stable periodic motions in the problem on passage through a separatrix. *Chaos*, 7(1):2–11, 1997.
- [NSTV08] A. Neishtadt, C. Simo, D.V. Treschev, and A. Vasiliev. Periodic orbits and stability islands in chaotic seas created by separatrix crossings in slow-fast systems. *Discr. Contin. Dyn. Syst. B*, 10(2):621–650, 2008.
- [NT01] P. Noble and S. Travadel. Non-persistence of roll-waves under viscous perturbations. *Discr. Cont. Dyn. Syst. B*, 1(1):61–70, 2001.
- [Num84] E. Nummelin. *General irreducible Markov chains and nonnegative operators*, volume 84 of *Tracts in Mathematics*. CUP, 1984.
- [NV99] A.I. Neishtadt and A.A. Vasiliev. Change of the adiabatic invariant at a separatrix in a volume-preserving 3D system. *Nonlinearity*, 12(2):303, 1999.
- [NV05] A.I. Neishtadt and A.A. Vasiliev. Phase change between separatrix crossings in slow-fast Hamiltonian systems. *Nonlinearity*, 18(3):1393–1406, 2005.
- [NV06] A.I. Neishtadt and A.A. Vasiliev. Destruction of adiabatic invariance at resonances in slow-fast Hamiltonian systems. *Nucl. Instr. Meth. Phys. Res. A*, 561:158–165, 2006.
- [NW99] M.E. Newman and D.J. Watts. Renormalization group analysis of the small-world network model. *Phys. Lett. A*, 263(4):341–346, 1999.
- [NW07] L. Noethen and S. Walcher. Quasi-steady state in the Michaelis–Menten system. *Nonl. Anal.: Real World Appl.*, 8(5):1512–1535, 2007.
- [NW11] L. Noethen and S. Walcher. Tikhonov’s theorem and quasi-steady state. *Discr. Cont. Dyn. Syst. B*, 16(3):945–961, 2011.
- [NWB⁺02] C.A. Del Negro, C.G. Wilson, R.J. Butera, H. Rigatto, and J.C. Smith. Periodicity, mixed-mode oscillations, and quasiperiodicity in a rhythm-generating neural network. *Biophysical J.*, 82:206–214, 2002.
- [NY10] S.L. Nguyen and G. Yin. Asymptotic properties of Markov-modulated random sequences with fast and slow timescales. *Stochastics*, 82(4):445–474, 2010.

- [OA82] R.E. O'Malley and L.R. Anderson. Time-scale decoupling and order reduction for linear time-varying systems. *Optim. Contr. Appl. Meth.*, 3:133–153, 1982.
- [OB03] N. O'Bryant. A noisy system with a flattened Hamiltonian and multiple time scales. *Stoch. Dyn.*, 3(1):1–54, 2003.
- [OC12] D. O'Malley and J.H. Cushman. Two-scale renormalization-group classification of diffusive processes. *Phys. Rev. E*, 86:011126, 2012.
- [OCA11] E. Olbrich, J.C. Claussen, and P. Achermann. The multiple time scales of sleep dynamics as a challenge for modelling the sleeping brain. *Philos. Trans. R. Soc. Lond. Ser. A*, 369(1952):3884–3901, 2011.
- [OCK03] B.E. Oldeman, A.R. Champneys, and B. Krauskopf. Homoclinic branch switching: a numerical implementation of Lin's method. *Int. J. Bif. Chaos*, 13(10):2977–2999, 2003.
- [OCN99] S.S. Oueini, C.-M. Chin, and A.H. Nayfeh. Dynamics of a cubic nonlinear vibration absorber. *Nonlinear Dyn.*, 20:283–295, 1999.
- [OD78] L.F. Olsen and H. Degn. Oscillatory kinetics of the peroxidase-oxidase reaction in an open system. Experimental and theoretical studies. *Biochim. Biophys. Acta*, 523(2):321–334, 1978.
- [Oda95] K. Odani. The limit cycle of the van der Pol equation is not algebraic. *J. Differential Equat.*, 115(1):146–152, 1995.
- [OE87] M. Orban and I.R. Epstein. Chemical oscillators in group VIA: The Cu(II)-catalyzed reaction between hydrogen peroxide and thiosulfate ion. *J. Am. Chem. Soc.*, 109:101–106, 1987.
- [OF80] R.E. O'Malley and J.E. Flaherty. Analytical and numerical methods for nonlinear singular singularly-perturbed initial value problems. *SIAM J. Appl. Math.*, 38(2):225–248, 1980.
- [OH98] N. Okazaki and I. Hanazaki. Photo-induced chaos in the Briggs–Rauscher reaction. *J. Chem. Phys.*, 109(2):637–642, 1998.
- [OHL03] J. Ockendon, S. Howison, A. Lacey, and A. Movchan. *Applied Partial Differential Equations*. OUP, 2003.
- [OK68] R.E. O'Malley and J.B. Keller. Loss of boundary conditions in the asymptotic solution of linear ordinary differential equations, II boundary value problems. *Comm. Pure Appl. Math.*, 21(3):263–270, 1968.
- [OK75] R.E. O'Malley and C.F. Kung. The singularly perturbed linear state regulator problem. II. *SIAM J. Contr.*, 13(2):327–337, 1975.
- [OK94] R.E. O'Malley and L.V. Kalachev. Regularization of nonlinear differential-algebraic equations. *SIAM J. Math. Anal.*, 25(2):615–629, 1994.
- [OK96] R.E. O'Malley and L.V. Kalachev. The regularization of linear differential-algebraic equations. *SIAM J. Math. Anal.*, 27(1):258–273, 1996.
- [OK09] R.E. O'Malley and E. Kirkikis. Examples illustrating the use of renormalization techniques for singularly perturbed differential equations. *Stud. Appl. Math.*, 122:105–122, 2009.
- [OK11] R.E. O'Malley and E. Kirkikis. Two-timing and matched asymptotic expansions for singular perturbation problems. *European J. Appl. Math.*, 22(6):613–629, 2011.
- [Okas87] H. Oka. Constrained systems, characteristic surfaces, and normal forms. *Japan J. Appl. Math.*, 4(3):393–431, 1987.
- [OKCRE00] M. Orban, K. Kurin-Csorgei, G. Rabai, and I.R. Epstein. Mechanistic studies of oscillatory copper(II) catalyzed oxidation reactions of sulphur compounds. *Chem. Eng. Sci.*, 55:267–273, 2000.
- [Øks03] B. Øksendal. *Stochastic Differential Equations*. Springer, Berlin Heidelberg, Germany, 5th edition, 2003.
- [Olv61] F.W.J. Olver. Error bounds for the Liouville–Green (or WKB) approximation. *Proc. Cambridge Philos. Soc.*, 57:790–810, 1961.
- [O'M68a] R.E. O'Malley. A boundary value problem for certain nonlinear second order differential equations with a small parameter. *Arch. Rat. Mech. Anal.*, 29(1):66–74, 1968.
- [O'M68b] R.E. O'Malley. Topics in singular perturbations. *Adv. Math.*, 2:365–470, 1968.
- [O'M69] R.E. O'Malley. On a boundary value problem for a nonlinear differential equation with a small parameter. *SIAM J. Appl. Math.*, 17(3):569–581, 1969.
- [O'M70a] R.E. O'Malley. A non-linear singular perturbation problem arising in the study of chemical flow reactors. *IMA J. Appl. Math.*, 6(1):12–20, 1970.
- [O'M70b] R.E. O'Malley. On boundary value problems for a singularly perturbed differential equation with a turning point. *SIAM J. Math. Anal.*, 1(4):479–490, 1970.
- [O'M70c] R.E. O'Malley. Singular perturbations of a boundary value problem for a system of nonlinear differential equations. *J. Differential Equat.*, 8:431–447, 1970.
- [O'M71a] R.E. O'Malley. Boundary layer methods for nonlinear initial value problems. *SIAM Rev.*, 13(4):425–434, 1971.
- [O'M71b] R.E. O'Malley. On initial value problems for nonlinear systems of differential equations with two small parameters. *Arch. Rat. Mech. Anal.*, 40(3):209–222, 1971.
- [O'M72a] R.E. O'Malley. Singular perturbation of the time-invariant linear state regulator problem. *J. Differential Equat.*, 12:117–128, 1972.
- [O'M72b] R.E. O'Malley. The singularly perturbed linear state regulator problem. *SIAM J. Contr.*, 10(3):399–413, 1972.
- [O'M74] R.E. O'Malley. Boundary layer methods for certain nonlinear singularly perturbed optimal control problems. *J. Math. Anal. Appl.*, 45(2):468–484, 1974.
- [O'M75] R.E. O'Malley. On two methods of solution for a singularly perturbed linear state regulator problem. *SIAM Rev.*, 17(1):16–37, 1975.
- [O'M76a] R.E. O'Malley. A more direct solution of the nearly singular linear regulator problem. *SIAM J. Contr. Optim.*, 14(6):1063–1077, 1976.
- [O'M76b] R.E. O'Malley. Phase-plane solutions to some singular perturbation problems. *J. Math. Anal. Appl.*, 54(2):449–466, 1976.
- [O'M78a] R.E. O'Malley. On singular singularly-perturbed initial value problems. *Applicable Analysis*, 8(1):71–81, 1978.
- [O'M78b] R.E. O'Malley. Singular perturbations and optimal control. In W.A. Coppel, editor, *Mathematical Control Theory*, volume 680 of *Lect. Notes Math.*, pages 170–218. Springer, 1978.

- [O'M79] R.E. O'Malley. A singular singularly-perturbed linear boundary value problem. *SIAM J. Math. Anal.*, 10(4):695–708, 1979.
- [O'M83] R.E. O'Malley. Shock and transition layers for singularly perturbed second-order vector systems. *SIAM J. Appl. Math.*, 43(4):935–943, 1983.
- [O'M88] R.E. O'Malley. On nonlinear singularly perturbed initial value problems. *SIAM Rev.*, 30(2):193–212, 1988.
- [O'M91] R.E. O'Malley. *Singular Perturbation Methods for Ordinary Differential Equations*. Springer, 1991.
- [O'M00] R.E. O'Malley. On the asymptotic solution of the singularly perturbed boundary value problems posed by Bohé. *J. Math. Anal. Appl.*, 242(1):18–38, 2000.
- [O'M01] R.E. O'Malley. Naive singular perturbation theory. *Math. Mod. Meth. Appl. Sci.*, 11:119–131, 2001.
- [O'M08] R.E. O'Malley. Singularly perturbed linear two-point boundary value problems. *SIAM Rev.*, 50(3):459–482, 2008.
- [O'M10] R.E. O'Malley. Singular perturbation theory: a viscous flow out of Göttingen. *Ann. Rev. Fluid Mech.*, 42:1–17, 2010.
- [OM11] M. Oh and V. Mateev. Non-weak inhibition and phase resetting at negative values of phase in cells with fast-slow dynamics at hyperpolarized potentials. *J. Comput. Neurosci.*, 31:31–42, 2011.
- [Oor00] F. Oort. Newton polygons and formal groups: conjectures by Manin and Grothendieck. *Ann. Math.*, 152(1):183–206, 2000.
- [OP11] M. Ottobre and G.A. Pavliotis. Asymptotic analysis for the generalized Langevin equation. *Nonlinearity*, 24(5):1629, 2011.
- [ØPO03] L. Øyehaug, E. Plathe, and S.W. Omholt. Targeted reduction of complex models with time scale hierarchy - a case study. *Math. Biosci.*, 185(2):123–152, 2003.
- [OQ11] E. O'Riordan and J. Quinn. Parameter-uniform numerical methods for some linear and nonlinear singularly perturbed convection diffusion boundary turning point problems. *BIT Numer. Math.*, 51:317–337, 2011.
- [OR75] P. Ortoleva and J. Ross. Theory of propagation of discontinuities in kinetic systems with multiple time scales: fronts, front multiplicity, and pulses. *J. Chem. Phys.*, 63:3398–3408, 1975.
- [O'R79a] J. O'Reilly. Full-order observers for a class of singularly perturbed linear time-varying systems. *Int. J. Contr.*, 30(5):745–756, 1979.
- [O'R79b] J. O'Reilly. Two time-scale feedback stabilization of linear time-varying singularly perturbed systems. *J. Frank. Inst.*, 308(5):465–474, 1979.
- [O'R80] J. O'Reilly. Dynamical feedback control for a class of singularly perturbed linear systems using a full-order observer. *Int. J. Contr.*, 31(1):1–10, 1980.
- [OR07] F. Otto and M.G. Reznikoff. Slow motion of gradient flows. *J. Differential Equat.*, 237(2):372–420, 2007.
- [OS90] R.E. O'Malley and C. Schmeiser. The asymptotic solution of a semiconductor device problem involving reverse bias. *SIAM J. Appl. Math.*, 50(2):504–520, 1990.
- [OS91] E. O'Riordan and M. Stynes. A globally uniformly convergent finite element method for a singularly perturbed elliptic problem in two dimensions. *Math. Comput.*, 57(195):47–62, 1991.
- [OS95] E. Olivieri and E. Scoppola. Markov chains with exponentially small transition probabilities: first exit problem from a general domain. I. The reversible case. *J. Stat. Phys.*, 79(3):613–647, 1995.
- [OS96] E. Olivieri and E. Scoppola. Markov chains with exponentially small transition probabilities: first exit problem from a general domain. II. The general case. *J. Stat. Phys.*, 84(5):987–1041, 1996.
- [OS99] O.A. Oleinik and V.N. Samokhin. *Mathematical Models in Boundary Layer Theory*. Chapman & Hall, 1999.
- [Osi97] G. Osipenko. Linearization near a locally nonunique invariant manifold. *Discr. Cont. Dyn. Syst.*, 3:189–205, 1997.
- [OSS92] H.K. Ozcetin, A. Saberi, and P. Sannuti. Design for H^∞ almost disturbance decoupling problem with internal stability via state or measurement feedback-singular perturbation approach. *Int. J. Contr.*, 55(4):901–944, 1992.
- [OSTA12] H.M. Osinga, A. Sherman, and K. Tsaneva-Atanasova. Cross-currents between biology and mathematics: the codimension of pseudo-plateau bursting. *Discr. Cont. Dyn. Syst. A*, 32:2853–2877, 2012.
- [OSY92] O.A. Oleinik, A.S. Shamaev, and G.A. Yosifian. *Mathematical Problems in Elasticity and Homogenization*. North-Holland, 1992.
- [OT94] H. Okuda and I. Tsuda. A coupled chaotic system with different time scales: possible implications of observations by dynamical systems. *Int. J. Bif. Chaos*, 4(4):1011–1022, 1994.
- [OTA10] H.M. Osinga and K.T. Tsaneva-Atanasova. Dynamics of plateau bursting in dependence on the location of its equilibrium. *J. Neuroendocrinology*, 22(12):1301–1314, 2010.
- [OV05] E. Olivieri and M.E. Vares. *Large Deviations and Metastability*. CUP, 2005.
- [OW04] C.H. Ou and R. Wong. Shooting method for nonlinear singularly perturbed boundary-value problems. *Stud. Appl. Math.*, 112(2):161–200, 2004.
- [OW06] R.E. O'Malley and D.B. Williams. Deriving amplitude equations for weakly-nonlinear oscillators and their generalizations. *J. Comput. Appl. Math.*, 190(1):3–21, 2006.
- [OWS95] D.L. Olson, E.P. Williksen, and A. Scheeline. An experimentally based model of the Peroxidase-NADH biochemical oscillator: An enzyme-mediated chemical switch. *J. Am. Chem. Soc.*, 117:2–15, 1995.
- [PACNH09] J.-C. Poggiale, P. Auger, F. Cordoleani, and T. Nguyen-Huu. Study of a virus-bacteria interaction model in a chemostat: application of geometric singular perturbation theory. *Phil. Trans. R. Soc. A*, 367:4685–4697, 2009.
- [Pal82] K.J. Palmer. Exponential separation, exponential dichotomy and spectral theory for linear systems of ordinary differential equations. *J. Differential Equat.*, 46(3):324–345, 1982.
- [Pal84] K.J. Palmer. Exponential dichotomies and transversal homoclinic points. *J. Differential Equat.*, 55:225–256, 1984.
- [Pal88] K.J. Palmer. Exponential dichotomies and Fredholm operators. *Proc. Amer. Math. Soc.*, 104:149–156, 1988.
- [Pan96] C.L. Pando. Recurrent synchronism in the internal dynamics of CO₂ lasers. *Phys. Lett. A*, 210(6):391–401, 1996.

- [Pan00] D. Panazzolo. On the existence of canard solutions. *Publicacions Matemàtiques*, 44:503–592, 2000.
- [Pan02] D. Panazzolo. *Desingularization of nilpotent singularities in families of planar vector fields*, volume 752 of *Mem. Amer. Math. Soc.* AMS, 2002.
- [Pan05] R.L. Panton. *Incompressible Flow*. Wiley, 2005.
- [Pan06] D. Panazzolo. Resolution of singularities of real-analytic vector fields in dimension three. *Acta Math.*, 197:167–289, 2006.
- [Pap76] G.C. Papanicolaou. Some probabilistic problems and methods in singular perturbations. *Rocky Mountain J. Math.*, 6:653–674, 1976.
- [Pap77] G.C. Papanicolaou. Introduction to the asymptotic analysis of stochastic equations. In *Modern Modeling of Continuum Phenomena*, volume 16 of *Lect. Appl. Math.*, pages 109–147. AMS, 1977.
- [Pav05] G.A. Pavliotis. A multiscale approach to Brownian motors. *Phys. Lett. A*, 344(5):331–345, 2005.
- [Paz83] A. Pazy. *Semigroups of Linear Operators and Applications to Partial Differential Equations*. Springer, New York, 1983.
- [PB81] B. Porter and A. Bradshaw. Singular perturbation methods in the design of tracking systems incorporating inner-loop compensators and high-gain error-actuated controllers. *Int. J. Syst. Sci.*, 12(10):1193–1205, 1981.
- [PB93] Z. Pan and T. Basar. H^∞ -optimal control for singularly perturbed systems. Part I: Perfect state measurements. *Automatica*, 29(2):401–423, 1993.
- [PB11] Y. Pomeau and M. Le Berre. Critical speed-up vs critical slow-down: a new kind of relaxation oscillation with application to stick-slip phenomena. *arXiv:1107.3331*, pages 1–8, 2011.
- [PCA⁺09] P. Poletti, B. Caprile, M. Ajelli, A. Pugliese, and S. Merler. Spontaneous behavioural changes in response to epidemics. *J. Theor. Biol.*, 260(1):31–40, 2009.
- [PCS93] R.W. Penney, A.C.C. Coolen, and D. Sherrington. Coupled dynamics of fast spins and slow interactions in neural networks and spin systems. *J. Phys. A*, 26(15):3681–3695, 1993.
- [PDL11] Y. Park, Y. Do, and J.M. Lopez. Slow passage through resonance. *Phys. Rev. E*, 84:056604, 2011.
- [PDL13] Y. Park, Y. Do, and J.M. Lopez. Cooperation of intrinsic bursting and calcium oscillations underlying activity patterns of model pre-Bötzing complex neurons. *J. Comput. Neurosci.*, 34(2):345–366, 2013.
- [PE94] J. Puellet and B. Ermentrout. Stable rotating waves in two-dimensional discrete active media. *SIAM J. Appl. Math.*, 54(6):1720–1744, 1994.
- [PE01a] D.J. Pinto and G.B. Ermentrout. Spatially structured activity in synaptically coupled neuronal networks: I. Traveling fronts and pulses. *SIAM J. Appl. Math.*, 62(1):206–225, 2001.
- [PE01b] D.J. Pinto and G.B. Ermentrout. Spatially structured activity in synaptically coupled neuronal networks: II. Lateral inhibition and standing pulses. *SIAM J. Appl. Math.*, 62(1):226–243, 2001.
- [Peg89] R.L. Pego. Front migration in the nonlinear Cahn–Hilliard equation. *Proc. R. Soc. London A*, 422(1863):261–278, 1989.
- [Per29] O. Perron. Über Stabilität und asymptotisches Verhalten der Integrale von Differentialgleichungssystemen. *Math. Zeitschr.*, 29(1):129–160, 1929.
- [Per69] L.M. Perko. Higher order averaging and related methods for perturbed periodic and quasi-periodic systems. *SIAM J. Appl. Math.*, 17(4):698–724, 1969.
- [Per76] L.M. Perko. Application of singular perturbation theory to the restricted three body problem. *Rocky Mountain J. Math.*, 6(4):675, 1976.
- [Per81] S.C. Perseck. Hierarchies of iterated averages for systems of ordinary differential equations with a small parameter. *SIAM J. Math. Anal.*, 12(3):413–420, 1981.
- [Per82] S.C. Perseck. Asymptotic stability and the method of iterated averages for almost periodic systems. *SIAM J. Math. Anal.*, 13(5):828–841, 1982.
- [Per84] S.C. Perseck. Iterated averaging for periodic systems with hidden multi-scale slow times. *Pacific J. Math.*, 112(1):211–236, 1984.
- [Per94a] S. Pergamenshchikov. Asymptotic expansions for a model with distinguished ‘fast’ and ‘slow’ variables, described by a system of singularly perturbed stochastic differential equations. *Russ. Math. Surv.*, 49(4):1–44, 1994.
- [Per94b] M. Pernarowski. Fast subsystem bifurcations in a slowly varying Liénard system exhibiting bursting. *SIAM J. Appl. Math.*, 54(3):814–832, 1994.
- [Per98] M. Pernarowski. Fast and slow subsystems for a continuum model of bursting activity in the pancreatic islet. *SIAM J. Appl. Math.*, 58(5):1667–1687, 1998.
- [Per00] M. Pernarowski. Fast subsystem bifurcations in strongly coupled heterogeneous collections of excitable cells. *Bull. Math. Biol.*, 62:101–120, 2000.
- [Per01a] L. Perko. *Differential Equations and Dynamical Systems*. Springer, 2001.
- [Per01b] M. Pernarowski. Controllability of excitable systems. *Bull. Math. Biol.*, 63:167–184, 2001.
- [Pes77] Ya.B. Pesin. Characteristic Lyapunov exponents and smooth ergodic theory. *Russ. Math. Surv.*, 32(4):55–114, 1977.
- [Pes04] Ya.B. Pesin. *Lectures on Partial Hyperbolicity and Stable Ergodicity*. EMS, 2004.
- [PGS91] B. Peng, V. Gaspar, and K. Showalter. False bifurcations in chemical systems: canards. *Phil. Trans. R. Soc. Lond. A*, 337:275–289, 1991.
- [PH78] S.C. Perseck and F.C. Hoppensteadt. Iterated averaging methods for systems of ordinary differential equations with a small parameter. *Comm. Pure Appl. Math.*, 31(2):133–156, 1978.
- [PH93] A. Panfilov and P. Hogeweg. Spiral breakup in a modified FitzHugh–Nagumo model. *Phys. Lett. A*, 176(5):295–299, 1993.
- [Phi80] R.G. Phillips. Reduced order modelling and control of two-time-scale discrete systems. *Int. J. Contr.*, 31(4):765–780, 1980.
- [Phi83] R.G. Phillips. The equivalence of time-scale decomposition techniques used in the analysis and design of linear systems. *Int. J. Contr.*, 37(6):1239–1257, 1983.
- [Pik81] A.S. Pikovsky. A dynamical model for periodic and chaotic oscillations in the Belousov–Zhabotinsky reaction. *Phys. Rev. A*, 25(1):13–16, 1981.
- [Pin95] P.F. Pinsky. Synchrony and clustering in an excitatory neural network model with intrinsic relaxation kinetics. *SIAM J. Appl. Math.*, 55(1):220–241, 1995.

- [PJC⁺09] M. Peil, M. Jacquot, Y.K. Chembo, L. Larger, and T. Erneux. Routes to chaos and multiple time scale dynamics in broadband bandpass nonlinear delay electro-optic oscillators. *Phys. Rev. E*, 79(2):026208, 2009.
- [PYJ97] L.R. Petzhold, L.O. Jay, and J. Yen. Numerical solution of highly oscillatory ordinary differential equations. *Acta Numerica*, 6:437–483, 1997.
- [PK75] G.C. Papanicolaou and W. Kohler. Asymptotic analysis of deterministic and stochastic equations with rapidly varying components. *Comm. Math. Phys.*, 45(3):217–232, 1975.
- [PK81] R. Phillips and P. Kokotovic. A singular perturbation approach to modeling and control of Markov chains. *IEEE Trans. Aut. Contr.*, 26(5):1087–1094, 1981.
- [PK95] A.V. Panfilov and J.P. Keener. Re-entry in three-dimensional Fitzhugh-Nagumo medium with rotational anisotropy. *Physica D*, 84(3):545–552, 1995.
- [PK97] A.S. Pikovsky and J. Kurths. Coherence resonance in a noise-driven excitable system. *Phys. Rev. Lett.*, 78:775–778, 1997.
- [PK06] N. Popović and T.J. Kaper. Rigorous asymptotic expansions for critical wave speeds in a family of scalar reaction–diffusion equations. *J. Dyn. Diff. Eq.*, 18(1):103–139, 2006.
- [PKC82] G. Peponides, P. Kokotovic, and J. Chow. Singular perturbations and time scales in nonlinear models of power systems. *IEEE Trans. Circ. Syst.*, 29(11):758–767, 1982.
- [PL87] U. Parlitz and W. Lauterborn. Period-doubling cascades and devil’s staircases of the driven van der Pol oscillator. *Phys. Rev. A*, 36(3):1428–1434, 1987.
- [Pla81] R.E. Plant. Bifurcation and resonance in a model for bursting nerve cells. *J. Math. Biol.*, 11:15–32, 1981.
- [PLRF97] E. Peacock-Lopez, D.B. Radov, and C.S. Flesner. Mixed-mode oscillations in a self-replicating dimerization mechanism. *Biophysical Chemistry*, 65:171–178, 1997.
- [PM00] J.F. Painter and R.E. Meyer. Turning-point connection at close quarters. *SIAM J. Math. Anal.*, 31(4):541–554, 2000.
- [PMHC⁺10] P. Pierobon, J. Miné-Hattab, G. Cappello, J.-L. Viovy, and M. Cosentino Lagomarsino. Separation of time scales in a one-dimensional directed nucleation-growth process. *Phys. Rev. E*, 82:061904, 2010.
- [PMK91] M. Pernarowski, R.M. Miura, and J. Kevorkian. The Sherman-Rinzel-Keizer model for bursting electrical activity in the pancreatic β -cell. In *Differential Equations Models in Biology, Epidemiology and Ecology*, pages 34–53. Springer, 1991.
- [PMK92] M. Pernarowski, R.M. Miura, and J. Kevorkian. Perturbation techniques for models of bursting electrical activity in pancreatic β -cells. *SIAM J. Appl. Math.*, 52(6):1627–1650, 1992.
- [PNT94] L. Pohlmann, G. Neher, and H. Tributsch. A model for oscillating hydrogen liberation at CuInSe₂ in the presence of H₂O₂. *J. Phys. Chem.*, 98:11007–11010, 1994.
- [Poe03] C. Poetschke. Slow and fast variables in non-autonomous difference equations. *J. Difference Equ. Appl.*, 9(5):473–487, 2003.
- [Pon57] L.S. Pontryagin. Asymptotic properties of solutions with small parameters multiplying leading derivatives. *Izv. AN SSSR, Ser. Matematika*, 21(5):605–626, 1957.
- [Pop11] N. Popovic. A geometric analysis of front propagation in a family of degenerate reaction–diffusion equations with cut-off. *Z. Angew. Math. Phys.*, 62(3):405–437, 2011.
- [Pop12] N. Popovic. A geometric analysis of front propagation in an integrable Nagumo equation with a linear cut-off. *Physica D*, 241:1976–1984, 2012.
- [Por74a] B. Porter. Singular perturbation methods in the design of observers and stabilising feedback controllers for multivariable linear systems. *Electronics Lett.*, 10(23):494–495, 1974.
- [Por74b] B. Porter. Singular perturbation methods in the design of stabilizing feedback controllers for multivariable linear systems. *Int. J. Contr.*, 20(4):689–692, 1974.
- [Por76] B. Porter. Design of stabilizing feedback controllers for a class of multivariable linear systems with slow and fast modes. *Int. J. Contr.*, 23(1):49–54, 1976.
- [Por77] B. Porter. Singular perturbation methods in the design of full-order observers for multivariable linear systems. *Int. J. Contr.*, 26(4):589–594, 1977.
- [Pos78] T. Poston. *Catastrophe Theory and Its Applications*. Dover, 1978.
- [PP13] P. Pfafelhuber and L. Popovic. Scaling limits of spatial chemical reaction networks. *arXiv:1302.0774v1*, pages 1–50, 2013.
- [PPS09] A. Papavasiliou, G.A. Pavliotis, and A.M. Stuart. Maximum likelihood drift estimation for multiscale diffusions. *Stoch. Proc. Appl.*, 119(10):3173–3210, 2009.
- [PPZ09] A.V. Pokrovskii, A.A. Pokrovskiy, and A. Zhezherun. A corollary of the Poincaré–Bendixson theorem and periodic canards. *J. Differential Equat.*, 247(12):3283–3294, 2009.
- [PR60] L.S. Pontryagin and L.V. Rodygin. Approximate solution of a system of ordinary differential equations involving a small parameter in the derivatives. *Soviet Math. Dokl.*, 1:237–240, 1960.
- [PR64] S.S. Pul’kin and N.H. Rozov. The asymptotic theory of relaxation oscillations in systems with one degree of freedom. I. Calculation of the phase trajectories. *Vestnik Moskov. Univ. Ser. I Mat. Meh. (in Russian)*, 1964(2):70–82, 1964.
- [PR74] A. Prothero and A. Robinson. On the stability and accuracy of one-step methods for solving stiff systems of ordinary differential equations. *Maths. Comput.*, 28:145–162, 1974.
- [PR81] A.S. Pikovsky and M.I. Rabinovich. Stochastic oscillations in dissipative systems. *Physica D*, 2(1):8–24, 1981.
- [PR94] P.F. Pinsky and J. Rinzel. Intrinsic and network rhythmogenesis in a reduced Traub model for CA3 neurons. *J. Comput. Neurosci.*, 1(1):39–60, 1994.
- [PR12] G. Papamikos and M. Robnik. WKB approach applied to 1D time-dependent nonlinear Hamiltonian oscillators. *J. Phys. A: Math. Theor.*, 45:015206, 2012.
- [Pra05] L. Prandtl. Über Flüssigkeiten bei sehr kleiner Reibung. In *Verh. III - International Math. Kongress*, pages 484–491. Teubner, 1905.
- [Pri05] M. Prizzi. Averaging, Conley index continuation and recurrent dynamics in almost-periodic parabolic equations. *J. Differential Equat.*, 210(2):429–451, 2005.
- [Pro03] M. Procesi. Exponentially small splitting and Arnold diffusion for multiple time scale systems. *Rev. Math. Phys.*, 15(4):339–386, 2003.

- [Pro05] P. Protter. *Stochastic Integration and Differential Equations - Version 2.1*. Springer, 2005.
- [PRR⁺81] Y. Pomeau, J.-C. Roux, A. Rossi, S. Bachelart, and C. Vidal. Intermittent behaviour in the Belousov-Zhabotinsky reaction. *Journal de Physique Lettres*, 42:271–273, 1981.
- [PRSZ11] A. Pokrovskii, D. Rachinskii, V. Sobolev, and A. Zhezherun. Topological degree in analysis of canard-type trajectories in 3-D systems. *Appl. Anal.*, 90(7):1123–1139, 2011.
- [PS70] C. Pugh and M. Shub. Linearization of normally hyperbolic diffeomorphisms and flows. *Invent. Math.*, 10(3):187–198, 1970.
- [PS75a] B. Porter and A.T. Shenton. Singular perturbation analysis of the transfer function matrices of a class of multivariable linear systems. *Int. J. Contr.*, 21(4):655–660, 1975.
- [PS75b] B. Porter and A.T. Shenton. Singular perturbation methods of asymptotic eigenvalue assignment in multivariable linear systems. *Int. J. Syst. Sci.*, 6(1):33–37, 1975.
- [PS75c] C. Pugh and M. Shub. Axiom A actions. *Invent. Math.*, 29(1):7–38, 1975.
- [PS89] C. Pugh and M. Shub. Ergodic attractors. *Trans. AMS*, 312:1–54, 1989.
- [PS01] V.A. Pliss and G.R. Sell. Perturbations of normally hyperbolic manifolds with applications to the Navier-Stokes equations. *J. Differential Equat.*, 169(2):396–492, 2001.
- [PS02] P.E. Philipson and P. Schuster. Bistability of harmonically forced relaxation oscillations. *Internat. J. Bifur. Chaos Appl. Sci. Engrg.*, 12(6):1295–1307, 2002.
- [PS04a] N. Popović and P. Szmolyan. A geometric analysis of the Lagerstrom model problem. *J. Differential Equat.*, 199:290–325, 2004.
- [PS04b] N. Popović and P. Szmolyan. Rigorous asymptotic expansions for Lagerstrom's model equation - a geometric approach. *Nonlinear Anal.*, 59(4):531–565, 2004.
- [PS05a] G.A. Pavliotis and A.M. Stuart. Analysis of white noise limits for stochastic systems with two fast relaxation times. *Multiscale Model. Simul.*, 4(1):1–35, 2005.
- [PS05b] G.A. Pavliotis and A.M. Stuart. Periodic homogenization for inertial particles. *Physica D*, 204(3):161–187, 2005.
- [PS06] V.A. Pliss and G.R. Sell. Averaging methods for stochastic dynamics of complex reaction networks: description of multiscale couplings. *Multiscale Model. Simul.*, 5(2):497–513, 2006.
- [PS07a] G.A. Pavliotis and A.M. Stuart. Parameter estimation for multiscale diffusions. *J. Stat. Phys.*, 127(4):741–781, 2007.
- [PS07b] Y. Peng and Y. Song. Existence of traveling wave solutions for a reaction-diffusion equation with distributed delays. *Nonl. Anal.: Theory, Meth. & Appl.*, 67(8):2415–2423, 2007.
- [PS08] G.A. Pavliotis and A.M. Stuart. *Multiscale Methods: Averaging and Homogenization*. Springer, 2008.
- [PSS92] V. Petrov, S.K. Scott, and K. Showalter. Mixed-mode oscillations in chemical systems. *J. Chem. Phys.*, 97(9):6191–6198, 1992.
- [PSSM08] D.E. Postnov, O.V. Sosovtseva, P. Scherbakov, and E. Mosekilde. Multimode dynamics in a network with resource mediated coupling. *Chaos*, 18, 2008.
- [PSV10] M.A. Peletier, G. Savaré, and M. Veneroni. From diffusion to reaction via Γ -convergence. *SIAM J. Math. Anal.*, 42(4):1805–1825, 2010.
- [PSV12] M.A. Peletier, G. Savaré, and M. Veneroni. Chemical reactions as Γ -limit of diffusion. *SIAM Rev.*, 54(2):327–352, 2012.
- [PSZ07] G.A. Pavliotis, A.M. Stuart, and K.C. Zygalakis. Homogenization for inertial particles in a random flow. *Comm. Math. Sci.*, 5(3):506–531, 2007.
- [PT77] J. Palis and F. Takens. Topological equivalence of normally hyperbolic dynamical systems. *Topology*, 16(4):335–345, 1977.
- [PT00] A.V. Pronin and D.V.E. Treschev. Continuous averaging in multi-frequency slow–fast systems. *Reg. Chaotic Dyn.*, 5(2):157–170, 2000.
- [PT13] R. Prohens and A.E. Teruel. Canard trajectories in 3D piecewise linear systems. *Discr. Cont. Dyn. Syst. A*, 33(10):4595–4611, 2013.
- [PTK⁺11] M. Pradas, D. Tseluiko, S. Kalliadasis, D.T. Papageorgiou, and G.A. Pavliotis. Noise induced state transitions, intermittency, and universality in the noisy Kuramoto-Sivashinsky equation. *Phys. Rev. Lett.*, 106(6):060602, 2011.
- [PTVF07] W.H. Press, S.A. Teukolsky, W.T. Vetterling, and B.P. Flannery. *Numerical Recipes 3rd Edition: The Art of Scientific Computing*. CUP, 2007.
- [PTW05] M. Percu, R. Temam, and D. Wirosoetisno. Renormalization group method applied to the primitive equations. *J. Differential Equat.*, 208(1):215–257, 2005.
- [Pug10] C. Pugh. *Real Mathematical Analysis*. Springer, 2010.
- [Puhi13] A.A. Puhaliskii. Large deviations of coupled diffusions with time scale separation. *arXiv:1306.5446v1*, pages 1–74, 2013.
- [PV01] E. Pardoux and Yu. Veretennikov. On the Poisson equation and diffusion approximation. I. *Ann. Probab.*, 29(3):1061–1085, 2001.
- [PVK05] F. Plenje, H. Varela, and K. Krischer. Asymmetric target patterns in one-dimensional oscillatory media with genuine nonlocal coupling. *Phys. Rev. Lett.*, 94, 2005.
- [PW00] D.B. Percival and A.T. Walden. *Wavelet Methods for Time Series Analysis*. CUP, 2000.
- [WPWK10] S. Pillay, M.J. Ward, A. Peirce, and T. Kolokolnikov. An asymptotic analysis of the mean first passage time for narrow escape problems: Part I Two-dimensional domains. *Multiscale Mod. Simul.*, 8(3):803–835, 2010.
- [PZ92] G. Da Prato and J. Zabczyk. *Stochastic Equations in Infinite Dimensions*. Cambridge University Press, 1992.
- [PZ03] D.E. Pelinovsky and V. Zharnitsky. Averaging of dispersion-managed solitons: existence and stability. *SIAM J. Appl. Math.*, 63(3):745–776, 2003.
- [PZ08] A. Pokrovskii and A. Zhezherun. Topological degree in analysis of chaotic behavior in singularly perturbed systems. *Chaos*, 18(2):023130, 2008.
- [QG92] M.T. Qureshi and Z. Gajic. A new version of the Chang transformation. *IEEE Trans. Aut. Contr.*, 37(6):800–801, 1992.
- [QGNR97] D. Quinn, B. Gladman, P. Nicholson, and R. Rand. Relaxation oscillations in tidally evolving satellites. *Celestial Mech. Dynam. Astronom.*, 67(2):111–130, 1997.

- [RA00a] S. Rajesh and G. Ananthakrishna. Effect of slow manifold structure on relaxation oscillations and one-dimensional map in a model for plastic instability. *Physica A*, 270:182–189, 2000.
- [RA00b] S. Rajesh and G. Ananthakrishna. Incomplete approach to homoclinicity in a model with bent-slow manifold geometry. *Physica D*, 140:193–212, 2000.
- [RA03] C.V. Rao and A.P. Arkin. Stochastic chemical kinetics and the quasi-steady-state assumption: application to the Gillespie algorithm. *J. Chem. Phys.*, 118(11):4999–5010, 2003.
- [RA05] R. Raghavan and G. Ananthakrishna. Long tailed maps as a representation of mixed mode oscillatory systems. *Physica D*, 211:74–87, 2005.
- [Rab57] A.L. Rabenstein. Asymptotic solutions of $u^{iv} + \lambda^2(zu'' + \alpha u' + \beta u) = 0$ for large $|\lambda|$. *Arch. Rat. Mech. Anal.*, 1(1):418–435, 1957.
- [Rad05] J.D.M. Rademacher. Homoclinic orbits near heteroclinic cycles with one equilibrium and one periodic orbit. *J. Differential Equat.*, 218:390–443, 2005.
- [Rad13] J.D.M. Rademacher. First and second order semistrong interaction in reaction–diffusion systems. *SIAM J. Appl. Dyn. Syst.*, 12(1):175–203, 2013.
- [Rak00] D.A. Rakhlina. Enhanced diffusion in smoothly modulated superlattices. *Phys. Rev. E*, 63(1):011112, 2000.
- [Ran94] R.H. Rand. *Topics in Nonlinear Dynamics with Computer Algebra*. Gordon and Breach, 1994.
- [Rat06] J.G. Ratcliffe. *Foundations of Hyperbolic Manifolds*. Springer, 2006.
- [Rau12] J. Rauch. *Hyperbolic Partial Differential Equations and Geometric Optics*. AMS, 2012.
- [Raz78] V.D. Razevig. Reduction of stochastic differential equations with small parameters and stochastic integrals. *Int. J. Contr.*, 28(5):707–720, 1978.
- [RB88] J. Rinzel and S.M. Baer. Threshold for repetitive activity for a slow stimulus ramp: a memory effect and its dependence on fluctuations. *Biophys. J.*, 54(3):551–555, 1988.
- [RBT10] M.J. Rempe, J. Best, and D. Terman. A mathematical model of the sleep/wake cycle. *J. Math. Biol.*, 60:615–644, 2010.
- [RC78] R.D. Russell and J. Christiansen. Adaptive mesh selection strategies for solving boundary value problems. *SIAM J. Numer. Anal.*, 15(1):59–80, 1978.
- [RCG12] H.G. Rotstein, S. Coombes, and A.M. Gheorghe. Canard-like explosion of limit cycles in two-dimensional piecewise-linear models of FitzHugh–Nagumo type. *SIAM J. Appl. Dyn. Syst.*, 11(1):135–180, 2012.
- [RCR08] V. Rajagopalan, S. Chakraborty, and A. Ray. Estimation of slowly varying parameters in nonlinear systems via symbolic dynamic filtering. *Signal Processing*, 88:339–348, 2008.
- [RD13] J. Ren and J. Duan. A parameter estimation method based on random slow manifolds. *arXiv:1303.4600*, pages 1–16, 2013.
- [RDdRvdK04] M. Rietkerk, S.C. Dekker, P. de Ruiter, and J. van de Koppel. Self-organized patchiness and catastrophic shifts in ecosystems. *Science*, 305(2):1926–1929, 2004.
- [RDJ12] J. Ren, J. Duan, and C.K.R.T. Jones. Approximation of random slow manifolds and settling of inertial particles under uncertainty. *arXiv:1212.4216v1*, pages 1–26, 2012.
- [RDKL11] J. Rankin, M. Desroches, B. Krauskopf, and M. Lowenberg. Canard cycles in aircraft ground dynamics. *Nonlin. Dyn.*, 66(4):681–688, 2011.
- [RE89] J. Rinzel and B. Ermentrout. Analysis of neural excitability and oscillations. In C. Koch and I. Segev, editors, *Methods of Neural Modeling: From Synapses to Networks*, pages 135–169. MIT Press, 1989.
- [REG11] A. García Cantú Ros, J.-S. Mc Ewen, and P. Gaspard. Effect of ultrafast diffusion on adsorption, desorption, and reaction processes over heterogeneous surfaces. *Phys. Rev. E*, 83:021604, 2011.
- [Rei71] E.L. Reiss. On multivariable asymptotic expansions. *SIAM Rev.*, 13(2):189–196, 1971.
- [Rei80] E.L. Reiss. A new asymptotic method for jump phenomena. *SIAM J. Appl. Math.*, 39(3):440–455, 1980.
- [Rei99a] S. Reich. Multiple time-scales in classical and quantum-classical molecular dynamics. *J. Comput. Phys.*, 151:49–73, 1999.
- [Rei99b] S. Reich. Preservation of adiabatic invariants under symplectic discretization. *Appl. Numer. Math.*, 29:45–56, 1999.
- [Rei00] S. Reich. Smoothed Langevin dynamics of highly oscillatory systems. *Physica D*, 138:210–224, 2000.
- [Res92] S.I. Resnick. *Adventures in Stochastic Processes*. Birkhäuser, 1992.
- [RESG06] C. Roussel, T. Erneux, S.N. Schiffmann, and D. Gall. Modulation of neuronal excitability by intracellular calcium buffering: from spiking to bursting. *Cell Calcium*, 39(5):455–466, 2006.
- [RF91a] M.R. Roussel and S.J. Fraser. Accurate steady-state approximations: implications for kinetics experiments and mechanism. *J. Phys. Chem.*, 95(22):8762–8770, 1991.
- [RF91b] M.R. Roussel and S.J. Fraser. Geometry of steady-state approximation: perturbation and accelerated convergence methods. *J. Chem. Phys.*, 95:8762–8770, 1991.
- [RF91c] M.R. Roussel and S.J. Fraser. On the geometry of transient relaxation. *J. Chem. Phys.*, 94:7106, 1991.
- [RF92] J. Rinzel and P. Frankel. Activity patterns of slow synapse network predicted by explicitly averaging spike dynamics. *Neural Comput.*, 4(4):534–545, 1992.
- [RF01] M.R. Roussel and S.J. Fraser. Invariant manifold methods for metabolic model reduction. *Chaos*, 11(1):196–206, 2001.
- [RG04] S. Rinaldi and A. Gragnani. Destabilizing factors in slow–fast systems. *Ecol. Model.*, 180:445–460, 2004.
- [RG12] S. Revzen and J.M. Guckenheimer. Finding the dimension of slow dynamics in a rhythmic system. *J. R. Soc. Interface*, 9:957–971, 2012.
- [RG13] A. Roberts and P. Glendinning. Canard-like phenomena in piecewise smooth planar systems. *arXiv:1311.5192*, pages 1–22, 2013.
- [RGG00] C. Rocscoreanu, A. Georgescu, and N. Giurgiteanu. *The FitzHugh–Nagumo Model - Bifurcation and Dynamics*. Kluwer, 2000.
- [RGZL08] O. Radulescu, A.N. Gorban, A. Zinoviyev, and A. Lilienbaum. Robust simplifications of multiscale biochemical networks. *BMC Syst. Biol.*, 2(1):86, 2008.
- [RH80] R.H. Rand and P.J. Holmes. Bifurcation of periodic motions in two weakly coupled van der Pol oscillators. *Int. J. Non-Linear Mech.*, 15(4):387–399, 1980.

- [RH85] R.M. Rose and J.L. Hindmarsh. A model of a thalamic neuron. *Proc. Roy. Soc. London B*, 225:161–193, 1985.
- [RH89a] R.M. Rose and J.L. Hindmarsh. The assembly of ionic currents in a thalamic neuron I. The three-dimensional model. *Proc. Roy. Soc. London B*, 237:267–288, 1989.
- [RH89b] R.M. Rose and J.L. Hindmarsh. The assembly of ionic currents in a thalamic neuron II. The stability and state diagrams. *Proc. Roy. Soc. London B*, 237:289–312, 1989.
- [RH89c] R.M. Rose and J.L. Hindmarsh. The assembly of ionic currents in a thalamic neuron III. The seven-dimensional model. *Proc. Roy. Soc. London B*, 237:313–334, 1989.
- [RH12] M. Rafei and W.T. Van Horssen. Solving systems of nonlinear difference equations by the multiple scales perturbation method. *Nonlinear Dyn.*, 69:1509–1516, 2012.
- [RH13] J. Rinzel and G. Huguet. Nonlinear dynamics of neuronal excitability, oscillations, and coincidence detection. *Comm. Pure Appl. Math.*, 66(9):1464–1494, 2013.
- [RHD11] M. Raghib, N.A. Hill, and U. Dieckmann. A multiscale maximum entropy moment closure for locally regulated space-time point process models of population dynamics. *J. Math. Biol.*, 62:605–653, 2011.
- [RHMN09] J.E. Rubin, J. Hayes, J. Mendenhall, and C. Del Negro. Calcium-activated nonspecific cation current and synaptic depression promote network-dependent burst oscillations. *Proc. Natl. Acad. Sci.*, 106(8):2939–2944, 2009.
- [Ria08] R. Riaza. *Differential-Algebraic Systems. Analytical Aspects and Circuit Applications*. World Scientific, 2008.
- [Ric11] M.P. Richardson. New observations may inform seizure models: very fast and very slow oscillations. *Prog. Biophys. Molec. Biol.*, 105:5–13, 2011.
- [Rin75] J. Rinzel. Spatial stability of traveling wave solutions of a nerve conduction equation. *Biophys. J.*, 15(10):975–988, 1975.
- [Rin77] J. Rinzel. Repetitive activity and Hopf bifurcation under point-stimulation for a simple FitzHugh–Nagumo nerve conduction model. *J. Math. Biol.*, 5(4):363–382, 1977.
- [Rin84] C.A. Ringhofer. On collocation schemes for quasilinear singularly perturbed boundary value problems. *SIAM J. Numer. Anal.*, 21:864–882, 1984.
- [Rin85] J. Rinzel. Bursting oscillations in an excitable membrane model. In *Ordinary and Partial Differential Equations*, pages 304–316. Springer, 1985.
- [Rin86] J. Rinzel. A formal classification of bursting mechanisms in excitable systems. *Proc. Int. Congress Math., Berkeley*, pages 1578–1593, 1986.
- [Rin87] J. Rinzel. A formal classification of bursting mechanisms in excitable systems. In *Mathematical Topics in Population Biology, Morphogenesis and Neurosciences*, pages 267–281. Springer, 1987.
- [Rin94] S. Rinaldi, Laura and Petrarch: an intriguing case of cyclical love dynamics. *SIAM J. Appl. Math.*, 58(4):1205–1221, 1994.
- [Rin09] S. Rinaldi. Synchrony in slow–fast metacommunities. *Int. J. Bif. Chaos*, 19(7):2447–2453, 2009.
- [Ris96] H. Risken. *The Fokker–Planck Equation*. Springer, 1996.
- [RJ72] R.J. Field, E. Körös and R.M. Noyes. Oscillations in chemical systems II. Thorough analysis of temporal oscillations in the Ce – BrO₃-malonic acid system. *J. Am. Chem. Soc.*, 94:8649–8664, 1972.
- [RJM95] J. Rubin, C.K.R.T. Jones, and M. Maxey. Settling and asymptotic motion of aerosol particles in a cellular flow field. *J. Nonlinear Sci.*, 5:337–358, 1995.
- [RK73] J. Rinzel and J.B. Keller. Traveling wave solutions of a nerve conduction equation. *Biophys. J.*, 13(12):1313–1337, 1973.
- [RK83] J. Rinzel and J.P. Keener. Hopf bifurcation to repetitive activity in nerve. *SIAM J. Appl. Math.*, 43(4):907–922, 1983.
- [RK86] B. Riedle and P. Kokotovic. Integral manifolds of slow adaptation. *IEEE Trans. Aut. Contr.*, 31(4):316–324, 1986.
- [RK99] M. Rachwalska and A.L. Kawczynski. New types of mixed-mode oscillations in the Belousov–Zhabotinsky reaction in continuously stirred tank reactors. *J. Chem. Phys. A*, 103:3455–3457, 1999.
- [RK01] M. Rachwalska and A.L. Kawczynski. Period-adding bifurcations in mixed-mode oscillations in the Belousov–Zhabotinsky reaction at various residence times in a CTSR. *J. Chem. Phys. A*, 105:7885–7888, 2001.
- [RK02] V. Rottschäfer and T.J. Kaper. Blowup in the nonlinear Schrödinger equation near critical dimension. *J. Math. Anal. Appl.*, 268:517–549, 2002.
- [RK03] V. Rottschäfer and T.J. Kaper. Geometric theory for multi-bump, self-similar, blowup solutions of the cubic nonlinear Schrödinger equation. *Nonlinearity*, 16:929–961, 2003.
- [RK06] H.G. Rotstein and R. Kuske. Localized and asynchronous patterns via canards in coupled calcium oscillators. *Physica D*, 215:46–61, 2006.
- [RKS13] E. Reznik, T. Kaper, and D. Segré. The dynamics of hybrid metabolic-genetic oscillators. *Chaos*, 23(1):013132, 2013.
- [RKZE03a] H.G. Rotstein, N. Kopell, A.M. Zhabotinsky, and I.R. Epstein. A canard mechanism for localization in systems of globally coupled oscillators. *SIAM J. Appl. Math.*, 63(6):1998–2019, 2003.
- [RKZE03b] H.G. Rotstein, N. Kopell, A.M. Zhabotinsky, and I.R. Epstein. Canard phenomenon and localization of oscillations in the Belousov–Zhabotinsky reaction with global feedback. *J. Chem. Phys.*, 119(17):8824–8832, 2003.
- [RL86] J. Rinzel and Y.S. Lee. On different mechanisms for membrane potential bursting. In *Nonlinear Oscillations in Biology and Chemistry*, pages 19–33. Springer, 1986.
- [RL87] J. Rinzel and Y.S. Lee. Dissection of a model for neuronal parabolic bursting. *J. Math. Biol.*, 25(6):653–675, 1987.
- [RL88] S. Rajasekar and M. Lakshmanan. Period-doubling bifurcations, chaos, phase-locking and devil’s staircase in a Bonhoeffer–van der Pol oscillator. *Physica D*, 32:146–152, 1988.
- [RL99] H.-G. Roos and T. Linß. Sufficient conditions for uniform convergence on layer-adapted grids. *Computing*, 63(1):27–45, 1999.
- [RM63] M.L. Rosenzweig and R.H. MacArthur. Graphical representation and stability conditions of predator-prey interactions. *American Naturalist*, 97:209–223, 1963.
- [RM80] J. Rinzel and R.N. Miller. Numerical calculation of stable and unstable periodic solutions to the Hodgkin–Huxley equations. *Math. Biosci.*, 49(1):27–59, 1980.

- [RM92] S. Rinaldi and S. Muratori. Slow-fast limit cycles in predator-prey models. *Ecol. Model.*, 61:287–308, 1992.
- [RM00] A.V. Rao and K.D. Mease. Eigenvector approximate dichotomic basis method for solving hypersensitive optimal control problems. *Optim. Control Appl. Meth.*, 21:1–19, 2000.
- [RMSaSL12] V.M. Rozenbaum, Yu.A. Makhnovskii, I.V. Shapochkina, S.-Y. Sheu, D.-Y. Yamg and S.H. Lin. Adiabatically slow and adiabatically fast driven ratchets. *Phys. Rev. E*, 85:041116, 2012.
- [RMW99] C. Rhodes, M. Morari, and S. Wiggins. Identification of low order manifolds: validating the algorithm of Maas and Pope. *Chaos*, 9(1):108–123, 1999.
- [Rob83] C. Robinson. Sustained resonance for a nonlinear system with slowly varying coefficients. *SIAM J. Math. Anal.*, 14(5):847–860, 1983.
- [Rob86] S.M. Roberts. An approach to singular perturbation problems insoluble by asymptotic methods. *J. Optimization Theory and Applications*, 48(2):325–339, 1986.
- [Rob01] J.C. Robinson. *Infinite-Dimensional Dynamical Systems*. CUP, 2001.
- [Rob03] Derek J.S. Robinson. *An Introduction to Abstract Algebra*. Walter de Gruyter, 2003.
- [Rob08] A.J. Roberts. Normal form transforms separate slow and fast modes in stochastic dynamical systems. *Physica A*, 387:12–38, 2008.
- [Rob09] A.J. Roberts. Model dynamics across multiple length and time scales on a spatial multigrid. *Multiscale Model. Simul.*, 7(4):1525–1548, 2009.
- [Rob13] R.C. Robinson. *An Introduction to Dynamical Systems: Continuous and Discrete*. AMS, 2013.
- [Roo94] H.-G. Roos. Ten ways to generate the Il'in and related schemes. *J. Comput. Appl. Math.*, 53(1):43–59, 1994.
- [Roo98] H.-G. Roos. Layer-adapted grids for singular perturbation problems. *Z. Angew. Math. Mech.*, 78(5):291–309, 1998.
- [Ros86] B. Rossetto. Trajectoires lentes des systèmes dynamiques lents-rapides. In *Analysis and Optimization of Systems*, Lecture Notes in Contr. Inform. Sci., pages 680–695. Springer, 1986.
- [Ros89] B. Rossetto. Geometrical structure of attractors of slow–fast dynamical systems: the double scroll chaotic oscillator. In *Differential Equations*, Lecture Notes in Pure and Appl. Math., pages 621–628. Dekker, 1989.
- [Ros93] B. Rossetto. Chua's circuit as a slow–fast autonomous dynamical system. *J. Circuits Systems Comput.*, 3(2):483–496, 1993.
- [Ros06] S. Ross. *A First Course in Probability*. Pearson Prentice Hall, 2006.
- [Rou98] R. Roussarie. *Bifurcations of Planar Vector Fields and Hilbert's Sixteenth Problem*. Springer, 1998.
- [ROWK06] H.G. Rotstein, T. Oppermann, J.A. White, and N. Kopell. The dynamic structure underlying sub-threshold oscillatory activity and the onset of spikes in a model of medial entorhinal cortex stellate cells. *J. Comput. Neurosci.*, 21:271–292, 2006.
- [Roz62] N.H. Rozov. Asymptotic calculation of nearly discontinuous solutions of a second-order system of differential equations. *Dokl. Akad. Nauk SSSR (in Russian)*, 145:38–40, 1962.
- [Roz64] N.H. Rozov. On the asymptotic theory of relaxation oscillations in systems with one degree of freedom. II. Calculation of the period of the limit cycle. *Vestnik Moskov. Univ. Ser. I Mat. Meh. (in Russian)*, 1964(3):56–65, 1964.
- [RP12] I. Ratas and K. Pyragas. Pulse propagation and failure in the discrete FitzHugh–Nagumo model subject to high-frequency stimulation. *Phys. Rev. E*, 86:046211, 2012.
- [RPVG07] Z. Ren, S.B. Pope, A. Vladimirs, and J.M. Guckenheimer. Application of the ICE-PIC method for the dimension reduction of chemical kinetics coupled with transport. *Proceed. Combust. Inst.*, 31:473–481, 2007.
- [RR92] Y. Ren and R.D. Russell. Moving mesh techniques based upon equidistribution, and their stability. *SIAM J. Sci. Stat. Comput.*, 13(6):1265–1286, 1992.
- [RR94] M.E. Rush and J. Rinzel. Analysis of bursting in a thalamic neuron model. *Biol. Cybern.*, 71(4):281–291, 1994.
- [RR95] M.E. Rush and J. Rinzel. The potassium A-current, low firing rates and rebound excitation in Hodgkin–Huxley models. *Bull. Math. Biol.*, 57(6):899–929, 1995.
- [RR00] P.J. Rabier and W.C. Rheinboldt. *Nonholonomic Motion of Rigid Mechanical Systems from a DAE Viewpoint*. SIAM, 2000.
- [RR04] M. Renardy and R.C. Rogers. *An Introduction to Partial Differential Equations*. Springer, 2004.
- [RRAA87] P. Richetti, J.C. Roux, F. Argoul, and A. Arneodo. From quasiperiodicity to chaos in the Belousov–Zhabotinskii reaction. II. Modeling and theory. *J. Chem. Phys.*, 86(6):3339–3355, 1987.
- [RRBV81] J.-C. Roux, A. Rossi, S. Bachelart, and C. Vidal. Experimental observations of complex dynamical behaviour during a chemical reaction. *Physica D*, 2(2):395–403, 1981.
- [RRCL00] S. Ramdani, B. Rossetto, L.O. Chua, and R. Lozi. Slow manifolds of some chaotic systems with applications to laser systems. *Int. J. Bif. Chaos*, 10(12):2729–2744, 2000.
- [RRE13] J.J. Rubin, J.E. Rubin, and G.B. Ermentrout. Analysis of synchronization in a slowly changing environment: how slow coupling becomes fast weak coupling. *Phys. Rev. Lett.*, 110(20):204101, 2013.
- [RS75a] P. Reddy and P. Sannuti. Optimal control of a coupled-core nuclear reactor by a singular perturbation method. *IEEE Trans. Aut. Contr.*, 20(6):766–769, 1975.
- [RS75b] S. Rosenblat and J. Shepherd. On the asymptotic solution of the Lagerstrom model equation. *SIAM J. Appl. Math.*, 29:110–120, 1975.
- [RS81] J.-C. Roux and H.L. Swinney. Topology of chaos in a chemical reaction. In C. Vidal and A. Pacault, editors, *Nonlinear Phenomena in Chemical Dynamics*, pages 38–43. Springer, 1981.
- [RS84] J. Rinzel and I.B. Schwartz. One variable map prediction of the Belousov–Zhabotinskii mixed mode oscillations. *J. Chem. Phys.*, 80(11):5610–5615, 1984.
- [RS93] P.F. Rowat and A.I. Selverston. Modeling the gastric mill central pattern generator of the lobster with a relaxation-oscillator network. *J. Neurophysiol.*, 70(3):1030–1053, 1993.
- [RS96] J.-P. Ramis and R. Schäffke. Gevrey separation of fast and slow variables. *Nonlinearity*, 9:353–384, 1996.
- [RS99] C. Reinecke and G. Sweers. A positive solution on \mathbb{R}^N to a system of elliptic equations of FitzHugh–Nagumo type. *J. Differential Equat.*, 153(2):292–312, 1999.

- [RS00] S. Rinaldi and M. Scheffer. Geometric analysis of ecological models with slow and fast processes. *Ecosystems*, 3:507–521, 2000.
- [RS03] D. Rachinskii and K. Schneider. Delayed loss of stability in systems with degenerate linear parts. *Zeitschr. Anal. Anwend.*, 22(2):433–454, 2003.
- [RSK89] J. Rubinstein, P. Sternberg, and J.B. Keller. Reaction-diffusion processes and evolution to harmonic maps. *SIAM J. Appl. Math.*, 49(6):1722–1733, 1989.
- [RSS83] J.-C. Roux, R.H. Simoyi, and H.L. Swinney. Observation of a strange attractor. *Physica D*, 8(1):257–266, 1983.
- [RSS11] E. Reznik, D. Segré, and W.E. Sherwood. The quasi-steady state assumption in an enzymatically open system. *arXiv:1103.1200v1*, pages 1–28, 2011.
- [RST96] H.-G. Roos, M. Stynes, and L. Tobiska. *Numerical Methods for Singularly perturbed Differential Equations: Convection-Diffusion and Flow Problems*. Springer, 1996.
- [RT82a] J. Rinzel and D. Terman. Propagation phenomena in a bistable reaction–diffusion system. *SIAM J. Appl. Math.*, 42(5):1111–1137, 1982.
- [RT82b] J. Rinzel and W.C. Troy. Bursting in a simplified Oregonator flow system model. *J. Chem. Phys.*, 76(4):1775–1789, 1982.
- [RT00] J.E. Rubin and D. Terman. Analysis of clustered firing patterns in synaptically coupled networks of oscillators. *J. Math. Biol.*, 41:6, 2000.
- [RT02a] J.E. Rubin and D. Terman. Geometric singular perturbation analysis of neuronal dynamics. In B. Fiedler, editor, *Handbook of Dynamical Systems 2*, pages 93–146. Elsevier, 2002.
- [RT02b] J.E. Rubin and D. Terman. Synchronized activity and loss of synchrony among heterogeneous conditional oscillators. *SIAM J. Appl. Dyn. Syst.*, 1:1, 2002.
- [RT12] J.E. Rubin and D. Terman. Explicit maps to predict activation order in multi-phase rhythms of a coupled cell network. *J. Math. Neurosci.*, 2:4, 2012.
- [RTK02] O. Runborg, C. Theodoropoulos, and I.G. Kevrekidis. Effective bifurcation analysis: a time-stepper-based approach. *Nonlinearity*, 15(2):491–511, 2002.
- [RU03] H.-G. Roos and Z. Uzelac. The SDFEM for a convection-diffusion problem with two small parameters. *Comput. Meth. Appl. Math.*, 3(3):443–458, 2003.
- [Rub77] L.A. Rubenfeld. The passage of weakly coupled nonlinear oscillators through internal resonance. *Stud. Appl. Math.*, 57:77–92, 1977.
- [Rub78] L.A. Rubenfeld. On a derivative-expansion technique and some comments on multiple scaling in the asymptotic approximation of solutions of certain differential equations. *SIAM Rev.*, 20:79–105, 1978.
- [Rub06] J. Rubin. Bursting induced by excitatory synaptic coupling in non-identical conditional relaxation oscillators or square-wave bursters. *Phys. Rev. E*, 74:021917, 2006.
- [Rud76] W. Rudin. *Principles of Mathematical Analysis*. McGraw-Hill, 1976.
- [Rud91] W. Rudin. *Functional Analysis*. McGraw-Hill, 1991.
- [Rul02] N.F. Rulkov. Modeling of spiking-bursting neural behavior using two-dimensional map. *Phys. Rev. E*, 65(4):041922, 2002.
- [Rus77] R.D. Russell. A comparison of collocation and finite differences for two-point boundary value problems. *SIAM J. Numer. Anal.*, 14(1):19–39, 1977.
- [Rus79] R.D. Russell. Mesh selection methods. In *Codes for Boundary-Value Problems in Ordinary Differential Equations*, volume 74 of *Lecture Notes in Computer Science*, pages 228–242. Springer, 1979.
- [RV98] J.-M. Roquejoffre and J.-P. Vila. Stability of ZND detonation waves in the Majda combustion model. *Asymp. Anal.*, 18(3):329–348, 1998.
- [RVSA06] M.I. Rabinovich, P. Varona, A.I. Selverston, and H.D. Abarbanel. Dynamical principles in neuroscience. *Rev. Mod. Phys.*, 78(4):1213–1265, 2006.
- [RW77] L.A. Rubenfeld and B. Willner. Uniform asymptotic solutions for linear second order ordinary differential equations with turning points: formal theory. *SIAM J. Appl. Math.*, 32(1):21–38, 1977.
- [RW88] J.R. Rohlicek and A.S. Willsky. Multiple time scale decomposition of discrete time Markov chains. *Syst. Contr. Lett.*, 11(4):309–314, 1988.
- [RW95a] L.G. Reyna and M.J. Ward. Metastable internal layer dynamics for the viscous Cahn–Hilliard equation. *Meth. Appl. Anal.*, 2:285–306, 1995.
- [RW95b] L.G. Reyna and M.J. Ward. On the exponentially slow motion of a viscous shock. *Comm. Pure Appl. Math.*, 48(2):79–120, 1995.
- [RW01] V. Rottschäfer and C.E. Wayne. Existence and stability of traveling fronts in the extended Fisher–Kolmogorov equation. *J. Differential Equat.*, 176:532–560, 2001.
- [RW05] X. Ren and J. Wei. Nucleation in the FitzHugh–Nagumo system: interface-spike solutions. *J. Differential Equat.*, 209(2):266–301, 2005.
- [RW07] J. Rubin and M. Wechselberger. Giant squid - hidden canard: the 3D geometry of the Hodgin-Huxley model. *Biological Cybernetics*, 97(1), 2007.
- [RW08] J. Rubin and M. Wechselberger. The selection of mixed-mode oscillations in a hodgkin-huxley model with multiple timescales. *Chaos*, 18, 2008.
- [RW12] H.G. Rotstein and H. Wu. Swing, release, and escape mechanisms contribute to the generation of phase-locked cluster patterns in a globally coupled FitzHugh–Nagumo model. *Phys. Rev. E*, 86:066207, 2012.
- [RWJWZ13] A. Roberts, E. Widiasih, C.K.R.T. Jones, M. Wechselberger, and M. Zaks. Mixed mode oscillations in a conceptual climate model. *arXiv:1311.5182*, pages 1–26, 2013.
- [RWK08] H.G. Rotstein, M. Wechselberger, and N. Kopell. Canard induced mixed-mode oscillations in a medial entorhinal cortex layer II stellate cell model. *SIAM J. Applied Dynamical Systems*, 7(4):1582–1611, 2008.
- [RWV11] A. Rasmussen, J. Wyller and J.O. Vik. Relaxation oscillations in spruce-budworm interactions. *Nonlinear Anal. Real World Appl.*, 12:304–319, 2011.
- [RX04] S. Ruan and D. Xiao. Stability of steady states and existence of travelling waves in a vector-disease model. *Proc. R. Soc. Edinburgh A*, 134(5):991–1011, 2004.
- [RY12] B. Ryals and L.-S. Young. Horseshoes of periodically kicked van der Pol oscillators. *Chaos*, 22:043140, 2012.

- [Ryb87] K.P. Rybakowski. *The Homotopy Index and Partial Differential Equations*. Springer, 1987.
- [SA89] M. Schell and F.N. Albahadly. Mixed-mode oscillations in an electrochemical system. II. A periodic-chaotic sequence. *J. Chem. Phys.*, 90:822–828, 1989.
- [Sab87] A. Saberi. Output-feedback control with almost-disturbance-decoupling property - a singular perturbation approach. *Int. J. Contr.*, 45(5):1705–1722, 1987.
- [Sac69] R. Sacker. A perturbation theorem for invariant manifolds and Hölder continuity. *J. Math. Mech.*, 18:705–762, 1969.
- [Sak90] K. Sakamoto. Invariant manifolds in singular perturbation problems for ordinary differential equations. *Proc. Royal Soc. Ed.*, 116:45–78, 1990.
- [Sal85] D. Salamon. Connected simple systems and the Conley index of isolated invariant sets. *Trans. AMS*, 291:1–41, 1985.
- [Sam91] S.N. Samborski. Rivers from the point of view of the qualitative theory. In E. Benoît, editor, *Dynamic Bifurcations*, volume 1493 of *Lecture Notes in Mathematics*, pages 168–180. Springer, 1991.
- [San74] P. Sannuti. Asymptotic series solution of singularly perturbed optimal control problems. *Automatica*, 10(2):183–194, 1974.
- [San75] P. Sannuti. Asymptotic expansions of singularly perturbed quasi-linear optimal systems. *SIAM J. Contr.*, 13(3):572–592, 1975.
- [San77] P. Sannuti. On the controllability of singularly perturbed systems. *IEEE Trans. Aut. Contr.*, 22(4):622–624, 1977.
- [San78] P. Sannuti. On the controllability of some singularly perturbed nonlinear systems. *J. Math. Anal. Appl.*, 64(3):579–591, 1978.
- [San79] J.A. Sanders. On the passage through resonance. *SIAM J. Math. Anal.*, 10(6):1220–1243, 1979.
- [San80] J.A. Sanders. Asymptotic approximations and extension of time-scales. *SIAM J. Math. Anal.*, 11(4):758–770, 1980.
- [San83a] J.A. Sanders. On the fundamental theorem of averaging. *SIAM J. Math. Anal.*, 14(1):1–10, 1983.
- [San83b] P. Sannuti. Direct singular perturbation analysis of high-gain and cheap control problems. *Automatica*, 19(1):41–51, 1983.
- [San95] B. Sandstede. Constructing dynamical systems having homoclinic bifurcation points of codimension two. *J. Dyn. Diff. Eq.*, 9(2):269–288, 1995.
- [San98] B. Sandstede. Stability of N -fronts bifurcating from a twisted heteroclinic loop and an application to the FitzHugh–Nagumo equation. *SIAM J. Math. Anal.*, 29(1):183–207, 1998.
- [San01] B. Sandstede. Stability of travelling waves. In B. Fiedler, editor, *Handbook of Dynamical Systems*, volume 2, pages 983–1055. Elsevier, 2001.
- [Sar78] W. Sarlet. On a common derivation of the averaging method and the two-timescale method. *Celestial Mech.*, 17(3):299–311, 1978.
- [Sau80] P.T. Saunders. *An Introduction to Catastrophe Theory*. CUP, 1980.
- [SB82] V.R. Saksena and T. Basar. A multimodel approach to stochastic team problems. *Automatica*, 18(6):713–720, 1982.
- [SB85] P.R. Sethna and K.R. Meyer A.K. Bajaj. On the method of averaging, integral manifolds and systems with symmetry. *SIAM J. Appl. Math.*, 45(3):343–359, 1985.
- [SB97] C. Schütte and F.A. Bornemann. Homogenization approach to smoothed molecular dynamics. *Nonl. Anal.*, 30:1805–1814, 1997.
- [SB99] C. Schütte and F.A. Bornemann. On the singular limit of the quantum-classical molecular dynamics model. *SIAM J. Appl. Math.*, 59(4):1208–1224, 1999.
- [SB03] R. Suckley and V. Biktashev. Comparison of asymptotics of heart and nerve excitability. *Phys. Rev. E*, 68:011902, 2003.
- [SB04] B.F. Smith and P.E. Børstad. *Domain Decomposition: Parallel Multilevel Methods for Elliptic Partial Differential Equations*. CUP, 2004.
- [SB08] K. Sriram and S. Bernard. Complex dynamics in the Oregonator model with linear delayed feedback. *Chaos*, 18(2):023126, 2008.
- [SB11] R.D. Simitev and V.N. Biktashev. Asymptotics of conduction velocity restitution in models of electrical excitation in the heart. *Bull. Math. Biol.*, 73(1):72–115, 2011.
- [SBB⁺09] M. Scheffer, J. Bascompte, W.A. Brock, V. Brovkin, S.R. Carpenter, V. Dakos, H. Held, E.H. van Nes, M. Rietkerk, and G. Sugihara. Early-warning signals for critical transitions. *Nature*, 461:53–59, 2009.
- [SBJM00] B. Sandstede, S. Balasuriya, C.K.R.T. Jones, and P. Miller. Melnikov theory for finite-time vector fields. *Nonlinearity*, 13(4):1357, 2000.
- [SBO01] W.M. Schaffer, T.V. Bronnikova, and L.F. Olsen. Nonlinear dynamics of the peroxidase-oxidase reaction. II. Compatibility of an extended model with previously reported model-data correspondences. *J. Phys. Chem.*, 105:5331–5340, 2001.
- [SC81] V.R. Saksena and J.B. Cruz. Nash strategies in decentralized control of multiparameter singularly perturbed large scale systems. *Large Scale Syst.*, 2:219–234, 1981.
- [SC82] V.R. Saksena and J.B. Cruz. A multimodel approach to stochastic Nash games. *Automatica*, 18(3):295–305, 1982.
- [SC83] M.A. Salman and J.B. Cruz. Team-optimal closed-loop Stackelberg strategies for systems with slow and fast modes. *Int. J. Contr.*, 37(6):1401–1416, 1983.
- [SC84] V.R. Saksena and J.B. Cruz. Robust Nash strategies for a class of non-linear singularly perturbed problems. *Int. J. Contr.*, 39(2):293–310, 1984.
- [SC86] J.A. Sanders and R. Cushman. Limit cycles in the Josephson equation. *SIAM J. Math. Anal.*, 17(3):495–511, 1986.
- [SC03] M. Scheffer and S.R. Carpenter. Catastrophic regime shifts in ecosystems: linking theory to observation. *TRENDS in Ecol. and Evol.*, 18(12):648–656, 2003.
- [SCC05] A. Shilnikov, R.L. Calabrese, and G. Cymbalyuk. Mechanism of bistability: tonic spiking and bursting in a neuron model. *Phys. Rev. E*, 71(5):056214, 2005.
- [SCCA02] B. Song, C. Castillo-Chavez, and J.P. Aparicio. Tuberculosis models with fast and slow dynamics: the role of close and casual contacts. *Math. Biosci.*, 180(1):187–205, 2002.

- [SCF⁺01] M. Scheffer, S.R. Carpenter, J.A. Foley, C. Folke, and B. Walker. Catastrophic shifts in ecosystems. *Nature*, 413:591–596, 2001.
- [Sch80] Z. Schuss. Singular perturbation methods in stochastic differential equations of mathematical physics. *SIAM Rev.*, 22(2):119–155, 1980.
- [Sch85a] S. Schechter. Persistent unstable equilibria and closed orbits of a singularly perturbed equation. *J. Differential Equat.*, 60:131–141, 1985.
- [Sch85b] C. Schmeiser. Finite deformations of thin beams, asymptotic analysis by singular perturbation methods. *IMA J. Appl. Math.*, 34(2):155–164, 1985.
- [Sch88] S. Schechter. Stable manifolds in the method of averaging. *Trans. Amer. Math. Soc.*, 308(1):159–176, 1988.
- [Sch89] C. Schmeiser. On strongly reverse biased semiconductor diodes. *SIAM J. Appl. Math.*, 49(6):1734–1748, 1989.
- [Sch95a] G. Schneider. Validity and limitation of the Newell-Whitehead equation. *Math. Nachr.*, 176:249–263, 1995.
- [Sch95b] C.G. Schröer. First order adiabatic approximation for a class of classical slow-fast systems with ergodic fast dynamics. In *Hamiltonian Systems with Three or More Degrees of Freedom*, pages 563–567. Kluwer, 1995.
- [Sch96] G. Schneider. The validity of generalized Ginzburg-Landau equations. *Math. Meth. Appl. Sci.*, 19(9):717–736, 1996.
- [Sch98] G. Schneider. Justification of modulation equations for hyperbolic systems via normal forms. *Nonl. Diff. Eq. Appl. NoDEA*, 5(1):69–82, 1998.
- [Sch01] G. Schneider. Bifurcation theory for dissipative systems on unbounded cylindrical domains – an introduction to the mathematical theory of modulation equations. *ZAMM Z. Angew. Math. Mech.*, 81(8):507–522, 2001.
- [Sch02] S. Schechter. Undercompressive shock waves and the Dafermos regularization. *Nonlinearity*, 15(4):1361–1377, 2002.
- [Sch04] S. Schechter. Existence of Dafermos profiles for singular shocks. *J. Differential Equat.*, 205(1):185–210, 2004.
- [Sch06] S. Schechter. Eigenvalues of self-similar solutions of the Dafermos regularization of a system of conservation laws via geometric singular perturbation theory. *J. Dyn. Diff. Eq.*, 18(1):53–101, 2006.
- [Sch08a] S. Schechter. Exchange lemmas 1: Deng's lemma. *J. Differential Equat.*, 245(2):392–410, 2008.
- [Sch08b] S. Schechter. Exchange lemmas 2: general exchange lemma. *J. Differential Equat.*, 245(2):411–441, 2008.
- [Sch09a] M. Scheffer. *Critical Transitions in Nature and Society*. Princeton University Press, 2009.
- [Sch09b] Z. Schuss. *Theory and Applications of Stochastic Processes: An Analytical Approach*. Springer, 2009.
- [Sch10] I.V. Schurov. Ducks on the torus: existence and uniqueness. *J. Dynamical and Control Sys.*, 16(2):267–300, 2010.
- [Sch11] I.V. Schurov. Duck farming on the two-torus: multiple canard cycles in generic slow-fast systems. *Discr. Cont. Dyn. Syst. Suppl.*, pages 1289–1298, 2011.
- [Sco94] S.K. Scott. *Oscillations, waves, and chaos in chemical kinetics*. Oxford University Press, 1994.
- [SCR07] A. Shpiro, R. Curtu, J. Rinzel, and N. Rubin. Dynamical characteristics common to neural competition models. *J. Neurophysiol.*, 97:462–473, 2007.
- [SD93] S. Sen and K.B. Datta. Stability bounds of singularity perturbed systems. *IEEE Trans. Aut. Contr.*, 38(2):302–304, 1993.
- [SD99] P. Shi and V. Dragan. Asymptotic H_∞ control of singularly perturbed systems with parametric uncertainties. *IEEE Trans. Aut. Contr.*, 44(9):1738–1742, 1999.
- [SD03] B. Sicardi and V. Dubois. Co-orbital motion with slowly varying parameters. *Celestial Mech. Dynam. Astronom.*, 86(4):321–350, 2003.
- [SDT91] C. Sueur and G. Dauphin-Tanguy. Bond graph approach to multi-time scale systems analysis. *J. Frank. Inst.*, 328(5):1005–1026, 1991.
- [Ser13] O.S. Serea. Characterization of the optimal trajectories for the averaged dynamics associated to singularly perturbed control systems. *J. Differential Equat.*, 255:4226–4243, 2013.
- [Set95] P.R. Sethna. On averaged and normal form equations. *Nonlinear Dyn.*, 7:1–10, 1995.
- [Sey94] R. Seydel. *Practical Bifurcation and Stability Analysis*. Springer, 1994.
- [SF84] J. Shinari and N. Farber. Horizontal variable-speed interception game solved by forced singular perturbation technique. *J. Optim. Theor. Appl.*, 42(4):603–636, 1984.
- [SF07] C. Sourdis and P.C. Fife. Existence of heteroclinic orbits for a corner layer problem in anisotropic interfaces. *Adv. Differential Equat.*, 12(6):623–668, 2007.
- [SFH⁺01] S.S. Azhchin, G. Feng, M.R. Heikal, I. Goldfarb, V. Sol'dshtein, and G. Kuzmenko. Thermal ignition analysis of a monodisperse spray with radiation. *Combustion and Flame*, 124(4):684–701, 2001.
- [SMFH05] R. Straubhaar, D. Flockerzi, S.C. Müller, and M.J. Hause. Reduction of chemical reaction networks using quasi-integrals. *J. Phys. Chem. A*, 109(3):441–450, 2005.
- [SG79] L.F. Shampine and C.W. Gear. A user's view of solving stiff ordinary differential equations. *SIAM Rev.*, 21(1):1–17, 1979.
- [SG00] H. Schlichting and K. Gersten. *Boundary-Layer Theory*. Springer, 2000.
- [SG03] K. Sriram and M.S. Gopinathan. Effects of delayed linear electrical perturbation of the Belousov-Zhabotinsky reaction: a case of complex mixed mode oscillations in a batch reactor. *React. Kinet. Catal. Lett.*, 79(2):341–349, 2003.
- [SG10] W.E. Sherwood and J. Guckenheimer. Dissecting the phase response of a model bursting neuron. *SIAM J. Appl. Dyn. Sys.*, 9(3):659–703, 2010.
- [SG13] L. Sacerdote and M.T. Giraudo. Stochastic integrate and fire models: a review on mathematical methods and their applications. In *Stochastic Biomathematical Models*, pages 99–148. Springer, 2013.
- [SGH77] R.A. Schmitz, K.R. Graziani, and J.L. Hudson. Experimental evidence of chaotic states in the Belousov-Zhabotinskii reaction. *J. Chem. Phys.*, 67(6):3040–3044, 1977.
- [SGH01] G. Schmid, I. Goychuk, and P. Hänggi. Stochastic resonance as a collective property of ion channel assemblies. *Europhys. Lett.*, 56(1):22, 2001.

- [SGK03] C.I. Siettos, M.D. Graham, and I.G. Kevrekidis. Coarse Brownian dynamics for nematic liquid crystals: bifurcation, projective integration, and control via stochastic simulation. *J. Chem. Phys.*, 118(22):10149–10156, 2003.
- [SGL93] C.G. Steimetz, T. Geest, and R. Larter. Universality in the peroxidase-oxidase reaction: period doublings, chaos, period three, and unstable limit cycles. *J. Phys. Chem.*, 97:5649–5653, 1993.
- [SGS92] W.C. Su, Z. Gajic, and X.M. Shen. The exact slow–fast decomposition of the algebraic Riccati equation of singularly perturbed systems. *IEEE Trans. Aut. Contr.*, 37(9):1456–1459, 1992.
- [SH87] R. Seydel and V. Hlavaceka. Role of continuation in engineering analysis. *Chem. Eng. Sci.*, 42(6):1281–1295, 1987.
- [SH96] K.R. Schenk-Hoppé. Bifurcation scenarios of the noisy Duffing–van der Pol oscillator. *Nonlinear Dyn.*, 11:255–274, 1996.
- [SH98] K.R. Schenk-Hoppé. Random attractors - general properties, existence and applications to stochastic bifurcation theory. *Discr. Cont. Dyn. Syst. A*, 4(1):99–130, 1998.
- [SH08] A. Surana and G. Haller. Ghost manifolds in slow–fast systems, with applications to unsteady fluid flow separation. *Physica D*, 237(10):1507–1529, 2008.
- [SH13] J. Shen and M. Han. Bifurcations of canard limit cycles in several singularly perturbed generalized polynomial Liénard systems. *Discrete Contin. Dyn. Syst.*, 33(7):3085–3108, 2013.
- [Sha61] A.N. Sharkovskii. The reducibility of a continuous function of a real variable and the structure of the stationary points of the corresponding iteration process. *Dokl. Akad. Nauk SSSR*, 139:1067–1070, 1961.
- [Sha64a] A.N. Sharkovskii. Co-existence of cycles of a continuous map of the line into itself. *Ukrainskii Matematicheskii Zhurnal*, 16(1):61–71, 1964. English translation: *Int. J. Bif. Chaos* 5(5), pp. 1263–1273, 1995.
- [Sha64b] A.N. Sharkovskii. Fixed points and the center of a continuous mapping of the line into itself. *Dopovid Akad. Nauk Ukr. RSR*, 1964:865–868, 1964.
- [Sha65] A.N. Sharkovskii. On cycles and structure of a continuous mapping. *Ukrainskii Matematicheskii Zhurnal*, 17(3):104–111, 1965.
- [Sha66] A.N. Sharkovskii. The set of convergence of one-dimensional iterations. *Dopovid Akad. Nauk Ukr. RSR*, 1966:866–870, 1966.
- [Sha94] R. Shankar. Renormalization-group approach to interacting fermions. *Rev. Mod. Phys.*, 66(1):129–192, 1994.
- [Sha04] Z.H. Shao. Robust stability of two-time-scale systems with nonlinear uncertainties. *IEEE Trans. Aut. Contr.*, 49(2):258–261, 2004.
- [She03] E. Schepakina. Black swans and canards in self-ignition problem. *Nonl. Anal. Real World Appl.*, 4(1):45–50, 2003.
- [She08] W.E. Sherwood. *Phase response in networks of bursting neurons: modeling central pattern generators*. PhD thesis, Cornell University, Ithaca, USA, 2008.
- [Shi65] L.P. Shilnikov. A case of the existence of a denumerable set of periodic motions. *Sov. Math. Dokl.*, 6:163–166, 1965.
- [Shi73] M.A. Shishkova. Analysis of a system of differential equations with a small parameter at the higher derivatives. *Akademii Nauk SSSR, Doklady*, 209:576–579, 1973.
- [Shi83] J. Shinar. On applications of singular perturbation techniques in nonlinear optimal control. *Automatica*, 19(2):203–211, 1983.
- [Shi91] G.I. Shishkin. Grid approximation of singularly perturbed boundary value problem for quasi-linear parabolic equations in the case of complete degeneracy in spatial variables. *Russ. J. Numer. Anal. Math. Mod.*, 6(3):243–262, 1991.
- [Shi97] G.I. Shishkin. On finite difference fitted schemes for singularly perturbed boundary value problems with a parabolic boundary layer. *J. Math. Anal. Appl.*, 208(1):181–204, 1997.
- [Shi05] G.I. Shishkin. Robust novel high-order accurate numerical methods for singularly perturbed convection–diffusion problems 1. *Math. Mod. Anal.*, 10(4):393–412, 2005.
- [Shi12] A. Shilnikov. Complete dynamical analysis of a neuron model. *Nonlinear Dyn.*, 68:305–328, 2012.
- [SHK89] S. Sastry, J. Hauser, and P. Kokotovic. Zero dynamics of regularly perturbed systems may be singularly perturbed. *Syst. Contr. Lett.*, 13(4):299–314, 1989.
- [SHPC09] C. Soria-Hoyo, F. Pontiga, and A. Castellanos. A PIC based procedure for the integration of multiple time scale problems in gas discharge physics. *J. Comput. Phys.*, 228(4):1017–1029, 2009.
- [SHX08] Y. Shen, Z. Hou, and H. Xin. Transition to burst synchronization in coupled neuron networks. *Phys. Rev. E*, 77:031920, 2008.
- [Sib62a] Y. Sibuya. Asymptotic solutions of a system of linear ordinary differential equations containing a parameter. *Funkcial. Ekvac.*, 4:83–113, 1962.
- [Sib62b] Y. Sibuya. Formal solutions of a linear ordinary differential equation of the n -th order at a turning point. *Funkcial. Ekvac.*, 4:115–139, 1962.
- [Sib63a] Y. Sibuya. Asymptotic solutions of initial value problems of ordinary differential equations with a small parameter in the derivative, I. *Arch. Rat. Mech. Anal.*, 14:304–311, 1963.
- [Sib63b] Y. Sibuya. Simplification of a linear ordinary differential equation of the n -th order at a turning point. *Arch. Rat. Mech. Anal.*, 13:206–221, 1963.
- [Sib81] Y. Sibuya. A theorem concerning uniform simplification at a transition point and the problem of resonance. *SIAM J. Math. Anal.*, 12(5):653–668, 1981.
- [Sib00] Y. Sibuya. The Gevrey asymptotics in the case of singular perturbations. *J. Differential Equat.*, 165:255–314, 2000.
- [SIB01] J. Stark, P. Iannelli, and S. Baigent. A nonlinear dynamics perspective of moment closure for stochastic processes. *Nonl. Anal.*, 47:753–764, 2001.
- [Sie13] J. Sieber. Longtime behaviour of the coupled wave equations for semiconductor lasers. *arXiv:1308.2060*, pages 1–33, 2013.
- [Sij85] J. Sijbrand. Properties of center manifolds. *Trans. Amer. Math. Soc.*, 289:431–469, 1985.
- [Sil04] W.T. Silfvast. *Laser Fundamentals*. CUP, 2004.

- [Sim83] B. Simon. Semiclassical analysis of low lying eigenvalues. I. Non-degenerate minima: Asymptotic expansions. *Ann. IHP (A) Phys. Théor.*, 38(3):295–308, 1983.
- [Sim84] B. Simon. Semiclassical analysis of low lying eigenvalues, II. Tunneling. *Ann. Math.*, 120:89–118, 1984.
- [Sin82] R.N.P. Singh. The linear-quadratic-Gaussian problem for singularly perturbed systems. *Int. J. Syst. Sci.*, 13:92–100, 1982.
- [SJLS05] S.N. Simic, K.H. Johansson, J. Lygeros, and S. Sastry. Towards a geometric theory of hybrid systems. *Dynamics of Continuous, Discrete and Impulsive Systems, Series B*, 12(5):649–687, 2005.
- [SK69a] P. Sannuti and P. Kokotovic. Near-optimum design of linear systems by a singular perturbation method. *IEEE Trans. Aut. Contr.*, 14(1):15–22, 1969.
- [SK69b] P. Sannuti and P. Kokotovic. Singular perturbation method for near optimum design of high-order non-linear systems. *Automatica*, 5(6):773–779, 1969.
- [SK84] A. Saberi and H. Khalil. Quadratic-type Lyapunov functions for singularly perturbed systems. *IEEE Trans. Aut. Contr.*, 29(6):542–550, 1984.
- [SK85a] A. Saberi and H. Khalil. Stabilization and regulation of nonlinear singularly perturbed systems - composite control. *IEEE Trans. Aut. Contr.*, 30(8):739–747, 1985.
- [SK85b] W.M. Schaffter and M. Kot. Nearly one dimensional dynamics in an epidemic. *J. Theor. Biol.*, 112:403–427, 1985.
- [SK93a] G.M. Shroff and H.B. Keller. Stabilization of unstable procedures: a recursive projection method. *SIAM J. Numer. Anal.*, 30:1099–1120, 1993.
- [SK93b] D. Somers and N. Kopell. Rapid synchronization through fast threshold modulation. *Biol. Cybern.*, 68(5):393–407, 1993.
- [SK95a] D. Somers and N. Kopell. Waves and synchrony in networks of oscillators of relaxation and non-relaxation type. *Physica D*, 89(1):169–183, 1995.
- [SK95b] P.E. Strizhak and A.L. Kawczynski. Regularities in complex transient oscillations in the Belousov–Zhabotinsky reaction in a batch reactor. *J. Phys. Chem.*, 99:10830–10833, 1995.
- [SK97] T.I. Seidman and L.V. Kalachev. A one-dimensional reaction/diffusion system with a fast reaction. *J. Math. Anal. Appl.*, 209(2):392–414, 1997.
- [SK07] J. Sieber and B. Krauskopf. Control-based continuation of periodic orbits with a time-delayed difference scheme. *Int. J. Bif. Chaos*, 17(8):2579–2593, 2007.
- [SK08] A. Shilnikov and M. Kolomiets. Methods of the qualitative theory for the Hindmarsh–Rose model: a case study - a tutorial. *Int. J. Bif. Chaos*, 18(8):2141–2168, 2008.
- [SK10] J. Sieber and P. Kowalczyk. Small-scale instabilities in dynamical systems with sliding. *Physica D*, 239(1):44–57, 2010.
- [SK11a] E. Shchepakina and O. Korotkova. Condition for canard explosion in a semiconductor optical amplifier. *J. Opt. Soc. Am. B*, 28(8):1988–1993, 2011.
- [SK11b] D.J.W. Simpson and R. Kuske. Mixed-mode oscillations in a stochastic, piecewise-linear system. *Physica D*, 240(14):1189–1198, 2011.
- [SK13] E. Shchepakina and O. Korotkova. Canard explosion in chemical and optical systems. *Discr. Cont. Dyn. Syst. B*, 18(2):495–512, 2013.
- [Ske82] R.D. Skeel. A theoretical framework for proving accuracy results for deferred corrections. *SIAM J. Numer. Anal.*, 19(1):171–196, 1982.
- [Ski81] L.A. Skinner. Note on the Lagerstrom singular perturbation models. *SIAM J. Appl. Math.*, 41(2):362–364, 1981.
- [Ski87] L.A. Skinner. Uniform solution of boundary layer problems exhibiting resonance. *SIAM J. Appl. Math.*, 47(2):225–231, 1987.
- [Ski94] L.A. Skinner. Matched expansion solutions of the first-order turning point problem. *SIAM J. Math. Anal.*, 25(5):1402–1411, 1994.
- [Ski11] L.A. Skinner. *Singular Perturbation Theory*. Springer, 2011.
- [SKK87] M.W. Spong, K. Khorasani, and P.V. Kokotovic. An integral manifold approach to the feedback control of flexible joint robots. *IEEE J. Robot. Autom.*, 3(4):291–300, 1987.
- [SKR04] G. Samaey, I.G. Kevrekidis, and D. Roose. Damping factors for the gap-tooth scheme. In *Multiscale Modelling and Simulation*, volume 39 of *Lecture Notes Comput. Sci. Eng.*, pages 93–102. Springer, 2004.
- [SKR06] G. Samaey, I.G. Kevrekidis, and D. Roose. Patch dynamics with buffers for homogenization problems. *J. Comput. Phys.*, 213(1):264–287, 2006.
- [SKR07] G. Samaey, I.G. Kevrekidis, and D. Roose. Patch dynamics: macroscopic simulation of multiscale systems. *PAMM*, 7(1):1025803–1025804, 2007.
- [SKR08] I. Sainz, A.B. Klimov, and L. Roa. Quantum phase transitions in an effective Hamiltonian: fast and slow systems. *J. Phys. A*, 41:355301, 2008.
- [Skr12] Y. Skrynnikov. Solving initial value problem by matching asymptotic expansions. *SIAM J. Appl. Math.*, 72(1):405–416, 2012.
- [SL91] C.G. Steinmetz and R. Larter. The quasiperiodic route to chaos in a model of the peroxidase-oxidase reaction. *J. Phys. Chem.*, 94(2):1388–1396, 1991.
- [SL13] A. Turi Savadkoohi and C.-H. Lamarque. Dynamics of coupled Dahl-type and nonsmooth systems at different scales of time. *Int. J. Bif. Chaos*, 23(7):1350114, 2013.
- [SLdL08] M. Storaie, D. Linaro, and E. de Lange. The Hindmarsh–Rose neuron model: bifurcation analysis and piecewise-linear approximations. *Chaos*, 18:033128, 2008.
- [SLW99] A.L. Sanchez, A. Linan, and F.A. Williams. Chain-branching explosions in mixing layers. *SIAM J. Appl. Math.*, 59(4):1335–1355, 1999.
- [SM96] P.E. Strizhak and M. Menzinger. Slow passage through a supercritical Hopf bifurcation: time-delayed response in the Belousov–Zhabotinsky reaction in a batch reactor. *J. Chem. Phys.*, 105:10905–10910, 1996.
- [SM01] S. Schechter and D. Marchesin. Geometric singular perturbation analysis of oxidation heat pulses for two-phase flow in porous media. *Bull. Braz. Math. Soc.*, 32(3):237–270, 2001.
- [SM03] E. Süli and D. Mayers. *An Introduction to Numerical Analysis*. CUP, 2003.
- [SM08] I. Siekmann and H. Malchow. Local collapses in the Truscott–Brindley model. *Math. Model. Nat. Phenom.*, 3(4):114–130, 2008.

- [SM11] T. Schäfer and R.O. Moore. A path integral method for coarse-graining noise in stochastic differential equations with multiple time scales. *Physica D*, 240:89–97, 2011.
- [SM13] D. Soudry and R. Meir. The neuron’s response at extended timescales. *arXiv:1301.2631*, pages 1–5, 2013.
- [Sma63] S. Smale. Diffeomorphisms with many periodic points. In S.S. Cairns, editor, *Differential and Combinatorial Topology*, pages 63–80. Princeton University Press, 1963.
- [Sma67] S. Smale. Differentiable dynamical systems. *Bull. Amer. Math. Soc.*, 289:747–817, 1967.
- [Sma00a] S. Smale. Finding a horseshoe on the beaches of Rio. *Math. Intelligencer*, 20:39–44, 2000.
- [Sma00b] S. Smale. Finding a horseshoe on the beaches of Rio. In R. Abraham and Y. Ueda, editors, *The Chaos-Avant-Garde*, pages 7–22. World Scientific, 2000.
- [Sma00c] S. Smale. On how I got started in Dynamical Systems 1959–1962. In R. Abraham and Y. Ueda, editors, *The Chaos-Avant-Garde*, pages 1–6. World Scientific, 2000.
- [Smi75] D.R. Smith. The multivariable method in singular perturbation analysis. *SIAM Rev.*, 17(2):221–273, 1975.
- [Smi85] D.R. Smith. *Singular-Perturbation Theory: An Introduction with Applications*. CUP, 1985.
- [Smi02] G.V. Smirnov. *Introduction to the Theory of Differential Inclusions*. AMS, 2002.
- [Smo94] J. Smoller. *Shock Waves and Reaction-Diffusion Equations*. Springer, 1994.
- [SMSG07] M. Sieber, H. Malchow, and L. Schimansky-Geier. Constructive effects of environmental noise in an excitable prey–predator plankton system with infected prey. *Ecol. Complex.*, 4(4):223–233, 2007.
- [SN03] A. Shilnikov and F.R. Nikolai. Origin of chaos in a two-dimensional map modeling spiking-bursting neural activity. *Int. J. Bif. Chaos*, 13(11):3325–3340, 2003.
- [SN13] D.L. Stein and C.M. Newman. Rugged landscapes and timescale distributions in complex systems. In *Emergence, Complexity, and Computation*. Springer, 2013. to appear.
- [SNBEB78] K. Showalter, R.M. Noyes, and K. Bar-Eli. A modified Oregonator model exhibiting complicated limit cycle behaviour in a flow system. *J. Chem. Phys.*, 69:2514–2524, 1978.
- [SO81] S. Schmidt and P. Ortoleva. Electric field effects on propagating BZ waves: predictions of an Oregonator and new pulse supporting models. *J. Chem. Phys.*, 74:4488–4500, 1981.
- [SO87] P.M. Sharkey and J. O’Reilly. Exact design manifold control of a class of nonlinear singularly perturbed systems. *IEEE Trans. Aut. Contr.*, 32(10):933–935, 1987.
- [SO88] P.M. Sharkey and J. O’Reilly. Composite control of non-linear singularly perturbed systems: a geometric approach. *Int. J. Contr.*, 48(6):2491–2506, 1988.
- [SO97a] A. Stevens and H.G. Othmer. Aggregation, blowup, and collapse: The ABC’s of taxis in reinforced random walks. *SIAM J. Appl. Math.*, 57(4):1044–1081, 1997.
- [SO97b] M. Stynes and E. O’Riordan. A uniformly convergent Galerkin method on a Shishkin mesh for a convection–diffusion problem. *J. Math. Anal. Appl.*, 214(1):36–54, 1997.
- [SOAM93] A.A. Sharp, M.B. O’Neil, L.F. Abbott, and E. Marder. Dynamic clamp: computer-generated conductances in real neurons. *J. Neurophysiol.*, 69(3):992–995, 1993.
- [Sob13] V. Sobolev. Canard cascades. *Discr. Cont. Dyn. Syst.*, 18(2):513–521, 2013.
- [SOK84] V.R. Saksena, J. O’Reilly, and P.V. Kokotovic. Singular perturbations and time-scale methods in control theory: survey 1976–1983. *Automatica*, 20(3):273–293, 1984.
- [SOLS08] J.V. Stern, H.M. Osinga, A. LeBeau, and A. Sherman. Resetting behavior in a model of bursting in secretory pituitary cells: distinguishing plateaus from pseudo-plateaus. *Bull. Math. Biol.*, 70(1):68–88, 2008.
- [Son93] H.M. Soner. Singular perturbations in manufacturing. *SIAM J. Contr. Optim.*, 31:132–146, 1993.
- [Son98] E.D. Sontag. *Mathematical Control Theory*. Springer, 2nd edition, 1998.
- [Son04] E.D. Sontag. Some new directions in control theory inspired by systems biology. *Syst. Biol.*, 1(1):9–18, 2004.
- [Sou13] M. Souza. Multiscale analysis for a vector-borne epidemic model. *J. Math. Biol.*, pages 1–14, 2013. accepted, to appear.
- [SOW+97] A. Scheeline, D.L. Olson, E.P. Williksen, G.A. Horras, M.L. Klein, and R. Larter. The peroxidase-oxidase oscillator and its constituent chemistries. *Chem. Rev.*, 97:739–756, 1997.
- [Sow01] R.B. Sowers. On the tangent flow of a stochastic differential equation with fast drift. *Trans. Amer. Math. Soc.*, 353(4):1321–1334, 2001.
- [Sow02] R.B. Sowers. Stochastic averaging with a flattened Hamiltonian: a Markov process on a stratified space (a whiskered sphere). *Trans. Amer. Math. Soc.*, 354(3):853–900, 2002.
- [Sow08] R.B. Sowers. Random perturbations of canards. *J. Theor. Probab.*, 21:824–889, 2008.
- [SP96] P. Soravia and E. Panagiotis. Phase-field theory for FitzHugh–Nagumo-type systems. *SIAM J. Math. Anal.*, 27(5):1341–1359, 1996.
- [SP10] I. Shlykova and A. Ponosov. Singular perturbation analysis and gene regulatory networks with delay. *Nonlinear Analysis*, 72:3786–3812, 2010.
- [Spa66] E.H. Spanier. *Algebraic Topology*. McGraw-Hill, 1966.
- [Spa82] C. Sparrow. *The Lorenz Equations: Bifurcations, Chaos, and Strange Attractors*. Springer, 1982.
- [SPC92] B. Siciliano, J.V.R. Prasad, and A.J. Calise. Output feedback two-time scale control of multilink flexible arms. *J. Dyn. Syst. Measur. Contr.*, 114:70–77, 1992.
- [Spi99] M. Spivak. *A Comprehensive Introduction to Differential Geometry*. Publish or Perish, 1999. Volumes 1–5.
- [Spi06] M. Spivak. *Calculus*. CUP, 2006.
- [Spi13a] K. Spiliopoulos. Fluctuation analysis and short time asymptotics for multiple scales diffusion processes. *arXiv:1306.1499v1*, pages 1–18, 2013.
- [Spi13b] K. Spiliopoulos. Large deviations and importance sampling for systems of slow–fast motion. *Appl. Math. Optim.*, 67(1):123–161, 2013.
- [SPKP13] M. Schmuck, M. Pradas, S. Kalliadasis, and G.A. Pavliotis. A new stochastic mode reduction strategy for dissipative systems. *arXiv:1305.4135v1*, pages 1–5, 2013.
- [SPM04] S. Schechter, B.J. Plohr, and D. Marchesin. Computation of Riemann solutions using the Dafermos regularization and continuation. *Discr. Cont. Dyn. Syst.*, 10:965–986, 2004.
- [SPT05] A. Samoilenko, M. Pinto and S. Trofimchuk. Krylov-Bogolyubov averaging of asymptotically autonomous differential equations. *Proc. Amer. Math. Soc.*, 133:145–154, 2005.

- [Spo00a] H. Spohn. The critical manifold of the Lorentz-Dirac equation. *Europhys. Lett.*, 50(3):287, 2000.
- [Spo00b] B. Sportisse. An analysis of operator splitting techniques in the stiff case. *J. Comput. Phys.*, 161(1):140–168, 2000.
- [SR73] P. Sannuti and P. Reddy. Asymptotic series solution of optimal systems with small time delay. *IEEE Trans. Aut. Contr.*, 18(3):250–259, 1973.
- [SR82] D.W. Storti and R.H. Rand. Dynamics of two strongly coupled van der Pol oscillators. *Int. J. Non-Linear Mech.*, 17(3):143–152, 1982.
- [SR86] D.W. Storti and R.H. Rand. Dynamics of two strongly coupled relaxation oscillators. *SIAM J. Appl. Math.*, 46(1):56–67, 1986.
- [SR88] H. Sira-Ramirez. Sliding regimes on slow manifolds of systems with fast actuators. *Internat. J. Systems Sci.*, 19(6):875–887, 1988.
- [SR91] A. Sherman and J. Rinzel. Model for synchronization of pancreatic beta-cells by gap junction coupling. *Biophys. J.*, 59(3):547–559, 1991.
- [SR93] C.L. Stokes and J. Rinzel. Diffusion of extracellular K⁺ can synchronize bursting oscillations in a model islet of Langerhans. *Biophys. J.*, 65(2):597–602, 1993.
- [SR97a] L.F. Shampine and M.W. Reichelt. The MatLab ODE suite. *SIAM J. Sci. Comput.*, 18(1):1–22, 1997.
- [SR97b] M. Stynes and H.-G. Roos. The midpoint upwind scheme. *Appl. Numer. Math.*, 23(3):361–374, 1997.
- [SR03] A. Shilnikov and N.F. Rulkov. Origin of chaos in a two-dimensional map modeling spiking-bursting neural activity. *Int. J. Bif. Chaos*, 13(11):3325–3340, 2003.
- [SR04] A. Shilnikov and N.F. Rulkov. Subthreshold oscillations in a map-based neuron model. *Phys. Lett. A*, 328(2):177–184, 2004.
- [SRK88] A. Sherman, J. Rinzel, and J. Keizer. Emergence of organized bursting in clusters of pancreatic beta-cells by channel sharing. *Biophys. J.*, 54(3):411–425, 1988.
- [SRK05] G. Samaey, D. Roose, and I.G. Kevrekidis. The gap-tooth scheme for homogenization problems. *Multiscale Model. Simul.*, 4(1):278–306, 2005.
- [SRS93] P. Smolen, J. Rinzel, and A. Sherman. Why pancreatic islets burst but single beta cells do not. The heterogeneity hypothesis. *Biophys. J.*, 64(6):1668–1680, 1993.
- [SRT04] J. Su, J. Rubin, and D. Terman. Effects of noise on elliptic bursters. *Nonlinearity*, 17:133–157, 2004.
- [SRV95] M.N. Stolyarov, V.A. Romanov, and E.I. Volkov. Out-of-phase mixed-mode oscillations of two strongly coupled identical relaxation oscillators. *Phys. Rev. E*, 54(1):163–169, 1995.
- [SS83] G.P. Syrmos and P. Sannuti. Singular perturbation modelling of continuous and discrete physical systems. *Int. J. Contr.*, 37(5):1007–1022, 1983.
- [SS87] A. Saberi and P. Sannuti. Cheap and singular controls for linear quadratic regulators. *IEEE Trans. Aut. Contr.*, 32(3):208–219, 1987.
- [SS89] L.A. Segel and M. Slemrod. The quasi-steady-state assumption: a case study in perturbation. *SIAM Rev.*, 31(3):446–477, 1989.
- [SS95] G. Sun and M. Stynes. Finite-element methods for singularly perturbed high-order elliptic two-point boundary value problems. I: reaction-diffusion-type problems. *IMA J. Numer. Anal.*, 15:117–139, 1995.
- [SS01] E. Shchepakina and V. Sobolev. Integral manifolds, canards and black swans. *Nont. Anal. Theor. Meth. Appl.*, 44(7):897–908, 2001.
- [SS04a] B. Sandstede and A. Scheel. Evans function and blow-up methods in critical eigenvalue problems. *Discr. Cont. Dyn. Syst.*, 10:941–964, 2004.
- [SS04b] S. Schecter and P. Szmolyan. Composite waves in the Dafermos regularization. *J. Dyn. Diff. Eq.*, 16(3):847–867, 2004.
- [SS04c] B.K. Spears and A.J. Szeri. Topology and resonances in a quasiperiodically forced oscillator. *Physica D*, 197(1):69–85, 2004.
- [SS05a] B. Sandstede and A. Scheel. Absolute instabilities of standing pulses. *Nonlinearity*, 18:331–378, 2005.
- [SS05b] E. Shchepakina and V. Sobolev. Black swans and canards in laser and combustion models. In *Singular Perturbations and Hysteresis*, pages 207–256. SIAM, 2005.
- [SS08a] J.M. Sanz-Serna. Mollified impulse methods for highly oscillatory differential equations. *SIAM J. Numer. Anal.*, 46(2):1040–1059, 2008.
- [SS08b] B. Schmalfuss and K.R. Schneider. Invariant manifolds for random dynamical systems with slow and fast variables. *J. Dyn. Diff. Eq.*, 20(1):133–164, 2008.
- [SS08c] L.B. Shaw and I.B. Schwartz. Fluctuating epidemics on adaptive networks. *Phys. Rev. E*, 77:(066101), 2008.
- [SS09] S. Schecter and P. Szmolyan. Persistence of rarefactions under Dafermos regularization: blow-up and an exchange lemma for gain-of-stability turning points. *SIAM J. Applied Dynamical Systems*, 8(3):822–853, 2009.
- [SS10] S. Schecter and C. Sourdis. Heteroclinic orbits in slow–fast Hamiltonian systems with slow manifold bifurcations. *J. Dyn. Diff. Equat.*, 22:629–655, 2010.
- [SS11a] A.M. Samoilenko and O. Stanzhytskyi. *Qualitative and Asymptotic Analysis of Differential Equations with Random Perturbations*. World Scientific, 2011.
- [SS11b] M. Sarich and C. Schütte. Approximating selected non-dominant timescales by Markov state models. *Comm. Math. Sci.*, 10(3):1001–1013, 2011.
- [SS13a] R.I. Saye and J.A. Sethian. Multiscale modeling of membrane rearrangement, drainage, and rupture in evolving foams. *Science*, 340:720–724, 2013.
- [SS13b] R. Singh and S. Sinha. Spatiotemporal order, disorder, and propagating defects in homogeneous system of relaxation oscillators. *Phys. Rev. E*, 87:012907, 2013.
- [SSB⁺87] W. Scharpf, M. Squicciarini, D. Bromley, C. Green, J.R. Tredicce, and L.M. Narducci. Experimental observation of a delayed bifurcation at the threshold of an argon laser. *Optics Commun.*, 63(5):344–348, 1987.
- [SSH06a] A. Singer, Z. Schuss, and D. Holzman. Narrow escape, part II: The circular disk. *J. Stat. Phys.*, 122(3):465–489, 2006.
- [SSH06b] A. Singer, Z. Schuss, and D. Holzman. Narrow escape, part III: Non-smooth domains and Riemann surfaces. *J. Stat. Phys.*, 122(3):491–509, 2006.

- [SSH07] Z. Schuss, A. Singer, and D. Holcman. The narrow escape problem for diffusion in cellular microdomains. *Proc. Natl. Acad. Sci. USA*, 104(41):16098–16103, 2007.
- [SSH08] A. Singer, Z. Schuss, and D. Holcman. Narrow escape and leakage of brownian particles. *Phys. Rev. E*, 78(5):051111, 2008.
- [SSHE06] A. Singer, Z. Schuss, D. Holcman, and R.S. Eisenberg. Narrow escape, part I. *J. Stat. Phys.*, 122(3):437–463, 2006.
- [SSI⁺11] M. Sekikawa, K. Shimizu, N. Inaba, H. Kita, T. Endo, K. Fujimoto, T. Yoshinaga, and K. Aihara. Sudden change from chaos to oscillation death in the Bonhoeffer–van der Pol oscillator under weak periodic perturbation. *Phys. Rev. E*, 84:056209, 2011.
- [SSL⁺09] I. Surovtsova, N. Simus, T. Lorenz, A. König, S. Sahle, and U. Kummer. Accessible methods for the dynamic time-scale decomposition of biochemical systems. *Bioinformatics*, 25(21):2816–2823, 2009.
- [SSP95] E. Sivan, L. Segel, and H. Parnas. Modulated excitability: a new way to obtain bursting neurons. *Biol. Cybernet.*, 72(5):455–461, 1995.
- [SSS03] K.R. Schneider, E.A. Shchepakina, and V.A. Sobolev. New type of travelling wave solutions. *Math. Meth. Appl. Sci.*, 26(16):1349–1361, 2003.
- [SSSI12] K. Shimizu, Y. Saito, M. Sekikawa, and N. Inaba. Complex mixed-mode oscillations in a Bonhoeffer–van der Pol oscillator under weak periodic perturbation. *Physica D*, 241:1518–1526, 2012.
- [SST05] A. Shilnikov, L. Shilnikov, and D. Turaev. Blue-sky catastrophe in singularly perturbed systems. *Moscow Math. Journal*, 5(1):269–282, 2005.
- [SSV06] L.F. Shampine, B.P. Sommeijer, and J.G. Verwer. IRKC: an IMEX solver for stiff diffusion-reaction PDEs. *J. Comput. Appl. Math.*, 196(2):485–497, 2006.
- [ST96] J. Sotomayor and M.A. Teixeira. Regularization of discontinuous vector fields. In *International Conference on Differential Equations (Lisboa)*, pages 207–223. World Scientific, 1996.
- [ST97] H. Suzuki and O. Toshiyuki. On the spectra of pulses in a nearly integrable system. *SIAM J. Appl. Math.*, 57(2):485–500, 1997.
- [ST01] C. Soto-Trevino. A geometric method for periodic orbits in singularly-perturbed systems. In C.K.R.T. Jones, editor, *Multiple Time Scale Dynamical Systems*, volume 122 of *The IMA Volumes in Mathematics and its Applications*, pages 141–202. Springer, 2001.
- [ST03] M. Stynes and L. Tobiska. The SDFEM for a convection-diffusion problem with a boundary layer: optimal error analysis and enhancement of accuracy. *SIAM J. Numer. Anal.*, 41(5):1620–1642, 2003.
- [Ste73] G.W. Stewart. *Introduction to Matrix Computations*. Academic Press, 1973.
- [Ste04] D.L. Stein. Critical behavior of the Kramers escape rate in asymmetric classical field theories. *J. Stat. Phys.*, 114(5):1537–1556, 2004.
- [STE05] R. Sharp, Y.-H. Tsai, and B. Engquist. Multiple time scale numerical methods for the inverted pendulum problem. In *Multiscale Methods in Science and Engineering*, pages 241–261. Springer, 2005.
- [Ste07] M. Steinhauser. *Computational Multiscale Modeling of Fluids and Solids: Theory and Applications*. Springer, 2007.
- [Sti98a] M. Stiefenhofer. Quasi-steady-state approximation for chemical reaction networks. *J. Math. Biol.*, 36(6):593–609, 1998.
- [Sti98b] M. Stiefenhofer. Singular perturbation with Hopf points in the fast dynamics. *Z. Angew. Math. Phys.*, 49(4):602–629, 1998.
- [Sti98c] M. Stiefenhofer. Singular perturbation with limit points in the fast dynamics. *Z. Angew. Math. Phys.*, 49(5):730–758, 1998.
- [STK96] C. Soto-Trevino and T.J. Kaper. Higher-order Melnikov theory for adiabatic systems. *J. Math. Phys.*, 37:6220–6250, 1996.
- [STKW96] C. Soto-Trevino, N. Kopell, and D. Watson. Parabolic bursting revisited. *J. Math. Biol.*, 35(1):114–128, 1996.
- [Sto49] H. Stommel. Trajectories of small bodies sinking slowly through convection cells. *J. Mar. Res.*, 8:24–29, 1949.
- [Sto61] H. Stommel. Thermohaline convection with two stable regimes of flow. *Tellus*, 13:224–230, 1961.
- [STR93] P. Smolen, D. Terman, and J. Rinzel. Properties of a bursting model with two slow inhibitory variables. *SIAM J. Appl. Math.*, 53(3):861–892, 1993.
- [Str00] S.H. Strogatz. *Nonlinear Dynamics and Chaos*. Westview Press, 2000.
- [Str01] S.H. Strogatz. Exploring complex networks. *Nature*, 410:268–276, 2001.
- [Str08] W.A. Strauss. *Partial Differential Equations: An Introduction*. John Wiley & Sons, 2008.
- [Str09] G. Strang. *Introduction to Linear Algebra*. Wellesley-Cambridge Press, 2009.
- [Sty05] M. Stynes. Steady-state convection-diffusion problems. *Acta Numerica*, 14:445–508, 2005.
- [Su93] J. Su. Delayed oscillation phenomena in the FitzHugh–Nagumo equation. *J. Differential Equat.*, 105(1):180–215, 1993.
- [Su96a] J. Su. Delayed bifurcation properties in the FitzHugh–Nagumo equation with periodic forcing. *Differen. Integral Equat.*, 9(3):527–539, 1996.
- [Su96b] J. Su. Persistent unstable periodic motions, I. *J. Math. Anal. Appl.*, 198(3):796–825, 1996.
- [Su97] J. Su. Effects of periodic forcing on delayed bifurcations. *J. Dyn. Differen. Equat.*, 9(4):561–625, 1997.
- [Su01] J. Su. The phenomenon of delayed bifurcation and its analysis. In C.K.R.T. Jones, editor, *Multiple Time Scale Dynamical Systems*, volume 122 of *The IMA Volumes in Mathematics and its Applications*, pages 203–214. Springer, 2001.
- [Su12] T. Su. On the accuracy of conservation of adiabatic invariants in slow–fast Hamiltonian systems. *Reg. Chaotic Dyn.*, 17(1):54–62, 2012.
- [Sub96] N.N. Subbotina. Asymptotic properties of minimax solutions of Isaacs–Bellman equations in differential games with fast and slow motions. *J. Appl. Math. Mech.*, 60(6):883–890, 1996.
- [Sug95] M. Suguri. Metastable behaviors of diffusion processes with small parameter. *J. Math. Soc. Japan*, 47(4):755–788, 1995.
- [Suz81] M. Suzuki. Composite controls for singularly perturbed systems. *IEEE Trans. Aut. Contr.*, 26(2):505–507, 1981.
- [SV96] R. Spigler and M. Vianello. WKB-type approximations for second-order differential equations in C^* -algebras. *Proc. Amer. Math. Soc.*, 124(6):1763–1771, 1996.

- [SVM07] J.A. Sanders, F. Verhulst, and J. Murdock. *Averaging Methods in Nonlinear Dynamical Systems*. Springer, 2007.
- [SW79] T. Steihaug and A. Wolfbrandt. An attempt to avoid exact Jacobian and nonlinear equations in the numerical solution of stiff differential equations. *Math. Comput.*, 33:521–534, 1979.
- [SW83] P. Sannuti and H. Wason. A singular perturbation canonical form of invertible systems: determination of multivariate root-loci. *Int. J. Contr.*, 37(6):1259–1286, 1983.
- [SW85] P. Sannuti and H. Wason. Multiple time-scale decomposition in cheap control problems - singular control. *IEEE Trans. Aut. Contr.*, 30(7):633–644, 1985.
- [SW86] C. Schmeiser and R. Weiss. Asymptotic analysis of singular singularly perturbed boundary value problems. *SIAM J. Math. Anal.*, 17(3):560–579, 1986.
- [SW00a] K.R. Schneider and T. Wilhelm. Model reduction by extended quasi-steady-state approximation. *J. Math. Biol.*, 40(5):443–450, 2000.
- [SW00b] P.R. Shorten and D.J. Wall. A Hodgkin–Huxley model exhibiting bursting oscillations. *Bull. Math. Biol.*, 62(4):695–715, 2000.
- [SW00c] X. Sun and M.J. Ward. Dynamics and coarsening of interfaces for the viscous Cahn–Hilliard equation in one spatial dimension. *Stud. Appl. Math.*, 105(3):203–234, 2000.
- [SW01] P. Szmolyan and M. Wechselberger. Canards in \mathbb{R}^3 . *J. Differential Equat.*, 177:419–453, 2001.
- [SW04] P. Szmolyan and M. Wechselberger. Relaxation oscillations in \mathbb{R}^3 . *J. Differential Equat.*, 200:69–104, 2004.
- [Swa83] R. Swanson. The spectral characterization of normal hyperbolicity. *Proc. Amer. Math. Soc.*, 89(3):503–509, 1983.
- [SWC89] K. Strehmel, R. Weiner, and H. Claus. Stability analysis of linearly implicit one-step interpolation methods for stiff retarded differential equations. *SIAM J. Numer. Anal.*, 26(5):1158–1174, 1989.
- [SWHH04] C. Schütte, J. Walter, C. Hartmann, and W. Huisenga. An averaging principle for fast degrees of freedom exhibiting long-term correlations. *Multiscale Model. Simul.*, 2(3):501–526, 2004.
- [SWR05] X. Sun, M.J. Ward, and R. Russell. The slow dynamics of two-spike solutions for the Gray–Scott and Gierer–Meinhardt systems: competition and oscillatory instabilities. *SIAM J. Appl. Dyn. Syst.*, 4(4):904–953, 2005.
- [SWW05] B.D. Sleeman, M.J. Ward, and J.C. Wei. The existence and stability of spike patterns in a chemotaxis model. *SIAM J. Appl. Math.*, 65(3):790–817, 2005.
- [SX12] S. Schechter and G. Xu. Morse theory for Lagrange multipliers and adiabatic limits. *arXiv:1211.3028v1*, pages 1–42, 2012.
- [SY04] T. Sari and K. Yadi. On Pontryagin–Rodygin’s theorem for convergence of solutions of slow and fast systems. *Electron. J. Differential Equat.*, 139:1–17, 2004.
- [SY10] F.J. Solis and C. Yebra. Modeling the pursuit in natural systems: a relaxed oscillation approach. *Math. Comput. Modelling*, 52(7):956–961, 2010.
- [SZ02] J. Shatah and C. Zeng. Periodic solutions for Hamiltonian systems under strong constraining forces. *J. Differential Equat.*, 186(2):572–585, 2002.
- [SZ04] H.L. Smith and X.-Q. Zhao. Traveling waves in a bio-reactor model. *Nonl. Anal. Real World Appl.*, 5(5):895–909, 2004.
- [SZB96] S.J. Stuart, R. Zhou, and B.J. Berne. Molecular dynamics with multiple time scales: the selection of efficient reference system propagators. *J. Chem. Phys.*, 105:1426–1436, 1996.
- [Szsm89a] P. Szmolyan. A singular perturbation analysis of the transient semiconductor-device equations. *SIAM J. Appl. Math.*, 49(4):1122–1135, 1989.
- [Szsm89b] P. Szmolyan. Traveling waves in GaAs semiconductors. *Physica D*, 39(2):393–404, 1989.
- [Szsm91] P. Szmolyan. Transversal heteroclinic and homoclinic orbits in singular perturbation problems. *J. Differential Equat.*, 92:252–281, 1991.
- [Szsm92] P. Szmolyan. Analysis of a singularly perturbed traveling-wave problem. *SIAM J. Appl. Math.*, 52(2):485–493, 1992.
- [Tak76] F. Takens. Constrained equations; a study of implicit differential equations and their discontinuous solutions. In P. Hilton, editor, *Structural Stability, the Theory of Catastrophes, and Applications in the Sciences*, volume 525 of *Lecture Notes in Mathematics*, pages 143–234. Springer, 1976.
- [TaI99] P. Tulkner. Stochastic resonance in the semidiabatic limit. *New J. Phys.*, 1(1):4, 1999.
- [TAORS10] K.T. Tsaneva-Atanasova, H.M. Osinga, T. Riess, and A. Sherman. Full system bifurcation analysis of endocrine bursting models. *J. Theor. Biol.*, 264(4):1133–1146, 2010.
- [Tar09] L. Tartar. *The General Theory of Homogenization - A Personal Introduction*. Springer, 2009.
- [TAWJ08] D. Terman, S. Ahn, X. Wang, and W. Just. Reducing neuronal networks to discrete dynamics. *Physica D*, 237(3):324–338, 2008.
- [TAZBS06] K.T. Tsaneva-Atanasova, C.L. Zimliki, R. Bertram, and A. Sherman. Diffusion of calcium and metabolites in pancreatic islets: killing oscillations with a pitchfork. *Biophys. J.*, 90(10):3434–3446, 2006.
- [TB91a] M. Tuckerman and B.J. Berne. Stochastic molecular dynamics in systems with multiple time scales and memory friction. *J. Chem. Phys.*, 95:4389, 1991.
- [TB91b] M. Tuckerman and B.J. Berne. Molecular dynamics in systems with multiple time scales: systems with stiff and soft degrees of freedom and with short and long range forces. *J. Chem. Phys.*, 95:8362, 1991.
- [TB11] N. Toporikova and R.J. Butera. Two types of independent bursting mechanisms in inspiratory neurons: an integrative model. *J. Comput. Neurosci.*, 30(3):515–528, 2011.
- [TBM91] M. Tuckerman, B.J. Berne, and G.J. Martyna. Molecular dynamics algorithm for multiple time scales: systems with long range forces. *J. Chem. Phys.*, 94:6811, 1991.
- [TBM94] M. Tuckerman, B.J. Berne, and G.J. Martyna. Reversible multiple time scale molecular dynamics. *J. Chem. Phys.*, 97(3):1990–2001, 1994.
- [TBR91] M. Tuckerman, B.J. Berne, and A. Rossi. Molecular dynamics algorithm for multiple time scales: systems with disparate masses. *J. Chem. Phys.*, 94:1465, 1991.
- [TCE86] J.L. Tennyson, J.R. Cary, and D.F. Escande. Change of the adiabatic invariant due to separatrix crossing. *Phys. Rev. Lett.*, 56(20):2117–2120, 1986.

- [TCN03] J.J. Tyson, K.C. Chen, and B. Novak. Sniffers, buzzers, toggles and blinks: dynamics of regulatory and signaling pathways in the cell. *Current Opinion in Cell Biology*, 15:221–231, 2003.
- [TdC11] D.J. Tonon and T. de Carvalho. Generic bifurcations of planar Filippov systems via geometric singular perturbations. *Bull. Belg. Math. Soc.*, 18(5):861–881, 2011.
- [TdS12] M.A. Teixeira and P.R. da Silva. Regularization and singular perturbation techniques for non-smooth systems. *Physica D*, 241(22):1948–1955, 2012.
- [Tem90] R. Temam. Inertial manifolds and multigrid methods. *SIAM J. Math. Anal.*, 21(1):154–178, 1990.
- [Tem97] R. Temam. *Infinite-Dimensional Dynamical Systems in Mechanics and Physics*. Springer, 1997.
- [Ter91] D. Terman. Chaotic spikes arising from a model of bursting in excitable membranes. *SIAM J. Appl. Math.*, 51(5):1418–1450, 1991.
- [Ter92] D. Terman. The transition from bursting to continuous spiking in excitable membrane models. *J. Nonlinear Sci.*, 2(2):135–182, 1992.
- [Tes12] G. Teschl. *Ordinary Differential Equations and Dynamical Systems*. AMS, 2012.
- [TGO8] J.H. Tien and J. Guckenheimer. Parameter estimation for bursting neural model. *J. Comput. Neurosci.*, 24:358–373, 2008.
- [TG09] M. Thomson and J. Gunawardena. Unlimited multistability in multisite phosphorylation systems. *Nature*, 460:274–277, 2009.
- [TGS12] P. Thomas, R. Grima, and A.V. Straube. Rigorous elimination of fast stochastic variables from the linear noise approximation using projection operators. *Phys. Rev. E*, 86:041110, 2012.
- [TGT95] D.N.C. Tse, R.G. Gallager, and J.N. Tsitsiklis. Statistical multiplexing of multiple time-scale Markov streams. *IEEE J. Selected Areas in Comm.*, 13(6):1028–1038, 1995.
- [Tia03] H. Tian. Asymptotic expansion for the solution of singularly perturbed delay differential equations. *J. Math. Anal. Appl.*, 281(2):678–696, 2003.
- [Tik52] A.N. Tikhonov. Systems of differential equations containing small parameters in the derivatives. *Mat. Sbornik N. S.*, 31:575–586, 1952.
- [Tin94] S.-K. Tin. *On the dynamics of tangent spaces near normally hyperbolic manifolds and singularly perturbed boundary value problems*. PhD thesis - Brown University, 1994.
- [Tin95] S.-K. Tin. Transversality of double-pulse homoclinic orbits in the inviscid Lorenz-Krishnamurthy system. *Physica D*, 83(4):383–408, 1995.
- [TIO77] K. Tomita, A. Ito, and T. Ohta. Simplified model for Belousov-Zhabotinsky reaction. *J. Theor. Biol.*, 68(1):459–481, 1977.
- [TK88] J.J. Tyson and J.P. Keener. Singular perturbation theory of traveling waves in excitable media (a review). *Physica D*, 32(3):327–361, 1988.
- [TKD13] J. Touboul, M. Krupa, and M. Desroches. Noise-induced canard and mixed-mode oscillations in large stochastic networks with multiple timescales. *arXiv:1302.7159v1*, pages 1–22, 2013.
- [TKJ94] S.-K. Tin, N. Kopell, and C.K.R.T. Jones. Invariant manifolds and singularly perturbed boundary value problems. *SIAM J. Numer. Anal.*, 31(6):1558–1576, 1994.
- [TL97] D. Terman and E. Lee. Partial synchronization in a network of neural oscillators. *SIAM J. Appl. Math.*, 57(1):252–293, 1997.
- [TL13] S. Tang and J. Liang. Global qualitative analysis of a non-smooth Gause predator-prey model with a refuge. *Nonlinear Anal.*, 76:165–180, 2013.
- [TLRB11] D. Terman, E. Lee, J. Rinzel, and T. Bem. Stability of anti-phase and in-phase locking by electrical coupling but not fast inhibition alone. *SIAM J. Appl. Dyn. Syst.*, 10(3):1127–1153, 2011.
- [TM88] M.C. Torrent and M. San Miguel. Stochastic-dynamics characterization of delayed laser threshold instability with swept control parameter. *Phys. Rev. A*, 38(1):245–251, 1988.
- [TMB90] M. Tuckerman, G.J. Martyna, and B.J. Berne. Molecular dynamics algorithm for condensed systems with multiple time scales. *J. Chem. Phys.*, 93:1287, 1990.
- [TMN03] A.R. Teel, L. Moreau, and D. Nesić. A unified framework for input-to-state stability in systems with two time scales. *IEEE Trans. Aut. Contr.*, 48(9):1526–1544, 2003.
- [TN94] M. Taniguchi and Y. Nishiura. Instability of planar interfaces in reaction-diffusion systems. *SIAM J. Math. Anal.*, 25(1):99–134, 1994.
- [TOM10] M. Tao, H. Owhadi, and J.E. Marsden. Nonintrusive and structure preserving multiscale integration of stiff ODEs, SDEs, and Hamiltonian systems with hidden slow dynamics via flow averaging. *Multiscale Model. Simul.*, 8(4):1269–1324, 2010.
- [TOM11] M. Tao, H. Owhadi, and J.E. Marsden. From efficient symplectic exponentiation of matrices to symplectic integration of high-dimensional Hamiltonian systems with slowly varying quadratic stiff potentials. *Appl. Math. Res. Express*, 2:242–280, 2011.
- [TOP96] E.B. Tadmor, M. Ortiz, and R. Phillips. Quasicontinuum analysis of defects in solids. *Phil. Mag.*, 73(6):1529–1563, 1996.
- [TP94a] M.E. Tuckerman and M. Parrinello. Integrating the Car-Parrinello equations. I. Basic integration techniques. *J. Chem. Phys.*, 101:1302–1315, 1994.
- [TP94b] M.E. Tuckerman and M. Parrinello. Integrating the Car-Parrinello equations. II. Multiple time scale techniques. *J. Chem. Phys.*, 101:1316–1329, 1994.
- [TQK00] C. Theodoropoulos, Y.H. Qian, and I.G. Kevrekidis. “Coarse” stability and bifurcation analysis using time-steppers: a reaction-diffusion example. *Proc. Natl. Acad. Sci.*, 97(18):9840–9843, 2000.
- [TR98] H.C. Tuckwell and R. Rodriguez. Analytical and simulation results for stochastic Fitzhugh-Nagumo neurons and neural networks. *J. Comput. Neurosci.*, 5(1):91–113, 1998.
- [Tra94] P. Tracqui. Mixed-mode oscillation genealogy in a compartmental model of bone mineral metabolism. *J. Nonlinear Science*, 4:69–103, 1994.
- [Tre96] D. Treschev. An averaging method for Hamiltonian systems, exponentially close to integrable ones. *J. Nonlinear Sci.*, 6(1):6–14, 1996.
- [Tre97] D. Treschev. The method of continuous averaging in the problem of separation of fast and slow motions. *Reg. Chaotic Dyn.*, 2(3):9–20, 1997.
- [Tre04] D. Treschev. Evolution of slow variables in a priori unstable Hamiltonian systems. *Nonlinearity*, 17(5):1803, 2004.

- [Tre07] V.A. Trenogin. The development and applications of the asymptotic method of Lyusternik and Vishik. *Russ. Math. Surv.*, 25(4):119, 2007.
- [Tro76] W.C. Troy. Bifurcation phenomena in FitzHugh's nerve conduction equations. *J. Math. Anal. Appl.*, 54(3):678–690, 1976.
- [Tro78] W.C. Troy. The bifurcation of periodic solutions in the Hodgkin–Huxley equations. *Quart. Appl. Math.*, 36:73–83, 1978.
- [Tro85] W.C. Troy. Mathematical analysis of the oregonator model of the Belousov–Zhabotinskii reaction. In R.J. Field and M. Burger, editors, *Oscillations and Traveling Waves in Chemical Systems*, pages 145–170. Wiley-Interscience, 1985.
- [TS77] D. Tenekezis and N. Sandell. Linear regulator design for stochastic systems by a multiple time-scales method. *IEEE Trans. Aut. Contr.*, 22(4):615–621, 1977.
- [TS95] H.C. Tseng and D.D. Siljak. A learning scheme for dynamic neural networks: equilibrium manifold and connective stability. *Neural Networks*, 8(6):853–864, 1995.
- [TS97] C.J. Tomlin and S.S. Sastry. Bounded tracking for non-minimum phase nonlinear systems with fast zero dynamics. *Int. J. Contr.*, 68(4):819–848, 1997.
- [TS10] J.M.T. Thompson and J. Sieber. Predicting climate tipping points. In B. Launder and M. Thompson, editors, *Geo-Engineering Climate Change: Environmental Necessity or Pandora's Box*, pages 50–83. CUP, 2010.
- [TS11a] J.M.T. Thompson and J. Sieber. Climate tipping as a noisy bifurcation: a predictive technique. *IMA J. Appl. Math.*, 76(1):27–46, 2011.
- [TS11b] J.M.T. Thompson and J. Sieber. Predicting climate tipping as a noisy bifurcation: a review. *Int. J. Bif. Chaos*, 21(2):399–423, 2011.
- [TS11c] J.-C. Tsai and J. Sneyd. Traveling waves in the buffered FitzHugh–Nagumo model. *SIAM J. Appl. Math.*, 71(5):1606–1636, 2011.
- [Tsa12] J.-C. Tsai. Do calcium buffers always slow down the propagation of calcium waves? *J. Math. Biol.*, pages 1–46, 2012. to appear.
- [TSG11] P. Thomas, A.V. Straube, and R. Grima. Limitations of the stochastic quasi-steady-state approximation in open biochemical reaction networks. *J. Chem. Phys.*, 135(18):181103, 2011.
- [TSO96] Y. Tang, J.L. Stephenson, and H.G. Othmer. Simplification and analysis of models of calcium dynamics based on IP3-sensitive calcium channel kinetics. *Biophys. J.*, 70:246–263, 1996.
- [TTB12] W. Teka, J. Tabak, and R. Bertram. The relationship between two fast/slow analysis techniques for bursting oscillations. *Chaos*, 22:043117, 2012.
- [TTFB07] J. Tabak, N. Toporikova, M.E. Freeman, and R. Bertram. Low dose of dopamine may stimulate prolactin secretion by increasing fast potassium currents. *J. Comput. Neurosci.*, 22:211–222, 2007.
- [TTV⁺11] W. Teka, J. Tabak, T. Vo, M. Wechselberger, and R. Bertram. The dynamics underlying pseudo-plateau bursting in a pituitary cell model. *J. Math. Neurosci.*, 1(12):1–23, 2011.
- [Tuc99] W. Tucker. The Lorenz attractor exists. *C.R. Acad. Sci. Paris*, 328:1197–1202, 1999.
- [Tur91] T. Turáňi. Rate sensitivity analysis of a model of the Briggs–Rauscher reaction. *React. Kinet. Lett.*, 45:235–241, 1991.
- [Tuw03] J.M. Tuwankotta. Widely separated frequencies in coupled oscillators with energy-preserving quadratic nonlinearity. *Physica D*, 182(1):125–149, 2003.
- [TW95] D. Terman and D.L. Wang. Global competition and local cooperation in a network of neural oscillators. *Physica D*, 81:148–176, 1995.
- [Tys81] J.J. Tyson. On scaling the oregonator equations. In C. Vidal and A. Pacault, editors, *Nonlinear Phenomena in Chemical Dynamics*, pages 222–227. Springer, 1981.
- [Tys84] J.J. Tyson. Relaxation oscillations in the revised Oregonator. *J. Chem. Phys.*, 80(12):6079–6082, 1984.
- [Tys85] J.J. Tyson. A quantitative account of oscillations, bistability, and traveling waves in the Belousov–Zhabotinskii reaction. In R.J. Field and M. Burger, editors, *Oscillations and Traveling Waves in Chemical Systems*, pages 93–144. Wiley-Interscience, 1985.
- [TZ11] B. Texier and K. Zumbrun. Nash–Moser iteration and singular perturbations. *Annales de l'Institut Henri Poincaré (C) Non Linear Analysis*, 28(4):499–527, 2011.
- [TZK12] J.-C. Tsai, W. Zhang, V. Kirk, and J. Sneyd. Traveling waves in a simplified model of calcium dynamics. *SIAM J. Appl. Dyn. Syst.*, 11(4):1149–1199, 2012.
- [ULFN04] N. Ulanovsky, L. Las, D. Farkas, and I. Nelken. Multiple time scales of adaptation in auditory cortex neurons. *J. Neurosci.*, 24(46):10440–10453, 2004.
- [Vak10] A.F. Vakakis. Relaxation oscillations, subharmonic orbits and chaos in the dynamics of a linear lattice with a local essentially nonlinear attachment. *Nonlinear Dyn.*, 61:443–463, 2010.
- [VAKA00] V. Vuković, S. Anić, and L. Kolar-Anić. Investigation of dynamic behaviour of the Bray–Liebhafsky reaction in the CSTR. Determination of bifurcation points. *J. Phys. Chem. A*, 104:10731–10739, 2000.
- [Van08] J. Vanneste. Asymptotics of a slow manifold. *SIAM J. Appl. Dyn. Sys.*, 7(4):1163–1190, 2008.
- [Var76] A.N. Varchenko. Newton polyhedra and estimation of oscillating integrals. *Functional Anal.*, 10(3):175–196, 1976.
- [Var84] S.R.S. Varadhan. *Large Deviations and Applications*. SIAM, 1984.
- [VAR07] J. Vigo-Aguilar and H. Ramos. A family of A-stable Runge–Kutta collocation methods of higher order for initial-value problems. *IMA J. Numer. Anal.*, 27(4):798–817, 2007.
- [Var08] S.R.S. Varadhan. Large deviations. *Ann. Probab.*, 36(2):397–419, 2008.
- [Vas63] A.B. Vasilieva. Asymptotic behaviour of solutions of certain problems for ordinary non-linear differential equations with a small parameter multiplying the highest derivatives. *Russian Math. Surveys*, 18:13–84, 1963.
- [Vas76] A.B. Vasilieva. The development of the theory of ordinary differential equations with a small parameter multiplying the highest derivative during the period 1966–1976. *Russian Math. Surveys*, 31(6):109–131, 1976.
- [Vas94] A.B. Vasilieva. On the development of singular perturbation theory at Moscow State University and elsewhere. *SIAM Rev.*, 36(3):440–452, 1994.
- [VB07] F. Verhulst and T. Bakri. The dynamics of slow manifolds. *J. Indones. Math. Soc.*, 13:73–90, 2007.
- [VBK95] A.B. Vasil'eva, V.F. Butuzov, and L.V. Kalachev. *The Boundary Function Method for Singular Perturbation Problems*. SIAM, 1995.

- [VBTW10] T. Vo, R. Bertram, J. Tabak, and M. Wechselberger. Mixed mode oscillations as a mechanism for pseudo-plateau bursting. *J. Comput. Neurosci.*, 28(3):443–458, 2010.
- [VBTW13] T. Vo, R. Bertram, J. Tabak, and M. Wechselberger. Multiple geometric viewpoints of mixed mode dynamics associated with pseudo-plateau bursting. *SIAM J. Appl. Dyn. Syst.*, 12(2):789–830, 2013.
- [VBTW12] T. Vo, R. Bertram, and M. Wechselberger. Bifurcations of canard-induced mixed mode oscillations in a pituitary Lactotroph model. *Discr. Cont. Dyn. Syst.*, 32(8):2879–2912, 2012.
- [VC93] A.F. Vakakis and C. Cetinkaya. Mode localization in a class of multidegree-of-freedom nonlinear systems with cyclic symmetry. *SIAM J. Appl. Math.*, 53(1):265–282, 1993.
- [VC01] M.I. Vishik and V.V. Chepyzhov. Averaging of trajectory attractors of evolution equations with rapidly oscillating terms. *Sbornik Math.*, 192(1):11, 2001.
- [VCDD06] N.P. Vora, M.-N. Contou-Carrere, and P. Daoutidis. Model reduction of multiple time scale processes in non-standard singularly perturbed form. In *Model Reduction and Coarse-Graining Approaches for Multiscale Phenomena*, pages 99–113. Springer, 2006.
- [VCG⁺06] M. Valorani, F. Creta, D.A. Goussis, J.C. Lee, and H.N. Najm. An automatic procedure for the simplification of chemical kinetic mechanisms based on CSP. *Combustion and Flame*, 146(1):29–51, 2006.
- [vD64] M. van Dyke. *Perturbation Methods in Fluid Mechanics*. Academic Press, 1964.
- [VD86] A.B. Vasilieva and M.G. Dmitriev. Singular perturbations in optimal control problems. *J. Math. Sci.*, 34(3):1579–1629, 1986.
- [VD13] F. Veerman and A. Doelman. Pulses in a Gierer–Meinhardt equation with a slow nonlinearity. *SIAM J. Appl. Dyn. Syst.*, 12(1):28–60, 2013.
- [vdB87] I. van den Berg. *Nonstandard Asymptotic Analysis*, volume 1249 of *Lecture Notes in Mathematics*. Springer, 1987.
- [vdB91] I.P. van den Berg. Macroscopic rivers. In E. Benoit, editor, *Dynamic Bifurcations*, volume 1493 of *Lecture Notes in Mathematics*, pages 190–209. Springer, 1991.
- [vdP20] B. van der Pol. A theory of the amplitude of free and forced triode vibrations. *Radio Review*, 1: 701–710, 1920.
- [vdP26] B. van der Pol. On relaxation oscillations. *Philosophical Magazine*, 7:978–992, 1926.
- [vdP34] B. van der Pol. The nonlinear theory of electric oscillations. *Proc. IRE*, 22:1051–1086, 1934.
- [vdPD05] H. van der Ploeg and A. Doelman. Stability of spatially periodic pulse patterns in a class of singularly perturbed reaction–diffusion equations. *Indiana Univ. Math. J.*, 54(5):1219–1301, 2005.
- [vdPvdM27] B. van der Pol and J. van der Mark. Frequency demultiplication. *Nature*, 120:363–364, 1927.
- [vdPvdM28] B. van der Pol and J. van der Mark. The heartbeat considered as a relaxation oscillation, and an electrical model of the heart. *Phil. Mag. Suppl.*, 6:763–775, 1928.
- [vdSDWE03] G. van der Sande, J. Danckaert, I. Wereてennicoff, and T. Erneux. Rate equations for vertical-cavity surface-emitting lasers. *Phys. Rev. A*, 67(1):013809, 2003.
- [VE03] E. Vanden-Eijnden. Numerical techniques for multiscale dynamical systems with stochastic effects. *Comm. Math. Sci.*, 1:385–391, 2003.
- [Vel97] V. Veliov. A generalization of the Tikhonov theorem for singularly perturbed differential inclusions. *J. Dyn. Control Sys.*, 3(3):291–319, 1997.
- [Ver76] J.G. Verwer. S-stability properties for generalized Runge–Kutta methods. *Numer. Math.*, 27(4): 359–370, 1976.
- [Ver94] R. Verfürth. A posteriori error estimation and adaptive mesh-refinement techniques. *J. Comput. Appl. Math.*, 50:67–83, 1994.
- [Ver96] R. Verfürth. *A Review of A Posteriori Error Estimation and Adaptive Mesh-Refinement Techniques*. Wiley-Teubner, 1996.
- [Ver05a] F. Verhulst. Invariant manifolds in dissipative dynamical systems. *Acta Appl. Math.*, 87(1):229–244, 2005.
- [Ver05b] F. Verhulst. *Methods and Applications of Singular Perturbations: Boundary Layers and Multiple Timescale Dynamics*. Springer, 2005.
- [Ver05c] F. Verhulst. Quenching of self-excited vibrations. *J. Eng. Mech.*, 53(3):349–358, 2005.
- [Ver06] F. Verhulst. *Nonlinear Differential Equations and Dynamical Systems*. Springer, 2006.
- [Ver07a] F. Verhulst. Periodic solutions and slow manifolds. *Int. J. Bif. Chaos*, 17(8):2533–2540, 2007.
- [Ver07b] F. Verhulst. Singular perturbation methods for slow–fast dynamics. *Nonlinear Dyn.*, 50:747–753, 2007.
- [Ver09] J.G. Verwer. Runge–Kutta methods and viscous wave equations. *Numer. Math.*, 112(3):485–507, 2009.
- [VF12] A. Vidal and J.-P. Francoise. Canard cycles in global dynamics. *Int. J. Bif. Chaos*, 22(2):1250026, 2012.
- [VFD⁺12] A.J. Veraart, E.J. Faassen, V. Dakos, E.H. van Nes, M. Lurding, and M. Scheffer. Recovery rates reflect distance to a tipping point in a living system. *Nature*, 481:357–359, 2012.
- [VGCN05] M. Valorani, D.A. Goussis, F. Creta, and H.N. Najm. Higher order corrections in the approximation of low-dimensional manifolds and the construction of simplified problems with the CSP method. *J. Comp. Phys.*, 209(2):754–786, 2005.
- [vGKS05] S. van Gils, M. Krupa, and P. Szmolyan. Asymptotic expansions using blow-up. *ZAMP*, 56:369–397, 2005.
- [VGVC07] M. Venkadesan, J. Guckenheimer, and F.J. Valero-Cuevas. Manipulating the edge of instability. *J. Biomech.*, 40:1653–1661, 2007.
- [vGZMF01] F. van Goor, D. Zivadinovic, A.J. Martinez-Fuentes, and S.S. Stojilkovic. Dependence of pituitary hormone secretion on the pattern of spontaneous voltage-gated calcium influx. *J. Biol. Chem.*, 276:33840–33846, 2001.
- [VH08] P. Várkonyi and P. Holmes. On synchronization and traveling waves in chains of relaxation oscillators with an application to Lamprey CPG. *SIAM J. Appl. Dyn. Syst.*, 7(3):766–794, 2008.
- [vHDK08] P. van Heijster, A. Doelman, and T.J. Kaper. Pulse dynamics in a three-component system: stability and bifurcations. *Physica D*, 237(24):3335–3368, 2008.
- [vHDK⁺11] P. van Heijster, A. Doelman, T.J. Kaper, Y. Nishiura, and K.-I. Ueda. Pinned fronts in heterogeneous media of jump type. *Nonlinearity*, 24:127–157, 2011.

- [vHDKP10] P. van Heijster, A. Doelman, T.J. Kaper, and K. Promislow. Front interactions in a three-component system. *SIAM J. Appl. Dyn. Syst.*, 9(2):292–332, 2010.
- [vHS11] P. van Heijster and B. Sandstede. Planar radial spots in a three-component FitzHugh–Nagumo system. *J. Nonlinear Sci.*, 21:705–745, 2011.
- [Vid85] M. Vidyasagar. Robust stabilization of singularly perturbed systems. *Syst. Contr. Lett.*, 5(6):413–418, 1985.
- [Vig97] A. Vigodner. Limits of singularly perturbed control problems with statistical dynamics of fast motions. *SIAM J. Contr. Optim.*, 35(1):1–28, 1997.
- [Vis93] M.I. Vishik. *Asymptotic Behaviour of Solutions of Evolutionary Equations*. CUP, 1993.
- [Vis94] A. Visintin. *Differential Models of Hysteresis*. Springer, 1994.
- [Vit79] M. Vitens. Error bounds in the method of averaging based on properties of average motion. *SIAM J. Math. Anal.*, 10:331–336, 1979.
- [vK07] N.G. van Kampen. *Stochastic Processes in Physics and Chemistry*. North-Holland, 2007.
- [VM06] I.B. Vivancos and A.A. Minzoni. Chaotic behaviour in a singularly perturbed system. *Nonlinearity*, 19:1535–1551, 2006.
- [VMMMO9] N. Vaissmoradi, A. Malek, and S.H. Momeni-Masuleh. Error analysis and applications of the Fourier–Galerkin Runge–Kutta schemes for high-order stiff PDEs. *J. Comput. Appl. Math.*, 231(1):124–133, 2009.
- [VMS00] S. Varela, C. Masoller, and A.C. Sicardi. Numerical simulations of the effect of noise on a delayed pitchfork bifurcation. *Physica A*, 283(1):228–232, 2000.
- [VNAZ12] A. Vasiliev, A. Neishtadt, A. Artemyev, and L. Zelenyi. Jump of the adiabatic invariant at a separatrix crossing: degenerate cases. *Physica D*, 241:566–573, 2012.
- [VNIM06] D.L. Vainchtein, A.I. Neishtadt, and I. Mezic. On passage through resonances in volume-preserving systems. *Chaos*, 16(4):043123, 2006.
- [vNS07] E.H. van Nes and M. Scheffer. Slow recovery from perturbations as generic indicator of a nearby catastrophic shift. *Am. Nat.*, 169(6):738–747, 2007.
- [Vor08] N.V. Voropaeva. Decomposition of problems of optimal control and estimation for discrete systems with fast and slow variables. *Automat. Remote Contr.*, 69(6):920–928, 2008.
- [Vor12] A. Voros. Zeta-regularization for exact-WKB resolution of a general 1D Schrödinger equation. *J. Phys. A: Math. Theor.*, 45:374007, 2012.
- [VP81] C. Vidal and A. Pacault. *Nonlinear Phenomena in Chemical Systems*. Springer, 1981.
- [VP09] M. Valorani and S. Paolucci. The G-scheme: a framework for multi-scale adaptive model reduction. *J. Comp. Phys.*, 228(13):4665–4701, 2009.
- [VRBR80] C. Vidal, J.-C. Roux, S. Bachelart, and A. Rossi. Experimental study of the transition to turbulence in the Belousov–Zhabotinskii reaction. *Annals of the New York Academy of Sciences*, 357(1):377–396, 1980.
- [Vri98] G. De Vries. Multiple bifurcations in a polynomial model of bursting oscillations. *J. Nonlinear Sci.*, 8(3):281–316, 1998.
- [Vri01] G. De Vries. Bursting as an emergent phenomenon in coupled chaotic maps. *Phys. Rev. E*, 64(5):051914, 2001.
- [vS87] S.J. van Strien. Normal hyperbolicity and linearisability. *Invent. Math.*, 87(2):377–384, 1987.
- [VS00] G. De Vries and A. Sherman. Channel sharing in pancreatic- β -cells revisited: enhancement of emergent bursting by noise. *J. Theor. Biol.*, 207(4):513–530, 2000.
- [VS01] G. De Vries and A. Sherman. From spikers to bursters via coupling: help from heterogeneity. *Bull. Math. Biol.*, 63(2):371–391, 2001.
- [vS03] W. van Saarloos. Front propagation into unstable states. *Physics Reports*, 386:29–222, 2003.
- [VS06] N.V. Voropaeva and V.A. Sobolev. Decomposition of a linear-quadratic optimal control problem with fast and slow variables. *Automat. Remote Contr.*, 67(8):1185–1193, 2006.
- [VSH96] V. Vukojević, P.G. Sørensen, and F. Hynne. Predictive value of a model of the Briggs–Rauscher reaction fitted to quenching experiments. *J. Phys. Chem.*, 100:17175–17185, 1996.
- [VTBWB13] T. Vo, J. Tabak, R. Bertram, and M. Wechselberger. A geometric understanding how fast activating potassium channels promote bursting in pituitary cells. *J. Comp. Neurosci.*, 2013. to appear.
- [vV78] M. van Veldhuizen. Higher order methods for a singularly perturbed problem. *Numer. Math.*, 30(3):267–279, 1978.
- [vV81] M. van Veldhuizen. D-stability. *SIAM J. Numer. Anal.*, 20:45–64, 1981.
- [vV83] M. van Veldhuizen. On D-stability and B-stability. *Numer. Math.*, 42(3):349–357, 1983.
- [VV09] F. Veerman and F. Verhulst. Quasiperiodic phenomena in the van der Pol–Mathieu equation. *J. Sound Vibr.*, 326(1):314–320, 2009.
- [vVK95] T.G.J. van Venrooij and M.T.M. Koper. Bursting and mixed-mode oscillations during the hydrogen peroxide reduction on a platinum electrode. *Electrochimica Acta*, 40(11):1689–1696, 1995.
- [VVV94] A.I. Volpert, V. Volpert, and V.A. Volpert. *Traveling Wave Solutions of Parabolic Systems*. Amer. Math. Soc., 1994.
- [VWM+05] J.G. Venegas, T. Winkler, G. Musch, M.F. Vidal Melo, D. Layfield, N. Tgavalekos, A.J. Fischman, R.J. Callahan, G. Bellani, and R.S. Harris. Self-organized patchiness in asthma as a prelude to catastrophic shifts. *Nature*, 434:777–782, 2005.
- [Wai11] G. Wainrib. Noise-controlled dynamics through the averaging principle for stochastic slow–fast systems. *Phys. Rev. E*, 84:051113, 2011.
- [Wal86] G. Wallet. Entrée-sortie dans un tourbillon. *Ann. Inst. Fourier*, 36:157–184, 1986.
- [Wal90a] G. Wallet. Singularité analytique et perturbation singulière en dimension 2. *Bull. Soc. Math. France*, 122:185–208, 1990.
- [Wal90b] G. Wallet. Surstabilité pour une équation différentielle analytique en dimension 1. *Ann. Inst. Fourier*, 120:557–595, 1990.
- [Wal01] D.F. Walnut. *An Introduction to Wavelet Analysis*. Birkhäuser, 2001.
- [Wal07a] A.H. Wallace. *Algebraic Topology: Homology and Cohomology*. Dover, 2007.
- [Wal07b] A.H. Wallace. *An Introduction to Algebraic Topology*. Dover, 2007.
- [WALC11] S. Wieczorek, P. Ashwin, C.M. Luke, and P.M. Cox. Excitability in ramped systems: the compost-bomb instability. *Proc. R. Soc. A*, 467:1243–1269, 2011.

- [Wan92] Z.-Q. Wang. On the existence of multiple, single-peaked solutions for a semilinear Neumann problem. *Arch. Rational Mech. Anal.*, 120:375–399, 1992.
- [Wan93] X.J. Wang. Genesis of bursting oscillations in the Hindmarsh–Rose model and homoclinicity to a chaotic saddle. *Physica D*, 62:263–274, 1993.
- [Wan98] X.J. Wang. Calcium coding and adaptive temporal computation in cortical pyramidal neurons. *J. Neurophysiol.*, 79(3):1549–1566, 1998.
- [War94] M.J. Ward. Metastable patterns, layer collapses, and coarsening for a one-dimensional Ginzburg–Landau equation. *Stud. Appl. Math.*, 91(1):51–93, 1994.
- [War96] M.J. Ward. Metastable bubble solutions for the Allen–Cahn equation with mass conservation. *SIAM J. Appl. Math.*, 56(5):1247–1279, 1996.
- [War05] M.J. Ward. Spikes for singularly perturbed reaction–diffusion systems and Carrier’s Problem. In C. Huu and R. Wong, editors, *Differential Equations and Asymptotic Theory in Mathematical Physics*, pages 100–188. World Scientific, 2005.
- [War06] M.J. Ward. Asymptotic methods for reaction–diffusion systems: past and present. *Bull. Math. Biol.*, 68:1151–1167, 2006.
- [Was85] W. Wasow. *Linear Turning Point Theory*. Springer, 1985.
- [Was02] W. Wasow. *Asymptotic Expansions for Ordinary Differential Equations*. Dover, 2002.
- [Wat71] A.M. Wattis. A singular perturbation problem with a turning point. *Bull. Austral. Math. Soc.*, 5:61–73, 1971.
- [Wat05] F. Watbled. On singular perturbations for differential inclusions on the infinite interval. *J. Math. Anal. Appl.*, 310:362–378, 2005.
- [WB98] H.Y. Wu and S.M. Baer. Analysis of an excitable dendritic spine with an activity-dependent stem conductance. *J. Math. Biol.*, 36(6):569–592, 1998.
- [WB04] K. Wierschem and R. Bertram. Complex bursting in pancreatic islets: a potential glycolytic mechanism. *J. Theor. Biol.*, 228(4):513–521, 2004.
- [WB13] M.A. Webber and P.C. Bressloff. The effects of noise on binocular rivalry waves: a stochastic neural field model. *J. Stat. Mech.*, 2013:P03001, 2013.
- [WB87a] D. Wycoff and N.L. Balazs. Multiple time scales analysis for the Kramers–Chandrasekhar equation. *Phys. A*, 146:175–200, 1987.
- [WB87b] D. Wycoff and N.L. Balazs. Multiple time scales analysis for the Kramers–Chandrasekhar equation with a weak magnetic field. *Phys. A*, 146:201–218, 1987.
- [WB87c] D. Wycoff and N.L. Balazs. Separation of fast and slow variables for a linear system by the method of multiple time scales. *Phys. A*, 146:219–241, 1987.
- [WPBK00] J.A. White, M.I. Banks, R.A. Pearce, and N.J. Kopell. Networks of interneurons with fast and slow γ -aminobutyric acid type A ($GABA_A$) kinetics provide substrate for mixed gamma-theta rhythm. *Proc. Natl. Acad. Sci. USA*, 97(14):8128–8133, 2000.
- [WC73] H. Wilson and J. Cowan. A mathematical theory of the functional dynamics of cortical and thalamic nervous tissue. *Biol. Cybern.*, 13(2):55–80, 1973.
- [WCAK80] J.R. Winkelman, J.H. Chow, J.J. Allemon, and P.V. Kokotovic. Multi-time-scale analysis of a power system. *Automatica*, 16:35–43, 1980.
- [WCB⁺81] J.R. Winkelman, J.H. Chow, B.C. Bowler, B. Avramovic, and P.V. Kokotovic. An analysis of inter-area dynamics of multi-machine systems. *IEEE Trans. Power Appar. Syst.*, 2:754–763, 1981.
- [WCM94] R. Wright, J. Cash, and G. Moore. Mesh selection for stiff two-point boundary value problems. *Numer. Algorithms*, 7:205–224, 1994.
- [WD07] W. Wang and J. Duan. Homogenized dynamics of stochastic partial differential equations with dynamical boundary conditions. *Comm. Math. Phys.*, 275:163–186, 2007.
- [WD09] W. Wang and J. Duan. Reductions and deviations for stochastic partial differential equations under fast dynamical boundary conditions. *Stoch. Anal. Appl.*, 27(3):431–459, 2009.
- [WDD07] W. Wang, D. Cao, and J. Duan. Effective macroscopic dynamics of stochastic partial differential equations in perforated domains. *SIAM J. Math. Anal.*, 38:1508–1527, 2007.
- [Wec98] M. Wechselberger. *Singularly perturbed folds and canards in \mathbb{R}^3* . PhD thesis, Vienna University of Technology, Vienna, Austria, 1998.
- [Wec02] M. Wechselberger. Extending Melnikov-theory to invariant manifolds on non-compact domains. *Dynamical Systems*, 17(3):215–233, 2002.
- [Wec05] M. Wechselberger. Existence and bifurcation of canards in \mathbb{R}^3 in the case of a folded node. *SIAM J. Appl. Dyn. Syst.*, 4(1):101–139, 2005.
- [Wec12] M. Wechselberger. A propos de canards (apropos canards). *Trans. Amer. Math. Soc.*, 364:3289–3309, 2012.
- [WED⁺13] L. Weicker, T. Erneux, O. D’Huys, J. Danckaert, M. Jacquot, Y. Chembo, and L. Larger. Slow–fast dynamics of a time-delayed electro-optic oscillator. *Phil. Trans. R. Soc. A*, 371(1999):20120459, 2013.
- [Wei84] R. Weiss. An analysis of the box and trapezoidal schemes for linear singularly perturbed boundary value problems. *Math. Comp.*, 42:537–557, 1984.
- [Wei12] S. Weinberg. *Lectures on Quantum Mechanics*. CUP, 2012.
- [WEJ⁺12] L. Weicker, T. Erneux, M. Jacquot, Y. Chembo, and L. Larger. Crenelated fast oscillatory outputs of a two-delay electro-optic oscillator. *Phys. Rev. E*, 85:026206, 2012.
- [Wel76] J.C. Wells. Invariant manifolds of non-linear operators. *Pac. J. Math.*, 62(1):285–293, 1976.
- [Wen26] G. Wentzel. Eine Verallgemeinerung der Quantenbedingungen für die Zwecke der Wellenmechanik. *Zeitschrift für Physik*, 38(6):518–529, 1926.
- [Wes39] A.J. Wesselink. Stellar variability and relaxation oscillations. *Astrophys. J.*, 89:659–668, 1939.
- [WF70] A.D. Wentzell and M.I. Freidlin. On small random perturbations of dynamical systems. *Russ. Math. Surv.*, 25:1–55, 1970.
- [WF73] A.D. Wentzell and M.I. Freidlin. Some problems concerning stability under small random perturbations. *Theory Probab. Appl.*, 17(2):269–283, 1973.
- [WGR95] X.J. Wang, D. Golomb, and J. Rinzel. Emergent spindle oscillations and intermittent burst firing in a thalamic model: specific neuronal mechanisms. *Proc. Natl. Acad. Sci. USA*, 92(12):5577–5581, 1995.

- [WH01] Z. Wang and H. Hu. Dimensional reduction for nonlinear time-delayed systems composed of stiff and soft substructures. *Nonlinear Dyn.*, 25(4):317–331, 2001.
- [Whi36] H. Whitney. Differentiable manifolds. *Ann. Math.*, 37(3):645–680, 1936.
- [WHK93] M.J. Ward, W.D. Heshaw, and J.B. Keller. Summing logarithmic expansions for singularly perturbed eigenvalue problems. *SIAM J. Appl. Math.*, 53(3):799–828, 1993.
- [Wid67] O.B. Widlund. A note on unconditionally stable linear multistep methods. *BIT Numer. Math.*, 7(1):65–70, 1967.
- [Wie85] K. Wiesenfeld. Noisy precursors of nonlinear instabilities. *J. Stat. Phys.*, 38(5):1071–1097, 1985.
- [Wie09] S. Wieczorek. Stochastic bifurcation in noise-driven lasers and Hopf oscillators. *Phys. Rev. E*, 79(3):036209, 2009.
- [Wig88] S. Wiggins. On the detection and dynamical consequences of orbits homoclinic to hyperbolic periodic orbits and normally hyperbolic invariant tori in a class of ordinary differential equations. *SIAM J. Appl. Math.*, 48(2):262–285, 1988.
- [Wig94] S. Wiggins. *Normally Hyperbolic Invariant Manifolds in Dynamical Systems*. Springer, 1994.
- [Wig03] S. Wiggins. *Introduction to Applied Nonlinear Dynamical Systems and Chaos*. Springer, New York, NY, 2nd edition, 2003.
- [Wil75] K.G. Wilson. The renormalization group: critical phenomena and the Kondo problem. *Rev. Mod. Phys.*, 47(4):773–840, 1975.
- [Wil81] M. Williams. Another look at Ackerberg–O’Malley resonance. *SIAM J. Appl. Math.*, 41(2):288–293, 1981.
- [Wil83] K.G. Wilson. The renormalization group and critical phenomena. *Rev. Mod. Phys.*, 55(3):583–600, 1983.
- [Wil91] D. Williams. *Probability with Martingales*. CUP, 1991.
- [Wil06] J.P. Wilber. Invariant manifolds describing the dynamics of a hyperbolic–parabolic equation from nonlinear viscoelasticity. *Dynamical Systems*, 21(4):465–489, 2006.
- [Win84] A.T. Winfree. The prehistory of the Belousov–Zhabotinskii reaction. *J. Chem. Educ.*, 61:661–663, 1984.
- [WK73] R. Wilde and P. Kokotovic. Optimal open-and closed-loop control of singularly perturbed linear systems. *IEEE Trans. Aut. Contr.*, 18(6):616–626, 1973.
- [WK74] K.G. Wilson and J. Kogut. The renormalization group and the ϵ expansion. *Phys. Rep.*, 12(2):75–199, 1974.
- [WK93] M.J. Ward and J.B. Keller. Strong localized perturbations of eigenvalue problems. *SIAM J. Appl. Math.*, 53(3):770–798, 1993.
- [WK96] C.J. Wilson and Y. Kawaguchi. The origins of two-state spontaneous membrane potential fluctuations of neostriatal spiny neurons. *J. Neurosci.*, 16(7):2397–2410, 1996.
- [WK01] M.W. Walser and C.H. Keitel. Geometric and algebraic approach to classical dynamics of a particle with spin. *Lett. Math. Phys.*, 55(1):63–70, 2001.
- [WK05] S. Wieczorek and B. Krauskopf. Bifurcations of n-homoclinic orbits in optically injected lasers. *Nonlinearity*, 18:1095–1125, 2005.
- [WKB97] S. Weibel, T.J. Kaper, and J. Baillieul. Global dynamics of a rapidly forced cart and pendulum. *Nonlinear Dyn.*, 13(2):131–170, 1997.
- [WKvdB12] Y.-F. Wang, M. Khan, and H.A. van den Berg. Interaction of fast and slow dynamics in endocrine control systems with an application to β -cell dynamics. *Math. Biosci.*, 235(1):8–18, 2012.
- [WLL⁺12] Y. Wu, W. Lu, W. Lin, G. Leng, and J. Feng. Bifurcations of emergent bursting in a neuronal network. *PLoS ONE*, 7(6):e38402, 2012.
- [Wlo05] J. Włodarczyk. Simple Hironaka resolution in characteristic zero. *J. Amer. Math. Soc.*, 18(4):779–822, 2005.
- [WLW08] Z. Wang, W. Lin, and G. Wang. Differentiability and its asymptotic analysis for nonlinear singularly perturbed boundary value problem. *Nonlinear Anal.*, 69(7):2236–2250, 2008.
- [WM06] B.P. Wood and J.R. Miller. Linked selected and neutral loci in heterogeneous environments. *J. Math. Biol.*, 53(6):939–975, 2006.
- [WMH⁺02] M.J. Ward, D. McInerney, P. Houston, D. Gavaghan, and P. Maini. The dynamics and pinning of a spike for a reaction–diffusion system. *SIAM J. Appl. Math.*, 62(4):1297–1328, 2002.
- [Woj97] P. Wojtaszczyk. *A Mathematical Introduction to Wavelets*, volume 37 of *LMS Student Texts*. CUP, 1997.
- [Wol77] D.J. Wolkowich. Singular perturbation techniques: a comparison of the method of matched asymptotic expansions with that of multiple scales. *SIAM Rev.*, 19(3):502–516, 1977.
- [Wol94] G. Wolansky. On the slow evolution of quasi-stationary shock waves. *J. Dyn. Diff. Eq.*, 6(2):247–276, 1994.
- [Woo93] S.L. Woodruff. The use of an invariance condition in the solution of multiple-scale singular perturbation problems: ordinary differential equations. *Stud. Appl. Math.*, 90(3):225–248, 1993.
- [Woo95] S.L. Woodruff. A uniformly valid asymptotic solution to a matrix system of ordinary differential equations and a proof of its validity. *Stud. Appl. Math.*, 94(4):393–413, 1995.
- [WORD03] S.J. Watson, F. Otto, B.Y. Rubinstein, and S.H. Davis. Coarsening dynamics of the convective Cahn–Hilliard equation. *Physica D*, 178(3):127–148, 2003.
- [WP74] A.E.R. Woodcock and T. Poston. *A Geometrical Study of the Elementary Catastrophes*, volume 373 of *Lecture Notes in Mathematics*. Springer, 1974.
- [WP10] M. Wechselberger and G.J. Pettet. Folds, canards and shocks in advection–reaction–diffusion models. *Nonlinearity*, 23(8):1949–1969, 2010.
- [WPJ11] K. Wang, J. Peng, and D. Jin. A new development for the Tikhonov theorem in nonlinear singular perturbation systems. *Nonl. Anal.*, 74:2869–2879, 2011.
- [WR76] B. Willner and L.A. Rubenfeld. Uniform asymptotic solution for a linear ordinary differential equation with one μ -th order turning point: analytic theory. *Comm. Pure Appl. Math.*, 29(4):343–367, 1976.
- [WR95] M.J. Ward and L.G. Reyna. Internal layers, small eigenvalues, and the sensitivity of metastable motion. *SIAM J. Appl. Math.*, 55(2):425–445, 1995.
- [WR02] S. Wirkus and R. Rand. The dynamics of two coupled van der Pol oscillators with delay coupling. *Nonlinear Dyn.*, 30(3):205–221, 2002.

- [WR12] W. Wang and A.J. Roberts. Average and deviation for slow–fast stochastic partial differential equations. *J. Differential Equat.*, 253(5):1265–1286, 2012.
- [WR13] W. Wang and A.J. Roberts. Slow manifold and averaging for slow–fast stochastic differential system. *J. Math. Anal. Appl.*, 398(2):822–839, 2013.
- [WRD12] W. Wang, A.J. Roberts, and J. Duan. Large deviations and approximations for slow–fast stochastic reaction–diffusion equations. *J. Differential Equat.*, 12:3501–3522, 2012.
- [WS72] H.A. Watts and L. Shampine. A-stable block implicit one-step methods. *BIT Numer. Math.*, 12(2):252–266, 1972.
- [WS00] D. Wirosoetisno and T.G. Shepherd. Averaging, slaving and balance dynamics in a simple atmospheric model. *Physica D*, 141:37–53, 2000.
- [WS01] H. Wang and Y. Song. Regularization methods for solving differential-algebraic equations. *Appl. Math. Comput.*, 119(2):283–296, 2001.
- [WS06a] J. Walter and C. Schütte. Conditional averaging for diffusive fast–slow systems: a sketch for derivation. In *Analysis, Modeling and Simulation of Multiscale Problems*, pages 647–682. Springer, 2006.
- [WS06b] L. Wang and E.D. Sontag. Almost global convergence in singular perturbations of strongly monotone systems. *Lect. Notes Contr. Inf. Sci.*, 341:415, 2006.
- [WS08] L. Wang and E.D. Sontag. Singularly perturbed monotone systems and an application to double phosphorylation cycles. *J. Nonlinear Sci.*, 18(5):527–550, 2008.
- [WS11] J. Wojcik and A. Shilnikov. Voltage interval mappings for activity transitions in neuron models for elliptic bursters. *Physica D*, 240(14):1164–1180, 2011.
- [WS12] Z.-L. Wang and X.-R. Shi. Chaos bursting synchronization of mismatched Hindmarsh–Rose systems via a single adaptive feedback controller. *Nonlinear Dyn.*, 67:1817–1823, 2012.
- [WSB04] T. Wellens, V. Shatokhin, and A. Buchleitner. Stochastic resonance. *Reports on Progress in Physics*, 67:45–105, 2004.
- [WSGR11] J. Wang, J. Su, H. Perez Gonzalez, and J. Rubin. A reliability study of square wave bursting beta-cells with noise. *Discr. Cont. Dyn. Syst. B*, 16:569–588, 2011.
- [WW03] M.J. Ward and J. Wei. Hopf bifurcation and oscillatory instabilities of spike solutions for the one-dimensional Gierer–Meinhardt model. *J. Nonlinear Sci.*, 13(2):209–264, 2003.
- [WW05] J. Wei and M. Winter. Clustered spots in the FitzHugh–Nagumo system. *J. Differential Equat.*, 213(1):121–145, 2005.
- [WW07] K. Wang and W. Wang. Propagation of HBV with spatial dependence. *Math. Biosci.*, 210(1):78–95, 2007.
- [WW09a] M. Wechselberger and W. Weckesser. Bifurcations of mixed-mode oscillations in a stellate cell model. *Physica D*, 238:1598–1614, 2009.
- [WW09b] M. Wechselberger and W. Weckesser. Homoclinic clusters and chaos associated with a folded node in a stellate cell model. *Discr. Cont. Dyn. Syst. S*, 2(4):829–850, 2009.
- [WWL11] L. Wang, Y. Wu, and T. Li. Exponential stability of large-amplitude traveling fronts for quasi-linear relaxation systems with diffusion. *Physica D*, 240(11):971–983, 2011.
- [WX13] X. Wang and Q. Xu. Spiky and transition layer steady states of chemotaxis systems via global bifurcation and Helly’s compactness theorem. *J. Math. Biol.*, 66(6):1241–1266, 2013.
- [WY01] Q. Wang and L.-S. Young. Strange attractors with one direction of instability. *Commun. Math. Phys.*, 218:1–97, 2001.
- [WY02] Q. Wang and L.-S. Young. From invariant curves to strange attractors. *Commun. Math. Phys.*, 225:275–304, 2002.
- [WZ05] Y. Wu and X. Zhao. The existence and stability of travelling waves with transition layers for some singular cross-diffusion systems. *Physica D*, 200(3):325–358, 2005.
- [WZY06] J.W. Wang, Q. Zhang, and G. Yin. Two-time-scale hybrid filters: near optimality. *SIAM J. Contr. Optim.*, 45:298–319, 2006.
- [XC03] J. Xu and K.W. Chung. Effects of time delayed position feedback on a van der Pol–Duffing oscillator. *Physica D*, 180(1):17–39, 2003.
- [XCKA08] Y. Xie, L. Chen, Y.M. Kang, and K. Aihara. Controlling the onset of Hopf bifurcation in the Hodgkin–Huxley model. *Phys. Rev. E*, 77(6):061921, 2008.
- [XDX11] Y. Xu, J. Duan, and W. Xu. An averaging principle for stochastic dynamical systems with Lévy noise. *Physica D*, 240(17):1395–1401, 2011.
- [XH00] J.X. Xin and J.M. Hyman. Stability, relaxation, and oscillation of biodegradation fronts. *SIAM J. Appl. Math.*, 61(2):472–505, 2000.
- [XHZ05a] F. Xie, M. Han, and W. Zhang. Canard phenomena in oscillations of a surface oxidation reaction. *J. Nonlinear Sci.*, 15(6):363–386, 2005.
- [XHZ05b] F. Xie, M. Han, and W. Zhang. Singular homoclinic bifurcations in a planar fast–slow system. *J. Dyn. Contr. Syst.*, 11(3):433–448, 2005.
- [XHZ06a] F. Xie, M. Han, and W. Zhang. Existence of canard manifolds in a class of singularly perturbed systems. *Nonlinear Anal.*, 64(3):457–470, 2006.
- [XHZ06b] F. Xie, M. Han, and W. Zhang. The persistence of canards in 3-D singularly perturbed systems with two fast variables. *Asymp. Anal.*, 47(1):95–106, 2006.
- [Xie12] F. Xie. On a class of singular boundary value problems with singular perturbation. *J. Differential Equat.*, 252:2370–2387, 2012.
- [Yad13] K. Yadi. Averaging on slow and fast cycles of a three time scale system. *J. Math. Anal. Appl.*, pages 1–26, 2013. accepted, to appear.
- [Yam93] M. Yamada. A theoretical analysis of self-sustained pulsation phenomena in narrow-stripe semiconductor lasers. *IEEE J. Quant. Electr.*, 29:1330–1336, 1993.
- [Yan87] E. Yanagida. Branching of double pulse solutions from single pulse solutions in nerve axon equation. *J. Differential Equat.*, 66:243–262, 1987.
- [Yan88] E. Yanagida. Existence of periodic travelling wave solutions of reaction–diffusion systems with fast–slow dynamics. *J. Differential Equat.*, 76:115–134, 1988.
- [Yan89] E. Yanagida. Stability of travelling front solutions of the FitzHugh–Nagumo equations. *Math. Comput. Modelling*, 12(3):289–301, 1989.

- [YD03] G. Yin and S. Dey. Weak convergence of hybrid filtering problems involving nearly completely decomposable hidden Markov chains. *SIAM J. Contr. Optim.*, 41(6):1820–1842, 2003.
- [YE06] J.Z. Yang and W. E. Generalized Cauchy-Born rules for elastic deformation of sheets, plates, and rods: derivation of continuum models from atomistic models. *Phys. Rev. B*, 74(18):184110, 2006.
- [Yin01] G. Yin. On limit results for a class of singularly perturbed switching diffusions. *J. Theor. Prob.*, 14(3):673–697, 2001.
- [YK73] R. Yackel and P. Kokotovic. A boundary layer method for the matrix Riccati equation. *IEEE Trans. Aut. Contr.*, 18:17–24, 1973.
- [YK99] G. Yin and M. Kniazeva. Singularly perturbed multidimensional switching diffusions with fast and slow switchings. *J. Math. Anal. Appl.*, 229(2):605–630, 1999.
- [YK05] G. Yin and V. Krishnamurthy. Least mean square algorithms with Markov regime-switching limit. *IEEE Trans. Aut. Contr.*, 50(5):577–593, 2005.
- [YKL06] N. Yu, R. Kuske, and Y.X. Li. Stochastic phase dynamics: multiscale behavior and coherence measures. *Phys. Rev. E*, 73(5):056205, 2006.
- [YKL08] N. Yu, R. Kuske, and Y.X. Li. Stochastic phase dynamics and noise-induced mixed-mode oscillations in coupled oscillators. *Chaos*, 18:015112, 2008.
- [YKU77] K.-K. Young, P. Kokotovic, and V. Utkin. A singular perturbation analysis of high-gain feedback systems. *IEEE Trans. Aut. Contr.*, 22(6):931–938, 1977.
- [YL11] Z. Yang and Q. Lu. Bifurcation mechanisms of electrical bursting with different-time-scale slow variables. *Int. J. Bif. Chaos*, 21(5):1407–1425, 2011.
- [YLK13] N. Yu, Y.X. Li, and R. Kuske. A computational study of spike time reliability in two cases of threshold dynamics. *J. Math. Neurosci.*, 3:11, 2013.
- [You02] L.-S. Young. What are SRB measures, and which dynamical systems have them? *L. Stat. Phys.*, 108(5):733–754, 2002.
- [YPMD08] P. Yanguas, J.F. Palacián, J.F. Meyer, and H.S. Dumas. Periodic solutions in Hamiltonian systems, averaging, and the lunar problem. *SIAM J. Appl. Dyn. Syst.*, 7(2):311–340, 2008.
- [YTE01] A.C. Yew, D.H. Terman, and G.B. Ermentrout. Propagating activity patterns in thalamic neuronal networks. *SIAM J. Appl. Math.*, 61(5):1578–1604, 2001.
- [YTHL11] P. Yordanov, S. Tyanova, M.-T. Hütt, and A. Lesne. Asymmetric transition and time-scale separation in interlinked positive feedback loops. *Int. J. Bif. Chaos*, 21(7):1895–1905, 2011.
- [Yvi13] R. Yvinec. Adiabatic reduction of models of stochastic gene expression with bursting. *arXiv:1301.1293v1*, pages 1–24, 2013.
- [YW10] S. Yanchuk and M. Wolfrum. A multiple time scale approach to the stability of external cavity modes in the Lang–Kobayashi system using the limit of large delay. *SIAM J. Appl. Dyn. Sys.*, 9(2):519–535, 2010.
- [YWDZ12] Z. Yang, Q. Wang, M.-F. Danca, and J. Zhang. Complex dynamics of compound bursting with burst episode composed of different bursts. *Nonlinear Dyn.*, 70:2003–2013, 2012.
- [YY77] K. Yokota and I. Yamazaki. Analysis and computer simulation of aerobic oxidation of reduced nicotinamide adenine dinucleotide catalyzed by horseradish peroxidase. *Biochemistry*, 16(9):1913–1920, 1977.
- [YY04] G. Yin and H. Yang. Two-time-scale jump-diffusion models with Markovian switching regimes. *Stoch. Stoch. Rep.*, 76(2):77–99, 2004.
- [YYYZ02] H. Yang, G. Yin, K. Yin, and Q. Zhang. Control of singularly perturbed Markov chains: a numerical study. *ANZIAM J.*, 45:49–74, 2002.
- [YZ94] G. Yin and Q. Zhang. Near optimality of stochastic control in systems with unknown parameter processes. *Appl. Math. Optim.*, 29(3):263–284, 1994.
- [YZ97] G. Yin and Q. Zhang. Control of dynamic systems under the influence of singularly perturbed Markov chains. *J. Math. Anal. Appl.*, 216(1):343–367, 1997.
- [YZ98] G.G. Yin and Q. Zhang. *Continuous-Time Markov Chains and Applications: A Singular Perturbation Approach*. Springer, 1998.
- [YZ00] G. Yin and Q. Zhang. Singularly perturbed discrete-time Markov chains. *SIAM J. Appl. Math.*, 61(3):834–854, 2000.
- [YZ02a] G. Yin and H. Zhang. Countable-state-space Markov chains with two time scales and applications to queueing systems. *Adv. Appl. Prob.*, 34(3):662–688, 2002.
- [YZ02b] G. Yin and Q. Zhang. Hybrid singular systems of differential equations. *Science China F*, 45(4):241–258, 2002.
- [YZ03] G. Yin and Q. Zhang. Discrete-time singularly perturbed Markov chains. In *Stochastic Modeling and Optimization*, pages 1–42. Springer, 2003.
- [YZ04a] L. Yang and X. Zeng. Stability of singular Hopf bifurcations. *J. Differential Equat.*, 206(1):30–54, 2004.
- [YZ04b] G. Yin and Q. Zhang. Two-time-scale Markov chains and applications to quasi-birth-death queues. *SIAM J. Appl. Math.*, 65(2):567–586, 2004.
- [YZ05] G.G. Yin and Q. Zhang. *Discrete-time Markov Chains: Two-Time-Scale Methods and Applications*. Springer, 2005.
- [YZ07] G. Yin and Q. Zhang. Singularly perturbed Markov chains: limit results and applications. *Ann. Appl. Prob.*, 17(1):207–229, 2007.
- [YZ08] G. Yin and Q. Zhang. Discrete-time Markov chains with two-time scales and a countable state space: limit results and queueing applications. *Stochastics*, 80(4):339–369, 2008.
- [YZ10] G.G. Yin and C. Zhu. *Hybrid Switching Diffusions: Properties and Applications*. Springer, 2010.
- [YZB00a] G. Yin, Q. Zhang, and G. Badowski. Asymptotic properties of a singularly perturbed Markov chain with inclusion of transient states. *Ann. Appl. Math.*, 10(2):549–572, 2000.
- [YZB00b] G. Yin, Q. Zhang, and G. Badowski. Occupation measures of singularly perturbed Markov chains with absorbing states. *Acta Math. Sinica*, 16(1):161–180, 2000.
- [YZB00c] G. Yin, Q. Zhang, and G. Badowski. Singularly perturbed Markov chains: convergence and aggregation. *J. Multivar. Anal.*, 72(2):208–229, 2000.
- [Z11] M. Zaks. On chaotic subthreshold oscillations in a simple neuronal model. *Math. Model. Nat. Phenom.*, 6(1):149–162, 2011.

- [ZD11] A. Zagaris and A. Doelman. Emergence of steady and oscillatory localized structures in a phytoplankton-nutrient model. *Nonlinearity*, 24(12):3437–3486, 2011.
- [ZDTS09] A. Zagaris, A. Doelman, N.N. Pham Thi, and B.P. Sommeijer. Blooming in a non-local, coupled phytoplankton-nutrient model. *SIAM J. Appl. Math.*, 69(4):1174–1204, 2009.
- [ZE10] E.P. Zemskov and I.R. Epstein. Wave propagation in a FitzHugh-Nagumo-type model with modified excitability. *Phys. Rev. E*, 82:026207, 2010.
- [Zee77] E.C. Zeeman. *Catastrophe Theory: Selected Papers, 1972–1977*. Addison-Wesley, 1977.
- [Zel13] S. Zelik. Inertial manifolds and finite-dimensional reduction for dissipative PDEs. *arXiv:1303.4457v1*, pages 1–60, 2013.
- [ZFM⁺97] M.G. Zimmermann, S.O. Firle, M.A. Matiello, M. Hildebrand, M. Eiswirth, M. Bär, A.K. Bangia, and I.G. Kevrekidis. Pulse bifurcation and transition to spatiotemporal chaos in an excitable reaction-diffusion model. *Physica D*, 110(1):92–104, 1997.
- [ZGB⁺03] M. Zhang, P. Goforth, R. Bertram, A. Sherman, and L. Satin. The Ca^{2+} dynamics of isolated mouse β -cells and islets: implications for mathematical models. *Biophys. J.*, 84(5):2852–2870, 2003.
- [ZGKK09] A. Zagaris, C.W. Gear, T.J. Kaper, and I.G. Kevrekidis. Analysis of the accuracy and convergence of equation-free projection to a slow manifold. *ESAIM: Math. Model. Numer. Anal.*, 43(4):754–784, 2009.
- [ZGO13] Q. Zhang, J. Gong, and C.H. Oh. Intrinsic dynamical fluctuation assisted symmetry breaking in adiabatic following. *Phys. Rev. Lett.*, 110:130402, 2013.
- [Zha64] A.M. Zhabotinsky. Periodic processes of malonic acid oxidation in a liquid phase (in Russian). *Biofizika*, 9:306–311, 1964.
- [Zha85] A.M. Zhabotinsky. The early period of systematic studies of oscillations and waves in chemical systems. In R.J. Field and M. Burger, editors, *Oscillations and Traveling Waves in Chemical Systems*, pages 1–6. Wiley-Interscience, 1985.
- [Zha95] Q. Zhang. Risk-sensitive production planning of stochastic manufacturing systems: a singular perturbation approach. *SIAM J. Contr. Optim.*, 33(2):498–527, 1995.
- [Zha96] Q. Zhang. Finite state Markovian decision processes with weak and strong interactions. *Stochastics*, 59(3):283–304, 1996.
- [Zha08] Z. Zhao. Solitary waves of the generalized KdV equation with distributed delays. *J. Math. Anal. Appl.*, 344(1):32–41, 2008.
- [ZJ07] J. Zinn-Justin. *Phase Transitions and Renormalization Group*. OUP, 2007.
- [ZJJ04] J. Zinn-Justin and U.D. Jentschura. Multi-instantons and exact results I: conjectures, WKB expansions, and instanton interactions. *Ann. Phys.*, 313:197–267, 2004.
- [ZKK04a] A. Zagaris, H.G. Kaper, and T.J. Kaper. Analysis of the computational singular perturbation method for chemical kinetics. *J. Nonlinear Sci.*, 14:59–91, 2004.
- [ZKK04b] A. Zagaris, H.G. Kaper, and T.J. Kaper. Fast and slow dynamics for the computational singular perturbation method. *Multiscale Model. Simul.*, 2(4):613–638, 2004.
- [ZKK05] A. Zagaris, H.G. Kaper, and T.J. Kaper. Two perspectives on reduction of ordinary differential equations. *Math. Nachr.*, 278(12):1629–1642, 2005.
- [ZKS11] W. Zhang, V. Kirk, J. Sneyd, and M. Wechselberger. Changes in the criticality of Hopf bifurcations due to certain model reduction techniques in systems with multiple timescales. *J. Math. Neurosci.*, 1:9, 2011.
- [ZMdB89] H. Zeghlache, P. Mandel, and C. Van den Broeck. Influence of noise on delayed bifurcations. *Phys. Rev. A*, 40:286–294, 1989.
- [ZNK13] A. Zakhrova, Z. Nikoloski, and A. Koseka. Dimensionality reduction of bistable biological systems. *Bull. Math. Biol.*, 75:373–392, 2013.
- [Zol87] H. Zoldekk. Bifurcations of certain family of planar vector fields tangent to axes. *J. Differential Equat.*, 67(1):1–55, 1987.
- [ZP08] J. Zhang and Y. Peng. Travelling waves of the diffusive Nicholson’s blowflies equation with strong generic delay kernel and non-local effect. *Nonl. Anal.: Theor. Meth. Appl.*, 68(5):1263–1270, 2008.
- [ZREK03] A.M. Zhabotinsky, H.G. Rotstein, I.R. Epstein, and N. Kopell. A canard mechanism for localization in systems of globally coupled oscillators. *SIAM J. Appl. Math.*, 63(6):1998–2019, 2003.
- [ZS84] A.K. Zvonkin and M.A. Shubin. Non-standard analysis and singular perturbations of ordinary differential equations. *Russ. Math. Surveys*, 39(2):69–131, 1984.
- [ZT88] E.C. Zachmanoglou and D.W. Thoe. *Introduction to Partial Differential Equations with Applications*. Dover, 1988.
- [ZVG⁺12] A. Zagaris, C. Vanderkerckhove, C.W. Gear, T.J. Kaper, and I.G. Kevrekidis. Stability and stabilization of the constrained runs schemes for equation-free projection to a slow manifold. *Discr. Cont. Dyn. Syst. A*, 32(8):2759–2803, 2012.
- [ZW10a] Y.G. Zheng and Z.H. Wang. Delayed Hopf bifurcation in time-delayed slow-fast systems. *Science China - Technological Sciences*, 53(3):656–663, 2010.
- [ZW10b] Y.G. Zheng and Z.H. Wang. The impact of delayed feedback on the pulsating oscillations of class-B lasers. *Int. J. Non-Linear Mech.*, 45(7):727–733, 2010.
- [ZW12a] Y.G. Zheng and Z.H. Wang. Relaxation oscillation and attractive basins of a two-neuron Hopfield network with slow and fast variables. *Nonlinear Dyn.*, 70:1231–1240, 2012.
- [ZW12b] Y.G. Zheng and Z.H. Wang. Time-delay effect on the bursting of the synchronized state of coupled Hindmarsh-Rose neurons. *Chaos*, 22:043127, 2012.
- [ZY96] Q. Zhang and G.G. Yin. A central limit theorem for singularly perturbed nonstationary finite state Markov chains. *Ann. Appl. Prob.*, 6(2):650–670, 1996.
- [ZY99] Q. Zhang and G.G. Yin. On nearly optimal controls of hybrid LQG problems. *IEEE Trans. Aut. Contr.*, 44(12):2271–2282, 1999.
- [ZY04] Q. Zhang and G.G. Yin. Exponential bounds for discrete-time singularly perturbed Markov chains. *J. Math. Anal. Appl.*, 293(2):645–662, 2004.
- [ZY05] S. Zhu and P. Yu. Computation of the normal forms for general M-DOF systems using multiple time scales. I. Autonomous systems. *Commun. Nonlinear Sci. Numer. Simul.*, 10:869–905, 2005.
- [ZY06] S. Zhu and P. Yu. Computation of the normal forms for general M-DOF systems using multiple time scales. II. Non-autonomous systems. *Commun. Nonlinear Sci. Numer. Simul.*, 11:45–81, 2006.

- [ZYL97] Q. Zhang, G.G. Yin, and E.K. Boukas. Controlled Markov chains with weak and strong interactions: asymptotic optimality and applications to manufacturing. *J. Optim. Theor. Appl.*, 94(1):169–194, 1997.
- [ZYL05] Q. Zhang, G.G. Yin, and R.H. Liu. A near-optimal selling rule for a two-time-scale market model. *Multiscale Model. Simul.*, 4(1):172–193, 2005.
- [ZYM07] Q. Zhang, G.G. Yin, and J.B. Moore. Two-time-scale approximation for Wonham filters. *IEEE Trans. Inf. Theor.*, 53(5):1706–1715, 2007.

Index

- A-stable, 301, 302
- absolutely continuous
 - conditional measure, 459
 - measure, 459
- absolutely stable, 301
- absorbing state, 510
- Ackerberg–O’Malley resonance, 69
- action, 646
 - functional, 514
- action-angle coordinates, 273, 316, 646
- active node, 698
- Adams–Bashforth method, 299
- adaptive
 - dynamics, evolution, 680
 - mesh, 308
 - network, 697
 - self-organized criticality, 700
- adiabatic
 - invariant, 648
 - theorem, 695
- adjoint operator, 481
- adjoint representation, 333
- admissible control, 606
- admissible time change
 - hysteresis operator, 635
- advection–reaction–diffusion, 572
- affine coordinates, 174
- Airy equation, 107
- Allee effect, 559
- alpha limit set, 527
- amplitude, 278
 - equation, 279, 283, 286
 - equation, PDEs, 614
- analytic continuation, 363
- angle, 646
- annealed network, 697
- appreciable hyperreal, 640
- approximate identity, 580
- approximation
 - geometrical optics, 262
 - physical optics, 262
 - zeroth-order, 102
- ARD, 572
- Arrhenius–Eyring–Kramers law, 517
- Arzelà–Ascoli, 610
- asymptotic
 - expansion, 15
 - expansion, Gevrey, 269
 - matching, 240, 243, 248
 - matching condition, 245
 - moment of falling, 364
 - moment of jumping, 364
 - phase, 340
 - rate foliation, 46
 - sequence, 15
 - sequence, logarithmic, 107
 - series, 16, 92
- asymptotically
 - flat (Gevrey), 269
 - flat (Poincaré), 269
- asymptotics
 - Poincaré, 270
 - via blowup, fold, 262
- atlas, 28
- attracting normally hyperbolic, 55
- attractor, 436
 - Axiom A, 460
 - Lorenz, 468

- maximal, 436
- strange, 436
- attractor–repeller pair, 527
- autocatalator, 674
- auxiliary canard, 420
- average, 542
- average connectivity, 699
- averaged equation, 266
- averaging, 265
 - fast subsystem, 267
 - theorem, 266
- Axiom A attractor, 460
- B-tipping, 655
- Bézout’s lemma, 379
- backward
 - differentiation formula, 302, 626
 - Kolmogorov equation, 481, 517
- Banach
 - contraction mapping theorem, 35
 - manifold, 588
 - space, 37
- Barkley model, 684
- basin of attraction, 514
- BDF, 302, 626
- Belousov–Zhabotinskii reaction, 398, 673
- Bernoulli shift, 438
- Berstein-type inequality, 488
- beyond all orders, 15, 248
- bi-infinite sequences, 438
- bifurcation, 53
 - critical transition, 656
 - cusp, 63
 - diagram, singular, 409
 - dynamic, 63
 - fold, 62
 - Hopf, 63, 361, 404
 - pitchfork, 265, 386
 - saddle node of limit cycles, 213
 - saddle-node, 62
 - transcritical, 63
- bilinear oscillator, 607
- block diagram, 665
- blowdown, 187
- blowup
- asymptotics, fold, 262
- directional, 168
- directional, repeated, 170
- directional, rescaled, 168
- example, polar, \mathbb{R}^2 , 161
- method, 160
- planar fold, 180
- polar, \mathbb{R}^2 , 160
- polar, \mathbb{R}^n , 162
- polar, rescaled, 164
- polar, weighted, 173
- quasihomogeneous, 173
- repeated, construction of, 165
- transcritical point, 231
- weighted, directional, 176, 177
- Boltzmann constant, 497
- Bornholdt–Rohlf model, 698
- boundary
 - condition, separated, 303
 - function, 257
 - function method, 255
 - layer, 693
 - manifold, 149
 - map, 536
- boundary value problem, 303
 - two-point, 303, 393
 - two-point, fast–slow, 149
 - two-point, linear, 76, 94
- box, 546
- Brownian motion, 478, 497, 506
 - scaling law, 482
- bundle
 - normal bundle, 23
 - plane bundle, 561
 - tangent bundle, 23
 - transversal bundle, 30
- Burgers’ equation, 563
- burst
 - initiation, 416
 - termination, 416
- bursting, 398
 - elliptic, 417
 - fold-homoclinic, 416
 - square-wave, 416
 - subHopf-foldcycle, 417
- BZ reaction, 673

- C-slow exit/entrance point, 543
canard, 200
auxiliary, 420, 423
cycle, 212
delayed Hopf, 361
explosion, 212, 315, 418, 643
faux, 215, 218
in \mathbb{R}^3 , node, saddle, 219
jump-back, 211
jump-forward, 212
maximal, 200, 355, 419
point, 200, 418, 632
secondary, 226, 228, 420
secondary, turning point, 228
singular, 215, 401
singular cycle, 211
turning point, Gevrey, 273
vrai, 218
with head, 212
without head, 211
candidate, 64, 462, 655
canonical
adaptive dynamics, 680
transformation, 646
cap, 547
carrier density, 590
carrier wave, 613
celestial mechanics, 685
cell problem, 598
center
folded, 218
manifold, 49
chain recurrent, 542
chaotic, 435, 456, 458
characteristic polynomial, 300
first, 299
second, 299
characteristics, 563
chart, 28
classical, 220
fold point, 181
rescaling, 220
Chern number, 561
classical chart, 220
close vector fields, 28
cocycle property, 506
coevolutionary network, 697
coherence resonance, 479
cohomological Conley index, 531
collapse time, 365
collocation, 307
conditions, 307
points, 307
compact perturbation, 591
complete orbit, 437
complex
fast–slow system, 271
phase, 365
composite expansion, 246, 520
computational singular perturbation
condition, 334
fast fiber, 340
method, 331
one-step method, 332, 334
two-step method, 332, 334
condition
asymptotic matching, 245
conditional measure, 458
conditioning, 308
constant, 310
ill, 308
well, 308
cone, 440
condition, 440, 454
conjugate
topologically, 438
Conley index, 531
connecting homomorphism, 536
connecting orbit, 528
connection
matrix, 538
problem, 149
conservation law, 562
constrained ODE, 620
continuation, 312
natural, 314
problem, 313
property, Conley index, 532
related by, 526
contraction mapping theorem, 35
control
admissible, 606

- curve, 272
- theory, 88
- convex hull, 373
- coordinates
 - affine, 174
 - chart, 28
 - homogeneous, 174
- corner layer, 255
- corrector problem, 598
- correlation, 504
 - function, 503
- cost, 516
- covariance ellipsoid, 485
- critical
 - set, 12, 229
 - set, for 1D map, 457
 - transition, 654, 655
- critical manifold, 12, 54
 - normally hyperbolic, 48
 - random, 509
 - S-shaped, 188
 - tame branch, 388
- CSP, 331
 - condition, 334
 - fast fiber, 340
 - one-step method, 334
 - two-step method, 334
- CU-system, 653
- curvature, 233
- cusp point, 63, 167, 469
- DAE, 11, 620
 - linear, 623
- Dafermos regularization, 568
- Dahlquist
 - barrier theorem, 301
 - test equation, 300
- damped harmonic oscillator, 274
- delay
 - equation, 602
 - fold, 360
- delay equation, 586
- delayed Hopf bifurcation, 361, 407
- delta-distribution, 580
- Descartes, folium, 376
- desingularization, 167
- diffeomorphism, 29
- differential
 - algebraic equation, 11, 620
 - form, 129, 646
 - form, basic, 130
 - form, projective, 130
 - inclusion, 605
- differentiation index, 620
- diffusion
 - matrix, 472, 481, 514
 - process, 480
 - term, 480
- Diophantine equation, 379
- direct sum, 23
- directional blowup, 168
 - transition maps, 183
- discontinuous vector field, 628
- disordered series, 104
- distinguished limit, 251
- domain
 - of validity, 244
 - sectorial domain, 269
- dominant balance, 251, 393
- Dorodnitsyn's formula, 111
- double limit, 494
- double-well potential, 512
- Drazin inverse, 623
- drift, 480
- drop curve, 463
- drop point, 109
- duck, 200, 212
- Duffing equation, 275
- Duhamel's principle, 484, 487, 594
- dynamic bifurcation, 63
- Dynkin's equation, 518
- early-warning sign, 654
- ecology, 679
- edge of a network, 696
- eigenspace
 - center, 48
 - stable, 48
 - unstable, 48
- eigenvalue
 - nontrivial, 47
 - operator, 554

- problem, operator, 554
- singular, 207
- trivial, 47, 555
- eikonal equation, 261
- ellipsoid, 485
- elliptic
 - bursting, 417
 - operator, 595
- entrance point, slow, 541
- envelope, 613
 - equation, 614
- epsilon-embedding method, 624
- equation-free, 344
- equicontinuity, 610
- error
 - equidistribution, 308
 - global, 296
 - HMM, 320
 - local truncation, 296, 320
- essential spectrum, 555
- Estrin–Kubin model, 667
- Euclidean norm, 4
- Euler method
 - explicit, 296
 - implicit, 299
 - modified, 298
- Euler–Lagrange equations, 515
- Euler–Maruyama, 318, 478
- Evans function, 555, 557
- evolution operator, 309
- evolutionary dynamics, 680
- exchange lemma, 129
 - C^0 -version, 129
 - C^1 -version, 129
 - differential form version, 130
 - MFDE, 577
 - strong version, 148
 - with exponentially small error, 148
- exchange of stability, 231
- excitable system, 684, 700
- excitation, 691
- existential transfer, 639
- exit
 - guide, slow, 543
 - point, immediate, 544
- point, slow, 541
- set, 530
- time, 481, 514
- expansion
 - composite, 246
 - in 1D maps, 457
 - inner, 241
 - outer, 241
 - post-Newtonian, 602
 - small noise, 493
- explicit method, 298, 299
- exponential dichotomy, 556
- extended domain of validity, 244
- extended system, 117
- exterior product, 130
- Eyring–Kramers law, 517
- family of cones, 440
- fast
 - flow, 12, 47
 - rotating phase, 273
 - subspace, 345
 - subsystem, 12, 54
 - time, 8
 - variable, 8
 - vector field, 12
 - wave, 142, 351
- fast–slow
 - differential inclusion, 607
 - Markov chain, 511
 - random differential equation, 507
 - system, 8
 - system, complex, 271
 - vector field, 8
- faux canard, 215, 218
- feasible control, 606
- feedback system, 665
- Fenichel
 - normal form, 73, 74
 - theorem, classical fast–slow, 48
 - theorem, fast–slow systems, 55, 328
 - theorem, foliations, 45
 - theorem, general manifolds, 28, 42
- FHN, 11

- fiber
 bundle, 45
 stable, 45, 46
 unstable, 45
 Field–Körös–Noyes mechanism, 673
 Filippov convex method, 628
 Fillipov system, 606
 finite differences, 306
 finite smoothness, 65
 first
 -order corrector, 598
 exit-time, 481, 514
 integral, 202, 646
 Lyapunov coefficient, 209, 372, 408
 Lyapunov exponent, 435
 FitzHugh–Nagumo equation, 11
 2D ODE, 10, 233, 314, 372
 2D PDE, 10, 120, 573, 649
 3D ODE, 141, 350, 406, 534, 650
 lattice model, 573
 symmetry, 650
 FitzHugh–Nagumo equation
 3D ODE, 11, 67
 FKN mechanism, 673
 flow, 11, 584
 box, 75
 skew-product, 507
 fluid dynamics, 691
 Fokker–Planck equation, 473, 481
 fold
 bifurcation, 62
 blowup, 180
 curve, 80, 353
 curve, nondegenerate, 80
 curve, normal form, 80
 in the slow flow, 433
 nonautonomous, 103
 point, 62, 632
 point, generic, 77, 103, 178, 359, 386, 489
 point, nondegenerate, 62
 point, normal form, 77, 80, 359
 saddle, 450
 fold-homoclinic bursting, 416
 folded
 center, 218
 focus, 218, 410
 node, 218, 353, 400, 408, 410
 saddle, 218, 410
 saddle, example, 214
 saddle-node, 218, 404, 410
 singularity, 409
 singularity in \mathbb{R}^2 , 198
 singularity in \mathbb{R}^3 , 216
 singularity, generic, \mathbb{R}^2 , 198
 foliation, 45
 asymptotic rate, 46
 folium of Descartes, 376
 forward Kolmogorov equation, 481
 frozen
 component size, 700
 node, 698
 full system, 12
 function
 input-output, 365
 functional differential equation
 mixed, 574
 retarded, 586
 functional equation, 39
 functional response, 559
 fundamental solution, 309, 483, 556, 696
 gain, 578
 block, 665
 medium, 676
 galaxy, 640
 Gaspard–Nicolis–Rössler model, 399
 gating variable, 669
 gauge function, 15
 Gauss points, 307
 Gaussian random variable, 484
 generating function, 647
 generator, 481
 infinitesimal, 482
 Markov chain, 510
 generic, 62
 1-parameter family, 198
 delayed Hopf, 363
 fold point, 77, 103

- geometric
desingularization, 160
singular perturbation theory, 53,
56
- geometrical optics, 262
- Gevrey
asymptotic expansion, 269
order, 269
- Gierer–Meinhardt equation, 682
- Ginzburg–Landau equation, 615
- global error, 296
- good rate function, 514
- gradient, 5, 132
system, 512, 516
- graph, 33, 696
transform, 34, 35
- Green’s function, 309
- Gronwall’s lemma, 32
generalized, 138
- GSPT, 53
- Hénon map, 455
- half-return map, 447, 462
- halo, 641
- Hamiltonian
Schrödinger equation, 695
system, 273, 316, 646, 652
system, time-dependent, 647
- harmonic average, 599
- harmonic oscillator, 274, 276, 646
damped, 274
- Hausdorff distance, 55
- heat equation, 585
- Heaviside function, 578, 690
- height
of an edge, 384
of the Newton diagram, 384
- Hermite polynomial, 222
- Hermitian conjugate, 590
- Hessenberg index-1, 621
- Hessian, 163
- heteroclinic
cycle, 628
orbit, 114, 527
orbit, connection problem, 150
- heterogeneous, 596
- heterogeneous multiscale methods,
315
- hidden constraint, 622
- high-gain amplifier, 666
- HMM, 315
- Hodgkin–Huxley equations, 669
- Holling functional response, 559
- holomorphic, 270
- homoclinic orbit, 114, 405
computation, FHN, 350
double loop, 471
existence, FHN, 142
Lorenz-type model, 470
MFDE, 576
n-homoclinic, 407
- homogeneous coordinates, 174
- homogenization, 595, 596
- homogenized tensor, 596
- homological Conley index, 531
- homology, 531
- homotopy, 470
method, computation, 354
- Hopf bifurcation, 63, 361
delayed, 361, 407
in van der Pol-type system, 208
singular, 315, 643
singular, \mathbb{R}^2 , 206, 207
singular, \mathbb{R}^3 , 404
subcritical, 414, 416
theorem, 209
- horizontal
part, 439, 441
surface, 440
- horizontally cylindric, 441
- horseshoe map, 437
- hydra, 681
- hyperbolic
conservation law, 571
manifold, 41
matrix, 48
normally, 41
splitting, 41
- hyperreal number, 638, 640
- hysteresis, 633
operator, 635

- ILDM, 345
- ill conditioned, 308
- implicit
 - Euler method, 299
 - function theorem, 59
 - method, 299
- index
 - bundle, 550
 - DAE, 620
 - Morse, 556
 - of nilpotency, 623
 - pair, 530
 - pair, singular, 544
 - triple, 536
- induced derivation, 146
- inequality
 - Łojasiewicz, 166
- inertial manifold, 595, 601
- infinitely
 - close, 641
 - large, 638
 - small, 638
- infinitesimal generator, 481, 482
- infinitesimal hyperreal, 640
- inflection point, 233
- inflowing
 - invariant manifold, 21
- inhibition, 691
- initial conditions
 - sensitive dependence, 435
- inner
 - expansion, 241
 - layer, 242
 - product, 5
- input-output function, 365
- integer programming, 388
- integrating factor, 137
- integrator block, 665
- integrodifferential equation, 578, 590
- interaction kernel, 578
- interior layer, 150, 242, 253
- intersection
 - transverse, 142
- interval, 529
- interval arithmetic, 449
- intrinsic low-dimensional manifold, 345
- invariance equation, 328, 336, 604, 632
- invariant
 - globally, 20
 - locally, 49, 55
 - manifold, 22
 - manifold, random, 508
 - measure, 458
 - negatively, 45
 - positively, 46
 - probability measure, 317
 - set, 587
 - subspaces, blowup, 184
- inverse function theorem, 30
- isola, 485
- isolating
 - block, 531
 - neighborhood, 526, 540
 - neighborhood, singular, 541
- Itô integral, 480
- Itô's formula, 480, 483
- iterative method
 - slow manifold, 347
- Jeffrey–Hamel flow, 691
- jet, 163
- jump, 97
 - back canards, 211
 - forward canards, 212
 - on set, 151
 - matrix, 510
 - point, 109, 188, 191
- Kepler's second law, 686
- kinematic viscosity, 692
- Kirchhoff's law, 668
- Kolmogorov's
 - backward equation, 481, 517
 - forward equation, 481
- Koper model, 354, 408
 - symmetric, 409
- Kramers law, 517

- Lagrangian viewpoint, 693
Landau notation
 big-O, 14
 little-o, 14
Langevin equation, 497
LAO, 399
Laplace method, 490
Laplace transform, 501
Laplacian, 5, 611
large deviation
 principle, 514
 theory, 514
large-amplitude oscillation, 399
laser, 590, 676
lattice differential equation, 573
layer
 equations, 12
 inner, 242
 interior, 150, 242, 253
 outer, 242
 problem, 12
LDP, 514
leaf, 45
Lebesgue space, 587
Liénard transformation, 9
Liénard transformation, 573
Lie bracket, 333
light amplitude, 590
limit
 distinguished, 251
 set, alpha, 527
 set, omega, 527
limited distance apart, 640
limited hyperreal, 640
Lin's method, 653
Lindstedt's method, 276
linear
 k -step method, 299
 DAE, 623
 multistep method, 298
 recurrence relation, 299
 stability, traveling wave, 555
 system, 86
link, 696
Liouville equation, 472
Lipschitz
 set-valued map, 606
local
 truncation error, 296, 320
 vector field, 177
locally invariant manifold, 22, 55
logarithmic equivalence, 515
logistic map, 433
Lojasiewicz inequality, 166
Lorenz attractor, 468
Lyapunov
 α -type numbers, 23, 40
 coefficient, Hopf bifurcation, 209, 408
 equation, 484
 exponent, 435
 exponent, first, 435
 number, 435
macro solver, 316
macroscopic variable, 316
magnifying glass, 85, 644
manifold, 6, 54
 boundary, 149
 center-stable, semiflow, 589
 center-unstable, semiflow, 589
 critical, 12, 54
 hyperbolic, 41
 inertial, 595, 601
 inflowing invariant, 21
 intrinsic low-dimensional, 345
 invariant, 22
 locally invariant, 22
 normally hyperbolic, 41, 48, 54
 overflowing invariant, 22
 slow, 56
 stable, 42
 unstable, 42
map
 rank-one, 456
 singularly perturbed, 455
Markov chain, 510
martingale, 488
mass action kinetics, 674
matched asymptotic expansion, 240, 243, 248
maximal canard, 200

- Maxwell–Bloch equation, 593
 measure
 F-invariant, 458
 -preserving, 506
 acc, 459
 conditional, 458
 physical, 459
 SRB, 459
 Melnikov
 method, 228, 684
 theory, 156
 membrane potential, 668
 mesh, 306
 adaptation, 308
 metastable, 481
 method
 of characteristics, 563
 of multiple scales, 277
 metric dynamical system, 506
 MFDE, 574
 Michaelis–Menten kinetics, 688
 Michaelis–Menten–Henri, 338
 micro solver, 316
 microscopic variable, 316
 mild solution, 594
 Minkowski sum, 373
 mitotic oscillator, 688
 mixed functional differential equation, 574
 mixed-mode oscillations, 398
 mixing, 436, 458
 MMH, 338
 MMO, 398
 modified Euler method, 298
 modulation equation, 614
 moment
 of falling, 364
 of jumping, 364
 Morris–Lecar model, 413, 416, 689
 Morse
 decomposition, 529
 index, 556
 moving
 frame, 339
 window, 658
 multi-index, 280, 377
 multiple
 scales method, 277, 596
 shooting, 306
 multiplier, 437
 multistep method, 298, 625
 natural continuation, 314
 near-identity transformation, 273
 negatively invariant, 45
 neighborhood
 isolating, 526
 Nernst potential, 668
 Netushil’s principle, 635
 networks, 696
 neural competition, 485
 neural field, 578
 neuroscience, 668
 Newell–Whitehead–Segel equation, 614
 Newton
 diagram, 374
 diagram, height, 384
 law of gravitation, 686
 method, 307
 open polygon, 375
 polygon, 373
 Newtonian expansion, 602
 nilpotency index, 623
 node
 folded, 218, 353
 of a graph, 696
 noise level, 493
 noise-induced
 effect, 479
 transition, 479
 nondegenerate
 fold curve, 80
 fold point, 62
 nonsmooth system, 628
 nonstandard analysis, 637
 nonwandering set, 443
 norm, 4
 sup-norm, 37
 Euclidean, 4
 normal
 bundle, 23

- form, 71
- hyperbolicity, semiflow, 588
- space, 23
- switching condition, 80, 191, 461
- normal form
 - Fenichel, 74
 - fold point, 77, 359
 - Hopf bifurcation, 361
 - linear system, 87
 - theory, 284
- normally hyperbolic
 - attracting, 55
 - manifold, 41, 48, 54
 - planar system, 98
 - repelling, 55
 - saddle type, 55
 - splitting, 41
- numerical continuation, 312
- ODE, 3
- omega limit set, 527
- one-step method, 298
- operator norm, 587
- orbit
 - complete, 437
 - heteroclinic, 114
 - homoclinic, 114
- order, 298
 - higher than, 14
 - not lower than, 14
 - partial, 529
 - total, 529
- Oregonator, 674
- Ornstein–Uhlenbeck process, 484, 503
- oscillation
 - bursting, 398
 - large-amplitude, 399
 - mixed-mode, 398
 - relaxation, 97
 - relaxation, simple, 97
 - small-amplitude, 399
- outer
 - expansion, 241
 - layer, 242
- overflowing invariant manifold, 22
- overlap domain, 244
- part
 - horizontal, 439, 441
 - vertical, 439, 441
- partial order, 529
- PDE, 4
- period
 - of oscillation, vdP, 108
 - of relaxation oscillation, \mathbb{R}^3 , 194
- perturbation
 - regular, 95
 - singular, 95
- phase
 - complex, 365
- physical measure, 459
- physical optics, 262, 695
- pitchfork bifurcation, 265, 386
- Planck's constant, 694
- plane bundle, 561
- plastic deformation, 667
- play operator, 633
- Poincaré asymptotics, 270
- Poincaré–Lindstedt method, 276
- point spectrum, 555
- polar blowup
 - \mathbb{R}^2 , 160
 - \mathbb{R}^n , 162
 - rescaled, 164
 - weighted, 173
 - weighted, rescaled, 173
- population inversion, 676
- positive averages, strictly, 542
- positively invariant, 46, 587
 - random set, 507
- post-Newtonian expansion, 602
- potential
 - double-well, 512
 - quasi-, 516
- power
 - positive, 458
 - ramp, 372
 - transformation, 377
 - transformation, unimodular, 377
- predator–prey, 558, 679
- predictor–corrector, 313
- principal solution, 309, 483, 556, 696

- probability
 - density, 480
 - distribution, 480
- projective space, 174
- propagation failure, 575
- propagator, 309
- pullback, 130
- pushforward, 130, 162
- set, 544
- Q-matrix, 510
- quantum adiabatic theorem, 695
- quantum Hamiltonian, 695
- quartic oscillator, 261
- quasihomogeneous
 - blowup, 173
 - fold, 180
 - function, 172
 - vector field, 172, 393
- quasipotential, 516
- quasistationary distribution, 512
- Radon–Nikodym derivative, 459
- ramp, 370
- random
 - critical manifold, 509
 - differential equation, 507
 - dynamical system, 506
 - equilibrium point, 509
 - invariant manifold, 508
 - set, 507
- rank-one map, 456
- Rankine–Hugoniot condition, 565
- rarefaction, 566
- rate
 - function, 514
 - independence, 635
 - independent memory, 635
- Rayleigh’s equation, 280
- RDE, 507
- RDS, 506
- reaction–diffusion equation, 554, 586
- recall, 29
- rectangle, 441
- rectification lemma, 75
- recurrence relation, 299
- reduced flow, 11
- reduced problem, 11
- reflection coefficient, 695
- region of absolute stability, 301
- regular
 - pair, 623
 - perturbation, 95
 - point, fast–slow, 58
- regularization
 - Dafermos, 568
 - nonsmooth, 630
 - viscous, 567
- related by continuation, 526
- relative homology, 531
- relaxation oscillation, 97, 188
 - asymptotics in \mathbb{R}^3 , 194
 - existence in \mathbb{R}^2 , 188
 - existence in \mathbb{R}^3 , 190
 - period, vdP, 108
 - simple, 97, 109
- renormalization, 285
- renormalization group, 279
 - condition, 280, 283
 - equation, 286
 - equation, k th-order, 289
 - transformation, 286
 - transformation, k th-order, 289
- repeated blowup, 165
- repelling normally hyperbolic, 55
- replica, 318
- rescaling, 83
 - chart, 220
 - time, 195
- resonance, 219
 - Ackerberg–O’Malley, 69
 - coherence, 479
 - stochastic, 479
- resonant term, 284
- retarded functional differential
 - equation, 586, 600
- Reynolds number, 692
- Riccati equation, 107
- Riemann
 - Dafermos solutions, 568
 - problem, 567

- Rosenzweig–MacArthur model, 558, 679
rotation
sector of, 403, 424
Runge–Kutta method, 298
- saddle
-focus, 407
-node bifurcation, 62
-node, folded, 218
-type slow manifold, 310, 348
node of limit cycles, 213
type, normally hyperbolic, 55
folded, 218
- sample path, 318, 478
SAO, 399
scale-invariant conservation laws, 568
scaling law, 658
Brownian motion, 482
fold, 360
- Schilder’s theorem, 515
Schrödinger equation, 260, 694
Schur
decomposition, 345
vector, 345
- SDE, 478
secondary canard, 226, 228, 420
section, 30, 33
sector of rotation, 403, 424
sectorial domain, 269
secular terms, 275, 687
self-organized criticality, 700
semiexplicit system, 620
semiflow, 584
semigroup, 584
sensitive dependence, 435
separation time, 365
series
asymptotic, 92
disordered, 104
uniformly convergent, 92
- set-valued map, 605
Lipschitz, 606
shadow, 641
- Sharkovsky
ordering, 434
theorem, 434
- shift
Bernoulli, 438
- shock, 564
- shooting
multiple, 306
simple, 305
- simple shooting, 305
- Sinai–Ruelle–Bowen measure, 459
- single-neuron models, 668
- singular
bifurcation diagram, 409, 649
canard, 215
canard cycle, 211
eigenvalue, 207
faux canard, 215
Hopf bifurcation, 315, 643
Hopf bifurcation, \mathbb{R}^2 , 206, 207
Hopf bifurcation, \mathbb{R}^3 , 404, 408
index pair, 544
isolating neighborhood, 541
limit, 12
perturbation, 95
point, fast–slow, 58
point, singularity theory, 58
trajectory, 65
transition matrix, 539
- singular perturbation
computational, 331
geometric theory, 56
problem, 95
- singularity
folded, in \mathbb{R}^3 , 216
transcritical, 229
- singularly perturbed map, 455
skew-product flow, 507
sleep–wake cycle, 689
- sliding
flow, 629
window, 658
- slow
entrance point, 541
entrance point, strict, 545
exit guide, 543

- exit point, 541
- flow, 11, 47, 54, 58
- manifold, 56
 - manifold, finite smoothness, 65
 - manifold, iterative, 347
 - manifold, saddle-type, 310, 348
 - subspace, 345
 - subsystem, 11, 54
 - time, 8
 - variable, 8
 - vector field, 11
 - wave, 142
- slowing down, 657
- Smale horseshoe, 437, 443
 - existence theorem, 441
- small-amplitude oscillation, 399
- smooth manifold, 54
- SMST algorithm, 348
- Sobolev space, 515
- special
 - flow, delay equation, 601
 - linear group, 377
 - solution, delay equation, 601
- spectral
 - gap, 696
 - gap, RDEs, 508
 - problem, 554
- spectrum, 554
 - essential, 555
 - point, 555
- spike, 399, 669
- spiral wave, 684
- splitting, 439
 - hyperbolic, 41
 - normally hyperbolic, 41
- square-wave bursting, 416
- SRB measure, 459
- stability polynomial, 300
- stable
 - absolutely, 301
 - fiber, 45, 46
 - manifold theorem, 20
 - subspace, 20
- standard
 - part, hyperreal, 641
 - rectangle, 439
- standing wave, 694
- state space form method, 625
- static network, 697
- stiff differential equation, 297
- stiffness ratio, 297
- stochastic resonance, 479
- Stokes number, 693
- Stommel flow, 625, 693
- Stommel–Cessi model, 659
- stop operator, 637
- strained coordinate, 276
- strange attractor, 436
- strict slow entrance point, 545
- strictly positive averages, 542
- structural stability, 443
- subHopf–foldcycle bursting, 417
- subordinate, 458
- subspace
 - fast, 345
 - slow, 345
 - stable, 20
 - unstable, 20
- sufficiently small, 8
- sup-norm, 37
- superslow, 418
- support function, 609
- surface
 - horizontal, 440
 - vertical, 440
- Swift–Hohenberg equation, 611
- symbol sequence for MMOs, 399
- symbolic dynamics, 438
- symmetry
 - FHN, 650
 - periodically forced vdP, 447
- symplectic 2-form, 646
- system
 - extended, 117
 - of first approximation, 83, 85, 222
- systems biology, 688
- tame branch, 388
- tangent
 - bundle, 23
 - invariant manifolds, 413
 - prediction, 313

- test function, 565
thermal conductivity tensor, 595
thermohaline circulation, 658
three-time-scale, 417
Tikhonov's theorem, 56
time
 rescaling, 195
 scale, 8
 step, 296
topologically
 conjugate, 438
 transitive, 436
total order, 529
tourbillon, 408
trait, 680
transcendentally small, 248
transcritical point, 63, 229
transfer principle, 639
transformation
 canonical, 646
 power, 377
transition
 function, nonsmooth, 630
 map, 177
 maps, blowup, 183
 matrix, 539
 matrix, singular, 539
 point, 655
 probability, 481, 511
transitive
 topologically, 436
translation invariance, 555
transmission coefficient, 695
transport equation, 261, 594
transversal
 bundle, 30
 intersection, 142
transversality, 29
 condition, fold, 77
 condition, fold curve, 80
 parametric, 1D maps, 457
trapezoid rule method, 299
traveling
 back, 120
 front, 120
 pulse, 120
pulse, neural field, 579
wave, 10, 120
wave train, 120
wave, nonlinear stability, 555
wave, spectral stability, 555
trivial eigenvalue, 555
truncation, 380
tube, 546
tubular neighborhood, 188
tunneling, 694
turning point, 62, 69, 272, 304, 695
 of canards, 228
twist, 401
two-body problem, 685
two-scale convergence, 599
two-timing, 277, 687
ultrafilter, 639
uniformity lemma, 26, 32
unimodal map, 433
unimodular power transformation, 377
universal transfer, 639
unlimited hyperreal, 640
unstable
 fiber, 45
 subspace, 20
upper semicontinuous, 608
van der Pol equation, 9, 16
 constant forcing, 9, 201, 233, 234, 305, 478, 642
 equation, 194
 periodically forced, 10, 13, 82, 97, 190, 222, 442, 460
 stochastic, 478, 494
 unforced, 9, 13, 59, 96, 102, 108, 252, 330, 541, 545
variable
 macroscopic, 316
 microscopic, 316
variation of constants, 484, 594
variational equation, 117, 451
vdP, 9
vector bundle, 23
vector exponent, 377

- vector field
 - discontinuous, 628
 - local, 177
 - perturbed, 28
 - quasihomogeneous, 172, 393
 - unperturbed, 28
- vertex, 696
- vertical
 - part, 439, 441
 - surface, 440
- vertically cylindric, 441
- viscosity, 692
- viscous profile criterion, 567
- viscous regularization, 567
- vrai canard, 218
- wandering set, 443
- Wang–Young theory, 456
- wave
 - fast, 142
 - function, 694
 - number, 612
 - slow, 142
 - speed, 10, 120
 - vector, 612
- way-in/way-out map, 365
- Wazewski property, 532
- weak solution
 - conservation law, 565
- Weber equation, 221
- wedge product, 130
- Weierstrass canonical form, 623
- weighted
 - directional blowup, 176, 177
 - polar blowup, 173
- well conditioned, 308
- Wentzel–Kramers–Brillouin, 259
- white noise, 472
- Whitney sum, 562
- Wiener
 - measure, 506
 - space, 506
- WKB, 259, 518
 - delayed Hopf, 371
- Yamada model, 678
- ZDP, 342
- zero section, 30
- zero-derivative principle, 342
- zoom, 85